

**57th SWST International
Convention
7th Wood Structure and Properties
Conference
6th European Hardwood
Conference**

June 23–27, 2014

**Technical University in Zvolen
Zvolen, Slovakia**

Edited by: H. Michael Barnes and Victoria L. Herian

***Overall General Co-Chairs: Michael Wolcott, Washington
State University, USA and Marian Babiak,
Technical University in Zvolen, Slovakia***

Table of Contents

Hardwood Research & Utilization

Session Co-Chairs: Rado Gazo, Purdue University, USA and Róbert Németh, University of West Hungary, Hungary

Rado Gazo, Juraj Vanek, Michel Abdul-Massih, and Bedrich Benes, Purdue University, USA
CT Scanning of Logs – Analysis and Optimization for Better Utilization of Hardwoods..... 15

Roman Réh, Technical University in Zvolen, Slovakia
Decorative Veneer Properties of Black Walnut (*Juglans nigra L.*)..... 16

Leandro Passarini, Université Laval; Cédric Malveau, Université de Montréal ; Roger Hernández, Université Laval, Canada
Distribution of the Equilibrium Moisture Content in Four Hardwoods Below Fiber Saturation Point by Magnetic Resonance Microimaging..... 22

Bryan Dick, Perry Peralta, and Ilona Peszlen, North Carolina State University, USA
Changes in the Anatomy of Exposed Roots of Some Hardwood Species..... 24

Szabolcs Komán, University of West Hungary, Hungary; Wilfried Beikircher and Christian Lux, University of Innsbruck, Austria
Mechanical Properties of Common Beech (*Fagus sylvatica L.*) after Microwave Drying in Comparison to Naturally and Laboratory Oven-dried Material..... 25

Róbert Németh, Dimitrios Tsalagkas and Miklós Bak University of West Hungary, Hungary
Protecting Effect of Beeswax Impregnation on the Modulus of Elasticity During Soil Contact..... 35

Solid Wood Manufacturing

Session Co-Chairs: Bob Rice, University of Maine, USA and Levente Dénes, University of West Hungary, Hungary

Douglas J. Gardner, Ashley A. Hellebrand, Barbara J.W. Cole, Raymond C. Fort Jr., University of Maine, USA
Processing Conditions Contributing to Formaldehyde Emissions from “Native” Wood..... 45

Thomas Krenke, Stephan Frybort, Oliver Vay, Kompetenzzentrum Holz GmbH, Austria ; and Ulrich Müller, BOKU – University of Natural Resources and Life Sciences, Austria
A New Method of Dynamic 3D-cutting Force Analysis of Wood..... 47

Yaroslav Sokolovskyy, Yu. Prusak and I. Kroshnyy, National Forestry University of Ukraine, Ukraine
Mathematical Modeling of Rheological Behaviour of Capillary- Porous Materials with Fractal Structure During Drying..... 53

Levente Dénes, Balázs Bencsik, Zsolt Kovács, János Kalmár, Viktória Csanádi, University of West Hungary, Hungary
Monte Carlo Simulation of Window’s Air Tightness Performance..... 61

Nikolay Skuratov and Anatoliy Vojakin, Moscow State Forest University, Russia
Decorative Finger Jointing of Valuable Wood..... 63

*Proceedings of the 57th International Convention of Society of Wood Science and Technology
June 23-27, 2014 - Zvolen, SLOVAKIA*

Forest Products Policy, Global Trade, and Value Chain Management
Session Co-Chairs: Eric Hansen, Oregon State University, USA and Mikulas Supin,
Technical University in Zvolen, Slovakia

Henry Quesada-Pineda, Edgar Arias, and Robert Smith, Virginia Tech, USA
Factors Impacting the Export of US Hardwoods in Germany, China and Vietnam..... 70

Manja Kuzman, Mirko Kariž, and Martina Zbašnik-Senegačnik, University of Ljubljana, Slovenia
Timber Passive House Technologies of Slovenian Contemporary Architecture..... 78

Yvonne Brodrechtova, Marek Trenčiansky, Daniel Halaj, Technical University in Zvolen, Slovakia
Dynamics of Slovakian Timber Market in Retrospect..... 89

Michael Burnard and Andreja Kutnar, University of Primorska, Slovenia
Restorative Environmental Design: Wood as a Material for Sustainable, Healthy Environments..... 97

**Alexandru Giurca, European Forest Institute, Sweden; Ragnar Jonsson, European Commission Joint
Research Centre, Italy; Marko Lovrić, European Forest Institute, Finland; and Ed Pepke, European
Forest Institute, France**
European Union Timber Regulation Impact on International Timber Markets.....105

**Erlend Nybakk, Norwegian Forest and Landscape Institute, Norway; Eric Hansen, Oregon State
University, USA; Andreas Treu, Norwegian Forest and Landscape Institute, Norway;
and Tore Aase, UMB School of Economics and Business, Norway**
Chemical Suppliers' Views and Impact on Innovation in the Wood Treating Industry.....120

Sustainable Forest Management
Session Co-Chairs: Ilona Peszlen, North Carolina State University, USA and Jaroslav Kmet',
Technical University in Zvolen, Slovakia

**Julie Bossu, CNRS, UMR Ecofog, French Guiana; Jacques Beauchêne, CIRAD, French Guiana,
Bruno Clair, CNRS, French Guiana**
Looking for "Paradoxical" Species for a Sustainable Forest Management in French Guiana.....127

Ubong Ime Udoakpan, University of Uyo, Nigeria
A Comparative Study of Wood Properties of *Pinus caribaea* (Morelet) in Two Plantation Ages in
Oluwa Forest Reserve, Ondo State, Nigeria.....136

**Anton Zbonak, Department of Agriculture, Fisheries and Forestry, Australia; Henri Bailleres and
Rob McGavin, Forest Products Innovation, QDAFF, Australia**
Veneering of Plantation Grown Sub-tropical Species from Thinning Experiments.....137

**Tahiana Ramanantoandro, Université d'Antananarivo, Madagascar; Miora F. Ramanakoto,
Institut Universitaire de Technologie de Tarbes, France; Patrick H. Rafidimanantsoa, Université
d'Antananarivo, Madagascar**
Influence of the Tree Diameter and Shade-tolerance on Wood Density and its Radial Variation
in Madagascar Rainforest..... 145

Perry Peralta, Ilona Peszlen, and Vincent Chiang North Carolina State University, USA
Bridging Forest Biotechnology and Biomaterials Engineering.....147

Lignocellulosic Material Science and Wood Quality
Session Co-Chairs: Barry Goodell, Virginia Tech, USA and Alfred Teischinger,
Universität für Bodenkultur, Austria

*Proceedings of the 57th International Convention of Society of Wood Science and Technology
June 23-27, 2014 - Zvolen, SLOVAKIA*

Roger Rowell, University of Wisconsin, USA Accessibility and Reactivity of Hydroxyl Groups in Wood.....	149
Barry Goodell, Virginia Tech, USA; Valdeir Arantes, University of British Columbia, Canada; Jody Jellison, Virginia Tech, USA Non-enzymatic Deconstruction Systems in the Brown Rot Fungi.....	155
Jerrold Winandy, University of Minnesota, USA; H.Michael Barnes and P.David Jones, Mississippi State University, USA Modeling Severity of Exposure Relationships Between Laboratory and Field Exposures for FRT Plywood.....	156
Chloé Maury, Khalil Jradi, and Claude Daneault, Université du Québec à Trois-Rivières, Canada Study of Mechanical Properties of Composites Based on TEMPO-oxidized Cellulose Gel and Silica Nanoparticles.....	160
Dimitrios Tsalagkas, University of West Hungary, Hungary; Rastislav Lagaña, Technical University in Zvolen, Slovakia; Levente Csóka, University of West Hungary, Hungary Morphological and Structural Changes of Ultrasound-treated Bacterial Cellulose.....	161
Stefan Pinkl, Kompetenzzentrum Holz GmbH, Austria; Stefan Veigel, BOKU, University of Natural Resources and Life Sciences, Austria; Erik van Herwijnen, Kompetenzzentrum Holz GmbH, Austria; Wolfgang Gindl-Altmutter, BOKU, University of Natural Resources and Life Sciences, Austria Fibrillation of Different Lignocellulose Suspensions and their Bonding Strength to Wood Compared with Nanocellulose.....	170
Yaroslav Sokolovskyy and O. Storozhuk, Ukrainian National Forestry University, Ukraine Determination of the Non-isotropic Elastic Features for Wood by an Ultrasonic Method.....	178
Galina Gorbacheva, Moscow State Forest University, Russia; Yuri A. Olkhov, Russian Academy of Sciences, Russia; Boris N. Ugolev and Serafim Yu. Belkovskiy, Moscow State Forest University, Russia Research of Molecular-Topological Structure at Shape-Memory Effect of Wood.....	187
Peder Gjerdrum, Norwegian Forest and Landscape Institute, Norway Grain Angle Variation in Norway Spruce: Overall Pattern and Stochastic Dissimilarities Within and Between Stems.....	196
Ilona Peszlen, Perry Peralta, Zachary Miller, Charles Edmunds, and Zhouyang Xiang; North Carolina State University, USA Variation in Cell Morphology of Genetically Engineered Aspen and Cottonwood.....	202
Hyeun-Jong Bae, Chonnam National University, Korea Rapid Hydrolysis of Lignocellulosic Wood Biomass.....	203
Veronika Kotradyova, Slovak University of Technology, Faculty of Architecture, Slovakia; Alfred Teischinger, BOKU – University of Natural Resources and Life Sciences, Austria Tactile Interaction and Contact Comfort of Wood and Wood Materials.....	204
Peter Niemz, Katalin Kranitz and Walter Sonderegger; ETH Zurich, Switzerland Effect of Natural Aging on Wood Properties.....	214
Stephen Frybort and Thomas Krenke, Kompetenzzentrum Holz GmbH, Austria; Ulrich Müller, Deformation Analysis of Cutting Processes of Wood.....	222

*Proceedings of the 57th International Convention of Society of Wood Science and Technology
June 23-27, 2014 - Zvolen, SLOVAKIA*

Wood Panels Composites

Session Co-Chairs: Marius Barbu, Transilvania University of Brasov, Romania and Sergej Medved, University of Ljubljana, Slovenia

Marius Barbu, Axel M. Rindler, Pia Solt, and Thomas Schnabel; Salzburg University of Applied Sciences, Austria

The Use of Waste Leather in Wood-based Panels.....227

Marius Barbu, Günther Kain, Marius-Catalin Barbu, Alexander Petutschnigg, Bettina Hauser, and Michael Mazzitelli; Salzburg University of Applied Sciences, Austria

Bark-based Insulation Panels Made of Different Softwood Barks.....236

Ayfer Donmez Cavdar and Hulya Kalaycioglu, Karadeniz Technical University, Turkey; Ertugrul Casur, Kastamonu Integrated Wood Industry & Trade Company, Turkey; Fatih Mengeloglu, Kahramanmaraş Sutcuimam University, Turkey

Some Properties of Fire Retardants and Sand Dusts of Medium Density Fiberboard Filled Wood Plastic Composites.....244

Kate Semple, University of British Columbia, Canada; Martin Smola, Fachhochschule Rosenheim, Germany; John Hoffman, FPInnovations, Canada; Gregory D Smith, University of British Columbia, Canada

Optimising the Stranding of Moso Bamboo (*Phyllostachys pubescens* Mazel) Culms Using a CAE 6/36 Disk Flaker.....257

Ahmad Jahan-latibari, Islamic Azad University Karaj Branch, Iran; Fardad Golbabaee, Institute of Forests and Rangeland, Iran

The Potential Of Urban Wood Residues in Particleboard Production.....270

Eike Alexander Mahrtdt and Hendrikus W. G. van Herwijnen, Wood K Plus, Austria; Wolfgang Gindl-Altmatter, BOKU – University of Natural Resources and Applied Life Science, Austria; Wolfgang Kantner and Johann Moser, Metadynea Austria GmbH, Austria; Ulrich Müller, BOKU – University of Natural Resources and Applied Life Science, Austria

A New Analytical Method to Study UF Resin Distribution within Particle Boards.....278

Johann Trischler, Linnaeus University, Sweden; Dick Sandberg, Luleå University of Technology, Sweden; Thomas Thörnqvist, Linnaeus University, Sweden

Classification of Lignocellulose Raw Materials Regarding Selected Material Properties and the Requirements of Three Competitors to Reveal Options for Alternative Use.....287

Christoph Wenderdel, Tino Schulz and Detlef Krug, Institut fuer Holztechnologie Dresden GmbH, Germany; Alf-Mathias Strunz, Papiertechnische Stiftung, Germany

Very Thin Medium Density Fibreboards (MDF) with Paperboard-like Properties as Reusable Packaging Material.....296

Anna Ślęzak and Stanisław Prosyk, Poznan University of Life Sciences, Poland

Investigations upon Resistance of Surfaces Panel Elements Bonding by Artificial Veneers from Hot Melt Adhesives.....305

Min Niu, Fujian Agriculture and Forestry University, China; Olle Hagman and Xiaodong (Alice) Wang, Luleå University of Technology, Sweden; Yongqun Xie, Fujian Agriculture and Forestry University, China

Fire Properties Improvement of an Ultralow Density Fiberboard.....312

Levente Dénes, Viktor Utassy, and Zsolt Kovács University of West Hungary, Hungary

Finite Element Modelling Simplification of Paper Honeycomb Panels by a Substituting Homogenous Core.....320

*Proceedings of the 57th International Convention of Society of Wood Science and Technology
June 23-27, 2014 - Zvolen, SLOVAKIA*

Wood Construction & Structures

Session Co-Chairs: Arijit Sinha, Oregon State University, USA and Bohumil Kasal, Fraunhofer Wilhelm Klauditz Institute, Germany

Andreja Kutnar, University of Primorska, Slovenia; Anthonie Kramer, Arijit Sinha, and Andre Barbosa, Oregon State University, USA

Cross Laminated Timber Panels Using Hybrid Poplar.....321

Karol Sikora and Annette M. Hart, National University of Ireland, Ireland; Daniel O. McPolin, Queen's University Belfast, UK

Durability of Adhesive Bonds in Cross-laminated Timber (CLT) Panels Manufactured.....323

Bryan Dick, North Carolina State University, USA; Miklos Horvath, Obuda University, Hungary; Perry Peralta, Phil Mitchell and Iona Peszlen, North Carolina State University, USA; Weichi Pang and Scott Schiff, Clemson University, USA; Robert White, U.S. Forest Products Laboratory, USA

Fire Performance of Adhesives Used for Southern Pine Cross-Laminated Timber.....332

Georg Stecher, Anton Kraler and Roland Maderebner, University of Innsbruck, Austria

“Radiusholz” – Curved Cross-laminated Timber Elements.....334

Marius Barbu and Josef Weissensteiner, Salzburg University of Applied Sciences, Austria; Timothy M. Young, University of Tennessee, USA

Cross Laminated Timber – Implementation of European Experiences in the USA.....342

Desmond Dolan, Mark McCaffrey and Annette Harte, National University of Ireland, Ireland

A Hybrid Input-Output LCA Analysis of Timber Construction Products Produced in Ireland.....349

David DeVallance, Gregory Estep and Shawn Grushecky, West Virginia University, USA

Spatial Analysis of Certified Wood Use in LEED Green Building Projects.....358

Jaromir Milch, Jan Tippner, Martin Brabec and Václav Sebera, Mendel University in Brno, Czech Republic

Experimental Verification of Numerical Model of Single and Double-Shear Dowel-Type Joints of Wood.....368

Energy, Fuels, Chemicals

Session Co-Chairs: Dave DeVallance, West Virginia University, USA and Margareta Wihersaari, Åbo Akademi University, Finland

Quy Nam Nguyen, Alain Cloutier, Alexis Achim, and Tatjana Stevanovic Université Laval, Canada

Fuel Pellets from Low Quality Hardwood Trees: Raw Materials and Pelletization Characteristics..377

Robert Rice, University of Maine, USA; Evan Chatmas, New Page Paper Company, USA;

Douglas Gardner and Adrian Van Heiningen, University of Maine, USA

Rapid Assessment of Pellet Ash Agglomeration Using Electrical Resistivity.....385

Bestani Benaouda and Benderdouche Noureddine, University of Mostaganem, Algeria

Chemically Treated Wood-based Material for the Removal of Phenol from Aqueous Media.....387

*Proceedings of the 57th International Convention of Society of Wood Science and Technology
June 23-27, 2014 - Zvolen, SLOVAKIA*

Wenliang Wang and Jianmin Chang, Beijing Forestry University, China; Liping Cai and Sheldon Q. Shi, University of North Texas, USA Fast Pyrolysis of Wastes and Bio-refinery for Value-added Products.....	397
Amy Falcon and Jingxin Wang, West Virginia University, USA Optimizing Urea Concentration for Woody Biomass Pretreatment.....	404
Richard Bergman and Hongmei Gu, US Forest Service Forest Products Laboratory, USA Life-cycle Inventory Analysis of Bio-products from a Modular Advanced Biomass Pyrolysis System.....	405
Md Sarwar Jahan, BCSIR, Bangladesh; Haitang Liu and Hui ren Hu, Tianjin University of Science and Technology, China; Yonghao Ni, University of New Brunswick, Canada Improvement of Furfural Production From Concentrated Pre- Hydrolysis Liquor (PHL) of a Kraft-Based Hardwood Dissolving Pulp Production Process.....	416
Melanie Blumentritt and Stephen M. Shaler, University of Maine, USA Electron Microscopic Study of Neat and Hot Water Extracted Aspen Wood by Means of Selective Electron Dense Staining and Immunogold Labeling.....	417
Milan Sernek and Matjaž ČOP, University of Ljubljana, Slovenia Curing Kinetics of Spruce Bark Tannin-Based Foams.....	425
Ru Liu and Jinzhen Cao, Beijing Forestry University, China Some Physical and Mechanical Properties of Two-step Organo-montmorillonite Modified Wood Flour/Polypropylene Composites.....	426
Michel Delmas, Bouchra Benjelloun-Mlayah and Nadine Tacho, University of Toulouse, France; Louis Pilato, Pilato Consulting, USA Biolignin™, a Renewable and Efficient Natural Product for Wood Adhesives.....	433
Advanced Wood and Polymer Composites Session Co-Chairs: Rupert Wimmer, BOKU Vienna, IFA Tulln, Austria and Joris Van Acker, Ghent University, Belgium	
Matthew Schwarzkopf and Lech Muszyński, Oregon State University, USA Strain Distribution and Load Transfer in the Polymer-wood Particle Bond in Wood Plastic Composites (WPCs).....	434
Gloria Oporto, Tuhua Zhong, Jacek Jaczynski and Ronald Sabo West Virginia University, USA Microstructure, Mechanical, Thermal and Antimicrobial Properties of Hybrid Copper Nanoparticles and Cellulose Based Materials Embedded in Thermoplastic Resins.....	441
Stephen Shaler, Nadir Yildirim and R. Lopez-Anid, University of Maine, USA Cellulose Nanofibril (CNF) Reinforced Open Cell Foams - Application of Cubic Array Foam Theory.....	451
Sheldon Shi, Changlei Xia and Liping Cai, University of North Texas, USA Vacuum Assisted Resin Transfer Molding Process for Kenaf Fiber Based Composites.....	459
David De Vallance and Nan Nan, West Virginia University, USA Bio-based Carbon/Polyvinyl Alcohol Piezoresistive Sensor Material.....	467
A. Emeran Neuhäuser and Hendrikus Van Herwijnen, Wood K Plus, Austria; Stefano D'Amico and Ulrich Müller, BOKU- University of Natural Resources and Life Sciences, Austria Lifecycle of a Novel Bio-based Wood Composite made of Sawmill Waste.....	475

*Proceedings of the 57th International Convention of Society of Wood Science and Technology
June 23-27, 2014 - Zvolen, SLOVAKIA*

Nadir Ayrilmis and Alperen Kaymakci, Istanbul University, Turkey; Turker Güleç, Artvin Çoruh University, Turkey Mechanical Performance of Wood Plastic Composite Containing Decayed Wood.....	482
Joris Van Acker, Imke De Windt, Wanzhao Li, and Jan Van den Bulcke, Ghent University, Belgium Moisture Dynamics of Plywood and Impact on Time of Wetness.....	488
Yonggun Park, Yeonjung Han, Jun-Ho Park, Yoon-Seong Chang, JuHee Lee, Sang-Yun Yang, Hwanmyeong Yeo, Seoul National University, Korea Properties of the Wood Dried and Heat-treated by Superheated Steam.....	489
Sheldon Shi, University of North Texas, USA; Jun Hua, Wei Xu, Guangwei Chen and Keqi Wang, Northeast Forestry University, China; Liping Cai, University of North Texas, USA Correlation Between Fracture Fractal Dimension and Wood Shear Properties after Hydrothermal Treatment.....	497
Roland Maderebner, Thomas Badergruber and Anton Kraler University of Innsbruck, Austria Artificially Aged Timber for Structural Components.....	510
Levente Dénes and Balazs Bencsik, University of West Hungary, Hungary Modification of Wood by Organometallic Processes.....	518
Poster Session and Student Poster Competition Session Co-Chairs: Douglas Gardner, University of Maine, USA and Jozef Kúdela, Technical University in Zvolen	
Turgay Akbulut and Zeki Candan, Istanbul University, Turkey Low Formaldehyde-Emitting Wood Composites by Nanotechnology.....	519
Abdulrazzak Raoof Alsulaiman, Mosul University, Iraq; Ahmed Younis Al-Khero, Ministry of Agriculture/Ninavah Agricultural Directorate, Iraq Phthalic Acid Unhydride for Wood Modification.....	524
Ioannis Barboutis, Aristotle University of Thessaloniki, Greece; Charalampos Lykidis, Hellenic Agricultural Organization "Demeter" The Effects of Bark on Fuel Characteristics of Some Evergreen Mediterranean Hardwood Species.....	533
Bogdan Bedeleian, Cristina Olarescu, and Mihaela Campean, Transilvania University of Brasov, Romania Predicting the Compression Strength Parallel to Grain of Heat Treated Wood Using Artificial Neural Networks: A Preliminary Study.....	541
Richard Bergman, US Forest Service Forest Products Laboratory, USA Life-Cycle Inventory Analysis of Cellulosic Fiberboard Production in North America.....	542
Wayan Darmawan, Dodi Nandika, Yusram Massijaya, Abigael Kabe, Irsan Alipraja, Istie Rahayu, Bogor Agricultural University, Indonesia; Barbara Ozarska, University of Melbourne, Australia Lathe Check Characteristics of Fast Growing Sengon Veneers and Their LVL Glue-Bond and Bending Strength.....	551
Levente Dénes, University of West Hungary, Hungary Wood Related Researches in Central Europe- A Review.....	565

*Proceedings of the 57th International Convention of Society of Wood Science and Technology
June 23-27, 2014 - Zvolen, SLOVAKIA*

Levente Dénes, University of West Hungary, Hungary User-chair Interaction Analysis of Different Age Groups.....	566
David DeVallance, West Virginia University, USA; Joshua Faulkner, University of Vermont Center for Sustainable Agriculture, USA; and Tom Basden, West Virginia University Extension, USA Use of Non-treated and Thermally-treated Biomass Media in Livestock Heavy-use Areas to Reduce the Environmental Impacts of Agriculture.....	567
Tuncer Dilik, Istanbul University, Turkey Surface Treatment, Layer Thickness and Surface Performance Relations of Wood Materials.....	568
Arsenio Ella, Emmanuel P. Domingo, and Florena B. Samiano, Forest Products Research and Development Institute, Philippines Wood Anatomy of Naturally Grown Philippine Teak (<i>Tectona philippinensis Benth. & Hook. F.</i>).....	574
Emine Seda Erdinler, Istanbul University, Turkey Relations Between Varnish Type and Color Changes of Wood Material.....	576
Tomasz Gałęzia, Pomorze Forest Inspectorate, State Forests National Forest Holding, Poland Comparing the Efficiency of Selected Methods of Logging Residue Chipping for the Energy Purposes.....	582
Peder Gjerdrum, Norwegian Forest and Landscape Institute, Norway Woods and Wood through the Ages of Western Culture – our Wooden Heritage.....	591
Galina A. Gorbacheva and Victor G. Sanaev, Moscow State Forest University, Russia; Anatoly V. Bazhenov, Institute of Solid State Physics of the RAS, Russia; Ivica Suchanova, Technical University in Zvolen, Slovakia FTIR-Study of Thermally Treated Beech Wood.....	592
Eric Hansen, Oregon State University, USA US Forest Sector Innovation During the Great Recession.....	599
Alyson Wade, Arijit Sinha, and Chris Knowles, Oregon State University, USA Industry Perspective on Wood as Structural Green Building Material.....	600
Eva Haviarova, Purdue University, USA and Henry J. Quesada-Pineda, Virginia Tech, USA New Approach to Sustainability Education for Study Abroad Programs.....	601
Eva Haviarova, Mesut Uysal, Carl A. Eckelman, Purdue University, USA Furniture Design and Product Development Principles Considering End-of-Life Options and Design for Environment Strategies.....	609
Salim Hiziroglu, Oklahoma State University, USA Wood-Plastic Composite Made from Eastern Redcedar.....	617
Richard Hrčka, Pavol Halachan, Marián Babiak and Rastislav Lagaňa, Technical University in Zvolen, Slovakia; Jan Tippner, Eva Troppová, and Miroslav Trecala, Mendel University in Brno, Czech Republic Transverse Isotropic Material Thermal Properties Measurement.....	622
Pavel Ihracký and Josef Kúdela, Technical University in Zvolen, Slovakia Morphological Changes on Spruce Wood Surface during Accelerated Aging.....	629

*Proceedings of the 57th International Convention of Society of Wood Science and Technology
June 23-27, 2014 - Zvolen, SLOVAKIA*

David Jones, Mississippi State University, USA Providing Wood Science Training to the Forest Products Industry or How Do You Provide Educational Programs to Employees with No Formal Education in Wood Science.....	630
Abolfazl Kargarfard, Iran Research Institute of Forests & Rangelands, Iran; Ahmad Jahan-Latibari, Islamic Azad University, Iran Investigation of The Effect of Resin Consumption on The Properties of Particleboard Made Using Cotton Stalks.....	631
Abolfazl Kargarfard, Iran Research Institute of Forests & Rangelands, Iran; Ahmad Jahan-Latibari, Islamic Azad University, Iran Investigation on the Influence of Nano-clay Addition on Mechanical Properties of Soy Straw-polypropylene Composite.....	637
Walid Aboudi Kasir, Mosul University, Iraq Using Pine And Oak Bark Tannin Extracts As An Adhesive For Particleboards Production.....	644
Alperen Kaymakci, Istanbul University, Turkey Effect of Wood Chemical Composition on Physical Properties of Biocomposites.....	650
Chul-Ki Kim, Seoul National University, Korea Improvement of Accuracy of Portable CT by Considering Penetrating Depth in Wood.....	656
Seon-Hong Kim, Ga-Hee Ryu, and Su-Yeon Lee, Seoul National University, Korea; Mi-Jin Park, Korea Forest Research Institute, Korea; In-Gyu Choi, Seoul National University, Korea Insecticidal Effect of Essential Oils from <i>Abies Holophylla Maxim</i> and its Chemical Constituents against <i>Dermatophagoides Farinae</i>	662
Kucuk Huseyin Koc, Istanbul University, Turkey Abrasion, Surface Treatment and Glossiness Relations of Wood Material.....	667
Suleyman Korkut and Zeki Candan, Istanbul University, Turkey Surface Characteristics of Thermally Modified Plywood Panels.....	674
Tomasz Krystofiak, Stanislaw Proszyk and Barbara Lis, Poznan University of Life Sciences, Poland Bio-friendly Systems for Finishing of Wooden Windows Elements.....	676
Andreja Kutnar, University of Primorska, Slovenia; Frederick A Kamke, Oregon State University, USA; Emil Engelund Thybring, ETH Zurich EMPA, Switzerland Sorption Properties of Viscoelastic Thermal Compressed (VTC) wood	677
Jin Heon Kwon and Seung-Hwan Lee, Kangwon National University, Korea; Nadir Ayrilmis, Istanbul University, Turkey; Tae Hyung Han, Kangwon National University, Korea Effect of Microfibrillated Cellulose Content on the Bonding Performance of Urea-formaldehyde Resin.....	683
Ahmad Jahan Latibari and Hanieh Ghasemi, Islamic Azad University, Iran; Abolfazl Kargarfard, Institute of Forests and Rangeland, Iran The Application of Canola Straw In the Reduction of the Particleboard Density.....	691
Su-yeon Lee, Chang-Young Hong, Seon-Hong Kim, In-Gyu Choi; Seoul National University, Korea Biotransformation of Geraniol by <i>Polyporus brumalis</i>	697

*Proceedings of the 57th International Convention of Society of Wood Science and Technology
June 23-27, 2014 - Zvolen, SLOVAKIA*

Erni Ma, Beijing Forestry University, China Dimensional Responses of Wood Subjected to Cyclic Temperature Changes.....	701
Miroslava Mamoňová and Ladislav Reinprecht, Technical University in Zvolen, Slovakia Spectrophotometric Analysis of the Accelerated Aged Wood Treated with Transparent Coatings for Exterior Constructions.....	709
Carl Morrow and Thomas M. Gorman, University of Idaho, USA; David E. Kretschmann, USDA Forest Service, Forest Products Laboratory, USA A Comparison of Latewood Measurements in Suppressed Douglas-fir.....	719
Leoš Mrenica, Technical University in Zvolen, Slovakia; Šmíra, P., Thermo Sanace Ltd., Czech Republic; Ihracký, P., Technical University in Zvolen, Slovakia; Nasswetrová, A., Thermo Sanace Ltd., Czech Republic; and Kúdela, J., Technical University in Zvolen, Slovakia Pre-treatment of Surface of Old Wood Construction Elements with Dry Ice.....	727
Monika Muszynska, Tomasz Krystofi ak, Stanisław Proszyk, and Barbara Lis, Poznan University of Life Sciences, Poland Silanes Adhesion Promoters Applied in Furniture Industry	737
Abdollah Najafi , Islamic Azad University, Iran Effect of Pretreatment of Rice Husk with Acetic Acid on Properties of Rice Husk/HDPE Composites.....	744
Elisha Ncube, Copperbelt University, Zambia Premature Failure of Creosote Treated Electricity Transmission Wood Poles in Zambia.....	745
Conan O'Ceallaigh, Annette Harte, and Karol Sikora, National University of Ireland, Ireland; Daniel McPolin, Queens University Belfast, Ireland Mechano-sorptive Creep in Reinforced Sitka Spruce.....	753
Jung-Kwon Oh, Jung-Pyo Hong, and Jun-Jae Lee, Seoul National University, Korea Compressive Strength of Cross-laminated Timber Panel.....	761
Sung-Jun Pang, Seoul National University, Korea Accelerated Leaching Test for Estimating Service Life of Preservative Treated Wood in Retaining Wall.....	769
Zoltán Pásztor, University of West Hungary, Hungary Log Homes Mitigate the Global Warming.....	773
Henry Quesada-Pineda, Edgar Arias, Robert Smith, Virginia Tech, USA Case Study: “Exports of U.S. Hardwood Products: Increasing Performance in Asia and Western Europe”.....	774
Vladimír Račko and Ol’ga Mišíková, and Blažej Seman Technical University in Zvolen, Slovakia Effect the Indentation of the Annual Growth Rings in Norway Spruce (<i>Picea Abies L.</i>) on the Shear Strength - Preliminary Study.....	780
Peter Rademacher, Mendel University in Brno, Czech Republic; Ditriech Meier, Thünen Institute of Wood Research, Germany; Petr Pařil, Jan Baar, Pavel Sáblík, Petr Čermák, and Radim Rousek, Mendel University in Brno, Czech Republic Improvement of Properties of Selected Woods using Different Modification Techniques.....	788

*Proceedings of the 57th International Convention of Society of Wood Science and Technology
June 23-27, 2014 - Zvolen, SLOVAKIA*

Péter Rébék-Nagy and Zoltán Pásztor, University of West Hungary, Hungary CO ₂ Balance of Wood Wall Constructions Compared to Other Types of Wall.....	799
Roman Réh, Technical University in Zvolen, Slovakia; Marius C. Barbu, Salzburg University of Applied Sciences, Austria; and Ayfer D. Çavdar, Karadeniz Technical University, Turkey Non-Wood Lignocellulosic Composites.....	801
Martin Riegler, Martin Weigl, and Ulrich Müller, Wood K Plus, Austria The Role of Fibre Characteristics for Online Process Adaptation in the Manufacturing of MDF....	806
Ildikó Ronyecz, Kristóf Mohácsi, and Zoltán Pásztor, University of West Hungary, Hungary Errors of Sampling Based Moisture Content Measurement of Wood.....	814
Matthew Schwarzkopf and Lech Muszynski, Oregon State University, USA Quantitative Analysis of the Micromechanical Load Transfer in Wood-Adhesive Bond Interphases.....	815
Václav Sebera, Jan Tippner, Peter Rademacher, and Rupert Wimmer, Mendel University in Brno, Czech Republic FE model of Oriented Strand Board Made By Two Different Geometry Generation Techniques...	821
Franz Segovia, Pierre Blanchet, Costel Barbuta, and Robert Beaugard, Université Laval, Canada Aluminium Laminated Wood Composites: Optimal Manufactured Parameters.....	828
Milan Simek, Mendel University, Czech Republic Development of Ready-to-Assemble Furniture Constructions.....	837
Tomislav Sinković, Faculty of Forestry, Croatia Defining of Wood Colour.....	847
Nikolay Skuratov, Moscow State Forest University, Russia Assessment of Drying Quality and Accuracy of Wood Processing.....	856
Yaroslav Sokolovskyy, Ukraine National Forestry University, Ukraine Mathematical Modeling of Timber Elastic-viscous-plastic Deformation in Drying Process.....	865
Péter Szeles, Szabolcs Komán, and Sándor Fehér; University of West Hungary, Hungary Mitigation of End Shakes on Oak Saw Timber as a Result of Storage by Applying Environmentally-friendly Methods.....	866
Radovan Tiňo, Zuzana Repanova, and Michal Jablonsky, Slovak University of Technology, Slovakia Activation of Wood Surfaces With Atmospheric Plasma Treatment.....	876
Jan Tippner, Mendel University in Brno, Czech Republic Probabilistic Numerical Analysis of Quasi-stationary Thermal Measurement of Medium Density Fiberboard.....	878
Johann Trischler, Linnæus University, Sweden; Dick Sandberg, Luleå University of Technology, Sweden Integrating the Surface Treatment of Monocotyledons into Particleboard Production Process to Provide a Substitute Raw Material.....	887
Eva Troppová, Mendel University, Czech Republic Thermal Conductivity and Water Vapor Transmission Properties of Wood-based Fiberboards.....	897

*Proceedings of the 57th International Convention of Society of Wood Science and Technology
June 23-27, 2014 - Zvolen, SLOVAKIA*

Inna Varivodina, Nikolai Kosichenko and Tamara Starodubtseva, Voronezh State Academy of Forestry and Technologies, Russia Interconnection of Strength, Porosity and Microstructure of Hardwood.....	903
Oliver Vay, Kompetenzzentrum Holz GmbH, Austria; Johannes Konnerth, Alfred Teischinger, and Ulrich Müller, BOKU - University of Natural Resources and Life Sciences - Vienna, Austria Cross Industry Innovation Process to Identify “New” Technologies for Mechanical Wood Disintegration.....	909
Xiping Wang, Steve Verrill, Eini Lowell, Robert J. Ross and Vicki L. Herian, US Forest Products Laboratory, USA Acoustic Sorting Models for Improved Log Segregation.....	915
Kyaw Ko Win, Seoul National University, Korea Heart Rots Detection on the Nasis of Sonic Velocity Based on Transducer’s Angles Orientation...	925
Sang-Yun Yang, Seoul National University, Korea Analysis of High Frequency Dielectric Curing of Phenol-Resorcinol Formaldehyde Resin used for Manufacturing Larch Glulam.....	933
Hwanmyeong Yeo, Yeonjung Han, Yoon-Seong Chang, Sang-Yun Yang, Chul-Ki Kim, Gi-Young Jeong, Jun-Jae Lee, Seoul National University, Korea; Yeonjung Han, Yoon-Seong Chang, Sang-Yun Yang, and Chul-Ki Kim, Seoul National University; Gi-Young Jeong, Chunnam National University; Jun-Jae Lee, Seoul National University Analysis of Laminar Yield for Manufacturing Cross Laminated Timber.....	940
Hwanmyeong Yeo, Yoon-Seong Chang, and Jun-Ho Park, Seoul National University, Korea; Whi-Lim Son, Joo-Saeng Park, and Moon-Jae Park, Korea Forest Research Institute, Korea Half-Life and Carbon Stock of Harvested Wood Products (HWP) Produced by Domestic Trees in Korea.....	945
Ales Zeidler, Vlastimil Boruvka, Guillermo Garcia Mayoral, Czech University of Life Sciences Prague, Czech Republic Wood Quality of Black Walnut Grown in Reclaimed Surface Mine in the Czech Republic.....	951
Student Poster Competition	
Adeyinka Saheed Adesope, Forestry Research Institute of Nigeria, Nigeria Effects of Particle Geometry on Dimensional Stability of Bamboo-reinforced Cement Composites.....	957
Melanie Blumentritt, Sasha Howes and Stephen M. Shaler, University of Maine, USA Life Cycle Assessment of Exported Torrefied Wood Pellets (TOP) from Maine to the European Union.....	958
Bryan Dick, North Carolina State University, USA Changes in the Anatomy of Exposed Roots of Some Hardwood Species.....	967
Charles Edmunds, North Carolina State University, USA Thermo-mechanical Properties of Genetically Modified <i>Populus trichocarpa</i>	968
Alexandra Himsel, Kompetenzzentrum Holz GmbH, Austria; Ulrich Müller, BOKU – University of Natural Resources and Applied Life Science, Austria; Hendrikus W. G. van Herwijnen, Kompetenzzentrum Holz GmbH, Austria Rheometer Method to Determine Factors Influencing Sticking Behaviour of Aminoplastic Resins.....	972

*Proceedings of the 57th International Convention of Society of Wood Science and Technology
June 23-27, 2014 - Zvolen, SLOVAKIA*

Chloé Maury and Khalil Jradi, Université du Québec à Trois-Rivières, Canada; Claude Daneault, Canada Research Chair in Value-added Paper, Canada Study of Mechanical Properties of Composites Based on TEMPO-oxidized Cellulose Gel and Silica Nanoparticles.....	979
Zachary Miller, North Carolina State University, USA Comparing Mechanical and Chemical Properties of Young Transgenic Black Cottonwood Trees Modified for Reduction of Specific Genes in Lignin Biosynthesis.....	980
Jimmy Thomas, The Rubber Board and University of Canterbury, New Zealand; David Anthony Collings, University of Canterbury, New Zealand Novel Imaging and 3D rendering Techniques to Visualise Spiral Grain in <i>Pinus radiata</i>	984

Hardwood Research & Utilization Session
Session Co-Chairs: Rado Gazo, Purdue University, USA
Róbert Németh, University of West Hungary, Hungary

**CT Scanning of Logs – Analysis and Optimization for
Better Utilization of Hardwoods**

Rado Gazo, Juraj Vanek, Michel Abdul-Massih, and Bedrich Benes

Department of Forestry and Natural Resources, Purdue University
West Lafayette, Indiana, USA

Abstract

The mission of the Hardwood Scanning Center at Purdue University is to increase the global competitiveness of the United States hardwood industry and to conserve the hardwood resource by development of manufacturing technologies which will enable hardwood industry to “see inside a tree” and use this information to make better processing decisions.

The Hardwood Scanning Center partnered with Microtek, GmbH of Italy in the development of an industrial grade log CT scanner. World’s first three industrial CT log scanners have been installed in last 12 months in mills around the world and we will briefly discuss their application. The Hardwood Scanning Center also developed visualization and optimization software for the hardwood veneer and sawmill operations. This presentation will provide an overview of state-of-the-art in CT scanning of logs.

Keywords: Hardwood, log, CT, scanning

Decorative Veneer Properties of Black Walnut (*Juglans nigra* L.)

*Roman Réh*¹

¹ Associate Professor, Department of Mechanical Technology of Wood, Faculty of Wood Science and Technology, Technical University in Zvolen, Zvolen, Slovak Republic.

reh@tuzvo.sk

Abstract

Black walnut (*Juglans nigra* L.) is an interesting species for wood processing worldwide and it can be fully recommended for the European woodworking industry as well. The quality of decorative veneer made from black walnut does not differ from the quality of the commonly used veneer for veneering in furniture industry when correct thickness is selected. In Europe selected introduced woody species suggest good perspectives in the coming years and the future quality and volume of the production may be secured providing systematic and intense tending of the forest stands takes place. Because of the shortage of the high quality traditional raw material for decorative purposes, it is the time to start to utilize the suitable minor trees from the European forests.

From the results of tests performed black walnut is an interesting species for veneering industry and the veneer thickness of 0.6 mm can be fully recommended for furniture industry and other purposes.

Black walnut is suitable for application in the furniture industry either as a replacement for some commonly used woody species or as a woody species widening the assortment of woody species utilized in furniture industry. The results obtained suggest that it is possible to recommend its cultivation in larger areas upon properly managed stands. It is still necessary to reach more accurate data on the nearest zoning and to realize a research of consumer market in the field of utilizing veneer made of black walnut.

Keywords: wood veneer, decorative veneer, properties of veneer, black walnut

Introduction

Potential products including decorative veneers can be manufactured from hardwoods that are considered as introduced (invasive) species (Brashaw et al. 2012). Because of the growth of veneer industries and the reduction of timber supplies of the well-known veneer species, the search continues for alternate species, either domestic or foreign. In screening

for new veneer species, it is helpful to know which factors are important for veneer use (Lutz 1971).

This paper includes the recommendations to use the species black walnut (*Juglans nigra* L.) for the production of decorative veneer and veneering. Black walnut is an important source of decorative veneer in the U.S.A. For Central European wood-processing industry is black walnut an introduced species. Black walnut has it specific interesting particularities: it is the only North American dark wood and in Europe it does not have any natural pests while growing.

Botanic name: *Juglans nigra*, L.

Family: Juglandaceae

Other names used for species: American walnut, Eastern black walnut

Black walnut is sought after for its great beauty and toughness. It is fairly straight grained but can be wavy with a coarse texture and a dark brown to purplish black color. Heartwood can range from a lighter pale brown to a dark chocolate brown with darker brown streaks. Color can sometimes have a grey, purple, or reddish cast. Sapwood is pale yellow-gray to nearly white. Figured grain patterns such as curl, crotch, and burl are also seen. Grain is usually straight, but can be irregular. Has a medium texture and moderate natural luster.

Black walnut is a hard, strong, heavy wood that weighs 600 - 660 kg.m⁻³ when seasoned. The wood requires care in drying to avoid checking and degradation. It has good shock resistance and is unusually durable. The timber works well with hand and machine tools, with a moderate blunting effect on cutting edges. It holds nails and screws well, and can be glued satisfactorily. Its workability is good and it glues well while holding it's bending properties (Barbu et al. 2014). It accepts natural wood finishes extremely well and can be polished to a fine finish.

Materials and Methods

Raw material for this research has Slovak origin and it was taken from Arborétum Mlyňany. 12 veneer logs with a length of 140 cm and with a diameter of 29 – 32 cm were dipped for a period of 2 months at the water temperature 20 °C. Veneers were manufactured by off-center cutting in the Development workshops and laboratories of the Technical University in Zvolen. By means of interrupted off-center cutting new and interesting grains and textures of black walnut were obtained. Veneers with the thicknesses of 0.6, 0.7, and 0.8 mm were dried up to a moisture content of 10 ± 1 % by drying at a temperature 100 °C.

Black walnut veneers were subjected to a number of technological test procedures. Our aim was to determine the most appropriate thickness of off-center cutting (eccentrically peeled) black walnut decorative veneer and values of optimal glue mixture spread which is needed for veneering technology.

Specific Glue Penetration to the Veneered Area. The glue penetration to the veneered area is usually determined on veneer specimens of the size of 250 x 300 mm. The most common construction material used is particleboard (thickness 16 mm) and we had to solve the proper glue amount (it was tested the range from 100 to 220 g.m⁻² in the glue spread gradation of 10 g.m⁻²). The evaluation of the amount of glue penetrated on the veneer surface was done with the help of a net with mesh size of 5 x 5 mm. For each value of the glue spread ten specimens had been pressed and the penetration was evaluated in percentage of the total area.

Veneering with urea-formaldehyde glue was carried out under the following conditions:

- Press pressure: 0.6 MPa
- Pressing temperature: 130 ° C
- Pressing time: 4 min.

Moisture Absorption of Veneer. Essence of the moisture absorption determination of veneers is to determine the equilibrium moisture content of the test specimens during long-term storage of veneer sheets in an environment in which the desired temperature and the desired relative humidity of air exists. The test is conducted under the terms of the technical standard. The test specimens with the dimensions 50 x 50 mm in the number of 60 specimens were conditioned in a chamber at a relative humidity of 95 ± 2 % and at a temperature of 20 ± 2 °C for 30 days. After completion of the conditioning the weight of test specimens was determined with an accuracy of ± 0.01 g. The test specimens were then oven dried to zero moisture content at the temperature 103 ± 2 ° C. Moisture absorption n_w (%) was calculated according to the formula:

$$n_w = \frac{m_w - m_o}{m_o} \cdot 100 \quad (1)$$

where m_w is specimen weight after conditioning and m_o is specimen weight after oven drying.

Tensile strength of veneers perpendicular to the grain. Test essence is to determine the tensile strength at maximum load which is exposed to the test specimen up to the failure of its strength perpendicular to the grain.

Results and Discussion

Specific Glue Penetration to the Veneered Area. Results of the specific glue penetration to the veneered area in dependence on the spread thickness are given in Table 1.

Table 1. Results of the Specific Glue Penetration to the Veneered Area in Dependence on the Spread Thickness

Veneer Thickness (mm)	Glue Spread (g.m ⁻²)												
	100	110	120	130	140	150	160	170	180	190	200	210	220
0.6	-	-	-	-	0.022	0.015	0.019	0.051	0.030	0.066	0.093	0.256	0.586
0.7	-	-	-	-	-	-	0.010	0.020	0.040	0.063	0.100	0.103	0.563
0.8	-	-	-	-	-	-	-	-	0.003	0.001	0.073	0.116	0.146

The test results on glue penetration to the veneered area revealed no substantial glue penetration within the spread range 140 – 160 g.m⁻², inclusive of followed thicknesses. Black walnut from the point of view of glue penetration to the veneered area proved good properties. In actually used spreads there is no danger of devaluation of the veneered elements. Glue spread 140 – 150 g.m⁻² was proposed for particleboard.

Moisture Absorption of Veneer. Results of the moisture absorption test are given in Table 2.

Table 2. Statistical characteristics of moisture absorption of black walnut veneer

Thickness [mm]	x	V _x	n [pcs]
	[%]		
0.6	21.24	7.21	60
0.7	20.92	8.16	60
0.8	20.67	7.56	60

(x – Average value; V_x - Variation coefficient; n – Number of measurements)

The values of moisture absorption of black walnut veneers move within the minimum interval of 20 – 21 % and they are decreasing insubstantially with the increasing veneer thickness. The variation coefficient of all measurements is at an acceptable level. The value of moisture absorption is relatively low. However, it corresponds to the equilibrium moisture content determined from sorption isotherm for lower range of standard test conditions (22.20 %) according to DeBoer and Zwicker isotherm.

Tensile strength of veneers perpendicular to the grain. Results of tensile strength of veneers perpendicular to the grain are given in Table 3.

Table 3. Statistical characteristics of tensile strength of black walnut veneers perpendicular to the grain (w = 12 %)

Thickness [mm]	x [MPa]	V _x [%]	n [pcs]
0.6	3.34	16.61	60

0.7	3.76	18.26	60
0.8	3.82	19.42	60

(\bar{x} – Average value; V_x - Variation coefficient; n – Number of measurements)

The value of tensile strength of black walnut veneers perpendicular to the grain increases with the veneer thickness.

Tensile strength of black walnut veneers perpendicular to grain could be theoretically equal to the tensile strength of wood in the same direction. Experimental results have shown that the average strength of veneers is significantly lower than the strength of the wood. This difference increases with decreasing veneer thickness. Cracks play a negative role in the case of tensile strength of veneers, whose frequency depends to a large extent on the veneers production technology.

Most importantly in terms of the mechanical properties of decorative veneer is that veneer must withstand as compact as possible during handling. From this perspective, tensile strength of black walnut veneers perpendicular to the grain is decisive. Mechanical properties of decorative veneers are negligible after veneering.

Conclusions

Black walnut as an interesting species for veneer industry is fully recommended. The quality of veneer made from black walnut does not differ from the quality of commonly used veneer and thickness 0.6 mm can be recommended for furniture industry. Glue spread 140 – 150 g.m⁻² was proposed for particleboard.

Selected introduced woody species suggest good perspectives in the coming years and the future quality and volume production may be secured providing systematic and intense tending of forest stands takes places. Black walnut is suitable for veneering of composites (particleboard, MDF) and it is suitable for application in the furniture industry either as a replacement for some commonly used woody species or as a woody species widening the assortment of woody species utilized in furniture industry.

The results obtained suggest that it is possible to recommend its cultivation in larger areas upon properly managed stands. It is still necessary to reach more accurate data on the nearest zoning in Central Europe and to realize a research of consumer market in the field of utilizing veneer made of black walnut.

References

Barbu M.C., Irle M., Reh R. (2014): Wood Based Composites, Chapter 1 in Aguilera A., Davim P., Research Developments in Wood Engineering and Technology. IGI Global. Engineering Science Reference. Hershey, PA, USA, pp.1-45.

Brashaw B. K., Ross R. J., Wang X., Wiemann M. C. (2012): Options for Urban Trees Infested by Invasive Species. University of Minnesota and U.S. Department of Agriculture, Forest Service, Forest Products Laboratory, Madison., 96 p.
http://spfnic.fs.fed.us/werc/finalrpts/09-DG-087_2.pdf

Lutz J. F. (1971): Wood and Log Characteristics Affecting Veneer Production. Forest Service research paper, Forest Products Laboratory, Madison, WI, 1971, pp. 1-35.
<http://www.fpl.fs.fed.us/documnts/fplrp/fplrp150.pdf>.

<http://www.fpl.fs.fed.us/documnts/usda/amwood/270bwaln.pdf>

<http://www.lewislp.com/woodchar.asp>

<https://www.osbornewood.com/woodtypes.cfm>

<http://www.piecesofwood.com/woods.html>

<http://www.wood-database.com/wood-identification/>

Acknowledgements

The research described in the paper presented was supported by grant No. 01/0345/12 from the Slovak Grant Agency (Interaction of the Components of Wood and High Temperatures during Pressing of Wood Composites and its Effect on the Formation of Composites Avoiding the Chemical Changes in Composition of Pressed Wood Particles and Elimination of the Fire Risk). The author would like to thank the grant agency for the support of this research.

Distribution of the Equilibrium Moisture Content in Four Hardwoods Below Fiber Saturation Point by Magnetic Resonance Microimaging

Leandro Passarini – Cédric Malveau – Roger Hernández

Abstract

The magnetic resonance imaging (MRI) is one of most powerful and versatile technique for wood characterization. It is non-invasive, relatively fast and allows the visualization of water in wood structure over a wide range of moisture contents. The main objective of this work was to use the MRI technique to study liquid and bound water distribution in small wood samples under equilibrium moisture contents (EMC) below FSP. Two hardwood species from the Amazon rainforest, namely huayruro (*Robinia coccinea* Aublet) and cachimbo (*Cariniana domesticata* (C. Martius) Miers), a plantation grown eucalyptus species (*Eucalyptus saligna* Smith) from Brazil, and a temperate species red oak (*Quercus rubra* L.) were used for this study. These species were chosen considering their diversity in terms of anatomical and physical properties. Desorption tests were carried out at 21°C in a single step procedure from full saturation state for huayruro, cachimbo, and red oak and from green condition for *E. saligna*. The EMC was reached under three desorption conditions (58, 76, and 90% RH). One sample was select to IRM test for each RH condition. Two images were obtained, one based on T₂ times and another based on 1H concentration. A scanning electron microscopy image was obtained for the same section scanned in order to help the MRI interpretation. The results showed that wood structure plays a major role in liquid water drainage and water diffusion. *E. saligna* and red oak presented liquid water entrapped, respectively, in axial parenchyma and rays, even below FSP. For cachimbo and huayruro woods, all liquid water was drained at 90 % RH. For these two species, even at EMC, the images showed that bound water was not uniformly distributed in wood structure, concentrating mainly in rays for cachimbo and in fibers for huayruro. Therefore, water concentration varied according to the wood tissue, reveling that some tissues are more hygroscopic than others.

Keywords: *magnetic resonance imaging, fiber saturation point, liquid water, wood hygroscopicity*

Leandro Passarini

PhD student, Centre de recherche sur les matériaux renouvelables, Département des Sciences du bois et de la Forêt, Pavillon Gene-H. Kruger, 2425, rue de la Terrasse, Université Laval, Québec, Qc, Canada, G1V 0A6. E-mail: leandro.passarini.1@ulaval.ca

*Proceedings of the 57th International Convention of Society of Wood Science and Technology
June 23-27, 2014 - Zvolen, SLOVAKIA*

Cédric Malveau

Research assistant, Laboratoire de RMN, Département de Chimie, Université de Montréal, Pavillon Roger-Gaudry (PRG), 2900, boul. Édouard-Montpetit Montréal (Québec) H3T 1J4. Email : cedric.malveau@umontreal.ca

Roger Hernández

Professor, Centre de recherche sur les matériaux renouvelables, Département des Sciences du bois et de la Forêt, Pavillon Gene-H. Kruger, 2425, rue de la Terrasse, Université Laval, Québec, Qc, Canada, G1V 0A6. E-mail: roger.hernandez@sbf.ulaval.ca

Changes in the Anatomy of Exposed Roots of Some Hardwood Species

Bryan Dick, Perry Peralta, and Ilona Peszlen

Abstract

Dendrogeomorphology, a subfield of dendrochronology, is a valuable tool for dating and estimating the rates of erosion and deposition of river banks, ephemeral channels, hillslopes, landslides and other mass movements. By determining the initial year of root exposure, exposed tree roots offer a means of determining erosion rates for both riverine and hillslope processes. While dendrogeomorphology is a well-established field, there is very little information available to researchers and practitioners in the way of specific responses of hardwoods by genus or classification of anatomical structure. Macroscopic and microscopic indicators of the date or root exposure include; the occurrence of eccentricity in growth rings, a transition of diffuse to ring porous arrangements of vessels (root-like to stem-like anatomy), a decrease in the size of vessels and fibers, fiber cell wall thickening, the occurrence of gelatinous fibers in tension wood and the occurrence of pith flecks (scarring and wound tissue). The observed macroscopic and microscopic changes in root wood anatomy of exposed roots of sugar maple (*Acer saccharinum*), slippery elm (*Ulmus rubra*) and common hackberry (*Celtis occidentalis*), water oak (*Quercus nigra*), green ash (*fraxinus pensylvannica*), water hickory (*Carya aquatica*), black willow (*Salix nigra*), and eastern cottonwood (*Populus deltoids*) will be presented. The difficulties associated with using some species will also be discussed, in order to assist with the planning of what is best used for future studies of soil erosion using exposed roots.

Keywords: dendrochronology, dendrogeomorphology, exposed roots of hardwoods

Bryan Dick, Ph.D. Student

bmdick@ncsu.edu

Perry Peralta, Associate Professor

+1919-515-5731; Fax: +191-3513-3496

Perry_Peralta@ncsu.edu

Ilona Peszlen, Associate Professor

+1-919-513-1265; Fax: +191-3513-3496

Ilona_Peszlen@ncsu.edu

Department of Forest Biomaterials

North Carolina State University

Campus Box 8005

Raleigh, NC 27695-8005

Mechanical Properties of European Beech Wood (*Fagus Silvatica* L.) after Microwave Drying in Comparison to Naturally and Laboratory Oven-Dried Material

*Wilfried Beikircher*¹ – *Christian Lux*² – *Szabolcs Komán*^{3*}

¹ Senior scientist, University of Innsbruck, Department of Engineering Science - Timber Engineering Unit, Technikerstr. 13, 6020 Innsbruck, Austria.

wilfried.beikircher@uibk.ac.at

² Assistant, University of Innsbruck, Institute of Ion Physics and Applied Physics, Technikerstr. 25/3, 6020 Innsbruck, Austria, Innsbruck, Austria.

³ Associate Professor, University of West Hungary, Simonyi Károly Faculty of Engineering, Wood Sciences and Applied Arts, Institute of Wood Sciences, Bajcsy-Zs. u. 4., 9400 Sopron, Hungary.

** Corresponding author*

szabolcs.koman@skk.nyme.hu

Abstract

This aim of this study to investigate the effect of the microwave drying process on mechanical properties of European beech (*Fagus silvatica* L.) in comparison to laboratory oven dried and natural dried material. The wood was dried in air at ambient temperature at about 20 °C, in a conventional laboratory oven at elevated temperatures at 103°C and in a microwave oven at two different power settings with target core temperatures of 65°C for the vacuum drying and at 100 °C for drying at atmospheric pressure. The drying experiments were performed at small clear wood specimens with the cross section of 30 mm and 500 mm in length, which were prepared for the mechanical tests. After drying, the mechanical properties as the three-point bending test, the compression strength parallel to the grain and the Brinell hardness were determined. The results of this systematic investigation show no influence by the microwave drying process on the mechanical properties as the modulus of rupture and the modulus of elasticity out of tree-point bending test and the compression strength parallel to the grain. The influence of drying rate and internal cracking affect the mechanical properties more as the drying process. Regarding the Brinell hardness some differences could be found within the artificial drying processes but in comparison to the natural dried Beech wood not at significant level.

Keywords: microwave wood modification, wood drying, mechanical properties, European beech (*Fagus silvatica* L.)

Introduction

The drying of wood can be a time and energy consuming process. The optimization of drying processes and the reduction of needed energy plays an important role in the industry. Several methods for drying are used in the timber industry. These include drying the wood at elevated temperatures by using convectional kiln drying, which is the most common method, drying in radio frequency or microwave ovens, or a combination of the two. In timber drying, mechanical properties may be changed due to treatment temperature and treatment duration. In general when increasing the kiln temperature, drying time is decreased and some timber properties are negatively affected. The occurrence of cracks, case hardening and loss of mechanical properties and undesired colour changes are major problems in wood drying. Attention should be given on the control of drying conditions in order to avoid these forms of defects.

Although investigations on microwave drying of wood have been performed since the late fifties, this drying process is little used for industrial timber drying processes. A comprehensive review on the drying of wood with high frequency electric current is given by Resch (2009) [1]. Studies by many authors [2], [3], [4],[4] [5], [6], [7] and [8] emphasize the advantages of microwave drying over convective drying.

A literature review where different drying methods and investigated wood species are presented is given by Oltean et al. (2011) [9]. This report deals with different temperature ranges and drying methods, but little information is available to quantifying the effect of the microwave drying method on the mechanical properties of the wood. In general mechanical properties at drying temperatures below 100 °C are not affected.

Investigations of different authors differ in the statements concerning the effect of the microwave drying process on mechanical properties of wood. As Hansson and Atti (2006)[10] found no change in the temperature range at 60-100 °C, Oloyede and Groomebridge (2000) [5] found up to 60 % lower strength properties. In comparison Taskini (2007) [8] found that microwave dried wood lead to higher strength as infrared and convectional drying processes. Due to these inconsistencies research work will be necessary for this topic and this study should support the actual knowledge.

In this study the changes in MOE, MOR and the compression strength parallel to the grain on European beech (*Fagus silvatica* L.) related to the drying process are investigated. In the present paper, the tests were carried out using laboratory size specimens with the dimensions of 30 x 30 x 500 mm. As target moisture content (MC) 12 % and 0 % was selected. Due to the small specimen size, short drying times were used and the results should therefore not be directly compared on full size specimens e.g. timber boards and beams.

Materials and Methods

Drying experiments

In this study, freshly sawn European beech (*Fagus silvatica* L.) from upper Austria was used for the investigations. The raw material was prepared in the way to get twin samples for optimal comparison of the microwave drying effect. For having an adequate material range the starting material selected was out of six trees, presented sapwood and heartwood. From each tree one core board and one side board was used. Out of the boards

three bars were cutted and from each bar one sample were randomly selected for the different drying processes (**Figure 1**). Because of the careful selection of the test series, with exception of the water stored material, the samples can be denoted as twin samples to generate meaningful results. The series TSA_100°C_12%_w and MWA_100°C_12%_w are in between directly comparable, because there were twin samples, but this series were made out of other trunks as the other six series. For every test series 36 samples were used. All drying samples were prepared to the dimension of 30 x 30 x 500 mm. After cutting, the bars were sealed on both cross sections with epoxide adhesive, in order to prevent drying from the cross sectional ends. Due to the material from the sawn mill the starting moisture content (MC) varied between 28 to 35 %. For a more intense effect of the drying processes on material properties additional two series were prepared and stored in water before drying. Those two series had a mean starting MC of 51 % (**Error! Reference source not found.**).

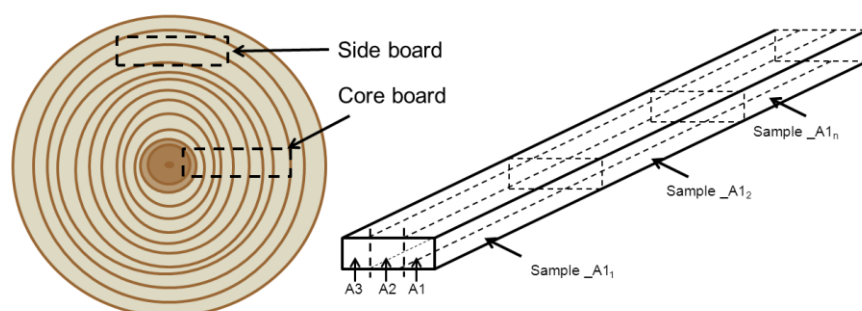


Figure 1. Sample preparation

The methods applied were vacuum-microwave drying, microwave and laboratory oven drying under atmospheric pressure and natural dried material was used as reference material. The drying schedules are summarized in **Error! Reference source not found.**

Identification	Description	Starting MC (%)	Target MC (%)	Drying temp. (°C)	Process time (h)
MWA_100°C_12%	MW-drying under ambient pressure	30 ±6	12	100 ± 2	3
MWA_100°C_0%	MW-drying under ambient pressure	28 ±5	0	100 ± 2	14
MWV_65°C_12%	MW-drying under vacuum (200mbar)	29 ±5	12	65 ± 2	4
MWV_65°C_0%	MW-drying under vacuum (200mbar)	34 ±4	0	65 ± 2	14
FLA_20°C_12%	Natural-drying in the storage room	35 ±6	12	20 ± 5	3.5 month
TSA_100°C_0%	Laboratory oven drying under ambient pressure	35 ±6	0	103 ± 3	126
TSA_100°C_12%_w	Laboratory oven drying under ambient pressure	51 ±8	12	103 ± 3	51
MWA_100°C_12%_w	MW-drying under ambient pressure	51 ±8	12	100 ± 2	12.5

Table 1. Drying parameters

Experimental equipment

Drying experiments were carried out with laboratory MW-drying equipment (Figure 2). For the drying tests the first five Magnetrons of the MW-kiln were used. The laboratory plant is equipped with 12 spirally positioned magnetrons at the whole length of 3 m. Each magnetron has a maximum power of 800 W and the working frequency is 2.45 GHz.

During the drying the core temperature was measured with a fiber optic sensor (FOTEMP1 Fa. OPTOcon GmbH), which was inserted to the core of one of the samples. The surface temperature was measured with an infrared spectral pyrometer. The core temperature was used for the manual regulation of the intensity of the MW-power. The drying started by using 50 % of the MW-power and then the power was manually regulated for holding the target core temperature. The core temperatures were regulated in the range of 100 ± 2 °C for the atmospheric drying process and 65 ± 2 °C for the vacuum drying process at 200 mbar.

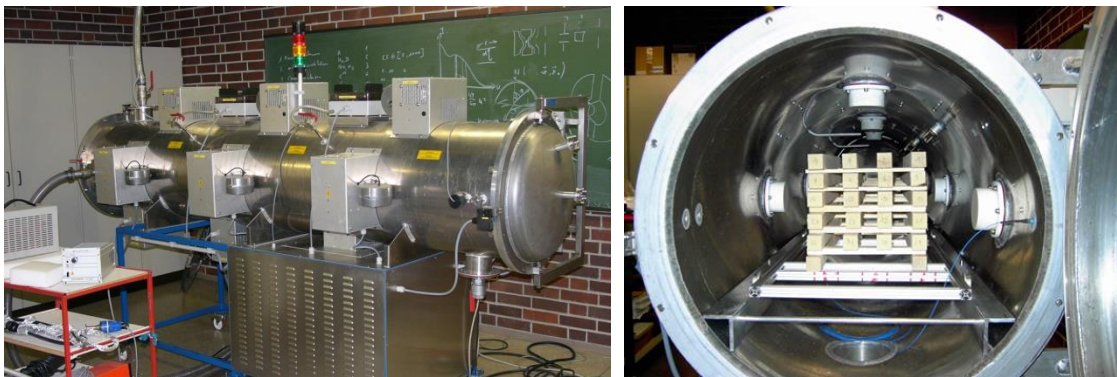


Figure 2. Microwave laboratory equipment and position of the samples

For the comparison of the MW-dried timber, natural dried and in a laboratory oven dried samples were used. The natural dried material was stored in a storage room at about 15-25 °C until the MC of about 12 % was reached. The drying steps for the laboratory oven were 24 hours with 50 °C following of 24 hours with 80 °C and finally until the target MC was reached the temperature of 103 °C were settled. The different drying experiments were carried out to get final target moisture content of 12 % and 0 % (Table 1). With exceptions of the natural dried material, this was only dried at the target MC of 12%. After drying all samples were conditioned in a climate chamber at 20 °C and 65 % relative humidity prior to testing until constant moisture content was reached.

Preparation of test specimens

The test material consisted of microwave dried, laboratory dried and natural dried control specimens according to the schedules described above. For the determination of the mechanical properties defect free specimens were produced after the drying at the final dimension of 20 x 20 x 360 mm for the bending tests and 20 x 20 x 60 mm for the compression strength and 20 x 20 x 30 mm for the Brinell hardness in radial and tangential direction.

Mechanical testing

The determination of the material properties were performed according to the Standards for small defect free wood samples. The material properties to be determined were: the density, the moisture content, modulus of elasticity and bending strength, compressive strength and Brinell hardness. The specified standards which were followed, as well as the devices and some remarks are presented in **Error! Reference source not found.** The material tests were performed at the TVFA (Technische Versuchs- und Forschungsanstalt) of the University of Innsbruck. All tests were performed after storage the material in a climate chamber at 20 °C and 65 % RH until the equilibrium moisture content (EMC) was reached.

Test	Standard	Devices	Remarks
Density	DIN 52182 (1976)	digital measuring slide, balance	balance accurateness 0,001 g
Moisture content	DIN 52183 (1977)	balance	accurateness 0,001 g
Compression test	DIN 52185 (1976)	Shimadzu Autograph AG-100 kN Testing Maschine	cross head speed 0,7 mm/min
Three point bending test	DIN 52186 (1978)	Shimadzu Autograph AG-100 kN Testing Maschine	cross head speed 7 mm/min
Brinell hardness	EN 1534 (2000)	Shimadzu Autograph AG-100 kN Testing Maschine	max. load 1000 N

Table 2. Details concerning the standards followed and devices used

Results and Discussion

The statistical processing of the data obtained is presented in **Table 1, Table 1. Number of samples, mean values and standard deviation for the density, the MOR and MOE out of the three point bending test** and **Table 2. Number of samples, mean values and standard deviation for the density and the compression strength**. For the drying processes carried out mean values were recorded between 107.13 and 126.72 MPa for MOR and from 12.27 to 13.08 GPA for MOE in the tree point bending test. In the case of compression tests parallel to the grain mean values of compression strength were recorded between 47.56 and 57.88 MPa. Remarkable lower values for the water stored material can be recognized for the compression strength s. **Table 1. Number of samples, mean values and standard deviation for the density, the MOR and MOE out of the three point bending test**. For the Brinell hardness in the radial direction HB 10/1000 mean values are between 34.03 to 38.44 N/mm² and for the tangential direction between 31.27 to 34.94 N/mm². After the drying macro cracks could be recognized within the water stored test series (TSA_100°C_12%_w and MWA_100°C_12%_w). Those cracks influence the mechanical properties of the wood [11]. The testing results with lower values for the water stored material at about 9 % for the compression strength in comparison to natural dried material are in agreement to this. The reason for the cracks can be assumed as result of the drying rate as the similar processes were used as for the material with lower starting MC [12].

Three point bending tests							
Test Series	n	Density (kg/m ³)		MOR (MPa)		MOE (GPa)	
		Mean	Std.dev.	Mean	Std.dev.	Mean	Std.dev.
MWA_100°C_12%	36	731	31.29	116.24	12.74	12.27	1.04
MWA_100°C_0%	36	723	33.29	126.72	13.68	13.08	1.27
MWV_65°C_12%	36	721	30.61	107.13	9.69	12.27	0.91
MWV_65°C_0%	36	722	28.66	111.72	12.23	12.44	1.23
FLA_20°C_12%	36	717	28.96	112.80	8.66	12.30	1.17
TSA_100°C_0%	36	716	28.07	120.53	12.42	12.98	0.89
TSA_100°C_12%_w	36	730	36.11	112.50	19.92	12.30	1.47
MWA_100°C_12%_w	36	731	33.99	121.79	10.94	12.94	1.26

Table 1. Number of samples, mean values and standard deviation for the density, the MOR and MOE out of the three point bending test

Compression strength parallel to the grain					
Test Series	n	Density (kg/m ³)		compression strength (MPa)	
		Mean	Std.dev.	Mean	Std.dev.
MWA_100°C_12%	36	729	30.40	51.81	5.66
MWA_100°C_0%	36	721	29.91	57.88	5.94
MWV_65°C_12%	36	718	27.53	50.73	5.15
MWV_65°C_0%	36	723	25.21	54.37	5.06
FLA_20°C_12%	36	716	28.21	53.54	4.49
TSA_100°C_0%	36	710	29.05	55.03	5.00
TSA_100°C_12%_w	36	726	35.20	47.56	5.79
MWA_100°C_12%_w	36	728	33.00	48.05	5.96

Table 2. Number of samples, mean values and standard deviation for the density and the compression strength

Brinell Hardness HB 10/1000							
Test Series	n	Density (kg/m ³)		HB rad. (N/mm ²)		HB tang. (N/mm ²)	
		Mean	Std.dev.	Mean	Std.dev.	Mean	Std.dev.
MWA_100°C_12%	36	731	31.29	35.29	4.60	33.36	3.96
MWA_100°C_0%	36	723	33.29	38.44	4.70	34.94	4.83
MWV_65°C_12%	36	721	30.61	34.34	4.29	31.69	3.68
MWV_65°C_0%	36	722	28.66	34.69	4.02	31.77	2.40
FLA_20°C_12%	36	717	28.96	34.03	5.39	31.27	4.10
TSA_100°C_0%	36	716	28.07	36.97	4.15	33.01	3.25
TSA_100°C_12%_w	36	730	36.11	33.89	6.78	33.16	3.14
MWA_100°C_12%_w	36	731	33.99	34.66	3.93	33.06	4.20

Table 5. Number of samples, mean values and standard deviation for the density and the Brinell hardness in radial and tangential direction

Three-point bending tests

The diagrams in Figure 3 and Figure 4 show the influence of the drying schedules applied on European beech wood at low and moderate temperature ranges on MOR and MOE in three-point bending tests. For both the MOR and MOE the series MWA_100°C_0%, TSA_100°C_0% and TSA_100°C_12%_w show higher values in comparison to the other drying processes, for which quite no difference can be seen for the MOE.

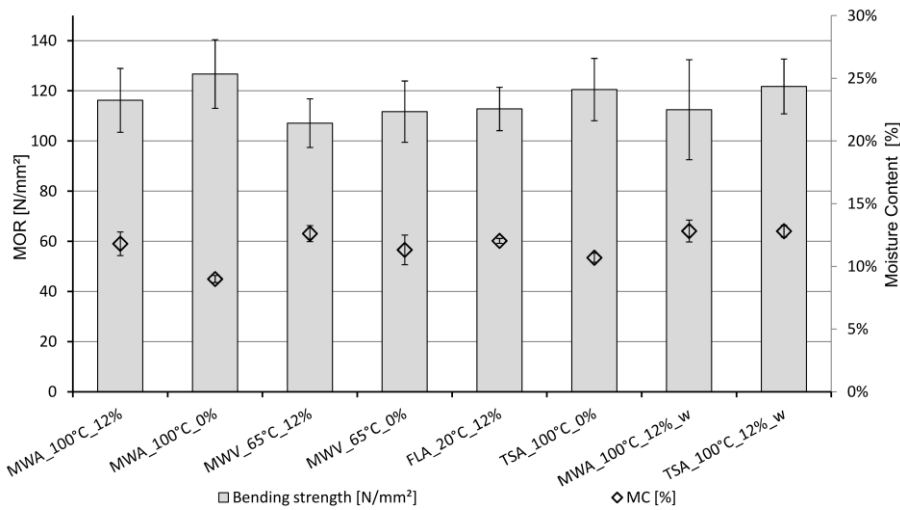


Figure 3. MOR out of the tree-point bending for different drying processes, the whiskers represent the standard deviation

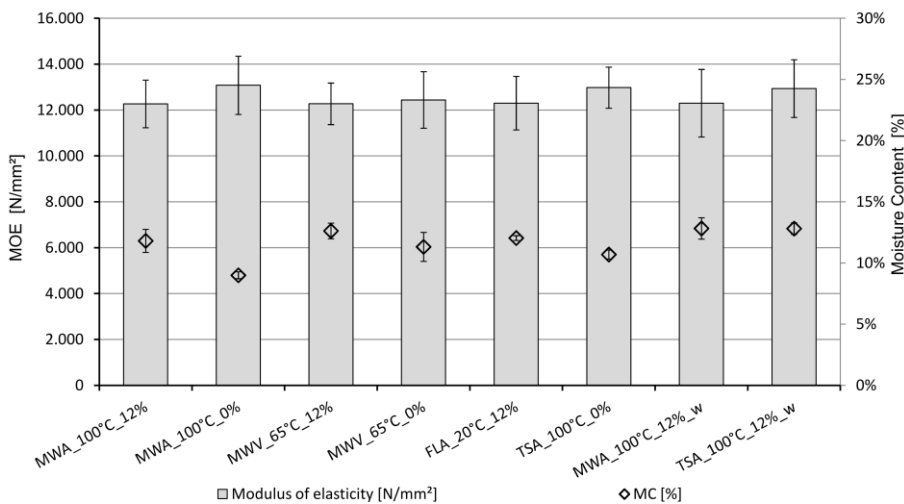


Figure 4. MOE out of the tree-point bending for different drying processes, the whiskers represent the standard deviation

Compression strength.

The compression strength of the eight drying processes is presented in Figure 5. The compression strength show remarkable lower values for the two processes TSA_100°C_12%_w and MWA_100°C_12%_w as for the other processes (Table 3 and Figure 5). The reason could be found in some slightly detectable cracks for those series. The series MWA_100°C_0% show remarkable higher values as all other series.

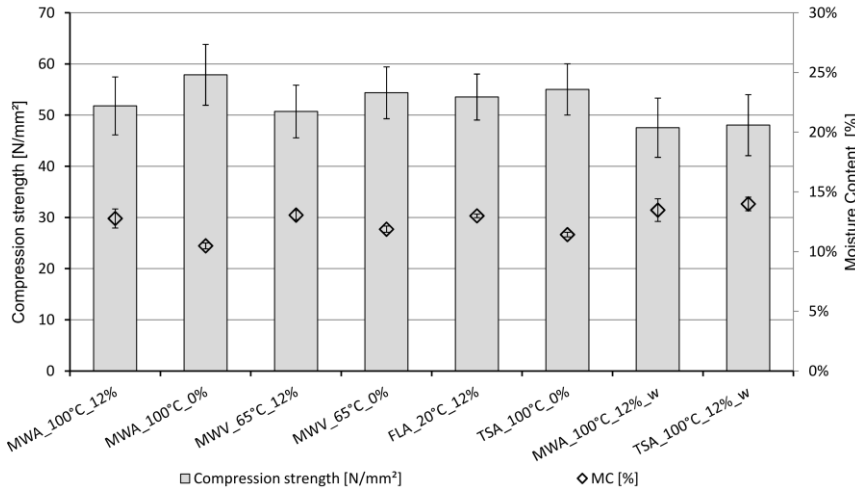


Figure 5. Compression strength parallel to the grain for different drying processes, the whiskers represent the standard deviation

Brinell hardness.

The diagram for the Brinell hardness in radial and tangential direction is presented in Figure 6. By facing natural dried material FLA_20°C_12% to the other series the results show remarkable higher values for the MWA_100°C_0% in radial direction and tangential direction and the TSA_100°C_0% series in radial direction. For all other series the Brinell Hardness show similar results as the natural dried material.

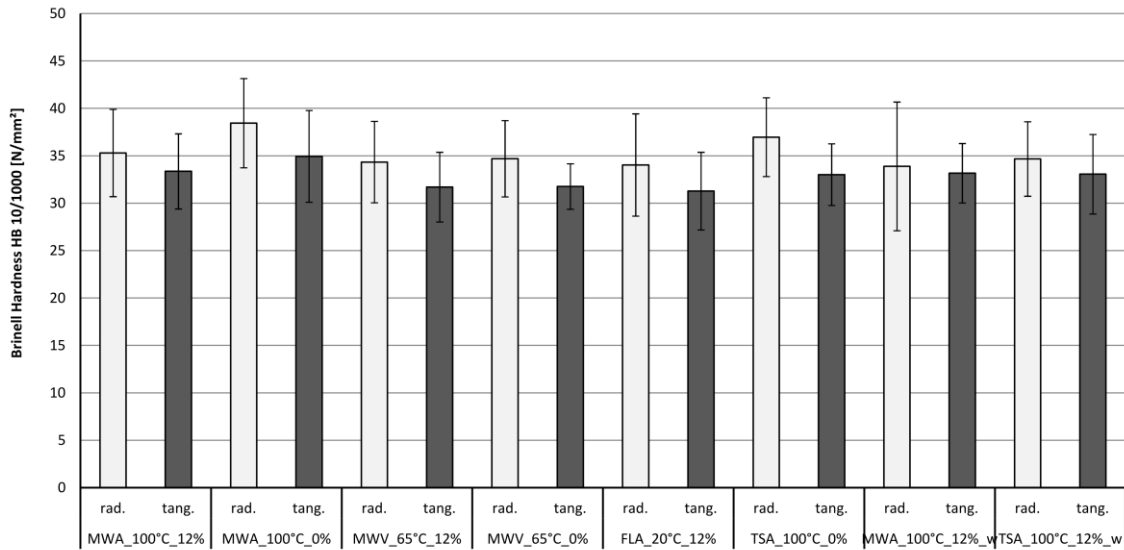


Figure 6. Brinell hardness in radial and tangential direction for different drying processes, the whiskers represent the standard deviation

Conclusion

As a conclusion it can be stated that the mechanical properties of European beech wood investigated, namely: the three-point bending strength and the compression parallel to the grain are not negatively influenced by the moderate temperature microwave and oven drying processes applied. Significant differences could be found for the compression strength of water stored material with a high starting MC due to cracks as result of the drying stresses by comparison with the natural dried material. Higher values for the Brinell hardness could be found in some cases in comparison to the natural dried material for the radial and tangential direction. In general the microwave dried material at 100 °C to the target MC of 0% show in most cases for all properties determined higher values as the other test series.

Acknowledgement

The presented work is financially supported by the “Tiroler Standortagentur” under the project “Physikalisch-chemische Untersuchungen der silikatischen Nano-Infiltration von Hölzern nach Mikrowellentrocknung” within the Translational-Research program.

References

- [1] Resch H (2009) Drying Wood With High Frequency Electric Current, Society of Wood Science and Technology, Madison WI 53726-2398 (USA), ISBN 978-0-9817876-1-9

- [2] Antti, A. L. 1992. Microwave drying of wood: simultaneous measurements pressure, temperature, and weight reduction, *Forest Products J.* 42 (1992) 49–54.
- [3] Turner, I. W. 1994 A study of the power density distribution generated during the combined microwave and convection drying of softwood, in: *Proceedings of the 9th International Drying Symposium, Gold Coast, Australia, August, 1994*, pp. 1–4.
- [4] Lehne, M., Barton, G. W., Langrish, T.A.G. 1999. Comparison of experimental and modelling studies for the microwave drying of ironbank timber, *Drying Technol.* 1999, 2219–2235.
- [5] Oloyede, A., Groombridge, P. 2000. The influence of microwave heating on the mechanical properties of wood, *Journal of Materials Processing Technology* 100, 67-73
- [6] Lee, H. W. 2003. Combined microwave and convective drying of Koreanwood species, in: *Proceedings of the 8th International IUFROWood Drying Conference, 2003*, pp. 146–149.
- [7] Masakasu, M., Harumi, K., Akihiko, S., Toyoji, K., Keji, T. 2003 Rapid pyrolysis of wood block by microwave heating, *J. Anal. Appl. Pyrol.* 2003, 1–13.
- [8] Taskini, J. 2007. Effect of Drying Methods on wood Strength: A comparison Between Microwave, Infrared and Conventional Drying, *Mech. & Aerospace Eng. J.* Vol. 3, No.1, 2007, 83-90
- [9] Oltean, L., Teischinger, A., Hansmann, Ch. 2011. Influence of low and moderate temperature kiln drying schedules on specific mechanical properties of Norway spruce wood, *Eur. J. Wood Prod.* 69, 451-457
- [10] Hansson, L., Antti, A.L. 2006. The effect of microwave drying on Norway spruce woods strength: a comparison with conventional drying, *Journal of Materials Processing Technology* 141, 41-50
- [11] Oltean, L., Teischinger, A., Hansmann, Ch. 2007. Influence of temperature on cracking and mechanical properties of wood during wood drying – a Review, *Bio resources* 2(4), 789-811
- [12] Shahverdi, M., Tarmian, A., Dashti, H., Ebrahimi, G., Tajvidi, M. 2012. Mechanical properties of poplar wood (*Populus alba*) dried by three kiln drying schedules, *Bio resources* 7(1), 1092-1099

Standards

- DIN 52182 Prüfung von Holz; Bestimmung der Rohdichte, 1976
- DIN 52183 Prüfung von Holz; Bestimmung des Feuchtegehalts, 1977
- DIN 52185 Prüfung von Holz; Bestimmung der Druckfestigkeit parallel zur Faser, 1976
- DIN 52186 Prüfung von Holz; Biegeversuch, 1978
- EN 1534 Parkett und andere Holzfußböden – Bestimmung des Eindruckwiderstandes (Brinell) – Prüfmethode, 2000

Protecting Effect of Beeswax Impregnation on the Modulus of Elasticity During Soil Contact

Róbert Németh^{1} – Dimitrios Tsalagkas² – Miklós Bak³*

¹ Associate professor, Institute of Wood Science, Simonyi Karoly Faculty of Engineering, Wood Sciences and Applied Arts, University of West Hungary
Sopron, Hungary.

** Corresponding author*

robert.nemeth@skk.nyme.hu

² PhD student, Institute of Wood Based Products and Technologies, Simonyi Karoly Faculty of Engineering, Wood Sciences and Applied Arts, University of West Hungary
Sopron, Hungary.

dimitrios.tsalagkas@skk.nyme.hu

³ Researcher, Institute of Wood Science, Simonyi Karoly Faculty of Engineering, Wood Sciences and Applied Arts, University of West Hungary
Sopron, Hungary.

miklos.bak@skk.nyme.hu

Abstract

During the outdoor utilization of wood, hazard class of soil contact is very high among the exposure classes (Use class 4, according to EN 335). In this case, very good protection or/and durable wood species are needed. The aim of this study was to use beeswax impregnation as a wood preservative method, in order to evaluate the suitability to protect wood species with low resistance. The advantage of beeswax is its biological origin, without any toxic agents. For this reason, poplar (*Populus × euramericana* cv. Pannonia) and beech (*Fagus sylvatica*) samples (20×20×300 mm) were impregnated with beeswax and exposed to soil contact for 18 months. Unimpregnated samples were used as control. MOE was determined initially at absolute dry state. Impregnated samples were separated into 3 groups, on the basis of the degree of pore saturation (DPS). With the progressing of the decay, load bearing capacity and MOE of wood decreased. After 1 month in soil contact, significant decrease in MOE could be observed, but it is explained by the increase of the moisture content. After 18 months control samples were completely decayed, thus no measurements could be accomplished. In spite of that, impregnated samples showed less decay and significant remaining load bearing capacity. Compared to the absolute dry state, MOE of beech and poplar wood decreased 65-80 % and 50-60 % respectively. Impregnation efficiency had significant effect on decay resistance, as higher DPS resulted in less decrease in MOE for both investigated species. Although beeswax is a bio-based material, it showed significant decay resistant effect against soft rot.

Keywords: beeswax, soil contact, soft rot, decay test, wood protection, beech, poplar

Introduction

The advantage of beeswax is its biological origin and its nontoxic nature. But therefore, natural waxes are in general not biologically stable (Schmidt, 2006), however they can delay the decay, because waxes are water repellent and with the impregnation method the cell lumens can be filled with wax. As a result of the hydrophobic properties and the lumen filling, fungi can decay wood only slower. Waxes have the effect of reducing termite damage as well, but they cannot protect wood completely (Scholz et al. 2010a). Another advantage of wax impregnation of wood is the improvement of mechanical properties, for example the hardness can be increased by beech wood up to 86-189% in longitudinal and lateral directions respectively (Scholz et al. 2010b). Different waxes, including beeswax are often used as conservation agent for wooden artifacts (Timar et al. 2010 and 2011). This shows that under appropriate conditions beeswax is suitable for wood protection. Chemical composition of beeswax presents a huge diversity of components because of its lipid nature. Beeswax is mainly composed by a mixture of hydrocarbons, free fatty acids, monoesters, diesters, triesters, hydroxy monoesters, hydroxy polyesters, fatty acid polyesters and some unidentified compounds. Each class of compounds consists of a series of homologues differing in chain length by two carbon atoms (Maia és Nunes, 2013).

During the outdoor utilization of wood, hazard class of soil contact is ranked to very high among the exposure classes (Use class 4, according to EN 335). For use in soil contact, very effective protection or/and durable wood species are needed. The aim of this study was to show, the effectiveness of beeswax against the degradation of less durable woods with different impregnation intensities in soil contact.

Materials and Methods

Poplar (*Populus × euramericana* cv. Pannonia) and beech (*Fagus sylvatica*) samples were impregnated with beeswax and exposed to soil contact for 18 months. Unimpregnated samples were used as control. The two wood species has different physical properties, but both of them are low resistant against decay without protection (Class 5 acc. to EN 350). Wood pores were completely filled with wax, or their surface was coated with wax as a result of the impregnation, depending on the degree of the impregnation. Beeswax was melted at 80°C in a closed chamber, and the dry samples (moisture content: 0%) were put into the melted beeswax. After that the pressure was decreased in the chamber to 150 mbar for 4 hours. Following the vacuum period the pressure was increased to atmospheric pressure and the temperature of the beeswax (with the samples) was kept at 80°C for 20 hours. Impregnated samples were separated into 3 groups, on the basis of the degree of pore saturation (DPS) (Table 1.). All these separated groups contained 25 samples, thus

we had 25 untreated samples as control and 75 impregnated samples from poplar and beech as well.

Group	Poplar1	Poplar2	Poplar3	Beech1	Beech2	Beech3
DPS (%)	20-40	40-55	55-70	60-75	75-90	90-100

Table 1: Sample groups according to the degree of pore saturation (DPS)

DPS was calculated as a ratio of the theoretical pore volume of wood material and the volume of the beeswax injected into the pores (Eq. 1).

$$DPS = \frac{V_{BW}}{V_{PTH}} \times 100 \quad (1)$$

Where: DPS: Degree of pore saturation [%]
 V_{BW} : Volume of the injected beeswax [cm³]
 V_{PTH} : Theoretical pore volume of wood [cm³]

Modulus of elasticity (MOE) was determined initially at absolute dry state both on the unimpregnated and impregnated samples, before the insertion of the samples in the soil. To determine the MOE, a standard 3-point bending method was used. Sample dimension was 20×20×300 mm. MOE was determined at a defined load, to not damage the samples. As the different load bearing capacity of the investigated wood species was taken into consideration, the load was 400N for poplar and 600N for beech.

The effect of outdoor exposure in soil contact was investigated under laboratory conditions. The soil was compost, collected in the Botanical garden of the University in Sopron. The area is under natural protection, without use of any biocides; the starting moisture content of the compost was 35%. Soil was collected into a plastic box and the samples were put into this soil to a depth of its 2/3 length (~20cm). To retain the moisture content of the soil the boxes were seal up with plastic foil, thus a wet climate could be maintained which is very favourable for the fungi (Figure 1.)



Figure 1. A plastic box with poplar samples in the soil after the opening of the foil

The first inspection of the MOE was made after one month soil contact. The load was the same than at the first determination in absolute dry state. The second inspection was made after 18 months soil contact. In this case the load was decreased according to the expected damage of the samples. Load was 300N by both wood species, but MOE was determined at 150N as well, because in some cases load bearing capacity of the samples was under 300N.

After 18 months in soil contact samples were investigated with SEM imaging, to determine the extent of the decay and the effect of beeswax on the decay. Furthermore, the location of the beeswax in the structure of the wood was studied.

Results and Discussion

The protecting effect of beeswax could be observed already with visual inspection, because the ends of both the untreated beech and poplar samples which were put into the soil were almost completely decayed after 18 months soil contact (Figure 2a-b.). The initial cross section was decreased significantly and the texture of the wood was disintegrated. The unimpregnated samples lost their load bearing capacity completely until the end of the investigated period, thus the determination of the MOE was impossible. In spite of that on the impregnated samples only surface decay could be observed and the initial cross section remained almost unchanged. It was not possible to make a difference with visual inspection between the impregnation groups.

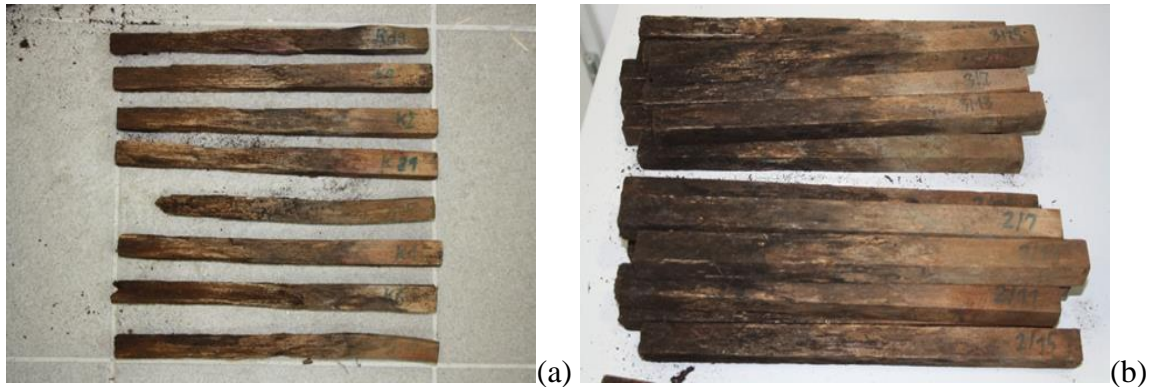


Figure 2. Unimpregnated (a) and impregnated (b) beech samples after 18 months soil contact

As a result of beeswax impregnation, MOE at absolute dry state increased significantly by 30-50% and 15-25% compared to the control samples by beech and poplar respectively, depending on the impregnation efficiency. The initially 12100MPa MOE of beech increased up to 13600-15000MPa depending on the impregnation efficiency. The initially 6200MPa MOE of poplar increased up to 8000-9200MPa depending on the impregnation efficiency. Interesting result was that the impregnation efficiency had opposite effect on the MOE. In case of poplar higher impregnation rates resulted in higher MOE, in spite of that by beech the opposite could be observed (Figure 3.)

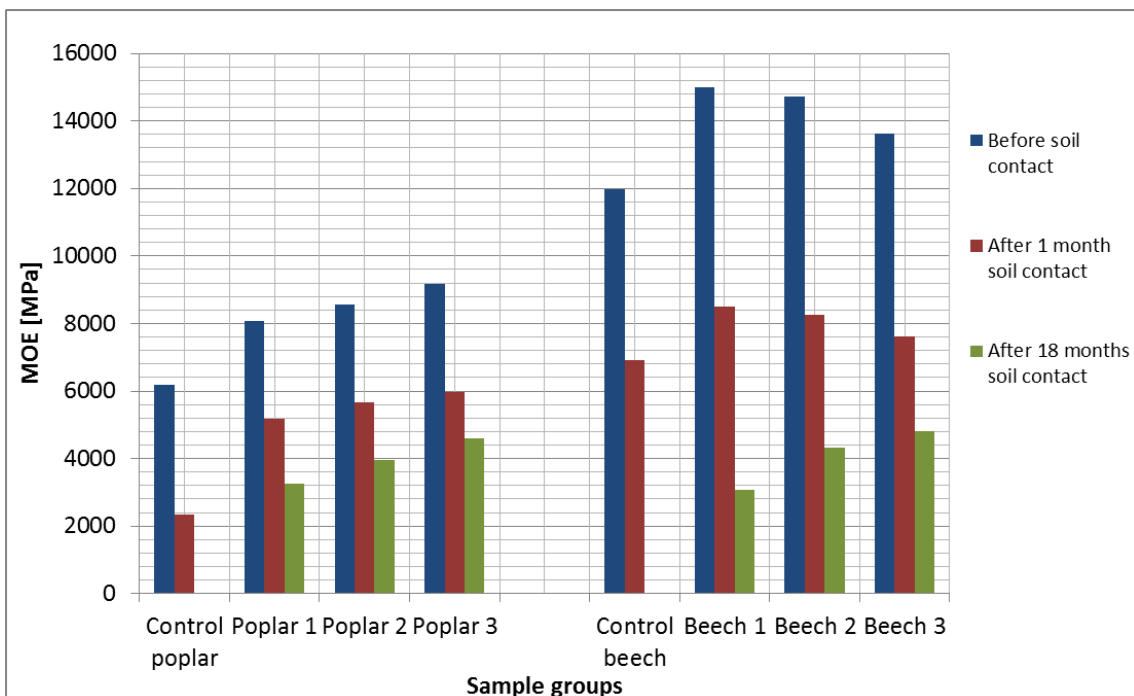


Figure 3. MOE of poplar and beech samples in the investigation periods

MOE decreased significantly during the exposure to soil (Figure 3.). A strong decrease (30-60%) could be observed in the MOE already after 1 month soil contact, but this is mainly explained with the increase of the moisture content in the samples. The initially

MOE was determined at absolute dry state of the samples, however after 1 month in soil contact the moisture content of the samples increased near to the fibre saturation point. This high moisture content increase can strongly decrease MOE. After 1 month in soil contact no significant decay is expected, but it can have a slight effect on the elastic properties of the wood. The values measured at absolute dry state are close to the theoretical maximum of the investigated samples, while MOE measured after 1 month soil contact can be considered as the MOE under utilization conditions. During the next 17 months soil contact the MOE decreased significantly forth. Untreated beech and poplar specimens lost their load bearing capacity completely, because their texture was destroyed by fungi. Accordingly, their MOE was 0MPa due to the heavy decay. In spite of that the load bearing capacity of impregnated beech and poplar specimens remained considerably. Accordingly, their MOE was measurable. Only a few samples were decayed at that large extent that the load bearing capacity was under the investigation load (150N). The DPS had significant effect on the decay. Higher DPS of both beech and poplar specimens resulted in higher MOE after 18 months soil contact. Even though, beech samples showed lower MOE at higher DPS values before soil contact. This result shows clearly that impregnation efficiency is an important factor in the wood protection against decay.

The decrease in MOE can be explained by visual inspection as well, because after cutting them by most samples the decay of the inner parts could be seen as well beside the decay of the surfaces. This decrease of the solid cross section decreases the load bearing capacity and the MOE forth. Beside all of the unimpregnated beech and poplar samples, some impregnated samples were damaged completely as well, because their load bearing capacity was far under 150N. Some samples had load bearing capacity over 300N, but they had extremely high deformation during the load. This indicates the strong degradation of the cell wall structure. The most of the samples probably could bear much higher loads.

Compared to the absolute dry state, after 18 month soil contact exposure, MOE of beech and poplar wood decreased by 65-80 % and 50-60 % respectively (Figure 4.). Impregnation efficiency had significant effect on decay resistance, as higher DPS resulted in less decrease in the MOE in both case of beech and poplar samples. The advantage of the beeswax impregnation is, that higher DPS resulted in higher MOE at absolute dry state (before soil contact) and this higher MOE decreased less during soil contact in case of beech and poplar wood. The decrease of the MOE was lower in case of poplar compared to the beech samples, thus beeswax impregnation was more effective by poplar in the prevention of MOE decrease during soil contact.

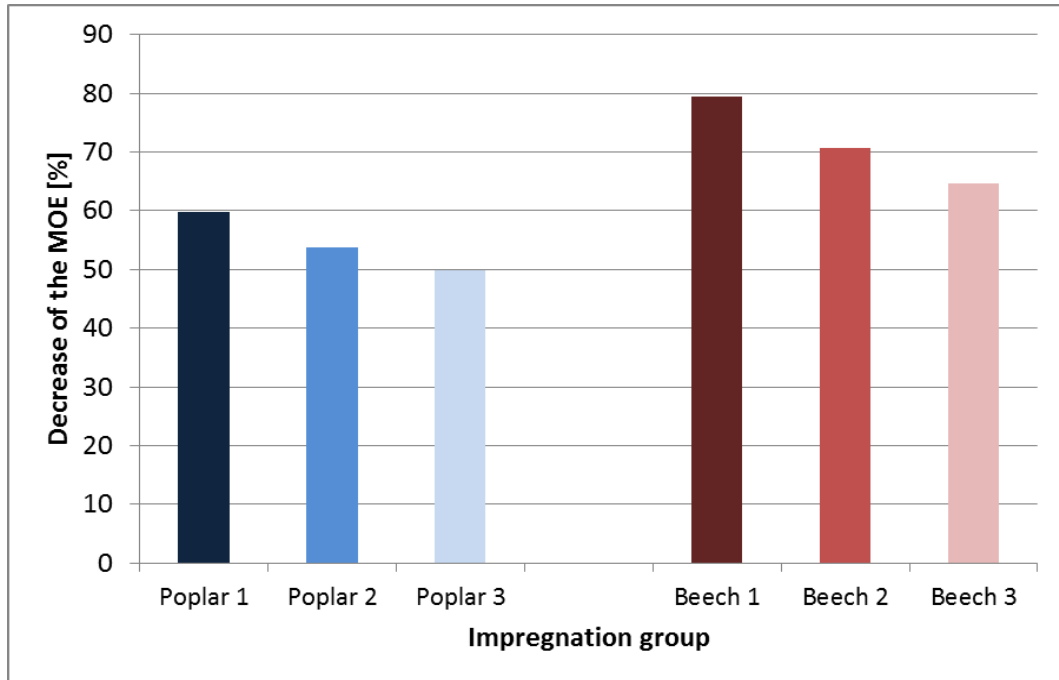


Figure 4. MOE decrease of beech and poplar samples after 18 months soil contact

The beeswax could be well identified with SEM imaging in the cell lumens, mainly in the vessels (Figure 5.). Beeswax fills the whole lumen in most cases, but sometimes it only coats the inner surface of the lumen like a protective layer. Hyphae could be observed only on the surfaces of the specimens with direct soil contact in large quantities. Hyphae in the inner structure of the specimens were rare to find, and only in lumens without any beeswax (Figure 6.). The spreading of the hyphae was physically inhibited with the presence of the beeswax in the lumens, and this slows the progression of the fungi in the wood. This can explain the slower decay of the impregnated samples. Higher ratio of filled lumens inhibits the spreading of hyphae better, which can explain the higher remaining MOE values of samples with higher DPS.

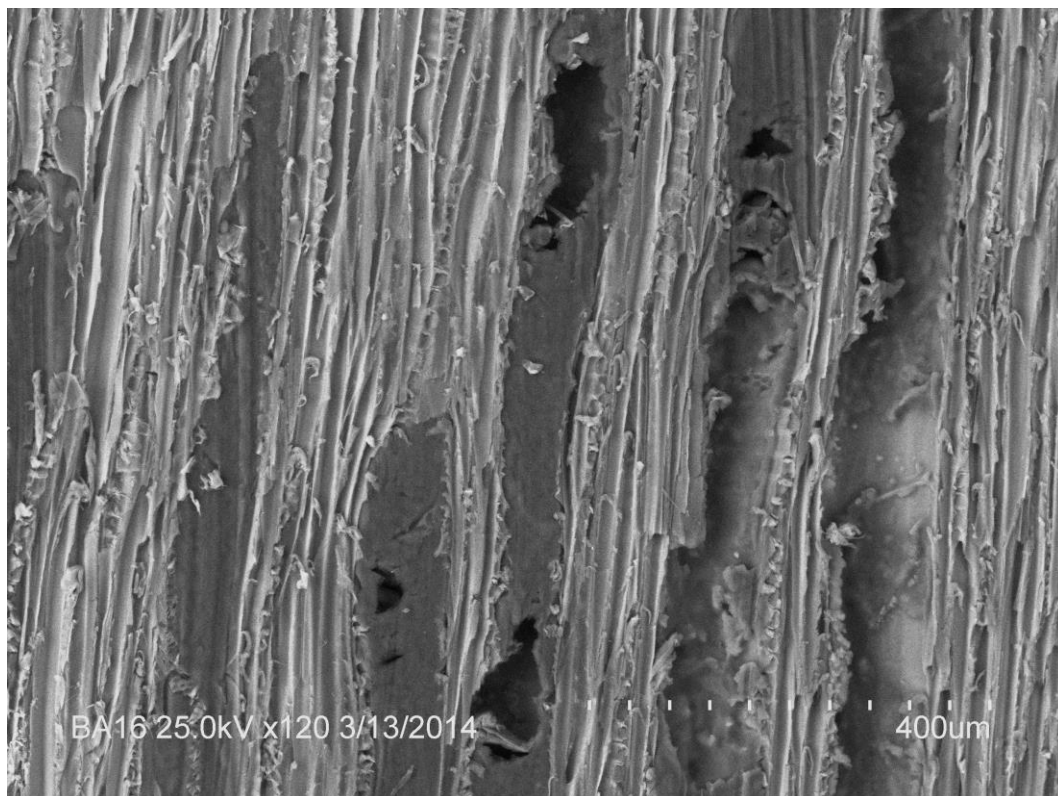


Figure 5. Beeswax in the cell lumens of poplar wood

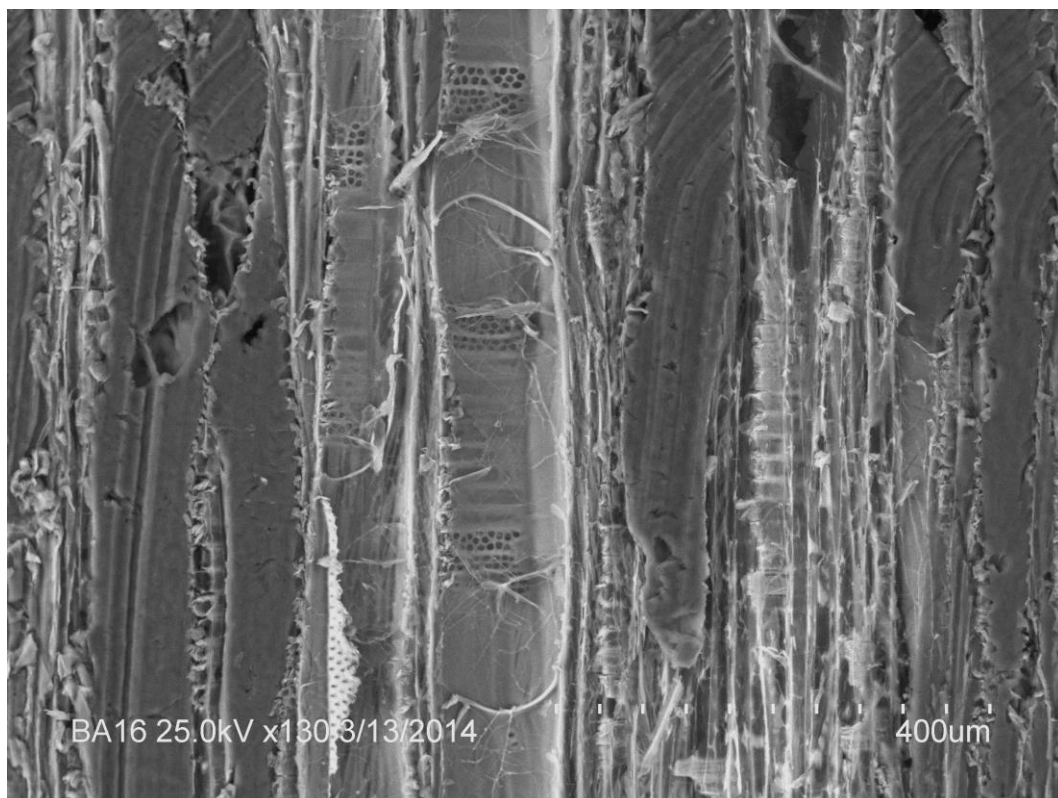


Figure 6. Hyphae in a beeswax free cell lumen of poplar wood

Conclusions

Beeswax impregnation increased MOE of beech and poplar wood. Unimpregnated beech and poplar samples were decomposed completely during the 18 months soil contact. In spite of that the damage of the impregnated samples was significantly lower. This was confirmed by the MOE measurements, which showed remarkable remaining MOE of impregnated samples after exposure. The impregnation improved the resistance against fungi, as higher DPS resulted in lower decrease of the MOE during the investigated period. SEM imaging showed that beeswax fills the lumens and separates the most of the cell walls from the hyphae, which slows the spreading of the fungi in the wood. This explains the protecting effect of the beeswax, even though it does not consist any “artificial” fungicide agents.

Although the impregnated wood was damaged remarkably by fungi, the experimental condition was the highest exposure class excepting seawater. If a beeswax impregnation with high DPS were used for wood species from higher durability classes (Class 4 or 3) or without soil contact, it could slow down the decay remarkably. But further investigations are needed to clarify this. Furthermore, it is an important factor that this treatment is entirely environmental friendly, because only biomaterials are used for the process. Even though beeswax is a bio-based material, it showed significant decay resistant effect.

References

- Timar, M.C., Tuduce, T.A., Porojan, M., Lidia, G. 2010. An investigation of consolidants penetration in wood. Part 1: General methodology and microscopy. *Pro Ligno*. 6(4): 13-27.
- Timar, M.C., Tuduce, T.A., Paľachia, S., Croitoru, C. 2011. An investigation of consolidants penetration in wood. Part 2: FTIR spectroscopy. *Pro Ligno*. 7(1): 25-38.
- Maia, M., Nunes, F.M. 2013. Authentication of beeswax by high-temperature gas chromatography and chemometric analysis. *Food Chemistry*. 136(2): 961–968.
- Scholz, G., Militz, H., Gascón-Garrido, P., Ibiza-Palacios, M-S., Oliver-Villanueva, J.V., Peters, B.C., Fitzgerald, C.J. 2010a. Improved termite resistance of wood by wax impregnation. *International Biodeterioration & Biodegradation*. 64(8): pp. 688-693.
- Scholz, G., Krause, A., Militz, H. 2010b. Beeinflussung der Holzfestigkeit durch Wachstränkung. *Holztechnologie*. 51(1): 30-35.
- Schmidt, O., 2006. *Wood and tree fungi*. Springer, Berlin Heidelberg New York

Acknowledgement

This study was supported by the Environment conscious energy efficient building TAMOP-4.2.2.A-11/1/KONV-2012-0068 project sponsored by the EU and European Social Foundation.

Solid Wood Manufacturing

***Session Co-Chairs: Bob Rice, University of Maine, USA and
Levente Dénes, University of West Hungary, Hungary***

**Processing Conditions Contributing to Formaldehyde
Emissions from “Native” Wood**

*Ashley A. Hellenbrand, Barbara J.W. Cole, Raymond C. Fort Jr., and
Douglas J. Gardner*

Abstract

Formaldehyde emissions from wood have long been linked to the adhesives used to produce wood composite materials. In recent years, formaldehyde has received increased attention and regulatory limits for formaldehyde emissions have been reduced. There is a growing body of literature suggesting that formaldehyde emanates from wood itself without it being processed into composites. The mechanism(s) by which formaldehyde is produced in or by “native” wood have not been established. This study will report on a project examining wood processing conditions and how they might contribute to native formaldehyde emissions. In this study, formaldehyde emitted by aspen (*Populus tremuloides*) wood under various processing conditions (temperature, moisture content, particle size) is being quantified, and the reaction conditions occurring in the wood are being ascertained to determine of the source of formaldehyde emissions. Formaldehyde emissions are collected using a Dynamic Microchamber and a Parr bench top micro reactor. The analytical method used involved derivatizing emissions with 2, 4, 6-trichlorophenylhydrazine (TCPH) and subsequent quantification using gas chromatography-mass spectrometry. Results to date suggest that processing temperature has a significant effect on the formation and emission of formaldehyde from aspen wood.

Keywords: formaldehyde, emissions, wood, processing, temperature, moisture

Douglas J. Gardner
University of Maine
School of Forest Resources and
Advanced Structures and Composites Center
35 Flagstaff Road
Orono, Maine 04469
+01-207-581-2846 FAX +01-207-581-2074
douglasg@maine.edu

*Proceedings of the 57th International Convention of Society of Wood Science and Technology
June 23-27, 2014 - Zvolen, SLOVAKIA*

Ashley A. Hellenbrand, Barbara J.W. Cole, Raymond C. Fort Jr.
University of Maine
Department of Chemistry
Orono, Maine 04469

A New Method of Dynamic 3D-Cutting Force Analysis of Wood

Thomas Krenke.^{1} – Stephan Frybort² – Oliver Vay³ – Ulrich Müller⁴*

¹ Junior Researcher, Division Wood Technologies – Wood K plus – Competence Centre for Wood Composites and Wood Chemistry, Tulln, Austria.

** Corresponding author*

t.krenke@kplus-wood.at

² Senior Researcher, Wood K plus – Competence Centre for Wood Composites and Wood Chemistry, Tulln, Austria.

³ Senior Researcher, Wood K plus – Competence Centre for Wood Composites and Wood Chemistry, Tulln, Austria.

⁴ Priv.-Doz., Institute of Wood Science and Technology, BOKU – University of Natural Resources and Life Sciences, Vienna, Austria.

ulrich.mueller@boku.ac.at

Abstract

Sustainable utilisation of the raw material wood is gaining more and more importance. Mechanical disintegration is one of the key processes in wood technology in general. Basic understanding of the cutting process can help to optimise existing mechanical disintegration technologies and to enable the development of alternative disintegration technologies. For measuring cutting forces by applying different cutting tools a test set-up was developed enabling measurement of cutting forces in three directions (i.e. feeding- or main cutting-force, lateral cutting force and cutting normal force). The main focus of the following work has been on data processing to analyse material specific influences on the cutting process. Previous investigations mainly applied curve smoothing on their data by moving average. However, by this method material specific information of the anisotropic inhomogeneous material is lost. For this examination cutting forces were measured directly beneath the cutting tool. The recorded data are adjusted for test-specific influences by the aid of a transmission function, which describes the relationship between input and output signal. Great efforts have been made to calibrate the dynamometer and to identify the possible sampling rate of the piezo-force sensor. As the cutting tool is mounted at the bottom dead end of the pendulum the whole cutting process can be observed by a high-speed camera. Examinations were done at a cutting speed of 6.8 m/s. First results of cutting force measurements are presented. Results of this study will be transferred to other cutting speeds of subsequent examinations.

Keywords: Cutting force analysis, transmission function, wood properties

Introduction

Cutting processes are the main principles in the wood working industry. Nevertheless, description of the cutting-process for wood and other anisotropic visco-elastic materials is mainly (Kivimaa, 1950) based on empirical parameters (Pahlitzsch, 1962). For optimizations of existing cutting technologies as well as development of new mechanical disintegration methods a basic understanding of the cutting process is required. Therefore, aim of this work is the development of a general method for a basic analysis of dynamic cutting processes. Thereby, the main focus has to lie on the inhomogeneous, anisotropic and visco-elastic material. Generally, measured data are highly influenced by the chosen test set-up as well as by subsequent data processing. For this reason results of former studies and their derived models are not transferable (Pahlitzsch, 1962; Martynenko 2006; Goli 2005). Additionally, description of previous experiments is poor as important information, like accurate data acquisition (cutting speed, sampling rate) and data processing (filtering, etc.), is missing. The frequently observed method of curve smoothing by moving average is not practicable as important material-specific information is lost (Ettelt 2004; Heisel 2001). Prior to measurement knowledge of cut-off frequency and stability of the measurement chain is required. Therefore, another important task is to enable interpretation of cutting force measurements by developing an appropriate filtering method.

Materials and Methods

Force sensor. For a detailed analysis of the interaction of cutting tool and raw material it is necessary to measure effective forces in 3D-directions. Therefore, the chosen measuring device is a force sensor based on the piezoelectric effect. Identification of an appropriate force sensor is fundamental. The sensor has to possess high sampling rate for sufficient measurement data and at the same time a high resolution for analyzing slight force differences. The minimum sampling rate was identified by the aid of the Nyquist-Shannon-sampling theorem (Meyer 2011). For high dynamic cutting processes superposition of the measuring signals has to be avoided. For this reason the sensor has to possess a high rigidity to quickly dissipate occurring vibrations. However, damping of the system must not happen by high masses, as measurement accuracy would significantly decrease. The output signal of a piezo force-sensor is a function of vibration characteristics and disturbance values which are accumulated by the principle of superposition. The challenge of using a piezoelectric force sensor is the subsequent evaluation of measured data, e.g. elimination of disturbing influences like vibration characteristics of the dynamometer. To enable interpretation of the data the output-signal needs to be related to a known input-signal. This mathematical relationship is called response function.

The chosen 3D-piezo force sensor 260A02 (PCB Piezotronics, New York, United States of America) has a sampling rate ranging from 0.01 Hz to 90 kHz. The sensitivity is given with 0.56 mV/N for the z-axis and 1.12 mV/N for the x- and y-axis. Due to the high sampling rate the sensor can be used for examination of cutting speeds up to 70 m/sec.

Measurement signal is amplified by an external signal conditioner 482C16 (PCB Piezotronics, New York, United States of America) and read-out from the software over a 4-channel analog PC input module NI 9215 with a 16-bit simultaneous resolution (National Industry, Salzburg-Bergheim, Austria). The measurement software is reading and saving the raw data and plotting the force-curve over the time.

Pendulum. For cutting-force measurement a pendulum (Wolpert, Vienna, Austria) was modified for analysis of linear cutting processes with cutting speeds of around 7 m/sec. Therefore a vertically adjustable machine table (IEF Werner, Furtwangen, Germany) is mounted on the bottom dead centre of the pendulum. The table enables adjustment of different cutting thicknesses in steps of $1\mu\text{m}$. The piezo force sensor is fixed between machine table and working tool (fig. 1). The test set-up enables measurement of main cutting force, cutting normal force and passive force. The samples with differing fiber directions are mounted at the adapted hammer. The comparatively high mass of the hammer (6 kg) enables a constant cutting speed during the cutting process.

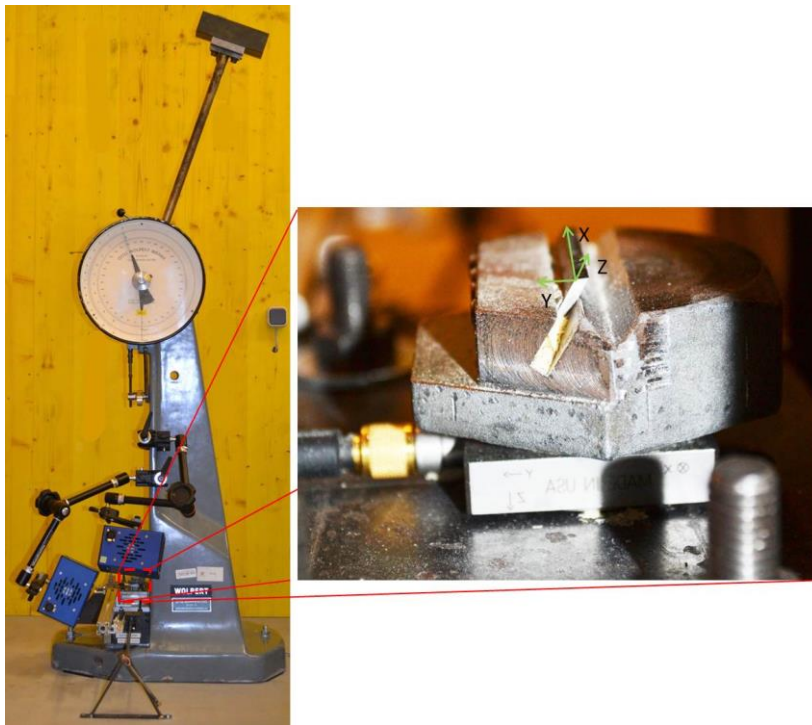


Figure 7: Cutting force measurement system; right image: detail of the force sensor and the work tool including the coordinate system

Data processing. As most filtering methods (e.g. curve smoothing by moving averages) delete specific inhomogeneous, anisotropic and visco-elastic influences of the workpiece on the cutting force, data processing is done with the saved raw data. To achieve unadulterated data the saved output signal will be filtered by the so-called system/transfer-function. The system/transfer function considers all influencing components of the test-setup as a black box whereby the relationship between input- and output-signal is described by the frequency response function. Therefore the output signal

is processed by the frequency response function eliminating all disturbing influences from signal acquisition.

Samples. For examination solid samples of flawless spruce (*Picea abies* Karst.) of differing fiber angles (0° ; $22,5^\circ$; 45° ; $67,5^\circ$ and 90°) were used. Sample geometry is shown in figure 2.

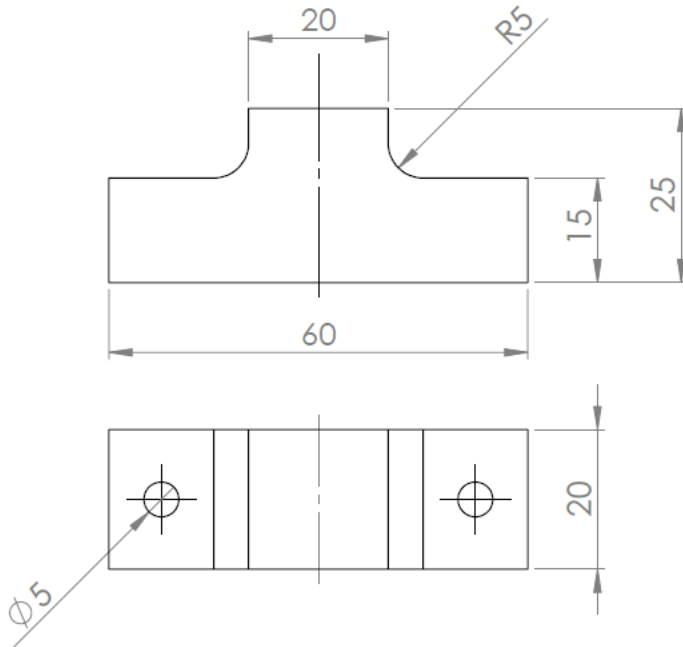


Figure 8: Sample geometry

High speed camera. To improve interpretation of the cutting process a high speed camera Motion NX 7 (IDT, Tallahassee, USA) was mounted onto the Pendulum. To achieve exposure times around $3 \mu\text{s}$ two cold-light sources, with each 800W were used (Optronis, Kehl, Germany).

Results

To enable measurements preliminary tests as well as calibration procedures are necessary. For identification of the appropriate sampling rate all test parameters have to be constant (cutting length, cutting speed, test set-up). Several cuts are performed and the main frequency of the cut is identified by the aid of a Fast Fourier Transformation (Meyer 2011). By following the Nyquist-Shannon-sampling theorem the minimum sampling rate has to be twice the measured frequency (Meyer 2011). For determination of the response-function the test set-up has to be fed with a known input signal. Common applicable input signals of signal processing are the step and the pulse signal. The pulse signal can be generated by a shot bullet test. For this study, a ball of known mass (5, 5970g) was dropped from a defined height level (30 cm) onto the measuring unit. The saved measurement values are the output signal of the so called black-box. The crux of generating a pulse signal by a shot bullet is that it is a more or less unknown input signal

as the measured output signal is superimposed by the transfer function. In order to calculate the transfer function the pulse signal has to be mathematically described. Therefore the input signal was simulated by a pulse generator in Simulink R2013b (MathWorks, Ismaning, Germany) identical to the signal of the shot bullet test. After generating the input signal the relationship between input and output signal is calculated.

To verify own measurements cutting force curves were compared with values from literature. To enable comparison own data was also smoothed by the inappropriate method of moving average. By doing so the same trend of cutting-forces and curve progression are observed. To illustrate the problem arising through this filtering method, an unfiltered cutting curve and the associated filtered curve is plotted in figure 3.

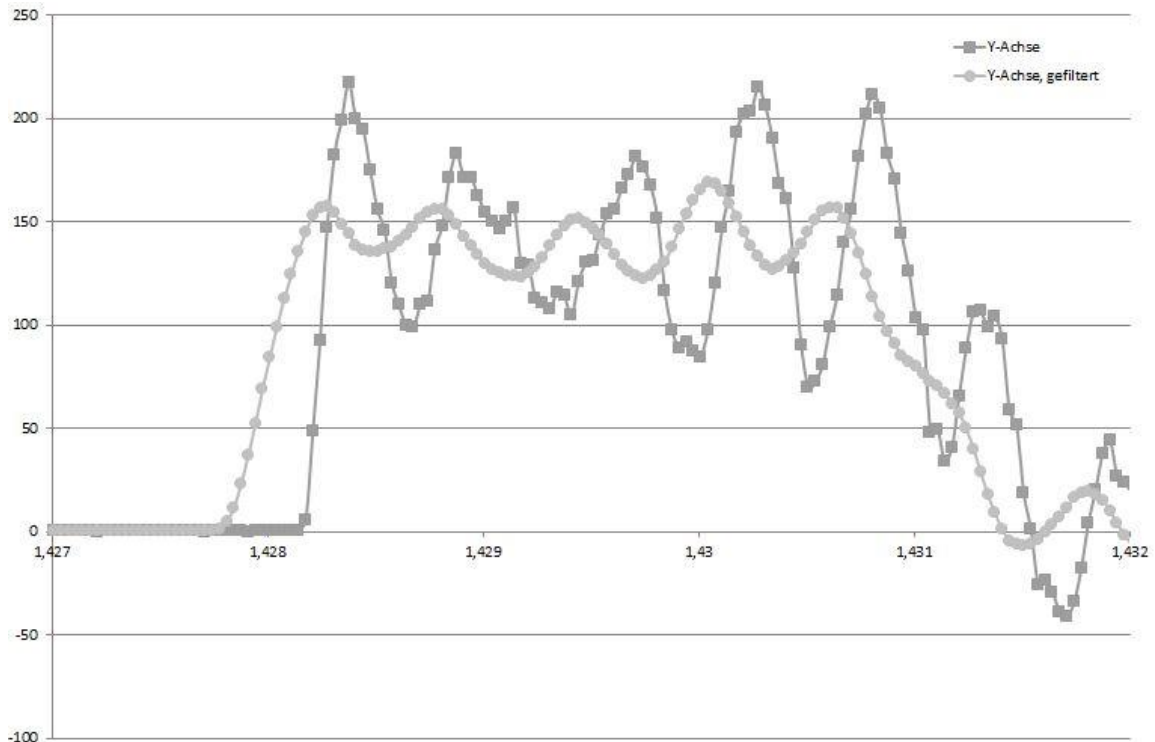


Figure 9: Influence of Low-Pass Filtering on measurement values; dark grey: original unfiltered values, light grey: smoothed values

As aforementioned, by curve smoothing all specific influences of the wood itself onto the cutting process are deleted and additionally time-delayed. The high-speed camera supports interpretability of the measured data by a visual analysis of the cutting process. By this method variability in cutting forces, i.e. pre-splitting, can be explained.

Conclusion

The modular design of the dynamometer enables examination of several cutting tools at dynamic cutting processes. The design of the test setup exhibits a high stiffness thereby guaranteeing a high stability of the test setup. Additionally, interfering effects are

significantly reduced by the chosen setup. Interpretability of measurement signals is improved in terms of the specific material influences. The so far used filtering method of moving average deletes important information of the cutting process. The response-function is therefore an adequate tool for examination of cutting-force measurements. The synchronized high speed camera enables a visually assisted analysis of the cutting process and the cutting force measurements.

References

Ettelt B, Gittel H-J (2004) Sägen, Fräsen, Hobeln, Bohren; Die Spannung von Holz und ihre Werkzeuge.3. Auflage: DRW-Verlag, Leinfelden-Echterdingen.

Goli G, Fioravanti M, Sodini N, Jiangang Z, Uzielli L (2005) Wood Processing: a contribute to the interpretation of surface origin according to grain orientation. 17th International Wood Machining Seminar, Rosenheim, Germany.

Heisel U, Tröger J (2001) Aktueller Handlungsbedarf zur Bestimmung der Kräfte am Schneidkeil (2). HOB Die Holzbearbeitung 47: 72 - 76.

Kienzel O (1952) Bestimmung von Kräften an Werkzeugmaschinen. Z-VDI 94: 299-305.

Kivimaa E (1950) Cutting force in woodworking. Valtion Teknillinen Tutkimuslaitoksen Julkaisuja 18: 102.

Kivimaa E (1952a) Die Schnittkraft in der Holzbearbeitung. Holz als Roh- und Werkstoff 10: 94-108.

Martyenko S, Scholz F, Tröger J (2006) Modellierung der Kräfte am Schneidkeil. Holztechnologie 47: 32-38.

Meyer M (2011) Signalverarbeitung - Analoge und digitale Signale, Systeme und Filter.6. Auflage: Vieweg und Teubner Verlag, Wiesbaden.

Pahlitzsch G (1962) Internationaler Stand der Forschung auf dem Gebiet des Sägens. Holz als Roh- und Werkstoff 20: 381-392.

Pahlitzsch G (1966) Internationaler Stand der Forschung auf dem Gebiet des Hobelns und des FräSENS von Holz und Holzwerkstoffen. Holz als Roh- und Werkstoff 24: 579-593.

Mathematical Modeling of Timber Elastic-Viscous-Plastic Deformation in the Drying Process

Ya. Sokolovskyy^{1} – Yu. Prusak² – I. Kroshnyy³*

¹ Prof. Dr.-Ing., Department of Information Technology, Ukrainian National Forestry University (UNFU), UKRAINE.

** Corresponding author*

[*sokolowskyyyar@yahoo.com*](mailto:sokolowskyyyar@yahoo.com)

² Postgrad, Department of Information Technology, Ukrainian National Forestry University (UNFU), UKRAINE.

[*yu.prsk@gmail.com*](mailto:yu.prsk@gmail.com)

³ Assistant Professor, PhD, Department of Information Technology, Ukrainian National Forestry University (UNFU), UKRAINE.

[*kroshny.igor@gmail.com*](mailto:kroshny.igor@gmail.com)

Abstract

In the paper there is described solving a current scientific problem of mathematical modeling of heat-mass transfer processes and elastic-viscous-plastic deformation taking into account the mechanics and sorption creep in hygroscopic capillary-porous materials with variable anisotropic heat and mechanics characteristics what is of importance for the rational choice and substantiation of energy conservative technologies of timber drying under the conditions of necessary qualitative production providing. There has been implemented the formulated mathematical model of timber deformation during the drying process which enables to identify two-dimensional intense-deforming state under the conditions of non-isothermal humidity transfer by means of the finite elements method. This method has been developed for the research of the two-dimensional anisotropic intense-deforming state during the capillary-porous materials drying process in an elastic-viscous-plastic area of deformation taking into account the mechanics and sorption creep.

There has been elaborated the applied software which consists of the documented classes and provides the possibility to automate the finite-elemental analysis of timber intense-deformation state during drying process.

The problem of timber drying process optimization has been formulated and solved which enables to define the parameters of the drying process conditions taking into consideration the restrictions on the intense-deforming state which does not exceed the solidity limit of the material.

Keywords: mathematical model, the method of finite elements, heat and mass transfer, elastic-viscous-plastic state, drying process.

Introduction

During drying of hygroscopic capillary-porous bodies irreversible physical processes arise up and cooperate between itself, there are phase transitions, which predetermine changes in physical mechanical properties of materials in general, initial form of body, formation of cracks in it and its possible destruction. The conducted analysis of mathematical models deformation-relaxation processes and methods of their calculation during drying of capillary-porous materials, especially woods, showed that the resilient and viscoelastic area of deformation is mainly investigated in unidimensional and two-dimensional cases for permanent mechanical descriptions, independent of temperature and humidity change [1,2,3,4,5]. Construction of mathematical models of wood deformation during drying taking into account resilient, viscoelastic, plastic deformation and features of their regeneration in a wide turn-down physical mechanical properties of wood is a complicated and not fully decided problem.

Taking into account difficult connected with each other processes of deformation and mass transfer during the design of the convective drying of hygroscopic capillary-porous materials substantially complicates mathematical models and requires the improvement of numeral methods for their realization and software development.

Synthesis of Mathematical Model

According to the basic laws of thermodynamics of irreversible processes, mechanics of the inherited environments, contraction of hygroscopic materials, the mathematical model of two-dimensional viscoelastic deformation is formed and heat-and-mass transfer in the process of drying of capillary-porous materials taking into account the anisotropy of heat-mechanical descriptions of material, resilient, viscoelastic, plastic deformations and deformations, caused by a mechanism of mechanical and sorption creep.

System of model equalizations for determination component of deformation vector $\varepsilon = (\varepsilon_{11}, \varepsilon_{22}, \varepsilon_{12})^T$, strains $\sigma = (\sigma_{11}, \sigma_{22}, \sigma_{12})^T$, temperature $T(X, \tau)$ and humidity content $U(X, \tau)$ during drying wooden bar during time $\tau \in [0, \tau_{dry}]$ in the area of cross-cut section $\Omega = \{X = (x_1, x_2); x_1 \in [0, l_1], x_2 \in [0, l_2]\}$ the center of which is combined with beginning of co-ordinates, and the axes of anisotropy coincide with co-ordinate axes, it is built so. The components of tensions vector are satisfied by equalizations of equilibrium with boundary conditions which take into account absence of external efforts:

$$\frac{\partial \sigma_{11}}{\partial x_1} + \frac{\partial \sigma_{12}}{\partial x_2} = 0; \frac{\partial \sigma_{12}}{\partial x_1} + \frac{\partial \sigma_{22}}{\partial x_2} = 0; \sigma_{ij} \Big|_{x_i=l_i, x_j=l_j} = 0. \quad (1)$$

Modeling of connection between the components of tensions and deformations during wood drying is based on Boltzmann-Volterra integral equalizations and laws of contraction of hygroscopic materials [1,6]. For an account mechanical and sorption deformations, predefined speed of change of humidity during drying, the functions of rheological conduct of materials are complemented correlations mechanical and sorption

creep. Therefore connection between tensions and deformations taking into account the anisotropy of mechanical properties in material looks like:

$$\begin{aligned}
 \sigma_{11}(\tau) &= C_{11}(T, U)[\varepsilon_{11}(\tau) - \varepsilon_{U1}] - C_{11}(T, U) \int_0^{\tau} R_{11}(\tau - s, T, U) \times [\varepsilon_{11}(\tau) - \varepsilon_{U1}] ds + \\
 &\quad + C_{12}(T, U)[\varepsilon_{22}(\tau) - \varepsilon_{U2}] - C_{12}(T, U) \int_0^{\tau} R_{12}(\tau - s, T, U) [\varepsilon_{22}(\tau) - \varepsilon_{U2}] ds; \\
 \sigma_{22}(\tau) &= C_{21}(T, U)[\varepsilon_{11}(\tau) - \varepsilon_{U1}] - C_{21}(T, U) \int_0^{\tau} R_{21}(\tau - s, T, U) [\varepsilon_{11}(\tau) - \varepsilon_{U1}] ds + \\
 &\quad + C_{22}(T, U)(\varepsilon_{22}(\tau) - \varepsilon_{U2}) - C_{22}(T, U) \int_0^{\tau} R_{22}(\tau - s, T, U) [\varepsilon_{22}(\tau) - \varepsilon_{U2}] ds; \\
 \sigma_{12}(\tau) &= 2C_{33}(T, U)\varepsilon_{12}(\tau) - 2C_{33}(T, U) \int_0^{\tau} R_{33}(\tau - s, T, U)\varepsilon_{12}(s) ds,
 \end{aligned} \tag{2}$$

where $\varepsilon_U = (\varepsilon_{U1}, \varepsilon_{U2}, \varepsilon_{U3})^T$ – a vector component of deformations, predefined the change of wood temperature and humidity content; C_{ij} – components of tensor of resiliency woods, which depend on the temperature and humidity.

For the modeling of mechanical and sorption deformations, predefined by humidity speed change in wood, such equalizations are used [7]:

$$\frac{\partial \varepsilon_M}{\partial \tau} = m(\sigma - E_m \varepsilon_M(\tau)) \left| \frac{\partial U}{\partial \tau} \right|, \tag{3}$$

where m – is a tensor of mechanical and sorption deformations, which depend on the temperature, in radial and tangential directions of wood anisotropy, the coefficients of which are determined with the help of experimental data.

For the modeling of plastic deformations in wood the Prandtl-Reuss equations of plastic flow is used. The relation between differentials of tensions and deformations for the flat tense state looks like:

$$d\sigma_{ij} = \frac{E}{2(1+\nu)} \left(d\varepsilon_{ij} + \frac{\nu}{1-2\nu} \delta_{ij} d\varepsilon_{ij} - s_{ij} \frac{s_{ke} d\varepsilon_{ke}}{s} \right); \quad s = \frac{2-\nu}{3} \sigma^2 \left(1 + \frac{2(1+\nu)}{3E} \right), \tag{4}$$

where s_{ij} – deviators of deformation, δ_{ij} – Kronecker's delta.

The functions of rheological conduct of wood during drying taking into account the mechanism of piling up of irreversible deformations choose in a kind:

$$R(\tau, U, T) = \left(a_0 - \sum_{i=1}^M a_i \exp(-b_i \tau) \right) h(\tau) h(\tau_0 - \tau) - a_0 - \sum_{i=1}^M \alpha_i \exp(-\beta_i (\tau - \tau_0)) h(\tau - \tau_0), \tag{5}$$

where $h(\tau)$ – Heaviside step function, and unknown coefficients $a_i, b_i, \alpha_i, \beta_i$ are determined by the method of the least squares on the basis of approximation of experimental information of creep of wood samples on-loading and after unloading. They are the functions of temperature and humidity.

During the convective drying of wood the two-dimensional mathematical model of heat-and-mass transfer taking into account the anisotropy of thermo-physical descriptions is described by the system of differential equalizations of non-isothermal humidity transfer:

$$\begin{aligned} c\rho \frac{\partial T}{\partial \tau} &= \frac{\partial}{\partial x_1} \left(\lambda_1 \frac{\partial T}{\partial x_1} \right) + \frac{\partial}{\partial x_2} \left(\lambda_2 \frac{\partial T}{\partial x_2} \right) + \varphi_0 r \frac{\partial U}{\partial \tau}; \\ \frac{\partial U}{\partial \tau} &= \frac{\partial}{\partial x_1} \left(a_1 \frac{\partial U}{\partial x_1} \right) + \frac{\partial}{\partial x_2} \left(a_2 \frac{\partial U}{\partial x_2} \right) + \frac{\partial}{\partial x_1} \left(a_1 \delta \frac{\partial T}{\partial x_1} \right) + \frac{\partial}{\partial x_2} \left(a_2 \delta \frac{\partial T}{\partial x_2} \right), \end{aligned} \quad (6)$$

Boundary conditions look like:

$$\begin{aligned} \lambda_i \frac{\partial T}{\partial n} \Big|_{x_i=l_i} + \rho_0 (1 - \varepsilon) \beta_i (U|_{x_i=l_i} - U_p) &= \alpha_i (t_c - T|_{x_i=l_i}); \\ \left(a_i \frac{\partial U}{\partial n} + a_i \delta \frac{\partial T}{\partial n} \right) \Big|_{x_i=l_i} &= \beta_i (U_p - U|_{x_i=l_i}); \quad \left(\alpha_i \frac{\partial U}{\partial n} + \alpha_i \delta \frac{\partial T}{\partial n} \right) \Big|_{x_i=0} = 0; \\ \frac{\partial T}{\partial n} \Big|_{x_i=0} &= 0; \quad U|_{\tau=0} = U_0; \quad T|_{\tau=0} = T_0, \quad i = 1, 2. \end{aligned} \quad (7)$$

Denotations used here: $T_0(X)$, $U_0(X)$ – primary apportionment of the temperature and humidity content in the material; $U_p(T_c, \varphi)$ – equilibrium humidity; $c(T, U)$ – heat capacity; $\rho(U)$ – density; $\lambda_i(T, U)$ – coefficients of heat-conducting in the directions of anisotropy; ε – coefficient of phase transition; ρ_0 – basic density; r – specific heat of vaporization; $\delta(T, U)$ – thermal-gradient coefficient; $a_i(T, U)$ – coefficients of hydraulic conductivity in the directions of anisotropy; $\alpha_i(T_c, v)$ – coefficient of heat exchange; $\beta_i(T_c, \varphi, v)$ – coefficient of humidity exchange; T_c – environment temperature; $\varphi(\tau)$ and $v(\tau)$ – relative humidity and rate of movement of drying agent; n – vector of external normal of area limit Ω ; τ – current time. During modeling of drying process in the period of the irregular mode the primary apportionment of humidity content in wood is accepted permanent, and in the period of the regular mode initial humidity content changes after a parabolic law.

For numeral realization of mathematical models of connected with each other processes of heat-mass transfer during wood drying (6) – (7) the Finite element method (FEM) is used [8]. Equivalent variation formulation of model is for this purpose got with assumption, that the change of humidity content in time is possible to show as a sum of constituents, related to the stream of mass transfer by the gradient of humidity content and temperature. Eventual system of equalizations for realization of mathematical model (6) – (7) after FEM looks like:

$$[C] \frac{\partial \{U\}}{\partial \tau} + [K] \{U\} + \{F\} = 0; \quad [\bar{C}] \frac{\partial \{T\}}{\partial \tau} + [\bar{K}] \{T\} + \{\bar{F}\} = 0, \quad (8)$$

where: $[C] = \int_V \rho_0 [N]^T [N] dV$; $[K] = \int_V [B]^T [D^*] [B] dV + \int_S \rho_0 \beta_w [N]^T [N] dS$; $\{F\} = \int_V [B]^T [H] [B] [T] dV - \int_S \rho_0 \beta U_p [N]^T dS$ – according to the matrix of thermo-physical properties of material, damping and loading, $\{N\}$ – matrix of form functions. Analogical matrixes are those $[\bar{C}]$, $[\bar{K}]$, $\{\bar{F}\}$, related with the coefficient of heat conductivity and heat exchange.

For the values of change of temperature $\{T\}$ and humidity $\{U\}$ in time the Finite difference method is used. Then numeral realization of mathematical model (6) – (7) is taken to the decision of the kind of system equalizations:

$$[A]\{U\}_{next} = \{R\}; \quad [A_r]\{T\}_{next} = \{R_r\}. \quad (9)$$

As thermo-physical descriptions of wood depend on a temperature and humidity, and equalization of model (6) – (7) are related with each other, the iteration process of equalizations realization (9) is carried out on every sentinel step taking into account additional iteration procedure, which specifies influence of humidity on apportionment of temperature in material and vice versa. Completing of iterations for equalizations (9) foresees implementation of conditions: $\{U_n\} - \{U_{n-1}\} \leq 10^{-4}$ i $\{T_n\} - \{T_{n-1}\} \leq 10^{-4}$.

For numeral realization of mathematical model (1) – (5) elastic-viscous-plastic deformation of wood during drying developed FEM for the research of wood deformation taking into account mechanical-sorption and plastic deformations and mechanism of regeneration of deformations. For this purpose on the basis of a minimum of complete potential energy equivalent variation formulation of tasks was received. Lagrange's equation, minimum of which coincides with the decision of mathematical model (1) – (5) is written down like:

$$\begin{aligned} \Omega = & \frac{1}{2} \int_V \left(\{U\}^T [B]^T [C] [B] \{U\} + 2 \{U\}^T [B]^T [C] \int_0^{\tau} [R(\tau, \tau')] [B] \{U\} d\tau' - \right. \\ & \left. - \{U\}^T [B]^T [C] \left(\{\alpha\} \Delta T + \{\beta\} \Delta U + [m] \left| \frac{dU}{d\tau} \right| \right) + \right. \\ & \left. + 2 \{U\}^T [B]^T [C] \int_0^{\tau} [R(\tau, \tau')] [B] \{U\} \left(\{\alpha\} \Delta T + \{\beta\} \Delta U + [m] \left| \frac{dU}{d\tau} \right| \right) d\tau' \right). \end{aligned} \quad (10)$$

From the condition of a minimum of functional $\delta\Omega = 0$ system of equalizations of algebra is received for finding of the unknown moving on every sentinel step $\Delta\tau_i$ ($i = \overline{1, M}$, M – an amount of sentinel intervals):

$$\sum_{n=1}^N [\bar{K}^{(n)}] \{U\} = \sum_{n=1}^N \{\bar{F}^{(n)}\} - \sum_{n=1}^N [\bar{K}^{(n)}] \left(\{\alpha\} \Delta T + \{\beta\} \Delta U + [m] \left| \frac{dU}{d\tau_i} \right| \right) \quad (11)$$

where, integrals $[\bar{K}^{(n)}]$ define the matrix of key inflexibility of material, which is defined by resilient or plastic characteristics of wood and geometrical sizes of elements of laying out. In case of resilient deformation it is taken that $[\bar{K}^{(n)}] = [K^{(n)}]$. For viscous-plastic deformation ($\sqrt{\sigma_{11}^2 + \sigma_{22}^2 - \sigma_{11}\sigma_{22} + 3\sigma_{12}^2} > \sigma_{pl}$) matrix of inflexibility consists of two matrices $[K^{(n)}]$ i $[K^{(n)pl}]$, and $[C^{(n)pl}]$ is calculated with the help of (4). The matrix of loading $\{\bar{F}^{(n)}\}$ is determined by the rheological conduct of wood, and also temperature and humidity descriptions of material. Vector of component to be found $\{U\}$ on the i -step after laying out on time is unknown in relation to calculations $\{U\}$ on previous $i-1$ steps depending on apportionment of temperature and humidity, which are determined on those steps using the algorithm from a previous paragraph.

Programmatic Realization of Mathematical Models

We described the application software for numeral realization of mathematical models of heat-mass transfer (6) – (7) and elastic-viscous-plastic deformation (1) – (5) of wood during drying developed within the limits of the object-oriented approach [9]. Programmatic complex, developed with the help of programming language *Java*, contains an informative model and interface of the programmatic system, which looks like packages of classes and relations between them with the use of graphic diagrams of UML, components of programmatic code, calculative charts of FEM realization. Developed classes represent the essence of the object-oriented realization of Finite element method. It creates possibility of integration of the developed programs to the existent systems of the automated modeling with the purpose of expansion of their functional possibilities.

There are separate packages for the classes, which realize: geometrical and physical and mechanical descriptions of researches object; laying out of area on finite elements with the help of mesh of knots and elements; determination of basic functions within the limits of eventual elements; calculable classes (squaring for numeral integration); interpolation functions; decision of the system of linear equations; classes, which are oriented on the concrete calculations of matrix and vectorial algebra; classes of saving loaded and received data; user interface.

Analysis of Modeling Results and their Discussion

Application of the developed mathematical models and applied programmatic facilities is shown for the research of processes of heat-mass transfer of the elastic-viscous-plastic state of wood during drying. For numeral experiments some thermo-physical descriptions of wood are specified. Especially, on the basis of working of experimental data dependence of coefficient of wood hydraulic conductivity as functions from a temperature and humidity is used: $a_{m1}(T, U) = a_{mt}(T) a_{mu}(U)$, $a_{m1} / a_{m2} = 1,25$. For determination of coefficient of humidity exchange we use the dependence: $\alpha = 0,95(T/\varphi \varepsilon \exp(-2\sigma V_p / rTR)) 10^{-9}$, where V_p , σ – molar volume and superficial strain of liquid, φ – relative humidity of environment. Value $r = r(U)$ have been received on the basis of wood

structure modeling by the system of inconstant capillaries of radius r , that depends on humidity.

To research the elastic-viscous-plastic state taking into account the mechanism of sorption creep resilient and mechanical-sorption descriptions were chosen according to the temperature and humidity change on the basis of approximation of known experimental data [5,7].

For determination of the module of wood plasticity used experimental data, according to which the determination of the modules of plasticity have been received.

The analysis of apportionment of temperature and humidity dynamics affirms that mathematical models enable to take into account interconnectivity of processes, their physical non-linearity, predefined by dependence of thermo-physical properties of material temperature and humidity.

On the basis of the developed mathematical models we investigated influence of anisotropy of viscous-plastic descriptions of wood, descriptions mechanical and sorption creep, withering coefficients on apportionment of two-dimensional stress-strain state of wood during drying taking into account an isothermal process. For this purpose during numeral modeling the probed index changed to the half of its value and the change of normal and tangential tensions on-the-spot and on the “near surface” layers of wood was probed.

Conclusions

1. We formulated a mathematical model of elastic-viscous-plastic deformation of wood during drying process, which takes into consideration plastic deformations, caused by mechanical-sorption creep and anisotropy of mechanical characteristics of the material and gives the opportunity to determine two-dimensional stress-strain state in the conditions of non-isothermal humidity transfer.
2. On the basis of the created mathematical models and methods of analysis application software is developed for the modeling of elastic-viscous-plastic state of capillary-porous materials during the convective drying, which consists of the above classes and gives the opportunity to automatize finite element analysis stress-strain state of wood during convective drying.
3. As a result of calculable experiments, conducted with the use of developed applied programmatic facilities regularity of anisotropy influence of thermo-physical and mechanical descriptions of wood were set, it initial humidity on changing of two-dimensional temperature-humidity and elastic-viscous-plastic state of wood during the convective drying.

References

1. B. Ugolev. Wood-forest with the basics of merchandising: a textbook for forestry schools. – Russian Ministry of Education: MGUL. – 2002. (Russian)
2. Ja. Sokolowsky, M. Dendyyuk, B. Pobereyko. Simulation of strain-relaxation processes in the wood during the drying // *Journal of Forest.* – Vol. 1. – 2007. – P. 75-83.
3. O. Dornyyak. Modeling of rheological behavior of wood during pressing // *Journal of Engineering Physics.* – Vol. 76, № 3. – 2003. – P. 150-155.
4. P. Akulich, K. Militzer. Modeling of non-isothermal moisture transport and stress in the wood during drying // *Journal of Engineering Physics.* – Vol. 71, №3. – 1998. – P. 404-411.
5. P. Perré, J. Passard. A physical and mechanical model able to predict the stress field in wood over a wide range of drying conditions // *Drying Technology Journal.* – Vol. 22, № 1-2. – 2004. – P. 27-44.
6. R. Kristensen. Introduction to the theory of viscoelasticity . – Moscov: Mir. – 1974. (Russian)
7. J. Rodic, A. Jayne. Mechanics of wood and composites. – New York: Van Nostrand Reinhold. – 1982.
8. L. Segerlind. Application of finite element method. – Moscov: Mir. – 1979. (Russian)
9. Ja. Sokolowsky, I. Kroshnyy. Algorithmic and software systems modeling and analysis of drying of capillary-porous materials // *Computer Science and Information Technology.* – Vol. 732. – 2012. – P. 306-315.

Monte Carlo Simulation of Windows Air Tightness Performance

*Balázs BENCSIK, Zsolt KOVÁCS, János KALMÁR, Viktória CSANÁDI,
Levente DÉNES*

Abstract

The ever-increasing energy prices and progressively more stringent directives constrain both users and designers to pay more attention on energy use of buildings; therefore the reliability of windows characteristics – one of the most vulnerable point of buildings – plays an important role in the overall evaluation of energy consumption. Test measurements demonstrated that in many cases the heat loss by filtration of the windows exceeds significantly the heat loss by transmission, especially at higher pressure values. First steps in window's performance reliability increase include the determination of influencing factors' effect and building a probability model thereafter able to predict the performance variation over time.

This article introduce a newly developed stochastic-deterministic model to simulate the windows air tightness variation over time in function of sash-frame gap deviations caused by repeated opening i.e. hinges wearing and internal stress relaxation of the sealings. Based on large number of Monte Carlo simulations the model predicts the air tightness of windows at certain stress levels in function of use time. Based on the simulation results and quality classes' threshold levels determined by standards, the model is able to forecast the time when the window does not fulfill these requirements anymore, with a confidence of 95%. Without any maintenance programs the air tightness will start to decrease rapidly after this time. Varying the model's input parameters in designed manner the sensitivity of the model have been determined. Based on the simulation results recommendations are formulated at the end to maintain the initial performance values of the windows.

Keywords: reliability, performance characteristic, air tightness, Monte Carlo simulation, stochastic-deterministic model

Balázs BENCSIK, bbencsik@fmk.nyme.hu

Zsolt KOVÁCS, zskovacs@fmk.nyme.hu

Levente DÉNES, dali@fmk.nyme.hu - corresponding author

University of West Hungary

College of Charles Simonyi Engineering, Wood Science and Art

Institute of Wood Based Products and Technology

Bajcsy Zs. 4.. H-9400, Sopron

János KALMÁR, kalmar@inf.nyme.hu

University of West Hungary

College of Charles Simonyi Engineering, Wood Science and Art

Institute of Informatics and Economy

*Proceedings of the 57th International Convention of Society of Wood Science and Technology
June 23-27, 2014 - Zvolen, SLOVAKIA*

Viktória CSANÁDI, vcsanady@emk.nyme.hu
University of West Hungary
College of Forestry
Institute of Mathematics

Decorative Finger Jointing of Valuable Wood

Nikolay Skuratov^{1} – Anatoliy Vojakin²*

¹ Professor, Department of Processes and Apparatuses in Woodworking Industry– Moscow State Forest University. 141005, Mytischki, Moscow Region, RUSSIA.

** Corresponding author*

skuratov@mgul.ac.ru

² Professor, Department of Machinery and Tools - Moscow State Forest University. 141005, Mytischki, Moscow Region, RUSSIA.

vojakin@mgul.ac.ru

Abstract

Finger jointing has become an increasingly popular method of reducing wood waste and utilizing short pieces of lumber. Defect free finger-jointed lumber is raw material for a wide range of wood products for structural and non-structural purposes, for external or internal uses, and for transparent or non-transparent finishes. Finger joint forms a zigzag or a straight line on the surface of the bonded parts. Such joints are not always suitable for wood products having a transparent finish. Monotone joints catch the eye, bring aesthetic damage to the product and reduce its cost.

The article gives the description of finger jointing which provides almost invisible joints. With the developed method, jointing fingers are of different heights and the line that bends around their tops is the curve. The profile of this curve depends on the texture of wood grain and may be a periodic function such as a sinusoid.

When tangential texture profile of the envelope line of larger amplitude, period, and height of fingers is more suitable. When radial texture which has finer and more monotonous pattern amplitude and period can be reduced without changing the height of the fingers. Numerous expert evaluations showed that curvilinear splice well masks joints and improves the aesthetic perception of glued products. This approach allows to provide higher value-output of blanks for furniture parts, decorative panels, baseboards etc. Joints are formed by two special cutters having direct and inverse profiles that can be set in conventional finger jointing lines with two cutting units. In the near future optimization of geometrical parameters of the compound and cutting tool design as well as carrying out strength tests are planned.

Keywords: Finger jointing, valuable wood, texture of wood grain.

Introduction

Finger jointing has been widely used in woodworking industry for many years. The finger jointing process is generally recognized to be the most effective method of timber longitudinal joints. The benefits of finger joints are well known: increasing output of lumber of given length from low grade raw material and reduction of waste. Defect free finger-jointed lumber is raw material for a wide range of wood products for structural and non-structural purposes, for external or internal uses, and for transparent or non-transparent finishes. Structural wood products are produced with the joints designed to have high mechanical properties. Strength of properly made finger joints is close to the strength of clear wood. General requirements for glued finger joints are well known. They are described in many standards and technical literature (ASTM D4688-99. 2005, EN 386. 2001, GOST 19414-90. 1991, ISO 10983. 1999, NLGA. 2002). The appearance of the joints in structural products is not the most important characteristic.

Finger jointed timber is used in non-structural applications, where clear wood is required. But conventional finger joint forms a zigzag or a straight line on the surface of the bonded parts which may be easy-to-see. Such joints are not always suitable for valuable wood products having a transparent finish. Monotone joints catch the eye, bring aesthetic damage to the product and reduce its cost.

The objective of this project was to develop the aesthetically acceptable finger joint profile for non-structural finger jointing of valuable wood.

Materials and Methods

To hide the actual finger joint effectively and to make it almost invisible, curved profile of the joint was selected. With the developed method jointing fingers are of different heights and the line that bends around their tops is the curve. In order to get away from the monotony fingers in the developed jointing are of different heights and the line that bends around their tops is the curve. But at the same time all fingers have the same slope (Fig. 1).

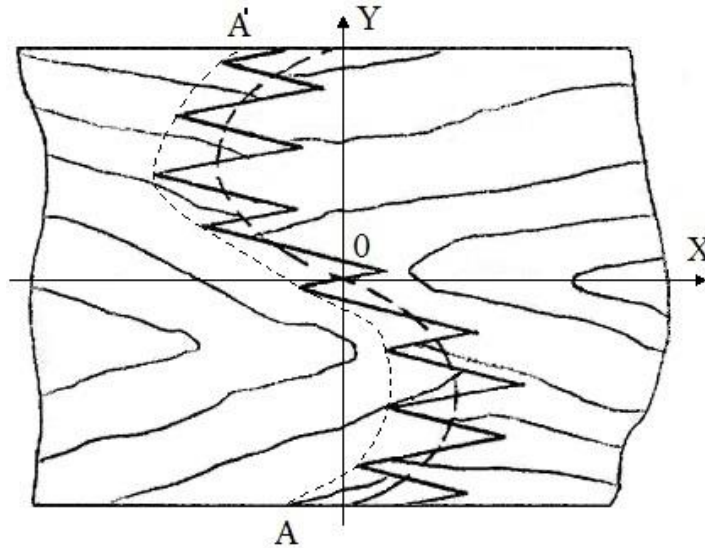


Figure 1. Curvilinear finger jointing

The profile of this curve depends on the texture of wood grain and may be a periodic function such as a sinusoid. Parameters of periodic function should match a texture of wood. When tangential texture profile of the envelope line of larger amplitude, period, and height of fingers is more suitable. For radial wood texture which has finer and more monotonous pattern amplitude and period can be reduced without changing the height of the fingers.

It is necessary to use wooden pieces of similar texture to produce high quality products of finger jointed lumber. Selection of the optimal finger joint profiles was based on the analysis of many of expert evaluations. Most of them showed that curvilinear splice better masks joints and improves the aesthetic perception of glued products.

If sinusoidal profile of joint is symmetrical with respect to the longitudinal axis X and the midpoint 0 , one cutter of such profile for simultaneous processing the ends of adjacent short pieces may be utilized (Fig. 1). For joining pieces into a single line every second of them should be deployed around the axis X on angle of 180° .

Results and discussion

Process diagram is shown in Figure 2. Work bay 1 is for matching of blanks for color, texture and the cross-section. The ends of workpieces are processed at work bay 2.

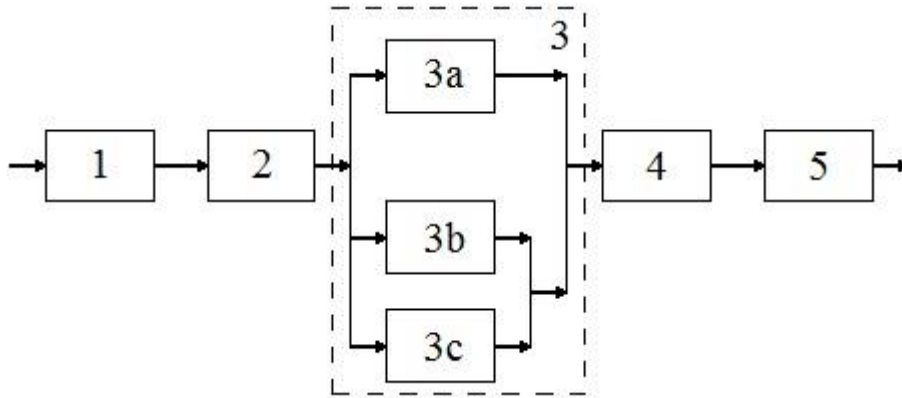


Figure 2. Process diagram of the decorative finger jointing: 1 – selection of wood pieces by color and fiber direction; 2 – trimming and removal of wood defects; 3 – finger cutting work bay (3a – with two units and alternate milling fingers at the ends of the workpieces; 3b – with two units when simultaneous milling fingers by two cutters at the ends of two adjacent workpieces; 3c – with one unit when simultaneous milling fingers by one cutter at the ends of two adjacent workpieces when centrally symmetric profile is used); 4 – longitudinal gluing workpieces in the press; 5 – processing defect free glued details by means of a planer.

At this work bay wood defects are removed by means of CNC band saw machine which makes curved cuts on the line A-A' along the envelope of the finger tops. Application of the curvilinear trimming will reduce the amount of waste and electricity consumption at subsequent milling. Next workpieces are moved to work bay 3 for cutting fingers by one of three ways. For an arbitrary curvilinear finger jointing the equipment with two cutters with forward and reverse profiles are needed.

In a conventional batch line with two cutting units (work bay 3a) fingers on the package of blanks are formed successively. The first unit forms the forward profile on the front ends of blanks and the second unit forms the reverse profile on opposite ends (Fig. 3). More productive line (work bay 3b) is designed for the simultaneous formation of the forward and reverse profiles at the ends of each blank (Fig. 4).

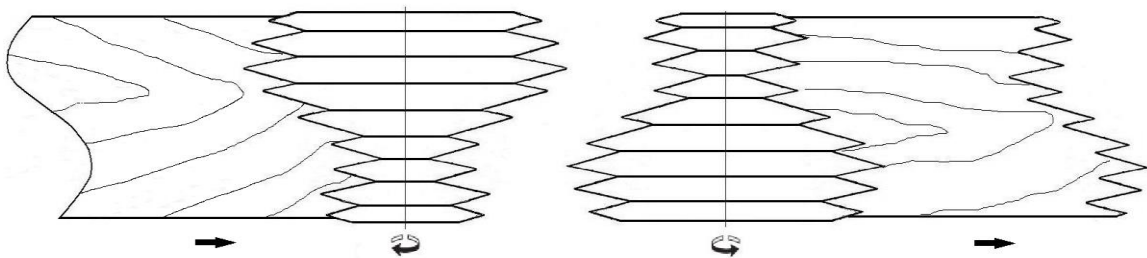


Figure 3. Alternate milling fingers by two cutters at the ends of the workpieces

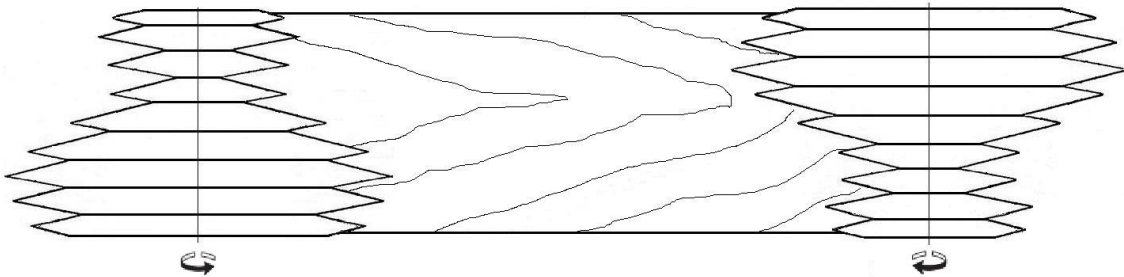


Figure 4. Simultaneous milling fingers by two cutters at the ends of two adjacent workpieces

For the formation of the centrally symmetric finger joints (Fig. 1) one cutting unit is needed (work bay 3c). Cutter forms simultaneously forward and reverse profiles on adjacent ends of two pieces. After turning over direct profile at the end of the first workpiece is transformed into reverse profile for the front end of the second workpiece (Fig. 5). To prevent chipping wood along the ends of the workpieces when milling the profiled supporting plates are to be used. Also, the latter method is applicable for batch cutting fingers if the turntable for basing package of blanks is used. Before entering the press every second workpiece must be turned over.

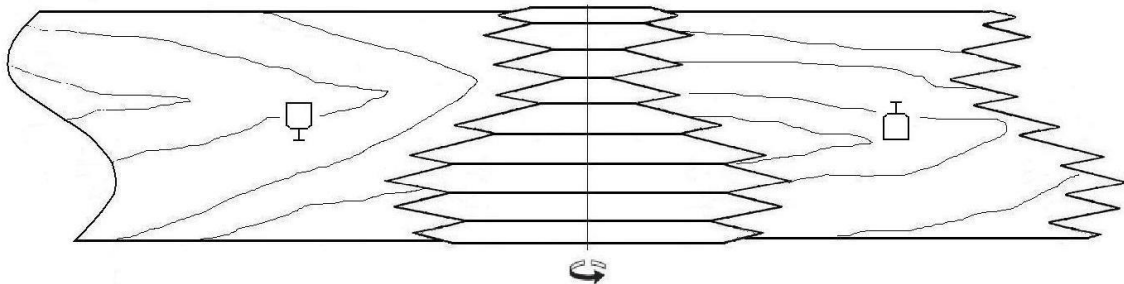


Figure 5. Simultaneous milling fingers by one cutter at the ends of two adjacent workpieces

Further the workpiece comes in press (work bay 4), where after applying the adhesive, they are compressed in the longitudinal direction to obtain long finger jointed lumber. Then the lumber is cut by circular saw into the details of a given length, which are moved on the accumulation table for curing of glue. At the final stage (work bay 5) defect free details are processed by means of a planer to form a cross-section of given shape and dimensions.

As a cutting tool the set of wing-finger jointing cutters of different diameters can be used. Each cutter in finger joint head processes one groove. Cutters are mounted on the mandrel through spacer rings of different thicknesses which is fixed on the machine spindle (Fig. 6). To reduce the dynamic loads when cutting the teeth of cutters are placed on a mandrel along a helical line.

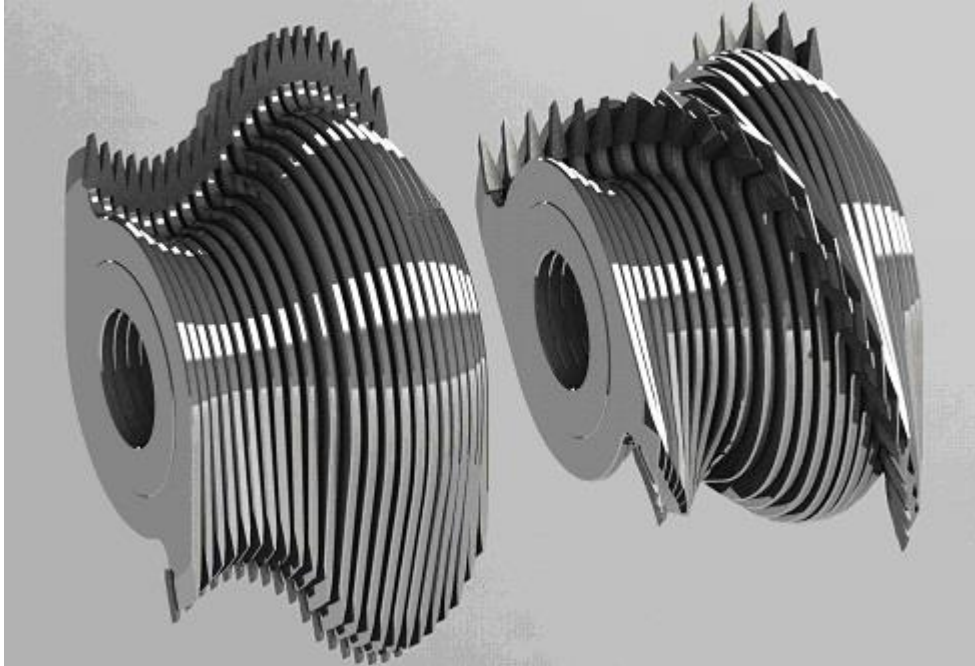


Figure 6. Cutterhead before (a) and (b) after turning wing cutters along the helix

Quality of finger jointing does not depend on the method of finger cutting. Correctly selected for the specific wood texture the curvilinear finger-joint profile better hides joints and improves the aesthetic perception of glued products including details of high profile (Fig. 7).

Conclusions

The proposed method can be used for finger jointing short pieces of expensive timber. Its application will improve the appearance and increase the utility value of products made of glued wood. Its application will improve the appearance and increase the utility value of products made of glued wood.

In the future finger jointing geometrical parameters and design of the cutting tool are going to be optimized and strength tests will be carried out.



Figure 7. Appearance of the curvilinear finger jointing oak pieces

References

ASTM D4688-99: 2005. Standard Test Method for Evaluating Structural Adhesives for Finger Jointing Lumber.

EN 386:2001. Finger jointed structural timber – Performance requirements and minimum production requirements. European Committee for Standardization. B – 1050 Brussels.

GOST 19414-90: 1991. Solid glued wood. General requirements for glued finger joints.

ISO 10983: 1999. Timber structures – solid timber finger-jointing – Production requirements. International Organization for Standardization. CH-1211 Geneva 20. Switzerland.

NLGA. 2002. Special products standard for fingerjointed structural lumber. NLGA SPS-I, National Lumber Grades Authority of Canada, Vancouver, BC, Canada.

Forest Products Policy, Global Trade, and Value Chain Management

Session Co-Chairs: *Eric Hansen, Oregon State University, USA and Mikulas Supin, Technical University in Zvolen, Slovakia*

Factors Impacting the Export of US Hardwoods in Germany, China and Vietnam

Edgar Arias, Henry Quesada-Pineda, Robert Smith

Department of Sustainable Biomaterials
Virginia Tech
Blacksburg, Virginia, USA

Abstract

The US hardwood industry used to benefit from high production volumes (above 10 billion board feet) between years 1997 and 2005. However, the production of the entire hardwood manufacturing industry fell to historically low levels after the collapse of the U.S. housing market in 2008. In order to remain competitive, the U.S. hardwood industry has turned to international markets as an opportunity to replace some of the local demand.

International exports of U.S hardwood represents today 17,3% of the volume of all eastern U.S. hardwood production (1,2 billion board feet). However, most of the U.S. hardwoods exports consist of primary products such as logs and lumber (together they represent 80%) of total volume traded. This fact leads to believe that a better understanding of the factors affecting the performance of exports to overseas markets should be conducted in order to increase the value-added of the products currently being exported.

In order to understand what factors that impact the export of U.S hardwoods, a case study methodology was formulated. A sample of 38 companies importing not just U.S. hardwoods but similar products from other countries was interviewed during 2013 in Germany, China, and Vietnam. Companies in these countries were selected because they represent the largest importing volumes of U.S. hardwoods. Interviews were conducted by contacting wood products importers that attended wood trade shows in those countries. Information was analyzed using qualitative and quantitative techniques.

Results indicate that on-time delivery, quality, and price are the most important factors that buyers in those three countries seek in their suppliers. For U.S. hardwood exporting business there seems to be opportunities to increase value-added in their products and services by providing more knowledge in U.S hardwood species, offering flexible dimensions, and providing better background data on lumber pricing models.

Keywords U.S. hardwoods exports, value-added products, international trade.

Background

The U.S. hardwood industry suffered a continued decline from 1999 through 2009, in part as a consequence of the collapse of the domestic housing market, and the overall economic recession that followed. Sawmill closures, a 37 percent reduction in employment in wood manufacturing (Bureau of Labor Statistics, 2014), and a 53 percent decrease in hardwood production (Hardwood Review, 2012), are some of the difficulties that the industry faced at the end of the first decade of the 21st century.

Hardwood exports

Improvements in the domestic and global economies have led to a slow recovery of the U.S. Hardwood industry, particularly on traditional markets such as pallets and crates, and non-traditional markets, as the exports sector for instance. The international trade is expected to account for a 13.2 percent of the total industry revenue in 2014 (Goddard, 2014), thereby exports have become the second market in importance for the industry, only after pallets. The value of hardwood exports has increased from 1.89 billion USD in 2009 to 2.99 billion USD in 2013 – almost a 58 percent increase, which also signifies a 2.14 percent increase vs. 2006, the year that held the highest exporting record until now. Even though exports haven't come to raise the industry's total production levels to match 1999 records (14 BBF), but they have certainly become a key market for short and long term growth (HMR, 2012). Hence there is no question as to the growing importance of international markets

Problem statement and goal

Firms need to have a good understanding of the characteristics and dynamics of markets to formulate proper strategies to increase growth and improve profits. Even though there has been extensive research on export performance, this field of study of International Business, still characterizes by fragmentation, diversity and inconsistency in results. The goal of this research is to identify opportunities to increase the export performance of U.S. hardwood firms in Asia and Western Europe. The focus was set on hardwood firms located in eastern U.S., and particularly those in the Appalachian region, considering the importance of its contributions to the total of hardwood exports.

Methodology

A comparative case study (Jan & Tony, 2008) was implemented between January 2013 and October 2013 to explore the importance of export performance factors found in the literature and assess the need of incorporating new ones in a model specifically adapted for the U.S. Harwood Industry.

The case study involved applying a survey interview to hardwood importing companies. The purpose of this phase is to capture the customers' opinions about the key elements in hardwood lumber supplier selection, customer service expectations, and opportunities for their suppliers to improve their competitiveness. To select the companies, the research team attended a series of trade fairs in Asia and Western Europe for suppliers to the furniture and interior finishing industries and identified the companies which utilized hardwood products as raw materials. Three trade fairs were visited in the following order:

- Interzum's Trade fair for suppliers to the furniture industry and interior finishing in Cologne, Germany; attended in May 2013
- The 14th International Furniture Fair in Chengdu (IFF), China; attended in July 2013
- The 11th Vietnam International Woodworking Industry Fair (VIWIF) in Ho Chi Minh City, Vietnam; attended in October 2013.

Questionnaire design

Table 1. Questionnaire Design

		Variable		
#	Type	Name	Description	Type
1	Close-ended	Hardwood Importer	Groups respondent in importers and non- importers	Categorical
2	Open-ended	Respondent Position	Job performed by respondent	Categorical
3	Open-ended	Respondent Location	Country where respondent's firm is located	Categorical
4	Open-ended	Supplier Location	Country where main hardwood supplier of respondent's firm is located	Categorical
5	Open-ended	Hardwood Species	Hardwood species imported by respondent's firm	Categorical
6	Close-ended	Hardwood Product Types Imported	Hardwood products imported by respondent's firm	Categorical
7	Open-ended	Order Qualifier 1	Main factor considered by responding firm when choosing supplier	Categorical
8	Open-ended	Order Qualifier 2	Responding firm's expectations that have not been fulfilled by hardwood suppliers	Categorical

9	Open-ended	Order Winner	Opportunities for hardwood suppliers to add value	Categorical
---	------------	--------------	---	-------------

(Bernard, 1995). An initial set of wood-based products manufacturers were selected among the exhibitors of the cited trade fairs. These companies were approached by the research team, and interviews were carried out with the representatives once it was determined that hardwood lumber was among their main raw materials. Altogether, the questionnaire was designed to explore the factors that may have an impact on the performance and competitiveness of their hardwood suppliers. The first six items of the questionnaire refer to the characteristics of the respondent's firm, its suppliers and the products imported from that later. In questions seven to nine, the respondents are asked to mention the minimum requirements expected from the hardwood suppliers. In other words, these factors, which were conceptualized as "order qualifiers" (Hofmann, Beck, Fuger, & SpringerLink, 2013), represent the characteristics of that a supplier must demonstrate in order for a customer to considering to establish a business relationship. The question eight refer to those order qualifiers in which respondents believe their expectations have not been fully met in the past. Finally, the question nine explore, the "order winners" –those characteristics of the product or service that motivates a customer to choose one supplier among its competitors (Hill, 2000). Table 1 provides a summary of the questionnaire design.

As Table 1 indicates, the variables measures through the questionnaire are categorical (Ott & Longnecker, 2010), which means, each variable has a measurement scale consisting of a set of categories. In this study, categorical data analyses (Agresti, 2002) were conducted to explore the behavior of each individual variable and the potential relationships among them; which included contingency tables, Chi-Squared tests for independence of one-way and two-way tables, and Fisher's Exact Test of independence of two-way tables.

Results and Discussion

A total of thirty-eight companies were included in the sample: fourteen from Interzum, ten from IFF, and fourteen from VIWIF. Respondents answered a set of nine questions distributed in two main areas firm's characteristics and hardwood product imports. Out of the 38 interviewed, 31 companies imported any form of hardwood products. The rest of the companies either acquired hardwood products from domestic suppliers or did not use hardwood species as part of their materials. See Table 2 for other demographic statistics on the sample.

Table 2. Distribution of Respondents by Trade Fair Location

Trade Fair Location	Frequency	Percent	Cumulative Frequency	Cumulative Percent
China	10	32.26	10	32.26
Germany	12	38.71	22	70.97
Vietnam	9	29.03	31	100.00

When asked about the location of their firm's main supplier, respondents indicate that in 48.39 percent of the cases, hardwood products are sourced from the United States (Figure 1). China accounts for 19.35 percent of responses, Thailand for 12.90 percent, Vietnam for 3.23 percent and the remaining 12.90 percent of cases correspond to other countries. The following item in the questionnaire asked for the three top species imported by interviewed firms. In 28.05 percent of the responses, a variety of Oak was accounted as the main hardwood species traded; followed by Ash and Walnut with 10.98 percent of responses each.

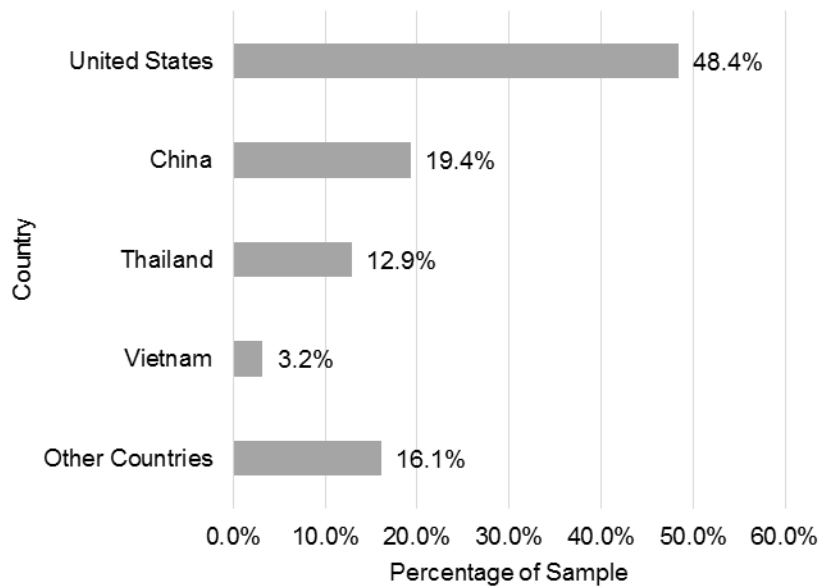


Figure 1. Distribution of Hardwood Suppliers by Country

In order to corroborate any potential relationship between the species traded and the geographic locations of either the interviewed firms or their suppliers, contingency tables and independence tests were performed for the analysis of categorical variables. Statistical independence was tested with Pearson Chi-Squared and Fisher's Exact Tests, the latter was necessary given the small size of certain combination of variables. First, the researchers were interested in studying the relation between the traded species and the location of respondents' firms. With a p-value of 0.1006, Fisher's Exact Test rejected the null hypothesis that species are independent of where respondents are located, with a significance level (alpha) of 0.05. In other words, it appears that each geographic region shows similar preferences for hardwood species. Next, independence of traded species was also tested against the geographic location of suppliers. As it was expected, a p-value of 0.0005 obtained also with Fisher's Exact Test, indicates that the varieties of hardwood commercially traded are dependent on the supplier's location, with a significance level of also 0.05.

Respondents were also inquired about aspects they value the most at the time of choosing trade partners (hardwood suppliers in particular), the obstacles and problems they have

faced in the past with their suppliers, and opportunities for the these to offer additional value. In question seven respondents were asked about the factors of concern to their firms in the selection of the main hardwood supplier, which, for the purpose of this study, will be named order qualifiers. Their answers to this open-end question were first coded into order qualifiers and then group in three main Order Qualifier Categories: product characteristics, service characteristics, firm (supplier) characteristics and others; according to the concepts of export performance studied in the literature review. A total of eighteen individual order qualifiers were coded by researchers, which are depicted in Figure 2. The category of product characteristics correspond to 65.08 percent of the responses obtained, whereas service characteristics, firm characteristics and others account for 28.57, 4.76 and 1.59 percent respectively. Price and quality stand out as the qualifiers with higher frequency counts -25.40 percent each, followed by color, customer service and species availability with 9.52, 7.94 and 6.35 percent respectively. The remaining 25.38 percent consists of six qualifiers, mostly within the service characteristics.

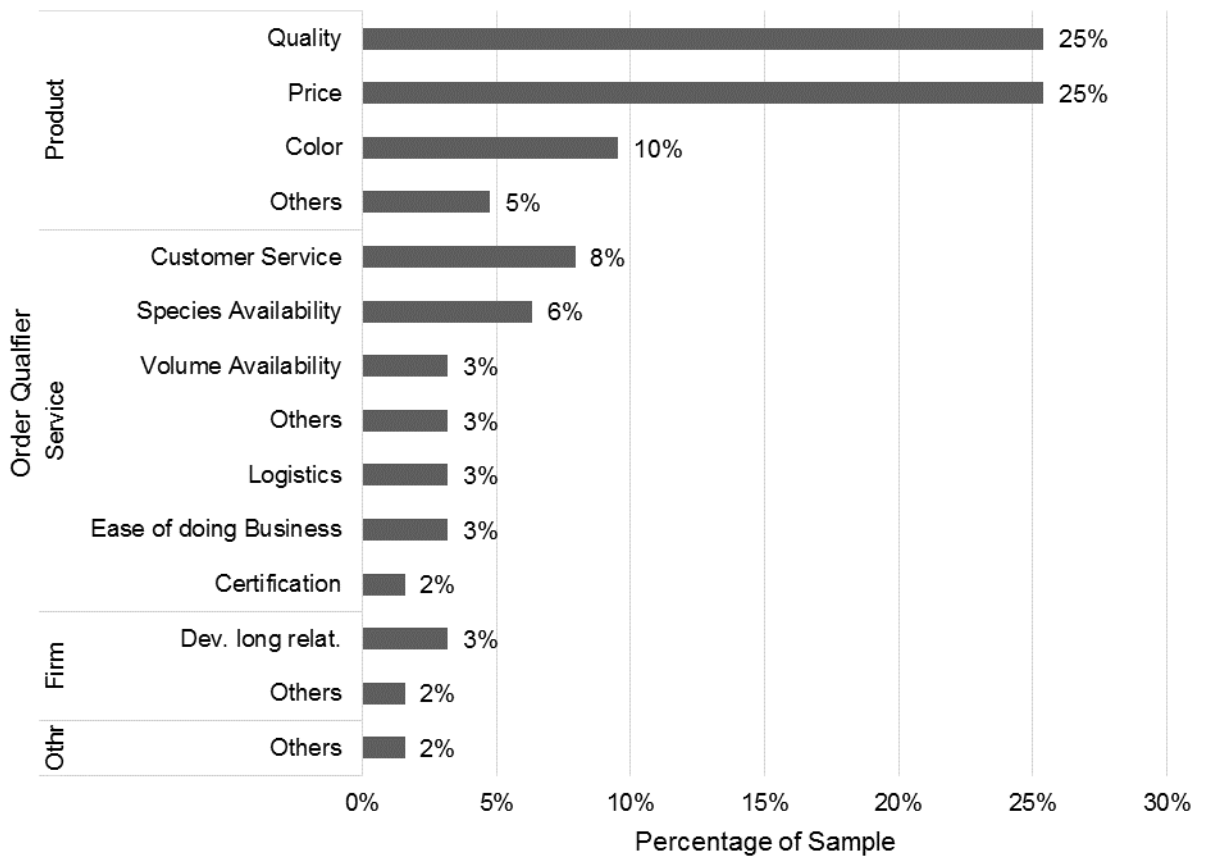


Figure 2. Most value aspects at the time of choosing trade partners

A Fisher's exact test was conducted to examine the relationship between the three order qualifier categories (product, service, firm and others) established in question seven, and the respondent's location. With a p-value of 0.3584, the researchers failed to reject the null hypothesis, which states that proportions of above factor categories remain the same for all geographic regions. This means that the distribution of factor categories depicted

in Figure 2 is independent from the regions considered in this study. Similarly, the Fisher's test conducted for order qualifiers as the response variable, and the supplier country as the explanatory variable, resulted in a p-value of 0.6874 with a significance level of 0.05. Therefore, there is not sufficient statistical evidence to reject the null hypothesis, which is that the distribution of order qualifier categories remains the same between suppliers (locations).

Respondents were asked to mention barriers or roadblocks (Figure 3) they have faced in their business relationships with suppliers of hardwood products. Just as in the previous question, the barriers and roadblocks proposed by respondents correspond to either features of the product supplied, the service, or the characteristics of the supplying firm. Given the similarities between the response items of this and the preceding question, the research team also coded the former as order qualifiers and order qualifier categories. With the distinction, however, that the latter correspond to aspects of the supplier, its products or services, where customer's expectations have not been fully met.

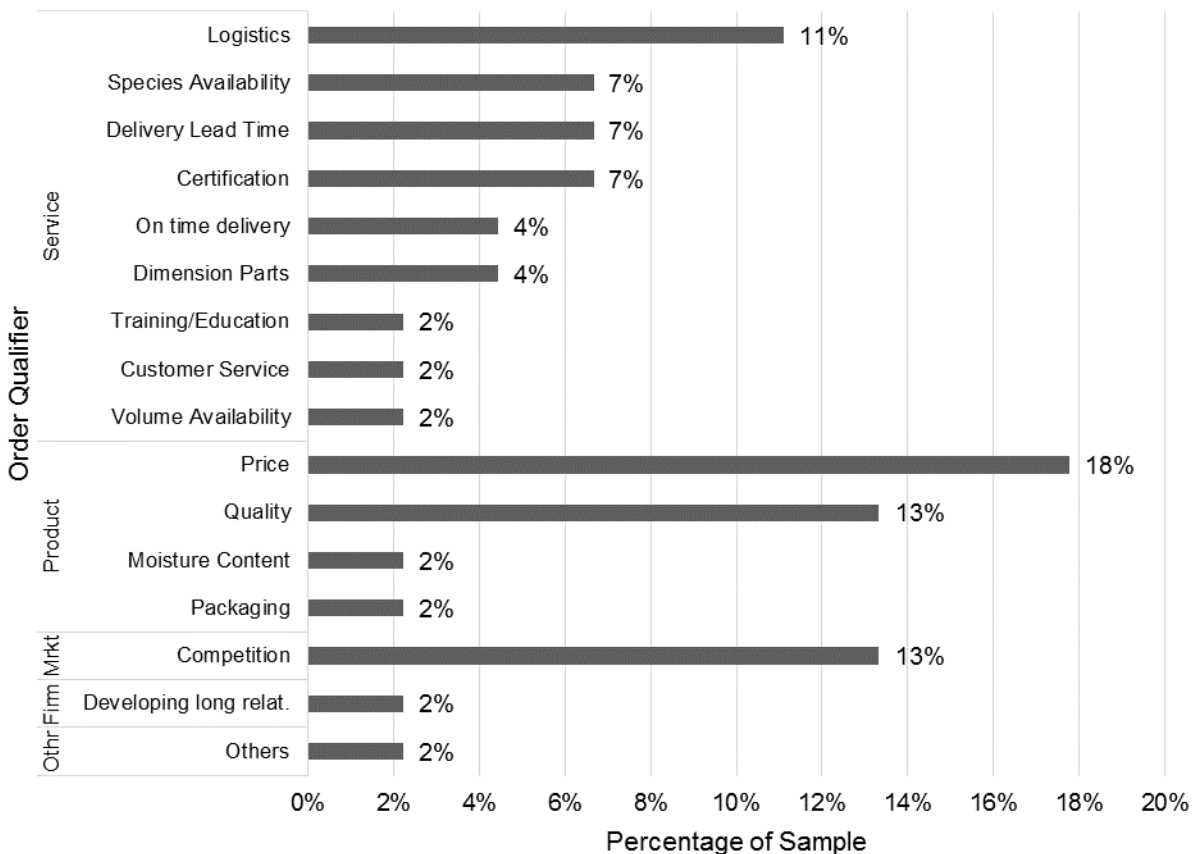


Figure 3. Barriers or roadblocks

Conclusions

Four main dimensions have been found to have a potential impact on export performance: characteristics of the Product, Service, Market and Firm (supplier). These categories together consist in a total of twenty-one factors, which have been divided into order

qualifiers and winners. The order qualifiers are the characteristics that customers perceive as necessary for a potential supplier to be considered for doing business. The order winners, account for those features that improve the supplier's position in the eye of customers, and therefore may lead to improving export performance. It has been found that product-related order winners (i.e. product characteristics) are the foundation for entering the export markets of hardwood products. Factors such as price, quality and color, are fundamental not only to join the competition, but to improve a hardwood firm's competitive advantage. However, any growth strategy should be accompanied by specific actions intended to improve multiple aspects of a firm's service, such as logistics, species & volume availability, delivery lead time, among others.

References

- Agresti, A. (2002). *Categorical Data Analysis*. New York: Wiley-Interscience.
- Bernard, H. R. (1995). *Research Methods in Anthropology: Qualitative and Quantitative Approaches*. Walnut Creek, CA: AltaMira Press.
- Bureau of Labor Statistics. (2014). Economic Releases, Series Report for Wood Products (CES3132100001). Retrieved March 26, 2014, from <http://data.bls.gov/cgi-bin/srgate>
- Goddard, L. (2014). Now boarding: Renewed construction demand will support industry growth *IBISWorld Industry Report 32111 Sawmills & Wood Production in the US* (pp. 1-41): IBISWorld.
- Hardwood Review. (2012). Turning Back The Clock: Why Annual Demand for U.S. Hardwoods Could Return to 14 BBF. *Hardwood Review Express*, 11(45), 2-4.
- Hill, T. (2000). *Manufacturing strategy: text and cases*. Boston, Mass: Irwin/McGraw-Hill.
- Hofmann, E., Beck, P., Füger, E., & SpringerLink. (2013). *The Supply Chain Differentiation Guide: A Roadmap to Operational Excellence*. Berlin, Heidelberg: Springer Berlin Heidelberg.
- Jan, D., & Tony, H. (2008). *Case Study Methodology in Business Research*. GB: Butterworth-Heinemann/Elsevier.
- Ott, L., & Longnecker, M. (2010). *An Introduction to Statistical Methods and Data Analysis*. United States: Brooks/Cole Cengage Learning.

Timber Passive House Technologies of Slovenian Contemporary Architecture

Manja KITEK KUZMAN

University of Ljubljana, Biotechnical Faculty
Department of Wood Science and Technology, Slovenia

Mirko KARIŽ

University of Ljubljana, Biotechnical Faculty
Department of Wood Science and Technology, Slovenia

Martina ZBAŠNIK-SENEGAČNIK

University of Ljubljana
Faculty of Architecture, Slovenia

Abstract

Energy efficiency is essential in the efforts to achieve a 20% reduction of primary power consumption by 2020. It is widely recognized that the potential of energy saving in buildings is large. Considering the tendencies of energy production and price, it is becoming urgent to reduce energy consumption in buildings. The choice of materials for a building with a high energy efficiency becomes much more important and strategies for reducing the use of primary energy for the production of materials and components becomes key. Renewable building materials should already be integrated into the early phases of building planning. The positive trend towards wooden construction is dictated by international guidelines, where a wooden building is an important starting point, not only for low-energy, but also low-emission building with exceptional health and safety aspects. In Europe, the most comprehensive and widely used is a concept of ultra-low energy house, more precisely, the passive house concept. Most Slovenian buildings combine contemporary styling with a degree of energy efficiency that comes close to passive house standards. It is widely recognised that the Slovenian construction industry is relatively advanced in the field of low energy buildings. In the light of the growing importance of energy-efficient building methods, it could be said that timber passive house would play an increasingly important role in the future.

Keywords: timber construction, energy efficiency, passive house, sustainable development, Slovenia.

1 Introduction

Timber as a material for load bearing construction represents a future challenge for residential and public buildings. Being a natural raw material, timber represents one of the best choices for energy efficient construction since it also functions as a material with good thermal properties if compared to other construction materials. In addition, it plays an important role in reduction of the CO₂ emissions (Natterer, 2009), has good mechanical properties and ensures a comfortable indoor living climate. Timber construction has better thermal properties than conventional brick or concrete construction methods, even with smaller wall thickness. Considering the growing importance of energy-efficient building methods, timber construction will play an increasingly important role in the future.

The dominating methods of timber construction in Slovenia include a timber-frame construction, balloon and massive construction (Figure 1).



Fig. 1 Panel construction, Wood frame construction, Solid wood construction

Currently, most Slovenian companies offer houses with timber-frame construction. Timber panel construction has had its own production in Slovenia for more than 35 years. Over the past thirty years, timber construction has undergone major changes. The most important (Žegarac Leskova and Premrov, 2013) are the following introduced changes: transition from on-site construction to prefabrication in a factory, transition from elementary measures to modular building and development from a single-panel to a macro-panel wall prefabricated panel system. All of these greatly improve the speed of building.

In timber-frame buildings the basic vertical load bearing elements are panel walls consisting of load bearing timber frames and sheathing boards. Dependant on the wall dimensions, one can distinguish between single-panel and macro-panel wall systems. The single-panel was based on the individual smaller elements in dimensions of 1.30 m (1.25 m) x 2.5 m to 2.65 m (Figure 2a). The height of the wall elements was meeting the height of the floor and the length of the ceiling elements the span of the bridged field. The macro-panel system was developed from the single-panel system in the last two decades and represents an important milestone in panel timber frame building. The aim of the system is that whole wall assemblies, including windows and doors, are totally constructed in a horizontal plane in a factory from where they are transported to the building-site. Prefabricated timber-frame walls as main vertical bearing capacity

elements, of usually typical dimensions with a width of 1.250 m and a height of 2.5–2,6 m, are composed of a timber frame and sheets of board-material fixed by mechanical fasteners, usually staples, to one or both sides of the timber frame (Figure 2c).

Between the timber studs and girders a thermal insulation material is inserted the thickness of which depends on the type of external wall. Composition of wall elements is in detail presented in Table 1(Premrov and Žegarac L., 2013) .

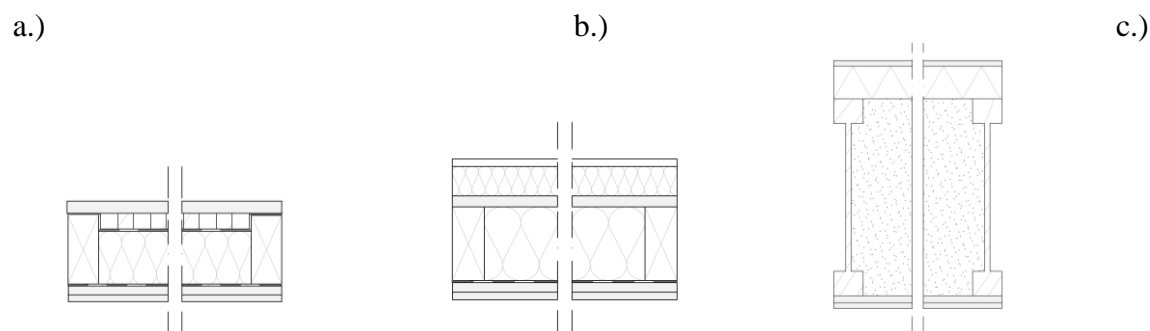


Fig. 2 a.) Single-panel system (TFCL2); b.) Renovated single-panel system (TFCL 3), c.) Timber-frame wall element with I-studs (TF 3).

Table 1 Composition of analysed macro-panel (TF 3) and single-panel (TFCL 2, 3) timber-frame wall elements.

TF		TFCL 2		TFCL 3 – renovation	
material	d/mm	material	d/mm	material	d/mm
rough coating	10	wooden planks	22	rough coating	10
wood fibreboard	60	/	/	mineral wool	40
/	/	TSS*** /open air	0.5	gypsum fibreboard	15
cellulose fibre /	360	TSS*** /open air	20	mineral wool / TF*	100
TF*		bitumen sheet	0.5		
		mineral wool / TF*	80		
OSB**	15	aluminium foil		aluminium foil	
gypsum	12.5	particleboard	13	particleboard	13
		gypsum plasterboard	10	gypsum	10
total thickness	457.5	total thickness [mm]	146	total thickness	188
U _{wall} -value	0.102	U _{wall} -value	0.48	U _{wall} -value	0.30
[W/(m ² K)]		[W/(m ² K)]		[W/(m ² K)]	

*timber frame, **oriented strand board, ***timber sub-structure.

The first single-panel systems in Slovenia were used by company Marles and company Jelovica. Those first pre-fabricated houses built in the early 70's had very good thermal properties of external envelope. Thermal transmittance of the best panel types was always much lower than it was defined by the regulations; for example thermal insulation was nearly three times better from 1963 to 1972, and after the year 1992 almost four times better than it was defined by the current national regulation (Figure 3).

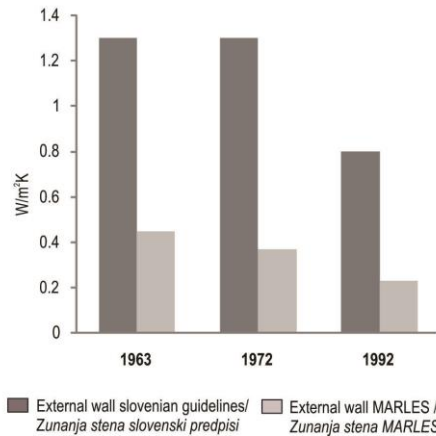


Fig. 3 Thermal transmittance of external wall elements - U-value comparison of the Marles' wall with the Slovene legislation in the period from 1963 to 1992.

Because of the reduction of energy losses in the newly built residential objects, the first measure introduced by the producers was gradual reduction of the thermal transmittance of the external wall elements, resulting in the increase of the timber-frame wall elements thickness, thus enabling thicker thermal insulation instalment. Detailed composition of the older single panel external wall elements construction, as well as newer macro-panel system, are explicitly presented in the Table 1, with additional graphic presentation in Figure 2.

Figure 3 shows data only till the year 1992, when external wall elements for the first time, even at any rate, met nowadays Slovene legislation regarding energy efficient construction, so that the thermal transmittance of external walls was for the first time lower than now prescribed limit value $U=0.28 \text{ W}/(\text{m}^2\text{K})$, i.e. it has nearly reached the value for light constructions, which is $U=0.20 \text{ W}/(\text{m}^2\text{K})$.

Therefore, all prefabricated timber framed objects set up before the year 1992 are considered as a fund needing energy efficient renovation till the year 2020. The latter refers to the wide-ranging package on climate change adopted by European Union, the overall 20-20-20 targets, which are binding for buildings as well. Therefore, energy performance of existing buildings has to be improved through a complex process of energy efficient renovation, likewise the sustainable new construction of energy-efficient buildings with the use of renewables has to be performed.

2 Energy-efficient buildings

Researching energy efficiency of buildings is not a matter of the last decade only, since the first intensive studies related to energy and buildings were already carried out in the seventies and eighties of the last century. Many studies focusing on the research of specific parameters influencing energy performance of buildings, such as Johnson et.al. (1984) and Steadman and Brown (1987) have been performed since then. From the existing research findings we summarize that the process of defining the optimal model of a building is very complex. The most important parameters influencing energy-

performance of buildings are listed below: location of the building and climate data for the specific location, orientation of the building, properties of installed materials, such as timber, glass, insulation, boards etc., building design (shape factor, length-to-width ratio, window-to-wall area ratio, building's envelope properties, windows properties), selection of active technical systems. According to the Slovene legislative framework, particularly to the Energy Act, the system of energy performance certification is defined in *Rules on the methodology of construction and issuance of building energy certificates (2009)*. On the basis of these rules, the classification of energy-efficient houses was carried, which is listed in Table 3.

Table 3 Classification of energy-efficient houses on the basis of “Rules on the methodology of construction and issuance of building energy certificates”.

Degree / Classification in accordance with the rules	Generally used classification in practice	Q_h* (kWh/m²a)	Variation of execution
Class C	minimal requirements for low-energy house	35 – 50 (60)	classical prefabricated construction, conventional heating system, contemporary windows (doors), no central ventilation system
Class B2	low-energy house	25 – 35	thermally improved building envelope conventional heating system, contemporary windows (doors).
Class B1	very low-energy house	15 – 25	thermally improved building envelope + HRV** + improved U-value of windows (doors)
Class A2	passive house	10 – 15	additionally thermally improved building envelope + HRV + improved U-value of windows (doors)
Class A1	passive house	≤ 10	additionally thermally improved building envelope + HRV + improved U-value of windows (doors)

* specific annual heating demand, **heat recovery ventilation

Table clearly shows that energy efficient objects can be constructed only by adequate combination of external envelope efficient insulation and high quality glazing installation. Respecting climate change conditions and the subsequent European directions related to energy performance of buildings, which are forcing the building industry into constructing a nearly zero energy house by 2020, searching for the optimal model of an energy-efficient house has therefore become of major importance.

2.1 Passive house

In Europe, the most comprehensive and widely used concept of ultra-low energy, more precisely, the passive house concept was developed by Dr. Wolfgang Feist of the Passive House Institute (Feist, 1998, Galvin and Sunikka-Blank, 2012). It sets forth the maximum

permissible energy consumption for the heating of the building and limits the total primary energy consumption. In its essence, it is an upgrade of the low-energy house standard. Passive houses are buildings that ensure a comfortable in-door climate during summer and winter without requiring a conventional heat distribution system (Feist, 1998). The passive house standard means that the space heating peak load should not exceed 10 W/m^2 living area in order to use supply air heating. The resulting space heating demand will approximately be 15 kWh/m^2 but will vary depending on climate (Feist, 2005).

The term ‘passive house’ refers to a construction standard that can be met through a variety of technologies, designs and materials such as solid (masonry, concrete, and aerated concrete) and wood structures. Different timber passive house technologies are presented in Figure 4.



Fig. 4 a) Panel construction (Jelovica houses), b) Timber-frame wall element with I-studs I-joists (Lumar), c) Solid wood construction (Riko houses).

The following considerations are particularly important when choosing the material and the construction type: the construction type should be standardized; the construction system should be based on natural and environmentally-friendly materials; the thermal envelope should meet the standards of a passive house; the construction should be wind-tight, airtight and diffusion open.

In order to design and implement a high-quality passive house project, attention should be paid to the materials used. The choice depends on personal preferences, in particular on the cost. There is a growing movement especially in Germany, Austria and Switzerland to build passive houses that are based on energy conservation measures and an efficient mechanical ventilation system with heat recovery. Over the past few years, the number of different types passive houses (Figure 5) has been seen a continuous increase in Europe as shown in Figure 6 (The International Passive House Association).



Fig. 5 Different types of passive houses: (a) Single family passive house, (b) Multy storey timber frame passive house, (c) Industrial building.

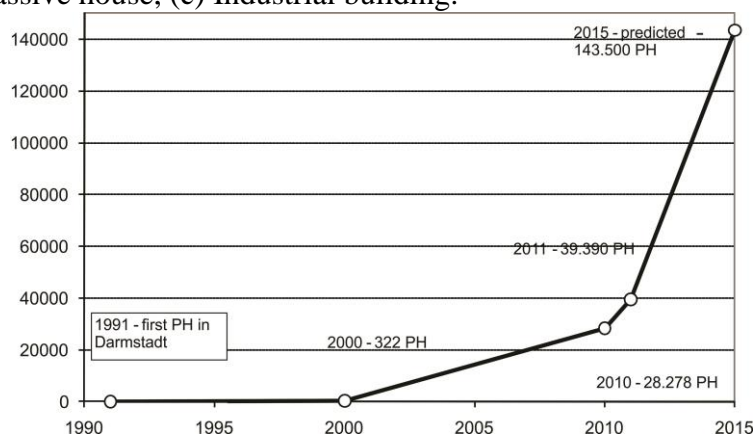


Fig. 6 The number of passive houses in 31 countries of Europe.

The greatest challenge facing civil engineers, wood science and technology engineers and architects today is how mitigate and adapt to climate change. They have recently focused their efforts on finding environmentally-friendly solutions and construction methods that bolster energy efficiency and thus reduce the environmental burden. The choice of a construction material is one of the most important decision with long-term consequences for the owner of the building (Johnson, 1990). The analysis by Kitek Kuzman et al. (2013) showed that wood as a renewable raw material is one of the best choices for energy-efficient construction. because it is also a good thermal insulator, has good mechanical properties, and ensures a comfortable indoor climate.

2.1.1. Certificates

In recent decades several methodologies have been developed to assess the quality of buildings: in the UK there is BREEAM (BRE Environmental Assessment Method) in France HQE (Haute Qualite Environnementale), the USA has LEED (Leadership in Energy and Environmental Design), Germany has DGNB (Deutsche Gessellschaft für Nachhaltiges Bauen) and so on. These certificates demonstrate the environmental and energy indicators of buildings, as well as the economic, socio-cultural and technical aspects of construction. For those buildings in the highest energy class, for instance passive houses, special systems of certification have been developed: in Switzerland the Minergie P and in Germany the Passive House Certificate. In some countries (Germany,

Austria and Switzerland), the two certificates are the basis for allocating subsidies for passive houses. Within the profession they are highly valued – as a good promotional tool representing a market advantage.

In the Slovenian market there are already a large number of components bearing the Passive House Certificate. Components with this certificate are most commonly manufactured by large foreign firms that have representatives in Slovenia, but also by a number of Slovenian firms that is growing each year. Currently there are few houses in Slovenia built with the Passive House Certificate and with the Minergie P certificate.

3 Case study: The Active House

Based on the active house concept, this highly energy-efficient structure makes best use of solar energy and offers utmost living comfort. The built-in smart home installations, the ceiling-mounted heating and cooling system, and the rooftop photovoltaic installations and solar collectors in combination with skylights are only one part of the concept. The idea of an environmentally friendly house is completed with an outside rainwater collector; collected water is used for flushing toilets, washing machines and the *automatic garden watering* system. The design follows the strict requirements set out by the municipal site plan for this area. The longer side of this two-story house with a symmetrical gable roof faces the southeast, ensuring a maximum gain from sun energy. All blinds, skylights, the watering system, and all mechanical and electrical installations are computer-controlled and automatic, allowing for maximized energy efficiency. Energy consumption can also be monitored online. (Figure 7 and Figure 8).

Location | Dragočajna, Year | 2013

Architect | Jernej Gartner, Brigita Babnik, Gregor Košorok, KOŠOROKGARTNER ARHITEKTI d.o.o.

Surface | 151 m²

Construction time | 1 year

Structural engineer | dr. Luka Pavlovčič, Lumar IG d.o.o.

Energy efficiency | plusenergy (PHPP 15 kWh/m²a)

U-value (W/(m²K)) | wall 0,1; roof 0,1; floor 0,12; window 0,87: glass 0,6; frame 0,86

Construction system | timber frame

Construction company | Lumar IG d.o.o.

Price | best practice Zeleni svinčnik 2013, ZAPS

House technique | air to water heat pump, floor heating, solar collector, photovoltaic power station, comfort ventilation with heat recovery, rain water collector

(a)

(b)



Fig. 7 (a) The house is built entirely of environmentally-friendly materials, which have the biggest impact on the environment in the stage of production. The house includes an photovoltaic power station, solar collectors for hot water, skylights, rainwater gathering for sanitary purposes and watering as well as smart installations, (b) The basic idea in the design was to produce a demonstration dwelling house used for the promotion and relevant explanation about 3 topics energy, indoor climate and environment. Active House is a network for knowledge sharing and demonstration of the feasibility of comfortable buildings in the future.

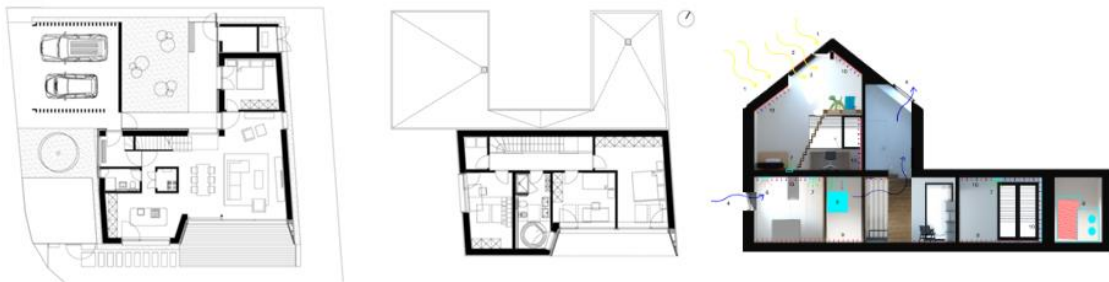


Fig. 8 Ground floor plane and first floor plane.

Conclusion

Most Slovenian buildings combine contemporary styling with a degree of energy efficiency that comes close to passive house standards. It is widely recognised that the Slovenian construction industry is advanced in the field of low energy buildings. In the light of the growing importance of energy-efficient building methods, it could be said that timber passive house would play an increasingly important role in the future.

References

- Feist, W. 1998. DAS PASSIVHAUS – BAUSTANDARD DER ZUKUNFT?. Protokollband Nr. 12, Passivhaus Institut, Darmstadt.
- Feist, W. 2005. QUALITÄTSSICHERUNG BEIM BAU VON PASSIVHÄUSERN. Protokollband Nr. 18, Passivhaus Institut, Darmstadt.
- Galvin, R., Sunikka-Blank, M. 2012. Including fuel price elasticity of demand in net present value and payback time calculations of thermal retrofits: Case study of German dwellings. *Energy and Buildings*. 50:219-228.
- Johnson, K. 1990. *Timber Bridge Design, Engineering and Construction Manual*. Wheeler Consolidated. St. Louse Park, MN.
- Johnson, R. et al. 1984. Glazing energy performance and design optimization with daylighting. *Energy and Buildings*. 6:305–317.
- Kitek Kuzman et al., 2013. Comparison of passive house construction types using analytichierarchy process. *Energy and Buildings*. 64:258–263.
- Natterer, J. 2009. Massivholz-konstruktionen: Herausforderung für eine nachhaltige Ökobilanz. In: Kitek Kuzman (Ed.): *Building with Timber, Challenge and Opportunity for Slovenia*. University of Ljubljana, Biotechnical Faculty, Ljubljana, pp. 18-21.
- Premrov, M., Žegarac L., V. 2013. *Energy-Efficient Timber-Glass Houses*. Springer, 178 p.
- Rules on the methodology of construction and issuance of building energy certificates, Official Gazette RS, 77/2009.
- Schnieders, J., Hermelink, A. 2006. CEPHEUS results: measurements and occupant's satisfaction provide evidence for Passive Houses being an option for sustainable building, *Energy Policy*, 34, pp. 151–171.

*Proceedings of the 57th International Convention of Society of Wood Science and Technology
June 23-27, 2014 - Zvolen, SLOVAKIA*

Steadman, P., Brown, F. 1987. Estimating the exposed surface area of the domestic stock. Energy and urban built form. Centre for Architectural and Urban Studies, University of Cambridge, pp. 113-131.

The International Passive House Association. Passive house. Darmstadt, Germany.
<http://www.passivehouse-international.org/>].

BREEAM, <http://www.breeam.org/> (Accessed December 2013)

HQE, http://www.interfaceflor.co.uk/web/sustainability/green_building/hqe (Accessed December 2013])

LEED, <http://www.usgbc.org/DisplayPage.aspx?CategoryID=19> (Accessed March 2014)

DGNB, <http://www.dgnb.de/> (Accessed March 2014)

Minergie P, <http://www.minergie.ch/> (Accessed March 2014)

Passivhaus Institut dr. Wolfgang Feist, www.passiv.de (Accessed March 2014)

Dynamics of Slovakian Timber Market in Retrospect

Yvonne Brodrechtova^{1} – Marek Trenčiansky² – Daniel Halaj³*

¹ Assistant Professor, Department of Economics and Management of Forestry, Faculty of Forestry, Technical University in Zvolen, Slovakia.

** Corresponding author*

brodrechtova@tuzvo.sk

² Assistant Professor, Department of Economics and Management of Forestry, Faculty of Forestry, Technical University in Zvolen, Slovakia.

trenciansky@tuzvo.sk

³ Assistant Professor, Department of Economics and Management of Forestry, Faculty of Forestry, Technical University in Zvolen, Slovakia.

halaj@tuzvo.sk

Abstract

Integration of round-wood markets, the introduction of renewable energy markets and sustainability issues, are among the many changes affecting the European forest products markets over the past two decades. With its simultaneously occurring institutional upheavals, Slovakia has been even more challenged by these changes. On the supply side, restitution has brought changes to forest ownership structures, while on the demand side, privatization introduced new forms of business. However, how and which changes have most influenced the timber market, particularly the demand and supply of wood assortments between 1990 and 2011 has not been clear. Therefore, the modelling of timber demand and supply and its influencing factors can provide a better understanding of the dynamics of timber markets. Although the application of time series econometrics in the forestry sector has in the recent years become less common in Europe, they still provide a quantifiable model that can be statistically verified. In the paper is described application of a linear econometric model for capturing the timber market in Slovakia and assessing key factors impacting it over the past two decades. Although modelling timber markets is a complex issue due imperfection of timber markets or problematic estimation of actual wood available to timber markets, the proposed simplified econometric model can still provide measurable information for more complex models that could be further used in policy analysis and forecasting the timber market or development of the forest sector.

Keywords: timber market, forest products trade, linear econometric model, Slovakia

Introduction

Forest sector modeling, particularly modeling of forest product markets has started in the 1950s. Various models such as econometrics, linear programming and system dynamics have been applied either alone or in combination, each showing unique strengths and weaknesses (Buongiorno 1996). An especially useful tool in presenting existing knowledge on how forest markets function and in providing forecasts and policy advice, is econometrics. The main advantage of econometric models lies in “the identification of causal connections between economic variables that makes them useful” (Hänninen 2004). Despite statistical problems in parameter estimation (e.g. quality and quantity of data) or structural equation problems (Buongiorno 1996, Hänninen 2004, Toppinen and Kuuluvainen 2010), econometrics provide a quantifiable model that can be statistically verified. Nevertheless, in the last decades the application of time series econometrics in forestry has declined (Toppinen and Kuuluvainen 2010) in Europe, with the notable exception of the Scandinavian countries. For instance, only a few studies with application of econometric analysis of forest products markets on Germany (e.g. Steinmeyer 1991, 1992), Austria (e.g. Schwarzbauer 1993, 2007) or Slovakia (e.g. Paluš 2002, Trenčiansky 2006) were identified, while in comparison their use in North America is much more popular.

As the last several decades the forest industries and their markets in Europe in general (Toppinen and Kuuluvainen 2010) and Slovakia in particular (Brodrechtova 2009) were challenged by internal and external structural changes, modelling the demand and supply of forest products might provide new information or missing scientific knowledge about forest products markets. Especially in Slovakia the last 20 years of institutional upheaval have shaped forest products demand and supply. On the demand side the privatization introduced new forms of business or the opening of new markets. On the supply side the restitution has brought changes to forest ownership structures or forest management practices. How and which changes have most influenced the timber market, particularly the demand and supply of wood assortments between 1990 and 2011 has not been clear. Therefore, the focus of the presented paper is to analyze the timber market, to identify and to quantify its main influencing factors. The result of the analysis is an econometric model of timber demand and supply.

Theoretical and Methodological Framework

Timber market model

Under assumption of perfect timber market, the proposed model consists of demand function Q_d , supply function Q_s and equilibrium condition: an intersection in which both curves result in an equilibrium price and an equilibrium volume. The demand function demonstrates the dependency between the timber volume, which are various subjects able and willing to buy and the timber price (Bergen 1996). In comparison to other goods that demand depends on available income of consumers, the timber demand could be replaced by production volume of processing companies and therefore is often termed as derived demand. In other words, timber demand derives from the production of semi-finished and

finished wood products, which demand in turn depends directly on consumers or on further processing (Schwarzbauer 2007, Trenčiansky 2006). Moreover, the prices of timber in the perfect market economy could be seen as one function of sawn timber prices (Mantel 1973, Schwarzbauer 2007). The higher the portion of timber costs on the whole timber processing and almost no possibilities for the substitute of timber resources, the higher correlation between these prices in the long-term. Accordingly, the first influencing factor of timber demand identified was the *price index of timber and paper-and pulp industry*. Furthermore, since building industry is considered as one of the largest timber consumers, the second factor identified and considered is the *production volume of construction industry*. Finally, timber demand could be also derived from macroeconomic indices such as Gross Domestic Product (GDP), interest rates, or export volume among others (Trenčiansky 2006). As these indices indicate demand in other sectors that might be potential consumers of semi-finished and finished wood products, *GDP in constant prices of 2005* was selected as a third influencing factor.

The supply function describes the dependency between the timber volume, which forest enterprises are able and willing to produce and sell, and timber price (Bergen 1996). Therefore, timber supply could be defined via *planned volume of yearly allowable cut* and was identified as a first factor influencing timber supply. As in the last decades the number and the intensity of calamities in Slovakia increased, and so did the volume of incidental felling. The *volume of incidental felling* was thus considered as a second influencing factor. Further, the timber price coupled with costs shape strategic behavior of forest enterprises (Trenčiansky 2006). Taking in consideration this experience and trying to eliminate the influence of inflation, as a third influencing factor of *averaged costs of timber felling-timber price ratio* was selected.

Methods

The goal of the paper is econometric analysis of timber market between 1990 and 2011 in order to design verifiable models of timber demand and supply with subsequent economic interpretations. An econometric model is a tool of econometrics, which uses sets of equations that explain the relationships and behavior of economic variables (Buongiorno 1996, Garaj and Šujan 1980). Put differently, the econometric model has to be not only statistically significant but also economically interpretable. For the purposes of this paper, linear regression equations and the estimation of its parameters by least squares was chosen (Garaj and Šujan 1980). Subsequently, for the econometric modelling of timber market theoretically justified influencing factors were considered (see *Timber market model*). Accordingly, the timber model depicting timber demand and supply in Slovakia was generally defined as (Garaj and Šujan 1980, Trenčiansky 2006):

$$Q_t = a + b_1 \cdot f_{1(t)} + b_2 \cdot f_{2(t)} + \dots + b_k \cdot f_{k(t)} + u_t \quad (1)$$

Specifically Q_t is timber demand, respectively timber supply in particular year (t ; $t = 1, 2, \dots, n$). a and b are estimated parameters of the model. What is more the linear dependency is summarized in random variable u_t . Variables $f_{1-k(t)}$ are price and non-price factors that influence timber demand, respectively supply and k defines the number of these factors.

Dynamics of the model are reached via inclusion of the time element. In other words, time delayed variables from previous year are used in the analysis of factors' influence:

$$Q_t = a + b_1 \cdot f_{1(t)} + b_2 \cdot f_{1(t-1)} + b_3 \cdot f_{2(t)} + b_4 \cdot f_{2(t-1)} + \dots + b_k \cdot f_{k(t)} + b_{k+1} \cdot f_{k(t-1)} + u_t \quad (2)$$

Data was sourced based on available statistics for 1990 – 2012 published in the form of Green reports between 1990 and 2013 by The Ministry of Agriculture and Rural Development of the Slovak Republic, and by available statistics for 1990 – 2012 published online by the FAOSTAT (2014).

Results

The results of the econometric analysis were an estimation of the equation for timber demand and supply in Slovakia.

$$Q_{dt} = -991,36 + 0,155GDP_t \quad (3)$$

$$Q_{st} = -4527,5 + 1,43E_t + 3171K_t \quad (4)$$

Where Q_{dt} and Q_{st} are the quantities of timber demanded and supplied in year t and m^3 , respectively GDP_t is the *gross domestic product* at constant prices of 2005 in €, E_t is the *planned volume of yearly allowable cut* in m^3 and K_t is the *proportional volume of incidental felling on the whole felling volume* in m^3 .

The simplified econometric models using time regression for the period 1990 – 2011 proved statistically significant with 5 % probability of error. Additionally, the multicollinearity and autocorrelation of residues was found to be statistically insignificant (Table 1). The result of the trimming process was the timber demand equation in which the *GDP* factor explained 93 % of variance of the probability distribution of demanded timber volume. In the timber supply equation the *planned volume of yearly allowable cut* (87 %) and the *proportional volume of incidental felling on the whole felling volume* (13 %) explained 95 % of variance of the probability distribution of supplied timber volume (Table 1).

Table 1: Statistical characteristics of the timber demand and supply equations

	Timber demand		Timber supply		
	a	b_1	a	b_1	b_2
T – test	2.32 (2.08)*	16.31 (2.08)*	6.49 (2.09)*	17.83 (2.09)*	2.73 (2.09)*
β		100 %		87 %	13 %
R^2	0.93		0.95		
R	0.96		0.98		

*critical values

F - test	266.13 (4.75)*	182.76 (3.98)*
von Neumann ratio	1.43 (1.27 – 3.04)*	1.83 (1.27 – 3.04)*
χ^2 - test		1.00 (6.63)*

The intensity of the factors' influence was

computed based on a 1 % relative change of the respective factor and on subsequent relative change in supplied volume, whereby for another factor average parameters from 1990 – 2011 were used. Estimated average elasticities of total demanded and supplied timber are presented in Table 2.

Table 2: Estimated relative elasticities of the timber demand and supply in Slovakia

Factors influencing timber demand	Relative change of demanded timber volume by 1 % increase of the factor in the year t (%)
<i>GDP</i>	+ 1.17
Factors influencing timber supply	Relative change in supplied timber volume by 1 % increase of the factor in the year t (%)
<i>Planned yearly allowable cut</i>	+ 1.43
<i>Proportion of incidental felling on the whole felling</i>	+ 0.79

The volume of demanded timber reacted to relative changes in *GDP* by elastic change in demand of + 1.17 %. The relationship between volume of supplied timber and relative change of allowable cut proved to be elastic, which indicated the significance of planned felling in forest management. In contrast, the change in the volume of incidental felling caused an un-elastic reaction of timber supply as a result of limited planned felling due to incidental felling. Thus, if planned allowable cut will increase by 1 %, then the volume of supplied timber will increase by 1.43 % at 0.79 % increase of incidental felling. Factual and estimated volume based on regression equation for demanded and supplied volume in Slovakia is captured in following figure 1 and 2.

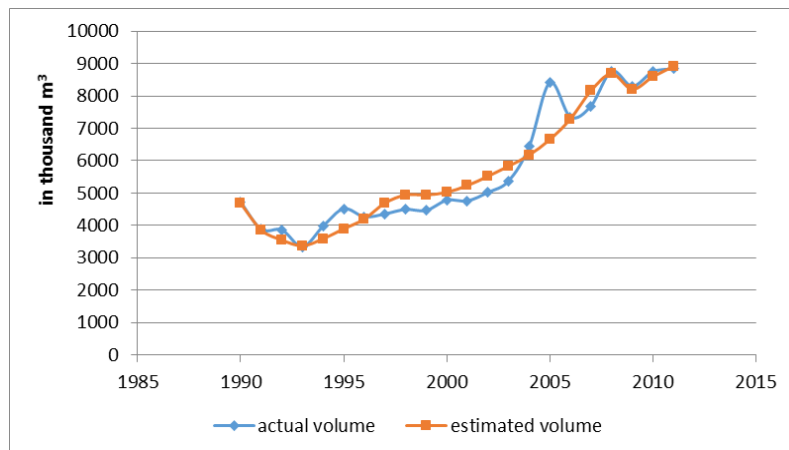


Figure 1: Time series of demanded timber volume

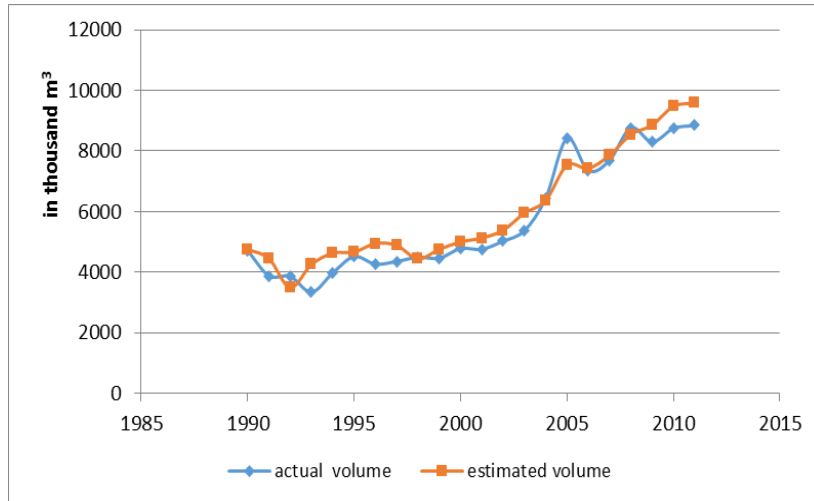


Figure 2: Time series of supplied timber volume

Conclusion

“Once tested, an econometric model can be used to forecast the variables determined within the model (endogenous), conditional on those determined outside the model (exogenous)” (Buongiorno 1996: 331). We assumed that GDP_t was the only exogenous variable, E_t and K_t being endogenous. Thus, in the case of the timber demand model, the regression equation could be defined based on GDP at constant prices. This factor affected timber demand in a positive direction as increasing GDP will increase timber demand. The last two decades of institutional upheavals such as the introduction of a market economy including the small size of Slovakia, the number of Slovakian residents and total economic power were mirrored in this parameter (The Ministry of Environment of Slovak Republic 2014). Perhaps for this reason, the identified *price index of timber and paper- and pulp industry* and the *production volume of construction industry* did not prove to be statistically relevant in the timber demand model. Put differently, under the assumption that the resulting model of the timber demand was driven by the factor GDP at constant prices, based only on its development it could be possible to produce timber market specific projections.

In the case of the timber supply model, the regression equation could be defined by the *volume of allowable cut* and by the *volume of incidental felling*. As both factors influenced supplied volume in the positive direction, then only their volume increase will lead to an increase in supplied timber volume. This explained why timber supplies aimed for the domestic market were not influenced by the economic factors such as *averaged costs of timber felling-timber price ratio*, but were rather conditioned and limited by the production possibilities of forest stands defined by their allowable cut and existence of unforeseen circumstances such as incidental felling. In other words, based on forest management plans upon consideration of increasing trends of incidental felling, it would be possible to design timber market trends.

Taken together, the simplified econometric model provided measurable information for more complex models that could be further used in policy analysis and forecasting the timber market or development of the forest sector (Toppinen and Kuuluvainen 2010, Trenčiansky 2006). However, this straightforward econometric approach in practical use showed two weaknesses. First, an estimation of the parameters was significant statistical problem as there were not suitable data for all the desired factors. Second, due to imperfection of economic theory the factual structural equations are never known (Buongiorno 1996). To overcome these shortcomings, search for more factors and testing of their parameters would be helpful. Moreover, due to volume and specifics of timber species and timber processing, the models of broadleaved and coniferous round wood, pulp wood or biomass would provide more details on how and which changes have most influenced the timber market in the last two decades in Slovakia. Nevertheless, “regardless of methodological shortcomings and data quality, a formal model that lays out all assumptions unambiguously, is a better way to study the forest sector than no model at all” Buongiorno 1996: 342).

References

Brodrechtova, Y. 2009. Export marketing strategy and its shaping factors in the context of transition - Theoretical perspectives and empirical testing in the forest products industries of Slovakia. In: Freiburger Schriften zur Forst- und Umweltpolitik, Band 21, Verlag Dr. Kessel.

Bergen, V. 1996. Holzmarktlehre. Institut für Forstökonomie G. A. Universität Göttingen, Göttingen [*not published*]

Buongiorno, J. 1996. Forest sector modeling: a synthesis of econometrics, mathematical programming, and system dynamics methods. *International Journal of Forecasting*. 12: 329-343.

FAOSTAT, 2014. Forestry data: roundwood, sawnwood, wood-based panels, paper and paperboards. <http://faostat.fao.org/> [*accessed 20.01.2014*]

Garaj, V., Šujan, I. 1980. *Ekonometria* [Econometrics]. Bratislava: Alfa.

Hänninen, R., 2004: Econometric models in forest sector forecasting. *Journal of Forest Economics*. 10: 57-59.

Mantel, K. 1973. *Holzmarktlehre. Ein Lehr- und Handbuch der Holzmarktökonomie und Holzwirtschaftspolitik*. Verlag J. Neumann – Neudamm, Melsungen.

Paluš, H. 2002. *Modelovanie dopytu po výrobkoch z dreva v SR* [Modelling of supply market with wood products in Slovakia]. Monograph 3/2002/A. Technical University in Zvolen.

Schwarzbauer, P. 1993. *Der Österreichische Holzmarkt im Modell*. Schriftreihe des Instituts für forstliche Betriebswirtschaft und Forstwirtschaftspolitik, Band 17, Eigenverlag des Instituts für forstliche Betriebswirtschaft und Forstwirtschaftspolitik, Wien.

Schwarzbauer, P. 2007. Einflüsse von Schaholz mengen auf Rohholzpreise. Eine quantitativ-statistische Analyse am Beispiel Österreichs. *Allgemeine Forst- und Jagdzeitung*. 178 (1): 1-8.

Steinmeyer, U. 1991. Das Laubstammholz – Angebot in der Bundesrepublik Deutschland von 1968 bis 1988 – eine ökonomische Analyse. Forst- und Jagdzeitung. 46 (17): 476-480.

Steinmeyer, U. 1992. Der deutsche Nadelstammholzmarkt. Eine aktualisierte Modellschätzung und Untersuchungen zu einem besitzarten spezifischen Angebotsverhalten von Forstbetrieben. Forstarchiv. 63: 106-111.

The Ministry of Environment of Slovak Republic 2014. Národná stratégia trvalo-udržateľného rozvoja Slovenskej Republiky [National Strategy of Sustainable Development of Slovak Republic] <http://www.minzp.sk/dokumenty/strategie-dokumenty/#obsah> [accessed 30.04.2014]

Toppinen, A., Kuuluvainen, J. 2010. Forest sector modelling in Europe – the state of the art and future research directions. Forest Policy and Economics. 12: 2-8.

Trenčiansky, M. 2006. Dynamika trhu so sortimentmi v SR. Monograph 4/2005/A. Technical University in Zvolen.

This research paper has been part of publications under the project VEGA no. 1/1099/12
“Economic efficiency of timber trade from the transaction costs perspective”

Restorative Environmental Design: Wood as a Material for Sustainable, Healthy Environments

Michael Burnard^{1*} – *Andreja Kutnar*²

¹ Andrej Marušič Institute - University of Primorska 6000-Koper, Abelium
d.o.o. 1000-Ljubljana, Slovenia.

** Corresponding author*

michael.burnard@iam.upr.si

² Assistant Professor, Andrej Marušič Institute and Faculty of Mathematics,
Natural Sciences and Information - University of Primorska 6000-Koper,
Slovenia.

andreja.kutnar@upr.si

Abstract

With swelling global populations the demand for buildings, and the construction materials they require, is placing significant pressure on natural resources. The buildings we construct are important both to the environment they are a part of, and to the occupants who use them. The USGBC estimates people spend an average of 80-85% of their time indoors, and ones environment is thought to have a significant effect on ones well-being. Restorative environmental design is a design paradigm addressing both sustainability and human well-being in buildings. Wood use as an exposed structural and decorative material can address both aspects of restorative environmental design. Wood is a valuable and widely used building material, derived from a renewable resource, whose value extends beyond its strength and mechanical values. Early research examining the health effects of wood in the built environment has provided suggestive evidence of reduced stress, and improved stress recovery in the presence of wooden products. This effect could provide significant benefit to workers, students and others who spend so much time indoors. Further research into the health impacts of wood in the built environment is required to inform building, interior, and product designers about wood use that is both sustainable and provides healthful benefits for the occupants/users. This presentation briefly introduces the elements of restorative environmental design and will cover the current state of research into wood and health in the built environment, and provide updates on ongoing research being conducted in Europe.

Keywords: design, health, indoor environment, stress, sustainability

Introduction

The goals of Restorative Environmental Design (RED) are to reduce environmental impacts of new buildings, and to ensure buildings provide healthful benefits to the occupants. Derr and Kellert (2012) believe RED is the next evolution of “green” design as combines the goals of environmental sustainability with providing healthful benefits to occupants and reinforcing the human-nature connection (Derr and Kellert, 2012). To achieve sustainability, society has to strive towards minimising consumption of matter and energy, reusability and recyclability of the material, human satisfaction, and minimising environmental impacts and embodied energy (Sinha et al., 2013). Healthful benefits for occupants and the promotion of the the human-nature connection can be achieved by implementing biophilic design, which is the inclusion of life and life-like processes into the building process (Kellert, 2005; Kellert, 2008).

Sustainable Design. Sustainable design principles emphasize reducing the impact of building construction, location and utilization on the environment by minimising the impacts of material choice, site choice, and energy use across all phases of the buildings lifetime (e.g., construction, occupancy) (Sinha et al., 2013). The methods or achieving these goals continue to evolve, as do the building certification schemes recognizing them. However, in Europe, some level of international standardization is being achieved through the implementation of Environmental Product Declarations (EPDs) under the Construction Products Regulation (305/2011). EPDs are statements of a product’s environmental impact and are comparable to similar products because they are produced according to Product Category Rules, which state how life cycle analysis should be used to for products of a certain category according to ISO 14025 (ISO, 2009).

Biophilic Design. Biophilic design is the incorporation of the principles of biophilia into building design (Kellert, 2005; Kellert, 2008). These principles are built around the concept of an innate human attraction to life, and life-like processes (Kellert, 2008).

There are six guiding principles of biophilic design. Briefly, they are (Kellert, 2008):

1. Environmental features – making design choices, which are readily recognizable as aspects of nature. These features may range from views of nature, to water features within the building, to including a wide variety of indoor plants.
2. Natural shapes and forms – using elements of the built environment to replicate naturally occurring elements (such as trees).
3. Natural patterns and processes – using elements of design (such as materials, spaces, lighting, etc.), which through visual recognition, touch, scent or sound remind occupants of growth, life, natural motion, and other elements of nature.
4. Light and space – diversity of color, natural light, and variability in lighting levels are reminiscent of nature. Further, difference in size, and shape of spaces in the built environment also remind us of nature.
5. Place-based relationships – connections to cultural and ecological elements linking geographically distinct locations with the built environment.

6. Evolved human relationships with nature – refers to connections humans have developed throughout our evolutionary history. For example, natural settings, such as forests, have provided shelter and safety, food and materials for survival.

Restoration and Restorative Environments

Though some design mechanisms are in place to bring nature into the built environment (Kellert, 2005; Kellert, 2008; Wilson, 2008) people often remain segregated from nature and its restorative effects while indoors. Therefore, the impetus to bring nature indoors is to bring the restorative qualities of natural outdoor environments to people where they spend most of their time. One readily available means to address the issue is to use wood as functional or decorative indoor material. Using wood for interior treatments in indoor environments has been shown to have positive impacts on occupants (Fell, 2010; Nyrud & Bringlimark, 2010; Rice et al., 2006; Sakuragawa et al., 2005; Tsunetsugu et al., 2007; Tsunetsugu et al., 2002).

Hartig (2004) defines restoration as a process of renewal that replenishes a depleted social, psychological or physical resource. These resources have most often been depleted by an individual's effort to adapt to their environment (Hartig, 2004). Early restoration theories focused on recovery from psychophysiological stress (Ulrich et al., 1991), and attention restoration (Kaplan & Kaplan, 1989). Psychophysiological stress recovery theory posits that natural environments, and even views of these environments, will aid recovery from stressful events, including psychological stress and physical stress (e.g., recovery from a surgery) (Ulrich, 1984; Ulrich et al., 1991; Ulrich, 1991). Attention Restoration Theory (ART) focuses on understanding how individuals replenish their ability to exert attention on common tasks, such as those at the workplace, that require directed attention (Hartig, 2004; Hartig et al., 1997; Herzog et al., 1997; Kaplan & Kaplan, 1989; Kaplan, 1995).

Though many studies have found empirical evidence to support these theories they remain open to elaboration as more evidence is collected regarding the restorative effects of nature (Hartig, 2004).

In the case of both ART and psychophysiological stress recovery theory, the natural environment provides the individual with a means to restore themselves to a more complete state. These restorative environments exist in nature and provide a model for bringing the desired effects indoors. According to Kaplan (1995), the components of a restorative environment are:

1. Being away – the sense of being in a different environment (distance is not a necessary component of being away.)
2. Fascination – when ones attention is focused on something. Attention of this sort is effortless.
3. Extent – feeling an area to be large. Well-designed paths can be used to make a small area seem larger.

4. Compatibility – the natural affinity humans seem to have for nature makes it a compatible environment.

Extent and being away seem contrary to the notion of restorative effects of nature occurring indoors. However, there are design practices, which can address these issues in buildings (Wilson, 2008). For example, Wilson (2008) suggests being away can be addressed with indoor gardens, views of nature, and other features occupants can view or visit, which differ from a typical workstation. Similarly, design features may provide extent by varying ceiling height, including natural lighting, and other mechanisms (Wilson, 2008). The concepts of fascination and compatibility fit more easily within the biophilic paradigm. Natural patterns, shapes and forms all provide targets of fascination, while compatibility is derived from evolved human relationships with nature (Kellert, 2008; Wilson, 2008).

Wood as an Element of Restorative Environmental Design. Wood is an ideal material for RED because it satisfies both general tenets of the design paradigm: sustainability and a connection to nature. Wood from healthy, well-managed forests is a renewable material, and provides carbon storage (Hashimoto et al., 2002). It is unsurprising such a product, when used in appearance applications, also provides a connection to nature (Masuda, 2004; Nyrud & Bringlimark, 2010; Nyrud et al., 2010; Rice et al., 2006).

Wood is an excellent building material because of its excellent strength to weight ratio and the variety of forms in which it can be used (e.g., in log form, lumber form, in fiber form, and in combination with other materials) (Kretschmann, 2010; Stark et al., 2010). In the United States, more than 90% of residential buildings are wood-framed and Japan is not far behind (Sinha et al., 2013). However, in the United States and Japan wood is predominately used in housing as a concealed structural component thereby limiting occupant interaction with it. Furthermore, wood use in non-residential construction is considerably less common than in residential construction (O'Connor et al., 2004). Beyond structural uses, wood is also an excellent architectural material for furniture and in decorative applications (Architectural Woodwork Institute, 1994). Though exposed wood is present in to some degree in many indoor environments, there are opportunities for greater utilization, which may contribute positively to occupant health (Fell, 2010; Nyrud & Bringlimark, 2010; Rice et al., 2006).

Current Research Into Using Wood in Restorative Environments

Though previous research has provided some evidence of the healthful benefit of using wood indoors, more research is required to better understand the phenomenon and translate research findings into evidence based building design practices. Studying the effects of wood on attention and physiological restoration in the built environment may produce helpful and enlightening results. These studies, which incorporate the healthful benefits of materials and design in buildings, are increasingly generating global interest. Currently, there are several projects in Europe approaching this subject in different ways. Generally, each seeks to identify key aspects of wood that contribute to the positive health impacts of using wood indoors, so that designers may implement the findings to improve

health in workplaces, schools, and homes where productivity, learning and general well-being.

The following European projects dealing with the health impacts and perceptions of wood in the built environment, in our opinion, will significantly contribute to knowledge in this developing field of research.

The Wood Life project (Aalto University, 2014) at Aalto University utilizes test houses to examine the energy saving potential of using fibre-based products and spatial design, wood modification and natural organic fibre surfaces, the thermodynamic interaction between wood and living spaces, and user experiences with related to these environments. The project expects to provide design guidance for energy efficient interiors that also promote human well-being.

An ongoing study related to user perceptions of building product naturalness expands a previous study by Nyrud et al. (2010). This study is a cooperate effort by the University of Primorska Andrej Marušič Institute (UP IAM), Aalto University School of Chemical Technology, Department of Forest Products Technology and the Norwegian Institute of Wood Technology. It examines how views of product naturalness, an integral part of material utilization in RED, vary between regions (e.g., Finland, Norway and Slovenia).

Researchers at UP IAM are conducting an investigation of human stress responses and stress recovery in rooms treated with different aspects of wood, including grain pattern, color and quantity of visible wood. The goal of this study is to identify which aspects of wood may impact how humans respond to stress in office-like environments, and also how recovery from stress is affected by the presence of wood in these environments.

Another promising project is Wood2New (WoodWisdom-Net, 2014) led by Aalto University. This project seeks to discover opportunities and limitations to wood use in indoor environments, assess the beneficial effects of indoor wood use on human well-being and develop sustainable, value added materials based on these findings that meet the needs of the marketplace.

Summary and Conclusions

Restorative environmental design expands the prevalent building design paradigm that focuses intently on minimizing the environmental harm of a buildings life. While the RED paradigm certainly calls for minimized environmental harm, it also calls for beneficial impacts of buildings for the environment and for occupants. The benefits include healthful indoor environments, which strengthen the occupants' connection to nature. In order for designers to effectively utilizing this design paradigm, though, evidence needs to be provided on how to achieve the healthful benefits. To this end, research must be conducted which examines how occupant health is affected by building design decisions. Current investigations into material choices will strengthen the understanding how design decisions may directly affect occupant health.

Future work in this field should include investigations in to other aspects of wood, investigations in different regions, the inclusion of other materials considered to be natural, and demonstration projects which implement the design suggestions and monitor occupant health. Furthermore, the results of these projects should be incorporated in to sustainable building rating systems to ensure buildings provide healthy living environments that play an important role in the lifestyle and health of the occupant. All parameters needed for occupant health should be taken into account when designing buildings. Human relationships with nature that may contribute to occupant well-being are a key parameter to consider. Material selection, especially, is an important component of designing healthy buildings for occupants.

As the number of projects in this field increases, and awareness of the RED paradigm grows in the construction sector, benefits to occupant health will surely become a tenet building rating systems. Currently, there are discussions regarding sustainability of the built environment, concerned that environmental performance alone does not address the full scope of sustainable design and construction practices. In order to address the full scope of sustainable design and construction practices, an expansion of the analysis framework to include social and economic indicators is necessary (Robertson et al., 2012). Therefore, research examining wood use in RED can deliver important knowledge to be used in contemporary timber architecture.

Acknowledgment

The authors would like to acknowledge the Slovenian Research Agency for financial support within the frame of the project Z4-5520 and the Italy-Slovenia Cross-border Cooperation Programme 2007-2013 for financial support within the project EnergyViLLab.

References

- Aalto University, 2014. *Wood Life Energy-efficient living spaces through the use of wooden interior elements - Aalto Energy Efficiency Research Programme - Aalto University*. [Online] Available at: <http://energyefficiency.aalto.fi/en/research/woodlife> [Accessed 28 April 2014].
- Architectural Woodwork Institute, 1994. *Architectural Woodwork Quality Standards*. 6th ed. Centerville, Virginia, USA: Architectural Woodwork Institute.
- Derr, V. & Kellert, S.R., 2012. Making Children's Environments "R.E.D": Restorative Environmental Design and Its Relationship to Sustainable Design. *Journal of Children, Youth and Environments*.
- Fell, D., 2010. *Wood in the human environment: restorative properties of wood in the built indoor environment*. Vancouver, B.C., Canada: University of British Columbia. Doctoral thesis.
- Hartig, T., 2004. Toward Understanding the Restorative Environment as a Health Resource. In *Open Space: People Space. Engaging with the Environment*. Edinburgh,

2004. OPENspace REsearch Centre.
<http://www.openspace.eca.ac.uk/conference/proceedings/PDF/Hartig.pdf> (accessed 24 Nov. 2013).
- Hartig, T., Korpela, K., G.W., E. & Gärling, T., 1997. A measure of Restorative Quality in Environments. *Scandinavian Housing and Planning Research*, 14, pp.175-94.
<http://dx.doi.org/10.1080/02815739708730435>.
- Hashimoto, S., Nose, M., Obara, T. & Moriguchi, Y., 2002. Wood products: potential carbon sequestration impact on net carbon emissions in industrialized countries. *Environmental Science & Policy*, 5(2), pp.183-93. [http://dx.doi.org/10.1016/S1462-9011\(01\)00045-4](http://dx.doi.org/10.1016/S1462-9011(01)00045-4).
- Herzog, T.R., Black, A.M., Fountaine, K.A. & Knotts, J.D., 1997. Reflection and attentional recovery as distinctive benefits of restorative environments. *Journal of Environmental Psychology*, 17, pp.165-70. <http://dx.doi.org/10.1006/jevp.1997.0051>.
- Kaplan, S., 1995. The restorative benefits of nature: toward an integrative framework. *Journal of Environmental Psychology*, 15(3), pp.169-82.
[http://dx.doi.org/10.1016/0272-4944\(95\)90001-2](http://dx.doi.org/10.1016/0272-4944(95)90001-2).
- Kaplan, R. & Kaplan, S., 1989. *The experience of nature: A psychological perspective*. Cambridge: Cambridge University Press.
- Kellert, S.R., 2005. *Building for Life: Designing and Understanding the Human-nature connection*. 1st ed. Washington, DC, USA: Island Press.
- Kellert, S.R., 2008. Dimensions, Elements and Attributes of Biophilic Design. In R.S. Kellert, J.H. Heerwagen & M.L. Mador, eds. *Biophilic Design: the theory, science and practice of bringing buildings to life*. First Edition ed. Hoboken, NJ: John Wiley & Sons, Inc. pp.3-19.
- Kretschmann, D.E., 2010. *Commercial Lumber, Round Timbers, and Ties*. General Report. Madison: United States Forest Service United States Forest Service.
- Masuda, M., 2004. Why wood is excellent for interior design? From vision physical point of view. In EWPA, ed. *Proceedings 8th world conference on timber engineering*. Lahti, Finland, June 2004. Engineered Wood Products Association. Paper 186.
- Nyrud, A. & Bringlimark, T., 2010. Is interior wood use psychologically beneficial? A review of psychological responses toward wood. *Wood and Fiber Science*, 42(2), pp.202-18.
- Nyrud, A., Bysheim, K. & Bringslimark, T., 2010. Health benefits from wood interior in a hospital room. In SWST, ed. *Proceedings of the international convention of Society of Wood Science and Technology and United Nations Economic Commission for Europe -- Timber committee*. Geneva, Switzerland, 11-14 October 2010. Society of wood science and technology and United Nations Economic Commission for Europe. Paper WS-56.
- O'Connor, J., Kozak, R., Gaston, C. & Fell, D., 2004. Wood in nonresidential buildings: opportunities and barriers. *Forest Products Journal*, 54(3), pp.19-28.
- Rice, J., Kozak, R.A., Meitner, M.J. & Cohen, D.H., 2006. Appearance Wood Products and Psychological Well-Being. *Wood and Fiber Science*, 38(4), pp.644-59.
- Robertson, G. P., S. L. Collins, D. R. Foster, N. Brokaw, H. W. Ducklow, T. L. Gragson, C. Gries, S. K. Hamilton, A. D. McGuire, J. C. Moore, E. H. Stanley, R. B. Waide, and M. W. Williams. 2012. Long-term ecological research in a human-dominated world. *BioScience* 62:342-353. <http://dx.doi.org/10.1525/bio.2012.62.4.6>

- Sakuragawa, S., Miyazaki, Y., Kaneko, T. & Makita, T., 2005. Influence of wood wall panels on physiological and psychological responses. *Journal of Wood Science*, 51(2), pp.136-40. doi: 10.1007/s10086-004-0643-1.
- Sinha, A., Gupta, R.K. & Kutnar, A., 2013. Sustainable development and green buildings = Održivi razvoj i zelena gradnja. *Drvena Industrija*, 64(1), pp.45-53. doi:10.5552/drind.2013.1205.
- Stark, N.M., Cai, Z. & Carll, C., 2010. *Wood-Based Composite Materials: Panel Products, Glued-Laminated Timbers, Structural Composite Lumber, and Wood-Nonwood Composite Materials*. General Report. Madison: United States Forest Service United States Forest Service.
- Tsunetsugu, Y., Miyazaki, Y. & Sato, H., 2002. The visual effects of wooden interiors in actual-size living rooms on the autonomic nervous activities. *Journal of Physiological Anthropology*, 21(6), pp.297-300. <http://dx.doi.org/10.2114/jpa.21.297>.
- Tsunetsugu, Y., Miyazaki, Y. & Sato, H., 2007. Physiological effects in humans induced by the visual stimulation of room interiors with different wood quantities. *Journal of Wood Science*, 53, pp.11-16. doi: 10.1007/s10086-006-0812-5.
- Ulrich, R., 1984. View through a Window May Influence Recovery from Surgery. *Science*, 224(4647), pp.420-21. DOI: 10.1126/science.6143402.
- Ulrich, R., 1991. Effects of interior design on wellness: theory and recent scientific research. *Journal of Health Care Interior Design*, 3(1), p.1991.
- Ulrich, R. et al., 1991. Stress recovery during exposure to natural and urban environments. *Journal of Environmental Psychology*, 11, pp.201-30. [http://dx.doi.org/10.1016/S0272-4944\(05\)80184-7](http://dx.doi.org/10.1016/S0272-4944(05)80184-7).
- Wilson, A., 2008. Biophilia in Practice: Buildings that connect people with nature. In S.R. Kellert, J.H. Heerwagen & M.L. Mador, eds. *Biophilic design: the theory, science and practice of bringing buildings to life*. First Edition ed. Hoboken, NJ, USA: John Wiley & Sons, Inc. pp.325-33.
- WoodWisdom-Net, 2014. *March 2014 Newsletter*. Newsletter. Helsinki: WoodWisdom-Net.

European Union Timber Regulation Impact on International Timber Markets

Alexandru Giurca^{1} - Ragnar Jonsson² - Marko Lovrić³ - Ed Pepke⁴*

¹Trainee, North European Regional Office (EFINORD) European Forest
Institute

Umeå, Sweden, SE-901 83

Tel. +46708196160

axgi0001@stud.slu.se

** Corresponding author*

²Senior Researcher, Forest Resources and Climate Unit, European
Commission Joint Research Centre

Ispra (VA), Italy, I-21027

Tel. +390332786592

Ragnar.Jonsson@jrc.ec.europa.eu

³Researcher, European Forest Institute, Yliopistokatu 6 80100 Joensuu
Finland

Tel. +358 01 773 43 61

Marko.Lovric@efi.int

⁴Senior Timber Trade and Policy Analyst, EU FLEGT Facility, European
Forest Institute, Sant Pau Art Nouveau Site, Sant Leopold Pavilion, St.

Antoni M. Claret, 167, ES-08025 Barcelona, Spain

Tel. +336 03 911 433

Ed.Pepke@efi.int

Abstract

The trade of illegal timber, often from illegal logging, has severe environmental, social and economic consequences. The EU's response to this problem came with the Forest Law Enforcement, Governance and Trade (FLEGT) Action Plan, with its specific goal to end illegal logging, thereby improving sustainability of forest resources. In March 2013, an additional step was taken by implementing the EU Timber Regulation (EUTR). The EUTR requires proof of timber's origin and legality to ensure that no illegal timber is imported into the EU. To this end the EU intends to block imports of any wood or wood product which comes from unknown sources. Certification of sustainable forest management will help EU importers minimize risk, which is an essential part of their required due diligence system. Monitoring organizations are established to assist trade

associations and businesses to construct comprehensive due diligence systems. National competent authorities are designated to follow the trade of the new FLEGT-licensed timber and timber products.

In the first year of the EUTR there are positive impacts, of which the most important is awareness of the disastrous situation with illegal logging, driven by exports of illegal timber. Another positive development is tropical timber exporters documenting the legality of their wood exports. Yet another positive feature is establishment of due diligence systems by EU importers. However, there are considerable problems for ensuring legal trade; for example the lack of comprehensive documentation of origin and legality.

Analysis of recent trends establishes changes in the European timber trade in terms of sourcing, substitution, diversion to less-demanding countries. Short-term forecasts of market trends and changes will enable further policy assessment to achieve the objectives of improved legality in international timber markets.

Keywords: EU Timber Regulation; FLEGT; illegal trade; market impacts; forest products policy;

Introduction

Illegal logging drives deforestation and has been proven to have detrimental environmental, economic and social effects (Moiseyev et al. 2010). In fact, the illegal trade of wood is believed to undermine legal trade by reducing prices and profits- estimates indicate that illegal logging reduces government revenues by approximately US\$ 5 billion per year and depresses timber prices considerably on the international market (Li et al. 2008).

The importance of legal and sustainable trade of forest products is increasingly recognized by governments, international organizations, non-governmental organizations, trade associations, timber traders and the wood processing industries alike. The European Union's (EU) response to illegal logging came with the Forest Law Enforcement Governance and Trade (FLEGT) Action Plan (European Commission 2003) and more recently, in March 2013, with the introduction of Regulation No 995/2010 commonly known as the EU Timber Regulation (EUTR) (European Commission 2013).

This paper and its presentation prepared for the "Joint International Convention of: Society of Wood Science and Technology; Wood Structure and Properties; and European Hardwood Conference 2014" focuses on the EUTR's impact on the international timber markets. Particular attention is given to recent trends in timber trade between the EU and its trading partner countries. Finally, a discussion on stakeholder's interpretation of the EUTR will be provided. The overall objective is to help improve the effective implementation of the EUTR and understand its impacts on the timber trade in order to ensure legality and avoid unwanted detrimental side effects on the international timber market.

EU Timber Regulation (EUTR)

In 2003 the EU established the FLEGT Action Plan acknowledging that the EU is an important export market for countries where levels of illegality and poor governance in the forest sector are high (European Commission 2003). In addition to actively combating illegal logging, the FLEGT Action Plan also focuses on encouraging policy reforms, transparency, and information sharing in timber producing countries (European Commission 2013).

The Action Plan focuses on seven broad areas (Pepke et al. 2013):

1. Support to timber exporting countries, including action to promote equitable solutions to the illegal logging problem;
2. Activities to promote trade in legal timber, including action to develop and implement Voluntary Partnership Agreements between the EU and timber exporting countries;
3. Promoting public procurement policies, including action to guide contracting authorities on how to deal with legality when specifying timber in procurement procedures;
4. Support for private sector initiatives, including action to encourage private sector initiatives for good practice in the forest sector, including the use of voluntary codes of conduct for private companies to source legal timber;
5. Safeguards for financing and investment, including action to encourage banks and financial institutions investing in the forest sector to develop due care procedures when granting credits;
6. Use of existing legislative instruments or adoption of new legislation to support the Plan, including the EU Timber Regulation;
7. Addressing the problem of conflict timber.

The Action Plan aims to achieve these endeavors through its Voluntary Partnership Agreements (VPAs) which are legally binding agreements between the EU and partner countries. Although VPAs are at first voluntary agreements, they become legally-binding when ratified. All of a VPA country's timber exports need to be verified as legal through a legality assurance system (LAS).

The LAS consists of legality definitions established through a multi-stakeholder process defining "legal timber¹", procedures for legality verification, tracking systems, issuing of FLEGT licenses and an independent audit. Once the LAS is in place, consignments will be awarded a FLEGT license. However, as of mid-2014, the first FLEGT licenses and therefore shipments of FLEGT -licensed timber are yet to be realized; they are expected in 2015.

In 2010 the EU took an additional step to combat global illegal logging by introducing the EU Timber Regulation (EUTR) which came into full effect in March 2013. VPAs and the

¹ Under the EUTR, the definition of legality is based on the country of harvest.

EUTR are meant to reinforce each other. The EUTR makes European operators² accountable for the products they bring into the EU and requires adequate documentation that wood products come from legal sources.

The EUTR sets out three requirements for European operators (European Commission 2013):

1. Prohibition -- it prohibits placing illegally harvested timber or products on the EU market;
2. Due Diligence System (DDS) -- operators can apply Due Diligence by themselves or by associating with Monitoring Organizations (MO) to support adequate application of DDS. Operators need to provide access to information on the timber (country of harvest, logging concession, species, sizes, quantities), implement risk assessment (evaluate the risk of occurrence of illegally harvested products) and implement risk mitigation measures and procedures to minimize risk of illegality; and
3. Traceability Obligation -- after placing timber on the market for the first time traders³, have to keep records with information from whom they bought and to whom they sold the timber.

Each EU Member State is responsible to determine how to control the legality of its imports and how sanctions are applied if necessary. For this, each EU Member State needs to designate a Competent Authority⁴, i.e. the competent authority for the Slovak Republic is the Ministry of Agriculture and Rural Development of the Slovak Republic, Forestry Section. The European Commission is accrediting Monitoring Organizations (MOs) to assist companies and trade associations with establishing adequate due diligence systems (European Commission 2013). As of mid-2014, four MOs are recognized by the EC: NEPCon, Conlegno, Control Union and Bureau Veritas⁵. Some of these MOs are national, and some international. The Commission expects to accredit more MOs.

The EUTR applies to a wide range of timber products, including roundwood, primary-processed products (i.e. sawnwood/lumber) and secondary-processed products (i.e. wooden furniture and paper products). The EUTR also covers fuelwood, particleboard, fiberboard, packaging, pallets, builders' joinery and carpentry and prefabricated wooden buildings.

Timber and timber products covered by FLEGT licenses or Convention on International Trade in Endangered Species of Wild Fauna and Flora (CITES)⁶ permits meet EUTR requirements thus creating a strong market advantage for such products. Certification of sustainable forest management will help EU importers minimize risk. Certified products

² Under the EUTR, "operators" are those who first place timber products on the EU market. They carry the main responsibility for the EUTR requirements.

³ Under the EUTR, "traders" are those who receive timber or timber products from "operators" and then trade on the European market;

⁴ List of competent authorities in each EU Member

State: http://ec.europa.eu/environment/forests/pdf/list_competent_authorities_eutr.pdf

⁵ Updated list of MOs recognized by the European Commission:

http://ec.europa.eu/environment/forests/timber_regulation.htm

⁶ For more information on CITES: <http://www.cites.org/>

provide evidence of legally sourced timber but certification alone does not necessarily ensure legality under the EUTR (Cashore and Stone 2012).

Importer's responses to the EUTR

The EUTR creates a new framework within which different actors (both from importing and exporting countries) involved in timber trade interact. Understanding how these different stakeholders interpret the EUTR is of great importance for the smooth implementation of the new regulation. Recent research shows that while some stakeholders see the EUTR as advantageous for their businesses, others consider it an impediment. Stakeholders raise issues such as: (weak) law enforcement, (lacking) guidance and (increased) bureaucracy. The trade-off between effective legislation and ease of trade seems to be concerning some stakeholders (Giurca and Jonsson expected 2014). Naturally such issues need to be further explored and addressed in order for the regulation to fulfill its prime objectives. The European Commission and EU FLEGT Facility⁷ at the European Forest Institute are working on resolving such issues.

Exporter's responses to the EUTR

Already before the EUTR came into force, many exporting countries had begun establishing different legality verification schemes to meet EUTR's requirements in order to prove the legality of their exports. All VPA partner countries⁸ are currently developing such systems. As of mid-2014 there are fifteen VPA countries including six which have signed agreements and are in the process of implementation (Cameroon, Central African Republic, Ghana, Indonesia, Liberia and the Republic of Congo) and nine which are negotiating agreements (Democratic Republic of Congo, Gabon, Guyana, Honduras, Ivory Coast, Laos, Malaysia, Thailand and Vietnam). In addition a number of other tropical timber producing countries are considering VPAs.

Timber exports from Central Africa represent a large share of tropical timber imports to the EU. In fact, the Central African region has the largest number of countries engaged in the VPA process (Eba'a Atyi et al. 2013). Partner countries in the region such as Ghana and Cameroon have been making considerable efforts to assure the legality of their exports, an ambitious process meant to cover products for EU and other international markets alike. As an example, Ghana made efforts towards establishing its Legality Assurance Systems (LAS) and in developing a chain-of-custody system for tracking timber along the supply chain through a Wood Tracking System (WTS).

An independent monitoring system to assure proper functioning of the legality assurance system was also introduced (Ghana-EU VPA 2008, Ochieng et al. 2013). A recent progress review in Ghana demonstrates that the country has made considerable progress in developing its legality assurance system and especially its verification protocols and wood tracking system (EU FLEGT 2013). Similarly, Cameroon made significant steps forward towards establishing legality verification procedures and traceability system development. Other countries in the region show similar positive developments.

⁷ <http://www.euflegt.efi.int/home>

⁸ Updated list of the VPA process and partner countries: <http://www.euflegt.efi.int/vpa-countries>

(Cameroon and EU 2012). Nevertheless, further progress needs to be achieved and more challenges are anticipated for VPA implementation in the Central African region.

Indonesia became the first Asian country to initiate a VPA with the EU and it raised efforts to meet EUTR's demands. For this, the Indonesian government launched a national Timber Legality Verification Information System (SVLK)⁹. All wood products manufacturers in Indonesia were required to comply with SVLK and secure third party verification (ITTO-TTM 2013). The EU Delegation in Indonesia has confirmed that operators placing timber on the EU market from Indonesia complying with SVLK requirements will fully comply with the EUTR requirements (FLEGT Asia 2013).

With most of the global tropical trade concentrated in the Asian region, China continues to consolidate its position as the dominant market for tropical timber imports (ITTO 2011). China also strengthened its position as a major exporter of furniture, exceeding Italy and Germany's combined exports since 2005 (CINTRAFOR 2011). However, much of China's timber exports are suspected to come from illegal sources (Global Witness 2009). As China is not a VPA country, the EU Commission has signed an agreement with China: "the EU-China Bilateral Coordination Mechanism on Forest Law Enforcement and Governance" in 2009. More recently, the China Timber Legality Verification Scheme (CTLVS)¹⁰ was established in order to meet the new timber legality requirements of the EUTR (Proforest 2011).

The CTLVS is based on China's domestic timber management and control system. The CTLVS system is based on a forest harvesting permit, a timber shipment permit and a timber processing permit. Chinese timber legality certificates are issued only by China-authorized organizations. These certificates are further checked by the Chinese customs before Chinese companies export timber products. A wood tracking system is needed for both schemes once timber products enter the country. Implementation of the CTLVS has yet to overcome many challenges before it reaches full effectiveness (Pepke et al. 2013). The EU is exploring the possibility to establish similar bilateral agreements with other major timber trading countries which would not be considered for a VPA, for example, India.

Russia, a major world resource for both softwoods and hardwoods, and a major export partner to the EU, is also expected to provide reliable documentation for exported products. The European Commission is currently engaged in dialogs with Russia to establish incentives regarding the potential for the forest-based sector in "the Partnership and Cooperation Agreement between the EU and Russia"¹¹.

⁹ More information on the SVLK: <http://www.mfp.or.id/about-the-svlk/>

¹⁰ More information on the CTLVS: <http://www.proforest.net/projects/experience.2010-09-17.5626429669>

¹¹ For more information on EU-Russia dialogue progress see: http://www.thinkforest.efi.int/files/attachments/events/2013/eu-pirkanniemi_thinkforest_13-12.pdf

Market Developments

Timber-trade trends

In this section we analyze timber-trade trends as indicated by international trade data and statistics. The EUTR impacts Europe's trade, hence the focus is on the trade between the EU and its VPA partners in a global context.

EU's total imports of primary-processed solid wood products (in this instance sawnwood, plywood and veneer) and industrial roundwood -- from both tropical and temperate softwood and hardwood sources -- grew steadily until 2007. Afterwards, due to the global economic crisis in 2008, imports have sunk rapidly only to pick up slightly in recent years (Fig. 1).

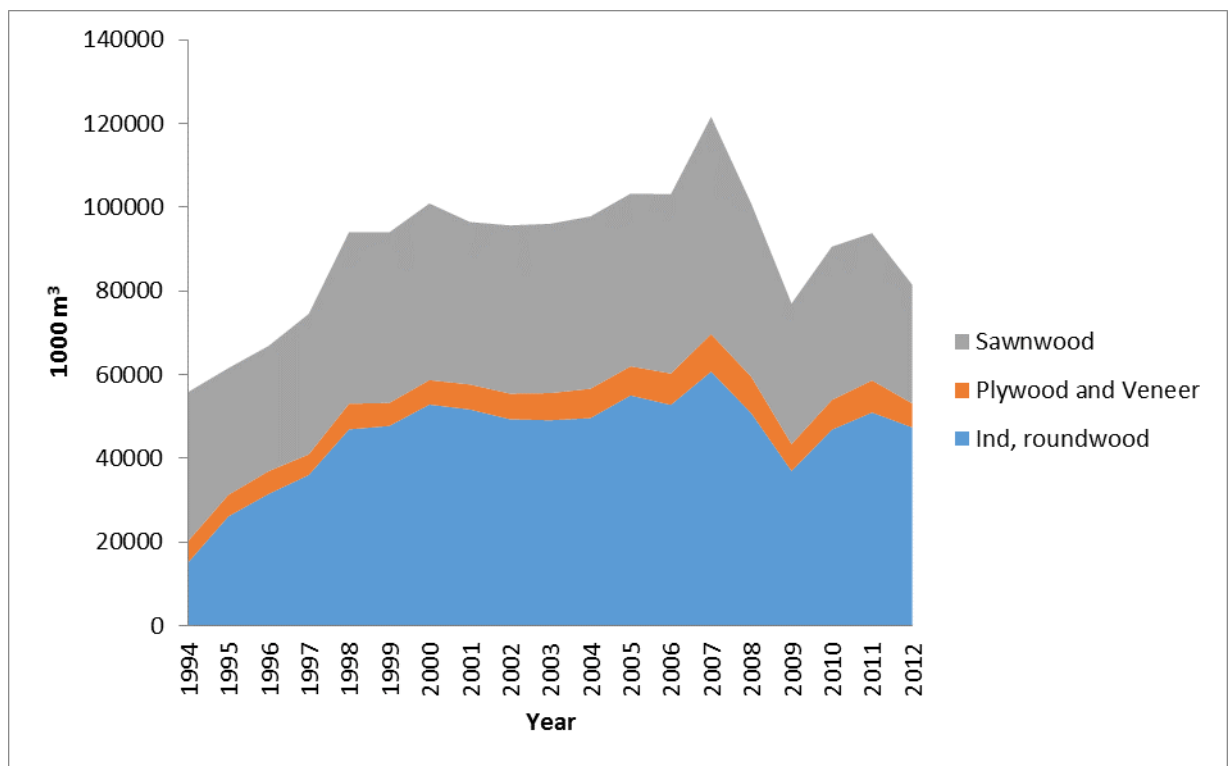


Figure 1 EU total imports of primary-processed products.

Source: ITTO 2014.

Primary-processed tropical timber (both softwoods and hardwoods) accounted for 34% of global trade in 2012 (Fig. 2). Tropical timber has a higher market share when measured in value than in volume. However, temperate timber (both hardwoods and softwoods) has a greater share of the volume on a global scale, accounting for 83% while only 17% is represented by tropical timber volume (ITTO 2013).

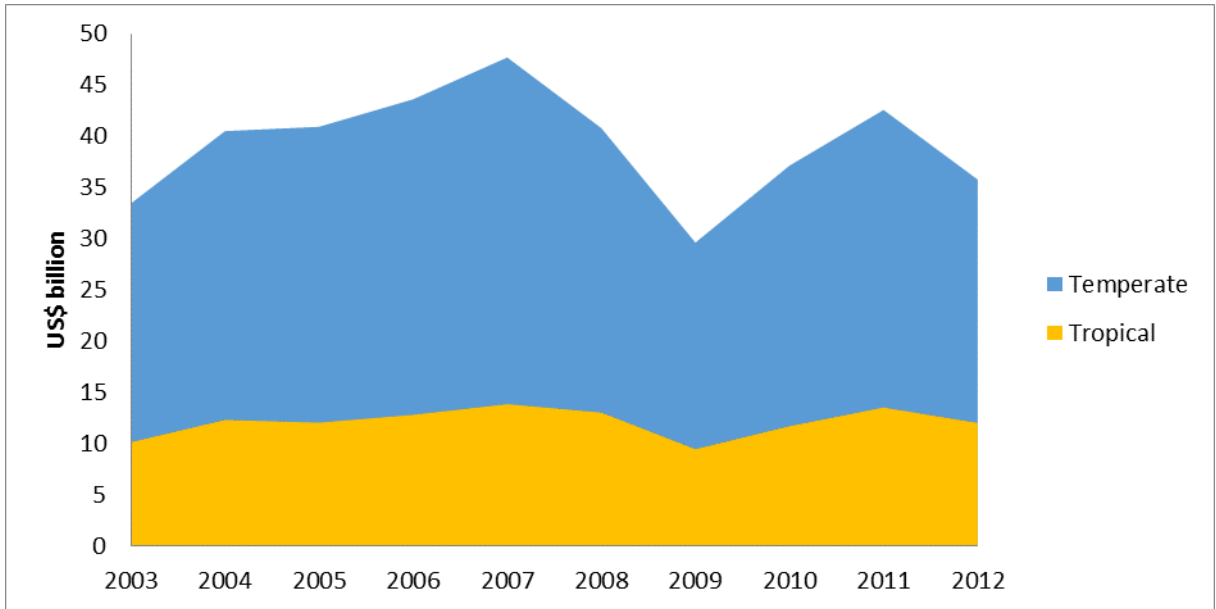


Figure 2 Tropical and temperate shares of global trade, 2003-2012.

Note: Based on 4 primary products: industrial roundwood, sawnwood, plywood and veneer.

Source: ITTO 2014.

For comparison, the EU’s share of temperate and tropical timber imports show a similar pattern to the global trend (fig. 3). In the early 2000s, the tropical share of EU imports was approximately 20%, but it has fallen to approximately 15% in 2012 (the latest statistics available from ITTO). There are multiple reasons for the declining EU tropical imports, including concern about illegal and unsustainable harvests in tropical countries, and uncertainty of the legality of imported timber.

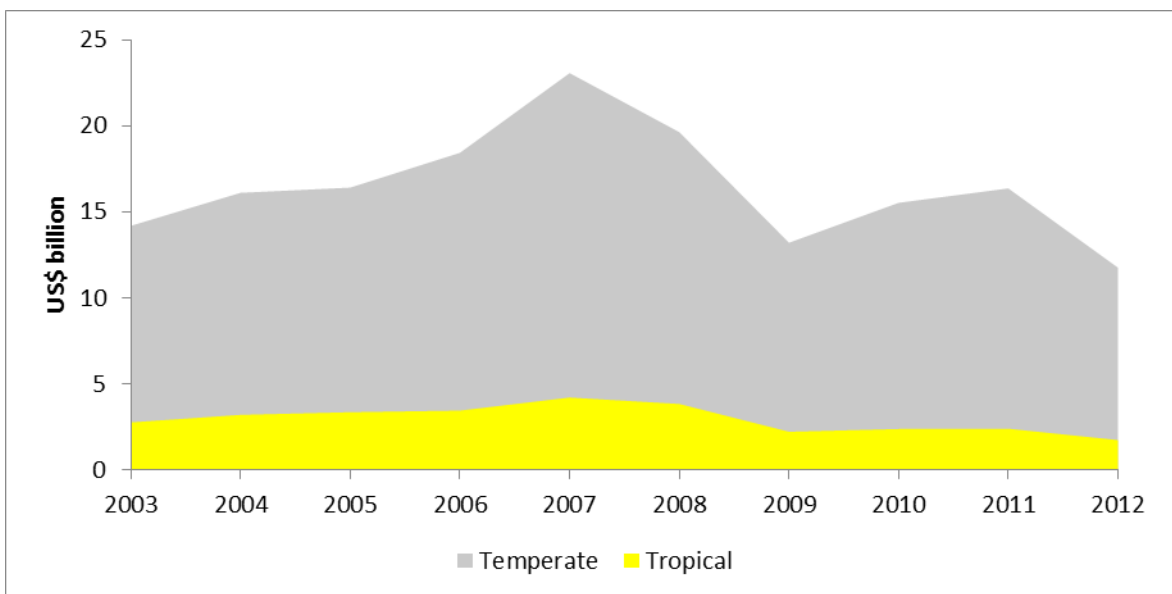


Figure 3 EU's import shares of temperate and tropical timber.

Source: ITTO 2014.

The EU's tropical timber imports show a clear overall decline during the last twenty years (Fig. 3). Again, a sharper decline in imports is clearly visible after the global economic downturn in 2008. However, the trend of decreasing imports continues even after this period.

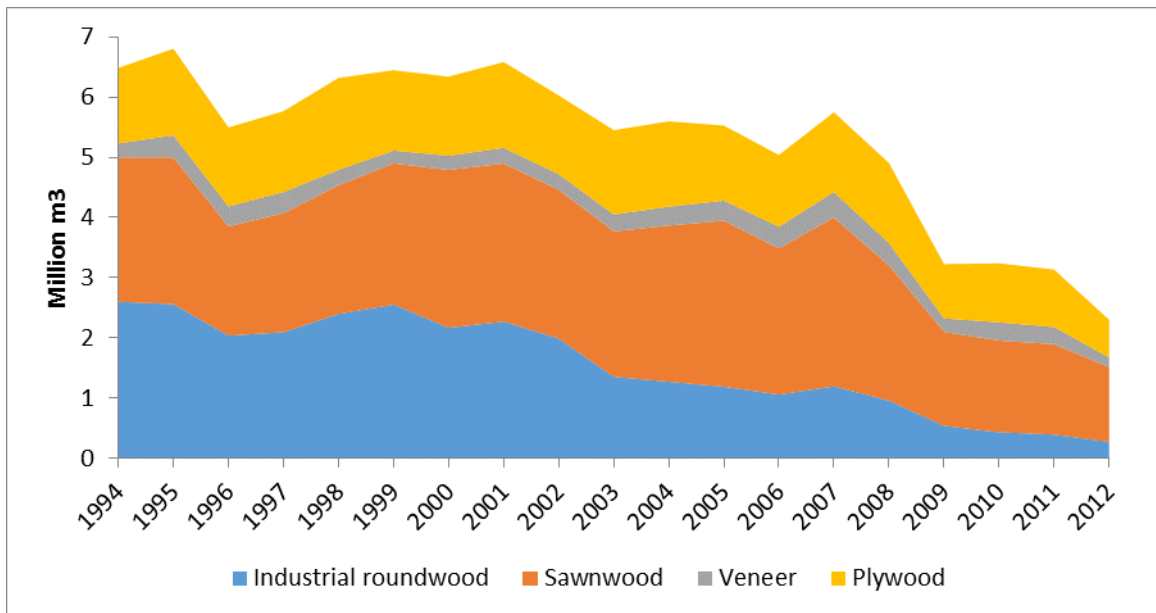


Figure 4 EU tropical timber imports.

Source: ITTO 2014.

More recent data suggests that EU tropical wood imports have declined by 13% in 2013. Imports of tropical hardwood logs were also down with 20% compared to the previous year. Value-wise, the EU imported tropical wood products with a total value of €1.91 billion in 2013, almost 12.6% less than in 2012 (ITTO-TTM 2014).

The majority, approximately 80%, of the EU's tropical sawnwood imports come from the current 15 VPA countries (Fig. 5). From the countries presented here, only the following have signed and are implementing a VPA as of mid-2014: Cameroon, Central African Republic, Ghana, Indonesia, Liberia and Republic of the Congo. The other 8 countries in the figure, plus Guyana, are negotiating a VPA as of mid-2014. Again, trade data analysis over the past decade shows similar trends, with tropical sawnwood imports steadily declining, and remaining relatively low after the global economic crisis in 2007-2008.

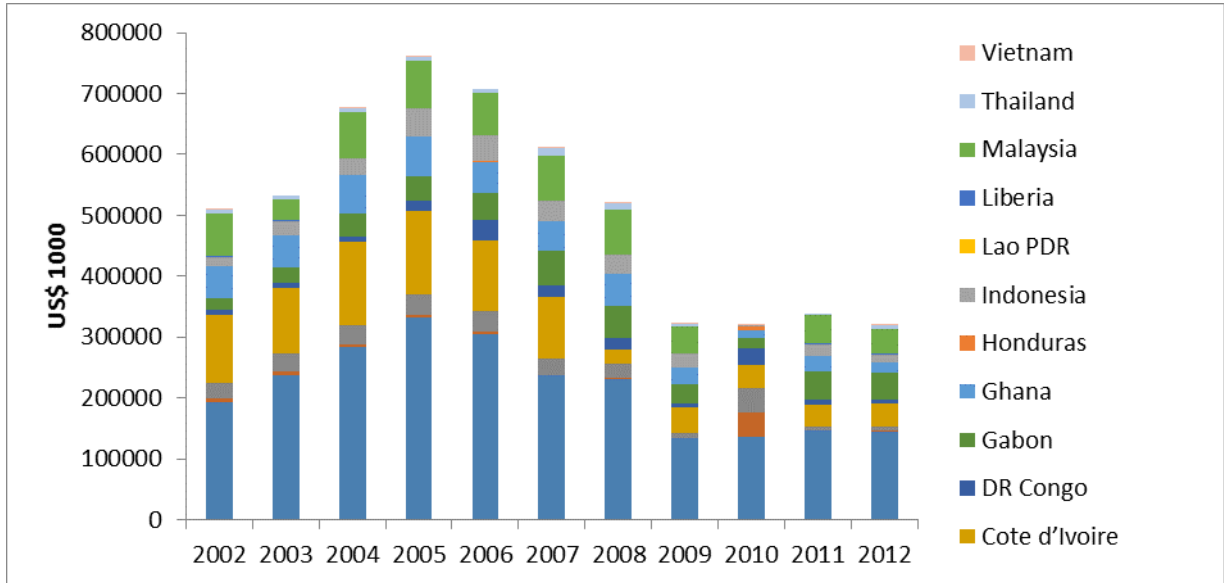


Figure 5 EU-27 imports of tropical sawnwood from VPA producers.

Note: No recorded exports of tropical sawnwood from Guyana to EU.

Source: UN COMTRADE 2014.

Imports of logs from all the leading supply countries (Congo, Cameroon, Central African Republic, and Liberia) have also continued to decline throughout 2013 (ITTO-TTM 2014).

Network analysis

A preliminary network analysis was performed on the EU27 level for the 1996-2006 period. Data on bilateral trade of all forest products was gathered from EFI's Forest Products Trade Flow Database. The network is very dense (85% of all possible trade flows), and all countries participate in the trade. Although Germany, Sweden, France and Finland together hold 48% of EU 27 exports, the overall centralization (both for import and export) is just 11%. For the observed period Germany stands out with highest trade volumes (import of 219 million m³ and export of 229 million m³). The top five exporting countries were Germany, Sweden, France, Finland and Austria. While Germany, France and Austria had balanced import-export trade flows, Sweden's exports were two times greater than imports, while Finland's exports were three times higher.

For analyzing cohesive subgroups, the following tests have been performed: components and factions routine, hierarchical clustering, clique analysis, structural and regular equivalence, categorical and continuous core-periphery analysis. Based on these tests, four cohesive subgroups have been identified. Countries within a subgroup have stronger ties within the group compared to the trade with countries outside the group, and the countries within the have similar patterns of trade flows. The following groups were identified:

- “Core countries”: Austria, Belgium, Finland, France, Germany, Italy, Netherlands and Sweden
- “Core dependent countries”: Bulgaria, Cyprus, Denmark, Greece, Luxembourg, Malta Poland, Portugal and Spain
- “Independent periphery”: Czech Republic, Estonia, Hungary, Latvia, Lithuania, Romania, Slovakia and Slovenia
- “Relative isolates”: Ireland and UK

These four groups can be illustrated with the magnitude of the bilateral trade between countries shown by the thickness of lines. The size of the arrowheads represents the strength of export and the size of the circles represents the volume of production of all forest products (Fig. 5). The more “central” a country is, the closer it is to the centre of the graph. The color coding for the 4 groups is: Core Countries in blue; Core Dependent Countries in green; Independent Periphery Countries in purple; and Relative Isolates in pink.

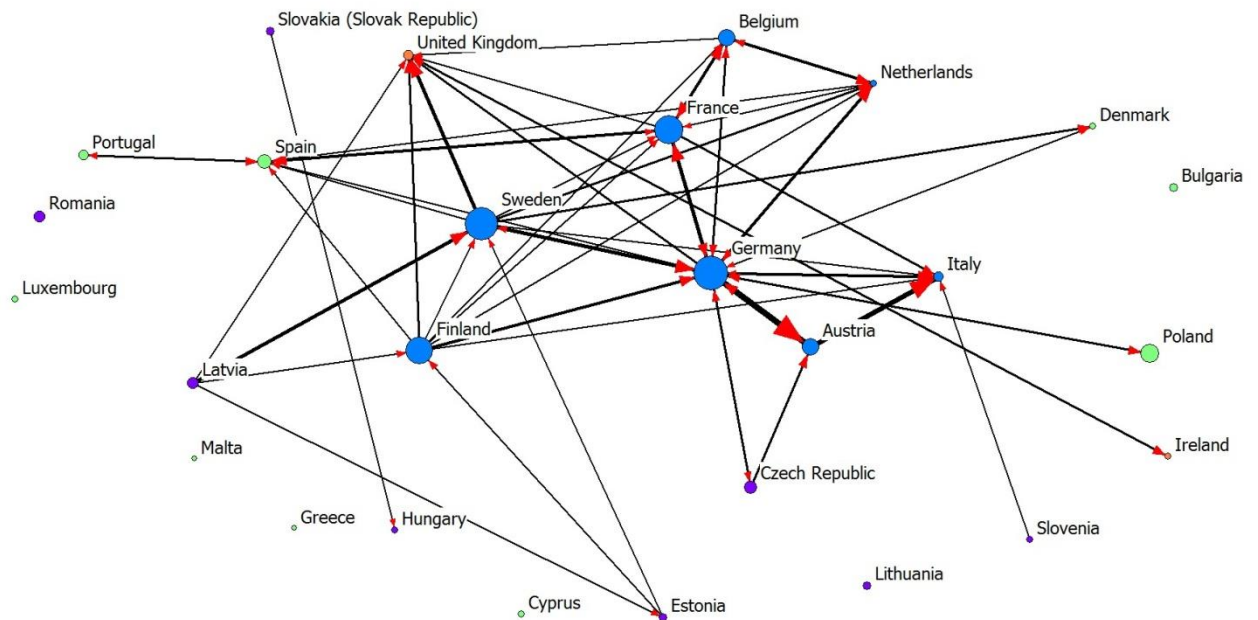


Figure 5 Trade flows in forest products in EU-27

Longitudinal SIENA type model has been constructed on the same data set, where descriptive attributes of countries are used as explanatory variables in the changes of trade flows. The most important of these attributes were the country-level numbers of Forest Stewardship Council (FSC) and Programme for the Endorsement of Forest Certification (PEFC) certificates. Having more FSC and PEFC certificates positively influence export, whereas the FSC influences the export by 9% more than PEFC. However, having more FSC certificates has no effect on import, whereas number of PEFC certificates has positive effect on import.

Discussion

The EUTR is expected to have positive impacts on the international timber trade. Once all legality verification systems will be in place and VPA partners will be able to provide FLEGT licensed timber, the EUTR will open up the market for legal and sustainably sourced timber products, especially from tropical producers. Not only will tropical timber exporting countries benefit from sustainable management of their forests achieved through legal harvesting, processing and exports, but a strong market demand for such products is likely to be reinvigorated. This is further indicated by the network analysis, indicating a positive influence on exports of certified forest products.

The EUTR will impact non-VPA countries (exporting to Europe) as well. Again, it is important to stress that China exerts a growing influence on global tropical timber trade flows and recent changes in EU's tropical timber trade have to be seen against this background. As mentioned above, China is developing its own verification system to comply with the legality demands of the EU but there are still efforts to be made.

Trade data analysis shows that the demand for tropical timber (especially hardwoods) has been weak since the 2008 global economic and financial crisis, and is still trying to regain momentum. Imports of timber products from all the leading supply countries in the tropics have continued to decline even throughout 2013. Important reasons behind the more recent decline in tropical timber trade could be increased ambiguity in the international timber trade. This ambiguity could originate as a side effect of the transition towards a stricter regulation for tropical timber. Ambiguity arises as the effects and requirements of the EUTR are not yet fully known or understood (Giurca et al. 2013). Empirical evidence in the economic literature shows that agents normally display aversion towards ambiguity. This implies that, when they take economic decisions, they tend to focus on worst case scenarios (cf. Camerer and Weber 1992, Etner et al. 2009).

As a result, substitution and trade diversion can be reasons behind EU's decreasing imports of tropical timber. On one hand, European importers, in doubt about the legality of timber coming from tropical countries, opt for products coming from countries with (perceived) more reliable documentation, such as temperate hardwood or softwood exporters (within the EU or North America). Hence, EU businesses choose safe sources, which lead away from less-documented tropical and temperate timber (both hardwoods and softwoods), or even substitute non-wood based commodities for wood. On the other hand, exporters of tropical timber, uncertain about the costs of complying with legal requirements, could opt to trade with partners with less stringent regulatory frameworks (Giurca et al. 2013).

Temperate species are often a viable substitute for tropical timber. New temperate softwood and hardwood products have been marketed as an alternative for traditional tropical hardwoods, performing equally in many applications (e.g. for exterior uses exposed to weather). More recently, temperate hardwoods such as oak have consolidated leading market positions in the European flooring and joinery sectors while tropical hardwoods have continued to lose market share (ITTO 2011). Research indicates

significant positive cross-price elasticity for oak, implying that oak and tropical lumber are indeed substitutes (Giurca et al.2013).

Substitution and trade diversion can thus be seen as causing market effects leakage. Market effects leakage occurs when policy actions in one place indirectly create incentives for third parties to increase activities elsewhere and is caused by a shift in market equilibrium (Jonsson et al. 2012), e.g., legality verification and certification, reducing the share of illegally sourced timber on the market, and thus increasing prices and pressures on temperate forests, e.g., in Eastern Europe or North America.

Transparent and consistent application of the EUTR, with clear guidelines for exerting due diligence, should diminish unwanted side-effects such as trade diversion and substitution of temperate timber for tropical timber. However, smooth implementation requires further understanding of stakeholder's interpretation/perceptions and problems (bureaucracy, guidance, law enforcement) related to the EUTR. Structural aspects of the regulation need to be addressed in order to avoid conflict of interest in the private sector and with consideration for international trade (Giurca and Jonsson expected 2014).

Conclusion

One year after its introduction, the EUTR's impacts on timber trade can already be felt on the global market. European companies and trade associations have clearly made efforts to establish viable due diligence systems for mitigating the risk of dealing with illegal timber. Producing countries have also made noteworthy efforts to establish reliable systems to tackle illegal logging and comply with the EUTR.

However, the full impact of EUTR on global timber trade will only be quantifiable as soon as the first fully FLEGT-licensed shipments arrive in Europe. Only then will the success of the new regulation be judged appropriately. For now, further attention needs to be focused on stakeholder's interpretation of the EUTR, the problems they face, and on providing viable solutions for facilitating a smooth and effective implementation of the regulation.

Ambiguity needs to be reduced as much as possible in order to avoid potential unwanted detrimental side effects such as substitution and trade diversion. Hence, efforts need to be put into assuring that the EUTR manages to fulfill its objective of eliminating illegal logging from international trade in timber, and of promoting sustainable forest management, good forest governance and equitable trade.

References

Camerer, C. and Weber, M. 1992. Recent Developments in Modeling Preferences: Uncertainty and Ambiguity. *Journal of Risk and Uncertainty*. 5:235-370.

Cameroon and EU 2012. Joint Annual Report 2012 on VPA implementation in Cameroon; Available online: <http://www.euflegt.efi.int/documents/10180/72377/Joint+Annual+Report+2012+on+VPA+implementation+in+Cameroon/c5bcd0b-3c4a-4ada-9704-0c6a83d33aa3> Accessed 12 April 2014

Cashore, B. and Stone, M.V. 2012. Can legality verification rescue global forest governance? Analyzing the potential of public and private policy intersection to ameliorate forest challenges in Southeast Asia. *Forest Policy and Economics*. 18: 13-22.

CINTRAFOR. 2011. Economic and Environmental Aspects of China's Wood Products Industry. <http://www.cintrafor.org/publications/newsletter/c4news2011winter.pdf>. Accessed 12 April 2014

Eba'a Atyi, R., Assembe-Mvondo, S., Lescuyer, G. and Cerruti, P. 2013. Impacts of international timber procurement policies on Central Africa's forestry sector. The case of Cameroon. *Forest Policy and Economics*.32: 40-48.

Etner, J., Jeleva, M. and Tallon, J-M. 2009. Decision theory under uncertainty. *Documents de Travail du Centre d'Economie de la Sorbonne*. No. 64

European Commission 2003. Communication from the Commission to the Council and the European Parliament—Forest Law Enforcement Governance and Trade (FLEGT)—Proposal for an EU Action Plan; European Commission: Brussels, Belgium

European Commission 2013. Timber regulation http://ec.europa.eu/environment/eutr2013/index_en.htm Accessed 01 November 2013

EU FLEGT 2013. News: Ghana reports progress in verification procedures and timber tracking system; Available online: http://www.euflegt.efi.int/news/-/asset_publisher/VoA92AEdZlro/content/ghana-reports-progress-in-verification-procedures-and-timber-tracking-system Accessed 13 April 2014

FLEGT Asia 2013. Indonesia and the EU adopt new timber trade legality rules in a move expected to boost bilateral timber trade. <http://www.euflegt.efi.int/portal/news?bid=988>. Accessed 28 February 2013

Giurca, A., Jonsson, R., Rinaldi, F., Priyadi, R.H. 2013. Ambiguity in timber trade from efforts to combat illegal logging- potential impacts on trade between South-east Asia and Europe. *Forests*. 4: 730-750.

Giurca, A. and Jonsson, R. expected 2014. Stakeholders' evaluation of the European Union Timber Regulation (EUTR): perceived risks, benefits and uncertainty. Manuscript submitted for publication.

Ghana-EU VPA Agreement 2008. Voluntary Partnership Agreement between the European

Global Witness 2009. A Disharmonious Trade. China and the continued destruction of Burma's northern frontier forests. A review by Global Witness.
http://www.globalwitness.org/sites/default/files/import/a_disharmonious_trade_pages_1_15.pdf. Accessed 20 May 2013

ITTO 2011. Annual Review and Assessment of the World Timber Situation 2011. Division of Economic Information and Market Intelligence: Yokohama, Japan

ITTO-TTM 2013. Tropical Timber Market Report Vol 17, Nr2, 16th-31st January 2013.

ITTO-TTM 2014. Tropical timber Market Report Vol 18, Nr6, 31st March 2014.

Jonsson, R., Mbongo, W., Felton, A., Boman, M. 2012. Leakage Implications for European Timber Markets from Reducing Deforestation in Developing Countries. *Forests*. 3:736-744

Li, R., Buongiorno, J., Turner, J.A., Zhu, S., Prestemon, J. 2008. Long-term effects of eliminating illegal logging on the world forest industries, trade, and inventory. *Forest Policy and Economics*. 10: 480-490.

Moiseyev, A., Solberg, B., Michie, B., Kallio, I., Maarit, A. 2010. Modeling the impacts of policy measures to prevent import of illegal wood and wood products. *Forest Policy and Economics*. 12: 24-30.

Ochieng, R.M., Visseren-Hamakers, I.J., Nketiah, K.S. 2013. Interaction between the FLEGT-VPA and REDD+ in Ghana: Recommendations for interaction management. *Forest Policy and Economics*. 32: 32-39.

Pepke, E., Giurca, A., Jonsson, R., Lovric, M. 2013. European Union Timber Regulation Impacts Global Hardwood Markets. In: Conference Paper prepared for International Scientific Conference on Hardwood Processing—2013; 7-9 October; Florence, Italy; ISCHP 13 Organizing Committee.

Proforest 2011. Update on China: Timber legality verification scheme. http://forest-trends.org/documents/files/doc_2777.pdf. Accessed 13 April 2014

UN COMTRADE 2013.

<http://comtrade.un.org/db/mr/rfCommoditiesList.aspx?px=H1&cc=4407> Accessed 13 February 2013

Chemical Suppliers and the Wood Treating Industry - Innovation in Buyer-Supplier Relationships

Erlend Nybakk.^{1} – Eric Hansen² - Andreas Treu³ - Tore Aase⁴*

¹ Reseacher, Norwegian Forest and Landscape Institute, Postbox 115, 1431
Ås, Norway.

** Corresponding author
nye@skogoglandskap.no*

² Professor, Department of Wood Science and Engineering, Oregon State
University, 119 Richardson Hall, Corvallis, OR 97331

³ Reseacher, Norwegian Forest and Landscape Institute, Postbox 115, 1431
Ås, Norway..
@skogoglandskap.no

⁴ Master student, UMB School of Economics and Business, Postbox 5003,
N-1432 Ås, Norway

Abstract

Recent challenges to maintaining competitiveness by forest sector firms have driven strong interest in the potential for innovation to create new opportunities for competitive advantage. Suppliers are a major source of innovation for many forest sector firms, yet little research has investigated their role in the innovation process. Using a qualitative case study approach, we explore how chemical companies who produce registered end-use products for wood protection perceive innovation in the wood treating industry and how they feel that they impact innovation among wood treating firms. Our findings indicate that chemical company managers view the wood treating industry as conservative and not particularly innovative. Additionally, retailers play a special hampering and directing role regarding innovation in the wood treating industry. Chemical company managers feel that they have an important impact on innovation within their customer firms, partially because they see limited possibilities for differentiating wood products without value-added additions, such as chemical treatments. Currently, various mechanisms for coloring wood products, along with standard chemical treatments, are the focus of innovation efforts. Chemical company managers also view their role with customers as a problem solver, providing a package of benefits in the spirit of the total product concept. Finally, strong relationships between chemical suppliers and key innovative customers play an important role in creating and implementing innovations in the industry.

Keywords: wood treating industry, innovation, chemical suppliers

Introduction

The Great Recession and housing crisis have placed extreme pressure on the forest products industry (Hansen et al. 2013). Even before these events, global competition caused losses of thousands of jobs across the sector and low profitability levels in many of the surviving firms. Various levels of government around the world have introduced strategies to boost innovation in an effort to increase industry competitiveness and financial performance based on a commonly held belief and growing evidence in the forest sector literature of the positive impact of innovation on firm financial performance. Often, innovations adopted by forest sector companies originate from suppliers. Some researchers argue that this reliance on, especially equipment and instrument suppliers, may explain some of the lack of innovation in the sector (Anderson, 2006) and this tendency does not contribute to competitiveness since innovations by suppliers are easily available to competitors (Nakamura, 2003)

This study is theoretically positioned within the innovation literature. The use of the term “innovation” has proliferated in recent decades and scholars have used multiple definitions in the literature (Garcia and Calantone, 2002). In this study, we define innovation as something new, such as a product, service, or business system, that is put into use or commercialised in the marketplace. In the last decade many innovation studies have been conducted within the wood product industry (e.g. Rametsteiner and Weiss 2006, Van Horne et al. 2006), Hansen et al. 2007, Stendahl and Roos 2008, Nybakk et al. 2011, Nybakk 2012, Nybakk and Jenssen 2012, Crespell et al. 2006, Crespell, Hansen 2008, Hansen 2010, Knowles et al 2008, Hansen et al. 2011, However, none of these describe the impact of chemical suppliers on innovation in the wood treating industry or wood industry in general.

There is little research that characterizes the relationship between forest sector firms and their suppliers and how that relationship influences innovation. With this gap in mind, we chose to study the wood treating industry where we expected suppliers of wood protection chemicals to be important contributors to innovation in wood treating companies.

Our primary objectives were to determine how chemical suppliers view the state of innovation in the wood treating industry and how they see themselves impacting innovation in the wood treating industry.

Materials and Methods

In this study, we employed a qualitative methodology for this work because the main questions under investigation were “how” in nature (Yin, 1994). Although often referred to as a “case study” approach, we emphasize that in this situation, the “case” is the phenomenon “supplier views of and impacts on innovation in the wood treating industry” rather than the sampled companies. The study attempts to identify how relationships between buyers and suppliers in the wood treating industry affect innovation. The

research was not designed for generalisability, and readers should carefully consider this fact as they explore the results and discussion below.

Basic qualitative data analyses techniques were employed. In total 14 managers were interviewed. Interviews were conducted within three chemical suppliers and three customer companies. Two chemical suppliers were based in Europe, and one was based in the US. The three customer companies were from Norway, Germany, and the US.

The semi-structured interviews (mostly face-to-face interview) lasted from 40 to 100 minutes. All interviews were recorded and later transcribed. The transcribed interviews consisted of approximately 144 pages of double-spaced text. The text was analysed using traditional qualitative method analyses techniques (Yin, 1994).

Results

Views from Suppliers. Chemical company managers see the industry as conservative, not especially innovative, and reactive rather than proactive.

“... the industry is quite conservative, so it is not so easy to bring in new technologies into this market.” – European Manager, chemicals

“...this industry is quite conservative, so customers like to do business as they have done it for the past twenty years.” – US Manager, chemicals

Big box retailers have an important impact on innovation in the sector. Low cost/price is supremely important for these retailers and the pressure they place on wood treaters to provide low-cost products limits the ability of treaters to explore new options.

“...I think the sawmilling industry has a huge problem... retail with lots of negotiation power.” – European Manager, chemicals

“I will tell you that big boxes always want something for nothing. They want everything, but they don't necessarily want to pay for it.” – US Manager, chemicals

This sort of pressure from customers reinforces the well-documented tendency among forest sector companies to pursue low-cost strategies rather than, for example, differentiation strategies. Recent evidence suggests some evolution by forest sector companies but many still rely on low-cost strategies and suffer from a commodity mentality. It is likely that a low-cost, production orientation has prevented industry from sufficiently investing in development of new or value added products

Impact of Suppliers. Each of the chemical companies participating in this research had a strong R&D department and each utilized a structured approach to new product development. Each was actively engaged in cooperation with research institutes and universities. Given this and the history of new chemical formulations entering the market,

it is clear that chemical companies are major drivers of innovation in the treated wood sector. Past research has shown the forest industry to be a “supplier-dominated” sector where a majority of new innovations come from suppliers rather than from within the industry itself (Pavitt, 1984)

Interviewees mentioned a number of product innovations, but the most current and prevalent topic was with respect to additives that color the final wood products. On the wood treating side of the industry, companies were focused on improved treatment processes as well as what the chemical suppliers could provide for product enhancements such as improved penetration, durability of a color, improved appearance, and product stability.

“Color is the product innovation. The new generation will maybe have something else than green. We are screening the market, so we try to adapt by adding colors. But the technology today is not good enough” - Scandinavian Manager, wood treater

“With wood preservative products it is quite rare to have new products for the market, but once in a while we achieve that with our color paste product range.” – European Manager, chemicals

Beyond pure R&D-based innovation, chemical suppliers see themselves as problem solvers for their customers and believe they are well-connected to the marketplace. Managers consistently spoke of their ability to bring both ideas and problems back from the marketplace into their companies and develop solutions for their customers. They referred to this ability in the spirit of providing a complete product offering to their customer, meaning a package far beyond a chemical formulation, including a variety of supporting services.

“So we help them solving this problem by chemical means, giving technical support, maybe also marketing and regulatory support.” – European Manager, chemicals

“So we are definitely not just a chemical company that sells chemicals. We definitely have a full package. There are some chemicals we offer, plus a service package.” European Manager, chemicals

As outlined above, chemical company managers see the wood treating sector as traditional, conservative, and lacking innovation. However, each of the chemical companies that participated in this research pointed us to a customer that they knew to be quite innovative. Managers tended to discuss customers in two groups: innovative and non-innovative.

“...you will find that are prone to innovation and there are of course some that are just price buyers.” – European Manager, chemicals

“So I would say when you are talking about a customer innovation standpoint, you got 85% of them, they are just waiting on us to bring them something. Then about 15% of

them, there is good communication and they are trying to think ahead of the game.” – US Manager, chemicals

It is with those more innovative customers that the chemical companies develop especially close relationships. The building of trust over time with these “key customers” translates to a situation where the customers are essentially facilitators of innovation development and implementation in the industry.

“You build trust obviously when you are developing these relationships and they are more willing to be our guinea pig when we have a new product.” – US Manager, chemicals

“So we help them solving this problem by chemical means, giving technical support, maybe also marketing and regulatory support. They may also get a reduced price to act as a test customer.” European Manager, chemicals

Although big box retailers were seen to limit innovation in the industry because of their sharp focus on low price, a US manager described a situation where the retailers drove innovation by demanding a more stable product. Ironically, the big box retailer, instead of going to its supplier of treated wood, went directly to the chemical company seeking an improved product.

Conclusions

As indicated in earlier research, our findings show that suppliers to forest products manufacturers play an important role in the innovation that takes place in their customer companies. In the context of our work, the suppliers were important for both product and process innovations. Generally, chemical company managers saw the wood treating industry as conservative and rather non-innovative. This doesn't paint a strong innovation-focused future scenario for the wood treating industry. However, the customers interviewed during this study were outliers, clearly pushing the envelope with respect to developing innovations. In fact, one of the customer companies had recently hired an innovation manager, a rare thing in the forest sector.

Big box retailers, because of their intense low-cost focus, were described as a bit of a villain in the marketplace, discouraging innovation by their customers. Chemical company managers were clear in their description that it was exceedingly difficult for treating companies to reap any rewards from big box retailers on the innovation front. Still, examples were cited where the retailer went directly to the chemical company seeking specific product improvements. Accordingly, retailers can also be a strong force for innovation in the sector.

References

Anderson, F. 2006. A comparison of innovation in two Canadian forest service support industries. *Forest Policy and Economics*. 8(7):674-682.

- Crespell, Pablo, Chris Knowles, and Eric Hansen. 2006. Innovation in the North American Sawmilling Industry. *Forest Science*. 52(5):568-578.
- Crespell, Pablo and Eric Hansen. 2008. Work Climate, Innovativeness, and Firm Performance: In search of a conceptual framework. *Canadian Journal of Forest Research*. 38(7):1703-1715.
- Garcia, R., Calantone, R., 2002. A critical look at technological innovation typology and innovativeness terminology: A literature review. *Journal of Product Innovation Management*. 19, 110-132.
- Hansen, E. 2010. The Role of Innovation in the Forest Products Industry. *Journal of Forestry*. 108(7):348-353.
- Hansen, Eric, Heikki Juslin, and Chris Knowles. 2007. Innovativeness in the Global Forest Products Industry: Exploring New Insights. *Canadian Journal of Forest Research*. 37(8):1324-1335.
- Hansen, E., E. Nybakk, L. Bull, P. Crespell, A. Jélvez, and C. Knowles. 2011. A Multinational Investigation of Softwood Sawmilling Innovativeness. *Scandinavian Journal of Forest Research*. 26(3):278-287.
- Hansen, E., Nybakk, E. & Panwar, R. 2013. Firm performance, business environment, and outlook for social and environmental responsibility during the economic downturn: findings and implications from the forest sector. *Canadian Journal of Forest Research* 43: 1137-1144.
- Knowles, Chris, Eric Hansen and Steve Shook. 2008b. Assessing Innovativeness in the North American Softwood Sawmilling Industry Using Three Methods. *Canadian Journal of Forest Research*. 38(2):363-375.
- Nakamura, M., Nelson, H., and Vertinsky, I. 2003. Cooperative R&D and the Canadian forest products industry. *Managerial and Decision Economics*. 24(23):147-169.
- Nybakk, E. (2012). Learning Orientation, Innovativeness and Financial Performance in Traditional Manufacturing Firms: A Higher-Order Structural Equation Model. *International Journal of Innovation Management*., 16(5), 28.
- Nybakk, E., P. Crespell and E. Hansen. (2011). Climate for Innovation and Innovation Strategy as Drivers for Success in the Wood Industry: Moderation Effects of Firm Size, Industry Sector, and Country of Operation. *Silva Fennica*, 45, 415-430.
- Nybakk, E. and J. I. Jenssen. (2012). Innovation Strategy, Working Climate, and Financial Performance in Traditional Manufacturing Firms: An Empirical Analysis. *International Journal of Innovation Management*, 16(2), 26 pp.

*Proceedings of the 57th International Convention of Society of Wood Science and Technology
June 23-27, 2014 - Zvolen, SLOVAKIA*

Pavitt, K. 1984. Sectoral patterns of technical change: Towards a taxonomy and a theory. *Research Policy*. 13(6):343-373.

Rametsteiner, E. and G. Weiss. 2006. Innovation and Innovation Policy in Forestry: Linking Innovation Process with Systems Models. *Forest Policy and Economics*. 8:691-703.

Van Horne, C., D. Poulin, and J.M. Frayret. 2012. Innovation and Value Creation in University-Industry Research Centres in the Canadian Forest Products Industry. *Canadian Journal of Forestry Research*. 42:1884-1895.

Van Horne, C., J.M Frayret, and D. Poulin. 2006. Creating Value with Innovation: From Centre of Expertise to the Forest Products Industry. *Forest Policy and Economics*. 8(x):751-761.

Yin, R.K., 1994. *Case study research: Design and methods*. Sage Publications, Thousand Oaks.

Sustainable Forest Management

Session Co-Chairs: *Ilona Peszlen, North Carolina State University, USA and Jaroslav Kmet', Technical University in Zvolen, Slovakia*

Looking for “Paradoxical” Species for Sustainable Forestry Management in French Guiana. *Bagassa Guianensis* and *Cordia Alliodora* Combine a Rapid Growth Rate and Superior Wood Quality

Julie Bossu^{1*} – *Jacques Beauchêne*² – *Bruno Clair*³

¹ PhD Student, Université Antille-Guyane, EcoFoG Research Unit (Ecologie des Forêt de Guyane). Kourou-FRENCH GUIANA.

* *Corresponding author*

julie.bossu@ecofog.gf

² Co Supervisor, CIRAD, EcoFoG Research Unit (Ecology of Guianese Forest). Kourou-FRENCH GUIANA.

³ Supervisor, CNRS, Wood Science Laboratory, EcoFoG Research Unit (Ecologie des Forêt de Guyane). Kourou-FRENCH GUIANA.

bruno.clair@ecofog.gf

Abstract

Wood construction costs appear to be offset by efficient traits such as high photosynthetic rates and optimized architecture with a small crown aperture. Current thinking holds that wood density results as a tradeoff between strength and price, with the rapid growing light-dependent tree species generally related to low wood quality (density, specific modulus, durability). However, certain tropical rainforest tree species represent both wood with good technological characteristics and high growth rates. This study aims to understand what the specific characteristics of these “paradoxical” tree species are and confirm their potential for new forest management models in French Guiana. Physical and mechanical wood properties were tested to evaluate wood quality; technological characteristics were analyzed in parallel with tree development, in relation to tree architecture and functional traits (leaf, cost-stem), to give a new understanding of these species. We identified *Bagassa guianensis* and *Cordia alliodora* as very promising species and results confirmed remarkable wood properties, exceptional for heliophilous species, with an optimized development strategy combining climax and pioneer growth

characteristics throughout ontogeny. Wood construction costs appear to be offset by efficient traits such as specific gravity, implying specific gradient of wood properties within the trunk. Nevertheless, despite this wood heterogeneity *Cordia alliodora* showed a homogeneous dimensional stability. Deformations registered for *Bagassa guianensis* were more variable in the tree but shrinkage seems to be influenced by specific gravity only in sapwood. Compared to current local species, these are characterized by highly reduced values of shrinkage for such a low density, which is a real advantage at the industrial scale. Continuation of this project will aim to compare the properties on plantation trees to confirm their wood quality for future forest exploitation in order to propose new sustainable models for the French Guiana logging production and forest management, valuing these native species with very strong potential.

Keywords: French Guiana, long-lived pioneers, density, wood quality, tree growth strategy.

Introduction

French Guiana forest management is specific and adapted to its small dimensions. The forest cover represents 96% of the whole region and is well protected. Across this area, about 1500 species have been identified and we consider that 500 are available for exploitation. However, currently only 70 exploited and 3 of these represent 70% of local production (*Dicorynia guianensis*, *Qualea rosea*, *Sextonia rubra*). In comparison to many areas in South America, French Guiana's forest is still rich and well preserved and as such could be an ideal region to develop new models for sustainable tropical forest management. The current wood production is small and adapted to existing population levels. However, current birth rates are equivalent to emerging countries, and thus the actual system needs rapid adaptations to avoid a monospecific tertiary system built on massive imports. In the field of timber, we must develop sustainable projects using fast growing species, adapted to plantations and with quality wood suitable for use as timber. The considerable richness of the Guianese rainforest entails a great diversity of growth strategies employed by different tree species. Crossing growth monitoring and technical databases, we isolated two singular species referred to as "paradoxical" species regarding their unique behavior: *Bagassa guianensis* Aubl and *Cordia alliodora* (Ruiz and Pav.) Oken. *Bagassa guianensis* Aubl. (Commercially known as Tatajuba), is a large and an infrequently tree in French Guiana (Royer, 2012). It only grows on secondary and anthropised forest. *Cordia alliodora* (Ruiz and Pav.) Oken is a deciduous secondary forest tree with a native range from latitude 25°N (Mexico) to 25°S (Argentina) in the American neotropics (Hummel, 1999) where it is commercially known as Laurel. But CA is not well distributed in French Guiana, instead concentrated next to the region of Saul. Already largely employed in South America, they both are rarely used in French Guiana. A large range of ecological, physical and mechanical traits have been measured in order to describe their unique development and highlight their interest for the local logging industry. In this study we focused on basic physical wood properties but always in the view of analyzing precisely their radial and longitudinal gradients in the tree.

Materials and Methods

Specific gravity and wood shrinkage are crucial technical characteristics for future wood products, but also good indicators of tree development. Specific gravity is now considered as the integrator of wood properties in the “wood economics spectrum” given its importance in structure, storage, and translocation (Chave et al., 2009). Wood is also known to be an anisotropic composite material, with a complex multi-scale structure. Wood shrinkage is representative of this heterogeneity and a useful wood trait to isolate the different types of wood observed in the trunk. These two traits describe well the “paradoxical” character of these two singular species and may help to explain their specific growth strategy.

Materials

Two species, *Bagassa guianensis* Aubl. (later noted Bg) and *Cordia alliodora* (Ruiz and Pav.) Oken (noted Ca) were tested. For each species we selected 9 individuals following a homogeneous distribution of the diameter to explore every stage of development. Material was collected at three different heights along the trunk and samples were taken using the same orientation and cutting process from the bark to the pith. For each property to be measured, the sample dimensions were different, but they all referred to a precise radial position that allowed us to compare samples almost of the same cambial age. Bg individuals were sampled next to the experimental station of Paracou, on a trail plot opened almost 30 years ago. Ca were sampled at the vicinity of the city of Saul. Both in Bg and Ca, trees DBH were ranged from a diameter of 15 to 55 cm.

Specific gravity

Basic Specific Gravity (SG) of wood is a measure of the amount of structural material a tree species allocates to support and strength. It is the ratio between dry mass (M0%) and saturated volume (VSat), (Kollmann&Cote, 1968. Williamson&Wiemann, 2010). We measured VSat by the inversed principle of Archimede method, observing the accurate water displacement of the sample immersed into a beaker of water loaded on a top-loading Sartorius CP224S scales, with a precision of 0.2 mg. Thanks to the dry and green mass, we can also calculate the Moisture Content (MC) and the Saturated Humidity (H%Sat). Then, considering 1.5 as the theoric density of woody matter, we calculated the Cavity Ratio of the sample (C%) to deduce the accurate proportion of Water (%W), Gas (%Gas) and Dry wood mass (%Dwm) contained in the sample. The following equations detail the main steps in obtaining the result:

$$\begin{array}{l}
 SG = \frac{M0\%}{VSat} = \frac{M0\%}{Mv - Mi} \rightarrow \\
 MC = \frac{Mv - M0\%}{M0\%}
 \end{array}
 \left. \begin{array}{l}
 H\% Sat = \frac{1}{SG} - \frac{1}{1.5} \\
 C\% = 1 - \frac{SG}{1.5}
 \end{array} \right\}
 \begin{array}{l}
 \%Gas = \frac{H\% Sat - MC}{H\% Sat} \times 1 - \frac{SG}{1.5} \\
 \%W = \frac{MC}{H\% Sat} \times 1 - \frac{SG}{1.5} \\
 \%Dwm = \frac{SG}{1.5} - 1
 \end{array}$$

Shrinkage

To analyze the dimensional stability of our anisotropic material, we calculated the dimensional variations due to shrinkage in each direction. To describe properly each phenomenon, it is necessary to use methods adapted to the scale of observation, and as such the following two were selected: (i) large samples (R×T×L=20×20×80mm) to evaluate radial and longitudinal shrinkage according to the method developed by François Sassus (Sassus, 1998). Tangential and longitudinal dimensions were measured with two comparators (Mitituyo) fixed to the frame of the measuring device with respect to standard metal shim used as reference. This is a fast and accurate process but this relative measure requires a precise positioning of the sample to keep the same reference for all the measures. (ii) and small samples (R×T×L=20×20×20mm) to measure the radial, tangential and longitudinal variations for a few growth rings. Here, we used a Mitituyo (model ID-H0530) that gives a precise absolute measure of the dimensions. We use the same measurement point during the whole process, marking each side with a standard gage. Saturated condition of the sample is ensured maintaining the samples in water since sawing. It then pass through several moisture content stages: 25% in an enclosure with K₂SO₄ salts, 10% in the laboratory air conditioning, 7% in an enclosure with MgCl₂ salts. Oven-dried sample is obtained with 3 days in the oven at 103°C.

Results

High change in density during ontogeny

First, the specific gravity analysis revealed significant and uncommon wood variability within the trunk for both species: we observed a remarkable radial gradient from the pith to the bark, especially for *Bg* that showed an outstanding factor two between juvenile and mature wood for specific gravity. Wood density is a common wood trait well related to tree construction costs (Larjavaara, 2010). This result helped to identify what types of wood are produced along a tree's life. In general, long-lived climax species tend to have high wood density, while pioneers have low wood density (Muller-Landau 2004). Here, *Bg* and *Ca* share both pioneers and long-lived climax characteristics, using one specific growth strategy during juvenile stage and then moving to another when older. Here is one of the outstanding particularities which classify these species to the rank of "paradoxical" ones: the ability to mix different growth strategies optimizing the qualities of each model and using them at the most suitable stage of the tree development.

A very low shrinkage

Growth rate is an important characteristic in species selection, yet wood quality takes precedence over all. That unavoidable condition combines a large range of physical and mechanical characteristics of which is the dimensional stability. The main results from the shrinkage analysis we carried out for the two species is presented in the Table 1.

Shrinkage (%)	Radial	Tangential	Longitudinal	Volumic
<i>Bagassa guianensis</i>	3.599 3.293	4.922 4.557	0.221 0.149	8.742 7.999

<i>Cordia alliodora</i>	3.077 2.892	5.764 5.283	0.181 0.165	9.022 8.340
-------------------------	-----------------------	-----------------------	-----------------------	-----------------------

Table 1– Global results of the shrinkage analysis (with means in bold, medians in italics)

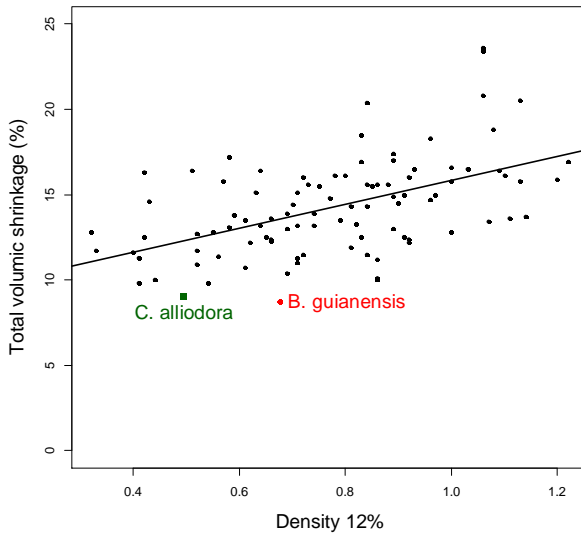


Figure 1 – Link between dimensional stability and wood density for common Guianese species.

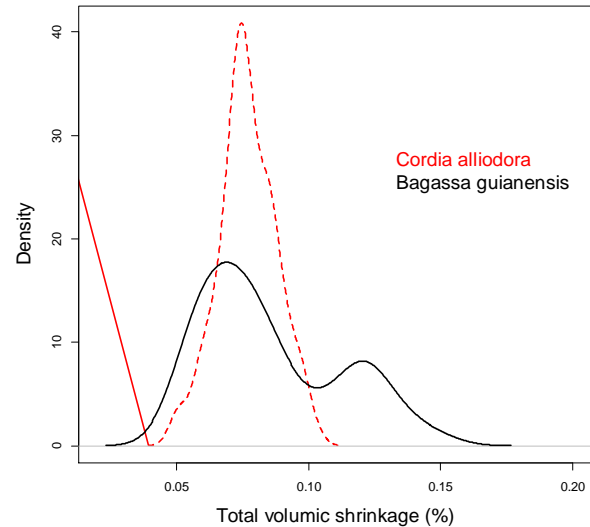


Figure 2 – Distribution of shrinkage measures for the two species.

Ba and *Ca* are characterized by a very low volumic shrinkage, especially for such a mean density. Figure 1 illustrates how these two species stand out and differ from the global tendency over 94 others current local species. We can notice that *Ba* and *Ca* are respectively the most stable species in their range of density. The existing ideas on the tradeoff between density and wood quality can be revised here. Wood products from paradoxical species represent a real advantage at the industrial scale in the sense that these light building materials enable an easy handling in constructions but do not have similar shrinkage problems that can be observed in other species of the medium density.

Parameters affecting wood shrinkage – *Bagassa guianensis* specific aspects

We then analyzed the variability of the dimensional stability within the tree for the two species. During the drying process, samples from *Ba* showed the largest shrinkage dispersion. In the density plot (Fig.2) that compares the distribution of the measures for the two species, *Ca* stands out: its wood is more homogeneous than *Bg*. Focusing on *Bg*, it clearly appears that samples are divided into two different groups. We then asked about the parameters that may influence wood shrinkage. Density is known to be properly linked with wood shrinkage since wall thickness directly influences the apparent density of wood (Kellogg, 1969). We expected a global tendency with dimensional variations increasing proportionally to wood density when drying, but final results showed two groups dissociating clearly heartwood and sapwood samples and different responses to drying for each type of wood (Fig.3). The influence of specific gravity on total shrinkage

is stronger in sapwood than heartwood. The radial gradient of the deformations is reduced in heartwood. Secondary metabolites responsible for heartwood formation in *Bg* might be responsible for this phenomenon. Most of these compounds are polyphenols and are synthesized by the plant as the sapwood is converted into heartwood.

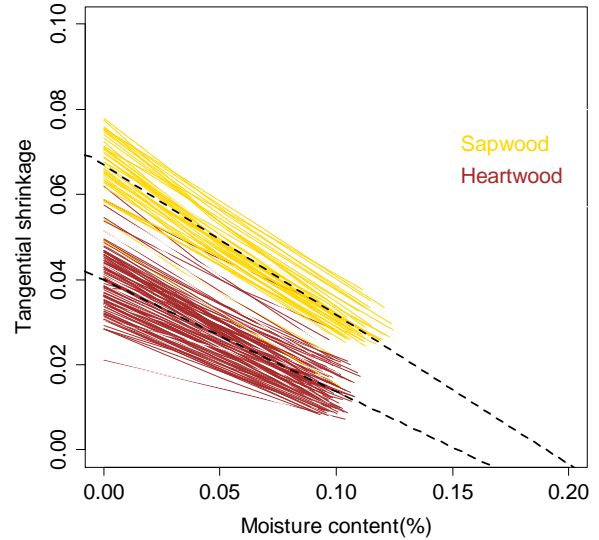
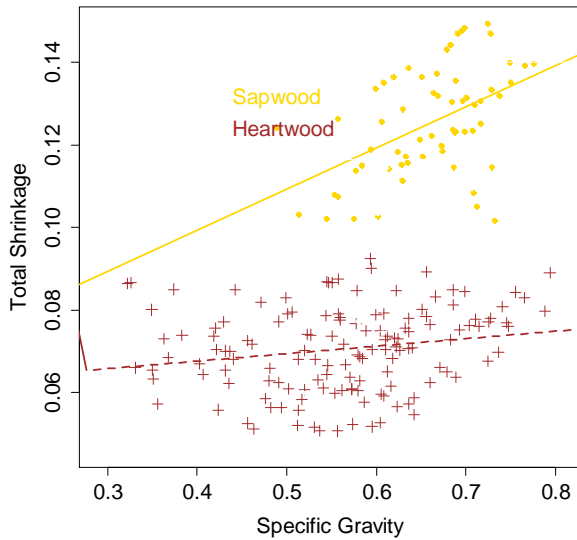


*Figure 3 – Influence of specific gravity for sapwood and heartwood on shrinkage in *Bagassa guianensis*.*

*Figure 4 – Tangential deformation in sapwood and heartwood according to the successive stages of moisture content in *Bagassa guianensis*.*

These extractives are known to bring natural resistance to *Bg*'s heartwood thanks to a complex synergism between active and inactive polyphenols, mainly stilbenes, representing almost 70% of the isolated polyphenolic compounds extracts (Royer, 2012). The important quantity of extractives in *Bg* apparently has an impact on the wood physical characteristics of and shrinkage behavior. Heartwood shows a lower anisotropy over the radial profile, reducing the probability of appearance of defects on the logs during the drying process.

What is a good fiber saturation point?

Using the results of the successive tangential deformations for each stage of humidity, we calculated the fiber-saturation point (FSP): we observed a significant difference between heartwood and sapwood (Fig.4). Sapwood's FSP (21%) is significantly bigger than heartwood's one (16.4%). FSP valor predetermines the minimum of humidity acceptable for wood storage without deformations. In that sense the heartwood is more convenient. A limit to this analysis is the relation between moisture content and relative humidity due to water diffusion into wood in across-the-fiber directions, which is variable depending of the wood porosity. The important specific density radial gradient induces high variability of water diffusion. The humidity distribution is more homogeneous in sapwood than heartwood and we know that humidity gradient directly impacts on shrinkage defects like deformations, cracks or collapse. Heartwood pieces are easier to stock before shrinking, but passing from a humidity stage to another, sapwood might stabilize faster than heartwood. It leads us to revise our views about what is a good wood product with regards to shrinkage behavior. Indeed, a question that emanates from these results is the criterion to be retained to select a species over another. It is clear that the FSP is not sufficient to predict properly the potential deformations of a wooden product in its conditions of use. The slope of the mean drying profile used to determine the FSP is also relevant. After an industrial drying process, a wood product is still subjected to a certain range a humidity variations in its conditions of use. In a region characterized by high annual humidity variation, if we consider two species with the same FSP, the species with a lower slope in shrinkage profile will imply largest risks of deformation. This example shows that it is important to take into account the whole shrinkage behavior of a certain type of wood to be able to conclude about its dimensional stability and recommend it for specific conditions of use.

Detailed description of the different types of wood in *Bagassa guianensis*

Bg is characterized by a strong specific gravity radial gradient and significant variability of the dimensional stability between heartwood and sapwood. However, heartwood and sapwood division may not be sufficient to describe this variability. Further statistical analysis on the whole dataset from *Bg* sampling helped us to identify other wood types. We used a general agglomerative hierarchical clustering procedure, where the criterion for choosing the pair of clusters to merge at each step is based on the optimal value of an objective function (Ward, 1963) and a principal component analysis to observe all the steps of the clustering. It enables us to identify how samples are successively separated to eventually form smaller groups with roughly the same characteristics. This analysis showed that it exists a more accurate classification than the simple dissociation

sapwood/heartwood: (i) *internal heartwood* (low specific gravity and low volumic shrinkage); (ii) *external heartwood at the base of the trunk* (medium specific gravity and low volumic shrinkage), (iii) *external heartwood higher in the trunk* (high specific gravity and low volumic shrinkage) and (iv) *sapwood* (high specific gravity and high shrinkage). We manually carried out the same separation on our database and measured the physical characteristics and shrinkage behavior for each group to verify the statistical analysis' results: this wood types classification is thus justified.

Conclusion

Paradoxical species represent a real opportunity for the local logging field. A combination of medium density (0.68 for *Bagassa guianensis* and 0.49 for *Cordia alliodora*) and low shrinkage (average volumic shrinkage of respectively 8.7% and 9%) is well adapted for industrial use. The high variability in specific gravity observed from the pith to the bark enables the two species to reach an efficient growth rate until reaching the canopy, before quickly producing good quality wood. *Bagassa guianensis* wood showed small shrinkage values but appeared to be less stable than *Cordia alliodora*. The important quantity of extractives in *Bagassa guianensis* heartwood has a non negligible effect on shrinkage behavior. To create a model of the physical properties in the tree, the different types of wood need to be differentiated. One pattern for the whole trunk depending only on the height and the radial position is not accurate. What is surprising with paradoxical species is their ability to produce a certain kind of wood for certain conditions or maturation stages. Such flexibility in a tree's wood production is an example of an optimized tradeoff between strength and cost of construction. This uncommon tree development is interesting from a technical point of view but also regarding plantation, as both species are well adapted to growth in open spaces. Plantation projects demand efficiency, and neighboring experience has already shown that *Bagassa guianensis* and *Cordia alliodora* are promising species for future exploitation. We are now studying the variations of interlocked grain in *Bagassa guianensis*. Grain angle showed a periodic and increasing evolution from the pith to the bark, reaching up to 25° for the biggest individuals. It is an advantage for the tree (mainly to support radial compression) but has a strong negative impact on specific modulus. But it can be considered as an additional benefit if we use this specificity as the species does, focusing on tenacity. We are testing the radial tenacity on several samples of variable interlocked grain and expect a good correlation between the distance from the pith and radial tenacity. Studying these species leads us to the following questioning: What is a good wood product? What is an interesting species for future exploration? Current productive system in French Guiana requires rapid adaptations and such species appear really promising as regards their characteristics and growth strategy. *Bagassa guianensis* and *Cordia alliodora* represent local species of interest that deserved to be further studied and employed in future plantations projects.

References

- Chave J. 2009. Towards a worldwide wood economics spectrum. *Ecology Letters* (12): 351–366.
- Hummel, S. 2000. Height, diameter and crown dimensions of *Cordia alliodora* associated with tree density. *Forest Ecology and Management* (127):31–40.
- Kellogg, R.M. 1969. Variation in the cell-wall density of wood. *Wood Fiber Sci* (1):180–204.
- Kollmann, F.F.P. and W.A. Cote. 1968. Principles of wood science and technology (I). Solid Wood. Springer-Verlag. Berlin. 592.
- Larjavaara, M. 2010. Rethinking the value of high wood density. *Functional Ecology* (24): 701–705.
- Muller-Landau, H.C. 2004. Interspecific and inter-site variation in wood specific gravity of tropical trees. *Biotropica*, (36): 20–32.
- Royer, M. 2012. Efficacy of *Bagassa guianensis* Aubl. extract against wood decay and human pathogenic fungi. *International Biodeterioration & Biodegradation*, (70): 55–59
- Sassus, F. 1998. Déformations de maturation et propriétés du bois de tension chez le hêtre et le peuplier : mesures et modèles. Sciences du bois Thesis, ENGREF, Montpellier.
- Ward, J. H., Jr. 1963. Hierarchical Grouping to Optimize an Objective Function. *Journal of the American Statistical Association*, (58): 236–244.
- Wiemann, M.C. & Williamson, G.B. 1989. Radial gradients in the specific gravity of wood in some tropical and temperate trees. *Forest Science*, (35): 197–210.

A Comparative Study of Wood Properties of *Pinus caribaea* (Morelet) in Two Plantation Ages in Oluwa Forest Reserve, Ondo State, Nigeria

UDOAKPAN, Ubong Ime

Forestry and Wildlife Department, University of Uyo, Nigeria
P.M.B. 1017
ubongudoakpan@gmail.com
+2348087973202

Abstract

This paper examines and compares the effects of variation on wood density, ring width and anisotropic shrinkage of *Pinus caribaea* (Morelet) among two plantations in Oluwa forest reserve (a world bank assisted pulpwood plantation). The wood samples were collected from a 16 and 17 year-old plantation with an area of 25 ha. Each of the plantations was divided into 5 partitions with an area of 5ha each. 2 trees each with good bole form with a diameter equal to the mean diameter of all the trees in each of the partitions were randomly selected from the two plantations for the study. Wood samples were collected from five levels of each tree merchantable length: 10%, 30%, 50%, 70% and 90% and also radially among the wood types: inner wood, middle wood and outer wood portions of the stem according to standard procedures. T-test and descriptive statistics were used in the data analysis of the obtained results. The result showed the variation in wood density between the wood types and merchantable length of the 16 and 17 year old plantations were not significantly different from each other ($p>0.05$). Among the two plantations, ring width variation decreased along the wood types and merchantable length, although there was no significant difference between them ($p>0.05$). However, there was a positive correlation between the density and shrinkage properties of the two plantations, including the ring width and anisotropic shrinkage properties. Thus, the use of wood density and grain orientation biometrics to predict anisotropic shrinkages of the *Pinus caribaea* (Morelet) and its dimensional stability is important for pulp and paper making, and production of suitable wood based panels..

Key words: Density, Ring width, anisotropic shrinkage, *Pinus caribaea* (Morelet), Nigeria

Veneering of Plantation Grown Sub-tropical Species from Thinning Experiments

Anton Zbonak^{1*} – *Henri Bailleres*² – *Rob McGavin*³

¹ Team Leader, Forest Value; Queensland Department of Agriculture, Fisheries and Forestry (QDAFF). Brisbane Qld, AUSTRALIA.

* *Corresponding author*

anton.zbonak@daff.qld.gov.au

² Team Leader, ³ Research Facility and Project Manager; Forest Products Innovation; QDAFF. Salisbury Qld, AUSTRALIA.

Abstract

Small spindleless veneer lathe technology was used as an alternative processing option to optimise the utilization of small log plantation hardwood resource. Trees were sampled from thinned (300 spha) and unthinned control (1000 spha) plantings of 10.5-year-old *Corymbia citriodora ssp. variegata* (CCV) and *E. dunnii* (Dunn's white gum) grown in two contrasting sites in Queensland. Veneer samples taken at regular intervals along the length of the veneer ribbon were tested for stiffness and veneer density.

Overall veneer gross recoveries ranged from 50% to 70%, which were up to 5 times higher than what has been reported to be achieved from similar plantation resources when converted to sawn timber products. Major limiting factors preventing veneer from meeting higher grades were the presence of kino defects and encased knots. Splits in *E. dunnii* veneer also contributed to reduced grade quality.

Differences between two thinning treatments for veneer properties and grade recovery were generally small. There was significant evidence of site and species differences on veneer quality. The good quality site with higher rainfall produced denser and stiffer veneers with higher grade recoveries. Significant trend was observed between radial trajectories of veneer traits and drought period in studied sites.

The results demonstrated that sub-tropical plantation hardwoods can produce veneer with superior mechanical properties and high recoveries. This relatively young plantation resource has attributes suited to a range of engineered wood products including plywood and laminated veneer timber.

Keywords: peeling, *E. dunnii*, CCV, veneer stiffness, veneer recovery

Introduction

Sub-tropical eucalypt plantations established in Queensland and New South Wales total slightly less than 150,000 ha, which is 15% of Australia's hardwood plantation estate (Gavran and Parsons 2010). The rate of plantings accelerated after 2000 when private forestry companies, many using managed investment schemes (MIS), became active in the region. The two most important species by area are Dunn's white gum (*Eucalyptus dunnii*, DWG) and spotted gum (*Corymbia citriodora* spp. *variegata*, CCV), which together comprise approximately 54,000 ha of the subtropical plantation estate. Much of the DWG plantation area was established for pulpwood production, whereas plantations of CCV have been targeted more at solid wood production (Nichols et al. 2010).

This paper summarizes the peeling performance and veneer quality of logs from trees of both species sourced from two contrasting sites and thinning treatments: thinned to 300 stems ha⁻¹; and an unthinned control. A significant increase in the rate of stem diameter growth following thinning was demonstrated for both species at both sites (Glencross et al 2011). Billets from two different tree heights were peeled. This enabled the effects of site, species, thinning treatment and billet height, and their interactions to be examined. Standing tree acoustic wave velocity was assessed before the selected trees were felled and the effectiveness of this non-destructive assessment method in predicting veneer stiffness was evaluated.

Materials and Methods

Sampling. CCV and DWG logs were sourced from plantations established by Forest Enterprises Australia in subtropical eastern Australia. Both sites had similar management histories. Reid's plantation is located at Ellangowan, 50 km south-west of Lismore in north-east NSW; Barron's plantation is 15 km south-west of Kingaroy in south-east Queensland, and Tingoora plantation is 40 km north of Kingaroy (Table 1). Rainfall conditions during the life of the plantations contrasted between Ellangowan and the sites near Kingaroy. The mean annual rainfall for the 2001–2010 period at Ellangowan was 1096 mm, which is close to the long-term average (97% of long-term mean rainfall), whereas at Kingaroy, the mean annual rainfall for 2001–2010 was 783 mm, which is 23% below the long-term average for this region.

Table 1. Summary information for CCV and *E. dunnii* plantations in two locations

Parameters	Ellangowan		Kingaroy	
	CCV	<i>E. dunnii</i>	CCV	<i>E. dunnii</i>
Species	CCV	<i>E. dunnii</i>	CCV	<i>E. dunnii</i>
Site	Reid's	Reid's	Tingoora	Barron
Stocking prior to thinning	1050	1270	950	930
Age thinned (year, month)	7 y 9m	7y 9m	6y 9m	6y 9m
Age when harvested (year)	10.5	10.5	10.5	10.5
Mean annual rainfall (mm)	1096	1096	783	783
Elevation (m)	52	52	449	465

Thinning treatments had been implemented at age seven years and nine months old and six years and nine months old at the Ellangowan and Kingaroy sites respectively (Table 1). For each site, the thinning treatments of 300 stems ha⁻¹ and 500 stems ha⁻¹ and an unthinned control treatment (with stocking in the range 950-1270 stems ha⁻¹) were applied in a randomised complete block design with four replicates.

Two contrasting treatments, 300 stems ha⁻¹ and an unthinned control, were targeted for sampling. For each species and thinning treatment, at each site, five dominant trees with above-average stem diameters were selected. The aim was to assess the potential of trees that would be retained as final crop trees for veneer log production. From each tree, two 1.5 m long billets were removed: a butt billet from 0.3-1.8 m above ground and a top billet from a height of approximately 5.5-7.0 m. In total, 80 billets were cut: 2 species × 2 sites × 2 treatments × 2 height positions × 5 trees per treatment.

Prior to sampling, a Fakopp microsecond timer was used to assess the time of flight for an acoustic signal on each selected standing tree.

Processing. The billets were transported to the Salisbury Research Centre (Department of Agriculture, Fisheries and Forestry, Queensland) for veneer processing. The billets were heat-treated to a core temperature of 90°C prior to peeling, to facilitate easier peeling. Core temperature elevation was achieved by exposing the billets to full steam conditions for 24 hours before peeling. After heat treatment the billets were assessed for splitting and then merchandised to 1.3 m in length (trimmed equally from both sides to reduce any end splitting).

The billets were peeled on an Omeco spindleless lathe. The full ribbon was produced with a target green thickness of 2.8 to 3.0 mm. The veneer ribbon was peeled until a core diameter of approximately 45 mm was attained. The full length of ribbon was laid out on the conveyor for easy evaluation.

Veneer assessment. After peeling, the ribbon was trimmed into 1.55 m wide (tangential dimension) sheets and 0.15 m wide veneer assessment samples. The first assessment sample was removed from the ribbon position closest to the peeler core and others removed sequentially after each 1.55 m veneer sheet. The veneer assessment samples were conditioned to 12% equilibrium moisture content and analysed for veneer density and dynamic modulus of elasticity (stiffness, MOE), measured with resonance frequency using the BING system (Brancheriau and Bailleres 2003).

Following peeling, the veneer sheets were dried by a commercial veneer company using a Jet box dryer to target final moisture content of less than 10%.

The veneer sheets were visually graded to the Australian/New Zealand Standard (2008) to establish grade recovery in accordance with the existing industry standard. This standard is designed for face veneer grade segregation only, as most plywood panel products are manufactured with D-grade (the lowest grade) veneer. Each veneer sheet was assessed for presence and severity of defects such as knots, gum veins, holes, splits, discoloration, compression and roughness. The final veneer grades assigned were based on the worst limiting defect. A-grade is the highest grade followed by B-, C- and then D-grade.

Gross recovery was calculated as the percentage by volume of dried veneer, recovered from its respective green billet volume, meeting AS/NZS 2269 D-grade and higher. Grade recovery is the percentage by volume of each grade of dry veneer, assessed according to AS/NZS 2269, from its respective green billet volume.

Results and Discussion

Veneer gross and graded recoveries. The gross recovery from individual billets varied substantially for individual species-site combinations (Fig. 1). Overall veneer gross recoveries, as site averages, ranged from 50% to 70%. The logs from these veneer trials were younger and had smaller diameters than traditional plywood resources, so higher recoveries should be achieved from older, larger diameter logs. In this sense the veneer recoveries reported here are quite encouraging as they are 2–3 times higher than typical green off-saw recoveries from sawing logs of similar diameters (Leggate et al 2000).

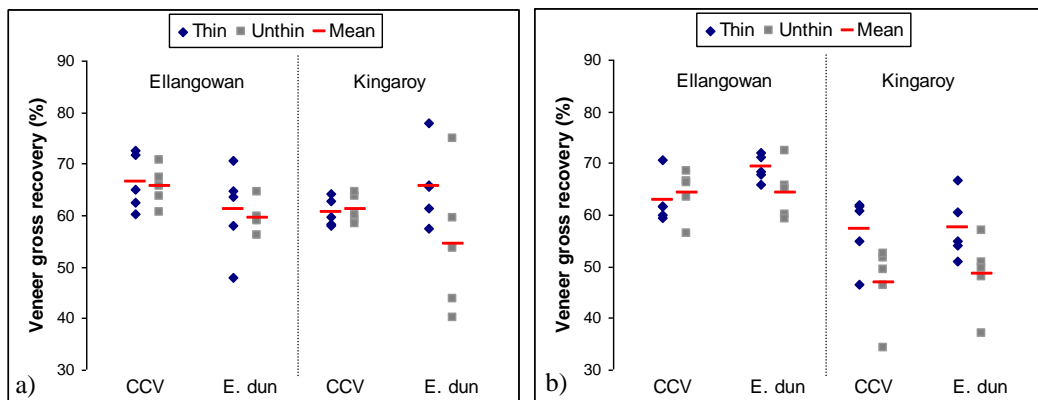


Figure 1. Veneer gross recovery for butt log (a) and top log (b) for two thinning treatments for CCV and *E. dunnii* from two sites.

Overall gross recovery was significantly influenced by site for both species. This effect was more pronounced for top logs, with recovery being lower from the drier Kingaroy site (Fig. 1). The thinning treatment significantly affected recovery for *E. dunnii* only, with unthinned trees producing less veneer recovery than those from the 300 spha thinning treatment.

The main factor affecting recovery was the short radius measured at the billet's small end ($r=0.52$). Recovery is expected to be less from small-diameter trees, as the diameter of the core is fixed regardless of the billet size, so proportionally less of the billet volume can produce veneer.

For comparison, green recoveries from billets from plantation-grown *E. nitens* from Tasmania, of larger diameter and aged 22 years, were around 47% for unpruned and 58% for pruned trees (Blakemore et al 2010). Thomas et al (2009) reported that green off-lathe recovery for *E. dunnii* for three age classes (12-year-old, 17-year-old and 34-year-old) ranged from 30 to 55%. However, different veneering systems were used in these other trials, and larger diameter residual cores remained after peeling, which accounts in part for the lower recoveries.

Most of the veneer recovered was D-grade, the lowest grade quality (Fig. 2). This is not unexpected, given the known presence of knots and other defects in plantation eucalypt logs of the size and age processed. CCV trees from the Ellangowan site had up to 38% of C-grades and better. Slightly higher percentages of better grade were recovered from the thinned treatments, in the majority of species-site combinations. Top billets yielded less of the higher veneer grades than butt billets, which may reflect a higher incidence of knots from branches in the upper parts of the stem.

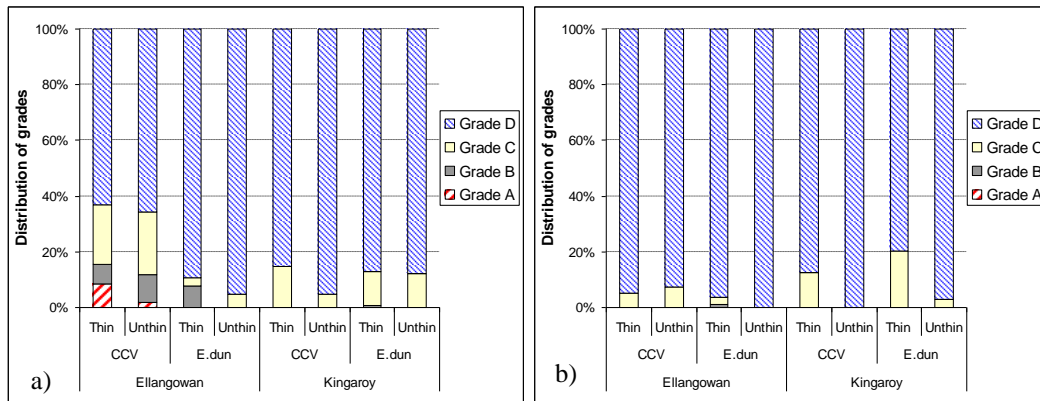


Figure 2. Proportions of different veneer grades recovered from butt logs (a) and top logs (b) for two thinning treatments for CCV and *E. dunnii* from two sites.

Some of the major limiting factors preventing veneer from meeting higher grade qualities were the high presence of kino defects and encased knots. Splits were also common in veneer from *E. dunnii* and significantly degraded its quality. The average veneer grade for individual billets based on the assessment of splits was strongly correlated with average billet end split area index from both ends. A logarithmic relationship provided better fit to data from butt billets ($R^2 = 0.68$), whereas the relationship between log end split area and veneer grade for top billets was better explained by a linear relationship ($R^2=0.48$).

Veneer properties Average veneer air-dry density ranged from 775 to 800 kg m⁻³ for CCV and 606 to 699 kg m⁻³ for *E. dunnii*. ANOVA results indicated ($p < 0.001$) that site was a significant factor influencing veneer density for *E. dunnii*. Veneer density for both species was not significantly affected by thinning treatment, billet position or their interactions.

Average veneer stiffness ranged from 13.1 to 18.2 GPa for CCV and 10.3 to 16.7 GPa for *E. dunnii*. Surprisingly, *E. dunnii* from the Ellangowan site exhibited relatively high values of veneer stiffness, similar to those of CCV, despite its significantly lower wood density. There was evidence of a significant effect of site on veneer stiffness for both species, with lower stiffness values from the drier Kingaroy site. Billet height was also shown to be significant factor for *E. dunnii* with the veneers from upper billets having greater mean stiffness. There was no significant effect of thinning treatment recorded for either species.

Despite the young age of this hardwood resource (10.5-year-old), both species display stiffness properties that are superior (or at the very least comparable) to mature plantation radiata pine, which typically has a veneer stiffness of around 10.5 GPa and is commonly used to manufacture structural plywood. Similar comparisons can be made with other species: veneer stiffness of 22-year-old plantation *E. nitens* from Tasmania achieved a maximum 10 GPa (Blakemore et al 2010) and mature 36- to 51-year-old Douglas fir from the USA averaged around 10.9 GPa (Todoroki et al 2012).

Individual trees displayed considerable radial variation in veneer stiffness (Figs. 3a, 4a) and veneer density (Figs. 3b, 4b). For about 90% of the samples, veneer stiffness ranged from 10.2 to 22 GPa for CCV and from 8.1 to 21.6 GPa for *E. dunnii*; veneer density ranged from 660 to 900 kg m⁻³ for CCV and 565 to 760 kg m⁻³ for *E. dunnii*. Radial trajectories varied from tree to tree, however there were few major changes in ranking; trees with lower veneer stiffness adjacent to the core generally had lower outer-wood stiffness.

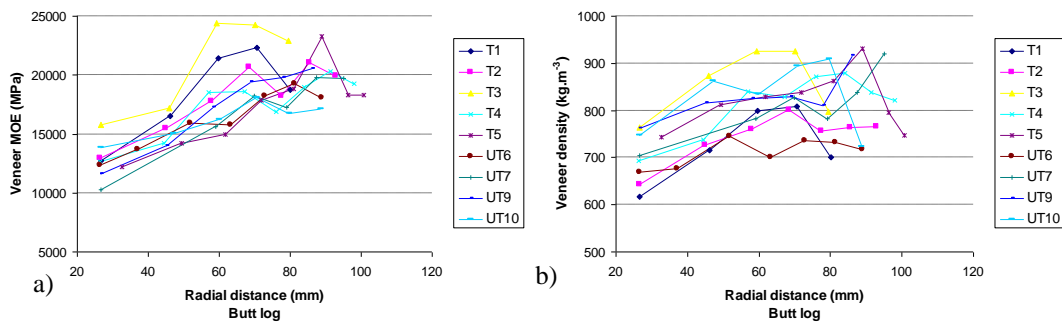


Figure 3. Example of variation in veneer properties for individual CCV trees along ribbon length from the more productive Ellangowan site: a) veneer stiffness; b) air-dry density

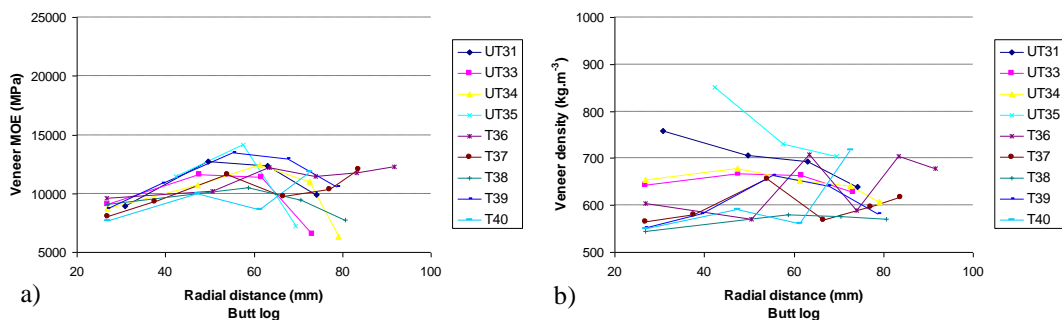


Figure 4. Example of variation in veneer properties for individual *E. dunnii* trees along ribbon from the drier Kingaroy site: a) veneer stiffness; b) air-dry density

Veneer stiffness and density in CCV increased from pith to bark at both sites, with no evidence of a major effect of site on radial trajectories (Figs. 3a, 3b). For *E. dunnii*, stiffness and density increased radially at the Ellangowan site only. At the drier Kingaroy site, veneer stiffness and density decreased outwards from middle radius to the billet periphery (Figs. 4a, 4b). It is known that wood properties are sensitive to fluctuations in

environmental conditions. Kingaroy experienced serious drought over the period 2005-2009, so drought stress may be the cause of the decline in veneer stiffness and density in the outer wood of *E. dunnii*. It appears that drought conditions at Kingaroy had less influence on the wood properties of CCV.

Standing tree acoustic velocity Standing tree acoustic velocity, determined by the Fakopp time of flight method, was a good predictor of mean veneer stiffness from butt billet, and returned significant coefficients of determination for CCV ($R^2=0.78$) and *E. dunnii* ($R^2=0.90$). Fakopp provided a reliable prediction of veneer stiffness not only from the outer part of the butt billet ($R^2=0.81$) but also from the heartwood zone ($R^2=0.74$).

Conclusions

Small spindleless veneer lathe technology is a promising processing option for producing veneer sheets from relatively small diameter logs that will optimise the recovery and use of this plantation resource. Results from veneering study indicate that relatively high veneer recoveries were achieved for the sub-tropical plantation hardwoods. When considered with the superior mechanical properties of these hardwoods, it is suggested that the veneers have attributes that are suited to several engineered wood products, including plywood and laminated veneer lumber.

References

- Blakemore P., Morrow A., Washusen R., Harwood C., Wood M. and Ngo D. (2010): Evaluation of thin-section quarter-sawn boards and rotary veneer from plantation-grown *Eucalyptus nitens*. CRC for Forestry Technical Report No. 202.
- Brancheriau L. and Bailleres H. (2003): Use of Partial Least Squares Method with Acoustic Vibration Spectra as Grading Technique for Structural Timber. *Holzforschung* 57: 644–652.
- Gavran M and Parsons M (2010): Australia's Plantations 2010 Inventory Update. National Forest Inventory, Bureau of Rural Sciences, Canberra.
- Glencross K., Palmer G., Pelletier MC. and Nichols JD (2011): Growth response to thinning in two subtropical hardwood species. CRC for Forestry Technical Report No. 217.
- Leggate W., Palmer G., McGavin R. and Muneri A. (2000): Productivity, sawn recovery and potential rates of return from eucalypt plantation in Queensland. In "The future of eucalypts for wood products". Proceedings of IUFRO conference. 19-24 March 2000, Launceston. Forest Industries Association of Tasmania.
- Nichols JD, Smith RGB, Grant J, Glencross K (2010): Subtropical eucalypt plantations in eastern Australia. *Australian Forestry* 73(1): 53-62.
- Standards Australia (2008): Plywood–Structural, Part 0: Specifications. AS/NZS 2269:2008. Standards Australia, Sydney.

Thomas D., Joe B., Austin S. and Henson M. (2009): Characterisation of plywood properties manufactured from plantation grown eucalypts. Forestry and Wood Products Australia Project No: PRB046-0809

Todoroki C., Lowell E., Dykstra D. and Briggs D. (2012): Maps and models of density and stiffness within individual Douglas-fir trees. New Zealand Journal of Forestry Science 42: 1-13.

Influence of the Tree Diameter and Shade-Tolerance on Wood Density and its Radial Variation in Madagascar Rainforest

Tahiana Ramananantoandro, Miora F. Ramanakoto, Patrick H. Rafidimanantsoa

Abstract

Wood is a material of biological origin with outstanding properties. One of its most important properties is the density. Indeed, it is connected to several functional traits of the tree and is correlated with some wood mechanical properties. This property then gives an indication of the potential uses of forest species. It is also an important parameter for estimating biomass and carbon stock of a forest resource.

Wood density varies according to various factors, such as environmental and intrinsic factors. The intrinsic factors which influence variation on wood density were studied in this research on 23 native hardwood species in natural rainforest of Mandraka (Madagascar). These factors were the tree diameter, the distance from pith and the species shade-tolerance. A total of 204 trees were studied. On each tree, core samples 1.5 mm in diameter were extracted from pith to bark at 1-1.5 m height. Measurements of wood density were performed on each 1 cm length segment cut from pith to bark. Within-tree and between-tree variations of wood density were analyzed.

The results showed that sciaphilous species have significantly higher average wood density than heliophilous species. Tree diameter doesn't have any influence on the average wood density. Concerning within-tree variation, wood density of light demanding species slightly increases from pith to bark with a positive slope of 0.002 to 0.004. That of shade-tolerant species decreases slightly with a negative slope equal to -0.001. Such information is important for understanding the behavior of the tree depending on intrinsic factors and to guide forest management activities. In addition, these results contribute to fill in the gap on wood properties database of Madagascar forest species.

Keywords: wood density, intrinsic factors, hardwood, forest, Madagascar.

Tahiana Ramananantoandro
Université d'Antananarivo
Ecole Supérieure des Sciences Agronomiques
Département des Eaux et Forêts
BP 175 Antananarivo 101, Madagascar
Tel : +261 32 44 332 25
ramananantoandro@gmail.com

Miora F. Ramanakoto
Institut Clément Ader, Université Paul Sabatier – Institut Universitaire de Technologie de
Tarbes, Département Génie Mécanique et Productique,
1 rue Lautréamont, BP 1624, 65016 Tarbes, France.
miora.ramanakoto@iut-tarbes.fr

Patrick H. Rafidimanantsoa
Université d'Antananarivo
Ecole Supérieure des Sciences Agronomiques
Département des Eaux et Forêts
BP 175 Antananarivo 101, Madagascar
rafidimanantsoa.patrick@gmail.com

A Graduate Program Bridging Forest Biotechnology and Biomaterials Engineering

Perry Peralta, Ilona Peszlen, Vincent Chiang

Abstract

Forest biotechnology is expected to play a major role in meeting future demand for wood as industrial material. Genetic engineering provides new sources of variation to traditional tree breeding and DNA transfer has been achieved to impart desired characteristics to several wood species. Tailoring specific transgenics to produce lines for optimal processing represents a significant potential for the forest products industry. It pushes the manipulation of wood properties upstream when chemical constituents and individual cells are being laid down by the tree.

Crucial to the integration of biotechnology and manufacturing are educational programs that marry materials science and tree biology. The approach is multi-disciplinary, addressing such diverse areas as tree improvement, genotype deployment, forest genetics, and wood materials science and engineering. The integration of the biological and engineering aspects of forestry will result in a cadre of researchers with the capability to tackle transformative issues such as global warming and sustainable alternatives to fossil fuel. North Carolina State University (NCSU) has developed an educational program designed to produce graduates who are proficient in forest biotechnology, biometrics, and wood engineering. This presentation describes the recruitment and selection of the fellows, their technical core and functional competencies, and their training program. Methods of assessing performance outcomes, and the resources needed for the program to be successful are also described. It is our aspiration that the presentation will encourage other universities to use the NCSU approach as a model to start their own programs that bridge Forest Biotechnology and Biomaterials Engineering.

Keywords: Graduate education program, biotechnology, genetic engineering, wood materials science and engineering

Perry Peralta, Associate Professor
Department of Forest Biomaterials
North Carolina State University, Campus Box 8005, Raleigh, NC 27695
Phone: +1-919-515-5731; Fax: +1-919-513-3496; perry_peralta@ncsu.edu

Ilona Peszlen, Associate Professor
Department of Forest Biomaterials
North Carolina State University, Campus Box 8005, Raleigh, NC 27695
Phone: +1-919-513-1265; Fax: +1-919-513-3496; ilona_peszlen@ncsu.edu

*Proceedings of the 57th International Convention of Society of Wood Science and Technology
June 23-27, 2014 - Zvolen, SLOVAKIA*

Vincent Chiang

Professor and Co-Director; Forest Biotechnology Group

Department of Forestry and Environmental Resources

North Carolina State University, Raleigh, NC 27695

Phone: +1-919-513-0098; Fax: +1-919-515-7801; vincent_chiang@ncsu.edu

**Lignocellulosic Material Science and Wood Quality
Session Co-Chairs: Barry Goodell, Virginia Tech, USA
Alfred Teischinger, Universität für Bodenkultur, Austria**

**Accessibility and Reactivity of Hydroxyl Groups in
Wood**

Roger Rowell

Professor Emeritus, Biological Systems Engineering, University of
Wisconsin, Madison, WI
rmrowell@wisc.edu

Abstract

In the reaction of wood with acetic anhydride, when no catalysis or decrystallizing solvent are used, there is always hydroxyl functionality remaining after the reaction has gone to “completion” as indicated by IR spectra. This indicates that not all hydroxyl groups have been involved in the reaction. Acetylation of wood is a good reaction to study in the accessibility and reactivity of wood as one acetyl group reacts with one hydroxyl group with no polymerization. The rate controlling parameter in this reaction is the accessibility of the reagent to the hydroxyl site. In the early stages of the reaction, lignin reacts the fastest due to the acetic phenolic hydroxyl. This is followed by the reaction with the hemicellulose polymers. No reaction seems to occur in the cellulose. Softwoods react with acetic anhydride faster and to a higher extent as compared to hardwoods. Primary hydroxyl groups react faster than secondary hydroxyl groups so woods high in xylans (hardwoods) show a slower rate of reaction and a lower level of hemicelluloses substitution as compared to softwoods. The primary intent of this research was to study the effects of acetylation on the change in equilibrium moisture content.

Key Words: Accessibility, hydroxyl groups, acetylation, reaction rate, hardwoods, softwoods.

Introduction

The polymers in the wood cell wall contain hydroxyl groups. Not all of those hydroxyl groups are accessible to moisture. The hydroxyl groups in crystalline cellulose and those buried in the lignin-carbohydrate matrix are probably not accessible to moisture. Only those hydroxyl groups in the non-crystalline portion of cellulose, and the hydroxyl groups on lignin and hemicelluloses that are not buried in the cell wall matrix are accessible to moisture.

The sorption of moisture in wood is presumed to be sorbed either as primary water or secondary water (“Figure 1”). Primary water is the water sorbed at primary sites with high-binding energies, such as the accessible hydroxyl groups. Secondary water is that water sorbed by less-binding energy – water molecules sorbed on top of the primary layer.

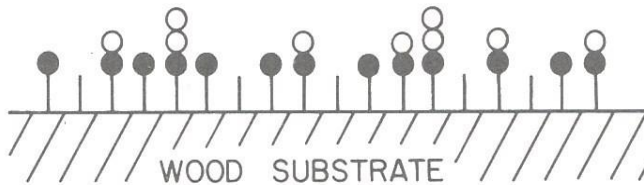


Figure 1 – Primary and secondary water on cell wall hydroxyo groups.

It is interesting that most sorption/desorption isotherms published for wood present a generic hysteresis curve, i.e. one curve fits all woods (“Figure 2”). While this may be generally true, different species of wood sorb moisture to different extents depending on amount of each cell wall polymer and extractive content (and probably on the cell wall architecture) [1]

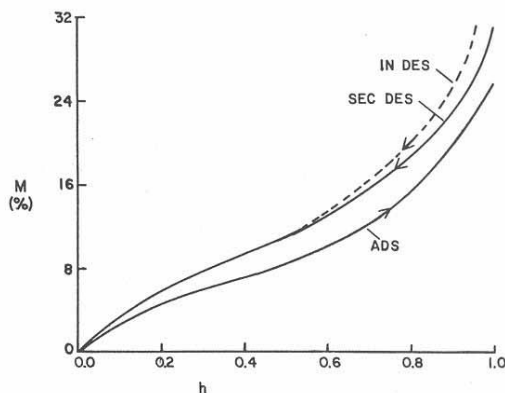
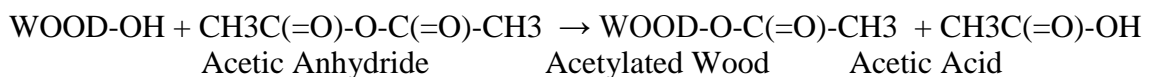


Figure 2 – Sorption/desorption isotherm for wood.

In the reaction of wood with acetic anhydride, it has been observed that softwoods react



faster and to a higher extent as compared to hardwoods (see “Table 1”). Since some of the hydroxyl sites are esterified with acetyl groups, there are fewer primary sites to which water sorbs. And since the wood is more hydrophobic due to acetylation, there may be less secondary binding sites available as well.

Table 1 - Weight gain due to reaction of Scots pine and aspen with acetic anhydride at various reaction times at 120 °C.

Wood	Weight gain (%) at reaction time (hrs)					
	0.25	0.5	1	2	4	24
Scots pine	13.7	15.4	19.5	20.7	24.9	23.7
Aspen	11.9	13.9	17.2	17.8	19.4	18.8

Isolated lignin reacts faster with acetic anhydride as compared to hemicelluloses and holocellulose (“Table 2”) [2] [3]. Kumar and Agawal reported that at an acetyl weight percent gain of 13.5, 86.4 % of the lignin was acetylated, 21.6 % of the hemicelluloses and 9.3% of the cellulose [2]. Reacting wood at 120 °C with acetic anhydride and no catalyst, at an acetyl weight gain of 16 to 19%, theoretically about 90% of the lignin is esterified, and 25% of the holocellulose [4]. It is assumed that all of the carbohydrate reactions takes place on the hemicellulose hydroxyl groups with little or no cellulose hydroxyls substituted. There may be a small amount of hydroxyls esterified on the surface hydroxyls in the amorphous regions of cellulose, however, this lack of reactivity of the isolated cellulose is based on the observation that pure wood cellulose showed no weight gain after several acetylation reactions.

Table 2 - Weight gain of pine wood and isolated cell wall polymers after reaction with acetic anhydride at 120 °C.

Substrate	Reaction Time (min)					
	15	30	45	60	120	180
Scots pine	3.8	7.1	11.2	15.0	17.8	18.4
Holocellulose	0.7	1.4	2.0	2.6	6.2	10.3
Hemicellulose	3.8	7.1	15.1	22.2	27.3	30.3
Lignin	9.8	12.7	13.7	14.8	16.7	16.9
Cellulose	0	0	0	0	0	0

“Table 3” shows the equilibrium moisture content for one soft wood (Scots pine, *Pinus sylvestris*) and one hard wood (aspen, *Populus tremuloides*) at four different relative humidity’s [5]. Note that the EMC for the hardwood is slightly lower at each RH as compared with the softwood.

Table 3 – Equilibrium moisture content of pine and aspen at different relative humidity's (27 °C)

Species	Equilibrium moisture content at:			
	30% RH	65% RH	80% RH	90% RH
Scots pine	5.8	12.0	16.3	21.7
Aspen	4.9	11.1	15.6	21.5

“Table 4” shows the cellulose, pentosans and lignin analysis for pine and aspen. Based on the data presented, it might be expected that aspen would have a slightly lower EMC as compared to pine because aspen contains a higher content of pentose polymers which do not contain a primary hydroxyl group [6].

Table 4 – Chemical composition of pine and aspen.

Wood	Alpha Cellulose	Pentosans	Klason Lignin
Scots pine	47.0	11.0	28.0
Aspen	49.0	19.0	19.0

A more detailed sugar analysis of Scots pine and aspen is given in “Table 5”. It is clear that pines, in general, have much less pentose sugars in its structure as compared to aspen.

Table 5 - Sugar analysis of Scots pine and aspen.

Wood	Percentage in Wood (%)				
	Glucose	Xylose	Galactose	Arabinose	Mannose
Scots pine	44.0	7.6	3.1	1.6	10.0
Aspen	49.0	17.0	2.0	0.5	2.1

EMC values for acetylated pine are proportional to the acetyl weight gain resulting from acetylation. A curve can be experimentally obtained and a graph can be made of EMC vs acetyl content (see “Figure 3”). The relationship is linear so that each hydroxyl group that is acetylated reduces the EMC in proportion. It might be expected that in the early stages of the reaction, the most accessible hydroxyl groups might be involved in the reaction and less available ones reacting later. But, this is not the case.

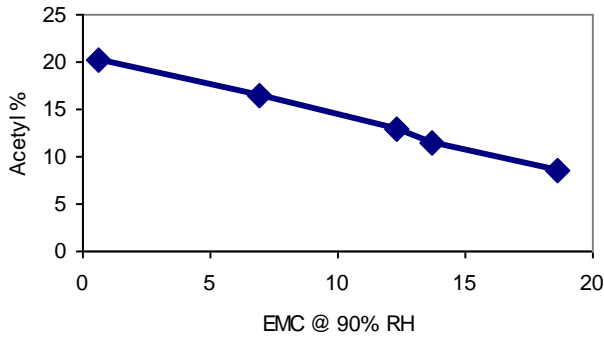


Figure 3 – Acetyl content of acetylated pine as a function of EMC.

“Figure 4” shows the sorption-desorption isotherms for acetylated spruce fibers [7]. The 10 minute acetylation curve represents a WPG of 13.2 and the 4 hour curve represents a WPG of 19.2. The untreated spruce reaches an adsorption/desorption maximum at about 35% moisture content (top), the 13.2 WPG a maximum of about 30% (middle), and the 19.2 WPG a maximum of about 10% (bottom). There is a larger difference between the adsorption and desorption (hysteresis) curves for the acetylated wood as compared to control which is not easy to explain since many of the hydroxyl groups are esterified in the acetylated samples as compared to the control.

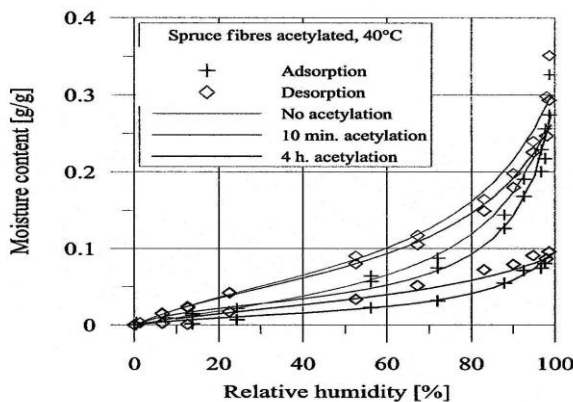


Figure 4 - Sorption Isotherm for control and acetylated spruce.

Conclusions

Acetylation of hardwoods is a slower reaction than acetylation of softwoods. The level of acetylation is lower for hardwoods as compared to softwoods. This difference may be due to more pentose sugars in the hemicelluloses in hardwoods which do not contain primary hydroxyl groups. The equilibrium moisture content decreases proportionate to the increase in acetyl content. Even at a high level of acetyl weight gain, there is still differences in the adsorption and desorption isotherm.

References

- [1] Rowell, R.M. Moisture properties, Handbook of wood chemistry and wood composites, Second Edition, Rowell, R.M., Ed, CRC Press, Boca Raton, FL, Chapter 4, 75-98, (2012).
- [2] Kumar, S. and S.C. Agarwal. Biological degradation resistance of wood acetylated with thioacetic acid. International Research Group on Wood Preservation IRG/WP/3223 (1983).
- [3] Rowell, R. M., R. Simonson, S. Hess, D.V. Plackett, D. Cronshaw, and E. Dunningham, Acetyl distribution in acetylated whole wood and reactivity of isolated wood cell wall components to acetic anhydride. Wood and Fiber Sci. 26(1):11–18 (1994).
- [4] Rowell, R.M. Distribution of reacted chemicals in southern pine modified with acetic anhydride. Wood Sci. 15(2):172-182 (1982).
- [5] Rowell, R.M., Tillman, A.-M. and Simonson. R. A simplified procedure for the acetylation of hardwood and softwood flakes for flakeboard production. J. Wood Chem. and Tech., 6(3): 427-448, (1986)
- [6] Rowell, R.M., R. Pettersen and M.A. Tshabalala. Cell wall chemistry. Handbook of wood chemistry and wood composites, Second Edition, Rowell, R.M., Ed, CRC Press, Boca Raton, FL, Chapter 3, 9-32 (2012).
- [7] Stromdahl, K. Water sorption in wood and plant fibers, PhD thesis, The Technical University of Denmark, Department of Structural Engineering and Materials, Copenhagen, Denmark, (2000).

Non-Enzymatic Deconstruction Systems in the Brown Rot Fungi

Barry Goodell¹, Valdeir Arantes², Jody Jellison¹

Abstract

Brown rot lignocellulose degrading fungi have evolved several times over the millennia to develop one or more unique mechanisms to depolymerize woody cell walls. Non-enzymatic free radical systems have been discovered which allow these fungi to at least partially eliminate the physiologically-expensive process of producing large extracellular enzymes for cell wall deconstruction. The first non-enzymatic system to be identified in *Gloeophyllumtrabeum* (Pers.) Murrill, and now found in several other brown rot species, is the chelator-mediated Fenton system (CMFS). The mechanism involves low molecular weight compounds, typically catecholates (hydroxybenzene derivatives), that bind iron from oxalate during a pH change, which occurs as these compounds diffuse from the environment immediately surrounding the fungal hyphae into the lignocellulose cell wall. Once in the buffered environment of the cell wall, the chelator-bound iron will react with peroxide within the lignocellulose cell wall, to generate the powerful hydroxyl radical oxidant via Fenton chemistry. This mechanism explains how reactive oxygen species can be generated at a distance from the fungal hyphae to protect the fungus from damage. Further it provides a basis for understanding how both cellulose and lignin are modified by brown rot fungi, with the cellulosic components being metabolized by the fungus and the lignin components re-polymerized to produce a highly recalcitrant "brown rot modified lignin" that will persist for centuries in the environment. This research helps to explain how biodegradation systems both cycle carbon back to the atmosphere, but also sequester carbon for many centuries in the soil. Further, the non-enzymatic deconstruction mechanism described, which employs reactive oxygen species, may provide a biomimetic model useful in pre-treatment systems that are required in feedstock production systems for bioenergy/biopolymer applications prior to enzymatic treatments.

Key Words: Fungi, Free Radicals, Lignocellulose Deconstruction, Bioenergy, Carbon Cycling

¹Department of Sustainable Biomaterials, 216 ICTAS II Building (0917), Virginia Polytechnic Institute and State University, Blacksburg, Virginia 24060 USA.

Goodell@vt.edu. Jody@vt.edu. Phone 01-540-231-8853

²Department of Wood Science, Faculty of Forestry, University of British Columbia, 2424 Main Mall, Vancouver, BC V6T 1Z4. valdeir.arantes@ubc.ca

Modeling the Relationship between Laboratory and Field Exposures for FRT Plywood

Jerrold E. Winandy^{1*} – *H. Michael Barnes*² – *P. David Jones*³

¹ Adjunct professor, Department of Bioproducts and Biosystems
Engineering, University of Minnesota, St. Paul MN, USA.

* *Corresponding author*

jwinandy@umn.edu

² Thompson Professor of Wood Science and Technology, Department of
Sustainable Bioproducts, Mississippi State University, Mississippi State,
MS, USA.

mbarnes@cfr.msstate.edu

³ Associate Professor, Department of Sustainable Bioproducts, Mississippi
State University, Mississippi State, MS, USA.

pdjones@cfr.msstate.edu

Abstract

Currently, no quantitative comparison exists to relate strength effects of wood samples exposed to high-temperature laboratory conditions to real-world field performance when exposed for an extended period of time as roof sheathing. Our understanding of how to interpret the laboratory-induced thermal degradation data and how it is related to real-world in-service performance of fire retardant (FR) systems is currently limited. This paper discusses critical issues that affect this relationship and then discusses our preliminary development of a theoretical model to relate the differential effects of laboratory and field exposures on strength loss in FR plywood.

Keywords: Plywood, Thermal degradation, Roof sheathing, Mechanical properties.

Introduction

Over the last 25-years a relatively large data base of plywood exposed to elevated temperatures at steady-state laboratory conditions as has been developed by the USFPL and others [Barnes et al 2008, 2010, Winandy 1997, 2001, Winandy et al 1991]. This work led to an ASTM Standard Test Method for FR-treated plywood [ASTM D 5516] and an ASTM Standard Practice for calculating bending strength design adjustment factors for fire-retardant-

treated plywood roof sheathing [ASTM D 6805]. However, the assumed exposure conditions used in the D6805 Standard Practice are based a non-verified roof temperature model and not on real-world roof temperature data. Earlier attempts at developing a steady-state versus cyclic exposure models were inconclusive [Levan et al 1996]. This paper describes an on-going project to develop a quantitative relationship between high-temperature, steady-state laboratory exposures and diurnal, seasonally-cyclic exposures in the real world because no definitive relationship based on matched data yet exists to relate the effects on wood strength loss between laboratory and field exposures..

Background

To model the quantitative relationship between thermal degradation of wood in a steady-state, high-temperature laboratory environment with that in a diurnal, seasonally-cyclic real world field exposure, we must first understand the relevant physical and environmental issues.

Materials

Plywood comes in many grades and lay-ups. Work to date has relied almost exclusively on higher grade plywood such a NN or AC. That decision was based on earlier chemical effects studies that found that higher grade materials usually experience greater treatment-related strength loss than did middle- to lower-grade materials (LeVan & Winandy 1990). Later, a specific study relation a wide range of plywood grades and thickness found little difference in either the initial or the elevated temperature effect of FRT on plywood strength (Lebow & Winandy 1998).

FR Chemicals

A number of FR-chemical treatments were evaluated and this data clearly showed that the magnitude of the initial effect of FRT on wood strength could be related to the difference in pH of the wood before and after FR treatment (Lebow & Winandy 2001).

Time-Temperature field relationships

To obtain actual field data on the temperatures and hours of exposure over the entire range of temperatures experienced for typical North American roof construction, matched test structures were built in Southern Wisconsin and Northern Mississippi. The sheathing and rafter temperature were recorded and modeled after collecting 8- and 4-years of actual field data in Wisconsin and Mississippi, respectively [Winandy et al 2000].

Modeling Laboratory & Field Data

In our modeling, matched specimens exposed in a steady-state environment of 65°C and 75% RH for 60- or 160-days were compared to field-exposed specimens, exposed for up three years in simulated roof structures in Mississippi (e.g. near Starkville, MS in Southeastern US). We analyzed for trends and quantitative relationships using non-parametric distributional analysis in which

10th, 25th, 50th, 75th and 90th percentiles of each group were modeled using regression analysis (Fig.1). For each treatment, the ratios of slopes for the mean and the five percentile levels were then averaged for laboratory and for field. Then the ratio of slopes between laboratory and field exposures can be calculated and used to develop comparative relationships for the differential rates of strength loss between cyclic-seasonal, diurnal field exposures and steady-state, high-temperature laboratory exposures. These relationships have been developed and show that depending on FR-treatment the Lab-to-Field relationship varies from 18:1 to 32:1 in a Mississippi climate (Winandy et al 2014).

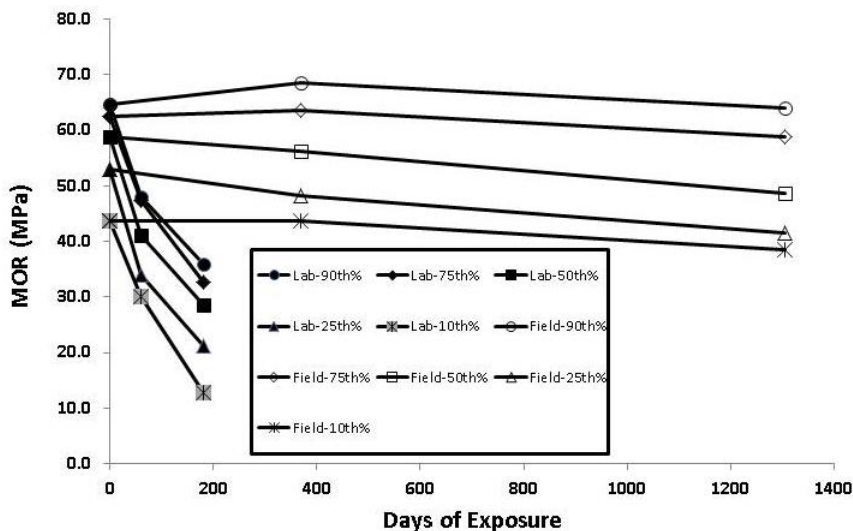


Figure 1. Comparative strength loss across the bending strength distributions for matched MAP-treated plywood exposed to high-temperature, steady-state laboratory exposure or diurnal, seasonally-cyclic exposure in Mississippi USA.

References

American Society for Testing and Materials International (2008a) Standard
American Society for Testing and Materials International (2008c) D5516-03
Standard test method for evaluating the flexural properties of fire-retardant treated softwood plywood exposed to elevated temperatures. Annual Book of ASTM Standards, Vol. 4.10. West Conshohocken, PA.

American Society for Testing and Materials International (2008c) D 6305-02 Standard practice for calculating bending strength design adjustment factors for fire-retardant-treated plywood roof sheathing. Annual Book of ASTM Standards, Vol. 4.10. West Conshohocken, PA.

Barnes, HM, Winandy, JE, McIntyre, CR (2008) Laboratory and Field Exposures of FRT Plywood: Part 1-Physical Test Data. Doc No IRG-WP 08-40426, Int Res Group on Wood Prot, Stockholm.

Barnes, HM, Winandy, JE, McIntyre, CR, Jones PD (2010) Laboratory and Field Exposures of FRT Plywood: Part 2-Mechanical Properties. *Wood Fiber Sci* 42(1):30-45.

Lebow, PK, Winandy, JE (1999) Verification of kinetics-based model for long-term effects of fire retardants on bending strength at elevated temperatures. *Wood Fiber Sci* 31(1):49-61.

Lebow, S. T., J. E. Winandy. 1998. The role of grade and thickness in the degradation of fire-retardant-treated plywood. *Forest Products Journal* 48(6):88-94.

LeVan, SL, Kim, JM, Nagel, RJ, Evans, JW (1995) Mechanical properties of fire-retardant-treated plywood after cyclic temperature exposure. *For Prod J* 46(5):64-71:

LeVan, S. L., J. E. Winandy. 1990. Effects of fire retardant treatments on wood strength: A review. *Wood and Fiber Science* 22(1):113-131.

Winandy, JE (1997) Effects of fire retardant retention, borate buffers, and redrying temperature after treatment on thermal-induced degradation. *Forest Products Journal* 47(6): 79-86.

Winandy, JE (2001) Thermal degradation of fire-retardant-treated wood: Predicting residual service-life. *Forest Products Journal* 51(2):47-54.

Winandy, JE (2013) Effects of fire-retardant treatments on chemistry and engineering properties of wood. *Wood Fiber Sci* 45(2):131-148.

Winandy, JE Barnes, HM, Hatfield, CA (2000) Roof temperature histories in matched attics in Mississippi and Wisconsin, Res. Pap. FPL-RP-589, USDA Forest Service, Forest Products Laboratory, Madison, WI, 24 p.

Winandy, JE, Barnes, HM, McIntyre, CR, Jones PD (2014) Laboratory and Field Exposures of FRT Plywood: Part 3-Modeling exposure relationships. *Wood Fiber Sci* 44(4):____-____. (In-Press).

Winandy, JE, Levan, SL, Ross, RJ, Hoffman, SP, McIntyre, CR (1991) Thermal degradation of fire-retardant-treated plywood: Development and evaluation of a test protocol, Res. Pap. FPL-RP-501, U.S. Dept. of Agriculture, Forest Service, Forest Products Laboratory, 21 p.

Elaboration of Hybrid Materials Based on TEMPO-Oxidized Cellulose Gel and Silica Nanoparticles

Chloé Maury¹; Khalil Jradi^{1,}; Claude Daneault^{1,2}*

¹ Lignocellulosic Material Research Centre, Université du Québec à Trois-Rivières, 3351 Des Forges, Trois-Rivières, Québec G9A 5H7, Canada;

² Canada Research Chair in Value-added Paper, 3351 Des Forges, Trois-Rivières, Québec G9A 5H7, Canada

* Corresponding author: Khalil Jradi (Khalil.jradi@uqtr.ca)

Abstract

In the present study, we report a simple and efficient approach for the fabrication of a hybrid material based on Tempo-oxidized cellulose gel (TOCgel) and silica nanoparticles (SilicaNPs) using the sol-gel process. The advantage in using the TOCgel material is clearly due to the presence of carboxylate (COOH) and hydroxyl (OH) moieties on the surface of TOCgel and also to the nano/micrometric size of their fibers.

In this work, silica NPS were incorporated in the cellulose nanofibers network through two routes: physical and chemical process. In the first one, Silica NPS were physically incorporated in TOCgel fibrous through hydrogen bound. However, the chemical process was accomplished firstly through the use of a cross-link agent (APTES) to realize the covalent coupling (amidation) between the carboxylate moieties of TOCgel and the APTES molecules, and secondly by the in-situ growth of SilicaNPs directly onto the surface of the TOCgel. Resulting composite films (SilicaNPs-TOCgel) were investigated by several techniques including Scanning electron microscopy, FTIR, EDX and XPS spectroscopy, mechanical tests and thermogravimetric analysis. Our results confirmed clearly the grafting state between APTES and TOCgel surface via the formation of amide bond at 1545 cm^{-1} and the strong reduction of the carboxylate moieties of the TOCgel. TGA analysis indicated the presence of silica NPS in the former composite (~ 30 %) for the both process. In the same context, SEM images indicated that the SilicaNPs seemed to be incorporated more homogeneously in the final composite obtained via the chemical process more than that obtained by the physical process. Consequently, mechanical test showed better properties for the former composite obtained through the chemical way than that for the physical one. Finally, because of the good mechanical properties and the well-aligned silica nanoparticles of the SilicaNPs-TOCgel composite films obtained in this work, they can be used as a promising material in applications of sensors, piezo-electric devices.

Keywords: Tempo oxidized cellulose; silica NPS; sol-gel process; amidation; characterization.

Morphological and structural Changes of Ultrasound treated Bacterial Cellulose

Dimitrios Tsalagkas^{1} – Rastislav Lagaňa² – Levente Csóka³*

¹ PhD student, Institute of Wood Based Products and Technologies, Simonyi Karoly Faculty of Engineering, Wood Sciences and Applied Arts, University of West Hungary, Sopron Hungary.

** Corresponding author*

dimitrios.tsalagkas@skk.nyme.hu

² Research scientist, Department of Wood Science, Faculty of Wood Science and Technology, Technical University of Zvolen, Zvolen Slovakia.

lagana@tuzvo.sk

³ Associate professor, Institute of Wood Based Products and Technologies, Simonyi Karoly Faculty of Engineering, Wood Sciences and Applied Arts, University of West Hungary, Sopron Hungary.

levente.csoka@skk.nyme.hu

Abstract

Bacterial cellulose (BC) is gaining importance in research and commerce due to numerous factors affecting the bacterial cellulose characteristics and application in different industries. Apart from crystalline structure, morphological dimensions of cellulose nanoparticles vary widely depending on the source of cellulosic material and the conditions under which extraction and purification is performed. High degree of crystallinity and size dimensions are of the most crucial parameters which make bacterial cellulose, suitable for several nanocomposite applications. Two important parameters temperature and distance of ultrasonic probe were examined to reveal the fibrillation of bacterial cellulose nanoparticles of purified nata de coco. The prepared bacterial cellulose dried thin films were characterized by Fourier transform infrared (FT-IR) spectroscopy and atomic force microscopy (AFM). Results showed that after ultrasound treatment new films were obtained with new microstructures and structural conformations, depicting differences in crystallinity and mechanical properties, depending the purification treatment.

Keywords: Bacterial Cellulose, Ultrasound, Structural Morphology, AFM, FTIR

Introduction

Bacterial cellulose is composed of a pure cellulose nanofiber mesh spun by bacteria mainly belonging to the genus *Acetobacter xylinum* and is produced mostly in static cultures (Bielecki et al. 2005). Bacterial cellulose network, due to its biosynthesis in the aqueous media binds large amounts of water – up to 99%. The reason of such interests in bacterial cellulose arises from the ease in producing a fully biobased cellulosic material which demonstrate unique properties including, very long polymer chains, high mechanical strength, high crystallinity, mimics to some extent extracellular matrix, high water holding capacity, high porosity, biocompatibility, the ability to obtain various shapes and forms and purity (Petersen and Gatenholm 2011, Gatenholm and Klemm 2010). Thus it is a useful biomaterial in many different applications including food industry applications, reinforced in paper manufacturing, biomedical applications (Gatenholm and Klemm 2010), loud speakers (Kim et al. 2009), electronic paper (Shah and Brown 2005) and biofilters for gas separation (Hosakun et al. 2014). Furthermore due to its large piezoelectric response (Csoka et al. 2012) potentially could be utilized in energy harvesting devices alone or reinforced with other piezoelectric materials (Tsalagkas and Csoka 2013).

The isolation of cellulose nanoparticles without serious degradation, at low costs and using an environmentally friendly method is always under investigation. Wang and Cheng (2009) examined the use of high intensity ultrasound to isolate fibrils from four cellulose sources: regenerated cellulose (lyocell), pure cellulose fiber, microcrystalline cellulose and pulp fiber. According to the authors, six factors may affect the efficiency of fibrillation such as power, temperature, time, concentration, size of the fibers and distance of the ultrasonic probe. Water retention value was used to evaluate and compare the effects of these factors. In general, water retention value was significantly increased by high intensity ultrasound treatment for all cellulose sources. Higher concentrations of cellulose suspensions, longer raw fibers and distance of the ultrasonic probe more than 10 mm resulted lower water retention values. In addition, higher temperature of the suspension was also helpful for cellulose microfibrillation. Furthermore, the water retention values of the fibers were increased as the treatment time increased. However, a longer treatment time could result in higher cellulose degradation.

Tischer et al. (2010) subjected bacterial cellulose pellicles to a high power ultrasonic treatment for 15, 30, 60 and 75 min. The ultrasonic treatment was carried out in an ice bath and the ice was maintained throughout the entire sonication time. Bacterial cellulose pellicles were prior purified by immersion in an aqueous solution of 0.1 M NaOH for one day. As reported by the authors this treatment was to avoid the mercerization of bacterial cellulose. Likewise, they refer, that, due to the intrinsic nature of polymerization and crystallization promoted by *Acetobacter xylinum*, the crystalline material formed is of type I and not of type II.

A two step purification process was presented by Gea et al (2011). The main objectives of this study were to just removing the organic impurities coming from the medium cultures of the high purity bacterial cellulose (in relation to plant cellulose) and to prevent

any polymorphic crystal transformation from cellulose I to cellulose II. As stated, this treatment with 2.5 wt% NaOH followed by 2.5wt.% NaOCl prevented any structural changes of the native fiber from cellulose I to cellulose II.

The purpose of this study was to analyze the effect of ultrasonic treatment on the reorganization of bacterial cellulose nanoparticles by using mild conditions and further to develop an easy, low cost and environmental friendly, optimized process to obtain nanocellulose films suitable for nanotechnology applications which require extensively high physical properties, as well as enhanced ability to be reinforced with other materials.

Materials and Methods

Nata de coco. Nata de coco is a chewy, jelly-like, translucent dessert, originated from Phillipines. Bacterial cellulose extracted from nata de coco meets the specification of pure cellulose, as was proven by FTIR, thermal properties and solubility studies and can be used as raw material for research of cellulose applications (Halib et al. 2012).

Purification of bacterial cellulose. Nata de coco cubes were washed and soaked in distilled water until the pH was neutral (pH 5-7), which could require 1-2 weeks, to remove the majority of sugar syrup. After this washing step, same amount of nata de coco (\approx 2.5-3.0 g of dried BC) were purified. In order to obtain pure bacterial cellulose, nata de coco was purified by alkaline treatment to remove the bacteria and any soluble polysaccharides and microorganisms. In the first method, nata de coco was purified by boiling a concentration of 0.5 (w/v %) in 0.1 M NaOH at 70° C for 2 h under continuous stirring. In the second treatment, nata de coco cubes were immersed overnight in 2.5 wt.% NaOH. This method hereafter referred to as one step purification. A third sample was prepared in the same way as the second sample, and successively treated with 2.5 wt.% NaOCl (two step purification). Bacterial cellulose was then rinsed with distilled water until neutral pH conditions. A fourth sample without any treatment, called untreated was used as control. After purification step, nata de coco was blended for a few minutes using a laboratory blender and homogenized, poured into silicon trays and dried up in the oven at 50° C.

Then, 0.1 wt% of dried cellulose films were added in 80 mL of distilled and was subjected to further grinding with a hand blender, prior to ultrasonication for 30 min. The concentration was estimated as solid weight percent of cellulose in distilled water. Two essential parameters of acoustic cavitation, temperature (no water bath, cold water bath and ice water bath) and distance of the ultrasonic probe (4 cm and 1 cm from the bottom of a 100 mL beaker) were investigated. Maximum power, time and volume of concentration were maintained stable. After this process, the ultrasonicated BC was reconstituted in the form of films and dried at 50° C once again.

Infrared analysis. Fourier transfer infrared (FTIR) spectra of the BC sheets were obtained using a Jasco FTIR 6300 spectrometer. Spectra were obtained in the mid infrared region ($4000-500\text{ cm}^{-1}$) at 4 cm^{-1} resolution and averaging of 50 scans by using a Diamond ATR PRO 470-H.

Atomic force microscopy. The topography and surface roughness of the cellulose films were determined using a Bruker Multimode 8 with Veeco V nanoscope analysis, using a V-shape cantilever, no-tapping mode. Width of bacterial cellulose nanofibrils was measured with Image-Pro Plus analysis software.

Results and Discussion

Temperature change. The temperature of water suspension during ultrasonication treatment changed significantly depending on time and the cooling methods used. Optical observation during process showed that maximum power needed more time to be reached when cold water and ice water bath are used. This means variations on the power also.

Effect of pretreatment by NaOH. One of the most significant treatments performed on cellulosic fibers to enhance properties such as crystallinity accessibility of unit cell structure, dimensional stability and tensile strength is mercerization. Pretreatment by NaOH swells the fibers and the fibers become more susceptible to fibrillation and remove impurities present in cellulose and affects the relative amounts of crystalline and amorphous regions and the amounts of cellulose I and cellulose II simultaneously (Colom and Carrillo 2002). Unfortunately, this mercerization process is often accompanied by an unwanted transformation of the crystal structure from cellulose I to cellulose II. Microfibrils keep its fibrillar morphology after treatments with NaOH solutions of less than 9% w/w, but change into irregular aggregates when treated with NaOH above 12% w/w corresponding to the crystal conversion to cellulose II. The crystallinity of the resulting cellulose II is very low after a brief alkali treatment (Shibazaki et al 1997).

FTIR. The FTIR spectra of bacterial cellulose prepared from nata de coco are shown in Figure 1. For further analysis, only the optimum processes of each treatment was chosen to depict the differences among them. The results of bacterial cellulose produced from nata de coco showed peaks that confirming the purity of cellulose produced. At the same time the N-H stretch peak from proteins and amino acids disappears even in the pure nata de coco. Additionally, no evidence of change in cellulose type (I to II) due to the of change in cellulose type II purification treatment was observed in the FTIR spectrum at this region, even in 0.1 M NaOH treated bacterial cellulose. This result is in accordance with Tischer et al. (.2010). 0.1 M NaOH treatment is a common method used for purification of bacterial cellulose for biomedical applications. Table 1 presents the characteristic absorption peaks and bands of bacterial cellulose obtained from nata de coco and these obtained from regenerated cellulose fibers.

The results of the infrared crystallinity ratios obtained from each film, as a function of different ultrasonic cavitation treatment are shown in Table 2. The total crystallinity (TCI) and lateral order (LOI) indices, proposed by Nelson and O'Connor (1964) and obtained from 1420/893 and 1375/2900 cm^{-1} absorbance ratios respectively, were used to study the crystallinity changes. TCI with substrates containing a high crystalline cellulose I content such as bacterial cellulose and LOI are useful to follow structural changes during caustic treatments (Colom and Carrillo 2002).

It can be seen that these infrared ratios produce different values which represent spectral differences, due to the different structural conformation of ultrasound treated cellulose. Films obtained after ultrasonication for 30 min in 4 cm cold water bath, pretreated with 2.5 wt% NaOH resulted the higher crystallinity.

Table 1: FTIR peak assignments for bacterial cellulose and cellulose II.

Bacterial cellulose (Halib et al. 2012)	Bacterial cellulose (Gea et al. 2011)	Regenerated cellulose (Colom and Carrillo, 2002)
3440 ν O-H cellulose II	3443 ν O-H cellulose II	1420 δ_s CH ₂
2926 ν CH	3345 ν O-H cellulose I	1376 δ C-H b
1440 δ CH ₂	3150-3220 ν_s N-H	1336 in plane δ C-OH
1300 δ CH	2930, 2860 ν_a CH ₂	1316 CH ₂ wagging
1163 ν C-O-C	1425-1435 in plane δ CH ₂ , C-OH	1278 δ C-H
1040 δ C-O	1146-1160 ν_a COC	1235 in plane δ C-OH
	1111 ν C-C ring (polysaccharides, cellulose)	1227 in plane δ C-OH
	870-900 out of plane CH δ vibrations	893 γ ν_s (COC) in plane

ν = stretching, δ = bending, s = symmetric, a = asymmetric

Table 2. Infrared crystallinity indexes of ultrasound treated and untreated bacterial cellulose films

Treatments	TCI A_{1372}/A_{2900}	LOI A_{1430}/A_{898}	HBI A_{3308}/A_{1330}
BC untreated	0.67	1.25	4.11
BC untreated 1 cm cold water	0.69	1.16	3.04
0.1 M NaOH untreated	0.71	1.39	3.84
0.1 M NaOH 1 cm cold water	0.72	1.27	3.68
One step pur. Untreated	0.69	1.51	3.75
One step pur. 4 cm cold water	0.88	1.28	3.31
Two step pur. Untreated	0.67	1.50	3.72
Two step pur. 1 cm ice water	0.74	1.30	3.63

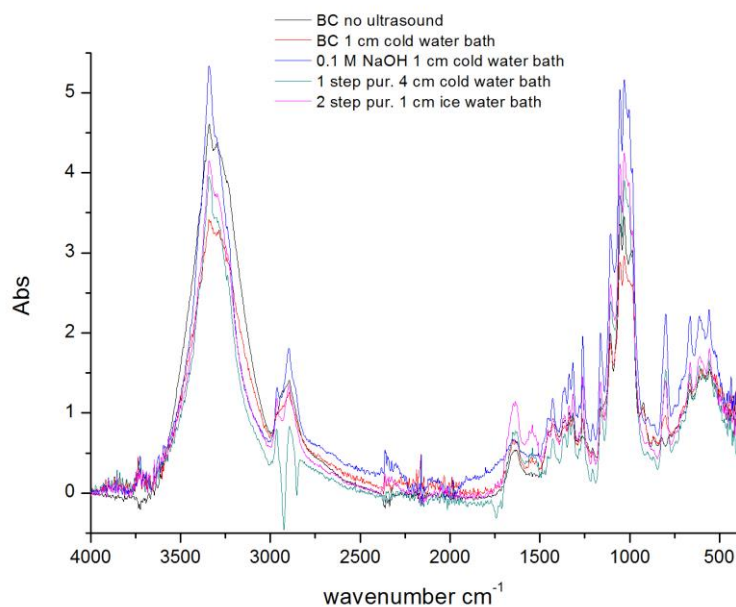


Figure 1: FTIR spectra of untreated and ultrasound treated bacterial cellulose from nata de coco

Atomic force microscopy. A polarized optical microscopy image of nata de coco is shown in Image 1. The surface morphology of cellulose microfibrils is important factor in

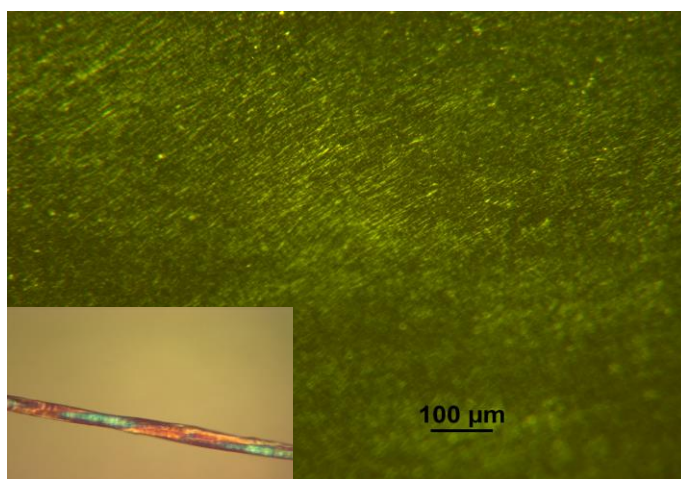


Image 1: Polarized optical microscopy of crude nata de coco.

interfacial interactions. Thus, the surface changes in width of bacterial cellulose, were determined. The mean width of the ribbons before ultrasonication, in the untreated bacterial cellulose was determined to be 39.95 (\pm 9.5) nm. In the 0.1 M NaOH treated 31.44 (\pm 9.2) nm, in one step purified 36.11 (\pm 7.6) nm and in two step purified 32.84 (\pm 10.8) nm. In 0.1 M NaOH and two step purified bacterial cellulose was apparently a

reduction in the width. In the bacterial cellulose samples that were ultrasonicated, only a slightly reduction was observed after ultrasonication. However, the estimated width of the measured microfibrils is in accordance with literature (Habibi et al. 2010). A possible explanation for the obtained width values of no-ultrasonicated bacterial cellulose is the two times grinding with high power blenders.

Yet, the ultrasonic treatment changed the microfibrillar arrangement, leading to a film with a different nanostructure. Analysis of the atomic force images illustrated more homogeneous films, more separated individual ribbons and less aggregated microfibrils. The ultrasound energy is transferred through searing and cavitation to the glucan chains, promoting the conversion of amorphous material into crystalline material (Tischer et al. 2010). The Image 2a shows the surface of untreated film, while Image 2b displays the changes in ultrasound treated bacterial cellulose.

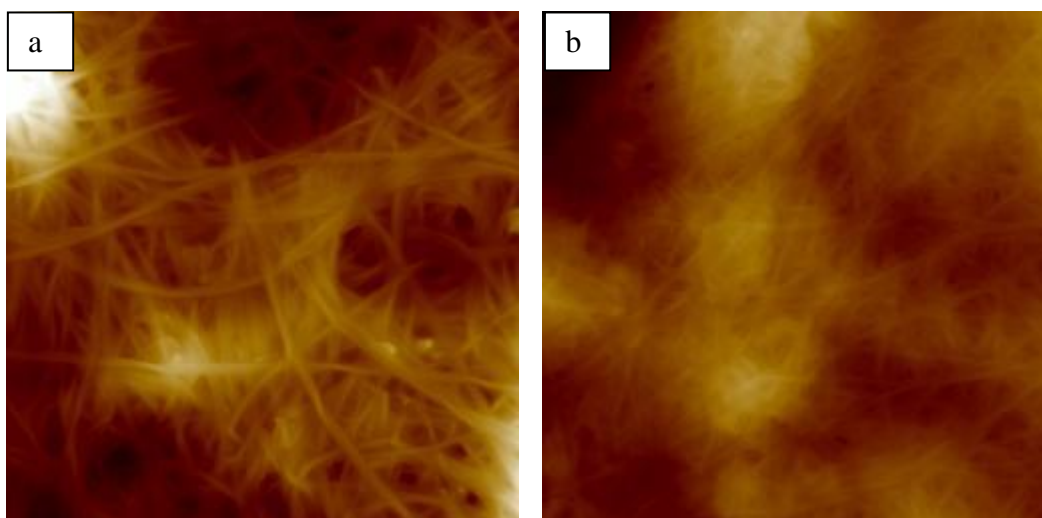


Image 2. Atomic force microscopy no tapping-mode height images of bacterial cellulose thin film: untreated (a) and ultrasonicated (b)

Conclusions

In this present work, we have demonstrated that ultrasonic processing in mild conditions was effective in changing the microfibrils structure of bacterial cellulose. The great advantage of these ultrasound treatments is that we can obtain nice, homogenous thin films, while after mechanical blending in majority cellulose nanoparticles exists as aggregates. FTIR and AFM results, revealed that ultrasound transformed the crystalline structure and consequently the mechanical properties of the obtained bacterial cellulose films. Even though FTIR spectra analysis, presents these changes, still TCI and LOI are empirical values. Thus, further analysis with XRD, TGA-DSC curves and stress-strain curves are needed in order to further verify the results.

References

- Bielecki, S., Krystynowicz, A., Turkiewicz, M., Kalinowska, H. 2005. Polysaccharides and polyamides in the food industry. Volume 1 // Wiley-Vch (edited by Alexander Steinbüchel and Sang Ki Rhee): 31-84.
- Colom, X. and Carrillo, F. 2002. Crystallinity changes in lyocell and viscose-type fibres by caustic treatment. *European Polymer Journal*. 38 (11): 2225-2230.
- Csoka, L., Hoeger, I., Rojas, OJ., Peszlen, I., Pawlak, JJ., Peralta, PN. 2012. Piezoelectric effect of cellulose nanocrystals thin films. *ACS Macro Lett*. 1 (7): 867-870.
- Gatenholm, P. and Klemm, D. 2010. Bacterial nanocellulose as a renewable material for biomedical applications. *MRS Bulletin*. 35 (03): 208-213.
- Gea, S., Reynolds, CT., Roohpour, N., Wirjosentono, B., Soykeabkaew, N. Bilotti, E., Peijs T. 2011. Investigation into the structural, morphological, mechanical and thermal behavior of bacterial cellulose after a two-step purification process. *Bioresource Technology*. 102 (19): 9105-9110.
- Habibi, Y. Lucia. LA., Rojas, OJ. 2010. Cellulose nanocrystals: Chemistry, self assembly and applications. *Chemical Reviews*. 110 (6): 3299-3850.
- Halib, N., Amin, MCIM., Ahmad, I. 2012. Physicochemical properties and characterization of nata de coco from local food industries as a source of cellulose. *Sains Malaysiana*. 41 (2): 205-211.
- Hosakun, Y., Wongkasemjit, S., Chaisuwan, T. 2014. Preparation of bacterial cellulose membranes from Nata de coco for CO₂/CH₄ separation. In: *Proceedings, ICCEE 2014: International Conference on Chemical and Environmental Engineering, Barcelona, Spain, 2014, February 27-28*.
- Kim, JH., Yun, S., Kim, JH., Kim, J. 2009. Fabrication of piezoelectric cellulose paper and audio application. *Journal of Bionic Engineering*. 6 (1): 18-21.
- Nelson, ML., O'Connor, RT. 1964. Relation of certain infrared bands to cellulose crystallinity and crystal lattice type. Part II. A new infrared ratio for estimation of crystallinity in cellulose I and II. *J. Appl. Polym. Sci*. 8 (3): 1325-1341
- Petersen, N. and Gatenholm, P. 2011. Bacterial cellulose-based materials and medical devices: current state and perspectives. *Applied Microbiology and Biotechnology*. 91 (5): 1277-1286.
- Shah, J and Brown, RM Jr. 2005. Towards electronic paper displays made from microbial cellulose. *Appl. Microbiol. Biotechnol*. 66 (4): 325-355.

Shibazaki, H., Kuga, S., Okano, T. 1997. Mercerization and acid hydrolysis of bacterial cellulose. *Cellulose*. 4 (2): 75-87.

Tischer, PCSF., Sierakowski MR., Westfahl H., Tischer CA. 2010. Nanostructural reorganization of bacterial cellulose. *Biomacromolecules*. 11 (5): 1217-1224.

Tsalagkas, D., Csoka, L. BCNs films and its potential as energy harvesting material. 2013. In: *Proceedings, Science for Sustainability, International Scientific conference for PhD students, Győr, Hungary, 2013, March 19-20.*

Wang, S., Cheng, Q. 2009. A novel process to isolate fibrils from cellulose fibers by high-intensity ultrasonication, Part 1: process optimization. *Journal of Applied Polymer Science*. 113 (2): 1270-1275.

Fibrillation of Different Lignocellulose Suspensions and their Bonding Strength to Wood Compared with Nanocellulose

Stefan Pinkl^{1} – Stefan Veigel² – Erik van Herwijnen³ –
Wolfgang Gindl-Altmutter⁴*

¹ Junior Researcher, Division Wood Materials Technologies, Wood K plus - Competence Centre for Wood Composites and Wood Chemistry, Konrad Lorenz Strasse 24, 3430 Tulln, AUSTRIA.

s.pinkl@kplus-wood.at

** Corresponding author*

² University Assistant, Department of Material Sciences and Process Engineering, Institute of Wood Science and Technology, BOKU, University of Natural Resources and Life Sciences, Tulln, AUSTRIA.

³ Senior Researcher, Division Wood Materials Technologies, Wood K plus - Competence Centre for Wood Composites and Wood Chemistry, Tulln, AUSTRIA

⁴ Professor, Department of Material Sciences and Process Engineering, Institute of Wood Science and Technology, BOKU, University of Natural Resources and Life Sciences, Tulln, AUSTRIA.

wolfgang.gindl-almutter@boku.ac.at

Abstract

Plant biomass consists of various biopolymers like cellulose, hemicellulose, lignin and pectin. For the production of nanofibrils cellulose is isolated from the natural compound and used for instance for very strong papers or as fibrils for purposes of reinforcement. Here the suitability for fibrillation in a high-pressure homogenizer of native and partially chemically digested cell walls from beech & spruce wood and sugar beet pulp is compared with cellulose from chemical wood pulp. Fibrillation of native cell walls is worse in comparison to wood pulp shown by mechanical paper tests and microscopy (electron, atomic force and light microscopy). However, for the bonding of wood non-cellulosic biopolymers could be helpful. Bonding tests of spruce wood (based on EN 302-1) show that cell wall fragments, which still contain non-cellulosic biopolymers, perform not less than nanofibrillated cellulose.

Keywords: self-adhesive force, lignocellulose, micro-and nanofibrils

Introduction

In 2012 the worldwide production volume of sawn lumber was 413 million m³ while 301 million m³ of wood-based materials were produced (FAO 2014). Particularly in the last two decades the wood-based materials industry recorded a massive growth, despite short-term reductions due to the global economic crisis. In addition to the wood properties subjected the anisotropy, the restricted dimensions because of natural tree growth contribute to the necessity of wood-based materials. The necessary adhesives almost base on fossil raw materials, why the interest for alternatives out of renewable resources is great.

Wood consists of three main biopolymers, cellulose, hemicellulose and lignin, which prove already different adhesive properties. For Pizzi it was possible to glue wood alone with friction. Those joints show strengths over 10MPa. NMR-studies revealed a cross linking action between lignin and furfural originated from hemicellulose, as well as a self-polymerization of furfural. Images show fused fibrillated cells whose network is newly twisted and then embedded in the new and hardened polymer matrix (Pizzi 2006). For many hundreds of years paper had been produced out of cellulose and its cohesion is possible completely without adhesives. Mechanical entanglement, hydrogen bonds and van der Waals forces among other things are enough, to produce today papers from Nanocellulose, those strengths reach those of steel, without any adhesive (Klemm, Kramer et al. 2011).

Outgoing from previous experience with Nanocellulose in this work the fibrillation of different lignocelluloses in a high-pressure homogenizer was examined. An interaction between the polymers of the wooden cell wall and the fibrillated lignocelluloses will be expected due to the area enlargement after the finest disintegration. Which biopolymers interact better with the wooden cell wall will be evaluated by glue attempts, to obtain a better understanding for future research about natural binders.

Materials and Methods

Materials. Different plant materials from different origin and pulping process were used for fibrillation. This ranges from never dried beech pulp from Lenzig AG (Austria) and already nanofibrillated cellulose out of kraft pulp from Daicel Finechem Ltd. (Japan). For lignocellulosic materials dried wood, spruce and beech from the institute belonging carpentry is used but also byproducts of food industry, particularly sugar beet pulp from CO Agrana (Austria). Respective dry content is listed in Table 3.

Table 3 Dry weight of different materials

never dried beech pulp (NFCs)	77,1%	beech (Be)	93,2%
nanocellulose (Daicel) (NFCK)	8,6%	spruce (Sp)	91,7%
sugar beet pulp (SBP)	27,2%		

Methods. The nanofibrillation takes place in a high-pressure homogenizer (APV1000) between 600 and 800bar, a dry matter of 0,5% and is repeated for 20 passages. Wood is previously milled at dry state in a cutting mill (Retsch) with a 0,2mm sieve and later wet (7% dry matter) in a toothed colloid mill (FrymaKoruma MZ80) at narrowest mill gap, repeated 5 times. Sugar beet pulp is previously milled only in the toothed colloid mill to enable the subsequent nanofibrillation.

Additionally all variants are modified in a previous chemical digestion before the homogenization step. A TEMPO mediated carboxylation of cellulose is applied for never dried beech pulp (**tNFCs**). The reaction performs for two hours at 60°C under neutral pH conditions (Saito, Hirota et al. 2009). To modify the chemical structure of wood, the milled wood flour is treated with 0,125M NaOH at room temperature for two hours under permanent stirring (**cBe**, **cSp**) (Gregorova, Wimmer et al. 2009). Sugar beet pulp is treated in 0,5M NaOH at 80°C for two hours, afterwards washed with deionized water, then NaOH and again with water. In a further step the pulp is bleached with NaClO₂ at 70°C for two hours, followed again by a washing step with water (**cSBP**) (Leitner, Hinterstoisser et al. 2007). A part of the fibrillated suspensions is used for film casting in PTFE coated petri dishes under the fume hood to produce later tensile test samples (55x10x<1mm). Their material properties (tensile strength, Young's Modulus, elongation) are tested in a universal testing machine (ZwickRoell020+LaserExtensometer) at 22°C and 50±5%RH. A microscopic characterization and analysis of fibrillation degree is done with a light microscope (Carl Zeiss Axioplan2ie MOT), scanning electron microscope (FEI Quanta FEG 250) and an atomic force microscope (Bruker Dimension icon with Scan Asyst). The adhesive properties are tested based on standard EN 302-1 but with spruce instead of beech with the upper named universal testing device with lap shear test samples. Therefore, the suspensions are concentrated after the homogenization step to 3% dry matter in a drying kiln at 80°C. After that, the suspensions are applied on newly planed spruce lamellas (thickness 5mm) with a spatula (application quantity 30, 60 and 120g/m²). In a hydraulic press (Langzauner LZT-OK 175L) the lap shear samples are pressed at a pressure of 0,5MPa and 50°C for 3 days and later conditioned at 20°C and 75%RH. Variants pressed at 120°C stay in press for 15 minutes and are conditioned fixed to avoid warp. For light-microscopic analysis of adhesive joint samples (4x4x2mm) from the lap shear samples are embedded in epoxy resin (Agar Scientific Low Viscosity Resin KIT R1078) whose surfaces are finished with a microtome.

Results and Discussion

Differences between the homogenized suspensions are obvious after a few hours in a beaker by different sedimentation rates. Sugar beet deposits very fast, Be and Sp less quickly, whereby chemically modified variants deposit more slowly. NFCs, NFck, tNFCs and cSBP suspensions stay homogenous over months what refers to a high degree of fibrillation.

Microscopy: Distinguishing for rapid deposition are large unfibrillated bundles that are present at SBP, Be and Sp. cSBP and tNFCs are fibrillated to such small sizes that no particles can be detected under the light microscope. No distinction between the two unmodified cellulosic variants is visible.

Under the scanning electron microscope, the differences are clearer. NFCs, NFCk and cSBP are better fibrillated compared to Be, cBe, Sp and cSp, so the microfibrils are no longer bundled. At tNFCs the microfibrils are especially fine and visibly not bundled anymore. On the surface of dried films the isolated fibrils are also present at Be, cBe, Sp and cSp, otherwise the fibrilbundles are fibrillated only superficially.

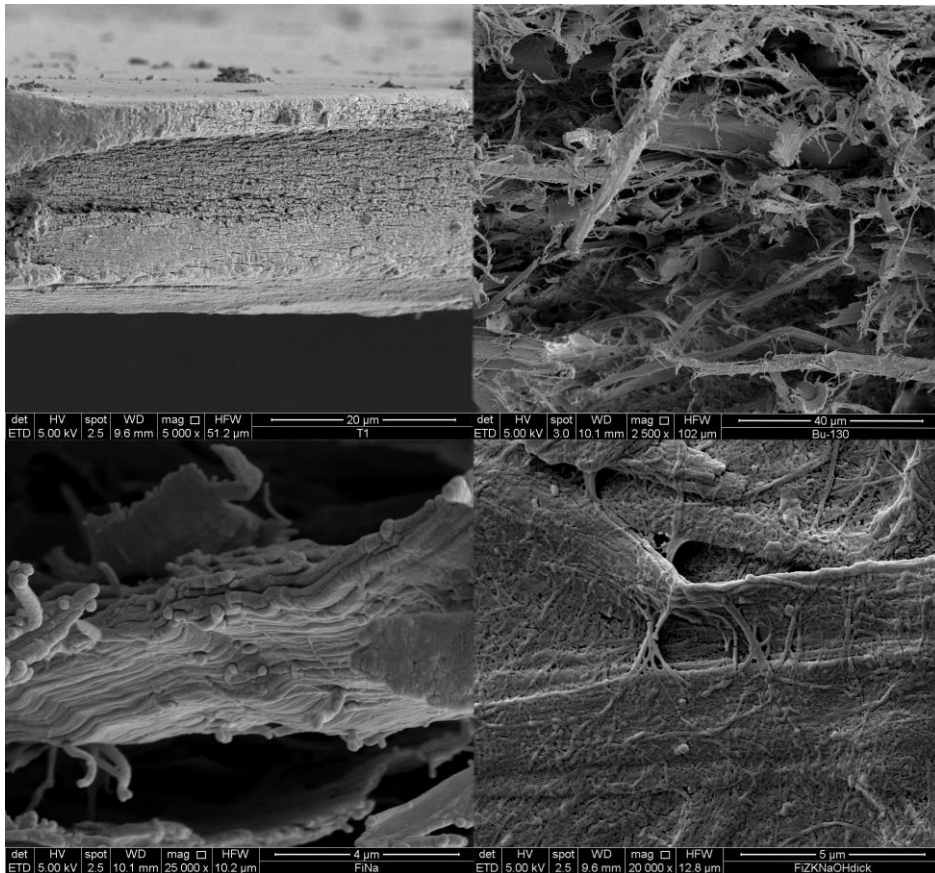


Figure 10 top left: tNFCs, fine fibrillated network; top right: Be, bundles only fibrillated on its surface; down left: cSP, fibrils still in bundles; down right: separated fibrils on films surface.

Under the atomic force microscope even fine fibrils and their diameter over the height can be analyzed. At all variants, nanofibrils with diameter below 10nm exist, especially at cSBP and tNFCs are many elementary fibrils until 1,5nm detectable.

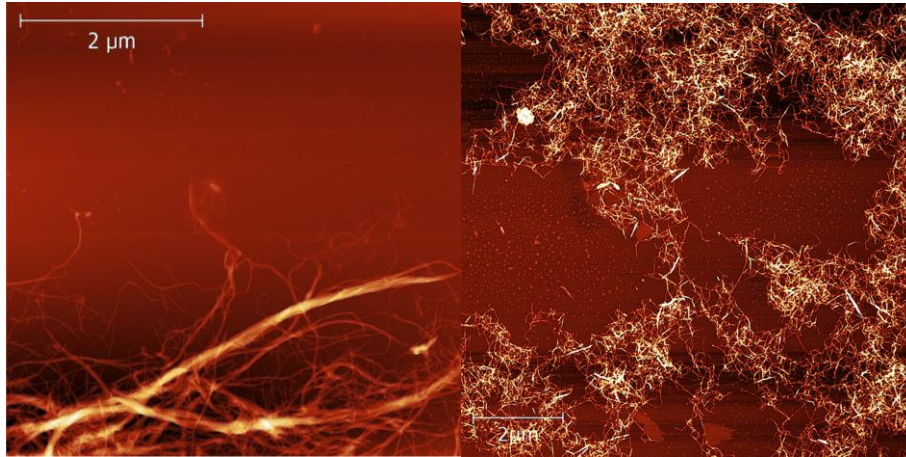


Figure 11 Atomic force microscopy: *left*: cSBP with elementary fibrils measuring 3-4nm in diameter; *right*: tNFCs elementary fibrils measuring 1,5-2nm.

Mechanical properties of dried films: Cohesive strength of adhesives is one critical property in bonding theory. Tension tests of samples out of the casted, dried films show that tNFCs feature tension strength over 150MPa. Also NFCs and NFCk are in the area of 100MPa. Untreated lignocelluloses form very fragile films that do not get over 20MPa. By chemical pretreatment the strengths climb clearly, particularly cBe and cSBP reach the NFCs level almost under 100MPa, even though many undissolved polymers beside Cellulose are contained.

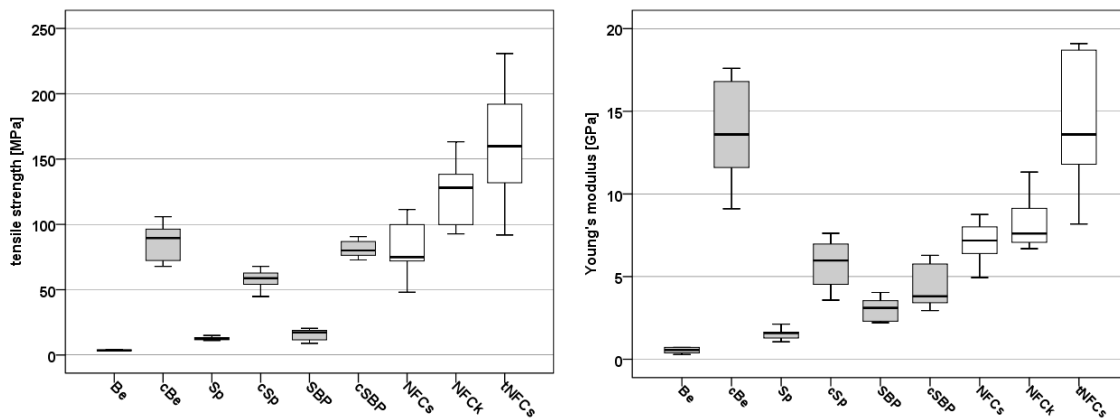


Figure 12 Results of films tensile test: gray=lignocellulose, white=cellulose; *left*: tensile strength (MPa) of films from dried homogenized suspensions; *right*: Young's modulus of same specimens.

The linear elastic behavior of the different films shows for the celluloses similar results with up to 19GPa Young's Modulus. For the lignocelluloses, the untreated variants are once more very fragile and less stiff. However, the chemical treatment causes a clear increase in stiffness particularly for beech. Possibly, because of increased crystallinity after alkaline treatment since more free hydroxyl groups exist (Das and Chakraborty 2006). For sugar beet pulp, the stiffness increases little but the base level is generally something over the other untreated variants.

Films with notably high strain yield the variants cSBP, NFCs and NFCk with up to 10% breaking elongation. That enables the known slide-stick mechanism of hydroxyl groups from cellulose chains, which form again hydrogen bonds after break. This phenomenon is apparent also in force progression, where after a plastic deformation the curve again rises before the test specimen cracks. Half as extendible are films from tNFCs. All further variants remain under 3%.

Adhesive quality: Beside cohesive strength, the adhesion of the bonding agent plays a major role in bonding theory. The testing of adhesives quality following standard EN 302-1 proves the shear strength of glue line where also adhesion influences results. The 3 cellulosic variants achieve no higher shear strengths than lignocelluloses. Untreated sugar beet has a higher adhesive quality compared to the other variants with the exception of cBe and tNFCs ($p < 0,05$). This indicates that high cohesive strengths are not necessarily conterminous with high adhesive quality. SBP features particularly low cohesive strengths when testing adhesives quality values above 3MPa are achievable.

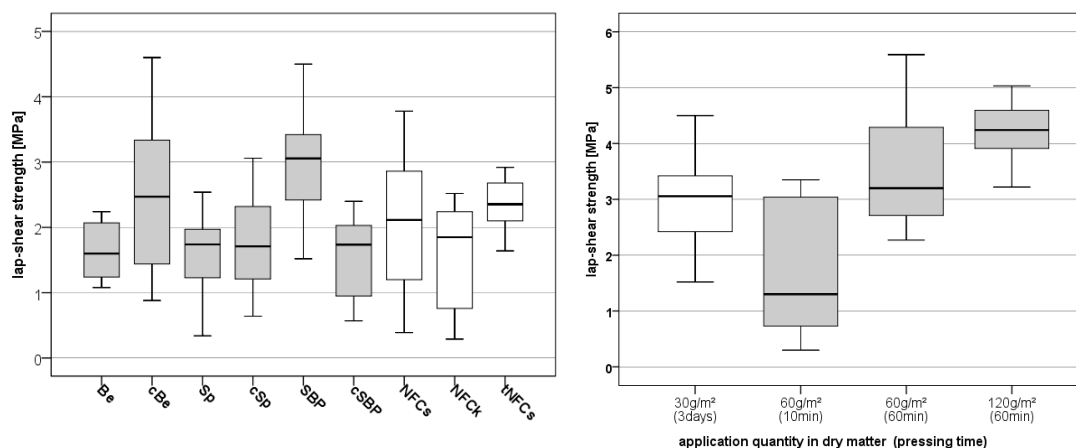


Figure 13 *left:* lap-shear strength of homogenized suspensions as adhesive for spruce wood; *right:* lap-shear strength of fibrillated sugar beet at different pressing conditions (white=cold, gray=120°C).

Commercially available adhesives for wood-based materials have to reach higher shear strengths. They have to be tested on beech because according to standard 10MPa have to be achieved where the shear strength of spruce is already exceeded. In a second experiment, the pressing time is shortened by raising pressing temperature and application amount is approached to usual industrial quantities (Figure 13). As a result, strengths increase further over 4MPa what approximately is half the shear strength of spruce (Konnerth and Gindl 2006). The evaluation of surface of break shows partial wood break in the form of fiber coating on the adhesive.

The temperature was kept low at the tests to modify wood and adhesive very little. For explanation, why SBP suits best the conversion of hemicellulose to furfural that has known bonding properties can more or less be excluded. In SBP beside hemicellulose and cellulose great amounts of pectin and proteins are contained (27 or 7%) (Dinand, Chanzy et al. 1999). Bonding properties of proteins are known and were used before the petrochemical renaissance. Pectins are located in the middle lamella between the wood

cells. The microscopic analysis of glue lines shows that fibrillated cells are too big for entering lower cell rows of wood-components. Few fibrils adhere on S3 which surface is apolarer (Obersriebnig, Konnerth et al. 2013). A huge part of gluing area make newly cut cells and cell-spaces where percentage of Pectin is higher.

Conclusion

In the high-pressure homogenizer lignocelluloses fibrillate not as fine as pure cellulose or carboxylated cellulose those fibrillation is possible until elementary fibrils. On the basis of diameter reduction of fibrils and fibril bundles the probability for failures and irregularities inside the material reduces which indicate high tension strengths of “glue films”. Only a chemical pretreatment and a partial destruction of noncellulosic matrix polymers induce to higher cohesive strengths. To asses adhesives quality adhesion plays also an important role for which noncellulosic matrix polymers may be more suitable. So show untreated sugar beets the highest shear strengths over 4MPa what corresponds to the half shear strength of spruce. Cellulose may form hydrogen bonds to cellulose. If wood is glued the cellulose fibrils however are not accessible but enclosed from lignin, hemicellulose and pectin. Hence, it would be an asset if development of natural binders is rather based on this biopolymers.

References

- Das, M. and Chakraborty, D. (2006). "Influence of mercerization on the dynamic mechanical properties of bamboo, a natural lignocellulosic composite." Industrial & Engineering Chemistry Research **45**(19): 6489-6492.
- Dinand, E., Chanzy, H. and Vignon, M. R. (1999). "Suspensions of cellulose microfibrils from sugar beet pulp." Food Hydrocolloids **13**(3): 275-283.
- FAO (2014). 2012 Global Forest Products Facts and Figures. Rome, Forest Economics, Policy and Products Division. FAO Forestry Department.
- Gregorova, A., Wimmer, R., Hrabalova, M., Koller, M., Ters, T. and Mundigler, N. (2009). "Effect of surface modification of beech wood flour on mechanical and thermal properties of poly (3-hydroxybutyrate)/wood flour composites." Holzforschung **63**(5): 565-570.
- Klemm, D., Kramer, F., Moritz, S., Lindström, T., Ankerfors, M., Gray, D. and Dorris, A. (2011). "Nanocelluloses: A new family of nature-based materials." Angewandte Chemie - International Edition **50**(24): 5438-5466.
- Konnerth, J. and Gindl, W. (2006). "Mechanical characterisation of wood-adhesive interphase cell walls by nanoindentation." Holzforschung **60**(4): 429-433.
- Leitner, J., Hinterstoisser, B., Wastyn, M., Keckes, J. and Gindl, W. (2007). "Sugar beet cellulose nanofibril-reinforced composites." Cellulose **14**(5): 419-425.

Obersriebnig, M., Konnerth, J. and Gindl-Altmutter, W. (2013). "Evaluating fundamental position-dependent differences in wood cell wall adhesion using nanoindentation." International Journal of Adhesion and Adhesives **40**: 129-134.

Pizzi, A. (2006). "Recent developments in eco-efficient bio-based adhesives for wood bonding: opportunities and issues." Journal of Adhesion Science and Technology **20**(8): 829-846.

Saito, T., Hirota, M., Tamura, N., Kimura, S., Fukuzumi, H., Heux, L. and Isogai, A. (2009). "Individualization of Nano-Sized Plant Cellulose Fibrils by Direct Surface Carboxylation Using TEMPO Catalyst under Neutral Conditions." Biomacromolecules **10**(7): 1992-1996.

Determination of the Anisotropic Elastic Features for Wood by an Ultrasonic Method

Ya. Sokolovskyy¹ – O. Storozhuk²

¹ Prof. Dr.-Ing., Department of Information Technology, National Forestry University (UNFU), Ukrainian.
sokolowskyyyar@yahoo.com

² Assistant Professor, PhD, Department of Information Technology, National Forestry University (UNFU), Ukrainian.
storozhuk@nltu.lviv.ua

Abstract

The range of problems which are related to an establishment of wood strength properties regular dependence with the parameters of ultrasonic waves taking into account temperature and humidity of a material.

Mathematical model of acoustic wave spreading in such anisotropic elastic materials as wood further developed, that establishes a relationship between the mechanical properties of wood and spreading of acoustic waves with the changing temperature and humidity of material, for the first time a mathematical model of acoustic waves spreading in a wood proposed, which takes into account exponential type functions with rheological behavior of wood and allows determination of viscoelastic properties, methods of determining a speed of acoustic waves spreading in a wood developed, which reduced measurement error significantly.

Also the appliance and equipment developed for ultrasonic examinations which allowed ensuring a possibility of carrying out of the experimental acoustic studies in a wide spectrum of the moisture and temperature conditions.

The results allow to predict the mechanical properties of wood for the acoustic waves spreading with the changing temperature and humidity of the material; acoustic methods simplify and speed determination of wood mechanical properties, device which was designed and developed provides contactless determination of the speed of acoustic waves spreading in a wood; algorithms for processing acoustic signals developed as well.

On the basis of estimated dependences between the ultrasonic wave speed of spreading and wood strength properties, the new acoustic method for qualimetry of wood assorting by its strengths for coniferous and a hardwood species on structural function of rectangular cut is developed.

Keywords: wood, a tensor of elasticity moduluses, anisotropy, temperature, moisture, ultrasonic methods, speed of an ultrasonic wave distribution.

Introduction

Wood refers to the capillary-porous materials and has the anisotropy of mechanical characteristics, which leads to some difficulties in the process of its investigation. In recent decades, the possibility of experimental determination of the wood and wood composite materials' mechanical characteristics by non-destructive methods of control, particularly acoustic is outlined in scientific articles. Mostly, the experimental acoustic studies performed in room temperature conditions and in a limited range of humidity are described. Only a few studies were conducted in a wide range of temperature and humidity changes [2,4-7]. Today the topic of wood mechanical characteristics determination with the help of acoustic methods is not enough investigated. In particular, the analysis of literature showed that nowadays the development of mathematical models that could describe the acoustic waves spreading in the wood as a viscoelastic material is of vital importance.

Materials and Methods

Theoretical results. A spatial mathematical model of the acoustic waves spreading in anisotropic elastic materials concerning the wood which establishes a relationship between the wood mechanical properties and the speed of acoustic waves spreading is accomplished.

The equation of motion, which is derived from the fundamental law of dynamics, taking into account Hooke's law can be written as:

$$\rho \frac{\partial^2 u_i}{\partial t^2} = c_{ijkl} \frac{\partial^2 u_l}{\partial x_j \cdot \partial x_k} \quad (1)$$

where: ρ – density of material (mass per unit volume), u_i – movement along the axis i , c_{ijkl} – the components of the elasticity tensor of elasticity, t – time.

The spreading of a plane sinusoidal wave in the wood can be written as:

$$u_i = A_i \cdot e^{i(\omega t - kx)} = A_i \exp[i(\omega t - kx)] \quad (2)$$

where: A – the wave amplitude, k – the wave vector, ω – the cyclic frequency, $i^2 = -1$.

By substituting the relations (2) in (1) after the mathematical transformations we obtain the equation of the following form

$$c_{ijkl} A_l n_k n_j - \rho A_i v_\phi^2 = 0 \quad (3)$$

By introducing the tensor of the second rank $\Gamma_{il} = c_{ijkl} n_k n_j$, the equation (3) can be written as follows :

$$\left(\Gamma_{il} - \rho \delta_{il} v_\phi^2 \right) P_m = 0 \quad (4)$$

where: δ_{il} – the Kronecker symbol, $P_m(p_1, p_2, p_3)$ – the unit vector component in the direction of displacement (polarization).

Expression (4) is a system of three homogeneous linear equations which provide the ratio between the components of the elasticity tensor c_{ijkl} and the phase velocity v_ϕ of the acoustic wave which spreads in the homogeneous anisotropic elastic medium.

In order to ensure that the system of equations (4) have a solution different from $p_1 = p_2 = p_3 = 0$, it is necessary that the determinant consisting of $(\Gamma_{il} - \rho\delta_{il}v_\phi^2)$, was equal to zero.

Because of the symmetry of the elastic moduli the tensor Γ_{il} is also characterized by the symmetry conditions $\Gamma_{li} = c_{ljki}n_jn_k = c_{kilj}n_jn_k = c_{ikjl}n_jn_k = c_{ijkl}n_jn_k = \Gamma_{il}$.

Since the wood is considered as an orthotropic material, the number of independent tensor components of elastic moduli decreases from twenty one to nine.

Thus, the Christoffel tensor for the wood as the orthotropic material takes the form:

$$\begin{aligned} \Gamma_{11} &= c_{11}n_1^2 + c_{66}n_2^2 + c_{55}n_3^2, \Gamma_{22} = c_{66}n_1^2 + c_{22}n_2^2 + c_{44}n_3^2, \Gamma_{12} = (c_{12} + c_{66})n_1n_2, \\ \Gamma_{33} &= c_{55}n_1^2 + c_{44}n_2^2 + c_{33}n_3^2, \Gamma_{13} = (c_{13} + c_{55})n_1n_3, \Gamma_{23} = (c_{23} + c_{44})n_2n_3, \\ \Gamma_{21} &= \Gamma_{12}; \Gamma_{31} = \Gamma_{13}; \Gamma_{32} = \Gamma_{23}. \end{aligned} \quad (5)$$

Now we consider the system of equations (4) in the case of acoustic bulk wave spreading along the axis of the wood symmetry. By substituting the appropriate values of the Christoffel tensor (5) we obtain:

$$\begin{aligned} (c_{11}n_1^2 + c_{66}n_2^2 + c_{55}n_3^2 - \rho v_\phi^2) \times (c_{66}n_1^2 + c_{22}n_2^2 + c_{44}n_3^2 - \rho v_\phi^2) \times \\ (c_{55}n_1^2 + c_{44}n_2^2 + c_{33}n_3^2 - \rho v_\phi^2) = 0 \end{aligned} \quad (6)$$

From the equation (6) it follows that along each axis of symmetry depending on the polarization fluctuations it is possible to have three types of acoustic waves, longitudinal and two transverse ones. Thus, by considering the acoustic waves spreading along the axis of the symmetry wood, we can determine the six diagonal tensor components of the elastic moduli $c_{\alpha\alpha} = \rho v_\phi^2$, $a = 1...6$. The off-diagonal tensor components of the elastic moduli can be calculated, provided the acoustic wave spreading in the direction that does not coincide with the symmetry axes [1].

The problem of the acoustic waves spreading in the wood, taking into account its viscoelastic properties is of vital importance nowadays. Synthesized mathematical model of the acoustic waves spreading with regard for the exponential type of relaxation kernel wood.

The solution to the equation of motion (1) can be represented as:

$$u(x, \tau) = G(x, \tau) ** F(x, \tau) + \gamma^2 \left[\dot{G}(x, \tau) * \varphi(x) + G(x, \tau) * \psi(x) \right]; \quad (7)$$

$$\sigma(x, \tau) = G_\sigma(x, \tau) ** F(x, \tau) + \gamma^2 \left[\dot{G}_\sigma(x, \tau) * \varphi(x) + G_\sigma(x, \tau) * \psi(x) \right]; \quad (8)$$

where: $G(x, \tau)$ – the dominant function for interchange, $F(x, \tau)$ – the massive power, $G_\sigma(x, \tau)$ – the dominant function for stress, φ and ψ – scalar and vector potential of the movement vector u , γ – the ratio setting of the acoustic waves spreading rate, * – the convolution in time.

In order to find these functions it is necessary to apply consistently the integrated Fourier transforms on the spatial coordinates x (q – the transformation parameter, marked "F" for the Fourier transforms) and the Laplace transform in time τ (s – the transformation parameter, marked "L" for the Laplace transform).

Inverse transformations are performed consistently. We first determine the original of the dominant function by Fourier

$$G^L(x, s) = \frac{k(s)}{2s\gamma} e^{-\gamma|x|k(s)}; \quad G_\sigma^L(x, s) = -\frac{\text{sign}(x)}{2\eta_\alpha} e^{-\gamma|x|k(s)}. \quad (9)$$

where: $\text{sign}(x)$ – signature x , η_α – the parameter that depends on the Poisson coefficient, $k(s)$ – the function which takes into account the core of wood relaxation.

After a series of mathematical operations the end result can be presented in a such form:

$$G_\sigma^L(x, s) = -\frac{\text{sign}(x)}{2\eta_\alpha} e^{-syk(s)} = -\frac{\text{sign}(x)}{2\eta_\alpha} e^{-sy} f^L(y, s + \beta) \quad (10)$$

$$f^L(y, s) = f_1^L(y, s) f_2^L(y, s);$$

$$f_1^L(y, s) = e^{-syk_1(s-\beta)} = e^{-sy \sum_{m=1}^{m^*} a_m [s^L(s-\beta)]^m} = e^{-sy \sum_{m=1}^{m^*} a_m \left(\frac{A}{s}\right)^m} = e^{\sum_{m=1}^{m^*} -y a_m A^m s^{1-m}};$$

where: $f_2^L(y, s) = e^{-syk_2(s-\beta)} e^{\beta y [k_1(s-\beta) + k_2(s-\beta)]} = \sum_{m=0}^{\infty} \frac{c_m(y)}{s^m} =$

$$= \sum_{j=0}^{\infty} \frac{1}{j!} \left[\frac{-y(s-\beta)A^{m^*+1}}{s^{m^*+1}} \sum_{m=0}^{\infty} \frac{a_{m+m^*+1} \cdot A^m}{s^m} \right] \cdot \sum_{k=0}^{\infty} \frac{1}{k!} \left[\beta y \sum_{m=1}^{m^*} \frac{a_m A^m}{s^m} \right]^k,$$

A, a, β – physical properties of the material.

$$G^L(x, s) = \frac{1}{2s\gamma} k(s) e^{-syk(s)} = \frac{1}{2s\gamma} e^{-sy} g^L(y, s + \beta) \quad (11)$$

$$g^L(y, s) = f_1^L(y, s)g_2^L(y, s); g_2^L(y, s) = k(s - \beta)e^{-syk_2(s-\beta)}e^{\beta y[k_1(s-\beta)+k_2(s-\beta)]} =$$

$$\text{where: } = \sum_{m=0}^{\infty} \frac{d_m(y)}{s^m} = \left(1 + \sum_{m=1}^{m^*} \frac{a_m A^m}{s^m} + \frac{A^{m^*+1}}{s^{m^*+1}} \sum_{m=0}^{\infty} \frac{a_{m+m^*+1} \cdot A^m}{s^m} \right) \times$$

$$\times \sum_{j=0}^{\infty} \frac{1}{j!} \left[\frac{-y(s-\beta)A^{m^*+1}}{s^{m^*+1}} \sum_{m=0}^{\infty} \frac{a_{m+m^*+1} \cdot A^m}{s^m} \right] \cdot \sum_{k=0}^{\infty} \frac{1}{k!} \left[\beta y \sum_{m=1}^{m^*} \frac{a_m A^m}{s^m} \right]^k.$$

The coefficients $c_m(y)$ are determined by the rules of the power-series [3].

Development of the experimental equipment. In order to ensure the conduction of the experimental studies series in the acoustic variable climatic conditions the experimental setup of acoustic studies (Fig. 1) and the laboratory climatic chamber have been outlined and developed at the Department of Information Technology, National Forestry University (UNFU), Ukraine (Fig. 2).

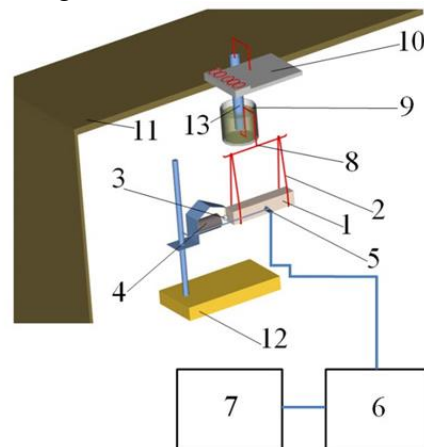


Figure 1. Axonometric block diagram of the experimental setup of acoustic researches. 1 – pattern in the shape of a parallelepiped; 2 – suspension; 3 – pendulum mechanism; 4 – electromagnet; 5 – microphone; 6 – filter; 7 – frequency meter; 8 – oil seal thrust for weighing the samples in a climate chamber; 9 – bath with oil; 10 – electronic weight; 11 – wall of the climatic chamber; 12 – anchor installation; 13 – oil seal tube.

In order to control the chamber mechanisms and systems a two-channel controller RD2 of NPF “REGMIK” production is used, the controller is equipped with RS232/RS485/USB interface for its connection with a PC. This allows: to use the PC software “system of data collection”, which provides the possibility to read, view and record the information from the device and the humidity and temperature sensor; to display the information in tabular or graphical form; to conduct rapid change in the regulatory parameters of the device. [6,7].

Obtained by the method of free oscillation data rate of acoustic waves penetration in the temperature range (from 18 to 60⁰C) and moisture content of wood (inside) is shown in (Fig. 3). The speed of acoustic oscillations (SAO) (acoustic free oscillation method) was determined by means of sample frequency and size in appropriate direction:

$$C = 2 \cdot l \cdot f = 2 \cdot l \cdot (n / T) \quad (12)$$

where: C – the speed of acoustic oscillations; l – the sample size in the direction of oscillation; f – the resonant frequency; n – the number of periods in the selected area of the timing diagram; T – the length of selected area of the timing diagram.

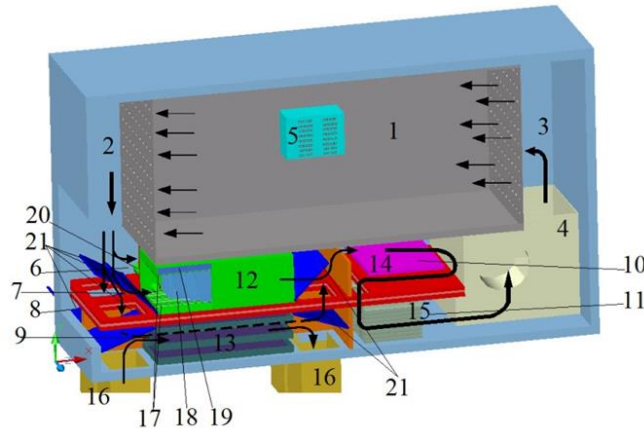


Figure 2. Axonometric block diagram of the working area and channels of the climate chamber airflow circulation.

1 – the working area of the chamber; 2,3 – the capacities for air pressure equalization with the flow lenses; 4 – double-speed fan; 5 – signal connectors; 6 – direct channel; 7 – hydration channel; 8,9 – two drainage channels; 10 – heat channel; 11 – cooling channel; 12 – hydration cassette; 13 – drying cassette № 1; 14 – heating element of the heating cassette; 15 – aluminum radiators installed on the cold side of the six Peltie elements; 16 – channel of the units silica gel regeneration in drying cassettes; 17 – two rows of needles; 18 – blade evaporator; 19 – cassette holding tank; 20 – one of the three drainage pipes; 21 – simultaneous doors for the channels opening and closing.

The metrological support of experimental research is done. Time diagrams of the experiments conducted were investigated with the help of digital oscilloscope with a sampling rate of 10 MHz, and the computer's sound card with a clock frequency of 192 kHz.

For sound card a relative error of the resonance frequency is $\delta f = \{ n / t \} = \partial n + \partial t = \Delta t / t = [(1 / 192000) / 0.032375] \cdot 100\% = 0.02\%$. For example, the absolute error of the sample size measured by the caliper is 0.05 mm, while the sample size $l = 101$ mm, is $\partial l = \Delta l / l = (0.00005 / 0.101) \cdot 100\% = 0.0495\%$.

The relative error of SAO was found for each measurement, $\partial C = \pm 0.0695\%$. The SAO absolute error of the sample for the value 1234.79 m/s is $\pm \Delta C = \pm C \cdot \partial C = \pm 1234.79 \cdot 0.0695\% = \pm 0.86 \text{ m/s}$, which is less than the well-known studies.

Results and discussion. The statistical analysis of the experimental results allowed to obtain the dependence of the third order regression with the coefficient of multiple determination $R^2 = 0,9985$.

$$c = b_0 + b_1 \cdot W + b_2 \cdot W^2 + b_3 \cdot W^3 + b_4 \cdot T^3 + b_5 \cdot W \cdot T^3 + b_6 \cdot W^2 \cdot T^3 \quad (13)$$

where: $b_0 = 1303,52; b_1 = -12,04; b_2 = 0,1132; b_3 = -0,0004;$
 $b_4 = -0,0005; b_5 = 8,89E - 06; b_6 = -7,86E - 08;$

Previous investigations make it possible to establish the dependence of the elastic moduli tensor component c_{55} from the changes in temperature and moisture content for the pine wood. Using the established patterns of connection between the speed of acoustic waves and elastic moduli $c_{\alpha\beta}$ it is possible to identify other components of the elastic moduli tensor. Further we will continue to record $c_{55} = G_{13}$ as G_{13} .

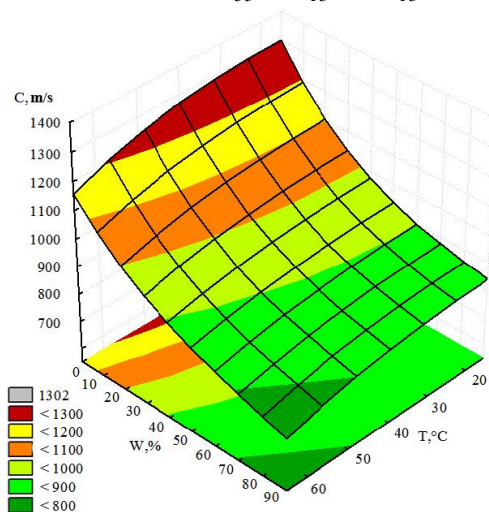


Figure 3. The dependence of SAO (VLT) from changes in temperature and moisture content for pine wood (acoustic method of free oscillations)

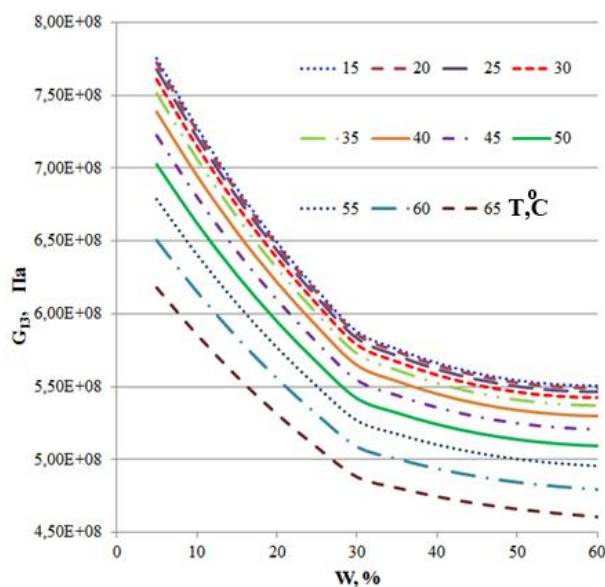


Figure 4 The dependence of the shear modulus G_{13} from the changes in temperature and moisture content of pine wood.

Conclusions

- Mathematical model of acoustic wave spreading in the wood as an orthotropic elastic material allows to determine the wood elastic moduli tensor coefficients taking into account the variable temperature and humidity environmental conditions with the purpose to measure the velocity of acoustic oscillations. To assess the influence of viscoelastic wood properties a new mathematical model of the acoustic waves spreading in the wood has been developed. The kernel of wood relaxation is taken into account in the model in exponential form.
- The designed and developed device of acoustic researches provides contactless determination of SAO in the wood. There is no direct mechanical contact of excitation devices and the reception of oscillations according to the pattern. The rate that does not change despite the changing environments is used which provides the measurement error of SAO the short sample with the length of 10 cm no more than $\pm 1M/c$.
- The designed and developed chamber provided the climatic conditions in such ranges: temperature range $+10 \div +125^{\circ}C$ and humidity range $2 \div 98\%$. The design of the chamber and developed specialized modules allow to conduct the acoustic studies of the wood and wood materials in a wide range of temperature and humidity changes, directly in the working area of the chamber without removing the samples.
- On the basis of the established relationships between SAO and wood mechanical properties, a new method of quality control is introduced, in particular the acoustic way to sort the soft and hardwood wood of constructional purposes rectangular in strength according to the standard EN338.

References

1. Dieulesaint, E., Royer, D. 1982. Ondes elastiques dans les solides, M: Nauka.
2. Dikrallah, A., Hakam, A. 2006. Experimental analysis of acoustic anisotropy of green wood by using guided waves. In: Proceedings of the ESWM-COST Action E35. 149-154.
3. Gorshkov, A.G., Medvedskij, A.L., Rabinskij, L.N., Tarlakovskij, D.V. 2004. Volny v sploshnyh sredach, M: Fizmatlit.
4. Istvan A, Veres, Mahir B, Sayir. 2004. Non-destructive testing of wood by wave propagation. Center of Mechanics, ETH Zentrum, CH-8092 Zurich, Switzerland XXI International Congress of Theoretical and Applied Mechanics Warsaw, Poland, August 15-21
5. Reinprecht, L., Panek, M. 2009. Detection of rot in wood beams by ultrasound method – model and practical studies. Technical University of Zvolen, Slovakia International Conference on Wooden Cultural Heritage: Evaluation of Deterioration and Management of Change, (Hamburg, Germany; October 7-10).
6. Sokolovskyy, Ya., Kens, I., Storozhuk, O., Borysov V. 2011. Eksperimentalnoe issledovanie vliyaniya temperatury i vlazhnosti na rasprostranenie akusticheskikh voln v drevesine. *Aktualnye problemy lesnogo kompleksa*. 30: 228-235.

7. Storozhyk. O., Borysov, V., Sokolovskyy, Ya., Kens, I. 2011. Investigation of sound velocity in wood by non-contact method. *Forestry, Forest, Paper and Woodworking Industry*. 37.2: 84-90

Research of Molecular-Topological Structure at Shape-Memory Effect of Wood

Galina A. Gorbacheva^{1} – Yuri A. Olkhov²–Boris N. Ugolev³–*

Serafim Yu. Belkovskiy⁴

¹Associate Professor, Department of Wood Science, Moscow State Forest University, Mytischki, Moscow Region, Russia.

** Corresponding author*

gorbacheva-g@yandex.ru

² Senior Researcher, Department of Polymers and Composite Materials Institute of Problems of Chemical Physics of the Russian Academy of Sciences, Chernogolovka, Moscow Region, Russia.

olkhov@icp.ac.ru

³Professor, Department of Wood Science, Moscow State Forest University, Mytischki, Moscow Region, Russia.

ugolev@mgul.ac.ru

⁴Phd student, Department of Wood Science, Moscow State Forest University, Mytischki, Moscow Region, Russia

belkovskiy@ro.ru

Abstract

Wood is a natural «smart» material which possesses «shape-memory effect. The model of hygro-thermo-mechanical strains of wood as an elastic-viscous-plastic material describes deformative conversions at this phenomenon. This model is taking into account formation of elastic-viscous frozen strains. The quazi-residual frozen strains are the result of temporary reconstruction of wood nanostructure. For quantification of the shape-memory effect of wood the quantities of this effect of polymers, such as R_r (strain recovery rate), R_f (strain fixity rate) were used. Results of a quantitative assessment of shape memory effect at moisture content changing on the bent samples of beech sliced veneer are presented. Changes of molecular-topological structure of wood polymers at the implementation of the shape memory effect were investigated by method of thermo mechanical spectrometry. Thermo mechanical curves, quantitative and molecular relaxation characteristics in topological blocks of wood are presented.

Keywords: A. Memory Effect of Wood, C. Quantification of the Shape-Memory Effect of Wood, B. Thermomechanical Spectrometry, A. Molecular-Topological Structure

Introduction

The so-called functional materials – the properties of which allow to meet particular purpose become more common (Ozerin 2008). In the class of functional materials can be erected a subclass of so-called "smart" materials that are based on the achievements of modern materials and computer science. The way the entire system – of a "smart" material is arranged allows it to perform a self-controlled "intelligent" action, it is capable of "thinking" like a living organism, to adopt and implement the solution. Alloys, ceramics and polymers with shape memory effect belong to smart materials (Hiltz 2002, Lendlein and Kelch 2002, Kauymov and Strahov 2011). They are capable to keep the temporary shape received as a result of deformation under certain conditions (programming). At return to initial physical conditions the sample remembers a permanent shape, i.e. there is a recovery of an original shape. Thus, the sample remembers two forms – permanent and temporary. Some polymers remember three forms (Lendlein and Kelch 2002), there were data on polymer which four forms can remember (Xie 2010).

Wood as a complex of biopolymers is a natural smart material possessing a shape memory effect. As an environmentally friendly, technically advanced material, wood and wood composites are gaining importance among modern materials. Comparing with artificial materials – the wood has the competitive advantages such as possibility of giving of a complex of new properties, effective application of coatings, recycling, waste disposal, etc.

Background

The memory effect of wood was experimentally discovered at the end of the 1970s (Ugolev 1986). Further research of various aspects of this phenomenon were mostly of qualitative character (Ugolev 1976, Ugolev 2011). Research of deformative conversions at various histories of deformation were conducted (Gorbacheva 2000, Ugolev et al. 2011, Ugolev 2014). It was shown that wood can remember the kind of applied loading. The Shape Memory Effect (SME) is latent property of wood. Visualization and quantification of SME on bent mini-samples of sliced, rotary-cut and fine-line veneer of birch, beech, pine and obeche were carried out at temperature and moisture content change. The multi-shape memory effect of wood also was investigated (Ugolev et al. 2013).

For quantitative assessment of this dominant feature of wood as a natural smart material two important quantities – for shape-memory polymers – were used (Lendlein and Kelch 2002):

- R_r is the strain recovery rate, it describes the ability of the material to memorize its permanent shape and is a measure of how far a strain that was applied in the course of the programming is recovered.
- R_f is strain fixity rate, it describes the ability to fix the mechanical deformation which has been applied during the programming process and so memorize its temporary shape.

The shape memory effect of wood is based on frozen strains. They were detected by us in wood fastened specimen at drying in the early 1960s (Ugolev 1961). The quasi-residual frozen strains are the result of temporary reconstruction of wood nanostructure. It takes place under the controlling load influence while wood stiffness increases at drying or cooling (Ugolev 2014). They disappear at wetting and heating. Using the model of hygro(thermo)-mechanical strains of wood (Ugolev 2005, Ugolev 2011, Ugolev 2014), based on the integral law of wood deforming under loading and moisture content and/or temperature changing (Ugolev and Lapshin 1971, Ugolev 1976) equations for the calculation of the shape memory effect quantities R_r and R_f were obtained .

The strain recovery rate R_r is determined as follows:

$$R_r = \frac{\varepsilon_{evp} - \varepsilon_p}{\varepsilon_{evp}} \quad (1)$$

here, ε_{evp} is the total hygro(thermo)-mechanical strain, ε_p is irreversible, plastic strain. The strain fixity rate R_f is calculated by the formula:

$$R_f = \frac{\varepsilon_s}{\varepsilon_{evp}} = \frac{\varepsilon_f + \varepsilon_p}{\varepsilon_{evp}}, \quad (2)$$

here ε_s is set strain after unloading; $\varepsilon_f = \varepsilon_{ev1} - \varepsilon_{ev2}$ is frozen strain equal to the difference between the elastic-viscous strains of the wood at the initial and final temperature and moisture content conditions.

Hence:

$$\varepsilon_f = \varepsilon_{evp}(R_r + R_f - 1) \quad (3)$$

SME is based on changes in wood structure. Wood material can be presented as a composite material consisting of cellulose microfibrils embedded in the lignin-hemicellulose matrix (Erinsh 1977, Salmen 2004). The spatial structure of the matrix is a superposition of three interpenetrating networks: H-net is a network of hydrogen bonds between carbohydrates, and also between lignin and carbohydrates; LH-net is a network with covalent bonds between lignin and hemicelluloses; L-net is a physical one between lignin macromolecules (Erinsh 1977).

Our earlier research conducted in collaboration with the Institute of Solid State Physics of RAS (Ugolev et al. 2007) by FTIR-spectroscopy method showed that drying of the loaded birch wood led to changes first of all in amorphous areas of cellulose, and also in network of hydrogen bonds of wood. The degree of orientation in amorphous area of cellulose additionally increases at mechanical loading as a result of reorientation of molecular chains. Such a structural rearrangement occurs during the cooling of loaded wood. At the same time concentration of hydrogen bonds plays an important role. In research (Jakes et al. 2012) shape memory effect at twist of pine wood microsample with RH changes was investigated . To clarify the mechanism of the memory effect the experiments by nanoindentation were carried out. Authors propose that hemicelluloses dominate shape fixity mechanism (R_f) and lignin dominates shape recovery (R_r).




However, this assumption is debatable, and additional researches in this area are necessary.

To detect changes in the wood structure during the formation of frozen strain responsible for the memory effect of wood, research by a method of thermomechanical spectrometry was conducted.

Materials and Methods

Samples and Procedure. For research of molecular-topological structure samples of beech sliced veneer along the grain (200x15x0,6 mm) at different test procedure were used. As an example, Table 1 shows the data for one set of tested specimens.

Table 1. Testing and measured characteristics

No of sample	Test procedure	Shape of sample	Strain	Quantities of SME
1-Bk-140	Before testing (initial conditions)	Permanent shape 	$\varepsilon=0$	
1-Bk-142	Programming Wetting at $t=80^{\circ}\text{C}$ to $W_1>100\%$, bending, drying under load at $t=80^{\circ}\text{C}$ to $W_2\approx 9\%$, unloading	Temporary shape 	$\varepsilon=\varepsilon_s=\varepsilon_f + \varepsilon_p$	$R_f = 0,9872$
1-Bk-143	Recovery of initial conditions Wetting at $t=80^{\circ}\text{C}$ to $W_1>100\%$, bending, drying under load at $t=80^{\circ}\text{C}$ to $W_2\approx 9\%$, unloading, wetting at $t=80^{\circ}\text{C}$ to $W_2>100\%$	Shape recovery 	$\varepsilon=\varepsilon_p$	$R_r = 0,8932$

Thermomechanical spectrometry. The thermomechanical spectrometry (TMS) (Ol'khov et al. 1992, Olkhov and Jurkowski 2005) is non-solution method of diagnostics of a molecular-topological structure of polymers, was developed at the Institute of chemical physics of the RAS. It allows to carry out complex molecular-topological testing of polymers during one experiment practically as express analysis (Ol'khov et al. 1996, Ol'khov and Irzhak 1998, Bazarnova et al. 2002).

Using this method in molecular mass and the topological analysis of the matrix of wood (hemicellulose, lignin) without solvents and multistage operations solubilizing cellulose

simplifies and makes more reliable analysis. Thermomechanical curves (TMC) of beech wood were obtained at perpendicular orientation vectors of application thermomechanical load and grain direction in the temperature scanning range from -100 to 300°C.

Results and discussions

Relaxation parameters, the phase state and molecular characteristics of the fragments of the macromolecules in the structure of topological blocks of wood were determined. Figure 1 gives an example of TMC of sample with temporary form, in Table 2 characteristics of molecular topological structure for all samples are presented. All the samples are characterized by rubbery mobility of cross-linked chains in a pseudo-network of an amorphous block, atypical for native wood. This is explained by a multi-stage processing of sliced veneer samples.

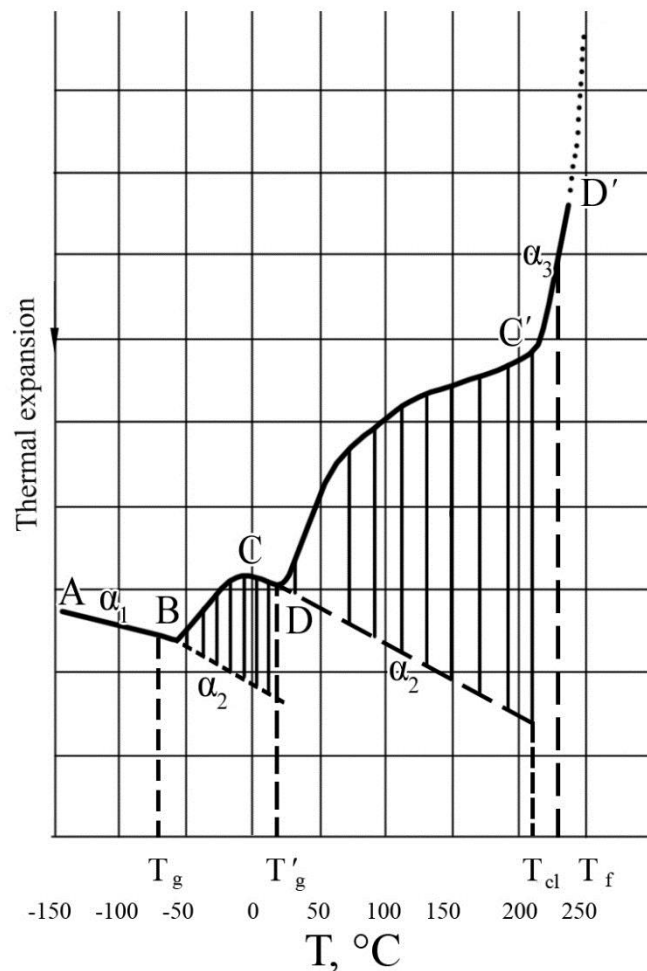


Figure 1 The thermomechanical curve of wood sample having a temporary shape

As shown in Table 2, the original beech wood has topologically diblock amorphous-cluster structure of the pseudonetwork structure with a ratio of blocks 0.76:0.24. As a result of programming the sample remembered the temporary shape, the frozen strains are formed. Thus there is a significant transformation of the topological structure, it becomes triblock. The high-temperature amorphous block of pseudonetwork structure with $T_c = 19\text{ }^\circ\text{C}$ (molecular-mass characteristics $M'_{cn} = 2790$, $M'_{cw} = 4640$, $K = 1.66$) is formed.

The part of more ordered cluster block is increased. The ratio of low - and high-temperature amorphous and cluster blocks is 0.26:0.3:0.44. In the amorphous block the molecular masses are significantly reduced that indicates the destruction of the three-dimensional networks formed of lignin and hemicelluloses, lignin-carbohydrate and hydrogen bonds. In the cluster block temperature of the beginning of a segmental relaxation in a cluster rises, molecular mass of clustered chains almost doubles.

Table 2 Molecular-topological structure of beech wood

Wood characteristic	1-Bk-140- permanent shape	1-Bk-142- temporary shape	1-Bk-143- shape after recovery
Amorphous block of pseudo-network structure			
$T_g, ^\circ\text{C}$	-73	-77	-71
$\alpha_1 \times 10^5 \text{ K}^{-1}$	6.67	6.28	8.82
$\alpha_2 \times 10^5 \text{ K}^{-1}$	19.8	17.2	23.8
V_f	0.072	0.064	0.052
M_{cn}	2830	125	2500
M_{cw}	5000	180	4670
K	1.77	1.45	1.87
φ_a	0.76	0.26	0.83
$T_\infty, ^\circ\text{C}$	193	3	213
High-temperature amorphous block of pseudo-network structure			
$T'_g, ^\circ\text{C}$	---	19	---
M'_{cn}	--	2790	---
M'_{cw}	---	4640	---
K'	---	1.66	---
φ'_a	0.00	0.30	0.00
$T'_\infty, ^\circ\text{C}$	---	213	---
Cluster block of pseudo-network branching			
$T_{cl}, ^\circ\text{C}$	196	225	216
$\alpha_3 \times 10^5 \text{ K}^{-1}$	-285.7	-284.9	-286.9
M_{cl}	17780	35480	2200
φ_t	0.530	0.520	0.520
φ_{cl}	0.24	0.44	0.17
$T_f, ^\circ\text{C}$	216	250	223

Moisture content, %	9.3	7.6	10.2
---------------------	-----	-----	------

Here: T_g , T'_g are glass transition temperatures; $\alpha_1, \alpha_2, \alpha_3$ are coefficients of linear thermal expansion; M_{cn} , M'_{cn} are number-average molecular weights; M_{cw} , M'_{cw} are weight-average molecular weights; K , K' are polydispersity indexes; φ_a , φ'_a are weight volumes of amorphous blocks; T_∞ , T'_∞ are temperatures of an output on a high elastic plateau; T_{cli} is temperature of the beginning of a segmental relaxation in a cluster; M_{cl} is molecular weight of the clustered fragments of chain; φ_t is weight volume of topological cross-links; φ_{cl} is weight volume of the clustered fragments of chain; T_f is temperature of the beginning of molecular flow.

Transition at 19 °C, determined by the TMS for beech wood, obviously, can be explained by fluctuations in the liberated OH groups after the breaking of hydrogen bonds in the components of wood (Goring 1963).

When returning to the initial conditions the frozen strains disappeared and the permanent shape is recovered. However, the full recovery of an initial form doesn't occur because of irreversible plastic strains (Table 1). Here takes place complete structural degradation of the high-temperature block, initial diblock structure of wood with some quantitative changes of molecular relaxation characteristics is restored. The portion of the amorphous block increases, ratio of blocks is 0.83:0.17, the geometrical free volume V_f decreases. In the cluster block considerable decrease in molecular mass of the cluster fragments of chains is noted, at the increasing of temperature of the beginning of a segmental relaxation in a cluster T_{cl} , and temperatures of molecular flow T_f .

Conclusions

The research conducted by the method of thermomechanical spectrometry, showed relationship between quantities of shape memory effect and changes in the molecular-topological structure. While forming the temporary shape there happens a substantial transformation of topological structure of wood, the high-temperature amorphous block of pseudo-network structure is formed. At recovery of permanent shape full structural degradation of the high-temperature block is observed, the initial topological structure of wood is restored with some quantitative changes of molecular and relaxation characteristics.

Results of this research belong to the area of fundamental wood science. They can be used for the developing of new smart materials based on wood with a set of specified properties and for the improvement of existing technologies.

References

- Bazarnova, N.G., Ol'hov, Yu.A., Markin, V.I., Katrakov I.B. 2002. The comparative study of structure of wood, cellulose and lignin by thermomechanical spectrometry. In: Proceedings, 2nd Conference «Chimia i tehnologia rastitelnih veschestv», June 2002 Kazan, Russia (In Russian).
- Erinsh, P.P. 1977. Structure and properties of wood as multicomponent polymeric system. *Chimia drevesini*. 1: 8-25. (In Russian).
- Gorbacheva, G.A. 2000. The method of experimental study of thermomechanical strains at bending. *Proc. MSFU*. 312:12–15 (in Russian)
- Goring, D.A.1963. Thermal softening of lignin, hemicellulose and cellulose. *Pulp and Paper Magazin of Canada*. 64(12): 517-527.
- Hiltz, J. A. 2002. Shape Memory Polymers. Literature Review. Technical Memorandum DRDC Atlantic TM 2002-127 August 2002.
- Jakes, J. E., Nayomi, N., Zelinka, S., Stone, D. 2012. Water-activated, Shape Memory Twist Effect in Wood Slivers as an Inspiration for Biomimetic Smart Materials. In: Proceedings, 2012 International Conference on Nanotechnology for Renewable Materials, Quebec, Canada.
- Kauymov, R.A., Strahov, D.E. 2011. Prediction of deformation in time of high polyethylene fibers with different temperatures. *Izvestija KGASU*, 2(16): 196-199. (In Russian).
- Lendlein, A., Kelch, S. 2002. Shape-Memory Polymers. Reviews. *Angew. Chem. Int. Ed.* 41: 2034 – 2057.
- Ol'khov, Yu. A., Baturin, S. M., Irzhak, V.I. 1996. Effect of Molecular Mass Distribution on the Thermomechanical Properties of Linear Polymers. *Polymer Science, Series A. Polymer Physics*. 5: 849-856.
- Ol'khov, Yu. A., Irzhak, V.I. 1998. Thermomechanical Analysis for Determination of the Molecular Mass Distribution of Bulk Polymers. *Polymer Science, Series B. Polymer Chemistry*. 10: 1706-1714.
- Ol'hov, Yu.A., Irzhak, V.I., Baturin, S.M. 1992. The way of definition of molecular-mass distribution of polymers. Patent №1763952 of Russian Federation.
- Olkhov, Yu.A., Jurkowski, B. 2005. On the more informative version of thermomechanical analysis at compression mode - A review. *Journal of Thermal Analysis and Calorimetry*. 81(2): 489-500.

- Ozerin, A.N. 2008. About functional and «smart» materials in «Nanotechnologies in Russia». *Nanotechnologies in Russia*. 3 (5-6): 8-9.
- Salmen, L. 2004. Micromechanical understanding of the cell wall structure. *C. R. Biologies*. 327 (9-10): 873-880.
- Ugolev, B., Gorbacheva, G., Belkovskiy, S. 2013. Quantification of wood memory effect. In: *Proceedings, annual IAWS meeting «Wood the Best Material for Mankind» and the 5th International Symposium on the «Interaction of Wood with Various Forms of Energy», September, 2012, Zvolen: Publishing House of Technical University in Zvolen.*
- Ugolev, B.N. 1961. Method of research of wood rheological properties at changing moisture content. *Zavodskaja laboratoria*. 27(2): 199 – 203 (In Russian).
- Ugolev, B.N. 1976. General laws of wood deformation and rheological properties of hardwood. *Wood Science and Technology*. 10(3): 169-181.
- Ugolev, B.N. 1986. Effect of “freezing” wood deformations at complex force and heat actions. In: *Proceedings, 2nd International Symposium on wood rheology, 1986, Rydzina, Poland.*
- Ugolev, B.N. 2005. Wood Drying Strains. In: *Proceedings, 9th International IUFRO Wood drying conference, Nanjing, China.*
- Ugolev, B.N. 2011. Nanotechnology and nanomaterials in forestry complex. Moscow : MGUL (In Russian).
- Ugolev, B.N. 2014. Wood as a natural smart material. *Wood Science and Technology*. 48(3): 553-568.
- Ugolev, B.N., Galkin, V.P., Gorbacheva, G.A., Axenov, P.A., Bazhenov, A.V. 2007. Changes of wood nanostructure at frozen strains during drying. *Bulletin of MSFU*. 338 : 9-16. (In Russian).
- Ugolev, B.N., Galkin, V.P., Gorbacheva, G.A., Kalinina, A.A. 2011. Frozen shrinkage of wood. In: *Proceedings, 6th International symposium IUFRO -TUZVO «Wood Structure and Properties'10», Zvolen, Slovakia.*
- Ugolev, B.N., Lapshin, Ju.G. 1971. On deforming of wood when loaded in the condition of drying. *Lesnoy Zhurnal*. 3: 63 – 65 (In Russian).
- Xie, T. 2010. Tunable polymer multi-shape memory effect. *Nature*. 464: 267-270.

Grain Angle Variation in Norway Spruce: Overall Pattern and Stochastic Dissimilarities Within and Between Stems

Peder Gjerdrum^{1*}

¹ Senior scientist, Section Wood Technology, Norwegian Forest and Landscape Institute, Ås, Norway.

** Corresponding author*

peder.gjerdrum@skogoglandskap.no

Abstract

Grain direction is influential for numerous wood properties: Appearance either in round, sawn or planed wood, strength, distortion, workability, etc. This paper describes fiber pattern and models for fiber directions in stem cross-cuts and along stems. Deviations in the general pattern are introduced by naturally occurring phenomena like apex undulation corresponding to pith eccentricity, out-of-roundness of stem cross-cuts, knots in general and in particular ‘udder-shaped’ branches, butt end irregularities, curved stems, etc. While grain angle in a stem cross-cut can be modeled with just two random parameters: grain angle changes linearly with distance from pith, four parameters are needed for an idealized stem model, and still substantial model errors must be expected. Including out-of-roundness in the model would add a handful of parameters for a cross-cut model and innumerable parameters for the stem model. The same argument applies to models including knots or other complex phenomena: A deterministic model for any given stem would require a prohibitive large number of parameters, leaving such analyses to stochastic models.

Keywords: Fiber distortion, spiral grain, pith undulation, branch swelling, curly grain

Introduction

Grain direction is influential for numerous wood properties: Appearance either in round, sawn or planed wood, strength, distortion, workability, etc. Wood is frequently described as an anisotropic material with three distinct directions: Longitudinal along the stem, radial outwards from the pith and tangential to the circular annual rings. Correspondingly, location within a stem is commonly given in cylindrical coordinates, (r, a, h) (i.e. radius from pith, azimuth, height from base). In an idealized stem, the grain (*i.e.* fiber, tracheid) direction is considered to coincide with the stem direction, and so even in timber sawn from round logs. However, a number of naturally occurring factors in a tree affect the grain directions. The objective of this paper is to give an overview of grain angle (GA) variation and models for grain angle in naturally growing trees. Damages to the growing

tree are not described. The description is mainly based on Norway spruce, but most of the description will even be valid for Scots pine.

Spiral grain

Qualitative description. Strange and atypical phenomena in nature has always triggered man's curiosity, and heavy spiral grain as can be seen in old and gnarled trees, certainly is among such spectacles. Often one will find neighboring trees similar in all respects other than grain direction: One straight-grained, the other strongly spiraled. The reason for these differences is still not settled and must be sought in the genetic origin. For a long time the term "spiral grain" was applied mostly for fibers that can be observed on the stem surface. Qualitative terms were used, *e.g.* 'a left spiral during youth passing through zero spiral to right spiral at maturity' (Northcott 1957), or trees were classified into distinct groups of different grain pattern (Bues 1992). Traditional knowledge in Scandinavia advises that while logs with any grain angle in the usual right-handed direction can well be used in loghouse constructions (Fig. 1), 'wrong-twisted' (i.e. left-handed) must be avoided as they otherwise would 'twist out of the wall' (Høeg 1974).



Fig. 1 A log with heavily twisted grain included in a loghouse construction along with more straight-grained logs.

Grain angle in cross-cuts.

Ormarsson (1995) was first to propose a linear model for GA outside of the juvenile wood, where a_i are parameters related to the given cross-cut:

$$GA = a_0 + a_1 \cdot r$$

This model has later been verified (Gjerdrum *et al.* 2002). That is, in the juvenile zone near the pith, there is a rather abrupt change in GA, followed by a constant change rate (Fig. 2). This model worked equally well



Fig. 2 Spruce opened with the split-disk method. GA changes rapidly in the juvenile wood, and subsequently linearly with distance from pith.

for radius r given in spatial distance or in cambial age (*i.e.* number of rings from the pith). The parameters a_0 and a_1 were bi-normally distributed and slightly correlated ($r = -0.3$ to -0.5). The background for the constant change rate was later explained by Schulgasser and Witztum (2007): Stresses between tracheids during maturation due to the microfibril angle in the cell wall.

Grain angle variation along the pith. A first guess would be that grain angle is constant along the stem, at least for corresponding radii. However, a recent study revealed some variation – and some new challenges to deal with (Gjerdrum and Bernabei 2009, Gjerdrum 2011). An augmented model including a couple of additional parameters was suggested:

$$GA = a_0 + a_1 \cdot r + (a_0 + a_2) \cdot \exp(r^{a_3})$$

The additional parameter a_2 accounts for local pith angle and a_3 for GA transfer from pith through juvenile to mature wood; \exp is the Euler function. Consequently, this formula models the GA all through the stem, juvenile wood inclusive. The four parameters are random and must be settled: a_0 , a_1 and a_3 for each stem, and a_2 for each location along each stem. Model error for stem model amounts to 2.3° , as compared to 1.6° for the disk model. A major challenge is to identify a precise definition of the longitudinal axis. One option would be to take the local pith direction, another to align along the cross-cut disk's outer shape. As can be seen from Figure 3, these do not necessarily coincide. Analyses indicate that neither work better; indeed, neither work very well at all. The above model was based on outer shape, and pith angle variation (*i.e.* standard error for a_2) was estimated to 2.2° .

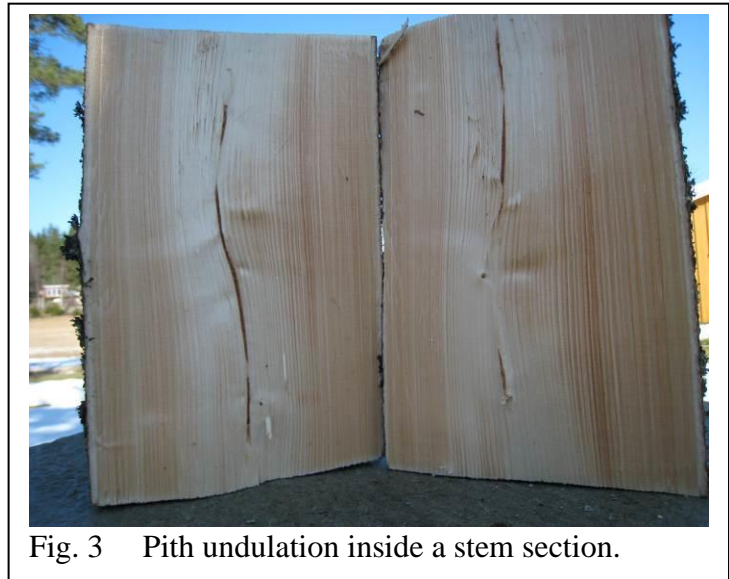
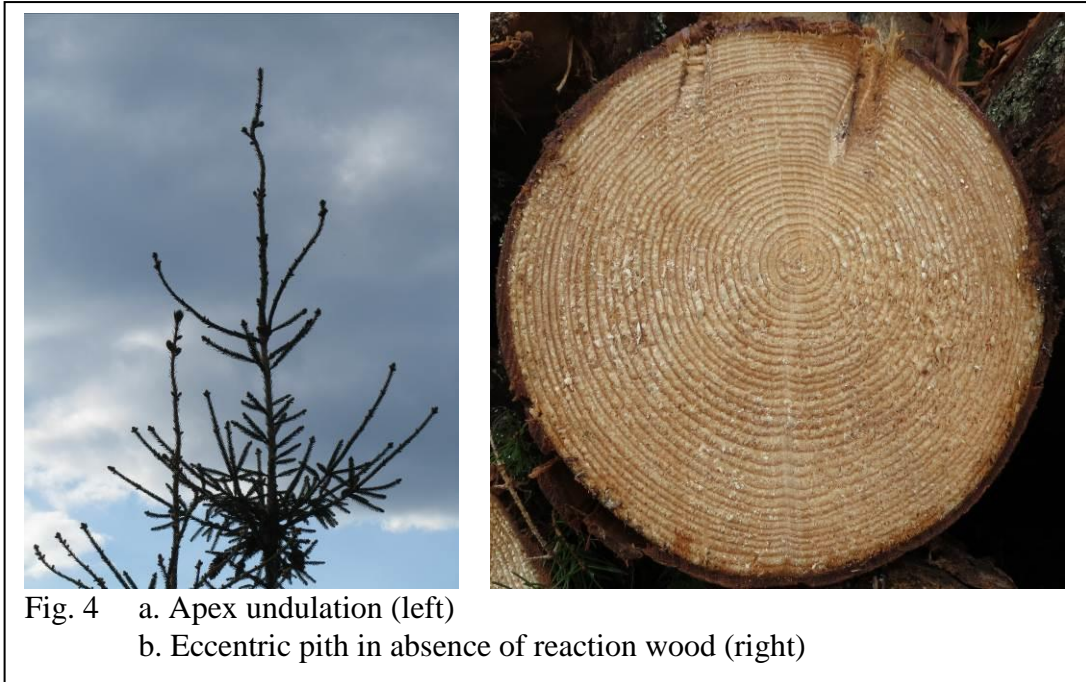


Fig. 3 Pith undulation inside a stem section.

Other Grain-affecting Traits

Apex undulation and pith eccentricity. Eccentric pith might well originate from reaction wood with wider rings in one part of the stem, *e.g.* due to a leaning tree. However, a lesser or stronger degree of eccentric pith (Fig. 4b) will be found in virtually every stem cross-cut, also perfectly devoid of compression wood. One reason for this, alongside azimuth variation in ring width, is the never perfectly straight apex (Fig. 4a). Nevertheless, the growing tree has an intrinsic ability to smoothen this irregularity, and after some years the outer surface of the stem appears quite smooth and straight, even for

pronounced apex deviation (Fig. 3). No representative observation of the magnitude of this eccentricity is known, but practical experience from sawmill operation indicates a standard deviation for the radial pith eccentricity in any direction in the magnitude of 10 mm. As already described in the previous paragraph, the change rate along the pith is equivalent to standard deviation for pith angle 2.2° .



Out-of-roundness. Pith eccentricity implies a form of out-of-roundness in that the radius (observed from the pith) varies considerably around the disk. However, out-of-roundness is a wider trait, including any radius variation with azimuth. The typical cross-shape of a spruce and pine disk is neither circular nor elliptical, but rather irregular (Skatter and Høibø 1998): Five to seven parameters are needed for an appropriate model. No representative analysis for shape variation along stems is known. For sawn timber, out-of-roundness only affects the radial vs. the tangential fiber directions in boards, which usually is of lesser significance than altering the longitudinal direction. Most trees tend to be more irregular near the base; this trait is most outspoken in Scots pine (Fig. 5).



Fig. 5 Severe out-of-roundness is found near the stem base, and more in pine (picture) than spruce

Representative knots have been modeled by numerous authors and in numerous ways. Here is not the place for a full overview, so just one example will be given. In her doctoral thesis on effects of knots in structural timber, Foley (2003) clearly demonstrated the intricacy of modeling knots in wood, with size, direction, live or dead knot, and then accounting for the distinct transfer zone between clear wood and the knot wood (Fig. 5). And that is for a single knot, before adding the complexity related to knot formation in stems: Distance between whorls and number and direction of knots in and between each whorl.



Fig. 6 Transfer zone between clear wood and knot wood

Complex fiber structures related to knots and branches. Some trees grow atypical, yet completely normal, grain patterns. Although most trees grow slight out-of-roundness pattern near the branches, in a few trees this can be found in very pronounced forms. Some trees form cavities, but more often noticeable bumps can be found, sometimes referred to as udder branches (Fig. 7a). This occurs more in spruce than pine, usually in solitary or dominant trees. In a stem, fibers can be visualized as ‘flowing’ around knots much like water flowing slowly past a rock in a river. And just like water forms whirls when water speed increases, similar complex, curly ‘eddies’ can occasionally be found in the transfer zone (Fig. 7b.). Grain whirls are mostly found in old trees. Udder branches can cause some extra trouble for the debanching and debarking operation. That apart, udder branches, grain whirls and similar phenomena are rare with little practical impact; they can rather be considered nature’s gift to trigger human curiosity. And so, the modeling of these phenomena will be appealing – but with little commercial impact.



Fig. 7 a. Some trees develop ‘udder branches’ (left)
b. Complex grain whirls in the transfer zone surrounding the knots (right)

Conclusions

Although plain spiral grain in stem cross-cuts is easily modeled and just takes two parameters for an adequate estimation, a mathematical prediction model has only been available for two decades. A stem grain angle model has been suggested, but higher model errors must be expected, probably mostly due to the undulating pith and problems to define an exact direction for the longitudinal axis. Fiber direction in connection with a knot can be modeled, but when it comes to knot locations in a stem, only stochastic models useful for simulation are at hand. The same is valid for out-of-roundness and more complex fiber structures: Models describing single cases might enlighten the understanding and significance of such phenomena, but deterministic models for predictive use seems far out of question.

References

- Bues, T. 1992 Zum Drehwuchs bei Fichten. Allg. Forstz. 19: 1040-1045. (In German.)
- Foley, C. 2003 Modeling the Effects of Knots in Structural Timber. Dr. thesis, Lund University. Report TVBK-1027, 174 p
- Gjerdrum, P., Säll, H. and Storø, H.M. 2002 Spiral grain in Norway spruce: Constant change rate in grain angle in Scandinavian sawlogs. Forestry, 75 (2): 163-170
- Gjerdrum, P. and Bernabei, M. 2009 Three-Dimensional Spiral Grain Pattern in Five Large Norway Spruce Stems. Silva Fennica 43(3): 457-464
- Gjerdrum, P. 2011 Analysis of three-dimensional grain angle variation in Norway spruce stems. Technology and Ergonomics in the Service of Modern Forestry, Krakow, ISBN 978-83-60633-51-9, page 413-420.
- Høeg, O. A. 1974 Planter og tradisjon. Universitetsforlaget, Oslo. 751. pp. ISBN 82-0008930-4. (In Norwegian.)
- Northcott, P. L. 1957 Is spiral grain the normal growth pattern? For. Chron. 33:333-352
- Ormarsson, S. 1995 A finite element study of the shape stability of sawn timber subjected to moisture variations. Lic. thesis. Lund University, Lund. Report TVSM-3017. 91 pp
- Schulgasser, K. and Witztum, A. 2007 The mechanism of spiral grain formation in trees. Wood Sci. Technol. 41: 133-156
- Skatter, S. and Høibø, O.A. 1998 Cross-sectional shape models of Scots pine (*Pinus sylvestris*) and Norway spruce (*Picea abies*). Holz als Roh- und Werkstoff 56: 187-191

Variation in Cell Morphology of Genetically Engineered Aspen and Cottonwood

*Ilona Peszlen, Perry Peralta, Zachary Miller, Charles Edmunds, &
Zhouyang Xiang*

Abstract

To meet specific needs of the wood and fiber industries, trees with modified chemical components are desired. Lignin-modified transgenic trees have the potential to benefit the paper making, fiber and bioethanol industries, which require huge amount of energy and cause environmental problems when dealing with the unwanted. In addition, genetic engineering of trees provides unique opportunities to explore the roles and effects of single woody cell wall chemical components such as cellulose, hemicelluloses, and lignin in order to gain new insights on cell wall biosynthesis, tree growth, and wood properties. The overall objective of our research program is to investigate various wood and fiber properties in relation to the chemical composition of the cell walls to gain new insights for specific utilization including solid wood, fiber, composites, and energy. This presentation will discuss the effect of the chemical alterations in transgenic poplar trees on cell wall formation and cell morphology. Transgenic aspen (*Populus tremuloides*) and cottonwood (*Populus trichocarpa*) clones with modified chemical composition were used for this investigation. Trees were harvested after six-month of growth in the greenhouse. From each sample tree, scanning electron microscope images and image analysis of transverse microtome sections were used to assess variation in cell wall formation and cell morphology. Vessels and fibers characteristics were measured and analyzed in order to improve our understanding on woody cell wall components biosynthesis as it relates to cell wall formation and secondary xylem development.

Keywords: cell morphology, chemical composition of cell wall

Ilona Peszlen, Associate Professor
+1-919-513-1265; Fax: +191-3513-3496
Ilona_Peszlen@ncsu.edu

Perry Peralta, Associate Professor
+1919-515-5731; Fax: +191-3513-3496
Perry_Peralta@ncsu.edu

Zachary Miller, Ph.D. Student
Charles Edmunds, Ph.D. Student
Zhouyang Xiang, former MS Student

Department of Forest Biomaterials
North Carolina State University
Campus Box 8005
Raleigh, NC 27695

Rapidly Hydrolysis of Lignocellulosic Wood Biomass

Hyeun-Jong Bae

Chonnam National University, Gwangju
South Korea

Abstract

Lignocellulosic wood biomass is an abundant, cheap and renewable resource on earth which can be converted to liquid transportation fuels. However, it is widely recognized that bioethanol production from wood biomass is limited by inefficient and economical extraction of recalcitrant lignin under mild conditions and with minimal loss of polysaccharides.

The economical production of biofuels is hindered by the recalcitrance of lignocellulosic biomass to bio-processing, causing high amount of consumption of enzymatic bioconversion and impeding hydrolysis of pretreated lignocellulosic biomass. We tested and determined the major rate-limiting factor in the hydrolysis of pre-treated wood biomass by examining cellulase adsorption to lignin and cellulose, amorphogenesis of lignocellulose, and re-hydrolysis. Based on the our results, equivalence between enzyme loading and the open structural area of cellulose was required to significantly increase productive adsorption of cellulase and to accelerate enzymatic saccharification of lignocellulose. Specially, Amorphogenesis of lignocellulose by acid treatment to expand open structural area of the cellulose fibers resulted in twofold higher cellulase adsorption and increased the yield of the first re-hydrolysis step. The total yield from wood biomass was increased to 70% after 3 h. These results provide evidence that cellulose structure is one of important effects on the enzymatic saccharification.

Keywords: Enzymatic bioconversion; Amorphogenesis; Lignocellulose

Hyeun-Jong Bae
Chonnam National University
Bioenergy Research Center
300 Yongbong dong
Gwangju, South Korea 500-757
+82-062-530-2097 FAX: +82-062-530-2098
baehj@chonnam.ac.kr

Tactile Interaction and Contact Comfort of Wood and Wood Materials

Veronika Kotradyová^{1} – Alfred Teischinger²*

¹ Associate Professor , Intsitute of Interior and Exhibiton Design, executive director of Body conscious Design Lab, Faculty of Architecture, Slovak University of Technology, Slovakia

** Corresponding author*

[*kotradyova@fa.stuba.sk*](mailto:kotradyova@fa.stuba.sk)

² Professor, Institute of Wood Science and Technology, Scientific director of the Competence Centre for Wood Composites and Wood Chemistry (Wood K plus) , BOKU Vienna, Austria

[*alfred.teischinger@boku.ac.at*](mailto:alfred.teischinger@boku.ac.at)

Abstract

The paper deals with the nature of contact comfort by tactile and behavioural interaction of human and wood/wood materials as a part of body conscious design/ human-centered design. After considering the complexity of contact comfort we suggest to set the following parameters or indicators for expressing the feeling of contact comfort: thermal comfort related to thermal conductivity, effusivity and thermal contact conductance of the surface, roughness of surface, hardness of surface including the elasticity of the supporting material layer, sorption activity of the surface in terms of absorbing the external moisture (e.g. sweat or humidity of air/its condensates), having control over body position, possibilities of maintenance connected with cultural background of users, individual mental and physical setting that creates overall feeling of comfort. One can express most of them by measurable parameters and all of them by subjective references of respondents. In this paper we will focus on the first two parameters and also their relation to the other ones mentioned above.

Roughness is extremely important for the overall feeling of contact comfort and it has direct relation to the other features. The paper presents the methodology and results of the pilot study of contact comfort. Different wood based materials and wood species with different types of surface finishing in comparison with other materials were investigated by using a test chair. The paper presents some examples of the cooperation of the two authors within the research project “Interaction of Man and Wood”, since 2011.

Keywords: tactile interaction, contact comfort, human, wood, surface, temperature, roughness

Introduction

In the clothing and textile industry there is a lot of research about comfort which is related to “contact comfort” as specific term for comfort sensations. According to Das and Alagirusamy (2011) the factors influencing the clothing comfort sensations of the wearer can be divided into three groups: physical factors (deals with the human-clothing-environment system); psycho-physiological factors of wearer; and psychological filters of the brain. The comfort status of the wearer depends on all these factors and their complex interactions and synchronizations. The most common clothing comfort related sensory attributes are thermal, moisture, tactile, hand and aesthetic experiences. The experts in the field of sensory attributes can easily identify the difference between these attributes. When the level of human activity or the temperature and humidity of a microclimate change, the changes in various sensory perceptions, like warmth, chilliness, scratchiness, dampness etc. can be very easily detected.

Table 1 List of related measurable parameters linked with indicators of contact comfort and how they contribute to contact comfort

Indicators of contact comfort	MEASURABLE PARAMETERS	Unit	Increasing (+) or decreasing (-) attitude of the variable towards (or in relation) to contact comfort
THERMAL COMFORT	Thermal conductivity (λ)	W/mK	-
	thermal effusivity/diffusivity (a)	m ² /s	-
	Thermal contact conductance (hc)		-
ROUGHNESS	Roughness (R_a)	μ m	+
HARDNESS	Brinell hardness (HB)	N/mm ²	-
SORPTION PARAMETERS	Water sorption coefficient (A)	kg.m ⁻² .s ^{-1/2}	+
	Apparent moisture diffusivity (K)	m ² /s	+
	Diffusion coefficient ($D_{(u)}$ or D_e)	m ² /s	+
	Water vapor diffusion resistance coefficient (μ)		-
	Water vapor diffusion permeability (σ)	S	+

This paper examines tactility and “contact comfort” as a more general expression, from both a technical/physical and a social/psychological point of view. Assessing the complexity of “contact comfort” of a person touching a material, we suggest the following parameters or indicators for expressing this contact comfort:

- thermal comfort related to thermal conductivity, effusivity and thermal contact conductance of the surface
- roughness of the surface
- hardness of the surface including the elasticity of the supporting material layer

- sorption activity of the surface in terms of absorbing the external moisture (e.g. sweat or humidity of air/its condensates)
- having control over the body position (e.g. in the case of a seat shell)
- possibilities of maintenance connected with cultural background of users
- individual mental and physical setting that creates an overall feeling of comfort.

Most of them can be expressed by measurable parameters and all of them can be assessed by subjective preferences of respondents. Tab. 1 lists related measurable parameters linked to contact comfort together with a hypothetic or expected contribution to contact comfort expressed by signs (+) for increasing of the variable and (-) for decreasing (e.g. the lower the thermal conductivity, the higher the contact comfort).

Materials and Methods

In order to assess the sitting comfort (as a special case of “contact comfort”) we developed a test chair which shows the following features (fig. 1): exchangeable seat, backrest and armrest made of different materials with different types of finishing that are usually used in the production of chairs. The skeleton of the chair is designed according to contemporary ergonomic standards in order to offer a usual somatic comfort so as to allow the respondent to concentrate on the contact comfort.

The following test materials were used:

1. polypropylene
2. aluminium
3. thin plywood board set with PUR-lacquer finishing- high glance spruce glued board set without finishing
4. beech glued board set with PUR-lacquer finishing - high glance
5. beech glued board set with flax oil finishing
6. beech glued board set without finishing
7. spruce glued board set with PUR-lacquer finishing - high glance (focus to “sliding effect”)
8. spruce glued board set with flax oil finishing

In second extended phase of the tests three more materials were added (tested with respondents in Slovakia only).

9. WPC (Wood Plastic Composites)
10. Plexiglas
11. Cork

The materials were selected according to their usual contemporary presence for manufacturing seating furniture for indoor and outdoor purposes or according to their potential to be used in this field.



Fig. 1 Testing chair with exchangeable sets of seat, arm rests and backrests, arm rests are also usable for testing the edge radius preferences.

We tested the materials by short-term interaction like an initial first impression (after 1-2 minutes of contact) and medium-term interaction (after 10 minutes of contact) in a typical office environment at a room temperature of about 22°C by artificial air-conditioning. One part of the test was performed in Austria (in an institute surrounding of the authors) and the second part of the test was executed in Slovakia at the Faculty of Architecture in summer 2012 where the rooms were naturally ventilated with no air-conditioning and a room temperature of about 25 °C (summer condition). The difference in the microclimatic conditions has contributed to the mapping of the both situations that are common with seating furniture. After each test cycle with the respondents (assessing the immediate contact comfort and the medium-term contact comfort of 10 minutes) the chair was equipped with another test material.

Due to the explanatory approach of the study only 12 test persons in Austria and 12 persons in Slovakia were asked to participate in the study (24 respondents altogether). There was no further statistical and gender related approach in the current investigation. The following questionnaire was used for the response of the respondents.

cold	—————	warm
smooth	—————	rough
hard	—————	soft
wet	—————	dry
poor control over sitting position	—————	good control over sitting position

The last question about comfort/discomfort should mirror an overall impression.

discomfort	—————	comfort
------------	-------	---------

The respondents were asked to make a simple cross on the line of each of the bars with opposite characters. Using this method we wanted to make the decision easier about their

feeling the contrasting features (e.g. hard or soft). When analysing the questionnaires, a scale from 0 to 10 was put on each of the lines with the contrasting features and the specific numerical value was taken into account for the further evaluation.

Results

In Tab. 2 we can see all results of the subjective preferences. Here the higher rating, the warmer the surface was felt and thus provided higher thermal comfort. The overall comfort also depends on the kinds of clothes the respondents were wearing. By testing the *thermal comfort* of the material (*characteristic cold/warm*), the highest rating of all had cork (8,0/8,5) followed by spruce raw (7,3/7,5), and the lowest rating had aluminium (0,7/2,2). WPC composites with (3,1/4,3) exhibits tactile characteristics nearer to plastics than to wooden materials. Almost in all cases the thermal comfort increased with running time as the body is “heating up” the surface and the material with the passing time (additional explanation to the effect is provided in Fig. 2).

Considering the indicators *smooth/rough* the smoothest material was polypropylene (2,0/2,1) with aluminium right behind. From the wood based materials, the smoothest was solid beech wood lacquered followed by lacquered plywood. Solid spruce wood with no finishing together with cork was considered like the roughest. Polypropylene with high glance finishing caused very similar reaction as aluminium.

Tab. 2 Evaluation of all criteria considered by contact comfort by all tested materials. There are always two ratings, first by first contact - I. milestone and second for the II milestone after 10 minutes

Average values from tests in Austria and Slovakia together

Features of Material	cold / warm		smooth / rough		poor/good control oversitting		hard / soft		wet / dry		discomfort/ comfort	
	I.	II.	I.	II.	I.	II.	I.	II.	I.	II.	I.	II.
Milestones												
polypropylen	3,1	4,3	2,0	2,1	3,7	4,3	3,3	3,1	4,4	4,2	3,9	4,1
aluminum	0,7	2,2	2,1	2,2	4,0	4,4	2,6	3,2	3,5	4,1	2,9	2,8
beech plywood (5mm thick) lacquered	4,4	5,3	3,1	3,3	4,9	5,1	4,4	4,5	4,7	4,3	4,2	4,4
solid beech glued board (25mm thick) lacquered	4,5	5,4	2,0	2,6	4,9	4,6	4,8	4,7	4,2	4,0	4,9	4,4
solid beech glued board (25mm thick) oiled	5,5	6,3	5,3	5,1	6,7	5,9	5,3	4,4	5,8	5,8	5,9	5,2
solid beech glued board (25mm thick) raw	5,2	6,1	5,1	5,1	5,9	5,6	4,7	4,3	5,4	5,5	5,2	4,9
solid spruce glued board (18 mm thick) lacquered	5,8	6,7	2,4	2,8	4,6	4,9	4,1	4,1	5,5	5,5	4,6	4,6
solid spruce glued board (18 mm thick) oiled	6,8	7,1	4,5	4,1	6,4	6,4	5,9	5,6	5,6	6,6	6,0	5,6
solid spruce glued board (18 mm thick) raw	7,3	7,5	5,6	4,9	7,4	7,0	5,9	5,9	6,8	6,5	6,3	5,8
WPC (22mm thick)	3,0	3,9	4,5	4,9			3,9	3,2	4,9	4,9	4,8	3,2
plexiglass, (8mm thick)	1,9	3,1	3,1	3,1			2,6	2,8	4,8	4,7	3,5	2,2
cork raw (8mm thick)	8,0	8,5	5,6	5,6			6,2	6,9	6,9	7,0	6,3	6,9

By the parameter *control over the sitting position* we mean preventing a sliding effect that occurs on high glance finishing with low friction of seats or sitting shells. Here we can see the parallel between the parameter smooth/rough, thus the results were according to this correlation. The poorest control over sitting position was reached on polypropylene 3,7/ 4,3, where with passing time we can see a tiny improvement of the feeling of control. Here the higher the rating, the better the control over the sitting

position. The highest rating (and the best control over sitting position) was achieved by raw solid spruce wood (7,4/7,0), the second was solid spruce wood oiled (6,4/6,4).

There was the hypotheses that the more times passes, the more intense the hardness is felt, but the test didn't shown such an attitude. Aluminium (2,6/3,2) and Plexiglas (2,6/2,8) were considered the hardest materials.

By evaluating *sorption activity*, (tested by the parameter *soft/dry*), we think it is necessary to interact with the material for a much longer time. Most of materials were rated quite high which means as "dry" between 3,5/4,1 by aluminium and 4,4/4,2 by polypropylene and 6,8/6,5 by raw spruce and by cork (6,9/7,0). The warmer and rougher the materials were felt, the drier they were felt, too.

The parameter *discomfort/comfort* is to express the overall comfort, regarding mental setting to, whereas the higher the rating is, the higher the comfort. It is interesting to observe that the rating was similar as by the other parameters, the highest rating had both raw solid spruce (6,3/5,8) and cork (6,3/6,9) and the lowest rating had aluminium and Plexiglas so we can state that the previous testing of the single parameters had influenced this evaluation.

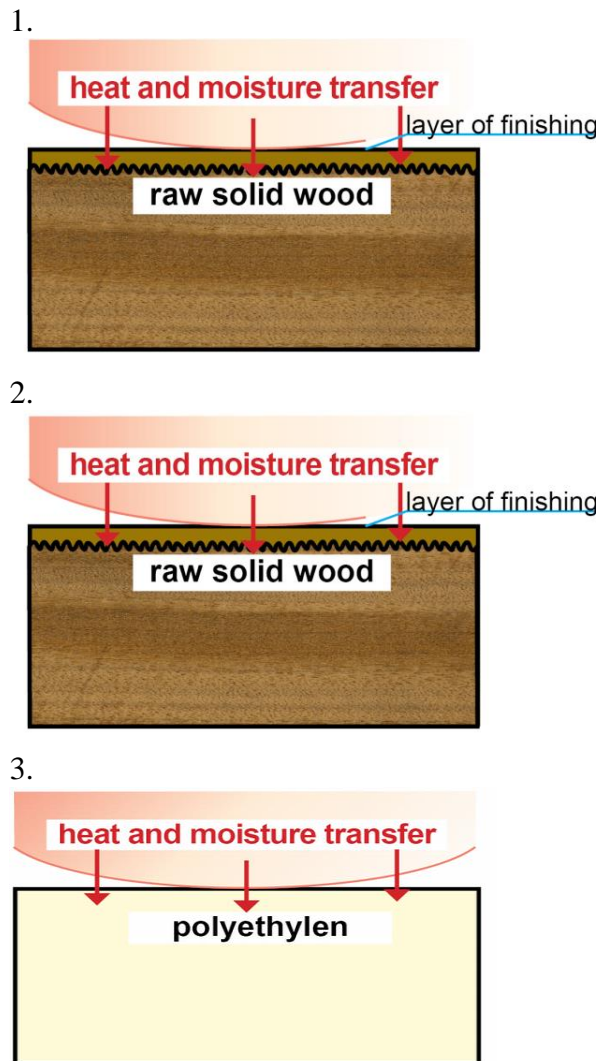


Fig. 2 Schematization of the interaction of the human body with materials with different setting of surface finishing

Tab.3 Comparison of subjectively expressed rating of indicators of contact comfort with measurable parameters by single materials. Average subjective rating (ASR) and objective parameter from reference (OPR)

Materials	Thermal comfort		Optimal roughness		Hardness		Sorption abilities	
	ASR cold / warm	OPR thermal conductivity λ [W/(m*K)]	ASR for property smooth / rough	OPR Roughness Average R_a [μm]	ASR for property hard / soft	OPR HB [N/mm ²]	ASR for property wet / dry	OPR Absorption coefficient μ [cm ² /g]
Polypropylene	3,7	0,22 ^[1]	2,1		3,2	70 ^[8]	4,2	10000 ^[13]
Aluminum	1,5	200 ^[2]	2,2		2,9	80 ^[8]	4,0	∞ ^[3]
beech plywood (5mm thick) lacquered	4,9	0,17 ^[1]	3,2		4,5	-	4,5	67-72 ^[10]
solid beech glued board (25mm thick) lacquered	5,0	^[4]	2,3		4,8	33 ^[8]	4,1	2000-40000* ^[14]
solid beech glued board (25mm thick) oiled	5,9	^[4]	5,2		4,9	-	5,8	-
solid beech glued board (25mm thick) raw	5,7	0,20 ^{[3][4]}	5,1		4,5	34 ^[9]	5,5	50/400 ^[10]
solid spruce glued board (18 mm thick) lacquered	6,3	^[4]	2,6	0,8 ^[7]	4,1	12	5,5	2000-40000 ^[14]
solid spruce glued board (18 mm thick) oiled	7,0	^[4]	4,3		5,8	-	6,1	-
solid spruce glued board (18 mm thick) raw	7,4	0,15 ^{[3][4]}	5,5	7 ^[7]	5,9	15,6 ^[10]	6,7	50/400 ^[10]
WPC (22mm thick)	3,5	0,24 ^[5]	4,4			28 ^[11]	4,9	
plexiglass, (8mm thick)	2,5	0,18 ^[6]	3,1		2,7	180-200 ^[12]	4,8	50000 ^[6]
cork raw (8mm thick)	8,3	0,045 ^[3]	5,6		6,6		7,0	5-10 ^[6]

^[1]Willems, W.M., Schild, K., Dinter, S., Stricker, D. 2007. *Formeln und Tabellen Bauphysik, 1. Auflage, Wiesbaden*

^[2]Schotz, W., Huse, W. 1999. *Baustoffkenntnis, 14. Auflage, Werner Verlag*

^[3]Handbuch für Energieberater, 1994. Joanneum Research

^[4]There were not found particular values for the different surface finishing of spruce and beech

^[5]<http://terrassenshop.ch/terrassendielen/holz-kunststoff-verbund-wpc/upm-profi-deck.html>

^[6]Willems, W.M., Schild, K., Dinter, S., Stricker, D. 2007. *Formeln und Tabellen Bauphysik, 1. Auflage, Wiesbaden, Vieweg Verlag*

^[7]Wagenführ, A., Scholz, F. 2012. *Taschenbuch der Holztechnik, Hanser Verlag*

^[8]Comparison of Brinell, Vickers and Rockwell hardness (according to DIN 50150). In: http://www.strack.de/pdf_upload/info/vickerst.pdf?sid=1&opentree=28

^[9]<http://www.gunreben.de/index.php/holzhe-brinellhe-informationen-299.html>

^[10]Dunky, M., Niemz, P., 2002. *Holzwerkstoffe und Leime, Heidelberg, Berlin, Springer Verlag*

^[11]<http://terrassenshop.ch/terrassendielen/holz-kunststoff-verbund-wpc/upm-profi-deck.html>

^[12] Eyerer, P., Elsner, P., Hirth, T., 2005, *Die Kunststoffe und ihre Eigenschaften*, 6. Auflage, Heidelberg, Berlin, Springer Verlag

^[13] Willems, W.M., Schild, K., Dinter, S., Stricker, D., 2007, *Formeln und Tabellen Bauphysik*, 1. Auflage, Wiesbaden, Vieweg Verlag

^[14] PVC paint has absorption coefficient μ 2000-10000 cm²/g and by water Water-thinnable clear varnish it is 2500-10000 cm²/g and by epoxid paints it is 10000-40000 cm²/g

It was possible to evaluate every element separately (seat, backrest, armrest) because there are different demands from the ergonomic perspective, but in this pilot study it would be too much time demanding and the attention of respondent would be diminished a lot with too many question to answer and this tiredness could be contra-productive for our goal. The less contacted part is the armrest and the most intensive contact is at the seat, which is heated by own human heat in the most intensive way.

Tab. 3 shows a comparison of subjectively expressed ratings of contact comfort with measurable parameters of single materials. The attitude is similar. These relations will be further explored.

Thermal comfort and roughness of surface are closely related to each other. The rougher the surface, the better thermal comfort is felt thanks to the presence of air in the contact zone between the body and a material (fig. 2) The rougher, regular or balanced rough the surface, the higher a contact comfort is achieved, because the thermal contact resistance will be greater for rough surfaces as an interface with rough surface will contain more air gaps with low thermal conductivity. An interface acts like a very thin layer of insulation, and thus the thermal contact resistance is only significant for highly conducting materials like metals. This hypothesis was verified in our tests.

The comparison between natural oils and synthetic lacquer shows that the oils are perceived as warmer and rougher. The comparison between contact with natural wood even with synthetic finishing and contact with laminates, the laminates are perceived as colder and smoother. Roughness is a strategic feature also for all other parameters.

Discussion and Conclusion

According to a literature review and our own field research we have synthesised following parameters that play an important role in creating contact comfort such as:

- surface temperature thermal conductivity/effusivity
- roughness of surface
- hardness of surface
- sorption activity of surface in terms of absorbing the external moisture from the human contact area
- having control over body position
- possibilities of maintenance – socio-cultural influence
- individual mental and physical setting that creates an overall feeling of comfort.

If we compare the finishing of different wood materials, in general all parameters were evaluated higher with raw surfaces and lowest with lacquered surfaces (Tab. 2). The Thickness of the material does not play and considerable role, thus the evaluation of

5 mm thick lacquered plywood was very similar to solid beech wood board with the same finishing. In our pilot study we explored them more deeply and created a methodology on how to get a feedback from users. The pressing of the veneers in the plywood production process causes a densification of the wood and the density increases about 5-10%. Therefore the thermal conductivity is increased (a and λ), too and standard plywood moulded elements as used as sitting shells, are to be felt as colder. These characteristics can be assessed by various measurement methods and due to this knowledge one can generate particular qualities of material surfaces that are in immediate contact with human body. In some cases an optimised surface performance with regard to contact comfort gives a trade-off with other important parameters such as mechanical, water and chemical resistance of the surface. This has to be considered at the final decision for a product design.

The choice of material by creating any kind of built-environment is influential for later behaviour, well-being, health and performance of occupants. That is the reason why the aim of our research is to show “human factors of materials”, too. In the on-going research project we will do the necessary measurements of missing parameters important for the different kind of comfort (with focus on contact comfort), especially for the different surface finishing of materials. We will also evaluate dependencies between subjective and objective parameters.

We will create some tool for the evaluation of materials regarding their human friendliness - overview of characteristics important for interaction of human and material - properties important for supporting users' well-being or complex comfort which includes health, social and economic importance, too. It will be summarized in an interactive database that will be an easy tool for professionals (architects, designers, engineers) but also for the public.

Acknowledgment

This study was created within research project “Interaction of Human and Wood” and the paper was supported by the Slovak Research and Development Agency under the contract No. APVV-0594-12 – Interaction of Human and Wood.

References

- Berger, G.; Katz, H.I.; Petutschnigg, A.J. 2006. What consumers feel and prefer: Haptic perception of various wood flooring surfaces. In: Forest Products Journal vol, 56, No. 10
- Cranz, G. 2000. The Chair, rethinking culture, body and design, Norton paperback, New York, p. 187, ISBN 0-393-04655-9
- Das, A.; Alagirusamy, A. 2011. Science in Clothing Comfort, Woodhead Publishing India, ISBN 1845697898
- Hall, E. 1992. The Hidden Dimension. Peter Smith Pub Inc.
- Harlow, H. F. 1958. The Nature of Love. In *American Psychologist*, 13, p. 673-685
- Haviarová, E., Babiak, M., Nemeč, Ľ., Joščák, P. 1996. Temperature sense of a person and thermal properties of chosen materials and wood species used at the complex interior

formation. In: Acta fakultatis xylogologiae (Zborník vedeckých prác Drevárskej fakulty) 1996/2, Zvolen, Vydavateľstvo TU. s. 7-14.

Teischinger, A; Zukal ML; Kotradyova V . 2012. Exploring the possibilities of increasing the contact comfort by wooden materials - tactile interaction of man and wood.

Innovation in Woodworking industry and engineering design, Sofia, BULGARIA, 27.10.2011. In: University of Forestry, Sofia (Hrsg.), innovation in woodworking industry and engineering design, Vol.01

Kotradyová, V. 2010. Tactile Characteristics of Wooden Interior Elements, in: Wood Structure and Properties 2010, September 6–9, 2010, Grand Hotel Permon – Podbanske, High Tatras, Slovakia, P. 123-126. ISBN 978-80-968868

Kotradyova, V. 2010. Body and mind conscious design (habilitation thesis), FA STU Bratislava, 122 Pages

Mandal, A.C.1981. Seated man (Homo Sedens), Applied Ergonomics, Oxford

Madhusudana, C.V. 1996. Thermal Contact Conductance, Springer Verlag, New York

Meyer, S. 1999. Produkthaptik, DUV, ISBN 3-8244-7225-2

Niemz, P. 1995. Physik des Holzes und der Holzwerkstoffe, DRW- Verlag. ISBN-10: 3871813249

Obata, Y.; Takeuchi K.; Furuta, Y.; Kanayama, K. 2005. Research on better use of wood for sustainable development: Quantitative evaluation of good tactile warmth of wood Energy - Dubrovnik Conference on Sustainable Development of Energy, Water and Environment

Comparison of Brinell, Vickers and Rockwell hardness (according to DIN 50150). In: http://www.strack.de/pdf_upload/info/vickerst.pdf?sid=1&opentree= 28

Lehmuskallio, E. 2001. Cold Protecting Emollients and Frostbite. Chapter 2.1.

Thermophysiology of man in the cold. In: <http://herkules.oulu.fi/isbn9514259882/>

Effect of Natural Aging on Wood Properties

Katalin Kranitz^{1} Walter Sonderegger^{2*} and Peter Niemz^{3*}*

¹ PhD student, ETH Zurich, Institute for Building materials, Wood Physics Group, Stefano-Francini-Platz 3, 8093 Zurich, Switzerland

kranitzk@ethz.ch

²Dr. Walter Sonderegger ETH Zurich, Institute for Building materials, Wood Physics Group, Stefano-Francini-Platz 3, 8093 Zurich, Switzerland

walter-sonderegger@bluewin.ch

³Professor, ETH Zurich, Institute for Building materials, Wood Physics Group, Stefano-Francini-Platz 3, 8093 Zurich, Switzerland

corresponding author

niemzp@ethz.ch

Abstract

The properties of wood are well documented and have been the focus of intensive research. Contrary to that, very little is known about the aging process of wood or the properties of the aged material, although such information is necessary to properly conserve wooden cultural heritage objects, as well as for the re-use of aged wood. Another challenge are the contradictory results and statements of studies on this topic. Therefore for many properties of aged wood no definite conclusions exist. A wide range of experiments on the chemical, physical and mechanical properties of aged wood were carried out to obtain results. Supplementary investigations on the role of factors influencing the properties of recent wood were conducted and a thorough literature study done. Based on the collected information, possible relationships between different properties were considered. It could be shown, that aging is governed by chemical changes. Even for specimens with 120 years of age a decrease in the extractive and hemicellulose content and signs of degradation of lignin were detected. Additionally, color changes were observed, namely an increase in redness and yellowness and a decrease in lightness. However, no significant influence of the mentioned chemical processes on the hygroscopic or mechanical properties were found, at least for up to 200 years of age (investigated in this work). Furthermore, it was confirmed that the aging process is dependent on the storage and service conditions and on the wood species as well.

Keywords: wood, aging, physical properties, chemical properties, mechanical properties

Introduction

The aging process of wood and the properties of aged wood have been scarcely investigated so far. In addition, the results of the studies are often contradictory and hard to compare to each other, as both, the wood species and the age of the specimens, vary and often the used methods differ.

The current study aims to fill this scientific gap and to contribute to the knowledge about the aging process of wood.

The main objectives were:

- delivering a complete characterization of wood aged in dry air,
- providing the necessary parameters for modelling wooden structures (furniture, simulating stresses induced through changing climatic conditions),
- reviewing of the assumptions and contradictions in earlier publications,
- describe the aging process and its effect on selected physical and mechanical wood properties.

Materials and Methods

Chemical tests and physical-mechanical properties:

To this aim, a wide range of experiments were performed on three different wood species commonly used in Europe: Norway spruce (*Picea Abies* L. Karst.), silver fir (*Abies alba*) and European oak (*Quercus robur* resp. *petraea*). Additionally new wood was investigated as reference material to the aged samples. Only defect-free clear specimens of sound wood were used for the investigations.

The age was determined with dendrochronology.

Grading from boards:

For a grading with ultrasound, aged wood (Norway spruce) used in an old buildings was obtained from companies that deal with wood from deconstructed buildings. Thus, the origin and history of the material is not known in detail.

The following investigations were carried out according to EN or DIN:

- Chemical investigations: determination of the proportion of the main components of wood (lignin, cellulose, hemicellulose, extractives and ash) by wet chemical methods; estimation of the crystallinity of cellulose and the cellulose/lignin ratio based on Raman spectra; analysis of extractives by means of gas-chromatography/mass spectroscopy (GC/MS);
- Investigations on the microstructure by means of environmental scanning electron microscopy (ESEM);
- Color measurements;
- Investigations on the hygroscopic behavior: determination of sorption isotherms and swelling coefficients for a single and repeated climate cycles,

- Investigations on strength and elastic properties: determination of bending strength as well as elastic and shear moduli with ultrasound (different testing devices)
- Investigations on the fracture behavior: determination of impact bending strength and fracture toughness; assessment of the proportional limit and the breaking strain in bending; analysis of fracture surfaces.

In order to be able to isolate the effects of aging, a multiple linear regression analysis was applied to the measured data. With this information about the influence of various factors on the investigated properties was examined. Besides specimen age, the factors density, annual ring width and moisture content were included in the model for regression analysis.

Results

Table 1 give an overview on changes due to aging based on values determined for recent species.

Chemical properties (table 2)

Chemical investigations revealed a decrease in the hemicellulose content with increasing age in the fir and oak samples. Additionally, their degradation products were detected by means of GC/MS investigations on the extractive compounds. The findings coincide well with literature, as almost all studies that considered the hemicelluloses in the aged samples reported a decrease of their proportion or some kind of modification, both in softwoods and hardwoods. However, no changes were found for the 120 years old fir samples. This could be due to the species, but also because of a more favorable storage conditions. As no earlier results are available regarding hemicellulose content in this species, the reason for this behavior cannot be determined.

Similar to earlier investigations carried out by different authors on specimens younger than 400 years, no significant difference between the cellulose content of aged and recent wood was found for softwood. Next to the ratio of cellulose, its crystallinity was investigated as well. The results indicate that no significant changes occurred in the samples. Kohara and Okamoto (1955) suggested that the crystallinity of cellulose in softwoods increases during the first hundred years of aging, followed by a decrease, while no increase occurs in hardwoods. Results of the current study are in agreement with this theory, as most other publications. However, an increase in crystallinity was reported for hardwood samples up to 180 and 260 years by (Popescu et al. 2007; Gawron et al. 2012). The reason behind this discrepancy may be the accuracy and differences between the applied methods (Thygesen et al. 2005; Agarwal et al. 2010).

Similar to cellulose, the proportion of lignin in the samples did not vary considerably among the samples. This included the reference material. However, degradation products of lignin among the extractives were found through GC/MS analysis. Degradation and oxidation of the lignin structures due to aging has already been reported in literature (Borgin et al. 1975a; Ganne-Chédeville et al. 2011). Some authors observed a change in

the proportion of lignin, namely an increase for samples between 300 and 800 years of age (Narayanamurti et al. 1961; Tomassetti et al. 1990) and a decrease for wood older than 4100 years (Van Zyl et al. 1973). The higher relative amount of lignin may be a consequence of a loss in the holocellulose fraction, but weight gain due to oxidation may contribute to this effect as well.

After summarizing the available literature and the current results, it can be stated that the chemistry of wood undergoes small changes during aging.

Physical and mechanical properties

The color of wood is determined by its chemical structure, thus any change in its chemistry can affect its color. As expected, the executed color measurements showed clear differences between aged and recent samples. An increase in redness and yellowness and a decrease in lightness was observed for all three investigated species. This is in accordance with the results of other studies on aged wood (Kohara and Okamoto 1955; Oltean et al. 2008; Miklečić et al. 2012). The pictures in Fig. 1 illustrate the differences between recent and aged wood.

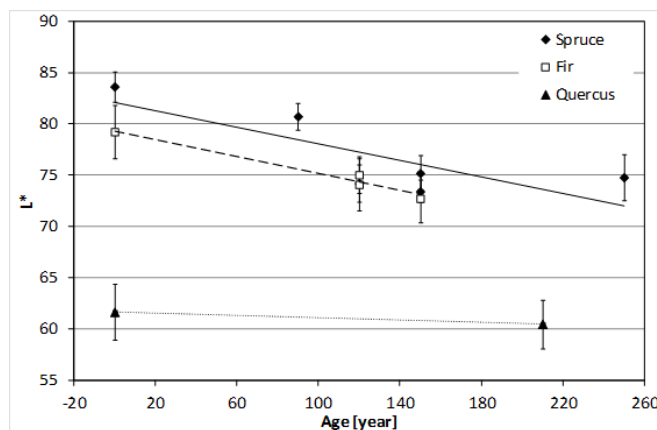


Fig. 1: Lightness as function from wood age

Hygroscopic behaviors

During investigations on the hygroscopic behavior of the samples, swelling coefficients and sorption isotherms were determined, for some specimens during multiple climate cycles. In contrast to results of previous studies and the beliefs of craftsmen about the improved dimensional stability of aged wood, no significant difference between the EMC and swelling properties of recent and aged samples were found. The exposure to cycling humidity resulted in a small decrease in the EMC, but did not affect the swelling coefficients from aged wood.

Table 1: Overview of the trends in property changes during aging, based on current results and literature values \uparrow : increasing; \downarrow : decreasing; \approx no change

material	age [year]	lignin content	cellulose content	hemicellulose content	crystallinity of cellulose	extractive content	ash content	porosity	lightness (L*)	redness (a*)	yellowness (b*)	chroma (C*)	Equilibrium moisture cont.	swelling coefficient radial	swelling coefficient tang.	swelling coefficient long.	bending strength	Young's mod. bending	Young's mod. eigentr.	Elastic modulus ultrasound	Shear modulus ultrasound	side hardness	impact bending strength	fracture toughness	fracture energy bending	elastic limit bending		
softwoods	current study																											
	spruce	90-210	\approx	\approx	\downarrow	\downarrow	\downarrow	\approx										\approx	\approx	\approx	\approx	\approx	\approx	\approx	\approx	\approx	\approx	\approx
		90-320							\approx	\downarrow	\uparrow	\uparrow	\uparrow		\uparrow/\approx	\uparrow/\approx												
	fir	120	\approx	\approx	\approx	\approx	\uparrow/\approx	\approx	\approx	\downarrow	\uparrow	\uparrow	\uparrow					\approx	\approx	\approx	\approx	\approx	\approx	\approx	\approx	\approx	\approx	\approx
		120-470												\approx	\downarrow/\approx	\downarrow/\approx												
literature																												
various species and age			\approx/\downarrow^2	\downarrow	\downarrow/\downarrow^3			\downarrow	\downarrow	\uparrow	\uparrow	\uparrow						γ^1	γ^1		$\gamma^{1,4}$	\downarrow	\downarrow					
hardwoods	current study																											
	oak	210-290	\approx	\uparrow	\downarrow	\downarrow	\downarrow	\approx	\approx	\downarrow	\uparrow	\uparrow	\uparrow	\approx	\approx	\approx	\approx											
		210-470												\approx	\approx	\approx	\approx											
literature																												
various species and age		\uparrow/\downarrow^5	\downarrow	\downarrow	γ^1	\uparrow	\uparrow		\downarrow	\uparrow	\uparrow	\uparrow	\downarrow	γ^1	γ^1		\downarrow	\downarrow			\downarrow^4	\downarrow	\downarrow					

¹ contradictory results; ² younger/older than 400 years; ³ change in trend around the age of 100 years; ⁴ determined by mechanical test; ⁵ increase by 300-800 years of age/decrease by 4100 year old samples

Table 2: Proportion of components determined by chemical analysis

sample	age	ash	extracts	cellulose	hemicellulose	lignin	Σ	
spruce	SA05	210 years	0.26%	1.29%	52.42%	19.88%	28.29%	102.14%
	SA06	150 years	0.33%	1.50%	52.95%	23.40%	29.48%	107.66%
	SA07	150 years	0.30%	1.84%	49.03%	27.11%	28.51%	106.78%
	SA08	120 years	0.32%	2.66%	49.03%	29.44%	30.50%	111.94%
	SR01	recent	0.26%	2.39%	53.01%	32.31%	29.00%	116.98%
fir	FA06	120 years	0.39%	2.95%	51.83%	19.32%	31.27%	105.76%
	FA07	120 years	0.40%	1.34%	56.43%	22.82%	29.90%	110.89%
	FR01	recent	0.29%	1.38%	52.26%	20.98%	28.14%	103.05%
oak	OA04	250 years	0.27%	5.24%	42.15%	17.37%	28.90%	93.92%
	OR03	recent	0.30%	11.96%	35.34%	29.09%	31.62%	108.31%

Mechanical properties

No significant differences wood were found between the mechanical properties of aged and recent in the current investigation (see Table 1). The correlation of density and moisture content with certain mechanical properties and the high variability of all properties is well known in wood science and was proven several times by regression analysis.

The dynamic elastic moduli for aged and recent spruce boards are plotted against the raw density in Figure 2. The values in this range and for this species correspond to the ones found in literature. The coefficients of determination and the slopes of the regression lines are quite similar for both groups of specimens and are compliant with well-known data for this type of measurement.

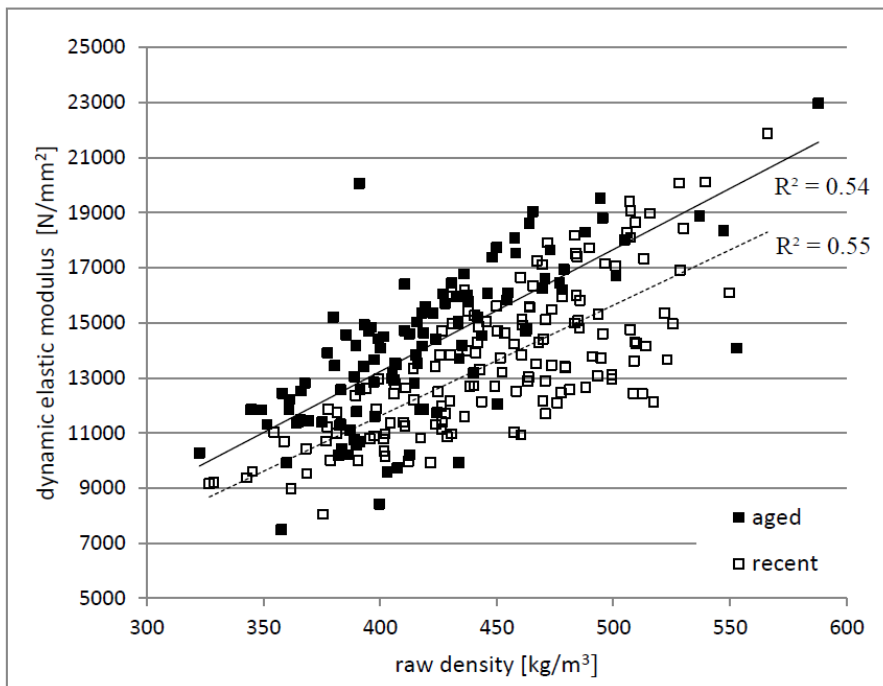


Fig. 2: Scatter plot of dynamic elastic modulus over raw density for aged and recent spruce wood (through testing of boards with ultrasound), Kranitz et al. 2014

Summary and Conclusions

The results suggest that the properties of wood stored under dry, indoor conditions change only to a small extent in the investigated time span of 200 years. The changes are mainly found regarding the chemical composition and color. This may not limit its usability. However, as storage conditions can remarkably affect the aging process, a condition assessment of aged wood based only on the age may be insufficient. As in most cases the history of the material is unknown, it is strongly recommended to further

investigate the aged material before processing, especially when it is intended to be used in a load-bearing role.

Table 3: MOE (E_B), bending strength (σ_b), fracture energy in bending (W_b), proportionality limit and breaking strain determined in bending (ε_b) for aged and recent wood

samples	age	n		ρ [g/cm ³]	arw [mm]	E_B [MPa]	σ_b [MPa]	W_b [J]	$\sigma_{0.1\%}$ [MPa]	$\sigma_{0.2\%}$ [MPa]	ε_b [%]	
spruce	SA06	150 years	4	mean	0.41	1.14	10385	77.2	7.70	63.5	70.4	1.17
				sd	0.02	0.10	619	3.0	0.49	1.8	1.9	0.03
				cov	4.0%	8.7%	6.0%	3.9%	6.4%	2.9%	2.7%	2.5%
	SA07	150 years	6	mean	0.46	1.60	12233	85.3	7.83	75.7	79.9	1.07
				sd	0.01	0.57	1275	5.2	2.58	1.1	6.5	0.21
				cov	3.0%	36.0%	10.4%	6.1%	33.0%	1.5%	8.1%	19.3%
	SA08	120 years	5	mean	0.44	2.47	12900	84.3	8.11	72.6	78.8	1.09
				sd	0.01	0.43	686	9.0	1.82	6.3	9.1	0.12
				cov	2.5%	17.5%	5.3%	10.7%	22.4%	8.7%	11.5%	11.4%
	SA09	120- 150 years	29	mean	0.42	2.63	11936	80.3	7.44	68.4	73.7	1.06
				sd	0.06	1.28	1584	10.8	2.16	7.2	10.5	0.17
				cov	13.6%	48.8%	13.3%	13.4%	29.0%	10.6%	14.3%	15.8%
SR01	recent	45	mean	0.41	2.60	11264	75.2	7.30	60.5	66.9	1.08	
			sd	0.02	0.96	2630	9.0	1.83	13.9	15.6	0.25	
			cov	5.6%	36.9%	23.3%	12.0%	25.0%	23.0%	23.3%	23.1%	
fir	FA08	150 years	4	mean	0.43	2.27	14325	77.2	7.45	60.7	69.0	1.09
				sd	0.04	0.60	2382	7.1	1.77	3.2	4.5	0.13
				cov	9.2%	26.4%	16.6%	9.2%	23.7%	5.2%	6.6%	11.6%
	FA06	120 years	6	mean	0.45	2.12	14117	86.8	8.32	72.2	80.7	1.09
				sd	0.02	0.32	1903	5.6	1.36	3.7	2.9	0.09
				cov	3.4%	14.9%	13.5%	6.5%	16.3%	5.1%	3.6%	8.2%
	FA07	120 years	3	mean	0.45	1.61	13767	69.7	5.12	59.0	58.9	0.83
				sd	0.01	0.24	1837	16.2	3.15	8.5	19.2	0.28
				cov	2.8%	14.6%	13.3%	23.2%	61.5%	14.5%	32.5%	34.2%
	FR01	recent	27	mean	0.48	2.40	14759	86.6	8.47	70.9	78.8	1.11
				sd	0.03	0.83	1664	8.9	2.14	7.4	7.1	0.15
				cov	6.1%	34.6%	11.3%	10.2%	25.3%	10.5%	9.0%	13.1%

References

Borgin, K., O. Faix and W. Schweers (1975a). "Effect of Aging on Lignins of Wood." *Wood Science and Technology* 9(3): 207-211.

Borgin, K., N. Parameswaran and W. Liese (1975b). "Effect of Aging on Ultrastructure of Wood." *Wood Science and Technology* 9(2): 87-98.

Ganne-Chédeville, C., A.-S. Jääskeläinen, J. Froidevaux, M. Hughes and P. Navi (2011). "Natural and artificial ageing of spruce wood as observed by FTIR-ATR and UVRR spectroscopy." *Holzforschung* 66: 163-170.

Gawron, J., M. Szczesna, T. Zielenkiewicz and T. Golofit (2012). "Cellulose crystallinity index examination in oak wood originated from antique woodwork." *Drewno* 55(188): 109-114.

Kranitz, K.: Effect of natural aging on wood. PhD thesis, ETH Zurich 2014

Kranitz, K.; Deublein, M.; Niemz, P.:

Determination of dynamic elastic moduli and shear moduli of aged wood by means of ultrasonic devices. *Materials and Structures* (2014) 47:925–936

Kohara, J. (1955). "Studies on the permanence of wood (X): Colorimetry on the old timbers by the trichromatic colorimeter." *Journal of the Japanese Forestry Society* 37(2): 63-66.

Kohara, J. and H. Okamoto (1955). "Studies of Japanese old timbers." *Sci Rep Saikyo Univ* 7(1a): 9-20.

Narayanamurti, D., S. S. Ghosh, B. N. Prasad and J. George (1958). "Note on Examination of an Old Timber Specimen." *Holz Als Roh-und Werkstoff* 16(7): 245-247.

Narayanamurti, D., B. N. Prasad and G. M. Verma (1961). "Untersuchungen an alten Hölzern 3. Ein altes Pterocarpus Holz aus Tirupathi." *Holz Als Roh-und Werkstoff* 19(2): 48-50.

Popescu, C. M., G. Dobeles, G. Rossinskaja, T. Dizhbite and C. Vasile (2007). "Degradation of lime wood painting supports evaluation of changes in the structure of aged lime wood by different physico-chemical methods." *Journal of Analytical and Applied Pyrolysis* 79(1-2): 71-77.

Thygesen, A., J. Oddershede, H. Lilholt, A. B. Thomsen and K. Stahl (2005). "On the determination of crystallinity and cellulose content in plant fibres." *Cellulose* 12(6): 563-576.

Tomassetti, M., L. Campanella and R. Tomellini (1990). "Thermogravimetric Analysis of Ancient and Fresh Woods." *Thermochimica Acta* 170: 51-65.

Van Zyl, J. D., W. J. Van Wyk and C. M. Heunis (1973). The effect of ageing on the mechanical and chemical properties of wood. IUFRO-5 Meeting: Wood in the Service of Man. Pretoria. 2: 1069-1080.

Deformation Analysis of Cutting Processes of Wood

Stephan Frybort^{1*} – *Thomas Krenke*² – *Ulrich Müller*⁴

¹ Senior Researcher, Division Wood Technologies – Wood K plus – Competence Centre for Wood Composites and Wood chemistry, Tulln, Austria.

* *Corresponding author*
s.frybort@kplus-wood.at

² Junior Researcher, Wood K plus – Competence Centre for Wood Composites and Wood Chemistry, Tulln, Austria.

³ Priv.-Doz., Institute of Wood Science and Technology, BOKU – University of Natural Resources and Life Sciences, Vienna, Austria.
ulrich.mueller@boku.ac.at

Abstract

Mechanical disintegration of wood is a central process in the woodworking industry. Optimisation of mechanical disintegration processes requires a basic understanding of the cutting process. However, a basic understanding of the influence of wood properties (e.g. fibre orientation, moisture content, temperature, etc.) on the cutting process as well as effects on surface quality, particle geometry, and mechanical weak boundary layer is lacking. The movement of the knife into the workpiece necessarily causes deformations around the process zone. Besides machining settings quantity and quality of deformation strongly depends on wood properties. Therefore, aim of this study was the development of a method to examine deformations at macro- and micro-scale during the cutting process. Analysis of the cutting process was done by means of a modified pendulum. The wood sample is fixed on the lower part of the fin, whereas the exchangeable cutting tool is positioned at the bottom dead centre of the pendulum. The actual cutting process happens when the fin is passing the knife at a cutting speed of around 6 m/s. For deformation measurements a so called randomised Speckle-pattern was applied on the surface of the sample to be examined. The cutting process was then observed by a high-speed camera. Images of the cutting process were analysed by the aid of Digital Image Correlation. For this preliminary study vertical deformation of spruce when cutting parallel to the grain (0°) was examined.

Keywords: deformation analysis, digital image correlation, cutting process, wood

Introduction

Cutting of wood is a central process in the woodworking industry (Maier 2001, Heisel and Tröger 2001). Beside the requested effect of disintegrating also undesired effects like deformation and irreversible damage of the surface of the workpiece is taking place

(Singh *et al.* 2002). The microscopically rounded cutting edge and the clearance surface of the knife cause a significant densification of the cell walls within the process zone. This more or less reversible densification process as well as irreversible deformation is the cause for the so called mechanical weak boundary layer (Stehr and Johansson 2000) which has a negative influence on subsequent process steps, e.g. bonding (Gardner 2002). To improve disintegration processes, concerning surface quality or particle geometry, the disintegration process has to be understood in more detail. For this reason it is necessary to examine the interaction between workpiece and cutting tool. Previous investigations of cutting processes addressed force analysis (Kivimaa 1952) and energy optimisation (Gottlöber 2003) of the cutting process as well as surface quality (Fischer and Gottlöber 2005) and surface energy (Frybort *et al.* 2014) of the freshly machined surface. To examine occurring deformations a method was developed enabling deformation measurements during the cutting process. Therefore an adapted pendulum was equipped with a high speed camera. Deformations of the workpiece during the cutting process were analysed by using Digital Image Correlation. For further studies this method will be combined with cutting-force measurements which deliver useful knowledge for a better understanding of disintegration processes.

Materials and Methods

Pendulum. For cutting-force measurements a pendulum (Wolpert, Vienna, Austria) was modified for analysis of linear cutting processes with cutting speeds around 6 m/sec (Krenke *et al.* 2014). Therefore a vertically adjustable machine table (IEF Werner, Furtwangen, Germany) is mounted on the bottom dead centre of the pendulum. The changeable knife HW: 30 x 12 x 1,5 (Leitz, Oberkochen, Germany) is fixed on the machine table. The wedge angle of the knife is 55°, the cutting angle δ was fixed at 65°. The table enables adjustment of different cutting thicknesses in steps of 1 μm . The sample is screwed on the adapted hammer (Fig. 1a). The comparatively high mass of the hammer (6 kg) enables constant cutting speed during the cutting process of 20 mm sample length. Cutting thickness was 100 μm .

Sample preparation. For deformation analysis solid samples of flawless spruce (*Picea abies* Karst.) were used (Fig. 1). To enable steady cutting through a more or less homogenous material without early- and latewood transition zones samples were prepared to allow cutting along the year ring. To analyze deformations by Digital Image Correlation a Speckle pattern is used on the surface to be investigated. The speckle pattern consists of randomly distributed dark spots, whereas necessary spot size is dependent on the resulting pixel size of the image. For the size of the image with 10 x 4 mm at the given resolution of 800 x 320 pixels a diameter of the dots of the Speckle pattern of around 40 μm is needed. To enhance contrast the samples were primed with white color prior to creating the Speckle pattern. A thick paint film has to be avoided to guarantee measurement of the wood sample instead of the paint. For creating the Speckle pattern an airbrush Evolution (Harder & Steenbeck, Norderstedt, Germany) with a nozzle of 0.15 mm in diameter was used.

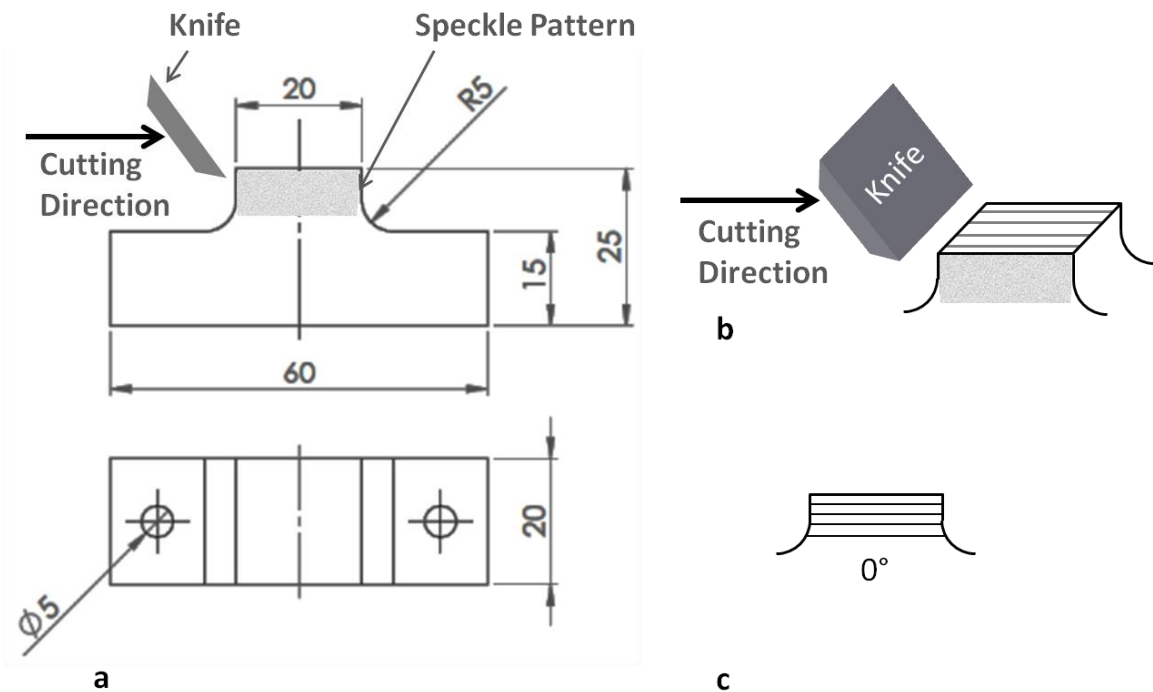


Figure 14: a Sample geometry, Speckle pattern and cutting direction, b cutting is happening on the flat surface with 20 mm in length along the year rings, c cutting direction 0°

High speed camera. To measure deformations during the cutting process a high speed camera Motion NX 7 (IDT, Tallahassee, USA) was mounted onto the Pendulum. To achieve exposure times 1 μ s two cold-light sources Marathon multiLED LT (Videal, Niederönz, Switzerland) were used. The cutting process was recorded with 16.500 fps.

Deformation measurement. For deformation analysis Vic-2D Digital Image Correlation Version 4.4.1 (Correlated Solutions, Columbia, USA) was used. For correlation procedure the reference image and three subsequent images and the scale of the images were defined. The area of interest was defined with 3 x 2 mm. Due to the large movement of the sample between the consecutive images an initial guess of three points was defined for each image to enable a correlation between the individual images. The subset size was defined with 21 and the step size with 5 and it was placed in a region of the sample where deformation is as small as possible. The amount of deformation was read out of the deformation plots.

Results and Discussion

For deformation analysis a high contrast of the Speckle pattern is mandatory. Therefore white background and clearly distinguished black dots of appropriate size are necessary. To enable short exposure times of 1 μ s an adequate illumination is needed. Reducing aperture (e.g. 1.2) is counterproductive as a deep depth of field is preferable for the more or less rough wood surface.

First results of cutting parallel to the fibre (0°) showed deformations of up to $30\ \mu\text{m}$ at the freshly cut surface (Figure 2). Deformation quickly decreases until a distance to the freshly cut surface of around $0,15\ \text{mm}$. An examination of Fischer (1980) with a similar experimental set-up and the same cutting thickness of $100\ \mu\text{m}$ showed deformations between $0.05\ \mu\text{m}$ for sharp knives and $100\ \mu\text{m}$ for blunted knives at the freshly cut surface. The study of Fischer (1980) showed deformation of 10 to $40\ \mu\text{m}$ at $8\ \text{mm}$ distance to the freshly cut surface. This high deformation is mainly thought to be attributed to the low cutting speed of $2.5\ \text{m/s}$ compared to this study with a cutting speed of $6\ \text{m/s}$. Comparing own results with values from literature is difficult as results from literature are somewhat contradictory. McKenzie (1960) did not find an influence of cutting speed (0.0002 to $142\ \text{m/s}$) on surface quality. In contrast, Ohta and Kawasaki (1995) reported that cutting mechanism is changing with cutting speed due to a change of the apparent stiffness of specimens under varying cutting speed. They observed high cell wall deformation at low cutting speeds ($0.00008\ \text{m/s}$) compared to less cell wall deformation and therefore to a rather smooth surface at higher cutting speeds ($5\ \text{m/s}$). Comparing results of this study with an unpublished examination at quasi static cutting speeds ($1\ \text{mm/min}$) confirm the influence of cutting speed on the degree and depth of deformation. To identify the minimum cutting speed concerning deformation quantity further studies are necessary.

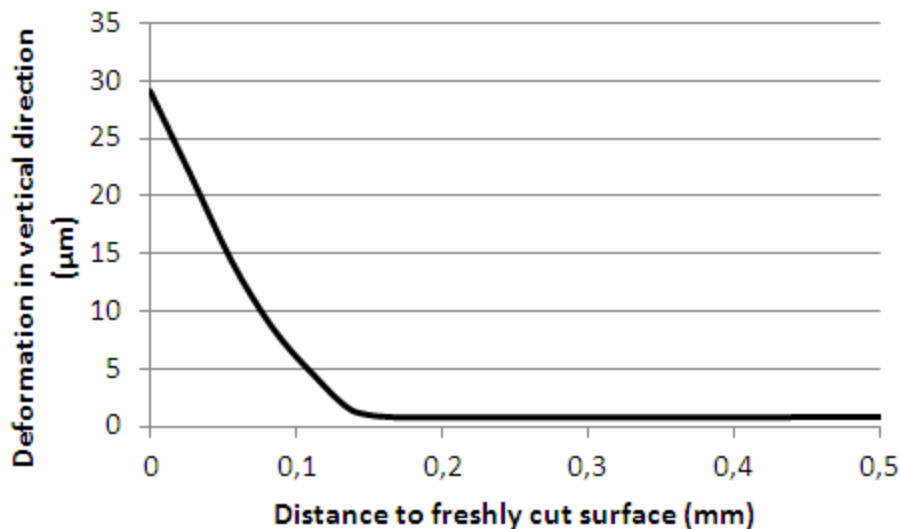


Figure 15: vertical deformation plotted against the distance to the freshly cut surface, cutting parallel to the grain (0°)

Conclusion

Measurement of deformation during the cutting process is possible by Digital Image Correlation. The influence of the cutting speed on the deformation behaviour could be shown. At higher cutting speed (e.g. $6\ \text{m/s}$) there is less deformation inside the sample

compared to lower cutting speed (e.g. 2.5 m/s). Further studies are needed to identify the minimum cutting speed concerning quantity of deformation and therefore surface quality.

References

- Fischer, R., Knüpfner, W., Regensburger, K. (1980) Orientierende Versuche zur Deformation beim Schneiden von Holz. *Holztechnologie* 21: 49-54.
- Frybort, S. Obersriebnig, M., Müller, U., Gindl-Altmatter, W., Konnerth, J. (submitted) Variability in surface polarity of wood by means of AFM adhesion force mapping. *Colloids Surf, A*.
- Gardner, D. J. (2002) Wood Surface Properties. 4th IUFRO Symposium “Wood Structure and Properties’02”, Zvolen, Slovakia: 87-89.
- Gottlöber, C. (2003) Spanungsprozesse in der Holzbearbeitung. *HOB* 10 66-70
- Fischer, R., Gottlöber, C. (2005) Grundlagen und Optimierung von Spanungsprozessen an Holz und Holzwerkstoffen. *Holztechnologie* 46: 44-51
- Heisel, U. and Tröger J. (2001) Aktueller Handlungsbedarf zur Bestimmung der Kräfte am Schneidkeil (2). *HOB* 47: 72 – 76.
- Kivimaa, E. (1952) Die Schnittkraft in der Holzbearbeitung. *Holz Roh Werkst* 10: 94-108.
- Maier, G. (2001) Was ist eigentlich ...? -Schnittleistung beim Spanen (3). *HOB* 47: 73 - 75.
- McKenzie, W. (1960) Fundamental aspects of the wood cutting process. *Forest Prod. J.* 10:447-456.
- Ohta, M. and Kawasaki, B. (1995) The effect of cutting speed on the surface quality in wood cutting--Model experiments and simulations by the extended distinct element method. 12th International Wood Machining Seminar, Kyoto, Japan: 56-62.
- Singh, A.P., Anderson, C.R., Warnes, J.M., Matsumura, J. (2002) The effect of planing on the microscopic structure of *Pinus radiata* wood cells in relation to penetration of PVA glue. *Holz Roh Werkst* 60:333–341.
- Stehr, M. and Johansson, I. (2002) Weak boundary layers on wood surfaces. *J Adhes Sci Technol* 14: 1211-1224.

Wood Panels Composites

Session Co-Chairs: *Marius Barbu, Transilvania
University of Brasov, Romania and Sergej Medved,
University of Ljubljana, Slovenia*

The Use of Waste Leather in Wood Based Panels

Axel M. Rindler.¹ – Pia Solt¹ – Marius C. Barbu^{1,2} – Thomas Schnabel¹

¹ Salzburg University of Applied Sciences
Forest Products Technology and Management
Markt 136a | 5431 Kuchl | Austria

axel.rindler@fh-salzburg.ac.at

² “Transilvania” University of Brasov
Faculty of Wood Engineering
Str. Universitatii nr.1 | 500068 Brasov | Romania

Abstract

A combination of the traditionally used and newly explored sources may reveal highly innovative ways.

The goal of this study is to provide an insight into the behaviour of the material and new applications of those fibre/particle wood and waste leather composites.

For this reason exclusively wood particles and fibres of spruce were used for the trials. Wet white (WW) leather particles, which are treated with herbal tannins and wet blue (WB) leather particles, which are tanned by using chromium-containing chemicals, were mixed with the wooden materials. To obtain meaningful comparisons, wood - leather combinations with 0%, 25%, 50%, 75% and 100% leather to wood content were produced. Besides the mechanical properties such as the internal bond (IB) the bending strength (MOR) and modulus of elasticity (MOE) was determined. Further physical properties as thickness swelling after 24h watering were investigated.

In the case of urea-formaldehyde (UF) bonded particleboard (700 kg/m³) the results show that all considered properties (IB, MOE, MOR) decrease with increasing leather content. If using UF bonded wood fibre (900 kg/m³) the results show an irregular improvement of the IBs with increasing leather content, whereas MOE and MOR decrease in equally. The

wood/leather samples show a significant difference in thickness swelling than 100% wood panels.

Keywords: Wet White Leather, Wet Blue Leather, Wood-Leather based panels,

Introduction

The ever-growing environmental consciousness of Western society increases the need for energy from biomass material [9] and better building material [17]. Thus the procurement of raw materials and resources for the wood products industry is significantly influenced. Because of this ever-growing demand of resources, the need cannot be met exclusively from sustainably harvested timber [16]. Therefore it is imperative to search for new and better alternatives [1] and proceed as resource saving as possible.

Investigations in nearly every section of new material resources have been made through the passed years. Most of these investigation aims were to up- or recycle a by-product to a composite material and to find possible supplements to the wood fibres and particles for wood based panel production [10]. Han [14] and Halvarsson [12][13] produced fibreboards from wheat and reed remains in combination with UF and UMF adhesives. Also exotic materials as coconut fibres [27], steam exploded banana bunch fibres [24], industrial hemp fibres [8], bamboo and rice straw [15] were investigated mechanically as well as physically and obtained meaningful insights into possible alternatives to conventionally produced fibre- and particleboards. Kargarfard [18] investigated encouraging agro-based materials as cotton and corn stalks in MDF panels. Lee [19] combined bagasse with other bio based materials, as bamboo, in particle panels and analysed their mechanical and physical properties.

Besides the bio-based materials also fossil-based materials, as plastic waste [2], were examined in combination with wood particles and fibres, and its degradability determined. A seminal way of by-product up cycling seems to be the usage of waste materials, as chicken feathers and leather shavings, which occur in the meat production [23], [20]. Most of these by-products are currently degraded thermally or getting landfilled on depositories in Central Europe [25] and the United States [28]. Winandy [28] manufactured and investigated medium density wood/chicken feather fibre composites and obtained interesting results in mechanical and physical properties. Investigations by Ostrowski [22] and Grünwald [11] describe the mechanical and physical effects of leather shavings in wood fibre materials with medium density and as insulating mats. Wieland and Stöckl [26] analysed the fire resistance of MDF boards with different leather contents and described a fire retarding behaviour of the wood/leather composite. This material combination of leather and wood, is issued in the European Patent by Lackinger (2009).

The aim of this study is to define the influence of leather type (Wet White=WW, Wet Blue=WB) and amount to the mechanical and physical properties of particle and high-

density fibreboards (HDF). Wood/leather combinations were mixed with leather contents 0-100% in 25% steps.

Materials and Methods

Materials

For this investigation the leather particles were provided by “Lackinger Consulting” Salzburg, Austria. Two different leather types, which are defined as wet white (WW) and wet blue (WB), were used. For the tanning process of WW a synthetically non-chromatic tanning is used whereas in WB chromium is connected with the proteins of the hides in a stable bond. Both leather types were dried to a moisture content of $8 \pm 1\%$ in a dry kiln. In a further step the dry particles were sieved to a grid size < 4 mm and separated into a fine and a rough part. The provided particles derived from spruce (*Picea abies*) were exclusively core layer particles with a length > 6 mm and a moisture content of $9 \pm 1\%$. The used wood fibres (*Picea abies*) were provided by MDF Hallein, Austria and had a moisture content of $8 \pm 1\%$. For this investigation all tested samples were prepared using the adhesive Urea- Formaldehyde “Prefere 10F102” by MetaDynea, Krems, Austria with a solid content of 66% and a 30 per-cent Amonium Sulfat-solution as a hardener.

Production of the panels

The particleboards with dimensions 450 x 450 x 12 mm and fibreboards with dimensions 450 x 450 x 4.5 mm were produced under laboratory conditions. Both panel types were manufactured with different leather to wood contents (0%, 25%, 50%, 75%, 100%) to provide a meaningful insight into the influence of the material content to the panel properties. Whereas the particleboards were prepared with a density of 700 kg/m^3 , for the fibreboards a density of 900 kg/m^3 was defined. Both panel types were produced with a resin amount of 10%, by using a Höfer HLOP 280 automated hot-press at 120°C with a pressing factor of 0.5 min/mm. After the pressing process the samples were stored in a standard climate (20°C / 65 % r.H.).

Testing Methods

The testing samples for both board types, for the modulus of rupture (MOR) and elasticity (MOE), were prepared by the formula $50 \text{ mm} \times (50 \text{ mm} + 20 \text{ mm} \times \text{thickness})$ which is in accordance to the EN 326-1:2005 [6] and the EN 310:2005 [3] with a crosshead speed of 10 mm/min. To analyse the internal bond (IB) the test was conducted according to EN 319:2005 [5] and therefore the testing samples were prepared in dimensions of 50 x 50 mm. To obtain meaningful results, each of the mechanical tests had an amount of 5 samples [n=5].

The samples for the thickness swelling after 24 hours watering were prepared in dimensions of 50 x 50 mm and the test was conducted in accordance to the EN 326-1:2005 [6] and the EN 317:2005 [4]. For the thickness swelling investigation 5 samples of the pure wood panels and leather/wood panels with leather contents of 50% and 100% were tested.

Results

Influence of the leather type and amount on mechanical properties

The mechanical investigations show, in all cases, a significant influence of the leather type and the leather amount to the mechanical properties of the particle- and fibreboards. As clearly visible in **Error! Reference source not found.** and **Error! Reference source not found.** the modulus of elasticity decreases with increasing leather content for both leather and both board types. Interestingly the 25% WW and WB HDF show a higher MOE mean than the pure wood high density panel. The particle boards in Figure 1 show a linear declining for higher WB and WW content. Although the WB values show a slight distortion at 75% in their development, it is not as significant as the MOE for the HDF on Figure 2. According to the analysis of variance ($\rho=0.05$) it is to say that the amount of leather is highly significant for both particle- and fibreboard, but the type of leather shows significant influence on particleboards only. Comparing between fibre- and particleboards, it is to say that the decreasing of MOE

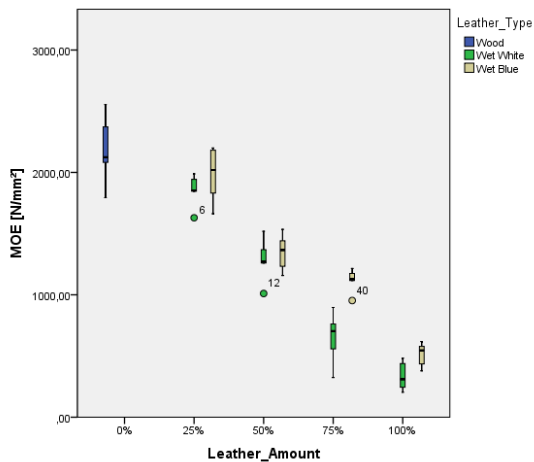


Figure 1: MOE of Particleboard

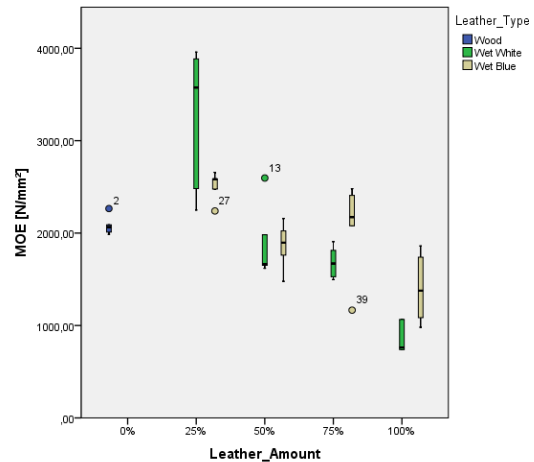


Figure 2: MOE of High Density Fibreboard

properties is more significant and in a high gear crucial for HDF than for particleboards. The MOR results show a similar behaviour of values to the MOE results. While HDF WW 25% and WB 25% indicate an explicitly stronger performance than the 100% wood based HDF panel, the particleboards show a decreasing MOR with increasing leather content. Interestingly in both types of panels the WB means show a non-linear, whereas the WW means show a clearly linear behavior for particleboards in correlation with the leather amount. The analysis of variance ($\rho=0.05$) shows that the amount as well as the type of leather significantly influences the MOR properties of the particleboards, but not the combination of both.

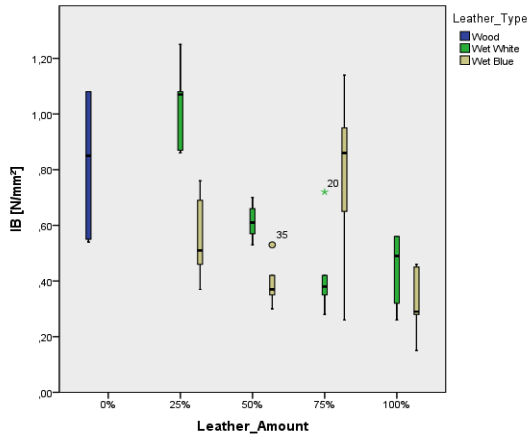


Figure 3: IB of Particleboard

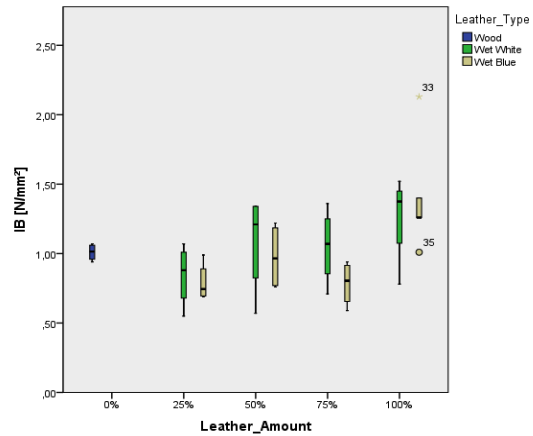


Figure 4: IB of High Density Fibreboard

Figure 3 and Error! Reference source not found. show the medians and standard deviations of the Internal Bond results, which indicate a relation between transverse tensile strength and leather content in the panels. It is to say that the IB is decreasing with increasing leather content in the particleboards. However, the IB results of WW 25% medians represent the strongest tensile strength properties, and also the median WB 75% samples show a higher IB (Fig. 3). As visible in **Error! Reference source not found.** the medians of the IB of HDF rise with increasing leather content. Both leather types show a higher performance in the board with 50% content than with 25% or 75% leather content. Except WW 25% every median of the WW panels shows a higher IB than the median of pure wood HDF. According to the analysis of variance ($\rho=0.05$) for the particleboards and the fibreboards the type of leather has no significant influence on the IB. For both panel types the amount of leather has a high significant influence, but the combination of leather amount and type is only significant for the particleboards.

Influence of leather type and amount on physical properties

Figure 5 and Figure 6 show that there is a significant difference of thickness swelling after 24h watering between particle- and fibreboards with various leather content and pure wood panels.

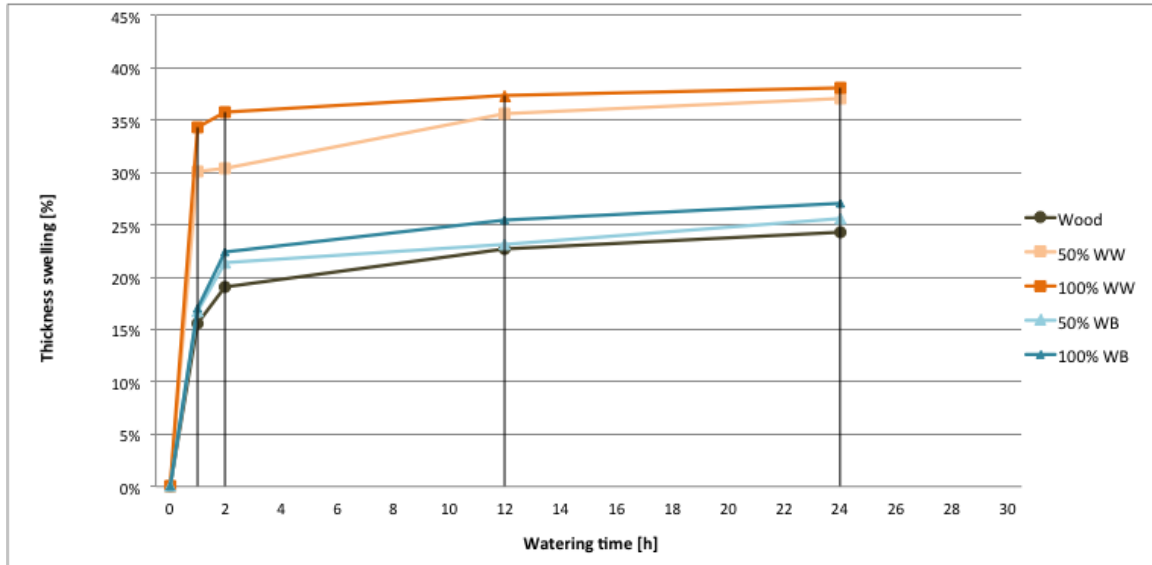


Figure 5: Particleboard Thickness Swelling after 24h Watering

The particleboards with leather show an intense hydrophilic behaviour compared to the pure wood particleboard. Whereas the wood particleboard shows an increase of thickness of around 24%, WW 50% and WW 100% swelled over 35% in thickness. WB 50% and WB 100% performed weaker and show slightly higher values than the wood particleboard.

Also the fibreboards show a similar behaviour in Figure 6 as the particleboards, although not as distinctively. Here the panel WW 100% with around 17% and WB 100% with around 13% show the strongest performance in swelling. WW 50% and WB 50% nearly reached the same increase of thickness of around 11%. According to the analysis of variance ($\rho=0.05$) there no significant influence of the leather type but of the amount of leather on the swelling behaviour.

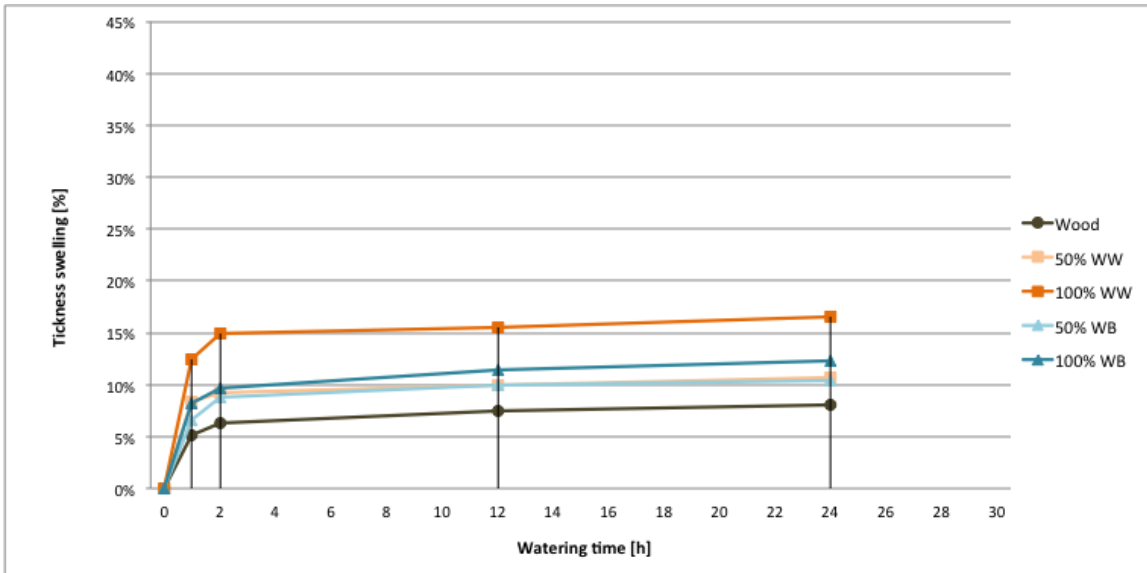


Figure 6: High Density Fibreboard Thickness Swelling after 24h Watering

Conclusions

1. The results for the modulus of rupture (MOR) and of elasticity (MOE) showed a decrease for particleboard and fibreboard with increasing leather content. Only the high-density fibreboards with 25% leather amount could achieve higher results than 100% wood fibreboards. A different linking behaviour between leather particles and UF resin and wood fibres and UF could be considered. To get certainty about this behaviour the linkage and penetration of UF to leather could be discovered in further research.
2. Regarding to the findings of the internal bond (IB) the results showed astonishing insight into the importance of the mixing proportion between leather particles and wood. Probably the correlation of the density of the panel and the particle size of the leather particles is a significant factor, which needs more research to obtain a better understanding
3. According to the results of the physical investigations the enormous hydrophilic behaviour of boards with higher leather content is to mention. To really use leather as an alternative to wood fibres in particle or fibreboards any kind of additive needs to be involved to reduce its water adsorption.

Acknowledgement

The authors gratefully acknowledge for the support of the Austrian Research Promotion Agency (FFG) under grant no.836988 and the partners from the industry.

References

- [1] BARBU, M.C., REH, R., IRLE, M. (2014): Wood-based Composites, Chapter 1 in Research Developments in Wood Engineering and Technology, edited by Aguilera,

- A.; Davim, P. IGI Global. Engineering Science Reference
- [2] BOEGLIN N., et al. (1997): A feasibility study on boards from wood and plastic waste: bending properties, dimensional stability and recycling of the board, *Holz als Roh- und Werkstoff* 55, p. 13-16, Springer.
- [3] CEN (2005), EN 310. "Particleboards and fiberboards – Determination of tensile strength perpendicular to the plane of the board"
- [4] CEN (2005), EN 317. "Particleboards and fibreboards - Determination of swelling in thickness after immersion in water"
- [5] CEN (2005), EN 319. "Wood-based panels – Determination of modulus of elasticity in bending and bending strength"
- [6] CEN (2005), EN 326-1. "Wood-based panels - Sampling, cutting and inspection - Part 1: Sampling and cutting of test pieces and expression of test results"
- [7] CEN (2011), EN 11925-2. "Reaction to fire tests - Ignitability of products subjected to direct impingement of flame - Part 2: Single-flame source test (ISO 11925-2:2010)"
- [8] CROWLEY J.G. (2001): The performance of cannabis sativa (hemp) as a fibre source for medium density fibre board (MDF), European Agricultural Guidance and Guarantee Fund, European Union.
- [9] DEMIRBAS, A. (2005): Potential applications of renewable energy sources, biomass combustion problems in boiler power systems and combustion related environmental issues, *Journal Progress in Energy and Combustion Science* 31 (2005) 171–192, Elsevier
- [10] DEPPE, H.J., ERNST, K. (1996): MDF – Mitteldichte Faserplatten, DRW – Verlag Weinbrenner GmbH & Co., Leinfelden – Echtingen.
- [11] GRÜNEWALD T. (2012): Structural Analysis and Mechanical Characterization of Wood-Leather Panels, Masterarbeit, Fachhochschule Salzburg.
- [12] HALVARSSON S., et al. (2008): Properties of medium-density fibreboard (MDF) based on wheat straw and melamine modified urea formaldehyde (UMF) resin, *Industrial Crops and Products* 28, p. 37-46, Elsevier.
- [13] HALVARSSON S., et al. (2009): Manufacture of non-resin wheat straw fibreboards, *Industrial Crops and Products* 29, p. 437-445, Elsevier.
- [14] HAN G., et. al. (2001): Development of high-performance UF-bonded reed and wheat straw medium-density fiberboard, *Journal of Wood Science* 47(5).
- [15] HIZIROGLU S., et al. (2008): Overlaying properties of fiberboard manufactured from bamboo and rice straw; *Industrial Crops and Products* 28, p. 107-111, Elsevier.
- [16] IRLE, M., BARBU, M.C., REH, R. et al. (2013): Wood Composites, Chapter 10 in *Handbook for Wood Chemistry and Wood Composites*, edited by Rowel, R. 2nd Edition. CRC Press Taylor & Francis Group LLC
- [17] IRLE, M., BARBU, M.C. (2010): Wood-Based Panel Technology, Chapter 1, in *Wood-Based Panels: An Introduction to Specialists*, edited by Thömen, H. et al. Brunel University Press.
- [18] KARGARFARD A., et al. (2011): The performance of corn and cotton stalks for medium density fiberboard production; *BioResources* 6(2), p. 1147-1157, Bioresources.
- [19] LEE S., et. al. (2006): Mechanical and physical properties of agro-based fiberboard. In *Holz als Roh-und Werkstoff* 64.

- [20] LMC International (2007): "Global Supply of hides and skins," In: Pocket Book for the Leather Technologist, BASF, p. 47.
- [21] MANTAU U., et al. (2010): "Wood resource balance results - Is there enough wood for Europe?" In: U. Mantau et al. (eds.): Real potentials for Changes in Growth and Use of EU Forests, University of Hamburg, pp. 19-34.
- [22] OSTROWSKI S. (2012): Entwicklung eines Wärmedämmstoffes aus den natürlichen Materialien – Holz und Leder, Masterarbeit, Fachhochschule Salzburg.
- [23] PARKINSON G. (1998): Chementator: A higher use for lowly chicken feathers?, Chemical Engineering, 105(3):21.
- [24] QUINTANA G., et al. (2009): Binderless fiberboard from steam exploded banana bunch; Industrial crops and Products 29, p. 60-66, Elsevier Verlag;
- [25] SCHRÖTER A., (1995): Versuch einer Wertung der Lederherstellung und Untersuchung wichtiger Schuhkomponenten unter ökologischen Aspekten, München, Diplomica.
- [26] STÖCKL U., (2013): Vergleichende Untersuchungen zum Feuerwiderstand und Aufzeigen neuer Einsatzgebiete feuerwiderstandsfähiger Plattenwerkstoffe aus Holz- und Lederfasern, Masterarbeit, Fachhochschule Salzburg.
- [27] VAN DAM J., et al. (2004): Production process for high density performance binderless boards from whole coconut husk, Industrial Crops and Products 20, p. 97-101, Elsevier.
- [28] WINANDY J.E., et al. (2007): Chicken feather fibre as an additive in MDF composites, Journal of Natural Fibers, 4:1, 35-48, Taylor & Francis;

Bark Based Insulation Panels Made of Different Bark Species

Günther Kain^{a,b}, Marius-Catalin Barbu^{a,c}, Alexander Petutschnigg^{a,d}, Bettina Hauser^a, Michael Mazzitelli^a,

a: Department of Forest Products Technology and Timber Construction,
Salzburg University of Applied Sciences, Markt 136, 5431 Kuchl, Austria;
gkain.lba@fh-salzburg.ac.at

b: Faculty for Wood Science, Technical University Munich, Winzererstraße
45, 80797 Munich, Germany

c: Faculty for Wood Engineering, University “Transilvania” Brasov, Str.
Universitatii 1, 500068 Brasov, Romania

d: BOKU University of Natural Resources and Life Science, Konrad
Lorenzstraße 24, 3430 Tulln, Austria

Abstract

This study focuses on bark-insulation boards made out of bark from several different tree species, aiming to find the ideal bark-species for thermal insulation. Therefore bark from fir/spruce-, larch-, pine- and oak- trees has been used to produce bark-insulation-boards (thickness ranging from 10 to 20 mm) with a density ranging from 0,3 g/cm³ up to 0,8 g/cm³, different particle sizes ($10 < x_1 < 30$ mm, $6 < x_2 < 10$ mm, $3 < x_3 < 6$ mm) as well as different adhesive systems (UF, MUF, Tannin) with varying resination. All boards were further tested on their mechanical properties (MOR, MOE, IB, TS and WA after 24h) as well as on their thermal conductivity (λ) values and were then statistically analyzed to determine the ideal board properties. Summarizing it was found that all the evaluated bark species can be used for insulation board use. Thermal conductivity is primarily influenced by panel density. With regard to panel stability all tested resin systems proved to be acceptable.

Introduction

Caused by the current situation of resource scarcity, the future trends and needs lead to a necessity to put on further research on alternative and sustainable solutions referring to raw-materials based on natural resources as adaptive and exchangeable building materials. The fact that an average amount of 10 % of a tree is bark (Xing et al. 2006), projected to the amount of sawn timber all over the world, and bark is hardly used as building, leads to the conclusion that there is a reasonable potential capacity for further research on this raw-material sector regarding the building industry (Kleinhempel 2005).

Inspired by the natural purpose of bark itself, protecting the tree stem from external influences, research was done on bark and its insulating properties. (Barbu 2011, Kain et al. 2012, 2013)

The aim of the following study was to compare bark of different tree species like fir (*Abies alba*), spruce (*Picea abies*), pine (*Pinus sylvestris*), larch (*Larix decidua*), oak (*Quercus spec.*), according to its thermal and mechanical properties. Therefore different bark panels with varying density, resination and particle size were produced. The different board types were further on tested, following standardized testing methods, and statistically analyzed to find the ideal species as well as technical properties.

Materials & Methods

As raw material bark from fir-, spruce-, larch-, pine-, and oak-trees was chosen and determined to be compared. Therefore bark from surrounding saw-mills in the area of Salzburg was gathered and subsequently dried in a vacuum dryer located at the Salzburg University of Applied Science in Kuchl. The bark, which was dried to an average moisture content of 5-10 %, was separated into 3 fractions sizes using fractioning machinery with different mesh sizes. In the following process, boards from all available kinds of fraction sizes as well as bark-species were produced with a density ranging from 0,3 g/cm³ up to 0,8 g/cm³, using three different adhesive systems with an adhesive-content varying from 8 % to 20 % (Table 1).

Table 1: Experimental design with the explanatory variables of the bark based insulation panels

Bark	Particle size	Target density	Resin type	Resin amount	No. sample
Oak	6/10	300	UF	8	1
				12	1
		350	MUF	8	1
				12	1
			UF	8	1
				12	1
		400	MUF	8	1
				12	1
			UF	8	1
				12	1
		450	MUF	8	1
				12	1
UF	8		1		
	12		1		
Spruce / Fir	3/6	400	MUF	8	1
				12	2
			UF	8	2
	6/10	400	MUF	8	2
				12	2
			UF	8	2
				12	2
		450	MUF	8	2
				12	2
	UF	8	2		
	12	2			
	Pine	13/30	200	S	0
250			S	0	1
400			UF	8	3
500			UF	8	3
				12	3
8/13		350	UF	12	1
		400	UF	8	2
				10	1
				12	0
		500	UF	6	1
				8	2
		12	3		
Larch	3/6	400	MUF	8	1
	6/10	250	Tannin	15	2
				20	2
			UF	15	1
		300	Tannin	15	2
				20	2
			UF	12	1
				15	1
		350	Tannin	10	2
				15	2
			UF	12	1
		400	MUF	8	1
				12	1
			Tannin	8	2
				10	2
	15			2	
	20			2	
	UF		8	1	
			12	1	
	450	MUF	8	1	
			12	1	
UF		8	1		
12	1				

	500	Tannin	5	2
			10	2
			15	2
			20	2
	800	Tannin	10	2

As binding agent two commonly used adhesives from the wood-industry have been used, urea-formaldehyde (UF) and melamin-urea-formaldehyde (MUF), and one innovative natural adhesive system based on tannins.

The UF adhesive systems were activated with 5% of an 25 % ammonium sulfate solution and possesses a solid content of about 60 %. For the tannin based adhesive systems, 50 % tannin powder and 50 % water was mixed carefully to a homogeneous viscous solution and following brought to a pH of about 9 by adding gradually a 32 % caustic soda solution. The viscous mixture was further added a 33 % hexamine solution to synthesize the binder before mixing it with the bark particles (Kain et al. 2014).

The particles were resonated in a laboratory ploughshare mixer and finally pressed with a common hot-press at a temperature of 180°C.

After pressing several different board types (Table 1), regarding to density, adhesive-type, binder-content, particle size and bark-species, the boards were tested on their thermal and physical properties. The thermal conductivity, as well as physical properties like MOR, MOE, IB regarding to panel boards, was determined by standardized testing equipment. Finally all test results were statistically evaluated in order to determine the best combination for a bark board.

Results and discussion

As a general result it can be said that thermal conductivity is improving by lowering density of bark boards relating to all tested bark-types (Figure 16). That fact was proven by coefficients of determination between 0.4 and 0.9 for the regression between panel density and thermal conductivity with the different bark species. An univariate analysis of variance showed bark species statistically very significantly ($p < 0.01$) influences the thermal conductivity, whereas the particle size doesn't show an effect in that respect. Boards out of spruce/fir bark showed an on average a 4 mW/(m*K) lower thermal conductivity than pine bark boards.

Focussing on the IB (as the most important mechanical board characteristic) again it is positively correlated with density showing coefficients of determination between 0.3 and 0.7 for the different resin systems (Figure 17). Also bark type and resin content showed highly significant ($p < 0.001$) influences on the IB whilst no statistical significant influence of the resin type was found. In that respect larch boards showed for a given density the best IB values and naturally a higher resination resulted in better internal panel stability. Particle size did not show a clear effect on the panels' IB (Figure 18). Moisture resistance of the bark panels was studied by the means of water absorption after 24 h of immersion. An univariate analysis of variance showed that density, bark species, resin type, and resin content highly significantly ($p < 0.001$) influence the water absorption. Although variation in water absorption is quite high, it could be clearly shown that density is negatively correlated with water absorption and that the natural

tannin resin system is competitive to the studied UF and MUF resin (Figure 19). The lowest water absorption was achieved with oak bark.

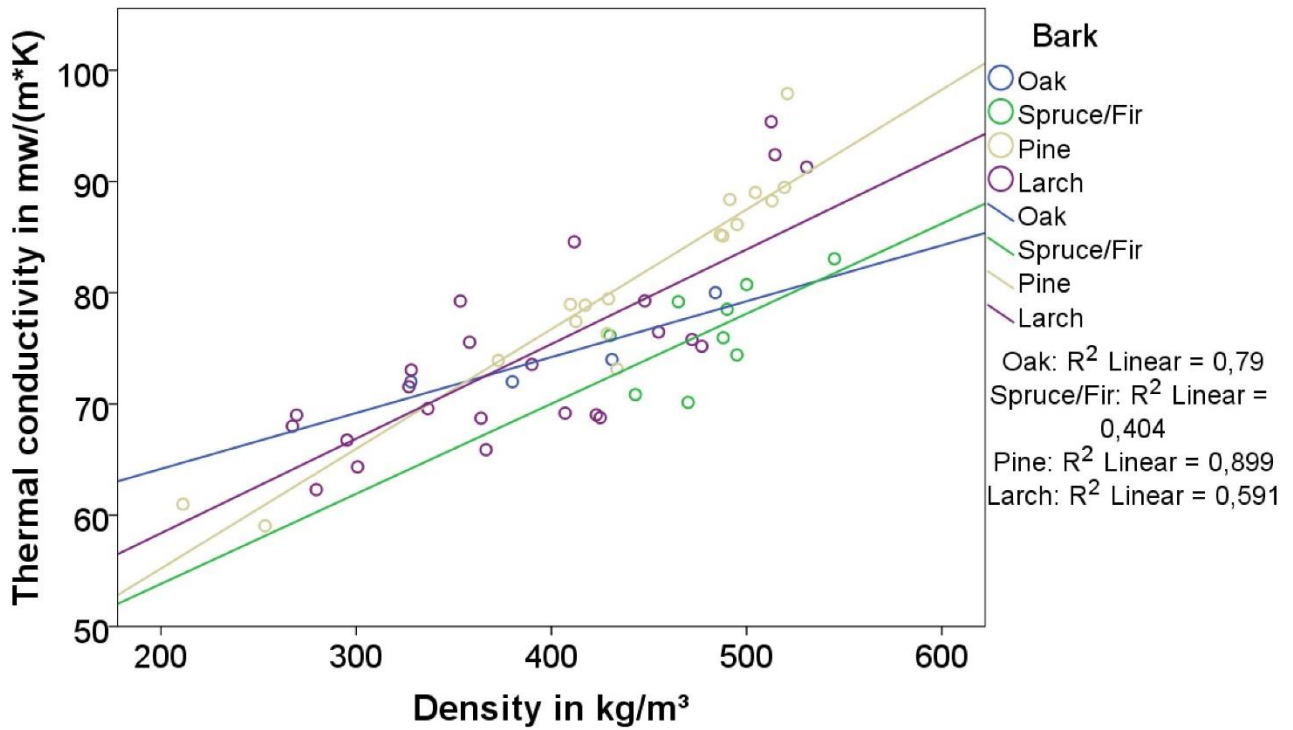


Figure 16: Panel density and bark species effect on thermal conductivity

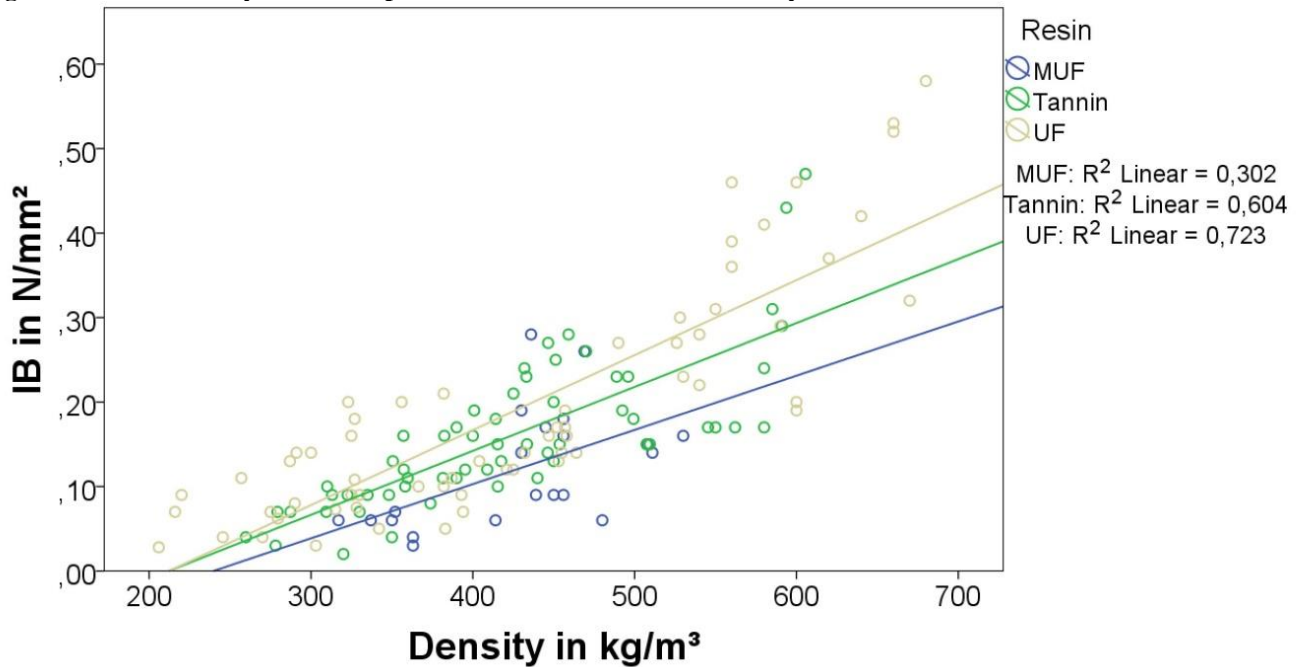


Figure 17: Panel density and adhesive type effect on IB

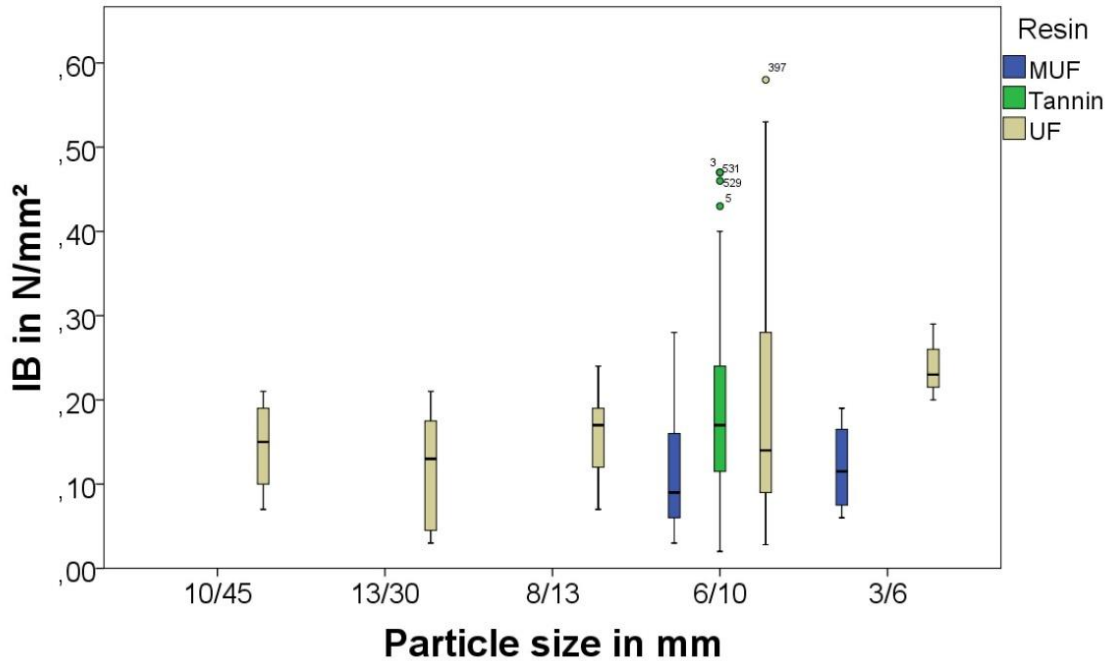


Figure 18: Particle size and adhesive type effect on IB

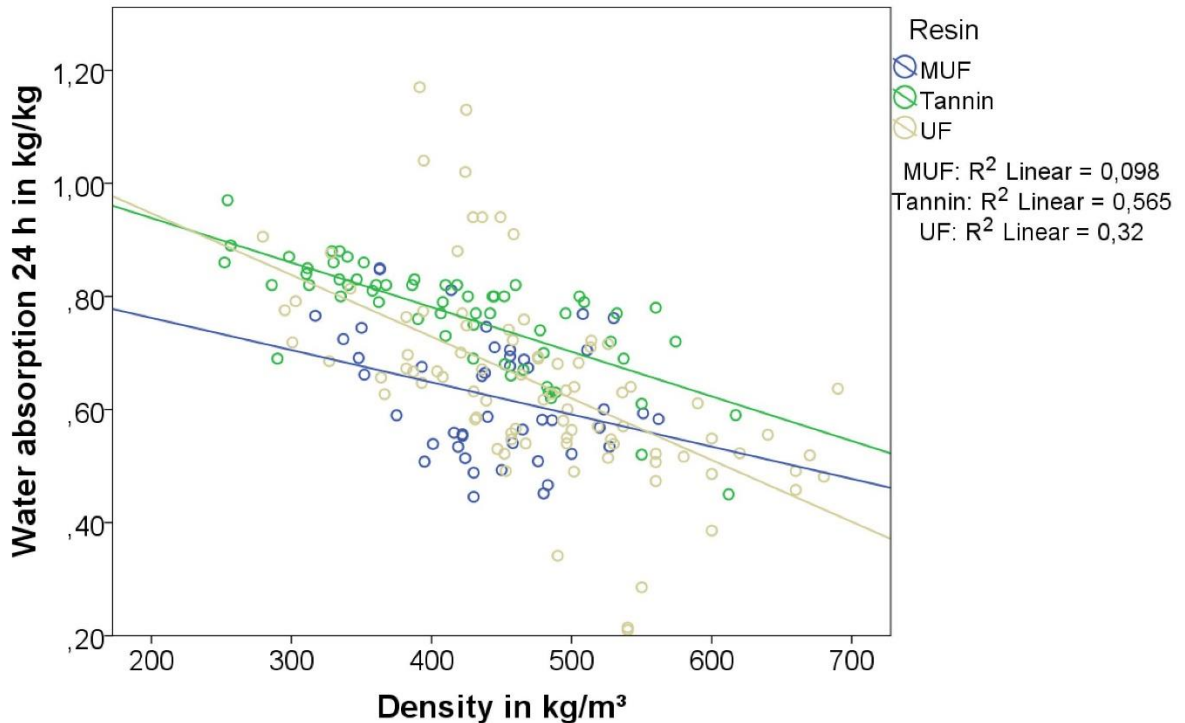


Figure 19: Water absorption after 24 hours depending on density and resin system

Panel thermal conductivity is nearly 4 times stronger influenced by panel density than is by bark type (shown by partial eta squared values in ANOVA). IB is twice as much influenced by density than it is by bark type or resin content. With regard to water absorption density has the highest explanatory power. Roughly half as good is the explanatory power of bark type and resin content. Whereas for further optimization higher resin boards out of oak bark would be beneficial for lower water absorption.

Conclusions

Generally it was found that all studied bark species are suitable for insulation panel production. Also, the three studied resin systems were proven to show sufficient strength properties. Overall it can be said that by dropping density the thermal conductivity is getting better, but internal bond however decreases. Therefore the most important task for future research activities will be an optimization of thermal conductivity and internal bond varying density, resin amount and probably particle size (as it is a key criterion for low density panels). The performance of the ecological tannin resin systems was as good as it is with UF or MUF resins and therefore ecological bark insulation panels can be produced without any hesitation.

Acknowledgment

The authors like to address their thanks to the companies Peter Graggaber GmbH in Unternberg for the and Wimmer Holz in Kuchl for the bark, to Egger GmbH in St.Johann/Tirol and Dynea (today Metadynea) in Krems/Donau for the resins, to Untha GmbH and Holztechnikum in Kuchl for chipping and screening and also to Mrs. Eva Troppova from Gregor Mendel University in Brno for her support during the Erasmus exchange term.

Literature

Barbu, M.C.(2011): Current developments in the forestry and wood industry. *ProLigno*7(4):111-124

Kain G., Teischinger A., Musso M., Barbu M.C., Petutschnigg A. (2012): Thermal insulation materials out of tree barks. *Holztechnologie* 53(4):31-37 (in German)

Kain G., Barbu M.C., Teischinger A., Musso M., Petutschnigg A. (2013a): Substantial bark use as insulation material. *Forest Product Journal* 62(6): 480-487

Kain G., Barbu M.C., Hinterreiter S., Richter K., Petutschnigg A. (2013b): Using bark as a heat insulation material. *Bioresources* 8(3): 3718-3731

Kain G., Güttler V., Barbu M.C., Petutschnigg A., Richter A., Tondi G. (2014): Density related properties of bark insulation boards bonded with tannin hexamine resin. *Eur. J. Wood Prod.*

Kleinhempel A. K. (2005): Innovative insulation materials in civil engineering – current state of research and market compendium. Department for Energy, University of Bremen (in German)

Xing C., Deng J., Zhang S. Y., Riedl B. and Cloutier A. (2006): Impact of bark content on the properties of medium density fibreboard (MDF) in four species grown in eastern Canada. For. Prod. Journal 56(3):64-69

Some Properties of Fire Retardants and Sand Dusts of Medium Density Fiberboard Filled Thermoplastic Composites

Ayfer D. Cavdar^{1}, Hulya Kalaycioglu², Ertugrul Casur³, Fatih Mengeloglu⁴*

¹ Assistant professor, Interior Architecture Department, Karadeniz Technical University, 61080 Trabzon, TURKEY

** Corresponding author
adonmez@ktu.edu.tr*

² Professor, Forest Industry Engineering Department, Karadeniz Technical University, 61080 Trabzon, TURKEY

³ Ph.D and Director, Kastamonu Integrated Wood Industry & Trade Company, 41400 Kocaeli, TURKEY

⁴ Professor, Forest Industry Engineering Department, Kahramanmaraş Sutcuimam University, 46100 Kahramanmaraş, TURKEY

Abstract

Physical, mechanical, thermal, fire and biological properties of sand dusts of medium density fiberboard filled thermoplastic composites incorporated with different contents of aluminum tri hydrate (ATH) and zinc borate (ZB) were investigated. In this study, the performance analysis of the composites produced with the extrusion method was accomplished by using sand dusts of medium density fiberboard (SD_MDF) as lignocellulosic materials and high density polyethylene (HDPE) and polypropylene (PP) as thermoplastic polymer. Coupling agents and fire retardants (FRs) were used to improve fire properties of the composites, and their effects on technological properties were evaluated. The performances of the composites were evaluated in aspect of physical, mechanical, thermal, fire, and biological properties. ATH had a positive effect on tensile modulus of the composites whilst ZB had adversely effect on that of the composites. However, strength properties of the composites slightly decreased with usage of FRs. In the light of obtained results, it was specified that use of FRs improved physical, biological, thermal and fire properties of SD_MDF filled thermoplastic composites.

Keywords: A. Sand Dusts of Medium Density Fiberboard, A. High density polyethylene, A. Polypropylene, A. Fire Retardants, B. Mechanical properties, B. Fire and thermal properties, B. Biological and physical properties

Introduction

Natural fiber filled thermoplastic composites or wood-plastic composites (WPC) are still new materials relative to other wood based composites. The most widespread use is in outdoor deck floors, but it is also used for railings, fences, landscaping timbers, cladding and siding, park benches, molding and trim, window and door frames, and indoor furniture (Clemons 2002). These composites are often considered a sustainable material because they can be made using the waste products of the wood industry (Mishra and Naik 2005, Kylosov 2007). For examples, a MDF plant of capacity of 314000 cubic meters per year is occurred in 12500 tons of sand dusts. Considering nearly five million m³ of MDF production per year in Turkey, it means 390000 tons of sand dusts in a year. Our previous study demonstrated that sand dust of MDF could be utilized as filler in polymer matrix (Donmez Cavdar et al. 2013).

Both wooden materials and plastics are in flammable material group. To Improve fire performance of these materials, fire retardant chemicals (FRs) are commonly used. FRs can be directly added during the processing into the furnishing material or polymer matrix (Kodowski et al. 1999). From past to present, several fire retardants have been used such as brominated FRs, phosphorus flame retardants (PFRs), boron compounds, metal hydroxides. Nowadays, halogen based FRs have been banned due to human health hazard and halogen free FRs has been became prominent in many countries (Joseph and Ebdon 2007).

The aim of this research was to determine the effects of halogen free and environmental friendly fire retardants, which are zinc borate and ATH, on the properties of sand dust of MDF filled thermoplastic composites. Mechanical, physical, thermal, fire and biological properties of the composites were determined.

Materials and Methods

Materials

In this study, sand dusts of MDF panels provided by Kastamonu Integrated Forestry Industry and Trade Inc., Turkey. The dusts (\approx 200 mesh) were generated from the sanding of the panels produced from beech, pines and oaks fibers and urea formaldehyde resin based on 65 % solid content. High density polyethylene (HDPE)(MFI/190°C/2.16 kg = 0.35 g/10 min) and polypropylene (PP) (MFI/230°C/2.16 kg = 5 g/10 min) produced by Petkim Petrochemical Co., Turkey were used as a thermoplastic matrix. Coupling agents, maleic anhydride grafted polyethylene (MAPE) and maleic anhydride grafted polypropylene (MAPP) were supplied by Clariant International Ltd, in Germany. As fire retardant chemicals (FRs), aluminum tri hydrate (ATH) and zinc borate (ZB) were used and purchased from Poliya Co. and Etibank Co., respectively.

Composite Manufacturing

SD_MDFs, coupling agent and FRs powders with HDPE or PP were mixed with high-speed mixer (Teknomatik, Turkey), speed range 5–1000 rpm, for 5 min. The

compounding was accomplished using a laboratory scale single screw extruder (Teknomatik, Turkey) to produce homogenous the composite pellets. The set temperatures of the extruder were controlled at 170°C, 175°C, 180°C, 185°C, and 190°C for five heating zones and the extruder screw speed was set to 40 rpm. Pellets were cooled in water and granulated. Granulated pellets were dried at 105 °C for 24 h and pressed under 100 bar pressure, at 200°C temperature for 20 min using a mould dimension of 20cm by 20cm by 0.5cm. After pressing, the composites were conditioned in a climatic room with the temperature of 20 °C and the relative humidity of 65%. The raw material formulations used for the composites are presented Table 1.

Table 1 Parameters of manufacturing the thermoplastic composites

Composite panel type	Plastic type	Coupling agent	FRs	Composite formulations (%)				
				FRs (phr)	SD_MDF Loading	Plastic	Coupling agent	Wax
Control_HDPE	HDPE	MAPE	-	-	40	54	3	3
Control-PP	PP	MAPP	-	-	40	54	3	3
A1	HDPE	MAPE	ATH	20	40	54	3	3
B1	HDPE	MAPE	ATH	40	40	54	3	3
C1	PP	MAPP	ATH	20	40	54	3	3
D1	PP	MAPP	ATH	40	40	54	3	3
A2	HDPE	MAPE	ZB	3	40	54	3	3
B2	HDPE	MAPE	ZB	6	40	54	3	3
C2	PP	MAPP	ZB	3	40	54	3	3
D2	PP	MAPP	ZB	6	40	54	3	3

Physical properties

Water absorption (WA) and thickness swelling (TS) of the thermoplastic composites were evaluated according to EN 317 (1993). Five samples, dimensions of 50mm*50mm*5 mm, from each group were used for the WA and TS tests. Before testing, samples were conditioned in a climatized room at 20°C and 65% relative humidity. The samples were weighed and their thicknesses were measured. The measured samples were dipped into water and their weight and thickness were measured periodically during 6 months (after 2 h, 24 h, 48 h, 72 h, 96 h, 120 h, 144 h, 168 h, 2 weeks, 3 weeks, 4 weeks, 2 months, 3 months, 4 months, 5 months, and 6 months). Before each measurement the surface of samples were wiped out with paper towel. The samples were weighed to the nearest 0.001 g and measured to the nearest 0.01 mm immediately. Five replicate samples were tested for each composite panel type.

Mechanical properties

Flexural and tensile properties and impact strength of the thermoplastic composites filled SD_MDFs and FRs were determined by ASTM D 638, ASTM D 790 and ASTM D 206, respectively. The flexural and tensile properties of all group samples were determined on Zwick Testing Unit with a capacity 10kN (1000 kg). Impact strength samples were notched with a Polytest notching cutter by RayRan™ and tested on a HIT5.5P impact testing machine manufactured by Zwick™. Test sample dimensions were in accordance with the respective ASTM standards and each obtained value represented the average of ten samples.

Thermogravimetric analysis (TGA)

Thermal properties of samples were investigated by Thermogravimetric Analysis (TGA) using a Shimadzu TGA-50 model thermal analyzer. All samples were performed under the dynamic nitrogen of a flow rate at 20 mL/min using a heating rate of 10°C/min from room temperature to 800°C.

Differential Scanning Calorimeter (DSC)

Differential scanning calorimeter (DSC) analysis was performed with Shimadzu DSC-60 in a dry nitrogen atmosphere (30 ml/min) with a heating rate of 10 °C/min from room temperature to 500 °C.

Fire Performance: Oxygen Index test (LOI)

Limiting oxygen index (LOI) analysis was performed with Dynisco brand LOI chamber which conforms to ASTM D 2863 standard. The limiting oxygen index is a measure of the percentage of oxygen that has to be present to support combustion of the plastic based materials - the higher the LOI the lower the flammability. In the LOI test, all samples with dimensions 100mm x 15mm x 5mm were supported in a vertical glass column, and a slow stream of oxygen/nitrogen mix was fed into the glass column. Each sample was ignited with a flame and burned downward into the unheated material. Then the minimum oxygen concentrations which would support combustion for all samples were recorded as a percentage.

Decay test

Decay test was carried out according to principles of EN113 with small modifications on sample dimensions, kolle flasks and total test period. Plastic sterile petri dishes were used instead of kolle flasks. A total of five replicate samples with dimension 10mm x 10mm x 5mm for each group were exposed to fungi attack. Beech (*Fagus orientalis* L.) and Scots pine (*Pinus sylvestris* L.) samples like composite samples were also exposed to fungal attack as a reference samples for validity of decay test. Prior to the test, samples were dried in an oven at a temperature of 103±2 °C until they reached constant weight, and were measured the weights, and then were sterilized in an autoclave for 55 min at temperature of 125 °C. Sterilized malt extract agar solution of 4.8% concentration was poured into each petri dish, and a brown-rot fungus (*Coniophora puteana*) was inoculated in the petri dishes. After incubation at 20°C and 65% RH for ten days, two samples were placed on the mycelium growing in each petri dish. The petri dishes were then incubated at 20°C and 65% RH. All samples were cleaned, dried at a temperature of 103±2 °C, weighed and the mass loss calculated on the basis of oven dry weight before and after fungal attack for 60 days. The weight losses of pine and beech samples for *C. puteana* attack were found to be 41.38 % and 15.41%, respectively. These results of weight loss verified the decay test was valid according to EN 113.

Results and Discussion

Physical Properties: Water Absorption (WA) and Thickness Swelling (TS)

The results of WA and TS tests of SD_MDF and FRs filled thermoplastic composites are shown in Figures 1 and 2. When the composites produced from HDPE, the lowest and

highest WA values were found as 1.67 % and 3.46% after 6 months immersion time. These values for PP based composites were found as 4.44 % and 8.06 % after the 6 months. Regarding TS values of HDPE based composites were ranged between 0.18% and 0.31 while those of PP composites were ranged between 0.62 % and 1.32 % after 6 months immersion time in water. The WA and TS values of all samples increased with increment of water immersion time.

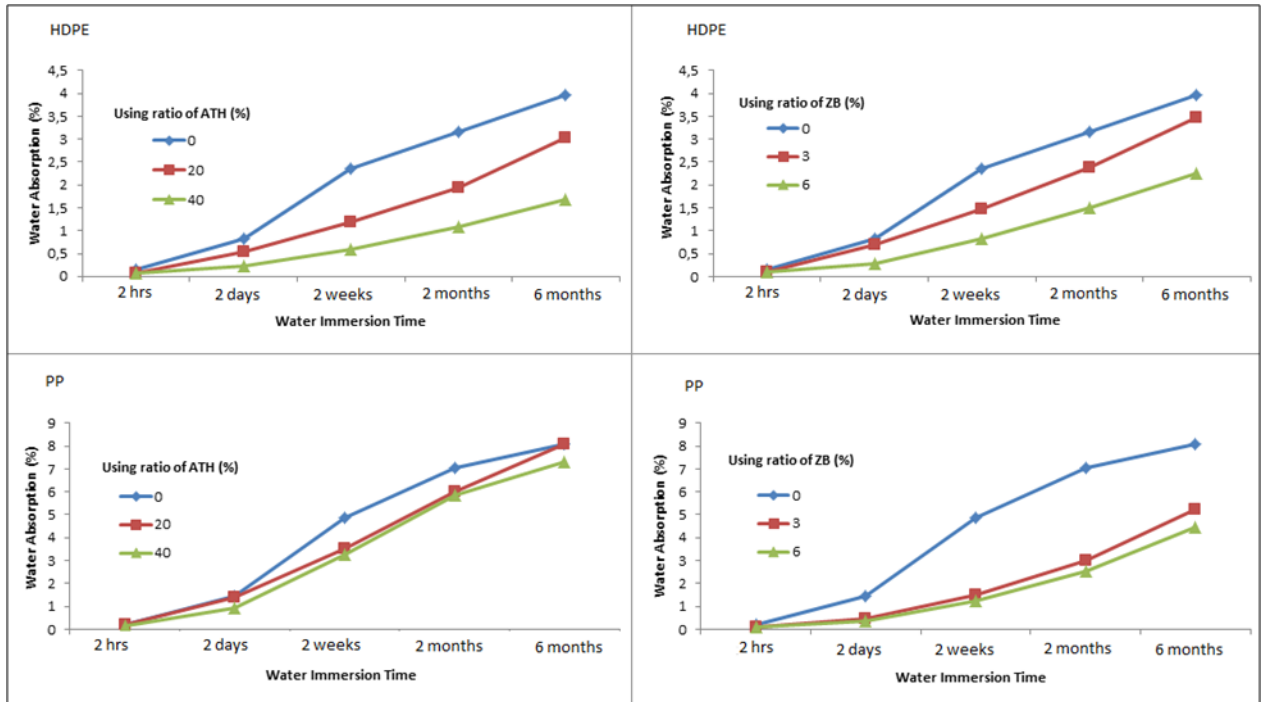


Figure 1. WA properties of SD_MDF and FRs filled thermoplastic composites

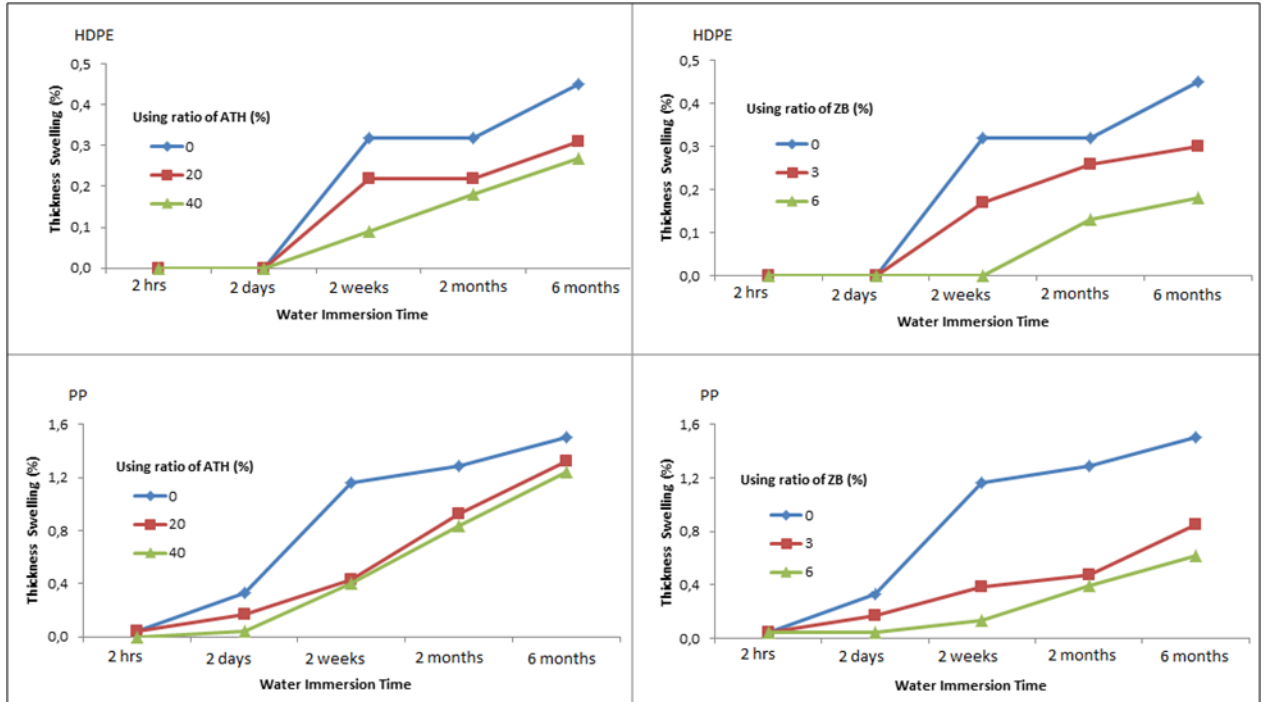


Figure 2. TS properties of SD_MDF and FRs filled thermoplastic composites

Usage FRs into the polymer matrix decreased WA and TS values. In previous studies, they have been reported that some of FRs (such as ZB) has also shown a water repellent property and improve dimensional stability of wood composites (Stark et al. 2003, Gnatowski and Burnaby 2005, Kylosov 2007). However, HDPE based composites had higher dimensional stability (low WA and TS) than PP based composites. This may happen due to the different characteristics between these plastics.

Mechanical Properties

The results of mechanical tests of SD_MDF and FRs filled thermoplastic composites are shown in Table 2.

Table 2. Mechanical properties of SD_MDF and FRs filled thermoplastic composites

ID	Flexural Properties		Tensile Properties			IS (J/m)
	FS (MPa)	FM (MPa)	TS (MPa)	TM (MPa)	EB (%)	
Control_HDPE	24.68 ¹	1692.57	12.82	598.38	2.71	21.68
	1.72 ²	34.91	0.14	9.90	0.18	3.60
Control_PP	32.01	1803.72	16.43	695.97	3.07	20.22
	0.50	80.61	0.95	22.60	0.09	0.56
A1	23.45	1269.99	14.04	586.25	2.86	19.10
	0.52	27.62	0.69	14.73	0.07	0.67
B1	23.38	1275.59	13.48	627.67	2.57	19.02
	0.79	75.54	0.80	20.61	0.07	1.60
C1	30.68	1549.64	16.43	721.73	2.58	18.94

	<i>1.46</i>	<i>31.64</i>	<i>1.27</i>	<i>27.89</i>	<i>0.23</i>	<i>1.50</i>
D1	30.05	1568.11	16.43	831.78	2.51	18.46
	<i>1.00</i>	<i>25.55</i>	<i>0.35</i>	<i>9.15</i>	<i>0.05</i>	<i>1.33</i>
A2	23.88	1134.26	15.01	586.99	3.08	19.28
	<i>0.46</i>	<i>26.49</i>	<i>0.31</i>	<i>10.63</i>	<i>0.15</i>	<i>0.72</i>
B2	22.54	1135.24	14.97	587.37	3.09	20.25
	<i>0.76</i>	<i>46.51</i>	<i>0.93</i>	<i>24.25</i>	<i>0.28</i>	<i>0.62</i>
C2	29.67	1156.00	15.64	607.47	3.11	20.24
	<i>0.81</i>	<i>58.62</i>	<i>3.00</i>	<i>34.93</i>	<i>0.48</i>	<i>0.73</i>
D2	29.17	1166.69	15.22	648.78	3.08	28.53
	<i>1.50</i>	<i>25.70</i>	<i>1.00</i>	<i>32.36</i>	<i>0.30</i>	<i>0.48</i>

(1) Mean, (2) Standard deviation FS: Flexural Strength, FM: Flexural Modulus, TS: Tensile Strength, TM: Tensile Modulus, EB: Elongation at Break, IS: Impact Strength

The highest flexural properties of the composites were obtained from control samples. Usage of FRs caused a small reduction on flexural properties of the samples. In previous studies were reported that metal hydroxides such as ATH, ZB or magnesium hydroxide had adversely effect on strength properties of thermoplastic composites (Katz and Milewski 1978, Yeh et al. 1995, Yeh et al. 1998, Ramazani et al. 2008, Wang et al. 2010, Goode et al. 2011, Kurt and Mengeloğlu 2011, Kurt et al. 2011). According to Song et al. (2004), this reduction is mainly due to agglomeration of FRs and phase separation between FRs and thermoplastics. Based on finding results, FRs (especially ATH) usage had not dramatically reduced strength properties of the composites samples. This is owing to the fact that addition of MAPE/MAPP can enhance the ductility of metallic hydroxides filled thermoplastics conceivably by improving the poor interfacial adhesion between PE/PP and metallic hydroxides and natural fibers (Yeh et.al. 1998, Kurt et al. 2011).

The tensile properties of the samples didn't negatively affect when FRs used in the polymer matrix. Many researchers have reported that usage of organic filler materials in polymer matrix has caused a reduction on tensile strength (Yeh et al. 1995, Chiu and Wang 1998, Ramazani et al. 2008, Hornsby 2010) but this is related to filler composition and matrix. If the stress is transferred from matrix to filler completely, tensile strength increases. Ramazani et al. (2008) found that ZB and ATH decreased the tensile strength of polymer composites without using a coupling agent and they concluded that MAPP served as a bridge for adhesiveness between filler surface's and matrix and prevented a probable decrease when to increase filler in polymer matrix. Also Goode et al. (2011) found that FRs used with coupling agents in polymer matrix had no adversely effect on the strength properties; even it was informed that some brome based FRs used with coupling agents in polymer matrix increased strength properties.

Tensile modulus of the composites improved with addition of ATH into polymer matrix by 5-20 %. When increase filler loading into polymer matrix, the elasticity of material decrease and it gets rigidity (Abu Bakar et al. 2010). However, ZB usage adversely affected on the modulus values of the composites, this decrease on the modulus of the composite was 2% and 13% for HDPE and PP, respectively. Elongation at break values

of the composite decreased with increment of ATH into polymer matrix alike those of tensile strength. Fillers such as lignocellulosic material and ATH have significant effect on brittleness of the composites. When addition the fillers into polymer matrix, the composite was more brittle than unfilled HDPE/PP. It is known that if rigidity increases elongation at break decreases in the material. In some researches, this situation was explained due to the fact that elastic strain properties of the solid interphase between polymer matrix and filler decreased (Zaini et al. 1996, Abu Bakar et al. 2007). Impact strength of the samples decreased when ATH used in the polymer matrix while the strength values increased by a 41% with increment of ZB in PP-matrix. This may be related to shape and grain size of FRs (Riley et al. 1990, Mareri et al. 1998, Suppakarn and Jarukumjorn, 2009). Some filler which has smaller grain size positively affects IS of the thermoplastic composites (Riley et al. 1990, Da Silva et al. 2002). Since the grain size of ZB is smaller than that of ATH, this may increase the IS values.

Thermal Properties (TGA and DSC)

Summary of TGA and DSC results which are onset degradation, peak temperature, residual weight after 500 °C, onset and melting temperatures of the composites were presented in Table 3. Thermal stability of the samples improves with increment of ATH and ZB loading into polymer matrix. The curves of TG gave similar peaks to the control samples. An increase of the residue char was observed after 500 °C. Also, it was seen a deceleration on weight loss rates of the composite filled with FRs during thermal degradation. It is known that metal hydroxides and borates promote the charring (Chen et al. 2006, Choi et al. 2009, Doğan et al. 2010). Metal hydroxides thermally decompose on heating to form oxides and water. This endothermic process attributes to cool the surface of material and improve the charring (Hilado 1998, Jang and Lee 2001, Kong et al. 2008, Li et al. 2010).

Table 3. Results of TGA and DSC analyses of the thermoplastic composites

ID	Thermo gravimetric data				DSC data		
	Onset Temperature (°C)	Peak Temperatures (°C)			Residue after 500 °C (%)	Onset Temperature (°C)	Melting Temperature (°C)
		1 st Peak	2 nd Peak	3 rd Peak			
Control_HDPE	290	335.7	475.1		13.5	121.4	133.9
Control_PP	282.6	362.3			4.25	151.3	162.9
A1	305.8	332.4	483.6		27.1	121.8	129.9
B1	305.5	324.9	479.3		33.2	120.4	130.3
C1	289.2	348.5			16.9	151.9	163.7
D1	289.2	351.5			21.3	152.3	163.3
A2	309.3	340.9	419.7	483.6	18.6	117.9	130.7
B2	314.9	337.7	463.5		21.5	117.9	130.7
C2	300.2	358.0			8.0	152.7	164.0
D2	301.3	365.5			11.5	152.3	164.0

According the DSC data, the curves of melting temperature for all samples gave one similar peak. The melting temperatures ranged from 130 to 134 °C and 163 to 165 °C for

HDPE- and PP- based composites, respectively. Also, the analysis results showed that FRs and SD_MDF didn't affect the melting temperature of polymer matrix.

Limiting Oxygen Index (LOI)

LOI levels of the samples were significantly increased by usage of FRs according to that of neat HDPE/PP. This is clearly seen in Figure 3.

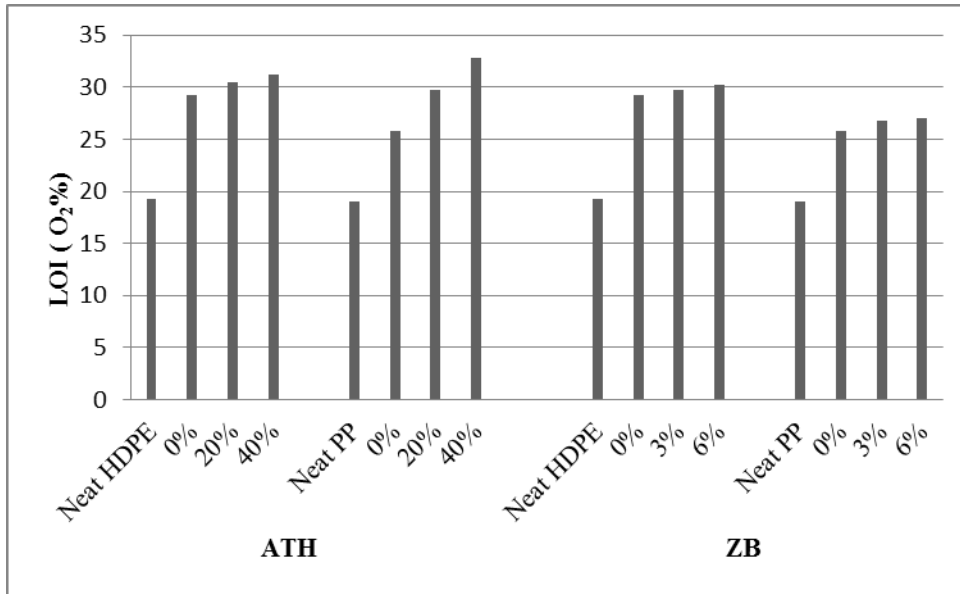


Figure 3. LOI levels of SD_MDF and FRs filled thermoplastic composites

The highest LOI levels were obtained from the thermoplastic composites filled ATH at 40 phr loading. Fire retardant materials need higher oxygen concentration to ignite than flammable materials (Sain et al. 2004). ATH and ZB act as heat sinks and prevent oxygen to set fire to flammable compounds by releasing water, or by forming a protective layer as a coating (Garcia et al. 2009, Hornsby 2010). Table 4 shows classification of all composite samples in this study according to ISO 4589.

Table 4. Fire Classification of the thermoplastic composites according to ISO 4589

LOI level	Classification of Fire	Composite Type
≤ 23	Combustible or Flammable Material	Neat HDPE, Neat PP
24–28	Limited Fire Retardant or Fire Resistance Material	Control PP, C2, D2
29–35	Fire Retardant or Fire Resistance Material	Control HDPE, A1, B1, C1, D1, A2, B2

Decay Test

Table 5 shows the results of decay resistance of SD_MDF and FRs filled thermoplastic composites. Although, the weight losses of pine and beech wood samples for *C. puteana* attack were found to be 41.38 % and 15.41%, respectively, the weight losses of all composites were found too low after decay test. FRs also decreased the weight losses of the samples and the lowest weight losses were obtained from ZB (6phr) filled

composites. It is known that boron compounds such as zinc borate effectively provide protection wood and wood composites from decay fungi etc (Laks and Palardy 1993, Tsunoda et al. 2002).

Table 5. Weight losses of the thermoplastic composites after decay test.

FRs Type	ATH						ZB					
Polymer Type	HDPE			PP			HDPE			PP		
Usage of FRs (phr)	0	20	40	0	20	40	0	3	6	0	3	6
Mean (%)	0.37	0.35	0.09	0.54	0.28	0.20	0.37	0.19	0.06	0.54	0.21	0.08
<i>S.D.</i>	<i>0.12</i>	<i>0.16</i>	<i>0.1</i>	<i>0.28</i>	<i>0.22</i>	<i>0.08</i>	<i>0.12</i>	<i>0.08</i>	<i>0.02</i>	<i>0.28</i>	<i>0.14</i>	<i>0.05</i>
Reference	Scotch pine 41.38 (8.64)						Beech wood 15.41(3.40)					

According to CEN/TC38/WG23 N34 the ranges of weight loss (%) in the five durability classes is as follows very durable ≤ 5 , durable > 5 to ≤ 10 , moderately durable > 10 to ≤ 15 , >15 to ≤ 30 and not durable >30 . In this study, all composite samples were located in the class of “very durable” due to their weight losses of less than 5 %. This is related directly to moisture content of materials since fungi need a minimum 18-20 % of moisture content to attack wood or wooden materials before decay begins (Schmidt and Czeschlik 2006). Although, wood plastic composites have high dimensional stability due to hydrophobic plastic if natural fiber reinforced composites content high fiber loading (especially more than 50%), they could be attacked by fungi, decay etc. This also has been corrected with some research (Kamdem et al. 2004). The WA values of all composites were found less than 20 % even after 6months in this study, therefore weight losses weren't seen remarkably after decay test. In addition, SD_MDF contents melamine and its known that the melamine is water resistant (Pizzi 2003).

Conclusions

This paper showed that FRs affected the properties of the filled thermoplastic composites. Mechanical properties of the samples slightly reduced with increment of the FRs while tensile modulus of those increased with increment of ATH. FRs improves dimensional stability by decreasing WA and TS values and thermal stability of the composites. Melting temperature of the composites didn't change with using FRs according to results of DSC analysis. FRs also increased the residue charring and LOI levels of the samples. Fire retardant performance of samples increased with the high loadings of ATH. FRs also improved resistance against decay fungi by decreasing the weight losses of the samples and the lowest weight losses were obtained from ZB (6phr) filled composites. In the light of obtained results, it was specified that use of FRs enhanced physical, biological, thermal and fire properties of SD_MDF filled thermoplastic composites.

References

- Abu Bakar, M.B., Leong, Y. W., Ariffin, A., Mohd Ishak, Z.A. 2007. Mechanical, Flow and Morphological Properties of Talc- and Kaolin-Filled Polypropylene Hybrid Composites. *Journal of Applied Polymer Science*. 104:434-441.
- Abu Bakar, M.B., Mohd Ishak, Z.A., Mat Taib, R., Rozman, H.D., Mohamad Jani, S. 2010. Flammability and Mechanical Properties of Wood Flour-Filled Polypropylene Composites, *Journal of Applied Polymer Science*. 116:2714–2722.
- Chen, X, Yu, J., Guo, S. 2006. Structure and Properties of Polypropylene Composites Filled with Magnesium Hydroxide, *Journal of Applied Polymer Science*, 102:4943–4951.
- Chiu, S.H., Wang, W.K. 1998. The Dynamic Flammability and Toxicity of Magnesium Hydroxide Filled Intumescent Fire Retardant Polypropylene. *Journal of Applied Polymer Science*. 67:989-995.
- Choi, S.W., Lee, B.H., Kim, H.J., Kim, H.S. 2009. Thermal Behavior of Flame Retardant Filled PLA-WF Bio-Composites. *Mokchae Konghak*. 37(2):155-163.
- Clemons, C., 2002. Wood–plastic Composites in the United States: The Interfacing of Two Industries. *Forest Products Journal*, 52(6):10–18.
- Da Silva, A.L.N., Rocha, M.C.G., Moraes, M.A.R., Valente, C.A.R., Coutinho, F.M.B. 2002. Mechanical and Rheological Properties of Composites Based on Polyolefin and Mineral Additives. *Polymer Testing*. 21:57-60.
- Doğan, M., Yılmaz, A., Bayramlı, E. 2010. Synergistic Effect of Boron Containing Substances on Flame Retardancy and Thermal Stability of Intumescent Polypropylene Composites. *Polymer Degradation and Stability*. 95:2584-2588.
- Donmez Cavdar, A., Kalaycıoğlu, H., Mengeloğlu, F., Casur, E. 2013. Physical and Mechanical Properties of Sand Dust of MDF Filled Thermoplastic Composites, 7th International Advanced Technologies Symposium (IATS'13), 411-416.
- García, M., Hidalgo, J., Garmendia, I., García-Jaca, J. 2009. Wood–plastics Composites with Better Fire Retardancy and Durability Performance, *Composites: Part A*, 40:1772–1776.
- Gnatowski, M., Burnaby, B.C. 2005. Water Absorption by Wood-plastic Composites Composites in Exterior, *Proceeding Book: 8th International Conference on Wood Fiber Plastic Composites*, 1- 27 May, Madison, Wisconsin, USA.
- Goode, M.J., Harscher, M., Sigworth, W.D., Lawlor, T.T. 2011. Flame Resistance Natural Fiber–filled Thermoplastics with Improved Properties, *United States Patent Application Publication*, Patent No: US 2011/0071237.
- Hilado, C.J. 1998. *Flammability Handbook for Plastics*. Product Safety Corporation, West Virginia, USA, 326p.
- Hornsby, P., 2010. Fire-Retardant Fillers, Chapter 7, *Fire Retardancy of Polymeric Materials*, Second Edition, Ed. Wilkie, C. A., Morgan, A.B.163-187.
- Jang, J., Lee, E. 2001. Improvement of the Flame Retardancy of Papersludge/ polypropylene Composite, *Polymer Testing*. 20: 7–13.
- Joseph, P., Ebdon, J. 2007. Recent developments in flame-retarding thermoplastics and Thermosets, Chapter 7, *Fire Retardancy of Polymeric Materials*, Second Edition, Ed. Wilkie, C. A., Morgan, A.B., 187-206.

- Kamdem, D. P., Jiang, H., Cui, W., Freed, J., Matuana L. M. 2004. Properties of Wood Plastic Composites Made of Recycled HDPE and Wood Flour from CCA-treated Wood Removed from Service. *Composites: Part A*. 35:347–355.
- Katz, H.S., Milewski, J.V. 1978. *Handbook of Fillers and Reinforcements for Plastics*, Van Nostrand Reinhold Company, Newyork, 652.
- Kong, X.J., Liu S.M., Zhao, J.Q. 2008. Flame Retardancy Effect of Surface-modified Metal Hydroxides on Linear Low Density Polyethylene. *Journal of Central South University of Technology*. 15:779–785.
- Kozłowski, R., Mieleniak, B., Helwig, M., Przepiera, A. 1999. Flame resistant lignocellulosic mineral composite particle boards. *Polymer Degradation and Stability*, 64 (3):523-528.
- Kurt, R., Mengeloğlu, F. 2011. Utilization of Boron Compounds as Synergists with Ammonium Polyphosphate for Flame Retardant Wood-polymer Composites. *Turkish Journal of Agriculture and Forestry*. 35:155-163.
- Kurt, R., Mengeloğlu, F., Meric, H. 2012. The Effects of Boron Compounds Synergists with Ammonium Polyphosphate on Mechanical Properties and Burning Rates of Wood-HDPE Polymer Composites. *European Journal of Wood and Products*. 70(1-3):177-182.
- Kylosov, A.A. 2007. *Wood Plastic Composites*, John Wiley&Sons, Inc.,NJ, USA, 698.
- Laks, P.E., Palardy, R.D. 1993. Properties and Process Considerations for Preservativecontaining Waferboards. *International Union of Forestry Research Organizations (IUFRO) Symposium on the Protection of Wood-Based Composite Products*, Orlando, FL, Forest Products Society. 12-17.
- Li, S., Long, B., Wang, Z., Tian, Y., Zheng, Y., Zhang, Q. 2010. Synthesis of Hydrophobic Zinc Borate Nanoflakes and Its Effect on Flame Retardant Properties of Polyethylene, *Journal of Solid State Chemistry*.183:957–962.
- Mareri, P., Bastide, S., Binda, N., Crespy, A. 1998. Mechanical Behaviour of Polypropylene Composites Containing Fine Mineral Filler: Effect of Filler Surface Treatment, *Composite Science and Technology*. 58:747–752.
- Mishra, S., Naik, J.B. 2005. Mechanical Properties of Wood Polymer Composites Prepared from Agro-Waste and HDPE. *Polymer-Plastics Technology and Engineering*. 44:511–522.
- Pizzi A. 2003. Melamine-formaldehyde resins. In: Pizzi A, Mittal KL, eds. *Handbook of adhesive technology*. NewYork: Marcel Dekker, 635–80.
- Ramazani, S.A.A., Rahimi, A., Frounchi, M., Radman, S., 2008. Investigation of Flame Retardancy and Physical-mechanical Properties of Zinc Borate and Aluminum Hydroxide Propylene Composites, *Materials and Design*. 29:1051-1056.
- Riley, A. M., Paynter, C. D., McGenity, P. M., Adams, J. M. 1990. Factors Affecting the Impact Properties of Mineral Filled Polypropylene, *Plastics and Rubber Processing and Applications*. 14:85-93.
- Sain, M., Park, S.H., Suhara, F. Law, S. 2004. Flame Retardant and Mechanical Properties of Natural Fibre–PP Composites Containing Magnesium Hydroxide. *Polymer Degradation and Stability*. 83:363–367.
- Schmidt, O., Czeschlik, D. 2006. *Wood and tree fungi biology, damage, protection, and use*. Berlin: Springer, 211.

- Song, L., Hu, Y., Lin, Z., Xuan, S., Wang, S., Chen, Z., Fan, W. 2004. Preparation and Properties of Halogen-free Flame-retarded Polyamide 6/organoclay Nanocomposite. *Polymer Degradation and Stability*. 86:535-540.
- Stark, N.M., Rowlands, R.E. 2003. Effects of Wood Fiber Characteristics on Mechanical Properties of Wood/polypropylene Composites. *Wood and Fiber Science*.35(2):167–174.
- Suppakarn, N., Jarukumjorn, K. 2009. Mechanical Properties and Flammability of Sisal/PP Composites: Effect of Flame Retardant Type and Content. *Composites:PartB*. 40:613–618.
- Tsunoda, K., Watanabe, H., Fukuda, K., Hagio, K. 2002. Effects of Zinc Borate on the Properties of Medium Density Fiberboard. *Forest Products Journal*. 52(11-12):62-65.
- Wang, F., Wang, Q., Wang, X. 2010. Progress in Research on Fire Retardant-Treated Wood and Wood-Based Composites: A Chinese Perspective. *Forest Products Journal*. 60(7-8):668-678.
- Yeh, J.T., Yang, H.M., Huang, S.S. 1995. Combustion of Polyethylene Filled with Metallic Hydroxides and Crosslinkable Polyethylene. *Polymer Degradation and Stability*. 50:229–234.
- Yeh, J. T., Yang, M.J., Hsieh, S. H. 1998. Combustion of Polyethylenes Filled with Metallic Hydroxides and Ethylene Vinyl Acetate Copolymer. *Polymer Degradation and Stability*. 61:465-472.
- Zaini, M. J., Fuad, M. Y. A., Ismail, Z., Mansor, M. S., Mustafah, J. 1996. The Effect of Filler Content and Size on the Mechanical Properties of Polypropylene/oil Palm Wood Flour Composites. *Polymer International*.40:51-55.

Acknowledgement

This work was supported by the Ministry of Industry and Trade. SANTEZ Project number: 00214.STZ.2007, and Kastamonu Integrated Inc., Turkey.

Optimising the Stranding of Moso Bamboo (*Phyllostachys Pubescens* Mazel) Culms Using a CAE 6/36 Disk Flaker

Kate E Semple¹, Martin Smola², John Hoffman³, Gregory D Smith^{1}*

¹Research Scientist, and Associate Professor, Department of Wood Science-Composites Group, University of British Columbia, 2900-2424 Main Mall, Vancouver, BC, Canada, V6T 1Z4. Email: kate.semple@ubc.ca, greg.smith@ubc.ca.

*Corresponding Author

²Undergraduate Applied Science Co-op Student, Fachhochschule Rosenheim, Hochschulstraße 1, 83024, Rosenheim, Germany. m.smola89@gmail.com.

³Senior Technician, FPInnovations (Western Division), 2665 East Mall, Vancouver, BC Canada, V6T 1Z4. John.Hoffmann@fpinnovations.ca.

Abstract

Giant timber bamboo such as Moso are potentially ideally suited to the production of engineered strand-based structural composite building materials. Conversion to strands utilizes a much higher proportion of the culm than the conventional milled, dried strips currently used to fabricate laminated bamboo lumber and boards, and also incorporates the fibre-rich, strongest portion of the culm located at the outer cortex into the composite. Previous studies have found Moso bamboo produces good quality strand-based composites, but commercial development of these for housing construction in China is thwarted by the lack of an efficient, automated technology for converting culm stock to strands. There are very few published details of experience in converting bamboo culms to strands, and how it contrasts with stranding wood logs. In this work we take an iterative approach to systematically assess the effects of different material and stranding parameters on bamboo strand dimensions and quality to arrive at an optimal set of conditions for converting re-saturated Moso bamboo culm stock to strands using a disk flaker. Adjustable material parameters included tissue moisture content and temperature, culm piece size, shape, orientation, slicing plane; and adjustable flaker parameters included knife projection and material feed rate. Optimum conditions involved stranding quartered culm pieces vertically, i.e. slicing along the fibre direction, to a nominal target thickness of 0.65 mm (knife projection = 0.726 mm), corresponding material feed rate of 0.47 m/sec. Optimum disk operating speed is 734 RPM and low counter knife angle of

40°. Further optimisation may be required to reduce the incidence of fibre damage on the rear face of strands.

Keywords: A. Bamboo, A. Aspen, C. Processing, C. Disk Stranding,

Introduction

Despite a plethora of mostly milled slat-based bamboo products available on the market for interior applications such as flooring and cabinetry, little of the vast resource that China grows is converted into building materials such as structural composite lumber (SCL) and panels (OSB and plywood), mainly due to strong consumer preference for inorganic building materials. Most current bamboo processing industries are highly labour intensive with very low product recovery from culm-stock, and loss of the strongest part of the culm from slat milling. Factories in China produce OSB from pine and poplar wood mainly for the export market, and there is one company, Yunnan Yung Lifa Forest Co Ltd, located in Hunnan Province, that has spent several years adapting OSB technology to bamboo driven by a niche market for tough, durable flooring to replace tropical timber plywood used in shipping containers (Anon 2012, Grossenbacher 2012). However, the main impediment to the efficiency and economic viability of this operation is the slow and still labour-intensive technique used to cut up culm stock and produce strands. At present there is no automated purpose-designed slicing machinery to convert the long, hollow bamboo culms to strands (Anon 2012a,b). A conventional disk flaker designed for logs is used at Yunnan Lifa to generate strands from culm sections that have been manually cut into short, node-free rounds in which small diameter rounds are stacked inside larger diameter ones (Boeck, F. 2013, Personal Communication). This is likely done so as to ensure maximum number of strands produced per machine running time. Nevertheless the OSB process still represents one of the best opportunities for automation and mass production of bamboo-based panel building materials. There has been some development work in China on producing strands and wafers from Moso bamboo for use in structural strand-based composites (Fu 2007a, b; Zhang et al. 2007). However there is almost no published information specifically relating to stranding bamboo in a parameter-controlled flaker. The objective of this work was to systematically investigate the effects on bamboo strand dimensions and quality of adjusting material parameters such as culm piece size, geometry and presentation to cutting blade, and flaker parameters including knife projection and feed speed.

Materials and Methods

Rewetting seasoned culm tissue. To develop a method for re-saturating culm tissue prior to stranding, forty 130-mm-long culm pieces (representing 10 different Moso stems) were randomly selected and divided into two batches of 20 pieces each, one soaked in water at 20°C for up to 4 days and the other boiled for 6 h followed by steeping overnight in cold water. Each piece was first weighed and its volume determined using the Archimedian method. Specimens were removed, drained and weighed at intervals of 1 h, 3 h, 6 h, 24 h, 48 h, and 96 h then oven dried at 105°C for 24 h to give to calculate MC.

Stranding. To minimise fines and damage to the flaker knives only bamboo tissue that had been saturated to the maximum capacity based on the findings of the re-wetting experiment was stranded. A 0.94-m diameter laboratory Disc Flaker (6/36 Lab Flaker) built by Carmanah Design and Manufacturing, Ltd, Vancouver BC, was used (Fig. 1). The flaker is designed to simulate the flaking action of a full size 37/118 disk flaker whose knife velocity at the blade mid-point is around 2585.3 m/min (Carmanah 2006). The thickness of the strands, and the amount of fines produced is mainly dependent on the finely balanced interaction between knife protrusion setting, disk rotational speed, ω , and the feed rate, F , of the material into the machining blade/s (Kruse et al. 2000). Knife angular velocity at the mid-point of the blade length is a function of disk radius to blade mid-point and disk rotation speed (RPM) as follows:

$$V_k = 2\omega\pi r/12 \text{ (Eqn. 1)}$$

where: V_k = knife velocity in mm/min; manufacturers recommendation for the scaled down, small diameter disk is 1404.5 m/min, ω = disc rotational speed in RPM, and r = radius to the mid-length of the knife blade (i.e. 30.48 cm). Rearranging Eqn. 1:

$$\omega = 12V_k/2\pi \text{ (Eqn. 2)}$$

gives a recommended disk rotational speed of 734 RPM which was used and kept consistent throughout all stranding trials for bamboo. To produce a particular desired strand target thickness at a fixed ω , the material feed rate (F) in mm per second is calculated as follows:

$$F = n_k t \omega / 60 \text{ (Eqn. 3)}$$

where: n_k = number of knives per disc (i.e. 1), t = target thickness of strands (i.e. 0.5 mm, 0.65 mm or 1.25 mm), and ω = 734 RPM. F for target thickness of 0.5 mm = 6.12 mm/sec; 0.65 mm = 7.95 mm/sec; and 1.25 mm = 15.29 mm/sec.

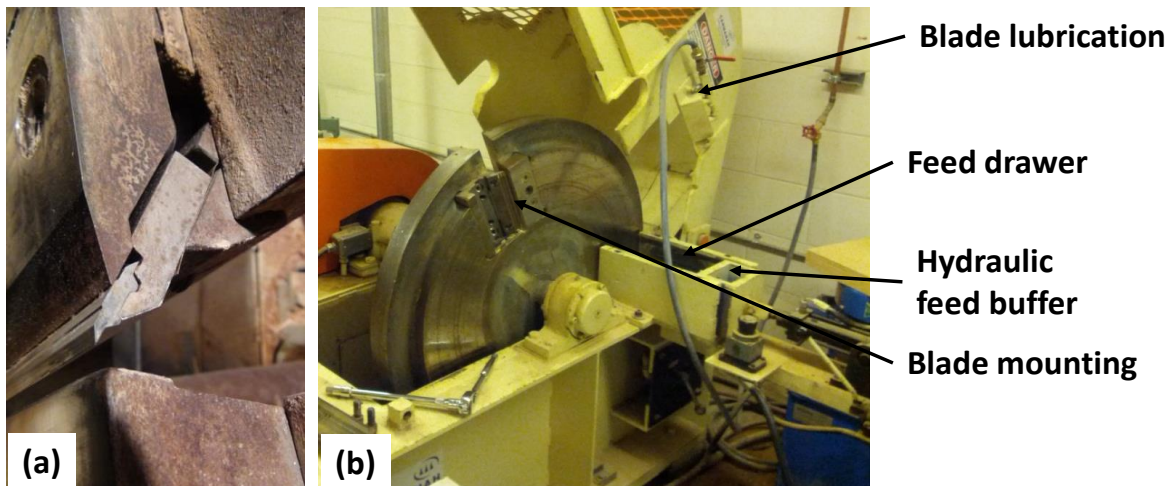


Figure 1 CAE 6/36 Lab Flaker showing (a) removable slicing blade, and (b) disk, housing and feed drawer.

Experimental parameters. Different flaker and material-related parameters were investigated in seven smaller experiments to arrive at an optimum set of processing conditions for stranding larger quantities of Moso bamboo. A fully balanced, multi factorial matrix design was heavily constrained by cost and time limits for the flaker. Instead, an iterative approach was taken to progressively build up an understanding of the stranding process and ensure bamboo strands as much as possible matched the quality and thickness distribution of industrial OSB strands of Aspen. Experiment designs are summarized in Table 1. Eventual best quality moso strands were compared with industrial face strands of Aspen (*Populus tremuloides* Michx.) supplied by the Weyerhaeuser OSB mill in Edson, AB.

Strand quality assessment. Strand length was constant at 130 mm, and measured strand physical parameters were thickness and width; with a visual and tactile surface smoothness classification into three broad groups. Depending on the experiment 200 or 250 strands from each of 14 different batches of dried strand types were randomly sampled in handfuls of approximately 50 strands each from the batch. The thickness and width of only intact strands (not fines or broken pieces) were measured using digital calipers and both visual and tactile assessment made as to whether the strand fell into one of three surface smoothness groupings: (1) rough on both sides, (2) smooth on one side and rough on the other, or (3) smooth on both sides.

Table 1 DoE for seven stranding experiments for different material and stranding conditions.

Experiment	Factor	Levels	Constants	Responses	<i>n</i>
1	Nominal Strand Thickness	1.25 mm	Form: quarters	Surface quality Strand thickness	250
		0.65 mm	MC: 140%		
		0.50 mm	Temp: 20°C		
2	Tissue Moisture Content	40%	Alignment: horizontal	Surface quality	200
			Orientation: radial		
		140%	Nom thickness: 1.25 mm	Strand width	200
			Feed rate: 15.29 mm/s		
		3	Tissue Temp.	20°C	Form: quarters
80°C	Alignment: horizontal				
	Orientation: radial				
		Nom thickness: 1.25 mm	Strand width	200	

			Feed rate: 15.29 mm/s		
4	Slicing Orientation	Radial Tangential	Form: quarters MC: 140% Temp: 20°C Alignment: horizontal Nom thickness: 1.25 mm Feed rate: 15.29 mm/s	Surface quality Strand thickness Strand width	200 200 200
5	Alignment	Horizontal Vertical	Form: whole rounds MC: 140% Temp: 20°C Nom thickness: 0.65 mm Feed rate: 7.95 mm/s	Surface quality Strand thickness Strand width	200 200 200
6	Culm shape	Whole rounds Half rounds Quarters	MC: 140% Temp: 20°C Alignment: vertical Nom thickness: 0.65 mm Feed rate: 7.95 mm/s	Surface quality Strand width	250 250
7	Feed rate	6.12 mm/s 7.95 mm/s	Form: whole rounds MC: 140% Temp: 20°C Alignment: vertical Nom thickness: 0.50 mm	Surface quality Strand thickness	200 200
8	Strand type	Best Moso strands Aspen mill strands	Form: quarters MC: 140% Temp: 20°C Alignment: horizontal Orientation: radial Nom thickness: 0.65 mm Feed rate: 7.95 mm/s	Surface quality Strand thickness Strand width	250 250 250

Results and Discussion

Culm re-saturation. The average tissue moisture content of culm pieces subjected to either cold water or hot water treatment at increasing time intervals is shown in Fig. 2. Starting moisture content was around 10%, and after 6 h soaking in cold water average tissue moisture content was 25.7%, and boiling for the same duration resulted in 46% MC, both of which were too low to enable adequate stranding. After 24 h the MC of cold water soaked tissue was only 38.5%, while MC of pieces boiled then steeped in cold water for a further 18 h was 126.6%. After a further 3 days soaking (to 96 h from start) the cold water specimens reached 75.2% MC, while the boiled and steeped pieces were 142.7%. Fresh Moso culm stock harvested and stranded by Lee et al. (1994) was 137% MC. We can therefore be confident that the tissue was fully re-saturated by boiling for 6 hours followed by steeping for 24 h or so as the tissue water content is similar to that measured for green culm stock. It is possible 6 hours boiling may not be necessary and a useful follow-up study would be to measure MC after boiling for 1 or 2 hours followed by cold water steeping.

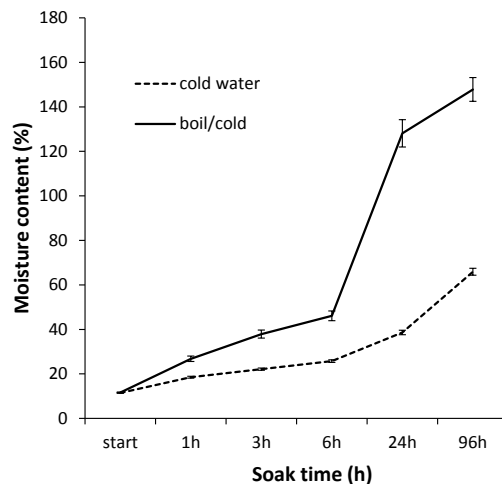
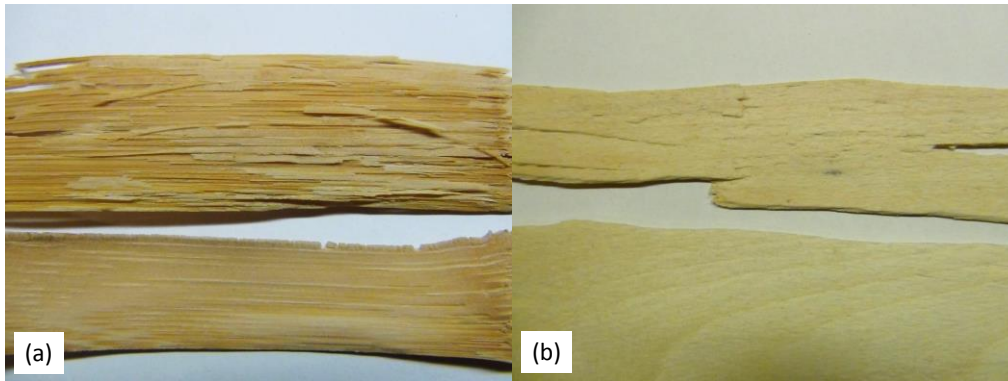


Figure 2 Average MC of Moso culm pieces at 0, 1h, 3h, 6h, 24h, and 96h exposure to cold or boiling water, $n = 20$. Boil/cold pieces were boiled for 6 h followed by steeping in cold water for 24 or 96 h.

Strand quality-surface smoothness. The visual appearance of ‘rough’ and ‘smooth’ strand surfaces of bamboo and aspen mill strands is shown in Fig. 3.



Scale = 20 mm

Figure 3 Appearance of the strand surface of (a) bamboo and (b) Aspen mill strands. Top strand has a ‘rough’ surface and bottom strand has a ‘smooth’ surface.

The proportions of strands in each of the three surface smoothness categories for different experimental parameters are given in Table 2. The greater proportion (60%) of industrial aspen strands were classified as smooth both sides, and 10% considered to be rough on both sides. Bamboo strand surface quality (i.e. maximising the proportion of strands that were smooth on both sides) was very sensitive to tissue moisture content, knife protrusion setting, material feed rate and whether the pieces were stranded horizontally or vertically. Full tissue saturation to above 130% MC, low knife protrusion setting, slower feed rate, and stranding vertically were all necessary to maximise the proportion of ‘smooth-both-sides’ strands. The high proportion of strands that were smooth one side, rough on the other is believed to be due to tensile stress and shearing forces on the backs of strands caused by the angled back of the cutting blade (designed to force sliced wood veneers to break up into narrower strands). A schematic diagram of illustrating this is shown in Fig. 4. Trying to produce strands above 1 mm in thickness resulted in many more strand quality issues than at narrow knife settings. Stranding the culm pieces horizontally, whereby the knife contacts the hard outer cortex first produced uneven strand thickness across strands, rougher surfaces and tendency for wide strands to curl along the grain with drying. Vertical culm slicing, and radial orientation so that the blade slices through the radial-longitudinal plane of the culm wall greatly improved strand quality and surface smoothness classification with greatly reduced propensity for curling during drying (Figure 5).

Table 2 Percentage of strands in each smoothness category, $n = 200$.

Parameter	levels	Rough both sides	Smooth-Rough*	Smooth both sides
Industrial aspen				
Industrial ring flaker		11	30	59
Bamboo				
Knife protrusion	1.25 mm	49	25	26
	0.65 mm	6	70	24
	0.50 mm	9	57	34

Tissue MC	40%	60	33	7
	Saturated	49	25	26
Tissue Temp	20°C	49	25	26
	80°C	63	30	7
Orientation	radial	49	25	26
	tangential	34	35	31
Alignment	Horizontal	27	43	30
	Vertical	9	57	34
Feed rate	0.37 m/s	9	57	34
	0.4 m/s	28	61	11
Piece Size	Whole rounds	6	70	24
	Half rounds	8	74	18
	Quarters	10	70	20

*Smooth-Rough: one surface smooth, the other rough

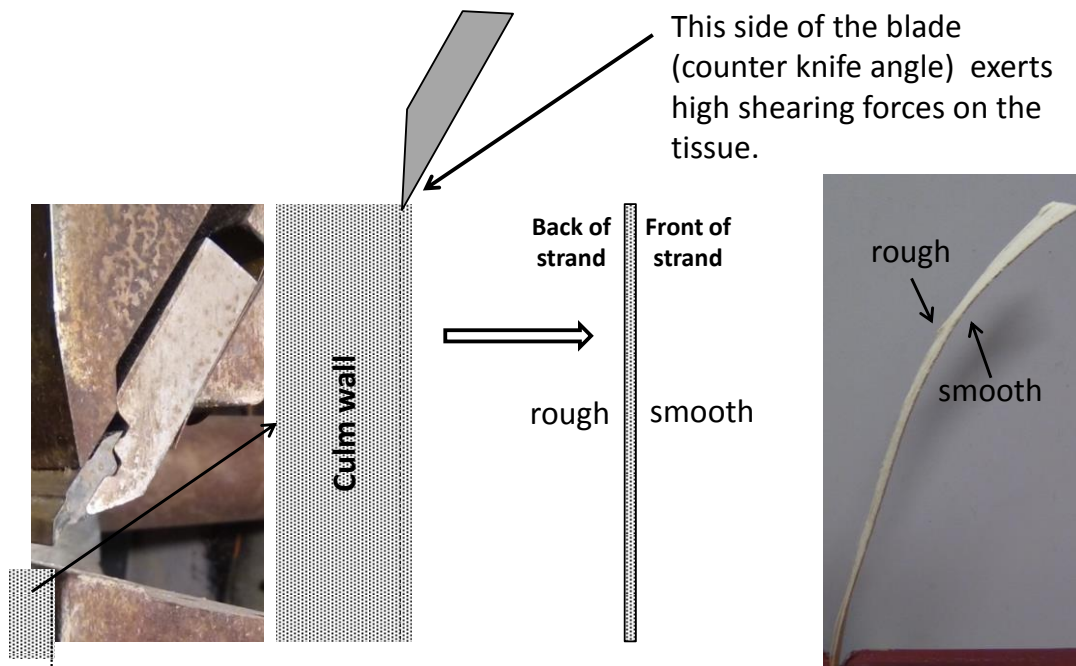


Figure 4 Slicing configuration for bamboo strands.

Strand quality-thickness and width distributions. The average and COV for strand thickness and width for all 16 stranding iterations plus industrial aspen strands are given in Table 3.

Table 3 Average strand thickness and width for different stranding conditions. COV- Coefficient of Variation.

Parameter	Setting	Strand thickness (mm)		Strand Width (mm)	
		Average	COV	Average	COV
		Industrial aspen			
		0.67	35.7	18.1	50.3

		Bamboo			
Knife protrusion	0.50 mm	0.47	40.8	NA	NA
	0.65 mm	0.65	37.7	NA	NA
	1.3 mm	1.32	31.9	NA	NA
Orientation	radial	1.32	31.9	11.6	23.7
	tangential	1.61	36.2	15.1	37.6
Tissue MC	40%	1.22	26.8	8.9	19.1
	Saturated	1.32	31.9	11.6	23.7
Tissue Temp	20°C	1.34	32.0	20.8	52.3
	80°C	1.63	35.7	11.6	23.6
Alignment	Horizontal	0.66	37.7	17.0	48.5
	Vertical	0.65	30.3	18.5	52.4
Feed rate	0.37 m/s	0.47	48.6	NA	NA
	0.4 m/s	0.84	40.6	NA	NA
Size	Whole	NA	NA	20.5	61.5
	Halves	NA	NA	17.6	39.9
	Quarters	NA	NA	12.88	30.7

NA = Not Applicable

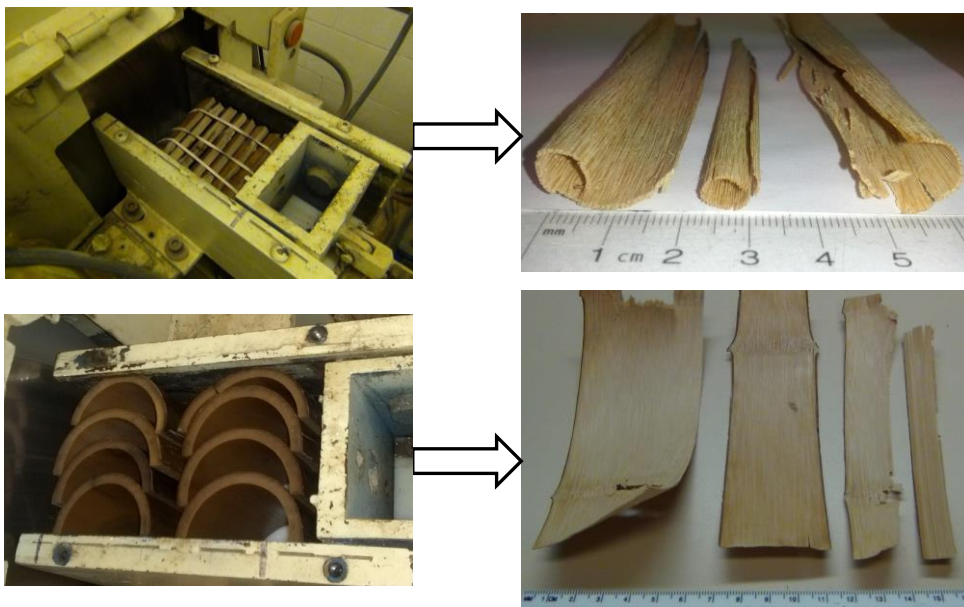


Figure 5 Culm piece alignment (horizontal, top; or vertical, bottom) in relation to strand curling after drying.

A comparison of the thickness and width distributions for optimum bamboo strands and Aspen mill strands is shown in Figure 6.

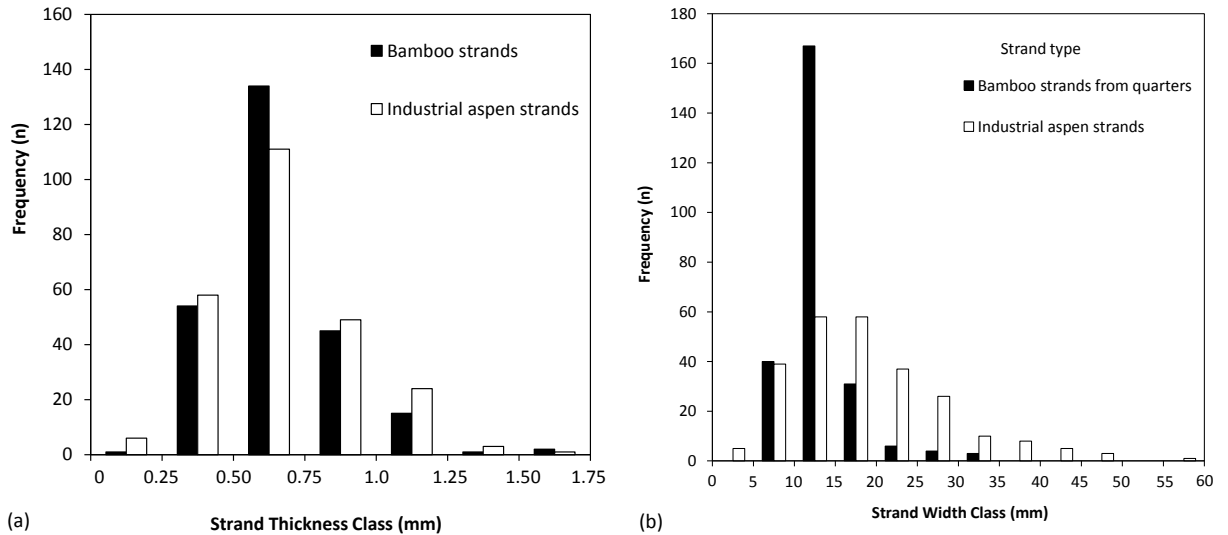


Figure 6 Frequency distributions for (a) strand thickness, and (b) strand widths for Moso bamboo and industrial Aspen mill strands. $n = 250$.

From Table 3 and Fig 6, optimal strand dimensions (average thickness, thickness distribution, and width distribution) was obtained when fully saturated culm pieces were quartered and stranded vertically at 734 RPM with a knife protrusion of 0.726 mm (nominal strand thickness = 0.65 mm), corresponding feed rate of 7.95 mm/s. Average strand thickness and coefficient of variation (0.65 mm and 37.7% COV) was very close to that found in industrial Aspen strands (0.67 mm and 35.7% COV). Vertical culm slicing resulted in a more consistent strand thickness distribution with 85% of strands falling within the thickness range of 0.25 to 0.75 mm. The culm wall thickness of the Moso ranges from around 8 to 15 mm, and so the average strand width was considerably lower (13 mm) than the average 18 mm width for sampled industrial Aspen strands.

Discussion

It should be noted that the industrial aspen strands are produced using a ring flaker, which have largely replaced disk flakers for reasons of efficiency and machine maintenance (Fodor, R. 2013 Personal Communication). Thick bundles of debarked logs are fed into a movable carriage mounted ring mounted with anywhere between 24 and 44 knife assemblies around the inside of the ring (Maietta et al. 2008). The wood is always sliced perpendicular to the grain direction, and spaced scoring knife tips determine the length of the strands. A typical ring flaker knife assembly for Aspen sets scoring knives 101 mm apart, a set-back distance and angle of the counter knife of 9.65 mm and 65° , respectively, to ensure most strands end up between about 25 and 50 mm in width (Maietta et al. 2008). Slicing bamboo culms perpendicular to the longitudinal axis (i.e. across the grain) is likely to be sub-optimal in terms of knife dulling, as it means with every cut the blade edge is hitting the hard outer wall first. If the culm wall is sliced along the grain, the cortex is confined to one edge of every slice. The rate and severity of blade dulling from slicing bamboo culms in different configurations should be investigated.

There are very few studies giving any specific details on stranding parameters for bamboo. The most detailed information given by previous workers on experimental stranding of bamboo is Barbu et al. (2009) and Malanit et al. (2011), who used a CAE 6/36 laboratory disk flaker similar to the one used here to produce 140 mm-long strands for fabricating OSB and OSL prototypes. The bamboo was *Dendrocalamus asper* Backer, commonly planted in Thailand. They converted the culms to node-free, 140 mm long half rounds and used the following specified stranding parameters; counter knife angle = 60°, knife projection = 0.736 mm, and scoring knife distance = 140 mm, and horizontal culm orientation (i.e. slicing perpendicular to grain direction). Average strand dimensions were 0.7 mm thickness, 140 mm length and 12.5 mm to 20 mm width, and strands screened through a 12.5 mm screen to remove fines. The RPM of the disk, feed rate and the fines fraction was not specified.

A PhD thesis (Fu 2007b) describes a method for ring flaker of producing industrial quantities of bamboo poles to strands. The usually 240-cm-long poles are first split into 8 sections or ‘flitches’ using a motorised splitting wheel common in the bamboo processing industry in China which also removes most of the central node plate, followed by grinding away the remaining node material from the inner wall so as to allow tight stacking. The flitches are clamped together in tight stacks of four rows of 15-20 flitches which are fed laterally against the inner knife-mounted wall of a ring flaker which cuts largely radial strands of a length determined by the spacing of the scoring knives. Slicing is also perpendicular to grain direction. Target strand dimensions were 110-120 mm long, 0.6 to 0.8 mm thick and strands were between about 9 to 15 mm in width. Why this method has not been adopted by the Yung Lifa bamboo OSB pilot plant is unclear, but may reflect the absence of a ring flaker.

Conclusions

1. Tissue re-saturation for stranding required up to 6 h of boiling followed by at least a further 18 h steeping in cold water; MC = 127%.
2. Optimal strand dimensions (average thickness, thickness distribution, and width distribution) was obtained for this particular strander configuration when fully saturated culm pieces were quartered and stranded vertically at 734 RPM with a knife protrusion of 0.726 mm (nominal strand thickness = 0.65 mm), corresponding feed rate of 7.95 mm/s. low counter knife angle of 40° was used.
3. Average strand thickness and coefficient of variation (0.65 mm and 37.7% COV) was very close to that found in industrial Aspen strands (0.67 mm and 35.7% COV). Average Moso strand width was around 13 mm compared with 18 mm for sampled industrial Aspen strands.
4. Further work aims to develop a model to calculate true numbers of strands and their sizes based on slicing a culm of given diameter and wall thickness into strands of a given nominal thickness. The computed strands can then be used to width distributions observed in real Moso strands from slicing different piece sizes and reveal the optimum ‘cutting-pattern’ for maximising strand production from Moso bamboo culms.

References

- Anon. 2012a. Focus on OSB: Another Good year's sales. Wood Based Panels International Issue 2 April 2012, pp 28-36.
<http://viewer.zmags.com/publication/9dac98f8#/9dac98f8/32>. Accessed 5 July 2013.
- Anon. 2012b. Aiming for domination. Wood Based Panels International Online, 18 June 2012. <http://www.wbpionline.com/features/aiming-for-domination/>. Accessed 10 April 2013.
- Barbu, M.C, Malanit, P., and A. Fruhwald, 2009. Development of oriented strand lumber made from *Dendrocalamus asper* Backer. Proceedings VIII World Bamboo Congress, Bangkok, Thailand, 16-18 September 2009, World Bamboo Organisation, Vol. 8: 113-124.
- Boeck, F. 2013. Personal communication of observations made during a visit to Yung LiFa bamboo OSB pilot plant, Yunnan Province, China in June 2012.
- Carmanah Design and Manufacturing Inc. 2006. 6/36 Lab Flaker Technical Manual. Carmanah Design and Manufacturing Inc., Vancouver BC, 28 pp.
- DeVallance, D.B., Gray, J.D. and S.T. Grushecky. 2012. Improving strand quality of upland oaks for use in oriented strand board. In G Miller, TM Schuler, KW Gottschalk, JR Brooks, ST Grushecky, BD Spong, JS Rentch eds, Proceedings of the 18th Central Hardwoods Forest Conference, 26-28 March 2012, West Virginia University, Morgantown, WV. USDA Forest Service Northern Research Station GTR-NRS-P-117: 284-291.
- Fodor, R. 2013. Personal Communication: Training and discussion on OSB flakers, FP Innovations, Vancouver, 27 March 2013.
- Fu, W. 2007a. Bamboo-A Potential Resource of Raw Material for OSB in China. China Forest Products Industry, 34: 21-24.
- Fu, W. 2007b. A Study on Flaking Technique and Manufacture of Bamboo OSB. PhD Dissertation, Northeast Forestry University, Harbin, China. 86 pp.
- Grossenbacher, M. 2012. Industrielle Herstellung von Bambus-OSB: Ein Erfahrungsbericht. In: 2nd Bieler Holzwerkstoff-Workshop, 28-29 November 2012, Biel, Switzerland.
- Kruse, K., Dai, C. and A. Pielasch. 2000. An analysis of strand and horizontal density distributions in oriented strand board (OSB). Holz als Roh- und Werkstoff 58(4): 270-277.
- Lee, A.W.C., B. Xuesong, and N.P. Perry. 1994. Selected physical and mechanical

properties of giant timber bamboo grown in South Carolina. Forest Prod.J. 44(9): 40-46.

Malanit, P., Barbu, M.C. and A. Fruhwald. 2011. Physical and mechanical properties of oriented strand lumber made from an Asian bamboo (*Dendrocalmus asper* Backer). European Journal of Wood Products 69: 27-36.

Maietta, A., Dexter, J., and T. House. 2011. Ring strander knife assembly and method of use. US Patent No. 7938155 B2. 20 pp.

Zhang, H., Du, F., Zhang, F., Liao, Z., Ye, X., Zheng, Z., and W. Wang. 2007. Research and Development of Production Technology of Bamboo Waferboard and Oriented Strand Board Based on Biological Characteristics and Timber Adaptability. Journal Of Bamboo Research, 26(2), 43-48.

Acknowledgements

This study was funded through an NSCERC (National Science and Engineering Research Council) G8 Tri-Council grant for a collaboration between UBC, MIT and Cambridge University on 'Structural Bamboo Products'.

The Potential of Urban Wood Residues in Particleboard Production

*Ahmad Jahan Latibari**

Professor, Department of Wood and Paper Science, Karaj Branch, Islamic
Azad University, Karaj, Iran

* Corresponding Author: latibari.aj@gmail.com

Fardad Golbabaee

Wood and Products Research Division, Institute of Forests and Rangeland,
Tehran, Iran

Abolfazl Kargarfard

Associate Prof., Wood and Products Research Division, Institute of Forests
and Rangeland, Tehran, Iran

Abstract

Based on the need and the importance of the urban wood residues to fulfill part of the wood raw material needed for particleboard production, and to increase its value as raw material, the potential of such material including residues from urban pine and sycamore trees as well as grape tree pruning for the production of particleboard was investigated. The results are compared with similar particleboards produced using particles from mixed hardwoods generated at the industrial scale. Laboratory boards at the density of 650 kg/m³ were made changing the resin dosages at three levels of 10, 11 and 12% based on the oven dry weight of the particles and then the strength and thickness swelling of the boards were measured as defined in relevant EN standards. Due to the lower bulk density of the particles from pine wood, boards produced using these particles generated highest MOR and MOE, and the lowest MOR and MOE were measured on boards produced using particles from mixed hardwoods. However, the IB of the boards from mixed hardwoods and the application of 12% resin was superior (1.18 MPa.) and the lowest IB (0.36 MPa.) was measured on boards produced using the mixture of 50% pine and 50% sycamore particles.

Keywords: Pine, Sycamore, Grape, Hardwoods, Particleboard, Strength, Thickness swelling

Introduction

The main objective of the early development of the particleboard production was the utilization of the residues generated in different wood working operations. The unique characteristics of particleboard opened its way into various applications and generated interest among different consumer sectors especially cabinet and home furniture. Such interest caused a very fast rate of expansion and implementation of new plants in industrial countries. Therefore, the wood raw material sources were diverted to forest residues as well as chips produced in saw mill operations. During the course of the rapid developments, plants were also erected in the developing regions as well. As a result, world particleboard production increased to almost 98.5 million m³ in 2012 (FAO 2013).

Interest in production and consumption of particleboard is not confined to industrial countries, and other regions especially developing countries are not exempt to such developments. However, these regions are faced with the severe shortage of wood as the main raw material and therefore regions such as Iran have been looking for alternative procedures to fulfill needed wood. Among them plantation of exotic fast growth species such as poplar and eucalyptus trees have been in the central point of research and developments. However, particleboard production is in intense competition with paper and MDF production industries to fulfill the required lignocellulosic raw material. In such competition, both paper and MDF industries are the winner since they are able to pay higher prices for the raw material and consequently particleboard is forced to find alternative and low cost raw material. In this course, lower quality raw material, fast growth, and small diameter wood have been the first candidates (Schneider et al. 2000).

Kiwi tree residues (Nemli et al. 2003), tea plants residues (Shi et al. 2006) and kenaf (Xu et al. 2004 and Kalaycioglu and Nemli 2006) were investigated as the potential sources of raw material for board production. Even though kenaf was used to reduce the resin consumption, but this procedure required the production of higher density boards which is not possible on the stand point of industrial production (Xu et al. 2004).

Attention has been focused on the reduction of the final board density as the possible way to reduce the raw material requirements. Wang and Sun (2002) utilized wheat straw and corn stalks to produce board of the required quality at lower density. However, the need to use isocyanate resin has limited the application of such material. Murathan et al. (2007) selected the waste carton boards as the potential raw material for board production, but the thickness of the boards was limited.

The production of particleboard using wood bark (Blanchet et al., 1998), pine tree needles (Nemli et al., 2008) , pine tree cones (Buyuksari et al. 2010) and bark and stem of the coffee branches (Bekalo and Reinhardt 2010) have been investigated.

The other alternative raw material investigated for particleboard production was urban and orchard tree pruning which is available in urban area and fruit tree plantations (Enayeti et al. 2008)

The severe shortage of wood raw material has forced the investigators to search and use the alternative, uncommon and unconventional wood supply especially urban wood residues. The availability of such wood in urban areas and limitations on wood supply necessitated the investigation to identify the suitability of such material for particleboard production. This was the objective of our research.

Materials and Methods

Material

Pine and sycamore branches were collected from urban tree pruning in the city of Karaj and the grape tree pruning was collected from grape tree yard in Takestan, Ghazvin. The collected material was transferred to Alborz Research Center, wood and paper research laboratory for particle preparation. Prior to particle preparation, all debris and leaves were separated from the branches. The larger diameter of the pine and sycamore tree branches was about five centimeters and the grape tree pruning diameter was very small because of the sizes of the grape tree branches.

Mixed hardwood particles were obtained from Iran Choub Particleboard plant located in the city of Ghazvin and were transferred to Islamic Azad University, Karaj Branch wood and paper research laboratory. The particles were used as received.

Urea-formaldehyde resin was purchased from Fars Chemical Company resin plant, Shiraz. The characteristic of the resin was as follow: gel time; 47 seconds (Bison Cup), density; 1.285, solid content; 63%, pH; 7.5 and viscosity; 45 seconds.

Hardener; industrial grade ammonium chloride was used.

Methods

Particle Preparation

All the wood residues were chipped using laboratory drum chipper, Pallmann PHT 120x430 and suitable chips were produced for particle production. Chips were then flaked using Pallmann ring flaker PZ8. Flake were dried in a laboratory rotating drum dryer equipped with electrical heating elements to reach final moisture content of 2% (dry basis). The dried particles were screened manually and fine portion was separated. The dried and screened particles were stored in polyethylene bags until used.

pH and Buffering Capacity and Bulk Density Measurement

The pH and buffering capacity of the dried particles from each wood was measured using the procedure outline by Johns and Niazi (1980). The bulk density of the particles was measure using a wooden box with the dimensions of 50x50x50 and result is reported in kg/m³.

Board Making and Testing

Particles were blended with a mixture of 10, 11 or 12 % resin (dry basis) and 1% hardener (based on dry weight of resin) at the concentration of 50%, utilizing rotary drum

blender and spray nozzle. Then the blended particles were hand formed using wooden mold. Board target density and thickness was selected as 650 kg/cm³ and 15 millimeters. Homogenous particle mats were pressed in laboratory press (Buerkle L100) applying 30 bar specific pressure, and five millimeters per seconds closing speed. Three boards for each combination of variables and total of 63 boards were produced. All boards were conditioned at 65% relative humidity and 21 °C for 15 days and then test samples were prepared from each board according to relevant EN standards. MOR and MOE was measured according to EN310/1996, internal bonding (IB), EN319/1996 and thickness swelling, EN 317/1996 standards. For each test, four samples were prepared from each board and tested. Different particles were used either pure or mixed.

Statistical Analysis

Factorial experimental design was used for statistical analysis of the generated data and in case the effect of variable(s) on the measured properties was significant at 99% or 95% level, then the averages were grouped using DMRT.

Results and Discussion

The results of pH and buffering capacities measurements are summarized in Table 1 and the results of strength and thickness swelling measurement on particleboards produced from different raw materials and the combination of the particles applying three different dosages of urea formaldehyde resin are shown in Table 2. Each value in table 2 is the average of 12 measurements (three replicate boards for each combination of variables and four sets of samples from each board).

pH and buffering capacity measurements indicated that the pH of the studied woods is close to the neutral pH with the acid buffering capacity in the range of 0.0065-0.02 ml 1 N NaOH per one gram of wood. The acid buffering capacity of grape tree residues is almost the same as mixed hardwoods and the acid buffering capacity of pine wood and sycamore is almost identical. Similar results are observed on alkaline buffering capacity measurements (Table 1).

The bulk density of mixed hardwood particles was higher than other material (Table 1). Mixed hardwood particles are produced using larger diameter lumber as well as log ends which contain mature and denser wood. However, pine and sycamore wood as well as grape tree residues consisted of small branch which is mostly juvenile wood and this wood upon chipping and flaking generates fluffy particles.

Table 1- The results of pH, buffering capacity and bulk density measurements

Chips	pH	Acid Buffering Capacity ¹	Alkaline Buffering Capacity ²	Bulk Density kg/m
Mixed Hardwood	5.36	0.02	0.065	245
Pine wood	4.90	0.007	0.007	153
Sycamore wood	4.85	0.0065	0.005	135
Grape tree residues	5.40	0.02	0.095	139

1- ml 1N NaOH/gram wood, 2- ml 1 N H₂SO₄/gram wood

The results showed that the type of the wood used for particle generation influences the strength of the boards and lower density wood (pine wood) which produces bulkier particles produces higher MOR and MOE. This is contributed to higher impaction between the particles in the boards. As it is observed from table 1, higher density hardwood particles produced weaker boards. The highest MOR was related to boards produced using pine particles and 11% resin and the lowest values were related to boards from mixed hardwood particles and 10% resin (Enayeti et al. 2008). Higher dosage of resin improved the MOR. The results of the statistical analysis indicated that both particle type and resin content statistically influenced the MOR of the boards at 99% significance level (Table 3). However, the interactive effect of two variables on MOR was not statistically significant. Similar results were reached on MOE of the boards except the interactive effect of two variables on MOE was statistically significant at 95% level (Table 3).

On the contrary to the results of the flexural strength and MOE of the boards, the highest internal bonding was measured on boards produced using mixed hardwood particles having higher bulk density. These particles are produced from denser woods and due to this factor, the specific surface area of the particles is lower than particles from lighter woods such as pine and sycamore. Therefore, resin coverage on mixed hardwood particles is more than others producing stronger bonds (Table 2). The influence of the either variable and the interactive effect of these variables on internal bonding of the boards was statistically significant at 99% level. The mixture of 50% mixed hardwood particles and 50% grape tree residues particles produced fairly high internal bonding which shows that the grape tree residues can be as a supplementary raw material in wood deficient regions with the potential of grape yards. Even though, other wood residues produced lower internal bonding, but the values are acceptable to EN requirements.

The thickness swelling of the boards is at acceptable level varying between 1.9-23.5% (2 hours soaking in water) and 7-26.1% (24 hours soaking in water). Lowest values were measured on boards produced from pine wood particles which contain resins and other organic soluble extractives and the highest values were measured on boards produced from sycamore wood particles having water soluble phenolic extractives which prevent urea formaldehyde resin bonding (Table 2). The influence of variables on thickness swelling of the boards was statistically significant at 95 or 99% level.

Table 2- The results of the strength and thickness swelling measurements on particleboards produced using different wood raw material

Wood Chip Composition				Resin Dosage (%)	MOR MPa	MOE MPa	IB MPa	Thickness swelling (%)	
Mixed hardwood	Pine wood	Sycamore wood	Grape tree residues	(%)				2 hours	24 hours
100	-	-	-	10	10.22	1215 ^{hi}	0.68 ^{efg}	11.6 ^{def}	14.6 ^{ef}
100	-	-	-	11	11.9	1605 ^{fghi}	1.06 ^{ab}	11.7 ^{def}	17.1 ^{bcde}
100	-	-	-	12	13.82	1812 ^{efg}	1.18 ^a	10.5 ^{efg}	17.8 ^{bcde}
-	100	-	-	10	20.08	2854 ^{ab}	0.66 ^{efg}	1.90 ^h	7 ^h
-	100	-	-	11	21.43	2926 ^a	0.64 ^{efg}	2.50 ^h	10.2 ^{gh}
-	100	-	-	12	21.26	2795 ^{ab}	0.81 ^{de}	1.70 ^h	11.7 ^{fg}
-	-	100	-	10	12.20	1616 ^{fhg}	0.49 ^{ghi}	23.5 ^a	26.1 ^a
-	-	100	-	11	12.75	1597 ^{fghi}	0.52 ^{ghi}	21.2 ^{ab}	27 ^a
-	-	100	-	12	16.5	1613 ^{fgh}	0.66 ^{efg}	15.9 ^{cd}	19.7 ^{bcd}
-	50	50	-	10	14.7	2167 ^{cde}	0.41 ^{hi}	7.2 ^g	18.8 ^{bcde}
-	50	50	-	11	15.82	2339 ^{cd}	0.36 ⁱ	10.4 ^{efg}	20.2 ^{bc}
-	50	50	-	12	16.36	2526 ^{bc}	0.59 ^{fgh}	19.3 ^{bc}	25.6 ^a
50	-	50	-	10	10.58	1415 ^{ghi}	0.65 ^{efg}	12.9 ^{de}	18.7 ^{bcde}
50	-	50	-	11	11.22	1475 ^{ghi}	0.80 ^{def}	13.3 ^{de}	18.6 ^{bcde}
50	-	50	-	12	10.34	1375 ^{hi}	0.83 ^{cde}	10.5 ^{efg}	14.9 ^{def}
50	50	-	-	10	12.51	1891 ^{ef}	0.72 ^{def}	11.9 ^{def}	16.4 ^{cde}
50	50	-	-	11	13.54	1937 ^{ef}	0.69 ^{efg}	8.4 ^{fg}	16 ^{cdef}
50	50	-	-	12	14.6	1973 ^{def}	0.69 ^{efg}	10.3 ^{efg}	15.5 ^{def}
50	-	-	50	10	11.21	1190 ⁱ	0.73 ^{def}	19.2 ^{bc}	21.5 ^b
50	-	-	50	11	11.45	1379 ^{hi}	0.91 ^{bcd}	12.9 ^{de}	19.2 ^{bcd}
50	-	-	50	12	12.22	1417 ^{ghi}	1.03 ^{abc}	11.4 ^{efg}	17.7 ^{bcde}

*- Superscript lower case letter indicated the DMRT grouping of the averages

Table 3- The results of the statistical analyses of the effect of variables of particleboard properties (F value and significance level)

Properties Variable	MOR	MOE	IB	2hours thickness swelling	24hours thickness swelling
Particle composition (A)	51.78**	95.75**	41.32**	83.07**	56.53**
Resin Dosage (B)	9.65**	9.34**	31.59**	3.01*	1.27 ^{ns}
AxB	1.21 ^{ns}	2.03*	4.14**	11.61**	6.27**

**-.99% significant level, *-95% significant level, ns- not significant

Conclusion

Wood industry is facing shortage of wood raw material, and the situation in countries located in forest deficient areas which are willing to operate board production facilities is severe. This indicates the need to look for alternative wood supplies. One such material can be urban tree pruning and fruit bearing tree residues with diverse characteristics and advantages and limitations. Therefore, in this study we investigated the impact of wood raw material type and the resin dosage on the strength and thickness swelling of the laboratory particleboard. The flexural strength (MOR) of the boards ranged from the lowest value of 11.21 MPa to the highest value of 21.43 MPa. Lower density pine wood produced strongest boards. However, other raw material and the combination of the raw material also produced suitable boards. Modulus of elasticity (MOE) followed the same trend as MOR. Mixed hardwood particles produced highest internal bonding, but the internal bonding of the boards produced using other raw material was more than the requirements of the ENB.

The results revealed that any combination of different urban and orchard tree residues can be utilized in particleboard production with the characteristics fulfilling the requirements of EN standard.

References

- Bekalo, S.A., Reinhardt, H.W. and Riedl, B. 2010. Fibers from coffee husk and hulls for the production of particleboard. *Materials and Structures*. 43:1049-1069.
- Blanchet, P. Cloutier, A and Riedl, B. 1999. Particle board made from hammer milled black spruce bark residues, *Wood Science and Technology*. 34(101): 11-19.
- Buyuksari, U., Ayrimis, N., Avci, E. and Koc, E. 2010. Evaluation of the physical and mechanical properties and formaldehyde emission of particleboard manufactured from waste stone pine (*Pinus pinea* L.) cones. *Boiresources Technology*. 101:255-259.
- Food and Agriculture Organization Statistics. (2013). Rome, Italy.
- Schneider, T. ; Roffael, E. ; Dix, B.. 2000. The effect of pulping process (TMP and CTMP) and pulping conditions on the physical and technological properties of medium density fiberboard (MDF). *Holz-als-Roh-und-Werkstoff*. 58(1-2):123-124.
- Enayeti, A., Yusefi, H., and Resoli, D. 2008. The possibility of using Apple tree pruning for particleboard making. *Iran Wood and Paper Research*. 28(1): 63-73.
- European Standard EN 319. 1996. Wood based panels, determination of tensile strength perpendicular to plane of the board. European Standardization Committee, Brussell.

European Standard EN 325-1. 1993. Wood based panels, Sampling, cutting and inspection. Sampling and cutting of test pieces and expression of test results. European Standardization Committee, Brussell.

European Standard EN 326-1. 1993. "Wood based panels, Sampling, cutting and inspection. Sampling and cutting of test pieces and expression of test results." European Standardization Committee, Brussell.

European Standars EN 310. 1996. "Wood based panels, determination of modulus of elasticity in bending and bending strength," European Standardization Committee, Brussell.

Johns, W.E. and Niazi, K. 1980. Effect of pH and buffering Capacity on the gelation time of urea-formaldehyde resin. *Wood and Fiber*. 12(4):255-263.

Kalaycoglu, H, Nemli, G. 2006. Producing composite particleboard from kenaf (*Hibiscus cannabinus* L.) stalks. *Industrial Crops and Products*. 24:177-180.

Marathan, A., Murathan, A.S., Guru, M. and Balbas, M. 2007. Manufacturing low density boards from waste cardboards containing aluminum. *Materials and Design*. 28:2215-2217.

Nemli, G. Kirel, H. Serdar, B. Av, N. 2003. Suitability of kiwi (*Actinidia sinensis* planch) pruning for particleboard manufacturing. *Industrial Crops and Products*. 17(1):39-46

Nemli, G, Yildiz, S, Gezer, E. D. 2008. The potential for using the needle litter of scoth pine (*Pinus sylvestris* L.) as a raw material for particleboard manufacturing. *Bioresource Technology* 99: 6054-6058

Shi, J.S., Li, J.Z., Fan, Y.M. and Ma, H.X. 2006. Preparation and properties of waste tea leaves particleboard. *For. Stud. China*. 8(1): 41-45.

Schneider, T. ; Roffael, E. ; Dix, B. 2000. The effect of pulping process (TMP and CTMP) and pulping conditions on the physical and technological properties of medium density fiberboard (MDF). *Holz-als-Roh-und-Werkstoff*. 58(1-2):123-124.

Xu, J., Sugawara, R., Widyorini, R., Han, G., Kawai, Sh. 2004. Manufacture and properties of low density binderles particleboard from Kenaf core. *J. Wood Sci*. 50:62-67.

Wang, D., and Sun, X.S. 2002. Low density particleboard from wheat straw and corn, *Industrial Crops and Products*. 15:43-50

A New Analytical Method to Study UF Resin Distribution within Particle Boards

Eike Mahrtdt,^{1} Hendrikus W. G. van Herwijnen,² Wolfgang Gindl-
Altmutter,³ Wolfgang Kantner,⁴ Johann Moser,⁵ Ulrich Müller,⁶*

- 1, Junior Scientist, Wood K plus, Competence Centre for Wood Composites and Wood Chemistry, Altenberger Str. 69, A-4040 Linz, Austria, Division Wood Materials Technologies, c/o Konrad Lorenz Str. 24, A-3430 Tulln, Austria, * *Corresponding author* e.mahrtdt@kplus-wood.at
- 2, Deputy area manager, Wood K plus, Competence Centre for Wood Composites and Wood Chemistry, Linz, Austria
- 3, Professor, BOKU – University of Natural Resources and Applied Life Science, Department of Material Science and Process Engineering, Institute of Wood Technology and Renewable Resources, Tulln, Austria
- 4, Product Development Manager, Metadynea Austria GmbH, Krems, Austria
- 5, Senior Development Chemist, Metadynea Austria GmbH, Krems, Austria
- 6, Professor, BOKU – University of Natural Resources and Applied Life Science, Department of Material Science and Process Engineering, Institute of Wood Technology and Renewable Resources, Tulln, Austria

Abstract

In the wood-based panel industry, particle boards are the main products and the most common binders for producing them are urea formaldehyde resins (UF). In order to optimise resin application, the knowledge of its distribution within wood-based boards is a first and crucial step. Due to the fact that UF resins are colourless they cannot be observed by using light microscopy without treatment. Existing analytical methods, in which the resin is stained before gluing particles and board making, have provided useful information. Nevertheless, on industrial scale, these methods are impractical, labour-intensive and expensive. Therefore, a simple, low-cost and efficient method was developed to investigate resin distribution. This new method is based on post-production staining of thin sections of industrial produced particle boards with a visible and a fluorescent dye and subsequent use of light microscopy for image recording. Pictures of cross sections were taken under halogen and fluorescent light. These image sections were matched and combined to make one new image, in which wood and adhesive are visible. By means of image processing software these images were further edited in order to calculate the adhesive distribution.

This efficient method is applied to study resin behaviour in industrial boards affected by different resin characteristics like viscosity and degree of condensation, and to investigate a potential influence of the distribution on mechanical board properties.

Keywords: fluorescence microscopy; particle board; post-added staining; resin distribution; UF resin

Introduction

Enormous amounts of amino resins are used to produce boards. For example, the European production of these types of resins was estimated to be 5.5×10^6 metric tons in the year 2004, from which approximately 95% were used in the particleboard and MDF production (Diem et al. 2010). Therefore, knowledge on the whereabouts of resin within industrially produced boards is of great importance. The distribution of the resin is one major aspect for the final quality of particleboards (Riegler et al. 2012). The most applied amino resins are Urea-Formaldehyde (UF) resins. Unfortunately, cured UF resins are nearly colorless and therefore difficult to observe under a conventional light microscope. An effective method of making UF resins visible is to label them with the fluorescent dye Acriflavin during resin synthesis (Grigsby and Thumm 2012). Labeled UF resin can then be incorporated into a commercial UF resin (Grigsby et al. 2004). By using this method, valuable information has been obtained. However, because the resin is marked in the liquid state and thus before boards are made, the method is limited to the study of laboratory boards. If one desires to study industrial boards, enormous amounts of resin have to be pre-stained because of the large scale on which boards are nowadays produced. Furthermore, it has to be decided in advance which specific charge of boards is to be investigated afterwards. If the need arises to analyse another charge which was not pre-stained, it is no longer possible. Therefore, in order to investigate industrial boards, another method is needed.

Sernek et al. (1999) used Brilliant Sulphaflavin to detect post-stained UF resins penetrated into beech veneer. Because of the selective reaction of Brilliant Sulphaflavin with amino groups (Leemann and Ruch 1972) the resin can be stained *after* the board has been pressed. Therefore, this dye played an important role in our studies.

Adhesive detection is just a first step or rather a tool towards an adequate knowledge of adhesive behaviour in particle boards. Furthermore, it has been used to draw a relation between adhesive distribution and its effect on bond performance.

Materials and Methods

For the present studies, three-layer particleboards were produced by Metadynea Austria GmbH (Austria), using urea formaldehyde (UF) resins. The boards were identical, except for the resin used.

Three types of resins were compared: UF1 is a low molecular weight resin with a low degree of condensation. UF2 is a middle molecular weight resin with a middle degree of condensation and UF3 is a high molecular weight resin with a high degree of condensation. The solid content of all three resins is similar and was balanced.

Table 1 shows resin properties and mechanical values of tested particle boards used for the resin evaluation. In this article three resins are compared in terms of their mechanical properties with different degrees of condensation (DOC).

Resin	Solid resin %	Viscosity mPas	DOC	Density kg/m ³	Bending strength N/mm ²	Internal bond N/mm ²	24h Swelling %
UF1	72	500	low	665	11,80	0,41	16,64
UF2	66	500	medium	666	12,38	0,42	13,95
UF3	63	500	high	659	11,75	0,36	18,57

Table 1. Characteristics of the resins and mechanical values of tested particle boards

Specimens (2x3x4 mm) were prepared out of a board, embedded in an epoxy resin, and cut into 2 µm thick cross sections. The thin sections were stained with Brilliant Sulphaflavine, which was used for labeling the adhesive, and another dye, Gentian violet, which was used for subsequently staining the wooden parts in order to obtain a better contrast. After each coloring step, the samples were rinsed with water to remove excess dye. Because of the embedment in epoxy resin, the samples could not swell. Afterwards, using a Zeiss Axioplan 2 microscope, pictures of the cross sections were taken under halogen (Figure 1) and fluorescence light (excitation at 438 nm, emission at 520 nm) (Figure 2). After microscopy, the two image sections were matched and combined to create one new image (Figure 3) using image processing software. In order to see both image aspects, one of them was made more lucent.

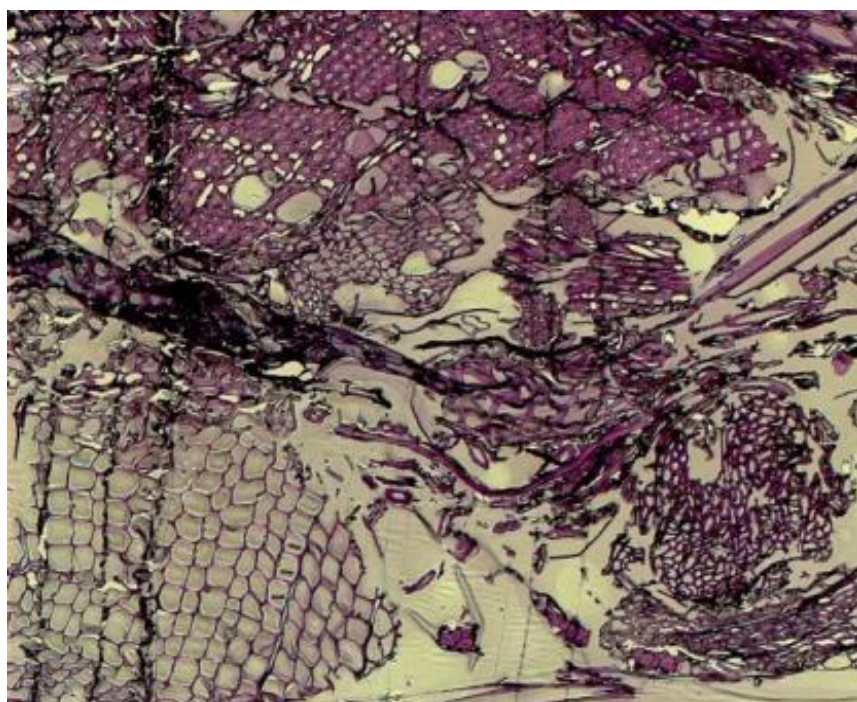


Figure 1. Microscopic picture of a particleboard sample bonded with UF resin under halogen light.

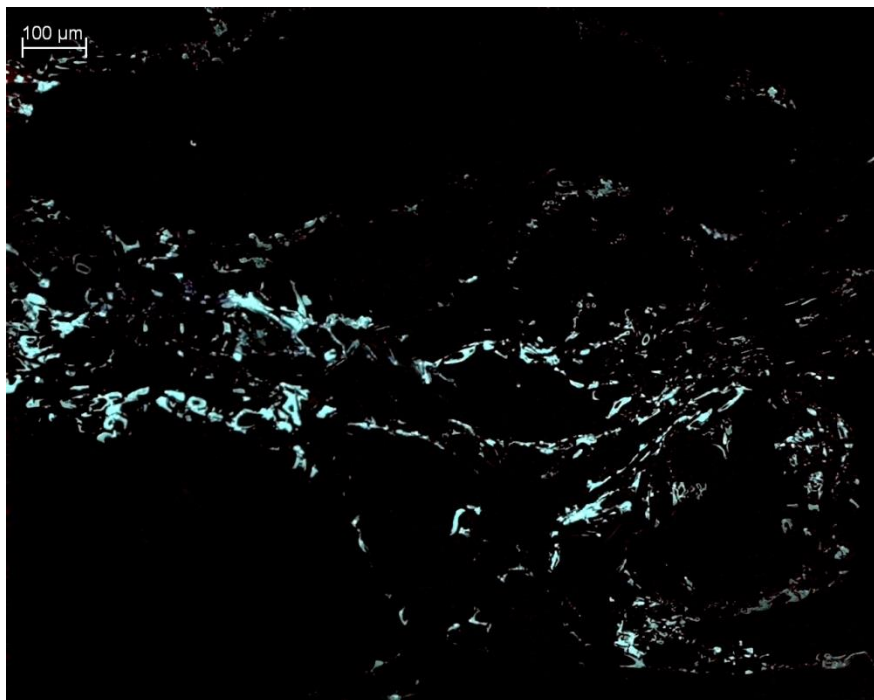


Figure 2. Microscopic picture of a particleboard sample bonded with UF resin (fluorescence picture).

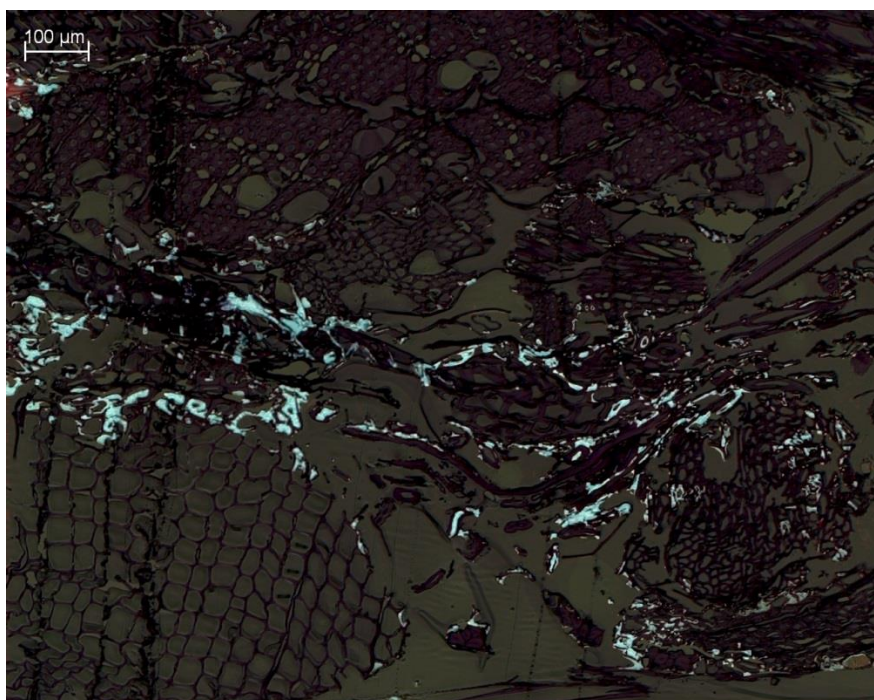


Figure 3. Particleboard sample bonded with UF resin as overlay of the halogen light picture with the fluorescence picture (Combination of figure 1 and 2).

In Photoshop all particle borders were contoured with a line to indicate the surface of wood particles. The bondline region was defined as an area of 25 μm around the surface line (12.5 μm in both directions). In addition, all particle lumen were filled in black. In Photoshop binary images of adhesive, penetrated areas and bondline regions were achieved. With these images, overlapping areas of adhesive and bondline region, as well as of adhesive and particle (penetration) were determined by the software ImageJ. Those areas could be added together and put in relation to the total adhesive. Resin not present inside bondline or particle was named “excess” resin. In this manner the adhesive distribution could be determined.

An additional parameter that was determined to characterize the board was “coverage”, defined as the surface area covered by resin divided by the total area surface. Coverage is expressed as percentage.

Results and Discussion

Figure 4 shows the resin coverage of particles of three different types of UF resins in the core layer of industrial particleboards. UF1, the resin with the lowest DOC shows the highest coverage, UF3 the lowest. UF2, the resin with the medium DOC is in between. It seems that the lower the DOC, the higher the coverage of the resin.

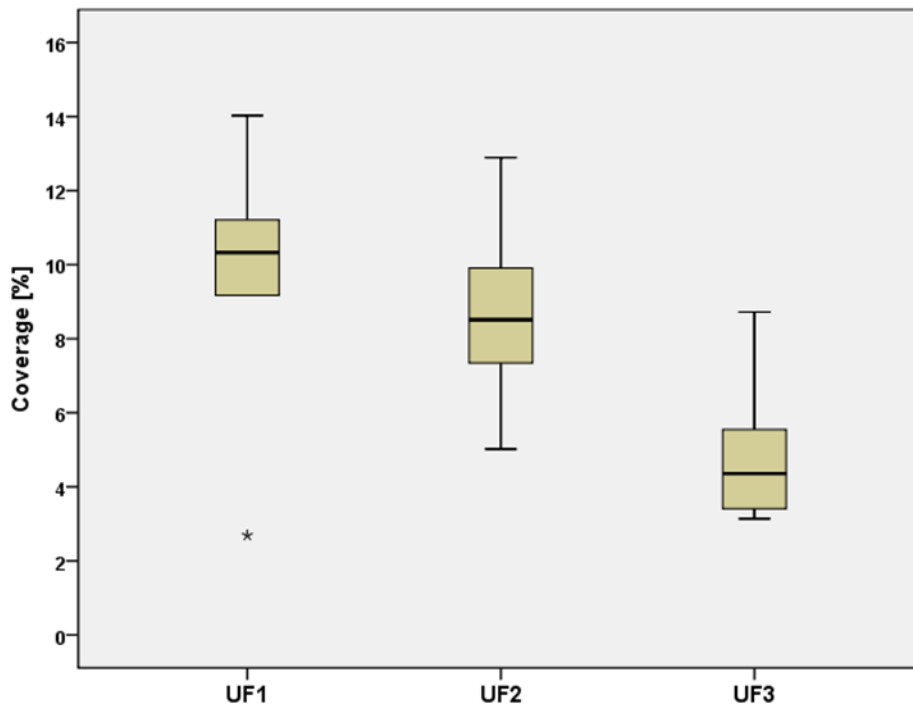


Figure 4. Coverage of the particles with UF resin in the core layer of three-layer particleboards.

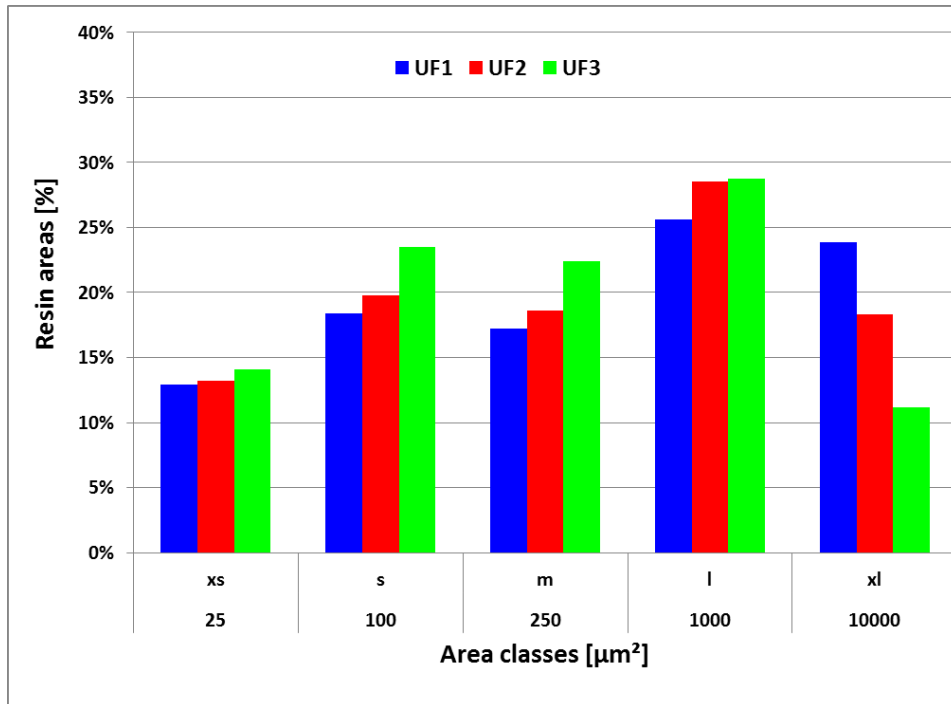


Figure 5. Resin area classes in the core layer of three-layer particleboards.

The resin size distribution can be seen in Figure 5. It shows for the low condensation resin more large resin areas whereas the high condensation resin has more smaller areas. One possible explanation in terms of different internal bond strengths might be due to the already mentioned shape formation. It is conceivable that the high condensation resin spread less on the particle surface and forms more and smaller resin drops. Whereas the low condensation resin may be tend to extended resin areas, which would lead to a bigger interface between wood and resin and therefore higher mechanical strengths.

Figure 6 shows the resin distribution of three different types of UF resin in the core layer of several particleboards. The values are average values of 8 samples taken from the board, as well as their standard deviations. Remarkable is the fact that only approximately half the resin formed a bondline, whereas the other half is penetrated or “excess” resin. Whereas the content of bondline adhesive of all three adhesives is slightly different the adhesive penetration shows a characteristic. In contrast to the assumption that the resin with the lowest DOC would results in the highest penetration both the high and low DOC resins are equal. This could be explained for the low condensation due to a larger spread of adhesive on the particle surface. As a result more resin might be remaining in the bondline and less penetrates into particles. However, for high condensation the low penetration could be an effect of larger resin molecules, which reduce the adhesive flow inwards the particle. The highest rate of penetration shows resin UF1 with medium degree of condensation. Apparently, the medium molecule size is able

to penetrate easier than bigger molecules and does not spread as much on the particle surface as the low condensation adhesive.

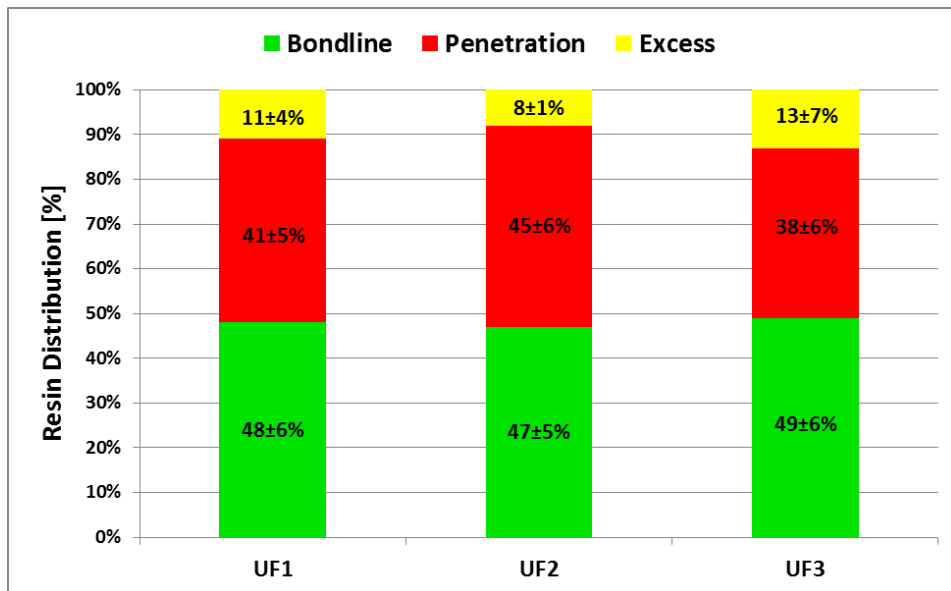


Figure 6. UF resin distribution within the core layer of three-layer particleboards.

Apart from an assumable influence of the bondline on mechanical bond performance adhesive penetration has been considered, too. As can be seen in Figure 1 the resin with the highest DOC results in the lowest internal bond strength (IB). An expected reason would be a low degree of adhesive penetration due to its high degree of condensation. Gavrilović-Grmuša et al. (2010) reported that a higher DOC causes a lower rate of penetration. In our case it partially applies but also other effects very likely overlap it. One of the possible effects could be best exemplified on the low condensation resin. The smallest resin molecules are expected to penetrate easily into particles and show the highest rate of penetration. Instead, the low DOC might leads to a higher spread of adhesive on the particle surface and this causes a decrease in penetration. Today it is widely recognised that a certain amount of adhesive penetration is necessary for a high bond performance. Kamke and Lee (2007) reported that a greater penetration is associated with more surface contact between adhesive and wood, thereby increasing the potential for additional bondings like secondary and covalent bonds. In the case of additional bonds, a greater mechanical performance could be presumed. In our case the adhesive with the highest rate of penetration results in highest bond strength. It seems there is more than just one influence regarding penetration. Many factors influence resin penetration, like those related to the fluid properties of the resin, anatomical characteristics of wood, and processing conditions (Kamke and Lee 2007). However, there is consensus that a specific amount of penetration is necessary for improving bonding quality but it is still questionable in which way penetration improves mechanical bonding quality and what the optimum adhesive penetration looks like. In literature there can be found several possible ways of reinforcement of bonding quality through adhesive penetration. The improvement might be derives from an enhanced mechanical interlocking effect, or from a fortification of subsurface wood areas

(Gavrilović-Grmuša et al. 2012). Also possible is for an improved bond performance a repairing effect of damaged cells and cracks by penetration (Kamke and Lee 2007).

Conclusions and Outlook

Effective methods are introduced that allow the analysis of UF resins in already produced industrial particle boards. It was found that inside particleboards approximately 50% of UF resin is present in the bondline and below 10% of the area of the particles is covered. The medium DOC seems to be the optimum in terms of bonding performance. Work is ongoing to understand the relation between resin parameters and bondline formation, resin penetration, and covering. Furthermore, the question in which way penetration improves mechanical bonding quality and what the optimum adhesive penetration looks like still has to be addressed.

References

- Diem, H., G. Matthias, and R. A. Wagner. 2010. Amino resins. in: Ullmann's encyclopaedia of industrial chemistry.
- Gavrilović-Grmuša I, J. Miljković, M. Điporović-Momčilović. 2010. Influence of the degree of condensation on the radial penetration of urea formaldehyde adhesives into Silver Fir (*Abies alba*, Mill.) wood tissue. *J Adhes Sci Technol* 24:1437-1453
- Gavrilović-Grmuša I, M. Dunky, J. Miljković, M. Điporović-Momčilović. 2012. Influence of the degree of condensation of urea formaldehyde adhesives on the tangential penetration into beech and fir and on the shear strength of the adhesive joints. *Eur. J. Wood Prod.* 70:655-665
- Grigsby, W., A. G. McDonald, A. Thum, and C. Loxton. 2004. X-ray photoelectron spectroscopy determination of urea formaldehyde resin coverage on MDF fibre. *Holz Roh Werkst.* 62, 358-364.
- Grigsby, W. J. and A. Thumm. 2012. Resin and wax distribution and mobility during medium density fibreboard manufacture. *Eur. J. Wood. Prod.* 70(1-3), 337-348.
- Kamke, F.A. and J.N. Lee. 2007. Adhesive penetration in wood – a review. *Wood Fiber Sci.* 39(2), 205-220
- Leemann, U. and F. Ruch. 1972. Cytofluorometric determination of basic and total proteins with sulfaflavine. *J. Histochem. Cytochem.* 20(9), 659-671.

Riegler, M., W. Gindl-Altmutter, M. Hauptmann, and U. Mueller. 2012. Detection of UF resin on wood particles and in particleboards: potential of selected methods for practice-oriented offline detection. *Eur. J. Wood Prod.* 70(6), 829-837.

Sernek, M., J. Resnik, and F. A. Kamke. 1999. Penetration of liquid urea-formaldehyde adhesive into beech wood. *Wood Fibre Sci.* 31(1), 41-48.

Classification of Lignocellulose Raw Materials Regarding Selected Material Properties and Regarding The Requirements of Three Competitors to Reveal Options for Alternative Use

Johann Trischler^{1} – Dick Sandberg² – Thomas Thörnqvist³*

¹ PhD student, Linnaeus University, SE-351 95 VÄXJÖ, Sweden

** Corresponding author*

[*johann.trischler@lnu.se*](mailto:johann.trischler@lnu.se)

² Professor of Wood Technology at Luleå University of Technology,
SE-931 87 SKELLEFTEÅ, Sweden

³ Professor of Forest Products at Linnaeus University, SE-351 95 VÄXJÖ,
Sweden

Abstract

According to different scenarios, the consumption of lignocellulosic raw material leading to competition is increasing for raw material for use in the board industry, the energy conversion industry, and the pulp and paper industry. The primary production of lignocellulosic raw material in some regions may therefore reach the limit of sustainability, and this means that the lignocellulosic raw material must be used more effectively to reduce the risk of a shortage. The physical and chemical properties of the lignocellulosic raw material of selected species have therefore been surveyed and the raw material properties which are important for each of the three competitors have been defined. A comparison between the properties of the various lignocellulosic raw materials and the requirements of the competitors for their products shows which raw materials face a high competition and which raw materials may open new opportunities, and at the same time lower competition because of their extraordinary properties.

The aim of the study is to characterise the lignocellulosic raw materials according to the three competing users and to show whether there is high or low competition. This is done by studying the restrictions found in the literature in combination with a statistical analysis. This method leads to results showing that the highest competition is for the coniferous species, while the properties of monocotyledons differ greatly from the properties of woody species resulting in low competition. Wood species grown in short rotation plantations show a high potential for all uses and not only for energy purposes.

Keywords: Bio fuel, Pulp and paper, Particleboard, Material properties.

Introduction

The competition for the lignocellulosic raw material between the particleboard industry, the energy conversion industry, and the pulp and paper industry is becoming increasingly tight. There are forecasts showing that already in 2020, the European consumption of wood can be as large as Europe's combined forest growth increment (Jonsson et al. 2011). An increasing proportion of the wood is expected to be used as fuel for heating, as propellant fuel or to generate electricity, i.e. applications that compete directly for the raw material used today in the particleboard and pulp and paper industries. Recently, approaches have been made to reduce the use of wood in particleboards by introducing other materials such as polymers, starch-based granulates, and monocotyledons like hemp or agricultural residues (Kharazipour et al. 2011; BASF 2013; ELKA 2013; Pfeleiderer 2013; WKI 2013). Monocotyledons not only give an opportunity to substitute wood but also have the advantage of reducing the weight of the boards (Boquillon et al. 2004). These developments lead towards specialized wood-based panels for certain applications and towards multi-component and multi-layered materials (Shalbafan et al. 2012). Nevertheless, not every raw material can be used for particleboards, as there are technical restrictions related to the material properties. For particle and fibreboards as well as OSB (oriented strand board) there is a relationship between the raw material and the board with regard to density, stiffness, strength, dimensional stability, internal bond strength, surface strength and appearance (Lundqvist and Gardiner 2011). Some properties like dimensional stability, internal bond strength, surface strength, and colour are influenced by additives during the production process (Grigoriou 2000; Frazier 2003; Frihart 2005; Xu et al. 2009; Saravia-Cortez et al. 2013) such as heat, pressure and closing speed of press (Kelly 1977; Kruse et al. 1997) or by the design of the particles and the product (Han et al. 1998; Hacke et al. 2001). A challenging feature is the contact area between particle and the adhesive, matrix, or environment.

For thermal energy recovery, important material properties are the moisture content, the calorific value, the proportions of fixed carbon and volatiles, the ash or residue content and the alkali metal content (McKendry 2002). The calorific value per mass is similar for different species, but the ash content and the ash softening point can differ strongly (Oechsner 2009). Among the European wood species, the softwood species have higher calorific values and higher ash melting points, but also higher ash contents than hardwood species (Schreiner 2009). Both, the ash content and the melting point are influenced by the chemical composition. The melting point decreases with increasing amount of potassium and sodium, while calcium, magnesium and aluminium increase the melting point (Biedermann and Obernberger 2005; Oechsner 2009). And low melting points, slagging, deposit formation, and corrosion cause problems in firing systems (Biedermann and Obernberger 2005). In general, all economically favourable lignocellulosic raw materials are nowadays used for thermal energy recovery, but density and moisture content have a strong impact on the transaction costs (Hamelinck et al. 2005; Altman et al. 2007; Möller and Nielsen 2007), and the calorific value per volume varies greatly (up to a factor of 20) depending on the species (Biedermann and Obernberger 2005).

For the pulp and paper industry, the dimensions, slenderness ratio, flexibility coefficient and Runkel-ratio of the plant fibres are important (Ververis et al. 2004). In particular, for paper made of fibres from hardwood, the length-to-diameter ratio is important because the fibres are shorter (Horn 1978). The strong influence of fibre length and cell wall thickness on the mechanical properties of paper has been shown in many tests (Horn 1978; Horn and Setterholm 1990), and there is a direct proportional relationship between tensile strength and cellulose content (Madakadze et al. 1999). Fibres for paper should generally be long (better fracture properties and wet strength of the paper) but not too long (negative influence on formation), thin-walled (better surface and optical properties) and flexible (positive for strength properties but negative for bulk) (Lundqvist and Gardiner 2011). According to the literature fibres with a long length, high slenderness ratio (>33) and low Runkel ratio (<1) are the best for pulping and papermaking (Xu et al. 2006). According to other sources the slenderness ratio of the fibrous material should be not less than 70 to be suitable for quality pulp and paper production (Shakhes et al. 2011) and the Runkel ratio should not exceed 1.25 (Antwi-Boasiako and Ayimasu 2012). The flexibility coefficient, which is an expression for the collapse of fibres resulting in surface contact and fibre-to-fibre bonding is also important and should exceed a value of 50 (Antwi-Boasiako and Ayimasu 2012).

Objectives

The objective of this study is to show the competition for different species by estimating the relatively best use of different lignocellulose raw materials for the particleboard industry, the thermal energy recovery industry and the pulp and paper industry, on the basis of some physical and chemical properties.

Materials and Methods

Literature data regarding the raw material properties of 21 species were collected. The species included 5 coniferous species (*Picea abies*, *Pinus sylvestris*, *Abies alba*, *Larix spp.*, *Pseudotsuga menziesii*), 12 broad-leaved species (*Betula spp.*, *Alnus glutinosa*, *Populus nigra*, *Populus tremula*, *Populus tremula x P. tremuloides*, *Salix spp.*, *Fraxinus excelsior*, *Fagus sylvatica*, *Quercus spp.*, *Tilia spp.*, *Acer plantanoides*, *Paulownia spp.*) and 4 monocotyledon species (*Miscanthus spp.*, *Phalaris arundinacea*, *Triticum spp.*, *Brassica napsus*).

The literature data include fibre properties (length, diameter, lumen, wall thickness), amount of fibres, wood density, contact angle of water, calorific value, ash content and melting point, and the pH-value. The raw material requirements of the industries including limitations or advantages are presented in Table 1.

The species are classified in relation to the properties of the raw material in two ways: (1) The species are compared relatively to each other and to the groups of competitors after the literature data have been standardised to a value between 0 and 1. This method

includes the selected limits presented in Table 1. (2) A hierarchical Cluster analysis (SPSS) also with standardized data in the range of 0 to 1. Ward's method with squared Euclidian distances as intervals was chosen for the cluster analysis. The monocotyledon species were excluded from the cluster analysis as their raw material properties differed too much. The combination of the relative method and the cluster analysis gives further information about the competition of the different species regarding their raw material properties.

Table 4. Overview of the criteria for classification of the raw material into those relatively best suited for particleboard production, thermal energy recovery and pulp- and papermaking including the limitations or advantages given in the literature. MC – moisture content.

	Criterion	Unit	Explained by	Limitations/ Advantages
Particleboard	Density	g/m ³	$\frac{\text{Mass at MC=15\%}}{\text{Volume}}$	X < average
	Wettability	°	Water drop contact angle	X < 70°
	pH-value	-	pH	X > average
	Amount of fibres	%	Percentage of fibres	X > average
Energy	Calorific value	MWh/m ³	$\frac{\text{Mass at MC=15\%}}{\text{Volume}}$	X < average
	Ash content	%	In percentage of mass at MC=15%	X < average
	Ash melting point	°C	chemical composition (Ca+Mg : K+Na)	X < average
Pulp and paper	Slenderness-ratio	-	$\frac{\text{Length of fibre}}{\text{Diameter of fibre}}$	X > 70
	Flexibility coefficient	-	$\frac{\text{Lumen diameter}}{\text{Diameter of fibre}}$	X > 70
	Runkel-ratio	-	$\frac{2 * \text{cell wall thickness}}{\text{Lumen diameter of fibre}}$	X < 1.25

Results and Discussion

The results of the relative classification are presented in Fig. 1, with the relative suitability for thermal energy recovery in the x-direction, that for pulp and paper in the y-direction and that for particleboard industry in z-direction.

The coniferous species show the highest suitability for all three competitors followed by some broad leaves species such as *Fraxinus excelsior*, *Alnus glutinosa* and *Betula spp.*. Species showing a relatively low suitability are *Tilia spp.*, *Populus nigra*, *Salix spp.*, *Populus tremula x P. tremuloides* and *Paulownia spp.*. The distance between the

monocotyledon species and the wooden species is relatively high due to the large differences in their raw material properties.

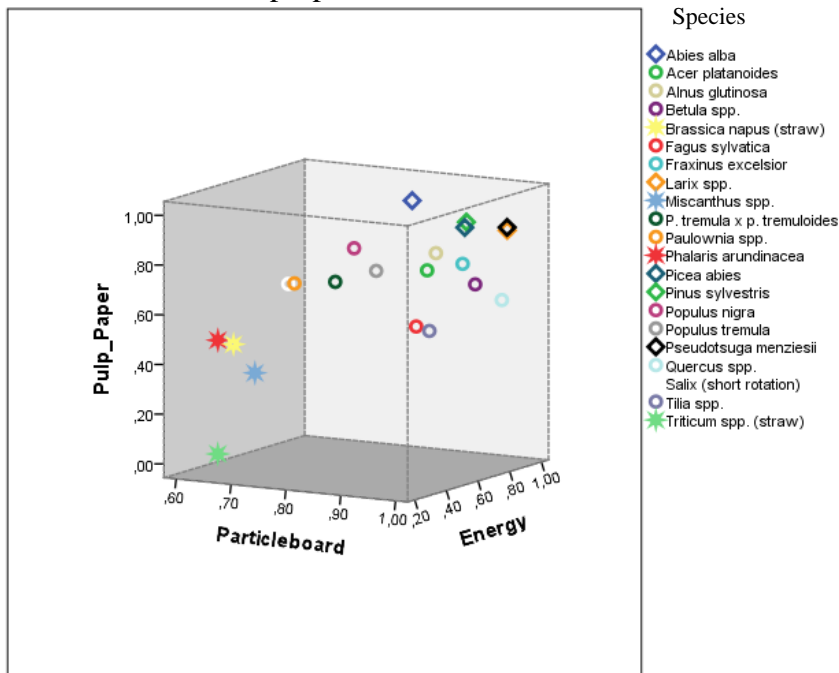


Fig. 1. *Relatively best use of raw material presented relative to each other and for use in the particleboard industry, for thermal energy recovery and for pulp- and papermaking.*

The dendrogram of the hierarchical Cluster analysis (Fig. 2) presents the distances of the wooden species from each other based on their raw material properties. Since the factor analysis gave a KMO of 0.531 with sig. $p < 0.000$ after excluding the monocotyledon species, no dimensional reduction of the properties as input data was made.

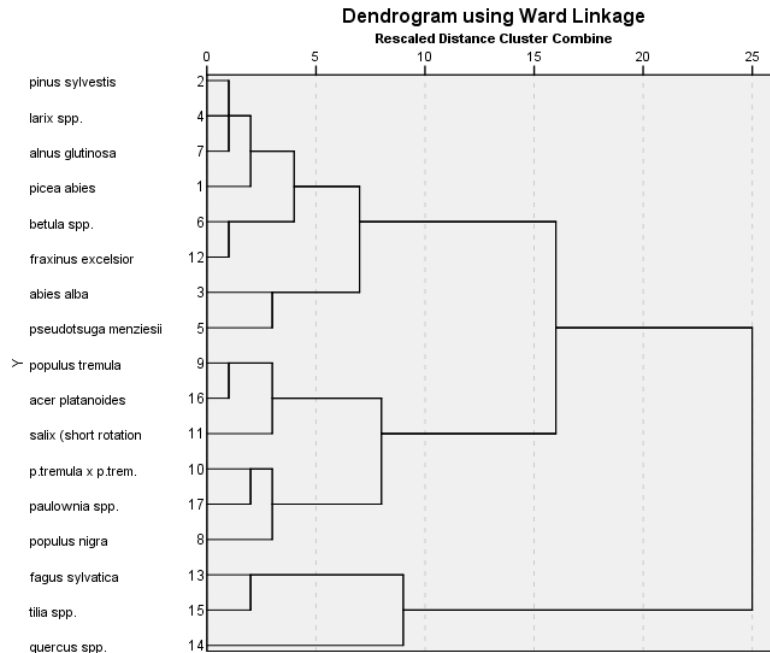


Fig. 2. Dendrogram of Cluster analysis of the wooden species using the Ward Linkage method.

The combination of both the “relative classification” and the “classification by the hierarchical Cluster analysis” can be interpreted as follows:

Cluster 1: highest competition: species which show values of at least 90% for one competitor and at least 60% for the other competitors in the relative classification. In the dendrogram, these are the species from *Pinus sylvestris* to *Pseudotsuga menziesii*.

Cluster 2: medium competition: species which show values between 60% and 90% in the relative classification. In the dendrogram, these are the species from *Populus tremula* to *Populus nigra*.

Cluster 3: low competition: species which show at least one value lower than 60% but still more than 50% for all values in the relative classification. In the dendrogram, these are the species from *Fagus sylvatica* to *Quercus spp.*.

Cluster 4: lowest competition: species which show values lower than 50%. These are the monocotyledon species in the relative classification not included in Cluster analysis as their raw material properties differ too much from those of the wooden species.

These two methods leave space for interpretation but their combination shows the relatively most suitable use and the competition, since the cluster analysis also groups the species regarding their distances but includes no further definition. Other competitors such as the sawmill or the cellulose fibre industry were not included in this classification. The group for thermal energy recovery was defined by raw material properties but in general all the species listed here can be used for energy production. The bioenergy sector with short rotation plantations, for example, nowadays uses exactly those species

which show the lower competition. This raw material might however be suboptimal for this purpose, as the calorific value per volume and the ash melting point are relatively low while the amount of ash and moisture content at harvest are relatively high compared to the species grouped as those most suitable for energy conversion. Nevertheless, this raw material might also be suboptimal for particleboard production because of the low density, amount of fibres etc. Overall, it is becoming obvious that it is very difficult for the particleboard industry to find alternative raw materials as either the competition is too high or the raw material properties are too low.

Conclusion

The aim of the study was to classify the raw materials of different species according to the needs of three competitors: the particleboard industry, the thermal energy recovery and the pulp and paper industry. This was done by combining two methods: (1) the species were classified relative to themselves with regard to the three competitors based on their relatively most suitable use. (2) A cluster analysis was used to give a more objective grouping and distances between the groups to see between which groups the pressure of competition is higher according to the material properties. The combination of both methods resulted in a ranking of the competition between the species. It can be concluded that in general (a) the coniferous species show the highest competition, being the most suitable for all three competitors, (b) the deciduous species with lower densities such as poplar, aspen and paulownia seem to have much less competition and seem to be to the same extent suitable for both particleboard production and thermal energy recovery, while (c) the monocotyledons were generally excluded as their raw material properties differ too much from those of the wooden species.

References

- Altman, I.J., Sanders, D.R., and Boessen, C.R. 2007. Applying Transaction Cost Economics: A Note on Biomass Supply Chains. *Journal of Agribusiness (Agricultural Economics Association of Georgia)* 25(1): 107.114.
- Antwi-Boasiako, C., and Ayimasu, A. 2012. Inter-family variation in fibre dimensions of six tropical hardwoods in relation to pulp and paper production. *Pro Ligno* 8(2): 19-36.
- BASF. 2013. Kaurit® Light: New lightweight Technology! Last Update 03 2013. <http://www.basf.com/group/corporate/chemistryworldtour/en/innovationen/kaurit-light>. [March, 18 2013].
- Biedermann, F., and Obernberger, I. 2005. Ash-related problems during biomass combustion and possibilities of a sustainable ash utilisation. <http://www.bios-bioenergy.at/uploads/media/Paper-Biedermann-AshRelated-2005-10-11.pdf>, [April, 23 2013].
- Boquillon, N., Elbez, G., and Schönfeld, U. 2004. Properties of wheat straw particleboards bounded with different types of resin. *Journal of Wood Science* 50(3): 230-235.
- ELKA. 2013. Lightweight chipboards. Last Update 03 2013. <http://www.elka-holzwerke.de/en/produkte/leichte-holzwerkstoffe/spanplatten-leicht/menu-id-236.html>. [March, 18 2013].

- Frazier, C.E. 2003. Isocyanate Wood Binders In: Handbook of Adhesive Technology, Revised and Expanded, A. Pizzi and K.L. Mittal, eds. 2003. New York: Taylor & Francis (Marcel Dekker Inc.).
- Frihart, C.R. 2005. Wood Adhesion and Adhesives, Boca Raton, FL: Taylor & Francis.
- Grigoriou, A.H. 2000. Straw-wood composites bonded with various adhesive systems. *Wood Science and Technology* 34(4): 355-365.
- Hacke, U.G., Sperry, J.S., Pockman, W.T., Davis, S.D., and McCulloh, K.A. 2001. Trends in wood density and structure are linked to prevention of xylem implosion by negative pressure. *Oecologia* 126(4): 457-461.
- Hamelinck, C.N., Suurs, R.A.A., and Faaij, A.P.C. 2005. International bioenergy transport costs and energy balance. *Biomass and Bioenergy* 29(2): 114-134.
- Han, G., Zhang, C., Zhang, D., Umemura, K., and Kawai, S. 1998. Upgrading of urea formaldehyde-bonded reed and wheat straw particleboards using silane coupling agents. *Journal of Wood Science* 44(4): 282-286.
- Horn, R.A. 1978. Morphology of Pulp Fiber from Hardwoods and Influence on Paper Strength. Department of Agriculture, Forest Service, Forest Products Laboratory, Madison, WI, <http://www.fpl.fs.fed.us/documnts/fplrp/fplrp312.pdf>, [March, 18 2014].
- Horn, R.A., and Setterholm, V.C. 1990. Fiber morphology and new crops, Portland, OR: Timber Press.
- Jonsson, R., Egnell, G., and Baudin, A. 2011. Swedish Forest Sector Outlook Study. United Nations, Geneva, http://www.unece.org/fileadmin/DAM/timber/publications/DP-58_hi_res.pdf, [March, 18 2014].
- Kelly, M.W. 1977. Critical literature review of relationships between processing parameters and physical properties of particleboards. USDA Forest Service, Forest Products Laboratory Madison, <http://www.fpl.fs.fed.us/documnts/fplgtr/fplgtr10.pdf>, [February, 05 2014].
- Kharazipour, A., Ritter, N., Werder, H.K.v., and Bohn, C. 2011. Entwicklung leichter dreischichtiger Spanplatten auf Basis nachwachsender Rohstoffe. *Holztechnologie* 52(5): 11-16.
- Kruse, K., Thömen, H., Maurer, H., Steffen, A., and León-Méndez, R. 1997. Optimierung des Spanplattenproduktionsprozesses mit Hilfe der Prozeßmodellierung. *Holz als Roh- und Werkstoff* 55(1): 17-24.
- Lundqvist, S.-O., and Gardiner, B. 2011. Key products of the forest-based industries and their demands on wood raw material properties. Joensuu, http://www.efi.int/files/attachments/publications/eforwood/efi_tr_71.pdf, [March, 23 2013].
- Madakadze, I.C., Radiotis, T., Li, J., Goel, K., and Smith, D.L. 1999. Kraft pulping characteristics and pulp properties of warm season grasses. *Bioresource Technology* 69(1): 75-85.
- McKendry, P. 2002. Energy production from biomass (part 1): overview of biomass. *Bioresource Technology* 83(1): 37-46.
- Möller, B., and Nielsen, P.S. 2007. Analysing transport costs of Danish forest wood chip resources by means of continuous cost surfaces. *Biomass and Bioenergy* 31(5): 291-298.
- Oechsner, H. 2009. Brennstoffeigenschaften von Biomasse. Heizen mit Getreide. Landesanstalt für Landwirtschaftliches Maschinen- und Bauwesen, Universität Hohenheim, Hohenheim, www.landwirtschaft-bw.info/servlet/PB/show/1200671/2006_Getreide_heizen_Drchsner_Hohenheim_Brennstoffeigenschaften.pdf, [March, 23 2013].
- Pfleiderer. 2013. Wood is replaced by annually-regenerating fibrous plants: BalanceBoard by Pfleiderer heralds a new generation of engineered wood-based products. Last Update 03 2013. <http://www.pfleiderer.com/en/news/press-release-868.html>. [March, 18 2013].

- Saravia-Cortez, A.M., Herva, M., García-Diéguez, C., and Roca, E. 2013. Assessing environmental sustainability of particleboard production process by ecological footprint. *Journal of Cleaner Production* 52(0): 301-308.
- Schreiner, M. 2009. Brennstoffdaten und Infos für Biomasse. Last Update 03 2012. http://energieberatung.ibs-hlk.de/planbio_brennst.htm. [March, 23 2013].
- Shakhes, J., Zeinaly, F., Marandi, M.A.B., and Saghafi, T. 2011. The effects of processing variables on the soda and soda-AQ pulping of kenaf bast fiber. *BioResources* 6(4): 4626-4639.
- Shalbafan, A., Welling, J., and Luedtke, J. 2012. Effect of processing parameters on physical and structural properties of lightweight foam core sandwich panels. *Wood Material Science & Engineering* 8(1): 1-12.
- Ververis, C., Georghiou, K., Christodoulakis, N., Santas, P., and Santas, R. 2004. Fiber dimensions, lignin and cellulose content of various plant materials and their suitability for paper production. *Industrial Crops and Products* 19(3): 245-254.
- WKI. 2013. Leichte Spanplatten aus Rückständen von Agrarpflanzen. Last Update 03 2013. <http://www.wki.fraunhofer.de/de/leistung/vst/projekte/spaplatten-aus-agrarpflanzen.html>. [March, 23 2013].
- Xu, F., Zhong, X.C., Sun, R.C., and Lu, Q. 2006. Anatomy, ultrastructure and lignin distribution in cell wall of *Caragana Korshinskii*. *Industrial Crops and Products* 24(2): 186-193.
- Xu, X., Yao, F., Wu, Q., and Zhou, D. 2009. The influence of wax-sizing on dimension stability and mechanical properties of bagasse particleboard. *Industrial crops and products* 29(1): 80-85.

Very Thin Medium Density Fibreboards (MDF) with Paperboard-like Properties as Reusable Packaging Material

Christoph Wenderdel^{1} – Tino Schulz¹ – Detlef Krug² – Alf-Mathias Strunz³*

¹ Scientists – Department Materials
Institut für Holztechnologie Dresden gemeinnützige GmbH,
Zellescher Weg 24, 01217 Dresden, GERMANY.

** Corresponding author*

Christoph.Wenderdel@ihd-dresden.de

Tino.Schulz@ihd-dresden.de

² Head of Department Materials,
Institut für Holztechnologie Dresden gemeinnützige GmbH,
Zellescher Weg 24, 01217 Dresden, GERMANY.

Detlef.Krug@ihd-dresden.de

³ Project leader – Paper and Fibre Pilot Plant,
Papiertechnische Stiftung,
Pirnaer Straße 37, 01809 Heidenau, GERMANY.

Alf-Mathias.Strunz@ptspaper.de

Abstract

Very thin MDF with cardboard-like properties (dry cardboard) were manufactured in lab-scale by combining chips of Scots pine with recovered paper as raw-material for the wood fibre pulp. The pulp was refined very finely, the fibre mat was produced with Airlaid-technology and the pressing conditions were adjusted. The mechanical properties of dry cardboards easily matched the requirements of cardboards for packaging purposes. The foldability, as required for folding boxes, was until now only achievable by producing multilayered dry cardboards.

Keywords: dry cardboard, ultra-thin MDF, foldability, folding behavior, burst index, folding box, packaging material, recyclability

Introduction

Due to sewage issues and a high drying effort for the production of fiberboards with the wet process technology, the dry process technology was developed in the 1960's (Šwidorski 1963, Lampert 1966). The advantages of the dry process were so convincing that today fiberboards are almost exclusively manufactured by this process. Calculations of current energy, water and raw material consumptions show that, in comparison to cardboard production on the basis of surface mass of 800 g / m², the dry process is energetically and economically favourable.

Regarding the development of MDF plants, where increasingly thin MDF can be produced (N.N. 2007a, 2007b, Schöler 2009, N.N. 2010), positive results are achieved compared to cardboard production with respect to the ecological and economic balances. This poses an enormous potential for the substitution of e. g. cardboard for packaging purposes by thin MDF.

The very different property profiles of the two products and additionally the high demands on the recyclability of packaging cartons are regarded as the main barriers for a direct substitution.

The aim of this study is a reduction of the mentioned barriers identified through the development of raw material and technology combinations, which allows the production of thin MDF with cardboard-like properties (hereinafter referred to as "dry cardboard"). The dry cardboards shall be suitable for further processing to packaging cartons and, compared to conventional cartons, shall have improved properties such as higher wet strength, smoother surfaces and, depending on the application, also have a distinctive density profile at the same or lower mass per unit area and furthermore allow the recyclability of the conventional used paper streams.

Preliminary studies have shown that the best results regarding folding behavior are achieved with finely refined fiber pulps, omitting the thermosetting condensation resins as a binder (Bartsch 2012, Wenderdel et al. 2012, Wenderdel et al. 2013). This paper focuses on the use of different bond effective additives, on different contents of recovered paper as well as on the difference of single and multilayered dry cardboards.

Materials and Methods

In this study, dry cardboards with different raw-materials and technologies were manufactured and board properties concerning the requirements of cardboards for folding boxes were characterised.

Materials

Different variants of fibre pulp were produced by varying the raw material. Logs of Scots pine [*Pinus sylvestris* L.] from the area "Dresdner Heide" were cut, debarked, chipped and sieved. Recovered paper of the grade 1.02 (household papers) was conditioned and

centrifuged. The dry mass content of the recovered paper differed from 0, 10, 20, and 30 to 50 %. The wood chips, in combination with the different recovered paper contents, were plasticised in a digester at a temperature of ~ 160 °C for 3 – 4 min, defibrated in a 12 inch laboratory refiner (Andritz) and dried in a lab flash drier. The grinding plate gap distance was 60 µm and the plate driving speed was 3,000 rpm. Refiner output of absolutely dry fibre was 60 kg/h with a sample size for each variant of 12 – 15 kg, while the inlet temperature of the flash drier was around 90 °C.

Table 5: Variants of different fibre pulp and additive combinations.

Additive	Recovered paper content / %				
	0	10	20	30	50
Starch	St_0	St_10			
Protein	Pr_0	Pr_10	Pr_20	Pr_30	Pr_50
Wheat flour	Wf_0	Wf_10			
PVAc	PV_0	PV_10			

Different bond effective additives such as starch, protein, wheat flour, and PVAc dispersion were added to the fibre pulps in the blowline (Table 5). The additive content amounted to 10 % with regard to absolutely dry mass of fibre pulp.

Methods

Manufacture of dry processed cardboard

The variants of fibre pulp and additive combinations were formed to fibre mats using the Airlaid technology (Figure 20).



Figure 20: Airlaid head and forming sieve with well distributed fibres.

The achieved grammages varied from 250 – 600 g/m². The fibre mats were rewetted to a moisture content of 13 ± 1 %. The hot pressing process was pressure controlled rather than distance controlled due to better repeatability regarding the target density of 700 kg/m³ (Wenderdel and Schulz 2013). Since the different pulps and additives led to different densification properties, the press process parameters had to be adjusted. Parameters were varied as follows: press time factor from 10 – 15 s/mm, pressing temperatures of 170 and 210 °C and specific pressure from 5 – 10 bar.

Multilayered cardboards were made of the above mentioned dry cardboard with a coating of 10 g/m² PVAc plus 80 g/m² printing paper and the same hot pressing parameters.

Characterisation of cardboard properties

The manufactured cardboards were characterised according to the following standards:

- Thickness DIN EN 20534
- Mass per unit area DIN EN ISO 536
- Burst index DIN 53141-1
- Bending stiffness DIN 53121
- Folding behavior DIN 55437-2 and DIN 55437-3
- Recyclability PTS-RH 021/97 and INGEDE-Methode 13

The standard regarding the folding behavior only considers passing or failing the test. Due to experiences from pre-trials the dry cardboards were most likely to fail the test, so that the results wouldn't allow assessing the influence of variations in raw materials and technology on the folding behavior. In accordance to DIN 55437-2 and DIN 55437-3 a method for assessing the folding behavior was established. The folding behaviors of the folded test specimens were graded from 1 (very poor) to 10 (very good) (Bartsch 2012).

Results

Due to process variability, the grammage, the thickness, and the density are not in the same range for every specimen. Therefore the results of the different properties are plotted against the parameter which is known to have the greatest influence:

- Burst index against density
- Bending stiffness against thickness
- Foldability against grammage

Influence of additive on cardboard properties

The earlier discovered correlation between density and burst index is covered by the different bond effective additives (Figure 21).

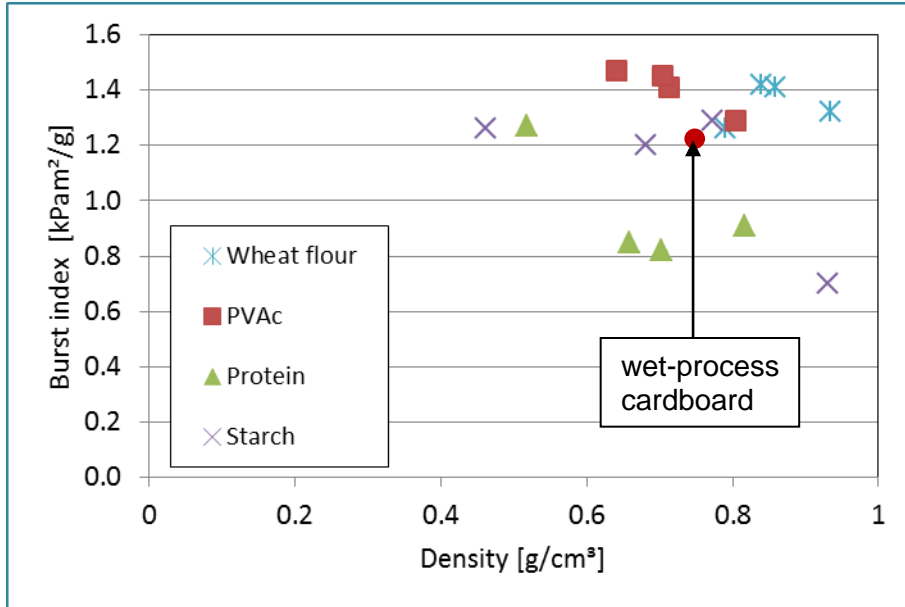


Figure 21: Burst index of dry cardboard bonded with different additives versus density.

Most burst index values of dry cardboard are equal or higher than for wet-process cardboard. The values are lower only for three variants of protein and one variant of starch bonded dry cardboard. The bending stiffness of the different bonded dry cardboards are comparable with the wet-process cardboards and differ only slightly regarding the correlation with thickness (Figure 22).

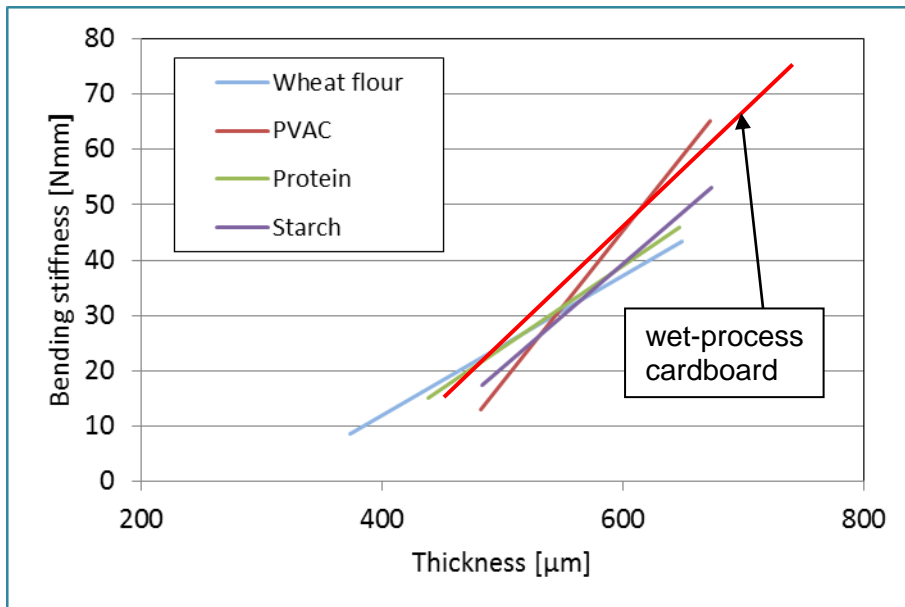


Figure 22: Bending stiffness of dry cardboard bonded with different additives versus thickness.

The foldability of all dry cardboards is only of medium quality, whereas the wet-process cardboard shows a very good foldability (Figure 23).

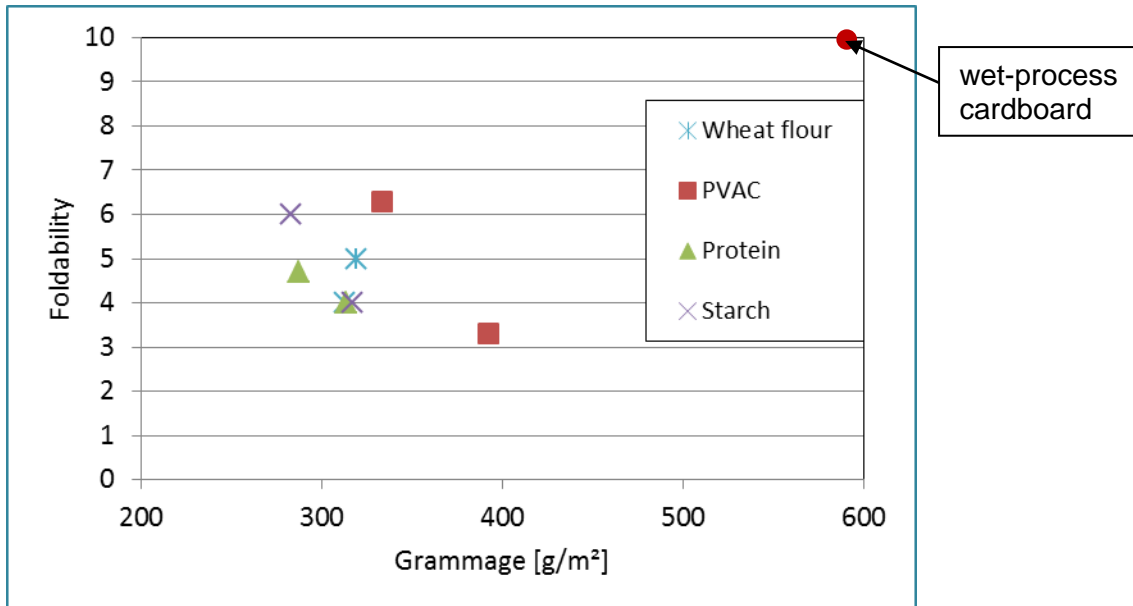


Figure 23: Foldability of dry cardboard bonded with different additives versus grammage.

Effect of different contents of recovered paper and multilayering

Exemplary for the influence of the content of recovered paper on cardboard properties, the burst index of protein bond dry cardboard with comparable grammage, thickness, and density is displayed in Figure 24. With 10 – 20 % content of recovered paper the burst index is slightly higher than with 0 % recovered paper. With higher contents of recovered paper the burst index decreases.

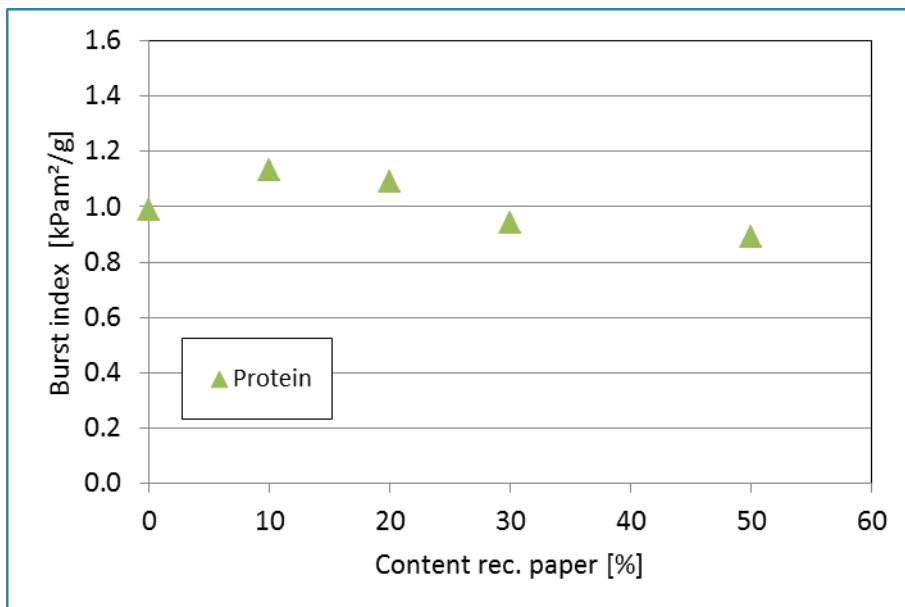


Figure 24: Burst index of dry cardboard bonded with protein versus content of recovered paper.

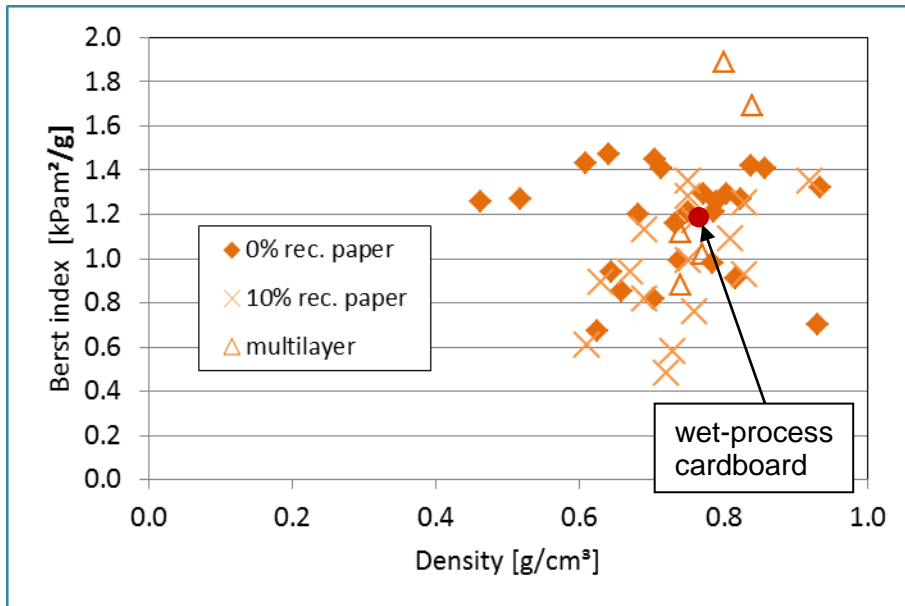


Figure 25: Burst index of dry cardboard bonded with different additives, different contents of recovered paper, and different layering versus density.

However, comparing all dry cardboards regarding the influence of the recovered paper, the effect of 10 % recovered paper on the burst index is rather negative (Figure 25). The burst index values of the multilayered dry cardboards differ from 0.9 to 1.9 kPam²/g. The content of recovered paper has only a small effect on bending stiffness, whereas the multilayer cardboards have a significant higher bending stiffness (Figure 26).

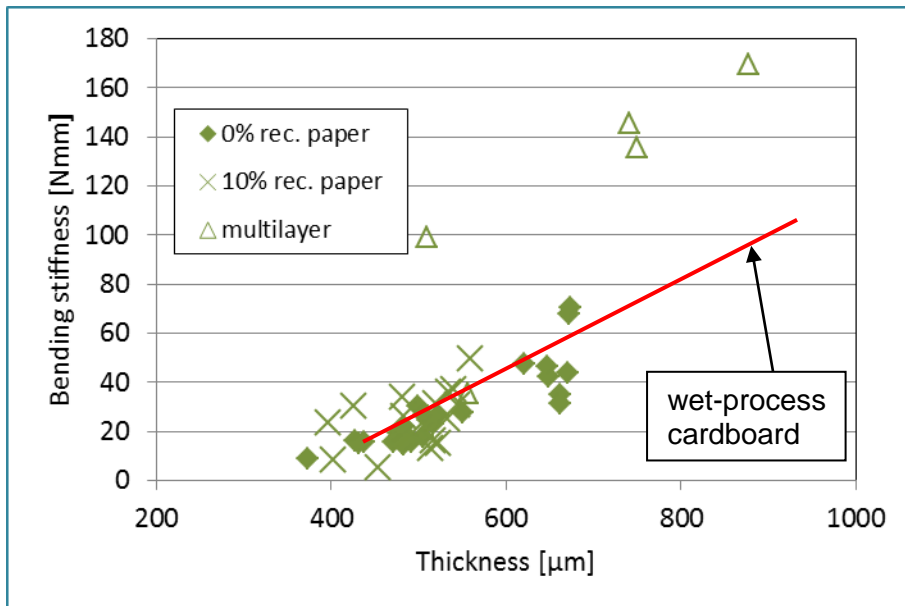


Figure 26: Bending stiffness of dry cardboard bonded with different additives, different contents of recovered paper, and different layering versus thickness.

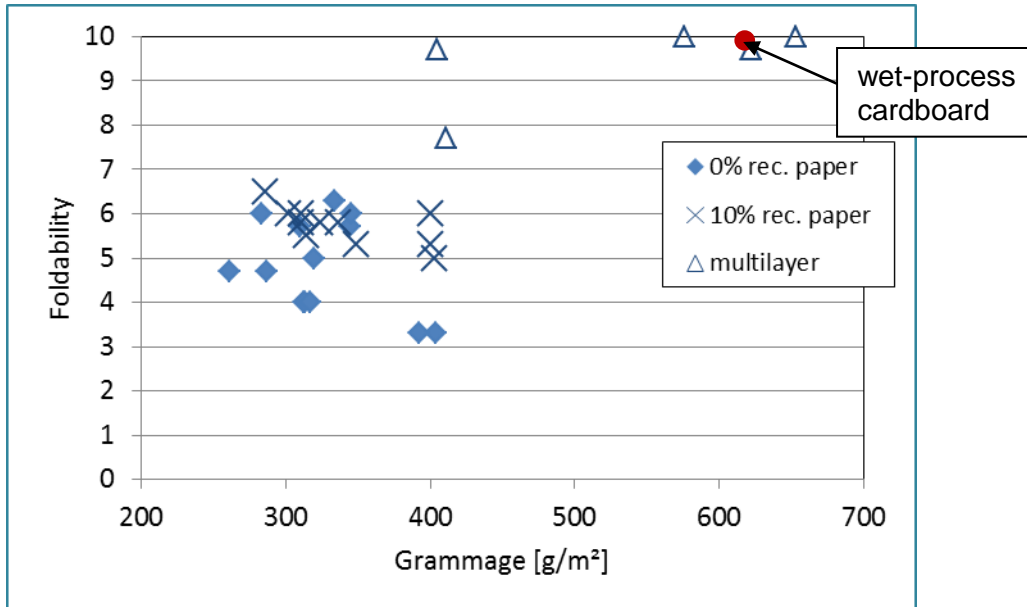


Figure 27: Foldability of dry cardboard bonded with different additives, different contents of recovered paper, and different layering versus grammage.

The usage of recovered paper has an impact on the foldability, but the quality is still only in the medium range. With a multilayer composition of the cardboards it is possible to increase the foldability to very good qualities, even in comparison to wet-process cardboard.

The recyclability was fully given for all dry cardboards described in this paper.

Conclusion

With a configuration of optimised raw-material combinations, an adaptation of the Airlaid technology and optimised pressing conditions, the production of dry cardboards with properties suitable for the manufacture of folding boxes is possible. Excellent mechanical properties are achievable with almost every raw material combination, however, to achieve a good foldability until now a coating of dry cardboard (multilayer) is necessary.

The optimum variant of this work consisted of fibre pulps refined with a very small grinding plate distance and an admixture of recovered paper of 50 %. The favourable bonding effective additive was PVAc and the coating consisted of 10 g/m² PVAc sprayed on the surface and an overlay of 80 g/m² printing paper.

Further work is planned to optimise the defibration process of the recovered paper in order to produce dry cardboard with suitable foldability without the necessity of constructing multilayer systems.

Acknowledgement

The presented work was supported by the German Federal Ministry of Economics and Technology at the decision of the German Bundestag (IGF: 16911 BG).

References

- Bartsch H (2012) Untersuchungen zur Herstellung von dünnen Faserplatten mit kartonähnlichen Eigenschaften im Trockenverfahren. Bachelor Thesis, Berufsakademie Dresden
- Lampert H (1966) Faserplatten. Fachbuchverlag, Leipzig
- N.N. (2007a) Dieffenbacher mit Dünn-MDF-Technologie erfolgreich. MDF-Magazin:28–34
- N.N. (2007b) Siempelkamp-Dünn-MDF-Technik geht bei Fantoni in Betrieb. MDF-Magazin:46–51
- N.N. (2010) Leichtbau-Konsequenz: Swedspan's neues UTHDF-Werk in Polen. MDF-Magazin:80–82
- Schöler M (2009) Verfahren zur Trockenkartonherstellung. PTS Energie-Symposium
- Šwiderski J (1963) Vergleich der Verfahren zur Herstellung von Hartplatten: Naß-, Halbtrocken- und Trockenverfahren. Holz als Roh- und Werkstoff 21(6):217–225
- Wenderdel C, Schulz T, Bartsch H, Schramm S (2012) Nicht von Papp. IHD und PTS prüfen Erzeugung dünner MDF für Verpackungen. MDF-Magazin:68–71
- Wenderdel C, Schulz T (2013) Extradünne, faltbare mitteldichte Faserplatten (MDF). In: VHI (ed) 4. Innovationsworkshop Holzwerkstoffe
- Wenderdel C, Schulz T, Schramm S (2013) Untersuchung zur Herstellung von Karton im Trockenverfahren. In: PTS (ed) PTS-Fachseminar: Roadmap 2050

Investigations upon Resistance of Surfaces Panel Elements Bonding by Artificial Veneers from Hot Melt Adhesives

Anna Ślęzak, Stanisław Proszyk

Poznan University of Life Science, Faculty of Wood Technology,
Department of Wood Based Materials, Division of Gluing and Finishing
of Wood, Poznan, Poland, e-mails: *anielaslezak@wp.pl*;
sproszyk@up.poznan.pl

Abstract

Production of furniture and furnishings of interior in Poland and on whole world develops in a very dynamic way. One of the most important directions of used wooden materials, in particular in furnishings of interior there are paneling, which are the products of new generation and their properties have become useful in a field of furniture industry and technology as well. It was worth emphasizing here, that the most important land are adhesives in producing processes, which determine the durability, resistance of finished manufactures. What is more, developments in adhesives for application in furniture industry are very fast as regards the industrial practice and innovating solutions. As a result of technical progress, the producers implement larger and larger qualitative needs. Those needs should provide the functionality, opportunely assessment of the aesthetic – decorative and also high durability to action of utylity factors. The surpass all expectations which are put to the various productions are in connection with used technology and quality of materials, which are used in furniture industry. Methods of resistance of surfaces panel elements bonding by artificial veneers from HM adhesives can be useful, universality and can show people how in easy way they should apply adhesives without expensive invensment and in what way people should use the panel elements to assure suitable durability and resistance. The investigations present the resistance upon surfaces panel elements from HM adhesives used to bonding by artificial veneers. For the investigations, there were used the paneling which were produced in industrial conditions, using LDF board, HM adhesives and artificial veneers.

Keywords: wall panel, LDF board, HM adhesive, artificial veneer, surface resistance

Introduction

The scope of applications hot melt (HM) adhesives practically started in the furniture industry from the end of sixties of last century and from now on it is widening in other fields connected with technology and wooden materials also. At present the assortment added variety of panel elements is being produced especially from LDF boards, which from the upper side are bonding by artificial veneers, usually in the version finish. The production of these veneers, relies on printing appropriate papers, next for impregnating them most often with acrylic composites and then finishing the surface by lacquers (Zenktelek 1996). The panel elements are intended above all rooms of destructive factors not exposed to the long-term influence of increased RH and outside (Malysheva i Bodrykh 2011). Additional advantage is a good thermal and acoustic isolation. The areas of discussed panel elements are quite immune to mechanical influences. The artificial veneers are intended to produce panels, offered in huge choice of assortments and quality classes. The collections of veneers are designed to current market trends, that is their colours drawn up by designers, effectively are raising visual advantages of get panel elements, granting finished form them. Their appearance is balanced very much what causes that they have a wide application, e.g. in architectural designs, of the production of furniture and furnishings interiors. From experience industrial, resulting from the production of panel elements it turns out, that every type of the artificial veneer, in the version finish it is important also and to a large extent it influences both to the process of bonding the surface, as well as properties of glue lines. In the process where the panel elements are bonding by artificial veneers the most important factors are relations which are deciding about properties in the arrangement substrate - adhesive - veneer. Binder based on ethylene – vinyl acetate (EVA) or polyolefine (PO) as the main element of applied HM adhesives, is deciding above all about appropriate adhesion artificial veneers to the surface of LDF boards, as well as about the forming of mechanical durability of finishing surfaces (Proszyk, Krystofiak and Lis 2012). A very important aspect which is determining the adhesion is compatibility of the polarity of base, adhesives and individual artificial veneers. They generally assume that it isn't possible to get a durable connection in case of polar materials, which are connected with glue about nonpolar character and inversely. In the mechanical aspect, they assume that the adhesion is manifesting itself as the biggest state of tensile stresses, acting on interphases surfaces which the moment of delaminating the arrangement is preceding (Gieldowski 1983, Krajaks et al. 2009; Proszyk, Bernaczyk and Krystofiak 1995a, b). The aim of work was to determine adherence of glue lines from Hot Melt adhesives used to bonding panel elements by LDF boards and artificial veneers.

Materials and Methods

For the investigations used the wall panels, which were produced in industrial conditions. To this destination using LDF panels (thickness 7 mm, density 650 kg/m^3 , MC 6 %), wrapping 6 artificial veneers (in decorative versions: pine, oak natural, pine natural, pine antic, marble cararra, ash mountain) by 3 HM adhesives, which based on EVA copolymers with fillers and without fillers and PO (Anonymous 2010). For determining

the resistance of glue lines in the attempt to tear away samples were used appropriately about dimensions 120 x 20 mm and aluminum plates 20 x 10 x 2 mm (fig. 1). Samples for indicating the durability of joints to tearing away were prepared according to guidelines drawn up by Zenkteler's (1983).

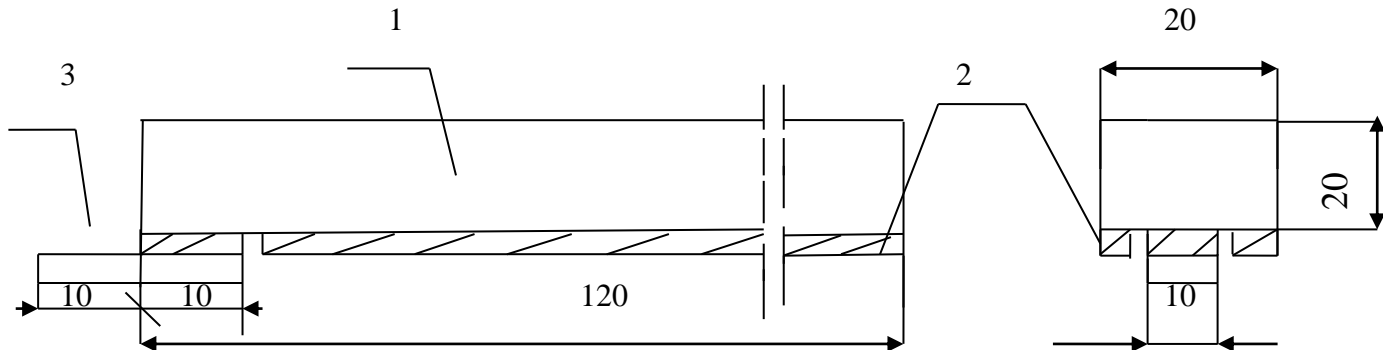


Fig. 1. Scheme of the sample with the stuck aluminium plate for determining the resistance to tearing away with the prototype MZ device:
1) LDF board, 2) artificial veneer, 3) aluminum plate

The sticking aluminum plates to the surface was an initial stage of veneers with 2 component glue silane - epoxy Jowat SE - Polymer 690.00. Next there was a conducted marking about the resistance of connections to tearing away, at using the prototype MZ device. Samples were fastened in the set stand, and then on sticking out from a distance 10 mm aluminum plate, a metal container was hung. Next a flow of water filling this container was started what all at the same time regular burdening the tested sample provided. In the moment of getting appropriate mass of the burden, tearing the aluminum plate away took place, with the simultaneous automatic blocking of the water supply into the container. Values of failure loads were being read off with the accuracy to 0.1 daN. For every sample additionally a degree of stratifications which took place in the attempt to tear away in the LDF surface, was being assessed expressed with so-called WFP indicator (Wood Failure Percent), which was being estimated with visual method with the accuracy up to the 25%. To determined adherence in system panels – adhesive - veneers used the samples of the size 120 x 30 mm, according to PN-EN ISO 4626. The initial stage there were sticking of metal measuring stamps to samples, at using SE-Polymer 690.00 adhesive. Before setting about determining the adhesion in the attempt to tear stamps away, examined part of the artificial veneer appropriately milled with cylindrical drill bit. PostiTest AT Adhesion apparatus was used for measurements testing machine, which is equipped with the plumbing drive of the team tearing away. It is possible to read off get values, expressed in MPa, in the automatic way from the electronic display of apparatus (Bordziłowski and Królikowska 2005). After tearing every stamp away, a visual evaluation of delaminated agreements was being conducted, with unarmed visual, making an appraisal of images of damage, according to the scale given in table 1.

Table 1

The markings of kinds of detachments in the method tearing away

Symbol	Type of tearing away
A	cohesion in substrate
A/B	disconnected in glue layer between substrate and veneer
B	cohesion in veneer
C	cohesion in the layer of glue
-/Y	disconnected of the glue – veneer system
Y	cohesion in SE adhesive layer
Y/Z	disconnected between SE adhesive and measuring stamp

Results

The results of investigations of the adhesion veneers to LDF boards in the attempt to tear away were presented on fig. 2. The lowest resistance were characterized the bonds with applying EVA adhesive with fillers, achieved average results were included in a range 1.0 - 3.5 daN, in addition lowest, comparable values were taken note for pine natural, pine antic and ash mountain (1.0 daN). However the highest value was stated for pine (3.5 daN), and a little bit lower parameters for oak natural and marble cararra. Next for samples of EVA adhesive without fillers were a little bit higher values (2.1 - 3.2 daN). In case of pine and pine antic, the lower values were recorded, whereas the highest for ash mountain and marble cararra. As by analogy as in case of analyzed previously properties, definitely the highest resistance of glue lines demonstrated PO adhesive, which this parameter was included in a range 2.8 - 3.9. In this variant, the highest values were for pine and oak natural, whereas the smallest for pine natural. Analyzing the appearance of delaminated connections in the attempt to tear away, they stated that all had adhesion character, being located between the veneer and substrate (A/B kind according to the scale from tab. 1). Chosen insults of damage were presented on fig. 3.

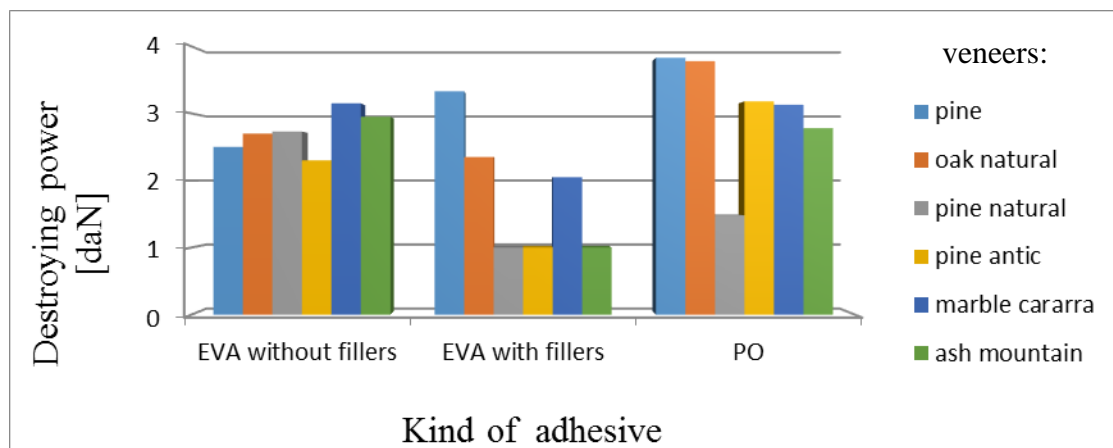


Fig. 2. Comparing results of the resistance of glue lines to tearing away of EVA adhesive without fillers, EVA with fillers, PO and different veneers

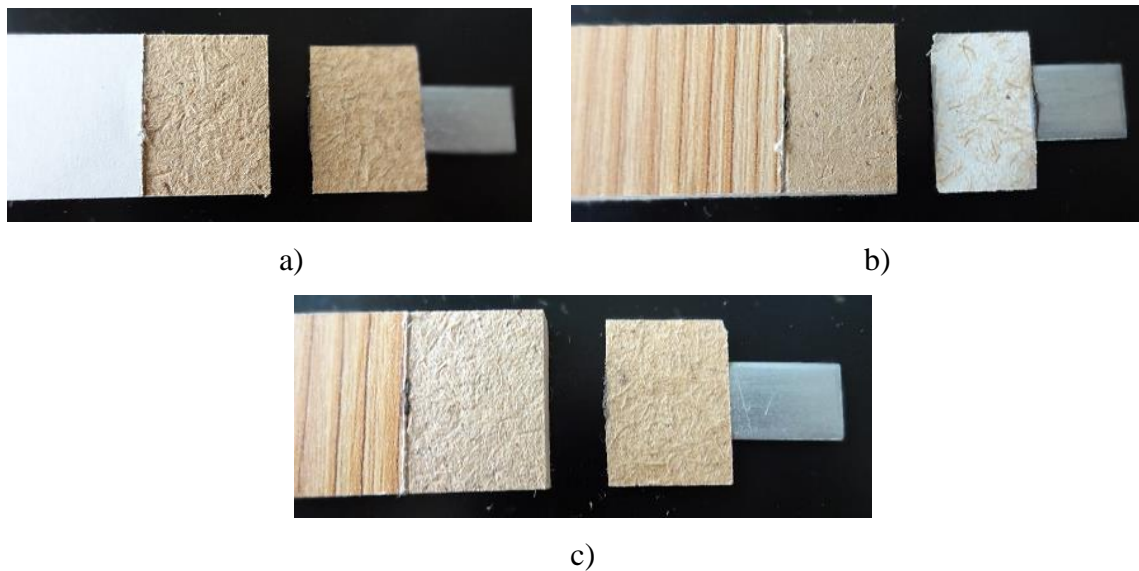


Fig. 3. Kinds of stratifications in the research on the resistance to tearing glue lines away of various adhesive: a) EVA without fillers, b) EVA with fillers, c) PO

The results of investigations of the adhesion of individual kinds of adhesives and veneers to base were placed in fig 4. In case of samples with applying EVA without fillers, achieved average results were included in range of values 0.56 – 0.87 MPa, however the highest value was stated for marble carrara, and the lowest for oak natural. Somewhat more profitable results were for ash mountain and for pine natural. Analyzing of the appearance of delaminated arrangements on the based of criteria which are given in table 1, they stated as dominating cohesive mechanism in substrate (A). However, the samples with EVA adhesive with fillers were characterized more profitable values (0.65 – 1.02 MPa). The least adhesion there were surfaces of such veneers as pine antic and marble cararra. However the highest values was stated for ash mountain and pine natural. Approximately a 50% of stratifications had adhesion character, appearing between the veneer and the LDF board, remaining whereas they categorised as cohesion in substrate. Next for panels with PO adhesive, the adherence was on the level moved close, and the data were located in range of values 0.60 – 0.96 MPa. In this variant, the highest values were get for oak natural, however the smallest for marble cararra. In this case as similarly as for EVA adhesive without fillers in all samples, cohesion character was stated in the substrate (A). Chosen images of damage arising in the researches of adhesion in the method tearing away were presented on fig. 5.

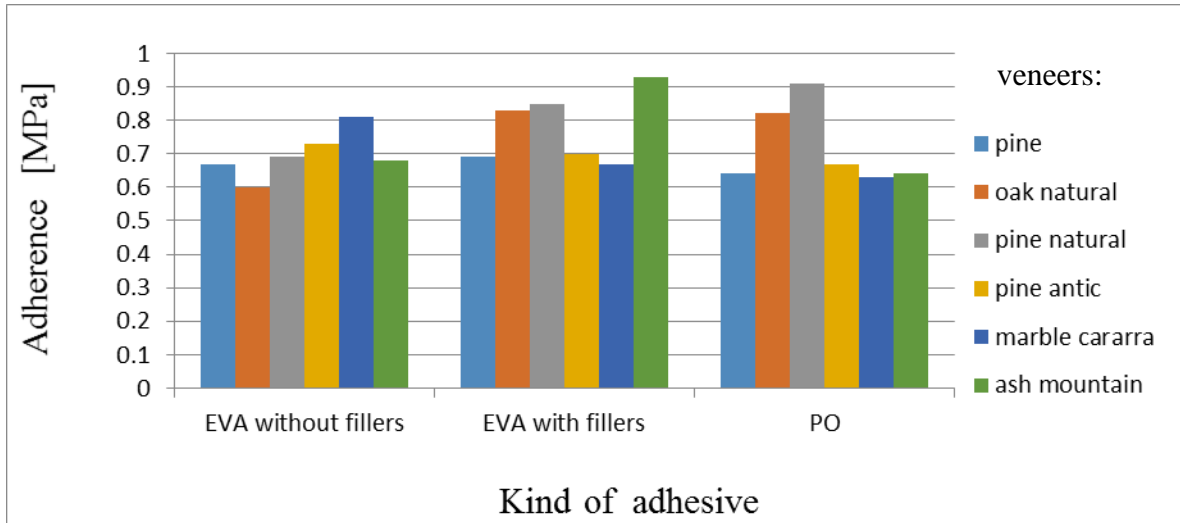


Fig. 4. The comparison results of adhesion of veneers to surfaces of LDF boards for glue lines from different HM adhesives and different artificial veneers



Fig. 5. The examples of images of damage arising in the researches of adhesion in the method tearing away

Conclusions

1. The adherence of artificial veneers to surface of wall panels in the test of tear off depended on kind of used adhesives, veneers and also panels. For EVA HM adhesives without fillers, the course in the range of values 2.50 – 3.15 daN, for EVA adhesives with fillers 1.0 – 3.33 daN, while for PO adhesives 1.48 – 3.83 daN. The most profitable values were for pine and oak natural veneers.

2. The highest adherence (acc. to PN-EN ISO 4626) of glue lines in the paneling from EVA adhesives with fillers and PO 0.63 – 1.02 MPa, while the least resistance of glue lines from HM adhesives, which based on EVA copolymers without fillers 0.56 – 0.87 MPa. Kind of artificial veneers do not have an influence on level of the resistance.

References

1. ANONYMOUS (2010): Karta produktu: Parametry fizykomechaniczne płyt LDF. Materiały firmy Kronopol.
2. BORDZIŁOWSKI J., KRÓLIKOWSKA A. (2005): Ocena przyczepności pokrycia lakierowego. *Lakiernictwo Przemysłowe* (1): 25-27.
3. GIEŁDOWSKI L. (1983): Zmodyfikowana metoda oznaczania przyczepności powłok lakierowych. *Przemysł Drzewny* 34 (9): 7-10.
4. KRAJAKS J.A., BAKRADZE G.G., VIKSNE A.V., REIHMANE S.A., KALNINS M.M., KRUTOHVOSTOV R. (2009): The use of polyolefins – based hot melts for wood bonding. *Mechanics of composite materials* 45 (6): 643-650.
5. MALYSHEVA G.V., BODRYKH N.V. (2011): Hot – melt adhesives. *Polymer Science Series D* (4): 301-303.
6. PROSZYK S., BERNACZYK Z., KRYSZTOFIK T. (1995A): Kleje topliwe stosowane w technologii opłaszczowania profili. *Przemysł Drzewny* 46 (6): 1-7.
7. PROSZYK S., BERNACZYK Z., KRYSZTOFIK T. (1995B): Kleje montażowe. Seminarium naukowo-techniczne na temat jakości w meblarstwie oraz stanu badań i normalizacji NOT – SITLiD Poznań: 97-105.
8. PROSZYK S., KRYSZTOFIK T., LIS B. (2012): Funkcjonalne taśmy obrzeżowe do oklejania wąskich powierzchni płytowych elementów meblowych. *Biuletyn Informacyjny OBRPPD w Czarnej Wodzie* (3-4): 115-124.
9. ZENKTELER M. (1983): Ćwiczenia z klejów i klejenia drewna. Skrypty AR w Poznaniu. Poznań: 57-64.
10. ZENKTELER M. (1996): Kleje i klejenie drewna. Wydawnictwo AR Poznań.
11. PN-EN ISO 4624 (2004): Farby i lakiery. Próba odrywania do oceny przyczepności.

Fire Properties Improvement of an Ultra-low Density Fiberboard Using Recycled Plant Fiber as a Matrix by Adding Si-Al Compounds

Min Niu¹ – Olle Hagman² – Xiaodong (Alice) Wang³ – Yongqun Xie^{4}*

¹ Lecture, Division of Wood Science and Technology, College of Materials Engineering, Fujian Agriculture and Forestry University, 350002, Fuzhou, Fujian, China
niumin521@163.com

² Professor, Division of Wood Science and Engineering, Department of Engineering Sciences and Mathematics, Luleå University of Technology, 93162, Skellefteå, Sweden
olle.hagman@ltu.se

³ Assistant Professor, Division of Wood Science and Engineering, Department of Engineering Sciences and Mathematics, Luleå University of Technology, 93162, Skellefteå, Sweden
alice.wang@ltu.se

⁴ Professor, Division of Wood Science and Technology, College of Materials Engineering, Fujian Agriculture and Forestry University, 350002, Fuzhou, Fujian, China
** Corresponding author
fafuxieyq@aliyun.com*

Abstract

An ultra-low density fiberboard was made of recycled plant fiber using a liquid frothing approach. It has a layered cross-linked interior structure and thus an ultra-low density of 10-90 kg/m³, a low thermal conductivity of 0.035 W/mK and a high sound reduction coefficient of 0.67. But the inflammability of plant fiber limited its application as a candidate of building insulation materials and packaging buffering materials. A single type of fire retardant does not have satisfactory fire retardation properties for the material, so Si-Al compounds was introduced into the foaming system to help another fire retardant improve its fire properties. The results from an energy dispersive spectroscopy suggested that the Si and Al relatively evenly covered the surface of the fibers, and their weight ratios in the material increased as a function of the amount of Si-Al sol-gel. The increasing weight ratios of Si and Al significantly affected the fire properties of the material, reducing the released amount of heat, smoke and off-gases such as CO and CO₂,

as well as decreasing the mass loss percent during combustion, shown through the use of a cone calorimeter. So Si-Al sol-gel has an evident synergistic effect on the halogen fire retardant; it can effectively restrain the fire hazard intensity and the yields of solid and gas volatiles.

Keywords: Ultra-low density fiberboard, Si-Al compounds, Energy dispersive spectroscopy, Fire properties, Cone calorimeter.

Introduction

A plant fiber-based ultra-low density fiberboard made by a liquid frothing approach is a new product different from the traditional fiberboard (Xie et al. 2003, 2008a, b). It uses plant fiber as a matrix and several additives as the reinforcement. No common adhesives, such as phenol-formaldehyde resin (PF) and urea-formaldehyde resin (UF), or heat pressing techniques are used in its preparation process, which is good for health issues and energy conservation. It can be used as a candidate for building insulation materials or package buffering materials. But a big problem is that the material has to be treated with fire retardants before its utilization. If no retardant treatment is employed, the fiber-based material will be highly flammable and burn up quickly, which is very dangerous for a building material. However, a single type of fire retardant generally does not impart satisfactory fire retardation properties to the material; other fire retardants are still needed to support it. Liu (2013) paid attention to the synergistic effect of several types of fire retardants; the results showed that a mixed retardant has a better effect on the fire properties of the material; halogen compound chlorinated paraffin can decrease total heat release and smoke release; and silicon compounds (silica as a main component) have a positive synergistic effect on other fire retardants. Besides silicon compounds, aluminum compounds also play an active role in resisting combustion. So in this study, chlorinated paraffin was used as a fire retardant, and a mixture water solution of Si and Al compounds was used to incorporate chlorinated paraffin to resist combustion.

Much attention has been paid to the manufacturing process and properties of the composites with inorganic substances as the matrix and plant fiber as the filler; however, few researchers have focused on the fire resistance of plant fiber-based materials. So using Si-Al compounds to enhance fire properties of fiber-based ultra-low density material is a very novel thought in the field of inorganic-organic combination, and little literature about fire properties of ultra-low density fiberboards with Si-Al compounds has been reported. Besides, because of the electrostatic effect of the Si-Al compounds clusters for absorption (Yang and Troczynski 1999), Si-Al compounds can adsorb poisonous suspended particles (such as printing ink and lead remaining in the newspaper), and thus there is less pollution of the water resource in the process of filtering water. Therefore, this also provides us an additional benefit in industrial production.

The combustion of the ultra-low density fiberboard is very similar to that of wood; it is also a degradation process of lignin, cellulose, and hemicellulose. A big difference from

wood is that the ultra-low density material has a network structure built by fibers. Thus the combustion of fibers is continuous at a low temperature and occurs in a flash at a high temperature. Through mechanically mixing the fibers and the additives together before frothing, Si-Al compounds accompanied by chlorinated paraffin can possibly wrap or cover the surface of fibers to effectively prevent the fibers from continuous combustion. The degradation products from Si and Al components can possibly absorb the heat released on the surface of the material, or the degradation products are some non-flammable gases to restrain heat and smoke release during combustion, thus lowering the fire and smoke intensity. The goal of the research presented here is to clarify the distribution of Si-Al compounds in the material and the interactions between the distribution and fire properties of material.

Materials and Methods

Materials. Newspaper (NP, collected in China) was utilized as a raw material to manufacture the ultra-low density fiberboard. Fiber length and fiber width of the raw material was 1047 (200-5310) μm and 23.5 (5-60) μm , respectively by MorFi Compact device.

Preparation of the ultra-low density fiberboard. Raw material was dispersed into fine fibers using a fiberizer. Water and Si-Al compounds, as a mixture solvent, were transferred into an open foaming tank attached to a pulp disintegrator (AB Lorentzen & wetter, Sweden), mixing fibers together to adjust fiber concentration to 5% wt. Preparation process of the specimens was the same as Xie et al. (2011). In this study, Si-Al compounds were prepared as a mixture of an aqueous solution of sodium silicate with 0.82% concentration and aluminum sulfate with 1.08% concentration. Its pH value was about 3.8. After foaming, the pH value of the solution was controlled to be 4.8 to 5.4 for by adding hydrofluoric acid of 10% wt. The adjustment of pH value was very important to get a desired foaming height. The amount of Si-Al compounds was set as two levels, 500 mL and 900 mL, to compare the fire property changes of the specimens. The amount of other additives was equal. For each specimen being suitable for the mould of 200 \times 200 \times 60 mm ($L\times W\times H$), total volume of water and Si-Al compounds solution was 1000 mL; the amount of absolute dry fiber, adhesive, AKD, chlorinated paraffin, and foaming agent (10% wt) was 50 g, 30 mL, 50 mL, 46 g, and 50 mL, respectively.

Distribution of Si-Al compounds in the ultra-low density fiberboard. A scanning electron microscope (SEM, Jeol JSM-6460, Japan) with an energy dispersive spectroscopy (EDS, INCA Energy EDS for X-ray analysis, Oxford Instruments) was used to localize and measure the weight ratios of silicon and aluminum in the fiberboard. The specimens were made by cutting a thin cross-sectional area. Their surfaces were unpolished and uncoated. The mapping was performed on an area displaying the additive and the matrix using an acceleration voltage of 25 kV, a current of 7 μA and a working distance of 10 mm. Detectable elements were registered during the mapping.

Testing of bulk density and fire properties. Bulk density of the specimen was measured using the same method as Xie et al. (2011). A cone calorimeter (FTT Co., England) is considered to be the most significant bench scale instrument for the testing of fire properties of a new product, adopted by the International Organization for Standardization (ISO 5660-1/2002) to evaluate the parameters of heat release, mass loss, smoke release and off-gases release as a function of time. The size of the specimens was 100×100×30 mm (*L×W×H*). The specimens were covered by aluminum foil except for the heating surface. The tests were performed at a heat flux level of 50 kW/m². The heat flow direction was vertical to the heating surface of the specimen and went down. The temperature on the surface of the specimen reached 780 °C, close to the temperature of an actual fire hazard.

Results and Discussion

Distribution of Si-Al compounds in the ultra-low density fiberboard

Figure 1 indicates micro morphology from SEM (left) and distribution of the element O, Al, Si and Cl from EDS (right) on the surface of fiberboard.

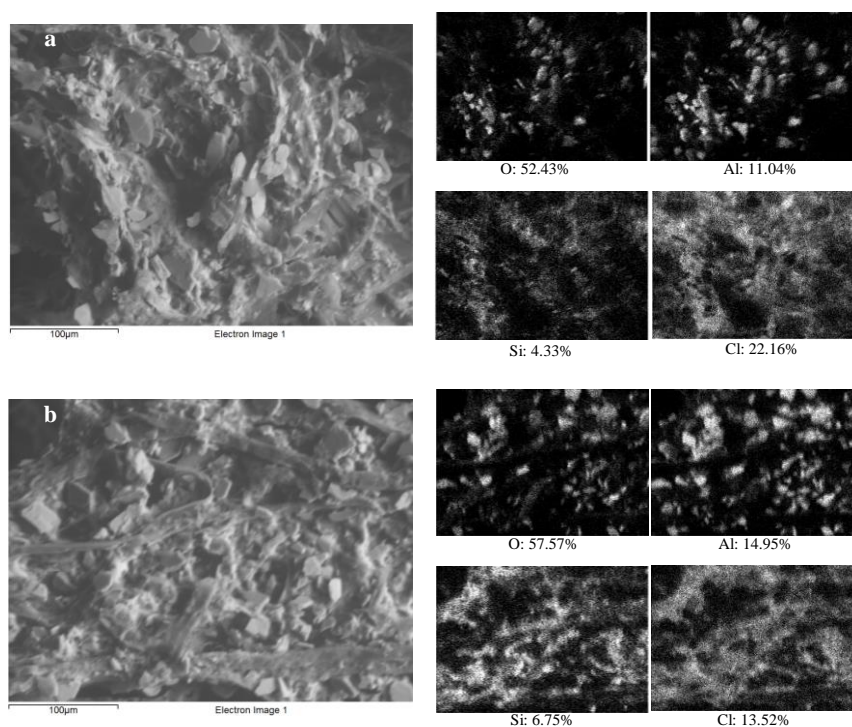


Fig. 1 Micro morphology (left), element mappings(right) and weight ratios at a certain region of the fiberboards at the levels of Si-Al compounds of 500 mL (a) and 900 mL (b).

Ultra-low density fiberboard made by using a liquid frothing technique has more interconnected holes in the network comprised of fibers. When Si-Al compounds were introduced into the foaming system, they dispersedly fill into these void spaces, thus improving the densification extent of the material, as is seen in Figure 1. The bulk density

of specimen with a and b was $55.67 (\pm 0.87)$ and $53.83 (\pm 1.29)$ kg/m^3 , respectively. The weight ratios from the four elements O, Al, Si, and Cl constituted almost 90% of the total weight, and their variations were more remarkable than those of other elements. When Si-Al compounds increased, weight ratios of O, Al and Si ascended and that of Cl descended. The increase of Si-Al compounds indeed resulted in more Si and Al elements being retained in the fiberboards. The increase of O was coincident with the element Al, which suggested that Al was present in the fiberboard in the form of oxides.

Fire properties of the fiberboard

Heat release and mass loss

The heat release rate (HRR) is a heat release value from the fiberboards with the same surface area ($100 \times 100 \text{ mm}^2$) at a certain time under the same heat flux. Combustion is inevitably accompanied by mass loss. Mass residual ratio, as a parameter of mass loss, is usually used to estimate the flammability or the combustion extent of the material. Figure 2 shows HRR (left), total heat release (THR, middle) and mass residual ratio (right) profiles as a function of time.

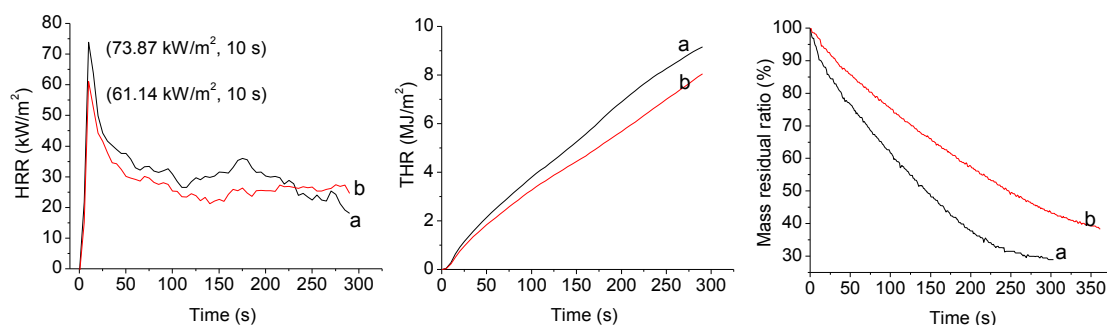


Fig. 2 HRR (left), THR (middle) and mass residual ratio (right) profiles of the specimens with 30 mm thickness at the levels of 500 mL (a) and 900 mL (b) Si-Al compounds at 50 kW/m^2

Two peaks can be seen in the HRR profiles. The first sharp one comes exactly at 10 s after ignition, and it is important for the evaluation of the fire intensity. The second peak appears around 200 s to 250 s when the surface of the specimen starts to break up and oxygen reaches the interior, and it is relative to the thickness of the specimen (Tsantaridis 2003). If the specimen is sufficiently thick, its second HRR peak will eventually reach a steady value and be inconspicuous. Mikkola (1990) and Moghtaderi (1996) also reported similar results for 38 mm thick spruce and 42 mm thick pacific maple.

The HRR maxima distinctly decreased when the amount of Si-Al compounds shifted from 500 mL to 900 mL. The lower the pkHRR , the less likely it was that flame was self-propagated on the material in the absence of an external flame or ignition source. It was also less likely that the material caused nearby objects to ignite. Furthermore, not only the peaks, but also the HRR curves in total time were lower. As suggested, that higher total weight ratio from Si and Al could effectively lower the HRR, in accordance with the

result of Gilman (1999). Gilman (1999) studied the flammability and thermal stability of the nanocomposite made from polymer and layered-silicate (clay), and indicated a 80% reduction in the pkHRR for the nanocomposite with only a mass fraction of 4% clay (a Si-Al compound). On the other hand, the time to pkHRR was the same. It meant that the fiberboards would simultaneously reach the maximum of the energy release and the fire would also simultaneously grow after ignition.

Total heat release (THR) represents the total heat release from the specimen in the total time. They increased almost linearly with time from Figure 2 (middle). The THR profiles for 900 mL Si-Al compounds were lower than those for 500 mL Si-Al compounds in the same time, possibly because of heat-trapping action of aluminum compounds and incomplete combustion of wrapped fibers by Si-Al compounds. Increasing Si-Al compounds indeed decreased heat release during the material burning. Mass loss differences between the two fiberboards with 500 mL and 900 mL Si-Al compounds were subjected to their THR differences. This was also the reason why the profiles about the mass residual ratios were similar to THR profiles. If the THR from pyrolysis and glowing reaction of char was lower, the residual ratio of carbonaceous matrix and Si-Al inorganic matrix would be higher.

Smoke and off-gases release

In fire hazards, people usually die from suffocation resulting from smoke and toxic gases, rather than being burned by high heat. So it is more important to study the smoke and off-gases release in the process of combustion of the building materials. The total smoke release (TSR, left), CO (middle) and CO₂ (right) concentration profiles are shown in Figure 3.

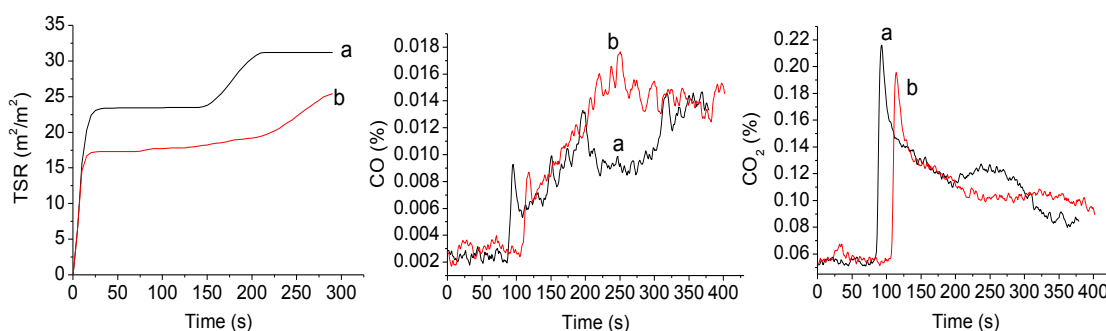


Fig. 3 TSR (left) profiles, CO (middle) and CO₂ (right) concentration profiles of the specimens with 30 mm thickness at the levels of 500 mL (a) and 900 mL (b) Si-Al compounds at 50 kW/m²

There was a sharp increase for the two TSRs at the beginning of combustion. When oxygen was insufficient, plenty of volatile matters with lower molecular weight contributed to the smoke due to incomplete combustion. After 150 s, one more big climb appeared in the TSR profile of the fiberboard with a. More smoke was possibly derived from burning residue and ash. For the fiberboard with label b, the second upward jump of TSR was not apparent. The amount of smoke did not increase, because more Si and Al

were distributed on the surface of the fibers and decreased the flammability of the fiberboard. Si-Al compounds had a significant smoke suppression function.

CO is a major safety concern because it is lethal at a relatively low concentration, with human death occurring within one hour at a concentration of about 1500 ppm (Mouritz *et al.* 2006). It is a product of the incomplete combustion of the flammable volatiles at the middle stage of combustion and sprays free carbon particles due to the surface cracks of the fiberboards at the later glowing combustion stage (Liu 2013). From Figure 3 (middle), CO concentration profiles were fluctuant and gradually increased as a function of time. The CO concentration of the fiberboard more or less increased after Si-Al compounds shifted from 500 mL to 900 mL. This was mainly because more Si and Al could insulate the fibers from outside oxygen and render the combustion of fibers incomplete. Liu (2013) also obtained the same results by comparing the CO concentrations of the materials before and after fire retardant treatment. According to the CO concentrations, we found that the release of CO mainly appeared in the process of glowing combustion of char, similar to that of basswood combustion after being treated by fire retardants FRW and Dricon (Li 2003).

More CO₂ can also make people and animals suffocate when a fire event occurs. The concentration of CO₂ is a mass ratio of CO₂ in the volatiles. From Figure 3 (right), CO₂ concentrations in flaming combustion were higher than those in glowing combustion, which was opposite to the CO production process. That is, CO₂ mainly came from the complete combustion of carbon at the flaming combustion stage. With the increase of Si-Al compounds, CO₂ concentration in volatiles more or less decreased because Si-Al compounds restrained flaming combustion of the material. CO₂ concentration can represent combustion intensity and it is also equal to the amount of heat released in combustion. CO₂ profiles of the fiberboards were very similar to the HRR profiles (in the left of Figure 2), which suggested that the heat release mainly came from the complete combustion of carbon in the early stage of combustion.

Conclusions

Because of the increase of Si-Al compounds, more Si and Al were distributed on the surface of fibers and thus their weight ratios in the material increased, which significantly affected fire properties of the material during combustion.

Si-Al compounds have an obvious restraint effect on fire intensity and the amounts of the volatiles. All the released amount of heat, smoke, and off-gases (CO and CO₂), as well as mass loss, were remarkably decreased as a function of the amount of Si-Al compounds.

References

Gilman, J. W. 1999. Flammability and thermal stability studies of polymer layered-silicate (clay) nanocomposites. *Applied Clay Science*. 15(1-2): 31-49.

- Li, J. 2003. Wood spectroscopy. Analysis Technology of Cone Calorimeter for Wood. Science Press, Beijing, China.
- Liu, J. H. 2013. Fire retardant properties and mechanism of ultra-low density wood fiber-based material. Dissertation, Fujian Agriculture and Forestry University.
- Mouritz, A. P. et al. 2006. Heat release of polymer composites in fire. *Composites: Part A*. 37(7): 1040-1054.
- Mikkola, E. 1990. Charring of wood. Technical Research Centre of Finland. VTT Research Report 689, Espoo, Finland.
- Moghtaderi, B. 1996. Combustion characteristics of solid fuels under fire conditions. Dissertation. the University of Sidney.
- Tsantaridis, L. 2003. Reaction to fire performance of wood and other building products. Dissertation. Royal Institute of Technology-KTH.
- Xie, Y. Q. et al. 2008a. Study on forming a truss-like reticular structure made from nature fiber under the effect of liquid frothing (in Chinese with English abstract). *Journal of Fujian College of Forestry*. 28(3): 203-207.
- Xie, Y. Q. et al. 2003. Study on foamed material from plant fibers (in Chinese with English abstract). *China Wood Industry*. 18(2): 30-33.
- Xie, Y. Q. et al. 2008b. Construction mechanism of reticular structure of plant fiber. *Journal of Korea Furniture Society*. 19(2): 106-110.
- Xie, Y. Q. et al. 2011. Manufacture and properties of ultra-low density fiberboard from wood fiber. *BioResources*. 6(4): 4005-4066.
- Yang, Q. Z., and Troczynski, T. 1999. Dispersion of alumina and silicon carbide powders in alumina sol. *Journal of the American Ceramic Society*. 82(7): 1928-1930.

Acknowledgments

The authors are grateful for writing correction from our colleagues who are working in Wood Products Engineering Division at Luleå University of Technology.

Finite Element Modelling Simplification of Paper Honeycomb Panels by a Substituting Homogenous Core

Viktor UTASSY, Zsolt KOVÁCS, Levente DÉNES

Abstract

Light-weight wood-based panel products have recently appeared as raw-material for furniture industry. Some information on their overall mechanical performance is either given by the manufacturers or can be obtained by simple testing. However, for an engineered utilisation of these complex sandwich-type products, in-depth understanding of their behaviour is needed. In this study, the authors demonstrate finite element modelling of honeycomb-core panel products with a view to assessing deformation, and stresses in the component materials under different loading situations. Material properties used in the model were determined by expedient testing; orthotropic material models were used where appropriate. Models were verified by comparing simulation results with test results on identical physical models; a good agreement with respect to maximum stresses and deformation could be achieved. Because of the complex geometry of honeycomb paper core the simulation of large scale models engages significant computer capacity and time, therefore any simplification speed up the modelling process. Based on the mechanical tests results a substituting homogenous material has been defined to replace the paper honeycomb core and reduce the modelling resource requirements. The behaviour of the sandwich panels with the newly defined “virtual” material was analysed and compared with the original structure.

Key words: furniture, sandwich construction, finite element, stressed, deformation

Viktor UTASSY, utassyv@gmail.com

Zsolt KOVÁCS, zskovacs@fmk.nyme.hu

Levente DÉNES, dali@fmk.nyme.hu - corresponding author

University of West Hungary

College of Charles Simonyi Engineering, Wood Science and Art

Institute of Wood Based Products and Technology

Bajcsy Zs. 4.. H-9400, Sopron

Wood Construction & Structures

Session Co-Chairs: *Arijit Sinha, Oregon State University, USA and Bohumil Kasal, Fraunhofer Wilhelm Klauditz Institute, Germany*

Cross Laminated Timber Panels Using Hybrid Poplar

Anthonie Kramer, Arijit Sinha, and Andre Barbosa

Abstract

Cross-laminated timber (CLT) is an engineered structural wood composite, which recently gained code acceptance in the US and is looking to make inroads in the construction marketplace. Several characteristics of the CLT have the design and build community excited about this product. The CLT technology has recently been used for residential and non-residential multi-story buildings and it has been identified as one of the ways for achieving tall timber building construction. CLT is generally made up of graded softwood species for structural use, such as Spruce or Douglas-fir. The development of CLT technology has opened up new avenues for low-density species, which have traditionally not been rated as construction-grade materials for structural engineering applications. As CLT gains acceptance in the industry, low-density wood species like poplar, not specified in current American National Standards Institute (ANSI) standards, need to be investigated for potentially successful use in CLT panels. This study reposts a preliminary investigation that demonstrates the viability of a certified sustainable plantation grown low-density hybrid-poplar species (marketed as Pacific Albus), for use in performance-rated CLT panels. Modulus of Elasticity (MOE) and bending strength of the panels were characterized through a series of long and short span bending tests. These tests were conducted according to ANSI/APA PRG 320-2012: Standard for Performance Cross-Laminated Timber and the results were compared to allowable design properties for use in the United States. Digital Image Correlation techniques were used to track the failure progression and gain a qualitative understanding of flexure behavior of the CLT panels. This research contributes to a wider perspective of innovative solutions regarding the use of low-density hardwood species in engineered wood products.

Keywords: Engineered wood products, green building material, wood mechanics, wood composite, digital image correlation

*Proceedings of the 57th International Convention of Society of Wood Science and Technology
June 23-27, 2014 - Zvolen, SLOVAKIA*

Arijit Sinha,
Assist. Professor
Department of Wood Sci. & Eng.
Oregon State University, Corvallis OR-97331
Ph: +1 541 737 6713; Fax: +1-541-737-3385
Arijit.sinha@oregonstate.edu

Anthonie Kramer, Graduate Research Assistant and Andre Barbosa, Assistant Professor,
School of Civil & Const. Eng.
Oregon State Univ., Corvallis OR-97331
Anthonie.kramer@oregonstate.edu
Andre.barbosa@oregonstate.edu

Durability of adhesive bonds in cross-laminated timber (CLT) panels manufactured using Irish Sitka spruce

Karol S. Sikora^{1} – Annette M. Harte² - Daniel O. McPolin³*

¹ Postdoctoral researcher, College of Engineering & Informatics, National University of Ireland, Galway, Ireland

** Corresponding author*

karol.sikora@nuigalway.ie

² Senior lecturer, College of Engineering & Informatics, National University of Ireland, Galway, Ireland

³ Lecturer, School of Planning, Architecture and Civil Engineering, Queen's University Belfast, UK

Abstract

The potential use of Irish-grown Sitka spruce for cross-laminated timber (CLT) manufacture is investigated as this would present new opportunities and novel products for Irish timber in the home and export markets. CLT is a prefabricated multi-layer engineered wood product made of at least three orthogonally bonded layers of timber. In order to increase rigidity and stability, successive layers of boards are placed cross-wise to form a solid timber panel. Load-bearing CLT wall and floor panels are easily assembled on site to form multi-storey buildings. This improves construction and project delivery time, reduces costs, and maximises efficiency on all levels.

The paper addresses the quality of the interface bond between the laminations making up the panels, which is of fundamental importance to the load-bearing capacity.

Furthermore, in order to assess the adhesive performance, which is an essential parameter in terms of the production process, three different values of pressure of 0.6 N/mm², 0.8 N/mm² and 1.0 N/mm² were used for specimens manufacturing. In total, 240 shear tests were carried out on glue lines and on reference solid wood specimens. Moreover, delamination tests were performed on samples subjected to accelerated aging, in order to assess the durability of bonds subjected to severe environmental conditions. The test results of bond quality presented in this study were within requirements of prEN 16351:2013. Even the lowest pressure of 0.6 N/mm² applied during manufacturing of the specimens is sufficient for Irish Sitka spruce in terms of the shear strength requirements. However, factors influencing this quality include: the adhesive type, the spread rate, the clamping pressure, and most importantly rolling shear. Therefore, in order to assess the potential use of Irish-grown Sitka spruce for CLT, all these factors need to be addressed in the ongoing project.

Keywords: Cross-laminated timber (CLT), Sitka spruce, Bonding, Delamination, Shear

Introduction

The construction industry like any other area of economic and social life undergoes continuous alterations and improvements in order to successfully comply with the requirements of sustainable development. Consumers demand materials with enhanced mechanical properties, more durable, less labour and service intensive at a competitive price. To meet these expectations numerous new engineered wood products have been developed over the last couple of decades. One of promising products satisfying such criteria is Cross-laminated timber (CLT).

CLT is a prefabricated wood product manufactured using at least three layers of parallel boards. The wood grains of each layer are orientated perpendicular to the wood grains of the layers with which it is in contact. These layers are bonded by gluing their surfaces together with an adhesive under a pressure for a period of time. The adhesives used for CLT production include: phenoplast- and aminoplast-adhesives, one-component polyurethane adhesives (1K-PUR) and emulsion-polymer-isocyanate adhesives (EPI). The number of laminates in CLT is odd, therefore face layers are parallel to each other. The advantages of this specific orientation between the laminates in regard to the load-displacement and failure behaviour of such composite include increase in load-bearing capacity against in-plane and out-of-plane stresses, rigidity and stability (Jobstl et al. 2008, Brandner 2012, 2013). The natural variations in timber strength, due to defects such as knots, are reduced in CLT in comparison with construction timber. Furthermore, it was reported that cross-lamination of the boards reduces the degree of anisotropy in properties in the plane of the panel (Jobstl et al. 2008, Mestek et al. 2008, Vessby et al. 2009, Fortune and Quenneville 2010). Moreover, load-bearing CLT wall and floor panels are easily assembled on site to form multi-storey buildings. This improves construction and project delivery time, reduces costs, and maximises efficiency on all levels (Brandner 2013, Leonardo da Vinci Pilot Project 2008, Crespell and Gagnon 2010, Rimetz 2011, Yeh et al. 2012).

In order to investigate the suitability and support the commercialisation of Irish-grown Sitka spruce for the manufacture of CLT panels, the development of necessary engineering data is required. The quality of the interface bond between the laminations making up the panels is of fundamental importance to the load-bearing capacity, a crucial property for every construction material. Shear tests of glue lines are required in the course of factory production control in CLT plants. Additionally, in order to assess the durability of bonds that are often subjected to severe environmental conditions, delamination tests on samples subjected to pressure soak-drying cycles are performed.

As a part of the testing programme of the project 'Innovation in Irish Timber Usage', these tests were carried out on samples manufactured using Irish Sitka spruce in order to investigate adhesive bonds' shear performance and durability.

Materials and Methods

Materials

In order to ensure a uniform moisture content in the specimens during the testing, boards of Irish Sitka spruce were stored in a conditioning chamber ($65\pm 5\%$ R.H., $20\pm 2^\circ\text{C}$) for 3 months before specimen preparation. Subsequently, all sides of the boards were planed by a specialised company to cross-sectional dimensions of 94 mm by 30 mm. A tight tolerance on the lamination thickness is required for the production of CLT due to the thin bond lines used. Because of this, thickness measurements were taken on the boards immediately after planing to determine whether the required tolerance of 0.1 mm was achieved. The boards that failed to meet the required tolerance were excluded when the test specimens were manufactured.

For the purpose of specimen manufacture for shear tests, boards were cut to lengths of 300 mm. Two blocks comprising 4 edge bonded 300 mm long boards were prepared. A single-component polyurethane adhesive, formulated for the manufacture of engineered wood products (PURBOND HB S309), was used to bond the edges of the shear test specimens. The 0.1 mm adhesive layer was applied on one surface of each glue line. Three different values of pressure, namely 0.6 N/mm^2 , 0.8 N/mm^2 and 1.0 N/mm^2 , were applied by a compressive testing machine for 120 minutes.

After reconditioning ($65\pm 5\%$ R.H., $20\pm 2^\circ\text{C}$), test bars were cut from the blocks. Each of the test bars comprised three glue lines. The dimensions of these tests specimens were in accordance with prEN 16351:2013 and were: 30 mm thick, 376 mm (4 glued pieces of 94 mm) long and 50 mm wide, as seen in Figure 1. In addition, solid wood specimens, without glue line, of the same cross-sectional dimensions were prepared.

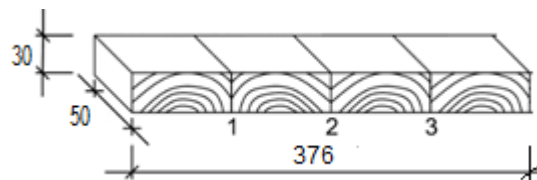


Figure 1. Shear test specimen dimensions

Table 1 presents the numbers of lines tested for different bonding pressures in end-grain and perpendicular to grain directions. The number of specimens for 1.0 N/mm^2 loaded perpendicular to the grain is very small, because this study is still ongoing.

Table 1. Numbers of shear tests

Bonding pressure	0.6 N/mm^2	0.8 N/mm^2	1.0 N/mm^2	Solid wood (unglued)
<i>End-grain</i>	36	36	27	36
<i>Perpendicular to grain</i>	36	24	9	36

In order to prepare specimens for the delamination tests, a sample CLT panel of 90 mm (3 layers of 30 mm) thickness, 600 mm length and 192 mm width was manufactured. The same adhesive, thickness of adhesive layer as for the shear tests samples was used and a

pressure of 0.8 N/mm² was applied. After reconditioning, specimens for the delamination tests of glue lines between layers were cut from this panel. Tests were carried out on 10 specimens of 105 mm by 96 mm by 90 mm.

Experimental techniques

The shear tests were carried out by applying a compressive force using a shearing tool adapted from prEN 16351:2013. The cylindrical bearing was able to self-align so that the test piece could load at the end-grain and perpendicular to grain with a stress field uniform in the width direction. A compressive testing machine was used to apply a compressive force to the shearing tool, as seen in Figure 2.

The prEN 16351:2013 standard requires loading tested specimens at the end-grain. However, since in CLT panels wood grains of each layer are orientated perpendicular to wood grains of layers with which it is in contact, the shear stresses occur in different planes of boards comprising CLT panels. Because of this, the additional tests were carried out for the specimens loaded perpendicular to grain, see Figure 2 (b). Loading was applied under displacement control at a rate of 3 mm/min, ensuring failure after no less than 20 s, which is in accordance with prEN 16351:2013 and studies by Steiger et al. (2010). Just after the shearing tests, four samples 50 mm long from each test bar (central parts between glue lines or glue line and end) were cut, and weighted in order to determine the density.

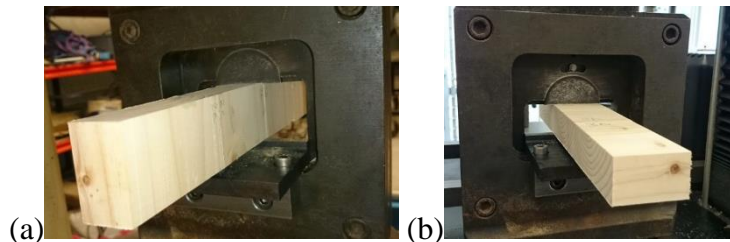


Figure 2. Test bar during testing in shearing tool loading end-grain (a) and perpendicular to grain (b)

Test pieces for the glue line delamination tests were placed in a pressure vessel and submerged in water at a temperature of about 15 °C. Then a vacuum of about 80 kPa was drawn and held for 30 min. Subsequently, the vacuum was released and pressure of about 550 kPa was applied for 2 h. Later, the test pieces were dried for a period of approximately 15 h in a circulating oven at a temperature of 70±5 °C. After removal from the oven, the delaminated length for each of the two glue lines was measured around the perimeter of the specimen. The maximum delamination length, $l_{\max, \text{delam}}$ is the greater of these two values and the total delamination length, $l_{\text{tot, glue line}}$ is the sum of these two values. The two glue lines were then split using a wedge and hammer, and the wood failure percentage was estimated visually. The lower of the wood failure percentages from the two glue lines, FF_{\min} , was recorded. The test programme and procedure were in accordance with Annex C of prEN 16351:2013.

Results and Discussion

Shear

The shear strength was determined for each of 3 glue lines from each test bar and the results are given in Figure 3, which presents the mean, 5-percentile and standard deviations of shear strengths for samples manufactured with different pressures and for solid wood specimens.

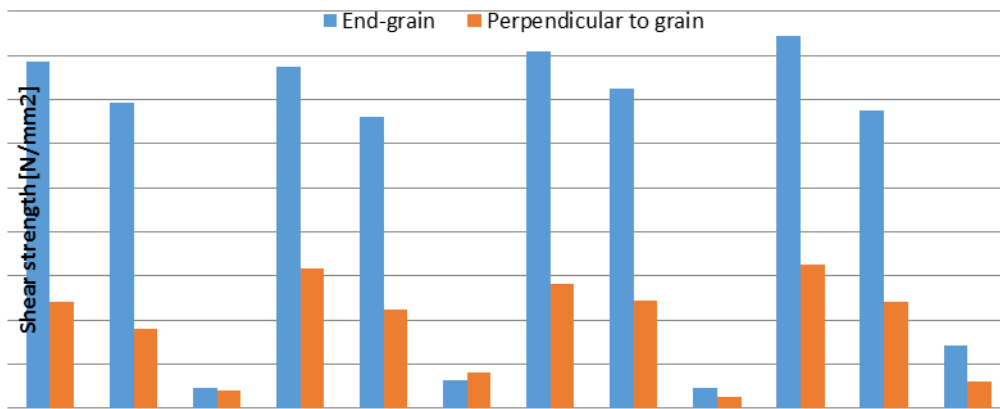


Figure 3. Shear strength values

The characteristic shear strengths, $f_{v,k}$, were 6.92 N/mm², 6.61 N/mm² and 7.24 N/mm² for glue lines loaded at end-grain and manufactured with pressures of 0.6 N/mm², 0.8 N/mm², 1 N/mm², respectively. These results were well in excess of the minimum requirement of 3.5 N/mm² for characteristic shear strength in accordance with prEN 16351:2013. Furthermore, 6.74 N/mm² was recorded characteristic shear strength, for solid wood specimens. This value is even lower than for specimens bonded at 0.6 N/mm² and 1 N/mm² pressures. These results give an indication that the lowest pressure of 0.6 N/mm² applied during manufacturing of the specimens is sufficient for Irish Sitka spruce in terms of the prEN 16351:2013 shear strength requirements.

The characteristic shear strengths were 1.81 N/mm², 2.24 N/mm², 2.44 N/mm², and 2.42 N/mm² for glue lines loaded perpendicular to grain, bonded at pressures of 0.6 N/mm², 0.8 N/mm², 1 N/mm², and solid wood, respectively. The characteristic shear strengths for glue lines loaded perpendicular to grain were lower by 74%, 66% and 66% in comparison to values for corresponding lines manufactured with different pressures loaded at end-grain. These values were consistent with result for solid wood specimens, for which a reduction of characteristic shear strengths of 64% between specimens loaded perpendicular to grain compared to those loaded at the end-grain.

The Student's *t*-test statistical comparison for the specimens loaded on the end-grain showed that the characteristic shear strength of specimens bonded at pressures of 0.6 N/mm² and 0.8 N/mm² were significantly different to the solid wood shear strength values. However, for the specimens loaded perpendicular to grain, the 0.6 N/mm² and 1.0 N/mm² bonded specimens were found to be significantly different to the equivalent

solid wood strength values. It should be noted, however, that the number of test results for the 1.0 N/mm² pressure case is very small. Nevertheless, considering the fact that the mechanical performance of CLT is largely determined by rolling shear and there is lack of available research on this property for Sitka spruce, the rolling shear strength of Sitka spruce should be comprehensively researched and established.

A mean density of 436.41 kg/m³ with standard deviation of 47.79 kg/m³ was obtained for all tested samples. The wood percentage failures (split glue area that is the ratio of the area with wood failures and the glued area before splitting) for 96% of all tested glue lines in both grain directions were above or equal 80%, and for 69% of the samples the wood percentage failures were 100%. These recordings have confirmed that wood failure percentages values for PUR type adhesives are generally very high and exhibit a small variation, which corresponds to results obtained by Steiger et al. (2010). The lowest wood failure percentage was 60% and occurred in a bond line manufactured with 0.8 N/mm² pressure and tested perpendicular to grain, see Figure 4 (a). It is likely that this low value was due to the presence of a large knot on one of the sheared faces. Figure 4 shows this glue line after testing in comparison to glue lines with 100% wood failure loaded perpendicular to grain (b) and at end-grain (c).

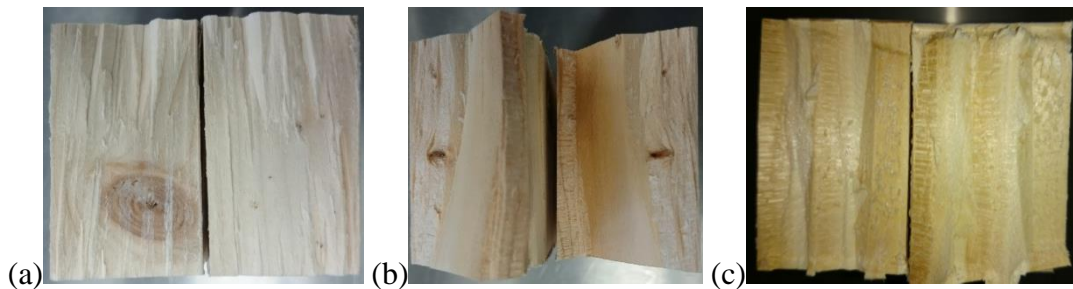


Figure 4. Glue lines with 60% wood failure loaded perpendicular to grain (a), 100% wood failure loaded perpendicular to grain (b), and 100% wood failure loaded at end-grain (c)

Delamination of glue lines

The total delamination $Delam_{tot}$ of each test piece was calculated from following Equation (1):

$$Delam_{tot} = 100 \frac{l_{tot,delam}}{l_{tot,glueline}} [\%] \quad \text{Equation (1)}$$

where:

$l_{tot,delam}$ is the total delamination length (in mm),

$l_{tot,glueline}$ is the sum of the perimeters of all glue lines in a delamination specimen (in mm).

The maximum delamination $Delam_{max}$ of a single glue line in each test piece was calculated from following Equation (2):

$$Delam_{max} = 100 \frac{l_{max,delam}}{l_{glueline}} [\%] \quad \text{Equation (2)}$$

where:

$l_{max,delam}$ is the maximum delamination length (in mm),

$l_{glueline}$ is the perimeter of one glue line in a delamination specimen (in mm).

The values of total delamination, $Delam_{tot}$ of each test piece and maximum delamination, $Delam_{max}$ of a single line in each test piece are shown in Table 2.

Since the delamination values exceeded the prEN 16351:2013 criteria of $Delam_{tot} \leq 10\%$ and $Delam_{max} \leq 40\%$ for all samples, the wood failure percentage of each split glued area was determined. All tested samples fulfilled the criteria of $FF_{min} \geq 50\%$, as presented in Table 2. Moreover, since the delamination occurred only in one of two glue lines for every tested specimen, the requirement of the minimum wood failure percentage of the sum of all split glued areas $\geq 70\%$ was also satisfied.

Table 2. Total and maximum delamination, and wood percentage failure

Specimen ID	$Delam_{tot}$ [%]	$Delam_{max}$ [%]	FF_{min} [%]
1	16.8	33.7	80%
2	17.6	35.2	75%
3	27.3	54.2	60%
4	16.0	32.0	85%
5	19.5	38.9	70%
6	21.7	43.7	65%
7	17.0	34.0	80%
8	23.1	46.2	65%
9	19.8	39.6	70%
10	28.2	56.3	60%

Although delamination results vary significantly between the test pieces, it is very likely that the mechanism resulting in the delamination of glue lines was the same for all specimens. In all cases, delamination occurred in one glue line on one side. Since the vacuum-pressure soak cycle resulted in swelling, which was much higher in the tangential and radial directions than the longitudinal direction for the timber, it induced significant internal shear stresses between the bonded surfaces. Furthermore, since there was no edge bonding of the boards in each CLT layer, the lowest bonding area to volume ratio was in the narrowest timber elements. Since these elements were placed in one side of the test piece, delamination occurred at their surfaces, which may be observed in Figure 5.

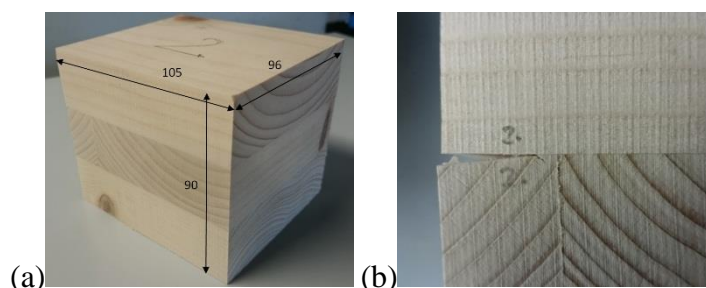


Figure 5. Specimen for delamination test before (a) and after vacuum-pressure cycle (b)

Moreover, the widths of the narrowest timber elements in each test piece determined the depth of delamination.

Conclusions

Preliminary investigations presented in this paper can lead to the following conclusions:

- the lowest pressure of 0.6 N/mm² applied during manufacturing of the specimens is sufficient for Irish Sitka spruce in terms of the prEN 16351:2013 shear strength requirements,
- it was confirmed that wood percentage failure results for PUR type adhesives are very high with small variations,
- the results presented for the shear strength and delamination were within the required limits given in prEN 16351:2013,
- the widths of the narrowest timber elements in CLT test piece determine the size of delamination.
-

Acknowledgments

This work has been carried out as part of the project entitled ‘Innovation in Irish timber Usage’ (project ref. 11/C/207) funded by the Department of Agriculture, Food and the Marine of the Republic of Ireland under the FIRM/RSF/COFORD scheme. The authors would also like to thank ECC Ltd. (Earrai Coillte Chonnacht Teoranta) for supplying the timber and Purbond AG for supplying the adhesive used in this project. The assistance of Ms. Vivienne McEvoy during the preparation of specimens and testing is kindly acknowledged.

References

- Brandner R. 2012. Stochastic System Actions and Effects in Engineered Timber Products and Structures, PhD Thesis, Institute of Timber Engineering and Wood Technology, Graz University of Technology, p. 467.
- Brandner R. 2013. Production and Technology of Cross Laminated Timber (CLT): A state-of-the-art Report, ECOST-MEETING-FP1004-210513-028873, ISBN 1 85790 181 9, p. 3-36.
- Crespell, P., and Gagnon, S., 2010. Cross Laminated Timber: a Premier, FPInnovations.
- Fortune, A.L., and Quenneville, P. 2010. Feasibility study of New Zealand radiata pine crosslam, in S. Setunge (ed.) Incorporating sustainable practise in mechanics and structures of materials, CRC Press.
- Jobstl, R.A., Bogensperger, T., and Schickhofer, G. 2008. In-plane shear strength of Cross Laminated Timber, CIB-W18/41-21-3, St. Andrews.
- Leonardo da Vinci Pilot Project. 2008. Handbook 1. Timber structures, Educational Materials for Designing and Testing Timber Structures – TEMTIS.
- Mestek, P., Kreuzinger, H., and Winter, S. 2008. Design of Cross Laminated Timber (CLT), WCTE 2008 - 10th World Conference on Timber Engineering, Miyazaki, Japan.
- prEN 16351:2013 Timber structures – Cross laminated timber – Requirements, CEN.

- Rimetz, B. 2011. Future of Wood Update / X Marks the Opportunity, ProSales.
- Steiger, R., Gehri, E., and Richter K. 2010. Quality control of glulam: shear testing of bondlines, Eur. J. Wood Prod. 68: 243–256.
- Vessby, J., Enquist, B., Petersson, H., and Alsmarker, T. 2009. Experimental study of cross-laminated timber wall panels, European Journal of Wood Products, 67, 211-218.
- Yeh, B., Gagnon, S., Williamson, T., Pirvu, C., Lum, C., and Kretschmann, D. 2012. The North American product standard for cross-laminated timber, Wood Design Focus, 22(2)13-21.

Fire Performance and Diffusion Coefficient of Adhesives Used for Southern Pine Cross-Laminated Timber

*Miklos Horvath, Bryan Dick, Perry Peralta, Phil Mitchell, Ilona Peszlen,
Weichiang Pang, Scott Schiff, Robert White*

Abstract

Cross-Laminated Timber (CLT) is a construction system that many foresee as having tremendous potential to displace concrete, masonry, and steel in low- and mid-rise residential and commercial construction. A collaborative CLT project involving NC State, Clemson University, and the US Forest Products Laboratory was initiated to foster the use of southern pine in the manufacture of CLT panels. Product performance data will feed into efforts to gain building code approval and eventual public acceptance of southern pine CLT. The research project will produce both laboratory- and full-size 3-layer and 5-layer CLT panels. Both solid and hollow-core panels will be evaluated. Bond evaluation of three different adhesives, measurement of hygrothermal properties, and evaluation of basic mechanical properties on laboratory size CLT panels will be performed. Fire and structural performance of full-size panels will also be tested. Structural and cost comparisons of CLT buildings and those made of concrete/steel will be performed. The research results will be communicated to stakeholders through the project's extension component. This presentation describes project results so far, especially those related to adhesives evaluation and moisture transfer properties. Fire tests following PS-1 procedures have been conducted to evaluate the fire performance of polyurethane, phenol resorcinol formaldehyde, and melamine formaldehyde adhesives. Moisture diffusion coefficients of the adhesives are currently being measured so that they can be incorporated into a moisture transfer model for the CLT panel.

Keywords: cross-laminated timber, adhesive, fire performance, diffusion, moisture transport

Perry Peralta

Phone: +1-919-515-5731; Fax: +1-919-513-3496; email: perry_peralta@ncsu.edu

Bryan Dick, Perry Peralta, Phil Mitchell, Ilona Peszlen

Department of Forest Biomaterials, North Carolina State University, Raleigh, NC 27695-8005

Miklos Horvath

Bánki Donát Faculty of Mechanical and Safety Engineering, Obuda University,
Budapest, Hungary

*Proceedings of the 57th International Convention of Society of Wood Science and Technology
June 23-27, 2014 - Zvolen, SLOVAKIA*

Weichiang Pang, Scott Schiff
Glenn Department of Civil Engineering, Clemson University, Clemson, SC 29634-0911

Robert White
Durability and Wood Protection Research, U.S. Forest Products Laboratory, One Gifford
Pinchot Drive, Madison, WI 5372-2398

“Radiusholz” – Curved Cross Laminated Timber Elements

Georg Stecher^{1} – Anton Kraler² – Roland Maderebner³*

¹ University Assistant, University of Innsbruck - Faculty of Engineering Science - Institute for Construction and Materials Science - Timber Engineering Unit.

** Corresponding author
georg.stecher@uibk.ac.at*

Abstract

The department of timber construction at Innsbruck University has been developing curved cross laminated timber elements (CLT) in cooperation with a timber company. The application of curved wooden components in timber construction occurred again and again but the use of curved CLT elements is still relatively new.

In the CLT development process the following effects need to be considered: construction orthotropy, internal stresses within the lamellas resulting from pre-curving, interactive rolling shear and tension perpendicular to the grain. To be able to test these effects in detail *experiments on 144 real-size specimens* are being carried out at the Innsbruck certified technical laboratory (TVFA).

The special shape of the specimens necessitates specific requirements on the test setup. In principle CLT-elements stress-tests are carried out on elements in vertical and horizontal position. For obtaining strength and stiffness values, bending and transverse tension stress tests are performed. The size of the curved radius plays a crucial role. In the medium third section the curved shape leads to additional transverse tension stress. These values are decisive in the calculation and they greatly impact the interactive rolling shear stress. The use of CE-certified timber lamellas did not necessitate additional tests.

Keywords: CLT, bending strength, tension perpendicular to the grain, rolling shear, shear strength, test setup

Introduction

Traditionally timber was used in construction for beam shaped components made of solid wood. Despite the industrialization at the beginning of the last century the use of the building material remained conventional.

The production of wood-based materials provided initial experiences with planar plate elements that were only limitedly used for static purposes. Initially from the middle of the 1990-ies solid wood elements could be used as plates and panels in the modern timber construction due to the cross laminated technology (Mesteck 2011). The cross section structure of cross laminated timber (CLT) is marked by orthogonal, glued together flat board layers (Jakobs 2005).

The increased use of CLT-elements has become an elegant and attractive solution for many constructional tasks in the recent past (Scholz 2004). However the large CLT-producers only offer flat elements for sale. In wood construction curved wooden components have been repeatedly applied but the use of curved CLT-elements is still relatively new. By the development of these elements a new diverse scope opens up for the modern wood construction.

This article primarily discusses the special requirements of the experimental setup at the material testing.

Materials and Methods

Materials. All in all 144 real-size specimens are tested at the University of Innsbruck. In principle it is distinguished between stress-tests on elements in vertical and horizontal position and here in turn between bending and shear load. Furthermore it is differentiated between 5-layer and 9-layer CLT-elements for the respective load. The specimens for the plate stress feature no curvature of the lamellas. The curved radius of the plates is chosen depending on the blade thickness according to equation (1) following EN 16351:2011:

$$t_{l,i} \leq \frac{r}{250} \cdot \left(1 + \frac{f_{m,j,dc,k}}{80}\right) \quad (1)$$

With:

$t_{l,i}$	final lamella thickness
r	curved radius
$f_{m,j,dk,k}$	characteristic value of the bending strength of the finger joints

The CE-certified timber lamellas are of strength class C24. Due to the CE marking no additional tests are necessary.

All specimens are conditioned in standard climate with 65% relative humidity and 20°C before the tests. The sample group is listed in table 1.

table 6: sample group

type	description	quantity	umber of layers	lamella thickness	radius
	[-]	[-]	[-]	[mm]	[m]
1	panel - bending	18	5	19	4,5
2	panel - bending	18	9	19	4,5
3	panel - thrust	18	5	32	6,5
4	panel - thrust	18	9	19	4,5
5	plate - bending	18	5	19	∞
6	plate - bending	18	9	19	∞
7	plate - thrust	18	5	32	∞
8	plate - thrust	18	9	19	∞

Test setup of the CLT plate elements. EN 16351:2011 is used as the normative basis for the performed tests though this norm does not include information on the test setup of curved plates. In consequence of the curved geometry of the tested elements special attention has to be payed to the load introduction. Small changes can have large effects on the test results. This fact is outlined in this paragraph resulting in a definition of a new proposed solution for the test of the single-curved CLT elements. In figure 1 to 3 different ways of the support geometry's design and the associated load introduction are shown, distinguishing between 3 different models:

- a) support geometry; cut support (figure 1)
- b) support geometry prEN 16351 - shim (figure 2)
- c) support geometry prEN 16351 - chock (figure 3)

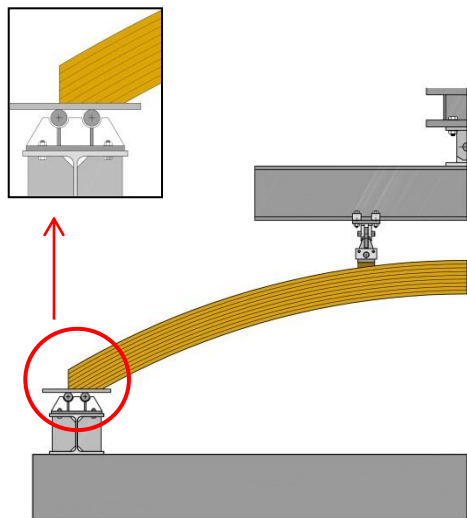


figure 28: support geometry (a)

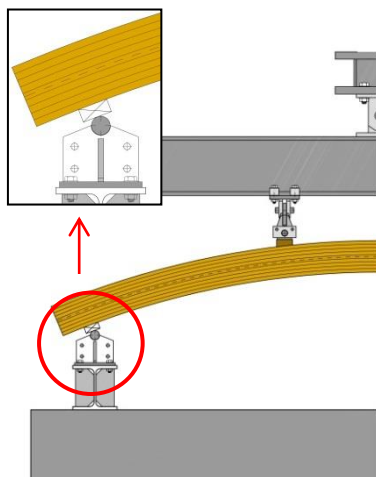


figure 29: support geometry (b)

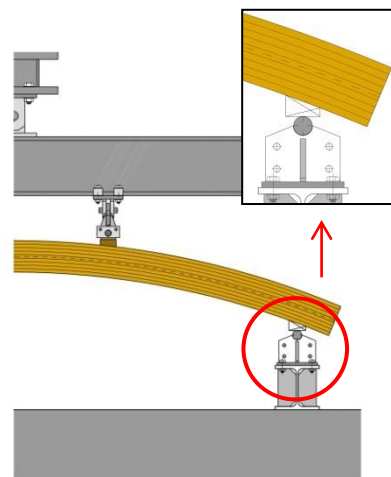


figure 30: support geometry (c)

Support geometry (a)

This support geometry contains a special cut in the sector of the load introduction points. A major disadvantage of this assembly is the variable span length during the load, which affects the assessing of the material parameters directly. Furthermore a loss of contact can occur in the outer roller bearings if the transfer of tensile forces causes the failure of the support. This can be expected since clamping torques would emerge otherwise. Consequently the assembly of a second support role in the outer sector is not expedient.

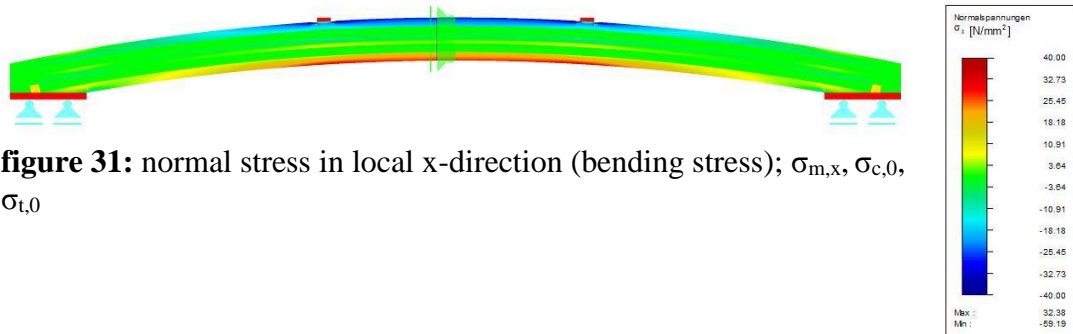


figure 31: normal stress in local x-direction (bending stress); $\sigma_{m,x}$, $\sigma_{c,0}$, $\sigma_{t,0}$

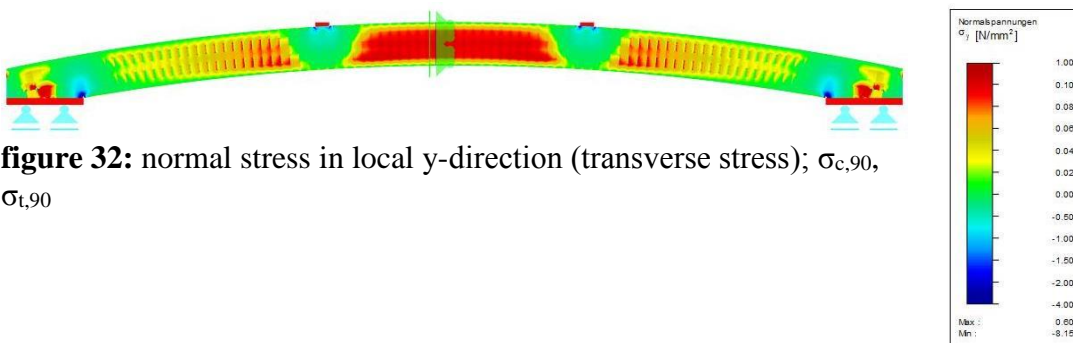


figure 32: normal stress in local y-direction (transverse stress); $\sigma_{c,90}$, $\sigma_{t,90}$

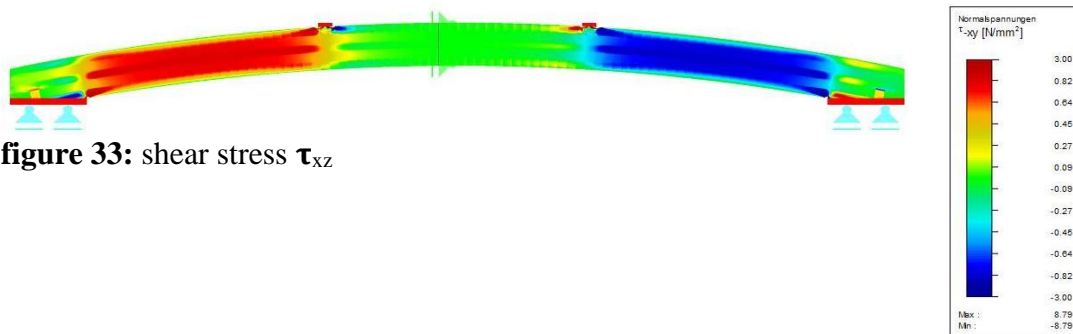


figure 33: shear stress τ_{xz}

Support geometry (b)

In accordance with the principles of EN 16351 for bending tests shims are used in the distance of $h/2$ from the ends of the plates to minimize local deformations. This assembly of the support geometry causes additional tensile stress in the curved elements. However a strain arc mostly emerges in usual constructions of this kind. Compared to the support geometry (a) the FE analysis shows a distinctive sector of transverse stress in the crown area of the elements.

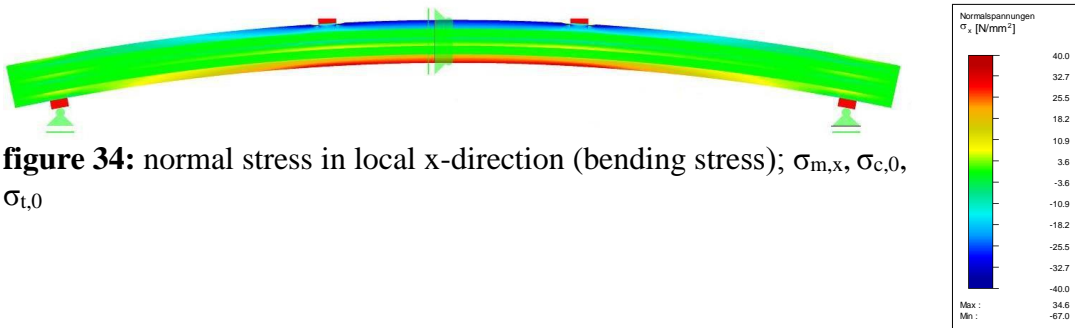


figure 34: normal stress in local x-direction (bending stress); $\sigma_{m,x}$, $\sigma_{c,0}$, $\sigma_{t,0}$

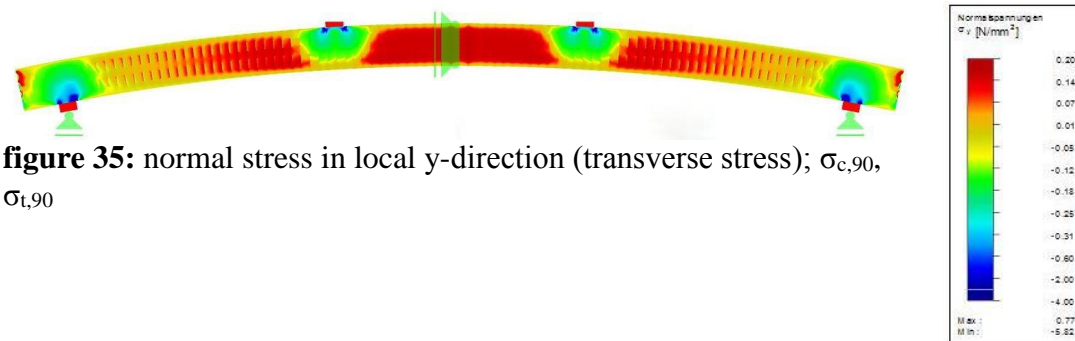


figure 35: normal stress in local y-direction (transverse stress); $\sigma_{c,90}$, $\sigma_{t,90}$

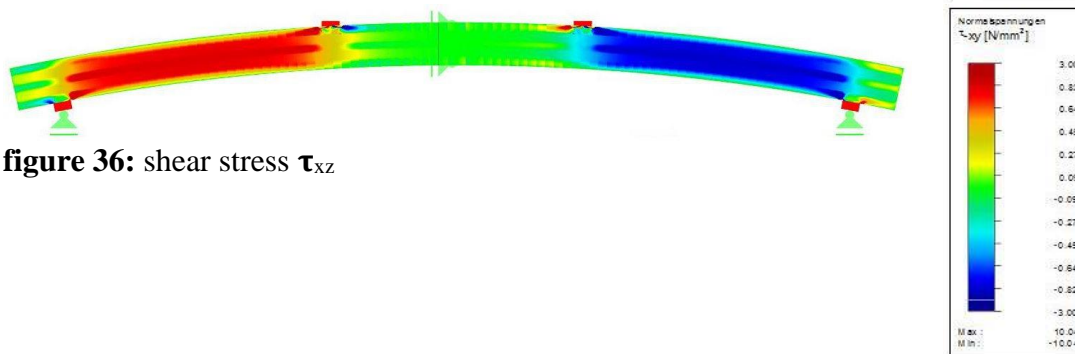


figure 36: shear stress τ_{xz}

Support geometry (c)

Instead of the shims chocks are used to eliminate the components of the tensile force described in support geometry (b). The direction of the load introduction is modified by the chocks so that compressive forces emerge in the arc element. As in support geometry (b) the FE analysis distinctly shows an appearance of transverse stress in the crown area of the elements.

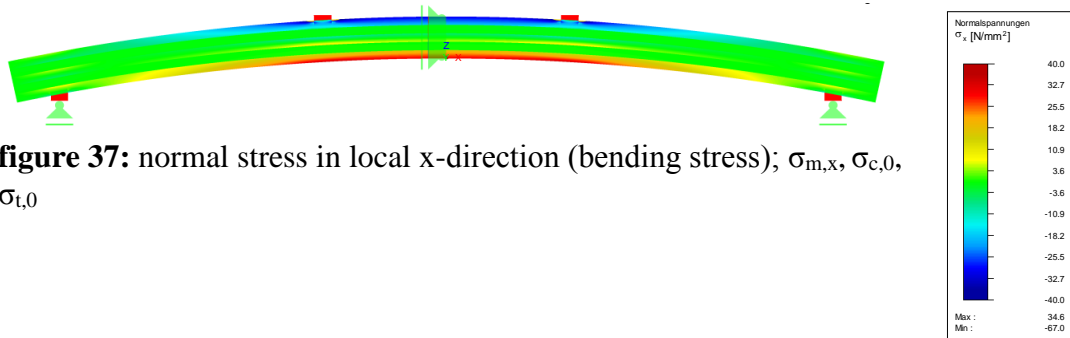


figure 37: normal stress in local x-direction (bending stress); $\sigma_{m,x}$, $\sigma_{c,0}$, $\sigma_{t,0}$

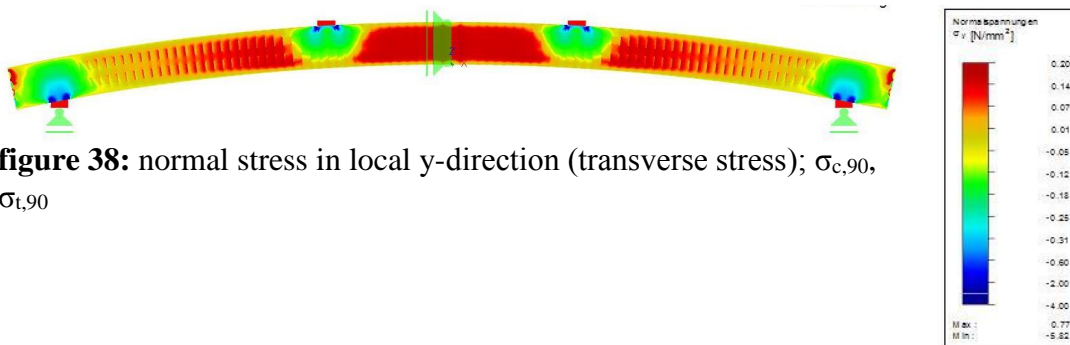


figure 38: normal stress in local y-direction (transverse stress); $\sigma_{c,90}$, $\sigma_{t,90}$

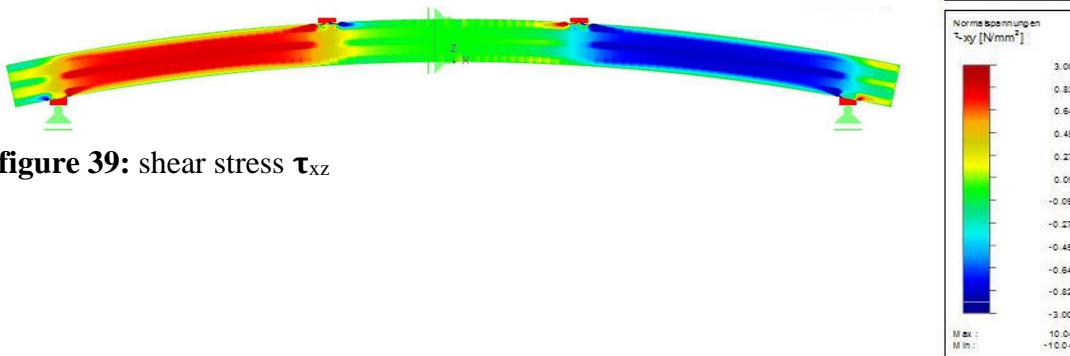


figure 39: shear stress τ_{xz}

Support geometry (c) was chosen for the tests.

Summary and Outlook

To determine the actual component parameters the support geometry (c) was chosen for the tests in the laboratory. The assembly of the chocks guarantees a load transfer without additional tensile forces which occur in support geometry (b). Currently the laboratory experiments on the curved CLT elements are run in the TVFA Innsbruck. In addition to the assessing of the stiffness (bending stiffness, shear stiffness) and the strength parameters (bending strength, shear strength) the deformations orthogonal to the plate thickness are measured to obtain conclusions on the transverse stresses. The first tests reveal that the interaction of bending stresses as well as rolling shear stresses with transverse stresses can never be neglected.

References

prEN 16351:2011. Timber structures - Structural timber and glued laminated timber - Determination of some physical and mechanical properties.

Mesteck P. 2011. Punktgestützte Flächentragwerke aus Brettsper Holz (BSP) - Schub bemessung unter Berücksichtigung von Schubverstärkungen, München: TU München Dissertation.

Jakobs A. 2005. Zur Berechnung von Brettlagenholz mit starrem und nachgiebigem Verbund unter plattenartiger Belastung mit besonderer Berücksichtigung des Rollschubes und der Drillweichheit, München: Universität der Bundeswehr München; Dissertation.

Scholz A. 2004. Ein Beitrag zur Berechnung von Flächentragwerken, München: Dissertation; Technische Universität München, 2004

Cross Laminated Timber – Implementation of European Experience in the USA

Josef Weissensteiner¹, Marius C. Barbu², Timothy M. Young³

1 – DipI.Ing. Josef Weissensteiner - HOLZagentur-weissensteiner, Liezen,
Austria,

weissensteiner@holz-weissensteiner.com

2 – Prof.Dr.Ing.Dr. - Salzburg University of Applied Sciences, Austria and
Faculty for Wood Engineering, "Transilvania" University Brasov, Romania

E-Mail: cmbarbu@unitbv.ro

3 – Prof.Dr. - Center for Renewable Carbon, University of Tennessee, USA

tmyoung1@utk.edu

Abstract

The European success story of Cross Laminated Timber (CLT) started more than one decade ago in many small capacity simple workshops in the Alps of Europe. Currently, Europe has over one dozen CLT manufacturers (>650,000 m³/y) which are extremely specialized, starting with eco-type (glue-free) to full glue applications, narrow (<1.25 m) to large (< 3 m) free size panels, short (<5 m) to long (16.5 m), handmade-to-fully automated lines able to produce engineered elements for walls, roofs, and floors. Traditionally CLT was delivered to the carpenters able to prepare cut-to-size elements for building construction which included the insulation layers, preparation of connectors, windows, doors etc. New CLT mills use CNC portal equipment working with their own architectural design departments that are able to shape the raw panels to the final construction element at the production site which may also include insulation, fire protection, finishing layers, windows, and doors. The final CLT delivery is a sophisticated ready-to-install product. Simplified working steps at the construction site allows for building erection that are much faster than traditional construction methods. However, this requires unique logistics, construction equipment, and trained workers in CLT construction. In Scandinavia and Central Europe the national building codes were forced to accept the new generation of multiple story buildings made from CLT, which now exceed 10 stories with a target of 20 stories. New challenges for earth quake, noise, fire, and summer heat protection were requested by owners and authorities. The European Norm (prEN 16351), specialized for CLT, was implemented in 2013. Intelligent solutions for the implementation of self-contained heat storage and generation; and indoor air conditioning are in development for the next generation of CLT based passive-energy houses. North America is the next logical market for pilot CLT construction projects and production facilities which will be based on the European experiences.

Key words: Cross Laminated Timber (CLT), X-Lam, building regulations

Technical Basis

The building regulations of CLT in Europe are issued by national approval from the construction authority such as the German Institute for Construction Technology (DIBt) or the European Technical Approvals (ETA). The approvals include minimum requirements for the products, the control mechanism and the designation. Furthermore the approvals include regulations and recommendations in regard to the structural, fire protection (analysis of load bearing structures) and thermal design of the building. For design of CLT based buildings the allowing for the specifications of the approval according to the national design standard DIN 1052 or the European design standard Eurocode 5-1-1 are requested or to fulfil. As a rule according to DIN 1052 the Service Classes 1 or 2 as well as a predominantly statically loading are available (Studiengemeinschaft Holzleimbau, 2010).

In USA the standard ANSI/ APA PRG 320- 2011, Standard for Performance- Rated CLT was introduced in 2011. This standard is based mainly on the productions standards for Glue Laminated Timber (GLT) and softwood lumber requirements for structural use.

Wood Preservation and Service Classes for CLT

CLT are permitted only for the Service Classes 1 and 2 in accordance to DIN 1052/2008, Design of Timber Structures - General Rules and Rules for Buildings, or DIN EN 1995-1-1/2010, Eurocode 5: Design of Timber Structures - Part 1-1: General - Common Rules and Rules for Buildings. The expected moisture content does not exceed 20% thus attack through fungi can be excluded. Preventive constructional measures in buildings are usually sufficient (Studiengemeinschaft Holzleimbau, 2010). The US- standard specifies only the moisture content during the production of CLT (max. 20%). Different national standards for use in construction may exist but were not studied.

Auxiliaries for CLT

Usually polyurethane (PUR) or melamine- urea- formaldehyde adhesives (MUF) are used as well as in smaller quantities polymer of isocyanates (EPI). The percentage of resin ranges from 0.1% (EPI) to 0.5% (PUR) in weight.

The formaldehyde emissions are established in accordance with the European standard draft prEN 16351/2011, Timber structures – Cross-Laminated Timber – Requirements, with reference to DIN EN 717-1, Wood-based Panels - Determination of Formaldehyde Release - Part 1: Formaldehyde Emission by the Chamber Method (Studiengemeinschaft Holzleimbau, 2010).

The ANSI 405- 2013, Standard for Adhesives for Use in Structural Glued Laminated Timber provides minimum requirements to evaluate adhesives for use in structural glued

laminated timber in the USA. Adequacy of the adhesive is established by meeting or exceeding the criteria outlined in Section 3. Alternative tests shall not be permitted to substitute for the tests prescribed in this standard. Although the test methods specified in this standard are primarily intended for evaluation of face bond adhesive, the minimum test requirements noted shall be used for evaluation of end joint adhesives by adapting the required face bond specimens to conform to required end joint adhesive curing conditions.

Fire Protection Concept

For height buildings is the Classification 5 (buildings with a fifth level not higher than 22 m) to be fulfilled. The fire resistance of 90 min as well as fire behaviour of the building material must fulfil certain requirements at least like the Fire Resistance Class A2 (mineral materials).

A case study was done for a 7 story building in down town area in Vienna. In order to fulfil all the requirements a compensation concept was examined by experts of the Technical University, Vienna and the Construction Authority of Vienna. The concept is an encapsulation of the load bearing wooden structure by mineral materials to prevent inflammation. The fire duration is calculated in accordance to the standard temperature curve where the same fire impact like with the normal (nature) fire is assumed. In case of an encapsulation of 30 minutes of the load bearing wooden structure with materials from the Fire Resistance Class A2 a fire load can be excluded. The report mentions the importance of encapsulating all cut outs and gaps. All installations are routed in the facing shell. Another option would be the installation of a sprinkler system where the fire load also can be controlled (Teibinger, 2008).

The standard “ANSI A190.1-2012- Standard for wood products- structural glued laminated timber” differs between two fire resistance ratings: Custom or non- custom member manufactured to provide a one- hour fire rating shall be manufactured to the specified layup except that a core lamination shall be removed, the tension zone moved inward, and the equivalent of one additional nominal 2 in. thickness outer tension lamination added. These members are permitted to be marked with a 1-h fire rating designation. Members manufactured to provide a 2-h fire rating shall be manufactured to the specified layup except that two core laminations shall be removed, the tension zone moved inward, and the equivalent of two additional nominal 2 in. thickness outer tension laminations added. These members are permitted to be marked with a 2-h fire rating designation.

Multi Story Timber Construction

Functionally efficient showcases are the 6- story building in Vienna’s Wagramerstrasse (completed 2012). Another residential complex with 255 apartments is also in Vienna’s Mühlweg. This building complex is still European largest residential complex built in a timber/masonry mix (Binderholz-Bausysteme, Subsidised Residential complex in an innovative timber and timber/ masonry mix, Wagramerstrasse, Vienna, A, 2012)

(completed 2008). Another 7- storey building is located in central Berlin (completed 2008) and a 8 storey building in Bad Aibling (close to Rosenheim) completed 2011. Also in UK a 9- storey free standing residential building near the centre of London was constructed entirely in wood (completed 2010). Also a residential complex in Milan open a new era of the CLT use and confirmed the quick building speed of a 9-stores (27 m) with 124 apartments in about one year (completed 2013) (HZB14, 2013)

Earthquake Safety of Buildings

The seismic performance of the CLT constructions was tested in a full scale (3 and 7 storey building) building by the Trees and Timber Research Institute (IVALSA) Trient in Italy on the world largest shake table in Miki, Japan. As the results show very little deformation due to the ductility of the wood and especially by the energy dissipation of the mechanical connectors. (FPIinnovations - Forintek Division - Canada's Wood Products Research)

Due to the ductility of the wood elements in combination with adequate mechanical connections the building's capacity to dissipate energy is comparably high to common materials such as concrete (Binderholz-Bausysteme, Earthquake safety of BBS buildings, 2010).

The earthquake tests at the "Laboratorio Nacional de Engenharia Civil" (LNEC) in Lisbon, organized by the Technical University in Graz (February 2012) showed very clear results. A building with 8 floors survived 32 earthquake tests with no severe damage. The test was carried out within two days. 75 sensors were installed to measure the deformations of the CLT and the connectors. A simulated earthquake with the magnitude of 7.3 (according the measurement of Richter) no damages were noted. In total 32 earthquakes were simulated whereat fasteners and connectors were partly removed. The final result showed very little damage (www.proholz.at, 2012).

Timber Tower and Chaneles

Environmental friendly and economical effective wind turbines made out of wood. The timber tower with a height of 100 m saves about 300 tons of sheet steel. The processing of wood saves energy, the material stores about 400 tons CO₂. There has been built one tower with a height of 25 m in Waffensen, Germany in 2010 as a pilot project. The tower serves for a simulation and further optimization for much higher towers (up to 100 m) in the near future. The current tower has a turbine with power of 1.5MW. The panels for the pilot tower were entirely prefabricated (including the connections and surface cladding) at the factory. For the transport standard trucks can be used. To transport a timber tower with a height of 100m about 10 trucks are required. First, the inside construction including multiple components such as light installations, cable system and the grid connectors and the operating platforms were constructed. Surrounding the inside structure the panels were attached. The weight of the power turbine on top is carried by

the panels. The splices of the panel surface sheeting are welded by using an integrated elevator system (www.timbertower.de, 2013).

In Melbourne timber+DESIGN currently designing a 10- story building which should be built starting 2014. This is a new dimension not only in Australia but also in UK and Central Europe.

Building Physics

Sound Insulation

Due to the crosswise composition of the CLT an acoustic light and in the same time stiff to bending exists. To reduce sound transmission flexible facing shell are used. For ceiling it is common praxis to decouple the facing shell from the construction.

(Studiengemeinschaft Holzleimbau, 2010)

Thermal insulation (winter/summer)

Due to the solid construction and therefore higher thermal capacity a balanced indoor climate can be assured.

Following are the example of specific values from CLT of 470kg/m³ made from spruce in accordance to DIN 4108:

Heat conductance: $\lambda_R = 0.13 \text{ W/mK}$

Specific thermal capacity $c = 2.10 \text{ kJ/kgK}$

conductibility of temperature $a = 1,317 \times 10^{-7} \text{ m}^2/\text{s}$ (www.binderholz-Bausysteme.com, 2012)

Allmost all companies provide proved build ups for wall, floor and roof constructions. Under standardized moisture content (m.c.) of 12% result in a thermal conductivity for CLT of 0.11 to 0.13 W/mK. An average value of 12 % is assumed for wood m.c., whereby less than 12 % wood m.c. should be expected in external walls during the relevant winter months. With less wood m.c., the actual thermal conductivity value reduces further. The Austrian standard ÖNORM EN 12524 specifies a rated thermal conductivity of 0.13W/mK for wood in the relevant bulk density range. (www.clt.com, 2013)

Airtightness

The airtightness depends upon the amount of layers and how they are glued together. Most of the CLT- producers have approved the airtightness of their products which is especially relevant for the 3 and 5 layer compositions. Basically with 5 layers all producer have approved the airtightness. Stora Enso also glues the boards sidewise which gives already a airtightness with 3 layers. Most of the companies have tested and confirmed the airtightness by the Wood Research Austria (HFA), German Institute for Construction Technology (DIBt) or the European Technical Approvals (ETA) (www.clt.com, 2013) The wind and airtightness of a building envelope (wall, ceiling and roof panels) are essential for several impacts such as indoor climate, noise load, indoor atmosphere and energy demand in of a building. In common frame structure buildings the airtightness

from inside is given by semipermeable sheet and the windtightness from outside given by windproof sheeting. CLT constructions do not need this additional sheeting by using a 5-layer structure. Due to this fact most of the taping with special tapes can be omitted. Additionally, dividing the structural layer from the insulation and other layers makes the construction methods much easier compared to timber frame buildings where the vapour barrier is very crucial and must be carried out with high precision by skilled people (www.clt.com, 2013).

Inadequate airtightness may cause deposition of condensation in the structure, reduced thermal protection and low surface temperature which results in poor living quality. If condensation occurs in the structure of the building the structure can be damaged, mold formation happens at increased moisture contents. Most of the insulation material have reduced thermal transmittance in case of high moisture (Riccabona, 2008).

The windtightness of a building is as important as its airtightness. Inadequate windtightness can cause similar phenomena like with inadequate airtightness. Standards for building physics are nationwide as part of the constructions requirements which was not object of the project.

Earthquakes in L' Aquilla, Italy

2009 the earthquakes in L' Aquilla in the Abruzzi have devastated a vast amount of buildings and infrastructure. About 300 people were killed and 70.000 people were left homeless. The earthquake had a power of 6.3 on the Richter scale and very few buildings resisted the multiple skakes. The few which are still standing must be proved if further use is reliable and approveable.

In the meantime the homeless people were sheltered in tents to have a "roof" above their head. Accordingly, the government of Italy was forced to build new houses before the winter arrives.

150 basements, supported by posts and reinforced by concrete were built. On this basements the buildings for each 25 to 30 apartments were contracted according 100 points system. 10 points were given for the realization time, 25 points for the costs and 65 points for the technic such as energy efficiency, sustainability, architecture, interior design, efficiency and residents concentration per area. The wood construction systems (CLT, frame building systems) won the competition.

CLT construction was delivered by BinderHolz Bausysteme, Unternberg, Austria and prefabricated by Schafferer Holzbau, Matrei, Austria. The ready elements (including part of the installations, insulation and cladding on the outside.

Within a construction time of 80 days thirty 3- story building with approximately 27.000m² living area were handed over to the people. The costs per m² are about € 1.200

and including the external costs about € 2.400. About 6.300 m³ of CLT was used for this project.

Additionally it must be mentioned that the use of wood in earthquake vulnerable areas has several advantages compared to concrete or steel. Due to the fact that ductile and lighter materials can absorb earthquake shakes in a higher degree wood has the weight of 1/6 of concrete and nearly 1/20 of steel. This was approved already in several full scale tests at different laboratories.

Big Players for CLT

In Austria there are basically five big CLT producer besides several small companies producing special CLT constructions (curved panels, different wood species, etc.) The big players are CLT (Stora Enso), BinderHolz Bausysteme, KLH, MM CrossPlan and Hasslacher with a total capacity of about 350.000m³/y CLT. Stora Enso and BinderHolz Bausysteme have already standardized thicknesses to full cm such as 6, 8, 9, 10, 12, 14, 15, 16, 18, 20, etc. up to 40cm. The maximum length of the produced is mostly about 16 to 18m and the max. width about 2.95m to 3.5m.

Various types of presses are in use. Besides the hydraulic press the vacuum press is very common for large scale presses.

References

- (2012, 03). Retrieved 03 2013, from www.proholz.at:
<http://www.proholz.at/bauphysik/erdbeben-grossversuch-in-lissabon/>
- (2012). Retrieved 04 2013, from www.binderholz-Bausysteme.com: www.binderholz-Bausysteme.com
- (2013). Retrieved 03 2013, from www.timbertower.de:
http://www.timbertower.de/downloads/?no_cache=1
- (2013). Retrieved 04 2013, from www.clt.com: <http://www.clt.info/index.php?L=2&id=6>
- Binderholz-Bausysteme. (2010). Earthquake safety of BBS buildings. Binderholz-Bausysteme.
- Binderholz-Bausysteme. (2012). Subsidised Residential complex in an innovative timber and timber/ masonry mix, Wagramerstrasse, Vienna, A.
- FPIInnovations - Forintek Division - Canada's Wood Products Research. (n.d.). Retrieved 03 2013, from www.forintek.ca
- mm-Kaufmann.com. (n.d.). Retrieved 04 2013, from www.mm-Kaufmann.com
- Riccabona, C. a. (2008). Baukonstruktionslehre 4 [Building construction theory 4]; 7th edition. Vienna: MANZ Verlag.
- Studiengemeinschaft Holzleimbau, e. (2010, 04). www.brettsperrholz.org. Retrieved 03 2013, from www.brettsperrholz.org
- Teibinger, M. (2008, September). Sonderthema im Bereich Holz, Holzwerkstoff und Holzbau. Zuschnitt.

Input-Output Hybrid LCA of Timber Construction Products Produced in Ireland

Desmond Dolan^{1} – Mark McCaffrey² – Annette Harte³*

¹ PhD Candidate, College of Engineering and Informatics – National University of Ireland, Galway - IRELAND.

** Corresponding author*

Desmond.dolan@nuigalway.ie

² Graduate M.Eng.Sc, College of Engineering and Informatics – National University of Ireland, Galway - IRELAND.

mark.mccaffrey@nuigalway.ie

³ Senior Lecturer, College of Engineering and Informatics – National University of Ireland, Galway - IRELAND.

annette.harte@nuigalway.ie

Abstract

Climate change is widely accepted as the greatest environmental challenge facing the world today, predominantly due to the increase of greenhouse gas emissions, especially CO₂. As buildings account for 36% of EU CO₂ emissions, the environmental impacts associated with building materials are becoming increasingly important. The use of sustainable construction materials, such as sawn timber and Oriented Strand board (OSB), have a major role to play in the reducing these CO₂ emissions.

The aim of this paper is to quantify the embodied energy and embodied carbon associated with the production of timber construction products in Ireland using a life cycle assessment IO Hybrid analysis methodology. This methodology incorporates the Central Statistics Office (CSO) “IO tables”, the Inventory of Carbon and Energy (ICE) database “process data”, and pricing data from the Irish Forestry and Forest Products association. Economic monetary flows are converted to energy flows and subsequently to carbon dioxide equivalents using the Intergovernmental Panel on Climate Change combustion emission factors.

The total embodied energy and embodied carbon for sawn timber were found to be 7.58 MJ/kg and 0.60 CO_{2e}/kg, respectively, and the total embodied energy and carbon associated with the production of OSB were 15.40 MJ/kg and 1.019 CO_{2e}/kg, respectively. These results are approximately between 2.1% and 3% higher than those found from the process LCA alone highlighting the fact some indirect emission are not being accounted for using a the process LCA methodology.

Keywords: Life Cycle Assessment, Input-Output Analysis, Hybrid Analysis, Timber Construction Products, Embodied Carbon, Embodied Energy.

Introduction

Climate change is widely accepted as the greatest environmental challenge facing the world today. Increases in the emission of green house gases (GHGs), especially CO₂, to the atmosphere as a result of human activity contribute to climate change. In Europe alone the European Union Climate and Energy Directives provide for a 20% reduction in CO₂ emissions by 2020 relative to 1990 and a 20% increase in energy efficiency over projected levels (European Commission 2007).

As buildings account for 36% of EU CO₂ emissions (European Commission 2010), the use of sustainable construction materials, such as timber, has a major role to play in the achievement of this objective. Buildings continue to reduce their operational energy requirements over their life cycle due to recent advances in energy management techniques. Due to this, the embodied energy (EE) and embodied carbon (EC) of the building are steadily becoming a larger proportion of the total energy used and GHGs emitted over a building's life cycle. The EE and EC refer to the energy required and emissions released in order to make the products that are used in the building. Understanding and accurately quantifying these emissions is vital in order to develop effective measures to reduce these increasing emissions and to comply with regulations. Due to major developments in timber construction and the introduction of new engineered wood products such as cross laminated timber, wood construction products can contribute to lowering the EE and EC of buildings.

The construction wood product industry in Ireland can be split up into 2 main sectors: sawmills and board mills. In Ireland, the sawmill industry produced 867,000m³ and 900,000m³ of sawn timber in 2011 and 2012, respectively (IFFPA 2014). The three main sectors that sawn timber is primarily used for in Ireland are construction and structural purposes, pallet and packing and also fencing. The panel products sector produced 704,000m³ of Medium Density Fiberboard and OSB in 2012 (IFFPA 2014). Other products that are produced from the forestry industry in Ireland include fire logs, furniture and bio-fuels, however, these are not considered within the scope of this study. Wood products have always been considered environmentally friendly products, however, in order to accurately quantify the total environmental impact of wood products and wood buildings they need to be analysed using a holistic environmental assessment technique such as LCA.

The aim of the current project is to quantify the total EE and EC associated with the production of timber construction products from Irish forests using LCA. This involves quantifying the inputs and outputs, such as the energy and material usage generated at each stage of a products life cycle and assessing the total environmental emissions associated with each. The development of robust and reliable methodologies for the assessment of a product's effects on sustainability and climate change is necessary. This

research presents a hybrid Input Output analysis methodology to account for sectoral energy and emissions intensities based on the energy and emissions associated per monetary unit, GJ/€ and kgCO_{2e}/€, respectively, to quantify the total environmental impacts of wood construction products produced in Ireland. The results of the LCA will also be important for the wood products industry in providing benchmarks of environmental performance for construction timber manufacturers and buildings products manufacturers alike. LCA studies are also important as they identify certain environmental hotspots throughout a products life cycle which can be used to prioritise future improvements

Life Cycle Assessment (LCA)

LCA is an environmental assessment tool that quantifies the total environmental impacts associated with a product over its life cycle. These environmental impacts are calculated by analysing the total inputs, such as raw material, energy and water and outputs such as co-products, solid waste and emissions associated with the production of a product at each stage of its life cycle and then quantifying the environmental burden associated with each. To ensure clarity, consistency and accuracy LCA studies are governed by the ISO standards which were published in 2006, most notably, ISO 14044 (ISO 2006).

There are a number of approaches to an LCA including process analysis, Input Output analysis (IO analysis) and hybrid analysis. These methodologies differ primarily due to their data collection methodology and their associated system boundaries. The system boundary refers to which processes and environmental impacts are to be included within the scope of a study and which are to be ignored.

The process analysis approach is the oldest and most commonly used method which involves a step by step analysis of the inputs and outputs to a product at each stage of its life cycle. The system boundary is typically defined by time, cost and data availability which often leads to issues ignoring certain indirect impacts. This is known as a truncation error.

IO analysis uses economic IO tables, which are unique to each economy, to track energy flows through an economy. The Irish IO tables (CSO 2009a) are separated into 55 sectors. From these the energy sectors are abstracted and disaggregated to calculate energy intensities of manufacturing or service sectors and the products therein. The advantage of using an I-O methodology is that the boundary for the analysis is defined by the economy and, therefore, the completeness of the analysis is improved as the indirect energy inputs are also included (Crawford 2008). However, IO analysis has a huge amount of uncertainties primarily due to the aggregation of dissimilar products within each sector.

Hybrid analysis takes advantage of both of the above methods and may be primarily process based or IO based. The energy intensity of typical products from a sector can be accounted for by IO analysis and incorporated into a process analysis if more detailed data is available for the inventory, and vice versa. There are also a number of

disadvantages associated with Hybrid analysis which include; aggregation, the proportionality assumption, the homogeneity assumption and errors relating to economic data, all of which have been discussed in detail by Treloar (1998) and McCaffrey (2011).

Methodology

This project uses a process based Input Output hybrid (PBH IO) analysis developed by Treloar (1998), Crawford (2009), McCaffrey (2011) and Goggins et al (2010a) in order to quantify the embodied carbon and embodied energy of sawn timber and OSB. A PBH IO analysis is an alternative and more comprehensive method than a process analysis and avoids some of uncertainty issues associated with an IO analysis.

The PBH IO model analyses each product by combining process LCA data to quantify the direct environmental impacts of a product and IO analysis data to account for the indirect emissions that would have been missed by the process analysis. Using this methodology the total EE and EC associated with the production of 1 kg of sawn timber or OSB will be expressed as the total Energy Intensity (EI_M) in MJ/kg and the total Carbon Emission Intensity (CI_M) in kgCO_{2e}/kg, respectively. They are found using Equation (1) and Equation (2) as shown below.

$$EI_M = PEI_M + (TEI_n - DEI_M) \times \epsilon_M \quad (1)$$

$$CI_M = PCI_M + (TCI_n - DCI_M) \times \epsilon_M \quad (2)$$

Where PEI_M and PCI_M are the process analysis energy and carbon emission intensities respectively (MJ/kg and kgCO_{2e}/kg); TEI_n and TCI_n are the total IO energy and carbon emission intensities of a given sector n (MJ/€ and kgCO_{2e}/€); DEI_M and DCI_M are the direct energy and carbon emission intensities of the IO (MJ/€ and kgCO_{2e}/€); and ϵ_M is the total price of the material (€/kg). Each input is described in more detail below.

Process LCA Data. (PEI_M and PCI_M)

The original Process data is taken from the Inventory of Carbon and Energy (ICE) database produced by Hammond and Jones (2011). The ICE database collated the results of many process LCA research studies on various materials and computed average weighted results for the EE and EC of the materials. It should be noted that the data may not be exactly suited to Ireland, but is the most reliable current estimate. Work is currently underway to quantify Irish specific process LCA data for construction wood products in produced in Ireland which will then be included in future analysis to improve the accuracy of the hybrid model (Dolan and Harte 2013). The environmental impacts associated with the process model tend to ignore certain indirect impacts which are then taken into account by the sectoral intensities from the IO analysis.

Sectoral intensities (TEI_n , DEI_M , TCI_n and DCI_M) and Basic Product Price. (ϵ_M)

In order to utilise the PBH IO analysis it is necessary to compute the indirect impacts associated with the product by initially calculating the total IO impacts and then subtracting the direct IO impacts. The IO model initially analyses the direct energy usage

and emissions associated with the sector inputs into the manufacturing process of the timber products (Stage 1, Direct intensities). In the case of sawn timber, the major inputs come from such sectors as ‘The products of forestry, logging and related services’ sector, the petroleum sector and numerous other sectors that contribute to the manufacture of wood products. The emissions into these sectors from all other sectors are then analysed (Stage 2) and in turn the emissions and energy into those sectors from all other sectors are analysed (Stage 3), and so forth. The summation of all these intensities calculated at each stage of a products production path will give the total IO impacts.

The Irish IO tables separate the economy into 55 sectors. The data required for this analysis comes primarily from 4 sectors: 3 energy sectors, in which 7 energy sources are aggregated, and also ‘The manufacture of wood and wood products’ sector.

In order to quantify these sectoral intensities, equations such as Equation (3), which is used to find total carbon emission intensity (TCI_n), are required. Three similar equations are necessary to calculate TEI_n , DCI_M , and DEI_M . They each use a series of coefficients and factors that ultimately convert the energy flows into each sector into energy required and carbon emissions associated with a given sector per monetary value (GJ/€ and kgCO_{2e}/€).

$$TCI_n = \sum_{e=1}^E C_d \times PEF \times T_{rc} \times T_e \times ECO_{2e} \quad (3)$$

Where C_d is the disaggregation constant, PEF is the primary energy factor for the energy source; T_{rc} is the total requirement coefficient relating to the energy requirement from the energy source by the sector being assessed (€/€); T_e is the average energy tariff for the energy source (GJ/€); ECO_{2e} is the emission factor for the energy source and E is the total number of energy sources (which is seven in this case).

The derived IO variables listed in Table 1, lists the 7 energy sources and the necessary variables derived for the IO analysis. These variables are applicable to ‘The manufacture of wood and wood products sector’ (sector 20).

Table 1: Necessary variables for sector 20 derived for the year 2005

	Peat	Crude	Coal	Petroleum Prods	Natural Gas	Non Renew Elect.	Renew Elect.
PEF	1.06	1.00	1.00	1.02	1.05	2.58	1.12
C_d	0.095	0.607	0.097	0.598	0.562	0.343	0.095
T_e	0.0781	0.1385	0.2791	0.0736	0.1206	0.0269	0.0960
D_{rc}	0.0000	0.0000	0.0000	0.0033	0.0148	0.0148	0.0148
T_{rc}	0.0008	0.0008	0.0008	0.0134	0.0211	0.0211	0.0211

Once the total and direct energy or carbon emission intensities are calculated the indirect energy or carbon emission intensity can be calculated by their difference. However, both of these are given per monetary value and as such need to be converted before being combined with the original process LCA by using the basic price of the product.

The prices utilised for construction wood products in the year 2005 were calculated using the export price of the material from detailed trade statistics from the forestry sector (CSO 2010 and IFFPA 2014). The use of the export price is assumed to be a fair representation of the market price, as other sources tend to have inflated retail prices instead of basic prices. The price was obtained from 2009 export data but was related back to 2005 prices by means of the wholesale price index (WPI) (CSO, 2009b).

Total EE and EC of Sawn Timber and OSB produced in Ireland

The total emissions intensity and direct emissions intensity of the “Manufacture of wood and wood products” sector were calculated as shown in Table. 2.

Table 2: Direct and Total energy and carbon emission intensities for the first ten product stages

Stage	Energy			Emissions		
	MJ/€	%	kg CO ₂ e/€	%		
1	DEI ₂₀ 1.7043369	58%	DCI ₂₀ 0.0977182	56%		
2	0.7141598	24%	0.0451609	26%		
3	0.3031027	10%	0.0199368	11%		
4	0.1179139	4%	0.0077421	4%		
5	0.0471149	2%	0.0030795	2%		
6	0.0192765	1%	0.0012562	1%		
7	0.0079650	0%	0.0005183	0%		
8	0.0032974	0%	0.0002144	0%		
9	0.0013628	0%	0.0000886	0%		
10	0.0005616	0%	0.0000365	0%		
Total	TEI ₂₀ 2.9190915	100%	TCI ₂₀ 0.1757513	100%		

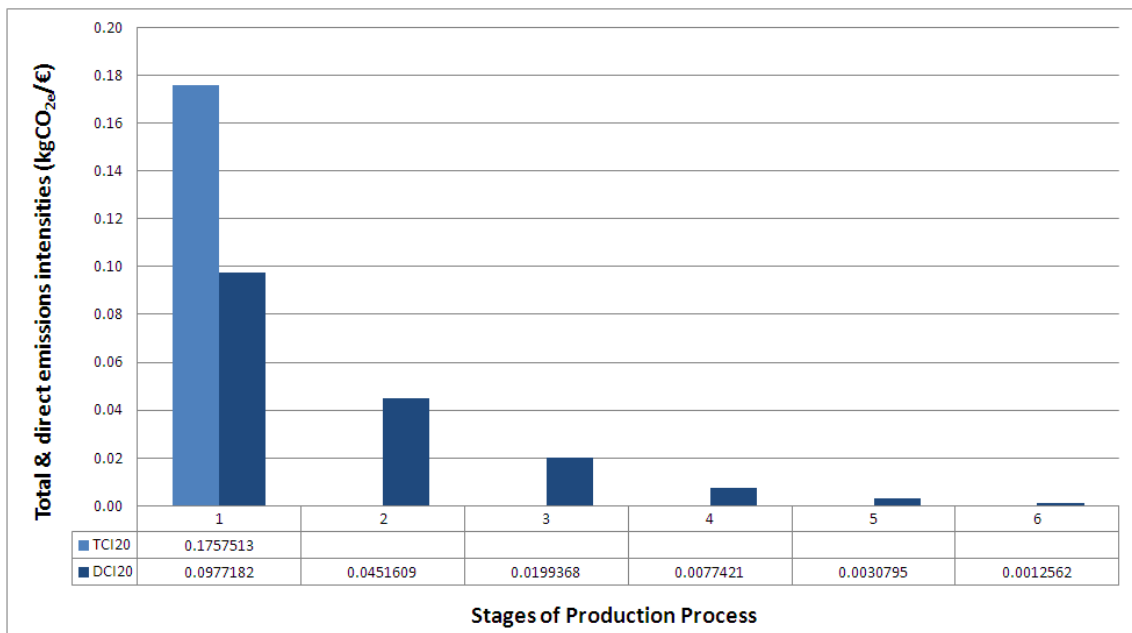


Figure 1: Total carbon emissions intensity value and direct carbon emissions intensity values per stage

Figure 1 highlights the importance of accounting for indirect carbon emissions associated with the production of wood products using the IO analysis. At Stage 1 only 56% of the emissions are accounted for. The remainder of the emissions are due to the indirect environmental impacts and would otherwise be ignored by a process LCA.

The process based direct energy intensity and carbon intensity for sawn softwood timber are 7.4MJ/kg and 0.59 CO_{2e}/kg, respectively (Hammond and Jones, 2011). The total quantity of exports from the sawn timber sector in the year 2009 was approximately 287,640,000kg with a value of €51,000,000 which equates to 0.155 €/kg after adjusting the price using WPI data to match the 2005 IO table (CSO2009b). Using Equation (1) and Equation (2) the PBH IO total EE and EC for sawn timber was found to be:

$$\begin{aligned}EI &= 7.4 + (2.91 - 1.70) \times 0.155 & EI &= 7.59 \text{ MJ/kg} \\CI &= 0.59 + (0.176 - 0.0977) \times 0.155 & CI &= 0.602 \text{ kgCO}_2\text{e / kg}\end{aligned}$$

This represents a 2.5% increase from the process based direct energy intensity and a 2.1% increase in carbon emission intensity

Similarly the process based direct energy intensity and carbon intensity for OSB, are 14.95MJ/kg and 0.99 CO_{2e}/kg, respectively (Hammond and Jones, 2011). The total quantity of exports was approximately 348,000,000kg with a value of €147,000,000 which equates to 0.369 €/kg after adjusting the pricing WPI data to match the 2005 IO table (CSO 2009b). Using Equation (1) and Equation (2), the PBH IO total EE and EC is calculated to be:

$$\begin{aligned}EI &= 14.95 + (2.91 - 1.70) \times 0.369 & EI &= 15.40 \text{ MJ/kg} \\CI &= 0.99 + (0.176 - 0.0977) \times 0.369 & CI &= 1.019 \text{ kgCO}_2\text{e / kg}\end{aligned}$$

This represents a 3.0% increase from the process based direct energy intensity and a 2.92% increase in carbon emission intensity.

Conclusions

Due to climate change and current legislation there is a growing need for ‘greener’ construction materials such as wood based products. The environmental impacts of such products need to be assessed using a holistic environmental assessment tool such as LCA. To date the majority of research done in analysing the environmental burdens of wood products over their life has focused on using process based LCA models. Due to the system boundaries set these process models ignore certain indirect environmental impacts. Although the difference between the total EE and EC found for wood products here compared to the process model alone is relatively small it does show that a certain amount of indirect energy emissions are not being accounted for. For large structures the aggregated total of these differences for all of the construction materials used can lead to a significant portion of total impact of the building on the environment being ignored.

There remains a certain level of uncertainty when using the ICE database as a source for the process LCA data, particularly in relation to the environmental impacts of wood products due to varying growing conditions, tree species etc. As no data is currently available for the Irish timber construction products industry, work is currently being undertaken to fill this knowledge gap using actual production data. These results can then be incorporated into the PBH IO model described in this study to truly quantify the total environmental impacts associated with wood production products and timber buildings produced in Ireland.

Acknowledgments

The authors would like to acknowledge the financial support of both Coillte and the Irish Research Council to this project.

References

- Crawford R. H. 2008. Validation of a hybrid life-cycle inventory analysis method. *Journal of Environmental Management* 88(3): 496-506. (Crawford 2008)
- Crawford R. H. 2009. Life cycle energy and greenhouse emissions analysis of wind turbines and the effect of size on energy yield. *Renewable and Sustainable Energy Reviews* 13(9): 2653-2660. (Crawford 2009)
- CSO (Central Statistics Office). 2009a. Supply and Use and Input-Output Tables for Ireland 2005. Central Statistics Office. Dublin, Stationary Office.
- CSO (Central Statistics Office). 2009b. Wholesale Price Index Retrieved on 20th of March 2011, from http://www.cso.ie/releasespublications/pr_pricesarchive2005.htm.
- CSO. 2010. Input-Output analysis and trade statistics. Retrieved on various dates 2010-2011.
- Dolan, D. and Harte, A. 2013. Gate to Gate Life Cycle Assessment of OSB products. In *Proceedings: International Panel Products Symposium 2013*.
- European-Commission: 2007. 2020 Vision: Saving our Energy.
- European-Commission. 2010. www.europa.eu: Retrieved 15/ 5/ 2012, from ec.europa.eu/energy/efficiency/buildings_en.htm 2010 36%
- Goggins J., Keane T. and Kelly A. 2010. The assessment of embodied energy in typical reinforced concrete building structures in Ireland. *Energy and Buildings* 42(5): 735-744.
- Hammond G. P. and Jones C. I. 2011. Inventory of carbon and energy (ICE) Version 2.0. Retrieved on 16th of April 2013, from <http://www.bath.ac.uk/mech-eng/sert/embodied>.

IFFPA (Irish Forestry and Forest Products Association) . 2014. An Overview of the Irish Forestry and Forest Product Sector 2013.

ISO-14044.2006. Environmental Management - Life Cycle Assessment - Requirements and Guidelines, ISO.

McCaffrey M. 2011. An I-O hybrid methodology for environmental LCA of embodied energy and carbon in Irish products & services - A study of reinforced concrete, in School of Engineering & Informatics. National University of Ireland: Galway.

Treloar G. J. (1998). A Comprehensive Embodied Energy Analysis Framework. Phd. Faculty of Science and Technology. Deakin University, Melbourne.

Spatial Analysis of Certified, Local, and Low-Emitting Wood Material Use in LEED Green Building Projects

David DeVallance¹ – Gregory Estep² – Shawn Grushecky³

¹ Assistant Professor and Program Coordinator, Division of Forestry and Natural Resources, West Virginia University, Morgantown, WV, USA
david.devallance@mail.wvu.edu

² Graduate Research Assistant and PhD Candidate, Division of Forestry and Natural Resources, West Virginia University, Morgantown, WV, USA
gdestep@mix.wvu.edu

³ Assistant Director – Appalachian Hardwood Center, Division of Forestry and Natural Resources, West Virginia University, Morgantown, WV, USA
shawn.grushecky@mail.wvu.edu

Abstract

There is a growing demand for green building products within the United States. Because of this increased demand and interest in green products, there exists potential for wood products manufacturers to gain increased market share opportunities within the green building sector. The overall objective of this research was to use spatial analysis techniques to evaluate the growth of green building projects and the use of certified, wood products within these projects. The focus of this research was on green building projects certified as part of the U.S. Green Building Council's (USGBC) Leadership in Energy and Environmental Design (LEED). Using spatial analysis techniques, the research was able to identify geographic areas where wood products are used and awarded points towards green building certification. The research also investigated the relative availability of certified wood products as it related to increasing use of wood products in LEED green building projects. Results indicated a trend of LEED green building projects to be more geographically concentrated over time. The research identified various "Hot Spots" for LEED green building projects and the use of certified wood materials. The results of the research are expected to help improve the availability of wood products by indicating potential green building marketing regions for wood products producers.

Keywords: green building, certified wood, LEED, spatial analysis

Introduction

Growing environmental impacts have influenced the evolution of less impactful building standards commonly known as “green” building. As an industry with the potential to cause significant reduction in environmental impacts, the United States (U.S.) building sector has been the focus of improved construction standards. To set benchmarks for green building practices, green building standards such as Leadership for Energy and Environmental Design (LEED), Green Globes, National Green Building Standard, and others have been developed as a guideline to help ensure buildings are built with lower environmental impacts as compared to standard construction practices. Varying levels of certification by these standards are often based on the point accumulation of successfully meeting the requirements for several categories such as: Site Development, Water Efficiency, Energy Efficiency, Material Use, and Indoor Environmental Quality. Although the particulars of each program differ, the root goal of all these programs is to lower the overall environmental impact of a building.

The recent and forecasted growth of green building projects in the United States (US) has identified the green building industry as a viable and increasing market for construction materials. A recent study published by McGraw Hill (2013) indicates that the green market made up 48% of all 2012 building project activity in the US. Additionally, respondents that reported having green building project comprising at least 60% of their work are expected to reach 53% in 2015, up from 40% in 2012. The top reported sectors where respondents plan to have green projects are: new commercial buildings, retrofits of existing buildings, and new institutional buildings. The continued growth of the green building market in the U.S. may present a local or regional opportunity for environmentally friendly construction material providers such as wood products manufacturers. In particular, those providing environmentally certified wood materials may have additional opportunities to include their products in various green building standards for specific point accumulations.

The most recognized green building standard in the U.S. is the Leadership in Energy and Environmental Design (LEED) program developed by the United States Green Building Council (USGBC) in 1998 (USGBC 2013.a). Since its inception, the LEED certification program has undergone 5 evolutions (LEED v1.0, LEED NCv2.0, LEED NCv2.2, LEEDv3, and LEEDv4) and currently lists 62,525 registered and certified U.S. based projects (USGBC 2013b). As a significantly popular standard in the green building industry, building projects pursuing LEED certification represent a large potential market for manufacturers of environmentally low-impact construction materials.

Wood products have low environmental impacts as compared to other construction materials such as steel or concrete (Gustavsson et al. 2006a, Gustavsson et al. 2006b, Lippke et al. 2004, Buchanan A. H. and Levine S. B. 1999, Peterson A.K and Solburg B. 2002, Peterson A.K and Solburg B. 2003, Upton et. al. 2008, Puettmann and Wilson 2005). LEED specifically encourages the use of certified wood products (CWP) by granting one point for the use of Forest Stewardship Council (FSC) certified wood, given

that at least 50% (cost based) of all wood based materials are FSC certified. However, the inclusion of wood product use in the LEED standard is not limited to only certified wood products. Other opportunities for credit accumulation exist for uncertified wood products in categories such as recycled content, indoor environment quality, locally sourced materials, and rapidly renewable materials. The sales opportunities for wood product producers interested in pursuing green building projects under LEED, therefore, are not limited to those participating in FSC wood product certification.

The inclusion of certified wood products in the green building sector has been a recent topic of research interest. One study suggests that non-wood products may have an unfair advantage in that green building programs require wood to be accompanied by an environmental certification to comply with particular point generating categories (Bowyer 2007). However, the singling-out of wood products may also provide an opportunity to educate others on the environmentally friendliness of the material (Falk 2009). Recommendations have been made to manufacturers who may be interested in diversifying their current sales market with the green building sector by becoming certified to produce FSC labeled products and to track new marketplace developments (Tardif et. al. 2009). A different study focused in western U.S., however, has suggested that design professionals have little incentive to include the use of wood products in the structural material selection of green buildings, even though wood was viewed as a more environmentally friendly material when compared to steel and concrete (Knowles et al. 2011). The use of certified wood products appears to also be growing in the Affordable Housing sector within the U.S. Appalachian Region. Estep et al. (2013) found that 50% of respondents planned to use CWPs in future affordable housing projects, up from the 14% that specifically looked to purchase CWPs in the previous year. Although the general use of certified wood products in green building projects have been explored, there is no known research that explores the spatial and temporal growth of certified wood product utilization in the largest green building certifying standard in the U.S. (LEED). Research in this area could help CWP manufacturers understand the geographic trends associated with the use of CWPs in the green building sector. Therefore, this research was initiated to evaluate the spatial growth trends for FSC certified wood products in LEED projects and to identify geographic regions where the use of FSC certified wood is more prominent.

To identify geographic trends of FSC use in the LEED rating system, it was important to explore certified project locations as well as influencing factors that may be associated with that region. By collaborating with the USGBC and the FSC, the spatial growth of LEED projects utilizing FSC certified wood to gain points towards building certification may indicate specific areas of market potential for FSC manufacturers. Information obtained through this research may help identifying specific market areas for FSC product manufacturers and help to indicate geographic market conditions for future growth trends.

The goal of this project was to assess the spatial growth trends of LEED certified projects within the U.S. that were awarded the certified wood credit. Specific objectives of this research were to identify the geographical distribution of LEED certified projects that

were awarded the certified wood credit and to evaluate particular areas of concentrated use of CWPs in certified LEED projects.

Materials and Methods

The United States Green Building Council (USGBC), the governing entity for the LEED certification program, was contacted to obtain the most accurate and updated list of LEED certified projects. This dataset contained all non-confidential projects located in the U.S. up to August 13th, 2013 that received LEED certification. LEED for Homes projects were not included in this dataset due to confidentiality restrictions. The dataset initially included 13,436 projects that were spread across six different LEED rating program types: LEED for Commercial Interiors (CI), LEED Core and Shell (CS), LEED existing Building Operation and Maintenance (EBOM), LEED for Schools, LEED for Healthcare, and LEED for New Construction (NC). The intent of this project was to identify possible markets for wood product producers. Because Alaska and Hawaii are located outside of typical sales markets for most wood product producers in the continental U.S., the projects located in these states (105) were removed from the list of data. Additionally, 2,007 projects listed as EBOM were removed from this study because of the lack of a certified wood credit in this rating program. Therefore, the working dataset for this project contained 11,324 LEED certified projects.

Accompanied in the list of certified projects, the following attributes specific to each project were also obtained: gross square footage of project, owner type, certification date, certification level, latitude and longitude coordinates of the project, industry type, space use type, rating program, and if the project achieved the certified wood credit. Additionally, specific category achievements were obtained from the USGBC for: material reuse recycled content, composite wood and agrifiber products, and regional materials. Although these categories may not be limited to the use of wood products specifically, there are opportunities for non-certified wood products to satisfy these categories. Therefore, this data was acquired to explore possible relationships between the achievement of these category credits and that of the certified wood credit.

The individual projects located in the continental U.S. were geocoded and uploaded to Geographic Information Systems (GIS) software (ESRI ArcGIS 10.1) for spatial analysis. All project locations and maps were projected to “USA Contiguous Equidistant Conic” prior to spatial analysis. Individual project locations were grouped for analysis by joining the LEED data with the respective county centroid. It is understood that uniform areas (unlike county borders) are preferred when spatially analyzing data, however, county level analysis was applied due to the availability of complementary data such as electricity rates, income, population, and other census-based data obtainable on the same geographic level. Additionally, county level analysis provided a satisfactory level of precision to draw trend conclusions. The number of projects found in a county essentially weighted that county for further spatial analysis.

Spatial analysis was performed on the continental U.S. as a whole to indicate country-wide growth trends for LEED certified projects. As a precursor to the Getis-Ord G_i^* test (Hot Spot Analysis) (ESRI 2014a) for cluster locations, a Moran's I test (ESRI 2014b) was initially conducted on the data to determine if spatial autocorrelation existed. Results from the Moran's I test indicated there were statistically significant ($P < 0.05$) clustered patterns which allowed for further hotspot analysis. Hotspot analysis was then performed on county level data to indicate the location of statistically significant clustering and/or dispersion of data points within a determined threshold distance (or neighborhood). Statistical significance of the hot spot analysis was determined based on the resulting z-scores. Resulting z-scores of -1.96 to -2.58 were significantly dispersed at the $p < 0.05$ level. Resulting z-scores smaller than -2.58 were significantly dispersed at the $p < 0.01$ level. Resulting z-scores of 1.96 to 2.58 were significantly clustered at the $p < 0.05$ level. Resulting z-scores larger than 2.58 were significantly clustered at the $p < 0.01$ level. Threshold distance was determined based on a distance that contained approximately eight neighboring data points (county centroids) (ESRI 2014a). Distance threshold was initially determined by measuring the distance needed to encompass the centroids of the eight largest neighboring counties within the area of analysis. The distance was then input to an incremental spatial autocorrelation analysis tool to determine the highest ranked distance threshold, relative to the input distance, based on significance level. The resulting threshold distance, 121,856 meters, was used to analyze data for the continental U.S.

To determine growth trends of LEED certified projects, Moran's I was calculated for each year (2000 – 2013). The resulting Moran's I value signifies if the data is significantly clustered, dispersed, or simply of random arrangement. Increasing Moran's I values indicate higher levels of clustering patterns. Therefore, by comparing the results for each year within the U.S., building patterns for LEED projects were determined. To indicate geographic trends in certified wood product use, a similar analysis was performed on LEED certified projects that earned the certified wood credit.

Results and Discussion

Results of the spatial analysis indicated that certified LEED projects have experienced significant spatial growth throughout the country between the years 2000 and 2013 (Fig. 1). Results from Moran's I testing showed that the growth pattern in LEED projects is becoming generally more clustered from one year to the next (Fig. 2). This clustering result suggests that areas that have experienced high volumes of LEED certified projects may likely continue to see future growth in the number of LEED certified projects.

Results from Moran's I testing indicated that the growth pattern of LEED projects that obtained the certified wood credit were generally more clustered from one year to the next (Fig. 2). Therefore, geographic areas that have experienced high volumes of LEED certified projects that have obtained the certified wood credit may likely see continued growth of LEED certified projects and use of FSC-certified wood.

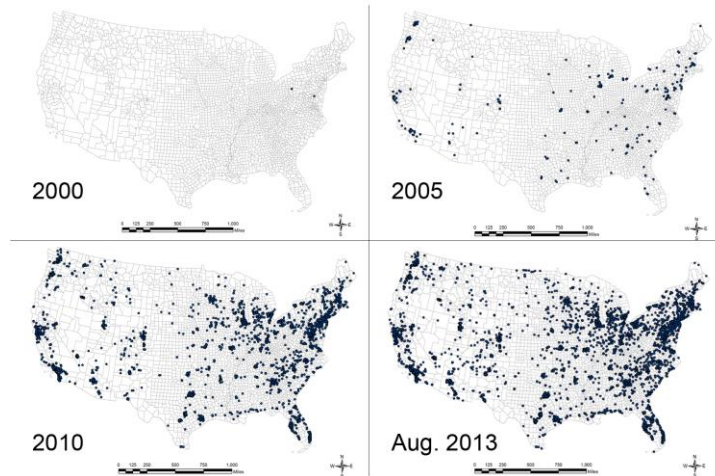


Figure 1 - LEED certified project location in sample data by year 2000, 2005, 2010, and August 2013.

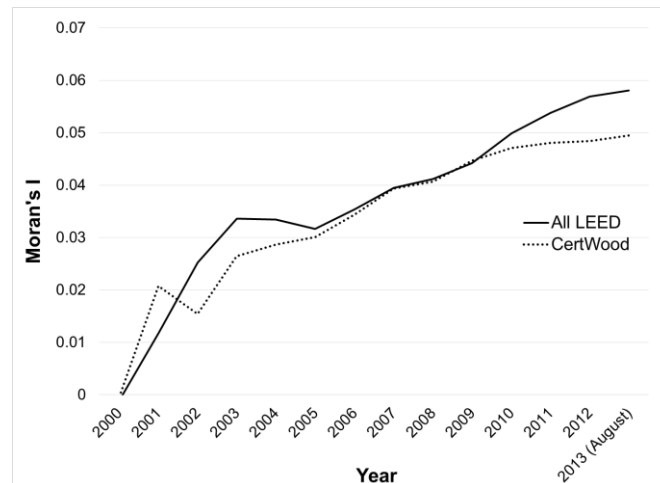


Figure 2 - Moran's I for all LEED certified projects and all LEED certified projects that obtained the certified wood credit in sample data.

LEED certified projects, contained in the sample data, were present in 1,189 (38%) of the 3,109 counties located in the continental U.S. (Fig. 3). A Hot Spot Analysis identified statistically significant clustering of counties weighted by the number of LEED certified projects the county contained. No statistically significant dispersion of counties weighted by the number of LEED certified projects were identified. Several Hot Spot counties were identified throughout the country (Fig. 4). Groups of adjacent Hot Spot counties are observed near the large metropolitan areas of: Seattle, WA; Portland, OR; San Francisco, CA; Los Angeles, CA; Denver, CO; Houston, TX; Chicago, IL; Washington, D.C.; Baltimore, MD; Philadelphia, PA; New York, NY; Boston, MA; Orlando, FL; and Miami, FL. These counties contained a statistically significant high concentration of

LEED certified projects within the neighborhood analysis distance (121,856 Kilometers) and are expected to be a viable future market for green construction materials.

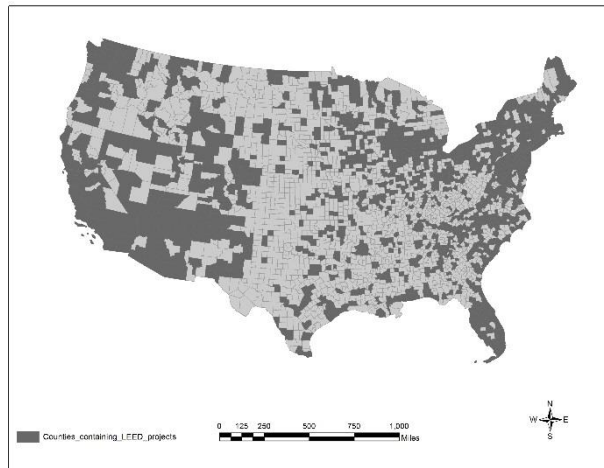


Figure 3 - U.S. counties that contain at least one LEED certified project, based on sample data.

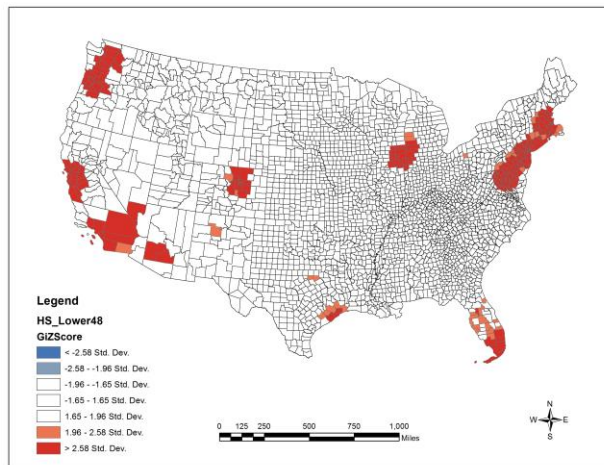


Figure 4 - Hot Spot locations of statistically significant (z -score of 1.96 or higher = $P < 0.05$) clustering of counties containing LEED certified projects in the continental U.S.

Likewise, a Hot Spot Analysis was also performed on LEED certified projects throughout the continental U.S. that obtained the certified wood credit. Of the 3,109 counties, 718 (23%) contained at least one LEED certified project that obtained the certified wood credit. Significant clustering of these projects is similar to the Hot Spot Analysis results of all LEED certified project (Fig. 5). Some differences can be seen, however, in a reduced number of significant counties within the state of Florida. Based on the significantly clustered growth pattern of these projects, these specific counties may be a viable future market for FSC certified wood material providers.

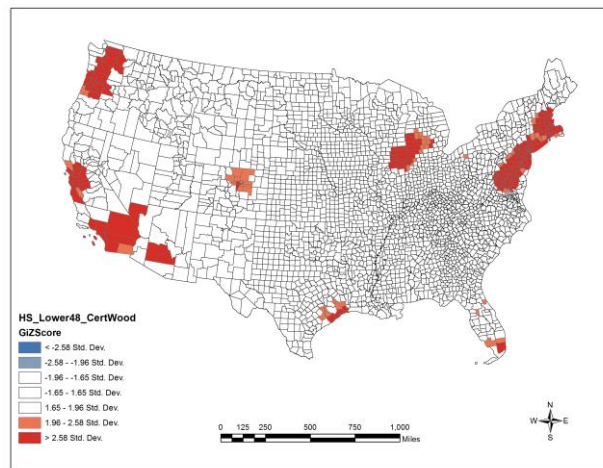


Figure 5 - Hot Spot locations of statistically significant (z-score of 1.96 or higher = $P < 0.05$) clustering of counties containing LEED certified projects that obtained the certified wood credit in the continental U.S.

Summary and Conclusions

This research focused on determining high-use areas for certified wood products in LEED certified projects within the United States. Specifically, the results of this study pinpointed the county-level Hot Spots for certified wood product use in LEED certified projects. LEED projects have high levels of spatial autocorrelation and continue to be constructed near existing LEED certified projects. Given the trend of spatial growth, the Hot Spot counties indicate regions of continued growth for both environmentally certified and non-certified wood products in future LEED projects.

Results indicated nine areas of statistically significant clustered LEED certified projects that obtained the certified wood credit (Figure 5). These areas contain at least three adjoining counties that are statistically significant at the $P < 0.05$ level. These areas indicate increased use of certified wood products for LEED projects and are likely to be growing market areas for providers of FSC certified wood products. In general, these areas are similar to the geographic areas containing increased numbers of LEED projects (Figure 4). The overlapping areas between these two groups of data may indicate target markets not only for FSC-certified wood products but also non-FSC-certified wood products. Additionally, manufacturers of point gaining products

that are looking to supply the LEED green building industry may increase their success by focusing on these areas of concentrated project locations.

The results of this research, however, are relative to the use of LEED certified green building projects and are not intended to be representative of other green building standards. Therefore, future studies are needed to identify additional regions of high wood product use in the various other green building standards in an effort to fully identify key green building markets for wood product manufactures.

References

- Bower J. 2007. Green Building Programs – Are They Really Green? *Forest Product Journal*. 57(9):6-17.
- Buchanan A. H. and S. B. Levine. 1999. Wood-based building materials and atmospheric carbon emissions. *Environmental Science & Policy*. 2: 427-437.
- Construction, McGraw Hill. 2013. World Green Building Trends. Available at: <http://analyticsstore.construction.com/index.php/world-green-building-trends-smartmarket-report-2013.html>
- ESRI. 2014a. Hot Spot Analysis (Getis-Ord G_i^*) (Spatial Statistics) Usage tips. Available at: http://resources.esri.com/help/9.3/arcgisengine/java/gp_toolref/spatial_statistics_tools/hot_spot_analysis_getis_ord_gi_star_spatial_statistics_.htm
- ESRI. 2014b. Spatial Autocorrelation (Global Moran's I) (Spatial Statistics). Available at: <http://resources.arcgis.com/en/help/main/10.1/index.html#//005p0000000n000000>.
- Estep, G. D., D. B. DeVallance, & S. Grushecky. 2013. Affordable Home Builder Demand for Green and Certified Wood Products. *Forest Products Journal*, 63(1): 4-11.
- Falk, B. 2009. Wood as a Sustainable Building Material. *Forest Products Journal*. 59(9): 6-12.
- Gustavsson L., R. Madlener, H. F. Hoen, G. Jungmeier, T. Karjalainen, S. Klohn, K. Mahapatra, J. Pohjola, B. Solberg, and H. Spelter. 2006b. The Role Of wood Material For Greenhouse Gas Mitigation. *Mitigation and Adaptation Strategies for Global Change*. 11: 1097–1127.
- Gustavsson L., K. Pingoud, R. Sathre 2006a. Carbon Dioxide Balance of Wood Substitution: Comparing Concrete- and Wood-Framed Buildings. *Mitigation and Adaptation Strategies for Global Change*. 11: 667–691.
- Knowles, C., C. Theodoropoulos, C. Griffin, J. Allen. 2011. Oregon design Professionals views on structural building products in green buildings: implications for wood. *Canadian Journal of Forest Resources*. 41: 390-400.

Lippke B., J. Wilson, J. Perez-Garcia, J. Bowyer, and J. Meil 2004. Corrim: Life Cycle Environmental Performance of Renewable Building Materials. *Forest Products Journal*. 54(6): 8-19.

Petersen A. K. and B. Solberg 2002. Greenhouse gas emissions, life-cycle inventory and cost-efficiency of using laminated wood instead of steel construction. Case: beams at Gardermoen airport. *Environmental Science & Policy*. 5: 169–182.

Petersen A. K. and B. Solberg 2003. Substitution between floor constructions in wood and natural stone: comparison of energy consumption, greenhouse gas emissions, and costs over the life cycle. *Canadian Journal of Forest Resources*. 33: 1061-1075.

Puettmann M.E. and J.B. Wilson. 2005. Life-Cycle Analysis of Wood Products: Cradle-To-Gate Lci Of Residential Wood Building Materials. *Wood and Fiber Science - Corrim Special Issue*. 37: 18 – 29.

Tardif P. and J. O’Conner. 2009. Selling Wood Products to the Green Building Market. *FPIInnovations Forintek*. Version 1.0 – February 2009.

Upton B., R. Miner, M. Spinney, L. Heath. 2008. The green House Gas and Energy Impacts of Using Wood Instead of Alternatives in Residential Construction in the United States. *Biomass and Bioenergy*. 32: 1-10.

USGBC 2013a. USGBC History. Available at: <http://www.usgbc.org/about/history>.

USGBC 2013b. USGBC Profile. Available at: <http://www.usgbc.org/profile>

Experimental Verification of Numerical Model of Single and Double-Shear Dowel-Type Joints of Wood

Jaromír Milch^{1} – Jan Tippner² – Martin Brabec³ – Václav Sebera⁴*

¹ PhD. student, Department of Wood Science - Mendel University in Brno.
Zemědělská 3, 61300 Brno.

* *Corresponding author*

xmilch@mendelu.cz

² Researcher, Department of Wood Science - Mendel University in Brno.
Zemědělská 3, 61300 Brno

jan.tippner@mendelu.cz

³ PhD. student, Department of Wood Science - Mendel University in Brno.
Zemědělská 3, 61300 Brno

martin.brabec@mendelu.cz

⁴ Researcher, Department of Wood Science - Mendel University in Brno.
Zemědělská 3, 61300 Brno

vaclav.sebera@mendelu.cz

Abstract

Mechanical analysis of dowel-type timber joints connection by 1) Finite Element Method (FEM) and 2) experimental testing with use of Digital Image Correlation (DIC) is presented in this paper. Norway spruce (*Picea abies* L. Karst.) one of the most important construction wood in Czech Republic for reconstruction of historic buildings was used; wooden dowels which were made from English oak (*Quercus robur* L.) were chosen as connection. Dimensions of samples were derived from the dowel diameter - 8 mm. Experimental tests were carried out according to the European standards EN 383 and EN 26891. Both single-shear and double-shear joints were loaded parallel to grain. Numerical (FEM) 3D model was built in software Ansys® ver. 14.5. Numerical model was based on the linear orthotropic mechanic theory. This model was verified using experimental data (displacements and forces mainly). The second part of experiment was focused on monitoring of surface deformations around dowel. Area around forehead dowel was scanned using stereovision system during the loading in testing machine with acquisition time interval of 250 ms. Strain distribution in this area was calculated by DIC technology. Results of numerical simulations showed correspondence with experimental part. Deformations around forehead dowel described by Finite Element Method were in agreement with deformations analyzed by Digital Image Correlation.

Keywords: single-shear, double-shear, dowel-type joints, Finite Element Method, Digital Image Correlation

Introduction

The connections are the most common the critical places in the timber structures, being responsible for the decrease locally continuity of overall structures. This fact (about in 80 % of cases) may leads to a reduction in the overall strength and stability of the structure (Itany and Faherty, 1984; Santos et al. 2009).

In the past was carried out and discussed many studies of this issue (such as Johansen 1949; Bouchair and Vergne 1995; etc.). The first mathematical model (European Yield Model) for strength of joints was proposed by Johansen in 1941. He applied the model to timber connection with a steel dowel but only for ductile failure modes, but some parts of this model were unfinished (Johansen 1949; Santos et al. 2009). Larsen (1973) continued and completed/developed Johansen's theory. The validity of this method was confirmed by experimental investigations (Möller 1950; Shanks et al. 2008; etc.). Brungraber (1985) such as one of the first performed the experimental tests on individual joints. These joints were tested in the full-scale of dimensions for the purpose of detect possible failures.

Historical timber construction used traditional all-wood joints with wooden connecting means – pegs/dowels. Many studies about construction joints with wooden pegs were investigated. Kessel and Augustin (1995, 1996) recommended minimum end distance (1.5 times peg diameter) for optimal placement of the oak pegs of full-scale joints. Bulleit et al. (1999) performed structural analysis for individual timber joints as well as full-scale frame using analytical and empirical approach.

Nowadays, considering to a renewed interest about all-wood connections were performed many studies of this issue by using tools such as finite element method (FEM) and digital image correlation (DIC) for predict possible failures (Chen et al. 2003; Hong and Barrett 2008; Oudjene, and Khelifa 2009, 2010; Dias et al. 2010; Ukyo et al. 2010). These tools especially FEM may simplify the optimization of the timber joints according to various parameters in comparison with the experimental testing. Therefore, the numerical modeling is usually undertaken as an approach to study timber joints (Chen et al. 2003).

Surface strain distributions can be observed by 1) FEM and 2) DIC techniques. Finite element analysis is one of much solution for obtaining the strain distribution. However, there are difficulties associated with the modeling of constitutive law of failure wood. As more practical solution, experimental strain measurement using DIC technique can be utilized to analyze surfaces strain distribution (Ukyo et al. 2010).

This paper deals with experimental verification of numerical model of single and double-shear dowel-type timber joints. The first objective was numerical analysis of dowel-type joints by FEM which was based of experimental results - displacements and forces mainly. As a secondary objective for verification, was focused of strain distribution around dowel using DIC technology.

Materials and Methods

Experimental test. Two types of joints were tested under various load: single-shear longitudinal tension (ss-T) (Fig. 1a), double-shear longitudinal tension (ds-T) (Fig. 1b) and double-shear longitudinal compression (ds-C) (Fig. 1c). The samples were prepared of Norway spruce (*Picea abies* L. Karst.). The components of all joints were cut parallel to grain with length and in the tangential direction with the thickness (detail of Fig. 1d). English oak (*Quercus robur* L.) was used to make the connection (dowel). The diameter of drill - 8 mm was used to bore the holes. The dowels ($d = 8$ mm) inserted into drill-holes were essentially without clearance. Wooden dowels were inserted so that the grain on the cross section were oriented parallel to the load direction. Experimental tests were carried out according to the European standards EN 383 and EN 26891. Both single-shear and double-shear joints were loaded parallel to grain. Figure 1 describes the configurations of tests samples including the geometric parameters which were derived from the dowel diameter (d).

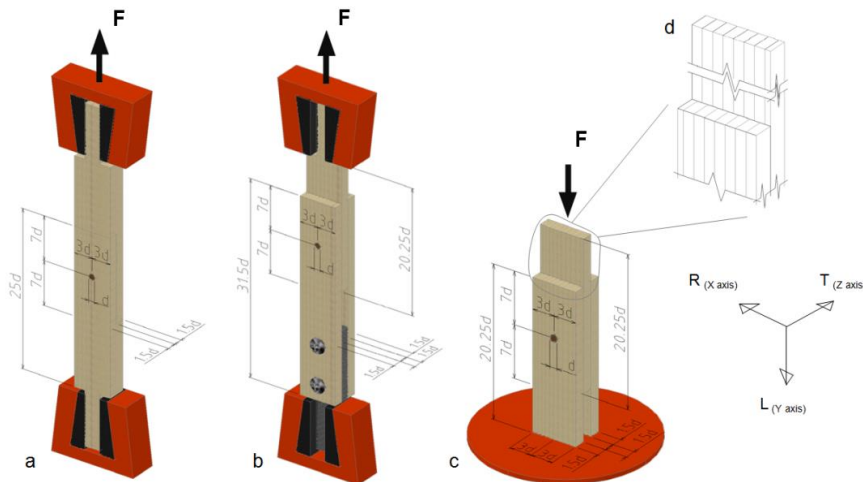


Figure 1: Experimental test configurations: a) ss-T; b) ds-T and c) ds-C.

Table 1 summarizes average density and experimental conditions of tests joints with dowels. All joints were assembled of components (side and middle members) with similar density. The density of components with moisture content (MC) of 12 % varies from 412 to $614 \text{ kg}\cdot\text{m}^{-3}$. The average density of dowels was $660 \text{ kg}\cdot\text{m}^{-3}$. All tests were done using of universal testing machine with 50 kN load capacity. The displacement from crosshead was recorded in an acquisition interval of $0.25 \text{ s} = 4 \text{ Hz}$. An automatic stop was triggered when the load decreased by 60% of the F_{max} or was reached time by 400 s .

Series	Number of samples	Density ($\text{kg}\cdot\text{m}^{-3}$)		Load direction	Displacement rate ($\text{mm}\cdot\text{s}^{-1}$)
		Average	VOC (%)		
ss-T	10	535.22	12.0	parallel to grain	0.025
ds-T	10	527.07	12.4	parallel to grain	0.025
ds-C	10	529.55	12.3	parallel to grain	0.025

Diameter	Length	Density ($\text{kg}\cdot\text{m}^{-3}$)	Load direction	-
----------	--------	---	----------------	---

(mm)	(mm)	Average	VOC (%)		
dowel - 8	26 or 38	660	9.4	radial	-

VOC - variation of coefficient

Tab. 1: Summary of average density and experimental conditions.

Numerical model. Numerical (FEM) 3D model was built in software Ansys® ver. 14.5. The model was built using the Ansys Parametric Design Language – APDL. The discretization of the wood members and wood dowel was consisted of 20-node hexahedral finite elements (SOLID186). Three contact pairs in the case of single-shear type joints and five contact pairs in the case of double-shear type joints were used. The contact between the dowel and wood members surfaces were modelled by the contact elements using surface-to-surface option. The elements CONTA174 and TARGE170 were used to model. These contact surfaces were set as flexible. The used friction coefficient (μ) was 0.33. Numerical model was based on the linear orthotropic mechanic theory. The wood dowel and wood members were modelled as homogeneous elastic material. Table 2 shows mechanical properties of all components of modelled joints.

Normal moduli of elasticity (GPa)	Wood members	Dowel
	<i>(Picea abies L. Karst.)</i>	<i>(Quercus robur L.)</i>
E_L	10.2	13.79
E_T	0.689	1.57
E_R	0.289	1.02
Poisson's Ratio		
ν_{LR}	0.023	0.056
ν_{RT}	0.557	0.044
ν_{TL}	0.014	0.566
Shear moduli (GPa)		
G_{LR}	0.523	1.324
G_{LT}	0.424	1.082
G_{RT}	0.053	0.112
Density ($\text{kg}\cdot\text{m}^{-3}$)	420	670

Tab. 2: Material properties of components of joints.

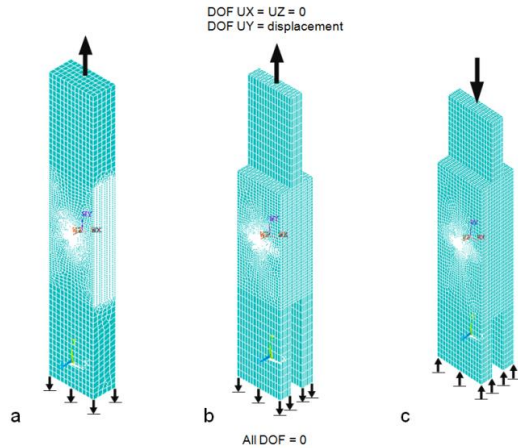


Figure 2: FE mesh of dowel type joints: a) ss-T; b) ds-T and c) ds-C.

The linear elastic behavior was assumed for materials. The models in this paper are only determined for simulation of the joints elastic stiffness. The loads of models were applied using maximum displacement which was set 1 mm for all models. The conditions of loading were applied with constant step of displacement (16.67 μm) in the 60 substeps. Figure 2 shows FE models of the joints with individual meshing.

Digital image correlation. Strain distributions were investigated using Digital Image Correlation (DIC) technique. Two surfaces (Fig. 3a and 3b) around forehead dowel was captured using stereovision system during the loading joints. Images were taken using two pairs of cameras – 2 \times 3D configurations (Fig. 3). Acquisition time interval was 250 ms. Area of interest (AOI) by a high-contrast speckle pattern needed to the DIC measurement was covered. Strain distribution in these areas was calculated by software Vic-3D (Correlated Solutions).

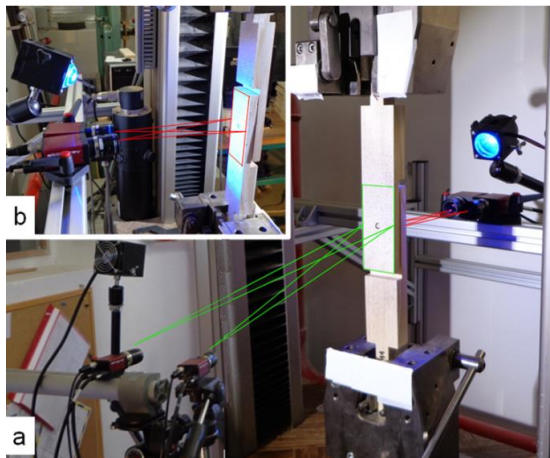


Figure 3: Stereovision scanning system (2 \times 3D system): a) front area; b) back area.

Results and Discussion

Global joints behavior. Single-shear and double-shear type joints were tested under various loading. The verification of the numerical models was done using displacement obtained from DIC analysis. Displacements calculated using Vic-3D are more accurate than displacements obtained from crosshead of testing machine. The average displacements from crosshead of single-shear type joints loaded in tension (ss-T), double-shear type joints loaded in tension (ds-T) and double-shear type joints loaded in compression (ds-C) were compared with displacement calculated by DIC. The displacements of ss-T, ds-T and ds-C measured by crosshead were higher (16%, 108% and 2%, respectively) compared to results from DIC. In the cases of joints loaded in tension, the differences were can be justified by slip, especially of metal member of joints, in the clamping wedges. Further, the compression deformation of joint grips induced by tension load allows displacement of clamping wedges in jaws. It should be of concern when loading wood joints in tension mode.

Verification of numerical models. The first objective was comparison and verified numerical models of dowel type joints. In a fact, numerical models highly depend on the material properties and on the loading conditions, especially on the applied step of displacement. Despite, the load-displacement curves exhibit the good agreement between the experiments and numerical models but only in the range of elastic deformation behaviour of tested joints (Fig. 4b).

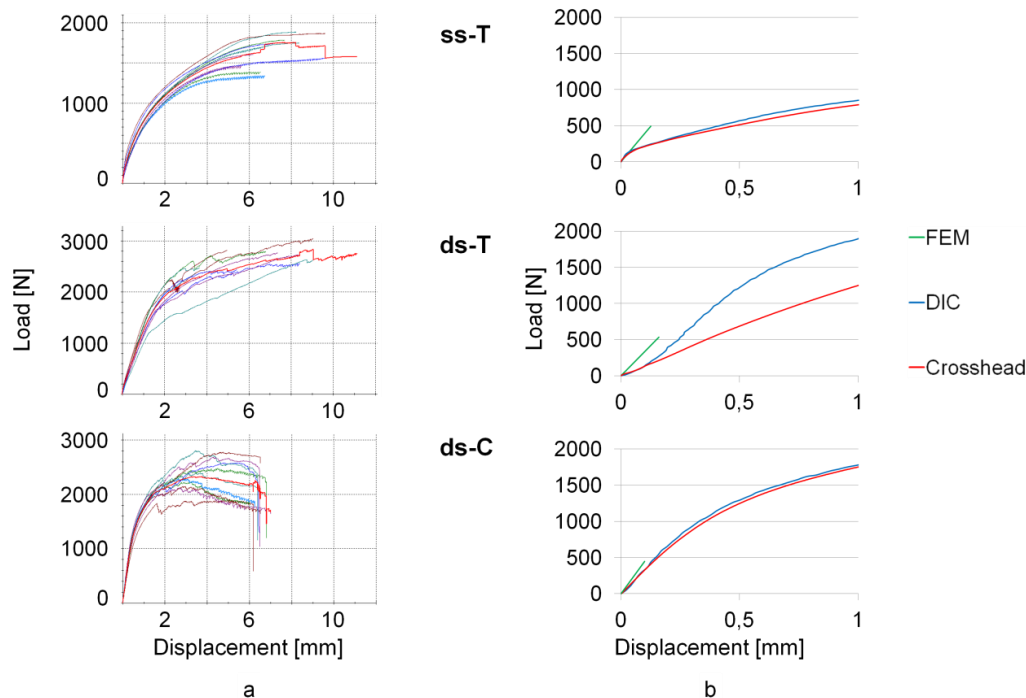


Figure 4: Load-displacement curves: a) experimental curves; b) comparison between experimental and numerical solution in the linear part; ss-T; ds-T and ds-C.

Figure 4a displays the load-displacement curves from experimental testing. The red curves represent the average of them. From these curves are apparent the differences in deformation (mainly failure) behaviour of single- vs. double-shear dowel type joints and joints loaded in

tension vs. compression. The ss-T exhibits the continual opening of joints, i.e. pulling out of dowel from holes; meanwhile ds-T is opened discontinuously. In this case, the dowel is alternately fixed and pulled out for a certain time interval. These differences can be justified by concentric (ds-T) and eccentric (ss-T) load of dowel. The dowel of ss-T is loaded by two contrary tension forces which don't shear the same axis. The dowel of ds-T is loaded by one higher and two half forces arranged in symmetric way relative to higher one. The failure of ds-T is gradual due to the bending load of dowel which is induced by "opening effect" of joint. Conversely, the dowel of ds-C is loaded in shear stress which leads to the abrupt failure of it which is enforced by "closing effect" of joint. The mentioned behavioral specifics were particularly observed also on the numerical models, especially in case of "opening" and "closing effect" of double shear joints or pulling out of dowels.

Strain distribution around dowel. Figure 5 shows normal strain in load direction (Y axis) and shear strain distribution at displacement of 0.1 mm. The numerical models show the good agreement of strain distribution with full-field strain calculated by DIC.

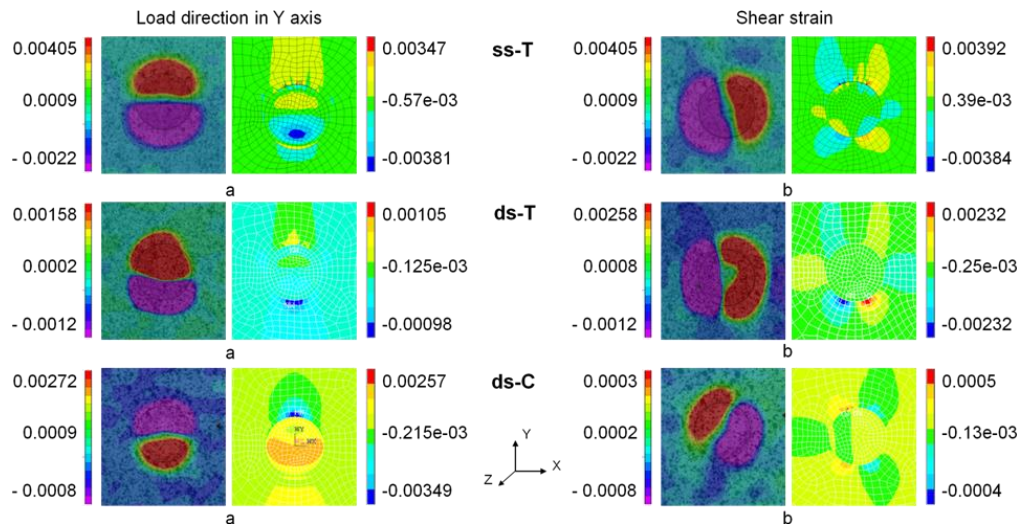


Figure 5: Normal strain and shear strain distribution around dowel: a) load direction in Y axis; b) shear strain.

Conclusion

This paper presents verification of numerical models based on the experimental tests. The differences in deformation behaviour of joints and failure mode of dowels were found. They are caused firstly due to single- and double-sheared loaded joints related to the pulling out of dowels, secondly due to character of loading (tension and compression) related to the arrangement of forces affecting the dowels. The numerical models demonstrated good agreement with experimental analysis. Because of linear orthotropic mechanic theory used for the numerical simulations, the numerical models correspond to experiments behaviour only in the range of elastic deformations of joints. Further, it was found that the behavioral specifics can be particularly investigated using of linear FE models. Material models with non-linear behaviour will be needed for future extended utilization of numerical models.

Acknowledgements

This article is supported by the project "Design and Assessment of Timber Joints of Historical Structures" reg. No, DF12P01OVV004 of Ministry of Culture Czech republic.

References

- [1] Bouchair, A., Vergne. 1995. An application of the Tsai criterion as a plastic flow law for timber bolted joint modelling. *Wood Science and Technology*. (30), 1:3-19.
- [2] Brungraber, R.L. 1985. Traditional timber joinery: a modern analysis, Ph.D dissertation. Stanford University, Palo Alto, CA.
- [3] Brungraber, R.L. 1985. Traditional timber joinery: a modern analysis. PhD thesis, Department of Civil Engineering, Stanford University, Palo Alto, CA.
- [4] Bulleit, W. M., Sandberg, L. B., Drewek, M. W., and O'Bryant, T. L. 1999. Behavior and modeling of wood-pegged timber frames. *Journal of structural engineering*, 125(1), 3-9.
- [5] Chen, C. J., Lee, T. L., and Jeng, D. S. 2003. Finite element modeling for the mechanical behavior of dowel-type timber joints. *Computers & structures*, 81 (30), 2731-2738.
- [6] Dias, A. M. P. G., Van de Kuilen, J. W., Cruz, H. M. P., and Lopes, S. M. R. 2010. Numerical Modeling of the Load-Deformation Behavior of Doweled Softwood and Hardwood Joints. *Wood and Fiber Science*, 42(4), 480-489.
- [7] Hong, J., Barrett, D. 2008. Wood material parameters of numerical model for bolted connections-Compression properties and embedment properties. In: *10th World Conference on Timber Engineering*.
- [8] Itany R.Y., Faherty K.F. 1984. Structural wood research, state-of-the-art and research needs. New York, ASCE.
- [9] Johansen, K. W. 1941. Forsög med Träförbindelser. Danmarks Tekniske Höjskole Medd. No. 10 (in Danish). Copenhagen: Laboratoriet for bygningsteknik.
- [10] Johansen, K.W. 1949. Theory of timber connections. Inter. Assoc. of Bridge and Struct. Engr., Lisabon, Portugal. (9): 249-262.
- [11] Kessel, M. H., Augustin, R. 1995. Load behavior of connections with oak pegs. *Peavy, MD and Schmidt, RJ, trans. Timber Framing, Journal of the Timber Framers Guild*, (38): 6-9.
- [12] Kessel, M. H., Augustin, R. 1996. Load behavior of connections with pegs II. *Timber Framing, Journal of the Timber Framers Guild*, (39): 8-10.
- [13] Larsen H J 1973. The yield load of bolted and nailed connections. Proceedings of International Union of Forestry Research Organisation Division V Conference, pp 646-655
- [14] Möller, T. 1950. En ny metod för beräkning av spikförband: New method of estimating the bearing strength of nailed wood connections (in Swedish and English translation). Rep. No. 117. Gothenburg, Sweden: Chalmers Tekniska Högskolas Handlingar.
- [15] Oudjene, M. and Khelifa, M. 2009. Elasto-plastic constitutive law for wood behaviour under compressive loadings. *Construction and Building Materials*, 23.11: 3359-3366.
- [16] Oudjene, M. and KHELIFA, M. 2010. Experimental And Numerical Analyses Of Single Double Shear Dowel-Type Timber Joints. In: *11th World Conference on Timber Engineering 2010*. Trentino: WCTE, June, pp. 476-482.

- [17] Santos, C. L., De Jesus, A. M., Morais, J. J., and Lousada, J. L. 2009. Quasi-static mechanical behaviour of a double-shear single dowel wood connection. *Construction and Building Materials*, 23(1), 171-182.
- [18] Shanks, Jonathan David; Chang, Wen-Shao and Komatsu, Kohei. 2008. Experimental study on mechanical performance of all-softwood pegged mortice and tenon connections. *Biosystems engineering*, 100.4: 562-570.
- [19] Ukyo, Seiichiro, Masahiko KARUBE, Masaki HARADA and Hideki AOI. 2010. Damage Detection in Bolted Timber Connections Using Acoustic Emission Monitoring. In: *11th World Conference on Timber Engineering 2010*. Trentino, June, pp. 498-506.

Energy, Fuels, Chemicals

Session Co-Chairs: *Dave DeVallance, West Virginia University, USA and Margareta Wihersaari, Åbo Akademi University, Finland*

Fuel Pellets from Low Quality Hardwood Trees: Raw Materials and Pelletization Characteristics

Quy Nam Nguyen, Alain Cloutier, Alexis Achim, and Tatjana Stevanovic*

Centre de recherche sur les matériaux renouvelables (CRMR)
Département des sciences du bois et de la forêt
2425 rue de la Terrasse
Université Laval, Québec, QC, G1V 0A6, Canada.

* *Corresponding author:* alain.cloutier@sbf.ulaval.ca

Abstract

Past harvesting practices in the temperate hardwood forests of the Province of Québec, Canada consisted of selecting the most valuable stems of both sugar maple and yellow birch for the production of hardwood lumber. This practice left a large amount of low quality trees with little commercial value. From the forest management standpoint, the presence of these unused low vigor and low quality trees has a negative effect on forest health and value. To palliate to this situation, harvesting priority is now given to low vigor trees for which market demand is low. This current availability of low quality hardwood logs raised interest for their use as raw material for the production of fuel pellets. Therefore, the objectives of this project were to characterize the chemical composition of low quality hardwood logs and their suitability for fuel pellets production.

Results indicated that the low vigor trees had higher contents of extractives, ash, and lignin than the healthy trees. In addition, there was no significant difference in the higher heating value of wood among tree vigor classes and between unextracted and extracted wood samples. This can be considered as a value-added advantage. Results also indicated that wood particles from low vigor trees are more favorable than those from the healthy trees for making pellets because they caused less friction in the pelletizer and resulted in higher strength pellets. The current study also pointed out an optimum pelletizing temperature of 100 °C and raw material moisture content of 11.2%, according to which the pelletizing process should be performed in order to minimize

friction force and maximize density and strength of the pellets produced. Additionally, using an appropriate combination of milling screen size with other optimal material and process variables could also be beneficial to the pelletizing process in terms of reduction in friction and energy consumption.

Keywords: Low quality hardwood, chemical composition, higher heating value, fuel pellets, value-added uses.

Introduction

Past harvesting practices in the temperate hardwood forests of the Province of Québec, Canada consisted of selecting the most valuable stems of both sugar maple and yellow birch for the production of hardwood lumber. This practice left a large amount of low quality trees with little commercial value. From the forest management standpoint, the presence of these unused low vigor and low quality trees has a negative effect on forest health and value. To palliate to this situation, harvesting priority is now given to low vigor trees for which market demand is low. The unused available annual forest biomass in the Province of Québec, Canada, is estimated at 6.4 million anhydrous metric tons including 3.5 million tons in the form of tree trunks and 2.9 million tons in the form of crowns and branches. More than half (55%) of this volume is coming from low vigor trees not suitable for lumber production (Ministère des Ressources naturelles et de la Faune, 2009). The current availability of unused low quality hardwood trees in the Province of Québec, Canada could thus represent a significant source of feedstock for the production of biofuel.

In recent years, a clear interest arose for the use of forest biomass as biofuels. This was motivated not only by its low environmental impact and carbon emissions, but also because meeting the global increase in energy consumption may not be achievable without the contribution of biofuels (Hunt, 2009; Masia et al., 2010). It has been argued recently that a better use of biomass would be to burn it in the form of solid fuel for the generation of electricity to power electric vehicles (Campbell et al., 2009). Particularly, modern solid fuel combustion technology has been developed with much cleaner and efficient combustion than in the past. Solid biomass fuel, e.g. in the form of pellets, could thus become a more important energy commodity (SFU, 2012; Stephan, 2013). The homogeneity in size, shape and quality of pellets makes them well-suited for fully automated feed systems. Pellets could be used as fuel directly in several applications from residential heating stoves to central heating boilers. They can even be used as a fuel source in large-scale power plants, or as part of the process to produce liquid fuels. Wood pellets are standardized and traded at both national and international levels. These features combined with their advantages such as environmental benefits, high energy content due to their high density and low moisture content, and relative convenience of transportation and storage explain the rapid growth of the global wood pellets market, both in terms of production and consumption. From a technical standpoint, almost all kinds of forest biomass could be pelletized. However, knowledge on raw material characteristics is of great significance for the optimal successes in pelletization. Therefore, the objectives of this project were to characterize the chemical composition of low quality hardwood logs and their suitability for fuel pellets production.

Materials and Methods

The material used in this study was harvested in July 2010 from two hardwood stands composed mainly of sugar maple and yellow birch located in the vicinity of Mont-Laurier, Québec, Canada (46°39'40"N, 75°36'30"W and 46°39'5"N, 75°36'25"W). Sugar maple trees were classified according to the tree vigor (MSCR) classification system proposed by Boulet (2007). Based on external traits, each tree of the stand was classified into one out of the four vigor classes as follows: trees of reserve stock (class R) are free of any symptoms of disease or damage and are considered as healthy trees with highest probability of survival; growing trees (class C) have minor defects but are not biologically declining and are expected to survive until the next harvest without risk of imminent wood decay; low quality or defective trees (class S) are considered to be declining in terms of vigor, wood quality and volume increment, and are not expected to survive until the next harvest; and moribund trees (class M) show signs of either lethal pathological infection or severe damage with high risk of trunk breakage.

After classifying each tree according to its corresponding tree vigor classes, nine sample trees were selected and cut. The selected trees were assigned to one of the three following categories: R - vigorous (healthy) tree, M - moribund (dead or dying) tree, and S - weakened (defective) tree. After felling, the trees were measured and marked, three sample logs were extracted from each one. The first logs of about 60 cm long at a distance of approximately 70 cm from the root collar were used for chemical analyses. The two other (second and third) logs of 1.2 m long at a height of 1.3 m and at one-third of the trunk length down from the crown base, respectively, were used for pelletization. Various types of equipment including a band saw, a chipper, a hammer mill, and a Pallmann ring refiner were used to convert the sample logs into particles with proper size for pellets production. The refiner screen sizes used in the present study were 4.0 mm, 2.5 mm and 1.5 mm. The results of particle size distribution presented in Figure 1 show that most ground material obtained with the 1.5 mm refiner screen size was retained on the sieves with openings of 0.25, 0.5, and 1.0 mm. The find grind fraction for trees of class M was significantly higher than that of trees of the more vigorous classes (S and R) at any specific refiner screen size.

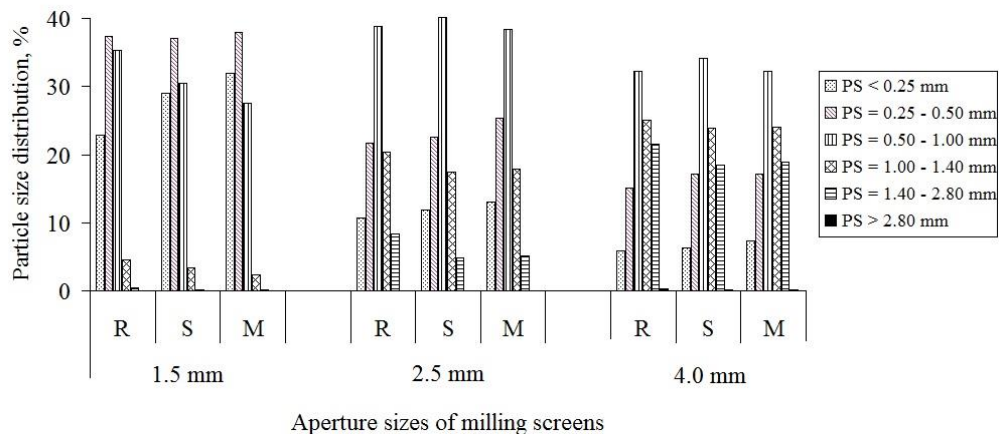


Figure 1. Particle size distribution by tree vigor classes.

The raw material characteristics were analyzed in the present study including contents of ash, extractives and lignin, and higher heating value (HHV). The HHV, based on the weight of the oven-dry sample was calculated according to CEN/TS 14918:2005:

$$HHV_d = HHV_w \times \frac{100}{(100 - MC)}$$

- where: - HHV_d is higher heating value at constant volume of the dry (moisture-free) fuel;
 - HHV_w is higher heating value at constant volume of the fuel as analysed;
 - MC is moisture content in the analysis sample, in percentage (dry basis).

The pelletizing characteristics were investigated in the present study including friction, pellets density and pellets strength. Pellets produced individually in a single pelletizer as demonstrated in Figure 2a, under controlled conditions as indicated in Table 2. The die wall friction during pellet compaction and ejection was recorded as indicated in Figure 2b. Compressive strength of pellets produced was determined using a universal MTS testing machine (50 kN load cell, 6 mm min⁻¹). The experimental plan is a three-level factorial design in 81 independent experiments/runs as described in Table 3.

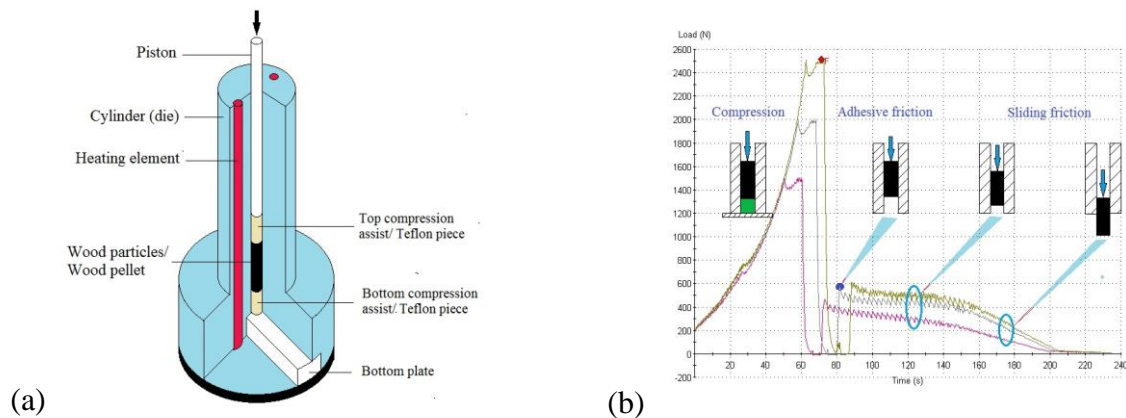


Figure 2. Schematic diagrams of the single pelletizer (left) and the measurement of frictional force at the wall of press channel (right).

Table 2. Experimental ranges and levels of independent variables.

Independent variables	Code	Coded variable levels		
		0	1	2
Temperature (°C)	X ₁	75	100	125
Moisture content (%)	X ₂	8.1	11.2	17.2
Compressive force (N)	X ₃	1500	2000	2500
Particle size (mm)	X ₄	< 0.25	0.25 - 0.50	0.50 - 1.00

Table 3. Experiment order.

X ₃ X ₄ X ₁ X ₂	Reserve (R) class									Moribund (M) class								
	0 0	0 1	0 2	1 0	1 1	1 2	2 0	2 1	2 2	0 0	0 1	0 2	1 0	1 1	1 2	2 0	2 1	2 2
Replication 1																		
0 0	37	30	39	40	31	42	47	46	29	37	30	39	40	31	42	47	46	29
0 1	50	51	49	41	52	35	48	54	28	50	51	49	41	52	35	48	54	28
0 2	32	44	45	36	43	34	33	53	38	32	44	45	36	43	34	33	53	38

1 0	10	3	12	13	4	15	20	19	2	10	3	12	13	4	15	20	19	2
1 1	23	24	22	14	25	8	21	27	1	23	24	22	14	25	8	21	27	1
1 2	5	17	18	9	16	7	6	26	11	5	17	18	9	16	7	6	26	11
2 0	64	57	66	67	58	69	74	73	56	64	57	66	67	58	69	74	73	56
2 1	77	78	76	68	79	62	75	81	55	77	78	76	68	79	62	75	81	55
2 2	59	71	72	63	70	61	60	80	65	59	71	72	63	70	61	60	80	65
Replication 2	81 runs in the order of replication no. 1									81 runs in the order of replication no. 1								
Replication 3	81 runs in the order of replication no. 1									81 runs in the order of replication no. 1								
Total	243 runs x 3 dependent variables = 729 runs									243 runs x 3 dependent variables = 729 runs								

Results and Discussion

Chemical composition. The chemical composition of sugar maple wood is presented in Table 3. The mean ash content of sugar maple wood by vigor category of trees varied from 0.38% in R tissue to 0.73% in S tissue and 0.97% in M tissue. The M tissue in sugar maple had a higher ash content than the two other higher quality (S and R) tissue. The mean values of total extractives content was 5.4%, 4.8%, and 7.3% for wood samples from sugar maple trees of categories R, S, and M, respectively. The M tissue had more extractives than R tissue. Amount of total and Klason lignin in sugar maple varied significantly from 25.0% and 21.4% in R tissue to 26.4% and 22.8% in S tissue, and 26.8% and 23.5% in M tissue, respectively.

Table 3. Chemical composition by tree vigor class. Standard deviations are shown in parentheses.

Tree vigor	Ash (%)	Extractives		Total extracts	Klason lignin		Acid soluble lignin		Total lignin	
		Ethanol-toluene	Hot water		Non-extracted wood	Extracted wood	Non-extracted wood	Extracted wood	Non-extracted wood	Extracted wood
Vigorous (R class)	0.38 ^c (0.03)	3.17 ^{ab} (0.22)	2.27 ^b (0.11)	5.44 ^b (0.20)	21.46 ^b (0.33)	22.70 ^b (0.38)	3.59 ^a (0.49)	3.80 ^a (0.51)	25.06 ^b (0.35)	26.46 ^b (0.35)
Poor foliage (S class)	0.73 ^b (0.07)	2.39 ^b (0.24)	2.48 ^b (0.11)	4.88 ^c (0.31)	22.89 ^{ab} (0.76)	24.06 ^{ab} (0.87)	3.53 ^a (0.40)	3.71 ^a (0.42)	26.40 ^{ab} (0.52)	27.76 ^{ab} (0.64)
Fungi attacked (M class)	0.97 ^a (0.05)	3.40 ^a (0.40)	3.92 ^a (0.37)	7.32 ^a (0.03)	23.53 ^a (0.83)	25.40 ^a (0.90)	3.29 ^a (0.08)	3.55 ^a (0.09)	26.83 ^a (0.75)	28.93 ^a (0.85)

Note: different letters for each composition means indicate a significant difference at 95%.

Calorific value of wood. The higher heating value (HHV) of sugar maple wood is presented in Table 4. The HHV ranged from 19.59 to 19.68 MJ/kg for unextracted wood samples and from 19.56 to 19.64 MJ/kg for extracted wood samples. In general, HHV of wood did not change measurably between the tree vigor classes. The results of the present study also indicate that the removal of extractives did not alter the HHV of sugar maple wood.

Table 4. Mean of higher heating values (HHV) by tree vigor class. Standard deviations are shown in parentheses.

Tree vigor	HHV of sugar maple (MJ/kg)	
	Non- extracted wood	Extracted wood
Vigorous (R class)	19.59 ^{abc} (0.08)	19.57 ^{abc} (0.07)

Poor foliage (S class)	19.68 ^{ab} (0.10)	19.64 ^{abc} (0.07)
Fungi attacked (M class)	19.62 ^{abc} (0.12)	19.56 ^{abc} (0.05)

Note: different letters for each composition means indicate a significant difference at 95%.

Pelletization characteristics. The results obtained from the ANOVA show that the linear terms of all main effects (temperature, moisture content, compression force and raw material particle size) were significant at the $P < 0.001$ level for all three dependent variables (friction, pellet density and pellet strength) indicating their strong effect on these properties. The interactions were also all significant at the $P < 0.02$ level or less.

The main effects and interaction plots are displayed in Figures 3 and 4. By visualizing the main effect plots and comparing the F-value obtained for each main effect, the factor raw material particle size (X_4) was the most important for friction, followed by factors moisture content (X_2), compression force (X_3) and temperature (X_1). Moisture content was the most important factor for pellet density followed by temperature, compression force and raw material particle size. Temperature was the most important factor for pellet compression strength, followed by compression force, raw material particle size and moisture content. Factor temperature appeared to have a greater effect on pellet strength, with a steeper slope.

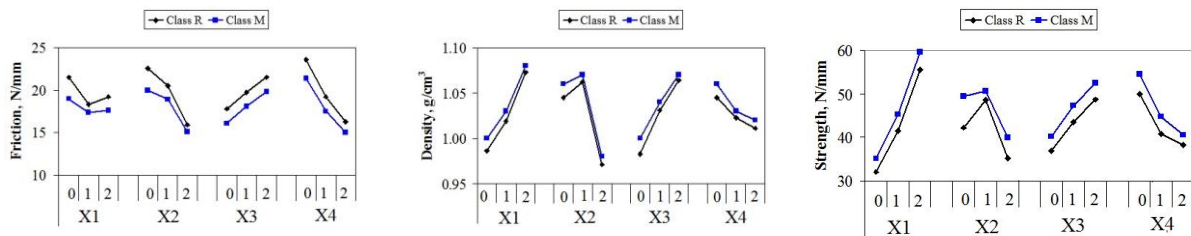
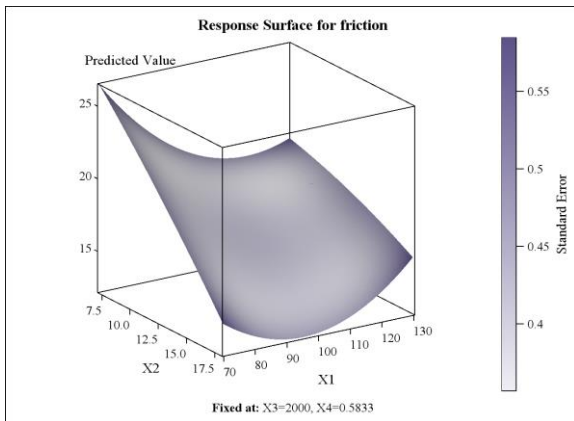
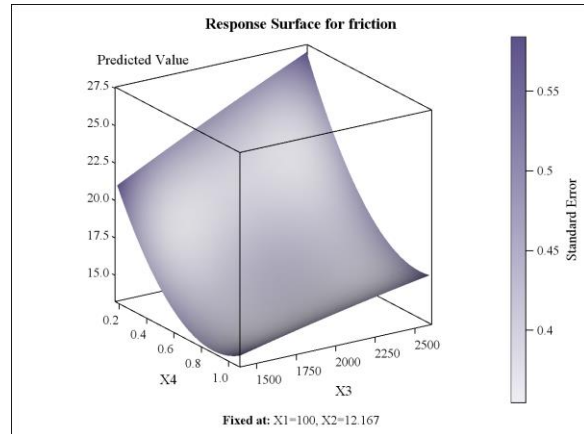


Figure 3. Main effects plots of friction (left), density (middle), and compression strength (right) for pellets pressed from particles of the most vigorous trees (class R) and the least vigorous trees (class M). Temperature (X_1) at three levels (0, 1 and 2) of 75°C, 100°C and 125°C. Moisture content (X_2) at three levels (0, 1 and 2) of 8.1, 11.2 and 17.2 %. Compression force (X_3) at three levels (0, 1 and 2) of 1500, 2000 and 2500 N. Particle size (X_4) at three levels/ranges (0, 1 and 2) of smaller than 0.25 mm, within 0.25 to 0.50 mm and within 0.50 to 1.00 mm.

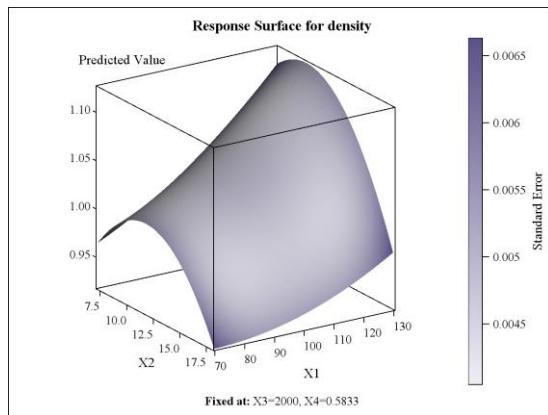
By examining the main effects plot and interaction plots in Figures 3 and 4 that correspond to the significant effects identified in the ANOVA, the most obvious findings are that level 1 (about 11.2%) of the moisture content should be chosen to maximize pellet density and pellet strength, while level 1 (about 100 °C) of the temperature should be chosen to minimize friction force. Also a strong effect of particle size on die wall friction was observed. The smaller particle size resulted in the higher friction during pellet compression and ejection. This finding in combination with the result of particle size distribution presented in Figure 1 suggest that using an appropriate (2.5 mm or larger) milling screen size in combination with other optimal material and process variables could be beneficial to the pelletizing process in terms of reduction in frictional force and energy consumption. Additionally, wood particles obtained from low quality trees (class M) are more favorable for making wood pellets than wood particles from high quality trees (class R).



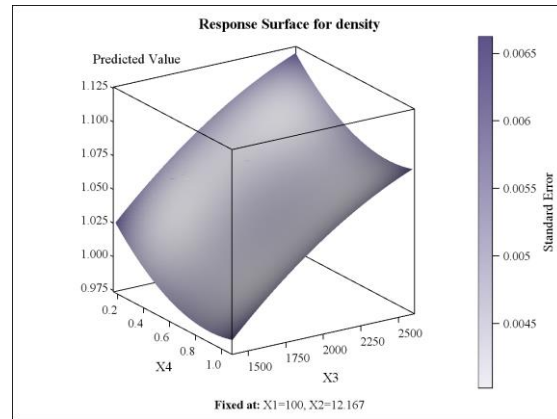
(a)



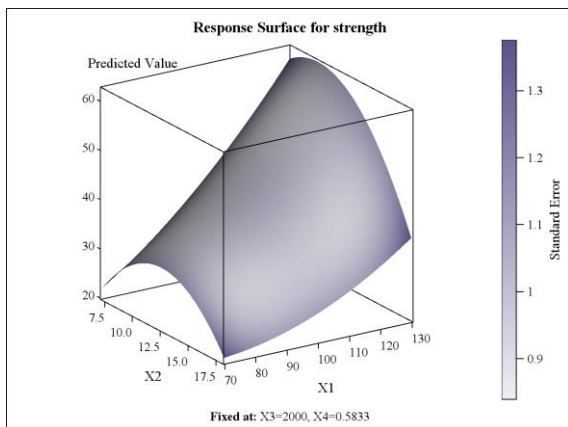
(b)



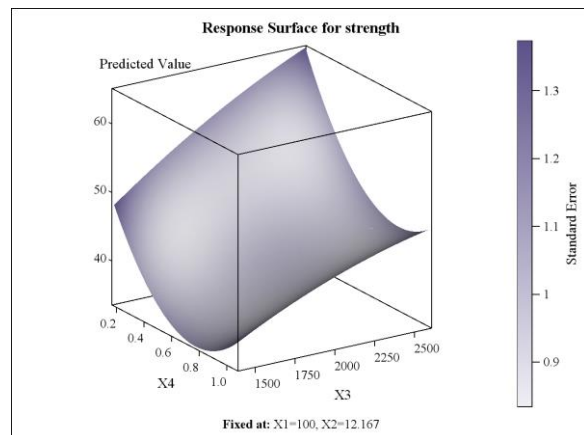
(c)



(d)



(e)



(f)

Figure 4. Interaction plots of friction in N/mm (a and b), density in g/cm³ (c and d), and compressive strength in N/mm (e and f) for pellets pressed from particles of the most vigorous trees. X1: temperature, X2: moisture content, X3: compressive force, and X4: particle size.

Conclusions

Tree vigor in sugar maple had significant effects on the chemical compositions including the amounts of ash, extractives, and lignin in wood.

No significant difference in the higher heating value of wood among tree vigor classes and between extracted and non-extracted wood samples was found.

Compared to particles from healthy trees, the use of particles from the less vigorous trees reduces friction, and increases the compression strength of the pellets produced. This means that wood particles from low quality trees are more favorable than those from the healthy trees for making pellets.

Acknowledgments

The authors would like to acknowledge Fonds de recherche du Québec - Nature et technologies, and Government of Vietnam - Project 322 for providing financial support for this research work.

References

Boulet B., 2007. Défauts et indices de la carie des arbres: guide d'interprétation. 2e édition. Ministère des Ressources naturelles et de la Faune, Québec, Canada.

Campbell J.E., Lobell D.B., Field C.B., 2009. Greater transportation energy and GHG offsets from bioelectricity than ethanol. *Science*, 324, 1055-57.

Hunt C.A.G., 2009. Carbon sinks and climate change - Forests in the fight against global warming. Cheltenham UK - Northampton, MA, USA: Edward Elgar Publishing Inc.

Masia P.N., Scheffran J., Widholm J.M., 2010. Plant biotechnology for sustainable production of energy and co-products. Springer-Verlag Berlin Heidelberg.

Ministère des Ressources naturelles et de la Faune, 2009. Developing the value of forest biomass. An Action Plan. Available at:
<http://www.mrn.gouv.qc.ca/english/publications/forest/publications/biomass-action-plan.pdf>.

Simon Fraser University (SFU), 2012. Sustainable use of biomass in a low-carbon Canada. Available at: <http://resources.carbontalks.ca/guides/CarbonTalks-DiscussionGuide-Biomass.pdf>.

Stephan D., 2013. Power from pellets - Technology and application. Springer-Verlag Berlin Heidelberg.

Rapid Assessment of Pellet Ash Agglomeration Using Electrical Resistivity

*Robert W. RICE, Evan CHATMAS, Douglas GARDNER and Adrian VAN
HEININGEN*

Abstract

The use of wood pellets for residential heating has grown exponentially in the United States. Along with increased pellet usage, ash related problems, such as corrosion and sintering, are also increasing and in some cases can be traced to the origin and chemical composition of the pellets. One approach that may prove useful to rapidly assess the potential for agglomeration and sintering related problems is to assess the electrical resistivity of the ash. Ash collected from burning commercial wood pellets at several temperatures was profiled with several analysis methods including SEM imaging, ICP-OES, and electrical resistivity measurements. The electrical resistivity of the wood pellet ash samples showed a curvilinear increase in response to temperature, with statistically significant differences seen when comparing the samples collected at low and high temperatures. The elemental analysis varied with increasing temperature and showed substantial changes in the total carbon content and in the K₂O levels relative to CaO; a strong indicator of fusion and potential sintering and slagging. Smaller changes were found in the percentages of a number of other elements. The SEM images showed geometric changes in some of the ash ranging from irregular through spheroidal and to crystalline. The changes in composition along with the ash structure are thought to be responsible for the variability in resistivity as the temperature of ash collection changed. All of the data show that the use of electrical resistivity is a rapid assessment technique for measuring the sintering potential of biomass fuels.

Keywords:

Wood pellets, biomass fuels, ash formation, electrical resistivity, energy

Principal Authors' contact details:

Robert W. Rice

Professor of Wood Science and Technology

University of Maine

Orono, Maine. 04469 USA

Robert_rice@umit.maine.edu or RWRice@maine.edu

Phone: 01-207-581-2883 FAX: 01-207-581-2875

Rice, Gardner and Van Heiningen are affiliated with the University of Maine; Chatmas is affiliated with the New Page Paper Company, Rumford, Maine.

Acknowledgments

This work was supported by a special grant from the Wood Education Resource Center (WERC). Any opinions, findings, conclusions, or recommendations expressed are those of the authors and do not necessarily reflect the view of the U.S. Department of Agriculture. Appreciation is expressed to the U.S. Green Building Council's (USGBC) Leadership in Energy and Environmental Design (LEED) for their assistance in the project.

Chemically Treated Wood-Based Material for the Removal of Phenol from Aqueous Media

Bestani Benaouda^{1} – Benderdouche Noureddine²*

¹ Professor, Département de Génie des Procédés, Faculté des sciences et de la technologie – Université Abdelhamid Benbadis - Mostaganem-ALGERIE.

** Corresponding author*

bestanib@yahoo.fr

² Professor, Département de Génie des Procédés, Faculté des sciences et de la technologie – Université Abdelhamid Benbadis - Mostaganem-ALGERIE.

benderdouchen@yahoo.fr

Abstract

This study aimed to compare the effectiveness of activated carbon in the purification of aqueous effluents charged with phenols. The activated carbons used were prepared starting from the sawdust, according to the following mode of activation using phosphoric acid as a chemical agent (PAAC). The characterization of the porosity of carbons as well as the chemical nature of their surface is carried out by the determination of the iodine and the methylene blue indexes for microporosity and mesoporosity respectively; and the functional groupings by infra-red FTIR. Various parameters influencing the adsorption capacity such as contact time, pH, adsorbate initial concentration and the temperature. The simulated adsorption isotherms are correctly described by Langmuir model. The maximum capacity of adsorption was enhanced by the chemical treatments to reach 192.32 mg of phenol/g of AC. The kinetics of adsorption was analyzed by the Lagergreen model and found to follow a second pseudo-order with good correlation factor ($R^2 > 0.98$). Thermodynamic parameters showed the endothermicity ($\Delta H > 0$) and the spontaneity ($\Delta G < 0$) of the adsorption mechanism. The capacity of adsorption depends on activated carbon porosity, of the medium pH and the solubility of the organic compound.

Keywords: Sawdust, chemical treatment, Adsorption, activated carbon, phenol, isotherm

Introduction

Water pollution caused by releasing wastewater charged with organics such as phenolic compounds is becoming one of the leading sources of pollution worldwide and causing widespread environmental and health problems. These pollutants can have a negative environmental impact when discharged directly into receiving wastewater system without any prior treatments. They are used in many industries as a chemical intermediates for the manufacture of drugs, pesticides, dyestuffs, and tanning agents. A growing awareness of industrial pollution and its consequences has led to tighter restrictions on pollution caused by this

type of toxic pollutants (Zhen-Mao et al., 2007). Different methods such as extraction, aerobic and anaerobic biodegradation, ion exchange by resins and oxidation by ozone have been proposed to remove these pollutants from wastewater.

Nowadays, adsorption using activated carbon is the most common method used for water treatments since it is proved to be one of the most effective and the most frequently used technique for these purposes (Ayranci and Duman, 2005; Alvarez et al., 2005).

Among a variety of solid, activated carbon is by far the preferred adsorbent, and it is generally derived from a selection of natural products as alternatives to the commercial activated carbons. In this study, attention was focused on the removal by adsorption of phenol as pollutant from assimilated wastewater using local sawdust as a lignocellulosic-based activated carbon.

Materials and Methods

In this study, phosphoric acid as chemical agent was used to modify and to functionalize the surface of local sawdust as solid waste in order to prepare activated carbons for toxic organic pollutant from assimilated wastewater.

Materials.

Stock Solutions and Adsorbents Preparation

As shown in Figure 1, Phenol (C_6H_5OH) supplied by Merck was chosen as an adsorbate in this study because of its strong uptake onto solids. A stock solution of Phenol (1g/L) was prepared by dissolving the required amount in homemade distilled water. Successive dilutions were used to prepare further solutions with desired concentrations.

The sawdust as a raw material was washed with distilled water, dried, then ground using a jar mill to pass through a 0.071 mm sieve. The amount of 50 g of sawdust was mixed with 500 mL of H_3PO_4 (20 %,) solution at 160 °C during 2 hours. The obtained mixture was filtered, oven dried overnight and then pyrolysed at 600 °C for 3 hours. The obtained chemically activated carbon was washed with hot distilled water until constant pH is reached. The dried (110°C overnight) sawdust based activated carbon obtained was first tested for its porosity by determining iodine number et Methylene blue index which give an indication of microporosity and mesoporosity respectively

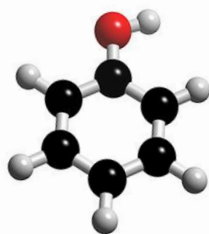


Figure 1: Phenol molecular structure

Batch Adsorption studies

Adsorption tests of Phenol onto prepared activated carbon were studied using batch process by placing 0.1g of adsorbent in a stoppered conical flask and 25 ml of phenol solution of a known concentration. The mixture was agitated magnetically until equilibrium is reached. Measurements were performed on phenol solutions at 275 nm using a UV-visible 2121 OPTIZEN spectrophotometer to determine the equilibrium concentration at ambient temperature against water as solvent reference. Solutions were diluted as required so that their absorbance remained within the calibration linear range of the calibrating curve established previously according to Beer-Lambert relationship given by the $A=0.0138 C$ equation. Experiments were carried out in triplicate at room temperature and the average value was reported. The equilibrium adsorption capacities (q_e) at different concentrations were determined according to the mass balance on the adsorbate according to equation 1.

$$q_e = \frac{(C_0 - C_{eq})}{m} V \quad (1)$$

Microporous and Mesoporous Available Areas

The activated carbon obtained was also characterized by measuring its iodine number (mg/g) which gives an indication of the adsorption capacity of activated carbon in micropores using 0.1 N standardized iodine solutions. The titrant used was 0.1 N sodium thiosulfate solution (Bestani et al. 2008). The adsorption of Methylene blue as a large organic molecule is also used for specific surface area determination (Kaewprasit et al., 1998) especially mesoporosity. The adsorption process of methylene blue was studied by mixing 0.1 g of Sawdust with 25 mL of dye solution at different concentrations for 2 h. After filtration the supernatant was analyzed for equilibrium concentration determination. The adsorption capacity obtained by Langmuir model is used to evaluate the available area for mesopores (S_{MB}) using the following equation:

$$S_{MB} = b \frac{N_A}{M_{MB}} \sigma_{MB} \quad (2)$$

Where b is the adsorption capacity (mg/g) obtained from previous Langmuir curves, N_A is Avogadro's number ($6.023 \cdot 10^{23}$), M_{MB} is the molecular weight of methylene blue (319.86 g/mol) and σ_{MB} is the area occupied by an adsorbed methylene blue molecule (119 \AA^2).

Activated carbon	H ₃ PO ₄ activation	Merck Activated carbon
Iodine number (mg/g)	832	826
Methylene blue index	286	157

Table 1. Iodine number and Methylene blue index values for PAAC and Merck-AC

Results and Discussions

Effect of Contact Time

In order to assess the contact time necessary for each adsorption system to come to equilibrium, preliminary tests were conducted and, for experimental purposes, each system was given a contact time in excess of this period. To determine the equilibrium time, 25 ml of solution of known concentration of phenol were mixed successively with 0.2 g of the prepared adsorbents and Merck activated carbon, and agitated during time intervals ranging from 60 to 300 min at room temperature. The resulting supernatants were analyzed and the equilibrium concentrations were determined as shown in Figure 2. Rapid equilibrium of 100 min was attained using all adsorbents.

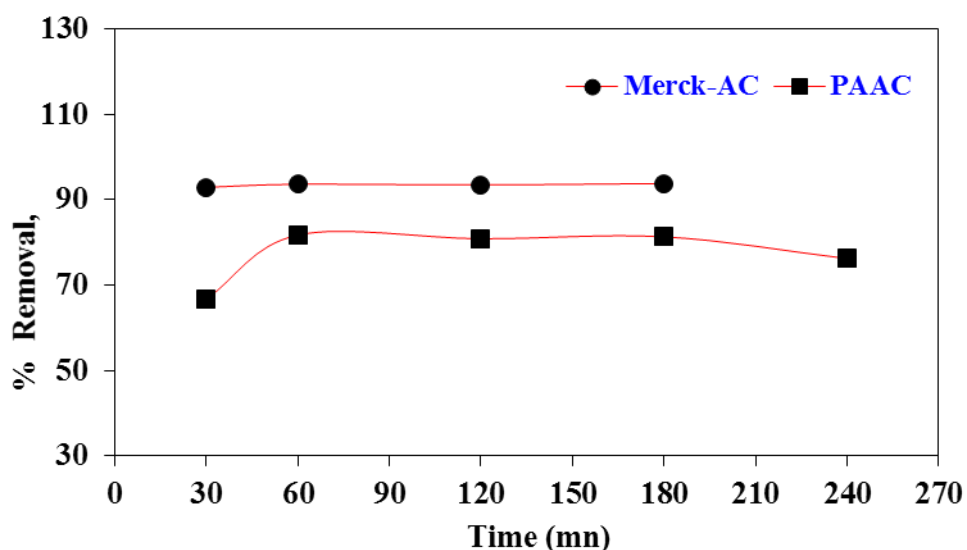


Figure 2: Contact time effect on Phenol adsorption onto both considered adsorbents.

pH Effect

As shown in Figure 3, initial pH of the Phenolic solution was varied from 2 to 12, by adding either 0.1 N NaOH or 0.1 N HCl solutions, to assess the effect of pH on phenol adsorption onto the PAAC and Merck AC. The experiments were performed using 8g/L adsorbents dose for a 120-min equilibrium time at room temperature. Higher values of the phenol uptake were observed at lower pH values. Neglected rate has been observed with increasing pH, the uptake efficiency was maximum and slightly affected by pH up to 10 for both adsorbents. The % removal then decreases with increasing pH due to the presence of phenolate.

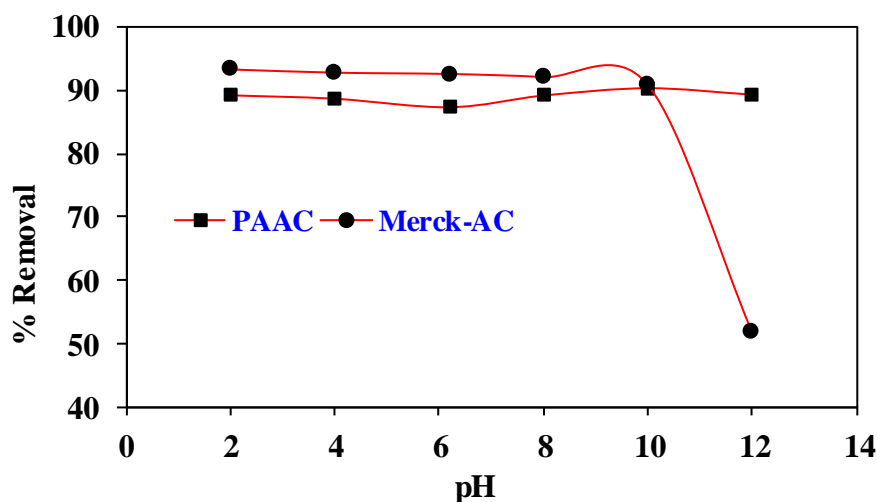


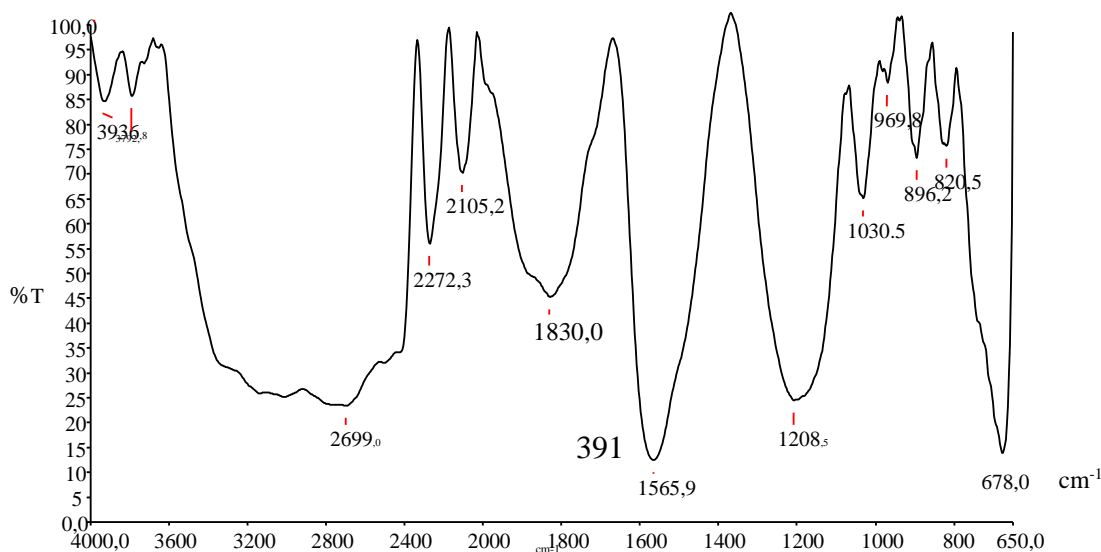
Figure 3: pH effect on Phenol adsorption onto both considered adsorbents.

Adsorbent Dose Effect

Among other parameters influencing the adsorption rate, the adsorbents dose is particularly important. It determines the rate of adsorption and the cost of activated carbon per unit of treated solution. 25 mL of phenol solutions of known concentrations were mixed and agitated at fixed pH with different adsorbent dosages (ranging from 4 to 20 mg/L) for 2 hours. After filtration, the supernatant was analyzed for final concentration determination. The study shows an increase of phenol uptake with increasing dosage of the adsorbent because of the availability of sites until saturation is reached (figure not shown).

Functional Groups Determination

Figure 4 shows the FT-IR spectra of the prepared adsorbents (PERKIN-ELMER Spectrometer) over the range 4000 – 400 cm⁻¹ using KBr pellets in order to determine the functional groups responsible for phenol adsorption. Due



functional groups responsible for phenol adsorption. Due

to their complex structure, the materials used in this study show a number of adsorption peaks. In all cases, spectrum exhibits fine peaks in the frequency range 3500-3200 cm^{-1} corresponding to the hydroxyl group (O-H) stretching vibrations. Intense peak at 2700 cm^{-1} for PAAC may be due to stretching vibrations of the (C-H) group. Another peak in the range of 1600 cm^{-1} due to the stretching vibration of carbonyl group CO, whereas in the case of Merck AC the peak in the range of 1640 cm^{-1} was due to the presence of an amide group. A weak band at 1384 cm^{-1} may indicate the presence of carboxylate ion COO^- . A weak band appears at 1062 cm^{-1} , due to the vibration of the C-O group.

Figure 4: IRFT spectra for the prepared PAAC.

Adsorption Isotherms

The equilibrium adsorption isotherms are of fundamental importance in the design of adsorption systems. In a batch system equilibrium is established between the liquid phase (free solution) and solid phase (adsorbent-attached solute) concentrations and can be described by adsorption isotherms determined at a fixed temperature. In most adsorption systems phenol-adsorbents, Langmuir and Freundlich isotherms have been applied to describe the equilibrium between liquid-solid phases (Benderdouche *et al.*2003, Batzias and Sidiras 2004, Malik 2003, Grag *et al.*2003).

Langmuir Isotherm

The linear plot of $C_{eq}/(q_e)$ versus C_{eq} yields the Langmuir constants b and K (equation 5a). The adsorption isotherms of phenol studied on the chemically activated sawdust compared to Merck powdered activated carbon used as a reference are presented in Figure 5a. Table 2 shows the results obtained from Langmuir fitting to the data obtained for the chemical activations and Merck AC systems. It can be seen that this model describes well the adsorptive properties of the PAAC and Merck AC with correlation coefficients >0.98 for all considered adsorbents. In addition, the Phenol uptake was significantly improved (up to 193 mg/g for PAAC).

$$\frac{C_{eq}}{q_e} = \frac{1}{k b} + \frac{1}{b} C_{eq} \quad (3)$$

Where q_e is amount of solute adsorbed per unit weight of adsorbent (mg/g), C_{eq} is the concentration of solute remaining in solution at equilibrium (mg/ L), b (mg/g) is the maximum adsorption capacity corresponding to complete monolayer coverage and K is a constant related to the energy or net enthalpy.

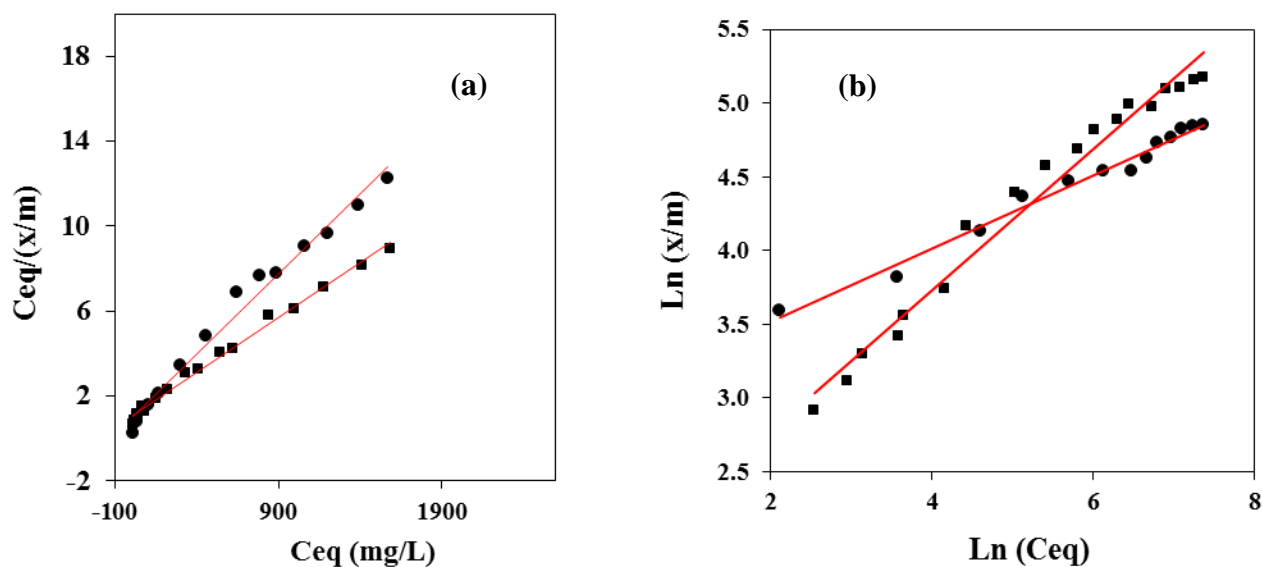


Figure 5: Plot of (a) Langmuir and (b) Freundlich adsorption isotherm of Phenol uptake onto PAAC (•) and Merck-Activated Carbon (■).

Freundlich Isotherm

The Freundlich model has been widely used to characterize the adsorption experiments and the uptake of phenol occurs on a heterogeneous adsorbent surface. It is assumed that the stronger binding sites are occupied first and that the binding strength decreases with the increasing degree of site occupation. The linearised form of Freundlich (equation 4)

$$\log q_e = \log k_f + \frac{1}{n} \log C_{eq} \quad (4)$$

Where K_f and n are the Freundlich constants related to adsorption capacity and adsorption intensity can be obtained from the intercept and slope of $\log q_e$ versus $\log C_{eq}$ plot, shown in table 2. For phenol adsorption, Freundlich fitted plots of the data for PAAC and Merck-AC presented in Figure 5b show linear behaviour, with correlation coefficients of 0.98 and 0.96 for both adsorbents. As shown in Table 2, the chemically activated sawdust exhibits small iodine number compared to the commercial Merck AC. Usually adsorbents with a high iodine number have a high surface area and are suitable for adsorbing small compounds (Noszko 1984).

Adsorbent	Langmuir model			Freundlich model		
	b (mg/g)	K_L (L/mg)	R^2	n	K_f	R^2
PAAC	192.31	0.0051	0.993	1.84	4.58	0.978
Merck-AC	133.33	0.007	0.982	4.02	40.94	0.984

Table 2. Langmuir and Freundlich isotherms parameters for PAAC and Merck-AC

Phenol Adsorption Kinetics

In this study, the applicability of the pseudo-second-order models and the intra-particle diffusion models were tested for the sorption of phenol onto both adsorbents in order to describe the mechanism of mass transfer (Duong 1998, Ho and McKay. 2003, Waranusantigul *et al.* 2003).

Represented by (equation 4), where k_2 is the equilibrium rate constant of pseudo-second-order adsorption (g/(mg min)). The linear relationship of the plot t/q_t versus t and the higher correlation coefficients ($R^2=0.99$) shown in Table 2 indicate clearly that the adsorption of phenol from aqueous solutions on both considered adsorbents obeys well pseudo second-order kinetics. This can be also confirmed by the experimental value of q_{exp} and the calculated one q_{cal} which are rather close.

$$\frac{t}{q_t} = \frac{1}{k_2 q_e^2} + \frac{1}{q_e} t \quad (5)$$

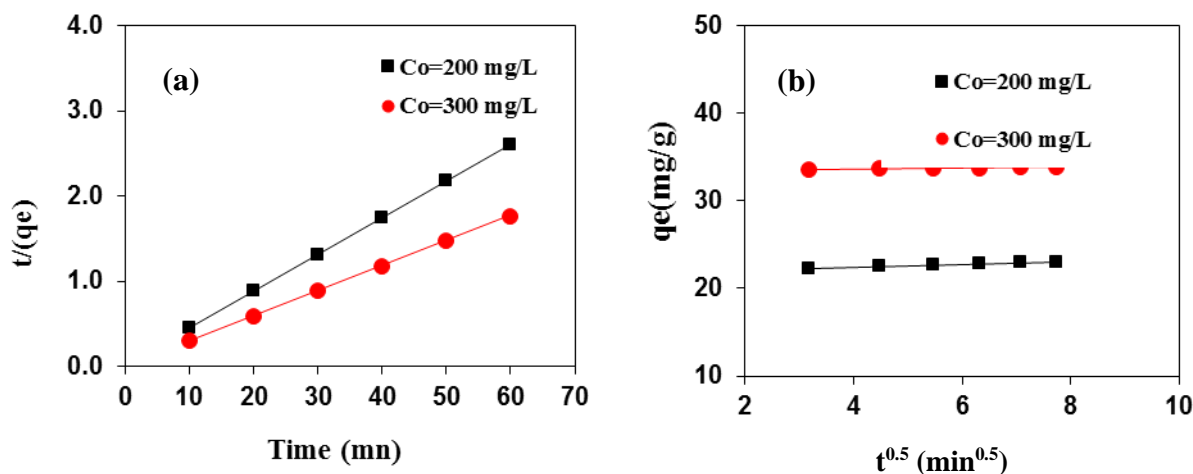


Figure 6: Kinetic Plot of (a) Pseudo-second order and (b) intra particle diffusion of Phenol adsorption onto PAAC and Merck-AC.

Thermodynamic Parameters

Temperature effect study on adsorption process will give an idea about its spontaneity and heat change. Thermodynamic parameters such as enthalpy change (ΔH), Gibbs free energy change (ΔG) and entropy change (ΔS) are very important and can be estimated by using equilibrium constants changing with temperature. These thermodynamic parameters can be estimated using equilibrium constants as a function of T and related by equation 6 (Tan *et al.* 2008, Gupta *et al.*; 2003). K_c values obtained from the Langmuir model at different temperature can be used to compute the standard enthalpy and entropy changes. The slope and the intercept of plot between $\ln K_c$ and $1/T$ are used to evaluate ΔH and ΔS respectively. Values of all thermodynamic parameters are listed in Table 3. The positive value of ΔH indicates the endothermic nature of the

process associated with physical link (Chen *et al.* 2007). Negative values of ΔG shown in Table 3 confirms the spontaneity of the adsorption process of phenol by all three adsorbents and, also that the interface is more efficient with increasing temperature.

$$\Delta G = T\Delta S - \Delta H = -RT \ln k_c \quad (6)$$

Adsorbent	Thermodynamic functions				
	ΔH (kJ/mol)	ΔS (kJ/mol °K)	- ΔG (kJ/mol) at T (°K)		
			298	303	313
PAAC	-4.84	1.39	5.78	5.83	5.84
Merck-AC	2.68	6.61	1.98	1.73	2.15

Table 3. Thermodynamic functions for phenol adsorption onto PAAC and Merck-AC

References

- Zhen-Mao, Ai-Min, L. J. Jian-Guo, C. Quan-xin, Z. 2007. Adsorption of phenolic compounds from aqueous solutions by aminated hypercrosslinked polymers. *Journal of Environmental Sciences* (19): 135–140
- Bestani, B. Benderdouche, N. Benstaali B. Belhakem, M. Addou, A. 2008. Methylene blue and iodine adsorption onto an activated desert plant. *Bioresource technology.* (99): 8441–8444.
- Kaewprasit, C. Hequet, E. Abidi, N. Gurlot, J.P. 1998. Application of Methylene Blue Adsorption to Cotton Fiber Specific Surface Area Measurement: Part I. Methodology. *The Journal of Cotton Science.* (2):164-173
- Benderdouche, N. Bestani, B. Benstaali, B. Derriche, Z. 2003. Enhancement of the adsorptive properties of a desert *Salsola Vermiculata* species. *Adsorption science and technology.* (21): 739-750
- Batzias, F. A. Sidiras, D.K. 2004. Dye adsorption by Calcium chloride treated beech sawdust in batch and fixed-bed systems. *Journal of hazardous materials* (18): 167–174.
- Malik, P.K. 2003. Use of activated carbons prepared from sawdust and rice-husk for adsorption of acid dyes: A case study of acid yellow 36. *Dyes and pigments.* (56): 239–249
- Grag, V.K. Renuka, G. Anu Bala, Y. Rakesh, K. 2003. Dye removal from aqueous solution by adsorption on treated sawdust. *Bioresource technology.* (89): 121–124
- Duong, D. D. 1989. *Adsorption analysts: Equilibria and kinetics*, Series on chemical engineering Imperial College, London.
- Noszko, L. Bota, A. Simay, A. Nagy, L. 1984. Preparation of activated carbon from the by-products of agricultural industry. *Periodica Polytechnica. Chemical engineering.* (28): 293–297

- Ho, Y. S. McKay, G. 2003. Sorption of dyes and copper ions onto adsorbents. *Process biotechnology*. (38): 1047–1061
- Waranusantigul, P. Pokethitiyook, P. Kruatrachue, M.R. Upatham, E. S. 2003. Kinetics of basic dye (Methylene blue) biosorption by giant duckweed (*Spirodella Polyrrhiza*). *Environmental pollution*. (125): 385-392
- Tan, I.A.W. Ahmad, A.L Hameed, B.H. 2008. Adsorption of basic dyes on high-surface area activated coal prepared from coconut husk: Equilibrium, Kinetic and thermodynamic studies. *Journal of hazardous materials*. (154): 337-346
- Gupta, V.K. Ali, I. Mohan, D. 2003. Equilibrium uptake and sorption dynamics for the removal of a basic dye (Basic red) using low cost adsorbents. *Journal of colloid and interface science*. (265): 2228-2230
- Chen, C. Li, X. Zhao, D. Tan, X. Wang, X. 2007. Adsorption kinetic thermodynamic and desorption studies of Th(IV) on oxidized multi-wall carbon nanotubes. *Colloids and surfaces A: Physicochemical Engineering aspects*. (302): 449–454

Quality Enhancement of Pyrolysis Char and Oil from Waste Rubber by Incorporating Sawdust

Wenliang Wang¹ – Jianmin Chang^{1} – Liping Cai² – Sheldon Q. Shi²*

¹ Doctor, College of Material Science & Technology, Beijing Forestry University, Beijing, China.

growth_1989@sina.com

¹ Professor, College of Material Science & Technology, Beijing Forestry University, Beijing, China.

** Corresponding author*

cjianmin@bjfu.edu.cn

² Professor, Mechanical and Energy Engineering Department, University of North Texas, Texas, USA.

liping.cai@unt.edu

² Professor, Mechanical and Energy Engineering Department, University of North Texas, Texas, USA.

sheldon.shi@unt.edu

Abstract

Pyrolysis of biomass and/or used rubber is a promising solution for the recycling of wastes by producing bio-oil, liquid fuel, and casinghead fuel gas and of commercial char as a solid product. This work was aimed at improving the quality of pyrolysis char and oil from waste rubber by adding larch sawdust. The contents of sawdust in rubber were gradually increased from 0%, 50%, 100% and 200% (w%). Two strategies of pyrolysis were carried out: (a) the sawdust and rubber were pyrolysed in fluidized bed reactor separately, then the pyrolysis chars from rubber and sawdust were mixed with different ratios mechanically; (b) the sawdust and rubber were mixed with different sawdust contents and then pyrolysed in a pyrolysis reactor.

Using a thermo-gravimetric (TG) analyzer coupled with Fourier transform infrared (FTIR) analysis, the weight loss characteristics under different contents of sawdust were observed. Using the pyrolysis-gas chromatography (GC)-mass spectrometry, the vapors from the co-pyrolysis processes were collected and the compositions of the vapors were examined. The physical and chemical characteristics of pyrolysis char were investigated.

The following conclusions were drawn from this work:

1. The efficiency of pyrolysis was increased as the percentage of sawdust increased.
2. The incorporation of sawdust significantly improved the pyrolysis oil quality by reducing the polycyclic aromatic hydrocarbons (PAHs) content.
3. The pyrolysis char produced in Strategy (b) was more efficient than that produced in Strategy (a) due to the occurrence of synergistic effect in Strategy (b).

Keywords: Waste rubber, Sawdust, Pyrolysis oil, Pyrolysis char.

Introduction

Used tire disposal has been a growing issue all over the world because the complex composition and structure of tire rubber and its additives make it highly resistant to natural degradation. Due to the increasing amounts of rubber waste and limited landfill capabilities, innovative methods of recycling and reuse of waste tires need to be developed. Numerous efforts have been made to utilize the used tires effectively and environmentally. A method to use the scrapped tires for leachate drainage layer materials was developed by Edil et al. [2004]. In one of our previous studies, rubber particles were pre-treated by a microwave oven and added into wood particles for fabrication of wood/rubber composites [Xu and Li, 2012]. The results indicated that the mechanical properties and dimensional stability of the wood/rubber composites were improved due to the adding of rubber particles.

Pyrolysis of car-tire shreds is a promising solution for the recycling of used tires by producing mazut, liquid fuel, and casinghead fuel gas and of commercial carbon as a solid product [Kalitko, 2008]. Bernardo et al. [Bernardo, et al. 2012] carried out the experiments for a multistep upgrading of chars obtained in the co-pyrolysis of plastic wastes, pine biomass and used tires. Jin et al. [Jin, et al. 2012] examined the composition and characteristics of permanent gases that evolved during co-pyrolysis of sawdust and waste tires.

Although rubber pyrolysis oil has high calorific values, it is difficult to be converted into fuel oil because it consists mainly of hydrocarbon that has a great amount of PAHs, nitrogen and sulfur. PAHs and nitrogen and sulfur compounds in oil can directly affect its efficiency of combustion in engine and has a negative environmental influence [Cao, et al. 2009]. To increase the efficiency of rubber pyrolysis and improve the value of pyrolysis oils and chars, larch sawdust was incorporated into waste rubber pyrolysis. Our hypothesis was that the incorporation of sawdust into rubber pyrolysis would improve the pyrolysis oil and char quality.

Materials and Methods

Materials. The rubber particles with an average size of 80-90 screen meshes were purchased from Ketai Rubber Scrap Mill, Tianjin, China. Sourced from Small Xing-An Mountain, China, the larch wood was dried and smashed into particles. Using a screen, particles with an average size of 80-100 screen mesh were sorted out. Table 1 presents the composition of the sawdust and rubber used in this study.

Table.1 Proximate analysis and ultimate analysis of waste rubber and Larch sawdust

Materials	Ultimate analysis (w%)					Proximate analysis (w%)			
	C	H	O	N	S	M _{ad} ^a	V _{ad}	FC _{ad}	A _{ad}

Rubber	84.1	6.6	2.44	0.3	1.6	4.70	54.53	26.28	14.49
	0	9		9	1				
Sawdust	53.4	4.6	37.1	0.1	0.0	10.2	71.59	17.35	0.79
	0	4	9	1	0	7			

^a Subscript “ad” stands for air-dried condition.

There were seven kinds of bio-char samples in this study. The contents of sawdust in rubber were gradually increased from 0%, 50%, 100% and 200% (w%). Two strategies of pyrolysis were carried out: (a) the sawdust and rubber were pyrolysed in a fluidized bed reactor separately, then the pyrolysis chars from rubber and sawdust were mixed with different ratios mechanically (0 w%-1, 50 w%-2, 100 w%-3, 200 w%-4); (b) the sawdust and rubber were mixed with different sawdust contents and then pyrolysed in a pyrolysis reactor (0 w%, 50 w%, 100 w%, 200 w%).

Methods. Using a special connection manner, the NETZSCH STA449F3 thermo-gravimetric analyzer was coupled with Bruker TENSOR 27 Fourier transform infrared analyzer (TG-FTIR). With a flow rate of 50 mL/min and a heating rate of 10°C/min, nitrogen was used as a protection gas in the chamber. The pyrolysis temperature ranged from 30 to 900°C. During the experiment, the FTIR mode number of 4000-600/cm, 4-time scans/s and a resolution of 1/cm were used.

The CDS 5150 pyrolyzer coupled with GCMS-QP2010Plus gas chromatography-mass spectrometry (Py-GC/MS) was used to observe the weight loss characteristics of the heat under different mixtures of sawdust/rubber. GC/MS had EI source, DM-5 (60m×0.25mm×0.25µm) and NIST08 MS data base. A heating rate of 20°C/s, a temperature of 600°C and a time-duration of 10 s were used for Py. An inlet temperature of 250°C, a He gas flow rate of 1.0 mL/min and a flow split-ratio of 100:1 were used for GC. A heating schedule was pre-set as: the temperature remained at 50°C for 5 min, increased to 250°C at a rate of 10°C/min and then remained for 15 min. A junction temperature of 250°C, an ion temperature of 200°C, an EI source electron energy of 70eV and a scan range of 40-450 u were used in this study.

The chars obtained in the pyrolysis experiments were carbonized particulate residues impregnated with the pyrolysis oil. A solvent extraction (CH₂Cl₂) was performed using the Soxhlet method for 6 h. And then a demineralization procedure was performed in order to decrease the ash content of the chars with 1 M HCl for 1 h. A KOH activation procedure was carried out to increase the surface area of the chars. The ash content of bio-chars was detected by the ASTM standard of D 1726-84 Standard Test Method for Chemical Analysis of Wood Charcoal.

Results and Discussion

TG and DTG analysis

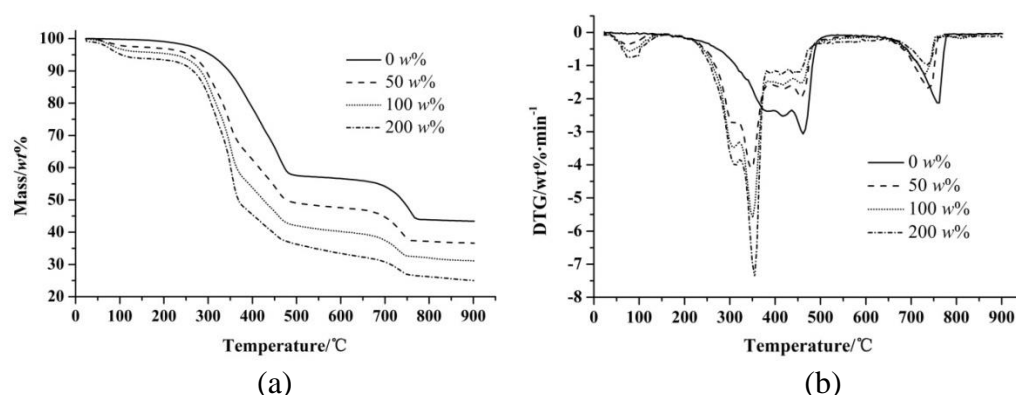


Fig.1 TG (a) and DTG (b) curves of pyrolysis of waste rubber modified by adding woody biomass

(Sawdust contents: 0 w%, 50 w%, 100 w%, 200 w%)

(1) Fig.1(a) shows that there were four stages in the pyrolysis process: pre-pyrolysis stage (30-270°C), principal pyrolysis stage (270-480°C), small molecular gas generation stage (480-750°C) and ash degradation stage (750-900°C). When 0 w%, 50 w%, 100 w% and 200 w% sawdust was added, the final residual carbon (900°C) was 43.4 w%, 36.6 w%, 31.1 w% and 24.9 w%, respectively, indicating that the incorporation of sawdust significantly increased the pyrolysis efficiency.

(2) Fig.1(b) shows that the weight loss rate reached its highest values between 270 and 480°C. The adding of sawdust reduced the maximum weight loss temperatures. The higher the sawdust content in the rubber, the higher the rates of weight loss were obtained. It was revealed that the adding of sawdust accelerated the vapor release in the samples, resulting in a reduced residual carbon.

FTIR analysis

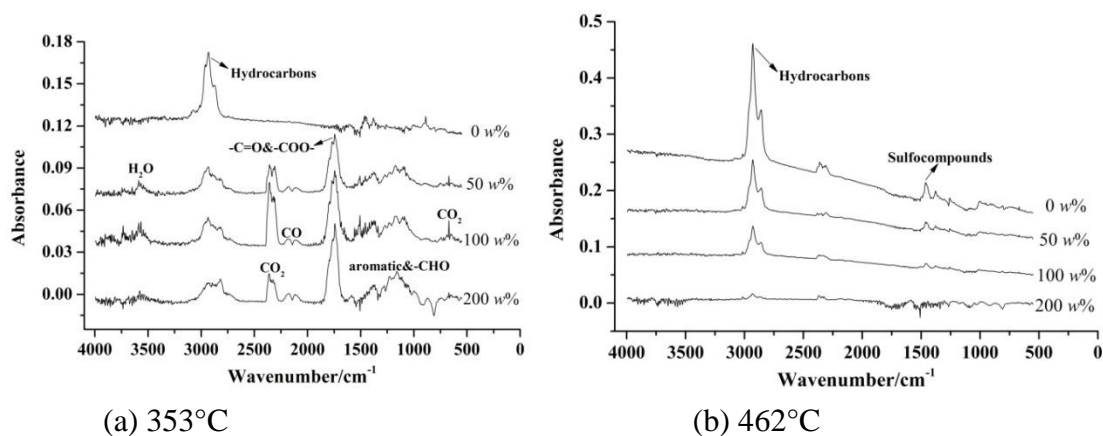


Fig. 2 FTIR spectra of pyrolysis of waste rubber modified by woody biomass (Sawdust contents: 0 w%, 50 w%, 100 w%, 200 w%)

- (1) The peaks of the four samples were found at the temperatures of 353°C and 462°C. Sawdust played a leading role at the temperature of 353°C in the pyrolysis process. Rubber played a primary role at the temperature of 462°C in the pyrolysis process.
- (2) The oxygen free radicals accelerated the decomposition of macromolecular substances in rubber, leading to an easier conversion from the hydrocarbons to oxygen compounds. In addition, the vibration peaks of sulfur compounds were detected.

Py-GC/MS analysis

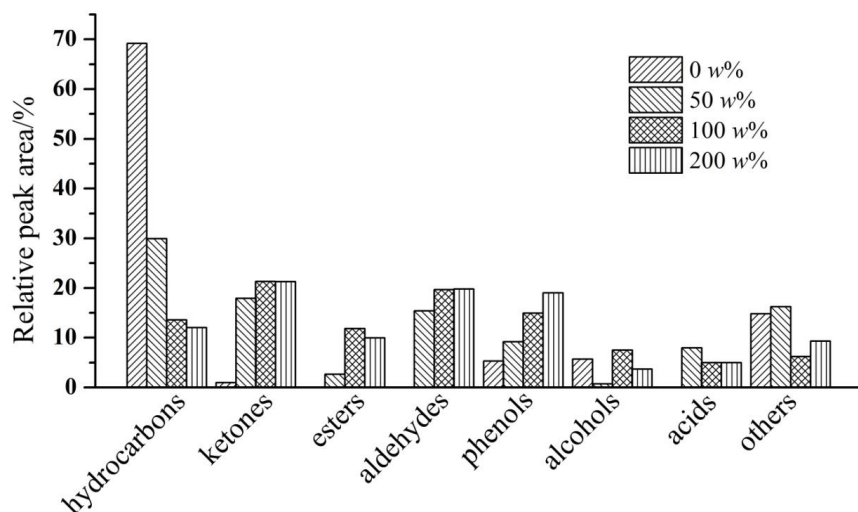


Fig. 3 The component distribution of pyrolysis vapors (Sawdust contents: 0 w%, 50 w%, 100 w%, 200 w%; Others: nitrogen and sulfur compounds)

- (1) The thermal vapor from rubber was mainly composed of hydrocarbons and small amounts of nitrogen and sulfur-containing materials. While the sawdust content increased, a rapid reduction in hydrocarbon content and the increase in contents of phenolic, ketones, aldehydes, acids and esters substances were observed. When 100 w% sawdust was added into the rubber, the contents of nitrogen and sulfur compounds were significantly reduced.
- (2) It can be seen that when 100 w% sawdust was added, although the hydrocarbon content in the pyrolysis vapor was reduced, the nitrogen and sulfur compounds were also significantly reduced, resulting in a considerable improvement in pyrolysis vapor quality.

Physical properties of pyrolysis oils and chars

Table 2 Properties of pyrolysis oils and chars

Samples	Bio-oils			Bio-oils yield/%	Bio-chars yield/%
	pH(20°C)	Moisture content/%	Kinetic viscosity(20°C) / (mm ² ·s ⁻¹)		
0 w% ^a	7.75	1.24	16.89	22.55	26.70
50 w% ^a	3.85	33.87	12.14	28.39	21.55
100 w% ^a	4.01	27.29	12.11	32.51	25.02

200 w% ^a	3.00	20.26	9.68	30.98	17.74
---------------------	------	-------	------	-------	-------

^a Sawdust contents: 0 w%, 50 w%, 100 w%, 200 w%.

(1) The yield of bio-oils and bio-chars reached the maximum when the sawdust content was 100 w%.

(2) After the sawdust was added, the pyrolysis-oil presented a strong acid owing to the generation of formic acid and high moisture contents, leading to an increase in pyrolysis oil yields.

Demineralization of bio-chars

Table 3 Ash content of the char samples before and after the extraction and activation

samples	Before extraction	After extraction	After activation
0 w% ^a	28.70	13.19	16.18
50 w% ^a	22.68	7.72	10.36
100 w% ^a	23.68	8.03	10.02
200 w% ^a	18.16	5.30	7.38
50 w%-1	22.43	10.66	12.72
100 w%-1	19.31	9.09	11.08
200 w%-1	16.27	7.40	9.33

^a Sawdust contents: 0 w%, 50 w%, 100 w%, 200 w%.

The ash content in bio-char of rubber was higher than the bio-chars after adding sawdust. After extraction with HCl, the ash content in bio-chars decreased significantly. But after activation of KOH activation, the ash content in activation chars was increased because some volatiles released in the process of activation.

Yields of bio-chars after demineralization and activation chars

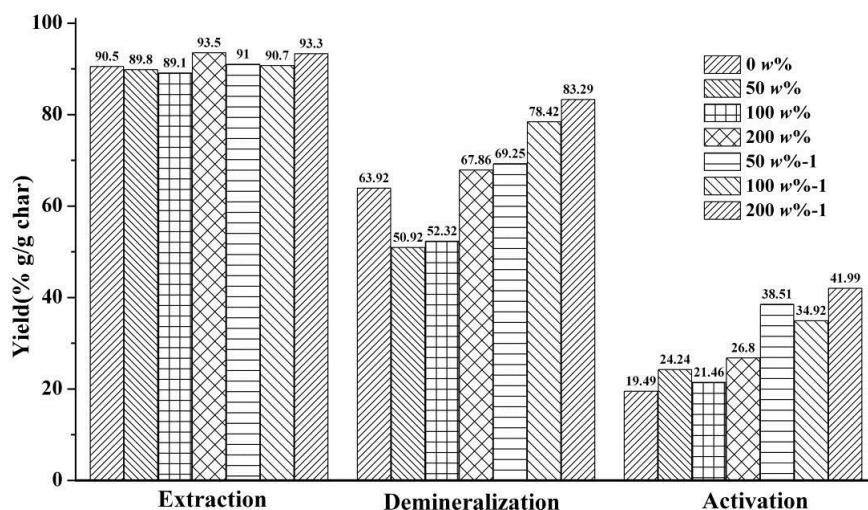


Fig. 4 Yields of bio-chars after demineralization and activation chars

The extraction yields obtained from different samples showed that about 10% residual bio-oils were eliminated. The demineralization yields showed that much more minerals (ash) were desorption in strategy (b). The activation yields showed that lower yields obtained in strategy (b) than strategy (a).

Conclusions

1. The percent of sawdust in the mixture had a great influence on the yield of pyrolysis oil and elemental composition. The higher the ratio of sawdust/rubber was used, the higher the efficiency of pyrolysis so that less ash was obtained.
2. A extraction, demineralization and activation procedures were successfully applied for biochars obtained from pyrolysis of different sawdust content in rubber.

Acknowledgements

The authors are grateful for the financial support from the Specialized Research Fund for the Doctoral Program of Higher Education of China (20130014110015) and the National High Technology Research and Development Program of China (863 Program, 2012AA101808-06)

References

- [1] Bernardo M, Lapa N, Goncalves M, Mendes B, Pinto F, Fonseca I, Lopes H. 2012. Physico-chemical properties of chars obtained in the co-pyrolysis of waste mixtures. *J Hazard Mater*, 219-220: 196–202.
- [2] Cao Q, Jin LE, Bao WR, Lv YK. 2009. Investigations into the characteristics of oils produced from co-pyrolysis of biomass and tire. *Fuel Process Technol*, 90: 337–42.
- [3] Edil TB, Park JK, Kim JY. 2004. Effectiveness of scrap tire chips as sorptive drainage material. *J Environ Eng*, 130: 824–31.
- [4] Kalitko VA. 2008. Steam-thermal recycling of tire shreds: Calculation of the rate of explosion-proof feed of steam. *J Eng Phys Thermophys*, 81: 781–6.
- [5] Jin LE, Wang LL, Su L, Cao Q. 2012. Characteristics of gases from co-pyrolysis of sawdust and tires. *Int J Green Energy*, 9: 719–30.
- [6] Xu M, Li J. 2012. Effect of adding rubber powder to poplar particles on composite properties. *Bioresour Technol*, 118: 56–60.

Optimizing Urea Concentration for Woody Biomass Pretreatment

Amy Falcon and Jingxin Wang

Abstract

Biomass pretreatment is one of the major key techno-economic factors affecting the yield and economics of bioenergy production. Ammonia pretreatment of lignocellulosic materials usually yields optimal hydrolysis rates due to the ammonia reacting with the lignin and also causing the decrystallization of cellulose. Using urea to catalyze the hot water extraction process of woody biomass has the potential to enhance the separation process, thus allowing for easier conversion into downstream products. Urea contains two parts ammonia, thus when urea is broken into its component chemicals under high temperatures, it can be utilized for the same purposes as ammonia. Response surface modelling is used to optimize the urea concentration for maximum sugar yield. Temperature, holding time, and urea concentration are varied from initial starting points (temperature: 160°C-180°C; holding time: 40-80 minutes; and urea concentration (0-20% (w/w)) with the response surface model covering levels in between. The method of steepest ascent is used to extrapolate the maximum concentration outside of the initial ranges. Pretreated materials were analyzed according to the National Renewable Energy Laboratory (NREL) Analytical Procedures for the determination of structural carbohydrates and lignin, and sugar yields were tested at the USDA Forest Products Laboratory.

Keywords: woody biomass, chemical pretreatment, urea, sugar yield

Amy K. Falcon
West Virginia University
Division of Forestry & Natural Resources
P.O. Box 6125
Morgantown, WV 26505
304-293-0041
aeverman@mix.wvu.edu

Jingxin Wang
West Virginia University
Division of Forestry & Natural Resources
P.O. Box 6125
Morgantown, WV 26505
304-293-7601
jxwang@wvu.edu

Life-Cycle Inventory Analysis of Bioproducts from a Modular Advanced Biomass Pyrolysis System

Richard Bergman^{1*} -- *Hongmei Gu*²

¹ Research Forest Product Technologist, U.S. Forest Service Forest Products Laboratory, Madison, Wisconsin, USA

**Corresponding author*

[*rbergman@fs.fed.us*](mailto:rbergman@fs.fed.us)

² Forest Product Technologist, U.S. Forest Service Forest Products Laboratory, Madison, Wisconsin, USA

Abstract

Expanding bioenergy production has the potential to reduce net greenhouse gas (GHG) emissions and improve energy security. Science-based assessments of new bioenergy technologies are essential tools for policy makers dealing with expanding renewable energy production. Using life cycle inventory (LCI) analysis, this study evaluated a 200-kW_e modular advanced biomass pyrolysis system, referred to as the Tucker renewable natural gas (RNG) unit. Similar to pyrolysis systems except no bio-oil is produced, the Tucker RNG unit converts forest and woody residues at high temperatures in an extremely low oxygen environment to synthesis gas (syngas) and biochar. Mass and energy balances, cumulative energy consumption, and LCI flows including environmental outputs were determined. Feedstock consumption for the Tucker RNG unit was estimated at 263 kg/h of whole-tree coniferous micro-chips at 8% moisture content. A 1-h system run test was done to collect production data and sample products. The Tucker RNG unit showed a net energy gain of 12.0 MJ/kg of dry chips from the system when excluding chip transportation. Consequentially, the system had a positive (over 1.0) fossil energy replacement ratio (FERR) of 2.54, which means 2.54 MJ of bioenergy products (syngas and biochar) were produced for every 1 MJ of fossil energy consumed in the system. Including chip transportation of 4,000 km, emission data summarized from the LCI flows through SimaPro modeling showed biomass and fossil CO₂ emissions of 0.43 g and 734 g, respectively, per kilogram of chips processed. The fossil CO₂ emission contributions were as follows: wood chip transportation (48.7%), propane combustion (50.2%) and electricity use (1.1%). A FERR of 2.54 shows, from a life cycle perspective, that the Tucker RNG unit has a net energy gain. Additionally, co-locating the Tucker RNG unit and the wood chip source would substantially lower GHG emissions while saving energy.

Keywords: Life-cycle inventory, biochar, syngas, pyrolysis, wood chips, modular, renewable natural gas

Introduction

Biomass as feedstock for producing bioenergy and bioproducts has raised considerable attention. The U.S. Department of Energy and the U.S. Department of Agriculture are both strongly committed to expanding the role of biomass as an energy source (Perlack et al. 2005), and envision a 30% replacement of the current U.S. petroleum consumption with biofuels by 2030. Biomass fuels and products are one way to reduce the need for oil and gasoline imports while supporting the growth of agriculture, forestry, and rural economies. Also, expanding biofuels and bioproducts production from biomass has the potential to reduce net greenhouse gas (GHG) emissions and improve local economy and energy security. The 2007 Energy Independence and Security Act (EISA) sets aggressive goals for moving biofuels into the marketplace to reduce the nation's dependence on foreign sources of energy and reduce greenhouse gas emissions by increasing the supply of renewable fuels from 4 billion in 2006 to 36 billion gallons by 2022 with 16 billion gallons being cellulosic biofuel (EISA 2007). Cellulosic biofuel refers to renewable fuel derived from any cellulose, hemicellulose, or lignin sources and has life-cycle GHGs that are at least 60% less than the baseline life-cycle GHGs from gasoline or diesel as transportation fuel for the year 2005.

Our study determined the cumulative energy and environmental outputs from a 200-kW_e modular advanced biomass pyrolysis system, which will be referred to in this paper as the Tucker renewable natural gas (RNG) unit. The system uses high temperature conversion (>750 °C) in an extremely low oxygen environment to convert forest thinning and mill residue feedstock into syngas for heat or biofuel and biochar for soil amendment or filtering products after activation. Eventually, the modular unit is expected to be integrated into existing forest industry operations and forest management to assist in environmental and economic sustainability measures. Because of its 20 dry tonne per day production and modular size, the Tucker RNG unit has the potential to be deployed at forest industry facilities of various sizes. Furthermore, the potential to produce high-value activated carbon from treatment residues and mill waste is highly desirable to mills that are unlikely to make investments in new conversion technologies that produce only heat and power.

Method

On a per production unit basis, the present study listed material flow, energy consumption, and emissions for the Tucker RNG unit production process. Primary data were collected from a 1-h continuous run of the Tucker RNG unit located in Locust, NC, using micro wood chips (<13 mm in the largest dimension) made and shipped from a lumber mill located in St. Regis, MO. Secondary data were collected according to CORRIM guidelines (CORRIM 2010) from peer-reviewed literature. Mass and energy balances for the system were then constructed using a spreadsheet algorithm. Energy present in the incoming feedstock was not considered in the analysis. With the material and energy inputs and reported emissions, the life-cycle inventory (LCI) model for of the Tucker system was built in SimaPro 8 to estimate the environmental outputs and cumulated energy consumption (PRé Consultants 2014). LCI can be thought of as a detailed mass and energy balance with all inputs and outputs accounted for.

Scope. The goal of this study was to find the emission profile and determine the mass and energy balances for the Tucker RNG unit using LCI analysis. To achieve this goal, we modeled the gate-

to-gate LCI for the Tucker RNG unit thermochemical process according to the ISO 14040 and 14044 standards (ISO 2006a; 2006b). In the analysis, the input gate begins with the chips leaving the lumber mill and being transported to the conversion site in North Carolina for processing. The trees chipped for feedstock were small-diameter logs from National Forests with a mix of conifer species dominated by lodgepole pine (*Pinus contorta*), Douglas fir (*Pseudotsuga menziesii*), and ponderosa pine (*Pinus ponderosa*). The output gate is at the outlet of Tucker RNG unit with the two primary output products, syngas and biochar. Before feeding the Tucker RNG unit, the chips were re-dried to ~8% moisture content (MC) to remove the ambient moisture absorbed during transportation and storage. However, this re-drying process was not considered in the LCI modeling since the re-drying of the feedstock will not be necessary if the pyrolysis unit co-locates with a lumber mill, which is the configuration considered in this study.

Eventually, this analysis will become part of an our overall project goal that covers the cradle-to-grave environmental impact for the Tucker RNG unit from forest extraction to wood chip processing and transportation, to thermochemical conversion, to downstream products' transportation and end use. In addition, the LCI data developed in this project will help conduct a comparative life-cycle assessment (LCA) for secondary biobased products to their corresponding fossil fuel-based commercial products in terms of the cumulative energy consumption, air pollution, water pollution, solid waste production, and climate change impacts. These secondary products will include electricity generated from the synthesis gas (syngas) and activated carbon manufactured from the biochar. The primary data for developing the LCI model of the Tucker RNG unit were collected from a 1-h continuous run in March 2013 in Locus, NC. Secondary LCI data used in the study including electricity and natural gas as a proxy for propane have already been developed by previous LCI work. We were able to use these (secondary) LCI data because the developed data are found in the US LCI database (NREL 2014) as part of the LCA modeling software, SimaPro 8 (PRé Consultants 2014). The energy densities for the two gases were considered when inputting the data into the LCI model.

Functional unit. Functional unit is the reference unit used to quantify the environmental performance of a product system. It is also a reference related to the inputs and outputs. The functional unit for the present study is 1 kg of whole tree chips at 10% MC being processed in the Tucker RNG unit. Material flows, energy use, and emission data are standardized based on the functional unit within the system boundaries. The GHG emissions as well as other emissions and raw material consumption will be allocated based on the mass content of the two primary products from system; i.e., mass allocation.

Unit process. Tucker RNG unit is a production-oriented advanced pyrolysis system comprised of two sections (i.e., chambers), Mable (active) and Ethyl (passive) (Figure 1). The system is engineered to maximize methane-rich syngas output in an extremely low oxygen reaction chamber at a temperature between 760 and 870 °C. The Mable section is heated by three propane burners providing continuous heating. When all the operating parameters are within the specified ranges and the system has stabilized, feedstock is fed in by an air-locked auger system to the Mable section. The injector feeding system is designed to prevent backflow from the Mable chamber as the system operates under a low-positive pressure. Temperature in Mable section is 870 °C. The gasified volatiles and solids generated from the feedstock leave Mable and enter into the Ethyl passive section (Figure 1), which operates at approximately 760 °C using the

residual heat from Mable section passed through the three pipes connected between the two sections. The feedstock entering Ethyl moves through two 3.0-m-long retorts for a total of 6 m of retort or condensing, whereby additional conversion of higher molecular chain gases to methane occurs from using a catalyst in the retort. The temperature measured at the entry of Ethyl is ~760 °C and ~510 °C at the exit of Ethyl. The residence time for the feedstock in the Tucker RNG unit is estimated at 3 minutes for the complete reaction (1.5 minutes/section).

Syngas leaving the passive section is cooled in a tar condenser. The tar condenser has twin screws to remove buildup of tar from the condensing caused by the cooling of the syngas. The tar condenser uses potable water for cooling. Water temperature and flow rate can be monitored during operations. The residual tars from the condenser are then augured back into a smaller retort inside the Mabel section to generate a low-Btu syngas that could be used to augment the propane gas currently used to heat the Mabel section. This occurs in conjunction with the production of the product syngas, a medium-Btu syngas. After cooling, the medium-Btu syngas goes through a misting chamber (Figure 1) that removes oil and tars before leaving the Tucker system for outside gas storage. The two primary products from the system, biochar and medium-Btu syngas are collected at separated outlets. The medium-Btu syngas is stored in a gas tank with very little compression although the syngas can be compressed to higher pressures as needed. After forced air cooling to remove heat from the biochar and thus prevent instantaneous combustion, the biochar is collected in a bin outside the building housing the Tucker RNG unit. The flue gas from the burning propane is emitted to the atmosphere without cooling or filtering.

Project Limitations. Human labor and the manufacturing LCA of the machinery and infrastructure were outside the system boundaries and therefore not modeled in this analysis.

Cut-off Rules. If the mass/energy of a flow is less 1% of the cumulative mass/energy of the model flow it may be excluded, provided its environmental relevance is minor. This analysis included all energy and mass flows for primary data.

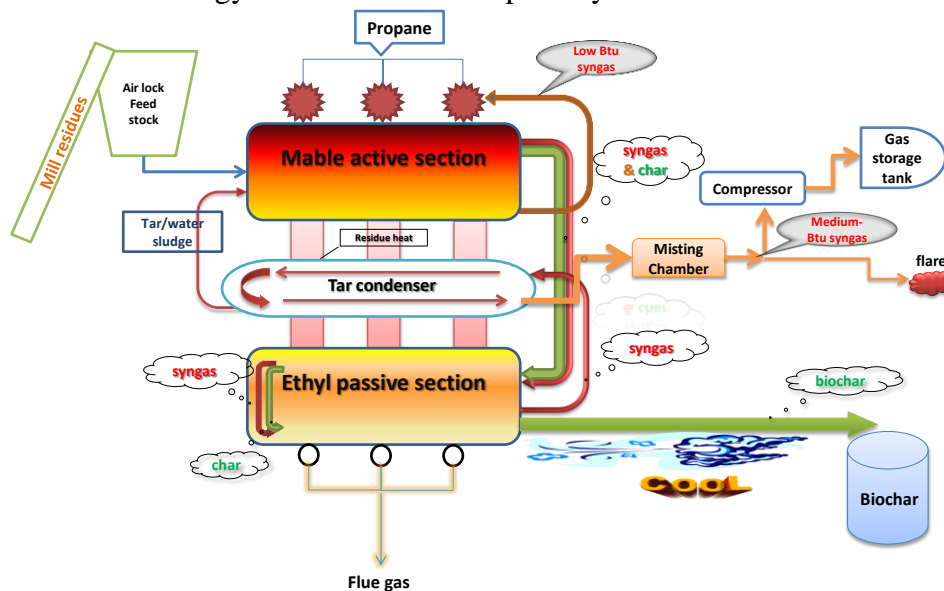


Figure 40. Process flow diagram for Tucker advanced pyrolysis system.

System boundary. Defining the system boundary selects the unit processes to be included in the system. Based on our goal to determine the cumulative energy consumption and emissions associated with the Tucker RNG unit, we drew our system boundary to include the entire conversion process within the Tucker RNG unit and the materials and energy inputs into the Tucker RNG unit. The thermochemical process includes feedstock conveyance, active reacting, passive reacting, condensing, tar cracking, cooling, collecting, and storing. Figure 2 shows the system boundary defined for this gate-to-gate LCI study. Transportation of the feedstock from the lumber mill to the Tucker RNG unit was not included when calculating the mass and energy balances of the Tucker RNG itself but was included when reporting air and water emissions.. Two system boundaries were considered. One, shown as solid line in Figure 2, is the cumulative system boundary including both on- and off-site emissions for all material and energy consumed by Tucker RNG unit. Fuel and electricity use for the converting process were included in the cumulative boundary to calculate the total emissions. The other (on-site) system boundary, shown as dotted line in Figure 2, covered emissions occurring only within the Tucker RNG unit. The off-site emissions include the grid electricity production, transportation of feedstock to the Tucker processing site, and fuels produced off-site but consumed onsite.

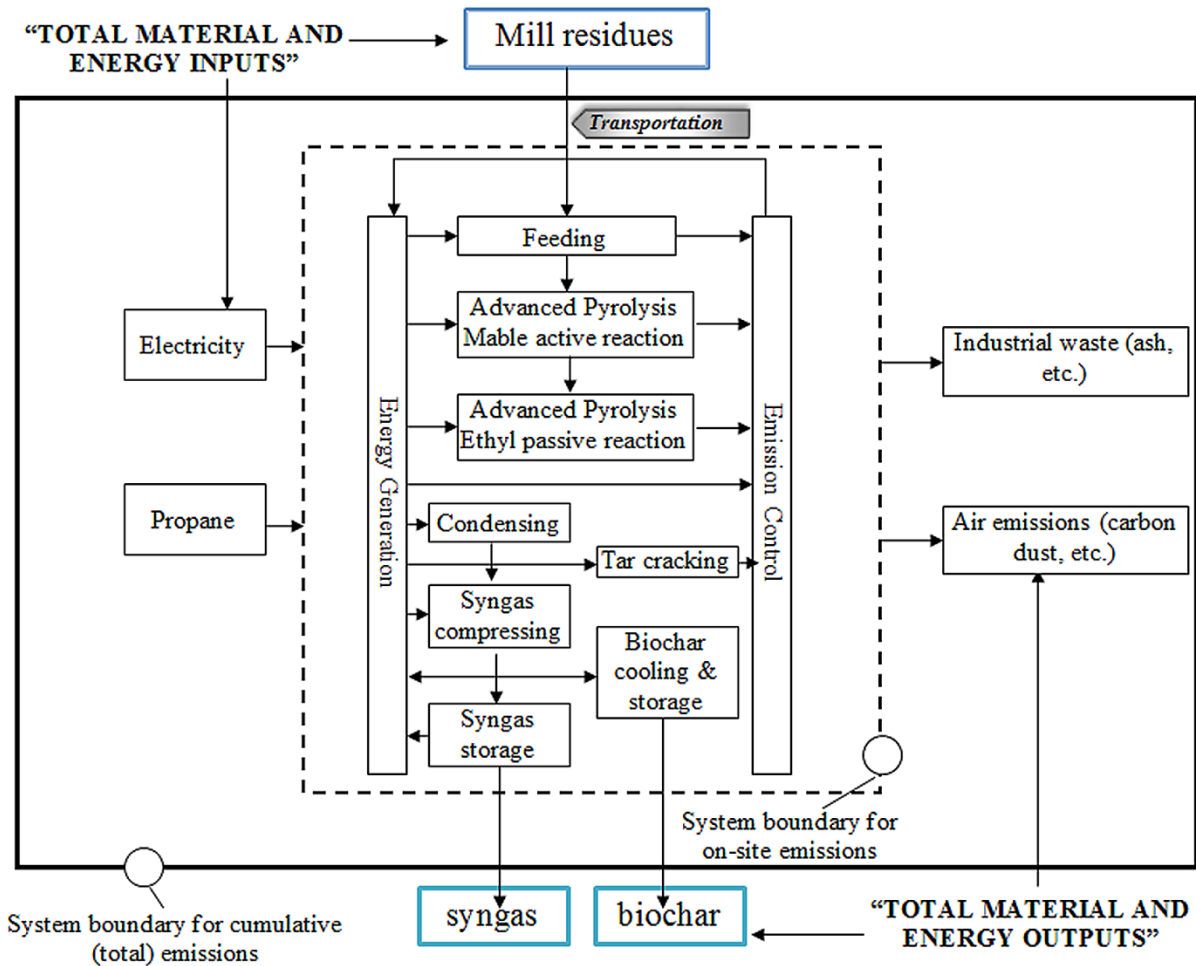


Figure 41. System boundaries for Tucker renewable natural gas unit.

Results and Discussion

The Tucker RNG unit is a modular, high-temperature pyrolysis system capable of converting multiple organic feedstocks into medium-BTU gas and biochar. For our study, the biomass feedstock was from whole trees chipped at a lumber mill in Montana, dried to ~10% MC, and shipped to North Carolina. In this analysis, wood chip transportation was not included in the inputs and outputs of the Tucker RNG unit and not for the net energy gain calculation as well. However, wood chip transportation was included when reporting cumulative energy consumption and environmental outputs.

The energy and mass balances account for the energy and mass flowing across the system boundary. This includes the parasitic loads to operate the input feeder, augers, and fans. Table 1 provides the mass and energy inputs into the Tucker system within a 1-h continuous operation. The feeding system on the Tucker RNG unit operated at 263 kg/h for wood chips. During the 1-h run, a computer monitored flow for propane, product (syngas) gas, and flue gas, pressure of product gas, temperatures at various locations, and power consumption by various electrical components. Table 1 shows the propane consumption and electricity use calculated during the 1-h run.

Table 7. Inputs into the Tucker advanced pyrolysis unit for 1-h operation.

MASS and ENERGY INPUTS				
Source	Mass (kg)	Energy (MJ/kg)	Total Energy (MJ)	Percent (%)
Feedstock	263	18.41 ⁽¹⁾	4,850	72.0
Propane	36.4	51.83 ⁽²⁾	1,880	28.0
Total thermal Input			6,730	100
Parasitic				
Electrical power	2.87 kWh	3.6 (MJ/kWh) ⁽²⁾	10.3	

⁽¹⁾ As measured from wood chips with 8.19% moisture (wt).

⁽²⁾ Propane and electricity unit energy HHV values are taken from Franklin Database. <http://www.fal.com/lifecycle.htm>.

Table 2 gives the mass and energy outputs from the system after the 1-h run. Heat loss to the atmosphere was not measured and is accounted for by the difference in energy in and out. Samples of biochar and syngas were collected to conduct the analysis for the constituents and chemical energy content. The ASTM-D3588 standard test was conducted on the syngas to obtain the heat of combustion value of 522 Btu/ft³. It was then converted to 18.0 MJ/kg based on the conversion factor and syngas density calculated from the gas chromatography test (ASTM-D1945) for gas constituents. The proximate analysis was performed on the feedstock and solid product biochar to determine the fixed carbon, volatile matter, and moisture and ash percentages. Then the ultimate analysis was done to provide the composition in percentage weight of the major components in the feedstock and biochar, such as carbon, hydrogen and oxygen, as well as sulfur and nitrogen after complete combustion of the samples. The high heating value (HHV) of the feedstock and biochar shown in Tables 1 and 2 were from the proximate and ultimate analysis.

Table 8. Outputs from the Tucker advanced pyrolysis unit of 1-h run.

MASS and ENERGY OUTPUTS					
Source	Mass (kg)	Mass (%)	Energy ⁽³⁾ (MJ/kg)	Total Energy (MJ)	Percent
Syngas	172	65.4	18.0	3,090	64.1

*Proceedings of the 57th International Convention of Society of Wood Science and Technology
June 23-27, 2014 - Zvolen, SLOVAKIA*

Tar, oil/water	54.3	20.6	10.5	572	11.9
Biochar	36.4	13.8	31.7	1,160	24.0
Total	263	99.8		4,820	100.0

⁽³⁾ Unit energy values for biochar and tar oil/water were obtained from the proximate and ultimate analysis, syngas unit energy value obtained from ASTM-D1945/3588 standard tests.

Net energy gain or energy balance is calculated as the difference between the energy contents in the output products and the fossil fuel energy consumed to produce the products. The total output energy in Table 2 from Tucker RNG unit is 4,820 MJ. To produce this amount of bioenergy, it required a total of 1,890 MJ of fossil fuels (propane and electricity) as shown in Table 1. This gives a net energy gain of 2,930 MJ for the total input feedstock of 263 kg, as shown in Table 3. Converting to 1 oven-dry kg (OD-kg) feedstock of wood chips to be processed by the Tucker RNG unit into syngas and biochar, the net energy gain is 12.0 MJ/OD kg chips (Table 3). Fossil Energy Replacement Ratio (FERR) is defined as the ratio of bioenergy output from the system over the fossil energy input into the system. For the Tucker RNG unit, the FERR is 2.54, which means for every 1 MJ of fossil fuel input into the system, there is 2.54 MJ of bioenergy output produced. This indicates 1.54 times more MJs are available in the bioenergy produced than in the fossil fuels that went into producing these bioenergy products. Therefore, on the basis of fossil energy inputs, using propane and grid electricity is an effective use of a finite energy resource.

Table 9. Net energy gain from Tucker RNG unit pyrolysis process.

NET ENERGY CALCULATION				
Total energy gain	Unit net energy gain	Fossil energy input into the system	Bioenergy output from the system	Fossil energy replacement ratio
(MJ)	(MJ/OD kg)	(MJ/OD kg)	(MJ/OD kg)	(MJ/MJ)
2,920	12.0	7.79	19.8	2.54

Other research has shown support of such efficiency for bioenergy conversion over fossil fuel operations. Zaines and others (2013) reported the Energy Return on Investment (EROI = fuel energy output/life cycle energy in) for miscanthus and switchgrass to convert into biofuel for bioelectricity use at about 2.5 to 4.5 MJ/MJ. Gaunt and Lehmann (2008) showed a net energy gain for a slow pyrolysis-based bioenergy system for biochar and energy production. They found an energy yield as syngas of 2–7 MJ/MJ when biochar is retained for soil amendment and an increase energy yield to 3–9 MJ/MJ when biochar is used as an energy source instead. The avoided emissions are between 2 and 5 times greater when biochar is applied to agricultural land than used solely for fossil energy offsets. To compare with the production of ethanol from corn, the corresponding energy yield is about 0.7–2.2 MJ/MJ according to Patzek (2005) and Metzger (2006). Steele and others (2012) reported an EROI of 2 for cradle-to-grave production and use of bio-oil derived from southern pine whole tree chips.

Gate-to-gate LCI model for 1-kg wood chips processed in Tucker RNG unit was constructed in the SimaPro 8 LCA modeling software (PRé 2014). Table 4 shows the cumulative energy consumption within the system boundary (Figure 2) from the input gate of wood chips leaving the lumber mill to the output gate of bioenergy (syngas) and bioproduct (biochar) produced from Tucker RNG unit. A total of 12.6 MJ was consumed for 1-kg of feedstock thermochemical conversion. We used natural gas as a proxy in SimaPro for modeling the gas phase of propane combustion to generate heat for the endothermic reaction. This is the closest approximation within the U.S. LCI database for propane combustion reaction. About 59% of the energy was

used to heat up the active reaction chamber to the high temperature of 870 °C. Crude oil provided almost 38% of the cumulative energy needed and was primary due to chip transportation. Chip transportation is included in our system boundary (Figure 2). For this study, feedstock was transported 4,000 km as part of the larger project examining feedstock from the Rocky Mountain region. This transportation distance is only used for this initial study and model set up. The model can be easily updated with any transportation distance and integration. A more realistic deployment of the system would be closer to the feedstock supply, potentially co-located at the sawmill, which would eliminate the energy use and GHG emissions from chip transportation.

Table 10. Cumulative energy calculated from the SimaPro LCI modeling for 1-kg of wood chips.

Substance	Unit	Mass allocation			Total	NG HHV (MJ/m ³)	HHV (MJ/kg)	Energy	
		Syngas	Biochar					(MJ)	(%)
Coal, 26.4 MJ per kg	kg	0.00962	0.00204	0.0117	38.4	26.2	0.305	2.4	
Gas, natural/m ³	m ³	0.16048	0.03397	0.1945					
Uranium oxide, 332 GJ per kg, in ore	kg	2.12E-07	4.48E-08	2.56E-07	332,000	45.5	0.085	0.7	
Oil, crude	kg	0.08605	0.01822	1.04E-01					
Total							12.60	100	

Table 5 allocates the environmental outputs from 1 kg of the feedstock processing to the two primary products – syngas and biochar based on their mass allocation. Emission data summarized through SimaPro modeling for biogenic and fossil carbon dioxide were 0.43 g and 735 g, respectively, per kilogram of chips used. The total air emission from the system is 747 g/kg of wood chips, of which 98% is fossil CO₂ emitted primarily from fossil fuel use in the heating of the reaction chamber and transportation of the feedstock. From the SimaPro model analysis output, we also identified the process contribution to the total fossil CO₂ emissions, chips transportation (48.7%), propane combustion (50.2%), and electricity use (1.1%). Biogenic CO₂ is extremely low because no biomass is consumed on-site to aid in the thermochemical conversion process. In addition, the release of biogenic CO₂ to the atmosphere from burning woody biomass is considered to be equal to the CO₂ absorption by forest regrowth. Therefore, as long as the forest carbon growth is equal or greater than the forest carbon lost through sustainable harvesting practices, burning woody biomass is assumed to be carbon neutral. Suspended solids (unspecified) and chloride generated the highest emissions to water at 45.4 and 35.6 g/kg of wood chips, respectively (see Table 5). Suspended solids (unspecified) and chloride are released during the extraction and production of fossil fuels. Although these environmental outputs are indirect, they are still accounted for, which is standard LCA practice

Table 11. Environmental outputs from thermochemical conversion of one oven-dry kg of wood chips.

Substance	Unit	Mass allocation		Sum	Percent
		Syngas	Biochar		
Air emission					
Carbon monoxide, fossil	g	1.782	0.377	2.160	0.289
Carbon dioxide, biogenic	g	0.358	0.076	0.434	0.058
Carbon dioxide, fossil	g	606.203	128.333	734.54	98.351
Formaldehyde	g	0.000	0.000	2.42E-04	0.000
Methane	g	1.749	0.370	2.119	0.284
Methane, fossil	g	0.233	0.049	0.283	0.038
Mercury	g	1.05E-06	2.22E-07	0.000	0.000
Nitrogen oxides	g	2.308	0.489	2.797	0.374
NMVOC, non-methane volatile organic compounds, unspecified origin	g	0.170	0.036	0.206	0.028
Particulates, > 2.5 um, and < 10um	g	0.055	0.012	0.067	0.009

Particulates, unspecified	g	0.034	0.007	0.041	0.006
Sulfur monoxide	g	0.289	0.061	0.350	0.047
Sulfur dioxide	g	2.923	0.619	3.542	0.474
VOC, volatile organic compounds	g	0.197	0.042	0.239	0.032
Total				746.86	
Water effluents					
Suspended solids, unspecified	g	37.449	7.928	45.377	46.694
Chloride	g	29.414	6.227	35.641	36.675
Chloride	g	8.295	1.756	10.051	10.343
Sodium	g	2.617	0.554	3.171	3.263
Calcium	g	0.546	0.116	0.662	0.681
Lithium	g	0.520	0.110	0.630	0.649
Barium	g	0.512	0.108	0.620	0.638
Total				97.18	

Conclusion

The Tucker RNG unit and other new bioenergy systems show a net energy gain. Based on our analysis of converting 1-kg dry wood chips from whole tree chips into bioenergy products, the Tucker pyrolysis unit produces 2.54 MJ of bioenergy for every 1 MJ of fossil fuel energy inputted into the system. Therefore, the Tucker RNG unit is an energy efficient system and thus will help in providing renewable energy at a distributed scale. In addition, the unit has the potential to assist lumber mills and other manufacturing facilities to manage biomass byproducts and convert them into useful co-products.

New bioenergy systems are becoming important to mitigate climate change impacts by lowering GHG emissions per unit of energy output. As for GHGs, CO₂ is of primary concern. For the Tucker RNG unit, fossil CO₂ was the major air emission and was primarily from burning propane to maintain the endothermic reaction and from burning diesel fuel for chip transportation. Co-locating bioenergy systems to the feedstock source or replacing the propane with syngas or by redesigning the bioenergy system to burn wood will substantially reduce fossil CO₂ and thus lower GHG emissions. As for biogenic CO₂, with the biochar and syngas thermally converted from biomass, the energy values of these two products are roughly related to their carbon contents. Release of this energy by combustion is considered renewable and is largely carbon neutral except for the fossil fuel consumed in their production. If the carbon in the biochar is not burned but rather used as a soil amendment or activated for use in filtering application, the carbon can be equated to the CO₂ sequestered over the long term in soils or landfills. In addition, some energy generated by bioenergy systems (e.g., the Tucker RNG unit) is currently being lost as waste heat. That energy can substitute for fossil fuel energy, especially in feedstock drying. This will further avoid fossil CO₂ emissions in the process. The sum of these effects could provide an even greater reduction of GHG emission than shown in the present study.

For future research, the authors will look at the associated environmental impacts upstream at material resources extraction and downstream at secondary conversion to higher value products of electricity and activated carbon. The authors will also look to characterize the system in its first commercial deployment, which is currently being installed in Charlotte, NC.

Acknowledgement

We thank Richard Tucker and David Barbee (Tucker Engineering Associates) for the technical assistance provided. In addition, the authors especially thank Mark Knaebe and Mark Dietenberger (USDA Forest Service Forest Products Laboratory) and Nathaniel Anderson (USDA Forest Service Rocky Mountain Research Station) for their peer review of this paper. Financial assistance for this research project provided by the U.S. Department of Agriculture (USDA) National Institute of Food and Agriculture Biomass Research and Development Initiative (BRDI) award no. 2011-10006-30357 is gratefully acknowledged. BRDI is a joint effort between the USDA and the U.S. Department of Energy.

References

- CORRIM. 2010. Research guidelines for life-cycle inventories. Consortium for Research on Renewable Industrial Materials, Inc., University of Washington, Seattle. 40 pp.
- EISA. 2007. Legal Reference—Energy Independence and Security Act of 2007. GPO (Government Printing Office).
- Gaunt, J. and J. Lehmann. 2008. Energy balance and emissions associated with biochar sequestration and pyrolysis bioenergy production. College of Agriculture and Life Sciences, Cornell University. *Environmental Science & Technology* 42: 4152–4158.
- ISO. 2006a. Environmental management—life-cycle assessment—principles and framework. ISO 14040. International Organization for Standardization, Geneva, Switzerland. 20 pp.
- ISO. 2006b. Environmental management—life-cycle assessment—requirements and guidelines. ISO 14044. International Organization for Standardization, Geneva, Switzerland. 46 pp.
- Metzger, J. 2006. Production of liquid hydrocarbons from biomass. [*Angewandte Chemie, International Edition*](#) 45: 696–698.
- NREL. 2014. Life-cycle inventory database project. National Renewable Energy Laboratory. Golden, CO. <https://www.lcacommons.gov/nrel/search>. (1 May 2014).
- Patzek, T. and D. Pimentel, 2005. Thermodynamics of energy production from biomass. *Critical Reviews in Plant Sciences* 24:327–364.
- Perlack, P.D., L.L. Wright, A.F. Turhollow, R.L. Graham, R.J. Stokes, D.C. Erbach. 2005. Biomass as feedstock for a bioenergy and bioproducts industry: The technical feasibility of a billion-ton: Annual supply. April 2005. A joint study sponsored by U.S.
- Department of Energy and the U.S. Department of Agriculture.
http://www1.eere.energy.gov/bioenergy/pdfs/final_billionton_vision_report2.pdf

PRé Consultants. 2013. Life-Cycle assessment software package SimaPro 8 Update Instructions. Stationsplein 121, 3818 LE Amersfoort, The Netherlands. <http://www.pre-sustainability.com/simapro-software-update-instructions>

Steele, P., M.E. Puettmann, V.K. Penmetsa, and J.E. Cooper. 2012. Life-cycle assessment of pyrolysis bio-oil production. *Forest Products Journal* 62(4):326–334.

Zaimes, G.G., K.A. Kaminsky, and V.Khanna. 2013. Environmental life cycle evaluation of fast pyrolysis derived drop-in-replacement biofuels. Department of Civil and Environmental Engineering, University of Pittsburgh, Pittsburgh, PA. LCA XIII conference, Orlando, FL. Oct. 1st, 2013.

Improvement of Furfural Production from Concentrated Pre-Hydrolysis Liquor (Phl) of a Kraft-Based Hardwood Dissolving Pulp Production Process

M. Sarwar Jahan Haitang Liu, Hui ren Hu, Yonghao Ni

Abstract

The commercial kraft-based dissolving pulp production process is a good example of an integrated forest biorefinery process. In the kraft based dissolving pulp production process, pre-hydrolysis is carried out prior to pulping to remove hemicelluloses from the lignocelluloses at high temperature and pressure. The main sugars of dissolved hemicelluloses in pre-hydrolysis liquor (PHL) are xylose/xylan that can be a good source of furfural production, which is an important renewable, non-petroleum based platform chemical. For PHL, a furfural yield of 48.4% was obtained with 0.4% sulfuric acid addition at 170 °C in 100 min and a low sugar concentration of 3.5%; while the furfural yield was only 2.3% when the sugar concentration increased to 17.5%. The reaction rate of sugar consumption and furfural destruction in PHL was higher than those of model xylan and xylose systems, which may be due to the side reactions of lignin with sugars and carbonization of oligomeric sugars. In order to minimize these side reactions, the results showed that steam stripping of generated furfural was effective in increasing the furfural yield from the concentrated PHL.

KEYWORDS: Biorefinery, Pre-hydrolysis liquor, Sugars conversion, Acetic acid, Furfural yield, Carbonization rate

M. Sarwar Jahan
Pulp and Paper Research Division,
BCSIR Laboratories, Dhaka,
Dr. Quadrat-iKhuda Road, Dhaka-1205, Bangladesh,
Ph # 8801715078023, Fax# 88028613022, E-mail: sarwar2065@yahoo.co.uk

Haitang Liu and Hui ren Hu
Tianjin Key Laboratory of Pulp and Paper, Tianjin University of Science and Technology,
Tianjin 300457, China

Yonghao Ni
Limerick Pulp and Paper Centre, Department of Chemical Engineering, University of New Brunswick, P.O. Box 4400, Fredericton, NB, Canada E3B 5A3

Electron Microscopic Study of Neat and Hot Water Extracted Aspen Wood by Means of Selective Electron Dense Staining and Immunogold Labeling

Melanie Blumentritt^{1*} –*Stephen M. Shaler*²

¹ PhD Candidate, School of Forest Resources/ Advanced Structures and Composites Center, University of Maine, Orono ME, USA

* *Corresponding author:*

melanie.blumentritt@maine.edu

² Director and Professor School of Forest Resources, Associate Director Advanced Structures and Composites Center University of Maine, Orono ME, USA

shaler@maine.edu

Abstract

Generating renewable fuels and chemicals independent from fossil sources is a major objective of many research areas. Pre-extraction of hemicelluloses from lignocellulosic feedstock has been a research focus during the last decade within the context of lignocellulosic-biorefineries. While a significant amount of research has been conducted studying and optimizing extraction and conversion rates, little attention has been paid to the effects of hemicelluloses extraction on the remaining material, which in the case of wood can be used to produce conventional wood composites (e.g. particle board, OSB, etc.).

In this study we investigate the effect of hot water extraction on the topochemistry and ultrastructure of aspen wood (*Populus spec.*) by means of scanning electron- (SEM) and transmission electron microscopy (TEM) paired with selective electron dense staining for lignin using mercurization and potassium-permanganate and immunogold labeling of hemicelluloses.

We show that hot water extracted wood differs significantly in its ultrastructure from neat wood e.g. spongy distorted cells and lignin and extractive agglomeration in the lumen. Furthermore, immunogold labeling results indicate that extracted hemicelluloses in the initial stages of extraction are closely associated with lignin and cellulose, for example in lignin-carbohydrate-complexes (LCCs) and both concentration and distribution within the wood cell wall layers are effected. However, labeling intensity is strongly influenced by the accessibility of hemicelluloses (porosity of the cell wall structure and association with lignin and/or cellulose) and for xylan an increase in labeling intensity with extraction can be observed, making it difficult to relate extraction rates to labeling data.

Results from this study will help to better understand mechanical properties and adhesion related questions regarding the use of hot water extracted wood for wood-composite production.

Keywords: Aspen, Electron Microscopy, Hot-Water Extraction, Immunogold Labeling, Mercurization

Introduction

While for many traditional applications wood is used in its solid form, a myriad of industrial applications exist that require an efficient fractionation of wood into individual components. For chemical pulp and paper, for example, only the cellulose is desired. The separated lignin and hemicelluloses resulting from the pulping process are burned for energy - which is the lowest value use possible. The ability to fractionate the raw material beforehand or to process residuals to produce additional products therefore offers significant potential of added value to the raw material. In the last decade extensive studies have been conducted investigating the principles, mechanisms, advantages and disadvantages of lignocellulosic-biorefineries in combination with pulp and paper and wood composite industries (Lui et al. 2006, van Heiningen 2006, Amidon et al. 2008, Gravitis et al. 2008, Amidon and Lui 2009, Söderholm and Lundmark 2009, Mikkonen and Tenkanen 2012, Rodríguez-López et al. 2012, Sanglard et al. 2013). Studies conducted in association with wood composite industries evaluated hot-water extracted wood for wood composite production (e.g. OSB, particle board, MDF board, WPC). The hydrothermal treatment removes mainly hemicelluloses from the wood for further conversion into other products like ethanol and acetic acid. It was verified that it is possible to produce high quality wood composites from hydrothermally modified raw materials (Paredes et al. 2008, Sattler et al. 2008, Paredes et al. 2009, Blumentritt 2010, Hosseinaei et al. 2011, Pelaez-Samaniego Manuel et al. 2013). However, those studies also show that some composites made from modified wood exhibit a significant reduction in two important mechanical properties, flexural and internal bonding strength, compared to conventional material (Paredes et al. 2008, Paredes et al. 2009, Hosseinaei et al. 2011). More research needs to be done to understand the underlying mechanisms and possible ways to prevent these reductions, since mechanical strength properties are a key to product quality and performance. Both flexural and internal bonding strength are to a large part dependent on the quality of the bond between the adhesive and wood. Paredes et al. (2009, 2010) identified an increase in porosity and corresponding structural and chemical changes (e.g. surface energy) of the wood cell wall ultrastructure as key factors for the decrease in mechanical properties. While significant research has been done on fractionation and extraction efficiencies little attention has been paid to ultrastructural changes of treated wood and corresponding impacts to performance properties.

In order to better understand the impact of material removal by a hydrothermal treatment, in this study, we describe the ultrastructure and distribution of xylans in both hydrothermally treated and untreated wood using immunolocalization and labeling methods paired with transmission electron microscopy (TEM) and scanning electron microscopy (SEM).

Material and Methods

Early in 2012 an approximately 50 year old Aspen (*Populus spp.*) tree was harvested at the University of Maine campus in Orono, Maine, USA. Wood from year rings 18-24 was used in this study. A hot-water extraction, to remove hemicelluloses, was conducted in a 500ml Parr

reactor with a stirrer. 1.8g of wood was combined with 100ml of deionized water and heated up to 160°C. To monitor the severity of extraction a severity factor (SF) was calculated. Upon completion of the extraction run the wood was separated from the liquid phase and air dried, oven dried, or stored moist in 50% ethanol. Mercurization of unextracted (SF0) and extracted (SF2.9 and SF3.5) material was conducted according to Westermarck et al. (1988) (with modifications) with a solution of mercuric acetate and acetic acid at 95°C with methanol as solvent.

For TEM, small slivers of unextracted, extracted, and mercurized wood were dehydrated through a graded ethanol series and infiltrated with a mixture of LR White resin and ethanol. After infiltration the slivers were embedded in fresh LR White resin and cured at 60°C for 48 hours.

Immunogold labeling was conducted according to procedures described previously in Kim and Daniel (2012) with minor modifications. Transverse ultrathin sections (ca. 90-100nm) were cut from the LR White embedded blocks with an ultramicrotome (Leica EM UC6) and a diamond knife (Diatome, 45°) and mounted on nickel grids. The grids were incubated in blocking buffer (pH 8.1, tris-buffered saline (TBS) containing 1% w/v BSA and 0.1% w/v NaN₃) for 30min at room temperature. Afterwards grids were incubated with xylan specific antibodies (PlantProbes, UK). After three washes with blocking buffer for 15min each, grids were incubated with secondary antibodies. For control, some grids were only incubated with secondary antibodies. After washing three times in changes of blocking buffer and two times in di-water for 15min each, some grids were post-stained with 1% potassium-permanganate (KMnO₄) for 5min and afterwards rinsed 5 times in deionized water. Examination of the sections was carried out using a Phillips CM10 TEM at 100kV.

Specimen for SEM (Zeiss NVision40) were dehydrated, trimmed with razor blades, mounted on stubs and sputter coated with a thin layer of gold-palladium or carbon coated.

Results and Discussion

Structural Differences between Extracted and Unextracted Xylem

Cell structure and integrity of the xylem of hot-water extracted wood is altered corresponding to the severity of extraction. Cells appear distorted and swollen from their natural shape and the compound middle lamella (CML) looks shifted in some places. Deformations are likely due to the softening of the cell wall due to high temperature, moisture penetration and agitation during the extraction process. TEM micrographs show that most cells have a layer and/or globules of extraction deposits on the lumen wall. The globules are most likely lignin deposits based on lignin's tendency of self-aggregation into spherical forms (Fengel and Wegener 1984, Shulga et al. 2012) while the layers are probably more a mix of lignin and polysaccharides. A higher concentration of such deposits in smaller diameter cells suggests that extractives preferentially deposit in areas with a low liquid flow rate (tips of cells or cells with fewer pits). Dislocations and deposits are also more pronounced in fibers compared to vessels. "Figures 1a and 1b" show a side by side comparison of unextracted and extracted wood and "Figures 2a and 2c" illustrate cell deformations and lumen deposits of extracted xylem.

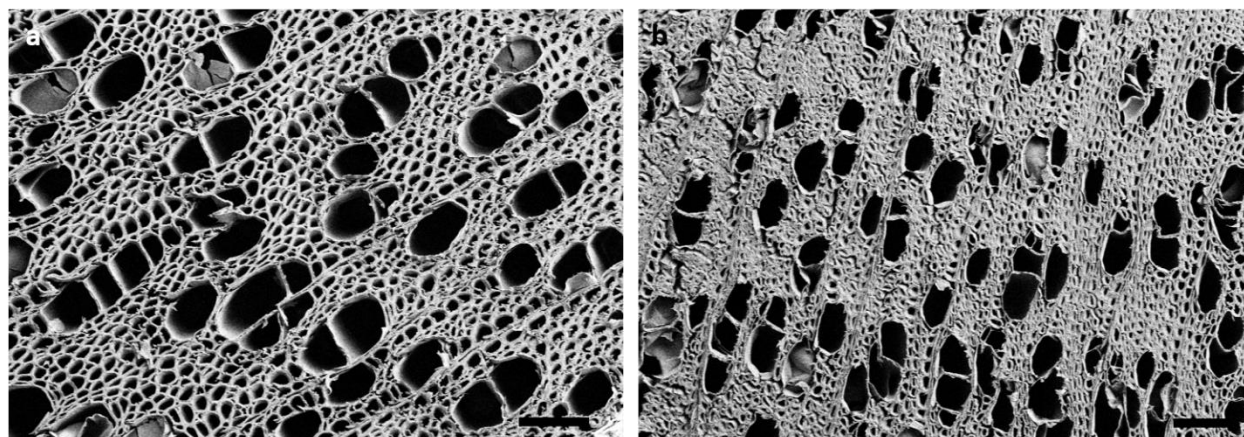


Figure 1 - SEM micrographs comparing: a) unextracted (SF0) and b) extracted (SF3.5) aspen wood. Scale bars: 100 μ m.

Occasionally, some individual fiber cells have an almost translucent layer in place of the S₃ against the inner face of the S₂. These are likely gelatinous layers (G-layers). Aspen is known to exhibit occasional G-layers in libriform fibers among normal fibers and not just in tension wood (Panshin and de Zeeuw 1980). The G-layers translucent appearance in the TEM (Fig. 2c) is due to its composition being composed of mainly highly crystalline cellulose which does not respond to contrasting with KMnO₄ (Panshin and de Zeeuw 1980, Joseleau et al. 2004). As can be expected no correlation was found between the occurrence of G-layers in fibers and the severity of extraction.

Immunogold Localization of Xylans

Labeling of LM10 is present across the whole secondary cell wall with a stronger labeling concentration in the outer rather than inner secondary cell wall of fibers (Fig. 2b and c). This pattern is more apparent in the untreated material compared to treated material. In SF3.5 material, a concentration of labels can be observed around areas with a higher lignin concentration (based on KMnO₄ contrast) in the S₂ layer of fibers. LM11 is more uniformly distributed over the whole secondary cell wall of fibers and vessels without strong apparent patterning (Fig. 2c). LM10 is specific to no- or low substitution xylan whereas LM11 is specific for low substitution xylan (McCartney et al. 2005). An increase in observed label intensity for LM10 with treatment is likely to be caused by hydrolysis of the acetic- and glucuronic acid groups from the xylan backbone due to the autohydrolysis conditions during the hot-water extraction.

Xylan deposition occurs in two phases during cell wall assembly. Initially, a type with an unsubstituted backbone is deposited in close relation with cellulose during the cell wall formation, while later, a more branched type preferably bonds with lignin during the lignification of the cellulose fibrils. This second type is also more likely to form lignin-carbohydrate complexes (LCCs) which can serve as anchor sites for further lignin polymerization (Awano et al. 1998, Awano et al. 2002, Ruel et al. 2006).

Overall, labeling intensity between the treatments is difficult to interpret because of the fact that hemicelluloses might be masked and/ or entangled in other compounds of the wood cell wall and thus are inaccessible for labeling or on the other hand become accessible by hot-water extraction. Work on enzymatic treatments of pulp fibers and wood fractions discuss both a limited access to hemicelluloses by entanglement in cellulose (Várnai et al. 2011) and binding to LCCs (Gübitz et al. 1998), but also limited accessibility of lignin for bleaching due to entrapment of lignin in hemicelluloses in the fiber wall (Suurnäkki et al. 1997). Either way, it is clear that hemicelluloses are closely linked to both lignin and celluloses and can be masked for immunolabeling.

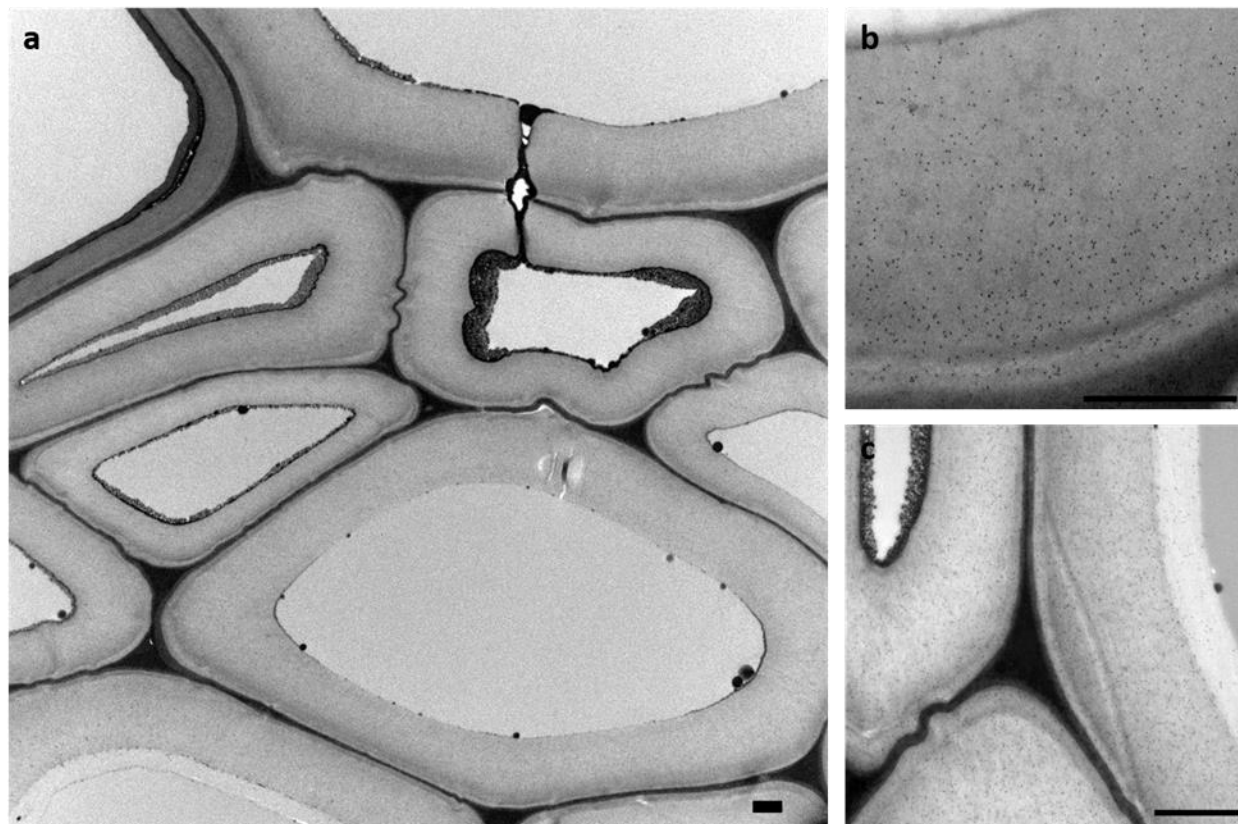


Figure 2 – a) Low magnification TEM micrograph of SF3.5 material showing cell deformation, deposits and a gelatinous layer; b) Higher magnification micrograph of a SF0 fiber wall labeled with LM10; and c) SF3.5 fibers labeled with LM11 and also showing CML deformation, deposits and gelatinous layer. Scale bars: 1 μ m.

Mercurization

Mercurization incorporates mercury into the aromatic nucleus of the lignin and thus makes lignin detectable based on atomic number contrast (Fig. 3). We found that for TEM, KMnO_4 contrasting gives more satisfactory results than mercurization. In SEM, with a back-scatter or in-lens detector the mercurization yields satisfactory results at low magnifications but becomes unstable under higher electron beam irradiation at high magnifications. Furthermore, the mercurization process removes extraction deposits observed by TEM of hot-water extracted wood.

Conclusions and Future Work

Hot-water extracted wood differs significantly in its ultrastructure from unextracted wood e.g. spongy distorted cells and lignin and extractive agglomeration in lumens. Furthermore, immunogold labeling results indicate that extracted hemicelluloses in the initial stages of extraction are closely associated to lignin and cellulose, for example in lignin-carbohydrate-complexes (LCCs) and both concentration and distribution within the wood cell wall layers are effected. However, labeling intensity is strongly influenced by the accessibility of hemicelluloses (porosity of the cell wall structure and association with lignin and/or cellulose) and for xylan an increase in labeling intensity with extraction can be observed, making it difficult to relate extraction rates to labeling data. To better understand labeling intensity to severity of extraction we will be counting labels per area of cell wall in vessels and fibers. Furthermore, we will be adding labels for glucomannans, the minor groups of hemicelluloses in hardwoods, and quantify lignin distribution with SEM-EDXA technique based on mercurization to gain a more holistic view of how hot-water extraction effects the ultrastructure and chemistry of wood.

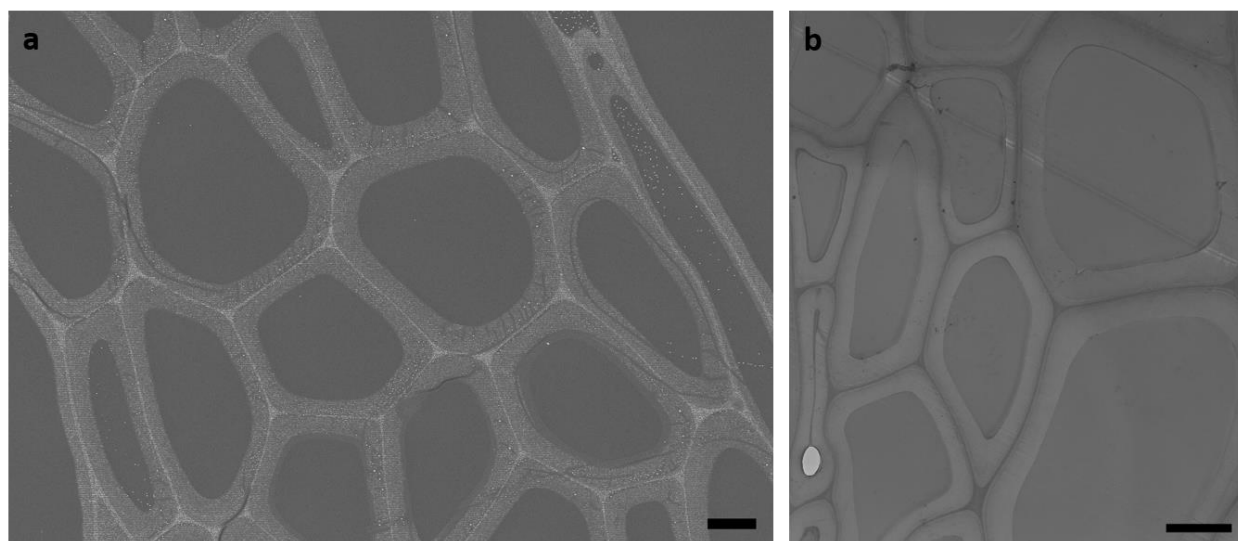


Figure 3 – Micrographs of mercurized unextracted wood (SF0). a) SEM image taken at 3kV with energy selective backscattered (ESB) detector showing areas high in lignin/ mercury in white. b) TEM micrograph showing areas high in lignin/ mercury as dark contrast. The lower left part shows an example of the susceptibility of mercury to electron irradiation. Scale bars: 5µm.

References

- Amidon, T.E. and Lui, S. 2009. Water-based woody biorefinery. *Biotechnology Advances*. 27: 542-550.
- Amidon, T.E., Wood, C., Shupe, A.M., Wang, Y., Graves, M. and Lui, S. 2008. Biorefinery: Conversion of woody biomass to chemicals, energy and materials. *Journal of Biobased Materials and Bioenergy*. 2(2): 100-120.
- Awano, T., Takabe, K. and Fujita, M. 1998. Localization of glucuronoxylans in Japanese beech visualized by immunogold labelling. *Protoplasma*. 202(3-4): 213-222.

- Awano, T., Takabe, K. and Fujita, M. 2002. Xylan deposition on secondary wall of *Fagus crenata* fiber. *Protoplasma*. 219(1-2): 106-115.
- Blumentritt, M. (2010). Influence of hot water extraction on selected particle board properties. Master's Thesis, University of Göttingen, Germany.
- Fengel, D. and Wegener, G. 1984. Wood – chemistry, ultrastructure, reactions. De Gruyter.
- Gravitis, J., Abolins, J. and Kokorevics, A. 2008. Integration of biorefinery clusters towards zero emissions. *Environmental Engineering and Management Journal*. 7(5): 569-577.
- Gübitz, G.M., Stebbing, D.W., Johansson, C.I. and Saddler, J.N. 1998. Lignin-hemicellulose complexes restrict enzymatic solubilization of mannan and xylan from dissolving pulp. *Applied Microbiology and Biotechnology*. 50(3): 390-395.
- Hosseinaei, O., Wang, S., Rials, T.G., Xing, C., Taylor, A.M. and Kelley, S.S. 2011. Effect of hemicellulose extraction on physical and mechanical properties and mold susceptibility of flakeboard. *Forest Products Journal*. 61(1): 31-37.
- Joseleau, J.-P., Imai, T., Kuroda, K. and Ruel, K. 2004. Detection in situ and characterization of lignin in the g-layer of tension wood fibres of *Populus deltoides*. *Planta*. 219(2): 338-345.
- Kim, J. and Daniel, G. 2012. Distribution of glucomannans and xylans in poplar xylem and their changes under tension stress. *Planta*. 236(1): 35-50.
- Lui, S., Amidon, T.E. and Francis, R.C. 2006. From forest biomass to chemicals and energy - biorefinery initiative in New York state. *Industrial Biotechnology*. 2(2): 113-120.
- McCartney, L., Marcus, S.E. and Knox, J.P. 2005. Monoclonal antibodies to plant cell wall xylans and arabinoxylans. *Journal of Histochemistry & Cytochemistry*. 53(4): 543-546.
- Mikkonen, K.S. and Tenkanen, M. 2012. Sustainable food-packaging materials based on future biorefinery products: Xylans and mannans. *Trends in Food Science & Technology*. 28(2): 90-102.
- Panshin, A.J. and de Zeeuw, C. 1980. Textbook of wood technology, McGraw-Hill Book Co.
- Paredes, J.J., Jara, R., Shaler, S.M. and van Heiningen, A. 2008. Influence of hot water extraction on the physical and mechanical behavior of OSB. *Forest Products Journal*. 58(12): 56-62.
- Paredes, J.J., Mills, R., Shaler, S.M., Gardner, D.J. and van Heiningen, A. 2009. Surface characterization of red maple strands after hot water extraction. *Wood and Fiber Science*. 41(1): 38-50.
- Pelaez-Samaniego, M. R., Yadama, V., Lowell, E., Amidon T. E. and Chaffee T.L. 2013. Hot water extracted wood fiber for production of wood plastic composites (WPCs). *Holzforschung*. 67: 193.
- Rodríguez-López, J., Romaní, A., González-Muñoz M. J., Garrote, G. and Parajó J.C. 2012. Extracting value-added products before pulping: Hemicellulosic ethanol from *Eucalyptus globulus* wood. 66: 591.
- Ruel, K., Chevalier-Billosta, V., Guillemain, F., Sierra, J.B. and Joseleau, J.P. 2006. The wood cell wall at the ultrastructural scale - Formation and topochemical organization. *Maderas. Ciencia y tecnología*. 8(2): 107-116.
- Sanglard, M., Chirat, C., Jarman, B. and Lachenal, D. 2013. Biorefinery in a pulp mill: Simultaneous production of cellulosic fibers from *Eucalyptus globulus* by soda-anthraquinone cooking and surface-active agents. *Holzforschung*. 67: 481-488.
- Sattler, C., Labbé, N., Harper, D., Elder, T. and Rials, T. 2008. Effects of hot water extraction on physical and chemical characteristics of oriented strand board (OSB) wood flakes. *CLEAN - Soil, Air, Water*. 36(8): 674-681.

- Shulga, G., Vitolina, S., Shakels, V., Belkova, L., Cazacu, G., Vasile, C. and Nita, L. 2012. Lignin separated from the hydrolyzate of the hydrothermal treatment of birch wood and its surface properties. *Cellulose Chemistry and Technology*. 46(5-6): 307-318.
- Söderholm, P. and Lundmark, R. 2009. The development of forest-based biorefinery: Implications for market behavior and policy. *Forest Products Journal*. 29(1/2): 6-16.
- Suurnäkki, A., Tenkanen, M., Buchert, J. and Viikari, L. 1997. Hemicellulases in the bleaching of chemical pulps. *Biotechnology in the pulp and paper industry*. K.E.L. Eriksson et al. (eds.), Springer Berlin Heidelberg. 261-287.
- van Heiningen, A. 2006. Converting a kraft pulp mill into an integrated forest biorefinery. *Pulp and Paper Canada*. 107: 38-43.
- Várnai, A., Huikko, L., Pere, J., Siika-Aho, M. and Viikari, L. 2011. Synergistic action of xylanase and mannanase improves the total hydrolysis of softwood. *Bioresource Technology*. 102(19): 9096-9104.
- Westermarck, U., Lidbrandt, O. and Eriksson, I. 1988. Lignin distribution in spruce (*Picea abies*) determined by mercurization with SEM-EDAX technique. *Wood Science and Technology*. 22(3): 243-250.

Acknowledgements

Funding support for this project was provided by the USDA McIntire-Stennis program (Project ME041413) and a Maine Economic Improvement Fund (MEIF) Dissertation Fellowship. Thanks to the Electron Microscopy Laboratory and the Laboratory for Surface Science and Technology at the University of Maine, for help and advice regarding sample preparation and equipment use. Additional acknowledgements are in order for Mr. Kelly Edwards, Dr. Douglas G. Gardner, Dr. Scott Collins, and Dr. Barbara Cole.

Curing Kinetics of Spruce Bark Tannin-Based Foams

Milan SERNEK^{1,}, Matjaž ČOP¹*

Abstract

The use of renewable resources has a positive impact on nature preservation and has recently increased steeply recently due to both environmental and economic reasons. Development of new bio-based tannin foams could make a significant contribution to the more efficient use of forest biomass resources. Tannin-based foams are networked structures that are obtained by polycondensation of polyflavonoid tannins and furfuryl alcohol, with good insulation and resistance properties (to chemicals and fire) comparable to those of synthetic foams. The objective of this study was to characterize the impact of tannin and catalyst content on foam curing kinetics and its properties. It was found that the curing of foams was faster at higher temperatures. Differential scanning calorimetry (DSC) revealed that the increased amount of tannin slowed down the conversion, whereas the increased amount of catalyst accelerated the foaming reaction. Advanced model free kinetics (AMFK) software was found as a suitable way for predicting the conversion of foams at isothermal conditions. The density of foams decreased with an increased amount of tannin, whereas the amount of added catalyst had no significant effect.

Keywords: curing, DSC, foam, spruce bark, tannin

¹ Department of Wood Science and Technology, Biotechnical Faculty, University of Ljubljana, Rozna dolina, C. VIII/34, 1001 Ljubljana, Slovenia

* Corresponding author: Tel: +386 1 320 3623, Fax: +386 1 257 2297
e-mail: milan.sernek@bf.uni-lj.si

Some Physical and Mechanical Properties of Two-Step Organo-Montmorillonite Modified Wood Flour/Polypropylene Composites

*Ru Liu, Jinzhen Cao**

MOE Key Laboratory of Wooden Material Science and Application, Faculty of
Material Science & Technology, Beijing Forestry University, Qinghua East Road
35, Haidian 100083, Beijing, China

** Corresponding author*

caoj@bjfu.edu.cn

Abstract

In this study, wood flour (WF) was modified by sodium-montmorillonite (Na-MMT) and didecyl dimethyl ammonium chloride (DDAC) in a two-step process to form organo-montmorillonite (OMMT) inside the WF with varied MMT concentration (0.25, 0.5, 0.75, and 1%, respectively). Then, the modified WF was mixed with polypropylene (PP) to produce WF/PP composites. Some physical and mechanical properties including the water sorption, thickness swelling, flexural, tensile, and impact properties of the composites were tested. Besides, the X-ray diffraction (XRD) and scanning electron microscopic (SEM) analyses were tested for further explanation. The results showed that: (1) the modification process of Na-MMT and DDAC inside WF was successful according to the existing of OMMT characteristic diffraction peak in XRD results; (2) the addition of OMMT improved the water repellency, dimensional stability, flexural and tensile properties of the composites compared with the pure composite, whereas the impact strength decreased; (3) most of the physical and mechanical properties of WF/PP composites increased with the increasing of MMT concentration at first until reaching the maximum at MMT concentration of 0.5% and then dropped, suggesting the 0.5% MMT concentration served as a critical point to the composites; (4) SEM analysis proved the interracial adhesion of WF and PP became better at MMT concentration lower than 0.5%, whereas it became poor at excessive MMT concentrations.

Keywords: A. Wood flour (WF); A. Polypropylene (PP); A. organo-montmorillonite (OMMT); A. Composite

Introduction

Recently, natural fibers have been found increasingly used in applications as reinforcements in polymer composites because of the advantages of natural fibers in low density, high specific strength, easy availability, renewability and relatively low cost compared with plastics (Kazayawoko et al., 1999; Li et al., 2013). Among natural fibers, wood flour/fiber (WF) is one of

the most widely used types. However, the main polymer chains of WF (especially cellulose and hemicellulose) contain large amounts of hydroxyl groups, making WF hydrophilic. The highly hydrophilic character of WF makes it incompatible with hydrophobic thermoplastics (George et al., 2001; Kuang et al., 2010). This incompatibility leads to poor interfacial adhesion between filler and matrix, which results in poor mechanical properties because stress cannot be transferred properly from the matrix to the filler. In order to reduce the hydrophilic character of WF and make it compatible with plastics, various treatments have been developed and used. Nanocomposite technology with layered silicate nanoclays as *in situ* reinforcement has been intensively investigated in recent years (Messersmith and Giannelis, 1995; Vertuccio et al., 2009). It offers new opportunities for the modification of wood products and polymers.

In our previous study (Liu et al., 2013), Na-MMT and DDAC were used to modify WF in a two-step process to form OMMT inside the WF. Subsequently, the modified WF was mixed with poly (lactic acid) (PLA) to prepare WF/PLA composites. Significant improvements were found in physical and mechanical properties of the composites at MMT concentration of 0.5%. Meanwhile, the enhancements were more obvious in coarse WF than fine one.

WF/polypropylene (PP) composite is one kind of the most widely used types of WPC in market. However, there are some drawbacks of WF/PP composite such as its low dimensional stability and mold resistance with water existing. Besides, its mechanical properties were also important. In this study, WFs were modified by the same process and then combined with PP to make WF/PP composites. Therefore, the X-ray diffraction (XRD) analysis of the WF was firstly carried on to prove the successful modification process. Thus, the physical and mechanical properties of the WF/PP composites, including water uptake, thickness swelling, flexural, tensile, and impact properties were tested. The fracture surfaces of the composites were observed by using scanning electron microscope (SEM) for further explanation.

Materials and Methods

Materials. The Wood flour of poplar (*Populus tomentosa Carr.*) with size 10 to 60 mesh was supplied by Xingda Wood Flour Company, Gaocheng, China. It has an average length of 1.5mm and average diameter of 0.2 mm. Polypropylene (PP) (K8303; Sinopec Chemical Products Sales Company, China) with a density of 0.9 g/cm³ was purchased from Beijing Yanshan Petrochemical Co. Ltd., China. It had a melt point around 165°C and a melt flow index of 1.5 to 2.0 g/10 min at 230°C. Na-montmorillonite (Na-MMT) was purchased from Zhejiang Fenghong Clay Chemical Co. Ltd., Huzhou, China. It is hydrophilic clay powder with volatiles below 4% at 105 °C for 2 h. The viscosity of 3% w/w Na-MMT in distilled water is 3000 mPa·s with pH of 8 to 10. The mean interlayer distance of Na-MMT is 1.459 nm with particle sizes of 76 µm. The cation exchange capacity of Na-MMT is 90 mmol/100 g. The modifier was didecyl dimethyl ammonium chloride (DDAC, 70%), which was purchased from Shanghai 3D, Bio-chem Co. Ltd., Shanghai, China. Polyfluotetraethylene (PTFE) films were used as demoulding materials to avoid sticking board during hot-pressing.

Modification of wood flours. The first step was to impregnate WF with Na-MMT suspensions at four concentrations (0.25, 0.5, 0.75, and 1%, respectively) through vacuum-pressure process. First, WF was put into a beaker in a treating tank and then vacuum treated at 0.01MPa for 30min.

Afterwards, Na-MMT suspension, which was dissolved in the distilled water, was let in to completely submerge WF with pressure treated at 0.6MPa for 1 h. The average particle size of Na-MMT suspension was 1.215 μ m as tested by Laser Particle Analyzer (DelsaTM Nano C, Beckman coulter, USA). The impregnated WF was taken out from Na-MMT suspension with a 100-mesh sieve and dried in an oven at 103 \pm 2 $^{\circ}$ C to constant weight. The weight percent gains of treated WF were 0.18, 0.62, 3.84 and 6.25%, respectively. The treated WF was then put into a beaker and submerged in DDAC solution in the second step. The concentration of DDAC was calculated according to the concentration of Na-MMT at a ratio of the cation exchange capacity of Na-MMT of 0.7:1. The beaker was placed in a water bath at 60 $^{\circ}$ C for 2h with a mechanical stirring at speed of 80r/min. Then, WF was taken out and dried at 103 \pm 2 $^{\circ}$ C to constant weight. The weight percent gains of modified WF were achieved another 3-3.5% compared to the first step. Besides, the “unmodified” control WF was treated with distilled water by using the same process.

Preparation of composites. The raw materials for WF/PP composites contain 50 wt% of unmodified or modified WF and another 50 wt% PP. They were mixed in a high speed blender at about 2900 rpm for 4 min. The mixture was then dried at 103 \pm 2 $^{\circ}$ C for 2h. After drying, the mixture was extruded via a co-rotating twin-screw extruder (KESUN KS-20, Kunshan, China) with a screw diameter of 20 mm and a length-to-diameter ratio of 36/1. The corresponding temperature profile along the extruder barrel was 165/170/175/180/175 $^{\circ}$ C, and the screw speed was 167 rpm. The extruded rods were cut into small particles about 5mm, and then the blends were dried again at 103 \pm 2 $^{\circ}$ C for 2 h and taken out for hand matting. A hot press (SYSMEN-II, China Academy of Forestry, Beijing, China) was used to produce the composites by compressing the mat at 180 $^{\circ}$ C with a pressure of 4 MPa for 6 min. The target density of the composites was 1.0 g/cm³ at size of 270 mm \times 270 mm \times 3 mm. Prior to demoulding, the formed mat was cooled down at 4MPa for another 6 min at room temperature. After that, all the mats were cut into required dimensions for further tests.

Physical and mechanical tests. The determination of water absorption was carried out according to the Chinese standard GB/T 17657-1999. Composites samples with dimensions of 50 mm \times 50 mm \times 3 mm (thickness) were completely immersed into distilled water at 20 \pm 2 $^{\circ}$ C for 8 days. After immersions for 6, 24, and 48 h and thereafter at 48 h intervals, the samples were taken out with removal of excess water on the surface and weighed. The water uptakes were calculated based on the weight percent gains at each stage. The thickness swelling rates were calculated based on the mid-span thickness changes till the final. Four replicates of the samples were used for each group, based on which the standard deviations were calculated. The flexural tests were carried out according to the Chinese standard GB/T 9341-2000, which involved a three-point bending test at a crosshead speed of 1 mm/min. The sizes of the samples were 60 mm \times 25 mm \times 3 mm. Five samples of each group were tested for standard deviations. The modulus of rupture (MOR) and modulus of elasticity (MOE) were calculated to evaluate the flexural property. The tensile tests were carried out according to American standard ASTM D638 at a testing speed of 2 mm/min. Five samples with dog-bone shapes of each group were tested for standard deviations. The tensile strength and Young's modulus were calculated to evaluate the tensile properties. Izod impact testing was carried out according to Chinese standard GB/T 1043.1-2008. Six samples with size of 80 mm \times 15 mm \times 3 mm were performed on a CEAST model 6957 impact tester and the average value was reported.

SEM analysis. The fracture surfaces of WF/PP composites were observed by a Hitachi (S-3400, Japan) SEM with an acceleration voltage of 5 kV. The samples were sputter-coated with gold prior to observation.

Results and Discussion

XRD analysis. The X-ray diffraction (XRD) scans for sodium-montmorillonite (Na-MMT), unmodified and 1% montmorillonite (MMT) modified WFs are shown in Fig. 1. The positions of the diffraction peaks for crystal planes (101), (002) and (040) in cellulose for WF at $2\theta=17^\circ$, 22.5° , and 35° did not change after being modified with OMMT, suggesting the modification did not influence the main crystalline structures of WF. However, a new peak was found at $2\theta=3.26^\circ$ after OMMT modification in WF, which was related to the crystalline structure of OMMT with the d-spacing of 2.707 nm. The d-spacing of OMMT modified with Na-MMT and DDAC was 2.323 nm. Therefore, a conclusion could be drawn that Na-MMT was transformed to OMMT after the two-step treatment process. Meanwhile, the enlarged d-spacing of OMMT indicated that WF might be intercalated into OMMT layers.

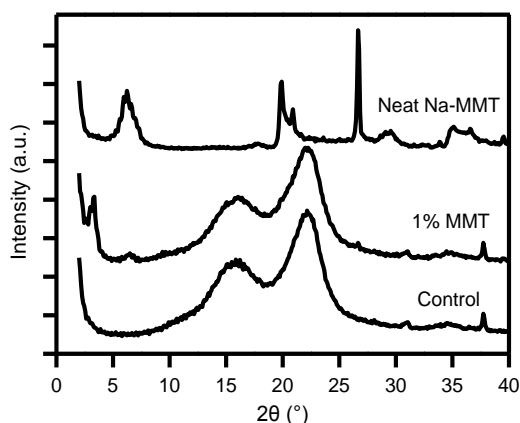


Fig. 1. XRD patterns of neat Na-MMT and WF samples

Water uptake and thickness swelling. The results of water absorption test are shown in Fig. 2. The water uptakes of WF/PP composites prepared with OMMT modified WF were significantly less than that of the WF/PP control (Fig. 2a). Irrespective of OMMT concentration, OMMT modified WF/PP composites absorbed about 3.5% while the WF/PP control absorbed 4.6% after 196h of immersion, with a reduction in water uptakes of over 20% in all cases. This might be due to the barrier effects of the silicate fillers inhibiting the water absorption (Drozdov *et al.* 2003) or the reduction of accessible OH groups in modified WF as proved in our previous study (Liu *et al.* 2013). Water in WPC can exist in three regions, namely, the WF lumen, WF cell walls, and gaps between filler and matrix in the interface region (Karmaker 1997). The reduction of OH groups in WF could lead to decrease in hygroscopicity of WF. Meanwhile, the combination of PP with modified WF could be stronger than pure WF. The improved compatibility of matrix and filler could reduce the gaps between them and limit the penetration of water into these gaps. These all contributed to the water repellency of WF/PP composites. For different MMT concentration

groups, it seemed that the 0.5% MMT modified group absorbed the least water. The increase in water uptake at high OMMT loadings might be caused by the agglomeration of OMMT on WF surface, which might cause weak interface bonding to the composites. Similar to the results of water uptakes, OMMT modified groups exhibited lower thickness swelling values than the control group, suggesting the introducing of silicate fillers was a positive factor to restrict the hydro-expansion of WF/PP composites. The thickness swelling rates were decreasing with the increase of MMT concentration until reaching the minimum value of 2.6% at 0.5% MMT concentration, which is nearly one-fourth of that of the WF/PP composite control. The increase in thickness swelling rate after 0.5% MMT concentration could be owing to the poor interface adhesion at excessive OMMT loading on WF surface.

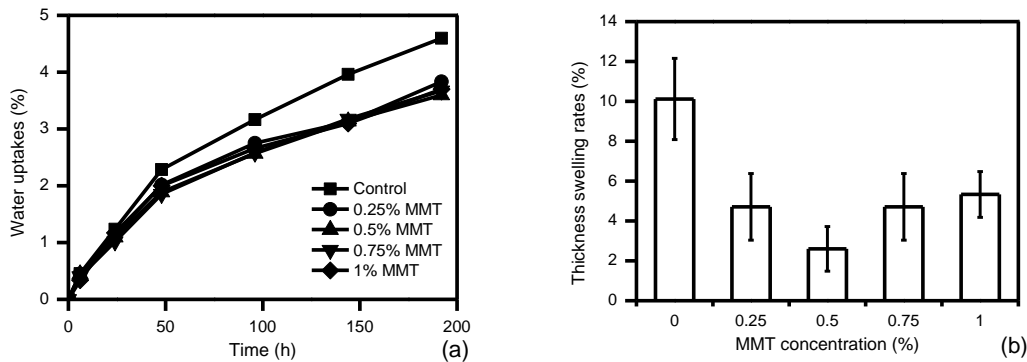


Fig. 2. Water uptakes (a) and thickness swelling rates (b) of WF/PP composites

Mechanical properties. The mechanical properties of WF/PP composites are listed in Table 1. The trends of the flexural and tensile properties of the composites were almost similar. The concentration of OMMT had an obvious influence on the mechanical properties of the composites. For flexural and tensile properties, composite prepared by 0.5% OMMT modified WF displayed higher flexural and tensile strength and modulus values than unmodified group and other OMMT modified groups. This is consistent with the results of water uptake and thickness swelling, which was attributed to the increased compatibility between modified filler and matrix. With OMMT concentration increasing, the flexural and tensile properties decreased, due to a large amount of OMMT attached on WF surface, resulting in embrittlement of WF. However, OMMT had negative effects on the impact strength of the composites because OMMT itself was a brittle particle.

Table 1. Mechanical properties of WF/PP composites

MMT concentration (%)	Flexural strength (MPa)	Flexural modulus (GPa)	Tensile strength (MPa)	Tensile modulus (GPa)	Impact strength (J/m ²)
0	29.57(1.37)	1.56(0.19)	17.63(2.99)	1.28(0.29)	5.80(0.82)
0.25	32.32(1.85)	1.73(0.19)	18.29(1.45)	1.35(0.20)	4.56(0.98)
0.5	33.22(1.29)	2.07(0.13)	20.86(2.04)	1.80(0.32)	4.65(0.65)
0.75	30.84(0.89)	1.96(0.19)	20.03(1.38)	1.64(0.21)	4.34(0.55)
1	30.05(0.34)	1.83(0.20)	18.99(0.84)	1.32(0.26)	3.73(0.76)

Note: The values in parentheses represent the standard deviations of replicates.

SEM analysis. The fracture surfaces of WF/PP composites are shown in Fig. 3. Some cracks were observed between filler and matrix in the control group (Fig. 3a), while less voids and cracks were found in 0.5% OMMT modified group. Besides, its WF surfaces were uniformly covered by PP and showed a better continuous phase than control, suggesting the improved interfacial adhesion and well embedded of the WF in PP matrix (Fig. 3b). The image of Fig. 3c shows some big cracks surrounding the WF, separating WF from matrix. This feature implied the considerable weakened interfacial adhesion of WF and PP while OMMT was overloaded. The SEM results proved the physical and mechanical results.

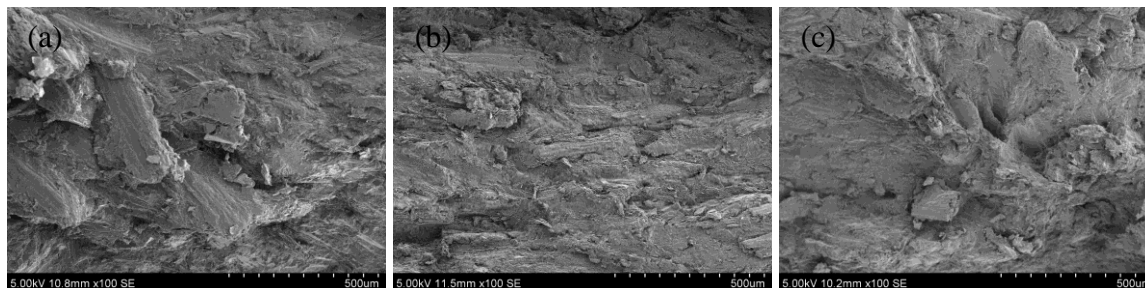


Fig. 3. SEM images of fracture surfaces of WF/PP composites made of unmodified (a), 0.5% MMT modified WF (b), and 1% (c) MMT modified WF.

Conclusion

The OMMT modified WF prepared with Na-MMT and DDAC in this study was successfully for application in WF/PP composites. After the modification, the interlayer distance of OMMT in WF samples was further enlarged, suggesting the intercalated structures of some OMMT layers in WF samples. This modification benefited to the physical and mechanical properties of WF/PP composites except for the impact strength. Among the four concentrations used in this study, the concentration (0.5%) seemed the optimal loading level for preparing WF/PP composites within the experiment range for the best interfacial compatibility between WF and PP matrix.

Acknowledgements

This study was financially supported by the National Natural Science Foundation of China (No. 31170524) and the Fundamental Research Funds for the Central Universities in China (No. BLYJ201414).

References

- Drozdov, A.D., deC Christiansen, J., Gupta, R.K., Shah, A.P. 2003. Model for anomalous moisture diffusion through a polymer-clay nanocomposite. *J. Polym. Sci. Polym. Phys.* 41: 476-492.

- George, J., Sreekala, M.S., Thomas, S. 2001. A review on interface modification and characterization of natural fiber reinforced plastic composites. *Polym. Eng. Sci.* 41: 1471-1485.
- Karmaker, A.C. 1997. Effect of water absorption on dimensional stability and impact energy of jute fiber reinforced polypropylene. *J. Mater. Sci. Lett.* 16: 462-464.
- Kazayawoko, M., Balatinecz, J.J., Matuana, L.M. 1999. Surface modification and adhesion mechanisms in woodfiber-polypropylene composites. *J. Mater. Sci.* 34: 6189-6199.
- Kuang, X., Kuang, R., Zheng, X., Wang, Z. 2010. Mechanical properties and size stability of wheat straw and recycled LDPE composites coupled by waterborne coupling agents. *Carbohyd. Polym.* 80: 927-933.
- Li, X., Lei, B., Lin, Z., Huang, L., Tan, S., Cai, X. 2013. The utilization of organic vermiculite to reinforce wood-plastic composites with higher flexural and tensile properties. *Ind. Crop. Prod.* 51: 310-316.
- Liu, R., Luo, S., Cao, J., Peng, Y. 2013. Characterization of organo-montmorillonite (OMMT) modified wood flour and properties of its composites with poly(lactic acid). *Compos. Part A-Appl. Sci.* 51: 33-42.
- Messersmith, P.B., Giannelis, E.P. 1995. Synthesis and barrier properties of poly(ecaprolactone)-layered silicate nanocomposites. *J. Polym. Sci. Polym. Chem.* 33: 1047-1057.
- Vertuccio, L., Gorrasi, G., Sorrentino, A., Vittoria V. 2009. Nano clay reinforced PCL/starch blends obtained by high energy ball milling. *Carbohyd. Polym.* 75: 172-179.

Biolignin™, a Renewable Raw Material for Wood Adhesives

*Bouchra Benjelloun-Mlayah^{1,2}, Nadine Tachon^{1,2}, Louis Pilato³,
Michel Delmas^{1,2}*

1- Université de Toulouse
Chemical Engineering Laboratory
4 allée Emile Monso
31432 Toulouse Cedex 4, France

2 - CIMV
109 rue Jean Bart, Diapason A
31670 Labege, France

3 - Pilato Consulting, Bound Brook, NJ 08805

Abstract

Biolignin™, a lignin extracted from wheat straw by CIMV process, based on organic acids, was tested to replace at least 50% of the phenol in phenol-formaldehyde (PF) resin, in a one-step synthesis.

The Biolignin™ can be used without any previous modification, due to its particular properties, related to the extraction process conditions: linear structure (Mass spectrometry), low molecular weight (SEC chromatography) high functionality (¹³P NMR) and high purity (AIL-ASL content).

The parameters, such as reaction time, temperature and formaldehyde to phenol+Biolignin™ mass ratio, were optimized in order to achieve the required pH, viscosity, dry matter and residual free formaldehyde, for wood adhesives application.

The substitution rate of about 70%, can be achieved. The optimum formaldehyde to phenol+Biolignin™ ratio has been determined and fixed to 47%. The Biolignin™-Phenol-Formaldehyde (BPF) resin synthesized in these conditions showed physico-chemical properties and chemical structure (¹³P NMR) close to standard phenol-Formaldehyde resins (free formaldehyde: 0,18%).

The mechanical properties of these based resins were analyzed in DLTMA and the Biolignin™-Phenol-Formaldehyde (BPF) resin was successfully tested in the manufacturing of particle boards and plywood panels without formaldehyde resin due to Biolignin™ which acts as very efficient formaldehyde scavenger which allows a very low formaldehyde release (0,008mg/l).

Advanced Wood and Polymer Composites
Session Co-Chairs: *Rupert Wimmer, BOKU Vienna, IFA Tulln,
Austria and Joris Van Acker,
Ghent University, Belgium*

**Strain Distribution and Load Transfer in the Polymer-Wood
Particle Bond in Wood Plastic Composites**

Matthew Schwarzkopf

PhD Candidate, Wood Science and Engineering, Oregon State University
173 Richardson Hall
Corvallis, OR 97331
matthew.schwarzkopf@oregonstate.edu

Lech Muszyński

Associate Professor, Wood Science and Engineering, Oregon State University
106 Richardson Hall
Corvallis, OR 97331
lech.muszynski@oregonstate.edu

Abstract

Wood plastic composite (WPC) material has been prepared in the form of thin films using high density polyethylene (HDPE). The load transfer between wood particles and the HDPE matrix was analyzed by observation of the strain patterns on the film surface after subjecting the material to tensile loading. The applied optical measurement technique is based on the principle of digital image correlation (DIC). Interpretation of the results in terms of load transfer between the wood particles and the HDPE matrix below the surface proved to be challenging and required a structured approach. In this paper, a selection of quantitative descriptors were proposed as synthesized metrics to support the quantitative interpretation of the measured strains. X-ray computed tomography (XCT) scans helped assess the effect of the position of the particles in the film specimens on the strain patterns, which were observed on the surface.

Keywords: digital image correlation (DIC); load transfer; micromechanics; optical measurement; short fiber composites theory; wood plastic composites (WPC)

Introduction

Mechanical performance of wood plastic composites (WPCs) is determined by their morphology, mechanical properties of their individual components, and the internal bonds providing effective load transfer between these components. Bulk mechanical properties of particulate composites like WPCs can be determined by means of standard tests. Predicting or modeling the WPC properties is still a serious challenge, if new and improved composites should be developed.

Clyne (1989) and Noselli et al. (2010) showed a strain field disturbance in the matrix surrounding a rigid embedded particle during tensile loading (Figure 42G and 1H). Noselli et al. (2010) embedded a steel inclusion in a flexible polymer matrix and observed the photoelastic fringe patterns produced when tension was applied (Figure 42G). Figure 42H from Clyne (1989) is a simplified schematic illustration of the strain field disturbance. The particles in these studies are different to that of wood in WPCs and the results may not be comparable.

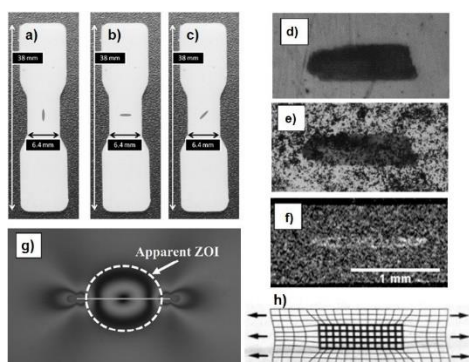


Figure 42. a, b, c) WPC test specimens; d, e) embedded wood particle before and after speckle application; f) XCT scan of embedded particle; g) photoelastic fringe patterns of particle in tension (Noselli, Dal Corso et al. 2010) h) schematic illustration of elastic strain around a rigid cylinder (Clyne 1989)

The present study is part of a larger project, in which a multimodal experimental characterization was coupled with morphology-based modeling techniques and inverse problem methodology in order to describe correlations between morphology, micromechanics of the internal bonds, and bulk properties of bio-based composites (Sebera and Muszynski 2011; Muszynski et al. 2013). The specific objective is to develop an efficient method for the measurement of strain distribution patterns in the embedding plastic matrix. The expectation is that the method will give quantitative data for characterization of load transfer between wood particles and polymer matrices in WPCs. The main question is whether the results verify the proposed analytical theories and numerical models.

Materials and Methods

The general approach of this study was to use optical measurement techniques based on the digital image correlation (DIC) principle to measure the strain patterns in thin films of high density polyethylene (HDPE) with embedded wood particles subjected to tensile loading.

Specimen preparation: Fortiflex HDPE is from Solvay Polymers (Houston, Texas). Southern yellow pine (SYP) flour (40-mesh, no. 4020) was obtained from American Wood Fibers (Schofield, Wisconsin). Particles from this source have a wide size distribution with the median

dimensions 0.77 mm x 0.27 mm and have a median aspect ratio of about 2.85 (Wang 2007). The particles dried overnight at 103°C in an approx. 30 mm thick layer in an aluminum tray. Dried particles were compounded with HDPE by means of a counter-rotating, twin screw Intelli-Torque Plasti-Corder® mixer (C.W. Brabender® Instruments, Inc.). HDPE (29.93 g) was added to the mixing chamber preheated to 180°C. The mixing speed was set to 30 rpm. When the torque reached a constant level, a pinch of wood particles was added to the mixing chamber. This small amount of particles was used to create a sparse composite, in which individual particles could be easily identified and analyzed, and that the particle-matrix interaction would not be affected by neighboring embedded particles. Once the torque level was constant, 6 g of the compounded melt material was transferred to a square mold with internal void dimensions of 102 x 102 x 0.85 mm³ and pre-heated in a small-scale Carver Inc. (Auto M-NE, H 3891) hot press to 180°C. The mold assembly with hard stops was held under hot pressure for 5 min and then transferred to a cold-press until cool to the touch. Test specimens were punched out of the wood-HDPE coupon with a steel dog bone shaped die. The coupon was manipulated in such a way so that a single wood particle was located in the center of the specimen with the orientation at 0°, 45°, and 90° with respect to the loading axis (Figure 42a, 1b, and 1c).

In addition to wood particles, idealized specimens with 1 mm sections of tin coated 0.2 mm copper wire embedded in a HDPE matrix served as references. The wire sections had similar dimensions to the median wood flour particles but were solid (non-porous), isotropic, and had a regular cylindrical geometry, which met some of the assumptions of the short fiber theories previously described. The surface was roughed with 120 grit sandpaper in an attempt to improve the bonding surface. All together nine reference specimens and nine wood specimens were prepared.

Generally, due to the random nature of the manufacturing process, the wood and wire particles naturally resided throughout the thickness of the specimens. Wang et al. (2007) determined the position of wood particles in their WPC composites by XCT scans. In the present study, all specimens were scanned in a MicroCT XCT scanner (by ScanCo) at a resolution of 10 µm/voxel (Figure 43) for determining the particle positions.

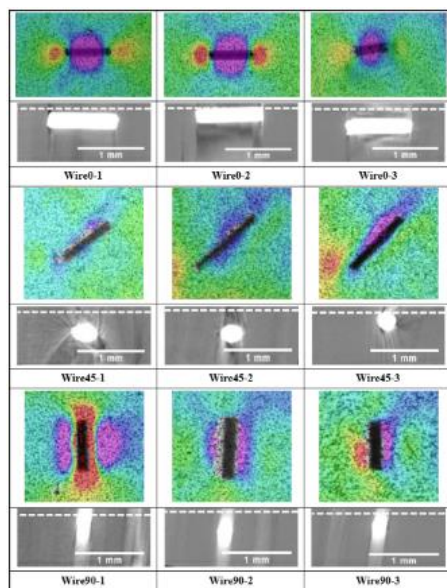


Figure 43. ϵ_1 strain plots of reference wire/HDPE composites with corresponding XCT images of particle depth. Specimen surface is marked with a dotted line. Note: Blurry images and shadows in the XCT data are artifacts from the metal particle affecting the x-ray beam.

Speckle pattern: The applied speckle pattern material was toner powder from a Hewlett Packard (Palo Alto, California) Q2612A cartridge. A uniform pattern was transferred on specimens by means of a custom made air deposition apparatus (Sutton 2010).

Tensile test: Specimens were tested in tension in an Instron ElectroPuls E1000 test machine at a ramp rate of 0.5 mm min^{-1} (strain equivalent to 0.02 mm min^{-1}) for 2 min. The force was measured with a 2527 Series Dynacell load cell ($\pm 2 \text{ kN}$ capacity). Force and displacement of the cross head was recorded throughout the test with a data acquisition (DAQ) unit.

Optical measurement: Changes in strain distribution patterns in the matrix material surrounding embedded wood particles were measured by an optical measurement system. During the test, images of the specimen surface in the immediate neighborhood of the embedded particles (field of view, $7.18 \text{ mm} \times 6.00 \text{ mm}$) were recorded every 1 s for 2 min with the VIC-Micro 3DTM system (by Correlated Solutions, Inc). The basic hardware components for this system consist of two synchronized cameras and a stereomicroscope. The image sequences were processed with VIC-3D 2010 software (by Correlated Solutions, Inc). For each test, an area of interest (AOI) including a single particle and the surrounding was selected for analysis manually (Figure 44). The output generated by VIC-3D 2010 software is numerical and can also be presented in the form of color coded maps plotted and overlaid on the deformed specimen images.

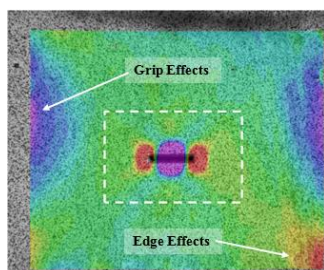


Figure 44. The effect from the tensile grips (blue/purple) seen on the left and right of the particle and an edge effect in the bottom right. The dotted box shows the area of analysis.

Data analysis: The area of local strain field disturbance in the matrix marked with a dotted circle in Figure 42G will be considered and referred to as the embedded particle's zone of influence (ZOI). For a quantitative analysis of the data, a number of descriptors were developed that refer to the extent, position, and shape of the ZOI around the embedded particle. A summary of the descriptors can be found in Table 12.

Table 12. Quantitative descriptors and their derivation.

Quantitative descriptors	Derivation
Particle length [mm]	Measured
Particle orientation [degrees from X]	Measured
Particle distance from the surface [mm]	Measured
Area of ZOI surface section [mm ²]	Measured
Equivalent radius of ZOI	$r_E = \sqrt{\left(\frac{A_Z}{\pi}\right) \cdot d^2}$
Circularity of ZOI [r ²]	Calculated
Ratio of ZOI equivalent radius to the particle length for 0° and 90° specimens [mm mm ⁻¹]	$R_{r_E-l} = \frac{r_E}{l}$
Ratio of ZOI minor dimension to the particle depth for 45° specimens [mm mm ⁻¹]	$R_{Z_m-d} = \frac{Z_m}{d}$

Where: r_E = equivalent radius; A_Z = the area of ZOI surface section; d = particle distance from the surface

l = particle length; Z_m = ZOI's minor dimension

This paper will focus on the area of ZOI surface section (Figure 42G and Figure 45C) and its relationship with the depth of the embedded particle. Each DIC point in this area has a physical area associated with it and these areas were added to find the total area.

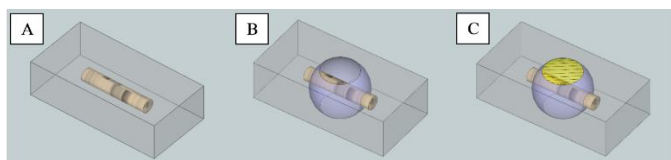


Figure 45. Idealized schematic of an embedded particle and its influence on the surrounding matrix: A) an idealized wood particle embedded in a polymer matrix. B) partial orb surrounding the particle representing its ZOI. C) Crosshatched circular section signifying the measured section of the ZOI.

Results and Discussion

During the test, as the matrix is loaded, and the load is gradually being transferred along the length of the fiber from the fiber end through shear forces (due to the difference in compliance between the fiber and matrix) so that more of the tensile load is gradually carried by the fiber and less so by the surrounding matrix until the strains in the fiber match the strain gradient in the matrix. In particles with low aspect ratios like those in WPCs, the load transfer zones from both ends overlap. In effect, the central part of the fiber never reaches the state in which the strains in the fiber are matching the strain gradient in the matrix (Cox 1952; Clyne 1989; Sretenovic, Müller et al. 2006; Wang 2007).

The evaluated data was restricted to that from a designated rectangular area surrounding the particle in a way to eliminate the effect of the tensile grips and the edges seen in Figure 44. The areas selected for specimens oriented at 0° , 45° and 90° were $4 \times 2 \text{ mm}^2$, $3 \times 3 \text{ mm}^2$, and $2 \times 2 \text{ mm}^2$, respectively. These areas were centered with the particle's center coordinates.

Figure 43 shows nine color-coded full-field maps of major principal strain, ϵ_1 , of the reference wire/HDPE specimens. Directly below these maps are their corresponding XCT scans locating their depth within the film.

Generally, the extent and the shape of the ZOI is affected by the bonding efficacy. However, while the actual ZOIs surrounding the embedded particles are three dimensional, the optical measurements are limited to the effects detectable on the specimen's surface where it intersects with the particle's ZOI (Figure 45C). The deeper the particle is buried below the specimen surface the smaller is the ZOI area detectable on the surface. Comparing the depth of the wire particles below the surface with the area of the ZOI intersection on the surface shows a distinct trend. For instance, Wire0-1 was found 0.020 mm from the surface and had a ZOI intersection area of 0.62 mm^2 , while the depth of Wire0-3 was 0.100 mm and had a ZOI intersection area of 0.41 mm^2 (first row in 2). This shape and extent of the zone may additionally be affected by the particle geometry, length, and orientation.

This analysis found that a quantitative analysis of the ZOI area alone can hardly be used for the assessment of the efficacy of load transfer between polymer matrices and embedded particles. It is expected that better results may be obtained by employing morphologically accurate numerical models of the analyzed specimens. This approach as well as results from embedded wood particles will be reported in a separate publication.

Conclusions

The overall goal of this research was to develop an efficient method for the measurement of strain distribution patterns in the matrix material surrounding embedded wood particles. This paper has presented a measurement methodology using optical measurement techniques, compounded WPC specimens, and multiple particle orientations.

It was found that the patterns observed on the surface of the specimen were substantially affected by the particle distance from the surface. This distance is a critical parameter for any comparison of strain patterns. Due to this significant effect, analysis of the load transfer behavior in the polymer-wood particle bond would be best conducted in conjunction with predictive modeling tools.

References

- Clyne, T.W. 1989. A Simple Development of the Shear Lag Theory Appropriate for Composites with a Relatively Small Modulus Mismatch. *Mater. Sci. Eng. A122*: 183-192.
- Cox, H.L. 1952. The elasticity and strength of paper and other fibrous materials. *Br. J. Appl. Phys.* 3: 72-79.
- Muszynski, L., Kamke, F.A., Nairn, J.A., Schwarzkopf, M., Paris, J.L. 2013. Integrated Method for Multi-Scale/Multi-Modal Investigation of Micro-Mechanical Wood-Adhesive Interaction. International Conference on Wood Adhesives, 2013, Toronto, Ontario, Canada.
- Noselli, G., Dal Corso, F., Bigoni, D. 2010. The stress intensity near a stiffener disclosed by photoelasticity. *Int. J. Fracture* 166(1/2): 91-103.
- Sebera, V., Muszynski, L. 2011. Determination of local material properties of OSB sample by coupling advanced imaging techniques and morphology-based FEM simulation. *Holzforschung* 65: 811-818.
- Sretenovic, A., Müller, U., Gindl, W. 2006. Mechanism of stress transfer in a single wood fibre-LDPE composite by means of electronic laser speckle interferometry. *Composites Part A* 37: 1406-1412.
- Sutton, M.A. (2010) Personal Communication.
- Wang, Y. 2007. Morphological Characterization of Wood Plastic Composite (WPC) with Advanced Imaging Tools: Developing Methodologies for Reliable Phase and Internal Damage Characterization. M.S., Oregon State University.
- Wang, Y., Muszynski, L., Simonsen, J. 2007. Gold as an X-ray CT scanning contrast agent: Effect on the mechanical properties of wood plastic composites. *Holzforschung* 61(6): 723-730.

Microstructure, Mechanical, Thermal and Antimicrobial Properties of Hybrid Copper Nanoparticles and Cellulose Based Materials Embedded in Thermoplastic Resins

Gloria S. Oporto^{1,2}, Tuhua Zhong³, Jacek Jaczynski⁴, and Ronald Sabo⁵*

¹ Assistant Professor Wood Science and Technology,
West Virginia University, Morgantown WV 26506

** Corresponding author*

gloria.oporto@mail.wvu.edu

² Unidad de Desarrollo Tecnológico-Universidad de Concepción,
Camino a Coronel km 25, Coronel, CHILE

³ PhD Student, Wood Science and Technology,
West Virginia University, Morgantown WV 26506

⁴ Associate Professor, Division of Animal and Nutritional Sciences,
West Virginia University, Morgantown, WV 26506

⁵ Research Materials Engineer, USDA Forest Service
Forest Product Laboratory, Madison WI 53726, USA

Abstract

Hybrid materials of copper nanoparticles synthesized “in situ” on carboxymethyl cellulose (CMC) and TEMPO-oxidized cellulose nanofibers (CNFs) were embedded in thermoplastic resins consisted of polypropylene (PP) and polylactic acid (PLA). Composites were prepared using a twin-screw extruder followed by both injection molding process and a dry film formation process. Morphological and copper elemental mapping analyses were performed using scanning electron microscopy-energy dispersive X-ray microscopy (SEM-EDX). Thermal and mechanical properties of the extruded-injected composites were analyzed using differential scanning calorimetry (DSC) and through a tensile test (ASTM D638), respectively. The morphological analysis of those composites revealed that a large amount of the hybrid material remained as aggregates. The tensile strengths of PP and PLA composites decreased in average up to 19.2% after the incorporation of the hybrid copper nanoparticles-cellulose based material. Thermal analysis showed no distinctive changes in the glass transition temperature and melting temperature for both PP and PLA composites after the incorporation of the hybrid material. The concentration of copper ions released from the hybrid materials embedded in thermoplastic resins was determined using Atomic Absorption Spectrometry (AAS). The preliminary results showed that even though copper ions are migrating from the surface of films, the rate of this migration is too slow that is not affecting the antimicrobial properties of the films against *E.coli* DH5 α .

Keywords: Carboxymethyl cellulose, cellulose nanofibers, copper nanoparticles, polypropylene, polylactic acid, nanocomposites.

Introduction

The feasibility to incorporate antimicrobial materials as active nanocomponents into thermoplastic resins has opened novel opportunities of application in areas such as packaging, medicine, safety, etc. (Zhang et al 2007; Duncan 2011). However, little work has been performed regarding the capability to release the active component and how the mechanical properties of the final composites are affected after the incorporation of the active material (Fernandez et al 2010; Fortunati et al 2010; Echegoyen and Nerin 2013; Fortunati et al 2013). Based on this fact, our long term goal is to develop a composite based on hybrid cellulose-copper nanoparticles embedded in thermoplastic resins with an effective copper release rate and appropriate mechanical properties to serve as antimicrobial material in active food packaging. In our research we were using cellulose based materials not only as a template and stabilizer of copper nanoparticles, but also with the aim to provide an improved and controlled release of copper ions. In our preliminary research we used commercial carboxymethyl cellulose (CMC) as template for synthesizing “in situ” copper nanoparticles, a potent biocide (Zhong et al 2013). The results demonstrated that copper nanoparticles with 10- and 20-nm diameter were synthesized on CMC using sodium borohydride as copper reducing agent. The resulting hybrid materials confirmed their antimicrobial effectiveness against the nonpathogenic surrogate of foodborne pathogen *Escherichia coli*.

Materials and Methods

Preparation of the Hybrid Carboxymethyl Cellulose (CMC)-Copper Nanoparticles

The general procedure used for the preparation of the hybrid carboxymethyl cellulose-copper nanoparticles has been described previously (Zhong et al 2013). Hybrids with copper concentrations of 305 $\mu\text{g/mL}$ and 582 $\mu\text{g/mL}$ were prepared. Some of the mixtures were subjected to a washing stage before the addition of the reducing agent (Table 1), where the excess of cupric ions were removed. Hybrid carboxymethyl cellulose-copper nanoparticles solutions were subsequently dried on a VirTis Genesis Freeze Dryer (Warminster, USA) for 1 week. The solid hybrid material with two different copper concentration was grinded to powder using a Waring Commercial Blender.

Table 1. Preparation of the Hybrid Carboxymethyl Cellulose (CMC)-Copper Nanoparticles

Na-CMC solution #	Sample Codes	Na-CMC (g)	Deionized water (mL)	CuSO ₄ solution (0.1 mol/L) (mL)	Treated with washing process. Yes / No	NaBH ₄ solution (0.5 mol/L) (mL)
1	CMC-Cu (1)	1	99	5 ^a	Yes	2
2	CMC-Cu (2)	1	99	10 ^b	Yes	4
3	CMC-Cu (3)	1	99	5 ^a	No	2
4	CMC-Cu (4)	1	99	10 ^b	No	4

CMC-Cu: carboxymethyl cellulose-copper nanoparticles

a - Expected copper concentration: 305 $\mu\text{g/mL}$

b - Expected copper concentration: 582 $\mu\text{g/mL}$

Preparation of the Hybrid Cellulose Nanofibers (CNF)-Copper Nanoparticles

Sixteen grams of TEMPO-oxidized cellulose nanofibers gel containing 0.67% cellulose nanofibers (TEMPO-oxidized cellulose nanofibers, Forest Product Laboratory, Madison, USA) were dissolved in 84 mL of deionized water under vigorous magnetic stirring. An hybrid material

with copper ion concentration of 51.2 $\mu\text{g/mL}$ was prepared. The powders of hybrid copper nanoparticles and cellulose nanofibers were obtained using freeze-drying followed by grinding process as described above.

Preparation of Composites: Hybrid Cellulose-Copper Nanoparticles Embedded in Thermoplastic Resins

Polypropylene (PP) (Certene PHM-20AN, Muehlstein and Co., Norwalk, CT) and polylactic acid (PLA) (Ingeo 4043D, NatureWorks LLC, Minnetonka, MN) pellets were dried in an oven overnight at 105°C. The resulting hybrids of cellulose-copper nanoparticles were incorporated into the thermoplastic resins polypropylene (PP) and polylactic acid (PLA) using extrusion-injection and extrusion-film processes. Extrusion was performed using a DSM Xplore twin-screw micro-extruder and injection process was performed using a DSM 10cc Micro Moulding Machine (Geleen, Netherlands). The extrusion process was performed at 180 °C and 190 °C for PP and PLA respectively; the injection processes was performed at 180 °C and 195 °C for PP and PLA, respectively.

In addition, preliminary PLA films embedded with the hybrid cellulose-copper nanoparticles were prepared by using DSM Xplore twin-screw micro-extruder followed by DSM Film Device Machine (Geleen, Netherlands).

Field Emission Scanning Electron Microscopy - Energy Dispersive X-ray Spectroscopy Characterization (FESEM-EDX)

The morphological and copper elemental mapping analyses of the hybrid cellulose-copper nanoparticles were characterized by using a Hitachi S-4700 FESEM with an EDX brand Energy dispersive spectroscopy detector (Tokyo, Japan).

Mechanical Strength - Tensile Testing

The tensile strength of the extruded-injected composites were measured using an Instron 810 Material Test System (Norwood, USA) according to the ASTM D638 standard. Five specimens were tested for each material.

Differential Scanning Calorimetry (DSC) Characterization

The thermal behavior of the produced composites was studied using a TA Instruments Q20 differential scanning calorimeter equipped with refrigerated cooling system (New Castle, USA). The temperature of analysis ranged from 25°C to 250°C with a heating rate of 10°C/min. The glass transition temperature (T_g), cold crystallization temperature (T_{cc}), melting temperature (T_m), cold crystallization and melting enthalpies (ΔH_{cc} , ΔH_m) were determined from the first heating scan. The degree of crystallinity of PP composites was calculated according to Bahar et al. The enthalpy of melting for 100% crystalline PP has been reported as value of 209 J/g (Fan et al, 2011). The degree of crystallinity of PLA composites was calculated according to Fortunati et al 2010. The enthalpy of melting for 100% crystalline PLA has been reported as 93 J/g (Tsuji and Ikada, 1996).

Atomic Absorption Spectroscopy (AAS) Characterization of Copper Ion Release from Thermoplastic Composites in an Aqueous Medium.

To monitor the copper ion release from the produced composites, extruded-injected specimens obtained from extrusion and injection molding processes were stored in bottles containing 100 mL deionized water. The analytes collected from such storages were used for quantification of copper ion released from the specimens at one-week interval for a month using a Perkin-Elmer 2380 Atomic Absorption Spectrometer (AAS) (Waltham, USA). A rectangular piece from each composite was prepared (length 100 mm and width 30mm). Two pieces of each composite were

immersed into the 100 mL of deionized water. The analytes collected from such storages were used for quantification of copper ion released from the films at one-week interval for a month using AAS.

Antimicrobial Properties of Composite Film of PLA containing Hybrid Cellulose Nanofibers-Copper Nanoparticles

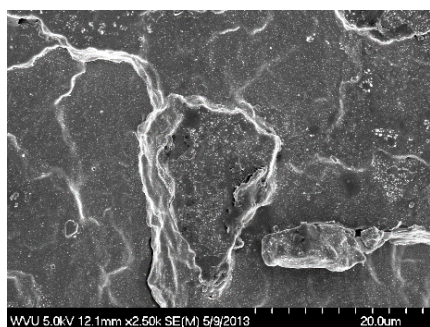
The procedure developed by Black et al. (2006) was followed to enumerate *E. coli*. Since only for PLA films was appreciated copper release, the preliminary antimicrobial test was performed only on these samples. A 1.5-mL aliquot of initial *E. coli* culture was transferred to a neat PLA film surface and PLA/CNF-Cu film surface and incubated at room temperature for the following time: 2 h, 1 week, and 2 weeks. All bacterial enumerations were performed in duplicate. Mean values are reported as CFU/mL.

Results and Discussion

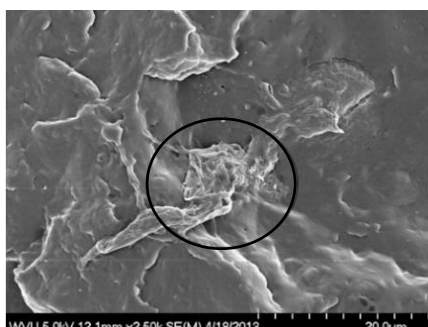
Morphological and copper elemental mapping of the hybrid cellulose-copper nanoparticles.

After the freeze-drying process it was difficult to reduce the size of the material. Aggregates of the cellulose-based material were easily formed. The copper elemental mapping showed a well distributed copper on the cellulose raw material (CMC and CNF).

Microstructure of the Hybrids Carboxymethyl Cellulose (CMC)-Copper Nanoparticles and Cellulose Nanofibers (CNF)-Copper Nanoparticles Embedded in Thermoplastic Resins (extruded-injected specimens). Several SEM pictures were taken and in Fig 1 (a) and (b) are presented representative examples of the cryo-fractured surfaces of pure polypropylene (PP) and one example of the PP composites. Some of the hybrid material remained as aggregates, as observed in Fig 1 (b) (inside black circle). Similar situation is observed for PLA composites, but in this case an example with no agglomeration is presented (Fig 1 (d)). Additionally, pure PLA and PLA composites exhibit a porous structure (Fig 1(c) and (d)), which might be attributed to residual moisture present in the original polymer.



(a)



(b)

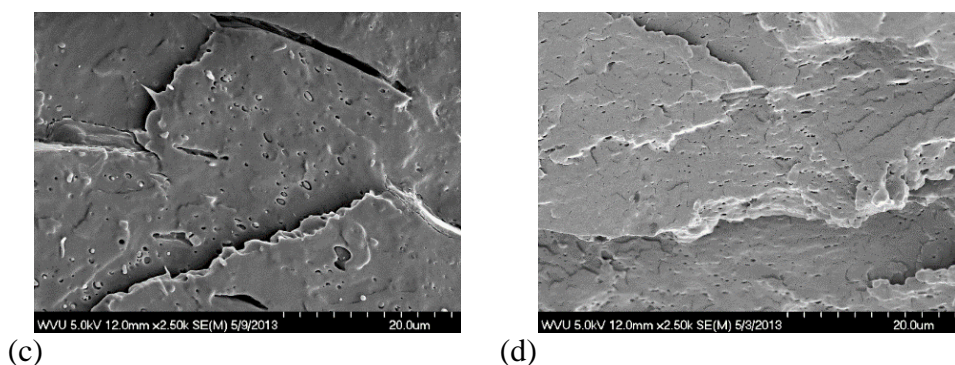
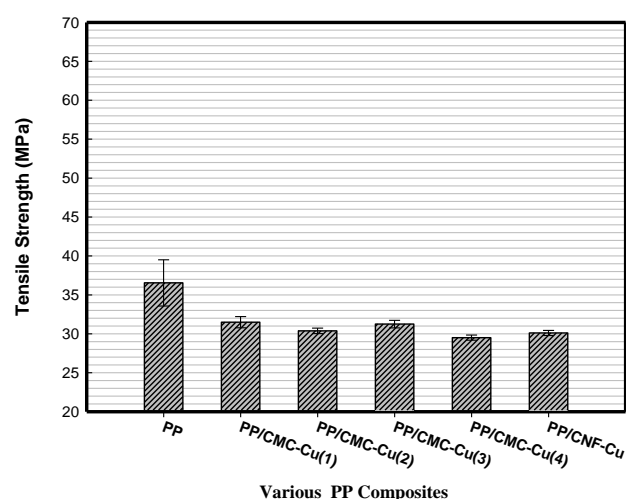


Figure 1. Scanning electron microscopy images of cryo-fractured surfaces of: (a) pure PP, (b) PP/CMC-Cu (3), (c) pure PLA, and (d) PLA/CMC-Cu (3).

Mechanical Strength –Tensile Testing on the Hybrids CMC-Copper Nanoparticles and CNFs-Copper Nanoparticles Embedded in Thermoplastic Resins (Extruded-Injected Specimens). In general, all composites (PP and PLA) resulted with tensile strength lower than the correspondent pure matrix (Fig.2). This reduction is attributed to the agglomeration of the hybrid material, porous formation and debondings between cellulose based materials and matrices. Agglomerates create stress concentration zones which in turn can act as a crack initiator. As traditionally recognized, tensile strength is governed by the interfacial adhesion between cellulose based materials and matrices.

A reduced effect in the composites tensile strength can be attributed to copper concentration for both PP and PLA composites. From Fig 2(a) and Fig 2(b), higher concentrations of copper in the hybrid material (solution number 2 and 4 from Table 1) resulted in slightly lower tensile strength values compared with lower copper concentrations.



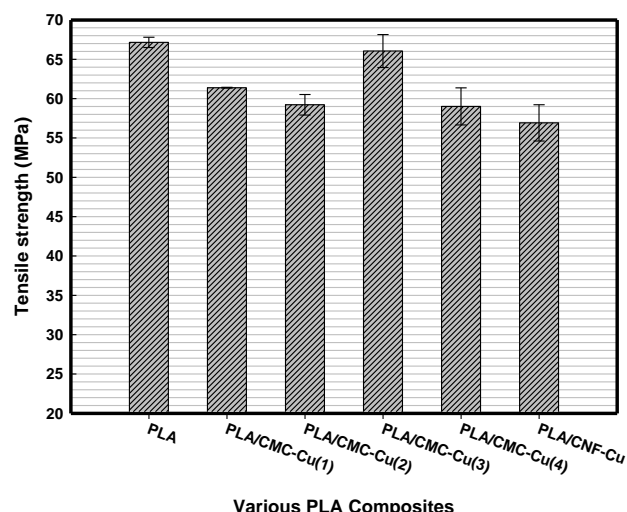
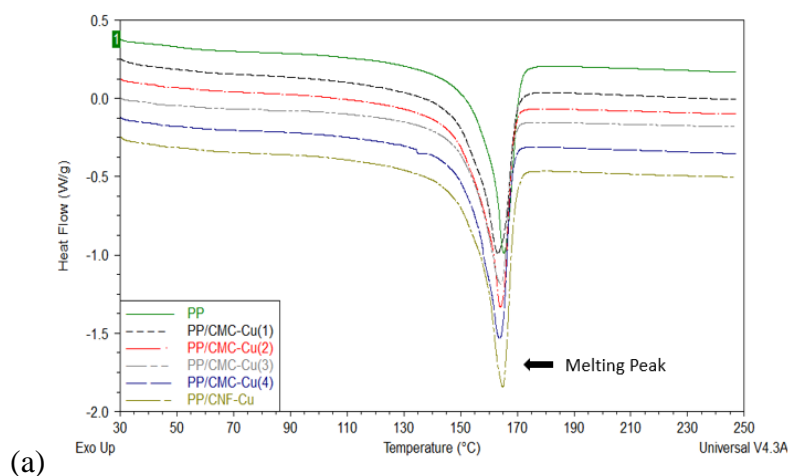


Figure 2. Tensile strength of (a) PP and PP composites, and (b) PLA and PLA composites.

Thermal Properties of Hybrid Copper Nanoparticles and Cellulose Based Materials in Thermoplastic Resins (Extruded-Injected Specimens). Fig 3(a) and Fig 3(b) present the thermal properties (melting temperature, glass transition temperature and the cold crystallization peak) for PP, PLA and their respective composites. The melting temperature of PP and PLA composites slightly decreased when compared with pure PP or PLA; this result might be attributed to the formation of more defective and less ordered crystals caused by heterogeneous nucleation in both composites. Two peaks of melting temperature are noticeable in Fig 3b for PLA and its composites. Each melting peak might be assigned to different crystalline lamellae population essentially characterized by its thickness or its perfection or the melting-recrystallization-melting mechanism (Tsuji and Ikada, 1996). A sharp endothermic peak associated to the glass transition of PLA is observed in Fig 3b. The peak is typically attributed to stress relaxation on heating of PLA. Here it is possible to appreciate a slight reduction of the glass transition temperature when PLA was embedded with the hybrids CMC-Cu and CNF-Cu. This reduction might be attributed to the formation of more defective and less ordered crystals caused by heterogeneous nucleation in PLA composites.



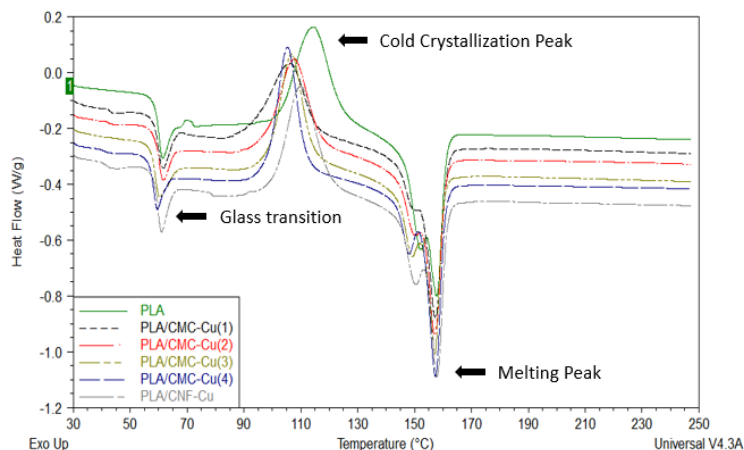


Figure 3. Differential Scanning Calorimetry analysis for (a) PP and PP composites, and (b) PLA and PLA composites.

The cold crystallization peaks for PLA composites shifted to lower temperature in comparison with the cold crystallization of pure PLA (Fig 3b). The lower of cold crystallization temperature could be the indication of faster crystallization, which might be induced by the hybrid materials. Cellulose based materials and metal nanoparticles are acting as nucleating agents for enhanced crystallization and therefore decreasing the cold crystallization temperature.

There is an increase in the degree of crystallinity for both PP and PLA composites compared to pure PP and PLA, respectively. Carboxymethyl cellulose and cellulose nanofibers might be acting as nucleating agents, and therefore contributed to the increased crystallinity of composites for both PP and PLA matrices. The increase in crystallinity of PLA after the addition of cellulose based materials have been reported for others (Mathew et al 2006). They determined increases up to 130% for instance, after the incorporation of 25% wt of wood flour (particles size: 20-30 μm) in PLA matrices.

The washing step is also affecting the crystallinity of the final composites for both, PP and PLA. For PP composites treated with a washing process (solution 1 and 2), the degree of crystallinity increased up to 22.5% in both cases. For those PP composites prepared with the hybrid materials without washing treatment (solution 3 and 4), the degree of crystallinity was increased up to 4.9% and 8.4%, respectively. A more dramatic effect of the washing treatment for those PLA composites on their crystallinity compared with PP composites was observed. For PLA composite prepared with hybrid materials that were treated by a washing process (solution 1 and 2), the degree of crystallinity resulted increased up to 356.2% and 393.8%, respectively. For those PLA composites prepared with the hybrid materials without washing treatment (solution 3 and 4), the degree of crystallinity was increased up to 268.8% and 250.0%, respectively. Washing process removed excess of copper on the cellulose surface and then the remnant copper nanoparticles might have a better ability to favor the nucleation and the growth of crystals in the thermoplastic resins. For composites prepared with PP and PLA embedded with CNF-Cu without washing treatment, the increase in the degree of crystallinity was in average up to 24.9% and 106.2%, respectively. Finally, the hybrid materials CMC-Cu and CNF-Cu seems to have higher ability to act as nucleation agents and increase the crystallinity of PLA matrices compared with PP matrices.

Copper Ion Release from Extruded-Injected Composites and Film Composites in Aqueous Media. Copper ion release was evaluated from the extruded-injected composites (PP and PLA composites) and from the extruded-film formation composites (PLA composites). Copper ions were not detected from the aqueous media in which extruded-injected specimens were immersed over one month. That might be attributed to the fact that the hybrid material was distributed through the whole composite and no much copper was available in the surfaces. The thickness of those extruded-injected composites of about 1.5 mm retarded copper ion leaching from the matrices. In terms of the evaluation of copper release from PLA films (thickness about 0.2 mm) it is possible to mention that just for those composites fabricated with the hybrid cellulose nanofibers-copper nanoparticles, copper release was evidenced (Table 2). After 2 days of immersion copper ions were determined in the aqueous solutions and the copper release continued over a period of a month.

Table 2. Copper ions released from PLA film composites.

Time (days)	Copper Ion Concentration (ppm)
	PLA/CNF-Cu
2	0.29
9	0.42
16	0.49
30	0.62

Antimicrobial Properties of pure PLA Film and PLA/CNF-Cu Film against E.coli DH5 α .

Since no copper release was determined from those extruded injected composites, only extruded-film composites (PLA/CNF-Cu) were evaluated in terms of their antimicrobial properties. The initial concentration of *E.coli* DH5 α culture this study corresponded to 1.9×10^8 CFU/mL. The concentrations of *E.coli* culture from the sample surfaces for both PLA film and PLA/CNF-Cu film slightly increased with the increase in the exposure time, indicating both PLA film and PLA/CNF-Cu film did not have antimicrobial activity against *E.coli* DH5 α . Considering that the hybrid cellulose-copper nanoparticles demonstrated excellent antimicrobial activity against *E.coli* DH5 α [7] and even though some copper migration was evidenced from some of the film composites, the reason why these composite films did not show antimicrobial properties might be because of the copper concentration. The concentration was likely not high enough to induce copper migration that would result in inactivation of *E. coli*.

Conclusions

The incorporation of the hybrid cellulose based materials-copper nanoparticles in both polypropylene (PP) and polylactic acid (PLA) matrices decreased their tensile strength. The reduction was considerably higher for those composites prepared with PP (19.2%) than for PLA (12.1%). Even though copper concentration is apparently affecting negatively the tensile strength of the composites, the presence of cellulosic agglomerates in the matrices and therefore the poor interfacial adhesion between them and matrices might be the most important reason for the mechanical property reduction. The agglomerations might be produced mainly during the drying freeze process and therefore a different process to dry is being currently evaluated.

The melting temperature and glass transition temperatures were slightly reduced for both, PP and PLA composites after the incorporation of the hybrid material, compared with the pure matrices. This result might be attributed to the formation of more defective and less ordered crystals caused

by heterogeneous nucleation in both composites. Similar effect might cause the reduction in the cold crystallization temperature for PLA composites.

Higher degree of crystallinity for both PP and PLA composites were demonstrated after the incorporation of the hybrid material. As published for others previously, cellulose based materials have favored nucleation and crystal growth and therefore the crystallinity of thermoplastic resins.

In terms of copper release from our composites after being immersed in an aqueous medium for a month, the preliminary results indicate that they were able to migrate only from PLA films. Copper ions were not able to migrate from the extruded-injected PP or PLA composites. The copper migration achieved for some PLA films was insufficient to inactivate of *E.coli*. Therefore, in the condition of the experiment no antimicrobial activity against DH5 α was demonstrated.

Acknowledgments

Funding for this work was provided by NIFA-McStennis WVA00098 “Efficient utilization of biomass for biopolymers in central Appalachia” and NIFA-USDA Grant/Contract No. 2013-34638-21481 “Development of novel hybrid cellulose nanocomposite film with potent biocide properties utilizing low quality Appalachian hardwoods”.

References

- ASTM (2010) D 638-10 Standard test method for tensile properties of plastics, West Conshohocken, PA.
- Bahar E, Ucar N, Onen A, Wang Y, Oksuz M, Ayaz O, Ucar M, Demir A (2012) Thermal and mechanical properties of polypropylene nanocomposite materials reinforced with cellulose nano whiskers. *J Appl Polym Sci* 125: 2882-2889.
- Black JL, Jaczynski J (2006) Temperature effect on inactivation kinetics of *Escherichia coli* O157:H7 by electron beam in ground beef, chicken breast meat, and trout fillets. *J Food Sci* 71(6):M221-M227.
- Duncan TV (2011) Applications of nanotechnology in food packaging and food safety: barrier materials, antimicrobials and sensors. *J Colloid Interface Sci* 363:1-24.
- Echegoyen Y, Nerin C (2013) Nanoparticle release from nano-silver antimicrobial food containers. *Food Chem Toxicol* 62:16-22.
- Fan Y, Zhang C, Xue Y, Zhang X, Ji X, Bo S (2011) Microstructure of two polypropylene homopolymers with improved impact properties. *Polymer* 52:557-563.
- Fernandez A, Soriano E, Hernandez-Munoz P, Gavara R (2010) Migration of antimicrobial silver from composites of polylactide with silver zeolites. *J Food Sic* 75(3):186-193.
- Fortunati E, Armentano I, Iannoni A, Kenny JM (2010) Development and thermal behaviour of ternary PLA matrix composites. *Polym Degrad Stabil* 95:2200-2206.
- Fortunati E, Peltzer M, Armentano I, Jimenez A, Kenny JM (2013) Combined effects of cellulose nanocrystals and silver nanoparticles on the barrier and migration properties of PLA nanobiocomposites. *J Food Eng* 118:117-124.
- Frone AN, Berlioz S, Chailan JF, Panaitescu DM (2013) Morphology and thermal properties of PLA–cellulose nanofibers composites. *Carbohyd Polym* 91:377-384.
- Mathew AP, Oksman K, Sain M (2006) The effect of morphology and chemical characteristics of cellulose reinforcements on the crystallinity of polylactic acid. *J Appl Polym Sci* 101:300-310.

- Tsuji H, Ikada Y (1996) Blends of isotactic and atactic poly (lactide)s: 2. Molecular-weight effects of atactic component on crystallization and morphology of equimolar blends from the melt. *Polymer* 37(4):595-602.
- Zhang W, Zhang Y, Ji J, Yan Q, Huang A, Chu PK (2007) Antimicrobial polyethylene with controlled copper release. *J Biomed Mater Res Part A* 83(3):838-844.
- Zhong T, Oporto GS, Jaczynski J, Tesfai AT, Armstrong J (2013) Antimicrobial properties of the hybrid copper nanoparticles-carboxymethyl cellulose. *Wood Fiber Sci* 45(2):215-222.

Cellulose Nanofibril (CNF) Reinforced Open Cell Foams; Application of Cubic Foam Theory

Nadir Yildirim³ – R. Lopez-Anido² – Stephen M. Shaler. ^{1}*

^{1*}Professor & Director // School of Forest Resources, University of Maine, 5755
Nutting Hall, Orono, ME 04469-5755

Associate Director // Advanced Structures & Composites Center, University of
Maine, 35 Flagstaff Road, Orono, ME, 04469-5793

* *Corresponding author*
shaler@maine.edu

²Professor // Civil Engineering & Advanced Structures & Composites Center,
University of Maine, 35 Flagstaff Road, Orono, ME, 04469-5793
RLA@maine.edu

³PhD. Candidate // School of Forest Resources, University of Maine, 5755 Nutting
Hall, Orono, ME 04469-5755
Graduate Research Assistant // Advanced Structures & Composites Center,
University of Maine, 35 Flagstaff Road, Orono, ME, 04469-5793
nadir.yildirim@maine.edu

Abstract

Cellulose nanofibril (CNF) reinforced open cell foams were produced using cellulose nanofibrils (up to 1.5% by weight), corn starch (up to 6% by weight), and water in conjunction with a freeze-drying process. As indicated in previous studies, starch foams are extremely friable and have low mechanical performance. The compressive performance of foams were significantly enhanced through incorporation of CNF. An inverse modeling scheme utilizing cubic array foam theory and the rule of mixtures for the CNF/starch foam wall material was used to predict the modulus of elasticity of the CNF component. Microscopic techniques (SEM and AFM) were used to measure the unit cell dimensions (beam/strut) as a function of CNF volume fraction. The prediction was that the CNF has a 1.8 GPa compression modulus. Future studies will include the investigation of CNF compression modulus using AFM and nanoindentation techniques and will focus on the enhancements of mechanical properties.

Keywords: Cellulose nanofibrils, micromechanics, foam modeling, scanning electron microscope (SEM), atomic force microscope (AFM)

Introduction

Cellular materials are made up from small compartments called cells. These cells have unique structures and interconnected through the cell walls, edges, faces or corners (Gibson and Ashby

1998). Cellular materials or cellular solids refer to a variety of porous structures including honeycombs, open-cell foams or closed cell foams. Raw materials for foam production can be polymers, metals, ceramics or organic materials. In addition, foams can be found in nature with wood, cork, and bone as good examples (Michalska and Pecherski 2003). Foams are popular in applications which require materials with low thermal conductivities. Mechanical properties of the foams mostly depend on the materials that have been used to produce the foams (Gan et al. 2005) as well as density. In this study, we produced starch-based foams reinforced with cellulose nanofibrils. The main reason for using cellulose and starch is they both are biopolymers, compatible with each other and abundant in nature. Cellulose can be obtained from trees, a broad range of plants and even sea animals (Moon et al. 2010) while starch can be obtained from corn, potato, rice wheat and etc. (Shogren et al. 1998).

The compression properties of organic composite foams were investigated using a hybrid theoretical model consisting of cubic array theory for the cellular structure with the rule of mixtures used to describe the mechanical properties of the CNF/starch foam wall material.

Materials and Methods

Five different organic composite foam combinations were produced with a variety of CNF/Starch/Water combinations (Table 1). Materials were corn starch and cellulose nanofibrils produced at the University of Maine pilot plant. Details on the manufacturing process can be found in Yildirim et al. 2014.

Table 1. Weight percent composition of freeze drying foam mixtures.

Foam Combinations	Solid –Water Content
0.5% CNF+ 0.5% Starch	1%-99%
1% CNF	1%-99%
1.5% CNF+ 3% Starch	4.5%-95.5%
1.5% CNF+ 6% Starch	7.5%-92.5%
7.5% Starch	7.5 %-92.5%

Density was measured for each material combination according to ASTM C303-10. Porosity measurements (calculations) were performed using a liquid porosimetry method followed by calculation provided in equation 1 (Gibson et al. 1982).

$$\phi = 100 \left(1 - \frac{\delta_{\text{bulk}}}{\delta_{\text{material}}} \right) \quad \text{Eq. 1}$$

where;

ϕ = porosity

δ_{bulk} = foam bulk density

δ_{material} = material density

Morphological properties and measurements of the cellular dimensions were conducted using scanning electron microscopy (Zeiss Nvision 40 FIB-SEM). Compression tests were conducted according to ASTM C165-07. Specimen displacements were obtained from the cross-head

displacement. All physical and mechanical tests were conducted under the laboratory conditions of 25 ± 2 °C temperature and 50% relative humidity.

Experimental Results

Produced foams were tested and investigated in our previous study (Yildirim et al. 2014). Foams produced in this study exhibited highly porous structures (93.5 % - 99.1 %) and super low densities (0.013 g/cm^3 - 0.098 g/cm^3). Morphological investigations showed that foams have mostly open cell structures (Figure 1a) and the cell wall structure is a plate of CNF material embedded within a starch matrix (Figure 1b,c). The fibril diameters typically ranged between 20 and 200 nm (Figure 1c).

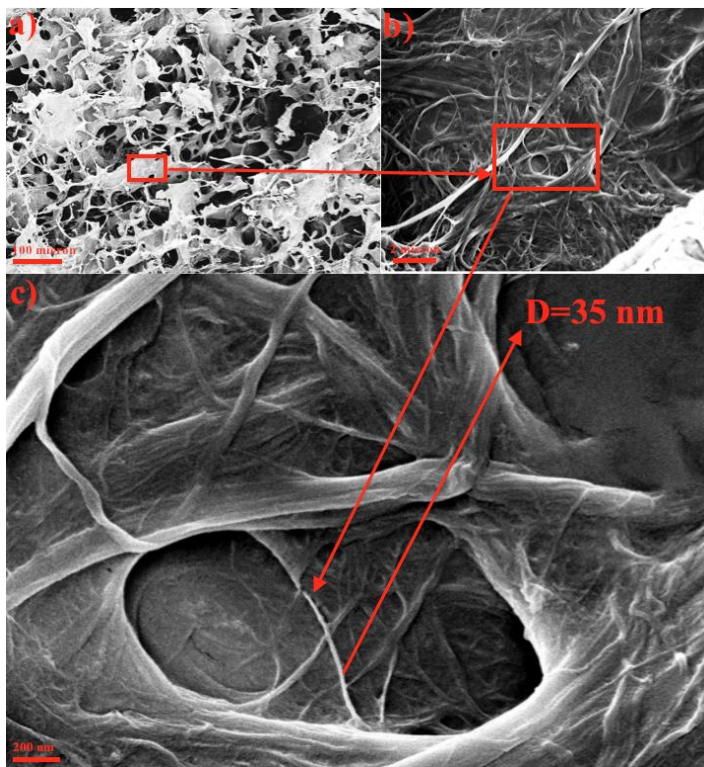


Figure 1. Representative SEM images of foams (1.5%CNF+6%S), (a) cellular structure, (b) distribution of nanofibrils in 2 micron scale bar and (c) fibril diameter measurements.

A typical stress-strain curve for the compression tests is given in Figure 2. The compression modulus (E) was obtained from the linear portion of the stress-strain curve.

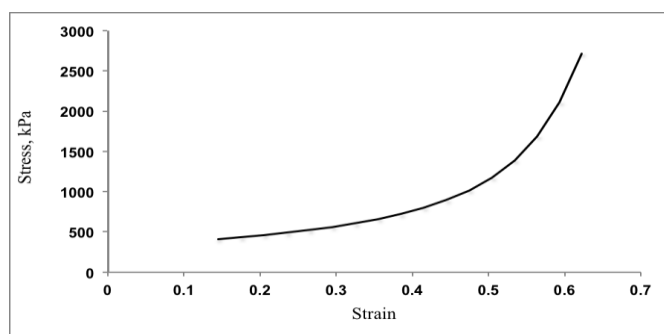


Figure 2. Typical stress-strain curve for compression tests of foams.

Compression properties are summarized in Table 2. Detailed information and comparison with other studies can be found in Yildirim et al. 2014.

Table 2. Compression properties of the foams.

Sample	Bulk Density (σ/cm^3)	Compression Modulus (kPa)	Compressive Strength (kPa)
.5% CNF+	0.014 (0.0010) C	15.0 (2.0) C	144 (44.0) C
1% CNF	0.014 (0.0016) C	30.0 (7.0) C	359 (63.0) C
1.5% CNF+	0.053 (0.0011) B	496 (82) B	2753 (203) B
1.5% CNF+	0.076 (0.0020) A	907 (171) A	3330 (249) A
7.5% Starch	N/A	N/A	N/A

Parentheses indicate the standard deviation. A, B, C and D letters indicates the significant differences between the treatments.

Microstructural Modeling Results

Cubic array foam theory for open cell foams was used (Gibson and Ashby, 1998). It was assumed that the produced foams were isotropic and that the cell wall material was linear-elastic. Relative density is defined as the ratio of bulk density (δ_{bulk}) to cell wall density (δ_{material}) (Eq. 2). For open cell foams, this relative density can be predicted from the idealized structure dimensions (Eq. 2.1).

$$\delta_{\text{relative}} = \frac{\delta_{\text{bulk}}}{\delta_{\text{material}}} \quad \text{Eq. 2}$$

For open cell foams;

$$\delta_{\text{relative}} = C_2 \left(\frac{t}{l} \right)^2 \quad \text{Eq. 2.1}$$

where;

t= beam thickness (7 microns, Table 3)

l=beam length or beam width (19 microns, Table 3)

$C_2 = 3/8$, numerical constant (Gibson and Ashby 1998)

There are different calculations and correction factors (D_1, D_2, D_3, D_4) for foam structure determination (open cell foam or closed cell foam) but these correction factors can be significant when the relative density, which provides information about the cell wall thickness and the pore spaces, is equal or larger than 0.2 (Gibson and Ashby 1998). Since relative density of the experimental foams was around 0.05 - none of these corrections were necessary. The application of this approach is provided for foam combination 4 (1.5% CNF+ 6% Starch). The measured bulk density (δ_{bulk}) was 0.076 g/cm³ and the material density (δ_{material}) was assumed to be 1.5 g/cm³.

The unit cell (cubic cell) column and beam dimensions (thickness and length) for a foam produced from 1.5% weight CNF and 6% weight starch were measured using scanning electron microscopy. A minimum of 15 measurements were conducted for each dimension and the average values are reported (Table 3).

Table 3. Material properties of experimental CNF/starch foam.

	Material Properties	1.5% CNF+ 6%Starch
Unit cell dimensions	t, thickness (μm)	7
	L, length (μm)	19
Physical properties	δ_{material} , material density	1.5
	δ_{bulk} , foam bulk density	0.076
	Relative density	0.051
	Φ , porosity (%)	94.95
Mechanical properties	E, compression modulus	907

In open cell foams like the foam that was produced in this study, cell walls bend under compression forces (Gibson and Ashby 1998).

The cubic array formula for foam modulus (Equation 3) was rearranged and the required beam/column modulus was predicted based on experimentally determined foam modulus.

$$E_{\text{foam}} = E_{\text{material}} * C_1 * \left(\frac{\delta_{\text{bulk}}}{\delta_{\text{material}}} \right)^2 \quad \text{Eq. 3}$$

where;

E_{material} = Modulus of the beam and columns

E_{foam} = Foam modulus

C_1 = 1, Numerical constant (Gibson and Ashby 1998)

The foam wall material is a composite material composed of starch (matrix) and CNF (fibers).

The properties of the cell wall material was assumed to be described by the rule of mixtures (Eq. 4 & Eq. 4.1) (Reuss 1929).

$$E_{\text{material}} = V_f * E_f + (1 - V_f) * E_m \quad \text{Eq. 4}$$

$$V_f = \frac{\text{Volume of Fibers}}{\text{Volume of fibers} + \text{Volume of matrix}} \quad \text{Eq. 4.1}$$

where;

E_{material} = Composite modulus (foam cell wall material)

E_f = Fiber modulus (modulus of elasticity of CNF)

E_m =Matrix modulus (modulus of elasticity of starch, 2.9 MPa (Glenn and Irving 1995))

V_f =Fiber volume fraction (0.2)

The material (composite cell wall) modulus predicted by Equation 3 was assumed to be equal to the E_{material} of equation 4. This resulted in an estimate of 1.8 GPa for the fiber (CNF) modulus. In the calculations given above (Eq. 4 and Eq. 4.1) rule of mixtures assumes all fibers are perfectly aligned and that the fibers are continuous, the aspect ratio of the CNF exceeds 100 and therefore the assumption of continuous fibers is reasonable.

Comparison of this indirect estimate of fiber modulus with direct experimental measures is relevant. Cheng and Wang studied the elastic modulus of a single cellulose fibril using atomic force microscopy. They applied 3 point bending test and determined that the elastic modulus of single cellulose fibre with 170 nm diameter was 93 GPa (Cheng and Wang 2008). (Eichorn and Young 2001) investigated the Young's modulus of microcrystalline cellulose using Raman spectroscopy and estimated the modulus to be 25 ± 4 GPa. A recent study were done by Moon et al on the elastic properties of crystalline cellulose I_{β} showed that Young's modulus varies in 3 directions, with estimates of 19 GPa at weakest axis and 206 GPa in the strongest axis (Moon et al. 2013). (Lahiji et al. 2010) investigated the single cellulose nanocrystal properties using atomic force microscopy and determined that the transverse modulus of single cellulose nanocrystals varies between 18 and 50 GPa. Another study on cellulose nanocrystals by (Wagner et al. 2011) and showed that the transverse elastic modulus of CNC is 8.1 GPa with a 95% confidence interval of 2.7-20 GPa. The predicted modulus of cellulose nano particles and nanofibrils varies significantly in each study. Many of the studies explored crystalline cellulose. However, the CNF in this study has an amorphous structures in the fibrils. This can be expected to decrease the mechanical properties significantly. Another reason for the lower estimate may be due to the irregularities and imperfections in the foam structure (Figure 3). Imperfections due to shape differences, gaps and cracks (Fig. 3a) can be caused because of drying process. In addition, there are some heterogeneities (poor fibril dispersion) and there was variation in the embedment of CNF in the foam wall starch matrix (Fig. 3b). Any foam beam/column element which were primarily starch would be expected to fail at lower stresses.

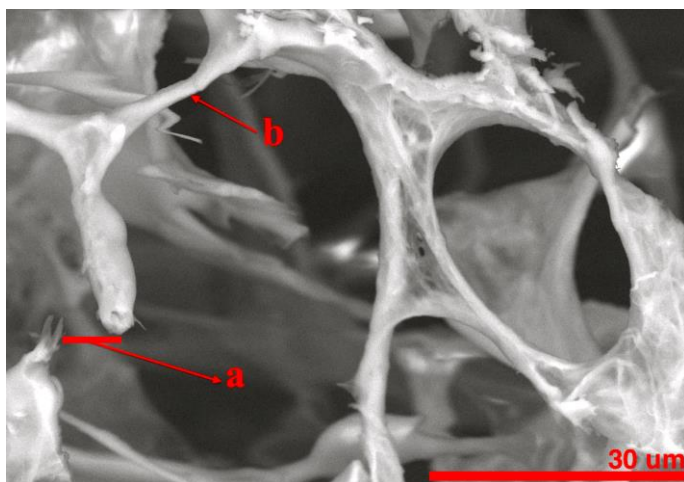


Figure 3. Structure imperfections and irregularities

Discussions and Conclusions

In this paper, the compression modulus of cellulose nanofibrils were predicted using bulk property measurements and an inverse hybrid theoretical model composed of foam theory and the rule of mixtures. As expected, density had a significant effect on the mechanical properties of the foams with lower density correlated with lower mechanical performance. The mechanical performance of the foam can be enhanced by modifying the foam structure during production process or can be increased by the addition of cellulose nanofibrils. The CNF modulus was predicted to be 1.8 GPa using the inverse hybrid modeling approach. Literature values from direct experiments on crystalline cellulose are significantly higher. The idealized open cell foam model did not account for a variety of factors (e.g. structural irregularities, imperfections, different fibril diameters and heterogeneous fibril dispersion).

References

1. Lorna J. Gibson and Michael F. Ashby 1998. Cellular Solids; Structure & Properties. Cambridge, United Kingdom.
2. M. J. Michalska and R. B. Pecherski 2003. Macroscopic Properties of Open-Cell Foams Based on Micromechanical Modeling. *Technische Mechanik* 23,2-4, 234-244
3. Y.X. Gan, C. Chen, Y. P. Shen 2005. Three-dimensional Modeling of the mechanical property of linearly elastic open cell foams. *Internayional Journal of Solids and Structures* 42, 6628-6642
4. Robert J. Moon; Ashlie Martini, John Nairn, John Simonsen and Jeff Youngblood 2010. Cellulose nanomaterials review: structure, properties and nanocomposites. *Chem. Soc. Rev.* 40, 3941-3944
5. R. L. Shogren; J. W. Lawton, W. M. Doane and K. F. Tiefenbacher 1998. Structure and morphology of baked starch foams. *Polymer*, 39, 6649-6655
6. L.J. Gibson, M. F. Ashby, G. S. Schajer and C. I. Robertson 1982. The mechanics of two-dimensional cellular materials. *Proc. R. Soc. Lond. A* 382, 25-42
7. N. Yildirim, S. M. Shaler, D.J. Gardner, R. Rice and D.W. Bousfield 2014. Cellulose Nanofibril (CNF) Reinforced Starch Insulating Foams. *MRS Proceedings*, 1621
8. Reuss, A. 1929. Calculation of the flow limits of mixed crystals on the basis of the plasticity of mono-crystals. *Z. Angew, Math. Mech.* 9, 49-58
9. G. M. Glenn and D. W. Irving 1995. Starch-Based Microcellular Foams. *Carbohydrates, Cereal Chem.* 72(2), 155-161
10. Q. Cheng and S. Wang 2008. A method for testing the elastic modulus of single cellulose fibrils via atomic force microscopy. *Composites: Part A* 39, 1838-1843
11. S. J. Eichhorn and R. J. Young 2001. The Young's modulus of a microcrystalline cellulose. *Cellulose* 8, 197-207
12. F. L. Dri, L. G. Hector Jr., R. J. Moon and P. D. Zavattieri 2013. Anisotropy of the elastic properties of crystalline cellulose I_{β} from first principles density functional theory with Van der Waals Interactions. *Cellulose* 20, 2703-2718
13. R. R. Lahiji, X. Xu, R. Reifengerger, A. Raman, A. Rudie and R. J. Moon 2010. Atomic force microscopy characterization of cellulose nanocrystals. *Langmuir* 26 (6), 4480-4488

14. R. Wagner, R. J. Moon, J. Pratt, G. Shaw and A. Raman 2011. Uncertainty quantification in nanomechanical measurements using the atomic force microscope. *Nanotechnology* 22, 455703
15. P. K. Mallick 1993. *Fiber-reinforced composites: materials, manufacturing and design-2nd ed.* New York, United States.
16. B. D. Agarwal and L. J. Broutman 1980. *Analysis and performance of fiber composites.* New York, United States.

Vacuum Assisted Resin Transfer Molding Process for Kenaf Fiber Based Composites

Changlei Xia, Sheldon Q. Shi and Liping Cai*

Department of Mechanical and Energy Engineering, University of North Texas
Denton, Texas, USA

* Corresponding author: Sheldon.Shi@unt.edu

Abstract

In order to apply vacuum-assisted resin transfer molding (VARTM) technique to vegetable fiber reinforced polymer molding products, a comparison of the mechanical properties of composites fabricated by VARTM technique and traditional hot-pressing was completed. Using a cold-press, kenaf (*Hibiscus cannabinus*, L.) bast fibers were preformed into mat. The unsaturated polyester resin was infused into the preforms at a vacuum pressure of 10-12 torrs. The examination of the mechanical properties and microstructure of the fabricated composites indicated that, compared to the composites made using the traditional hot-pressing, the modulus of elasticity, modulus of rupture and the tensile strength of the composites made using VARTM technology were increased by 65.5%, 30.7% and 41.7%, respectively. The dynamic mechanical analysis revealed that the composite moduli at the temperatures of -50 to 200°C were significantly increased (over twice) when the VARTM technology was used. The scanning electron microscope observation and mercury porosimetry confirmed that the interfacial compatibility between the kenaf fibers and the polyester resin was substantially improved.

Keywords : Vacuum-assisted resin transfer molding, Vegetable fibers, Composite properties, Scanning electron microscope

Introduction

An increasing attention is being devoted to the use of kenaf fibers (*Hibiscus cannabinus*, *L. family Malvacea*) owing to its lightness, low cost and high specific strength (Akli et al. 2011, Liang et al. 2013). Kenaf is well known as a cellulosic source with both economic and ecological advantages. From the viewpoint of energy consumption, it takes 15 MJ of energy to produce 1 kg of kenaf, comparing to 54 MJ to produce 1 kg of glass fiber (Akli et al. 2011). Furthermore, numerous benefits were discovered through the life cycle assessment (LCA). Base on the LCA study (Wang et al 2013), less negative environmental impact was found from raw material extraction to fiber manufacturing (cradle to gate) in kenaf fibers compared to glass fiber. Kenaf fibers consume less energy than other fibers in the manufacturing. A lower overall environmental burden is obtained from kenaf fibers (Wang et al. 2013).

The vacuum-assisted resin transfer molding (VARTM) technology is one of the well-established processes used to fabricate high performance composites using synthetic fiber, such as fiber glass or carbon fibers. Numerous studies regarding its manufacturing and applications have been carried out. The influence of molding conditions on the tensile properties of flat braided glass fabric reinforced phenolic composite was explored by Morii et al. (2001). The effect of the sizing of the glass fiber bundle on the tensile properties is also investigated. The results indicated that the tensile strength was significantly improved when longer periods (from 20 min to 60 min) of resin impregnation were applied. Good resin impregnation suppressed matrix cracking at low strain levels, which played an important role in the improvement of the tensile strength in the braided fabric reinforced phenolic resin composite.

The effects of geometric variables on the structural integrity and the strength of different glass-fabric-reinforced polyester composites made using VARTM technology were investigated by Cecen and Sarikanat (2008). Two types of traditional glass fabrics, woven roving fabric and chopped strand mat, were used. A strong correlation was found between the inter-laminar shear strength values and fiber orientation angle in the woven fabric laminates.

To fabricate aircraft grade composite parts with high fiber volume fractions, a VARTM process with elevated temperatures (>150°C) was developed by Menta et al. (2013). Instead of single vacuum bagging infusion, double vacuum bagging infusion processes was used. First-class composite parts with a void content less than 1% was consistently manufactured.

Using the VARTM technique without using the distribution media, the fabrication of sandwich panels comprised of E-glass fiber/polyester resin face sheets and a rigid polyvinyl chloride foam core was experimentally investigated by Halimi et al. (2012). Six different hole-patterns on the foam core were tested. The results showed that, although the specimens' weight was increased by 3.6%, the mold filling time decreased by 40%, the bending critical load and yield absorbed energy were increased by 38% and 100%, respectively.

Uddin et al. (2006) applied the fiber reinforced polymer composites to a cracked bridge girder using the VARTM technology. It was found that the VARTM was a competitive technique for reinforcing large structures. The overall cost for the project was estimated and compared with traditional methods. Although the initial project costs of VARTM were very similar to the hand

lay-up techniques, the life expectancy and maintenance costs ultimately give a competitive advantage to the VARTM over hand lay-up.

Chang (2012) modified the VARTM process to be more flexible, and called it vacuum-assisted compression resin transfer molding. An extra elastic film was placed between the upper mold and the mold cavity. Since a loose fiber stack was present, the resin was easily introduced into the cavity by the vacuum during resin injection. Once enough amount of resin was injected, a compression pressure was applied on the film that then the preform was compressed so that the resin was driven through the preform. It was demonstrated that this method was a cost-effective process and could fabricate a part with better quality.

There have been limited studies regarding the manufacturing of vegetable fiber composites using VARTM technology. As an important driving force for the impregnation of the fiber tows, the capillary effect of vegetable fibers played a critical role in the VARTM process (Francucci et al. 2012). The capillary pressure of jute/vinylester composites and the impact of capillary forces on fabric permeability were examined. It was found that the capillary pressure was significantly higher in vegetal than that in the synthetic fiber fabrics. The experimental permeability was corrected using the measured capillary pressure, resulting in obtaining a more accurate modeling estimation.

The objective of this study was to investigate the mechanical properties and interfacial compatibility of vegetable fiber based molding products fabricated using the VARTM technology. As a cellulosic source with both economic and ecological advantages, kenaf is commercially grown in the U.S. and maintains a low price of about \$0.44 - \$0.55/kg as compared to E-glass at \$2.00 - \$3.25/kg (Mohanty et al. 2000, Zampaloni et al. 2007). In addition, processing kenaf takes less energy consumption than fiberglass (Akli et al. 2011). As the energy price continues to increase, the fuel economy becomes a priority on the list of national interests. The other advantages of VARTM over the traditional hot-press molding are that the manufacturing cost and volatile organic compound (VOC) emission can be reduced. In this study, the VARTM technology was used to enhance the physical and mechanical properties of the kenaf-based composites.

Materials and Methods

In this study, a three-step VARTM process was used:

- (1) Preparing a kenaf preform: Using an aluminum box, the kenaf fibers were manually formed into a mat 160 mm by 120 mm in size. The mat was prepressed at 3 MPa for about 30 min at a temperature of 50 °C. Each specimen had 40g Kenaf fibers and about 20 g resins. A 1x1-ft metal flat plate was used as the mold. After applying a mold-release agent on the surface of the mold, the preform was placed on the mold.
- (2) Preforming impregnation with resin: A flexible, gas impervious polyethylene sheet (commonly called a vacuum bag) was placed over the mold. Resin infusion and vacuum tubes were inserted in the bag. A vacuum was created between the mold and the bag using a vacuum pump as shown in Fig. 1. As a result, the catalyzed resin (1.5% tert-Butyl peroxybenzoate) was supplied to the infusion tubes. The vacuum pulled the resin along the distribution layer into the fiber reinforcement preform. A vacuum of 1.3-1.6 KPa was applied to the infusion system by a vacuum pulp (Vacmobile 20/2 System with Becker U4.20). The unsaturated polyester AROPOL Q 6585, provided by the Ashland Chemicals, was infused

into the preform at a temperature of 50°C. It took about 40 min for applying the vacuum and transferring the resins

- (3) Resin curing: The resin curing occurred in the hot-press with a pressure of 13 MPa. The resin-infused preforms were pre-cured at 100°C for 2 h, and then post-cured at 150°C for 2 h. Once the resin cured, the VARTM bag and distribution layer were removed.

In the traditional hot-pressing process, the hand lay-up kenaf fibers were pressed in a hot press at 100°C for pre-curing and 150°C for post curing (the same curing temperatures as the VARTM process). Twelve panels with a size of 100 mm wide × 180 mm long × 3 mm thick using either traditional hot-pressing or VARTM technology were fabricated (six each).

Two specimens sized 160 mm × 25 mm × 3 mm (length × width × thickness) were cut from each panel for examining the flexural strength and modulus of the composites using an Instron universal testing machine (model 5869, Canton, MA, USA) in accordance with the procedure described in ASTM D 790 standard. Three-point bending set-up was used with a span of 50 mm and a crosshead speed of 1.3 mm/min. The tensile strength of the specimens was tested at a room temperature in accordance with the procedures described in ASTM D 638 standard using the Instron tester. Twelve replicates (six for the traditional hot-press and six for the VARTM technology) were used. The specimen dimensions were 165 mm × 19 mm × 3 mm and the cross section of the narrow section was 57 mm × 13 mm (length × width). A crosshead speed of 5 mm/min. was used. The densities of each panel were measured in accordance with the ASTM D 792-08 standard.



Fig. 1 Vacuum pump

Dynamic mechanical analysis (DMA) is a technique used to characterize material behavior at different temperatures. A sinusoidal stress was applied and the strain in the sample was measured, allowing one to determine the complex modulus. The temperature of the sample and the frequency of the stress are often varied, leading to variations in the complex modulus. The TA Q800 Dynamic Mechanical Analyzer was used to examine the composite moduli in a temperature range from -50 to 200°C. A JSM-6500F scanning electron microscope (SEM) with an accelerating voltage of 20 kV and a magnification ranging from 10 to 500,000× was used to observe the fracture failure mode of the tensile specimens, such as fiber pull out or fiber failure. The failure modes are important to determine the interfacial bonding quality at the vegetable fiber and molding resin matrix interface.

Mercury porosimetry is a traditional technique to determine the porosity of samples, which provides the information of porosity, pore size distribution, total pore volume, and etc. Mercury porosimetry relies on the non-wetting nature of mercury and analyzes the porosity by applying various levels of pressure to a sample immersed with mercury. The Micromeritics' AutoPore IV 9500 instrument (Fig. 2) was used for the porosity measurements of the specimens in this study. The procedure for the measurement of the porosity was described as follows: The samples were dried overnight at 105 °C before the measurement. The penetrometers for powdered samples, which had 3 cm³ capacity and 0.412 cm³ steam volume, were used. With a mercury filling pressure of 0.5 psi (3.4KPa), the mercury injection measurements were carried out at pressures ranging from 0.5 - 33,000 psi (3.4KPa - 228MPa).

Results and Discussion

Mechanical properties The results of bending tests (modulus of elasticity, MOE and modulus of rupture, MOR) and tensile strength were summarized in Table 1. Compared to the traditional hot-pressing method, MOE, MOR and the tensile strength of the composites made by the VARTM method were increased by 65.5%, 30.7% and 41.7%, respectively (Table 1). ANOVA tests ($\alpha=0.01$) indicated that MOE, MOR and the tensile strength were significantly increased for the VARTM method as compared to the traditional hot-press method. Table 1 also illustrates that the standard deviations of the three properties were reduced, which suggested that more uniform properties could be achieved when the VARTM method was applied.



Fig. 2 Micromeritics' AutoPore IV

Table 1 Mechanical properties of kenaf reinforced composites

	Sample size	Density (kg/m ³)		Moisture content (%)		MOE ¹ (MPa)		MOR ² (MPa)		Tensile strength (MPa)	
		Mean	Sd. ³	Mean	Sd. ³	Mean	Sd. ³	Mean	Sd. ³	Mean	Sd. ³
Traditional hot-press	12	1112.9	43.1	4.8	0.3	4185.6	1058.5	52.3	8.0	31.4	4.4
VARTM technology	12	1159.4	44.5	4.5	0.5	6927.5	646.7	68.3	6.5	44.5	3.8
Increase (%)						65.5	-38.9	30.7	-19.2	41.7	-11.9

1. MOE-Bending Modulus of Elasticity
2. MOR-Bending Modulus of Rupture
3. Sd-Standard deviation

DMA tests The results of DMA tests for the specimens fabricated from the traditional hot pressing method and the VARTM method are presented in Fig.3. Modulus E from DMA is stress divided by strain at the slope of the straight line portion of a stress-strain diagram:

$$E = \frac{\sigma_L}{\epsilon_L}$$

where σ_L and ϵ_L are the stress and strain in the line portion of the stress-strain diagram. Compared to the composites made using hot-

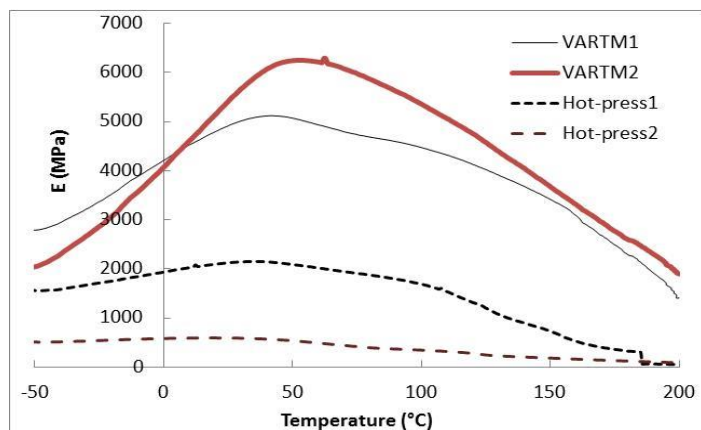


Fig. 3 A comparison of DMA results of the specimens made from hot-pressing (Hot-press1 and 2) and VARTM (VARTM1 and 2)

pressing, the elastic moduli of the specimens at the temperatures ranging from -50 to 200 °C were significantly increased by 2.3 to 11.1 times when the VARTM technology was used.

SEM observation The tensile fracture surfaces of the composites were observed by SEM under four different magnification levels are shown in Fig. 4. The specimens made from the traditional hot-pressing showed clean holes in the matrix and uncoated kenaf fiber surfaces (Fig. 4 a1-a4). It was apparent that a number of kenaf fibers and bundles protruded from the fracture plane. Fiber pullout played an important role in the failure mechanism of the kenaf fiber-reinforced composites. The pullout fibers did not adhere to the resin matrix. The specimens had an adhesive failure in the single-fiber pullout region at the interface. The de-bonding between the fibers and matrix may be due to the poor interfacial adhesion. However, much less fiber pullout was observed on the fracture surfaces of the specimens made using the VARTM technology. The interfacial bonding between the fibers and resin was much improved when VARTM was used. The higher interfacial bonding will result in a stronger adhesion between the fibers and matrix contributing to the higher tensile strength of VARTM composites.

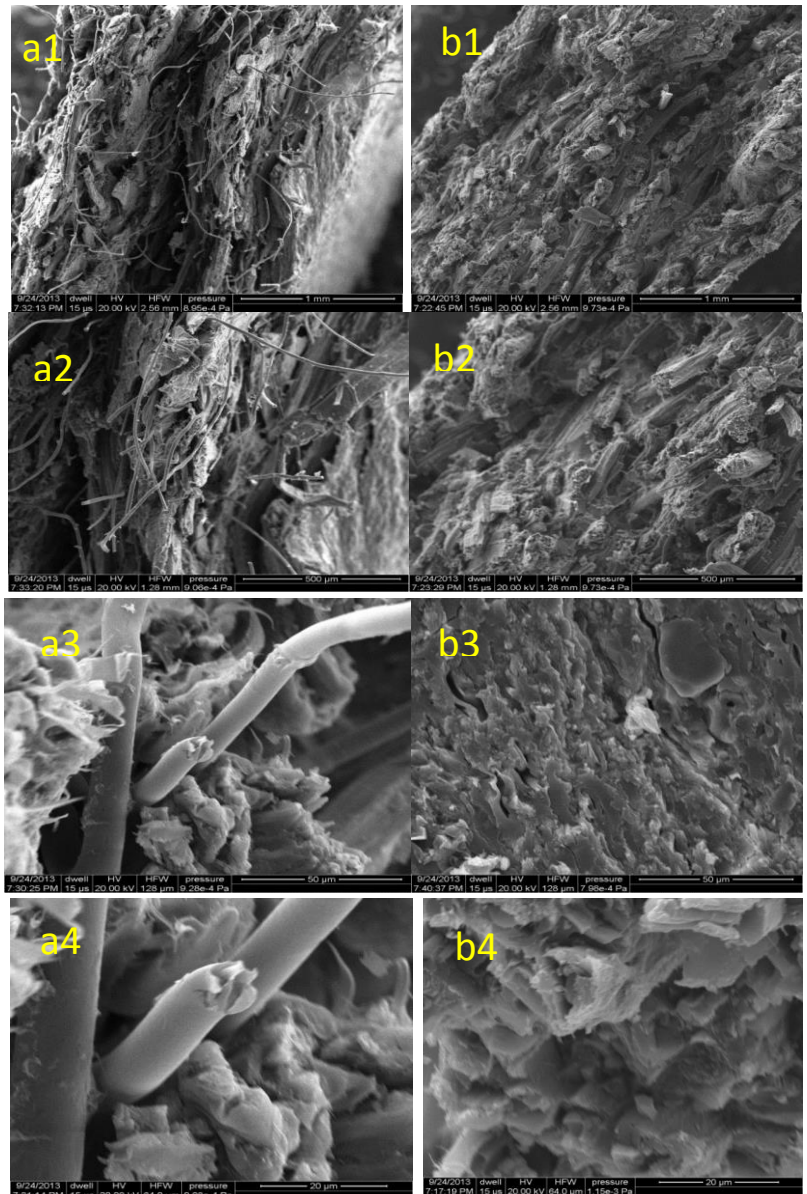


Fig. 4 Composites made by hot-pressing (a1-a4) and VARIM (b1-b4) at four magnifications

Mercury porosimetry Table 2

presents the results of mercury porosimetry tests, including the total pore area, median pore diameter, average pore diameter and porosity of the composites processed by both VARTM and traditional hot-press. Using the VARTM technique, a 30.8% reduction in total pore area was found as shown in Fig. 5. The median pore diameter was reduced from 5.535 μm to 1.209 μm, while the average pore diameter was reduced from 0.072 μm to 0.041 μm (Fig. 6). The porosity of the composites was reduced by 76%. The reduced porosity in composites leads to an increase in the mechanical properties of the materials.

Table 2 Mercury intrusion porosimetry results of kenaf reinforced composites

Total Pore Area	Median Pore Diameter (μm)	Average Pore Diameter	Porosity (%)
-----------------	---------------------------	-----------------------	--------------

	(m ² /g)		(μm)	
Composites by VARTM	5.393	1.209	0.041	3.628
Composites by traditional hot-press	7.795	5.535	0.072	15.220

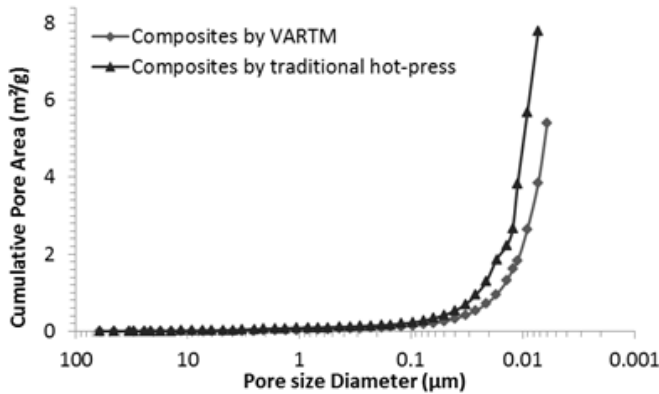


Fig. 5 Cumulative pore area comparison by mercury intrusion porosimetry

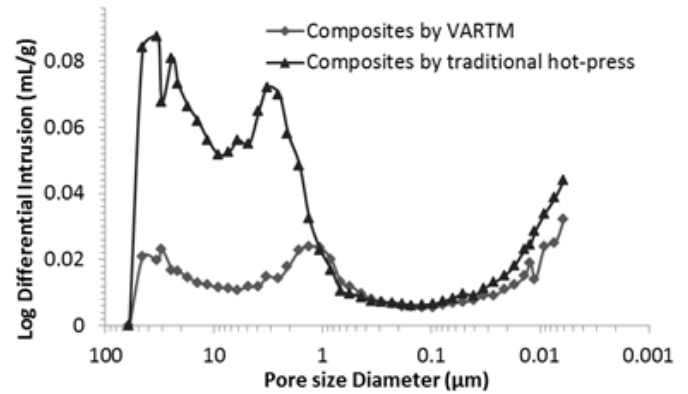


Fig. 6 Pore size distributions measured by mercury intrusion porosimetry

Conclusions

Compared to traditional hot-pressing composites, the VARTM composites showed a 65.5% improvement in MOE, 30.7% in MOR and 41.7% in tensile strength. From DMA tests, the elastic moduli of the VARTM specimens at temperatures ranging from -50 to 200°C were increased by 2.3 to 11.1 times compared to the hot-press composites. Single-fiber pullout was observed in the hot-pressing specimens. Much less kenaf fiber pullouts, less porosity and smaller pore size were observed on the VARTM composites, resulting in an increase in contact areas and an improvement in interfacial bonding between the fibers and polyester matrix.

References

- Akil, H.M., Omar, M.F., Mazuki, A.A.M., Safiee, S., Ishak, Z.A.M., Abu Bakar, A. (2011) Kenaf fiber reinforced composites: A review. *Materials and Design* 32: 4107–4121
- American Society for Testing and Materials (ASTM), (2010) Standard test method for flexural properties of unreinforced and reinforced plastics and electrical insulating materials. Vol. 04.10. ASTM D790-10.
- American Society for Testing and Materials (ASTM), (2010) Standard test method for tensile properties of plastics. Vol. 04.10. ASTM D638-10.
- American Society for Testing and Materials (ASTM), (2010) Standard test method for density and specific gravity of plastics by displacement. Vol. 04.10. ASTM D792-8.
- Cecen, V., Sarikanat, M. (2008) Experimental Characterization of Traditional Composites Manufactured by Vacuum-Assisted Resin-Transfer Molding. *Journal of Applied Polymer Science* 107: 1822-1830
- Chang, C.Y. (2012) Experimental analysis of mold filling in vacuum assisted compression resin transfer molding. *Journal of Reinforced Plastics and Composites* 31(23): 1630–1637

- Ehrenstein, G.W., Riedel, G., Trawiel, P. (2003) Praxis der Thermischen Analyse von Kunststoffen, second ed., Carl Hanser Verlag, München.
- Francucci, G., Vazquez, A., Ruiz, E., Rodriguez, E.S. (2012) Capillary Effects in Vacuum-Assisted Resin Transfer Molding With Natural Fibers. *Polymer Composites* 33(9): 1593-1602
- Halimi, F., Golzar, M., Asadi, P., Beheshty, M.H. (2012) Core modifications of sandwich panels fabricated by vacuum-assisted resin transfer molding. *Journal of Composite Materials* 47(15): 1853–1863
- Jeska, H., Schirpb, A., Corneliusb, F. (2012) Development of a thermogravimetric analysis (TGA) method for quantitative analysis of wood flour and polypropylene in wood plastic composites (WPC). *Thermochimica Acta* 543: 165-171.
- Liang, K., Shi, S.Q., Nicholas, D.D., Sites, L. (2013) Accelerated weathering test of knaf fiber unsaturated polyester sheet molding compounds. *Wood and Fiber Science* 45(1): 1-7
- Menta, V., Vuppalapati, R., Chandrashekhara, K., Schumanb, T., Sha, J. (2013) Elevated-temperature vacuum-assisted resin transfer molding process for high performance aerospace composites. *Polym Int* 62: 1465-1476
- Mohanty, A. K., Misra, M., Hinrichsen, G., (2000) Biofibres, biodegradable polymers and biocomposites. An overview. *Macromolecular Materials and Engineering* 276/277:1-24.
- Moriia, T., Tanakaa, A., Hamadab, H. (2001) Influence of molding condition on tensile properties of flat braided fabric reinforced phenolic composite. *Composites: Part A* 32: 1505-1511
- Uddin, N., Vaidya, U.K., Shohel, M.S., Serrano-Perez, J.C. (2006) Vacuum-Assisted Resin Transfer Molding. *Concrete International* (Nov 2006): 53-56.
- Wang, J., Shi, S.Q., Liang, K. (2013) Comparative Life-cycle Assessment of Sheet Molding Compound Reinforced by Natural Fiber vs. Glass Fiber. *Journal of Agricultural Science and Technology B3*: 493-502
- Zampaloni, M., Pourboghra, F., Yankovich, S.A., Rodgers, B.N., Moore, J., Drzal, L.T., Mohanty, A.K., Misra, M. (2007) Kenaf natural fiber reinforced polypropylene composites: A discussion on manufacturing problems and solutions. *Composites, Part A: Applied Science and Manufacturing* 38A(6): 1569-1580.

Bio-based Carbon/Polyvinyl Alcohol Piezoresistive Sensor Material

David B. Devallance^{1*} – *Nan Nan*²

¹ Assistant Professor and Program Coordinator, Wood Science and Technology Program, Division of Forestry and Natural Resources, West Virginia University, Morgantown, WV, USA

david.devallance@mail.wvu.edu

** Corresponding author*

[*david.devallance@mail.wvu.edu*](mailto:david.devallance@mail.wvu.edu)

² PhD Student and Graduate Research Assistant, Division of Forestry and Natural Resources, Davis College of Agriculture, Natural Resources and Design, West Virginia University, Morgantown WV, USA.

[*nnan@mix.wvu.edu*](mailto:nnan@mix.wvu.edu)

Abstract

Biochar, a by-product of slow and fast pyrolysis processes used to produce gas and bio-oil, has the potential to serve as an attractive alternative to conventional carbon materials used in composites. Biochar from wood is traditionally used in relatively low-value applications such as soil amendments and heating fuel. The carbonization of wood, however, is a promising field of research for creating pre-cursor material to be used for sensor and energy storage applications. Our previous work indicated that commercially produced hardwood biochar can be combined with polyvinyl alcohol (PVA) to form a film material. These PVA/biochar film materials have a unique potential to be used as sensor materials in a variety of applications. The objective of this research was to evaluate the piezoresistive properties of sensors films developed using bio-based carbon (i.e., biochar) as the electrical conductive filler material. Sensor film material was prepared by mixing biochar particles into a PVA solution (10% PVA). Biochar particles were added in three filler loading levels of 8%, 10%, and 12%. After mixing, the sensor films were produced via film casting and degassing. The resulting films were evaluated for piezoresistive properties when subjected to dynamical mechanical loading. The sensor materials' responses to quasi-static loading at room temperature were investigated and quantified. At the room temperature, addition of force to the sensor increased the resulting voltage response of PVA/Biochar sensors. Furthermore, the increasing of biochar particle loading level increased the voltage response of PVA/Biochar sensors.

Keywords: Bio-based carbon, piezoresistive sensors, biochar, electrical conductivity, wood carbonization

Introduction

Biochar is typically produced through the thermochemical decomposition of organic materials at elevated temperatures and in the absence of oxygen. Biochar is also a by-product obtained from

biomass pyrolysis processing to produce gas and bio-oil (Joseph 2010). The structure of biochar is mainly influenced by the nature of the biomass feedstock and the pyrolysis processing. The structure is essentially amorphous and contains some crystalline areas with layers of randomly cross-linked aromatic sheets (Joseph 2010). Similar to graphite, these crystalline areas exhibit excellent electrical conductivity. Jin et al. (2013) found that the nanostructured biochar-based carbons had high capacitance (more than 200F/g). Huggins et al. (2014) reported that biochar can be a sustainable material for microbial fuel cell electrodes with economic and environmental benefits. In recent years, biochar has mainly been used to improve soil productivity (Galinato et al. 2011; Sohi et al. 2010), and to remove pollutants like heavy metals, pesticides, and herbicides (Kookana et al. 2011). Some limited research has investigated using biochar as renewable fillers for composites. Peterson (2012) used the co-filler of corn starch and corn stover biochar, instead of carbon black, in styrene-butadiene rubber composites. The research indicated that the addition of biochar enhanced the toughness of the resulting composites. To date, there has been limited research on using biochar produced from wood in composite material applications. Ahmetli et al. (2013) reported that biochar from wood shavings can significantly improve the thermal stability, tensile strength, modulus, and surface hardness of an epoxy resin matrix. Given the potential for using biochar for conducting electricity and in composite material applications, this project was initiated to further expand on some composite research on polyvinyl alcohol (PVA)/Biochar films. Our previous work indicated that commercially produced hardwood biochar can be combined with polyvinyl alcohol (PVA) to form a film material by solution casting. However, this preliminary research did not evaluate the electrical conductivity of the films. As a result of the structure, and specifically the crystalline areas, biochar has good conductivity (Joseph 2010). Due to the potential conductivity, these PVA/Biochar film materials have a unique potential to be used as electrical sensor materials in a variety of applications. The main goal of this study was to investigate the piezoresistive properties of bio-composite sensors made using PVA that is dosed with conductive hardwood biochar particles and assess the suitability of these materials in touch sensor applications.

Objectives

The objectives of this research were to: 1) Investigate the influence of different biochar loading levels of 8wt%, 10wt%, and 12wt% on the piezoresistive properties of the bio-based sensor; 2) Determine the influence of film thickness on the piezoresistive properties of the sensors films developed using bio-based carbon (i.e., biochar) as the electrical conductive filler material; 3) Evaluate the repeatability and response of the bio-based sensor.

Materials and Methods

Materials

Mixed hardwood biochar manufactured by CharcoalHouse™ was ground using a Wiley Mill equipped with a 1 millimeter (mm) sieve. The resulting ground biochar was screened using a sieve shaker (U.S.A Standard Sieve Series, Model 11). The biochar used in this study was material which passed through a 60 mesh, 250 micron (µm) sieve. PVA solution at 10% by weight was made from PVA crystals (Acros Organics, MFCD-00081922).

Composites Preparation

The prepared PVA 10% solution and biochar particles were mixed manually at 3 different particle loading level: 8%, 10%, and 12% (w/w), and then further dispersed by ultrasonic treatment for 2 minute at 50% power. After mixing, the solutions were poured into Petri dishes and placed in desiccators to evaporate water at room temperature (20°C and relative humidity of 30%) and degassed with vacuum pump until films were formed (Fig. 1). The films were dried in an oven at 55°C for 6 hours. Upon cooling, the films were placed in sealed bags until testing. For each loading level, five different films were cast.

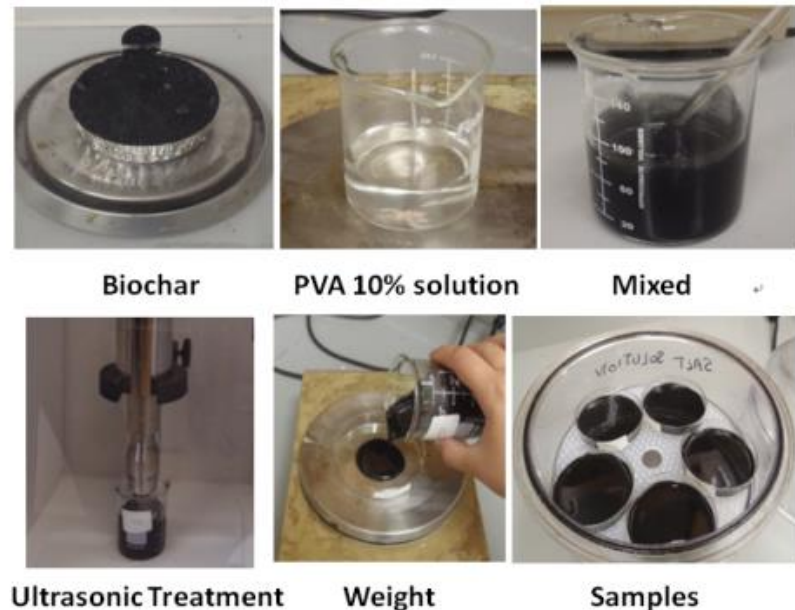


Figure 1. Process of making PVA/Biochar films.

Piezoresistive Testing

Testing was performed on samples using a TA Instruments Q800 dynamic mechanical analysis (DMA) instrument. A total of five sensors for each loading level were tested (one from each film that was cast). Both the static and active clamp surfaces were prepared with copper foil, providing smooth, full surface electrical contact with the sensor surface. A weather-resistant silicone compliance layer was used in series with the active clamp of the DMA to ensure full contact and homogeneous loading. The contact area for load application had a diameter of 8 mm (Fig. 2). Room temperature characterization of the sensor was performed using a quasi-static loading scheme with a rate of 2 kPa/second up to a maximum stress of 350 kPa. Electrical response was recorded with a NI USB-6210 16-bit DAQ system, using 5 V power source. In an effort to optimize the resolution of sensor response with this system, a circuit was fabricated to maximize ΔV during mechanical loading. Additionally, each specimen was loaded repetitively for five cycles with an increasing force from 1N to 18N, followed by immediate release to 1N. This circuit is depicted in Figure 2, and the sensor resistance can be determined using Equation 1.

$$R_{sensor} = \frac{5R_{ref}}{V_o} - R_{ref} \quad (\text{Equation 1})$$

Where: R_{sensor} is the resistance value of touch sensor; R_{ref} is the resistance value of reference resistor (15,000 ohms). V_o is the output voltage value; the all input voltage value is 5V.

For the purpose of this research, V_o was the value that was of interest to determine how well the sensor performed. Specifically, V_o as a function of film thickness and biochar loading level under various levels of stress was determined and analyzed.

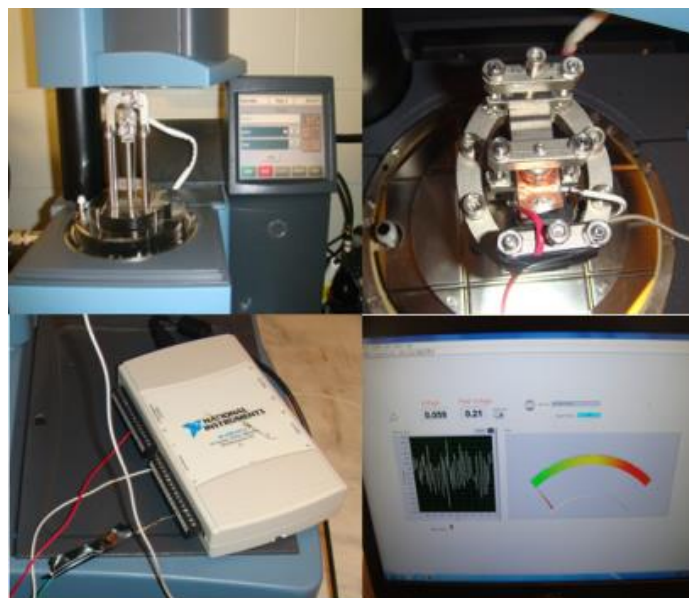


Figure 2. DMA setup for PVA/Biochar sensor piezoresistive testing.

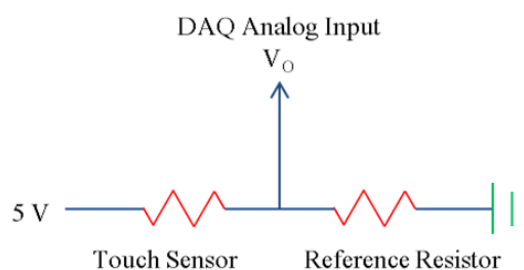


Figure 3. Circuit used for sensor testing.

Results and Discussion

The Effect of Loading Level

Piezoresistive response, displayed in terms of voltage, is shown in Figure 4. All sensor responses increased gradually with elevated stress from 0 to 350 kPa. As the compressive stress increased, it was evident that a more conductive path with reduced particle spacing was formed, which resulted in lower resistance and higher voltage output. The sensor loaded with 12% biochar filler exhibited the highest overall response as the stress approached 350 kPa. The sensor with 10% biochar filler showed the next highest overall voltage output. The sensor with 8% biochar filler

exhibited the smallest overall response. These results indicated that as the percentage of biochar filler increased, the voltage output of the sensor increased under a given set stress level.

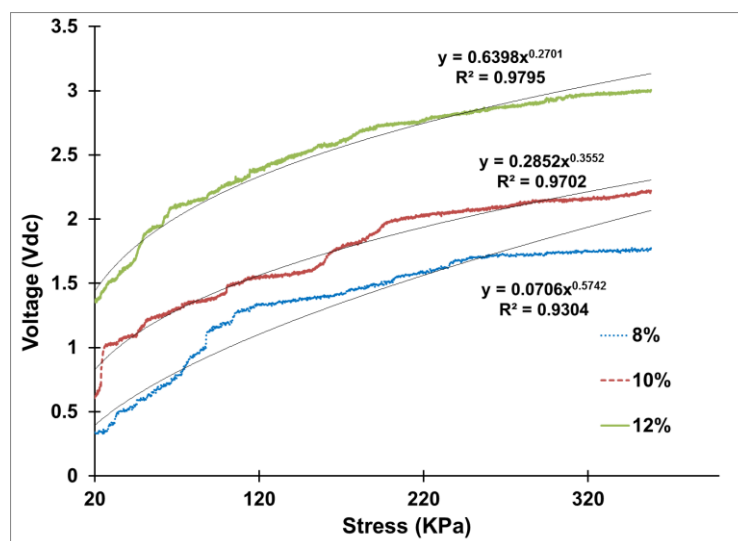


Figure 4. Piezoresistive sensors response at 8%, 10%, and 12% biochar loading.

These findings suggest that depending on the intended application, biochar-based sensor films could be fabricated with varying loading levels to reach a desired piezoresistive response. As evident in the voltage output shown in Figure 4, the resulting output was somewhat linear, with some initial non-linear behavior and followed more of a power function.

Influence of Film Thickness

The effect of film thickness was evaluated for each type of film material. Figure 5, 6, and 7 show the piezoresistive results (i.e., output voltage) of sensors fabricated from PVA/Biochar films with 8%, 10%, and 12% biochar filler, respectively.

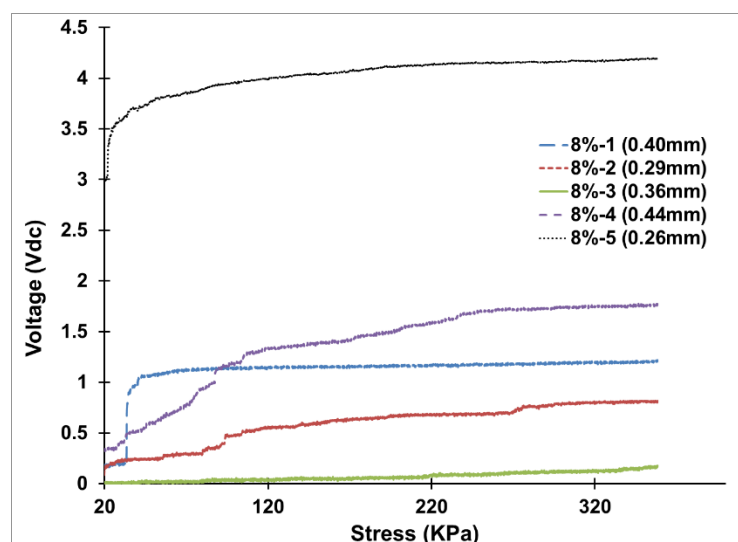


Figure 5. Sensor response with 8% biochar loading at different thicknesses.

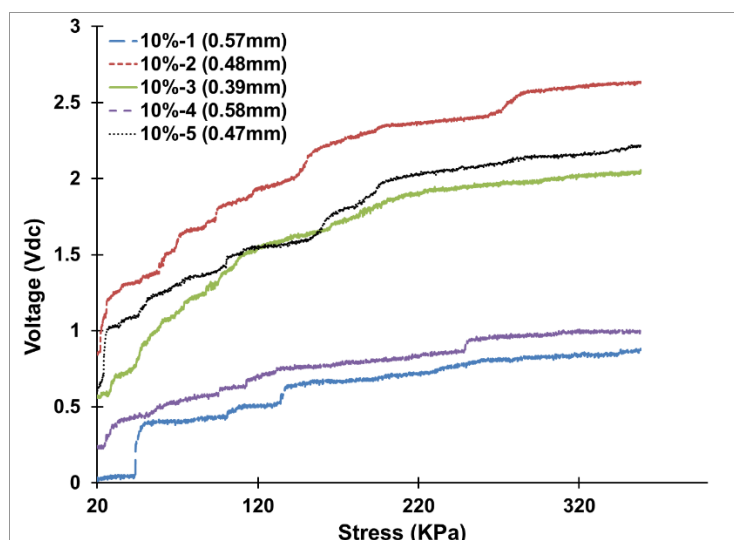


Figure 6. Sensor response with 10% biochar loading at different thicknesses.

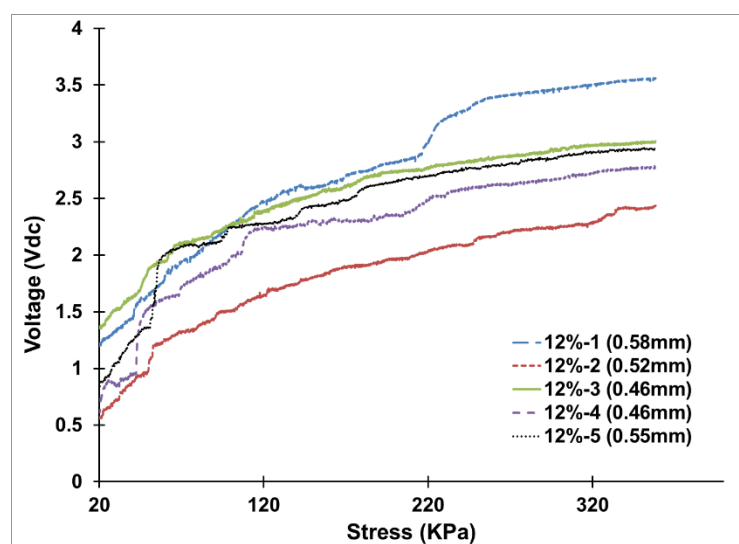


Figure 7. Sensor response with 12% biochar loading at different thicknesses.

For the 8% biochar filled sensor film, it appears that the thinnest film material exhibited the highest overall voltage output (i.e., lower resistance). Specifically, the 0.26mm film with an 8% biochar loading level had a very high voltage output and showed a significant increase at approximately 20 kPa. For the sensor films fabricated with 10% and 12% biochar loading, there did not appear to be a significant trend related to the thinner films having higher voltage output under stress. The effect of sensor thickness, however, requires more investigation. Some of the influential factors not specifically evaluated in this research were the influence of particle size and distribution on the voltage output and resulting thickness of the films. Without these key parameters being included in the analysis, the research was not able to provide a complete understanding of the influence of sensor film thickness on the performance of the sensor material. Research is currently underway to look at the effect of particle size on the resulting thickness and performance of bio-based carbon sensor materials.

Release Testing

Figures 8, 9, and 10 show the results of repeated pressure loading and the piezoresistive output from the PVA/Biochar sensor films with 8%, 10%, and 12% biochar loading, respectively. The release tests indicated that all of sensors types exhibited favorable recovery capability. Specifically, when the force was removed the voltage value returned to the original voltage (voltage at 1N of force) within one second. It was noted that the maximum voltage for the first cycle was slightly lower than the following cycles, which mean that the first cycle likely enhanced the stability of sensors. For each loading level of biochar, the second cycle to the fifth cycle of sensor loading resulted in similar piezoresistive response. These results indicated that the PVA/Biochar film has the potential to be used as a material for manufacturing a variety of piezoresistive sensors (e.g., in touch sensor applications).

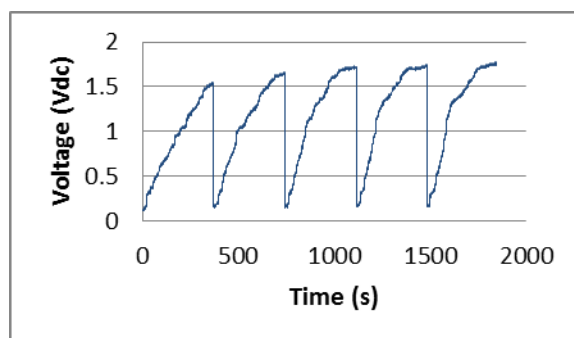


Figure 8. Release reaction of 8% PVA/Biochar piezoresistive sensors.

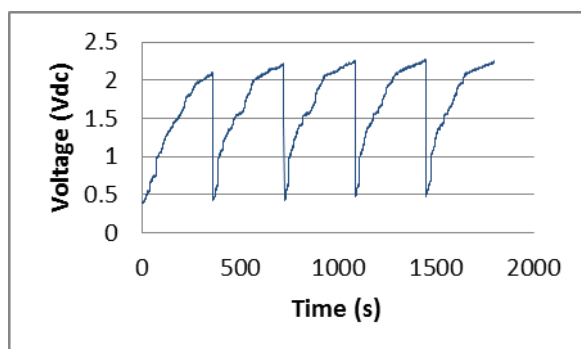


Figure 9. Release reaction of 10% PVA/Biochar piezoresistive sensors.

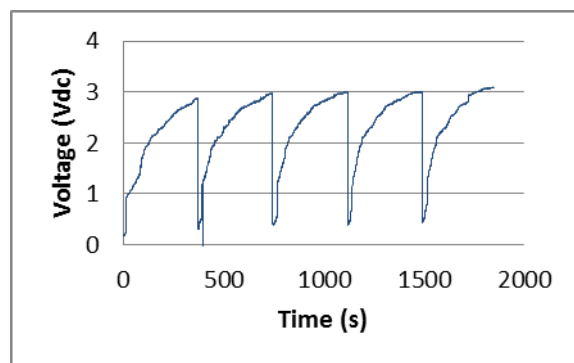


Figure 10. Release reaction of 12% PVA/Biochar piezoresistive sensors.

Conclusions

Under room temperature conditions, the voltage response of PVA/Biochar sensors gradually increased as pressure was applied. Also, as the biochar particle loading level increased, there was an increase in the voltage response of PVA/Biochar sensors. Additionally, the release tests indicated that all of the sensors types exhibited favorable recovery capability. The results indicated that biochar particle filled films possess suitable electrical conductivity and piezoresistive response and would be likely materials for piezoresistive sensors. Future work is needed, however, to investigate the influence of particle size and distribution on the piezoresistive properties of these film materials.

References

- Ahmetli, G., S. Kocaman, I. Ozaytekin, and P. Bozkurt. 2013. Epoxy Composites Based on Inexpensive Char Filler Obtained from Plastic Waste and Natural Resources. *Polymer Composites* 34 (4): 500–509.
- Galinato, S.P., J. K. Yoder, and D. Granatstein. 2011. The Economic Value of Biochar in Crop Production and Carbon Sequestration. *Energy Policy* 39 (10): 6344–50.
- Huggins, T., H. Wang, J. Kearns, P. Jenkins, and Z. J. Ren. 2014. Biochar as a Sustainable Electrode Material for Electricity Production in Microbial Fuel Cells. *Bioresource Technology* 157 (April): 114–19.
- Jin, H., X. Wang, Z. Gu, and J. Polin. 2013. Carbon Materials from High Ash Biochar for Supercapacitor and Improvement of Capacitance with HNO₃ Surface Oxidation. *Journal of Power Sources* 236 (August): 285–92.
- Joseph, S. and J. Lehmann. 2010. *Biochar for Environmental Management: Science and Technology*. New York, NY: Earthscan.
- Kookana, R.S., A.K. Sarmah, L. Van Zwieten, E. Krull, and B. Singh. 2011. Chapter Three - Biochar Application to Soil: Agronomic and Environmental Benefits and Unintended Consequences. *Advances in Agronomy*, Volume 112:103–43.
- Peterson, S. 2012. Evaluating Corn Starch and Corn Stover Biochar as Renewable Filler in Carboxylated Styrene–butadiene Rubber Composites. *Journal of Elastomers and Plastics* 44 (1): 43–54.
- Sohi, S.P., E. Krull, E. Lopez-Capel, and R. Bol. 2010. Chapter 2 - A Review of Biochar and Its Use and Function in Soil. *Advances in Agronomy*, Volume 105:47–82.

Lifecycle of a Novel Bio-based Wood Composite Made of Sawmill Waste

A. Emeran NEUHÄUSER^{1} - Hendrikus VAN HERWIJNEN² -*

Stefano D'AMICO³ - Ulrich MÜLLER⁴

¹ Junior Researcher, Kompetenzzentrum Holz GmbH – Division Wood Materials Technologies. Konrad Lorenz Straße 24, 3430 Tulln-Austria.

** Corresponding author*

[*e.neuhaeuser@kplus-wood.at*](mailto:e.neuhaeuser@kplus-wood.at)

² Senior Researcher, Kompetenzzentrum Holz GmbH – Division Wood Materials Technologies.

³ Senior Researcher, University of Natural Resources and Life Sciences, Vienna, Austria.

⁴ Priv.-Doz., University of Natural Resources and Life Sciences, Vienna, Austria.

Abstract

Politics and markets demand new materials to replace products based on fossil resources. Due to shortage of raw material the demand of bio-based products with reduced weight is steadily rising. On the other hand the question arises how to recycle and reuse manufactured products. Herein the presented novel bio-based wood composite meets these demands: it is light, totally bio-based and compostable.

The main component of material presented is fine sawdust from sawmills. Usually this sawdust is directly used for energy production at the production site. Beside the usage for WPC the application of this material is limited. The basic idea of the new composite is to blend fine wood particles with wheat flour, mix it with water and to use a fermentation process to create a foamed bio-composite. In the manufacturing process the structure of the foam is stabilized in an oven, comparable to the baking process in the food production. After gelatinization of the wheat matrix the material has to be dried in a kiln. After drying the panel can be further processed with common woodworking tools. The material is characterized by low density in a range of 350 kg/m³, good thermal insulation, compression strength higher than 1 N/mm² and outstanding acoustic properties. Feasible products could be e.g. acoustic panels, pin boards and door cores. After product life the material can be used for combustion or composted without concerns about contaminants.

Keywords: light weight panel, acoustic properties, recycling, sawdust, wood composite

Introduction

The development of new materials and products based on renewable resources is an important and growing research field. Due to increasing prices for energy and resources of fossil origin it becomes more feasible to use renewable resources and biological processes. Wood as an example of a renewable resource is already intensively used which lead to increasing prices recently. Therefore the material utilization of byproducts as for example saw dust gets more interesting. Saw dust is mainly used for energy production and due to the small particle size the usage for wood composites is limited. This paper presents a new developed material which comprises saw dust as main component. A further aim was to generate a biological material which has no synthetic contaminants. Affentranger (2002) developed a material which met this criteria based on saw dust glued with corn starch. This invention also implied the usage of yeast to foam the material on a biological way. Disadvantages of this combination were the low capability to trap the gas in the foaming process and the low strength properties. So this paper presents the production, the properties and some possible products of wood foam based on saw dust.

Wood Foam Production

Raw Materials

Substantial component of the presented material is saw dust. This contains mainly particles from Norway spruce and a low amount of silver fir. Due to the production process in sawmills a fine dust fraction accrues. With its extensive surface this dust particles would change the hygroscopic properties during the process and in the final product. Therefore the fraction below 500µm has to be sieved out.

To bond the particles wheat flour of type 480 Austrian notation was used with a ground size smaller than 120 µm. Wheat flour consists of about 70 % starch, 8 to 12 % proteins and fats, minerals and water (Belitz et al. 2008). The main part of the proteins is gluten, which is located in the endosperm of the wheat grain and has an important influence on product quality. Only wheat flour is able to form a viscoelastic and cohesive dough in a knead processes with water (Belitz et al. 2008). During kneading a three dimensional gluten network is formed, which is responsible for a high elasticity and an excellent gas retention of the dough. D'Amico et al. (2013) examined the wood bonding performance of native wheat gluten after different modifications. Highly hydrolyzed gluten showed best bonding strength and a higher resistance against moisture. Other tensile tests indicated a higher strength for specimens bonded with wheat flour compared to wheat starch (Müller et al. 2013).

The effect of temperature on the gluing performance of Norway spruce wood and wheat flour showed an optimum in wood failure with curing temperatures between 90°C und 105°C. This is the temperature range which is situated in the dough during the baking process (D'Amico et al. 2010). Further experiments after a storage period of one year showed low strength losses (D'Amico et al. 2012).

Yeast and its natural fermentation process are utilized to foam the material. In this process carbohydrates of the wheat flour are fermented to carbon dioxide and Ethanol (Sievert et al. 2000). With optimized process conditions the produced gas forms the porous structure of the final product. For the experiments 2-3 % (dry/dry) of commercial backer's yeast was dispersed in water before it was added to the mixture.

Water is an essential component of the entire process. The right amount of water is essential to form a dough like consistence. This is necessary for the dough to trap the fermented gas and to generate good bonding properties. The amount of water was more than 100% relatively to solid matter and different experiments showed evident changes in product properties with small deviations in the water content.

A further ingredient was propionic acid to increase the resistance against microorganisms. Moreover the acid changes the pH value to an optimum for the fermentation process. Essential advantages of propionic acid are that it does not affect the metabolism of yeast and it is widely used in food industry.

Production process

The production process of the here presented light weight panel is close to the bread making process (Neuhäuser et al. 2014). It consists of three main steps. First the above mentioned materials are mixed together and kneaded to a dough like mixture which is placed in a form. This form is heated up in the second step and the last step is drying and conditioning of the product (D'Amico and Müller 2013).

Due to the fact that the fermentation is based on a biological activity the production method has to be closely monitored. The amount of the different components has to be exact and the moisture content of every fraction has to be measured. Further temperature, kneading time and fermenting time have to be controlled accurately as they directly influence the activity of yeast.

The dough was prepared at room temperature and kneaded with a special dough hook to apply a consistent energy into the mixture. Alternation of kneading and fermenting split bigger CO₂ bubbles into smaller, homogeneous distributed bubbles. Furthermore oxygen is induced into the dough with a repeated kneading process which increases the growth of yeast (Siefert et al. 2000). As mentioned above the optimal stickiness of wheat flour is between 90 and 105 °C. In this range the ordered structure of starch is completely broken up and a crosslinking in the gluten matrix is built up which leads to optimal adhesive and cohesive strength (D'Amico et al. 2010; Lagrain et al. 2005). These temperatures are found through the entire cross section during baking above 200 °C which fixates the porous structure. Baking time varies with thickness of boards. During this process water vaporization of up to 20 % of the total water content could be observed.

Due to the high initial water content, water was more than 100 % of the mass after baking. The rapid removal of water to a final moisture content of 10% exhibits a big challenge. On the one hand a high drying rate is possible due to the very high porosity. This enables a drying scheme at high temperature with a high drying gradient. On the other hand a drying front with abrupt changes in the moisture content was measured for thick elements (see Figure 46). This could lead to typical drying defects as warp and cracks.

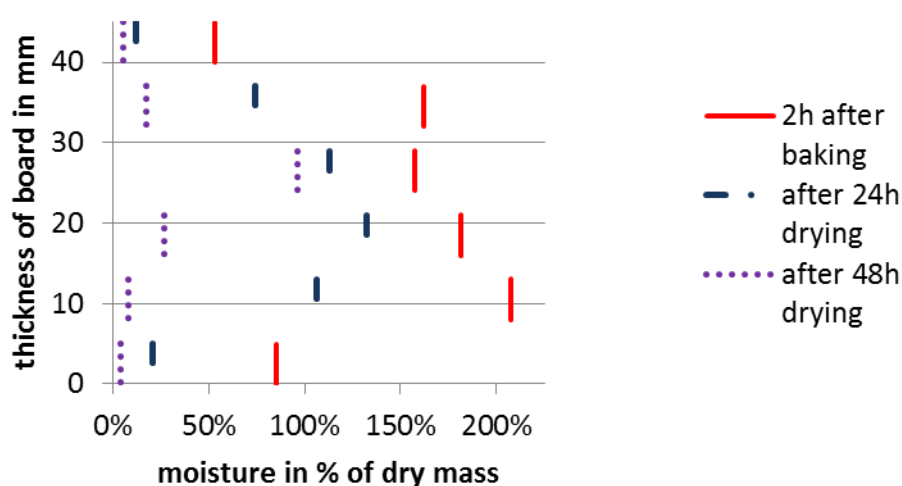


Figure 46 Vertical moisture profile after different drying times

Material Properties

Mechanical properties

The mechanical properties of wood foam are presented in

Table 13. Samples laminated with High Density Fiberboards (HDF) and non-laminated samples are compared. Basic wood foam has a density in a range of 350 kg/m³. Bending strength of the raw material is low with 1,1 N/mm². However this strength rises tenfold with the HDF cover. No difference was measured for tensile strength perpendicular and compression strength parallel to the surface. The resistance to axial withdrawal of screws in boards with HDF cover was nearly double as high as without. As there is no orientation in the panel, no difference was measured for tests in perpendicular and parallel direction of raw boards. The above mentioned results show that it is necessary to use a surface layer to get the required strength. Next to the strength properties another typical test method for wood materials is the swelling in thickness. The uncovered samples swelled 14 % in thickness after 2 h in water which increased to 15 % after 24 h. In comparison a maximum swelling of 13 % is allowed for particle boards according to EN312. Therefore, it is necessary to use hydrophobizing agents if the material could get in contact with water during product life. In contrast to this results were the findings for the interaction of the material with water vapor through moist air. Isotherms were measured with a dynamic vapor sorption apparatus (DVS Advantage, Surface Measurement Systems, London) at 25 °C and in 10 % measurement steps. Figure 47 shows the plots of adsorption and desorption for wood foam (dry mass: 25,3 mg) and particles of Norway spruce (dry mass: 23,9 mg). It can be seen that the adsorption and desorption behavior of the two materials is comparable. The adsorption of wood foam is slightly higher than the reference. This difference increases above 60 % relative humidity (RH) and has its maximum at 98 % RH with a moisture content (MC) of 25,3 % and 24,0 % for wood foam and spruce wood respectively. The higher moisture uptake of

wood foam might be explained by the baked starch. For the product application no different sorption behavior compared to solid wood is expected.

Table 13 Material properties of foamed wood



	Wood foam with cover	Wood foam without cover
Cover	2 mm HDF	none
Thickness	25,2 mm	21,4 mm
Density [kg/m ³]	440 (+/- 10)	340 (+/- 10)
Bending strength [N/mm ²] EN310	11 (+/- 1)	1,1 (+/- 0,2)
Compression strength [N/mm ²] EN789	1,3 (+/- 0,1)	1,1 (+/- 0,1)
Tensile strength [N/mm ²] EN319	0,4 (+/- 0,1)	0,4 (+/- 0,1)
Screw withdrawal [N] EN320		
surface	410 (+/- 10)	270 (+/- 30)
edge	260 (+/- 30)	260 (+/- 30)

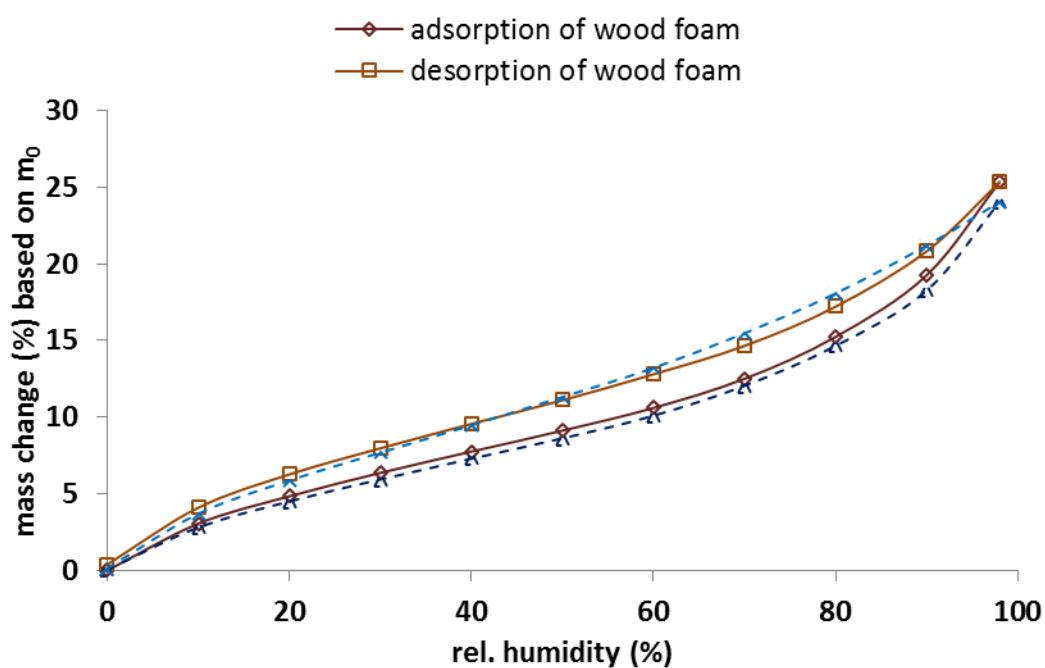


Figure 47 Isotherm of foamed wood and raw sawdust measured at 25°C in a DVS

Further properties

The reaction of the material to fire was tested accordingly to ÖNORM A 3800-1. These pretests let expect that the material is highly flame retardant which would correspond to classification B1. Fire properties can be further improved by using flame retardants.

An important factor for indoor use is sound absorption. The sound absorption coefficient of wood foam was measured in an impedance tube accordingly to EN ISO 10534-1. The tested specimens had a thickness of 18 mm and no gap was left between specimen and cover plate of the tube. Figure 48 shows the results for wood foam and other acoustic foams. This shows the good performance of wood foam for a frequency range from 125 Hz to 2000 Hz.

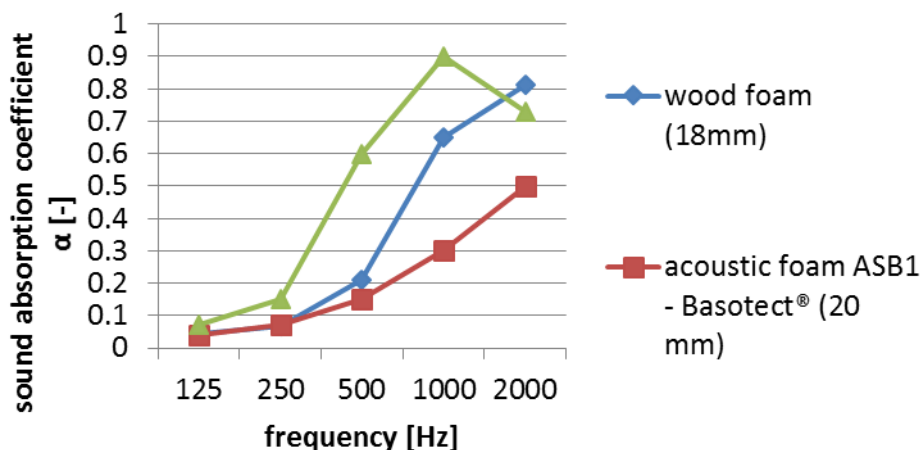


Figure 48 Comparison of the sound absorption coefficient α , quantified by the tube method following EN ISO 10534

A further material property which was tested was heat conductivity according to ISO 8302. A λ -10 value of 0.07 – 0.08 W/(m*K) was measured which is comparable to spruce wood.

Possible Products and Final Usage

The formability of the raw mixture gives the possibility to create 3D structures, although all data presented here refer to panel structures. Possible products for these panels could be acoustic elements due to the good sound adsorption. A further advantage of the porous structure is the good grip of pins wherefore it can be used as a pinboard. In general the material can be used where low density is needed and the restrictions in strength are no limitation. Examples are door core elements or kitchen worktops where the wood foam is strengthened and protected by a cover layer.

Due to the pure biological mixture of the material the combustion process is simple. It was not possible to take advantage of the very high water uptake and retention by replacement of turf in growth substrate. Maussymbayeva (2013) measured a good combination of soil nutrients and other relevant parameters. However experiments with plants showed highly reduced growth for substrate with wood foam particles. It was assumed that this was induced by fungal growth which was visible on the soil during the experiment. Another possible final use is combustion for the production of energy.

References

- Affentranger, C. (2002) Method for producing solid materials from plant material, material produced according to said method, use of the material in addition to a system for carrying out said method. WO 2002055722 A1 11.01.2002.
- Belitz, Hans-Dieter; Grosch, Werner; Schieberle, Peter (2008) *Lebensmittelchemie*. Berlin, Heidelberg Springer-Verlag.
- D'Amico, S.; Hrabalova, M.; Müller, U.; Berghofer, E. (2010) Bonding of spruce wood with wheat flour glue-Effect of press temperature on the adhesive bond strength. *Industrial Crops and Products* 31 (2), S. 255–260.
- D'Amico, S.; Hrabalova, M.; Müller, U.; Berghofer, E. (2012) Influence of ageing on mechanical properties of wood to wood bonding with wheat flour glue. *European Journal of Wood and Wood Products* 70 (5), S. 679–688.
- D'Amico, S.; Müller, U. (2013) Verfahren zur Herstellung von Leichtbauprodukten auf Basis von Holz. EP2615209A1 09.01.2013.
- D'Amico, S.; Müller, U.; Berghofer, E. (2013) Effect of hydrolysis and denaturation of wheat gluten on adhesive bond strength of wood joints. *Journal of Applied Polymer Science* 129 (5), S. 2429–2434.
- Lagrain, B.; Brijs, K.; Veraverbeke, W. S.; Delcour, J. A. (2005) The impact of heating and cooling on the physico-chemical properties of wheat gluten-water suspensions. *Journal of Cereal Science* 42 (3), S. 327–333.
- Maussymbayeva, D. (2013) Wood foam application in growth substrate formulation. Master's thesis. University of Natural Resources and Life Science, Vienna.
- Müller, U.; van Herwijnen, H.; Neuhäuser, A. E.; D'Amico, S. (2013) Natürlich geschäumte Holzstrukturen. In: *Bayern Innovativ* (Hg.): Holz als neuer Werkstoff. Regensburg, 06.11.2013.
- Neuhäuser, A. E.; D'Amico, S.; van Herwijnen, H.; Müller, U. (2014) Natürlich geschäumtes Leichtprodukt auf Holzbasis. *Holztechnologie* 56 (4), to be published.
- Sievert, D.; Hosoney, R. C.; Delcour, J. A. (2000) Bread and Other Baked Products. In: *Ullmann's Encyclopedia of Industrial Chemistry*. Wiley-VCH Verlag, Weinheim.

Mechanical Performance of Wood Plastic Composites Containing Decayed Wood

Nadir Ayrilmis^{1} – Alperen Kaymakci² – Turker Güleç³*

¹ Associate Professor, ² Research Assistant, Department of Wood Mechanics and Technology, Forestry Faculty, Istanbul University, Bahcekoy, Sariyer, 34473, Istanbul, Turkey

nadiray@istanbu.edu.tr, alperen.kaymakci@istanbul.edu.tr

* Corresponding author

³ Research Assistant, Department of Wood Mechanics and Technology, Forestry Faculty, Artvin Çoruh University, Artvin, Turkey

tgulec@artvin.edu.tr

Abstract

This study investigated the potential use of the decayed wood in the manufacture of wood plastic composite (WPC) panel. Scots pine (*Pinus sylvestris*) sound wood and decayed wood (brown-rot fungi) were used as wood material. Three levels of 30%, 40%, and 50% of sound wood and decayed wood, based on the composition by weight, were mixed with the polypropylene with 3% (based on weight) maleic anhydride grafted PP (MAPP) as a coupling agent. The compound pellets were prepared from twin screw co-rotating extruder. The WPC panels were produced by hot-press molding technique. The chemical properties of sound wood and decayed wood were investigated. The flexural and tensile properties of 3 mm thick WPC panels were determined according to ASTM standards. Although the holocellulose content of the decayed wood was significantly lower than that of the sound wood, there was no great difference between the flexural and tensile properties of the WPC panels containing decayed wood or sound wood. Based on the findings obtained from the present study, it can be said that a certain amount of the decayed wood can be incorporated into the composition of WPCs containing sound wood.

Keywords: wood plastic composite, decayed wood, mechanical properties.

Introduction

Wood-plastic composite (WPC) is composite materials made of wood fiber/wood flour and thermoplastic(s) (includes PE, PP, PVC etc.). WPC has gained popularity over the last decade especially with its properties and advantages that attracted researchers such as: high durability, low maintenance, acceptable relative strength and stiffness, fewer prices relative to other competing materials, and the fact that it is a natural resource (El-Haggar et al. 2011).

Wood decay is a deterioration of wood by primarily enzymatic activities of microorganisms. Brown-rot decay is the most common and most destructive type of decay of wood in use. The most serious kind of microbiological deterioration of wood is caused by fungi because they can cause rapid structural failure. Brown-rot fungi destroy wood by selectively degrading the hemicelluloses and cellulose without extensively changing the lignin (Flournoy et al. 1991). The rapid depolymerization of the wood carbohydrates is reflected by the substantial increase in alkali solubility products and the rapid decrease in strength properties of brown rotted wood. The lignin component also presents a barrier to wood decay because lignin is a complex aromatic polymer that encrusts the cell walls, preventing access of enzymes to the more easily degradable cellulose and hemicelluloses. In addition to these points, wood often contains potentially fungitoxic compounds, which are deposited in the heartwood (Green and Highley 1997).

Many countries face the problem of lack of woody raw material in forest products industry since most of their forested areas are unproductive. Sound wood can be used in the wood composite industry while decayed wood has no economic value in the wood composite. Although there have been a number of studies concerning the use of sound wood flour on the mechanical properties of WPC (Ayrilmis and Jarusombuti 2011, Ayrilmis et al. 2011, Ayrilmis and Kaymakci 2013), there is still no any study on the potential use of decayed wood in the manufacture of thermoplastic composites in the literature. The main objective of this study was to investigate potential use of decayed wood in the manufacture of WPC panel and compare the mechanical properties of the WPC panels with the WPC panels containing sound wood.

Materials and Methods

Materials

Wood material

Felled Scots pine (*Pinus sylvestris*) trees decayed by brown-rot fungi were supplied from plateau of *Kafkasor*, 8 km away from *Artvin province* on the Black Sea coast in the north-eastern corner of the country, on the border with Georgia. The sound Scots pine trees were harvested in the same location. The breast diameters of the decayed and sound trees were about 40 cm. The discs (10 cm thick) were taken from the 40 cm and 2.40 cm heights of the decayed and sound logs based on the ground level.

The wood particles were obtained from the decayed and sound wood discs using laboratory type drum chipper with three knives. The wood particles were then processed by using a laboratory *Fritsch* grinder. A vibratory sieve shaker (Fritsch Analysette) was used to obtain 60 mesh size wood flour for the WPC manufacture and 40-100 mesh size wood flour for the chemical analysis of sound and decayed wood. The wood flour used in the WPC manufacture was dried in a laboratory oven at 102°C for 24-h to a moisture content of 0-1% based on the oven-dry weight of wood. The dried wood flour was stored in a plastic bag.

Polymer matrix and coupling agent

The polypropylene (PP) (MFR/230°C/2.16 kg = 3,2 g/10 min, density: 0.91 g/cm³, isotactic index: 97.5%) produced by Borealis AG in Austria, was used as the polymeric material. The coupling agent, maleic anhydride-grafted PP (MAPP-Optim-425, MFI/190°C, 2.16 Kg = 120 g/10 min, density: 0.91 g/cm³), was supplied by Pluss Polymers Pvt. Ltd. in India.

Preparation of hot press molded WPC panels

The wood flour, polypropylene, and MAPP granulates were processed in a 30 mm co-rotating twin-screw extruder with a length-to-diameter (L/D) ratio of 30:1. The barrel temperatures of the extruder were controlled at 170, 180, 185, and 190°C for zones 1, 2, 3, and 4, respectively. The temperature of the extruder die was held at 200°C. The extruded strand passed through a water bath and was subsequently pelletized. The pellets were stored in a sealed container and then dried to the moisture content of 1-2% in a laboratory oven before the hot press molding. The pellets were compression molded in *Carver* hydraulic lab press. Press temperature, pressure, and press time were 170°C, 25 bar, and 5 min, respectively. At the end of the hot pressing cycle, the panel was moved from the hot press into a press at room temperature for cooling. Ten 3 mm thick panels were then trimmed to a final size of 130 mm × 130 mm. A total of 12 experimental panels, 2 for each type of panel, were manufactured. Finally, the specimens were conditioned at a temperature of 23 °C and relative humidity (RH) of 50% according to ASTM D 618. Air-dry density values of the specimens varied from 0.93 to 1.02 kg/m³. The raw material formulations used for the WPCs are presented in Table 1.

Table 1. Experimental design.

WPC code	Sound wood flour (% wt)	Decayed wood flour (% wt)	Polypropylene (% wt)	MAPP (% wt)
A	30	-	70	3
B	40	-	60	3
C	50	-	50	3
D	-	30	70	3
E	-	40	60	3
F	-	50	50	3

MAPP: maleic anhydride grafted polypropylene.

Chemical analysis of sound and decay wood specimens of Scots pine

For the determination of the chemical properties of the sound wood and decayed wood, the preparation of the test specimens was carried out according to TAPPI T 257 cm-85 standard. Alcohol-benzene, hot and cold water solubility's, and solubility in dilute alkali (1% Na OH) were determined according to TAPPI T 204 cm-97, TAPPI T 207 cm – 99, TAPPI T 212 cm – 98, respectively. Holocellulose and α -cellulose, and lignin contents were determined by the chlorite method (Wise and Karl, 1962), TAPPI T 203 cm – 99, and the *Runkel method* (Runkel and Wilke 1951), respectively. Ash content was analyzed by Tappi T 211 om-93.

Determination of mechanical properties

The flexural tests were conducted in accordance with ASTM D 790 using a Lloyd testing machine at a rate of 1.3 mm/min crosshead speed. Dimensions of the test specimens were 3.5 mm x 13 mm x 128 mm. The tensile tests were conducted according to the ASTM D 638. Tensile

specimens were tested with a crosshead speed of 5 mm/min in accordance with ASTM D 638. Seven specimens were tested for the tensile and flexural properties of each composite formulation.

Results and Discussion

The results of chemical analysis of sound wood and decay wood of Scots pine are presented in Table 2. Solubility in cold water, hot water, and dilute alkali (1% NaOH) of the decayed wood were considerably higher than those of the sound wood. The lignin content in the decayed wood increased from 28.24 to 50.75% as the sound wood degraded by brown-rot fungi while the α -cellulose content decreased from 43.15 to 14.42%.

Table 2. The results of chemical analysis of sound wood and decay wood of Scots pine.

Chemical analysis	Unit	Decayed wood	Sound wood
Solubility in cold water	%	5.49	3.12
Solubility in hot water	%	8.57	4.22
Solubility in dilute alkali (1% NaOH)	%	54.97	16.41
Solubility in alcohol-benzene	%	16.12	5.81
Lignin	%	50.75	28.24
Holocellulose	%	35.16	73.27
α - cellulose	%	14.42	43.15

The results of flexural and tensile tests are presented in Table 3. As expected, the strength values of the WPCs containing decayed wood were considerably lower than those of the WPCs containing sound wood. This was mainly due to the chemical changes of the wood degraded by brown-rot fungi. As shown in Table 2, the holocellulose of the decayed wood was found to be 35.16% while it was found to be 73.27% for sound wood.

Cellulose is primarily responsible for the strength of the wood fiber; therefore, reducing the length of the cellulose molecules (degree of polymerization) would cause a reduction in macro-strength properties of wood (Sweet and Winandy 1999). The brown-rot fungi accelerate depolymerization of the cellulose by breaking down the long chain cellulose (crystalline structure) to shorter chain. Depolymerization and shortening of the cellulose polymer adversely affect flexural and tensile properties of the wood.

There was no great difference between the flexural and tensile properties of the WPC panels containing decayed wood or sound wood. For example, at the same wood flour content (50 wt%), the flexural strength and modulus of the WPC containing 50 wt% sound wood was determined as 24.8 N/mm² and 3784 N/mm² while they were found to be 21.5 N/mm² and 3349 N/mm² for the WPCs containing 50 wt% decayed wood, respectively. Similar results were found for the tensile strength and modulus. Although the flexural and tensile strength of the WPCs containing sound

wood or decayed wood decreased with increasing wood flour content, the flexural and tensile modulus of the WPCs increased. The flexural and tensile modulus of the WPCs increased by 15.9% and 16.5 as the amount of the sound wood content increased from 30 to 50 wt% in the WPC. These properties were found to be 13.9% and 12.7% for the WPCs containing decayed wood.

Table 3. Density and mechanical properties of the WPC panels.

WPC code ¹	Density (g/cm ³)	Flexural strength (N/mm ²)	Flexural modulus (N/mm ²)	Tensile strength (N/mm ²)	Tensile modulus (N/mm ²)
A	0.97 (0.01)	33.3 (2.3) a	3263 (407)	21.0 (1.1)	2779 (485)
B	1.00 (0.01)	29.7 (1.2) b	3510 (141)	18.0 (0.9)	3063 (554)
C	1.02 (0.02)	24.8 (1.2)	3784 (157)	16.7 (1.3)	3239 (381)
D	0.94 (0.02)	28.6 (1.9)	2940 (128)	17.9 (2.0)	2577 (400)
E	0.95 (0.01)	24.4 (2.2)	3163 (372)	14.7 (3.1)	2769 (347)
F	0.98 (0.02)	21.5 (1.9)	3349 (185)	12.3 (1.3)	2906 (580)

¹ See Table 1 for WPC panel formulation. The values in the parentheses are standard deviations.

Conclusions

This study investigated the potential use of the decayed wood in thermoplastic composites as reinforcing filler. Although the holocellulose content of the decayed wood was significantly lower than that of the sound wood, there was no a great difference between the flexural and tensile properties of the WPC panels containing decayed wood or sound wood. Based on the findings obtained from the present study, it can be said that a certain amount of the decayed wood can be incorporated into the WPCs made using sound wood.

References

- Ayrilmis, N., Kaymakci, A. 2013. Fast growing biomass as reinforcing filler in thermoplastic composites: Paulownia elongata wood. *Industrial Crops and Products*. 43: 457–464.
- Ayrilmis, N., S. Jarusombuti, V. Fuengwivat, P. 2011. Bauchongkol. Effect of thermal treatment of wood fibres on properties of flat-pressed wood plastic composites. *Polymer Degradation and Stability*. 96(5): 818–822.
- Ayrilmis, N., S. Jarusombuti. 2011. Flat-pressed wood plastic composite as an alternative to conventional wood based panels. *Journal of Composite Materials*. 45(1): 103–112.

El-Haggar, S.M., Kamel, M.A. 2011. Advances in Composite Materials - Analysis of Natural and Man-Made Materials (Ed: Pavla Tesinova). Chapter 11: Wood Plastic Composites. Intechopen Publisher, Croatia.

Flournoy, D.S., Kirk, T.K., Highley, T.L. 1991. Wood decay by brown-rot fungi: changes in pore structure and cell wall volume. *Holzforschung*. 45: 383–388.

Green III, F., Highley, T.L. 1997. Mechanism of brown-rot decay: paradigm or paradox. *International Biodeterioration & Biodegradation*. 39(2–3): 113–124.

Sweet, M.S., Winandy, J.E. 1999. Influence of degree of polymerization of cellulose and hemicellulose on strength loss in fire-retardant-treated Southern Pine. *Holzforschung*. 53(3): 311–317.

Runkel, R.O.H., Wilke, K.D. 1951. Zur Kenntnis des thermo-plastischen Verhaltens von Holz. *Holz Roh Wokst*. 9: 260–270.

Wise, E.L., Karl, H L. 1962. Cellulose and Hemicellulose in Pulp and Paper Science and Technology, Vol:1, Pulp, Edited by Earl Libby Mc Graw Hill Book Co., New York.

Moisture Dynamics of Plywood and Impact on Time of Wetness

Joris Van Acker, Imke De Windt, Wanzhao Li, Jan Van den Bulcke

Abstract

Plywood intended for exterior applications seems to perform adequately in relation to service life expectations. However most such plywood type used under outdoor conditions (use class 3 according to EN 335) do not consist of durable wood species nor have been preservative treated against fungi. A fit for purpose approach revealed that next to intrinsic resistance against fungal decay also moisture dynamics are relevant. Many different plywood types have been exposed using a continuous moisture measurement (CMM) set up to obtain data on time of wetness (ToW) and matched samples were tested according to a laboratory floating experiment covering absorption/desorption to mimic this service life component. Significant differences were found and hence it can be underpinned that plywood product parameters like coating, wood species, glue-type and top veneer thickness are key in designing for longer service life under more adverse climatic conditions.

Keywords: Plywood, time of wetness, moisture dynamics, service life

Prof. Joris Van Acker
Ghent University (UGent)
Laboratory of Wood Technology (Woodlab)
Coupure links 653
9000 Ghent, Belgium
Phone: +32 9 2646120
Joris.VanAcker@UGent.be

Properties of the Wood Dried and Heat-treated by Superheated Steam

*Yonggun Park¹, Yeonjung Han¹, Jun-Ho Park¹, Yoon-Seong Chang¹,
JuHee Lee¹, Sang-Yun Yang¹, Hwanmyeong Yeo^{1,2*}*

¹ Department of Forest Sciences, College of Agriculture & Life Sciences, Seoul National University, Seoul, KOREA.

² Associate Professor, Research Institute of Agriculture & Life Sciences, Seoul National University, Seoul, KOREA.

** Corresponding author*

hyeo@snu.ac.kr

Abstract

Green pitch pine lumber (500 mm with longitudinal, 150 mm with radial and 50 mm with tangential) was dried and heat-treated by superheated steam. Drying and heat treatment were carried out simultaneously in an equipment. The thermodynamic condition of superheated steam is determined by temperature and pressure. It is important to find out proper temperature and pressure conditions of heat treatment that drying defects such as check and crack do not occur. Four superheated steam heat treatment conditions were tested; 0.1MPa-180°C, 0.1 MPa-220°C, 0.5MPa-180°C and 0.5MPa-220°C. Physical properties of wood heat-treated using superheated steam were compared to those treated by hot air (180°C and 220°C). Any drying checks did not occurred when green wood was dried and heat-treated with superheated steam of 0.5MPa-220°C. Superheated steam heat treatment decreased equilibrium moisture content (EMC) of wood. This lower EMC improved some physical and biological performances such as dimensional stability, compressive strength parallel to the grain, and decay resistance. This study shows that drying and heat-treating of green lumber without occurrence of drying checks is possible by using superheated steam.

Keywords: Wood Heat Treatment, Wood Drying, Superheated Steam, Physical Performance, Decay resistance, Pitch Pine

Introduction

Heat treatment (HT) in the range of 160°C~260°C is a conventional method to improve the physico-mechanical and biological performance of wood. The HT has effect on the performances of wood including hydrophobicity, dimensional stability, strength, and decay resistance with changes of some chemical components. Various methods of HT have been studied in Europe; ThermoWood process in Finland, Plato process in Netherland, Torrefied Process in France, and Oil Heat Treatment (OHT) process in Germany. Among these HT methods, ThermoWood process is a method using the superheated steam (SHS), which is a steam having a temperature above boiling point and has often used in drying green wood, as heat transfer medium. In

contrast to other HT methods treating a dried wood, the HT methods using SHS can treat a green lumber without pre-drying. However, when a temperature and a pressure of SHS during the process were not controlled severe drying defects, it could occur in the wood and at the wood surface.

Properties (equilibrium moisture content (EMC), shrinkage, hardness, compressive strength parallel to the grain, bending strength, and decay resistance) of superheated steam treated wood were compared to those of kiln-dried wood and hot-air heat-treated wood.

Materials and Methods

Materials. Twenty-one pitch pine green lumbers (150 mm × 50 mm × 600 mm) were prepared. Drying and HT were carried out with seven conditions; kiln drying, 180°C hot-air HT, 220°C hot-air HT, 0.1 MPa–180°C SHS HT, 0.1 MPa–220°C SHS HT, 0.5 MPa–180°C SHS HT, and 0.5 MPa–220°C SHS HT. It is to be noted that the length of these specimens is shorter than that of industrially dried lumber, but it is expected that the results of these lab-scale experiments can be used to design industrial-scale processes. Wood segments of 30 mm length were removed from both ends of the lumber to make all the samples uniform; 20 mm length of wood was cut from both ends of the remaining lumber to determine the initial moisture content (MC), and the remaining 500 mm lumber piece was heat-treated.

Heat treatment equipment. The equipment for HT consists of a reactor with a volume capacity of 15L, a feed tank, a condenser, and a vacuum pump. Sensors for measuring the temperature and pressure in the reactor and the temperature of the wood were attached to the reactor (Figure 1). The measurements were performed in real time, and the data were evaluated and controlled by a computer. The temperature sensor (K-type thermocouple, Fluke, WA, USA) detected the temperature of the vapor in the reactor and the temperature of the center of wood (Figure 1). The pressure sensor (PA21SR, Keller, NC, USA) detected the pressure in the reactor (Figure 1). The ceramic heater covered the internal surface of the reactor, and the insulation was made of glass wool.

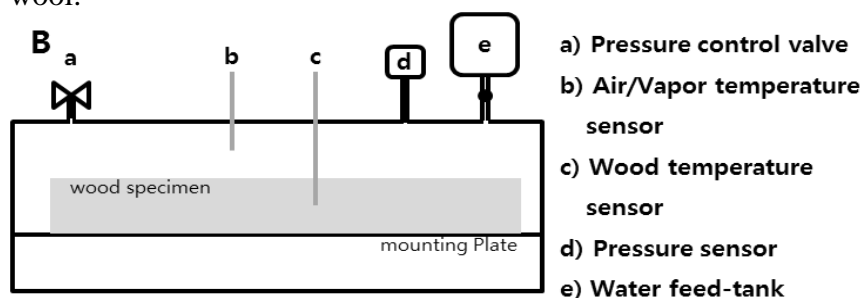


Figure 49. Side view of heat treatment reactor

Superheated steam heat treatment. During the SHS HT in the equipment, the water vapor pressures were maintained to 0.1 MPa (b.p. 100°C) and to 0.5 MPa (b.p. 151°C), respectively. The initial MC of all lumbers was in the range of 40%–50%. The processing time was fixed as 12 h for all the four treatment conditions. After closing the reactor in which wood specimen was placed, distilled water was injected into it. The amount of water was calculated based on the reactor size and the specific volume of the vapor. In the case of 0.1 MPa–180°C SHS HT, the specific volume is 2.08L/g, and the reactor volume is 15L. Therefore, 7.22 g water was injected. In the same manner, it was determined that 6.62 g of water was needed for 0.1 MPa–220°C,

37.04 g for 0.5 MPa–180°C, and 33.72 g for 0.5 MPa–220°C. Next, the air, including the oxygen and nitrogen in the reactor, was drawn off with a vacuum pump to reduce the fire risk and to enhance the water evaporation rate in the initial heating stage. The evacuated reactor was heated to the target temperature (180°C or 220°C), while the water added to the reactor was evaporated. The reactor became full of SHS, and the continuous water evaporation increased the pressure in the reactor. When the pressure exceeded the target pressure, the pressure control valve was opened automatically to remove the excess steam.

Kiln drying for comparison. Nine pieces of green pitch pine lumber were kiln-dried below 10% MC. Forest Products Laboratory (FPL) drying schedule (T12-C5) was applied to the lumber (Table 1). Three pieces of kiln-dried lumber were taken for 180°C air HT, and the other three were used for the 220°C air heat treatment.

MC (%)	Dry bulb (°C)	Wet bulb (°C)	RH (%)
Green~40	71.1	65.6	77.5
40~35	71.1	63.3	69.7
35~30	71.1	60.0	59.0
30~25	76.7	62.8	52.9
25~20	76.7	60.0	45.9
20~15	82.2	62.8	41.6
15~End	82.2	54.4	26.4

Table 14. FPL drying schedule for pitch pine wood with 5mm thickness (T12-C5)

Hot-air heat treatment. Three pieces of dried lumber were heat-treated in atmospheric pressure at 180°C, and another three were heat-treated at 220°C. The initial MC of all dried lumbars was approximately 8%–10% and the processing time was 12 h in all cases.

Observation of surface and internal checks. Pictures of cross sections were taken with a digital camera (EOS 50D, Cannon, Tokyo, Japan) before and after the HT for monitoring the checks occurrence. Internal checks were evaluated with small specimens cut from the lumber.

Equilibrium moisture content. Ten cubical specimens (20 mm × 20 mm × 20 mm) were prepared to evaluate EMC at each condition. All specimens were soaked in distilled water; then they were humidified in a thermo-hygrostat at 25°C and five different relative humidity conditions, 90%, 75%, 60%, 45%, and 30% RH, in desorption.

Shrinkage. Ten cubical specimens (20 mm × 20 mm × 20 mm) showing the exact *R* and *T* directions were prepared to evaluate the directional shrinkage of wood treated at each condition. Two measurement baselines were drawn along *R* and *T* directions at the cross section to measure the length of the same position. The lengths of wood were measured at water-saturated and oven-dried conditions. The volumetric shrinkage and the total shrinkage in the three anatomical directions were determined. It was supposed that there was no shrinkage along *L* direction.

Compressive strength and bending strength. For each treatment, 10 hexahedral specimens with a size of 30 mm (*L*) × 20 mm (*R*) × 20 mm (*T*) and 10 hexahedral specimens with a size of 280 mm (*L*) × 20 mm (*R*) × 20 mm (*T*) were prepared for evaluating the compressive strength parallel to the grain and the bending strength, respectively. All specimens were humidified in a thermo-hygrostat at 20°C and 65% RH until their weights were stabilized. The strength was measured by a UTM (10-ton UTM, Zwick, Ulm, Germany) with a loading rate of 3 mm/min.

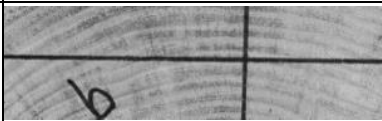
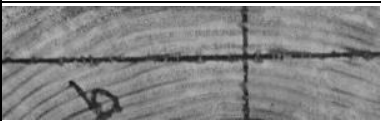
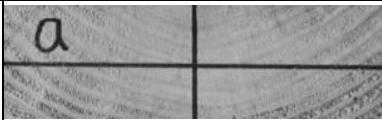
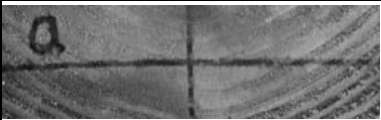
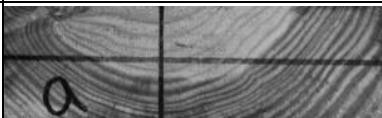
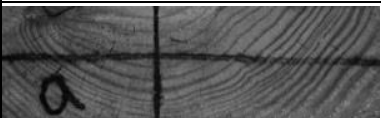
Hardness. To evaluate the Janka hardness, 15 cubical specimens (50 mm × 50 mm × 50 mm) were prepared for each treatment. In addition, the hardness of five specimens was determined in each directional section. All specimens were humidified in a thermo-hygrostat at 20°C and 65% RH until their weights were stabilized. When a metal ball with a diameter of 11.28 mm, which was installed in the UTM, indented the specimen to a 5.64 mm depth with a loading rate of 5 mm/min, the hardness was calculated by measuring the load delivered to the metal ball. Some specimens were destroyed before the metal ball had reached 5.64 mm depth. At this time, the hardness was calculated with the load until indenting to 2.82 mm.

Decay resistance. Decay test was determined in compliance with “method of test decay for wood” of Korean Standard (2004) (KS F 2213). The culture solution for growth of fungi was made with 2.5% glucose, 1.0% malt extract, 0.5% peptone, 0.3% potassium phosphate, 0.2% magnesium sulfate, and 95.5% water. The culture bottle was prepared by mixing 300 g sanitized sand and 80 ml culture solution in a glass bottle. After the fungi grew up, which was covered with the surface of sand in the bottle, six cubical specimens (20 mm × 20 mm × 20 mm) were put into the culture bottle and the bottle was placed in the thermo-hygrostat at 25°C and above 70% RH for 60 days. Mass loss (ML) was calculated by weights of specimens oven-dried at 105°C before and after decay.

Results and Discussion

Surface and internal checks after heat treatment. Figures 2 and 3 show cross sections and inside of wood specimens before and after HT. Severe checks were observable on the cross section and inside of wood along the *L* direction of the specimen treated at 0.1 MPa–180°C SHS (Figures 2 and 3a). In case of the specimen 0.1 MPa–220°C SHS HT, severe internal checks were not detectable but light cross section checks occurred. In contrast, after the treatment 0.5 MPa SHS HT, surface checks and internal checks were not observed (Figures 2 and 3b). In case of the air HT based on the pre-dried wood specimens (dried to 8%–10% MC before HT) surface and internal checks did not occur.

Equilibrium moisture content. Figure 4 shows adsorption isotherms at 25°C for each treatment condition. The EMCs of the untreated and the kiln-dried specimens are higher than those of the HT specimens. The EMCs of the wood treated at 0.5 MPa–220°C SHS HT at various RH conditions were the lowest. These low EMC values prove that the HT of green wood is satisfactory under the conditions 0.5 MPa–220°C SHS for 12 h. The

		Before	After	
Air HT	180°C			
	220°C			
SHS HT	0.1 MPa	180°C		

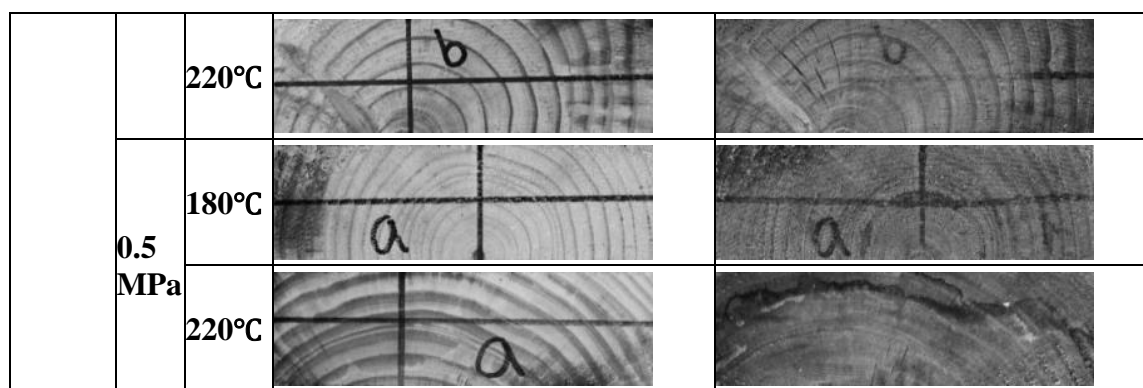


Figure 50. Cross section of wood specimens before and after HT

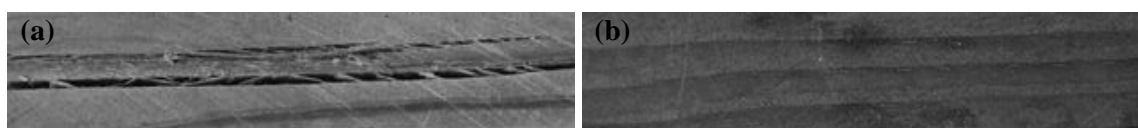


Figure 51. Inside of wood specimens (a) internal check to longitudinal direction in the specimen treated with 0.1 MPa-180°C SHS; (b) no internal checks in the specimen treated with 0.5 MPa-220°C SHS

EMCs of the wood varied as a function of the temperature and the heating time. More specifically, the EMC of the heat-treated wood was inversely proportional to the time spent in the heating chamber at wood temperatures above 170°C. The decrease in the EMC due to HT is related to the increase in cellulose crystallinity, plasticization of lignin, etc. It can be safely concluded that the low EMC values will be beneficial to many physico-mechanical and biological properties of the treated wood.

Shrinkage. The physico-mechanical properties of HT woods for each condition are listed in Table 2 and Table 3, including shrinkage, compressive strength parallel to grain, bending strength, hardness, and ML by fungi. The total *R* and *T* shrinkages shrinkage are in the range of 1%–5% and 1%–7%, respectively. The shrinkage of HT_{220°C} wood was lower than that of HT_{180°C}. In particular, both *R* and *T* shrinkages of the wood heat-treated by SHS at 0.5 MPa–220°C were with < 1% extremely low. Accordingly, SHS HT has a significant effect on the enhancement of the dimensional stability of wood.

Compressive strength. The compressive strengths and modulus of elasticity (MOE) parallel to the grain of the wood treated by the air HT and the 0.5 MPa–220°C SHS HT were higher than those of the non-treated wood. The reason is that the compressively loaded cross-sectional area of the specimens, which were heat-treated by air and 0.5 MPa–220°C SHS, was reduced without check. In contrast, small gaps between wood cells and drying checks occurred during the HT at 0.1 MPa, which might decrease the compressive strength. The strength of HT wood at 0.1 MPa was similar to or lower than that of the non-treated specimens. In the compressive strength test, non-treated specimens were destroyed normally with a little distortion, but HT specimens, especially those heat-treated at 0.1 MPa SHS were sometimes split with ring failures. This type of split may have occurred as a result of the internal checks that go parallel to grain. Cell structure, fiber direction, MC, specific gravity, and presence of defects may affect the wood strength.

Bending strength. Specimen used for the bending test is longer than that used for the compressive test. Thus the probability is higher that the specimens have checks or cracks, which

detract the results as it is well known that drying checks reduce bending strength. Especially the specimens treated at 0.1 MPa under SHS condition contained such

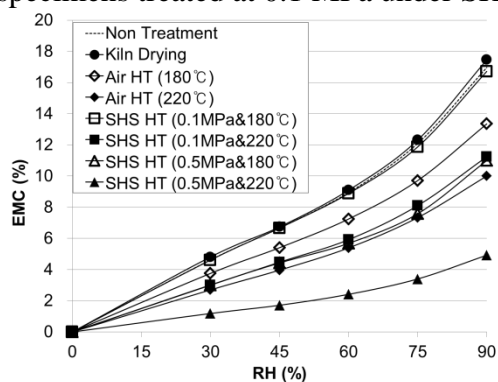


Figure 52. Desorption isotherm of each treated wood

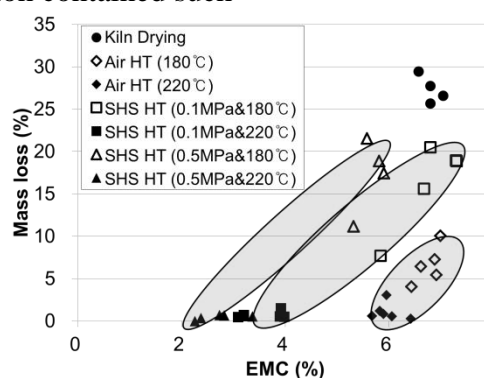


Figure 53. Relationship between EMC of wood humidified at 25 °C, 65% RH and ML by brown rot fungi (*Tyromyces palustris*)

damages, thus the lowered bending strengths were expectable. However, in case of SHS HT at 220 °C no checks were observed, but the bending strength was nevertheless decreased. This is probably due to the chemical changes in hemicelluloses and other chemical modifications. Most of the bending MOEs of HT specimens are higher than those of the non-treated specimens.

Hardness. Hardness and failure modes of wood are governed by the morphological or chemical characteristics of the small area loaded by the metal ball. Therefore, the statistical relevance of hardness tests is less reliable than that of other mechanical tests. The morphological characteristics are influenced by many parameters of drying, but the chemical properties are mainly influenced by the temperature. When the small area was weakened by shrinkage differences between early-wood and latewood, the cross section and transversal section of HT woods were destroyed along the annual ring and split along the grain, respectively, during the hardness testing. The hardness of the specimens of HT_{220 °C} was higher than that of HT_{180 °C} or that of untreated wood.

Decay resistance. The ML of the wood treated at 220 °C was lower than that of the wood treated at 180 °C (Table 3). The standard deviation is higher in case of HT at lower temperatures. As mentioned earlier, the EMC of wood is lowered by HT at high temperatures. It is known that the wood begins to decompose at around 165 °C, starting with hemicelluloses and then followed by cellulose and lignin. The decrease in the EMC value is closely associated with the decay resistance as fungi need moisture for their metabolism. The relationship between EMC of the wood humidified at 25 °C–65% RH and ML caused by brown rot fungi (*Tyromyces palustris*) is shown in Figure 5. The higher the EMC the higher is the ML, provided other parameters are kept constant. The relationship has a slightly linear tendency. Accordingly, the ML by brown rot can be predicted by evaluating the EMC of specimens humidified at 25 °C–65% RH.

Conclusions

To evaluate the effect of the temperature and pressure of the SHS on green pitch pine lumber, samples were dried and heat-treated by SHS at two temperatures and at two different water vapor pressures. The physico-mechanical properties of the SHS HT wood were compared with those of air-dried and kiln-dried wood and air heat-treated wood. The reproducibility of the experiments

was high. Through the SHS HT process, green wood was dried and heat-treated in one working step rapidly without drying checks, and the dimensional stability of the specimens was improved. When wood with 40% initial MC was submitted to SHS HT at 0.5 MPa–220°C, it reached an oven-dried state in 9 h without any drying checks. The EMC and the total volumetric shrinkage of wood SHS HT at 0.5 MPa–220°C were decreased to one-fourth and one-fifth of those of untreated wood. The compressive strength parallel to the grain and the hardness of the cross section of the wood could be increased by the treatment SHS HT at 0.5 MPa–220°C, although improvement of the bending strength did not occur. Finally, the ML of the wood SHS HT at 0.5 MPa–220°C was dropped to around zero and it can be concluded that chances are high that SHS HT could be developed and used for industrial applications.

TABLE 2. Total shrinkage and strength properties of treated wood. (standard deviation in brackets)

	<u>Total shrinkage*</u>				<u>Strength</u>					
	<u>L</u> (%)	<u>R</u> (%)	<u>T</u> (%)	<u>V</u> (%)	<u>Compressive Strength</u> (N/mm ²)	<u>Compressive MOE</u> (N/mm ²)	<u>EMC*</u> (%)	<u>Bending strength</u> th (N/mm ²)	<u>Bending MOE</u> (N/mm ²)	<u>EMC*</u> (%)
Non-treatment (Air drying)	0.58 (0.16)*	4.14 (0.28)	6.57 (0.19)	10.96 (0.43)	34.67 (1.40)	1494.79 (174.68)	11.86 (0.28)	71.36 (5.39)	4867.0 (508.04)	12.13 (0.17)
Kiln Drying	0.40 (0.20)	3.63 (0.77)	6.37 (0.59)	10.13 (1.05)	29.42 (7.34)	1535.47 (266.20)	11.68 (0.68)	68.95 (9.21)	4319.2 (1393.42)	12.12 (0.40)
Hot-air HT	180 °C (0.30)	2.93 (0.68)	4.19 (1.05)	7.55 (1.43)	47.49 (4.10)	2281.60 (221.89)	7.69 (0.29)	49.27 (20.12)	3700.7 (802.58)	6.72 (0.43)
	220 °C (0.05)	2.39 (0.47)	3.08 (0.43)	5.56 (0.77)	51.07 (3.03)	1634.00 (123.37)	5.60 (0.67)	45.97 (13.29)	6194.7 (1182.80)	4.99 (0.30)
0.1 SH MPa	180 °C (0.05)	5.31 (0.49)	6.84 (1.41)	11.87 (1.68)	43.74 (9.07)	1231.91 (322.83)	7.96 (0.78)	59.04 (25.60)	6645.6 (1378.90)	7.60 (0.76)
S HT	220 °C (0.22)	2.16 (1.06)	3.46 (1.44)	5.89 (2.21)	34.53 (8.00)	1386.77 (312.37)	3.63 (0.97)	34.02 (14.16)	5895.3 (1010.25)	5.18 (0.89)
0.5 MPa	180 °C (0.14)	1.88 (1.36)	2.88 (2.2)	4.95 (3.47)	38.08 (8.15)	1863.13 (200.32)	7.11 (1.45)	42.60 (22.17)	8068.9 (2215.1)	6.48 (1.36)

))	4))				27)
	-----							5018.8
220	0.36	0.77	0.97	2.09	56.75	1806.74	2.03	34.54
°C	(0.15	(0.36	(0.1	(0.58	(4.27)	(339.92)	(0.29)	(9.72)
))	7))				40)

* L: longitudinal, R: radial, T: tangential, V: volumetric. ** EMC at 25°C and 65% RH.
|| means parallel to grain

Table 3. Hardness and decay resistance for treated woods. (standard deviation in brackets)

	Hardness						Decay Resistance	
	C*	EMC**	R*	EMC**	T*	EMC**	Mass Loss	EMC**
	section	25/65	section	25/65	section	25/65	(%)	25/65
	(kN)	(%)	(kN)	(%)	(kN)	(%)		(%)
Non-treatment (Air drying)	3.47 (0.29)	11.76 (0.14)	1.35 (0.33)	11.68 (0.26)	1.71 (0.69)	11.92 (0.16)	13.36 (2.28)	7.65 (0.15)
Kiln Drying	3.76 (0.21)	11.41 (0.55)	1.66 (0.56)	11.09 (0.12)	1.26 (0.16)	11.19 (0.46)	25.58 (8.64)	6.81 (0.19)
Hor-air °C	3.43 (0.47)	6.83 (0.37)	2.43 (0.14)	7.04 (0.51)	2.05 (0.78)	7.23 (0.66)	5.57 (3.29)	6.77 (0.24)
HT 220 °C	4.66 (1.09)	4.78 (0.37)	2.64 (0.44)	5.06 (0.57)	2.56 (0.37)	5.02 (0.52)	1.07 (1.01)	5.98 (0.25)
SH S HT 0.1 MP a	2.98 (0.62)	6.56 (0.61)	1.51 (0.69)	4.91 (0.70)	2.04 (0.78)	5.96 (1.61)	15.14 (5.37)	6.79 (0.60)
SH S HT 0.5 MP a	4.02 (0.24)	5.69 (0.45)	1.47 (0.62)	6.14 (0.77)	1.72 (0.66)	6.19 (0.95)	1.41 (1.80)	3.63 (0.43)
SH S HT 0.5 MP a	2.48 (0.21)	8.35 (0.19)	0.60 (0.03)	8.01 (0.30)	0.71 (0.33)	8.74 (0.06)	13.10 (7.72)	5.66 (0.26)
SH S HT 0.5 MP a	4.57 (0.92)	3.86 (0.17)	1.36 (0.67)	3.76 (0.33)	1.61 (0.77)	3.42 (0.39)	0.47 (0.26)	2.79 (0.44)

*C: Cross, R: radial, T: tangential. ** EMC at 25°C and 65% RH

Correlation between Fracture Fractal Dimension and Wood Shearing Properties after Hydrothermal Treatment

Jun Hua^{1,*} – Wei Xu¹ – GuangweiChen¹ – KeqiWang¹ – LipingCai² – Sheldon Q. Shi²

¹*College of Electromechanical Engineering, Northeast Forestry University, box 310, Harbin, China;*

²*Department of Mechanical and Energy Engineering, University of North Texas, Denton, Texas, USA.*

**Corresponding authors: hua jun81@163.com*

Abstract

Fiber separation in refining is crucial for energy consumption in fiberboard manufacturing. Wood chips are broken down between two disks where one or both rotate in the refining process. Impact and shear forces are transferred to chips breaking them into progressively smaller pieces during the refining. To make the refining process more efficient, it is desired to understand the chip fracture characteristics under the two forces. This study focused on the examining of the surface fracture feature after the shear breaking using fractal dimension analysis.

Five species, i.e., white pine, poplar, pine, birch, and basswood, were hydro-thermally treated in a hermetical chamber with a temperature of 117°C (about 2-bar pressure) for 30 min. The specimens were broken under the longitudinal and transverseshearing forces using a lab-made mechanical testing machine. The fractal dimension of the fracture surfaces were measured with a vertical cross-sectional contour method. The linear relationships between fractal dimension and wood shear strength was found. The following conclusions were drawn from this work:

1. The shearing strength was significantly affected by thermal softening for the species of white pine, poplar, birch and basswood except for pine.
2. The surface fractal dimensions of the tested five species ranged between 2.047 and 2.133. Transvers shearing softened pine had the maximum value of 2.133 and transvers shearing birch with or without softening took the minimum value of 2.047.
3. Positive correlations between the transverse shear strength and fracture fractal dimensions were discovered for the five species.

Introduction

During the manufacturing process of fiberboards, refining of wood chips is one of the crucial steps in regard to the product quality and energy consumption. In the refining process, the wood chips are first heated up with steam in a heater, and then go through a mechanical break-down process using two refining disks in the refiner. By the movement, the chips are split into separate fibers finally (Hua et al. 2010). Marton and Eskelinen (1982) explored the effect of specimen thickness, tester gap, temperature, specific gravity, and moisture content on the impact strength

of Norway spruce. The results revealed that the refining energy consumption was greatly affected by the chip thickness. For Norway spruce, the impact strength in cleavage was about a quarter of that in forward shear. Thus it was suggested that changing the refining mode from shear to cleavage would be an effective method to reduce the energy consumption during refining. Huang et al. (2011) proposed the breakdown mechanism of Jack pine earlywood (EW) and latewood (LW) in thermo-mechanical pulping by means of microscopic observations. Characteristics such as fiber splitting, shortening, delamination (internal fibrillation), external fibrillation, etc. were evaluated. Physical changes in the EW and LW fibers were qualified and quantified with the aid of light microscopy and scanning electron microscopy. The impacts of the observed changes on pulp and paper properties were assessed to establish possible interrelation between the fiber characteristics and paper properties. Kekäläinen et al. (2012) examined the difference between the development of the softwood and hardwood fibers under controlled compression and shearing conditions. The results indicated that the shearing under the controlled compression at high consistency modified the softwood and hardwood fibers already at low-energy consumptions. The fiber length and width decreased, and the formation of curls and kinks was pronounced. However, the intensive mixing after in-pad attrition revealed that the fiber structure was not weakened under compression and shear forces; conversely, the fiber cell wall was more resistant for the intensive mixing. Fernando et al. (2013) compared the development of the internal and external fiber microstructure and ultrastructure of the primary refined softwood subjected to high-consistency (HC) or low-consistency (LC) secondary refining in the thermo-mechanical pulp process. It was found that broad sheet- and lamellae-type external fibrillation from the S2 was typical for HC refining, and these characteristics were rarely observed in the LC pulps. The cell wall characteristics (internal and external) of the pulp fibers appear to govern most of the physical and optical properties in handsheets.

Impact and shear forces are transferred to chips breaking them into progressively smaller pieces during the refining. Berg (2001) examined the effect of impact velocity on the fracture of wood during the refining. The result confirmed that the size reduction of chips during the refining was dependent on the refining intensity and the chip strength that was affected by the fracture mode, impact direction, chip dimension, temperature, rate of deformation and etc. Using a falling weight impact tester, it was found that the increase in impact velocity from about 2.7 to 4.8 m/s resulted in an increase in impact strength of about 50%. Berg et al. (2009) estimated the strain energy density required for defiberizing the chips by uniaxial tension or shear load using an analytical model. The results illustrated that the energy consumption was dependent on the micro-fibril angle in the middle secondary wall layers, the loading direction, the thickness of cell wall layers, the fiber separation mode, moisture content and temperature. The energy consumption for the fiber generated from earlywood was lower than that from latewood. Eskelinen et al. (1982) investigated the relationship between the mechanical properties of wood species and the mechanical pulping outcome. Two dynamic wood testing methods through the determination of 1) impact energy absorption and 2) torsion pendulum were used in the experiments. The results showed that a significant correlation existed between the refining energy consumption and the wood properties. Thus a property combining the transversal strength of wood and the energy absorption in failure was closely related to the fiber quality in mechanical pulping. No significant difference in impact energy with respect to the fracture direction (tangential, radial or longitudinal) was found.

The fractal dimension allows describing a general relation between the material structures and physical phenomena. The fractal characteristics of a series of fractured steel specimens were examined experimentally by Underwood and Baner (1986). The fractal data were obtained from

the fracture surfaces and their profiles. The physical nature of the fractal dimension was afforded by its close similarity to fracture roughness parameters that had simple physical meanings. To check for “self-similitude” of any irregular nature curve, the linearity of the entire fractal plot was examined by Underwood (1994). A reverse sigmoidal shape was found for the usual fractal plots of nature. Regardless of its angle or position, any sectioning plane that cuts an irregular surface is stereo-logically related to that surface. The fractal dimensions of metallic fracture surfaces in different states after the heat treatment were examined by Kotowski (2006), which included the influences of the mechanical notch radius in a compact specimen on the fractal dimension of the fracture surface, the distortion rate on the fractal dimension, the fatigue crack propagation rate on the fractal dimension, and the stress-intensity factor on the fractal dimension of the fracture surface. The results indicated that the fractal dimension of the fracture surface did not depend on the place of measurement. When testing the influence of the radius of the mechanical tip notch on the fractal dimension of a fracture surface, this dimension was determined in the places located at different distances from the tip of the mechanical notch. With respect to the radii up to 1.0 mm, no significant differences in fractal dimensions were found. With a range from 2.02 to 2.10, the same fractal dimensions of the fracture surface for all examined materials were found. The occurrence of fracture processes from images of fractures in specimens of molybdenum and porous iron was investigated based on the approaches of fractal geometry (Trefilov *et al.* 2001). It was suggested that the fractal dimension increased with a decrease in the size of the dimple and the test temperature in cast titanium tested under the conditions of uniaxial stretching. It was confirmed that the fractures had multi fractal (statistically self-similar) nature.

The applications of fractal models in porous media were explored by Kou *et al.* (2009). Based on the thermal-electrical analogy and statistical self-similarity of porous media, a fractal analysis of effective thermal conductivity for unsaturated fractal porous media was completed. Using a dimensionless expression of effective thermal conductivity, the effect of the parameters of fractal porous media on the dimensionless effective thermal conductivity was investigated. A simple method of quantitative assessment of surface roughness and texture was proposed by Klonowski *et al.* (2005). The method was developed from multiple disciplines and can be used for multidisciplinary applications. As a good measure of surface roughness, a greyscale 2-D image of a 3-D surface was employed for calculations of the surface fractal dimension. This method can be used for quality assessment of nano-sensors. The same analysis methods may be used for the processing of bio-signals generated by these nano-sensors. The effect of the fractal dimension of a fracture surface and spall contour on the characteristics of the loaded material was investigated by Barakhtin and Savenkov (2009). It was shown that an increase in the fractal dimensions of the spall contour leads to an increase in the material strength parameter in the tensile wave and spall strength, whereas an increase in the fractal dimension of the fracture surface reduced the spall strength.

Limited studies regarding the applications of fractal analysis in wood and wood-based materials were completed. The Griffith criterion that took into account the actual cracked wood surface induced by a crack extension was modified based on the scaling law describing the growth of roughness of fracture surfaces by Morel and Valentin (1999). It was found that the roughening leads to R-curve behavior where the fracture toughness depends on the crack length increment Δa as a power law. The link between morphology of fracture surface and fracture toughness also provided a size effect on the critical resistance. The critical energy release rate depended on the specimen size as a power law. Predicted results are confirmed by the comparison with fracture experiments made on Norway spruce and Maritime pine. The comparison of relation significance

of impact energy and linear combination of those fractal dimensions was carried out by Konas et al. (2009). Opposite to common way of estimating relation between impact energy and fractal dimension of fracture after impact loading (as quantitative of material toughness), sufficient amount of information about toughness in original state (before the loading) was provided for the estimation. Because of the complicated experimental assessment of the toughness, the work of impact loading as a measurable magnitude of material toughness was used. The fractal dimensions of void size (FDVS) in oriented strand boards were investigated using X-ray computer tomography images and a computer image processing technique by Li et al. (2013). The FDVS value was high in the panel surface layers and decreased toward the panel center. The decrease in FDVS was a linear function of the increased porosity. It was concluded that FDVS can be a useful additional parameter for characterizing the internal void structure of strand-based wood composites.

The objective of this study was to explore the relationship between the fracture fractal dimension and wood shear properties after hydrothermal treatment. These dimensions were determined for the vertical profile obtained by the profile technique with a camera and edited using the image graying method. By examining the fractal dimension values on the fractures from transverse and longitudinal shearing, the relationship between the impact ductility and the fracture fractal dimension would be established.

Material and Methods

Sourced from Heilongjiang Province, China, five species, white pine (*Pinus bungeana* Zucc. ex Endl.), poplar (*Liriodendron tulipifera*), pine (*Pinus sylvestris*), birch (*Betula papyrifera*), and basswood (*Tiliaceae*) were used in this study. Two types of specimens for the two shear directions, i.e., transversal and longitudinal directions, were prepared as shown in Fig. 1. In accordance with the Chinese standards GB/T 1929-2009 and GB/T 1937-2009, the same specimen cross sections of 10 mm × 25 mm (width × thickness) were prepared to compare the difference between the two shear directions (Fig. 1). The densities and moisture contents are presented in Table 1. The basic density was calculated as the following:

$$\rho_w = \frac{m_w}{V_w} \quad (1)$$

where, ρ_w is the basic density, g/cm³; m_w is the sample mass when the moisture content is $w\%$, g; V_w is the sample volume when the moisture content is $w\%$, cm³.

Table 1 The densities and moisture contents of the specimens

Species	White pine	Poplar	Pine	Birch	Basswood
Basic density (g/cm ³)	0.384	0.432	0.461	0.529	0.559
Initial moisture content (%)	14.11	12.64	13.10	11.15	15.88
The moisture content after softening (%)	91.2	157.8	75.7	115.0	102.6

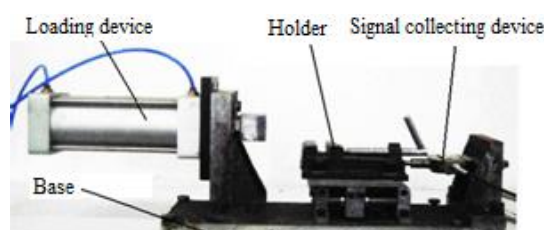
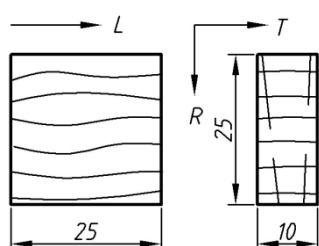


Fig. 1 Size of specimens (mm)

Fig. 2 Lab-made device of shearing strength

This study was aimed at investigating the relationship between the fracture fractal dimension and shear properties before and after hydrothermal treatment through the analysis of fracture profile contour lines on the specimen cross sections. The hydrothermal treatment was completed by placing the specimens in water in the YC3A-100 pressure container with a pressure of 0.8 bars for 30 min. Three shearing types, namely, transvers shearing, transvers shearing after softening and longitudinal shearing after softening, were tested.

Since the specimen sizes of wood shearing tests are much smaller than the sizes of the universal mechanical testing machine requires, a simple shearing device with high accuracy was developed as shown in Fig. 2. A specimen was placed on a holder and moved forward by an air cylinder.

With a cutting speed of 0.11m/s, a shearing force acted on the specimen until it was broken. The forces during the shearing process were measured using a pressure sensor and recorded in a computer.

The fracture Section and Shearing Strength

The shearing strengths of the five species were measured using the lab-made shearing device. Typical fracture profiles were selected from the tested specimens and the fracture specimen contours morphology sections were photographed using a camera. The profile contour images of the transvers and longitudinal shearing specimens after being softened are shown in Figs. 3, 4 and 5.

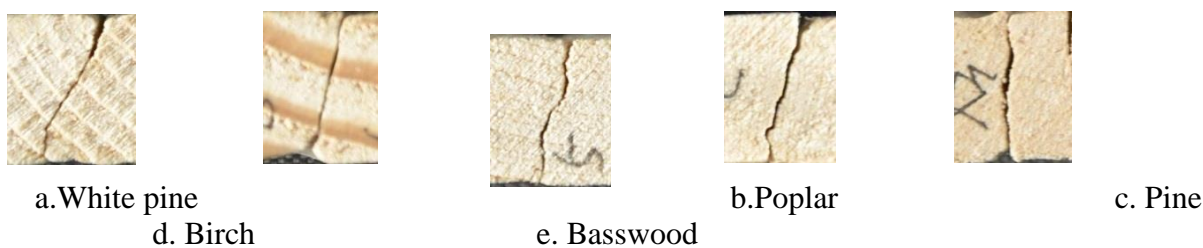


Fig. 3 Images of transvers shearing fracture profiles



Fig. 4 Images of transvers shearing fracture profiles after thermal softening

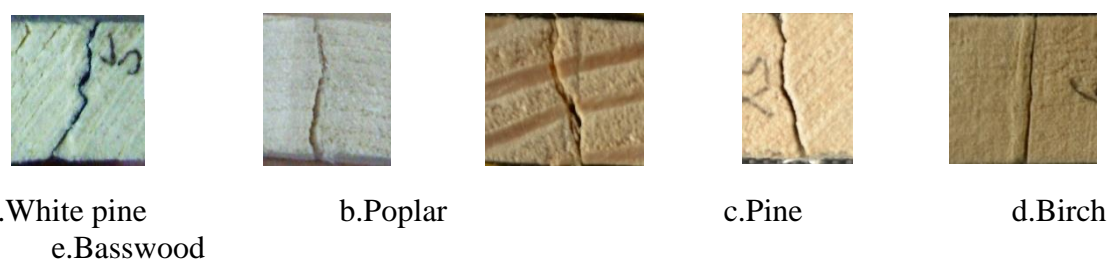


Fig. 5 Images of longitudinal shearing fracture profiles after thermal softening

When the specimens were cut through transvers shearing, the fractures occurred along fiber direction and curve fractures were obtained as shown in Fig. 3 (b). Greater bending curves were shown for white pine, poplar and pine, while relatively straight curves were observed for birch and basswood specimens.

When the thermal-softened specimens were tested by transvers shearing, most fractures occurred along the fiber direction curves as shown in Fig. 4 (b). The small bending curves and rugged curves along the shearing directions for white pine and pine were observed as illustrated in Fig. 4 (c). Greater bending curves and rugged curves as well as a few split fibers were found for poplar, birch and basswood specimens as shown in Fig. 4 (d).

When the thermal-softened specimens were tested by longitudinal shearing, linear fracture profile lines along the shearing directions were shown in Fig. 5 (b and e). The fracture profiles of the white pine and basswood were relatively flat, while the poplar, pine and birch specimens were rugged profiles.

Based on the Chinese standard GB/T1937-2009, the shearing strength was calculated according to the following equation:

$$\tau_w = \frac{0.96P_{\max}}{bl} \quad (2)$$

where, τ_w is the shearing strength (MPa) when the moisture content is $w\%$; P_{\max} is the maximum load (N); b is the width of the shearing in the specimen (mm); l is the length of the shearing in the specimen (mm).

The calculated shearing strengths are listed in Table 2.

Table 2 The shearing properties of the specimens (MPa)

Species	White pine	Poplar	Pine	Birch	Basswood
Transverse shearing strength	1.42	2.94	2.11	3.85	3.15
Transverse shearing strength after softening	0.98	1.32	1.27	1.71	1.55
Longitudinal shearing strength after softening	2.60	4.37	4.27	4.66	3.27

To investigate the effect of shearing direction on shearing strength before and after thermal softening, a statistical analysis was carried out. The variance analysis results of transverse and longitudinal shear strength are presented in Table 3 and 4.

As shown in Tables 3 and 4, all of the Probability Level (p-value) were greater than 0.05 except for pine ($p = 0.098712$), indicating that the shearing strength was significantly affected by thermal softening for the species of white pine, poplar, birch and basswood.

Table 3 Variance analysis results of transverse shearing strength

Species	Source of Variation	SS	df	MS	F	P	F—crit
White pine	Between Groups	0.744211	1	0.744211	6.797719	0.026164	4.964603
	Within Groups	1.094796	10	0.10948	—	—	—
	Total	1.839007	11	—	—	—	—

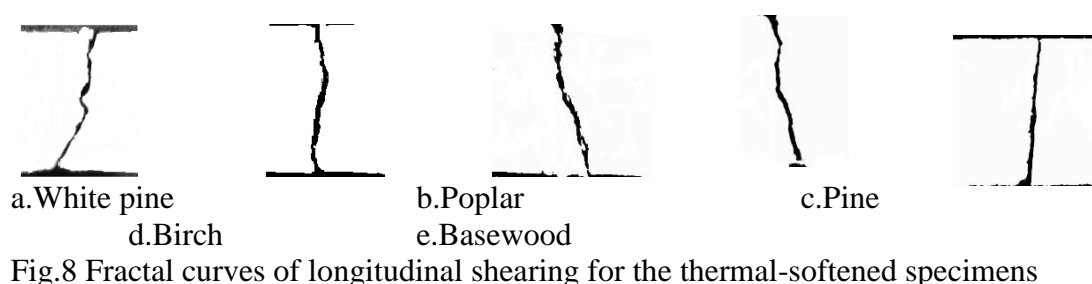
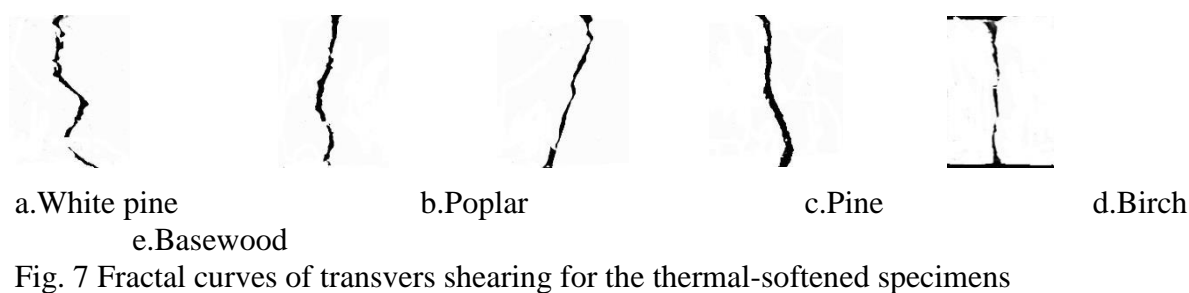
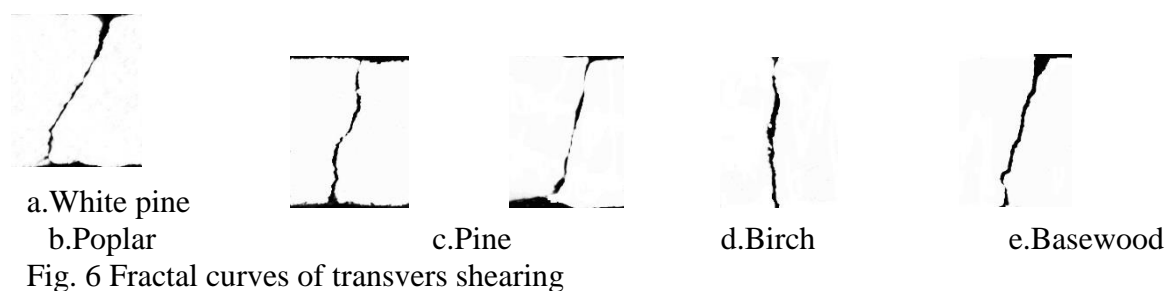
Poplar	Between Groups	8.322434	1	8.322434	50.77811	3.2e-05	4.964603
	Within Groups	1.638981	10	0.163898	—	—	—
	Total	9.961415	11	—	—	—	—
Pine	Between Groups	2.45738	1	2.45738	3.313862	0.098712	4.964603
	Within Groups	7.415457	10	0.741546	—	—	—
	Total	9.872837	11	—	—	—	—
Birch	Between Groups	14.67581	1	14.67581	559.9536	4.12e-10	4.964603
	Within Groups	0.26209	10	0.026209	—	—	—
	Total	14.9379	11	—	—	—	—
Basswood	Between Groups	9.436638	1	9.436638	16.17074	0.002433	4.964603
	Within Groups	5.835625	10	0.583562	—	—	—
	Total	15.27226	11	—	—	—	—

Table 4 Varianceanalysis results of longitudinal shearing strength

Species	Source of Variation	SS	df	MS	F	P	F—crit
White pine	Between Groups	13.06313	1	13.06313	159.9376	2.16e-10	4.413873
	Within Groups	1.470176	18	0.081676	—	—	—
	Total	14.53331	19	—	—	—	—
Poplar	Between Groups	46.52807	1	46.52807	1940.96	8.7e-20	4.413873
	Within Groups	0.43149	18	0.023972	—	—	—
	Total	46.95956	19	—	—	—	—
Pine	Between Groups	44.84636	1	44.84636	2115.336	4.04e-20	4.413873
	Within Groups	0.381611	18	0.021201	—	—	—
	Total	45.22797	19	—	—	—	—
Birch	Between Groups	43.82724	1	43.82724	1683.796	3.09e-19	4.413873
	Within Groups	0.468519	18	0.026029	—	—	—
	Total	44.29576	19	—	—	—	—
Basswood	Between Groups	14.99796	1	14.99796	147.6718	4.12e-10	4.413873
	Within Groups	1.828131	18	0.101563	—	—	—
	Total	16.82609	19	—	—	—	—

Shearing fracture fractal profiles and fractal dimension analysis

Using Photoshop CS5, the images of the fracture profile curves in Figs. 3, 4 and 5 were converted to greyscales by filtering noises, resulting fractal curves of longitudinal shearing fracture profiles as shown in Figs. 6, 7 and 8.

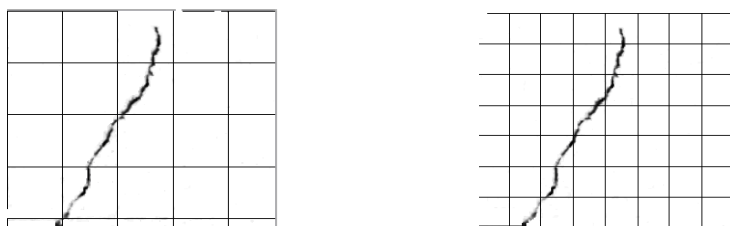


As shown in Figs. 6 and 7, after thermal softening, the fracture fractal curves were more complicated than that before the thermal treatment. The fractal curves were not smooth curves, but curves with saw-toothing or small zigzags.

By comparing the fracture fractal curves in Figs. 6, 7 and 8, the thermal-softened curves in longitudinal direction were not as complicated as that without softening. The thermal-softened curves were not smooth curves, but curves with saw-toothing or small zigzags.

Since the fractal curves of the fracture profile contour line were complicated and the peaks of the curves were distributed randomly, the structure had irregularly self-similar nature.

After the specimens were broken, the fractal dimensions of the fracture profiles were calculated using the grid covering method. At first, the fracture profiles and surfaces were observed closely, the typical profiles of the curves were determined. Using Photoshop CS5 software, these photos were edited by image graying and the curve was covered by grids. The yardstick δ was determined by adjusting the distance between the grid lines, as shown in Fig. 9b. The yardstick δ was changed by increasing the number of grids. Because the number $N(\delta)$ of grids that with curve was increased as yardstick δ reduced, a set of varied data $[\delta_i, N(\delta_i)]$ presented. After taking logarithms for $1/\delta_i$ and $N(\delta_i)$, a group of new data set $[\log(1/\delta_i), \log(N(\delta_i))]$ were obtained for linear regression. The slope K of the regression equation was the fractal dimension D_L of the fracture profile curve. Fig. 10 illustrates the linear regression result for the longitudinal shearing of birch specimens.



a. Fracture profiles and grid covering method with an increase in grid number

b. Fracture profiles and grid covering method

Fig.9 Calculating fracture profiles using the grid covering method

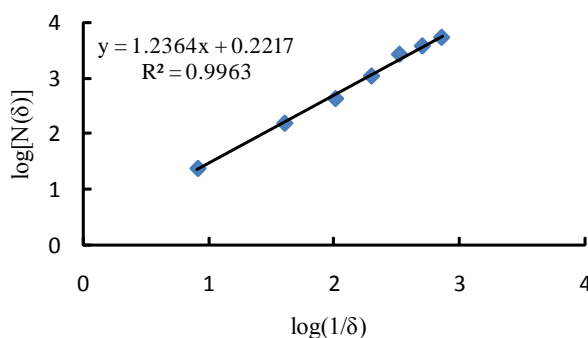


Fig.10 Linear

log(1/δ)

regression for the

longitudinal shearing of birch after thermal softening

Fig.10 shows an excellent linear relationship between $\log[N(\delta)]$ and $\log(1/\delta)$ ($R^2=0.9963$). An obvious similarity between the global and local fracture surface profile lines, namely, the profile line-shade fractal fracture characteristics was found. The slope of the linear regression was 1.2364, which was the fracture fractal dimension D_L . The following equation shows the relationship between the fracture profile dimension fractal D_L and the surface fractal dimension D_A (Underwood1994):

$$D_A = \frac{\ln \left[\frac{\pi \delta^4}{4(\delta^{1-D_L} - 1) + \pi} \right]}{2 \ln \delta} \quad (3)$$

It was calculated $D_A=2.1466$. Using this method, the surface fractal dimensions of the five species was calculated as shown in Table 5.

Table 5 Surface fractal dimensions of the five species

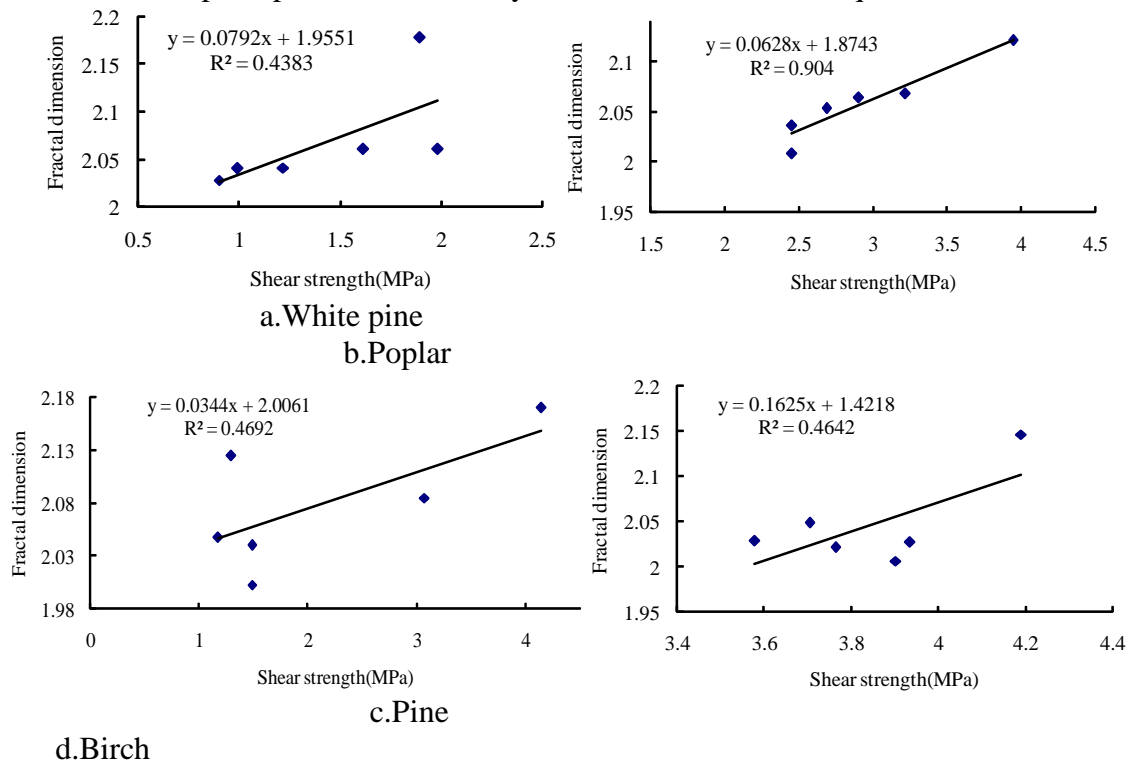
	White pine	Poplar	Pine	Birch	Basswood
Transvers shearing fracture fractal dimensions	2.069	2.081	2.079	2.047	2.105
Transvers shearing fracture fractal dimensions after softening	2.084	2.117	2.133	2.095	2.081
Longitudinal shearing fracture fractal dimensions after softening	2.066	2.080	2.049	2.047	2.073

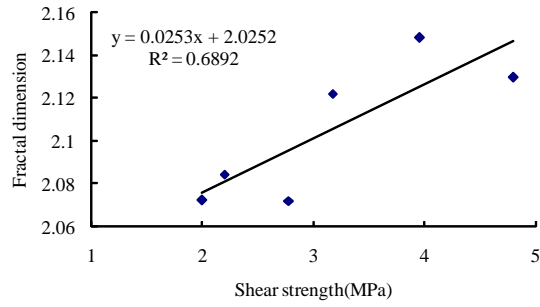
Table 5 indicates:

- For transvers shearing, the surface fractal dimensions of the tested five species were ranged between 2.047 and 2.105. The basswood had the maximum value of 2.105 and birch took the minimum value of 2.047, which made the difference was 0.058.
- After thermal softening, for transvers shearing, the surface fractal dimensions of the tested five species were ranged between 2.081 and 2.133. The pine was the maximum value of 2.133 and basswood took the minimum value of 2.081, which made the difference was 0.052.
- After thermal softening, for longitudinal shearing, the surface fractal dimensions of the tested five species were ranged between 2.047 and 2.080. The poplar had the maximum value of 2.080 and birch took the minimum value of 2.047, which made the difference was 0.033.

Correlation between Fracture Fractal Dimension and Shearing Property

Correlation between fracture fractal dimension and transvers shearing property. Fig. 11 shows the regression results of the transverse shear strength of the five species and the fracture fractal dimension. Positive correlations between the transverse shear strength and fracture fractal dimensions were discovered for the five species. Although a relatively low R squares were obtained for white pine, pine and birch, they still met the statistical requirements.

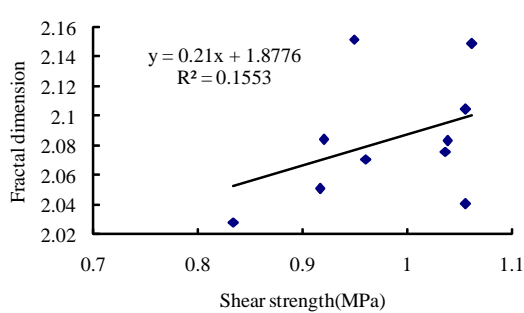




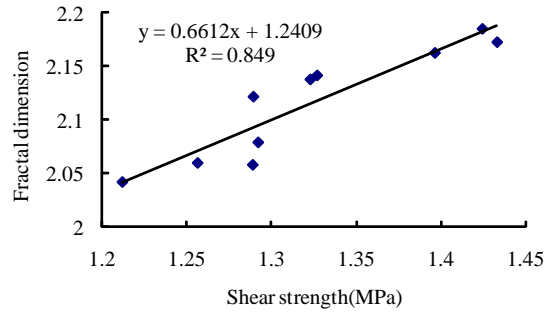
e. Basswood

Fig.11 Correlation between transvers shearing strength and fractal dimension

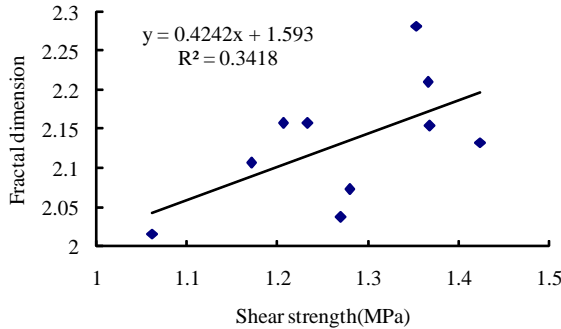
Correlation between fracture fractal dimension and transvers shearing property after softening. Fig. 12 shows the regression results of the transverse shear strength of the five species and the fracture fractal dimension after the thermal-softening. Positive correlations between the transverse shear strength and fracture fractal dimensions were found for the five species. Relatively low R squares were obtained for white pine, pine and birch, while high R squares were found for poplar and basswood.



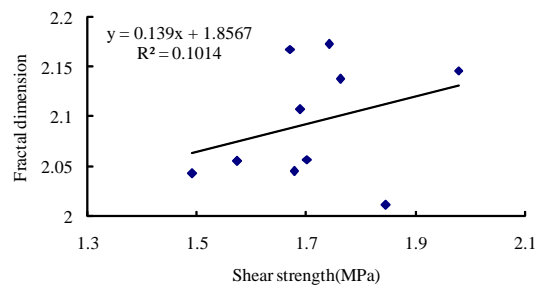
a. white pine



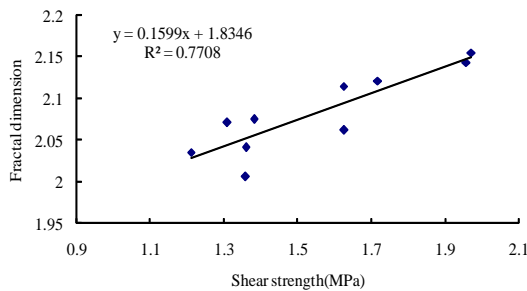
b. Paplar



c. Pine



d. Birch



e. Basswood

Fig.12 Correlation between transvers shearing strength and fractal dimension after thermal softening

Correlation between fracture fractal dimension and longitudinal shearing property after softening. Linear relationships between longitudinal shear strength and fracture fractal dimension were found as shown in Fig. 13. However, the correlations were low, which probably could not describe the shearing strength using fractal dimensions.

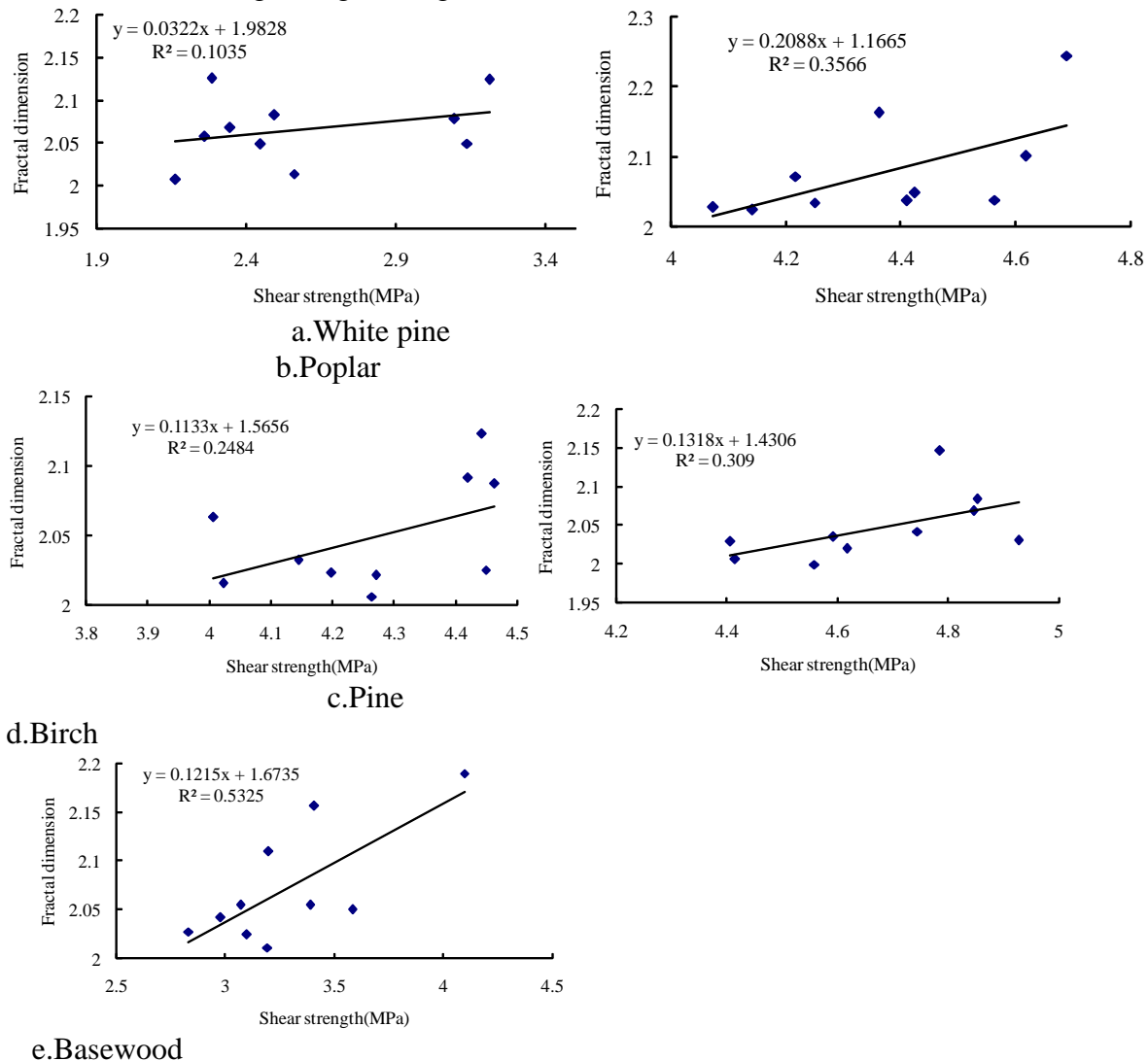


Fig.13 Correlation between longitudinal shearing strength and fractal dimension after thermal softening

Conclusions

The following conclusions were drawn from the shearing tests:

- When the specimens with and without thermal softening were broken by transvers shearing, all species were curvedly fractured along shearing direction and linearly fractured long fiber direction. After thermal softening, along shearing direction, linear fractures occurred.
- The shearing strength was significantly affected by thermal softening for the species of white pine, poplar, birch and basswood except for pine.
- The surface fractal dimensions of the tested five species ranged between 2.047 and 2.133. Transvers shearing softened pine had the maximum value of 2.133 and transvers shearing birch with or without softening took the minimum value of 2.047.

- d. Positive correlations between the transverse shear strength and fracture fractal dimensions were discovered for the five species.

Acknowledgement

This work was supported by the Natural Science Foundation of China (NSFC) through grant number 31070499.

References

- Barakhtin, B. K., and Savenkov, G. G. (2009). Relationship between spall characteristics and the dimension of fractal fracture structures, *J. Appl. Mech. Tech. Phy.* 50(6), 965-971.
- Berg JE. (2001) Effect of impact velocity on the fracture of wood as related to the mechanical pulping process. *Wood Science and Technology* 35: 343-351
- Berg, J.E., M.E. Gulliksson and P.A. Gradin. 2009. On the energy consumption for crack development in fiber wall in disc refining – a micromechanical approach. *Holzforschung.* 63: 204-210
- Eskelinen, E., Hu, SH, Marton, R (1982) Wood mechanics and mechanical pulping. *APPITA*360: 32-38
- Fernando, D.; Gorski, D.; Sabourin, M.; Daniel, G. 2013.Characterization of fiber development in high- and low-consistency refining of primary mechanical pulp.*Holzforschung*, 67(7): 735 - 745
- Hua, J., Chen, G., and Shi, S. Q. (2010).Effect of incorporating Chinese poplar in wood chips on fiber refining,*Forest Prod. J.* 60(4), 362-365.
- Huang, F., Lanouette, R. and Law, K-N. 2011. The breakdown mechanism of earlywood and latewood in refining. *Wood Science and Technology.* 46(5), 887 – 904
- Kekäläinen, K., Illikainen, M., and Niinimäki, J. 2012. Morphological changes in never-dried kraft fibers under mechanical shearing. *Cellulose.* 19(3): 879 – 889
- Klonowski, W., Olejarczyk, E., and Stepine, R. (2005).“A new simple fractal method for nanomaterials science and nanosensors,” *Mater. Sci. Poland* 23(3), 607-612.
- Konas, P., Buchar, J., and Severa, L. (2009).“Study of correlation between the fractal dimension of wood anatomy structure and impact energy,” *Eur. J. Mech. A* 28(5), 545-550.
- Kotowski, P. (2006). “Fractal dimension of metallic fracture surface,” *Int. J. Fract.* 141(3), 269-286.
- Kou, J., Liu, Y., Wu, F. Fan, J., Lu, H., and Xu, Y. (2009).“Fractal analysis of effective thermal conductivity for three-phase (unsaturated) porous media,” *J. Appl. Phys.* 106(4), 054905.
- Li, P., Wu, Q., and Tao, Y. (2013). “Fractal dimension analysis of void size in wood-strand composites based on X-ray computer tomography images,” *Holzforschung* 67(2), 177-182.
- Marton, R., and Eskelinen, E. (1982).“Impact testing in the study of chip refining,” *TAPPI J.* 65(12), 85-89.
- Morel, S., and Valentin, G. (1999).“Roughness of wood fracture surfaces and fracture toughness,” *1st RILEM Symposium on Timber Engineering*, Stockholm, Sweden, pp. 13-15.
- Trefilov, V. I., Kartuzov, V. V., and Minakov, N. V. (2001). “Fractal dimension of fracture surfaces,” *Met. Sci. Heat Treat.* 43(3-4), 95-98.
- Underwood, E. E. (1994). “Fractals in materials research,” *Acta Stereol.* 13/2, 269-276
- Underwood, E. E., and Baner, J. I. A. (1986).“Fractals in fractography,” *Mater. Sci. Eng.* 80(1), 1-14.

Artificially Aged Timber for Structural Components

Roland Maderebner^{1} – Thomas Badergruber¹ – Anton Kraler¹*

¹ University of Innsbruck, Faculty of Civil Engineering-Institute of Construction and Material Technology, Department of Timber Engineering

** Corresponding author*

roland.maderebner@uibk.ac.at

Abstract

The focus of this work is to examine the use of artificially aged wood for timber constructions. The artificial aging of wood is thereby obtained by a thermal treatment. In this conference paper, the results of the impact on the physical and elastic-mechanical properties by a comparison of treated and untreated specimens are presented. The results of preliminary tests on clear wood specimens are shown. The studies on the structural timbers are still in progress and will be presented to the scientific community as soon as possible. In order to enable the results of the clear wood specimens with the structural timbers the test setup is carried out in accordance to EN 408. The parameters bending strength, modulus of elasticity, shear modulus and gross density are determined. Particularly, the results of the shear moduli received by the shear field test method - one in the EN 408 relatively new recorded test method - are discussed. With regard to the data protection, details on the process of the artificial aging of wood can't be given in this work.

Keywords: Artificially aged timber, bending strength, global and local modulus of elasticity, shear modulus, shear field measurement, gross density, moisture content

Introduction

The process of thermal treatment leads to changes in the wood matrix, which must be taken into account. For the use of this material in timber constructions, it is necessary to know the effects, caused by the thermal treatment, on the physical and elastic-mechanical parameters.

In compliance with the requirements to the safety concept of the Eurocodes, the impact on the strength, stiffness and gross density of the material must be known. In order to neglect the influence of natural inhomogeneities, preliminary investigations of clear wood specimens (designated in this report as Clear-Wood "CW") are performed. By this procedure, the effects on the properties of wood by the chosen artificial wood aging process can be classified very well. For the planned use of the thermal treated material for timber constructions (designated in this report as Construction-Timber "CT") after the test series-CW, timber with typical timber cross section dimensions according to DIN 4074-1 (DIN 4074-1, 2012) is sorted visually, and tested according to the rules of the EN 408 (EN 408, 2013).

Materials and Methods

The specimens of the test series-CW are obtained of 50 mm thick boards from one tree trunk (figure 1). About half of the boards are artificially aged in a climate chamber. After the thermal treatment twin samples are cut of the tree trunk respectively of the boards. All tests are carried out on pieces, which are conditioned at the standard environment of $(20 \pm 2) ^\circ\text{C}$ and $(65 \pm 5) \%$ relative humidity. After conditioning, the specimens are prepared to the dimensions of 40/60/1050 mm for conducting bending tests to determine the bending strength, the global and local modulus of elasticity in bending and the shear stiffness. For the determination of bending parameters of small clear wood beams the DIN 52186 (DIN 52186, 1978) is often used as a basic concept. The scope of European Standard EN 408 specifies basically test methods for determining properties of structural timber and glued laminated timber and normally not for small clear (defect free) wood test pieces. However, in order to be able to produce the best possible causality and correlations between the test series CW and CT, the tests are carried out according to the same test setup. By doing so, a continuous documentation of the effects caused by artificial wood aging on specific technical parameter can be guaranteed. In Figure 1, the measuring devices for determining the deformations are shown. The test pieces are simply supported with symmetrically loaded in bending at two points over a span width of 18 times the depth. To minimize local indentations small steel plates are inserted between the pieces and the loading heads and supports. Due to the dimensions of the specimens it is unnecessary to use lateral restraints to prevent torsional buckling. For measuring the deformations of a total of 8 inductive sensors are used. The used load equipment Shimadzu AG-G 100 kN is capable of measuring the load applied to the test pieces to an accuracy of 1 %. The load is applied at a constant rate, so that the failure occurs within 300 ± 120 seconds.

Global Modulus of Elasticity in Bending, $E_{m,g}$: The shear modulus G in equation (1) can be taken as infinite if on the results of the experiments a classification to strength classes take place according to EN 384 (EN 384, 2010). In the test series-CW the shear modulus G is considered by measuring the shear field by the method described in the EN 408.

$$E_{m,g} = \frac{3 \cdot a \cdot \ell^2 - 4 \cdot a^3}{2 \cdot b \cdot h^3 \cdot \left(2 \cdot \frac{w_2 - w_1}{F_2 - f_1} - \frac{6 \cdot a}{5 \cdot G \cdot b \cdot h} \right)} \quad (1)$$

Local Modulus of Elasticity in Bending, $E_{m,l}$: In comparison to the global modulus of elasticity local indentations and shear deformations are not measured by the measuring principle of the local modulus of elasticity. Thus, the real bending stiffness is measured and can be determined using equation (2)

$$E_{m,l} = \frac{a \cdot \ell_1^2 \cdot (F_2 - F_1)}{16 \cdot I \cdot (w_2 - w_1)} \quad (2)$$

Shear Modulus $G_{tor,s}$: For the determination of the shear modulus G , the method by measuring the shear field according to EN 408 is used. At this point it should be noted that this method is especially recommended for glued laminated timber. This in the Austrian Standard Edition of the EN 408:2012 defined method for the determination of the shear modulus, based on studies by (Brandner). This method brings the benefit that the shear modulus can be measured in the course of bending tests. As this is a relatively new method, it still has to proof in the authors opinion, and assume a high accuracy of the test equipment. The calculation of the shear modulus can be determined with equation (3).

$$G_{tor,s} = \alpha \cdot \frac{h_0}{b \cdot h} \cdot \frac{(V_{s,2} - V_{s,1})}{(w_2 - w_1)} \quad (3)$$

with

$$\alpha = \frac{3}{2} - \frac{h_0^2}{4 \cdot h^2} \quad (4)$$

$$w_i = \frac{(|w_{i,1}| + |w_{i,2}|)}{h_0} \quad \text{mit } i=1, 2 \quad (5)$$

Gross density and moisture content: After the bending tests the determination of the gross density of the specimens takes place. Therefore a minimum of 20 mm wide block, free from knots and resin pockets, is cut as close as possible to the fracture over the whole cross section. To determine the moisture content and density, the volume and weight of this block of wood is determined. By the oven-dry method the moisture content and the gross density can be calculated.



Figure 1: Cutting of the specimens and test setup for measuring the bending strength, the global and local modulus of elasticity in bending and the shear modulus

Results

Bending Strength (table 1, figure 2)

The results of the bending strengths f_m show a strong impact of the thermal treatment on the material. The mean values have a difference of about 17 N/mm², which means a reduction of the bending strength of about 34 %. The statistical variability of the treated test pieces with 25% is about twice as large as for the untreated material. This fact is also reflected in the values of the 5%-quantile of the bending strength of around 28 N/mm² and 49 N/mm².

Global modulus of elasticity in bending (table 2, figure 3)

The mean values of the global modulus of elasticity in bending of the treated specimens are about 3,5% lower than those of the untreated specimens. Thus, the impact on the bending stiffness compared to the bending strength, seem to be significantly lower.

Local modulus of elasticity in bending (table 3, figure 4)

Both, the largest and the smallest value occurred on the treated specimens. The variability of the treated samples is 366 N/mm² higher than by the untreated tests. Due to low correlations of the load-displacement curves not all test results could be used.

Shear modulus (table 4, figure 5)

The shear modulus of the untreated specimens with 1015 N/mm² is 8 % higher than the treated samples. The statistical spread of the treated specimens with 120 N/mm² is 15 N/mm² lower than the variability of the untreated test pieces. However, the results in comparison with the known sizes of the shear modulus are much too high. Despite strict accordance with the experimental setup described in the EN 408 and very high correlations between the applied load and the shear deformations in the range between $0,1 \cdot F_{\max}$ and $0,4 \cdot F_{\max}$ it seems, that the measuring principle doesn't work for small samples.

Gross density (table 5, figure 6)

For both test series the gross densities are approximately equal. The max / min values are similar too. Thus, the thermal treatment has no impact on this material parameter.

Table 1: Bending strength f_m , statistical evaluation

		test series	n	max	min	mean	q_{0,05}	sd	
f_m [N/mm ²]		treated	48	72,40	26,66	50,62	28,39	12,81	
		untreated	40	85,28	47,01	67,61	48,98	8,82	
		<i>Total</i>	88	85,28	26,66	58,35	29,27	14,00	
		Niemz, 1993, untreated	-	116	42	66	-	-	
		Frühwald, 2007 treated	80°C	33	-	-	80,3*	-	9,2
			120°C	27	-	-	77,6*	-	8,4
		170°C	24	-	-	78,1*	-	8,4	

*) Median of f_m

Table 2: Global modulus of elasticity in bending, statistical evaluation

		test series	n	max	min	mean	q_{0,05}	sd	
$E_{m,g}$ [N/mm ²]		treated	48	1574 1	7188	1169 7	8844	1853	
		untreated	40	1449 1	8588	1129 6	8807	1631	
		<i>Total</i>	88	1574 1	7188	1151 5	8844	1758	
		Niemz, 1993, untreated	-	-	-	1000 0	-	-	
		Frühwald, 2007 treated	80°C	136	-	-	1190 0	-	1950
			120°C	121	-	-	1093 0	-	2200
	170°C		107	-	-	1106 0	-	1230	

Table 3: Local modulus of elasticity in bending, statistical evaluation

		test series	n	max	min	mean	q_{0,05}	sd
$E_{m,l}$ [N/mm ²]		treated	46	1803 8	6824	1257 7	8429	2831
		untreated	38	1771 8	7860	1231 6	8747	2465
		<i>Total</i>	84	1803 8	6824	1245 9	8747	2659

Table 4: Shear modulus, statistical evaluation

		test series	n	max	min	mean	q_{0,05}	sd
$G_{tor,s}$ [N/mm ²]		treated	45	1236	648	911	743	120
		untreated	39	1383	747	963	754	145
		<i>Total</i>	84	1383	648	935	747	134

Table 5: Gross density, statistical evaluation

ρ_{12} [kg/m ³]	test series	n	max	min	mean	q _{0,05}	sd	
		treated	48	516	384	439	387	42
	untreated	40	521	381	438	403	31	
	<i>Total</i>	88	<i>521</i>	<i>381</i>	<i>439</i>	<i>394</i>	<i>37</i>	
	Niemz [27], untreated	-	640	300	430	-	-	
	Frühwald [8], treated	80°C	136	-	-	448	-	39
		120° C	121	-	-	447	-	43
		170° C	107	-	-	447	-	31

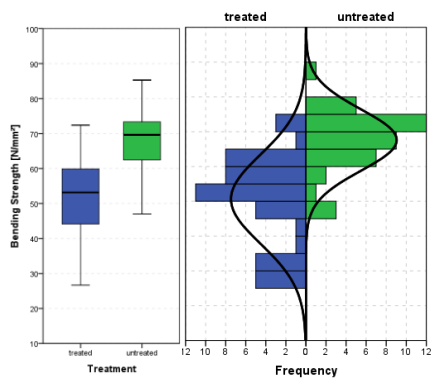


Figure 2: Bending strength

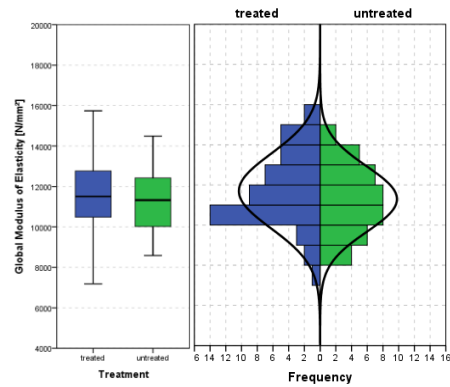


Figure 3: Global Modulus of Elasticity

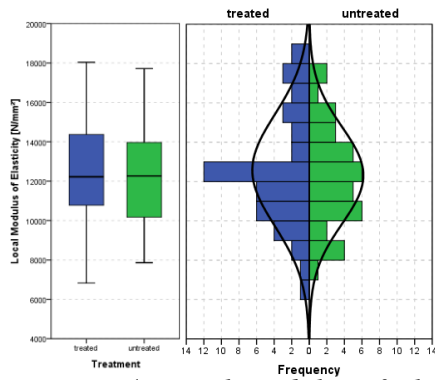


Figure 4: Local Modulus of Elasticity

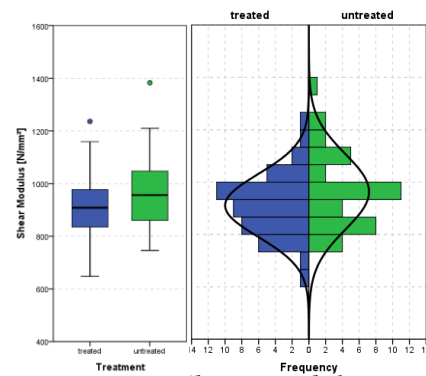


Figure 5: Shear Modulus

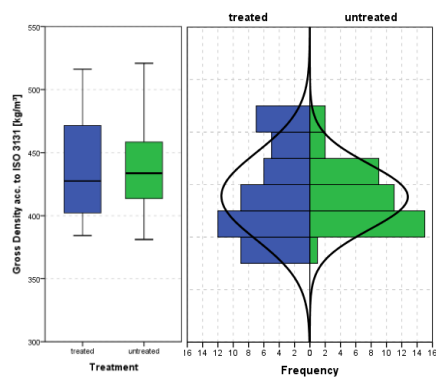


Figure 6: Gross Density

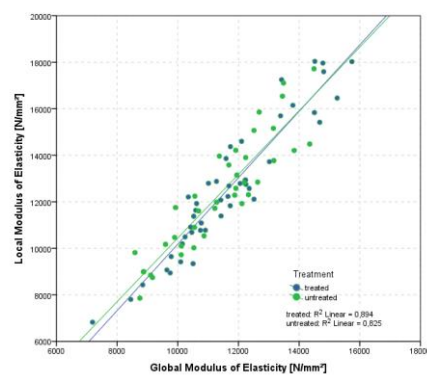


Figure 7: Scatterplot $E_{m,g}$, $E_{m,l}$

Conclusions

By the thermal treatment of the wood, the bending strength of the material is considerably affected. The treated test specimens have a 34 % lower bending strength. The calculated bending strengths of the untreated specimens coincide with those of Niemz (Niemz, 1993). However, in comparison to the data of Frühwald (Frühwald, 2007) the determined bending strengths are much lower.

The bending stiffness of the material is statistically not detectable influenced by the artificial aging process. The values of the global modulus of elasticity are higher than the data of Niemz and in the area of the investigations of Frühwald. It can be assumed that the shear stiffness is not adversely affected by the thermal treatment because the global and local modulus of elasticity have the same high correlations. According to EN 408 the method to determine the shear modulus by measuring the deformations of the shear field doesn't work with the used inductive sensors. The small dimensions of the specimens could be another reason.

References

DIN 4074-1, 2012. Sortierung von Holz nach der Tragfähigkeit - Teil 1: Nadelschnittholz Austrian Standards Institute, Vienna.

EN 408, 2012. Timber structures — Structural timber and glued laminated timber — Determination of some physical and mechanical properties. Austrian Standards Institute, Vienna.

DIN 52186, 1978. Testing of wood; bending test. Fachnormenausschuß Materialprüfung (FNM) im DIN Deutsches Institut für Normung e.V..

EN 384, 2010. Structural timber - Determination of characteristic values of mechanical properties and density. Austrian Standards Institute, Vienna.

Frühwald, E., 2007. Effect of high-temperature drying on properties of Norway spruce and larch. Holz als Roh- und Werkstoff, 65:8.

Niemz, P., 1993. Physik des Holzes und der Holzwerkstoffe. Holz : Anatomie - Chemie - Physik. DRW-Verlag. ISBN 9783871813245.

Brandner, R., et al.. Determination of modulus of shear and elasticity of glued laminated timber and related examinations. Bericht Holzforschungs GmbH, Graz.

Modification of Wood by Organometallic Processes

Balazs Bencsik

Assistant Professor
University of West Hungary
Institute of Wood-based Products and Technologies
E-mail: bbencsik@fmk.nyme.hu

Levente Denes

Associate Professor
University of West Hungary
Institute of Wood-based Products and Technologies
E-mail: dali@fmk.nyme.hu

Abstract

The life cycle of wooden objects, due their organic origin, is usually short. Wood is prone to be attacked by fungi and insects and in outdoor environment may deteriorate rapidly. The well-known hygroscopic properties make the solid wood instable in shape and dimensions. The combination of these disadvantages presents difficulties in design and applications on the various fields of the forest products industry.

This poster presentation deals with some preliminary results of research on organometallic processes for modification of wood. Several species were treated by vacuum injection to create silver layers on the capillary inner surfaces. The thickness of the formulated metallic layers was evaluated as a function of species, concentration of the AgNO_3 and treatment processes. Results were analyzed using scanning electron microscopy (SEM) and metallographic stereo microscopy (MSM). Findings indicated that the concentration and wood species have significant effect on the thickness of the silver layer. Additionally, the adhesion properties at the wood–silver interface were investigated by standard shear tests.

The lifecycle of metal treated wood may be doubled, because of improved mechanical and physical properties, better resistance against biological degradations (fungi and insects). In the long term, the introduction of organometallic solid wood or wood composites results in reduced volumes of harvested trees. Thus, it promotes sustainable forest management practices.

Key words: Organometallic, SEM, silver layer, solid wood.

Poster Session

Session Co-Chairs: *Douglas Gardner, University of Maine,
USA and Jozef Kúdela,
Technical University in Zvolen, Slovakia*

Low Formaldehyde-Emitting Wood Composites by Nanotechnology

Zeki Candan^{1} – Turgay Akbulut¹*

¹ Department of Forest Products Engineering, Istanbul University
Sariyer, Istanbul, Turkey
* *Corresponding author*
zekic@istanbul.edu.tr

Abstract

Nanotechnology has a number of advantages for wood composites to enhance their end-use properties. Formaldehyde emission of wood composite panels due by their formaldehyde-based adhesive content is disadvantage in many applications. In this research, development of environmentally friendly wood composites by nanotechnology application was objected. Urea-formaldehyde and melamine-urea-formaldehyde adhesives were reinforced with nanosilica, nanoalumina, and nanozinc oxide nanoparticles at different loading levels. Urea-formaldehyde was used as an adhesive in manufacture of the particleboard panels while melamine-urea-formaldehyde was used as an adhesive in manufacture of the plywood panels. Particleboard and plywood panels were manufactured using the thermosetting resins modified with the nanomaterials. Formaldehyde emission tests on the particleboard and plywood panels were conducted according to perforator method. The results showed that the lowest formaldehyde emission value was obtained in the plywood panels reinforced with nanoZnO at 1% loading level. The formaldehyde emission values of the plywood panels using 1% nanoZnO, 1% nanoAl₂O₃, and 3% nanoSiO₂ were decreased by 50.66%, 30.66, and 20%, respectively. The findings determined in this study revealed that all the particleboard panels had lower formaldehyde emission values than those of the control particleboard panels, except the particleboard panels reinforced with 3% nanoAl₂O₃. The maximum decrease in the formaldehyde emission was determined in these particleboard panels with 82%. In summary, formaldehyde emission property is of a great importance for particleboard and plywood panels which use especially furniture manufacture or interior design due to its carcinogenic effects on human health. The result of this research obviously indicates that nanoparticle reinforcement technology can help to develop novel particleboard and plywood panels having an environmentally friendly property.

Keywords: Nanotechnology; Formaldehyde emission; Plywood panels; Particleboard panels; Wood composites.

Introduction

Particleboard panels are generally used in furniture and decoration, while plywood panels are mostly used for structural applications. The production capacity of these composite panels is increasing annually. Turkey is one of the biggest wood-based panel producers in Europe. The formaldehyde emissions of wood composite panels due to their formaldehyde-based adhesive content are a disadvantage in many applications. Formaldehyde emissions are a crucial property to consider for particleboard and plywood panels that will be used in residential applications. It is known that formaldehyde has a carcinogenic effect on human health (National Cancer Institute 2012; Roffael 2006; Salthammer et al. 2010). Thus, there has recently been increased interest, in developed countries, in the development of wood composites having low formaldehyde emissions.

Nanotechnology can be defined as the manipulation of materials measuring 100 nm or less in at least one dimension. It is expected to be a critical driver of global economic growth and development in this century because it is a multi-disciplinary field of research that is providing glimpses into exciting new capabilities, and enabling materials, devices, and systems that can be examined, engineered, and fabricated on a nanoscale (Jones et al. 2005). Nanotechnology can be applied to many areas of research and development. Nanoscience and nanotechnology also have numerous advantages for wood composite materials. The use of nanotechnology in the manufacture of particleboard panels, plywood panels, and laminate flooring is of great importance to overcome the formaldehyde emission issue (Candan 2012; Candan and Akbulut 2012; Candan and Akbulut 2013; Ciraci 2005; Jones et al. 2005; Roughley 2005).

There is limited data in the literature on formaldehyde emissions of particleboard and plywood panels reinforced with nanomaterials at different loading levels. In this study, environmentally friendly wood composite panels were developed using nanotechnology. The effects of the nanomaterial type and loading level on the formaldehyde emission of the wood composite panels were evaluated.

Materials and Methods

Materials

Urea-formaldehyde adhesive, wood particles, hardener, and paraffin were supplied by Kastamonu Integrated Wood Industry and Trade Inc., located in Kastamonu, Turkey. The wood species used to manufacture particleboard panels in this study were *Pinus nigra*, *Populus tremula* L., *Fagus orientalis* Lipsky., and *Abies nordmanniana*. Melamine-urea formaldehyde adhesive, wood veneers, and additives were supplied by Cag Forest Products Inc., also located in Kastamonu, Turkey. The wood species used to manufacture plywood panels in this work were *Tetraberlinia bifoliolata* and *Populus × canadensis Moench*. The nanosilica, nanoalumina, and nanozinc oxide particles were used to modify both urea-formaldehyde and melamine-urea formaldehyde adhesives.

Methods

Panel manufacturing

Urea-formaldehyde and melamine-urea formaldehyde adhesives were reinforced with nanosilica, nanoalumina, and nanozinc oxide particles. The nanoparticles were added to each adhesive at loading levels of 1% and 3%. Urea-formaldehyde, NH_4Cl , and paraffin were used as adhesive, hardener, and hydrophobic additive, respectively, in the manufacture of the particleboard panels. Melamine-urea formaldehyde, $(\text{NH}_4)_2\text{SO}_4$, NH_3 , and flour were used as adhesive, hardener, buffer, and filler, respectively, in the plywood panels. Control panels without nanoparticles were also produced for comparison. Each type of panel was made with the three types of nanomaterials at the two tested loading levels.

Formaldehyde emission test

Formaldehyde emission tests were conducted on the particleboard and plywood panels according to TS 4894 EN 120 (1999). A perforator and spectrophotometer were used to determine the formaldehyde emission properties of the nanomaterial-reinforced composites.

Results and Discussion

The results indicated that the lowest formaldehyde emissions were obtained from the plywood panels reinforced with nanoZnO at a loading level of 1%, while the highest value was obtained from the plywood panels reinforced with nanoSiO₂ at a loading level of 1%. The formaldehyde emission values of the plywood panels using 1% nanoZnO, 1% nanoAl₂O₃, and 3% nanoSiO₂ decreased by 50.66%, 30.66, and 20%, respectively. The formaldehyde emission values from the plywood panels reinforced with 1% nanoSiO₂, 3% nanoAl₂O₃, and 3% nanoZnO were greater than those from the control panels.

The results of this study revealed that all of the nanomaterial-reinforced particleboard panels had lower formaldehyde emission values than the control particleboard panels, except for the particleboard panels reinforced with 3% nanoAl₂O₃. It was also shown that the particleboard panels reinforced with nanoZnO had the lowest overall formaldehyde emission values. The particleboard panels reinforced with 1% nanoAl₂O₃ or 3% nanoZnO had the lowest formaldehyde emission values. The maximum decrease in formaldehyde emissions of the particleboard panels was 82%.

Samarzija-Jovanovic et al. (2011) modified urea-formaldehyde adhesive with nanoSiO₂ particles and hexamethylenetetramine. It was stated that the formaldehyde content of the urea-formaldehyde adhesive decreased after using nanoSiO₂. Candan and Akbulut (2012) modified laminate flooring with nanoSiO₂, nanoAl₂O₃, and nanoZnO particles at different loading levels. It was reported that the nanoparticle type and loading levels significantly affected the formaldehyde emission values of the laminate flooring. The lowest formaldehyde emission value was determined from the laminate flooring reinforced with 1% nanoAl₂O₃.

Conclusions

Urea-formaldehyde and melamine-urea formaldehyde adhesives were modified with various nanomaterials at different loading levels in this work. The results showed that the nanomaterial type and nanomaterial loading level significantly affected the formaldehyde emission values of the particleboard and plywood panels. The use of nanoparticle reinforcement on adhesives can help to develop novel particleboard and plywood panels that are environmentally friendly. It can be concluded that nanoscience and nanotechnology offer important opportunities for the forest

products industry. The formaldehyde emission values of particleboard and plywood panels can be decreased using the proper nanomaterial type and loading level.

References

- Candan, Z. (2012). "Nanoparticles use in manufacture of wood-based sandwich panels and laminate flooring and its effects on technological properties," Ph.D. Dissertation, 309 pp., Istanbul University, Istanbul, Turkey.
- Candan, Z., and Akbulut, T. (2012). "Development of low formaldehyde-emitting laminate flooring by nanomaterial reinforcement," Proceedings of the 55th International Convention of Society of Wood Science and Technology, August 27-31, Beijing, China.
- Candan, Z., Akbulut, T. (2013). "Developing environmentally friendly wood composite panels by nanotechnology," *BioResources* 8(3): 3590 – 3598.
- Ciraci, S. (2005). "Science and technology at one of a billionth of a meter," Science and Technique, Tubitak, Ankara, Turkey.
- Jones, P., Wegner, T., Atella, R., Beecher, J., Caron, R., Catchmark, J., Deng, Y., Glasser, W., Gray, D., Haigler, C., Joyce, M., Kohlman, J., Koukoulas, A., Lancaster, P., Perine, L., Rodriguez, A., Ragauskas, A., and Zhu, J. (2005). "Nanotechnology for the forest products industry – Vision and technology roadmap," Report Based on Nanotechnology for the Forest Products Industry Workshop, Landsdowne, Virginia, USA, October 17-19, 2004, TAPPI Press, Atlanta, GA, USA.
- National Cancer Institute (2012). "Formaldehyde and cancer risk," <http://www.cancer.gov/cancertopics/factsheet/Risk/formaldehyde>.
- Roffael, E. (2006). "Volatile organic compounds and formaldehyde in nature, wood and wood based panels," *Holz als Roh- und Werkstoff* 64(2), 144-149.
- Roughley, D. J. (2005). "Nanotechnology: Implications for the wood products industry. Final Report," Forintek Canada Corporation, North Vancouver, Canada, 73.
- Salthammer, T., Mentese, S., and Marutzky, R. (2010). "Formaldehyde in the indoor environment," *Chem. Rev.* 110(4), 2536-2572.
- Samarzija-Jovanovic, S., Jovanovic, V., Konstantinovic, S., Markovic, G., and Marinovic-Cincovic, M. (2011). "Thermal behavior of modified urea-formaldehyde resins," *J. Therm. Anal. Calorim.* 104(3), 1159-1166.
- TS 4894 EN 120 (1999). "Wood based panels – Determination of formaldehyde content – Extraction method called the perforator method," Turkish Standard Institute (TSE), Ankara, Turkey.

Acknowledgements

The authors thank Istanbul University Research Fund for its financial support in this study (Project No: 4806 and Project No: 19515). The authors also would like to express their appreciation for the assistance provided by Kastamonu Integrated Wood Industry and Trade Inc. and Cag Forest Products Inc., located in Kastamonu, Turkey.

Effect Of Esterification By Phthalic Acid Anhydride On Some Mechanical Properties Of *Platanus Occidentalis* L. Wood

Abdulrazak R. Almalah, Ahmed Younis Al-Khero

Forestry Dept. / College of Agriculture and Forestry/ Mosul University - Iraq

Abstract

This study was performed to investigate the effect of esterification process on some mechanical properties of *Platanus occidentalis* L. wood, and studying the effect of wood type, (sap wood and heart wood), extracting type (extracted and unextracted) and 4 heating temperature 25, 80, 100, 120°C and comparing it with an unesterified wood, to find the best and most suitable esterification method which can increase age and wood efficiency. The results showed that the general mean value of untreated wood of Modulus of Rupture (MOR) and Modulus of Elasticity (MOE) and tension perpendicular to grain was higher than the treated wood. Sapwood showed a superiority compared to heartwood in static bending. The tension perpendicular to grain in treated heartwood was better compared to sapwood. The highest MOR and MOE and tension perpendicular to grain was in the extracted wood compared with the unextracted wood. Also, it was noticed that the highest mean of MOR was at 80 °C. The highest values of the tension perpendicular to grain and the MOE was at 120 °C. generally, 100 °C was the best for *Platanus occidentalis* L. wood esterification when using Phthalic acid anhydride to obtain the best physical and mechanical properties.

Corresponding author: Abdulrazak R. Almalah

Email : abdulrazakalmalah@yahoo.com

Key words: *Platanus occidentalis* L., esterification, Phthalic acid anhydride, MOE, MOR.

Introduction

Many scientists and researchers started to treat wood with chemicals to prevent or reduce wood infection by microorganism or insects. Most of wood stems and boards produced recently, exposed to deterioration during storage or usage due to the infection by micro organisms such as fungi or bacteria or by insects. Many wood preservatives have been used including water-born and oil-porn preservatives, some of them may be toxic or harmful to human health or to the environment (kasir et. al. 1993).

Recently, researcher began to use chemicals which have no effect to the humans or to the environment, and perform the same function as wood preservatives in increasing wood time usages. The best of these chemicals are the chemicals which were used for wood acetylation. Wood acetylation was used to improve physical and chemical properties of wood by using anhydride compounds which replace the free hydroxyl group of the wood with the acetyl group. It was believed that wood digestion by microorganism enzymes started from the free hydroxyl group which causes wood decay and deterioration. Acetylated wood was not toxic and has no harmful effect on the environment, and increase wood solidity, dimension stability, and increase resistance to fungi and insects. Wood acetylation using phthalic acid anhydride is the first to be performed in Iraq. Almalah and Al-khero (2013) stated that treated Sycamore wood with phthalic

acid anhydride will decrease swelling percent after immersion in water for 2 and 6 hrs, and decrease shrinkage percent. Risi and Arseneau (1957) and Pooper and Bariskam (1972) mentioned that wood acetylation can be carried out without using a catalyst. Some of the compounds used for wood acetylation are (ketene, Acetic acid anhydride, phthalic acid anhydride, Acetyllechloride). The best is by using phthalic acid anhydride because it is inexpensive and available in local markets. The chemical formula is $C_8H_4O_3$. The chemical reaction between phthalic acid anhydride and wood can be shown as in the following reaction:

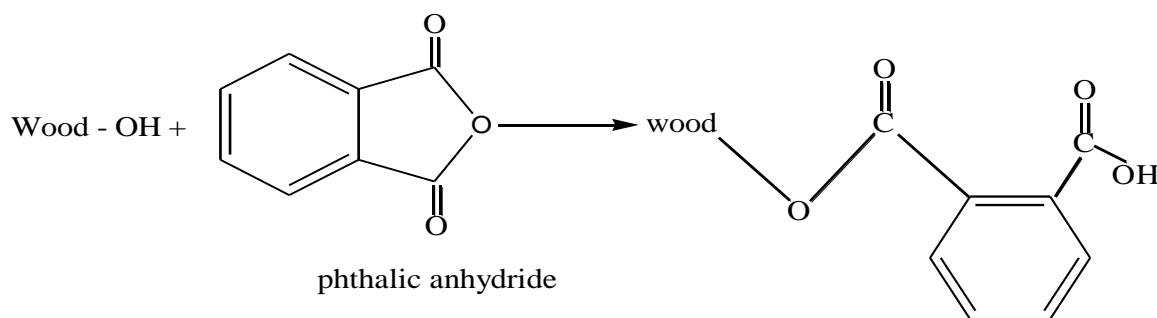


Figure (1): Reaction equation of ester group in phthalic acid anhydride with hydroxyle group of the wood.

Many studies have been conducted by researchers concerning the effect of acetylation on mechanical properties of acetylated wood, the results was varied from increasing mechanical properties or without any effects or minor decreasing of mechanical properties. Mohebbi and Hassani (2003) indicated that the process of hydroxyl group exchanging with acetylene group during acetylation will give a higher chance for mechanical properties improvement of acetylated woodboards. Birkinshaw and Hale (2002) found that wood acetylation did not affect strongly mechanical properties of soft wood (pine, larix and fir), mechanical properties have been tested for 4 meters long acetylated boards wood and the results was varied from increasing some mechanical properties to decreasing others. Dinwoodie (2000) explained that there were two main factors competed in affecting mechanical properties of the treated wood: the acetylation and temperature. Wood acetylation reduce and decrease equilibrium moisture content (EMC) of the wood associated with increasing of (MOE and MOR), while the hardness was decreased.

Baird (1969) noticed that when pine wood acetylated with acetic acid anhydride in the presence of Isocyanides butyl, the tension perpendicular to grain was decreased 10%. While Msden et. al. (1997) found that acetylated Scot pine wood gave small increase in tension perpendicular to grain. Bledzki et. al. (2008) found that when flax fiber treated with 250 ml toluene and 125 ml acetic acid anhydride at 60 °C for 1-3 hrs, the tension perpendicular to grain improved 25% when WPG was 18%.

The aim of this Study is to find the effect of phthaloylation process by using phthalic acid anhydride in some mechanical properties and choosing the best treatment which can give a suitable properties that increase wood utilization of many wood industrial manufacturing as well as increasing wood dimensional stability and decreasing the infection by fungi and insects.

Materials and Methods

Wood samples were taken from wood selling area (Sekala) at Mosul city, Iraq. *Platanus occidentalis* L. trees were felled at Shaqlawa provenance in Arbil governorate growing naturally at 966-970 meter over sea level. Five straight logs were chosen free from diseases, insects and wood defects, the logs had suitable diameter for wood sample manufacturing (table 1).

Table (1): Characteristics of trees used in the experiment.

5	4	3	2	1	(Log No.)
31.6	28.5	27.7	29.3	30.4	(DBH cm)
20	19	17	18	20	(Tree age)

Each log were divided to 4 sections and swan to 4 boards using tap saw (figure: 2) then the boards were air dried in a well ventilated room for two months at 17 °C with 28% relative humidity. The boards were sawn into 6x6x150 cm boards for each sapwood and heartwood free of defects, and left in the drying room for 15 days to get equilibrium moisture content with surrounding relative humidity.

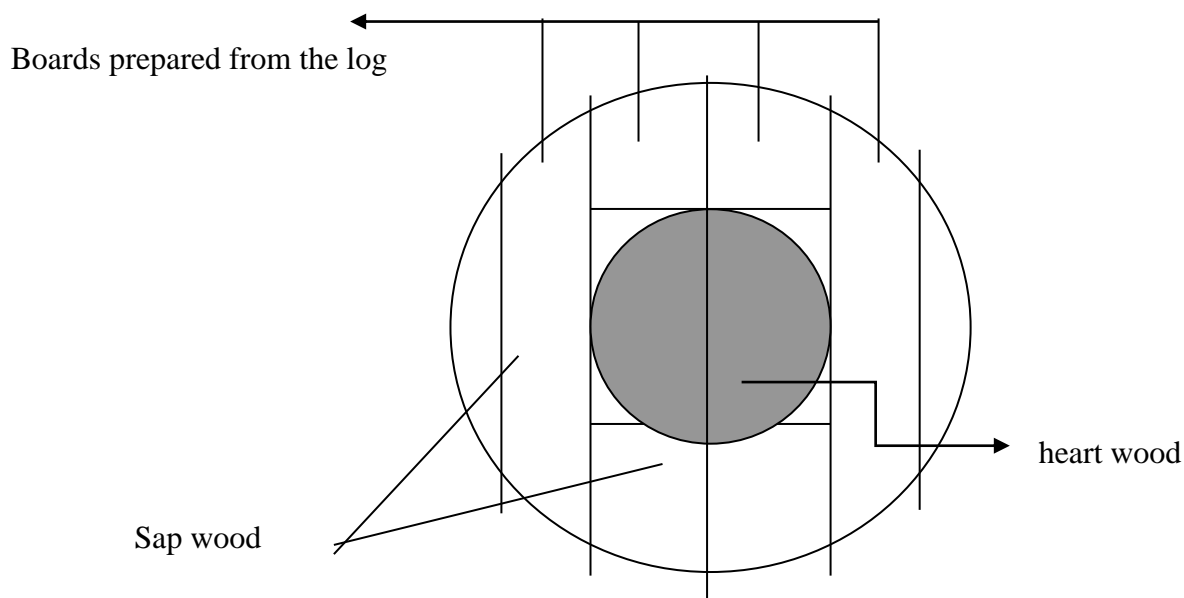


Figure (2): sketch showing the method of separation heart wood from sap wood and preparing the wood boards for sample test.

Extracting method and esterification process: after preparing samples test, half of them (sapwood and heartwood) were extracted from their extractives as mentioned by Fengel and Wagener, (1989).

Phthaloylation process was done by using phthalic acid anhydride after performing a primary test by dissolving (25, 50, 75 gm) of this material in one liter distilled water. After immersing the wood samples in the phthalic solution for 5 hrs, the best weight who gave the highest weight percent gain (WPG) was 75 gm. Four temperatures were used (25, 80, 100, 120) °C for 5 hours. Treated and untreated wooden samples were dried at 105 ± 2 °C for 24 hours, then they were conditioned in a the incubator at 22 °C and 50% relative humidity (RH) by using Calcium nitrate ($\text{Ca}(\text{NO}_3)_2 \cdot 4\text{H}_2\text{O}$), then size and weight were reported for all conditioned samples and the mechanical tests were performed.

Preparing and testing wood samples: wood samples for mechanical tests were prepared according to the national standards, samples of tension perpendicular to grain were selected for wood acetylation by phthalic acid anhydride because the samples have different surface shapes with less thickness which facilitate phthalic acid anhydride penetration into the wood. Dimensions of tension perpendicular to grain was 5x5x5 cm according to ASTM D-143-52, 78 standard (figure: 3).

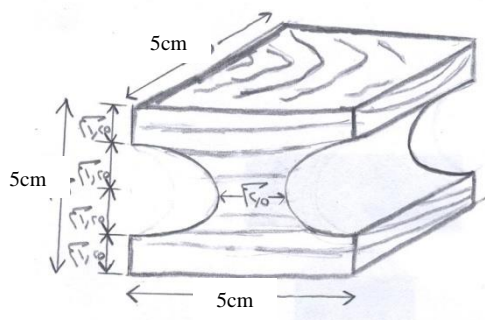


Figure (3): Dimension of test sample for tension perpendicular to grain.

Weight percent gain estimation (WPG): samples weight percent gain was estimated according to Ozmen, (2007).

Method of preparing and testing tension perpendicular to grain: The test was carried when tension area was at the radial face of the samples only, and tested according to ASTM D 143-52. (figure: 4).

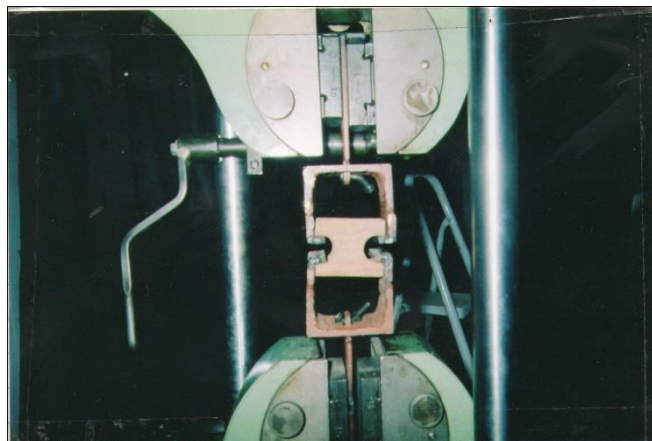


Figure (4): Amsler universal testing machine (20 ton) for testing tension perpendicular to grain test

After fixing the test sample to the machine, a tension load was applied at a constant speed of 2.5 ml/min. until rupture occurred at maximum load.

Method of preparing and testing static bending (MOE and MOR):

Wood samples dimensions for MOE and MOR test was 2x2x30 cm and tested according to (Kollman and Cote, 1968) (figure: 5).

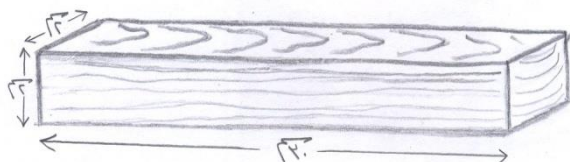


Figure (5): Dimensions of static bending test sample.

The static bending tests were performed at Mechanical lab of Engineering College at Mosul University.

Statistical analysis: Factorial Complete randomized design (CRD) was used to analyze the research data which composed of the following factors:

Wood type: two levels (sapwood and heartwood).

Extraction type: two levels (extracted and un extracted).

Treatment type: two levels (treated and un treated).

Temperatures: four levels (25, 80, 100, 120 °C).

Number of experimental units were $2 \times 2 \times 2 \times 4$ which gave 32 units, by adding 3 replications to each experimental units the total number of observation were 96. SAS statistical system (2001) were used to estimate ANOVA tables in addition to the significant differences between means using Duncan Method (Duncan, 1955) for all studied characters.

Results and Discussion

1- Modulus of Rupture (MOR): Duncan multiple range test (table 2) showed that MOR of treated sapwood (225.63 kg/cm^2) was better than heartwood (207.17 kg/cm^2), while untreated wood the table showed that sapwood was superior (304.09 kg/cm^2) than heartwood (215.04 kg/cm^2). The reason for the absence of significance between treated sapwood and heartwood may refer to the effect of esterification process in damaging some of wood cell wall by high temperatures and by the un hydride acid (Dinwoodie, 2000), knowing that there were no significant differences between SG values for acetylated sapwood and heartwood (table, 3) which may cause the un significance between them. The reason of MOR increased values for untreated sapwood compared to heartwood may refer to the increasing values of SG of untreated sapwood (0.515) compared to untreated heartwood (0.497) (table 3). Also Markwardt and Wilson, 1935 and Littleford, 1961 clarify that the reason for the mechanical properties variation of tree wood which may refer to the microfibril angles variation and direction and to secondary cell wall structure. Also, the interlocked grain of the fiber, especially for *Platanus* wood, may have an effect on wood variation strength.

MOR values of treated extracted wood was slightly better than treated un extracted wood but there were no significant differences between them, this may refer to the increased value of WPG of treated extracted compared to treated unextracted, also it may refer to the absence of significancy between SG values of treated extracted and unextracted wood samples (Table 3), and there were no significant differences between extracted and unextracted for untreated wood respectively for the same character mentioned above. However, MOR of untreated extracted wood was better than untreated and unextracted wood. This may related to the increasing value of SG of extracted untreated wood (0.513) compared to unextracted of untreated wood (0.499) (table 3). Similar results was obtained by Markwardt and Wilson (1935) which they found that there were no significant differences in mechanical properties of most tree type, and that this properties generally depend on growth conditions during wood formation.

Concerning temperatures effect on treated wood, table (2) shows that there were no significant differences in MOR of all studied temperature for treated and untreated wood.

For the general effect of treated and untreated wood on MOR, table (2) indicate that there were a reduction in MOR value of treated wood (216.40) compared to untreated wood (259.56 kg/cm²). These results were similar to the finding of Larsson and Simonson (1994). The increased general main value of SG for treated wood (0.518) compared to untreated wood (0.506) was low and not high enough to increase MOR of treated wood compared to untreated wood.

2- Modulus of elasticity (MOE): Duncan table (2) showed that treated sapwood was superior in increasing MOE compared to treated heartwood, this may refer to the higher WPG of sapwood compared to heartwood. The higher acetylation of sapwood compared to heartwood may increase MOE. Also, untreated sapwood was better in MOE than untreated heartwood, this may refer to the same reasons mentioned above in the effect of untreated wood type on MOR.

Also, the table indicate that extracted treated wood was superior in increasing MOE compared to unextracted treated wood. The reason may refer to the increase of WPG of extracted wood compared to unextracted wood, which increases esterification which may lead to increase MOE. Concerning untreated wood, the table showed that there were no significant differences of MOE between extracted and unextracted wood, knowing that MOE value of extracted untreated wood was higher than unextracted wood. These results may refer to the same reasons mentioned above for the effects of extracting type of untreated wood on MOR. Also, these results was similar to the finding of Markwardt and Wilson (1935).

Also, table (2) indicate that there were no significant differences in MOE of treated wood for temperatures (25, 80, 100, and 120 °C), and for untreated wood. The overall main effect of treated and untreated wood on MOE, shows that treated wood decreased slightly (55896 kg/cm²) compared to untreated wood (72724 kg/cm²) and the differences was not significant.

Table (2) effect of esterification by phthalic acid anhydride on MOR and MOE (kg/cm²)

Phthalic acid treatment type		WPG	Treatment levels	Treatments	characters
Untreated	Treated				
304.09 a	225.63 a	4.647 a	Sapwood	Wood type	MOR
215.04 b	207.17 a	3.581 b	Heartwood		
276.76 a	225.29 a	5.816 a	Extracted	Extraction type	
242.37 a	207.51 a	2.413 b	Unextracted		
252.32 a	52.212 a	0.152 c	25	Temperatures	
273.32 a	230.37 a	3.732 b	80		
244.87 a	197.92 a	8.859 a	100		
267.75 a	224.79 a	3.715 b	120		
259.56 a	216.40b	4.114	Mean		
a 5 11865	a71949	4.647 a	Sapwood	Wood type	
b 26793	b 39842	3.581 b	Heartwood		
a 86803	a 67754	5.816 a	Extracted	Extraction type	
a 58646	b4437	2.413 b	Unextracted		
a 74633	a44137	0.152 c	25	Temperatures	
a 76998	a 62440	3.732 b	80		
a 73819	a 49894	8.859 a	100		
a 65448	a 67111	3.715 b	120		
a 72724	a 55896	4.114	Main		

Different letters of each treatment mean that there were significant differences ($\alpha < 0.05$)

Table (3): effect of esterification process by phthalic acid anhydride in specific gravity.

Phthalic acid treatment type		Treatment Levels	Treatments
Untreated	Treated		
a 0.515	a 0.520	Sapwood	Wood type
b 0.497	a 0.516	Heartwood	
a 0.513	a 0.516	Extracted	Extraction Type
b 0.499	a 0.520	Unextracted	
a 0.503	b 0.503	25	Temperatures
a 0.505	a 0.529	80	
a 0.505	a 0.523	100	
a 0.511	a 0.517	120	
b 0.506	a 0.518	Main	

Different letters of each treatment mean that there were significant differences ($\alpha < 0.05$)

3- Tension perpendicular to grain: Duncan table (4) indicated that there were no significant differences between wood type of untreated sapwood, and heartwood and for untreated sapwood and heartwood in tension perpendicular to grain. Also, there were no significant differences between treated extracted wood and unextracted wood and between untreated extracted and unextracted wood for the same character mentioned above. These results were similar to the finding of Markwardt and Walson (1935).

Also, table (4) indicated that there were no significant differences in tension perpendicular to grain for treated wood between temperatures 25, 80, 100, and 120 °C, and for untreated wood for the same temperatures.

The general effects of treated and untreated wood on tension perpendicular to grain, table (4) showed that tension perpendicular to grain of treated wood reduced slightly (20.298 kg/cm²) compared to untreated wood (29.044 kg/cm²), these results agreed with Baird (1969) when he treated pine wood with acetic acid anhydride and found that tension perpendicular to grain was reduced 10%. This reduction may refer to the effect of acetylation process in deteriorating parts of wood cell wall by the presence of acetic acid anhydride (Dinwoodie, 2000).

Table (4) effect of wood acetylation by phthalic acid anhydride on tension perpendicular to grain (kg/cm²)

Phthalic acid treatment type		Treatment Levels	Treatments
Untreated	Treated		
a 33.286	a 16.983	Sapwood	Wood type
a 24.803	a 23.613	Heartwood	
a 24.905	a 23.817	Extracted	Extraction type
a 33.184	a 16.779	Unextracted	
a 26.962	a 23.017	25	Temperatures
a 26.928	a 18.733	80	
a 35.734	a 14.518	100	
a 26.554	a 24.922	120	
a 29.044	b 20.298	Main	

Different letters of each treatment mean that there were significant differences ($\alpha < 0.05$)

Conclusions: esterification process by phthalic acid anhydride can be used for increasing the preservation age of wood up to 10 years without any damage, and increasing painting period of acetylated wood up to 12 years ([Anonymous](#), 2010).

Also, treated unextracted *Platanus occidentalis* L. heartwood blocks are preferred for various wood manufacturing process. Untreated wood give MOR and MOE and tension perpendicular to grain slightly higher than treated wood. For both treated and untreated samples, sapwood is better than heartwood in static bending. Tension perpendicular to grain of treated heartwood is better than sapwood. Also, higher MOR and MOE and tension perpendicular to grain can be obtained from extracted wood, the highest MOE can be obtained at 120 °C. Generally, 100 °C is considered the best temperature for *Platanus occidentalis* L. wood esterification using phthalic acid anhydride to obtain better physical and mechanical properties.

References

- Almalah, A. R. and A. Y. Al-khero (2013). Effect Of Esterification By Phthalic Acid Anhydride On Some Physical Properties Of *Platanus occidentalis* L. Wood. Mesopotamia J. Agric. (online) vol. (41) No. (4) 2013. www.mesopotamia-j.com.
- Anonymous. (2010). www.accoya.info
- Antonios, P., P. Tountziarakis and Georgia Pougoula (2010). Fire resistance of two panel products made from chemically modified raw material.
- ASTMD-143-52, 78 (1979). Annual book of ASTM Standard, Wood; Adhesives. American Society for Testing and Materials, part 22. Philadelphia, PA.
- ASTM. D (1982). Standard methods of evaluating the properties of wood – base fiber and particle panel materials. ASTMD 1037-38, American standard for testing and materials, Philadelphia, PA.
- Baird, B. R. (1969). Dimensional stabilization of wood by vapor phase chemical treatments, wood and fiber 1:54-63.
- Birkinshaw, C. and HALE, M.D. 2002. Mechanical properties and fungal resistance of acetylated fast grown softwoods. I. Small specimens. Irish Forestry, 59(1-2), 49-58.
- Bledzki, A. A. Mamun, M. Lucka-Gaborl and V.S Gutowski (2008). The effects of acetylation on properties of flax fibre and its poly propylene composites 413-422. doi: 10.3144/express polymlett.
- Dinwoodie, J. M. (2000). Timber: its nature and behaviour. E. and F. N. spon, London, New York, 257P. This is the second edition of a very successful.
- Duncan, D. B. (1955). Multiple range multiple F-tests biometrics II: 1-42.
- Fengel, D. and G. Wegener, (1989). Wood Chemistry Ultrastructure Reactions. Walter de Gruyter & Co. Berlin. 613pp.
- Kollman, F. and W. Cote (1968). Principles of wood science and technology, part 1, Springer-Verlag, Berlin. Heidelberg. 592PP.
- Larsson P., R Simonson (1994). A study of strength, hardness and deformation of acetylated Scandinavian soft woods. Holz Roh werkst 52: 83-86.
- Little Ford, F. W. (1961). Variation of strength properties within trees and between trees in stand of rapid growth Douglasfir. (C.F. For Abs. Vol. 23(2): 305, 1962).
- Markwardt, L. O. and T. R. Wilson, (1935). Strength and related properties of woods grown in the United States U.S. Dept. of Agric. Washington, Tech. Bull. No. 479.
- Mohebbi and Hadji Hassani (2003). Moisture repellent effect of acetylation on poplar fibers.

*Proceedings of the 57th International Convention of Society of Wood Science and Technology
June 23-27, 2014 - Zvolen, SLOVAKIA*

- Msdén M J, Blake F S R, Fey N S. (1997). The effect of acetylation on the mechanical properties, hydrophobicity, and dimensional stability of pinus Sylvestris, wood Scitechnol 31: 97-104.
- Ozmen N. (2007) Dimensional stabilization of fast growing forest species by Acetylation. J. Applied Sc. 7:710-714.
- Pooper, R. and Bariskam (1972). "Acytelation of wood. Part1: the sorption behavior of water vapor" Holz Roh werkst off 30, 289-294.
- Risi, J. and D. F. Arseneau (1957). Dimensional stabilization of wood. I. acetylation, Forest Product Journal. 7: 210-213.
- SAS. (2001). SAS\ STAT\ Users Guide for personal Computers Release 6.12. SAS Institute Inc, Cary, NC, USA.

The Effects of Bark on Fuel Characteristics of some Evergreen Mediterranean Hardwood Species

Ioannis Barboutis^{1*} – *Charalampos Lykidis*²

¹ Associate professor, Department of Forestry and Natural Environment, Aristotle University of Thessaloniki, Thessaloniki, Greece.

* *Corresponding author*

[*jbarb@for.auth.gr*](mailto:jbarb@for.auth.gr)

² Researcher, Laboratory of Wood Anatomy and Technology, Institute of Mediterranean Forest Ecosystems and Forest Products Technology, Hellenic Agricultural Organization "Demeter", Athens, Greece.

[*lykidis@fria.gr*](mailto:lykidis@fria.gr)

Abstract

A significant proportion of Mediterranean forest vegetation consists of evergreen small diameter hardwood trees and shrubs which are traditionally used as fuelwood for domestic heating purposes. Nevertheless, their utilization in the form of pellets or briquettes could increase their energy efficiency. Due to differences in chemical structure, bark and wood present different fuel characteristics. In this study the higher heating value, lower heating value and ash content of wood and bark of five Mediterranean evergreen hardwoods (*Quercus coccifera*, *Quercus ilex*, *Arbutus unedo*, *Phillyrea latifolia* and *Erica arborea*) and two deciduous species (*Fagus sylvatica* and *Ostrya carpinifolia*) growing in northern Greece were investigated. For each species the stem diameter, bark thickness and wood : bark ratios were also determined. The results showed that the bark of all tested evergreen hardwood species presented significantly higher ash content than deciduous species did and can be used in pellet production only when carefully mixed with wood in order to keep ash content lower than 3%. *Quercus coccifera* bark showed the highest ash content values. All of the tested evergreen hardwoods showed heating values higher for wood than for bark, except for *Phyllirea latifolia* which showed significantly higher bark than wood heating value. The highest heating value of all investigated wood samples was presented by *Erica arborea*. Correlation of ash against higher and lower heating values for all species was found to be weak.

Keywords: Evergreen hardwoods, bark, wood, fuel, ash, heating value

Introduction

The constant quest for energy resources is one of the main characteristics of modern civilization. Nowadays, under the effects of global climate change, replacing fossil fuels with renewable energy sources is of key importance to meet the growing energy needs. The use of sustainable woody biomass for energy production might be an efficient way to fulfill the above requirements because there are many sources of such materials while at the same time, pelletizing of biomass

increases energy density, improves storability and reduces handling and transport costs (Telmo and Lousada 2011). Various alternative biomasses have been proposed or are already used as solid biofuels including sawdust, wood and other organic waste, agricultural waste, nonfood energy crops and forest biomass. (Haberl and Geissler 2000, Hoogwijk 2003, Perlack et al. 2005, Demirbas 2007, Filbakk et al. 2011.). The use of forest biomass originating from Mediterranean forest vegetation in particular has been acknowledged not only as a potential means to cover energy needs but also to prevent forest fires (Viana et al 2012). In Greece, many evergreen forests are short rotation (25-30 years) coppices and are exploited mainly with clear cuttings for the production of firewood and charcoal. Nevertheless, this widening of raw material base for biofuel utilization along with the opportunities it provides, also increases the need for detailed analysis and better understanding of the various proposed biomasses. This need is particularly important when it comes to forest biomass (logging residues, fire-prevention removals etc) which might contain various types of different plants and plant parts with different chemical composition and therefore differences in their thermal properties and handling efficiency. A representative example of this variability is the presence of bark, which has different chemical composition and generally higher ash content than pure wood does. It should also be noted that during traditional charcoal production bark is passively removed and therefore is wasted. On the other hand, in the case of pellet production bark could also be used.

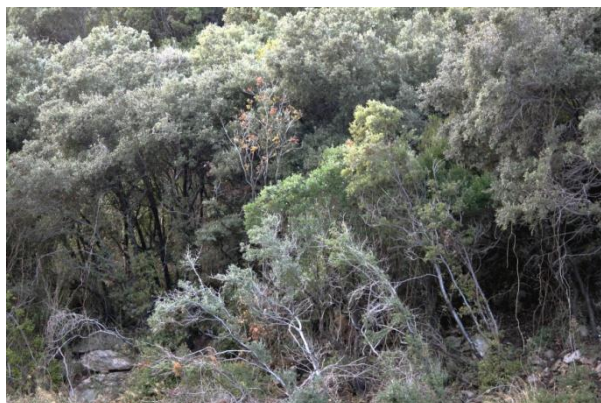


Fig. 1. Evergreen hardwoods forest



Fig. 2. Fuelwood from evergreen hardwoods for traditional production of charcoal

Concerning the effect of bark on the quality of biofuels Filbakk et al (2011) reported that the presence of bark in solid biofuels is related to increased tendency towards sintering during combustion and is therefore related to combustion problems. Concerning ash, Lehtikangas (2001) reported that increasing ash content results to lower heating value of the biofuel, implies the risk of sintering and negatively affects processing equipment. For this reason, in the recent related European norm for the quality characteristics of pellets the threshold ash content value is 3% (EN 14961-2:2011, European Pellet Council, 2013).

Taking into account the above facts, aim of this research was the assessment of calorific value and ash content for bark and wood of some Mediterranean hardwood species.

Materials and Methods

For the purposes of this work, wooden biomass from evergreen hardwood forest species was used namely: *Arbutus unedo*, *Quercus ilex*, *Quercus coccifera*, *Erica arborea* and *Phillyrea latifolia* samples consisting of stems having a mean diameter not larger than 10 cm was collected from the forests of East Chalkidiki, Greece. For comparison reasons material from *Fagus sylvatica* and *Ostrya carpinifolia* stems was also assessed because those species are present in the same forests and are also traditionally used as fuelwood. This bulk sample was reduced by a coning and quartering procedure to a representative sample of about 0.5 kg. The samples were subsequently air-dried and ground using a rotating-blade Wiley mill to pass a 0.7 mm sieve. All materials were gently dried for at least two weeks in a ventilated oven at $60\pm 1^\circ\text{C}$ until steady mass was achieved. The proportion of bark was calculated as the ratio of bark area in a transversal plane to the total stem area for the same plane. 30 measurements were carried out for each species.

For the determination of ash, the methodology described in EN 14775:2004 was used. The samples with mass of at least 1g were weighed to the nearest 0.1mg in pre-weighed porcelain crucibles and transferred in a cold muffle furnace (Heraeus MR 170) with a ventilation rate of about 5 changes per minute. The samples were then heated to 250°C within 50min and the temperature was kept constant for 60min. In the next step, the temperature was increased to 550°C within 60min and maintained in that level for 3h. Consequently the crucibles were transferred to an empty desiccator without lid for 5min followed by 15min with closed lid and then weighed. To ensure complete incineration the samples were reloaded in the hot furnace for 30min intervals and were reweighed until the mass changes were lower than 0.2mg. The ash content on dry basis was calculated using the following formula:

$$Ad = \frac{m_3 - m_1}{m_2 - m_1} \times 100$$

where:

m_1 : The mass (g) of the empty crucible

m_2 : The mass (g) of the crucible plus the dried test sample

m_3 : The mass (g) of the crucible plus ash

The ash measurements were carried out in 3 replicates for each tested material. The calorific value was expressed with Higher Heating Value (HHV) which is the absolute value of the specific energy combustion, in calories for unit mass of a solid biofuel burned in oxygen in a calorimetric bomb under specified conditions. HHV was determined in a Parr 1261 isoperibol bomb calorimeter according to the method described in the European Standard CEN/TS 14918:2005. Sample pellets with mass of $1.0\pm 0.1\text{g}$ and diameter of 13mm were produced using a hydraulic pellet press applying a load of about 7tn for about 1min. The pellets were weighed to the nearest 0,0001g in a stainless steel crucible and then placed in contact with 10cm of pre-weighed platinum ignition wire inside a Paar 1108 oxygen combustion bomb. The bomb was subsequently charged with oxygen (purity of 99.7%) at $30\pm 2\text{bar}$ and submerged in a stainless steel bucket containing 2000.0ml of distilled water. Prior to filling the bucket, the water was conditioned in a waterbath at $33\pm 0.5^\circ\text{C}$. The calorimeter jacket was maintained at constant temperature by circulating water at 35°C to maintain slightly higher temperature than the final temperature of the calorimeter and assure that evaporation losses were minimized. The HHV measurements were carried out in 6 replicates for each material. Prior to starting the above measurements, the calorimeter was calibrated and validated with 6 individual calibration runs

using benzoic acid pellets. HHV values were expressed in cal/g. Sulphur and chlorine adjustments were not carried out because they are present in low concentrations in wood fuels (Lehtikangas 2001).

Results and Discussion

The results of the determinations carried out in this research are presented in Tables 1-2 and Figures 3-5.

Table 1: Stem diameter, bark thickness and bark:wood bulk ratio for the tested species

Species	Stem diameter^a (cm)	Bark thickness^a (mm)	Bark (%)	Wood (%)
Quercus coccifera	6.2 (2.3)	1.7 (0.20)	10.7	89.3
Quercus ilex	7.5 (1.6)	1.5 (0.19)	7.8	92.2
Phillyrea latifolia	6.8 (1.3)	2.0 (0.28)	11.4	88.6
Arbutus unedo	6.4 (2.1)	1.3 (0.15)	7.9	92.1
Erica arborea	4.1 (0.9)	1.7 (0.22)	15.9	84.1
Fagus sylvatica	15.7 (3.2)	3.5 (0.34)	8.7	91.3
Ostrya carpinifolia	8.8 (1.9)	2.4 (0.41)	10.5	89.5

^a : Average of 30 measurements.
(S.D. in parentheses)

Table 2: Mean, standard deviation and coefficient of variation of ash and higher heating values of the samples

		Quercus coccifera		Quercus ilex		Phyllirea latifolia		Arbutus unedo		Erica arborea		Fagus sylvatica		Ostrya carpinifolia	
		wood	bark	wood	bark	wood	bark	wood	bark	wood	bark	wood	bark	wood	bark
Ash (%)	mean	1.62%	12.18%	1.14%	9.15%	0.67%	4.97%	0.83%	7.16%	0.39%	5.24%	0.50%	7.73%	0.44%	6.63%
	SD	0.06%	0.09%	0.03%	0.11%	0.05%	0.12%	0.06%	0.14%	0.04%	0.13%	0.07%	0.53%	0.09%	0.01%
	CV	3.53%	0.78%	2.25%	1.21%	7.96%	2.40%	6.99%	1.89%	9.55%	2.49%	14.43%	6.92%	20.69%	0.22%
	n	3	3	3	3	3	3	3	3	3	3	3	3	3	3
HHV (cal/g)	mean	4454.56	4228.35	4467.70	4121.77	4583.43	4956.91	4575.29	4334.84	4751.48	4764.42	4589.90	4442.59	4589.20	4382.1
	SD	18.31	10.25	10.81	15.22	7.77	30.77	14.53	2.93	14.96	21.64	9.62	1.90	12.30	3.92
	CV	0.41%	0.24%	0.24%	0.37%	0.17%	0.62%	0.32%	0.07%	0.31%	0.45%	0.21%	0.04%	0.27%	0.09%
	n	6	6	6	6	6	6	6	6	6	6	6	6	6	6

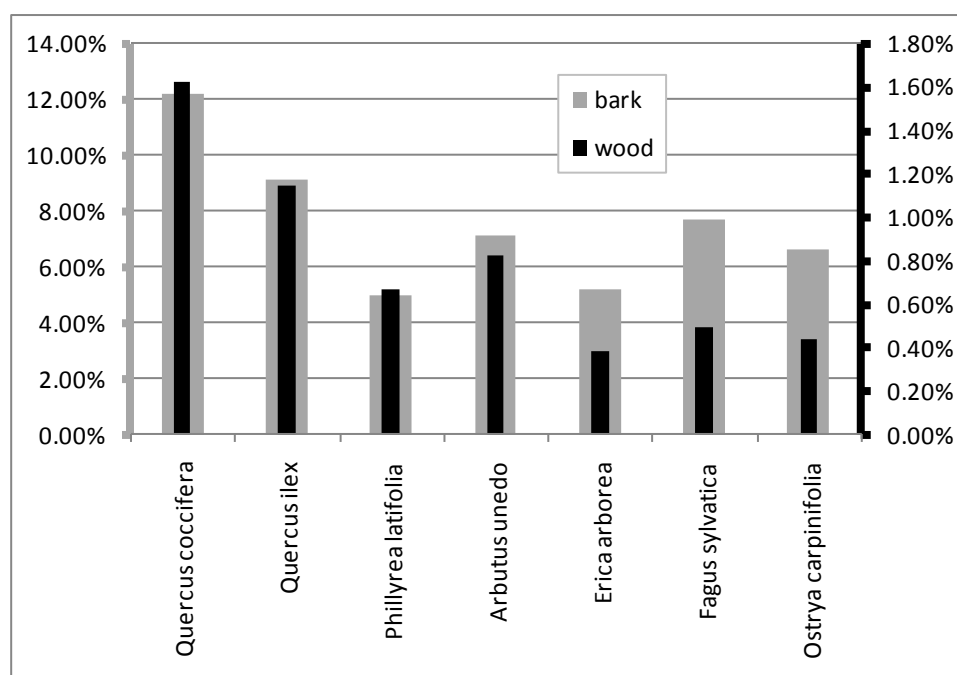


Fig. 3: Ash content of bark (left axis) and wood (right axis) for the tested samples

From Table 1 it can be drawn that the bulk bark content of the tested species varied between 7.8% for Quercus ilex and 15.9% for Erica arborea. As can be observed in Table 2 and Figure 3,

the ash content values among the tested materials varied between 0.39 - 12.18% while the HHV varied between 4121.77 - 4956.91 cal/g. The highest ash content among the tested species was presented both for bark (12.18%) and wood (1.62%) by *Quercus coccifera* while the lowest were presented by *Erica arborea* for wood (0.39%) and by *Phyllirea latifolia* for bark (4.97%). Among all tested species only *Erica arborea* showed lower wood ash content than *Fagus sylvatica* and *Ostrya carpinifolia*. In terms of bark ash content *Erica arborea* and *Phyllirea latifolia* showed lower values than *Fagus sylvatica* and *Ostrya carpinifolia*.

In terms of heating values, all tested materials met the requirements concerning the lower threshold values set by EN 14961-2 (ENplus-A1 class = 3940.96 cal/g, ENplus-A2 class = 3893.19 cal/g, EN-B class = 3821.53 cal/g). The highest HHV among the tested species was presented by *Erica arborea* for wood (4751.48 cal/g) and *Phyllirea latifolia* for bark (4956.91 cal/g). The lowest HHV was presented by *Quercus coccifera* for wood (4454.56 cal/g) and by *Quercus ilex* for bark (4121.77 cal/g). With the exception of *Phyllirea latifolia*, all tested species showed higher HHV for wood than for bark. For *Erica arborea* the HHV differences between bark and wood were not significant ($\alpha=0.05$). *Erica arborea* was the only one species among the ones tested in this work which showed heating value higher than than *Fagus sylvatica* and *Ostrya carpinifolia*. In terms of bark heating value *Erica arborea* and *Phyllirea latifolia* showed higher values than *Fagus sylvatica* and *Ostrya carpinifolia*.

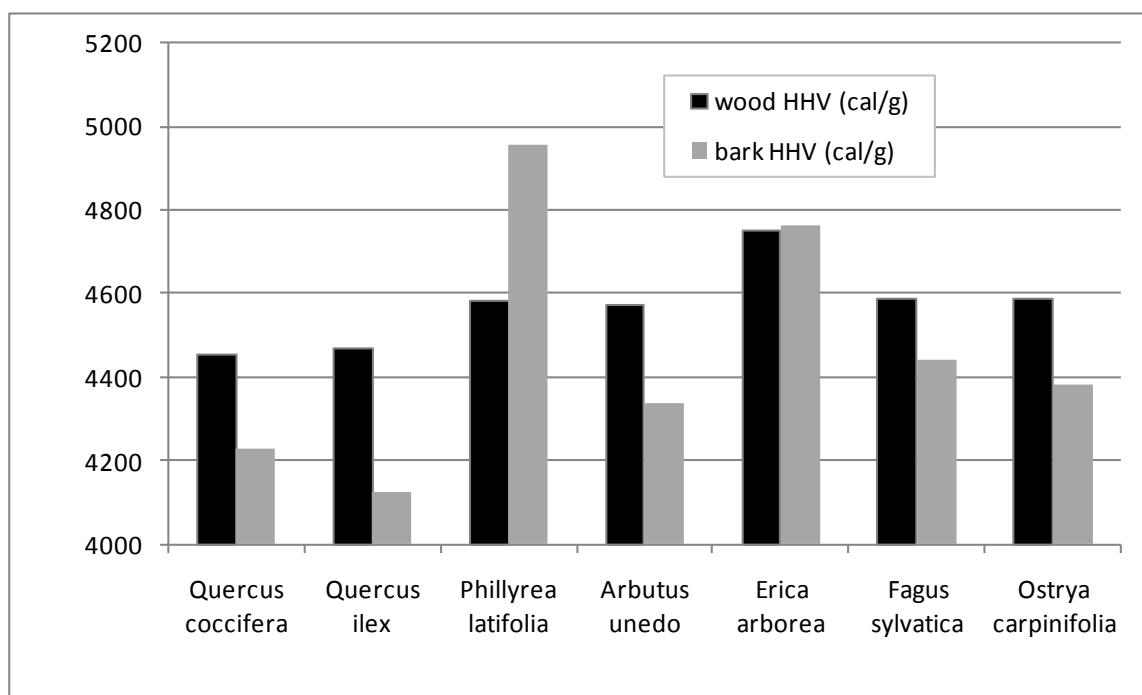


Fig. 4: Higher heating values of bark and wood for the tested samples

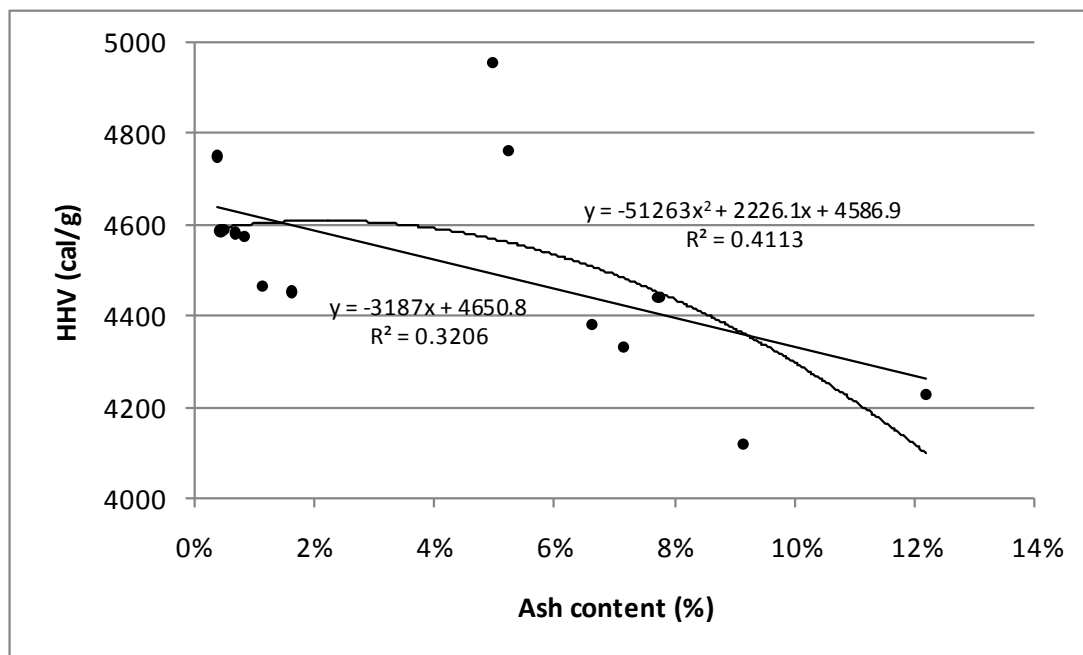


Fig. 5: Scatter graph of ash content against higher heating values and fit lines

Figure 5 represents a scatter graph of HHV against ash content values and 1st and 2nd degree polynomial fit lines. The Pearson correlation coefficient between HHV and ash content values was -0.57 indicating a moderate degree of linear dependence between the two variables for the tested materials. The correlation coefficient for both tested fit lines was low ($R^2 = 0.32$ for linear fit line and $R^2 = 0.41$ for 2nd degree curve) indicating a weak fit of the models to the data and leading to the conclusion that ash content cannot be used as a single means of estimating heating value and that other factors (e.g. other chemical components) should also be considered when constructing related models.

Conclusions

In general it can be concluded that, in terms of ash content and heating value, all wood samples could be used as raw materials for the production of pellets for non-industrial heating purposes since they meet the related threshold values for all three pellet quality classes. On the other hand, even though they all provided adequate heating values, none of the tested bark samples showed ash content values lower than 3% meaning that bark can only be carefully used in adequate mixtures with wood. According to the results Erica arborea, despite the lowest stem diameter and largest bark proportion among all tested species, presented the highest heating value for wood and second highest for bark.

References

- Demirbas A. Modernization of biomass energy conversion facilities. Energy Sources Part B 2007, 29:227-35.
EN 14961-2: 2011. Solid biofuels - Fuel specification and classes - Part 2: Wood pellets for non-industrial use

- European Pellet Council, 2013. Handbook for the certification of wood pellets for heating purposes. <http://www.enplus-pellets.eu> (Last accessed on 26/04/2014)
- Filbakk, T., Jirjis, R., Nurmi, J., Høibø, O. The effect of bark content on quality parameters of Scots pine (*Pinus sylvestris* L.) pellets (2011) *Biomass and Bioenergy*, 35 (8), pp. 3342-3349.
- Haberl H, Geissler S. Cascade utilization of biomass: strategies for a more efficient use of a scarce resource. *Ecol Eng* 2000;16:S111-21.
- Hoogwijk M, Faaij A, van den Broek R, Berndes G, Gielen D, Turkenburg W. Exploration of the ranges of the global potential of biomass for energy. *Biomass Bioenergy* 2003;25: 119-33.
- Lehtikangas P., (2001) Quality properties of pelletised sawdust, logging residues and bark, *Biomass and Bioenergy* 20, pp 351–360
- Perlack, R.D. et al. 2005. Biomass as Feedstock for a Bioenergy and Bioproducts Industry: The Technical Feasibility of a Billion-ton Annual Supply, DOE/GO-102005- 2135. Prepared by Oak Ridge National Laboratory for the U.S. Department of Energy and U.S. Department of Agriculture, Washington, DC.
- Telmo, C., Lousada, J. Heating values of wood pellets from different species (2011) *Biomass and Bioenergy*, 35 (7), pp. 2634-2639
- Viana, H., Vega-Nieva, D.J., Ortiz Torres, L., Lousada, J., Aranha, J. (2012). Fuel characterization and biomass combustion properties of selected native woody shrub species from central Portugal and NW Spain. *Fuel*, 102, pp. 737-745

Predicting the Compression Strength Parallel to Grain of Heat Treated Wood Using Artificial Neural Networks: A Preliminary Study

Bogdan Bedelean, Cristina Olarescu, Mihaela Campean

Abstract

The purpose of this study was to develop an artificial neural networks (ANN) model to be used to estimate the value of the parallel compression strength of heat treated compared to non-treated wood of the same species. The independent variables of the model were: species (spruce or black pine); density; treatment conditions (temperature within the range 180°C...200°C and duration within the range 1h...4h); wood origin (from mature trees or small-diameter trees). The dependent variable was the compression strength parallel to the grain. The dimensions of the samples were 20x20x60mm³. A dataset of 260 values was divided randomly in two subsets; one was needed for the training and testing phase (80%) and the other for the validation of the model (20%). The optimal structure of the ANN model was 4-7-1, respectively 4 neurons in the input layer, 7 neurons in the hidden layer and 1 neuron in the output layer. The selected network can be used to determine the parallel compression strength both for heat treated and non-treated spruce and black pine wood, with a mean absolute relative error (MRE) of 5.34%. The results showed that density is the most important variable that influences the parallel compression strength both for the heat treated and the non-treated wood. Further work is needed to increase the model accuracy and extend its applicability to other wood species, which are also suitable for heat treatment.

Key words: heat treated wood, spruce wood, black pine wood, compression strength, artificial neural networks

Bogdan Bedelean, Assistant
Transilvania University of Brasov,
Faculty of Wood Engineering,
Address: B-dul Eroilor nr. 29, 500036 Brasov, Romania
bedelean@unitbv.ro

Cristina Olarescu, PhD student
Transilvania University of Brasov,
Faculty of Wood Engineering,
Address: B-dul Eroilor nr. 29, 500036 Brasov, Romania
cristina.olarescu@yahoo.com

Mihaela Campean, Professor
Transilvania University of Brasov,
Faculty of Wood Engineering,
Address: B-dul Eroilor nr. 29, 500036 Brasov, Romania
campean@unitbv.ro

Life-Cycle Inventory Analysis of Cellulosic Fiberboard Production in North America

Richard D. Bergman^{1*}

¹ Research Forest Product Technologist, U.S. Forest Service Forest Products
Laboratory, Madison, Wisconsin, USA

* *Corresponding author*
rbergman@fs.fed.us

Abstract

Documenting the environmental performance of building products is becoming widespread because of many green-marketing claims made without scientific merit (i.e., green-washing). Developing environmental product declarations (EPDs) for building products is one way to accomplish this objective for scientific documentation and to counter green-washing. EPDs are based on life-cycle assessment (LCA) data and are similar to nutritional labels for food. To develop a business-to-business (B2B) EPD for uncoated cellulosic fiberboard, gate-to-gate life-cycle inventory (LCI) data must be developed to construct the cradle-to-gate LCA. This study used the internationally recognized LCI method to develop the needed gate-to-gate LCI data. Primary data were collected from seven cellulosic fiberboard plants that represented over 96% of cellulosic fiberboard production in North America. The primary data were then weight-averaged on a per-unit basis of one cubic meter of uncoated cellulosic fiberboard (254 oven-dry (OD) kg/m³) to calculate material flows and energy use. Cumulative allocated energy consumption associated with manufacturing 1.0 m³ of uncoated cellulosic fiberboard from 244 OD kg of various feedstocks was found to be 8.63 GJ/m³, with 6% of the primary energy provided by burning wood residues. Emission data produced through modeling the production process found that estimated biomass and fossil carbon dioxide emissions were 43.2 and 298 kg/m³, respectively. Our analysis estimated that 1.0 m³ of uncoated cellulosic fiberboard stores 477 kg CO₂-equivalents, assuming carbon content of wood to be 50%. The amount of carbon stored in cellulosic fiberboard exceeds the total carbon dioxide emissions during manufacturing by 30%. Therefore, cellulosic fiberboard's ability to store carbon when in use as a building product is a positive environmental attribute. From this study, the needed gate-to-gate LCI data can now be incorporated into the cradle-to-gate LCA to develop the B2B EPD.

Keywords: environmental product declaration, cellulosic fiberboard, LCA, life-cycle inventory, wood.

Introduction

Documenting the environmental performance of building products is becoming widespread because of many green-marketing claims made without scientific merit (i.e., green-washing). Developing environmental product declarations (EPDs) for building products is one way to accomplish this objective for scientific documentation and to counter green-washing (Bergman and Taylor 2011). Life-cycle inventory (LCI) data are the underlying data for subsequent

development of life-cycle assessments (LCAs) and EPDs. EPDs are similar to nutritional labels for food. At present, there are many EPDs for structural wood products made in North America.

LCI measures all raw material and energy inputs and outputs associated with the manufacture of a product on a per-unit basis within carefully defined system boundaries. These boundaries may be limited to only one stage within the product lifecycle (e.g., gate-to-gate). Multiple sequential LCI stages are usually included in an LCA. LCAs describe the total environmental impact for a particular product, referred to either as cradle-to-gate (raw material extraction to mill gate output) or as cradle-to-grave (raw material extraction to waste disposal) analysis.

Manufacturing cellulosic fiberboard uses a wet process that produces a low-density wood composition panel. Density for the final products ranges from 190 to 380 kg/m³ (Suchsland and Woodson 1986; USEPA 2002; Stark et al. 2010; ASTM International 2012). A thermo-mechanical process reduces the wood chip raw material and binds the fibers with a starch for recombination into cellulosic fiberboard. Other additives may include alum, clay, and wax. Asphalt may be added to improve strength properties. Furthermore, cellulosic fiberboard may be coated with asphalt for exterior uses. Final products include sheathing, sound-deadening board, roof fiberboards, and a wide variety of other products. Water is used to create a slurry (similar to the paper-making process) that produces the fiber mat. Large dryers are used to remove water; this process also releases volatile organic compounds into the atmosphere. Water usage is of particular concern because plants without any water conservation can use 100 tonnes of water per tonne (22,700 L/m³) of cellulosic fiberboard (Suchsland and Woodson 1986).

The goal of this paper is to document the gate-to-gate LCI of cellulosic fiberboard production for North America as part of a cradle-to-gate LCA. The paper documents material flow, energy type and use, emissions to air and water, solid waste production, and water impacts for the cellulosic fiberboard manufacturing process on a per unit volume basis of 1.0 cubic meter. Primary mill data were collected through a survey questionnaire mailed to cellulosic fiberboard plants. This survey tracked raw material inputs (including energy), product and by-product outputs, and pertinent emissions to water, air, and land for those unit processes. An industry-standard production unit (i.e., functional unit) was incorporated that can be translated to a metric production unit. Secondary data, such as pre-mill gate processes (e.g., wood and electricity production), were from peer-reviewed literature per CORRIM guidelines (CORRIM 2010). Material and energy balances were calculated from primary and secondary data. Using these material and energy data, the environmental impact was estimated by modeling emissions using the software package SimaPro 8 (Pré Consultants 2014), which follows internationally accepted standards and uses the U.S. LCI Database (NREL 2014).

A statistically significant sampling frame is required to attain valid results that can be generalized to the cellulosic fiberboard industry. CORRIM (2010) protocol targets a minimum of 20% to 50% of total production. Because there are only a few cellulosic fiberboard manufacturers, this study could realistically attain these levels by requesting participation and cooperation from the eight plants operated by North American Fiberboard Association (NAFA) members. Three of the eight North American mills are located in Canada and the other five in the United States.

Methods

Scope. This study covered the manufacturing stage of cellulosic fiberboard from forest landing to final product leaving the mill according to ISO 14040 and 14044 standards (ISO 2006a,b; ILCD 2010). LCI data from this study will help conduct a cradle-to-gate LCA for cellulosic fiberboard in preparation for developing an EPD, a Type III LCA-based eco-label (ISO 2006c). To construct a cradle-to-gate LCA, this manufacturing LCI will be linked to forest resources (upstream) LCI data from the U.S. LCI Database (NREL 2014). This manufacturing stage LCI provided a gate-to-gate analysis of cumulative energy of manufacturing and transportation of raw materials. Analyses included cellulosic fiberboard's contribution to cumulative energy consumption and emission data.

Seven of eight North American cellulosic fiberboard plants representing 96% of 2012 cellulosic fiberboard production provided primary data. In 2013, a site visit was conducted at one plant. The surveyed plants provided detailed annual production data on their facilities, including on-site energy consumption, electrical usage, log/chip volumes, and fiberboard production for 2012.

Functional unit. Defining system boundaries determined the unit processes to include and standardized material flows, energy use, and emission data. The present study selected a functional unit of 1.0 m³ of uncoated cellulosic fiberboard. Primary data and LCI flows were reported per 1.0 m³ of the final product, uncoated cellulosic fiberboard.

Unit processes. Ten main unit processes were identified in manufacturing cellulosic fiberboard. These included (1) resource transport, (2) storage yard, (3) feedstock preparation, (4) refining, (5) washing, (6) mixing, (7) wet forming, (8) board drying, (9) finishing, and (10) packaging, with energy generation considered an auxiliary process. All emissions (i.e., environmental outputs) and energy consumed were assigned to the cellulosic fiberboard and none to the co-products (i.e., molasses, culled boards, and fines) because these co-products were less than 4% of the total mass.

System boundary. Boundary selection helps track the material and energy flows crossing the boundary precisely. To track flows tied to cellulosic fiberboard production, two system boundaries were considered. One—the cumulative system boundary—is shown by the solid line in Figure 1 and includes both on- and off-site emissions for all material and energy consumed. Fuel resources used for the cradle-to-gate production of energy and electricity were included within the cumulative system boundary. The on-site system boundary (dotted line in Figure 1) covered emissions occurring only at the mill from the 10 unit processes involved. Off-site emissions include grid electricity production, transportation of feedstock and additives to the mill, and fuels produced off-site but consumed on-site. Ancillary material data such as motor oil, paint, and hydraulic fluid were collected and were part of the analysis.

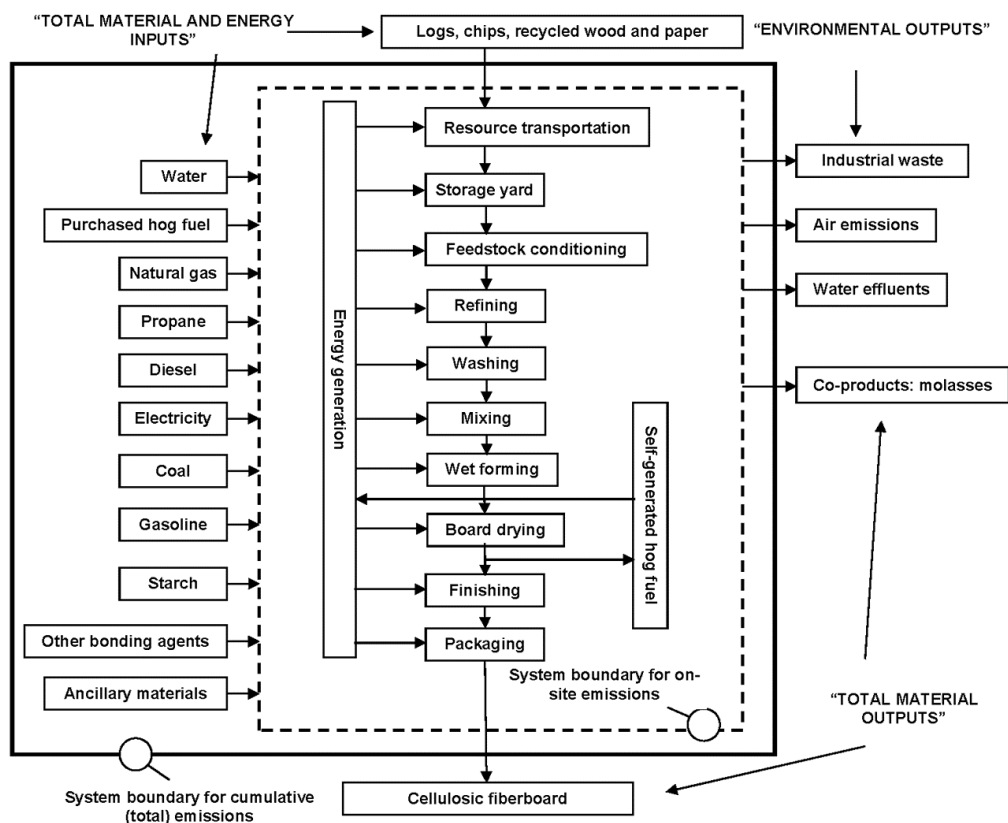


Figure 54 System boundaries for cellulosic fiberboard production

Results and Discussion

By surveying seven North American cellulosic fiberboard plants in 2012, detailed primary data on mass flow, energy consumption, and fuel types provided life-cycle information including air emission data. SimaPro 8 modeled weight-averaged survey data to estimate non-wood raw material use and emission data on a 1-m³ unit basis.

Material. To confirm the data quality, a mass balance was performed, and the results are summarized in Table 1. In performing the mass balance for cellulosic fiberboard, all unit processes located within the site system boundary were considered. Using a weight-averaged approach, 244 oven-dry (OD) kg of incoming feedstock and 21 OD kg of binding agents (additives) produced 1.0 m³ (254 OD kg) of cellulosic fiberboard along with some co-products (11 OD kg). Green chips made up the largest portion of feedstock at the facilities at 153 OD kg per m³ of cellulosic fiberboard made, with construction waste (31 OD kg) and dry shavings (30 OD kg) coming in distant second and third. Asphalt flakes made up the largest component of the additives at 10 OD kg/m³.

Table 15: Mass balance of cellulosic fiberboard manufacturing per m³

	Inputs (OD kg)	Mass (%)	CoV ^a (%)		Outputs (OD kg)	Mass (%)	CoV ^a (%)
Feedstocks				Products			
Logs	23	8.8%	-	Cellulosic fiberboard	254	96.1%	11.6%
Chips,	153	57.9%	134%	Co-Products			

green								
dry	Sawdust,	1	0.2%	-	Culled boards, wood fuel	1.1	0.4%	-
paper	Mixed	5	1.9%	153%	Molasses	5.8	2.2%	-
on waste	Constructi	31	11.8%	204%	Pins and fines	1.9	0.7%	-
pulper	Back to	1	0.3%	-	Other, not specified	1.5	0.6%	-
dry	Shavings,	30	11.3%	-	TOTAL, CO- PRODUCTS	11	3.9%	205%
TOTAL, FEEDSTOCK		244	92.1%	14.7%	TOTAL, OUT	265	100%	12.9%
	Additives							
	Starch	4.0	1.5%	148%				
flake	Asphalt	10	3.9%	97.7%				
	Alum	1.5	0.6%	122%				
	Wax	2.9	1.1%	94.1%				
black	Carbon	0.4	0.2%	216%				
	Clay	1.6	0.6%	204%				
aluminate	Sodium	0.15	0.1%	-				
	Other	0.02	0.0%	-				
TOTAL, ADDITIVES		21	7.9%	49.7%				
IN	TOTAL,	265	100.0%	13.7%				

^a Coefficient of variation

Carbon. Cellulosic fiberboard stores carbon. Carbon content for wood products is assumed to be 50% by mass of OD wood. Therefore, the carbon stored in the wood portion of 1.0 m³ (244 OD kg) of cellulosic fiberboard is equivalent to 447 kg CO₂¹² if left to decay.

Water. As mentioned previously, water impacts when producing cellulosic fiberboard have been a major concern because of the high volumes consumed. The cellulosic fiberboard industry has made substantial strides in reducing its water impacts. In this study, water was drawn from surface (1,230 L), ground (943 L), and municipality (353 L) sources for a total of 2,530 L/m³, with 63% of incoming water recycled. This has reduced water consumption by a factor of greater than 10 when not considering recycling and greater than 20 when considering recycling (Suchsland and Woodson 1986).

Raw material transportation. Feedstocks were transported a relatively short distance compared to the additives. The largest feedstock contributors, green chips, construction waste, and dry shaving, were transported 63, 29, and 33 km, respectively; starch and wax, which make up a far

¹² 244 OD kg wood * (0.5 kg carbon/1.0 OD kg wood) * (44 kg CO₂/kmole/12 kg carbon/kmole) = 477 kg CO₂

smaller portion of the uncoated cellulosic fiberboard, were transported 666 and 356 km, respectively.

Energy. Table 2 shows cumulative allocated energy consumption for a cubic meter of cellulosic fiberboard. Cumulative energy consumption for manufacturing cellulosic fiberboard was 8.63 GJ/m³, with wood fuel accounting for about 6%. Natural gas (59.5%), coal (22.8%), and uranium (6.4%) were the three highest energy resources consumed during product production. All but one facility uses natural gas for drying boards. In addition, natural gas provides the most power to the grid except for coal. Therefore, natural gas has the highest energy consumption for making uncoated cellulosic fiberboards. On-site energy consumption was estimated at 4.53 GJ/m³, with natural gas accounting for over 80% of the primary energy consumed.

Table 16: Cumulative energy (higher heating values (HHV)) consumed during production of cellulosic fiberboard—cumulative, allocated gate-to-gate LCI values^a

Fuel ^{b,c}	(kg/m ³)	(MJ/m ³)	(%)
Natural gas ^d	94.5	5,139	59.5
Coal ^d	75.2	1,968	22.8
Uranium ^d	0.00146	556	6.4
Wood residue	24	502	5.8
Crude oil ^d	9.00	410	4.7
Hydro	-	47	0.5
Wind	-	11	0.1
Energy, other	-	3	0.0
Total		8,630	100

^a Includes fuel used for electricity production and for log transportation.

^b Values are allocated and cumulative and based on HHV.

^c Energy values were found using their HHV in MJ/kg: 20.9 for wood oven-dry, 26.2 for coal, 54.4 for natural gas, 45.5 for crude oil, and 381,000 for uranium.

^d Materials as they exist in nature and have neither emissions nor energy consumption associated with them.

Wood products typically consume more energy during the manufacturing stage than any other stage (Puettmann and Wilson 2005; Winistorfer et al. 2005; Puettmann et al. 2010). For making oriented strandboard (OSB) in the southeastern (SE) United States, cumulative allocated energy consumption for 1.0 m³ of OSB is 11.0 GJ/m³, with 38% from wood fuel (Kline 2005). For making softwood plywood in the SE United States, cumulative allocated energy consumption for 1.0 m³ of plywood is 5.43 GJ/m³, with 38% from wood fuel (Wilson and Sakimoto 2005; Puettmann and Wilson 2005). The values listed in Kline (2005) and Wilson and Sakimoto (2005) use mass allocation. This study allocates all primary energy to cellulosic fiberboard and none to its residues. Primary energy is energy embodied in the original resources such as crude oil and coal before conversion. Energy consumption for cellulosic fiberboard falls between the cumulative allocated energy consumption of OSB and softwood plywood made in the SE United States.

Emissions. Table 3 lists allocated environmental outputs for manufacturing 1.0 m³ of cellulosic fiberboard for the cumulative and on-site system boundaries. The cumulative values included all

emissions and were higher than the on-site emissions. For the cumulative system boundary, biogenic CO₂ and fossil CO₂ were 43.2 and 298 kg/m³, respectively. Therefore, the amount of carbon stored in cellulosic fiberboard if allowed to decay is equivalent to about 130% of the total CO₂ emissions released during manufacturing. In addition, fossil CO₂ for the cumulative case was over two (298/133) times the fossil CO₂ emitted for the on-site case. For on-site, burning natural gas to dry boards was the main source of fossil CO₂. Major sources of air emissions were from board drying (on-site) and from the energy generation auxiliary process that includes grid electricity (off-site) and boiler operations (on-site).

Table 17: Environmental outputs for manufacturing one m³ of planed redwood decking

Substance	Cumulative (kg/m ³)	On-site (kg/m ³)
Water effluents		
BOD5 (Biological oxygen demand)	0.734	0.691
Chloride	8.78	3.77E-09
COD (Chemical oxygen demand)	0.274	0.203
DOC (Dissolved organic carbon)	1.11	1.11
Oils, unspecified	0.0200	0.0152
Suspended solids, unspecified	14.1	0.223
Industrial waste ^a		
Waste in inert landfill	5.63	5.63
Waste to recycling	8.83	8.83
Solid waste ^b	0.659	0.24
Air emissions		
Acetaldehyde	2.01E-02	2.01E-02
Acrolein	7.92E-03	7.92E-03
Benzene	3.33E-03	3.04E-03
CO	0.434	0.315
CO ₂ (biomass (biogenic))	43.2	42.1
CO ₂ (fossil)	298	133
CH ₄	0.932	7.00E-03
Formaldehyde	1.76E-02	1.75E-02
Mercury	1.36E-05	9.63E-06
Nitrous oxide	5.33E-02	4.87E-02
Non-methane VOC	1.51E-02	0
Particulate (PM10)	0.172	0.172
Particulate (unspecified)	0.777	0.193
Phenol	3.93E-03	3.93E-03
SO _x	2.62	0.591
VOC	.291	0.217

^a Includes solid materials not incorporated into the product or co-products but left the system boundary.

^b Solid waste was boiler ash from burning wood. Wood ash is typically used a soil amendment or landfilled.

Conclusions

EPDs present life-cycle data in a clear and transparent format to enable industry to counter green-washing. This study provides the underlying gate-to-gate LCI data for a cellulosic fiberboard EPD. Future efforts will work on incorporating the LCI data into a cradle-to-gate LCA and then eventually into a Business-to-Business EPD for uncoated cellulosic fiberboard.

Wood products such as cellulosic fiberboard used in building construction can store carbon for long periods. The amount of carbon stored in cellulosic fiberboard if allowed to decay is equivalent to about 130% the total carbon dioxide emissions released during manufacturing. Therefore, cellulosic fiberboard's ability to store carbon when in-use as a building product is a positive environmental attribute.

In the past, wet processes typically consumed huge volumes of water. However, water consumption in engineered wood products using a wet process such as that for cellulosic fiberboard manufacture has been substantially reduced over the past several decades. Therefore, industry water recycling efforts have been worthwhile in reducing water impacts, a critical environmental issue.

Acknowledgments

Primary funding for this project was through a cooperative agreement between the USDA Forest Service Forest Products Laboratory and the North American Fiberboard Association (13-CO-1111137-017). Additional funding was provided by FPInnovations. I especially thank Hongmei Gu (USDA Forest Service Forest Products Laboratory), Louis Wagner (North American Fiberboard Association), and Adam Taylor (University of Tennessee) for their peer review of this paper.

References

- ASTM International. 2012. Standard specification for cellulosic fiber insulating board. American Society for Testing and Materials. West Conshohocken, PA. 58-61.
- Bergman, R.D. and A. Taylor. 2011. Environmental product declarations of wood products—An application of life cycle information about forest products. *Forest Products Journal* 61(3):192-201.
- CORRIM. 2010. Research guidelines for life-cycle inventories. Consortium for Research on Renewable Industrial Materials (CORRIM), Inc., University of Washington, Seattle, WA. 40 pp.
- ILCD. 2010. International Reference Life Cycle Data System (ILCD) Handbook - General guide for Life Cycle Assessment—Detailed guidance. EUR 24708 EN. European Commission—Joint Research Centre—Institute for Environment and Sustainability. Luxembourg. Publications Office of the European Union. 417 pp.
- ISO. 2006a. Environmental management—life-cycle assessment—principles and framework.
- ISO 14040. International Organization for Standardization, Geneva, Switzerland. 20 pp.

*Proceedings of the 57th International Convention of Society of Wood Science and Technology
June 23-27, 2014 - Zvolen, SLOVAKIA*

- ISO. 2006b. Environmental management—life-cycle assessment—requirements and guidelines.
- ISO 14044. International Organization for Standardization, Geneva, Switzerland. 46 pp.
- ISO. 2006c. Environmental labels and declarations—Type III environmental declarations—Principles and procedures. ISO 14025. International Organization for Standardization, Geneva, Switzerland. 25 pp.
- Kline, E.D. 2005. Gate-to-gate life-cycle inventory of oriented strandboard production. *Wood and Fiber Science* 37 (Special Issue):74-84.
- NREL. 2014. Life-cycle inventory database project. National Renewable Energy Laboratory. <https://www.lcacommons.gov/nrel/search>. (accessed March 24, 2014).
- PRé Consultants. 2014. SimaPro 8 Life-Cycle assessment software package, Version 7. Plotter 12, 3821 BB Amersfoort, The Netherlands. <http://www.pre.nl/>. (accessed March 22, 2014).
- Puettmann, M.E. and J.B. Wilson. 2005. Life-cycle analysis of wood products: Cradle-to-gate LCI of residential wood building materials. *Wood and Fiber Science* 37 (Special Issue):18–29.
- Puettmann, M.E., R.D. Bergman, S. Hubbard, L. Johnson, B. Lippke, and F. Wagner. 2010. Cradle-to-gate life-cycle inventories of US wood products production—CORRIM Phase I and Phase II Products. *Wood and Fiber Science* 42 (CORRIM Special Issue):15–28.
- Stark, N.M., Z. Cai, and C. Carll. 2010. Wood-based composite materials: Panel products, glued-laminated timber, structural composite lumber, and wood–nonwood composite materials. In: *Wood handbook—wood as an engineering material*. General Technical Report FPL–GTR–113. Madison, WI: U.S. Department of Agriculture, Forest Service, Forest Products Laboratory. pp. 11-1–11-28.
- Suchland, O. and G.E. Woodson. 1986. Fiberboard manufacturing practices in the United States. *Agriculture Handbook* No. 640. Washington, DC: U.S. Department of Agriculture, Forest Service. 263 pp.
- USEPA. 2002. AP 42 Section 10.6.4 Hardboard and fiberboard manufacturing. United States Environmental Protection Agency. pp. 10.6.4-1-38. <http://www.epa.gov/ttn/chief/ap42/ch10/final/c10s0604.pdf> (accessed March 22, 2014)
- Wilson, J.B. and E.T. Sakimoto. 2005. Gate-to-gate life-cycle inventory of softwood plywood production. *Wood and Fiber Science* 37 (Special Issue):58-73.
- Winistorfer, P., Z. Chen, B. Lippke, J. and N. Stevens. 2005. Energy consumption and greenhouse gas emissions related to use, maintenance, and disposal of a residential structure. *Wood and Fiber Science* 37 (Special Issue):128-139.

Lathe Check Characteristics of Fast Growing Sengon Veneers and Their LVL Glue-Bond and Bending Strength

Wayan Darmawan^{(1)}, Dodi Nandika⁽¹⁾, Yusram Massijaya⁽¹⁾,
Abigael Kabe⁽²⁾, Irsan Alipraja⁽²⁾, Istie Rahayu⁽²⁾, Barbara Ozarska⁽³⁾*

⁽¹⁾Prof., Department of Forest Products, Faculty of Forestry,
Bogor Agricultural University (IPB), Bogor (16680), Indonesia.
Phone +62-251-8621285, Fax. +62-251-8621256
E-mail : wayandar@indo.net.id

* (Corresponding author)

⁽²⁾Research Assistant, Department of Forest Products, Faculty of Forestry,
Bogor Agricultural University (IPB), Bogor (16680), Indonesia.

⁽³⁾Professor, University of Melbourne, Australia

Abstract

Fast growing sengon (*Paraserianthes moluccana*) is largely rotary cut to produce veneer for core plywood production. In order to provide better information on veneer production and utilization, in this study the effects of wood juvenility and veneer thickness on veneer lathe checks of rotary-cut sengon veneers were evaluated. Before veneer manufacturing, sengon logs were boiled at 50 °C and 75 °C for 4 and 8 hours respectively. The boiled logs were peeled to produce veneer of 1 mm, 1.5 mm, 2 mm in thickness. Lathe checks of veneers were measured on the loosed side at every 5 mm veneer length under an optical video microscope and their frequency, depth, and length were characterized. Twenty sampling points of 5 mm veneer length were prepared from each segmented ring of 1 cm width from pith to bark. Isocyanate resin adhesive were used to produce laminated veneer lumber (LVL) of 20 mm thick, which consisted of 24-ply of 1 mm veneer thick, 14-ply of 1.5 mm veneer thick, and 11-ply of 2 mm veneer thick, for glue bond and bending strength test. Results showed that wood juvenility and veneer thickness determined the frequency, depth and length of lathe checks for the sengon rotary-cut veneers. In general, the frequency of lathe checks of the veneer increases with increasing veneer thickness, and also increases from pith to bark. Boiling of logs before rotary-cutting could decreases the frequency of lathe check of the veneer. The results indicated that boiling of logs at 50 °C for 8 h and at 75 °C at least 4 h before peeling the logs could minimize the frequency of lathe check in manufacturing rotary cut veneer thickness of 1 mm, 1.5 mm, and 2 mm from juvenile wood of fast growing sengon. The frequency of lathe check affect significantly glue bond strength of the sengon glue line, in which the glue bond strength decrease as the frequency of lathe checks increases.

Keyword : Lathe check, Rotary-Cut Veneer, Fast Growing Sengon, Boiling, Glue-bond, Bending strengt, Laminated veneer lumber

1. Introduction

Sengon (*Paraserianthes moluccana*) is a fast growing wood species widely planted by community in Indonesia. The sengon tress in the age of 7 years can reach breast height diameter up to 38 cm. Though all part of the tress in the age of 7 years are juvenile (**Darmawan et al., 2013**), however they have been felled in that age because demand of the sengon woods for wood industry is high, and are important incomes for the communities (**Krisnawati et al., 2011**). Sengon is the most common species used for packaging and pulp in Indonesia. Recently the wood is also used for laminated-wood products. Since the sengon wood is being used in the laminated wood industry, high bonding properties are expected. The bonding strength of the veneers depends upon a variety of factors. These factors are classified as veneers quality (moisture content, density, lathe checks, and surface roughness) and as adhesive quality (type of adhesive, mixture of adhesive, and its viscosity) and as bonding quality (glue spread, pressure time and temperature, relative humidity, and temperature of air) (**Dundar et al., 2008**). Among these factors, lathe check is one of the important factors on the bonding strength. The bonding strength decreases, probably because of the presence of important lathe checks. Also, the veneers with lathe checks require much more glue spread because of the degradation of veneer surface topography (**Daoui et al., 2011**). Veneers with lathe checks can also cause excessive resin use and may result in resin-bleed through the inside of veneer.

Veneer surface checks are formed when stress failures occur in the veneer. Failure will occur at the weakest part of the veneer which is generally over deep lathe checks, large pores, or other weakened areas on the veneer. Lathe checks are formed at the veneer's loose side as tension force of the lathe's knife pulls the veneer away from the peeler block and flattens the veneer from its natural curvature (**DeVallance et al., 2007**). There are many factors which contribute to the formation and severity of veneer lathe checks. It is usually very difficult to determine the exact cause of checking for any given incident. However, experience and research have taught us some of the most common and severe influences of veneer checking. Veneer lathe check can be affected by wood log's characteristic (specific gravity, wood pores, juvenile and mature wood). In addition, pretreatment and manufacturing conditions such as steaming or boiling, knife bevel and nose bar pressure, peeling temperature, peeling thickness and peeling speed, may also affect lathe checks.

The pretreatment and manufacturing factors affecting lathe check can be controlled to achieve better veneer surface. Log temperature at the time of peeling veneer significantly affects the quality of veneer. Low temperatures produce veneers with deeper and more spaced checks than high temperatures log (**Suh and Kim, 1988; Duplex et al., 2012**). Other studies indicated that higher peeling temperatures reduced the severity of lathe check depth (**Palka, 1974**). Most wood species are said to produce the best veneer quality when log temperatures are between 100 °F to 160 °F. The magnitude of compression applied to veneer surface was considered as important factor that affects peeled veneer quality. Pressure can be applied ahead of the knife by use of nose bar pressure. In eucalyptus veneer, the lathe check was found to decrease when the veneer was peeled with nose bar pressure up to 5% (ratio of lead gap opening to thickness). Between 0.5 to 5% pressures, deformation is within the elastic zone of the eucalyptus (**Acevedo et al., 2012**). Another study indicated that settings the nose bar pressure up to a certain point by adjusting the lead and exit gap lathe (5% to 20%) reduced lathe check depth in redwood veneer

(**Cumming and Collett, 1970**) and also showed a tendency to produce more frequent shallow lathe checks. Too little compression can result in deep lathe checks and rougher veneer surfaces, while too much compression can produce difficulties in veneer drying. Horizontal pressure ranging from 5% to 20% of the nominal veneer thickness can be typically applied for wood peeling operations. In many instances, higher horizontal pressures are needed for thicker veneers and lower pressure for thinner veneers, and in general, the thinner the veneer, the better the resulting peeled veneer quality. Rotary cutting speed (meter of veneer produced per minute) is another variable that affects veneer lathe check. An increase in cutting speed results in weaker veneer with deeper lathe checks (**Lutz, 1974**). An increase in speed causes reductions in nose bar pressure and can result in more severe lathe check formation.

Differences in log's wood properties have shown significant relationships to lathe check formation when peeled into veneer. In particular, tree growth rate, specific gravity, juvenility, and log conditioning have shown to affect veneer quality. A spindle-less rotary lathe allows manufacturers to peel smaller log's diameter and to produce more veneer sheet up to the log's core. When fast-grown logs were peeled, deeper lathe checking resulted. In general, it has been found that peeled quality is reduced as peeling from the log's sapwood to core material, due to factors such as lower specific gravity, highest growth rate, cutting speed, and highest angle of attack at the core material (**Palka and Holmes, 1973**). It has been noted that the best veneer was produced when peeling logs with growth rings orientated at 0° to the knife, while veneer quality decreased progressively as growth ring angle varied in either the plus or minus directions (**Cumming and Collett 1970**). Past research indicated that coarse grain, higher specific gravity veneer tends to check more significantly than does fine grain, lower specific gravity veneer. Lathe check depth was significantly less for fast growing trees (**Cumming et al. 1969**). Species of wood with fine pores check less than wood with large pores. This is because deep lathe checks and large pores create weak spots on the face veneer which provide less resistance to failure when the face veneer is under stress.

As the availability of slow growing trees from Indonesian tropical natural forest is diminishing, many plywood and LVL manufacturers are utilizing fast growing wood species and peeling veneer closer to the core. Peeling of fast growing sengon trees of smaller diameter logs continues to dominate the Indonesian veneer industry. As the smaller diameter logs are being peeled and much more juvenile woods are being utilized, severe lathe check veneer would *undoubtedly* be produced and manufactured. Therefore, it considerably needs to study lathe checks of veneer peeled from the sengon logs. The effect of lathe checks on glue-bond quality during LVL production should be also important by considering that the increasing of lathe check on the veneer would lead to lower glue-bond quality. Veneer with more frequent lathe checks may result in a higher incidence of delamination. To avoid delamination, the LVL may be typically produced by increasing the adhesive spread rate. Although increasing the adhesive spread rate is a common practice, however a question on how lathe checks affect the LVL glue-bond strength would exist. Investigation of lathe check characteristics of veneer from fast growing sengon and its LVL glue-bond and bending strength, gets less concern. Therefore it requires such study.

The objectives of this study were 1) to evaluate the effects of the juvenility, boiling temperature and veneer thickness on lathe checks of the rotary-cut sengon veneer (*Paraserianthes moluccana*); and 2) to determine the impact of veneer lathe checks on the LVL glue-bond and bending strength.

2. Material and Method

2.1 Sample tree origin

Sample trees were obtained from a plantation forest planted by community in 2007 at the West Java, Indonesia. The plantation site was located at Bogor region. Six sengon trees (*Paraserianthes moluccana*) were selected from the plantation site as representative specimens. The sample trees having straight stems and free external defects were chosen with the intent of minimizing tree-to-tree variation. The selected sample trees were 5 years old. The sample trees had a height of branch-free stem range from 6 to 8 m, and a diameter at breast height level (1.3 m above ground level) vary between 26 to 28 cm. After felling the trees, log sections (bolts) in length of 50 cm were taken from each tree from the bottom part up to the end of the free-branches tree stem. The sample logs were wrapped in plastic, kept cold, and maintained in the green condition before they were transported to the wood workshop for the rotary-cutting.

2.2 Logs preparation for rotary-cutting

Tree rings have been used for a long time in areas outside the tropics to characterize the presence of juvenile and mature wood. Considering distinct growth rings are absence in sengon tree, segmented ring was considered to be practically useful for characterizing their juvenility. A specified 1 cm width of segmented rings was made from pith to bark on the cross section of logs and numbered consecutively (No. 1-7) as shown in **Fig. 1a**. Veneer characteristics (veneer thickness, and veneer lathe checks) were measured at each segmented ring, and used to characterize the quality of sengon veneers.

Thirty bolts of minimum 26 cm in diameter were selected, thus the first six bolts were soaked in water at room temperature, and the other bolts were subjected to boiling process in hot water at 50 and 75 °C for 4 and 8 h, respectively. Subsequently, the bolts in each boiling treatment were peeled off to obtain veneers in the thickness of 1.0, 1.5, and 2.0 mm. For each boiling treatment, a sharp knife was used. The other factors such as knife angle, peeling angle, nose bar pressure, log temperature, peeling speed were kept constant in the study. The knife angle was 20°, and peeling angle was 21°. The veneers were peeled using a spindle less rotary lathe. The bolts were peeled up to core diameter of 6 to 8 cm in order to produce veneers from the 7 different segmented rings (**Fig. 1a**). The veneers were collected and grouped for each segmented rings and numbered consecutively from near the pith (number 1) to near the bark (number 7). Veneer in each segmented rings was measured for characterizing the density, shrinkage, lathe checks amplitude and frequency, thickness variations, and glue-bond.

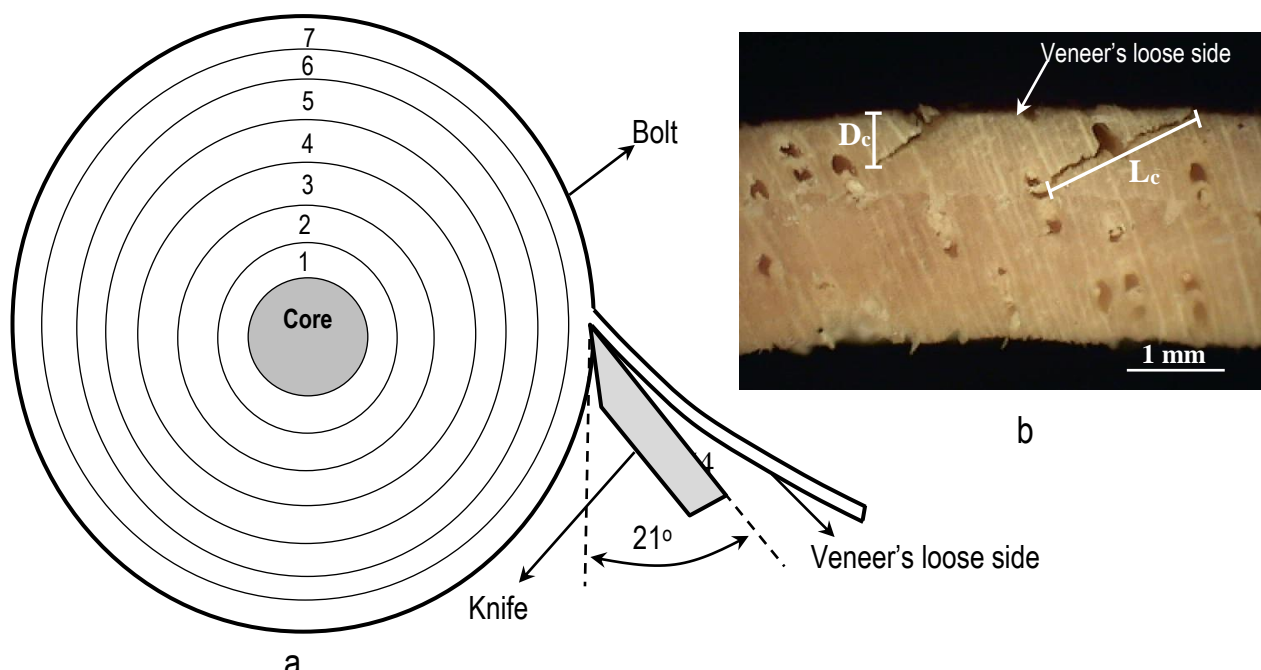


Fig. 1-Peeling diagram on the cross section of logs to produce veneers from segmented rings number 1 to 7 (a), and diagram for lathe checks measurement on veneer image (b)

2.3 Measurements

Veneer sheets produced from each segmented rings were collected and clipped to 30 cm x 50 cm veneer specimens. Ten specimens from each segmented rings were randomly selected and kept in plastic bags for test specimens. Two test specimens were used for the measurement of thickness variations. Six points of thickness measurement were marked on the side of each test specimens.

Lathe check frequency, depth, and length

The test specimens were kept in the green condition. Subsequently, an optical scanning system was used to evaluate lathe check characteristics of the veneers. In this study, an optical video microscope was used to capture images from the surface of veneer's loose side (**Fig. 1b**). Before capturing, veneer samples of 1.0, 1.5, and 2.0 mm in thickness were arched on their loose side over a pulley in diameter of 20, 35, and 50 mm respectively. Concerning the nature of veneer which is very fragile, then the success of measurement is strongly influenced by the choice of pulley diameter. Palubicki (2010) investigated that when diameter of the pulley is too small, the measurement process would lead to cracking and increased the depth of fissure thus the measure was not reliable. Otherwise, if diameter of pulley is too large, veneer cracks would not be opened so it was difficult to be detected by the camera. Palubicki (2010) recommended to apply pulley diameter between 10 to 70 mm for veneer thickness between 0.5 to 3.5 mm. The loose side of the arched veneers was set up on the table of optical video microscope under 30x magnification. Length of captured images on the loose side of the arched veneer was recorded to be 5 mm each. For each segmented rings, 20 images were captured and stored in a disk. The images then were analyzed using motic image software to count the lathe checks frequency, then measure their depth (D_c) and length (L_c) (**Fig. 1b**). The measurement technique was based on the opening of cracks occurring on the loose side of arched veneers. Frequency of lathe check was presented as the number of lathe check per 10 cm length of veneer.

Glue-Bond and bending strength Test

The veneer specimens were conditioned at relative humidity (RH) of 85% and temperature of 25 °C to an air-dry moisture content of 12%. Water based polymer Isocyanate resin adhesive was used for producing 20 mm thick of LVL panels. The isocyanate resin had a viscosity of 5000 - 15000 cps at 23°C, pH 6.5 – 8.5, solid material 40 - 44% and a density of 1.23 g/cm³. LVL panels with dimension of 20 mm x 30 mm x 500 mm were manufactured by 1 mm veneer thick (24-ply), 1.5 mm veneer thick (14-ply), and 2 mm veneer thick (11-ply) at each segmented rings. The spread volume of the isocyanate resin was 200 g/m² on single bonding surface of the veneers as recommended by the manufacture. The glue was uniformly spread on the surface of veneers by hand brushing. Assembled samples were pressed in a cold press at a pressure of 8 kg/m² for 5 hours. The resulting LVL panels were allowed to a stable condition for 72 h before cutting into test specimens.

Tests for the glue bond and bending strength properties were conducted on test specimens prepared from the LVL panels. Prior to the testing, the specimens were conditioned for 2 weeks at 25 °C and 85% relative humidity (RH) to air dry moisture content (around 12%). The air-dry glue bond and bending strength were tested. Five specimens were tested for each treatment combination. The glue bond and bending tests were carried out on an INSTRON universal testing machine. Perpendicular to the fiber and glue line (flatwise) modulus of rupture (MOR) and modulus of elasticity (MOE) tests were carried out according to JAS standard (JAS SE 11, 2003). Specimen size for the bending tests was 300 mm long by 20 mm wide by 20 mm thick of LVL. Glue-bond tests were also carried out according to JAS SE 11. The dimension of test samples was 50 mm length by 20 mm width by 20 mm thick. A loading rate of 10 mm/min was used in all tests according to the JAS SE 11. Loading on the glue bond test was continued until separation between the surfaces of the specimens occurred.

3. Results and Discussion

3.1 Characteristics of sengon tree

The breast height diameters for the sample sengon trees varied from 26 to 28 cm at the age of 5 years. The branches-free height of the sample sengon trees was between 6 to 8 m. Differences in diameter and in braches-free height among tress in this study reflect the sengon wood's sensitivity to environmental conditions. Sengon tree has been growing very fast and can flourish in tropical forests with an altitude of 0 to 1000 m above sea level. The breast height diameters indicate that the mean diameter growth for the sengon tree species would be about 5 to 6 cm/year. Investigation results for the sengon trees on the forest stand indicated that sengon tree stem has unique characteristics that are straight-trunked cylindrical and long braches-free height, which are very well used to manufacture veneers for plywood or LVL. In addition, density of sengon wood was reported to be 250 kg/m³ close to the pith, and to be 450 kg/m³ near the bark (Darmawan et al., 2013). This low density would bring a benefit in peeling the sengon trees for veneer production.

3.2 Characteristics of sengon veneer

Variation of veneer thickness

Uniformity of veneer thickness is a very important factor affecting the quality of glue bond strength in LVL or plywood. The result in **Fig. 2** shows that thickness variations of rotary-cut sengon veneers were slightly occurred. The thickness of sengon veneer peeled from some bolts, which was intended to be 1.0 mm, ranged from a minimum of 0.93 mm to a maximum of 1.08 mm, and the veneer thickness intended to be 2.0 mm ranged from a minimum of 1.95 mm to a maximum of 2.11 mm. Coefficient of variations of the veneer thickness from pith to bark calculated from the ranges was 5.3%, 5.8%, 5.9% for the intended veneer thickness of 1.0, 1.5, and 2.0 mm respectively. By considering the coefficient of variations less than 6%, the bolts of sengon were correctly peeled to maintain the thickness regularity.

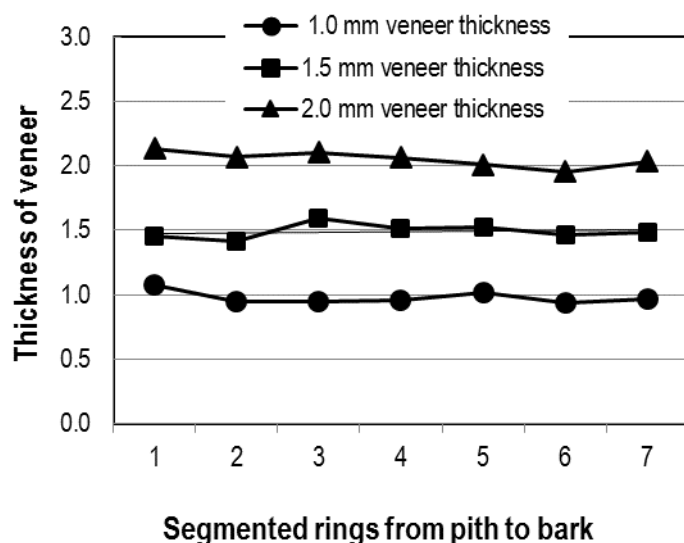


Fig. 2 - Variation of veneer thickness from pith to bark

Lathe check frequency, depth, and length

Basically, checking of veneer surface is caused by loss of moisture in the veneer surface resulting in shrinkage. As the dimensions of the veneer change, stresses are set up between the surface and the inside of veneers. When forces reach the point where they exceed the structural strength of the veneer, a rupture of the fiber takes place. This, in effect, appears as a “check” or “split” on the surface. These checks naturally follow the weak zones such as lathe checks, pores or splices in the veneer. In rotary-cut veneer manufacturing, when peeling starts, the wood tends to split along the grain. Lathe checks are formed at the veneer's loose side as tension force of the lathe's knife pulls the veneer away from the peeler block and flattens the veneer from its natural curvature. With respect to the cross section of the veneer, this advance splitting causes the formation of vertical cracks (known as lathe checks). The risk of this checking can be reduced by using a nosebar (Kollmann et al. 1975). However, recent spindle less rotary lathes, which are widely used to peel small log diameter of fast growing wood species, have not been completed with an adjustable nosebar. A boiling treatment of bolts would be considered to reduce the lathe check.

Fig. 3 shows average values of frequency of lathe check per 10 cm of veneer length taken from the loose side of the veneer. The average frequency of lathe check tended to decrease from pith to bark of the veneers. The veneers near to the piths showed larger frequency of lathe check. Large microfibril angle of wood fiber near the pith could be responsible for high frequency of lathe check of the veneers taken from the inner parts of the segment logs. Veneer with straight grain (radial face) has been shown to check less than veneer with a cathedral grain (tangential face). This is because shrinkage in wood is much greater tangentially than radially. Greater shrinkage creates greater stresses and thus, a higher chance of wood failure in the surface of veneer. Tanritanir et al. (2006) investigated the effect of steaming time on surface roughness of beech

veneer and they also found that the roughness of veneer sheets taken from heartwood (near pith) had higher values than those of sapwood (near bark).

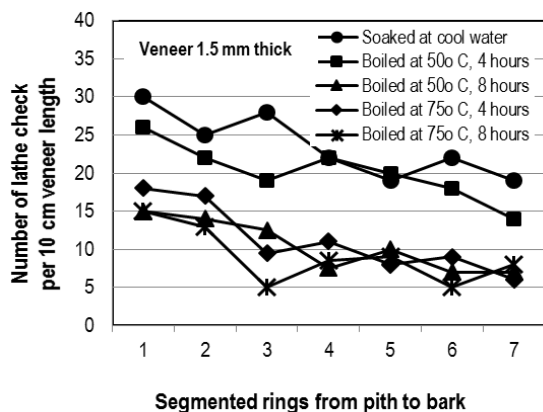


Fig. 3 - Variation of lathe check frequency from pith to bark for the 1.5 mm veneer thickness

The results in **Fig. 3** reveal that veneers with lower frequency of lathe checks were produced by bolts boiled for 4h and 8h at temperature of 75 °C, and for 8h at temperature of 50 °C, when compare to unboiled bolts. However, the bolts boiled for 4h at 50 °C produced the same frequency of lathe checks as the unboiled bolts. This result gives an indication that boiling at a higher temperature resulted in better surface properties of the veneers. It could be announced that sengon bolts boiled for 8h at 50 °C or 4h at 75 °C could be proposed before manufacturing veneers from the sengon wood. The boiling of sengon bolts at the temperatures and periods is considered to make the sengon veneers less plastic during the peeling so that sengon veneers with enhanced surface quality can be produced with less frequency of lathe check.

Fig. 4 shows the values of lathe check from pith to bark for different veneer thickness. Lathe check frequency of the veneers decreased from pith to bark. The lathe check frequency of veneers near the pith was twice larger than near the bark. The results in **Fig. 4** indicated that the lathe check frequency tended to increase as the veneer thickness increased. Increases in the veneer thickness decreased its elasticity, and resulted in much more cutting splits along the grain during the peeling. With respect to the cross section of the veneer, these greater splits caused the formation of more severe lathe checks. In addition, because the sengon has a high (27%) lignin content (Martawijaya et al. 2005), the elasticity of thick sengon veneers decreased.

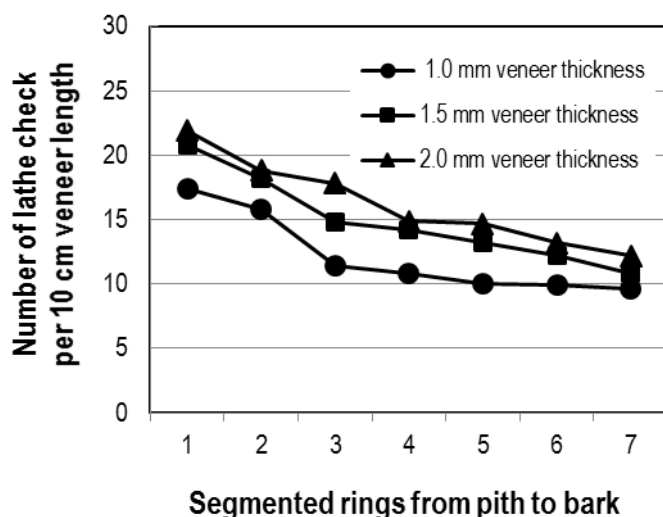


Fig. 4 - The effect of veneer thickness on the frequency of lathe checks

The second variable that is important in determining the veneer quality is deep lathe checks or shallow lathe checks. This study found that though the frequency of lathe checks decrease from pith to bark (**Fig. 4**), however the depths of lathe check in percent of veneer thickness are not significantly change from pith to bark (**Fig. 5b**), and did not differ prominently among the veneer thick. This result indicates that the thicker the veneer peeled, the deeper the lathe check will be (**Fig. 5a**). The average lathe check depths for the intended veneer thickness of 1.0 mm, 1.5 mm, and 2.0 mm were 0.28 mm, 0.41 mm, and 0.57 mm respectively.

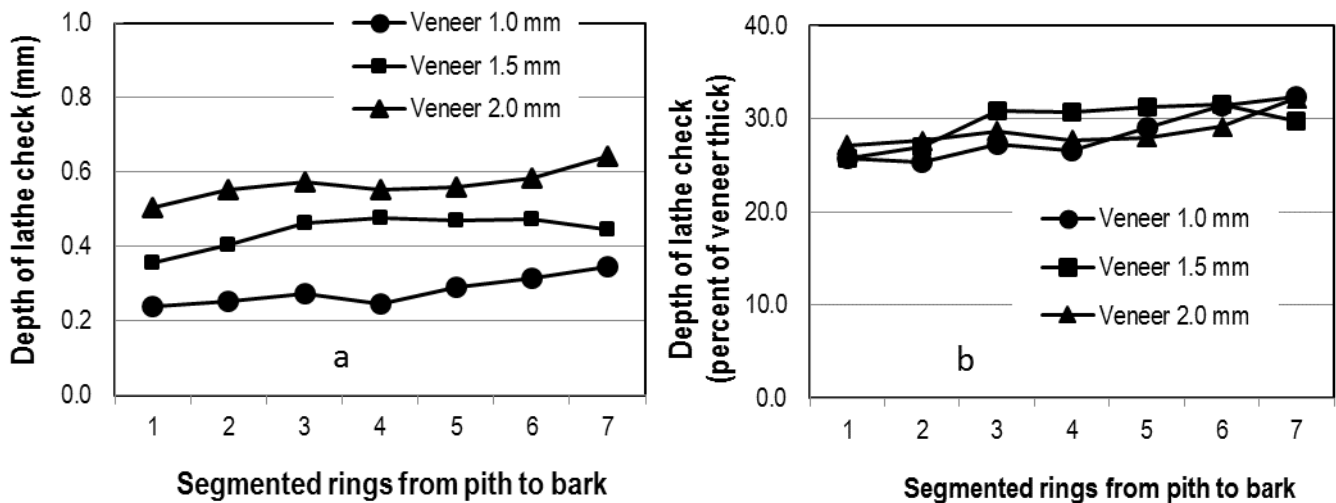


Fig. 5 - The progress of depth of lathe check from pith to bark

The other lathe check measured in determining veneer quality was length of lathe check. The lengths of lathe checks tended to slightly fluctuate from the pith to the bark. The length of lathe check follows the behavior of the depth of lathe check. The result in **Fig. 6** indicates that the thicker the veneer peeled, the longer the lathe check will be, however their depth and length ratio is almost the same. The average lathe check length for the intended veneer thickness of 1.0 mm, 1.5 mm, and 2.0 mm was 0.44 mm, 0.63 mm, and 0.88 mm respectively. The ratios between depth and length of the lathe check were 0.64, 0.65, and 0.65 for the veneer thickness of 1.0, 1.5, and 2.0 mm respectively. Therefore, these results suggest that obtaining higher glue bond strength will need to reduce the lathe check frequency rather than the depth and the length of lathe checks.

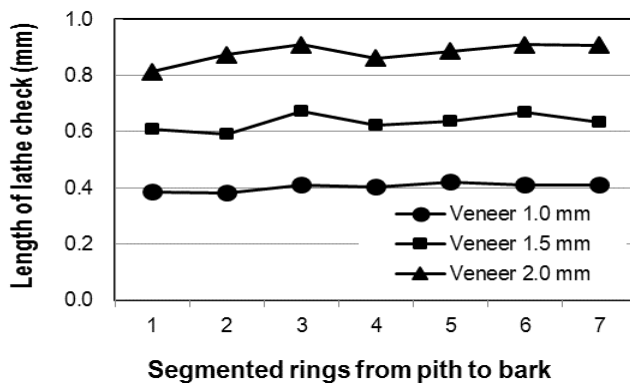


Fig. 6 - The progress of length of lathe check from pith to bark

3.3 Glue bond and bending strength

The bond strengths of veneer glue-line on the LVL increased from pith to bark (Fig. 7) for all veneer thickness. The results suggest that increasing proportion of veneer near the pith would decrease the glue-line's capacity to withstand concentrated shear stresses, thus resulting in higher amounts of glue-line failure and a reduction in percent wood failure. However, as the proportion of veneer near bark at the tight-side glue-line increased, percent glue-line failure decreased. This was attributed to an interaction between the juvenility (Fig. 7) and the frequency of lathe check (Fig. 8). The glue bond strength had a statistically significant, high, negative correlation to lathe check frequency, and its correlation coefficients according to the lines in Fig. 8 are summarized in Table 1. The results show that the regression coefficients for the glue bond strength linear equations depicted by the veneer thickness varied from -0.814 to -1.124. These variations indicate that the veneer thickness could also determine the glue bond strength of the sengon veneers. It appears that the glue bond strength would decrease as the veneer thickness increase, as comparing them for the same frequency of lathe check (Table 1).

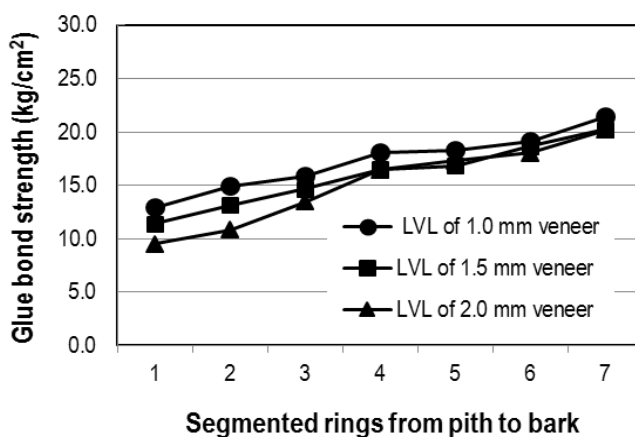


Fig. 7 - Development of glue bond strength from pith to bark for different veneer thickness

Lathe check frequency was the first variable analyzed to explain the glue bond strength. As lathe check frequency of veneers in between the glue line increased, the amount of "bridging" wood material between each lathe check decreases. This decrease would reduce contact between the

layers resulting in a weak glue line and low glue bond strength of the LVL. The results are in agreement with Kaneda et al. (1968), who reported that a high frequency of lathe checks results in lower strength.

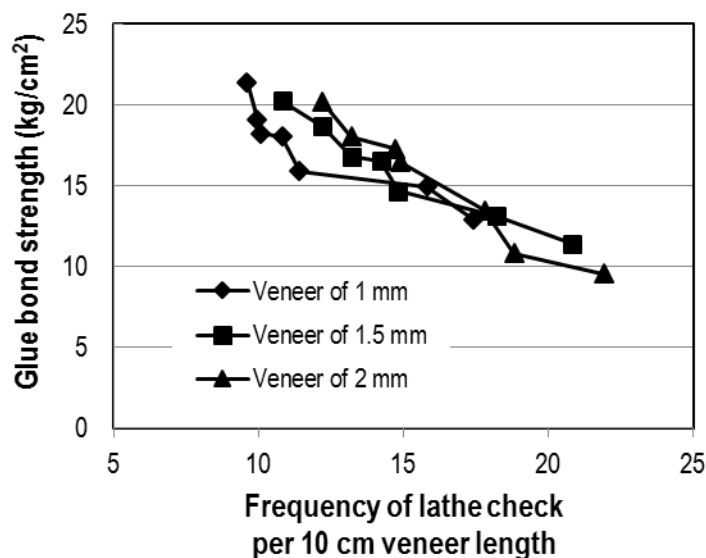


Fig. 8 - Relation between glue bond strength and frequency of lathe check

Table 1 - Linear regression equations and correlation coefficients according to Fig. 8

Veneer thickness	Linear equation	r
1.0 mm	$y = -0,814x + 27,10$	0.90
1.5 mm	$y = -0,857x + 28,68$	0.97
2.0 mm	$y = -1,124x + 33,33$	0.98

y = glue bond strength, x = frequency of lathe check, r = correlation coefficient

The behaviors of MOE and MOR from pith to bark for sengon solid wood was published (Darmawan et al. 2013). It was noted in the article that juvenile woods of sengon near pith have a significantly lower MOE and MOR than the juvenile wood near the bark. The lower MOE and MOR of juvenile wood near pith are due to larger microfibril angle, and lower density. Mean MOE and MOR values from pith to bark for sengon wood reported in the study were 43651 kg/cm² and 302 kg/cm², respectively. Martawijaya et al. (2005) also found out that the MOE and MOR of sengon were 44500 kg/cm² and 316 kg/cm², respectively. It was found in this study that MOE and MOR values of sengon LVLs are slightly lower compared to those of sengon solid woods. The average MOE for the sengon LVL made of 1 mm veneer thick (24-ply), 1.5 mm veneer thick (14-ply), and 2 mm veneer thick (11-ply) was 42953, 40172, and 38907 kg/cm², respectively, and their average MOR was 269, 233, 216 kg/cm², respectively.

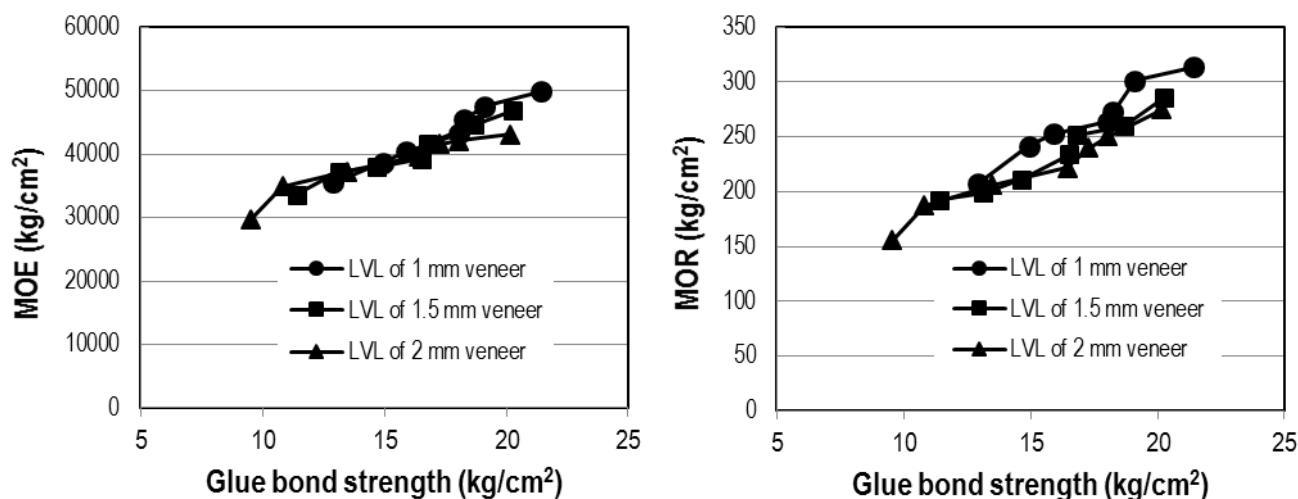


Fig. 9 - Relation between glue bond strength with MOE and MOR

The results in **Fig. 9** show that both MOE and MOR increased with an increase in glue bond strength. Though MOE are almost the same among the veneer thickness, however MOR among veneer thickness is slightly different. As shown in **Fig. 9** the 22-ply LVL had higher MOR compared to those of 14 and 11-ply. This is mainly due to the higher glue bond strength produced in the glue-lines between the plies of the 22-ply which consisted of veneers of less lathe check frequency. The thinner the veneer the higher amounts of glue were needed in the manufacturing process resulting in better compaction of the wood during the pressing. This strongly suggest that by using thinner veneers (higher number of ply), the LVL will exhibit higher strength compare to those thicker veneers in production of LVL. This finding confirms with results published by Kilic et al., 2006. It was reported in his article that the bending properties of LVL produced with thinner veneers were higher compared to those from thicker veneers.

4. Conclusion

In conclusion, we have found that the frequency of lathe check decreased from pith to bark. The increases in boiling temperature significantly decreased the lathe check frequency of the veneers peeled from the pith to the bark. When the logs boiled in water for 8 h at 50 oC, and 4 – 8 h at 75 oC, the veneers obtained from the pith to the bark of the logs showed significantly less lathe check than those boiled for 4 h at 50 oC. The thicker veneer peeled from the logs tend to produce larger frequency of lathe check compared to thinner veneer. The thin veneer provides better glue bond strength compared to thicker veneers, and the glue bond determines the value of MOE and MOR. Using thinner veneers in LVL manufacture improved the strength of the resulting panel.

Acknowledgments

The authors thank the Directorate for Research and Community Service of the Ministry of National Education for the Republic of Indonesia for the research grant and RISTEK for the research mobility to France

References

- [Acevedo, A., Bustos, C., Lasserre, J.P., Gacitua, W., 2012.](#) Nose bar pressure effect in the lathe check morphology to *Eucalyptus nitens* veneers. *Maderas, Cienc. Tecnol.* 14 (3), 289-301.
- Cumming, J.D., Fischer, C., Dickinson, F.E., 1969. Rotary veneer cutting characteristics of young-growth redwood. *Forest Prod. J.* 19 (11), 26-30
- Cumming, J.D., Collett, B.M., 1970. Determining lathe settings for optimum veneer quality. *Forest Prod. J.* 20 (11), 20-27.
- Darmawan, W., Nandika, D., Rahayu, I., Fournier, M., Marchal, R., 2013. Determination of juvenile and mature transition ring for fast growing sengon and jabon wood. *J Indian Acad Wood Sci.* 10 (1), 39-47
- DeVallance, D.B. 2003. Influence of veneer roughness, lathe check, and annual ring characteristics on glue-bond performance of Douglas-fir plywood. M.S. thesis, Oregon State Univ., Corvallis, OR
- DeVallance, D.B., Funck, J.W., Reeb, J.E., 2007. Douglas-fir plywood gluebond quality as influenced by veneer roughness, lathe checks, and annual ring characteristics. *Forest Prod. J.* 57 (1/2), 21-28
- [Duplex, A., Denaud, L., Bleron, L., Marchal, R., Hughes, M., 2012.](#) The effect of log heating temperature on the peeling process and veneer quality: beech, birch, and spruce case studies. *European Journal of Wood and Wood Products.* 71 (2), 63-171
- JAS SE 11 No. 237, 2003. Japanese agricultural standard for structural laminated veneer lumber. Japanese Agricultural Standard Association
- Kilic, Y., Colak, M., Baysal, E., Burdurlu, E., 2006. An investigation of some physical and mechanical properties of laminated veneer lumber manufactured from black alder (*Alnus glutinosa*) glued with polyvinyl acetate and polyurethane adhesives. *Forest Prod. J.* (56), 56-59.
- Kollmann, F., Kuenzi, E.W., Stamm, A.J., 1975. Principles of wood science and technology II, wood based materials. Springer Berlin Heidelberg, New York, pp. 123-132.
- Krisnawati, H., Varis, E., Kallio, M., Kanninen, M., 2011. *Paraserianthes falcataria* (L.) Nielsen: ecology, silviculture and productivity. CIFOR, Bogor, pp 1-23.
- Lutz, J.F., 1974. Techniques for peeling slicing, and drying veneer. USDA Forest Service Research Paper FPL 228.

Martawijya, A., Kartasujana, I., Kadir, K., Prawira, S., 2005. Atlas Kayu Indonesia. Forest Products Research Institute, Bogor

Neese JL, Reeb JE, and Funck JW. 2004. Relating traditional surface roughness measures to gluebond quality in plywood. Forest Prod. J. 54(1):67-73.

Palka, L.C., Holmes, B., 1973. Effect of log diameter and clearance angle on the peel quality of 0.125-inch-thick Douglas-fir veneer. Forest Prod. J. 23(7):33-41.

Palka, L.C., 1974. Veneer cutting review - factors affecting and models describing the process. Canadian Forestry Service, Western Forest Products Laboratory, Information Report VP-X-135, pp 1 – 54

[Suh, J.S.](#), [Kim, S.K.](#), 1988. Effects of softwood log pretreatments on the veneer peeling-, drying properties and plywood properties. The Research Reports of the Forestry Research Institute. 37, 63-71

Tanritanir, E., Hiziroglu, S., As, N., 2006. Effect of steaming time on surface roughness of beech veneer. Build. Environ. 41, 1494–1497.

Wood Related Researches in Central Europe- A Review

Levente DÉNES

Abstract

Central European region has a long tradition in forest and wood science education and research and all member countries have their own high education institution with departments and/or institutes related to wood processing. Many colleges also established state research centers for forest management, exploitation, primary and secondary processing of wood, wood based product design and furniture manufacturing, etc. Beside college operated research centers former socialist countries set up additional research and processing centers to fulfill the industry's needs. Nowadays most of these state owned and/or privatized centers were closed and the wood related researches are withdrawn to the colleges. This study overview the wood related research works of the last decade in the Central European region including countries like Austria, Czech Republic, Croatia, Poland, Romania, Serbia, Slovakia, Slovenia and Hungary. Research results, innovations and product developments completed in both academic and research institutions such as Holzforschung Austria, Natural Resources Research Center, etc. are introduced. The studied research fields include aspects of wood quality, wood modifications, energy related research by utilization of wooden waste generated during processing, design and reliability modeling of wood products, timber structures, cement and gypsum bonded panel, wood plastic composite development, comfort analysis of furniture, etc. The study comprise the introduction of the existing research infrastructure as well as the testing, inspection and service related activities of these institutions.

Keywords: wood research, Central Europe, wood science, infrastructure, testing and service

Levente DÉNES, dali@fmk.nyme.hu
University of West Hungary
College of Charles Simonyi Engineering, Wood Science and Art
Natural Resources Research Center
Bajcsy Zs. 4.. H-9400, Sopron

User-Chair Interaction Analysis of Different Age Groups

Noémi TAKÁCS, Levente DÉNES

Abstract

For long term users sitting comfort of chairs is critical to avoid the so called work-related musculoskeletal disorders (WMSD). Therefore, a special attention should be given in chair design to prevent the appearance of these injury types. Anthropometry, ergonomics, body pressure analysis, life cycle assessment and other methods support the chair design to minimize the appearance of WMSDs. This paper evaluates the body pressure distribution and distribution characteristics of different chairs in function of age groups, gender and body postures. Five age groups' sitting habits and comfort level were analyzed: age 3-6 (kindergarten), age 7-12 (primary school students), age 13-18 (secondary school students), age 19-23 (university students), (age 24 plus). During the measurements the incorrect postures, wrong sitting routines were observed and investigated.

Results of the study reveals the body pressure distribution differences associated with chair dimensions, adjustability features and different seating postures. Postures, movements, chair parts inclination and comfort rating data were collected from the subjects. Considerable effects of body built and chair type on pressure distribution and pressure changes were demonstrated. The results indicate an additional research to further explore the effect of other factors, i.e. foam type, elasticity, etc. on pressure distribution and discomfort measure.

Keywords: seat comfort, body pressure, chair ergonomics, pressure distribution, body postures

Noémi TAKÁCS,
Levente DÉNES, dali@fmk.nyme.hu - corresponding author
University of West Hungary
College of Charles Simonyi Engineering, Wood Science and Art
Institute of Wood Based Products and Technology
Bajcsy Zs. 4.. H-9400, Sopron

Use of Non-Treated and Thermally-Treated Biomass Media in Livestock Heavy-Use Areas to Reduce the Environmental Impacts of Agriculture

David DeVallance, Joshua Faulkner, and Tom Basden

Abstract

Nutrient enrichment of surface waters is a major cause of water quality impairment in the United States and around the World. Specifically, loss of nitrogen and phosphorus from agricultural operations plays a significant role in the degradation of the Chesapeake Bay, the Gulf of Mexico, and their tributaries. Manure is a primary source of these nutrients, and is often transported from livestock confinement areas due to stormwater runoff. In this research, a novel solution to this nonpoint source pollution was investigated. Specifically, the research focused on selecting the optimal biomass media for improving the water runoff from heavy-use livestock loafing areas. Bench-scale column study methods were used to select the biomass media system. The optimal biomass mixture was then implemented in an installation and renovation of an existing livestock confinement area at the West Virginia University Animal Sciences Farm. The findings from the monitoring of hydrologic performance, water quality, and biomass media characteristics will be presented and recommendations will be provided for using biomass as a chip pad material.

Keywords: wood chips, biofilter, torrefied wood, biochar, water quality

David B. DeVallance

Assistant Professor and Program Coordinator

david.devallance@mail.wvu.edu

Division of Forestry and Natural Resources, Wood Science and Technology Program

West Virginia University

PO Box 6125

Morgantown, WV 26506-6125

304-293-0029 FAX: 304-293-2441

Joshua Faulkner

Farming and Climate Change Coordinator

joshua.faulkner@uvm.edu

University of Vermont Center for Sustainable Agriculture

23 Mansfield Ave.

Burlington, VT 05401

Tom Basden

Extension Specialist, Nutrient Management and Extension Clinical Associate Professor

tom.basden@mail.wvu.edu

West Virginia University Extension

PO Box 6108

Morgantown, WV 26506

Surface Treatment, Layer Thickness and Surface Performance Relations of Wood Materials

Tuncer Dilik^{1}–K.Hüseyin Koç²–Ender HAZIR³–E.Seda ERDİNLER⁴*

¹ Associate Professor Dr., Istanbul University, Faculty of Forestry, Department of Forest Industry Engineering, 34473 Istanbul – Turkey

** Corresponding author*

[*tuncerd@istanbul.edu.tr*](mailto:tuncerd@istanbul.edu.tr)

² Professor Dr., Istanbul University, Faculty of Forestry, Department of Forest Industry Engineering, 34473 Istanbul – Turkey

[*hkoc@istanbul.edu.tr*](mailto:hkoc@istanbul.edu.tr)

³ Research Assistant, Istanbul University, Faculty of Forestry, Department of Forest Industry Engineering, 34473 Istanbul – Turkey

[*ender.hazir@istanbul.edu.tr*](mailto:ender.hazir@istanbul.edu.tr)

⁴ Assistant Professor, Istanbul University, Faculty of Forestry, Department of Forest Industry Engineering, 34473 Istanbul – Turkey

[*seda@istanbul.edu.tr*](mailto:seda@istanbul.edu.tr)

Abstract

Wooden material has an important place in manufacturing sector when evaluated in the means of its utilization fields and the added value it creates. Wooden materials are used more efficiently with respect to the technological development. Preventive surface treatment makes up the biggest share of the added value wooden material creates. Surface treatment applied on wooden material plays an influencing role on the discrimination of the consumer. Surface treatment appears as an important cost to the producers. Surface treatment applications of wood and wooden materials in the industry are made with qualitative methods. As the thickness of the paint layer can't be controlled numerically it inhibits the expected benefits of surface treatment. For this reason layer thickness, an important cost and aesthetic factor, should be determined quantitatively and evaluated in the means of surface properties. Thus, one of the important parameters to set a more efficient and controllable system in surface treatment applications would be taken under control. In this study, it is aimed to determine layer thickness in preventive surface treatment and evaluate the relationship between layer thickness and surface properties. It will be much easier to head to the appropriate surface treatment applications and save in surface treatment supplies and wages. International standards are used to determine the samples and sample sizes. Research is applied according to ASTM D 4541, TS 6884, TS EN ISO 4624 standards.

Keywords: A. Surface finishing, B. Coating thickness, C. Surface performance, D. Painting, E. Wooden.

Introduction

Surface treatments, as one of the final stages of production in wooden furniture and decoration applications, constitute the majority of production cost. In addition to this, it is effective in the performance of the products and the preferences of the customers. A good surface treatment increases the usage properties of the product, as well as facilitates its sales [1-5]. In surface treatments, factors such as surface roughness, adhesion resistance are influential in the surface performance. The use of MDF and particleboards gradually increases in furniture and decoration applications due to covering surface treatments. Although there are various national and international standards of surface treatments and their characteristics, it's seen that the required importance is not considered in application and the controls remain at subjective evaluation level [4]. Therefore, in the majority of the applications, the surface treatments may cause an increase in the production costs and prevent achieving the desired surface performance values [3, 5]. Various methods are being developed for a more effective and rational use in applying and evaluating the surface layer treatments with the recently developing technology. For this purpose, it's seen that surface modeling works, which allow objective evaluation of surface treatments, are also being carried out for wood materials [6-11].

In the literature, the general adhesion mechanisms between the wood material surfaces and protective layers have been examined with various studies and it's been stated that these materials are chemical, mechanical, electrostatic and acid-base adhesion. Furthermore, it's seen that adhesion resistance is determined by using different methods and the most commonly used methods are pull-off test and cross-cut test [4, 6, 8].

In this study, it is aimed to determine the thicknesses of the layers created with protective surface treatments to be applied on wood and wood-based materials and to explain the correlation between layer thicknesses and surface performance based on adhesion resistance. Thus, it's been considered that better applications can be carried out by taking the number of layers, layer thickness and surface performance expectation into account in industrial surface treatment applications. Therefore, the study is examined on two separate types of paint and two separate types of wood material with different layer thicknesses and different number of layers. The study is particularly limited with the wood materials and paint types commonly used in the industry. Thus, it's aimed to offer solutions for the problems related to layer structure as encountered in surface treatments and to ensure a more effective surface treatment application.

Materials and Methods

Materials: MDF board and Particleboard as wooden based materials and Cellulosic and Polyurethane paints as surface treatment materials are selected for the study.

Method: Test applications take the national and international standards into account. Test design and sample pattern are as shown in Table 1. During the study, the paint process, which is examined as surface treatment, is applied as minimum 3 layers and maximum 5 layers. Applications on 5 samples prepared for each application level are carried out with spray gun as 1, 2 and 3 finish paint on the primer layer. In this context, the layer thicknesses obtained have been measured with PosiTector Probe 200 and the adhesion resistance is measured with PosiTest AT-A Automatic Adhesion Tester [12-14].

Table 1: Test design and sample pattern used in the study ()*

Material type	Paint type	Applica- tion	No. of samp.	Treat. 1	Treat. 2	Treat. 3	Treat. 4	Treat. 5
MDF (Medium Density Fiberboard) (MDF board in calibrated 18x200x1000 mm size)	Cellulosic Paint	Applic-1	5	Primer	Primer	Finish		
		Applic-2	5	Primer	Primer	Finish	Finish	
		Applic-3	5	Primer	Primer	Finish	Finish	Finish
	Polyurethane Paint	Applic-1	5	Primer	Primer	Finish		
		Applic-2	5	Primer	Primer	Finish	Finish	
		Applic-3	5	Primer	Primer	Finish	Finish	Finish
PARTICLE BOARD (Particle board in calibrated 18x200x1000 mm size)	Cellulosic Paint	Applic-1	5	Primer	Primer	Finish		
		Applic-2	5	Primer	Primer	Finish	Finish	
		Applic-3	5	Primer	Primer	Finish	Finish	Finish
	Polyurethane Paint	Applic-1	5	Primer	Primer	Finish		
		Applic-2	5	Primer	Primer	Finish	Finish	
		Applic-3	5	Primer	Primer	Finish	Finish	Finish

(*) All applications are carried out on the surface treatment line of an industrial company according to the instructions of the producer companies with the same batch of paint.

Results

The arithmetic average values related to the layer thicknesses obtained and adhesion resistance measured in the study are provided in Table 2. From the examination of the values available in the table, it's been determined that higher values are achieved in MDF material compared to particleboard, provided that adhesion resistance directly effective on the surface performance is valid for both paint types.

However, the impact of layer thickness, obtained according to the number of layers applied according to the paint type and application levels, on the adhesion resistance could not be determined exactly. While the highest adhesion resistance in MDF is obtained as 3,62 MPa with 179 micron layer thickness and 3 layers of cellulosic paint application, the lowest adhesion resistance is obtained as 2,37 MPa with 239 micron layer thickness and 4 layers of polyurethane paint application. For the applications on particleboard, the highest adhesion resistance is obtained as 1,54 MPa with 322 micron layer thickness and 4 layers of cellulosic paint application, while the lowest adhesion resistance is obtained as 0,83 MPa with 249 micron layer thickness and 3 layers of cellulosic paint application.

Table 2: Results related to adhesion resistance and layer thicknesses obtained in the study.

Wood material type	Paint type	Application	Layer thickness (micron)	Standard Deviation (σ)	Adhesion resistance (MPa)	Standard Deviation (σ)
MDF (Medium Density Fiberboard) (MDF	Cellulosic Paint	Application 1	179	5,57	3,62	0,46
		Application 2	181	11,68	2,86	
		Application	236	5,51	2,78	

board in calibrated 18x200x1000 mm size)	Polyurethane Paint	3				
		Application 1	167	2,08	2,95	0,60
		Application 2	239	13,32	2,37	
Application 3	345	8,33	3,58			
PARTICLE BOARD (PB) (Particle board in calibrated 18x200x1000 mm size)	Cellulosic Paint	Application 1	249	13,89	0,83	0,38
		Application 2	322	19,08	1,54	
		Application 3	334	6,81	0,96	
	Polyurethane Paint	Application 1	199	10,54	0,85	0,16
		Application 2	295	3,06	1,16	
		Application 3	363	9,02	0,97	

The graphics showing the correlation levels of material and paint type, layer thickness and adhesion resistance according to the values in the table are as follows (Figure 1).

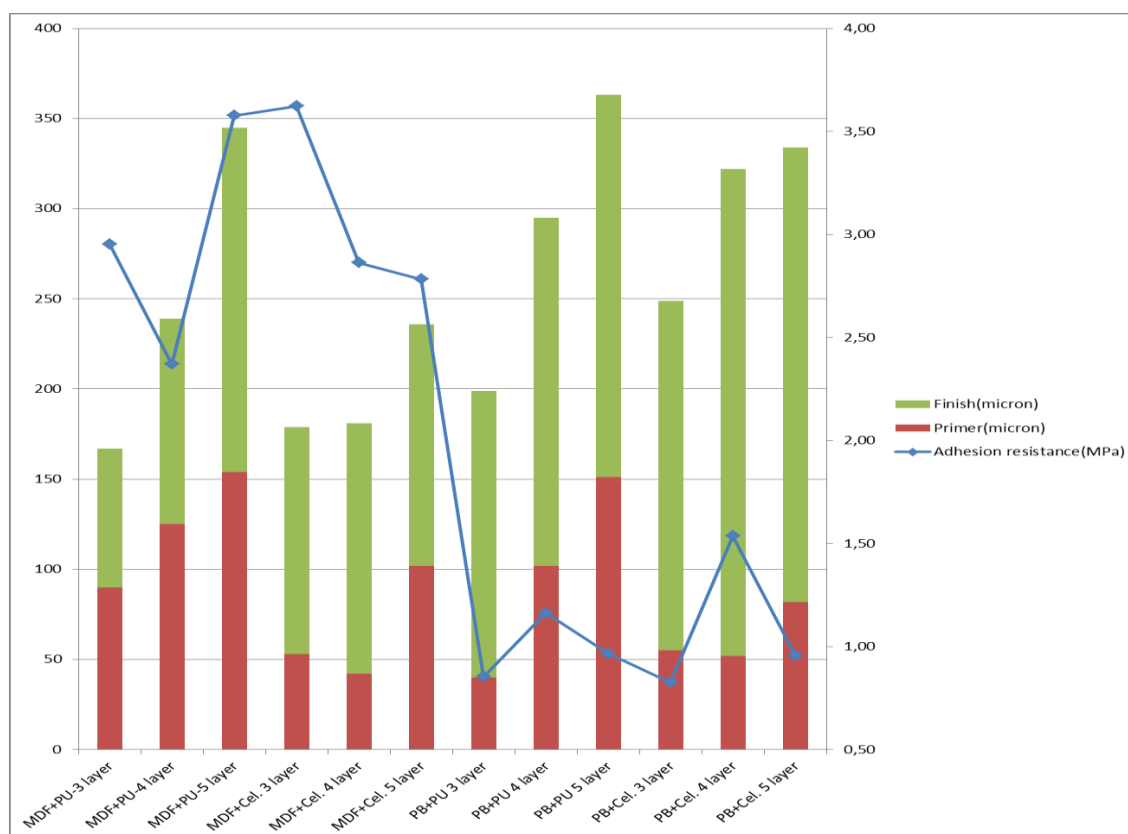


Figure 1: Relations between layer thickness and adhesion resistance with material and paint.

Conclusions

Accordingly, differences were found based on to the adhesion resistance values, material type, paint type and layer thicknesses. Examining the reasons for such difference, as it can be seen in the graphics, the layer thickness and surface performance correlation varies according to the wood material and paint types (Figure 1). During the tests, the breaking in paint layer is found out to appear between primer layer and wood material for all. Accordingly, it can be stated that finish layers on the primer paint layer is not directly effective on the adhesion resistance. This situation can be explained as the adhesion set between the primer layer and finish layer is higher than the adhesion developing between the primer layer and wood material.

These results generally reveal the importance of primer layer in order to ensure the desired surface performances in protective surface layer treatments, as well as the importance of working with one-layer application with the ideal layer thickness rather than working with multi-layer importance. A similar situation has tried to be explained with general adhesion mechanisms in various literature studies carried out for determining the adhesion resistance of varnish and paint types on the surfaces of different wood materials. [4, 5, 10, 16]

As a result, according to the findings of the study, it's been found out that the wood material type is important for the painting works of the furniture and decoration elements, which need to have high adhesion resistance, and it's also been considered that the primer layer is important rather than the layer thickness in the applications and a finish application with ideal layer thickness will be sufficient. However, more detailed studies will be beneficial for establishing a numerical and parametric correlation. As is known, the numerical value of the layer thicknesses is not known in the covering surface treatments with different numbers of layers applied on wood materials and the correlation between the number of layers and surface performance can be defined as a qualitative relation based on the number of layers. Therefore, the studies performed are insufficient for parametric evaluation of the relationship between the number of layers, layer thickness and surface.

References

- [1] Kurtoglu, A., 2000. Wood Material Surface Treatments, General Information, Volume 1, Istanbul University, Faculty of Forestry, Department of Forest Industry Engineering, Istanbul, 2000.
- [2] Şenok, A. S., 2000. Some Considerations Related to Pain Industry in Turkey, *ISO Journal*, p.32, March-2000.
- [3] Sönmez, A., 2000. Surface Layer Treatments in Wood Works I., Preparation and Coloring, Gazi University, Faculty of Technical Education, Çizgi Matbaacılık, Ankara, 2000.
- [4] Budakci, M. Sönmez, A., 2010. Determining the Adhesion Resistance of Some Wood Varnishes on Different Wood Material Surfaces, *J.Fac.Eng.Arch.Gazi Univ.*, Vol. 25, No:1, 111-118, 2010.
- [5] Çakicier, N., 2007. Changes Determined by Aging on Wood Material Surface Treatment Layers, *Doctoral Thesis*, Istanbul University Institute of Science, Istanbul, 2007.

- [6] Özdemir, T. – Hiziroglu, S., 2007. Evaluation of Surface Quality and Adhesion Strength of Treated Solid Wood, *Journal of Materials Processing Technology*, 186, pp. 311-314, 2007.
- [7] Hazir, E., 2012. A Modeling Work on Evaluating the Quality of Wooden Surface Quality, *Master Thesis*, Istanbul University Institute of Science, Istanbul, 2012.
- [8] Ahola, P., 1991. Adhesion Between Paint and Wood Substrate, *Surface Coatings International*, 74, No.5, 173-176, 1991.
- [9] Nejad, M.- Cooper, P., 2011. Exterior wood coatings.Part-2: Modeling correlation between coating properties and their weathering performance, *J.Coat technol.Res*, 8 (4) 459-467,DOI 10.1007/s11998-011-9331-4, 2011.
- [10] Mittal, K.L., 1995. Commentary, Adhesion Measurement of Films and Coatings, VSP, p.1-13, Utrecht, The Netherlands.
- [11] Jaic, M. – Zivanovic, R., 1997. The influence of the ratio of the polyurethane coating components on the quality of finished wood surface, *Holz als Roh- und Werkstoff*, 55, 319-322, 1997.
- [12] Nelson, G. L., 1995. Adhesion , Paint and Coating Testing Manuel, *Chapter 44, ASTM Special Technical Publication*, Philadelphia, P.A., 513-523, 1995.
- [13] ASTM D 4541, 1995. Standard test method for pull-off strength of coatings using portable adhesion testers, American Society for Testing and Materials, 1995.
- [14] TS EN ISO 4624, 2006. Paints and varnishes – Pull-off test for adhesion.
- [15] TS 6884, 2005. Wooden furniture surfaces – Determining the adhesion resistance of paint and varnish layers.
- [16] Dilik, T.- Hiziroglu, S., 2012. Bonding strength of heat treated compressed Eastern red cedar wood, *Materials and Design*, Volume 42, pages: 317-320, 2012.

Acknowledgement

This study is supported by Scientific Research Projects Coordination Unit of Istanbul University with project no. UDP-42282.

Wood Anatomy of Naturally Grown Philippine Teak (*Tectona philippinensis* Benth. & Hook. f.)

Arsenio ELLA, Emmanuel DOMINGO and Florena SAMIANO

Abstract

Filipino scientist and educators intend to utilize fully the country's endemic forest tree species like Philippine teak (*Tectona philippinensis* Benth. & Hook. f.) of the family Verbenaceae. The species is predominantly found in dry and exposed ridges of Lobo, Batangas. The wood of Philippine teak is classified as comparatively heavy and durable and can be substitute for molave (*Vitex parviflora* Juss.). The local residents in Batangas utilized them for posts and general construction often substituted for molave. Its potential as first class timber has not yet been investigated. Study of the basic wood anatomical and morphological characteristics would lead ultimately to the optimum utilization of the species.

Macroscopic observations and other physical attributes showed that the wood of Philippine teak is light yellow, grain is slightly wavy and texture is fine, glossy, hard and heavy. Fiber mensuration indicates that Philippine teak is medium-sized and thick-walled. Rays are observed to be of two kinds: uniseriate and multiseriate and are classified as extremely low. Philippine teak wood could be differentiated from teak (*Tectona grandis* L. f.) with the former having smaller pores and thinner rays. The most common anatomical features of the two *Tectonas* are the presence of whitish deposits and tyloses.

The study addresses a gap in technical information that will lead to harness the potential of the Philippine teak. Being heavy and hard wood species with relative density at 0.710 is an indicator that Philippine teak could be a strong potential for structural timber. Results of the study could possibly lead to establishments of plantations to raw materials source and benefit the researchers; Batangas farmers; and wood-using industries to maximize the full utilization of Philippine teak not only in raw form but also in engineered and other finished products.

Keywords: Wood Anatomy, *Tectona*, Philippine teak, Lobo, Batangas

Arsenio B. Ella
Scientist III
Forest Products Research and Development Institute
Department of Science and Technology
College, Laguna 4031 Philippines
+63-049-536-2377 FAX: +63-049-536-3630
Arsie_Ella@yahoo.com/Arsenioella@gmail.com

Emmanuel P. Domingo
Science Research Assistant
emandomingo@ymail.com

*Proceedings of the 57th International Convention of Society of Wood Science and Technology
June 23-27, 2014 - Zvolen, SLOVAKIA*

Florena B. Samiano
Science Research Specialist
flor_samiano@yahoo.com

Relations between Varnish Type and Color Changes of Wood Material

E.Seda Erdinler^{1}–Tuncer Dilik²–Ender HAZIR³–Emel Öztürk⁴*

¹ Assistant Professor E.Seda Erdinler, Istanbul University, Faculty of Forestry, Department of Forest Industry Engineering, 34473 Istanbul – Turkey

** Corresponding author*

[*seda@istanbul.edu.tr*](mailto:seda@istanbul.edu.tr)

² Associate Professor Dr, Istanbul University, Faculty of Forestry, Department of Forest Industry Engineering, 34473 Istanbul – Turkey

[*tuncerd@istanbul.edu.tr*](mailto:tuncerd@istanbul.edu.tr)

³ Research Assistant, Istanbul University, Faculty of Forestry, Department of Forest Industry Engineering, 34473 Istanbul – Turkey

[*ender.hazir@istanbul.edu.tr*](mailto:ender.hazir@istanbul.edu.tr)

⁴ Research Assistant, Istanbul University, Faculty of Forestry, Department of Forest Industry Engineering, 34473 Istanbul – Turkey

[*emelozt@istanbul.edu.tr*](mailto:emelozt@istanbul.edu.tr)

Abstract

Wooden material takes an important place in life with its natural structure and psychological effect. Color is an important parameter to emphasize the aesthetic appearance of the material and the surface. One of the important stages is varnishing. As known, varnish provides prevention as well as good appearance for wooden materials. Several varnish types are used in industrial applications with respect to the developing technology and the structure of the materials becomes more important with the environmental awareness. Varnish types may cause positive or negative effects on the color of wooden material. For this reason, determination of color changes of wood by investigating the changes in varnish types on wood according to their utilization is important. Varnish applications may have both positive and negative effects on natural wood color. Determination of these effects would be important to meet the expectations according to the utilization fields. In this frame, background for necessary information for appropriate application in the industry will be provided. The results from this study will be supported by future studies to determine varnish type and wooden material sufficiency. Appropriate varnish selection occurs by the determination of the effects of varnish types on different wooden materials. In the study color values are in accordance to TS 6611 EN ISO 3668 and ASTM D 2244-3.

Keywords: A. Color change, B. Wooden, C. Surface color, D. Varnish type, E. Surface treatment

Introduction

Wooden and wood based materials are one of the most widely used product groups. With their both industrial use and furniture and decoration use, wood based products directly affect the

quality of life. The basic reasons why wood based materials are used for industrial purposes can be listed as obtaining economic and wide surfaces, being used as a filling or bearing purpose and being able to be equipped with technological needs required by the setting. For the end-consumer use, wooden materials are preferred as first option due to their visual quality, warm life experience feeling and acoustic characteristics. The most important characteristic reflected by the wooden material in industrial use or end-consumer use is the rich natural color and appearance it offers. It's been endeavored to protect, feature or make this richness permanent in industrial applications. As is known, the natural beauty and live appearance of wooden material is affected more or less during the surface treatments. The color of the material changes after it is exposed to natural atmospheric conditions for a long time, changes. For example, the color of oak, walnut and mahogany under natural use becomes darker, while the color of maple and ash tree turns pale [1-7]. Coloring treatment is applied for changing the specific color of the wooden material, guaranteeing a unified appearance in mass production and removing the lines and spots arising from the natural appearance of the material. While color is a very positive characteristic when it can be taken under control and remain between esthetic lines, it can also cause undesired situations due to lack of application, method and material. Therefore, color measurements can be used in various fields in various industries such as food [8-11]. Considering the limited amount of studies carried out on the wooden materials, aging related color difference has always been an important study topic. The color of the wooden material may change due to various chemicals used in the production of surface treatment materials, and the color difference effect of varnish is also inevitable due to its own color. In this regard, the varnishes with highest color difference effect are the synthetic and polyurethane varnishes. Therefore, the expected color effect must be taken into account in all surface layer treatments [1, 3, 5, 6, 12].

Materials and Methods

Materials: Massive Abies is used in the study. Cellulosic and water based transparent varnish is selected as the surface treatment material to see its effect on the natural color system.

Method: Test applications take the national and international standards into account. Test design and sample pattern are as shown in Table 1. During the study, minimum 2 and maximum 4 layers of surface treatment is applied including the filling layer. In this context, the layer thicknesses obtained have been measured with PosiTector Probe 200 and color measurements have been carried out with HunterLab MiniScan EZ at D65/10⁰ according to CIEL* a*, b* basis [13-15].

Table 1: Test design and sample pattern used in the study ()*

Wooden material	Varnish type	Application	No. of samples	Treat. 1	Treat. 2	Treat. 3	Treat. 4
Abies (<i>Abies bornmulleriana</i> Mattf.) (Massive wood prepared in calibrated 18x100x1000 mm size)	Cellulosic Varnish	2 layers	5	Filling	Filling		
		3 layers	5	Filling	Filling	Finish	
		4 layers	5	Filling	Filling	Finish	Finish
	Water Based Varnish	2 layers	5	Filling	Filling		
		3 layers	5	Filling	Filling	Finish	
		4 layers	5	Filling	Filling	Finish	Finish

(*) All applications are carried out with spray gun according to the instructions of the company with the varnishes produced by the same company.

Results

The layer thicknesses obtained in the study and the color values measured are provided in Table 2. Based on these findings, the layer thickness and color correlation of different varnish types on color difference effect is illustrated in Figure 1. In the assessments, the color system of the non-varnish part is taken as the basis for natural color system as control sample. Therefore, it's been ensured that the varnished and non-varnished surfaces of the same part are subjected to the same preliminary preparation treatments before the application. Thus, the comparisons are made between the color systems of varnished and non-varnished surfaces of the same part and it's been tried to determine the effect of varnishes on color difference.

Table 1: Results related to layer thickness obtained in the study and color systems.

Varnish type	Application	Layer Thickn. (micron)	Natural Color System			Color difference (ΔE)1	Varnished Color System			Color difference (ΔE)2	Color Difference ⁽¹⁾ (ΔE)*
			L*	a*	b*		L*	a*	b*		
Cellulosic Varnish	2 Layers	76	90,88	- 2,61	- 18,48	90,81	86,11	- 2,61	- 20,95	88,25	2,56
	3 Layers	107	87,85	- 2,87	- 18,99	89,58	83,85	- 3,70	- 23,66	86,82	2,76
	4 Layers	120	89,20	- 2,88	- 18,81	90,89	86,21	- 2,02	- 20,14	88,13	2,76
Water Based Varnish	2 Layers	69	89,34	- 2,29	- 17,13	90,59	86,16	- 2,72	- 20,57	88,34	2,25
	3 Layers	73	90,31	- 2,30	- 17,59	91,54	87,35	- 2,89	- 20,01	89,07	2,47
	4 Layers	98	88,62	- 2,68	- 18,43	90,06	86,76	- 2,99	- 21,16	88,89	1,17

⁽¹⁾ (ΔE)* = (ΔE)1 - (ΔE)2

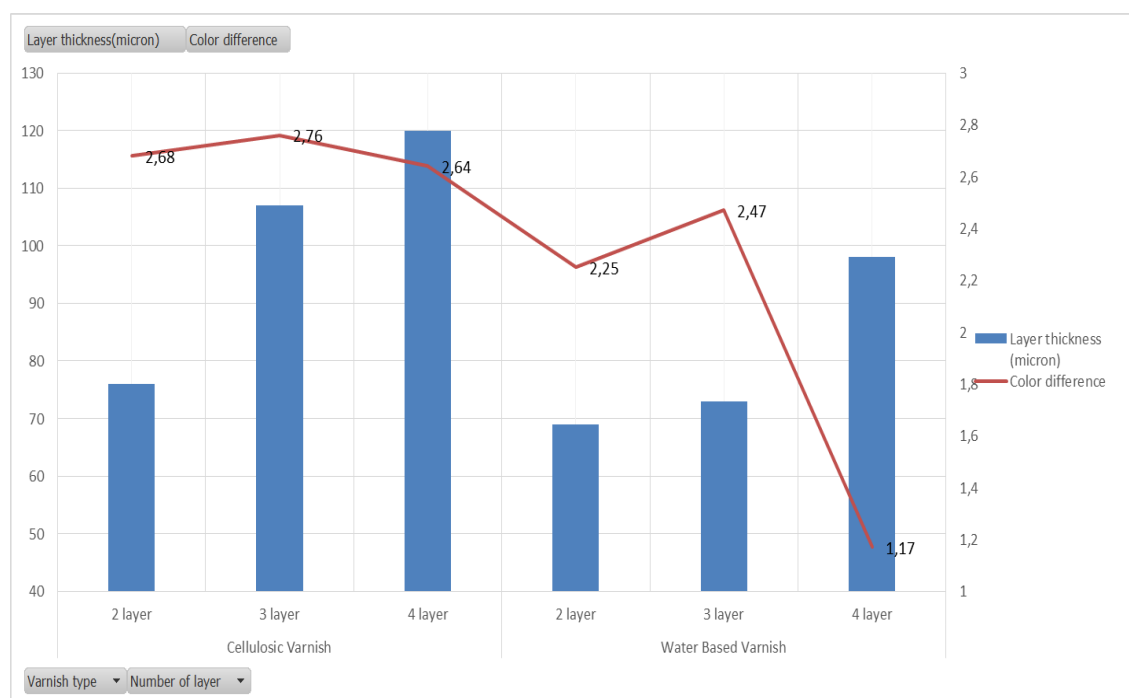


Figure 1: Layer thickness and color correlation in varnish application

As it can be seen from the examination of the values in the table and the graphics in the figure, for the color difference effect (ΔE)* of the varnishes on the natural color system, the highest value of 2,76 in cellulosic varnish is obtained in 3-layer and 4-layer applications, while the highest value of 2,47 in water based varnishes is obtained in 3-layer application. On the other hand, it's clearly seen that the varnish types have a changing effect on L* (color brightness value), a* (red color tone value) and b* (yellow color tone value) constituting the color system. As it can be seen in various studies [2, 7], this study also reveals the important effect of different layer thickness application on L*, a* and b* values. For the effect of varnish on color brightness, the highest value of 87,35 is determined in water based varnish with 3-layer application, while the lowest value of 83,85 is obtained in cellulosic varnish with 3-layer application. For the effect of varnish on red color tone, the highest value of 3,70 is obtained in cellulosic varnish with 3-layer application, while the lowest value of 2,02 is obtained in cellulosic varnish with 4-layer application. In water based varnish, the values are determined between 2,72 and 2,99. For the effect of varnish on yellow color tone, the highest value of 23,66 is obtained in cellulosic varnish with 3-layer, while the lowest value of 20,01 is obtained in water based varnish with 3-layer application. This allows observing the changing effect of varnish type and layer thickness on the natural color system and also reveals that cellulosic varnishes have higher color changing effect compared to water based varnishes on the same material. However, it's seen that color changing effect is more obvious in finish applications in cellulosic varnishes and more effective in filling layer applications in water based varnishes.

Conclusions

As a result, an evaluation, even partially, has been obtained on the degree the varnish type and number of layers, commonly used in the industrial application, meets the natural color appearance of the wooden material. It's been found out that the changing effect of the varnish type and layer thickness on the natural color system for the same material studied in this context is higher in cellulosic varnishes compared to water based varnishes. However, it's seen that color changing effect is more obvious in finishing applications of cellulosic varnish. In this case, the number of layers (layer thickness) in finishing applications of cellulosic varnish appears as a matter that should be taken into account. For the water based varnish application, it's seen that color changing effect is more effective in filling layer applications compared to finishing applications. Accordingly, the thing that should be taken into account in water based applications is the filling layer application. Thus, it's been considered that the results submitted would be effective in solving the problems and meeting the expectations related to coloring and appearance frequently encountered in protective surface layer treatments in the wood industry. However, it would be better to perform more detailed studies and control the layer thickness and color changing correlation in order to establish a complete numerical and parametric correlation.

References

- [1] Kurtoğlu, A., 2000. Wood Material Surface Treatments, General Information, Volume 1, Istanbul University, Faculty of Forestry, Department of Forest Industry Engineering, Istanbul, 2000.
- [2] Çakicier, N., 2007. Changes Determined by Aging on Wood Material Surface Treatment Layers, *Doctoral Thesis*, Istanbul University Institute of Science, Istanbul, 2007.
- [3] Bechere, I., 1998. Water and solvent based systems differences, *European Coatings Journal*, April 1998.
- [4] Anonim, 2006. Application of Colorimetry for Wood Appearance Products, value to wood, TP-05-01E.
- [5] Mitsui, K., 2006. Changes in color of Spruce by repetitive treatment, *Holz als Roh-und Werkstoff*, 64 (3), 243-244, 2006.
- [6] Bekhta, P.- Niemz, P., 2003. Effect of high temperature on the change in color, dimensional stability and mechanical properties of Spruce wood, *Holzforschung*, 57 (5):539-546, 2003.
- [7] Sogutlu, C. – Sonmez, A., 2006. Color changing effect of UV rays in some local trees treated with various preservatives, Gazi University, *Journal of Faculty of Engineering and Architecture*, 21 (1), 151-159, 2006.
- [8] Şahin, T., 2011. Color Changes in Wood Surfaces Modified by A Nanoparticulate Based Treatment, *Wood Research* 56(4):2011,525-532.
- [9] Uren, A., 1999. Three Dimensional Color Measurement Methods, *Food* (1999) 24(3):193-200.
- [10] Sönmez, A., 2000. Surface Layer Treatments in Wood Works I., Preparation and Coloring, Gazi University, Faculty of Technical Education, Çizgi Matbaacılık, Ankara, 2000.
- [11] Sonmez, A., 1989. Resistance of varnishes used in wood based furniture's surface layers against important mechanical, physical and chemical effects, *Doctoral Thesis*, Gazi University, Institute of Science, Ankara, 1989.
- [12] Budakci, M.- Sönmez, A., 2010. Determining the Adhesion Resistance of Some Wood Varnishes on Different Wood Material Surfaces, *J.Fac.Eng.Arch.Gazi Univ.*, Vol. 25, No:1, 111-118, 2010.
- [13] TS 6611 EN ISO 3668. Paints and varnishes – Visual comparison of the color of paints, Turkish Standards, Ankara, Turkey.
- [14] ASTM D-3023, 1998. Standard practice for determination of resistance of factory applied coatings on wood products of stain and reagents. American Society for Testing and Materials, 1998.

[15] ASTM D 2244-3, 2007. Standard practice for calculation of color tolerances and color differences from instrumentally measured color coordinates, American Society for Testing and Materials Standards, 2007.

Acknowledgement

This study is supported by Scientific Research Projects Coordination Unit of Istanbul University with project no. UDP-42338

Comparing the Efficiency of Selected Methods of Logging Residue Chipping for the Energy Purposes

Tomasz Gałęzia

State Forests National Forest Holding, Pomorze Forest Inspectorate
Pomorze 8, 16-506 Giby, Poland
tomasz.galezia@bialystok.lasy.gov.pl

Abstract

The aims of the research carried out in forest of Augustow Primeval Forest, Poland, were to compare the efficiency of various systems of forest residues comminution and to estimate the energy spent on preparation and transport of energetic biomass in form of chips.

Three systems of the forest residues comminution were analyzed: chipping non-piled residues at the clear-cut, chipping piled residues at the clear-cut and chipping piled residues at the roadside. Operations were performed by mobile chippers, farm tractors, forwarders and container trucks.

Quantity of the energy spent during technological process of biomass logging was a sum of the embodied energy and the energy of the fuel used in process of piling, extraction, chipping and transportation of the biomass. Energy input was compared to the amount of energy received by burning of the biomass in an oven of a power plant.

Data collection was carried out in ten final felling areas in four forest inspectorates of The State Forests National Forest Holding. During 88 hours of research 1980 m³ of chips was harvested. Surveys were performed using a working day activity study with an accuracy of 1 sec, which allowed identification of structure of a shift. Based on consumed fuel and its energy content, the energy input of each system was calculated. CO₂ emission was estimated using published data.

Keywords: Energy, Biomass, Chipping, Logging

Introduction

Polish economy bases strongly on fossil fuels as an energy source. Hard coal remains the main energy carrier for power and heat co-generation with its share of about 45 %. Considering decreasing resources of coal and the assumed average annual economic growth between 2.3% and 5.5%. (IAEA 2002) it is vital to look for alternative sources of energy.

Combustion of woody biomass seems to be the easiest way to reach the 15 % target for the Polish renewable energy share by 2020. The potential, annual supply of energy from forest residues reaches between 45 and 90 PJ y⁻¹ (depending on residue-to-stem) (Ericsson, Nilsson 2006). It must be said however, that the current regulations make combustion of merchantable timber in power plants economically ineffective, so the biomass from forest residues becomes the only source of forest biomass available for the Polish energy industry.

There are several ways of biomass harvesting depending on type and quantity of machines used in processes, type of supply chain or transportation distance (Hakkila 2004). The most popular biomass logging systems in Scandinavia are bundling and chipping and were analyzed by a number of researchers (Gustavsson et al. 2011, Iarocci 2009, Wihersaari 2005). The research concerning the biomass logging efficiency and energy inputs in Poland were performed by Róžański, Jabłoński (2009, 2010), Moskalik, Borkowska, Sadowski and Zastocki (2012). Bundling in mountainous conditions in Czech Republic was the subject of research by Liška, Klvač and Skoupý (2011). Fuel consumption during chip transportation was analyzed by Schwaiger and Zimmer (2001) in several EU countries and Goltsev, Tolonen, Syunev and Dahlin (2011) in Russia and Finland. A detailed review of different biomass logging systems used in United States was presented by Dempster, Gallo, Hartsough, Jenkins and Tittmann (2008). Efficiency of the process of chip production in Western Australia was analysed by Ghaffariyan, Brown and Spinelli (2013).

Materials and Methods

Research was carried out in the Augustow Primeval Forest in Northern-East Poland. The total area of this forest complex within Polish borders is 125 000 ha and is managed by six inspectorates of State Forests and one national park. Predominating are coniferous and mixed-coniferous forests (68.7% of the forest surface), coniferous species exceeding 83.6% (Sokołowski 2010).

Three systems of the forest residues comminution were analysed:

- i. chipping non-piled residues at the clear-cut (N-P/C),
- ii. chipping piled residues at the clear-cut (P/C),
- iii. chipping piled residues at the roadside (P/R).

For chipping mobile chippers, consisting of Bruks 803 CS, 804 CT and 805 CT built on John Deere 1410 or Ponsse Buffalo King forwarders. Piling of forest residues on a clearcut surface (P/C) was performed by Ursus C-360 farm tractor. Residue extraction (P/R) was made by Volvo BM Valmet 620 and Ponsse Elk forwarders or Ursus 1224 farm tractor with Palms 112 trailer. Hauling was performed by MAN FE 410 and Volvo 550 FH16 hook-container trucks in all cases.

Surveys took place in four forest inspectorates of The State Forests National Forest Holding: Augustow, Plaska, Pomorze and Szczebra, at ten clear-cut areas (nine clear fellings and one group shelterwood cutting), with the use of a working's day activity study. The accuracy of time measurement was one second. The productive machine hours (PMH) were based on readings of machine motor-hour counters (digital or analogue – in the case of Ursus C-360 tractor and the Volvo BM Valmet 620 forwarder). Fuel consumption was estimated on the basis of digital machine readings in the case of mobile chippers, modern farm tractors and transport trucks. The fuel consumption of non-computerised farm tractors and a forwarder was measured manually using a scaled gasoline can. In the energy balance, embodied energy of machinery has been taken into account. The embodied energy level for logging equipment was assessed at the level of 66 MJ kg⁻¹ and the mean lifetime for all machines was 18 000 operational productive hours (Athassiadis et al., 2002). Average transportation distance was 130 km (one way, but fuel consumption during the return journey was also included in calculations). CO₂ emissions were calculated based on the elaboration of Polish Ministry of Environment consisting the heating values and CO₂ emission factors for reporting in European Union Emissions Trading System

(Wartości opałowe..., 2013). The conversion factor for solid wood to chip volume was 2.63 (Kofman 2010).

Calculated for mobile chippers types of logging productivities included following operations during a shift:

- i. operational productivity: chipping, chip extraction, unloading, return to the clear-cut and change of workplace,
- ii. working productivity: chipping, chip extraction, unloading, return to the clear-cut, change of workplace, servicing and repairs,
- iii. exploitation productivity: all measured time components.

Parameters for chip combustion at the power plant were calculated basing on laboratory analysis.

Results

During 88 hours, 1980 m⁻³ lv of chips were harvested using three comminution systems. The percentage operation time (chipping, chip extraction, unloading, return to the clear-cut and change of workplace within a clear-cut area) using mobile chippers was 72 % (N-P/C), 77 % (P/C) and 71 % (P/R). Considering differences between N-P/C and P/C systems, the share of time of chipping was equal to 86 % in the case of non-piled residues and 92 % in the case of piled residues comparing to time of workplace change (14 % and 8 % respectively). Operation time for a single chipping cycle, production of 18 m⁻³ lv of chips (a full chipper load), ranged from 18.4 min (P/R) to 36.6 min (N-P/C) (Fig. 1). Statistical tests (T-test, $\alpha=0.05$, selected due to normal distributions of the data) showed significant differences of operational time among systems ($p=0.0000$).

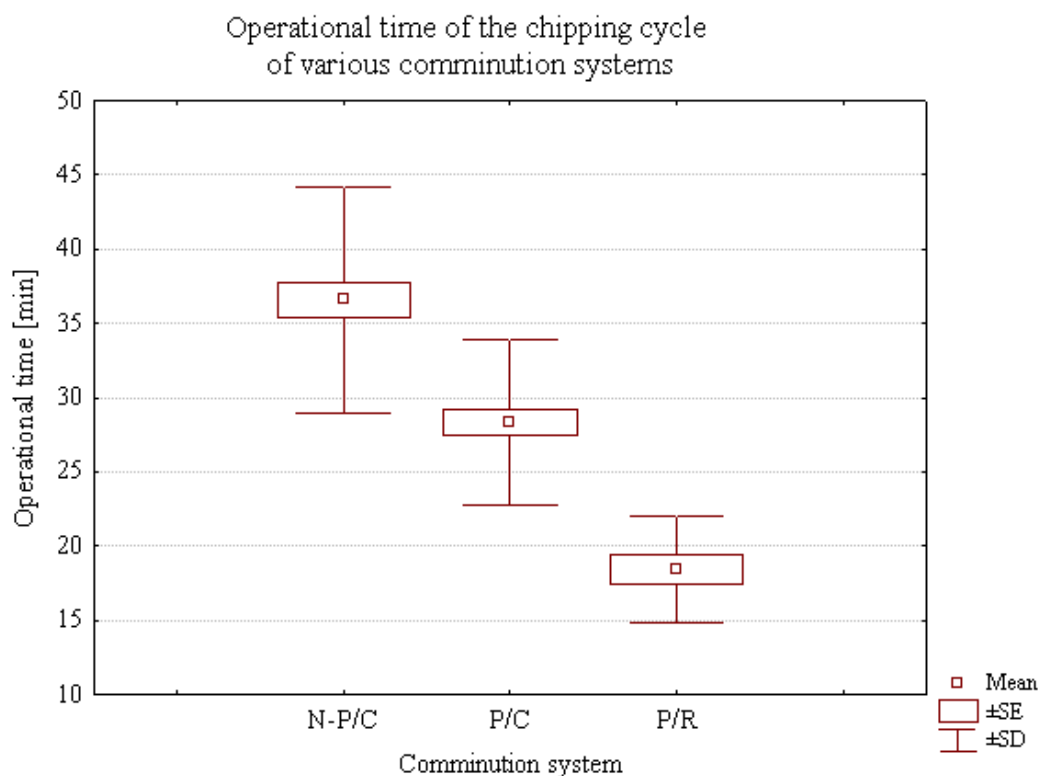


Figure 1. Operational time

The most time-consuming operation during mobile chipping was chipping itself in all systems used, ranging from 43 % to 58 %. Machine transportation time was between 10 and 17 %, and the breaks, a maximum of 2. The time spent on preparation of machines to work was equal in all cases (1%) (Fig. 2).



Figure 2. Operation duration (as percent of shift)

Operational productivity in the case of mobile chippers ranged from 29.6 m³ lv h⁻¹ (N-P/C) to 52.6 m³ lv h⁻¹ (P/R) (Fig. 3).

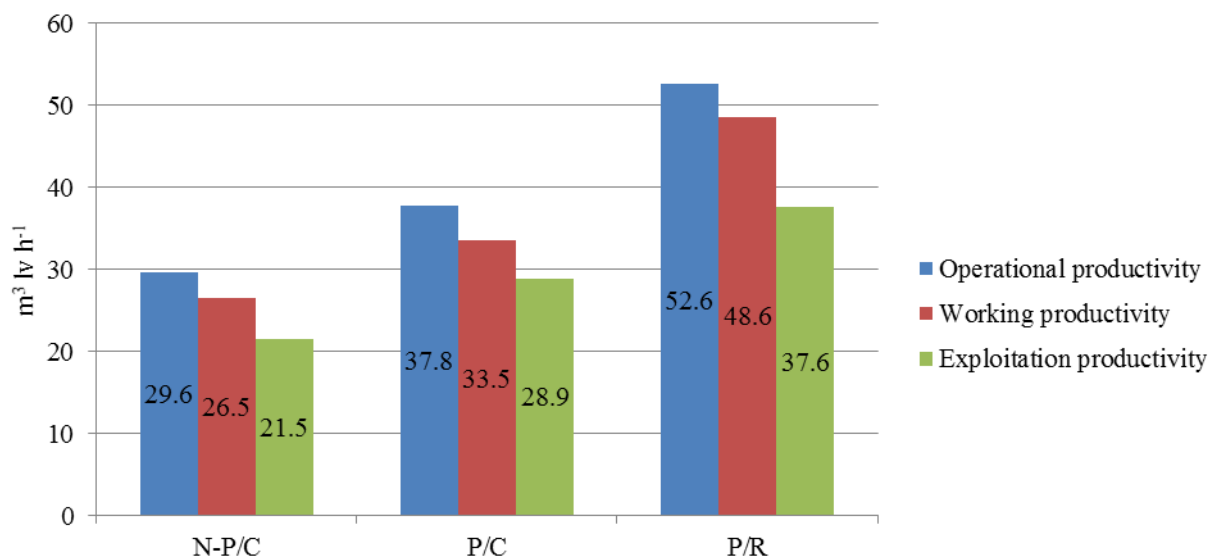


Figure 3. Mobile chipper productivity

A rake tractor (Ursus C-360) was used for piling residues on surface of the clear-cut. Raking (46 %), reversing (35 %) and change of workplace (11 %) were the most time-consuming activities. Breaks took 3 %.

Extraction of forest residues and piling at the roadside differed significantly (T-test, $\alpha=0.05$), depending on extraction mean ($p=0.0000$). Operational productivity of extraction of forest residues yielded 28.0 m³ lv (res.) h⁻¹ (Volvo BM Valmet 620), 75.4 m³ lv (res.) h⁻¹ (Ursus 1224 with the Palms 112 trailer) and 109.1 m³ lv (res.) h⁻¹ (Ponsse Elk) (Fig. 4). Predominating phases of the shift were loading (45 %), extraction (9 %), return to the clear-cut (9 %), change of workplace (9 %) and unloading (8 %).

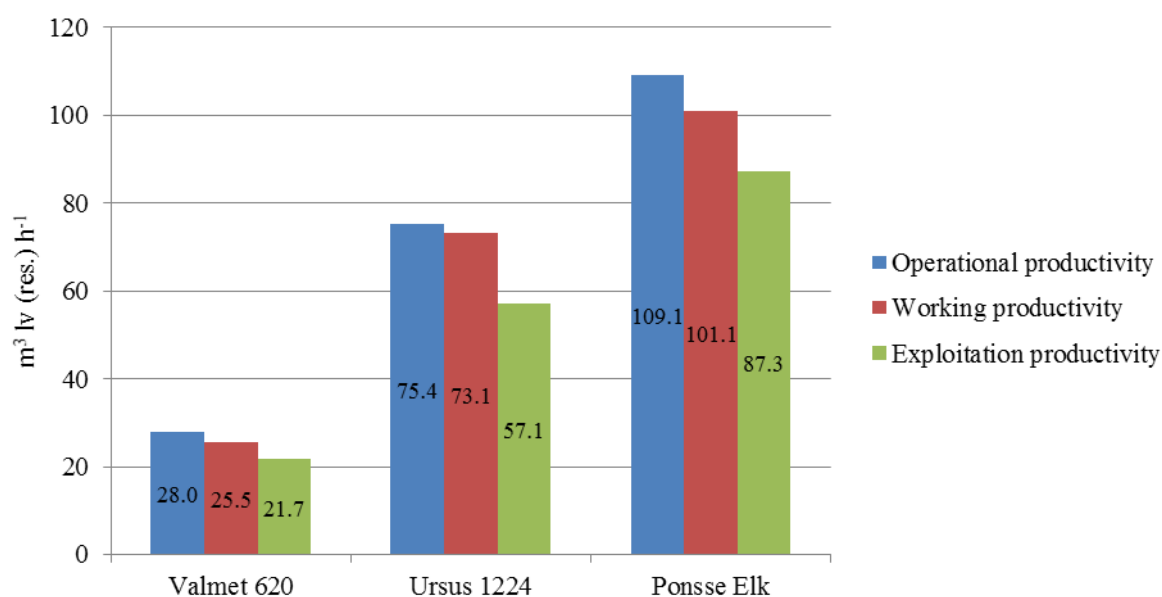


Figure 4. Productivity of residue extraction

The overall energy input was the greatest in the case of comminution of residues piled at the clear-cut surface, reaching $140.3 \text{ MJ m}^{-3} \text{ lv}$. Chipping at the roadside was slightly less energy-consuming ($139.9 \text{ MJ m}^{-3} \text{ lv}$) and chipping non-piled residues took $123.1 \text{ MJ m}^{-3} \text{ lv}$ (Fig. 5).

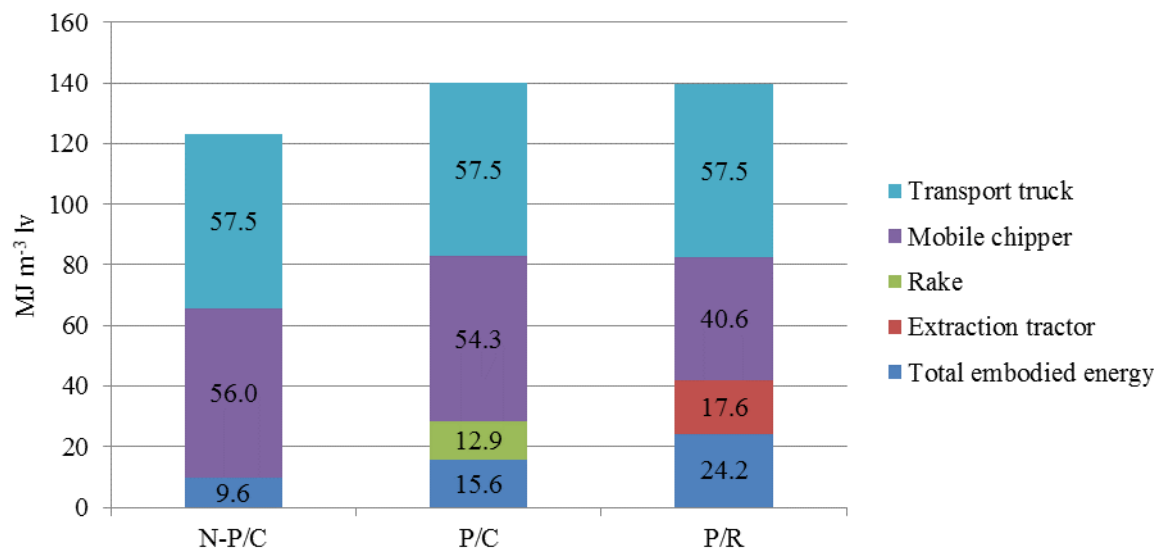


Figure 5. Input of energy inputs in comminution systems

Logging generated CO_2 emissions were $9.3 \text{ kg m}^{-3} \text{ lv}$, $8.5 \text{ kg m}^{-3} \text{ lv}$, and $8.4 \text{ kg m}^{-3} \text{ lv}$ respectively. Energy input was however significantly lower than energy generated in the oven of the power plant. Energy output was estimated at $3\,326.6 \text{ MJ m}^{-3} \text{ lv}$ from an oven equal of 84 % efficiency, with an average mass of $1 \text{ m}^3 \text{ lv}$ of chips of 333.0 kg of average moisture content of 37 %. The amount of CO_2 emitted during chip combustion was $434.7 \text{ kg m}^{-3} \text{ lv}$.

Discussion

Effective time of chipping in N-P/C system (43 %) is close to results gained by Cremer and Velazquez-Marti (2007) (38.8 %), but differences in P/R system are much more significant (49 % and 58.6 % respectively). Time of losses was smaller in the N-P/C than in P/R, as confirmed in literature quoted above.

The total energy input to the whole process of logging and transport of chips depended on the comminution system and ranged from $123.1 \text{ MJ m}^{-3} \text{ lv}$ to $140.3 \text{ MJ m}^{-3} \text{ lv}$. Estimated energy input was almost twice the value presented by Rózański and Jabłoński (2010), which was 191.39 MJ m^{-3} , but the difference result from the hauling distance (130 km in this study, compared with 50 km in the investigation mentioned above). It was also significantly larger than reported by Cremer and Velazquez-Marti (2007), however quoted researchers did not include long-distance hauling. The share of energy inputs to the P/R system is generally similar to results described by Rózański and Jabłoński (2010), although in their study, embodied energy was not calculated separately. Efficiency of chipping was about 30 % lower than reported by Rózański and Jabłoński (2009). Overall energy inputs in the case of P/C and P/R did not differ a lot ($0.4 \text{ MJ m}^{-3} \text{ lv}$). High level of inputs in the case of P/R was caused by difficult terrain conditions (slopes, muddy ground) in one of the locations (group shelterwood cutting in Pomorze Forest Inspectorate). That significantly enlarged fuel consumption.

The energy input – output ratio for chipping was between 3.7 % (N-P/C) and 4.2 % (P/C), similar to the results of Wihersaari (2005) (between 2.1 % and 2.6 %), Cremer and Velazquez-Marti (2007) (between 1.5 % and 2,0 %) or Marchi et al. (2011) (2.8 %) and lower than reported by Eriksson and Gustavsson (2010b) (12.4 %). CO₂ emissions were significantly higher (between 8.5 and 9.3 kg CO₂ m⁻³ lv) than those reported by Eriksson and Gustavsson (2010a) (about 3.3 kg CO₂ m⁻³ lv). Use of smaller number of machines in the case of N-P/C than in the case of P/C caused lower fuel consumption per unit of biomass, and therefore lower CO₂ emissions. Similar results were described by Marchi et al. (2011).

Chip transport figures as a major source of CO₂ emission (between 42 % and 47 %), confirming observations by Eriksson and Gustavsson (2010a).

The results do not significantly depart from those presented by other researchers, especially if the long haulage distance is considered. Average time for chip haulage (140 min for 130 km) was similar to those reported from Scandinavia (between Karelia and Finland) which averaged 97 min for 82 km (Goltsev et al. 2011). Fuel consumption of 0.6 l m⁻³ lv does not significantly differ from the European average (Schwaiger, Zimmer 2001).

In local conditions the least energy-consuming system for chip production seems to be for non-piled residues at a clear-cut surface (123.1 MJ m⁻³ lv). Its summary CO₂ emission is almost the lowest (only about 1 % higher than chipping at roadside). Nonetheless the operational productivity for chipping, being one of the most important components of the whole system, is the greatest in the case of roadside chipping, 52.6 m³ lv h⁻¹ (almost twice that for chipping of non-piled residues). Non-piled residue chipping at the clear-cut is organisationally simple, although transport must be punctual to avoid chipper idle time when waiting for chip transfer to haulage containers. There is no possibility of inter-operational storage of residues in any form. The system engages the fewest machines and employees so it may also be the cheapest method for biomass harvesting, although economics were not the focus of this paper.

Although Poland has a high index of energy self-sufficiency (above 80%), a steady decline of this value is projected over the next two decades to about 60% (IAEA 202). Increased biomass combustion should have a positive impact on fuel diversity that is beneficial to security of supply.

Conclusions

The greatest operational productivity for felling residue chipping was achieved at the roadside (52.6 m³ lv h⁻¹).

The least energy-consuming system was chipping of non-piled residues at the clear-cut surface, requiring 123.1 MJ to produce and deliver 1 m³ lv of chips.

For all comminution systems, transportation consumed more energy than any other input.

The lowest CO₂ emissions (8.4 kg CO₂ m⁻³ lv) were from chipping at the roadside.

All comminution systems are highly effective from the perspective of energy balance – energy input did not exceed 4.2 % of the energy generated by the biomass combustion.

References

- Athanassiadis D., Lidestav G., Nordfjell T., 2002: Energy use and emissions due to the manufacture of a forwarder. *Resources, Conservation and Recycling* 34 (2002): 149-160
- Cremer T., Velazquez-Marti B., 2007: Evaluation of two harvesting systems for the supply of wood-chips in Norway spruce forests affected by bark beetles. *Croatian Journal of Forest Engineering* 28(2007)2: 145-155
- Dempster P., Gallo N., Hartsough B., Jenkins B., Tittmann P., 2008: Final Report to State of California Department of Forestry and Fire Protection. Agreement Number 8CA05704
- Eriksson L., Gustavsson L., 2010a: Comparative analysis of wood chips and bundles – Costs, carbon dioxide emissions, dry-matter losses and allergic reactions. *Biomass and bioenergy* 34 (2010): 82-90
- Eriksson L., Gustavsson L., 2010b: Costs, CO₂ - and primary energy balances of forest-fuel recovery systems at different forest productivity. *Biomass and bioenergy* 34 (2010): 610-619
- Ericsson K., Nilsson L.J., 2006: Assessment of the potential biomass supply in Europe using a resource-focused approach. *Biomass and Bioenergy* 30 (2006): 1-15
- Ghaffariyan M.R., Brown M., Spinelli R., 2013: Evaluating Efficiency, Chip Quality and Harvesting Residues of a Chipping Operation with Flail and Chipper in Western Australia. *Croatian Journal of Forest Engineering* 34(2013)2: 189-199
- Goltsev V., Tolonen T., Syunev V., Dahlin B., 2011: Wood harvesting and logistics in Russia – focus on research and business opportunities. Working Papers of the Finnish Forest Research Institute No. 210, <http://www.metla.fi/julkaisut/workingpapers/2011/mwp210.htm>, accessed 19.12.2012
- Gustavsson L., Eriksson L., Sathre R., 2011: Costs and CO₂ benefits of recovering, refining and transporting logging residues for fossil fuel replacement. *Applied Energy* 88 (2010): 192-197
- Hakkila P., 2004: Developing technology for large-scale production of forest chips. Wood Energy Technology Programme 1999—2003. Technology Programme Report 6/2004
- Iarocci P., 2009: Biomass harvesting in Sweden. *Between the branches* No. 22: 4-7
- International Atomic Energy Agency, 2002: Comparative studies of energy supply options in Poland for 1997–2020. IAEA-TECDOC-1304, Vienna: 1-134
- Kofman P.D., 2010: Units, conversion factors and formulae for wood for energy. *Harvesting/Transportation* No 21, <http://www.coford.ie>, accessed 12.01.2012
- Liška S., Klvač R., Skoupý A., 2011: Evaluation of John Deere 1490D operation phase in typical conditions of the Czech Republic. *Journal of Forest Science* 57, 2011 (9): 394-400
- Marchi E., Magagnotti N., Berretti L., Neri F., Spinelli R., 2011: Comparing terrain and roadside chipping in Mediterranean Pine Salvaged Cuts. *Croatian Journal of Forest Engineering* 32(2011)2: 587-598

Moskalik T., Borkowska M., Sadowski J., Zastocki D., 2012: Efficiency of energy wood chip production from forest biomass. *Acta Scientiarum Polonorum, Silvarum*

Colendarum Ratio et Industria Lignaria 11(4): 27-36.

Róžański H., Jabłoński K., 2009: Economic effectiveness of logging residue bundling and chipping. *Acta Scientiarum Polonorum, Silvarum Colendarum Ratio et Industria Lignaria* 8(2) 2009: 47-51

Róžański H., Jabłoński K., 2010: Energy consumption in the production of chips and bundles from logging residues. *Acta Scientiarum Polonorum, Silvarum Colendarum Ratio et Industria Lignaria* 9(2): 25-30

Schwaiger H., Zimmer B., 2001: A comparison of fuel consumption and GHG emissions from forest operations in Europe, in Karjalainen T., Zimmer B., Berg S., Welling J.,

Schwaiger H., Finer L., Cortijo P., 2001 Energy, Carbon and Other Material Flows in the Life Cycle Assessment of Forestry and Forest Products. Results of Task 4, Working Group 1 (Production) in the COST Action E9. Discussion paper 10: 33-53

Sokołowski A. W., 2010: Puszcza Augustowska (*Augustow Primeval Forest*). CILP, Warszawa (in Polish)

Wartości opałowe (WO) i wskaźniki emisji dwutlenku węgla (WE) w roku 2011 do raportowania w ramach Wspólnotowego Systemu Handlu Uprawnieniami do Emisji za rok 2014, 2013: Opracowanie Ministerstwa Środowiska. Warszawa (*Heating values and emission factors in 2011 for reporting in European Emissions Trade System for 2014, 2013: Elaboration of Ministry of the Environment, Warsaw*) (in Polish)

Wihersaari M., 2005: Greenhouse gas emissions from final harvest fuel chip production in Finland. *Biomass and Bioenergy* 28 (2005): 435-443

Woods and Wood through the Ages of Western Culture – Our Wooden Heritage

Peder Gjerdrum

Abstract

Forests and timber always were integral parts of human life and society. That is evident already from the wide spread of similar words, e.g. tree, timber, birch and fir, indicating a common Indo-European origin thousands of years ago. The objective of this paper is to give a glimpse into the huge significance of wood and trees and forests and backwoods in our western society. Examples will be presented on wood and tree in word etymology and use in selected languages, poems and literature, mythology, folklore and tales, artefacts and art, tools and equipment, buildings and vessels, routes and bridges, defence and protection, heating, cooking and energy supply, mining and industry, rural life, hunting, pasturing, slash-and-burn and cultivation, etc., etc. all the way through society. Such examples and illustrations will be given from various geographic locations, from Mesopotamia via the Mediterranean and Alpine regions to Scandinavia, and from the Slavic domain via Finland and Britain to North America.

This topic should preferably be presented in a poster, offering space for a few sample texts from literature, graphs illustrating e.g. word relation and some drawings and pictures. Hopefully, such a presentation will even bring about new examples and input from other regions.

Key words: Forest, tree, timber, wooden tradition

Peder Gjerdrum
Dr.; senior scientist
Norwegian Forest and Landscape Institute
Section Wood Technology
Box 115
NO-1431 – Ås, NORWAY
+47 6494 9019 FAX: +47 6494 8001
peder.gjerdrum@skogoglandskap.no

FTIR-Study of Thermally Treated Beech Wood

Galina A. Gorbacheva^{1*} – *Anatoly V. Bazhenov*² – *Victor G. Sanaev*³ – *Ivica*

*Suchanova*⁴

¹ Associate Professor, Department of Wood Science, Moscow State Forest University, Mytischy, Moscow Region, Russia.

* *Corresponding author*

gorbacheva-g@yandex.ru

² Senior Researcher, Laboratory of Optical Strength and Diagnostics of Crystals, Institute of Solid State Physics of the Russian Academy of Sciences, Chernogolovka, Moscow Region, Russia.

bazhenov@issp.ac.ru

³ Professor and Rector, Moscow State Forest University, Mytischy, Moscow Region, Russia.

rector@mgul.ac.ru

⁴ Researcher, Department of Wood Science, Technical University in Zvolen Zvolen, Slovakia.

suchanovai@gmail.com

Abstract

Heat treatment is one of the perspective ways of wood modification. For developing new and improving existing technologies of heat treatment it is necessary to understand the changes in the structure of the wood at high temperatures. European beech (*Fagus sylvatica* L.) is one of the most common tree species in Slovakia. Beech wood samples were thermally modified at three temperature levels (160, 180, 200 °C) for 6 hours in air. Heat-treated and untreated samples were analyzed by Fourier transform infrared spectroscopy (FTIR). Most remarkable changes in peak area of the infrared absorbance spectra were found at 1502, 1592, 1650, 1238, 1370 и 1120 cm⁻¹. The influence of the heat treatment on chemical transformation in beech wood is shown.

Keywords: A. Beech Wood, C. Heat treatment, B. Fourier transform infrared spectroscopy (FTIR), A. Chemical transformation.

Introduction

Due to its mechanical and physical properties, the European beech (*Fagus sylvatica* L.) belongs to the most commonly used wood species at the different industrial sectors. However range of its applications is significantly reduced by its hygroscopicity. Thermal treatment seems to be one of the most perspective ways of its modification. Regardless of the large number studies of heat-treated wood (Babicki et al. 1977, Bekhta and Niemz 2003, Boonstra 2008, Boonstra et al. 2007, Gunduz et al. 2009, Hill 2006, Hofmann et al. 2008, Kocaefe et al. 2008, Majka et al. 2010, Salmen et al. 2008, Schwanninger et al. 2003, Skyba et al. 2009, Tajvidi and Mirzaei

2009, Windeisen et al. 2009), just a few of them are focused on the thermal treated beech wood (Babicki et al. 1977, Hofmann et al. 2008, Majka et al. 2010, Salmen et al. 2008, Schwanninger et al. 2003, Tajvidi and Mirzaei 2009). It is known that during exposition of wood to the high temperatures, chemical structure is being changed. This phenomenon results in weight loses, affects sorption properties of wood, decreasing swelling, wood density and mechanical properties. IR spectroscopy is one from the ways of investigation of wood structure. In the studies (Kocafee et al. 2008, Salmen et al. 2008, Schwanninger et al. 2003, Windeisen et al. 2009) changes at the wood structure of thermally treated wood by FTIR – spectroscopy are referred. In the work of Windeisen et al. (2009) analysis the influence of structural changes on the physical and mechanical properties of ash wood (EMC, MOE, MOR) was presented, Kocafee et al. (2008) analysed the influence on the mechanical properties of aspen and birch wood (MOE, MOR, hardness). However to make any detailed conclusions from the these results is very difficult, due to different chemical structure and natural variability of properties of different wood species, different processing conditions such as temperature levels, atmospheric parameters and duration of the heat treatment. Experimental research of physical properties (EMC, density, swelling, anisotropy of the swelling) of thermal treated beech wood were provided before (Suchanova and Gorbacheva 2012a, 2012b). Aim of this work is experimental study of the IR spectra of heat-treated beech for further determination of the relationship between the chemical treatment of wood components, heat treatment conditions and physical properties of wood.

Materials and Methods

Materials. The specimens were made from beech wood (*Fagus sylvatica* L.), which grows in the central part of Slovakia. Dimensions of the samples were 30×30×10 mm ($r \times t \times l$). The samples were dried to the absolute dry state at the temperature 103 +/- 2 °C, after that thermally treated in the environment dry air at three temperature levels - 160, 180 and 200 °C and treatment time 6 hours. Control samples (untreated) and thermally treated samples were investigated.

Sample preparation and FTIR –spectroscopy. FTIR-spectra were carried out with help of IR microscope of Fourier transform spectrometer IFS-113v. Thin longitudinal sections were prepared for FTIR-measurements. The transmittance spectra (T) of thin longitudinal sections of beech wood were measured at T=300 K. The area of section of diameter 80 µm was studied in the spectral range of 600-5000 cm⁻¹ with a resolution 4 cm⁻¹. Sections with thickness approximately of 20 µm were chosen. From transmittance spectra (T) the absorbance spectra (A) were calculated according to:

$$A = -\ln(T) \quad (1)$$

here, $A = kd$, where k is absorption coefficient, d is thickness of wood film.

Monotonous baseline was subtracted from the absorption spectra to remove the contribution of light scattering. The spectra were normalized at the intensity of the absorption line 1738 cm⁻¹.

Results and discussions

Figure 1 shows the absorption spectra of control and heat-treated samples in a wide spectral range containing the absorption lines, due to vibrations of the atoms of the wood. Very high absorption is observed for lines around 3400 cm⁻¹ (vibration of O-H bonds) and lines around 1100 cm⁻¹. Therefore, we exclude them from the analysis. The most notable changes are observed for the absorption lines in 1502, 1592, 1650, 1238, 1370 and 1120 cm⁻¹.

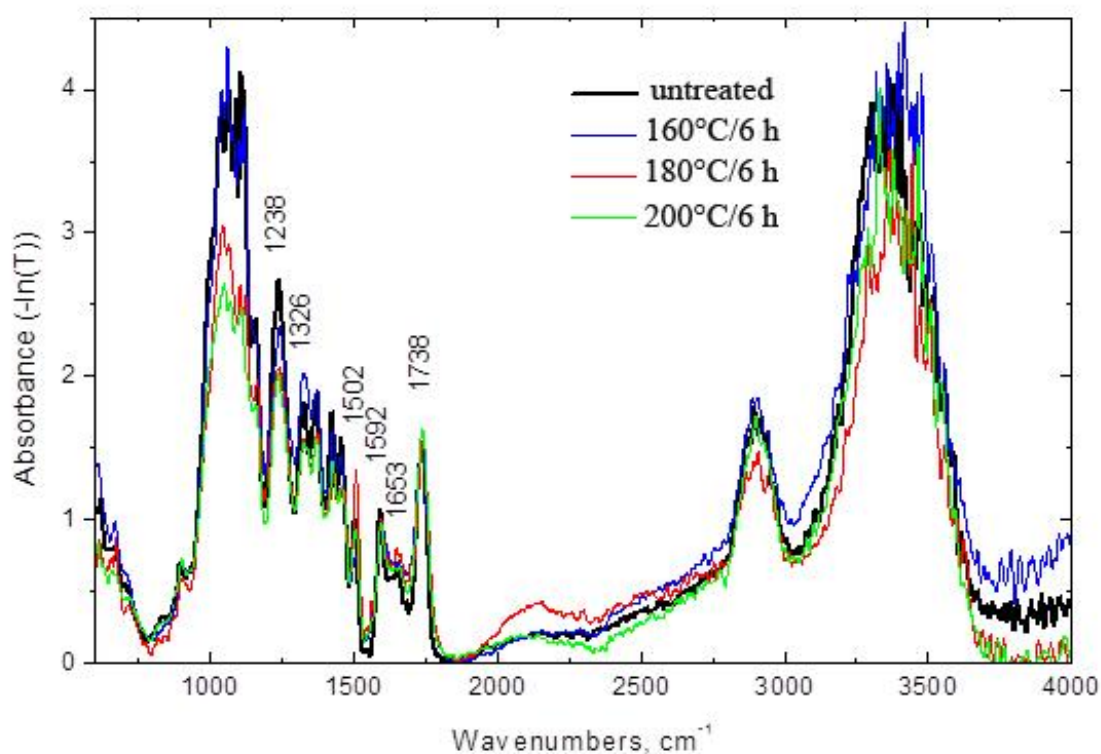


Figure 1. Absorption spectra of control and heat-treated samples of beech wood

The absorption spectra of control and heat-treated beech wood samples in the spectral range 1400-1800 cm^{-1} are shown in Figure 2. Lines 1502 and 1592 cm^{-1} are related to the lignin. In the paper (Karklin and Oherina 1975), this line was interpreted as a overlap of the two lines: 1495 cm^{-1} and 1515 cm^{-1} . This situation is the coexistence of two lines which is visible in Figure 2, in the spectrum of the specimen treated at the temperature 160 °C and duration 6 hours.

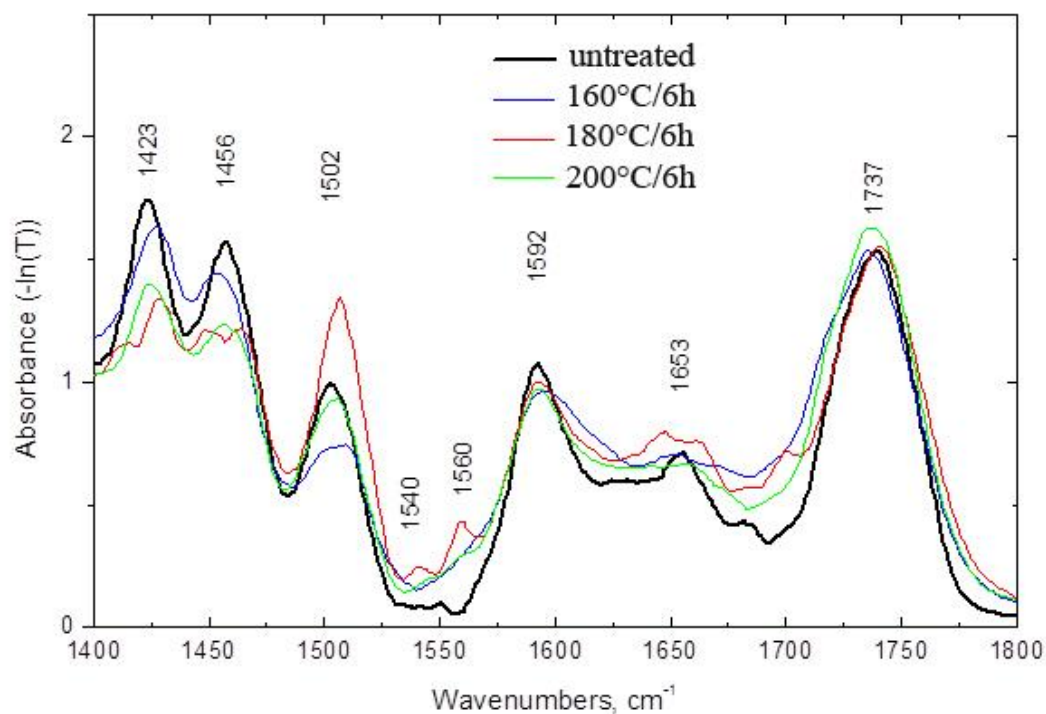


Figure 2. Absorption spectra of control and heat treated samples of beech wood in the spectral range of 1400-1800 cm^{-1}

For heat-treated beech wood (Salmen et al. 2008), birch and aspen wood (Kocafe et al. 2008) significant changes in the intensity of absorption lines 1508 and 1507 cm^{-1} , respectively, which increased with maximum heat treatment, were indicated.

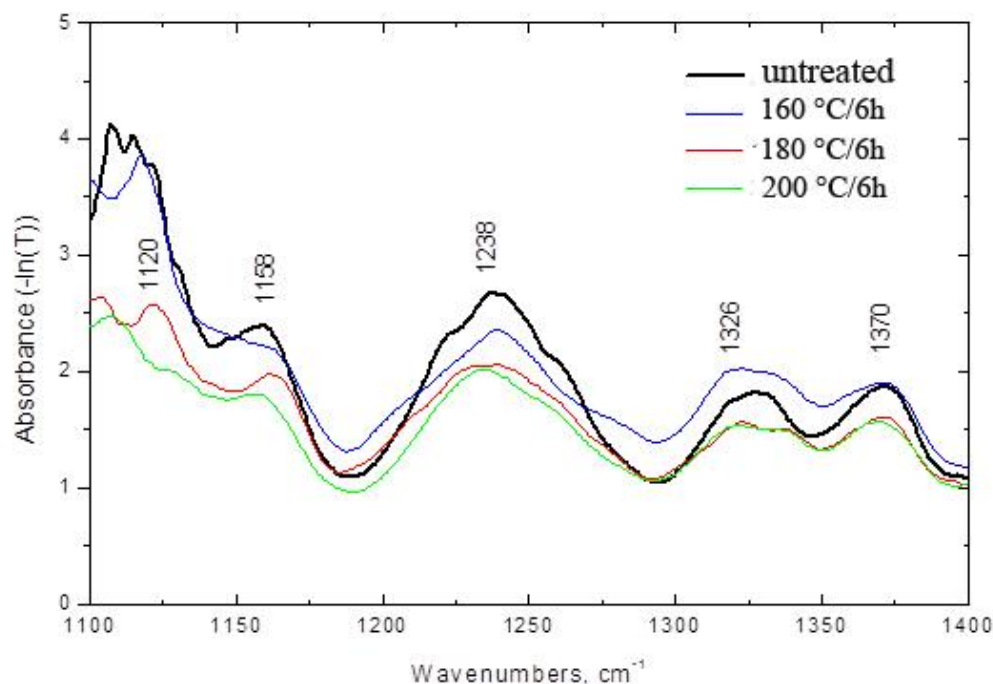
Line 1592 cm^{-1} , which contribute to lignin (69%) and holocellulose (31%), was considered in the study (Karklin and Oherina 1975). It was found that it is weakly dependent on the processes occurring during delignification. In our case, Figure 2 shows a significant high-energy broadening of this line as a result treatment of beech wood at 160 °C, indicated the transformation of lignin.

Schwanninger et al. (2003) for beech wood also described huge shift from 1507 to 1516 cm^{-1} and notable shift from 1595 to 1610 cm^{-1} with smaller decrease in intensity. For ash wood (Windeisen et al. 2009) slight shifts (1600, 1505 cm^{-1}) are noted.

Absorption line around 1650 cm^{-1} is caused by absorbed water. The splitting of the line is observed in the spectrum of the samples, treated at the temperature 180 °C. Perhaps it is caused by exposure of the heat-treated samples in ambient atmospheric conditions before the measurement of IR spectra. (Karklin and Oherina (1975) explained an absorption line 1737 cm^{-1} by hemicellulose contributions – 61 %, lignin – 25 % and the cellulose - 14%. In our case for beech wood such changes were not observed (Fig. 2, line 1737 cm^{-1}). Furthermore, in this study, this line was selected for normalization of spectra.

As a result of thermal treatment of ash wood (Windeisen et al. 2009) was found that for absorption lines 1730 cm^{-1} , corresponding to the light absorption by carbonyl and carboxyl groups, decrease of peak intensity, increasing the linewidth and its low-energy shift were observed. In the study of Schwanninger et al. (2003), was found a slight decrease in the intensity of the 1742 cm^{-1} at 205 °C and very fast intensity at the treatment temperature 220 °C, followed by shift of the line to 1733 cm^{-1} , due to release of the acetyl groups from hemicellulose. In the

study (Salmen et al. 2008), increasing the intensity of the 1735 cm^{-1} is explained by the contribution of xylan.



Figure

3. Absorption spectra of control and heat treated samples of beech wood in the spectral range of $1100\text{-}1400\text{ cm}^{-1}$

According to Karklin and Oherina (1975), the absorption lines 1238 and 1370 cm^{-1} by 70% and 80% are respectively related by holocellulose. From Figure 3 it is evident that its intensity is monotonically decreased as a result of heat treatment. The intensities of these lines are reduced by approximately 25 % when going from a control sample to treated sample at $200\text{ °C}/6$ hours. This indicates at least partial destruction holocellulose by thermal treatment.

For ash wood (Windeisen et al. 2009) the intensity of the absorption line 1245 cm^{-1} (it is characteristic of acetyl groups in hardwoods) significantly decreased as a result of thermal modification of wood, and the low-energy shift of the line was observed. Schwanninger et al. (2003) also described the decrease of intensity of the line 1245 cm^{-1} .

The absorption spectra show that the absorption line 1238 cm^{-1} (Fig. 3) in the spectrum of beech wood is an analogue of the absorption line 1245 cm^{-1} in the absorption spectrum of ash. In our case for beech wood changes of this absorption line is not so radical as for ash wood (Windeisen et al. 2009). Salmen et al. (2008) observed increasing the intensity in the range $1200\text{-}1285\text{ cm}^{-1}$, significant for the most heavily heat treatment, with a maximum duration.

For thermo-treated birch and aspen wood intensities of lines 1244 cm^{-1} diminish with increasing of treatment temperature (Kocaeffe et al. 2008). Small decrease of the line 1376 cm^{-1} was noted for beech wood (Schwanninger et al. 2003), and line 1373 cm^{-1} for birch wood (Kocaeffe et al. 2008).

Intensities of the rest bands in range 1100-1400 cm^{-1} (Fig. 3) decrease after heat treatment. It is worthy of note radical changes in intensity of line 1120 cm^{-1} . After thermal treatment it is shifted to high energy and becomes very weak in the samples treated at 200 °C / 6 h.

Karklin and Oherina (1975) noted that light absorption in this area of a range is more caused by carbohydrate part of wood and significantly smaller the lignin. Taniguchi et al. (1968) found that the intensities of the absorption lines 1110, 1060, 1040 cm^{-1} increase due to the desorption of water from wood. According to the authors (Taniguchi et al. 1968), this indicates an increase in the degree of orientation in the amorphous regions of cellulose due to the reorientation of the molecular chains in the wood as a result of desorption. In our case, we got the opposite result at this heat treatment schedule. Schwanninger et al. (2003) also reported about changes in range 1000-1200 cm^{-1} , they supposed that such changes do not depend on the moisture content of wood and could be due to extraction effects, volatile compounds will be liberated. It should be noted that in all the absorption spectra, without regard to wood species and schedule of thermal treatment, marked changes in the intensities of line in range 1502-1508 cm^{-1} («lignin band») related to the modification of lignin, and 1238-1245 cm^{-1} related with the decomposition of hemicelluloses.

Conclusions

1. High-temperature treatment of beech wood (*Fagus sylvatica L.*) changes its chemical structure. Disordering of bonds in the system of lignin and holocellulose, the transformation of lignin, holocellulose decomposition mainly due to decomposition of the hemicellulose were observed. It is reflected in changes of the intensities of the absorption lines 1502, 1592, 1650, 1370, 1238 and 1120 cm^{-1} .
2. For beech wood treated at our thermal conditions changes in the carbonyl and carboxyl groups (absorption line 1730 cm^{-1}) were not detected.
3. Absorption lines in the spectral range 1502-1508 cm^{-1} and band near 1238-1245 cm^{-1} are most sensitive to increased temperatures for different wood species and heat treatment methods.
4. Understanding the changes occurring in the structure of wood when exposed to higher temperatures, is necessary for the development of new technologies and improvement of existing technologies for heat treatment of wood, technological processes of wood processing, but also allows establishing effective wood composites.

References

- Babicki, R., Grzeczyński, T., Wróblewska, H. 1977. Effect of hydro-thermal treatment of green beech wood on its chemical and physico-mechanical properties. *Wood Science and Technology*. 11 (2): 125–131.
- Bekhta, P., Niemz, P. 2003. Effect of High Temperature on the Change in Color, Dimensional Stability and Mechanical Properties of Spruce Wood. *Holzforschung*. 57(5): 539–546.
- Boonstra M. A. 2008. Two-stage Thermal Modification of Wood. PhD Thesis University Ghent.
- Boonstra, M., Van Acker, J., Kegel, E., Stevens, M. 2007. Optimization of a two-stage heat treatment process: durability aspects. *Wood Science and Technology*. 41(1): 31-57.

- Gunduz, G., Aydemir, D., Karakas, G. 2009. The effects of thermal treatment on the mechanical properties of wild Pear (*Pyrus elaeagnifolia* Pall.) wood and changes in physical properties. *Materials and Design*. 30: 4391–4395.
- Hill, C. 2006. *Wood Modification. Chemical, Thermal and Other Processes*. Wiley, Chichester.
- Hofmann, T., Retfalvi, T., Albert, L., Niemz, P. 2008. Investigation of the chemical changes in the structure of wood thermally modified within a nitrogen atmosphere autoclave. *Wood Research*. 53(3): 85 – 98.
- Karklin, V.B., Oherina, E. A. 1975. IR-spectroscopy of wood and its main components. *Wood Chemistry*. 4: 49-58. (in Russian)
- Kocaefe, D., Poncak, S., Boluk, Y. 2008. Effect of thermal treatment on the chemical composition and mechanical properties of birch and aspen. *BioResources*. 3 (2): 517-537.
- Majka, J., Weres, J., Olek, W. 2010. Aliteration of wood hygroscopic properties after thermal modification. In: *Proceedings, Wood Structure and Properties '10*, edited by J. Kudela & R. Lagana, 2010, Arbora Publishers, Zvolen, Slovakia.
- Salmen, L., Possler, H., Stevanic, J.S., Stanzl-Tschegg, S.E. 2008. Analysis of thermally treated wood samples using dynamic FT-IR-spectroscopy. *Holzforschung*. 62: 676–678.
- Schwanninger, M., Gierlinger, N., Hanger, J., Hansmann, C., Hinterstoisser, B., Wimmer, R. 2003. Characterization of Thermally Treated Beech Wood by UV - Microspectrophotometry, FT-MIR and FT-NIR Spectroscopy. In: *Proceedings of 12 the ISWPC*, Madison, WI.
- Skyba, O., Niemz, P., Schwarze, F. W. M. R. 2009. Resistance of thermo - hygro - mechanically (THM) densified wood to degradation by white rot fungus. *Holzforschung*. 63: 639–646.
- Suchanova, I., Gorbacheva G.A. 2012. The influence of heat treatment on the density and swelling of beech wood (*Fagus sylvatica* L.). *Moscow State Forest University Bulletin – Lesnoj Vestnik* 2(85): 154-158. (in Russian)
- Suchanova, I., Gorbacheva G.A. 2012. The sorption of thermal treated of beech wood (*Fagus sylvatica* L.). *Moscow State Forest University Bulletin – Lesnoj Vestnik*. 2(85): 159-161. (in Russian)
- Tajvidi, M., Mirzaei, B. 2009. Effects of temperature on the mechanical properties of beech (*Fagus orientalis* Lipsky) and lime (*Tilia begonifolia*) wood. *Wood Material Science and Engineering*. 4 (3-4): 147–153.
- Taniguchi, T., Yoshimi, S., Harada, H., 1968. Changes in the infrared spectra of wood produced by desorption of water. *Bull. Kyoto Univ. For.* 40: 301-306.
- Windeisen, E., Bächle, H., Zimmer, B., Wegener, G. 2009. Relations between chemical changes and mechanical properties of thermally treated wood. *Holzforschung*. 63: 773-778.

US Forest Sector Innovation during the Great Recession

Eric Hansen

Professor of Forest Products Marketing
Department of Wood Science and Engineering
College of Forestry
Oregon State University
119 Richardson Hall
Corvallis, OR 97331
Eric.Hansen@oregonstate.edu

Abstract

The recent global recession has focused efforts toward better understanding firm response, and the outcome of that response, to recession. Firms tend to respond by being conservative, reducing costs, etc., or, proactively innovating. Data were collected from US forest sector manufacturing firms (SIC 24) in early 2013. In total, 142 valid responses were received, corresponding to an adjusted response rate of slightly over 15 percent. Respondents provided insights regarding the current innovativeness level of their firms as well as the level prior to the recession. Results show that innovativeness has important performance implications even in dire economic times. However, increasing innovativeness levels during decline is not shown to be superior to maintaining innovativeness. Findings provide limited evidence that decreasing innovativeness is not a desirable downturn strategy. Potential practical and theoretical implications of the findings are presented.

Key words: innovation, forest sector, Great Recession

Industry Perspectives on Wood as a Structural Green Building Material

Alyson Wade, Arijit Sinha, Chris Knowles

Oregon State University
Corvallis, OR, US

Abstract

Green building is becoming an increasingly popular trend around the world, creating positive growth in green building materials markets. The purpose of this research is to understand the role of wood as a green building material in the structural system of new buildings. The study also aims to identify areas in which information is lacking with respect to reducing the environmental burden of structural building materials and to identify gaps in access to or availability of green building materials. Semi-structured group interviews composed of industry professionals representing all stages of the design and build process (i.e. architects, engineers, contractors) and experiences in different scales and functionalities of buildings will be utilized to gather information for this study. Interviews will be conducted in different regions of Oregon, USA where the most growth is occurring including the Portland metropolitan region, Corvallis, Eugene, and Bend. Results will focus on the role of green building rating systems in material selection, resources used by industry professionals to research green building materials, and understanding constraints and biases against using wood for structural systems of green buildings.

Keywords: rating systems, green material availability, gap analysis

Alyson Wade, Alyson.wade@oregonstate.edu, 704-798-6380
Arijit Sinha, Arijit.sinha@oregonstate.edu, 541-737-6713
Chris Knowles, Chris.knowles@oregonstate.edu, 541-737-1438
Oregon State University
Department of Wood Science and Engineering
Richardson Hall
FAX: 541-737-3385

Incorporating Experiential Learning and Education for Sustainable Development into Study Abroad Programs

Henry J. Quesada-Pineda^{1} – Eva Haviarova²*

¹ Associate Professor, Department of Sustainable Biomaterials, Virginia Tech, 1650 Research Center Drive, Blacksburg, VA 24061 USA.

*Correspondant author (quesada@vt.edu)

² Associate Professor, Department of Forestry and Natural Resources, Purdue University, 175 Marsteller Street, West Lafayette, IN 47907 USA.

ehaviar@purdue.edu

Abstract

The goal of this study is to demonstrate the teaching effectiveness of incorporating experiential learning theory in a sustainability study abroad program. Although there is a large body of published research on sustainability, study abroad programs, and experiential learning, there is no research on how to effectively connect the three topics in a higher education course. The course was designed with the goal to introduce students enrolled in natural resources curricula to issues impacting the sustainability of natural resources in developing countries. Twenty-five activities were designed based on experiential learning theory principles. During the first part of the course, the delivered activities were designed to provide students with theory and facts about the topics being studied. During the field trip, the second part of the course, the activities that were conducted by the students focused on concrete experiences and active experimentation. Finally, students conducted activities categorized as reflective observation after students returned from the field trip. Dominant learning styles were determined for each student and statistical tests indicated that accommodating (concrete experience and active experimentation) was the most common dominant learning style in the group. Results of the student perceptions on the learning effectiveness of the course activities show that four activities were rated as moderate effective and 21 were rated as highly effective in helping the students to understand sustainability. This work successfully demonstrated the incorporation of experiential learning theory into a study abroad program while teaching sustainability and also provides a template for other potential study abroad programs.

Keywords: Experiential Learning; Education for Sustainable Development; Study Abroad Programs

Introduction

Sustainability continues to be a complex topic in higher education teaching (Wright, 2000, Fien and Tilbury 2002, and Blewitt and Cullingford 2012,) and today's trend is to incorporate sustainability either as a partial component of University's courses or as whole course (Wals and Jickling, 2002). Either way, the main challenge for university teachers is to create a course that is meaningful from the student's personal, civic, and academic perspectives where students can learn to develop critical reflection and potentially get engaged in sustainability actions. One way of overcoming this challenge and to create an effective way to teach sustainability is to design and deliver courses in education for sustainable development (ESD) through study abroad programs (Dunning, Meilan, and Jacobs, 2008). As UNESCO (2013) indicates, ESD promotes exemplary critical thinking, requires participatory teaching, and empowers learners with the goal to change behavior and engage in sustainability actions.

The domino effect of human actions can only be appreciated in many instances if sustainability students have the opportunity to experience how other cultures and geographical regions deal with the same issues (Hallows, Wolf, and Marks 2011). Therefore, study abroad programs could provide students with a great dose of experiential learning and even bigger opportunities to immerse in another culture (Hopkins, 1999). Furthermore, Kitsantas (2004) and Wilson (1982) reported that study abroad programs improved cross-cultural skills and global understanding of the studied topic. In a similar study by Chieffo and Griffiths (2004), the researchers concluded that even short-term study abroad programs have significant self-perceived impacts on students' intellectual and personal lives.

Even though study abroad programs might provide a good fit for ESD in a global context, Wals and Jickling (2002) stated that teaching sustainability in higher education requires enhancing the quality of the learning process by incorporating new teaching methods such as an experiential learning theory (ELT). Minnich (1999) indicated that one of the most important advantages of study abroad programs is that students learn by-doing almost all day. Hence, the incorporation of ELT seems to be a logical fit for effectively teaching sustainability through study abroad programs and the benefits of incorporating ELT into teaching programs have been reported in recent studies (Gitsham, 2012, MacVaugh and Norton, 2012).

Although there are a large number of publications related to study abroad programs (ESD, experiential learning, and learning styles), none of them seems to connect these three aspects in a meaningful and practical way. Domask (2007) reported that even though experiential learning in study abroad programs has a lot of benefits, higher education institutions are not incorporating this approach as they should be.

Approach

This paper focuses on the impact of incorporating ESD and ELT into a study abroad course as a way to increase students' learning on the topic of sustainability. While learning is a change in knowledge, beliefs, behaviors or attitudes (Ernest 1948), teaching focuses more on the skills and approaches that teachers need to develop to deliver meaningful knowledge to students (Gary and Soltis 1986). Although, both teaching and learning are very close related; measuring teaching effectiveness is not the objective of this paper.

What is the meaning of ESD (Education for Sustainable Development)? Current environmental issues such as forest depletion, greenhouse emissions, and pollution levels require solutions that could be created by increasing education, awareness, and training in sustainability.

What is the meaning of ELT (Experiential Learning Theory)? In the context of experiential learning, learning is defined as the process whereby knowledge is created through the transformation of experience. There are two ways of grasping experience: concrete experience and abstract conceptualization; and two ways or modes of transforming experience: reflective observation and active experimentation.

Current Gap and Factors impacting implementation of ESD and ELT: Inconsistent and unsystematic approach; financial support; logistic problems; unfit for curricula; little preparation of teachers; willingness and time allocation by universities; no real incentive or punishment for faculty.

Goal and Hypothesis

Hence, the goal of this paper is to provide a case study that describes and tests the effectiveness of ESD in study abroad course that incorporates ELT in the course design. This goal leads to the following null hypothesis:

H₀: ESD and ELT can be incorporated into a study abroad program for effective learning.

Methodology

Course description and recruiting. “Global Issues in Sustainability: Study Abroad in Costa Rica” is a three-credit hour course taught each semester at Virginia Tech by the Department of Sustainable Biomaterials and also adopted by the Department of Forestry and Natural Resources at Purdue. The goal of the course is to expose students from the College of Natural Resources and Environment and College of Agriculture to issues that impact the use and management of natural resources in an apparent high-ranked sustainable country. The course includes a field trip to Costa Rica, one of the most sustainable and environmentally friendly countries according to private and public organizations (YCELP, 2013 and NEF, 2013). A detailed review of the course design can be found in Quesada, Adams and Hammet (2010). Recruiting is conducted through different outlets such as emailing, study abroad fairs, and information sessions. The class is open for all majors but students are selected based on an application process where a statement of purpose, transcripts, and letters of recommendation are used to select the best candidates. Also, students will have to cover the cost of the trip. In some cases scholarships or stipends are provided depending on availability of funds.

Activities designed for the Global Issues in Sustainability Course. The designed activities for this class consider sustainability topic suggested by (Blewitt and Cullingford, 2012 and Shriberg, 2002) and the importance of traveling abroad to better understand the concept in study (Chieffo and Griffiths, 2004). The connection between Kolb’s four-mode learning cycles and the activities implemented in this course are shown in Figure 1.

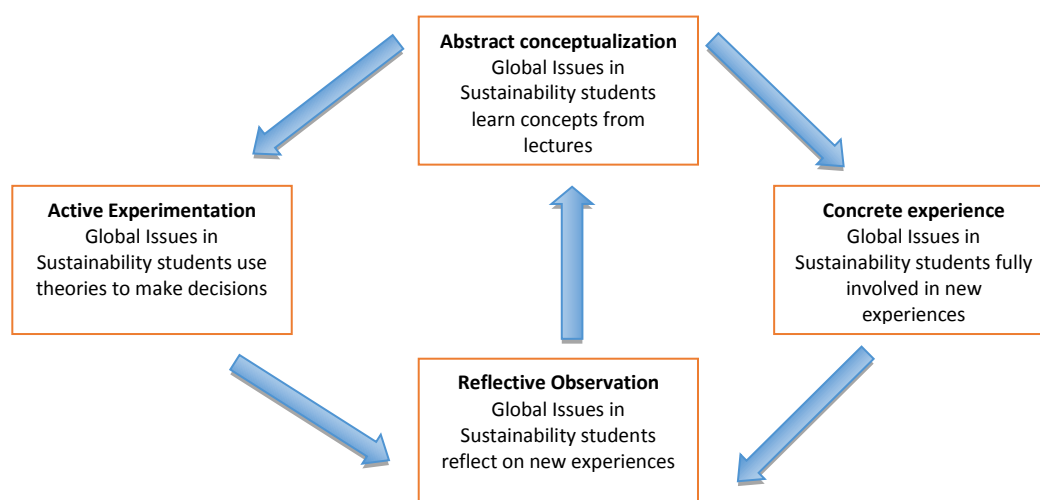


Figure 1. Relationship between Kolb's mode learning cycle and activities implemented in this course. The list of activities and their classification using Kolb's learning cycle is shown in Table 1. A total of 11 activities were designed to introduce the students to the most relevant concepts and theories related to the sustainability of natural resources and classified as abstract conceptualization activities.

Table 18. List of specific activities classified by Kolb's learning cycle

#	Issue/Theme	Goal	Classification
1	Introduction to Sustainability	Introduce students to sustainability	Abstract conceptualization
2	Sustainability update in Costa Rica	Highlight main aspects related to sustainability in Costa Rica	
3	Journal writing tips	Guidelines based on articulated learning for journal writing	
4	Water sanitation	Current issues impacting water sanitation	
5	Forestry issues in Costa Rica	Main aspects impacting forest management in Costa Rica	
6	Wood Products in Costa Rica	A review main wood products produced in Costa Rica and the current status of the industry	
7	Biology in Costa Rica	Biology's history in Costa Rica, main species, and current issues impacting wildlife in Costa Rica	
8	Ecotourism	Definitions and connection of ecotourism with pedagogy	
9	Waste management	Introduction on main practices for managing waste in tourist resorts	
10	Arenal hydroelectric power project	Description of the main hydroelectric power project in Costa Rica based on use of water, before, during, and after power is generated	
11	Introduction to Life Cycle Analysis	Introduction of a quantitative technique to measure impact of products and processes to human health, ecosystems, and the environment.	
12	Visit to Irazu Volcano National Park	Experience how the Costa Rican Park System manage its national parks	Concrete Experience
13	Hot Springs	Enjoy hot springs in a sustainable resort	
14	Visit to Fortuna Waterfall	Experience how local communities manage natural resources for profit and preservation of the environment	
15	Zip lining	Explore the forest from zip lines and observe how a private company can profit from the forest	Active Experimentation
16	EcoTec experience	Use of climate change's theories to explain changes in crocodile and butterfly populations and impact of the reduction of tropical forests on temperatures	
17	Wind power generation	Use of wind power to generate clean electricity	
18	Turtle hatchery	Exhumation of turtle nest to explain potential reasons for hatching failure	
19	Star finding	Use of astrology maps to locate stars, planets, and constellations in a non-polluted location	

20	Downtown tour of San Jose	Opportunity for students to observe the way of life, architecture, and people behavior in downtown San Jose	Reflective observation
21	Wildlife refuge	Guided-tour of a wildlife refuge to encourage student's reflections on how wild animals are impacted by human behavior	
22	Flooring mill tour	Guided-tour of a flooring manufacturing process to encourage student's reflection on use of renewable materials for the manufacturing of goods	
23	Plantation tour	Guided-tour of a fast-growth tropical species plantations to encourage student's reflections on the use of plantation wood vs. natural grown wood	
24	Field trip highlights and final reflections	Students' presentations to highlight and reflect on their most significant learning from the field trip	
25	Comparison between Costa Rica and Virginia	Students' presentations to introduce and compare sustainability initiatives between Costa Rica and Virginia	

Student's learning styles. Students' learning styles were determined at the start of the semester in order to get a better idea of the dominant learning style for the class. This was critical in order to make adjustments to the already designed activities. The instrument to determine learning styles was based on Kolb methodology (1984).

Descriptions of learning styles:

- Diverging: People in this category are imaginative, emotional, and tend to specialize in arts.
- Assimilating: Less focused on people and more interested in ideas and abstract concepts.
- Converging: People classified under this category are very good in finding practical uses for ideas and theories.
- Accommodating: Individuals with accommodating as the dominant learning style, have the ability to learn from hands-on experiences.

Determination of learning effectiveness of designed activities. Students rated all activities in Table 1 in terms of their effectiveness in helping them to understand sustainability. A five-point scale (not effective, a little effective, average effective, moderate effective, and highly effective) was used to rate statistically each activity. The Wilcoxon signed rank test for nonparametric data was used to test the null hypothesis (H_0 : *ESD elements and ELT can be incorporated into a study abroad program for effective learning*). The statistical procedure is testing if the rankings were equal or higher than 4. Activities ranked as four are considered moderately effective and the ones ranked as five are considered highly effective.

Evaluation of articulated learning. In addition to the rating of the effectiveness of the designed activities in understanding sustainability, students were asked to indicate their most significant learning outcome as well as to indicate how it was learned and to provide the main reasons why it matters. Finally, students were asked to indicate in what ways they will use their gained knowledge.

Data analysis. Nonparametric statistic tests were performed using the statistical package SAS. These tests were used to identify which activities were the most effective in helping students to understand sustainability. Also, learning style scores were analyzed and compared using statistical comparisons in order to point out the most dominant learning styles. The student's answers on articulated learning were analyzed using qualitative analysis techniques in order to better understand how students plan to engage in sustainability activities.

Sample description. 14 students (10 females, 4 males); 2 freshman, rest in senior or junior level; 10 from NRE, 2 in Liberal Arts, 1 in Engineering, and 1 in Agricultural Sciences.

Course implementation

Part 1: lectures at VT (6 weeks)

Part 2: excursion to Costa Rica (9 day) - lectures from Costa Rica Tech, industry visits, experiments and tours.

Part 3: analysis and reflexion at VT (6 weeks)

Results

Figure 2 shows the dominant learning styles by student where the majority of students (N=14) had an accommodative (active experimentation and concrete experiences) dominant learning style. Students that have characteristics of an accommodative learning style as the dominant style, emphasize greatly in concrete experience and active experimentation. The greatest strength of this style or orientation lies in doing things, formulating plans, and getting involved in new experiences.

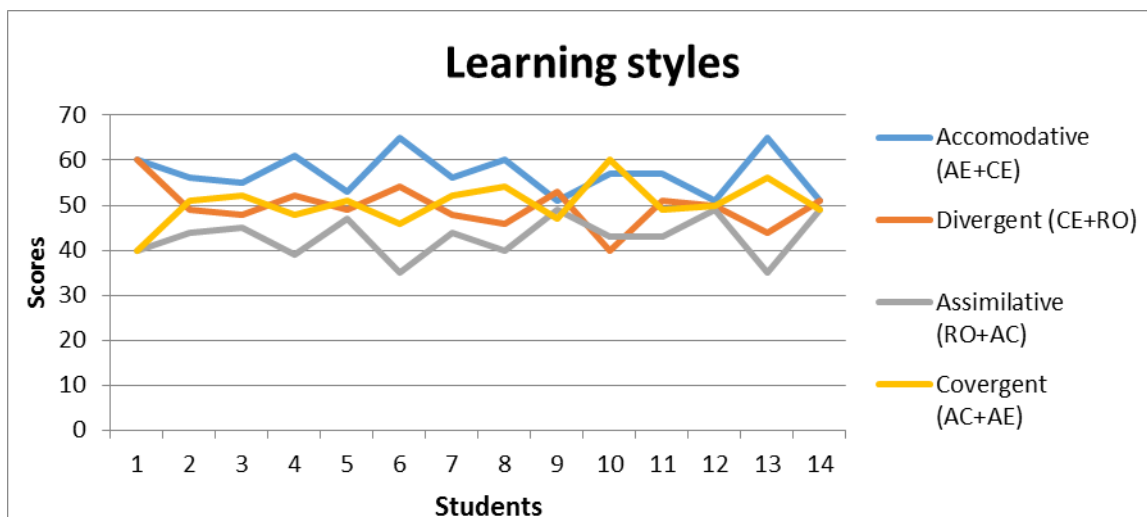


Figure 2. Students' learning styles.

Learning effectiveness of designed activities. The most significant result is that all activities except four (Water sanitation, Biology in Costa Rica, Downtown tour of San Jose, and Ecotourism) have a mode of 5 (highly effective). For all the other activities, the mode was 5. Among highly effective activities were EcoTec experience; Wind power project; Flooring mill tour; and Star finding.

Articulated learning. Students were asked to indicate their most significant learning from the course. The "Waste management" activity was cited by three students as the most significant learning. Two students identified cultural-related aspects such as "tie of sustainability with culture" and "being proud of being ecofriendly" as their most significant learning and two other students indicated educational issues "education as an effective tool to change policy and human

behavior” and “effective transitioning from learning in the classroom to the real world” as their most significant learning. Other most significant learning topics includes impact of light pollution, management of the forest, disadvantages and advantages of sustainability, ways of being sustainable, true meaning of sustainability, and the manufacturing of wood products (flooring mill tour). In most cases, it seems the students outlined a sound justification on why their most significant new learning matters. This particular result might indicate that students’ most significant learning is well connected with students’ previous knowledge, values, and perceptions. Students indicated that they will use their most significant learning in future personal, business, or community applications. These particular results could reflect in many ways the students’ personalities and future engagement with private and local organizations within their communities.

Finally, students had the opportunity to express through various activities such as journal writing, individual debriefing, group presentations, and a research paper to reflect on what was experienced and observed as a way to transition their new knowledge into a potential acting role.

Conclusions

- Learning is a continuous process that goes through different learning cycles.
- Using ELT is an effective mechanism to plan, organize, lead, and implement ESD in study abroad programs.
- This case study successfully connects study abroad programs, education for sustainable development (ESD), and experiential learning theory (ELT) in a meaningful way.
- Results provide strong support that designing study abroad courses using experiential learning theory is an effective learning strategy.
- Majority of students enrolled had an accommodative learning style (active experimentation and concrete experience) as their dominant learning style.
- In some cases the context could have induced “undesirable noise” by distracting students from the main purpose of some of the activities.
- It requires a lot of guidance from the instructor in order to provide the students with the theories and facts dealing with sustainability in the country to be explored.

Recommendations

This work successfully demonstrated the incorporation of experiential learning theory into a study abroad program while teaching sustainability and also provides a template for other potential study abroad programs. A new program based on the model is on the way to be designed in Eastern Europe (Sustainability in Slovak and Czech Republic).

References

- Blewitt, J., and Cullingford, C. 2012. The sustainability curriculum: The challenge for higher education. Earthsan, UK/USA.
- Chieffo, L., and Griffiths, L. 2004. Large-scale assessment of student attitudes after a short-term study abroad program. *Frontiers Journal* 10: 165-177.
- Domask, J. 2006. Achieving goals in higher education: an experiential approach to sustainability studies. *International Journal of Sustainability in Higher Education* 8:53-68.

- Dunning, J., Meilan, R., & Jacobs, D. 2008. Collaborative study abroad- combining efforts to improve undergraduate experience. *NACTA Journal* December: 20-24.
- Ernest, H. 1948. *Theories of learning*. Appleton-Century-Crofts, East Norwalk, CT.
- Fien, J. and Tilbury, D. 2002. The global challenge of sustainability. In Tilbury, D., Stevenson, R., Fien, J., and Schreuder, D., editors, *education and sustainability responding to the global challenge*. IUNC Commission on Education and Communication, Cambridge, UK p. 1-12.
- Gitsham, M. 2012. Experiential learning for leadership and sustainability at IBM and HSBC. *Journal of Management Development* 31: 298 – 307.
- Hallows, K., Wolf, P., and Marks, M. 2011. Short-term study abroad: a transformational approach to global business education. *Journal of International Education in Business* 4: 88-111.
- Hopkins, J.R. 1999. Studying abroad as a form of experiential education. *Liberal Education* 85(3): 36-41.
- Kitsantas, A. 2004. Studying abroad: The role of college students' goals on the development of cross-cultural skills and global understanding. *College Student Journal* 38(3): 441-452.
- Kolb, D. (1984). *Experiential learning: experience as the source of learning and development*. Prentice Hall, Englewoods Cliffs, NJ.
- MacVaugh, J. and Norton, M. 2012. Introducing sustainability into business education contexts using active learning. *International Journal of Sustainability in Higher Education* 13: 72–87.
- Minnich, E. 1999. Experiential education. *Liberal Education* 85(3): 36-41.
- New Economic Foundation (NEF). 2013. Happy planet index. <http://www.happyplanetindex.org> (accessed 1 June 2013).
- Piaget, J. 1954. Intelligence and affectivity: Their relationship during child development. *Annual Review Inc.*, Palo Alto, CA
- Quesada-Pineda, H.J., Adams, E. & Hammett, A.L. 2011. Incorporating experiential teaching methods in sustainable natural resources curriculum: A case study. *Journal of Natural Resources & Life Sciences Education* 40: 1-10.
- Shriberg, M. 2002. Institutional assessment tools for sustainability in higher education: strengths, weaknesses, and implications for practice and theory. *Higher Education Policy* 15: 153–167.
- Wals, A., and Jickling, B. 2002. Sustainability in higher education: From doublethink and newspeak to critical thinking and meaningful learning. *International Journal of Sustainability in Higher Education* 3: 221–232.
- Wilson, A. H. 1982. Cross-cultural experiential learning for teachers. *Theory Into Practice* 21(3): 184-192.
- Wright, T. 2000. Definitions and frameworks for environmental sustainability in higher education. *International Journal of Sustainability in Higher Education* 3: 203-220.
- Yale Center for Environmental Law and Policy (YCELP). 2013. Environmental performance index. <http://epi.yale.edu/epi2012/rankings> (accessed 4 June 2013)

Furniture Design and Product Development Principles Considering End-of-Life Options and Design for Environment Strategies

Mesut Uysal¹ - Eva Haviarova^{2} - Carl A. Eckelman³*

¹ Graduate Student, Department of Forestry and Natural Resources
Purdue University, West Lafayette, Indiana, USA.

uysalm@purdue.edu

² Associate Professor, Department of Forestry and Natural Resources
Purdue University, West Lafayette, Indiana, USA.

** Corresponding author*

ehaviar@purdue.edu

³ Professor, Department of Forestry and Natural Resources
Purdue University, West Lafayette, Indiana, USA.

eckelmac@purdue.edu

Abstract

During the last decades, environmental issues have come into prominence and some governmental or organizational regulations have been legislated to reduce environmental impacts of products over their life cycle. At the same time, consumers increasingly consider not only the price, quality, branding, uniqueness, and availability but also the environmental impacts, safety, and overall sustainability of the products they select. Therefore, producers are addressing the environmental impact of their products and are also making changes to their production process. This project addressed Design for Environment Strategies and End-of-Life (EoL) Options of wooden furniture in relation to feasible joinery systems. Two joinery systems – Ready-to-Assembly (RTA) and Permanent Glued Joinery – were compared in terms of strength, best suitability for construction, ease of assembly and disassembly, and reparability. RTA joinery systems included screws, bed bolts with dowel nuts, pinned round mortise and tenon, and pinned rectangular mortise and tenon. Permanent glued joinery systems included dowel, glued round mortise and tenon, and glued rectangular mortise and tenon. For all joint groups, T-joints, L-joints, and stool frames were constructed and tested. Static load joint tests and cyclic front-to-back load tests on stools were conducted to determine their load capacities. Higher load capacity levels were obtained with the permanent joinery systems in both the static joint tests and the cyclic stool-frame tests. Because of hardware costs, overall material costs for RTA joinery systems are higher than that for permanent glued joinery systems. In conclusion, permanent glued joinery system performed better than RTA joinery and thus could play an important role when considering End-of-Life Options and Design for Environment Strategies.

Key Words: Furniture Design, End-of-Life Options, Design for Environment, Static load joint test, cyclic load performance test.

Introduction

The ecological awareness of wood products manufacturers provides an important competitive advantage in foreign or home markets. As an example, the EU Timber Regulation, effective March 2013, requires manufacturers to demonstrate that their wood/wood products do not originate from illegal harvesting practices [7]. This opens the door for consumers and sellers to demand proof of compliance. The primary mechanisms for demonstrating this level of compliance are the Environmental Product Declarations (EPDs). EPDs assess the total environmental impact of a product or material. They are being developed by a broad spectrum of industries under a framework of international standards [8].

This study focuses on Design for Environment (DfE), End-of-Life (EoL) options in relation to wood products construction. Increasing product recovery for the 2nd life of products must be addressed as a whole because the recovery rate in the first life can only be increased through initial design and development for further use and environmentally friendly disposal. DfE strategies are considered in order to build easy-to-assemble and disassemble, durable, and, sustainable wooden furniture. EoL options are considered in order to provide better recovery rates for second life—considering mostly reuse, recycle and remanufacturing options.

The judicious use of timber resources, especially in disadvantaged countries of the world, dictates that furniture should be durable and easy to repair and if possible parts should be reusable. At present, however, chairs, tables, and other furniture are regularly discarded—sometimes owing to fractured legs and rails, but most often owing to loose or failed joints. In addition, given the ever-growing demand on world timber resources, it is important to investigate whether the structurally sound parts salvaged from broken or discarded furniture (that cannot be simply repaired) such as legs, rails, stretchers can be recycled, i.e., incorporated into "new" products. In this study, end of life options for wooden stools assembled with different joinery systems were investigated.

Material and Methods

Plan of Study

Static load test: 5 specimens were constructed for each of seven joint groups.

Cyclic front-to-back load test: 5 stools were constructed for each of seven joint groups.

Materials and Specimen Construction. All joint specimens and stools were constructed of Yellow Poplar (*Liriodendron tulipifera* L.) – specific gravity of 0.48 at 7% moisture content.

Screw joints: 76 mm long, #14 wood screws were used in the screw-joint tests.

Bed bolts with dowel nuts joints: primary connectors were 76 mm long by 6.35 mm root diameter bed bolts with 9.5 mm diameter dowel nut; 6.35 mm diameter dowels were used as locator pins.

Pinned/glued round mortise and tenon joints: tenons measured 38 mm long by 18.25 mm in diameter [3, 4] ; 6.35 mm diameter dowels were used as cross pins; joints were assembled with a 40% PVA adhesive.

Dowel joints: plain surface, 50 mm long by and 9.5 mm diameter white oak (*Quercus alba*) dowel were used; joints were assembled with a 40% PVA adhesive.

Pinned/glued rectangular mortise and tenon joints: tenons measured 50 mm long by 50 mm wide by 6.35 mm thick; joints were assembled with a 40% PVA adhesive.

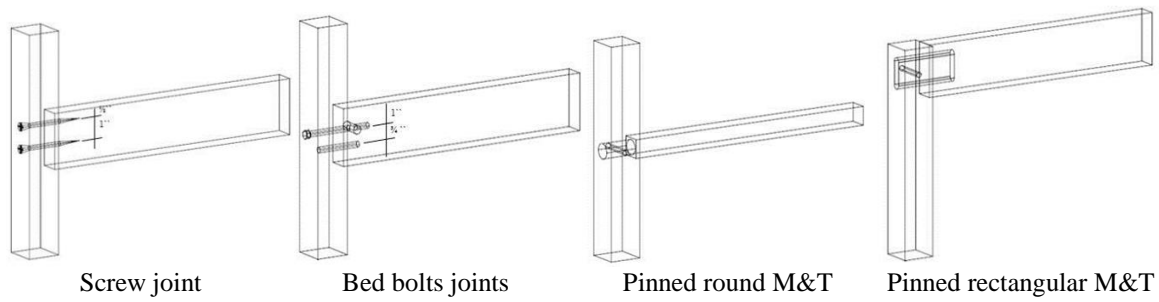


Figure 1: Ready-to-Assembly joinery systems specimen configuration for static joint load test.

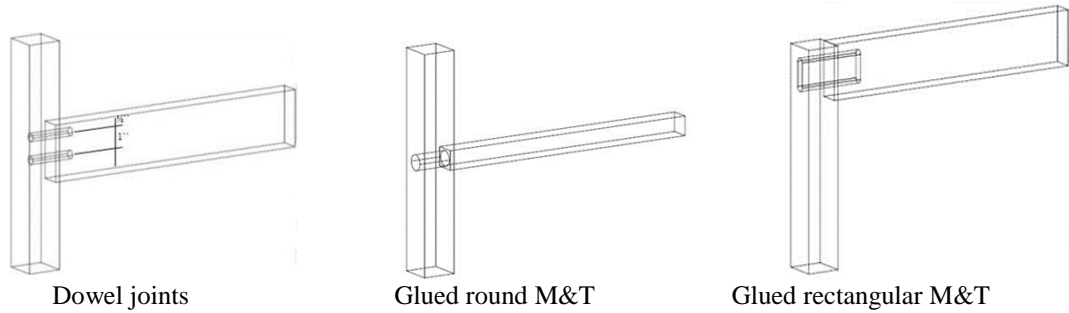


Figure 2: Permanent glued joinery systems specimen configuration for static joint test.

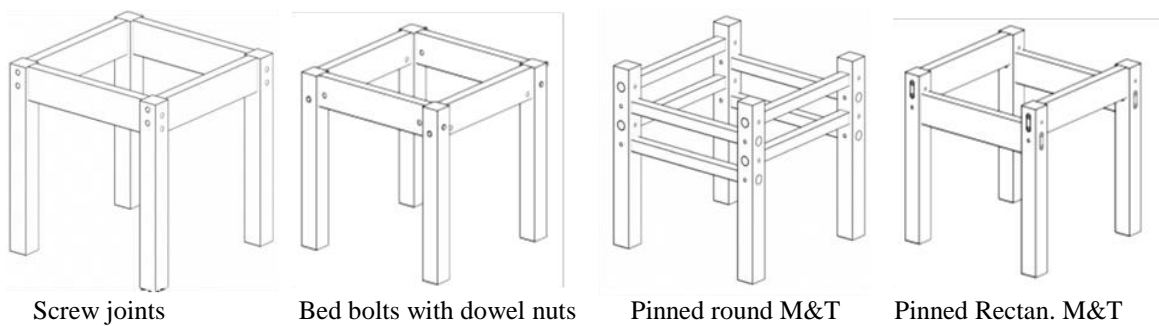


Figure 3: Stool configurations for cyclic front-to-back load test - RTA joinery systems.

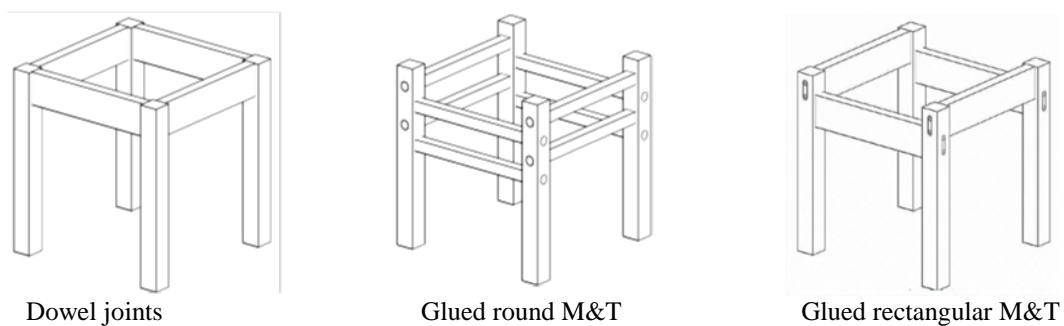
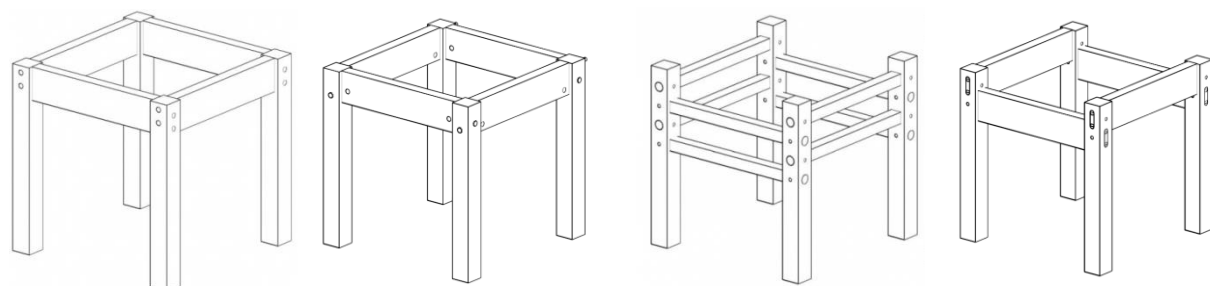


Figure 4: Stool configuration for cyclic front-to-back load test - permanent glued joinery systems.



Test Methods

Static load tests: Static load tests of joints were conducted on a Riehle 30 kip Universal Testing Machine at a cross head rate of 6.35 mm/min as shown Figure 5 [9]. Load was applied until non-recoverable drop off in load occurred.

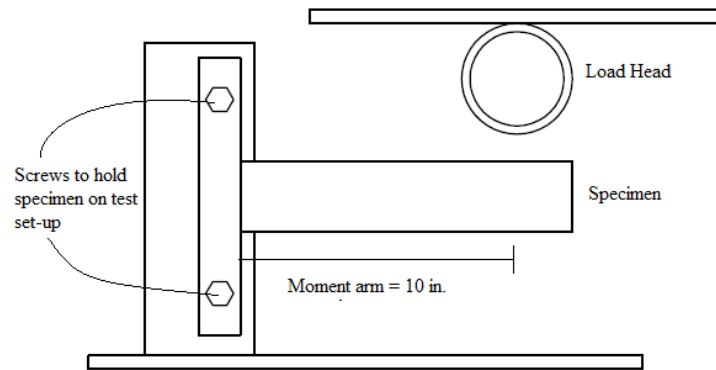


Figure 5: Static joint load test set up.

Cyclic front-to-back load test: Studies by the American Library Association [1] indicate that the most common damage to chair frames arises from cyclic front to back loading of the seats—mimicking a user sitting down in a chair and pushing backward or tilting backwards—which causes bending moments to be imposed on the rail and stretcher to front and back post joints. Hence, the front-to-back load test reported by the American Library Association was used to evaluate the chair frames included in this study.

The stools were mounted for testing as shown Figure 6. Cyclic horizontal loads were applied from front to back on stools at a rate 20 cycles per minute [1, 2]. Tests were started at the 222.4 N load level; loads were increased by 222.4 N after 25,000 cycles were completed at each preceding load level. This procedure was repeated until some type of structural failure occurred.

Following completion of the first life tests, the damaged parts were removed and the stools were reconstructed (new parts were used where needed) and 2nd life tests were conducted. Identical procedures were followed after completion of 2nd life testing, and 3rd life tests were conducted.

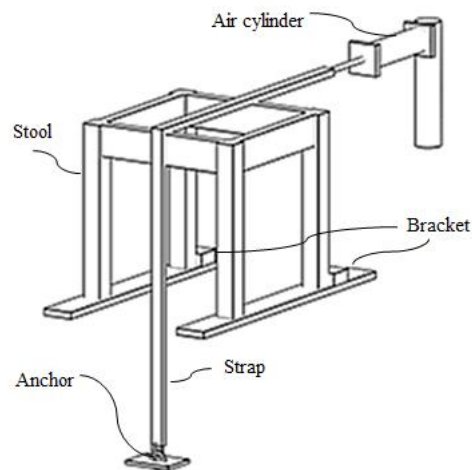


Figure 6: Cyclic front-to-back load test configuration.

Test Results and Discussions

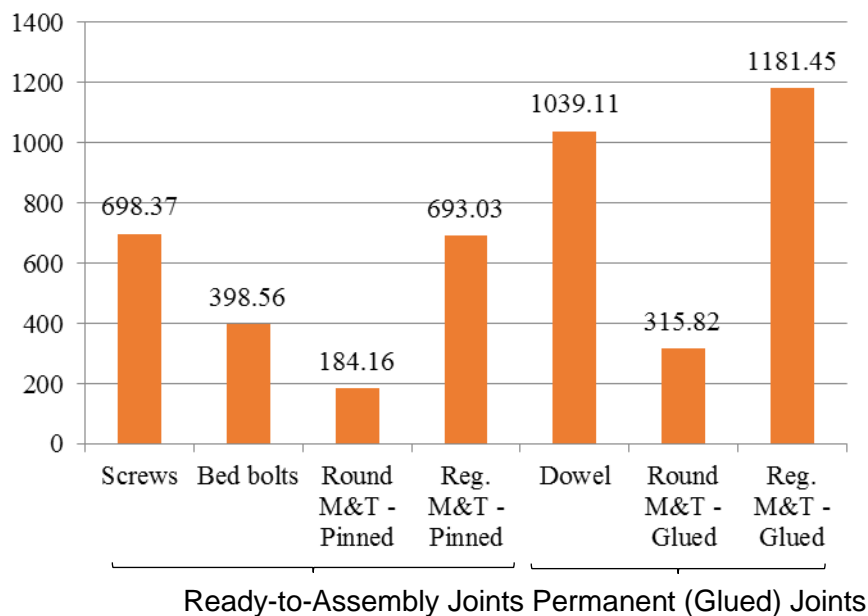


Figure 7: Static load capacity of joinery systems (N).

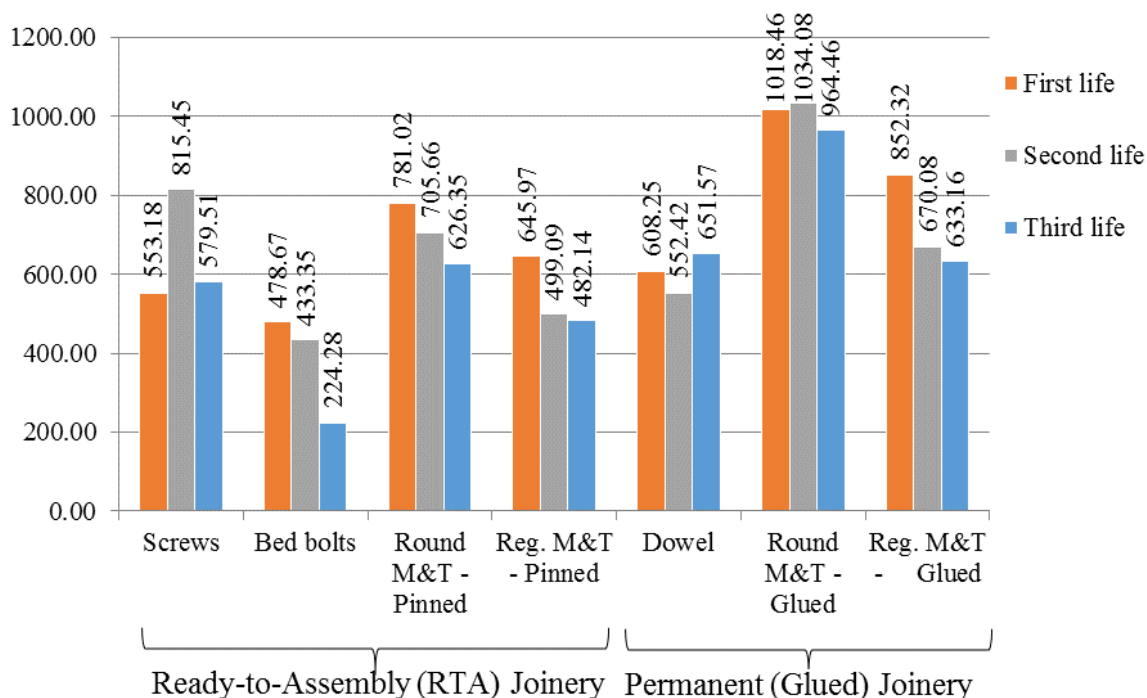


Figure 8: Cyclic front-to-back load capacity level of joinery systems (N).

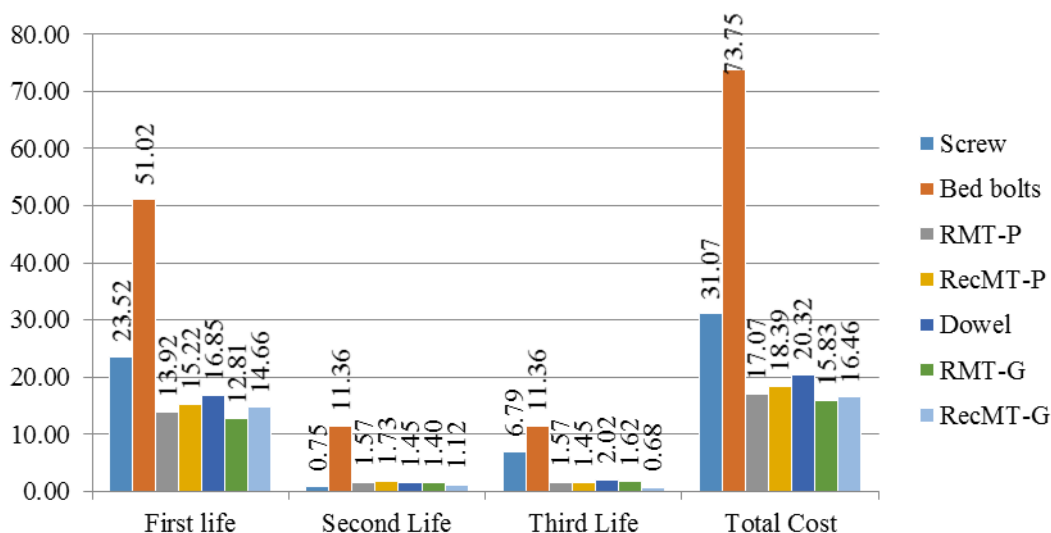


Figure 9: Material cost (wood material and hardware) per stools in each life (US Dollars).

Screw Joints. Screws can be used in joints in two ways, a) two screws can be used as a replacement for dowels—or for two bed bolts, or, b) as a replacement for a single bed bolt. Highest screw strength is obtained with sheet metal type screws. Pilot hole diameters should be equal to the root diameter of the screw.

Bed Bolt and Dowel Nut Joints. Joints constructed with bed bolts (with square nuts or dowel nuts) ordinarily fail owing to an initial split emanating from the slot or hole for the nut. Hence, nuts should be located an appropriate distance from the end of the rail—38 to 50 mm.

A problem with dowel nut construction is that the joint tends to loosen owing to shrinking and swelling of the back post. For this reason, it is recommended to countersink the head of the bolt in the back post (in order to lessen the perpendicular to grain distance between the underside of the bolt head and the face of the rail)—provided this does not weaken the back post unduly.

Glued/Pinned Round Mortise and Tenon Joints – Two Stretchers Stools. Round mortise and tenon joints constructed with adhesives subjected to an abusive static front to back load fail owing to fracture of the tenon at its point of entry into the back post subjected to cyclic loading normally fail. In the case of cyclic loading, normally a shear failure first develops near the neutral axis of the tenon followed by fracture of the tenon at its point of entry into the back post.

Round mortise and tenon joints with cross-pinned tenons ordinarily fail owing to shear failures that originate at the cross-pin hole. Overall, cyclic resistance is closely related to cross-pin hole diameter. Cross pins should not be larger than 3.175 mm in diameter. Also, it should be noted that cross-pinned round mortise and tenon joints have only about one-half the cyclic load capacity of glued round mortise and tenon joints.

Round-Shouldered Rectangular Mortise and Tenon. The structural characteristics of rectangular mortise and tenon joints depend largely on tenon length. The moment capacity of joints with short tenons depends primarily on the integrity of the adhesive bond between the sides of the tenon and the walls of the mortise, whereas the capacity of joints with long tenons depends

on the bending moment capacity of the tenon itself along with its axial shear strength. The moment capacities of joints with tenons of intermediate length are a function of both the resistance to bending of the tenon and the adhesive bond between the tenon and walls of the mortise.

The moment capacity of pinned joints is a function of both the resisting couple formed by the perpendicular-to-axis force exerted on the end of the tenon and the opposite perpendicular-to axis force exerted on the tenon at its point of entry into the mortise; and partially on the couple formed by the axial force acting on the cross pin and the resisting force exerted by the heel of the tenon member on the wall of the wall of the mortised member. The tenon is subjected to both longitudinal shear forces owing to bending of the tenon and to shear forces resulting from the forces exerted by the cross pin.

Dowels Joints. Dowel joints in the side rail of a chair ordinarily fail owing to one of the four causes; a) use of dowels that are too short; b) too loose a fit between the dowel and the walls of the dowel hole, and c) use of too little glue, and d) shear failure of the dowel owing to cross grain.

Use of short dowels (often 20 mm long with chamfered ends) and loose fits arise from the need for ease of assembly. Use of too little glue (along with improper gluing) occurs because of the need to avoid squeeze-out—which affects the finishing characteristics of the affected area.

Test Conclusions

Based on results of the static joint tests and cyclic stool performance tests, permanent glued joinery systems have higher load capacity levels than RTA joinery systems. Also, the material costs of permanent glued joinery systems are lower than those of RTA joinery systems. However, screw joints are the easiest to repair; bed bolts with dowel nuts joints are also easy to repair but require replacement of the rails in which they are embedded. While designing wooden furniture, selecting appropriate joinery is essential part of design for environment strategies.

References

1. Eckelman, C.A. 1995. Library chairs: An overview of the library technology reports tests methods with test reports on 30 chairs. American Library Association - Library Technology Reports. 31(2): 117-214.
2. Eckelman, C.A. 1999. Performance testing of side chairs. Holz Roh Werkst. 57: 227-234.
3. Eckelman, C.A., Erdil, Y.Z., Haviarova, E. 2003. School chairs for developing countries: Designing for strength and durability, simplicity, and ease of construction. Forest Products Journal. 53(2): 63-70.
4. Eckelman, C.A, Haviarova, E. 2006. Performance tests of school chairs constructed with round mortise and tenon joints. Forest Products Journal. 56(3): 51-57.
5. Eckelman, C.A., Haviarova, E., Erdil, Y., Tankut, A., Akcay, H., and Denizli, N. 2004. Bending moment capacity of round mortise and tenon furniture joints. Forest Products Journal 54(12): 192-197.

6. Eckelman, C.A., Haviarova, E., Zhu, H., Gibson, H. 2001. Consideration in the design and development of school furniture for developing regions based on local resources. *Forest Products Journal*. 51(6): 56-63.
7. European Commission (EC) 2010. EU timber regulation. Retrieved from http://ec.europa.eu/environment/forests/pdf/EUTR_Leaflet_EN.pdf. Last access February 2013.
8. Environmental Product Declarations (EDP). 2013a. An Introduction. Retrieved from <http://www.environmentalproductdeclarations.com>. Last access February 2013
9. Likos, E., Haviarova, E., Eckelman, C.A., Erdil, Y.Z., Ozciftci, A. 2013. Technical note: Static versus cyclic load capacity of side chairs constructed with mortise and tenon joints. *Wood and Fiber Science*. 45(2): 223-227.

Sandwich Type Panels Made from Rubberwood and Eastern Redcedar

Songklod Jarusombuti

Department of Forest Products, Faculty of Forestry
Kasetsart University
10900 Chatuchak, Bangkok, Thailand
E-Mail: fforsoj@ku.ac.th

Salim Hiziroglu

Department of Natural Resource Ecology & Management
Oklahoma State University,
Stillwater, OK 75078-6013
E-mail: salim.[hiziroglu @okstate.edu](mailto:hiziroglu@okstate.edu)

Abstract

This study evaluated the physical and mechanical properties of experimental sandwich type panels manufactured from rubberwood (*Hevea brasiliensis*) and Eastern redcedar (*Juniperus virginiana*). Panels with two density levels of 0.65 g/cm³ and 0.75 g/cm³ were made using 10% urea formaldehyde, combination of 3% urea formaldehyde and 10 % cassava starch and 10% cassava starch as binder. Three-layer samples having rubberwood fibers on the face layers and a mixture of 15% Eastern redcedar and 85% rubberwood particles in the core layer of the panels were manufactured for the experiments. Panels made with 10 % starch did not have sufficient mechanical properties and dimensional stability based on Japanese Industrial Standards (JIS). However panels made with 10% urea formaldehyde having 0.75 g/cm³ density resulted in the highest modulus of elasticity, modulus of rupture and internal bond strength values of 2,990 MPa, 34.72 MPa and 1.09 MPa. It appears that using mixture of low percentage of urea formaldehyde and cassava starch would be viable alternative binder to manufacture such panels with acceptable mechanical properties with enhanced surface quality.

Keywords: Rubberwood, Eastern redcedar, mechanical properties.

Introduction

Rubberwood (*Hevea brasiliensis*) is the most commonly used raw material to produce wood based composites in Thailand (Krukanont and Prasertsan, 2004, Falvey 2000). Lumber from rubberwood has been produced on a rather small scale in past but recently it has become much more common in planting as cash crop in Thailand. Rubberwood having strength properties similar to many tropical species became very important raw material for furniture and composite panel industry in South East Asian countries including Thailand. Waste material from furniture and lumber production along with low quality small logs are also the main raw material for

particleboard and fiberboard manufacture in Thailand (Falvey 2000, Fueangvivat et al, 2014, Hong and Sim,1994).

It has been determined that Eastern redcedar (*Juniperus virginiana* L.) which is considered an invasive species as spreads at a rate of around 50 trees per acres per year in the prairie land of Kansas (Hiziroglu et al 2002). It is a fact that the encroachment of redcedar is creating a significant ecological problem to the farmers in the form of depletion of ground water and risk of wild fires. Currently there is no effective and efficient use of small Eastern redcedar trees.

Urea formaldehyde and phenol formaldehyde adhesives are most commonly used binders in wood composite industry in many countries (Roffael 1993). One important disadvantage of phenolic based adhesives is formaldehyde emission from the manufactured panels. Several studies evaluated properties of wood based panels made using modified starch based and soybean binders (Yuan and Kaichang 2007, Zhongli et al 2006). Cassava (*Manihot esculenta*) is woody shrub native to South America and extensively planted as annual crop in many tropical countries including Thailand. Different characteristics of particleboards and fiberboards made from rubberwood and Eastern redcedar have been studied in previous experimental works (Hiziroglu et al 2002, Hong 1994, Fueangvivat et al. 2014). However there is little information on physical and mechanical properties of sandwich type panels with combination of both species using urea formaldehyde and cassava starch as potential green binder. Therefore the objective of this work was to determine basic properties of sandwich type panels made from two species using urea formaldehyde, cassava starch and their mixtures.

Materials and Methods

Rubberwood and Eastern redcedar chips were reduced into particles using a laboratory type hammermill. The particles were dried to 3 % moisture content in an oven. Rubberwood chips were also disintegrated in a defibrator using a pressure of 0.85 MPa and a temperature of 165 °C for 3 minutes for the material of face layers of the panels. The defibrated fibers were also dried to 3 % moisture content in an oven. Raw materials were mixed with 10% urea formaldehyde, 10% cassava starch and mixture of 3 % urea formaldehyde and 10% cassava starch as adhesive in a rotating drum equipped with pressured spray gun. Three-layer sandwich type panels having 25% rubberwood fibers on each face layer and 50% mixture of 85% rubberwood and 15% redcedar particles formed in a plexiglass box. A total of thirty six panels with a two target density levels of 0.65 g/cm³ and 0.75 g/cm³ were compressed in a computer controlled press using a pressure of 5.2 MPa at a temperature of 160 °C for 5 min to a target thickness of 1.0 cm. Bending, internal bond strength, dimensional stability, surface roughness characteristics of the samples were tested. Formaldehyde emission of the panels was also determined using perforator method based on European Standard (EN 120 1993). Surface roughness of the samples was determined employing a stylus equipment. Two roughness parameters, namely average roughness (R_a) and mean peak-to-valley height (R_z) were used for evaluation of the surface quality of the samples. Definitions and specification of these parameters have been discussed in past studies (ANSI 1985, Mummery 1993, Hiziroglu 1996).

Results and Discussion

Table 1 displays physical and mechanical properties of experimental panels. Modulus of elasticity and modulus of rupture values of 2,990 MPa and 34.72 MPa were found for the panels

having 0.75 g/cm³ density made with 10% urea formaldehyde as binder. Panels having 0.65 g/cm³ density made using 10% cassava starch resulted in the lowest corresponding values of 746 MPa and 3.81 MPa.

Panel Type	Binder Type	Density (g/cm ³)	MOE (MPa)	MOR (MPa)	IB (MPa)	TS (%)	WA (%)	Roughness Parameters (µm)	
								R _a	R _z
1	10% UF	0.65	2,183	23.50	0.98	21.09	77.09	5.15	39.56
2	3% UF&10% starch	0.65	1,625	13.59	0.29	41.58	118.8 2	6.05	45.75
3	10% starch	0.65	746	3.81	0.20	157.0 4	278.7 9	8.93	60.53
4	10% UF	0.75	2,990	34.72	1.09	23.35	69.34	5.02	38.91
5	3% UF & 10% starch	0.75	2,320	20.71	0.25	48.20	94.31	5.63	44.83
6	10% starch	0.75	1,358	8.67	0.07	164.3 9	256.4 6	9.03	59.59

Table 1. Average values of mechanical and physical tests of the samples.

It appears that panels using only starch as binder resulted in relatively lower bending characteristics than those samples made using urea formaldehyde resin. Starch bonded panels with 0.75 g/cm³ density had 1,358 MPa modulus of elasticity as shown in Figure 1. Panels made with only 10% cassava starch at both density levels did not meet JIS standard. However other samples including having a combination of 3% urea formaldehyde and 10 % cassava starch as binder satisfied JIS requirements regarding their bending properties. It seems that having 15% Eastern redcedar particles in the core layer of the panels did not make any adverse influence on bending properties of the panels.

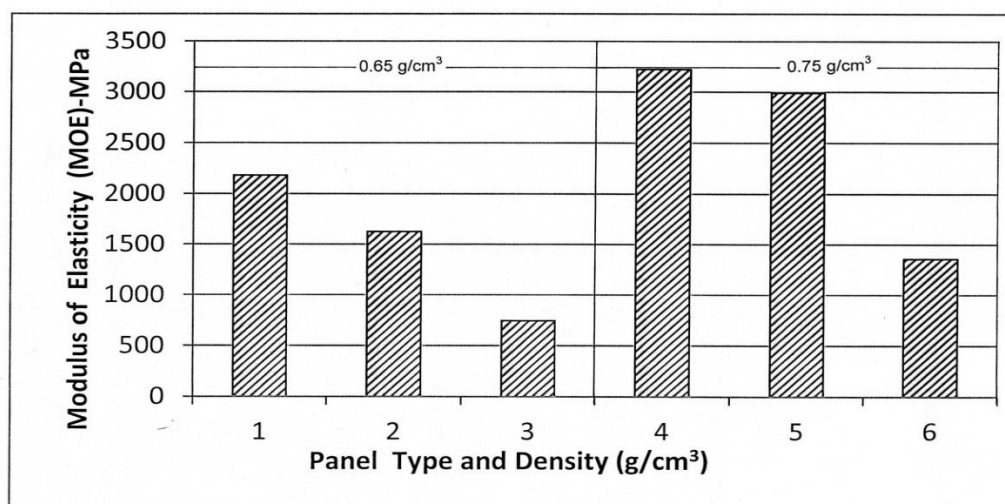


Figure 1. Modulus of elasticity and modulus of rupture values of the samples. (1:10% UF; 2:3% UF 10% starch; 3:10% starch)

Samples having 0.65 g/cm^3 density resulted in lower IB values. Starch bonded samples had average IB values of 0.13 MPa . It is clear that using only starch did not produce panels with accepted mechanical properties. Average thickness swelling and water absorption values of the samples at 2-hr water soaking ranged from 21.09% to 164.39% and from 77.09% to 256.46%, respectively. Panels made using starch as binder had substantially high dimensional instability values. Addition of 3% UF in the panels significantly improved their both thickness swelling and water absorption values. As shown in Table 1 panels made with 10% urea formaldehyde had the smoothest surface with an average R_a value of $5.08 \mu\text{m}$ followed by those made with combination of urea formaldehyde and starch as adhesive having $5.84 \mu\text{m}$. It appears that starch did not create high level of densification on the face layers in contrast to those manufactured with traditional type of resin. No sanding or any finishing was applied to the surface of the samples. Average formaldehyde emission values of the samples were 20 mg/100 g and 10 mg/100 g for the control samples made with 10% urea formaldehyde and mixture of 3% urea formaldehyde and 10% starch, respectively. It is clear that starch based samples had much lower emission values. All these values were within the limit of the E2 emission class (Moubarik et al 2010B, Roffael 1993, Nihat and Nilgun 2002).

Conclusions

Raw materials from rubberwood and Eastern redcedar were used to manufacture experimental sandwich type panels. It seems that starch reduced both mechanical and physical properties of the panels as compared to those of the control samples. As can be expected using fibers on the face layer resulted in smooth surface of the samples which would be ideal for overlaying applications.

References

American National Standards Institute (ANSI). 1985. Surface texture (surface roughness,

waviness, and lay) B46.1. The American Society of Mechanical Engineers, New York. 43 pp.

European Committee for Standardization (EN). 1993. Wood based panels. Determination of formaldehyde content. EN 120. European Committee for Standardization, Brussels.

Falvey, L. 2000. Thai Agriculture. Golden Cradle of Millennia. Kasetsart University Press, Bangkok, Thailand.

Fueangvivat, W., S. Jarusombuti, S.Hiziroglu., P.Bauchongkol. 2014. Properties of sandwich type of particleboard panels made from rubberwood and eastern redcedar. Forest Products Journal. 64 (1/2):72-76.

Hiziroglu, S., R. Holcomb, R. Q.Wu. 2002. Manufacturing Particleboard from Eastern Redcedar. Forest Products Journal. 52(7/8): 72-76

Hiziroglu, S. 1996. Surface roughness analysis of wood composites: A stylus method. Forest Prod. J. 46(7/8):67-72.

Hong, L. T. and H. C. Sim. 1994. Rubberwood processing and utilization. Malaysian Forest Record No. 39. Forest Research Institute of Malaysia, Kepong, Kuala Lumpur.

Japanese Industrial Standards (JIS). 1995. Particleboards. A-5908. Japanese Standards Association, Tokyo.

Krukanont, P. and S. Prasertsan. 2004. Geographical distribution of biomass and potential sites of rubber wood fired power plants in Southern Thailand. Biomass Bioenergy 26:47-59.

Moubarik, A., B. Charrier, A. Allal, F. Charrier, and A. Pizzi. 2010b. Development and optimization of a new formaldehyde-free cornstarch and tannin wood adhesive. Eur. J. Wood Wood Prod. 68(2):167-177.

Mummery, L. 1993. Surface Texture Analysis. The Handbook. Hommelwerke, Muhlhausen, Germany. 106 pp.

Nihat, S. C. and O. Nilgun. 2002. Use of organosolv lignin in phenol formaldehyde resin for particleboard production II. Particleboard production and properties. Int. J. Adhes. Adhes. 22:481-486.

Roffael, E. 1993. Formaldehyde release from particleboard and other wood based panels. Malaysian Forest Records No. 37. Forest Research Institute of Malaysia, Kepong, Kuala Lumpur.

Yuan, L. and L. Kaichang. 2007. Development and characterization of adhesive from soy protein for bonding wood. Int. J. Adhes. 27:59-67.

Zhongli, P., A. Cathcart, and D. Wang. 2006. Properties of particleboard bond with rice bran and polymeric methylene diphenyl diisocyanate adhesives. Ind. Crops Prod. 23:40-45.

Transverse Isotropic Material Thermal Properties Measurement

Richard Hrčka^{1} – Pavol Halachan¹ – Marián Babiak¹ - Rastislav Lagaňa¹ -*

Jan Tippner² – Eva Troppová² – Miroslav Trcala²

¹ Technical University in Zvolen, Slovak Republic.

² Mendel University in Brno, Czech Republic.

* *Corresponding author*

hrcka@tuzvo.sk

Abstract

The proposed method of measurement of transverse isotropic material thermal properties is based on the so called quasistationary method. The difference is in utilization of all three parts of measured temperature change in time, the first – the centre reaction on surface heat flux, the second - quasistationary part and the third – heat losses. Moreover, the measurement of specimens' density and surface heat flux can be transformed to mass specific heat capacity, two independent thermal diffusivities and two thermal conductivities. The principles of the method were proved by thermal properties measurement of MDF with finite dimensions, which revealed necessity of recognition of all three parts of temperature change in time. The precision and accuracy of the method depends on the precision of measurement and fulfilling the conditions used in the solution of heat conduction equation.

Keywords: MDF, quasistationary method, thermal properties

Introduction

We can often see material in the environment, where temperature changes (technologies, constructions) or there is some interaction of material with el. mag. field. As energy can not be created nor destroyed it is seemed to be reasonable that heat can only flow (be transported) and sources of heat can arise only as conversion of one form of energy to another. We often ask how much heat is needed to change the temperature of material, or how much heat flows through the wall, or how fast the different temperatures of material and its environment equilibrate. There are a lot of possibilities to get the answers to these questions. One of them is using the concept of properties and their definitions. The concept is really extensive and we often simplified it for material to be non-homogeneous continuum and rigid body. The first question relates to specific heat capacity, mostly the second one relates to thermal conductivity and third one to thermal diffusivity (Hrčka and Babiak 2012). The advantage of such description is also in reproducibility of measurement and its results. So, there is possibility to transport the results from one case to another, for example from research to practise and vice versa (Lübke and Ihnát 2013, Russ et al. 2013). The presentation of the method of measurement the transverse isotropic material thermal properties such as medium density fiberboard is the aim.

Material and Method

In this study we analyzed the possibilities of measurement the thermal properties of transverse isotropic material using quasistationary apparatus. The used material was medium density fiberboard (MDF).

Material. Sixteen specimens, made of MDF, have the parallelepiped shape with square base. The length of the side was 10.0cm and specimens differed in thickness (12 and 18mm). Prior to measurement, specimens were conditioned to equilibrium state in the environment of moist air with parameters: 65% relative humidity and temperature of 20°C. Afterwards, the average densities for different thicknesses were $719.2 \pm 2.4 \text{ kg} \cdot \text{m}^{-3}$ and $739.0 \pm 6.0 \text{ kg} \cdot \text{m}^{-3}$.

Method. The method is based on the solution of heat conduction equation under the following initial and boundary conditions:

1. Constant temperature throughout the specimen at the beginning of the experiment:

$$t(x,0) = t_0 \quad (1)$$

2. Constant heat flux φ at the surface of the specimen along the direction of thickness L:

$$\varphi = -\lambda_x \left. \frac{\partial t}{\partial x} \right|_{x=L} \quad (2)$$

3. There is no heat flux in the centre of the specimen.
4. Prescribed heat flux at boundary as function of temperature at boundary:

$$-\lambda_y \left. \frac{\partial t}{\partial y} \right|_{y=R} = \alpha_y (t(x, R, z, \tau) - t_0) \quad (3)$$

$$-\lambda_z \left. \frac{\partial t}{\partial z} \right|_{z=R} = \alpha_z (t(x, y, R, \tau) - t_0) \quad (4)$$

Then the solution has the form:

$$t(x, y, z, \tau) - t_0 = \frac{4\varphi}{Lcp} \sum_{r=1}^{\infty} \sum_{p=1}^{\infty} \sum_{m=1}^{\infty} \left(\frac{(\sin \mu_r)(\cos \frac{\mu_r}{R} z)}{(\mu_r + (\sin \mu_r)(\cos \mu_r))} \frac{(\sin \mu_p)(\cos \frac{\mu_p}{R} y)}{(\mu_p + (\sin \mu_p)(\cos \mu_p))} \cos \frac{m\pi}{L} x \right) \cdot \left(\frac{1 - e^{-\left((m\pi)^2 \frac{a_x}{L^2} + \mu_p^2 \frac{a_y}{R^2} + \mu_r^2 \frac{a_z}{T^2} \right) \tau}}{1 - e^{-\left((m\pi)^2 \frac{a_x}{L^2} + \mu_p^2 \frac{a_y}{R^2} + \mu_r^2 \frac{a_z}{R^2} \right) \tau}} \right) \quad (5)$$

where t_0 is constant temperature throughout the specimen at the beginning of the experiment; a_x , a_y are thermal diffusivities in perpendicular to plane and along with plane directions; L, R are

dimensions of board in thickness and width; x, y, z are coordinates of measurement; c specific heat capacity, ρ density; ϕ heat flux density from planar heat source to single specimen; τ time, μ_p, μ_r are nonnegative roots of the characteristic equations:

$$\mu_p \operatorname{tg} \mu_p = \mu_r \operatorname{tg} \mu_r = \frac{\alpha R}{\lambda_y} = H_r \quad (6)$$

where λ_x, λ_y are thermal conductivities in perpendicular to plane and along with plane directions; α , is heat transfer coefficients.

The kernel of this transform can be found in Luikov (1968). The solution for cylindrical specimen was obtained by Vozár and Šrámková (1997). The thin nickel-chrome foil (0,01mm) can be used as a heat source. The measuring device consists of one thermocouple 0,0125mm in diameter. The simplification of method is so called quasi-stationary method which does not account for heat losses from lateral surfaces. The thin nickel-chrome foil (0,01mm) can be used as heat source. It is necessary to know its properties (area S , electric resistance R) owing to the fact that all of the three thermal properties of wood are determined simultaneously. The arrangement of experiment is illustrated in fig.1.

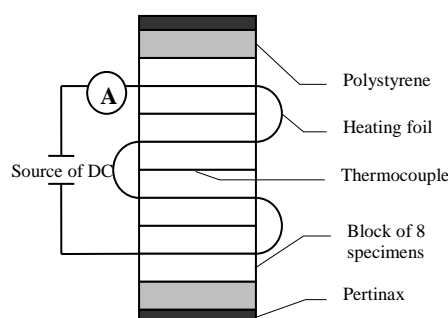


Figure 1. Apparatus scheme of quasi-stationary method and method used in this study.

We suppose that heat is symmetrically distributed to both adjacent specimens and heat flux is given by the equation:

$$\phi = \frac{RI^2}{2S} \quad (7)$$

I is the direct electric current flowing through the foil. Thin thermocouple is in the centre of the specimen block, $x=0$.

The whole apparatus is placed in the surrounding of air.

Results and Discussion

Typical temperature change in time as a result of their measurement is on fig. 2.

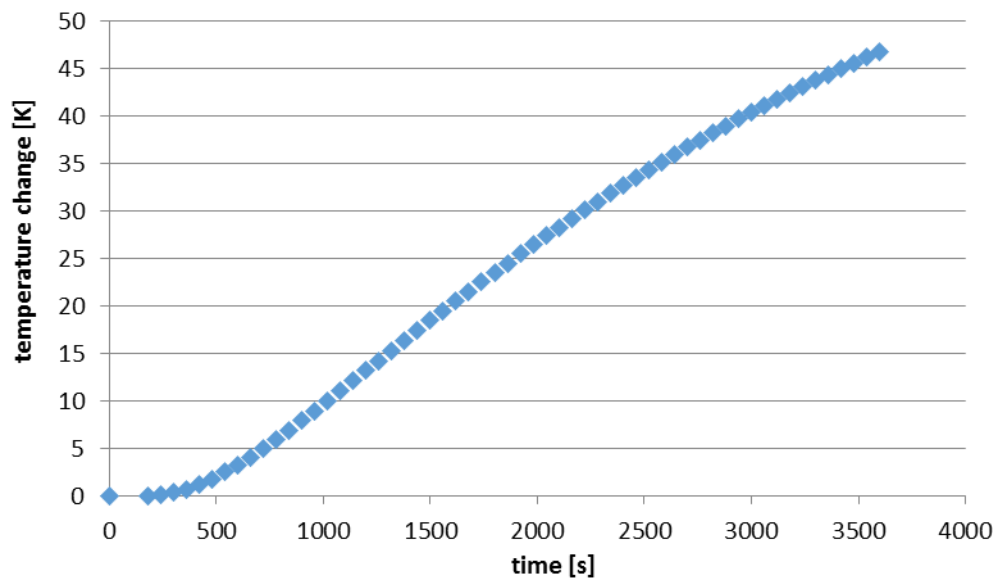


Figure 2: The graph of temperature change in time as was measured with assumed method ($\varphi=500W\cdot m^{-2}$, $L=18mm$, $R=50mm$, $\rho=700kg\cdot m^{-3}$, $c=2kJ\cdot kg^{-1}\cdot K^{-1}$, $a_x=1\cdot 10^{-7}m^2\cdot s^{-1}$, $a_y=2\cdot 10^{-7}m^2\cdot s^{-1}$, $H_r=10$).

There are three phases in the figure 2. The first one at the beginning of experiment is mainly influenced with thermal diffusivity perpendicular to plane direction, the second one with specific heat capacity is almost linear, and third one with thermal diffusivity in plane direction and heat transfer coefficient is curved to reach equilibrium temperature.

So there is a possibility for three different parts and along with known density and heat flux we can determine four unknown parameters. The possibility is given by the thickness to width ratio and possible creation of quasistationary or linear part. The sensitiveness analysis revealed this result.

Analysis of sensitivity. The sensitivity coefficient β_p is a measure of the temperature change caused by change of estimated parameter p (Vozár and Šrámková 1997) and is defined as:

$$\beta_p = p \frac{\partial t}{\partial p} \quad (8)$$

The fitting procedure does not work properly when sensitivity coefficients are small or linearly dependent on each other. Therefore, the analysis of the sensitive coefficients determines the time window in which the evaluation technique can be applied to the temperature response (Malinarič 2004).

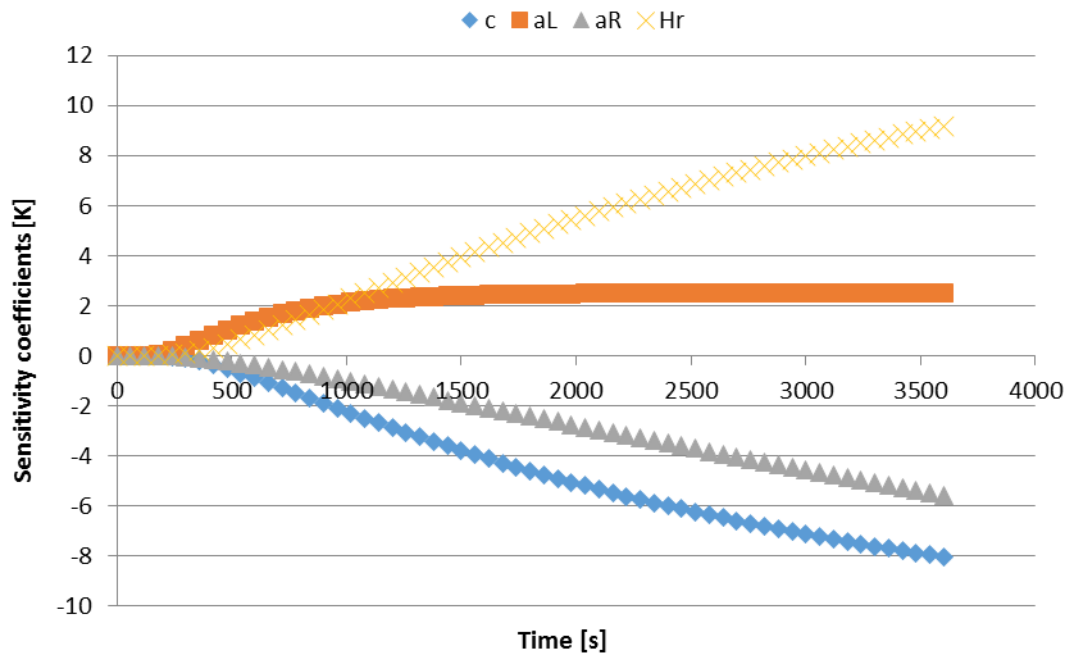


Figure 3: Sensitivity coefficients of specific heat capacity, thermal diffusivities and Biot number as depicted in figure 2.

The method hardly predicts differences between a_L and H_r during short time and c and a_R during long time. With respect to these facts, the final times around 1000s should be sufficient. If the width is cut to the half of the previous one, during this time interval is hard to estimate specific heat capacity and thermal diffusivity in plane, figure 4.

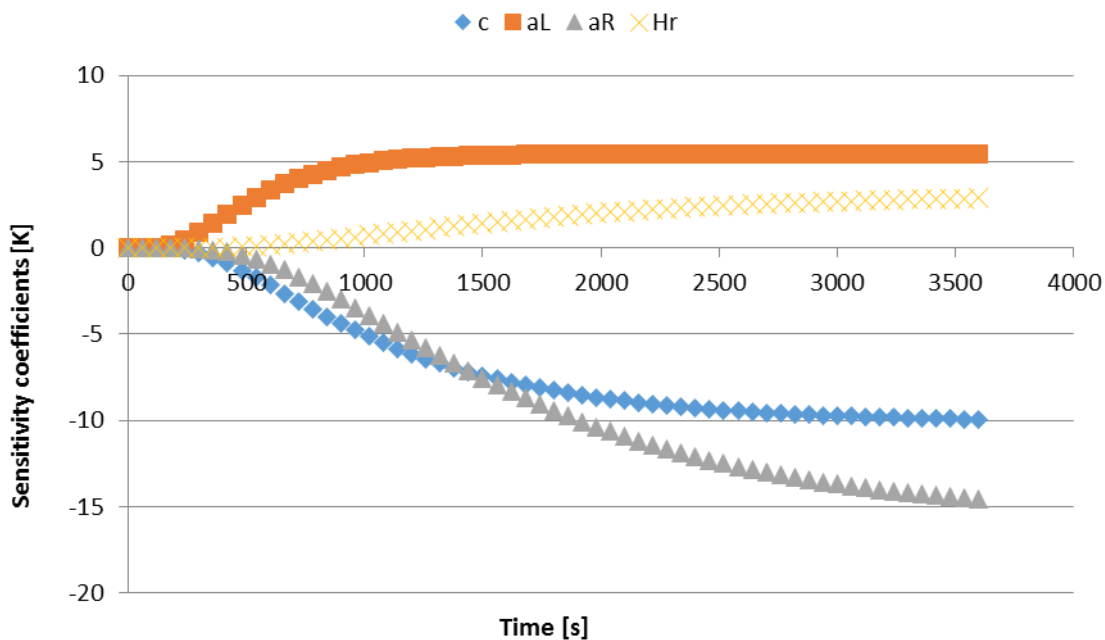


Figure 4: Sensitivity coefficients of specific heat capacity, thermal diffusivities and Biot number when thickness to width ratio was doubled.

Table 1: Average estimated parameters for MDF with different thicknesses.

L	R	c	a_x	a_y	λ_x	λ_y
[mm]	[mm]	[J·kg ⁻¹ ·K ⁻¹]	[m ² ·s ⁻¹]	[m ² ·s ⁻¹]	[W·m ⁻¹ ·K ⁻¹]	[W·m ⁻¹ ·K ⁻¹]
12.00	50.66	1940	1.1·10 ⁻⁷	2.2·10 ⁻⁷	0.15	0.30
18.00	50.68	1940	1.1·10 ⁻⁷	not estimated	0.16	not computed

The time of measurement was 800s and temperature change in the middle of block was not higher than 20°C since the flux of 600W·m⁻² was used. Thermal diffusivity a_y was not estimated because the short time of measurement.

The MDF significantly differed in thickness, i.e. the dimension parallel to heat flux. Specific heat capacity does not depend on thickness as it is a scalar quantity. The results are confirmed in Table 1.

Thermal diffusivity depends on the direction of flux which was proved for smaller thickness. Thickness did not influence thermal diffusivity significantly.

Thermal conductivity was computed as the product of thermal diffusivity, specific heat capacity and density. Therefore it is an anisotropic quantity like thermal diffusivity. We suppose that its larger value for thicker specimens 18mm is due to higher density of used samples.

Conclusions

The proposed method provides reasonable results as temperature is measured in some point of MDF body when heat is transported through it. Also thickness of specimens must be measured as it is involved in heat conduction solution for finite dimensions MDF body. The thickness does not influence the properties significantly. We assume that the larger value of thermal conductivity is due to the larger density. The measurement of thermal properties according the proposed method must involve all three part of temperature rise in time: time lag of temperature, quasistationary part and heat losses. The sensitiveness analysis revealed that the lasting of these parts depends on the ratios of samples dimensions.

Literature

HRČKA, R., BABIAK, M. 2012. Some non-traditional factors influencing thermal properties of wood. Wood research. 57(3), 367-373.

LUIKOV, A. V. 1968. Analytical heat diffusion theory. 2nd edition, Izd. "Vysshaya Shkola," Moscow 1967, Academic Press New York and London, 685 p.

LÜBKE, H., IHNÁT, V. 2013. Research on the properties of new insulating materials based on semichemical fiber. In.: Bridging research and practise, Sopron, p. 34-38.

MALINARIČ, S. 2004. Contribution to the Sensitivity Coefficients Analysis in the Extended Dynamic Plane Source (EDPS) Method. International Journal of Thermophysics, 25(6), 1913-1919.

RUSS, A., SCHWARTZ, J., BOHÁČEK, Š., LÜBKE, H., IHNÁT, V., PAŽITNÝ A. 2012. Reuse of old corrugated cardboard in constructional and thermal insulating boards. *Wood Research*. 58(3), 505--510.

VOZÁR, L., ŠRÁMKOVÁ, T. 1997 Step heating method for thermal diffusivity measurement. In: *New measurement challenges and visions*. Tampere, Finland, p. 8

Morphological Changes on Spruce Wood Surface During Accelerated Ageing

Ihracký, P. – Kúdela, J.

²⁾ Faculty of Wood Sciences and Technology, Department of Wood Science,
Technical University in Zvolen, Slovak Republic

**Corresponding autor*

[*ihrackypavel@gmail.com*](mailto:ihrackypavel@gmail.com)

Abstract

The subject of this work is monitoring and analysis of morphological changes on spruce wood surface induced by degradation effects of accelerated ageing. The morphological changes on wood surface were observed with a SEM, and they were also investigated through roughness parameters. The experimental results demonstrate that the degradation effects of accelerated ageing were reflected in increased surface roughness. The longer was the ageing process, the more distinct was the surface roughness, because the degradation of lignin and extractive substances. A selected mode of aging effects significantly the observed surface properties. In the case of simulated rain, morphological changes were more pronounced than in the dry mode. It has been shown that the degradation rates of early and late spruce wood were different. The faster erosion of early wood caused more diverse roughness patterns across the grain.

Keywords: Simulated ageing, Morphological changes, Roughness, Beech wood

Providing Wood Science Training to the Forest Products Industry or How Do You Provide Educational Programs to Employees with No Formal Education in Wood Science

P. David Jones

Abstract

Changes in the hiring practices of the forest products industry in the USA has led to a workforce that has little or no background in the fundamentals of wood science. They are producing primary and secondary products from wood and encountering a high number of problems that are easily solved with a background in the basic reactions of wood with its environment along with a basic understanding of the structures found in different wood species. These problems include drying defects, swelling, cracking, shrinkage, and decay. No matter the product being produced the educational resources must cover, Density/Specific Gravity, Anatomy, and Moisture Content, to solve the most basic problems inside and outside of the processing facility. Material must be presented in a series of lectures or webinars, and a session must be provided afterwards for questions that will arise from the new gained knowledge.

Keywords: Wood, Extension, Outreach

P. David Jones
Mississippi State University
Sustainable Bioporducts Department
Box 9820
Mississippi State, MS 39762
662-617-2820
pdjones@cfr.msstate.edu

Investigation on the Effect of Resin Consumption on the Properties of Particleboard Made Using Cotton Stalks

*Abolfazl Kargarfard**

Associate Prof., Wood and Products Research Division, Institute of Forests and Rangeland, Tehran Karaj Freeway. Tehran, Iran

*Corresponding Author: a_kargarfard@yahoo.com

Ahmad Jahan-Latibari

Professor, Department of Wood and paper Science and Technology, Karadj Branch, Islamic Azad University, Karadj, Iran

Abstract

The potential of cotton stalks residues for the production of particleboard was investigated. Three resin dosages (10% core,10% surface: 9% core :11% surface and 8% core :12% surface) and three press times (3,4 and 5 minutes) were selected as the variables to produce laboratory particleboards. Then the mechanical and physical properties of the boards were measured and statistically analyzed. The results of modulus of rupture (MOR) , modulus of Elasticity (MOE) and internal bonding (IB) measurements showed that as the resin dosage gradient increases, these properties increased and the effect of this variable on these properties was statistically significant. The highest values were reached when either 2 or 4% resin dosage gradient were applied. The effect of resin gradient on thickness swelling after 2 and 24 hours immersion in water was also statistically significant and these properties were improved. The effect of press time on thickness swelling was also statistically significant and the lowest thickness swelling was observed at 5 minutes press time. The results indicated that if 2 or 4% resin dosage gradient and either 4 or 5 minutes press time is applied for manufacturing of particleboard using cotton stalks residues, the specification of the boards meet the EN specification.

Keywords: Particleboard; Cotton stalks; Resin dosage gradient; Press time

Introduction

During the course of the particleboard production developments, plants were also erected in different regions of the world. As a result, world particleboard production increased to almost 98.5 million m³ in 2012 (FAO, 2013). Interest in production and consumption of particleboard has not been limited to industrial countries, and other regions especially developing countries have been active in this respect. However, these regions are faced with the severe shortage of wood as the main raw material and therefore these regions such as Iran have been looking for alternative procedures to fulfill the needed wood. Among them uncommon raw material such as agricultural wastes including wheat and rice straw and baggase have been investigated and used not only in fiber deficient regions but also in the industrial world.

Grigoriou and Natalos (1999) have investigated the production of particleboard from corn stalks and agricultural residues including wheat straw as the possible alternative raw material for wood using urea-formaldehyde/isocyanate resin system and expressed concerns on the bonding potential of corn stalks. Hague and Mclauchin (1998) and Gu and Gao (2002) also investigated the application of agricultural residues and other non-wood fiber resources for particleboard production and compared the characteristics of the boards with the particleboard from poplar tree small branches. The main limitation and drawback has been the existence of the waxy layer on the surface of the agricultural residues as the barrier for the sufficient bonding. Other research on the utilization of agricultural residues includes Sampathrajan et al. (1977) which attempted to use urea formaldehyde resin as the binder to produce lower density boards from agricultural residues. Meinschmidle et al. (2008) has expressed that the thin wall of the agricultural wastes and the expandable cells provide useful characteristics which enables the production of lower density boards.

The production of particleboard using bark and stem of the coffee branches (Bekalo and Reinhardt (2010) have been investigated. Kargarfard et al. (2006) manufactured particleboard using cotton stalks and eucalyptus particles and expressed that at higher dosages of the cotton stalks particles both MOR and MOE of the boards increased. Guler and Ozen (2004) also studied the performance of the cotton stalks particles in the production of the particleboards and mentioned that if the density of the board is in the range of 600 to 700 kg/m³, then the properties of the board will be at the acceptable level required for interior application. Khedar et al. (2004) used coconut fruit outer skin for particleboard production.

The shortage of wood raw material has forced the investigators to search and use the alternative, uncommon and unconventional fiber supply especially abundant agricultural residues. The availability of such material in rural areas and limitations on wood supply necessitated the investigation to identify the suitability of cotton stalks for particleboard production.

Materials and Methods

Material

Cotton stalks were collected from cotton plantation in the city of Varamin. The stalks were transferred to Alborz Research Center, wood and paper research laboratory for particle preparation.

Urea-formaldehyde resin was purchased from Fars Chemical Company resin plant, Shiraz. The characteristics of the resin was as follow: gel time; 47 seconds (Bison Cup), density; 1.285, solid content; 63%, pH; 7.5 and viscosity; 45 seconds.

Hardener; industrial grade ammonium chloride was used.

Methods

Particle preparation

All cotton stalks were chipped using laboratory drum chipper, Pallmann PHT 120x430 to obtain suitable chips for particle production. Chips were then flake using Pallmann ring flaker PZ8. Flake were dried in a laboratory rotating drum dryer equipped with electrical heating elements was used to reach final moisture content of 1% (dry basis). The dried particles were screen manually and fine portion was separated. The dried and screened particles were stored in polyethylene bags until used.

Board Making and Testing

Particles were blended with different dosages of resin (10% core, 10% surface: 9% core :11% surface and 8% core :12% surface) and 1% hardener (based on dry weight of resin) at the concentration of 50%, utilizing rotary drum blender and spray nozzle. Then the blended particles were hand formed using wooden mold. Board target density and thickness was selected as 700 kg/cm³ and 15 millimeters. Homogenous particle mats were pressed in laboratory press (Buerkle L100) applying 30 bar specific pressure, and five millimeters per seconds closing speed. Three pressing times of 3, 4 and 5 minutes were applied. Three boards for each combination of variables and total of 27 boards were produced. All boards were conditioned at 65% relative humidity and 21 °C for 15 days and then test samples were prepared from each board according to relevant EN standards. MOR and MOE was measured according to EN310/1996, Internal bonding (IB), EN319/1996 and dimensional changes, EN 317/1996 standards. For each test, four samples were prepared from each board and tested.

Statistical Analysis

Factorial experimental design based on randomized block design was used for statistical analysis of the generated data and in case the effect of variable(s) on the measured properties was significant at 99% or 95% level, then the averages were grouped using DMRT.

Results and Discussion

The results of statistical analysis on the effect of resin dosage gradient and the press time of flexural properties (MOR and MOE) of the produced boards revealed the significant effect of these variables on both MOR and MOE. The MOR and MOE of the boards varied between 11.78 MPa. and 2066 MPa. For boards produced without applying resin dosage gradient to 18.38 MPa. and 2535 MPa. for boards with 4% resin gradient. However, statistically significant difference was not observed between 2% and 4% resin gradient. The interactive effect of two variables on MOR and MOE of the boards was also statistically significant at 95% level. The results of MOR and MOE measurements of the boards are shown in figure 1. The DMRT grouping of the results are also shown in figure 1 using superscript lower case letters. It is observed that longer pressing times and application of the resin dosage gradient improved both MOR and MOE (Fig.1). The low bulk density of cotton stalks particles helped the development of sufficient flexural strength and MOE to meet the requirements of the both Iran and EN standards (Kargarfard et al., 2006, Guler and Ozen, 2004).

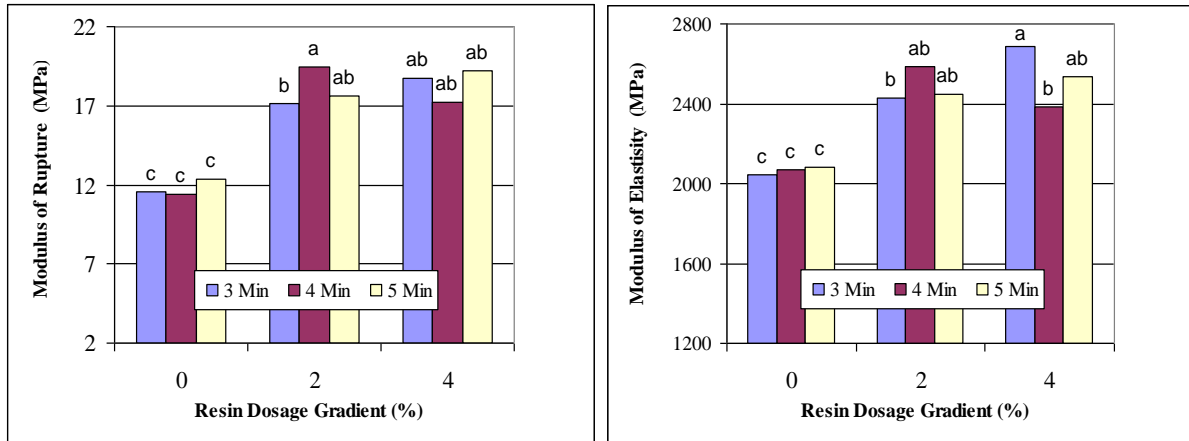


Fig. 1- Illustration of the effect of resin dosage gradient and pressing time on MOR and MOE of the boards produced using cotton stalks (Superscript lower case letters indicated DMRT grouping).

The impact of resin dosage gradient on internal bonding of the boards was statistically significant and as the resin gradient increases the IB of the boards increase from 0.856 MPa. to .0985 MPa. but significant difference was not observed between 2% or 4% resin gradient. However, the interactive effect of both variables on IB of the boards was not statistically significant (Fig.2).

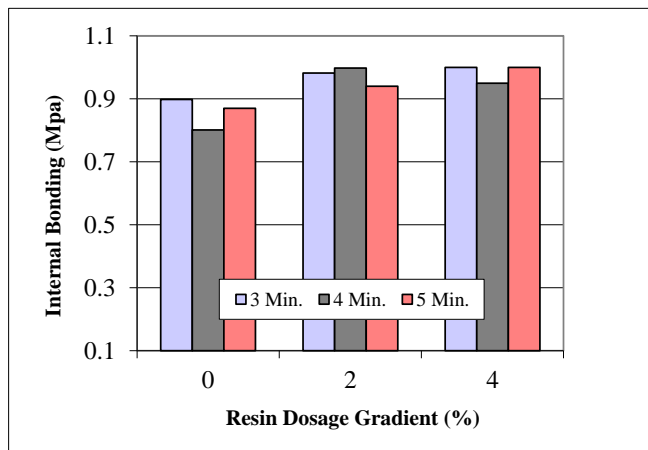


Fig. 2- Illustration of the influence of the resin dosage gradient and pressing time on internal bonding of the boards

The results thickness swelling measurement showed that the effect of resin gradient on both 2 and 24 hours thickness swelling is statistically significant at 99% level and lowest thickness swelling was measured on boards produced applying resin gradient. The impact of pressing times on thickness swelling was also statistically significant and as the pressing time increases, thickness swelling is reduced. The results of the thickness measurements are shown in Figure 3. The interactive effect of both variables on thickness swelling of the boards was statistically significant at 95% level. The results of the internal bonding and thickness swelling show that due to lower density of the cotton stalks, better bonding is developed between the particles (Moslemi, 1974, kargarfard et al., 2006, Guler and Ozen, 2004).

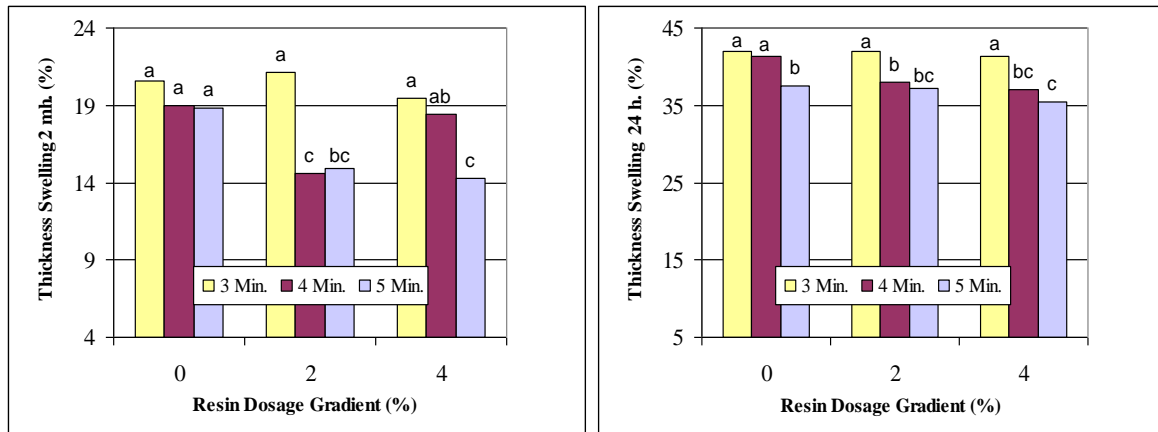


Fig. 3- Illustration of the effect of resin dosage gradient and pressing times on thickness swelling of the boards. Superscript lower case letters indicates DMRT grouping of the averages.

Conclusion

The potential of cotton stalks in the production of interior grade particleboard is studied. The results indicated that applying resin dosage gradient improves the flexural properties (MOR and MOE) of the particleboard. However applying longer pressing time will also improves the strength properties of the boards. Low bulk density of the cotton stalks particles facilitate the strength development of the produced boards. The properties of the cotton stalks particleboard surpass the requirement of both Iran and EN-312 standard requirements for interior grade particleboards.

References

- Bekalo, S.A., Reinhardt, H.W. and Riedl, B. 2010. Fibers from coffee husk and hulls for the production of particleboard. *Materials and Structures* 43:1049-1069.
- Food and Agriculture Organization Statistics. (2013). Rome, Italy.
- European Standard EN 310, 1996. Wood based panels, determination of modulus of elasticity in bending and bending strength. European Standardization Committee, Brussels.
- European Standard EN 312, 2003. Particleboards specifications, requirements for general purpose boards for use in general conditions. European Standardization Committee, Brussels.
- European Standard EN 317, 1996. Particleboards and fiberboards, determination of swelling in thickness after immersion. European Standardization Committee, Brussels.
- European Standard EN 319, 1996. Wood based panels, determination of tensile strength perpendicular to plane of the board. European Standardization Committee, Brussels.
- European Standard EN 326-1: 1993. Wood based panels, Sampling, cutting and inspection. Sampling and cutting of test pieces and expression of test results.
- Guler, C. ; Ozen, R.. (2004). Some properties of particleboards made from cotton stalks (*Gossypium hirsutum* L.). *Holz als Roh-und Werkstoff*. Vol. 62, No.1 P: 40-43.
- Grigouria. H. A, Natalos. A. G. 1999. Agro-waste panel bonded with UF and UF: PMDI resin. Presented at third European panel products symposium.
- Gu, J. and Gao, Z. 2002. A discussion on producing agro-residue composites with isocyanate resin. *Journal of Forestry Research*, 13(1):74-76.
- Kargarfard, A. Nourbakhsh, A. and Golbabaie, F. 2006. Investigation of the possibility of using cotton stalks in particleboard manufacturing. *Iran Wood and Paper Research* 21(2):95-104.
- Kargarfard, A. Nourbakhsh, A. and Golbabaie, F. 2006. Investigation of the possibility of using cotton stalks in particleboard manufacturing. *Iran Wood and Paper Research* 21(2):95-104.
- Khedar, J.; Nankongnab, N.; Hiranlabh, J.; Teekasp, S..2004. New low- cost insulation particleboards from mixture of durian peel and coconut coir. *Building and Environment J*. Volume 39. Issue 2. January 2004. Pp: 59-65.
- Meinschmidt, P. Schirp, A. Dix, B. Thole, V. Brinker, N. 2008. Agricultural Residues with light, parenchyma cells and Expandable filler Materials for the production of light weight particleboards. *International Panel Products Symposium; Braunschweig, Germany*, 179-188.
- Moslemi, A. A. (1974). Particleboard. Vol.2 : Technology. Carbondale III Southern Illinois Univ. Press.
- Meinschmidt, P. Schirp, A. Dix, B. Thole, V. Brinker, N. 2008. Agricultural Residues with light, parenchyma cells and Expandable filler Materials for the production of light weight particleboards. *International Panel Products Symposium; Braunschweig, Germany*, 179-188
- Sampathrajan, A. Vijayaraghavan, N.C. and Swaminathan, K.R. 1992. Mechanical and thermal properties of particleboards made from farm residues. *Bioresources technology*. 40:249-251.

Investigation on the Influence of Nano-clay Addition on Mechanical Properties of Soy straw-Polypropylene Composite

Abolfazl Kargarfard

Associate Prof., Wood and Forest Products Science Research Division, Research Institute of Forests and Rangelands, Tehran, Iran
Corresponding Author: a_kargarfard@yahoo.com

Ahmad Jahan-Latibari

Professor, Department of Wood and Paper Science and Technology, Karadj Branch, Islamic Azad University, Karadj, Iran

Abstract

The objective of this study was to produce natural fiber-plastic composite using soy straw powder as reinforcing component and to investigate the effect of nano-clay particles addition on the mechanical properties of the composite. Two levels of soy straw powder (35 and 45%, based on the weight of the composite), three levels of nano-clay (0, 3 and 6%) based on the weight of the polypropylene as the matrix was used. Five percent Maleic Anhydride Poly Propylene (MAPP) was added as the coupling agent. Composites compound was made and then the testing specimens were fabricated by injection molding and the mechanical strength were measured. The results were statistically analyzed using factorial experiment design. The results revealed that at higher dosage of the soy straw powder, the strength properties except impact strength values were reduced. At the higher addition of the nano-clay, the flexural strength and tensile strength were reduced and tensile and flexural modulus as well as the impact strength improved and the highest values were reached at 6% nano- clay addition.

Keywords; Natural-fiber; Polypropylene; Soy straw; Mechanical properties; Nano-caly

Introduction

New and advanced composites have been developed and used to utilize the advantages of the beneficial properties of each component and to eliminate the weakness and limitation of the

components used. These new materials often provide the useful properties compared to any of the constituents. Natural fiber reinforced composites resulting from the compounding of cellulosic material with thermoplastic polymer matrices have been developed to take the advantages of large quantity, annual renewability, low cost, light weight, excellent and competitive specific strength as well as environmental friendliness of such material (Oksman, 1994).

In general, in the course of natural fiber-plastic composites development and application, a wide range of lignocellulosic materials including wood powder and fibers, hemp fibers, linens, corns stalks, coconut shells, peanuts shells, wheat, and rice straws, etc., has been investigated by many research groups as fillers and/or reinforcing component for plastic matrices (Roger et al., 2000). Processing of such composite material is flexible, economical and ecological. Unfortunately, the incompatibility between polar lignocellulosic material and non-polar polymeric matrices affects the degree of dispersion of the fibers in the matrix and the overall homogeneity of the composite structure. Consequently, the use of compatibilizers in natural fiber reinforced polymer composites is required to improve poor interfacial attraction between hydrophilic fiber and hydrophobic polymer matrix. Therefore, most of the research on wood fiber reinforced composite has focused on improvement of interfacial interaction and the adhesion between wood fibers and plastic matrices by enhancing of the dispersion of fibers into the polymer matrix.

Nanotechnology is a recent development and has expanded very fast during last few decades and various sciences and technologies have benefited from this expansion. There has been continuing effort to take the advantages of recent advances in nanotechnology in the polymer sector as well, and composite material science and technology also showed interest in nanotechnology and research and development studies have been followed and a group of material called nanocomposites is produced (Lei et al. 2007). It has been demonstrated that application of nanoparticles in composite mixture improved the performance of noncomposites even at low level of addition compared to other common fillers, thanks to their special dimensions providing high aspect ratio (length to thickness) (Tjong et al. 2006).

Among different nanoparticles, nanoclay has attracted more interest as filler material and extensive research has been devoted on these nanoparticles as a filler material as well as reinforcing (Chooghee and naguib, 2007; Nourbakhsh et al. 2008). Even low levels of 1 to 5 parts per hundred (phr) have improved the strength properties of the nanocomposites (Faruk and Matuana 2008). It is believed that the nanocomposites are usually airtight, transparent, strong, and resistant to flame (Sinha et al. 2003). The impact of nanoclay on the physical and strength characteristics of nanocomposites have also been the objective of other studies (Nourbakhsh et al. 2008; Faruk and Matuana,2008; Chooghee and Naguib 2007; Yuan and Mira 2006; Wang et al 2006) and contradictory results have been reported.

The importance of nanocomposites and the global interest in application of waste material necessitates the development of alternative procedure to use such material in the production of value added products among them natural fiber-plastic composites. Therefore the objective of our study was directed to the application of soy straw powder and nanoclay particles in nanocomposite production.

Materials and Methods

Materials

Soy straw was collected from soy cultivating fields around the city of Gorgan, north of Iran. Soy straw was flaked using Pallmann ring flaker PZ8 and then the pith was separated. The depithed flakes were grounded in a grinding mill to produce suitable powder and the powder was classified using a set of 60 and 80 mesh screens. The portion of the powder passed 60 mesh and retained on 80 mesh screen was used as the filler. The powder was dried in air circulation oven at 80 °C to reach 1% moisture content required for compounding. The weight portion of the soy straw powder was either 35 or 45% of the total weight of the composite.

The polypropylene was purchased from Arak petrochemical Co. with density of 870 kg/m³ and melt flow index of 8 g/10 min. The flexural modulus, impact strength (Azod) and the tensile strength of the polypropylene were as 1100 MPa, 40J/m and 30 MPa respectively.

The nanoclay used was a refined montmorillonites, Cloisite 15A, made by US Southern-Clay Company, Texas, USA. The nanoclay dosage was at 0,3 and 6% of the total weight of the composite.

The maleic anhydride grafted polypropylene (MAPP) manufactured by the Aldrich was used as coupling agent. The coupling agent contained 1% (wt./wt.) grafted maleic anhydride, with the density of 934 kg/m³ and the viscosity of 4.0 poise, at 190 °C, M_n and M_w of 3900 (GPC) and 9100 (GPC) and the melting point of 165 °C, Five percent MAPP was used for all compounds.

Methods

Compounding and Sample Preparation

The compounding procedure was the direct blending procedure in which all components of the composite are mixed simultaneously, using Dr. Collin's counter-rotating twin screw extruder (Polymer and Petrochemical Research Center of Iran). The mixing temperature profile of 155-190 °C in different sections of the extruder, and the rotational speed of 70 rpm were selected. The extrudate produced was cooled to room temperature and then grinded to produce granules for further processing. Grinding was carried out in a laboratory mill and the granulated material was cooled to 85 °C before injection molding.

An injection molding machine set at 160-180 °C temperature was used to prepare test samples. At each molding operation, a complete set of specimens for different tests are produced.

Strength Evaluation

The specimens were conditioned at 65 ± 5% relative humidity and 20 ± 5 °C for two weeks prior to testing. Standard test methods used were as follow: tensile strength and modulus; ASTM D 638, three-point flexural; ASTM D 790, and impact strength; ASTM D 256. Factorial experiments was used for statistical analysis.

Results and Discussion

The results of the strength measurements on soy powder-PP nanocomposite produced incorporating different amounts of nanoclay and soy powder content are illustrated in Figures 1-

3. Each value in figures is the average of four measurements. Statistical analysis results using factorial experimental design are summarized in Table 1 showing the F-value and significance level. The results of statistical analysis revealed that the effect of soy powder content on flexural strength and modulus as well as the tensile strength of the nanocomposite was statistically significant at 95% level. The flexural strength and modulus of the nanocomposite containing 35% soy powder was higher than those containing 45% soy powder indicating that at higher dosage of soy powder, the bonding between polymer and powder is deteriorated. However the effect of this variable on tensile modulus and impact strength was not significant. The impact of nanoclay content on flexural strength and modulus and tensile strength was also statistically significant at 95% level and the effect of this variable on tensile modulus and impact strength was statistically significant at 99% level. As the dosage of the nanoclay increases, the flexural strength decreases and the flexural modulus increases which is the results of the addition of platelet nanoclay in the composite. However, the interactive effect of two variables on flexural and tensile strength was not statistically significant but the effect on flexural and tensile modulus and impact strength was statistically significant at 95% level (Table 1).

Table 1- The results of the statistical analyses of the effect of variables of nanocomposite properties (F value and significance level)

Properties Variable	Flexural strength	Flexural modulus	Tensile strength	Tensile modulus	Impact strength
soy powder content (A)	2.737*	2.375*	10.024**	0.530 ^{ns}	0.123 ^{ns}
nanoclay content (B)	3.472*	4.697*	3.161*	5.236**	10.318**
A*B	0.384 ^{ns}	4.609*	1.216 ^{ns}	3.512*	3.428*

**-99% significant level, *-95% significant level, ns- not significant

The nanocomposite containing higher dosage of nanoclay and soy powder exhibited higher tensile modulus compared to other combination of the nanoclay and soy powder (Fig. 1). However, the tensile strength of the nanocomposites containing different amount of nanoclay is almost similar. Even though, lignocellulosic fillers reinforce the composite, but sufficient adhesion between the reinforcing substance and the matrix is the prerequisite for good bonding (Nourbakhsh et al. 2008). On the contrary to common expectation that application of nanoparticles will improve the strength of the composites, but this is not always true and if the bond development condition is not provided, then the strength improvement is limited. The platelet shape and the high aspect ratio of nanoclay particles contributed to the development of the tensile modulus of elasticity of nanocomposites. Such configuration of the particles initiates better delamination and dispersion of nanoparticles in the matrix providing intercalation phenomenon and interlocking of nanoparticles with matrix (Faruk and Matuana 2008).

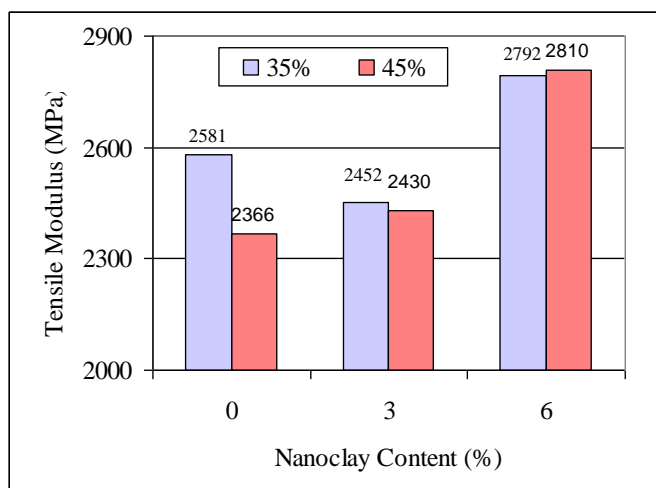


Figure 1. The influence of soy powder and nanoclay content on tensile modulus of soy powder/polypropylene nanocomposite.

Similar results were observed on flexural properties of soy powder/polypropylene nanocomposite. Soy powder/polypropylene nanocomposite showed higher flexural strength at lower content of either soy powder or nanoclay (Fig. 2). This is contradictory to the results of Nourbakhsh and Ashori (2010) indicating the influence of other factors such as the presence of different amount of MAPP. The flexural modulus of elasticity of the nanocomposite containing different contents of nanoclay and soy powder was the highest. The unique shape, favorable aspect ratio and delamination of nanoclay platelets and the presence of nanoclay as well as penetration of polymer chains in the open structure of the fibers provided denser nanocomposite and brittle material which produced higher flexural modulus of elasticity (Wang et al. 2006; Han et al. 2008).

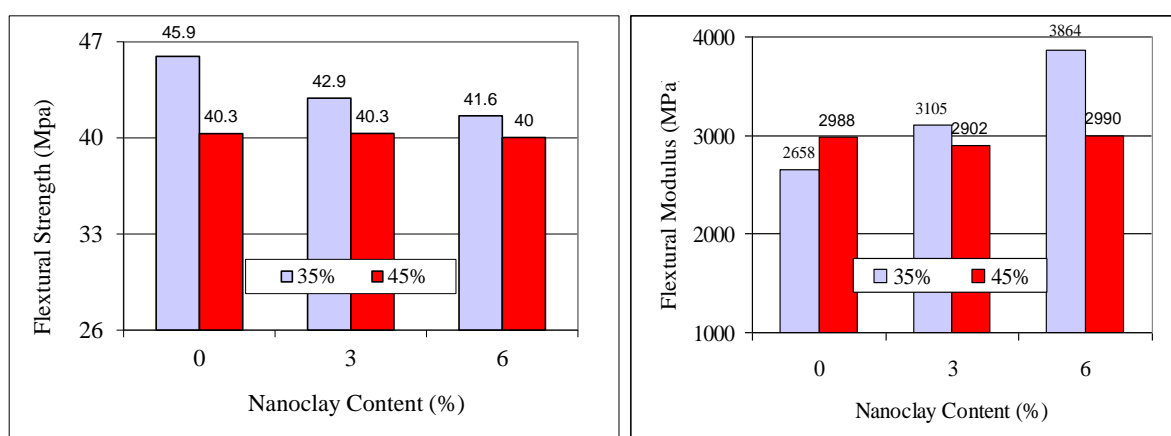


Figure 2. The influence of soy powder and nanoclay content on flexural strength and modulus of soy powder/ polypropylene nanocomposite

Higher addition of soy powder and nanoclay improved the impact strength of nanocomposites (Fig. 3). When nanoclay is incorporated in the composite, the density of the nanocomposite increased and brittle and fragile substance with lesser toughness was produced. Furthermore, the

presence of nanoclay particles in combination with ductile soy powder improve the bond formation between the matrix and the reinforcing component (Razavi-Nouri et al.,2006).

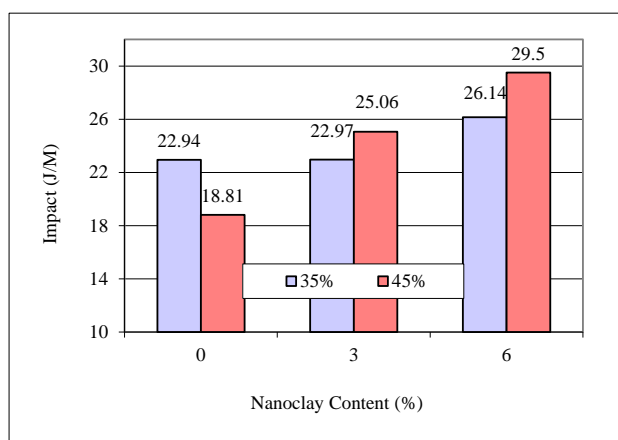


Figure 3. The influence of soy powder and nanoclay content on impact strength of soy powder/polypropylene nanocomposite.

Conclusion

Flexural and tensile strength of nonocomposites were decreased to response to increasing soy powder content from 35 to 45% indicating the deterioration of the bond between the lignocellulosic material and polymer. However, both tensile and flexural modulus of elasticity of nanocomposites was higher at higher content of either soy powder or nanoclay. The tensile modulus of elasticity of nanocomposites containing 6% nanoclay and 45% soy powder was at the highest values which show the interactive effect of these variables. The configuration of the nanoclay particles initiates better delamination and dispersion of nanoparticles in the matrix providing intercalation phenomenon and interlocking of nanoparticles with matrix. Higher soy powder content (45%) and higher content of nanoclay increased the impact strength of the nanocomposites. The results revealed that soy straw powder can be used as reinforcing filler in polypropylene matrix.

References

- ASTM annual book of standard testing methods, Part , Plastics. 2012. Philadelphia, PA., USA.
- Choonghee, J., and Naguib, H. E. .2007. .Effect of nanoclay and foaming condition on the mechanical properties of HDPE-Clay nanocomposites foams. *Journal of Cellular Plastics* 43(2):111-121.
- Faruk.O. and Matuana.L, 2008 Nanoclay reinforced HDPE as a matrix for wood-plastic composites, *Composites Science and Technology* 68: 2073-2077.
- Han, G., Lei, Y., Wu, Q., Kojima, Y., and Suzuki, S. 2008. Bamboo-fiber filled high density polyethylene composites: Effect of coupling treatment and nanoclay. *Journal of Polymers and the Environment* 16(2): 123-130.
- Lei .Y, Wu.Q, Clemons.C.M, Yao.F, Xu.Y. 2007 .Influence of nanoclay on properties of HDPE/wood composites, *J. of Applied Polymer Science*. 106:3958-3966.

- Nourbakhsh, A., Doosthosseine, K., Kargarfard, A., Golbabaie, F., and Haji-Hassani, R. 2008. Investigatoin of OCC fiber polymers composites in air-forming production. *Iranian Journal of Wood and Paper Science Research* 23(2): 91-101.
- Nourbakhsh, A.; Ashori, A. 2008. Influence of nanoclay and coupling agent on the physical and mechanical properties of polypropylene/bagasse nanocomposite. *Journal of Applied Polymer Science*. 112:1386-1390.
- Oksaman, K. 1994. Improved intraction between wood and synthetic polymers in wood/plastic composites. *Wood Science and Technology Journal*. 30(23): pp: 197-203.
- Razavi-Nouri, M., Jafarzadeh Dogouri, F., Oromiehie, A., and Ershad Langroudi, A. 2006. "Mechanical properties and water Absorption behavior of chopped rice husk filled polypropylene composites. *Iranian Polymer Journal* 15(9):757-766.
- Roger, M; Rowell, MR; Anand, R; Sanadi, Caulfield, DF; Rodney, E; and Jackson. 2000. Utilization of natural fibers in plastic composites: problems and opportunities, *Lignocellulosic/plastic composites*, pp: 5-23.
- Sinha Ray, S., and Okamoto, M. 2003. Polymer layered silicate nanocomposites; A review from preparation to processing. *Polymer Sci*. 28(11): 1539-1641.
- Tjong, S. C. 2006. Structural and mechanical properties of polymer nanocomposites: A review. *Journal of Material Science and Engineering* 53-73: 197pp.
- Wang, L., Wang, K., Chen, L., Zhang, Y., and He, C. 2006. Preparation, morphology and thermal/mechanical properties of epoxy/nanoclay composite. *Applied Science and Manufacturing* 37(11): 1890-1896.
- Yuan, Q., and Misra, R. D. K. 2006. Impact fracture behavior of clay-reinforced polypropylene nanocomposites. *Journal of Polymer Science* 47(12): 4421-4433.

Using Pine and Oak Bark Tannin Extracts as an Adhesives for Particleboards Production

Walid Kasir Ayad Aldaody Moneeb Mofty

Mosul University, Mosul, Iraq
Forestry Dept., College of Agriculture and Forestry

Abstract

In this study tannin extracts from the bark of two main species grown in Iraq namely; *Pinus brutia* Ten. And *Quercus aegilops* were used for particleboards production. Tannins were extracted from the parks, the two species examined appeared to have barks that are suitable for the production of tannins in sufficient amounts. Prior to panel manufacturing, the concentrated extracts were methylated by 10% of para formaldehyde as a hardener at extracted pH of 5.5. panels of laboratory scale particleboards were manufactured at two levels of tannin sources (pin and oak), two levels of press temperatures (170 and 190°C), and three levels of pressing time (8, 10, and 15 minutes). The physical and mechanical properties of the produced panels were tested according to ASTM standards. The results showed that pine park tannins gave better mechanical properties (MOR, MOE, and IB) of panels compared to oak bark tannin. Using press temperatures of 190 °C generally improved the mechanical properties of panels at 10 minutes pressing time. With regard to water absorption, thickness swelling and linear expansion, the results revealed tannins behavior, formaldehyde and wax content of pine and esters for oak as hydrophobic materials. Press temperatures (170°C) reduced moisture contents and increased panels resistance to water absorption at 15 minutes pressing time. Thickness swelling and linear expansion were lower in panels made from pine tannin compared to those manufactured from oak tannins. The results of this work proved that there is a possibility of using aqueous tannin extracts from the park of *p. brutia* and *Q. aegilops* after chemical modifications as a binder in particleboards production.

Key words: particleboards, binder, bark extracts, tannins, properties.

Part of Ph.D Thesis for Moneeb Mofty

Introduction

Adhesives play an important role in the manufacturing of wood-based products specially in particle boards mills. The resins manufactured are usually the range of amino and phenolic resins. For particleboards, only urea formaldehyde and phenol formaldehyde resins are being utilized. In the recent past, increasing attention has been paid to the use of natural adhesives as a binder in the wood-based panels industries. The idea of developing adhesives based on tannin-formaldehyde resins dated back for more than 50 years (Dalton, 1940 and Plomley et al. 1957, 1964). In 1971, an unfortified mimosa tannin adhesive for particleboards was formulated (Pizzi, 1977 and 1989). Several other tannin adhesive formaldehyde for manufacturing particleboards all

with good results, but all these are obtained by addition of fortified synthetic resin such as urea and phenol formaldehyde (Pizzi, 1978). In Iraq, research into the use of eucalyptus bark tannin started in the early years of 2002.

Al-Zaidbagy (2002) reported that the tannin content of *Eucalyptus camaldulensis* compared quite favorably with that of known commercial tannin sources and good properties of panels were produced from such source of tannin. Among the most common mountain forest in North of Iraq region are Oak and pine species. No work has been experienced in Iraq concerning the use of Oak and Pine barks tannin in particleboards manufacturing, therefore, the objective of this study were to:

1. Compare the strength and dimensional properties of particleboards bounded with Oak and Pine barks tannin with commercial synthetic urea-formaldehyde.
2. Determine the effect of partial replacements of bark tannin with urea-formaldehyde on the properties of the produced panels.

Material and Methods

Quercus aegilops and *Pinus brutia* barks were collected from trees growing in the Northern part of Iraq. The bark tannins were obtained as a liquid extract after extraction from bark by using three different sequences. The tannin extracts were concentrated to 50% solid content and then treated with 10% (based on oven dry weight) paraformaldehyde. The urea-formaldehyde as a commercial adhesive was obtained from Mosul furniture factory as a powder, the liquid urea was prepared by dissolving in water. The liquid urea-formaldehyde contained 50% solids. The mixed ratios of tannin-paraformaldehyde (TF) and urea-formaldehyde (UF) were prepared for particleboards studies as follows:

Five levels of mixing percentages of : UF namely (100:0; 75:25; 50:50; 25:75; and 0:100). 180 laboratory panels were manufactured at two levels of tannin sources, two levels of temperature (170 and 190 °C), and three levels of pressing time (8, 10, and 15 min). the panels were manufactured under pressure of 1250 psi. 10% resin content were used to get target density of 0.6 gm/cm³ at panel thickness of 18 mm. The physical and mechanical properties of the produced panels were tested according to ASTM standard 2559 (1961) after conditioning at 21 ± 2 °C and 65% R.H.

The statistical analysis system (SAS) was used to analyze the data the data obtained. The values given in tables are the means of six samples (each treatment replicated three times and two samples were taken from each replication).

Results and Discussion

Static bending and internal bond properties :

The results of the analysis of variance for MOR, MOE and IB) showed that there is a high statistical significance (at 1% level) differences between the strength values obtained when testing the different ratios of TF:UF, also, the analysis showed a significant effect of tannin sources, pressing temperature and pressing time on these properties. The results showed (Table 1) that *Pinus brutia* bark tannin gave better bending properties (MOR and MOE) and IB of

panels than *Quercus eagilops*. The averages of MOR, MOE and IB were 93.77, 5749.8 and 4.35 Kg/cm² for pine wood, while for Oak wood the averages were 82.90, 4935.0 and 3.84 Kg/cm² for MOR, MOE and IB respectively.

It is evident from duncans multiple range test (Table 1) that the highest values of MOR, MOE and IB regardless of the effect of tannin sources, pressing temperature and pressing time (147.29, 9456.6 and 6.84 Kg/cm² respectively) obtained from panels manufactured from 100% urea-formaldehyde and 0% tannin-formaldehyde, and the lowest values (27.05, 1287.0 and 2.33 Kg/cm²) of the same properties respectively were obtained from panels made from 100% tannin-formaldehyde and 0% urea-formaldehyde. It appeared that there is a decrease in the mechanical properties as the amount of tannin-formaldehyde increases in the ratios, similar results concerning MOR, MOE and IB were obtained by Kasir and Al-Zaidbagy (2004) in their study on the utilization of *Eucalyptus camaldulensis* bark extract fortified with UF and Goncalves et al.(2003) in there work on particleboards made with UF modified with tannin from mimosa.

Table (1): Averages of mechanical properties of produced particleboards.

Studied factors		MOR (Kg/cm ²)	MOE(Kg/cm ²)	IB(Kg/cm ²)
Tannin Source	Pine	93.77 a	5749.8 a	4.35 a
	Oak	82.90 b	4935.0 b	3.84 b
TF:UF * Ratios	100:0	27.05 e	1287.6 e	2.23 d
	75:25	50.54 d	2833.3 d	2.62 d
	50:50	91.78 c	5759.0 c	4.13 c
	25:75	125.01 b	7377.7 b	4.67 b
	0:100	147.29 a	9456.6 a	6.84 a
Pressing temperature(°C)	170	82.69 b	4709.1 b	3.68 b
	190	93.24 a	5796.6 a	4.52 a
Pressing time (min.)	8	85.53 b	4669.4 c	3.41 c
	10	94.24 a	5897.6 a	4.54 a
	15	85.24 b	5461.5 b	4.35 b

Averages followed by the same letter vertically are not significant at P<0.05

*: TF= Tannin-formaldehyde , UF=Urea-formaldehyde

It appeared that there is a possibility of fortifying tannin adhesives and getting better properties by using UF with 25 to 50% *pinus brutia* tannin and at 25% with *Quercus aegilops* tannin. Press temperature (190°C) also improved the mechanical properties of panels especially at 10 minutes pressing time. The value of MOR, MOE and IB were 93.24, 5976.6 and 4.52 kg/cm² respectively. The panels were also close in their mechanical values to the values mentioned in ASTM 2559, this may be attributed to the use of high platen temperatures and long pressing time during hot pressing, such conditions probably enhanced the polymerization and curing of adhesive. Similar results reported by sumadiwangsa (1985) who stated that there was a linear correlation between platen temperature and varios properties of particleboards, the higher the temperature, the better quality of the boards.

Water Absorption after 2 and 24 Hours Immersion:

With regard to water absorption after 2 and 24 hours, the results revealed tannins behavior, formaldehyde and wax content for pine and ester for Oak as hydrophobic materials. Both types of extracts (i.e. Pine and Oak extracts) improved the water absorption property, however, pine extract was a little bitter in reducing absorption compared to Oak extract. Tables (21 and 3)

shows that there is a significant differences between the water absorption values when testing the different ratios of adhesive blends after immersion in water for 2 and 24 hours. It is evident that the lowest values (59.85 and 71.35%) for absorption after 2 and 24 hours respectively obtained from panels made with 100% TF which differed significantly from other panels contained different amount of urea-formaldehyde in their blend, while the highest percents 82.83% after 2 hours and 95.33% after 24 hours immersion obtained from panels contained 100% urea-formaldehyde. This decreased in water absorption is probably due to the high amount of polyphenolic extractives in the bark as explained by Gokay et al. (2003). With respect to the effect of pressing temperature on water absorption, tables (2 and 3) shows that panels made at 170 °C were significantly better in water absorption than panels made at 190 °C. for both periods of immersion. Also, increasing pressing time reduced water absorption.

Thickness Swelling After 2 and 24 Hours Immersion:

The results of statistical analysis for thickness swelling showed that all studied had significant effects on this properties except for immersion for 24 hours. It appear that the lowest values (21.11% and 25.79%) for immersion after 2 and 24 hours obtained from panels made with 100% TF and the highest values (28.74% and 32.26%) for the same periods appeared in the panels made from 100% UF. It seems from the results that by reinforcing the tannin mix with urea, the thickness as property affected negatively (Tables 2 and 3). This decrease is probably due to the formation of condensation products with high bonding potential as explained by Gokay et al. (2003).

With regards to the effects of pressing temperatures and pressing time, it is found that panels made at 170 °C weresig better in thickness swelling after 2 and 24 h. than panels made at 190 °C while longer pressing time gave better results compared to lower pressing time.

Linear Expansion after 2 and 24 Hours immersion:

In the case of linear expansion test, it appeared from tables (2 and 3), that the linear expansion was slightly lower after 2 and 24 h. of immersion in panels made from Oak extract that from pine extractand panels made at 170 °C were lower in linear expansion than panels made at 190 °C. in the average pressing time analysis, 15 minutes pressing time was significantly lower than the other two levels especially after 2 hours of immersion. The slight reduction in linear expansion probably can be attributed to the irrecoverable movement resulting from the relief of the internal compressive stresses.

Conclusions

Generally, the results of this study conformed that there is a possibility of using aqueous extracts from the bark of *Pinus brutia* trees and *Quercus aegilops* trees after chemical modification as a binder in particleboards production. This work also has proved. That, incorporating Urea-formaldehyde with tannin-formaldehyde to produce good-quality adhesive for manufacturing particleboards for interior use.

Table (2): Averages of physical properties after immersion in water for 2 hours.

Studied factors		Water Absorption %	Thickness swelling %	Linear expansion %
Tannin Source	Pine	69.82 a	23.77 a	0.75 b
	Oak	74.94 b	26.29 b	0.64 a

TF:UF * Ratios	100:0	59.85 a	21.11 a	0.64 ab
	75:25	70.12 b	22.91 b	0.68 bc
	50:50	70.15 b	24.58 c	0.57 a
	25:75	78.96 c	27.81 d	0.78 cd
	0:100	82.83 d	28.74 d	0.84 d
Pressing temperature(°C)	170	71.02 a	24.78 a	0.66 a
	190	73.76 b	25.28 a	0.73 b
Pressing time (min.)	8	73.51 a	26.03 b	0.78 b
	10	72.08 a	24.77 a	0.75 b
	15	71.55 a	24.29 a	0.56 a

Averages followed by the same letter vertically are not significant at $P < 0.05$

*: TF= Tannin-formaldehyde , UF=Urea-formaldehyde

Table (3): Averages of physical properties after immersion in water for 24 hours.

Studied factors		Water Absorption %	Thickness swelling %	Linear expansion %
Tannin Source	Pine	84.07 a	29.27 a	0.98 a
	Oak	90.51 b	30.00 a	0.88 a
TF:UF * Ratios	100:0	71.35 a	25.79 a	1.02 b
	75:25	85.42 b	27.74 b	0.98 b
	50:50	89.45 c	30.24 c	0.75 a
	25:75	94.89 d	32.16 d	0.95 b
	0:100	95.33 d	32.26 d	0.98 b
Pressing temperature(°C)	170	86.19 a	29.10 a	0.86 a
	190	88.38 b	30.17 b	1.01 b
Pressing time (min.)	8	90.36 b	30.56 b	1.00 a
	10	86.23 a	29.75 b	0.93 a
	15	85.27 a	28.59 a	0.88 a

Averages followed by the same letter vertically are not significant at $P < 0.05$

*: TF= Tannin-formaldehyde , UF=Urea-formaldehyde

References

- Al-Zaidbagy, O. I. (2002). Utilization of *Eucalyptus camaldulensis* bark extract as an Adhesive for particleboards. Ph.D. Thesis, college of Agriculture and Forestry, Mosul University, Iraq.
- Dalton, I. K. 1950. Tannin-formaldehyde resin as adhesive for wood. Austr. J. Appl. Sci. 1:54-70.

- Gokay, N.; H. Kirci; A. Temiz, 2003. Influence of impregnating wood particles with Mimosa bark extract on some properties of particleboards. Elsevier, An International J. For Industrial Crops And Products, 20: 339-344.
- Kasir, W. A. and O. I. Al-zaidbagy, 2004. Improving the properties of particleboard bonded by fortified eucalyptus bark extract with urea-formaldehyde. Iragi J. for Agric. Sci. 5(4):69-76.
- Pizza, A. 1978. Chemistry and technology of cold and thermosetting wattle tannin-based wood adhesive. Ph.D. Thesis, Bloemfontein, South Africa. University of the Orange Free State.
- Pizza, A. 1977. Wattle based adhesive for exterior grade particleboards. For. Product J. 28(12):42-47.
- Plomely, K. F. 1964. Tannin-formaldehyde adhesives for wood. I. Mangrove Tannin Adhesives. Austr. J. Appl. Sci., 15:171-182.
- Plomely, K. F.; J. W. Gottstein; W. E. Hillis 1957. Tannin-formaldehyde adhesives. CSIRO Australian Forest Products Newsletter 234, Melbourne.
- SAS, 1979. Statistical analysis system. Carry, North Carolina, USA.
- Sumadiwangsa, S. 1985. Mangrove bark powder as particleboards adhesive. J. penelitian Hasil Hutan, 2(4): 1-7.

Effect of Wood Chemical Composition on Physical Properties of Biocomposites

Alperen Kaymakci^{1}-Nadir Ayrilmis²*

¹ Research Assistant ² Associate Professor, Department of Wood Mechanics and Technology, Forestry Faculty, Istanbul University, Bahcekoy, Sariyer, 34473, Istanbul, Turkey

alperen.kaymakci@istanbul.edu.tr

nadiray@istanbu.edu.tr,

* Corresponding author

Abstract

The effect of chemical composition of wood on physical properties of biocomposites was investigated. To meet this objective, the sound and decayed pine wood flour was compounded with polypropylene at 30, 40 or 50% (by weight) content with coupling agent, maleic grafted polypropylene with anhydride, in a twin screw co-rotating extruder. Test specimens were produced by compression moulding process from the pellets dried to moisture content of 1%. The effects of woods chemical composition on density, thickness swelling and water absorption properties of the produced biocomposites were determined. Based on the findings obtained from the present study, decayed pine wood flour could be successfully used in manufacture of biocomposites having high dimensional stability.

Keywords: biocomposites, chemical composition, water absorption, thickness swelling

Introduction

Composite materials produced from natural fiber and petroleum-derived non biodegradable polymers (polypropylene (PP), polyethylene (PE), epoxies, etc.) or biopolymers (poly(lactic acid) (PLA), polyhydroxyalkanoates (PHAs), etc.) are broadly defined as biocomposites (Mohanty et al., 2005). In manufacturing biocomposites natural organic fibers from renewable bioresources offer the potential to act as biodegradable reinforcing materials, alternative for the use of glass or carbon fibers and inorganic fillers. Compared to these materials, natural fibers present lower density; less abrasiveness; lower cost and are renewable and biodegradable (Mengelöglu and Karakus, 2012).

Coupling agents play a very important role in the improvement of compatibility and bonding strength between polar wood fibers and nonpolar thermoplastics in biocomposites. Maleated polypropylene (MAPP) has been extensively used in wood- biocomposites. The maleic anhydride (MAH) present in MAPP provides polar interactions, such as acid-base interactions, and can also covalently link to the hydroxyl groups on the lignocellulosic fiber (Ayrilmis et al., 2010)

Performance of biocomposites have been extensively investigated in previous studies (Lulianelli et al., 2010; Gassan and Bledzki, 1997; Sain and Kokta, 1993; Yang et al., 2007]. Most of the studies mainly focused on determining the reinforcing filler types and loading levels, modified fillers, or coupling mechanism on the properties of biocomposites. An extensive literature search did not reveal any information about the effect of of chemical composition of wood on physical properties of biocomposites. In this study, we aimed to determine effect of of chemical composition of wood on physical properties of biocomposites from sound and decayed pine wood flour and polypropylene with compatibilizing agent.

Materials and Methods

Materials

The pine wood flour (PWF) and decayed pine wood flour (DPWF) were obtained from Kafkasor plateau in Artvin, Turkey, granulated into 60 mesh size fiber using Thomas- Wiley mill, and dried before manufacturing. The polypropylene (PP) ($T_m = 165^\circ\text{C}$, $q = 0.91 \text{ g/cm}^3$, MFR/230°C/2.16 kg= 3.2 g/10 min) supplied by a Bolearis AG in Austria, was used as the polymeric material. The MAPP (Optim-E425) as the coupling agent was supplied by Pluss Polymers Pvt. Ltd. in India.

Chemical analysis of sound pine wood and decayed pine wood

Samples for chemical analysis were prepared according to TAPPI Standard Method T 257-os-76. Alcohol/benzene extracted samples were used for the determination of hollocellulose, alpha cellulose, lignin and ash. All measurements were repeated three times. The chemical composition of wood was determined by following

TAPPI standard procedures:

Holocellulose Wise's chloride method

Alpha cellulose TAPPI T 203 cm - 99

Lignin Runkel (1951)

Alcohol-benzene solubility TAPPI T 204 cm - 97

Hot and cold water solubility TAPPI T 207 cm - 99

1% NaOH solubility TAPPI T 212 cm – 98

Composite Manufacturing

The PWF and HDPE and with MAPE granulates were processed in a 30 mm co-rotating twin-screw extruder with a length-to-diameter (L/D) ratio of 30:1. The barrel temperatures of the extruder were controlled at 170, 180, 190, and 190°C for zones 1, 2, 3, and 4, respectively. The temperature of the extruder die was held at 200°C. The extruded strand passed through a water bath and was subsequently pelletized. Pellets were cooled in water and granulated. Granulated pellets were dried at 105°C for 24 h. Pellets then were pressed into a 3 mm-thick 130mm x 130 mm panels using a temperature of 170°C and a pressure of 25 bar for 20 min and cooled. After pressing, the composites were conditioned in a climatic room with the temperature of 20°C and the relative humidity of 50%. The composite group consists of PP, DPW, PWF and MAPP in varying proportions. The formulations of the composites are given in Table 1.

Table 1: The formulation of wood polymer composite

Composite Code	Pine Wood Flour (%)	Decayed Pine Wood Flour (%)	Polypropylene (%)	MAPP (%)
A	30	-	70	3
B	40	-	60	3
C	50	-	50	3
D	-	30	70	3
E	-	40	60	3
F	-	50	50	3

Property Testing

Physical properties (water absorption and thickness swelling, Water absorption (WA) and thickness swelling (TS) of the thermoplastic composites were evaluated according to EN 317 (1993). Five specimens, dimensions of 50 mm x 50 mm x 3 mm, from each group were used for the WA and TS tests. Before testing, samples were conditioned in a climatized room at 20 °C and 65% relative humidity. The specimens were weighed and their thicknesses were measured. The measured specimens were dipped into water and their weight and thickness were measured 2h and 24 hours. Before each measurement the surface of specimens were wiped out with paper towel. The percentage of WA and TS were calculated according to Equations (1) and (2), respectively:

$$WA_t = \left[\frac{W_t - W_0}{W_0} \right] \times 100 \quad (1)$$

$$TS_t = \left[\frac{T_t - T_0}{T_0} \right] \times 100 \quad (2)$$

Where WA_t is the WA value at time t , W_0 is the initial dry weight of specimens, W_t is the weight at time t , TS_t is the TS at time t , T_0 is the initial thickness of specimens, and T_t is the thickness at time t .

Result and Discussion

The results of chemical compositions of sound and decayed pine wood are shown in Table 2.

Table 2: Chemical compositions of sound and decayed pine wood

Chemical composition	Sound Pine Wood (%)	Decayed Pine Wood (%)	Changes (%)
Hollocellulose	73.27	35.16	- 52
Alpha cellulose	43.15	14.42	- 66
Lignin	28.24	50.75	+ 79
Alcohol benzene solubility	5.81	16.12	+ 177
Cold water solubility	3.12	5.49	+ 75
Hot water solubility	4.22	8.57	+ 103

1% NaOH solubility	16.41	54.97	+ 243
--------------------	-------	-------	-------

Densities of manufactured biocomposites were determined and are summarized in Table 3. Biocomposites in the density range of 0.93 to 1.02 were produced.

Table 3: Some physical properties of biocomposites filled with sound wood and decayed wood.

Composite Code ¹	Density (g/cm ³)	Water Absorption (WA) (%)	Thickness Swelling (TS) (%)
A	0.97	0.36	0.25
B	1.00	0.52	0.46
C	1.02	0.85	0.66
D	0.93	0.21	0.14
E	0.95	0.33	0.24
F	0.98	0.39	0.30

¹ See Table 1

According to Table 2, The lowest TS value was 0.14% for the samples containing 30% decayed pine wood flour (Group D), while the highest TS value was found as 0.66 % for the samples containing 50% sound pine wood flour (Group C) after 24h of submersion in water. The similar trends were also observed WA values. The lowest WA value was 0.21% for the samples containing 30% decayed pine wood flour (Group D), while the highest WA value was found as 0.85 % for the samples containing 50% sound pine wood flour (Group C) after 24h of submersion in water. The rates of water absorption and thickness swelling were higher in case of higher loaded pine wood flour in the polypropylene biocomposite. The reason behind this was the higher possibility of water absorption by hydrophilic nature of fibers, which proportionally increases the rate of water absorption with higher fiber loading. PP has very negligible or no water absorption ¹¹ and hence, it can be assumed that 99.9% of water is absorbed by the pine wood flour.

The moisture absorption in composites is mainly due to the presence of lumens, fine pores and hydrogen bonding sites in the wood flour, the gaps and flaws at the interfaces, and the micro cracks in the matrix formed during the compounding process (Stokke and Gardner, 2003). Water absorption by cellulose and hemicelluloses depends on the number of free hydroxyl groups thus the amorphous regions are accessible by water. Polar hydroxyl groups on the lignocellulosic material are contributed predominantly by holocellulose (cellulose and hemicellulose) and lignin (Aydin, 2004). Although amount of holocellulose which has a large of polar hydroxyl groups in the decayed pine wood flour is lower than its sound pine wood flour, composites containing the decayed pine wood flour showed lower TS and WA. This was attributed to the polar hydroxyl groups were mainly responsible for hydrogen bonds with polar adhesives polymers. The lower TS and WA values of the composites containing higher amounts of the sound pine wood flour can be related to higher amounts of holocellulose materials in the cell walls of the sound pine wood flour (See Table 2).

Conclusions

The results of this preliminary investigation showed that decayed pine wood flour could be successfully used in manufacture of biocomposites having high dimensional stability. The WA and TS of the biocomposites filled with sound pine wood higher than that of decayed pine wood. At the constant content of the wood flour (50 wt %), TS and WA values of the biocomposites filled with sound wood were found to be 0.66 and 0.85 while they were 0.30 and 0.39 for the biocomposites filled with decayed pine wood flour. This situation mainly due to chemical composition of wood. The lower TS and WA values of the composites containing higher amounts of the sound pine wood flour can be related to higher amounts of holocellulose materials in the cell walls of the sound pine wood flour.

References

- Mohanty, A. K., Misra, A. M., Drzal, L. T., Selke, S. E., Harte, B. R., and Hinrichsen, G. (2005). "Natural fibers, biopolymers, and biocomposites: Introduction," In: *Fibers, Biopolymers, and Biocomposites*, 1st Ed., A. K. Mohanty, M. Misra, and L. T. Drzal (eds.), Taylor and Francis, Boca Raton, pp. 1-36.
- Mengeloglu, F., Karakus, K. 2012. Mechanical Properties of Injection-Molded Foamed Wheat Straw Filled HDPE Biocomposites: The Effects of Filler Loading and Coupling Agent Contents, *BioResources* 7(3), 3293-3305.
- Ayrilmis, N., Buyuksari, U., Dundar, T. 2010. Waste Pine Cones as a Source of Reinforcing Fillers for Thermoplastic Composites, *Journal of Applied Polymer Science*, 117, 2324–2330.
- Lulianelli G, Tavares MB and Luetkmeyer B. Water absorption behavior and impact strength of pvc/wood flour composites. *Chemistry & Chemical Technology*. 2010; 4(3): 225-229.
- Gassan J and Bledzki AK. 1997. The influence of fiber surface treatment on the mechanical properties of jute—PP composites. *Composites Part A*. 28: 993–1000.
- Sain MM and Kokta BV. 1993. Effect of modified polypropylene on physical performance of saw dust filled polypropylene composite. *J. Adv. Polym. Technol*, 12 (2): 167–183.
- Anonymous, 1983, Tappi T-203 cm-99: Alpha-, Beta- and Gamma-Cellulose in Pulp, *TAPPI Test Methods*, Tappi Press, Atlanta Georgia.
- Anonymous, 1992, Tappi T-204 om-88: Solvent Extractives of Wood and Pulp, *TAPPI Test Methods*, Tappi Press, Atlanta Georgia, Vol 1.
- Anonymous, 1992, Tappi T-207 om-88: Water Solubility of Wood and Pulp, *TAPPI Test Methods*, Tappi Press, Atlanta Georgia, Vol 1.
- Anonymous, 1992, Tappi T-212 om-88: One percent Sodium Hydroxide Solubility of Wood and Pulp, *TAPPI Test Methods*, Tappi Press, Atlanta Georgia, Vol 1.

*Proceedings of the 57th International Convention of Society of Wood Science and Technology
June 23-27, 2014 - Zvolen, SLOVAKIA*

Wise, L.E., Murphy, M., D'addieco, A.A., 1946, Chlorite Holocellulose, its Fractionation and Beating on Summative Wood Analysis and Studies on the Hemicellulose, *Pap. Trade J.*, 122 (2), 35-43

Anonymous, 1992., TAPPI Test Methods 1992–1993, Tappi Press Atlanta, Georgia, USA.

Stokke, D. D.; Gardner, D. J. 2003. *J Vinyl Addit Technol*, 9, 96.

Aydin, I. Ph.D. Thesis, Black Sea Technical University, 2004.

Yang, H.S.; Wolcott, M.P.; Kim, H.S.; Kim, S.; Kim, H.J. 2007. Effect of different compatibilizing agents on the mechanical properties of lignocellulosic material filled polyethylene bio-composites, *Compos. Struct.* 79, 369-375.

Improvement of Accuracy of Portable CT by Considering Penetrating Depth in Wood

Chul-Ki Kim¹ – Jung-Kwon Oh² – Jun-Jae Lee^{3}*

¹ PhD Candidate, Department of Forest Science, Seoul National University, Seoul, KOREA

aries05@snu.ac.kr

² Research Professor, Department of Forest Science/Research Institute of Agriculture and Life Science, Seoul National University, Seoul, Korea

jkoh75@hotmail.com

³ Professor, Department of Forest Science/Research Institute of Agriculture and Life Science, Seoul National University, Seoul, Korea

junjae@snu.ac.kr

** Corresponding author*

Abstract

To apply X-ray CT (computed tomography) on site, a portable X-ray apparatus which generates soft X-rays having continuous wave length were used. The mass attenuation coefficient decrease as the penetrating depth in wood increase when using continuous wave length X-rays, unlike monochromatic X-rays. When X-ray CT was used for inspecting historical building, penetrating depth varies in an X-ray radiograph. Because the mass attenuation coefficient, which is related with X-rays attenuation, changes according to penetrating depth, CT image using portable X-ray apparatus could be less accurate. For that reason, penetrating depth in wood were considered by determining the equation of mass attenuation coefficient to improve accuracy of portable X-ray CT. In this study, X-ray tests were conducted on wood specimens of various depths. From the test results, the equation of mass attenuation coefficient according to penetrating depth ($\mu = -0.214\ln(t) + 0.7251$) was derived to convert radiographs to density radiographs. All projections were converted into density profiles using two method, average mass attenuation coefficient and the equation of mass attenuation coefficient. After that, a density distribution of wood cross-section was reconstructed by filtered back projection method. The equation of mass attenuation coefficient according to penetrating depth provided higher precision in density prediction than the average mass attenuation coefficient.

Keywords: Wood density, Computed Tomography, Soft X-rays, Continuous wave length X-rays, Mass attenuation coefficient.

Introduction

Non-destructive testing and evaluation has been developed in order to detect inner state of wood. Divos and Divos (2005) reported that the resolution of acoustic tomography was influenced by the wave length of the stress wave and the number of sensors. Nicolotti et al. (2003) showed that ultrasonic tomography with a frequency of 54kHz was effective tool for the detection of internal

decay when compared to electric or georadar tomography. Both of research group detect inner decay of specimen well, although acoustic techniques could not provide the inner density distribution.

X-rays have higher resolution compared with acoustic techniques. Moreover, X-rays can provide density information of specimen. The researches on X-rays attenuation has been conducted for verifying wood density. Olsen et al. (1988) derived the change of mass attenuation coefficient according to an electron volt for conifer wood. The X-rays energy between 5.13 and 5.69keV for 1mm thick wood samples provided the maximum attenuation difference between earlywood and latewood. Nakata et al. (1999) adopted soft X-ray image to investigate the MC distribution in Japanese cedars according to direction of wood. The methods using X-rays also can provide not only the size of a defect but the location of that when CT (computed tomography) is used. Macedo et al. (2002) reported CT quantification in terms of dry bulk density could be reconstructed for three different X- and gamma-rays energies (28.3, 59.5 and 662keV). Lindgren et al. (1992) reconstructed a density CT image of clear wood to determine physical properties in three direction of wood. Moberg (2000) and Oja and Temnerud (1999) analyzed CT images to locate internal knots and resin pockets to increase the production yield of lumber.

Despite the advantages of X-ray techniques, X-ray and CT techniques are difficult to use on site where structure or tree are located. The equipment of X-rays is more suitable for laboratory tests, and radiation shield have to be installed to prevent inspectors from radiation. However, installation of the radiation shield on site is difficult. For that reasons, soft X-rays from a portable X-ray apparatus have been used to solve the field applicability problems. If lower-energy intensity X-rays (soft X-rays) were used, researcher safety could be increased by positioning oneself a sufficient distance from X-ray source without radiation shield.

The attenuation behavior of soft X-rays is different from that of the hard X-rays used in previous studies. Attenuation of soft X-rays is governed by the penetrating depth of the object as well as its density, as the X-rays from portable apparatus have a continuous wave length. The longer wave length tend to be attenuated by scattering rather than absorption, and attenuation is more likely to be affected by scattering in a thicker object (Korean society of physics for radiosurgery, 2005). The effect of penetrating depth on density prediction for soft X-rays was investigated in this study. Also, CT images involving a density distribution were presented using the attenuation behavior of soft X-rays.

Materials and Methods

Materials. Specimens were prepared in this study; one was prepared for determination of mass attenuation of continuous wave length, and the other set for the validation of reconstructed CT image.

For determination of mass attenuation coefficient according to penetrating depth, 4 clear wood species (cedar, larch, pitch pine and red pine) were prepared for the first set. Table 1 shows the size, density and moisture content. The pitch pine round wood was also prepared for the validation of reconstructed CT image, its air-dry density and moisture content were 430kg/m³ and 12%, respectively.

Table 1. Details of clear wood for soft X-rays attenuation.

Species	Size (mm)			Density (kg/m ³)		MC (%)
	Width	Height	Length	Ave.	SD	
Cedar	31.51	33.37	80.00	328.07	40.66	12%
Larch	32.87	38.58		460.93	74.70	
Pitch Pine	31.50	33.58		505.11	26.63	
Red Pine	32.90	39.95		410.11	37.13	

Methods. Portable X-ray apparatus with X-ray tube, K-4 (Softex, Japan), and digital detector, NX (RF system, Japan), were used to determine of mass attenuation coefficient and to reconstruct CT image. Based on an experience of inspection on heritage building, the intensity of soft X-rays was chosen as 37kV and 2mA. The exposure time of digital detector to radiation was 5 seconds.

Mass attenuation coefficient with penetrating depth. Transmitted intensity of soft X-rays were measured to investigate characteristic attenuation as penetrating depth of clear wood specimens were changed. Beer's law was used to derive mass attenuation coefficient of soft X-rays, although it has continuous wave length.

Reconstruction of density CT image and verification of its accuracy. To make CT image, 180 radiographs were taken when round wood was turned every 2 degrees. 180 radiographs were converted into density radiographs using the equation of mass attenuation coefficient according to penetrating depth as well as constant mass attenuation coefficient. After that, density CT images were reconstructed by FBP (filtered back projection) algorithm using 180 density radiographs. Figure 1 shows how to make 30 small specimens to measure air-dry density by gravimetric method. Then, estimated density in reconstructed CT image were compared with air-dry density of 30 small specimens to verify accuracy of CT image.

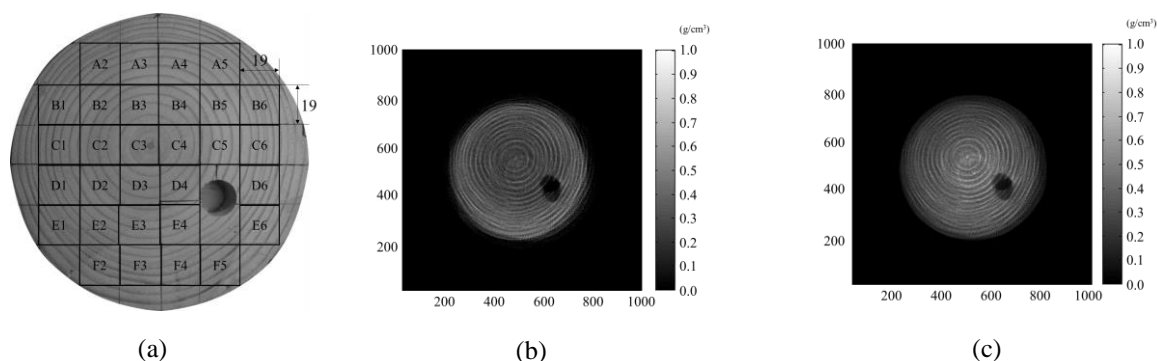


Figure 1. Location of 30 small specimens in round wood (a), reconstructed density CT image using constant mass attenuation coefficient (b), and the equation of mass attenuation coefficient (c)

Results and Discussion

Characteristic absorption of soft X-rays. Mass attenuation coefficient for the whole penetrating depth was 0.1844, but it seemed that mass attenuation coefficient decreased as penetrating depth in wood increased, as shown in Figure 2a. It means that quantity of transmitted soft X-ray increased as penetrating depth in wood increased. From these results, it thought that it is necessary to make the equation of mass attenuation coefficient according to penetrating depth in wood as $\mu = -0.214 \ln(t) + 0.7251$. The coefficient of determination (R^2) of the equation was 0.98.

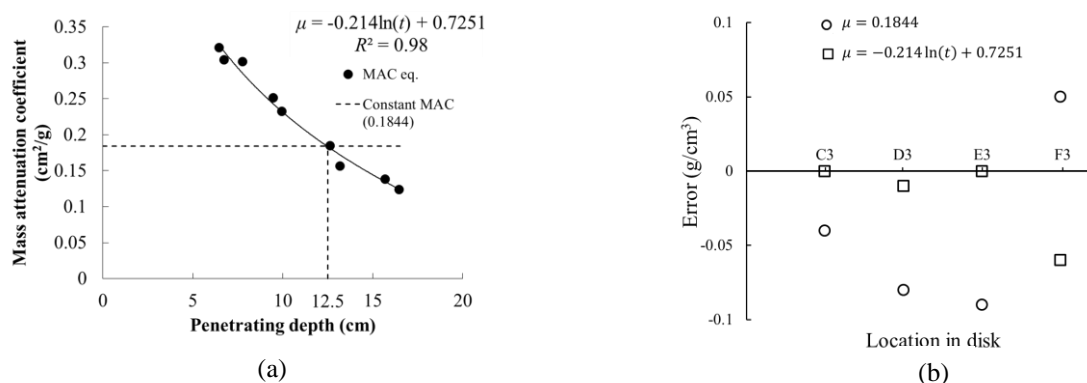


Figure 2. Mass attenuation coefficient according to penetrating depth (a) and comparison between air-density and estimated value in each density CT image (b)

Verification of density CT image accuracy. Two kinds of density CT image were reconstructed as shown in Figure 1a and b. In density CT image using constant mass attenuation coefficient, air-dry density in midsection of specimen was underestimated while the density of exterior parts was overestimated. In case of using the equation of mass attenuation coefficient, RMSE for estimating air-dry density was 41 kg/m^3 . This value was much smaller than using constant mass attenuation coefficient. It also confirmed that Figure 2b shows.

Conclusion

The present study aimed at investigating the effects penetrating depth on attenuation of soft X-ray to reconstruct density CT image and apply X-ray CT technique in field. Although digital

detector couldn't measure attenuation of soft X-ray passing short penetrating depth in exterior part of specimen, the CT technique using soft X-ray could be further developed to be used in field.

Reference

Divos F, Divos P (2005) Resolution of stress wave based acoustic tomography. In: 14th international symposium on nondestructive testing of wood, Shaker Verlag, Germany, pp. 307-314

Kaelbel EF (1967) Handbook of X-rays. McGraw-Hill, New York, pp 41(3)-41(24)
Korean society of physics for radiosurgery (2005) Radiation physics (in Korean). Komoonsa, Seoul, pp 209-211

Lindgren O, Davis J, Wells P, Shadbolt P (1992) Non-destructive wood density distribution measurements using computed tomography. *Holzforschung* 50(7):295-299

Macedo A, Vaz CMP, Pereira JCD, Naime JM, Cruvinel PE, Crestana S (2002) Wood density determination by X- and gamma-ray tomography. *Holzforschung* 56(5):535-540

Moberg L (2000) Models of Internal Knot Diameter for *Pinus sylvestris*. *Scand J For Res* 15(2):177-187

Nakada R, Fujisawa Y, Hirakawa Y (1999) Soft X-ray observation of water distribution in the stem of *Cryptomeria japonica* D. Don I : General description of water distribution. *J Wood Sci* 45(3):188-193

Nakada R, Fujisawa Y, Hirakawa Y (1999) Soft X-ray observation of water distribution in the stem of *Cryptomeria japonica* D. Don II : Types found in wet-area distribution patterns in transverse sections of the stem. *J Wood Sci* 45(3):194-199

National Research Institute of Cultural Heritage (2012) Conservation of wooden objects. Pointtech, Daejeon, pp 8

Nicolotti G, Socco LV, Martinis R, Godio A, Sambuelli L (2003) Application and comparison of three tomographic techniques for detection of decay in tree. *J of Arboric* 29(2):66-78

Olson JR, Liu CJ, Tian Y, Shen Q (1988). Theoretical wood densitometry: II. Optimal X-ray energy for wood density measurement. *Wood Fiber Sci* 20(1):187-196

Oja J, Temnerud E (1999) The appearance of resin pockets in CT-images of Norway spruce (*Picea abies* (L.) Karst.). *Holzforschung* 57(5):400-406

Acknowledgements

This study was supported by the Bio-industry Technology Development Program (project No. 111054-3), Ministry of Agriculture, Forestry and Fisheries.

Insecticidal Effect of Essential Oils from *Abies Holophylla* Maxim and its Chemical Constituents against *Dermatophagoides Farinae*

*Seon-Hong Kim*¹ – *Ga-Hee Ryu*² – *Su-Yeon Lee*³ – *Mi-Jin Park*⁴ –
In-Gyu Choi^{5*}

¹ Ph.D. Student, Department of Forest Sciences, College of Agriculture and Life Sciences, Seoul National University, Seoul, Korea.

sh98sh08@snu.ac.kr

² M.S. Student, Department of Forest Sciences, College of Agriculture and Life Sciences, Seoul National University, Seoul, Korea.

ryu1220@snu.ac.kr

³ Ph.D. Student, Department of Forest Sciences, College of Agriculture and Life Sciences, Seoul National University, Seoul, Korea.

goodday8508@snu.ac.kr

⁴ Ph.D., Department of Forest Resources Utilization, Korea Forest Research Institute, Seoul, Korea.

lionpmj@forest.go.kr

⁵ Professor, Department of Forest Sciences, College of Agriculture and Life Sciences, Seoul National University, Seoul, Korea.

* *Corresponding author*

cingyu@snu.ac.kr

Abstract

House dust mites are the main allergens involved in allergic symptoms such as asthma, atopic dermatitis, conjunctivitis, eczema and perennial rhinitis in those with sensitivities. Also, they are known to be causative agents of diseases that affect millions of people worldwide. They eat dead skin and dandruff from men and animals. And, there are always near human. Most of the best characterized allergens are from dust mites *Dermatophagoides farinae*. Essential oils are volatile and are formed by secondary metabolites. In nature, essential oils play an important role in the protection of the plants as antibacterials, antivirals, antifungals, insecticides and also against herbivores by reducing their appetite. *Abies holophylla* MAXIM essential oil and its constituents are excellent biologically active. So, in this study, the insecticidal effect of *A. holophylla* MAXIM essential oil and its constituents were evaluated against house dust mite, *Dermatophagoides farinae*. As a result, the insecticidal effect of *A. holophylla* MAXIM essential oil showed significantly high. And its constituents such as 3-carene, camphene, and caryophyllene were identified as effective constituents about insecticide. According to recent studies, essential oils have biological control activities because they consist of complex mixtures of terpenoids (hydrocarbons) and oxygenated compounds. So, essential oil and major constituents of *A. holophylla* MAXIM may use to be as raw materials of natural biocide.

Keywords: Anti Insecidal Effect, *Abies Holophylla Maxim*, Essential oil, *Dermatophagoides farina*.

Introduction

House dust mites are the main allergens involved in allergic symptoms such as asthma, atopic dermatitis, conjunctivitis, eczema and perennial rhinitis in those with sensitivities. Also, they are known to be causative agents of diseases that affect millions of people worldwide (Vandentorren, et al. 2003). Most of the best characterized allergens are from dust mites *Dermatophagoides farinae*. *D. farinae* is found in mattresses, carpets, central heating, space heating, more tightly sealed windows, poor ventilation, and soft furnishings, all of which allow the growth of house dust mites (An, et al. 2013). They eat dead skin and dandruff from men and animals. So, there are always near human.

Essential oils are volatile, natural, complex constituents characterized by a strong fragrance and are formed by secondary metabolites. In nature, essential oils play an important role in the protection of the plants as antibacterials, antivirals, antifungals, insecticides and also against herbivores by reducing their appetite. In addition, they also may attract some insects to favour the dispersion of pollens and seeds, or repel undesirable others (Bakkali, et al. 2008).

Abies holophylla MAXIM, also known as Manchurian Fir or Needle Fir, is an evergreen and coniferous tree that is widely distributed in Korea, China, and Russia. Several *Abies* species have been used in Korean folk medicine for the treatment of colds, stomach aches, indigestion, rheumatic diseases, and vascular and pulmonary diseases (Kim, et al. 2013). *A. holophylla* MAXIM essential oil has excellent biologically active about antifungal activity, antibacterial activity, and so on (Lee and Hong 2009).

As increasing public concern for human health, it is necessary to develop a natural insect repellent. So, in this study, the insecticidal effect of *A. holophylla* MAXIM essential oil was evaluated against house dust mite such as *Dermatophagoides farinae*. We also determined insecticidal effect of the major constituents of the *A. holophylla* MAXIM essential oils.

Materials and Methods

Materials. The leaves of *Abies holophylla* MAXIM grown in the south experiment forest of Seoul National University, South Korea, were collected in 2013. After sorting the leaves, those were stored at -39°C until essential oils were extracted. To examine the insecticidal effect, *Dermatophagoides farinae* was provided from Lab. of Bioactive Natural Products (WCU Biomodulation Major, Department of Agricultural Biotechnology, Seoul National University). The major constituents of the *A. holophylla* MAXIM oils, such as limonene, 3-carene, α -pinene, camphene, and β -caryophyllene were purchased from Sigma-Aldrich Korea.

Extraction of *A. holophylla* MAXIM essential oils. Essential oils of *A. holophylla* MAXIM leaves were extracted with distilled water on a lab-scale by steam distillation. The yield of extracted essential oils of *A. holophylla* MAXIM leaves was 3.2% based on dry mass (369 g) of initial leaves weight.

GC-MS analysis. The Gas chromatography column was an HP5 (model: Agilent 6890, Japan), and the carrier gas was helium. Analytical temperatures were 260 and 280°C in the injector and

detector, respectively. Initial oven temperature was kept at 120°C for 5 minutes and then increased by 4°C/min to 280°C, where it was held for 10 minutes. Mass spectrometry analysis used an Agilent 5973 (Japan) and was performed in EI mode. The chemical structures of the active constituents were analyzed by comparing the mass data of the active constituents peaks with the standard library data (Willy 7th ed).

Incubation of *D. farinae*. The stock cultures of *D. farinae* have been maintained in a temperature-controlled incubator without exposure to any known acaricide for more than 12 years. Mites were reared in plastic containers (12.5 × 10.5 × 5.0 cm) containing 40 g of sterilised diet (fry feed No. 1 + dried yeast; 1 : 1 (g/g)). The containers were incubated at 25 ± 1 °C and 70–80% relative humidity in darkness. The fry feeds and dried yeasts were purchased from Korea Special Feed Meal (Inchon, South Korea), and Daeheung Pharmaceutical (Seoul, South Korea), respectively.

Insecticidal effect of *A. holophylla* MAXIM essential oil and standard constituents.

Insecticidal effect against *D. farinae* was determined by residual film method. The samples were dissolved in ethyl alcohol in micro tube (samples 1, 0.5, 0.25, 0.125, and 0.0625 mg in 20 µL, respectively). And then, micro tube wall was coated with the sample solution by natural volatilizing ethyl alcohol. After then, 25~35 house dust mites were inserted in micro tubes coating by sample solutions, they were incubated at 25°C, relative humidity 75%, and incubated for 24 and 48 hours under dark condition. A control group was treated only with ethyl alcohol 20 µL. After 24 hours, each treatment sample was investigated the mortality rate by using electron microscopy (X20). The mortality rate was determined by ratio of dead mites to total mites ratio (Eqs. (1)). Just dead mites were considered immovable mites when stimulated with fine brush.

Eqs. (1): Insecticidal effect (%) = (Dead mites / Total mites) X 100

Results and Discussion

GC-MS analysis. Major constituents of *A. holophylla* MAXIM essential oil were identified by GC/MS analysis (**Table 1**). Major constituents are bornyl acetate, limonene, 3-carene, camphene, α-pinene, α-bisabolol, β-pinene, and borneol. Among them, the standard constituents such as limonene, 3-carene, camphene, α-pinene, and β-pinene were used for an experiment on insecticidal effect.

Table 1. Major constituents of the essential oil from *A. holophylla* MAXIM by GC-MS analysis

RI^a	Constituents	Relative proportion (%)
1285	Bornyl acetate	19.63
1138	Limonene	16.89
1009	3-Carene	14.02
950	Camphene	10.96
934	α-Pinene	10.74
1684	α-Bisabolol	5.42
945	β-Pinene	5.31
1174	Borneol	4.89

^a: Retention index relative to n-alkanes (C10~C25) on DB-5 capillary column, RI was identified based on comparison of retention index of the constituents compared with NIST08

Insecticidal effect of *A. holophylla* MAXIM essential oil and standard constituents. Figure 1 showed the insecticidal effect of *A. holophylla* MAXIM essential oil after 24 and 48 hours. The insecticidal effects turned up concentration dependent activation of *A. holophylla* MAXIM essential oil. The samples treated with *A. holophylla* MAXIM essential oil were effective compared to the sample treated with ethyl alcohol at every concentration. The insecticidal effect of *A. holophylla* MAXIM essential oil showed significantly high. The insecticidal effects also showed in **Figure 2** about major constituents of *A. holophylla* MAXIM essential oil. As a result, the toxicity of 3-carene was significantly higher than that of other constituents at 24 hours. On the other hand, camphene and caryophyllene showed insecticidal effects as much as 3-carene at 48 hours, while they have lower effect than 3-carene at 24 hours. For this result, 3-carene showed the insecticidal effects in a short time, and camphene and caryophyllen would need more time to have the insecticidal effects. Nevertheless, all of 3-carene, camphene, and caryophyllene were insecticidal effective constituents, because camphene and caryophyllene showed effective at 48 hours. According to recent studies, essential oils have biological control activities because they consist of complex mixtures of terpenoids (hydrocarbons) and oxygenated compounds (Lawless 2002). So, essential oil and major constituents of *A. holophylla* MAXIM were highly insecticidal effects, and may use to be as raw materials of natural biocide.

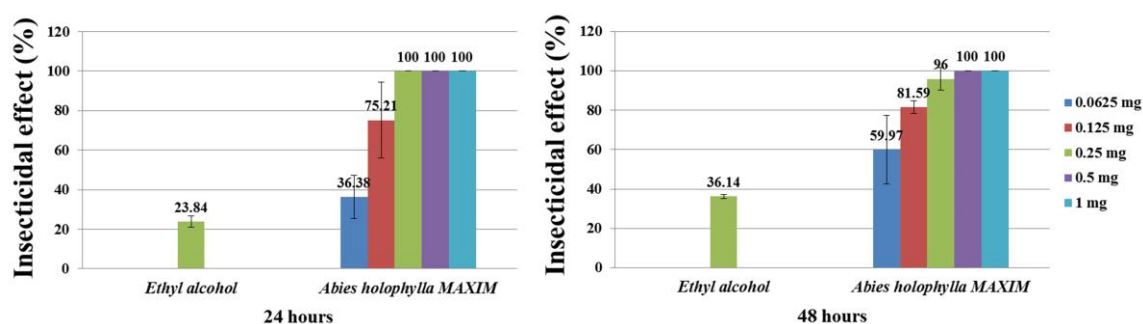


Figure 1. The insecticidal effect of *A. holophylla* MAXIM essential oil

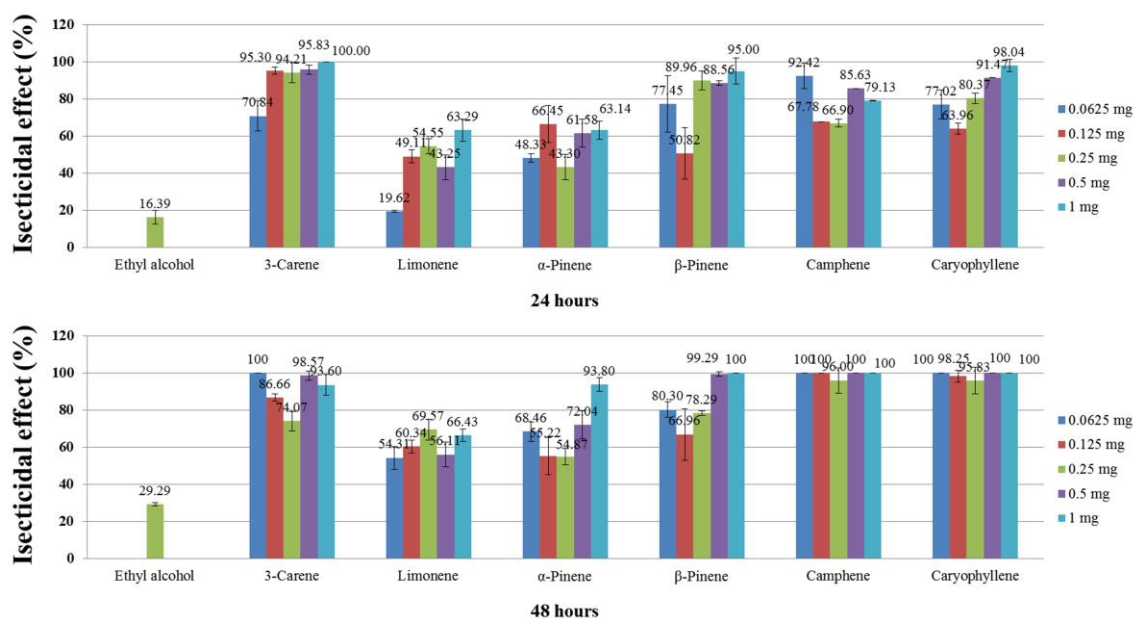


Figure 2. The insecticidal effect of major constituents of *A. holophylla* MAXIM essential oil

References

1. Vandentorren, S., Baldi, I., Maesano, I.A., Charpin, D., Neukirch, F., Filleul, L. *et al.* 2003 Long-term mortality among adults with or without asthma in the PAARC study. *European Respiratory Journal*, **21** (3), 462-467.
2. An, S., Chen, L., Long, C., Liu, X., Xu, X., Lu, X. *et al.* 2013 Dermatophagoides farinae allergens diversity identification by proteomics. *Molecular & Cellular Proteomics*, **12** (7), 1818-1828.
3. Bakkali, F., Averbeck, S., Averbeck, D. and Idaomar, M. 2008 Biological effects of essential oils—A review. *Food and chemical toxicology*, **46** (2), 446-475.
4. Kim, C.S., Kwon, O.W., Kim, S.Y. and Lee, K.R. 2013 Bioactive Lignans from the Trunk of *Abies holophylla*. *Journal of natural products*, **76** (11), 2131-2135.
5. Lee, J.-H. and Hong, S.-K. 2009 Comparative analysis of chemical compositions and antimicrobial activities of essential oils from *Abies holophylla* and *Abies koreana* activities of essential oils from *Abies holophylla* and *Abies koreana*. *Journal of microbiology and biotechnology*, **19** (4), 372-377.
6. Lawless, J. 2002 *The encyclopedia of essential oils: the complete guide to the use of aromatic oils in aromatherapy, herbalism, health & well-being*. HarperCollins UK.

Abrasion, Surface Treatment and Glossiness Relations of Wood Material

K.Hüseyin KOC¹ Ender HAZIR² E.Seda ERDINLER³ Emel OZTURK⁴

¹ Professor Dr., Istanbul University, Faculty of Forestry, Department of Forest Industry Engineerig, 34473 Istanbul – Turkey

** Corresponding author*

[*hkoc@istanbul.edu.tr*](mailto:hkoc@istanbul.edu.tr)

²Research Assistant, Istanbul University, Faculty of Forestry, Department of Forest Industry Engineerig, 34473 Istanbul – Turkey

[*ender.hazir@istanbul.edu.tr*](mailto:ender.hazir@istanbul.edu.tr)³

³ Assistant Professor , Istanbul University, Faculty of Forestry, Department of Forest Industry Engineerig, 34473 Istanbul – Turkey

[*seda@istanbul.edu.tr*](mailto:seda@istanbul.edu.tr)

⁴ Research Assistant, Istanbul University, Faculty of Forestry, Department of Forest Industry Engineerig, 34473 Istanbul – Turkey

[*emelozt@istanbul.edu.tr*](mailto:emelozt@istanbul.edu.tr)

Abstract

Wood material is used in many fields with its advantages such as its natural structure and aesthetic appearance. One of these fields is furniture either for indoor and outdoor. Mechanical and environmental conditions affect surface of wood material significantly. One of these important effects is abrasion surface treatment and glossiness. Important changes in surface appearance are a natural result of these effects. Glossiness effect visual admiration positively as it may effect it the other way round. In such cases besides glossiness, haze and orange peel are unwanted characteristic situations. For this reason the investigation of relationship between surface glossiness, surface treatment and abrasion is important.

In this study, it is aimed to determine the visual changes on wooden surfaces caused by abrasion and surface treatment. Change in surface glossiness is a natural result. For this reason the relationship between surface treatment, glossiness and abrasion makes up an important research field. It is aimed to determine the changes on surfaces due to different abrasion processes. It is considered that surface glossiness can be taken under control, as it is very important for visual perception and evaluation of quality and aesthetic expectations. In the study one of the important tree species and wood based material are used.

International standards are used to determine the samples and sample sizes. Abrasion techniques are applied according to ASTM standards and glossiness measures are applied according to TS 4318, EN ISO 2813.

Keywords: A. Wooden, B. Abrasion, C. Surface gloss, D. Varnish, E. Surface treatment

Introduction

Increasing demands and varied consumer requests related to the use of wood and wood based material and affordable and high quality product requests are important factors triggering the competition on sector basis [1, 2]. Offering the material more effectively, more efficiently and with better quality to the customer constitutes a critical phase in surviving from the domestic and international competition. Wood material is preferred by the consumers for its aesthetic appearance, functionality, long economic life and being a material gaining a different appearance as it is used. One of the important factors providing this is the surface layer treatment that influences the user, as well as protects the product against external impacts and makes the product more hygienic. Surface layer treatments also affect the product's color, glossiness and surface performance. However, changes may occur in the appearance of the wood material based on its usage conditions [3]. This might influence the user preferences positively or negatively. There are various studies displaying that there are changes in the surface glossiness with the abrasions arising by time and as a result of usage conditions and seeking for optimum condition on wood surface, and these studies emphasize that abrasion might affect the glossiness [4-12].

One of the most important factors effective on the abrasion of the wood materials throughout its economic life is the mechanical impact. In this study, it is aimed to examine the change in glossiness arising as a result of mechanical impacts. In addition to this, the studies on digitizing the abrasion related surface glossiness might constitute a base.

Materials and Methods

Materials: Abies type of tree is selected as the study material by considering its increasing natural usage area in furniture industry applications particularly including decoration, China cabinet, aesthetic perforator etc. For this purpose, Turkey's natural kind of *Abies Bormülleriana* Mattf. timber has been used. The samples have been prepared from timbers cut tangent according to TS EN 15185 2013 [13]. Cellulosic and Water Based transparent varnishes have been selected to determine the impact of varnish application, a common surface treatment application, on natural gloss.

Method: Test applications take the national and international standards into account. Test design and sample pattern are as shown in Table 1. During the study, GT-7012-T Taber Type Abrasion Tester device has been used for determining the abrasion impact. For abrasion, a rotating speed of 72 rpm/60 Hz, a load of 500 g and abrasion head of Taber S-42 have been used. The glossiness data on the surface was determined with RHOPPOINT Glossmeter (Trigloss+IQ) device by using various abrasion impacts in the test device. Wood surfaces have been subjected to abrasion at various abrasion levels (100-1000 rpm) and measured separately at 20, 60 and 85 degrees. TS EN ISO 2813 standards have been used for this purpose. [14-16].

Table 1: Test design and sample pattern used in the study ()*

MATERIAL	NO. OF SAMP LES	TREATMENT – APPLICATION	Gloss degrees		
			20°	60°	85°

(*)

Abies (<i>Abies bornmulleriana</i> Mattf.) (Massive wood prepared in calibrated 10x100x100 mm size) Natural	5X10	Natural gloss					
	5	Abrasion level (72 rpm)	Treatment-1	100	100	100	
	5		Treatment -2	200	200	200	
	5		Treatment -3	300	300	300	
	5		Treatment -4	400	400	400	
	5		Treatment -5	500	500	500	
	5		Treatment -6	600	600	600	
	5		Treatment -7	700	700	700	
	5		Treatment -8	800	800	800	
	5		Treatment -9	900	900	900	
	5		Treatment -10	1.000	1.000	1.000	
	5	Cellulosic varnish	2 layers				
	5		3 layers				
	5		4 layers				
	5	Water based varnish	2 layers				
	5		3 layers				
	5		4 layers				

The

treatments are carried out by taking five measurements from each sample.

Results

The glossiness values measured in the study based on the obtained abrasion level are provided in Table 2. The correlation of abrasion level and glossiness is shown in Figure 1. 3D images obtained from the study to better see the difference between abraded surface and non-abraded surface are given in Figure 2 a & b.

As it can be seen in Table 2, it's been determined that abrasion based gloss loss occurs at each abrasion level and according to natural gloss for each three measurements. For example, the natural gloss value is 1.78 at 20°, while it reduces to 1.72 at 100 rpm, 1.64 in 500 rpm and 1.57 at 1000 rpm. The same applies to 60° and 85°.

Also as it can be seen in Table 1; for the varnish treatment on surface, while the natural gloss value is 1.78 at 20°, it increase to 2.44 as a result of 2-layer cellulosic varnish application, 4.64 as a result of 3-layer varnish application and 6.06 as a result of 4-layer varnish application. The same values are measured respectively as 2.91, 4.78 and 10.94 as a result of water based varnish application. The findings show that the varnish applications on wood surfaces increase their surface glossiness by 3 to 27 times according to the type of varnish used and based on the number of layers.

Table 2: Glossiness results according to the abrasion levels obtained in the study

TREATMENT	Gloss degrees			Rate of change compared to natural gloss (%)		
	For 20 degrees	For 60 degrees	For 85 degrees	20°	60°	85°
Natural Gloss						

		AVG	ST	AVG	ST	AVG	ST			
		1,78	0,15	5,17	0,92	2,09	1,00			
Abrasion level (72 rpm)	100	1,72	0,15	4,11	0,57	1,23	0,44	-3,4	-20,5	-41,1
	200	1,71	0,09	4,43	0,46	1,59	0,52	-3,9	-14,3	-23,9
	300	1,63	0,14	4,09	0,44	1,24	0,48	-8,4	-20,9	-40,7
	400	1,67	0,10	4,02	0,50	1,11	0,28	-6,2	-22,2	-46,9
	500	1,64	0,07	3,17	0,45	1,33	0,45	-7,9	-38,7	-36,4
	600	1,60	0,10	3,89	0,56	1,79	0,60	-10,1	-24,8	-14,4
	700	1,61	0,15	3,52	0,69	1,17	0,49	-9,6	-31,9	-44,0
	800	1,62	0,06	3,59	1,09	1,07	0,61	-9,0	-30,6	-48,8
	900	1,47	0,10	3,63	0,75	1,07	0,40	-17,4	-29,8	-48,8
	1.000	1,57	0,19	3,59	0,73	1,09	0,39	-11,8	-30,6	-47,8
	AVG	-	0,11	-	0,62	-	0,47	-	-	-
Cellulosic varnish	2 layers	2,44	0,28	12,26	2,17	11,65	2,93	42,7	137,1	457,4
	3 layers	4,64	0,34	22,03	3,45	24,52	3,88	171,3	326,1	1073,2
	4 layers	6,06	0,25	28,30	2,21	36,09	4,45	254,4	447,4	1626,8
Water based varnish	2 layers	2,91	0,41	14,67	3,54	14,30	5,35	70,2	183,8	584,2
	3 layers	4,78	0,54	27,14	2,67	29,83	5,80	179,5	425,0	1327,3
	4 layers	10,94	1,55	44,89	6,47	59,08	8,82	539,8	768,3	2726,8

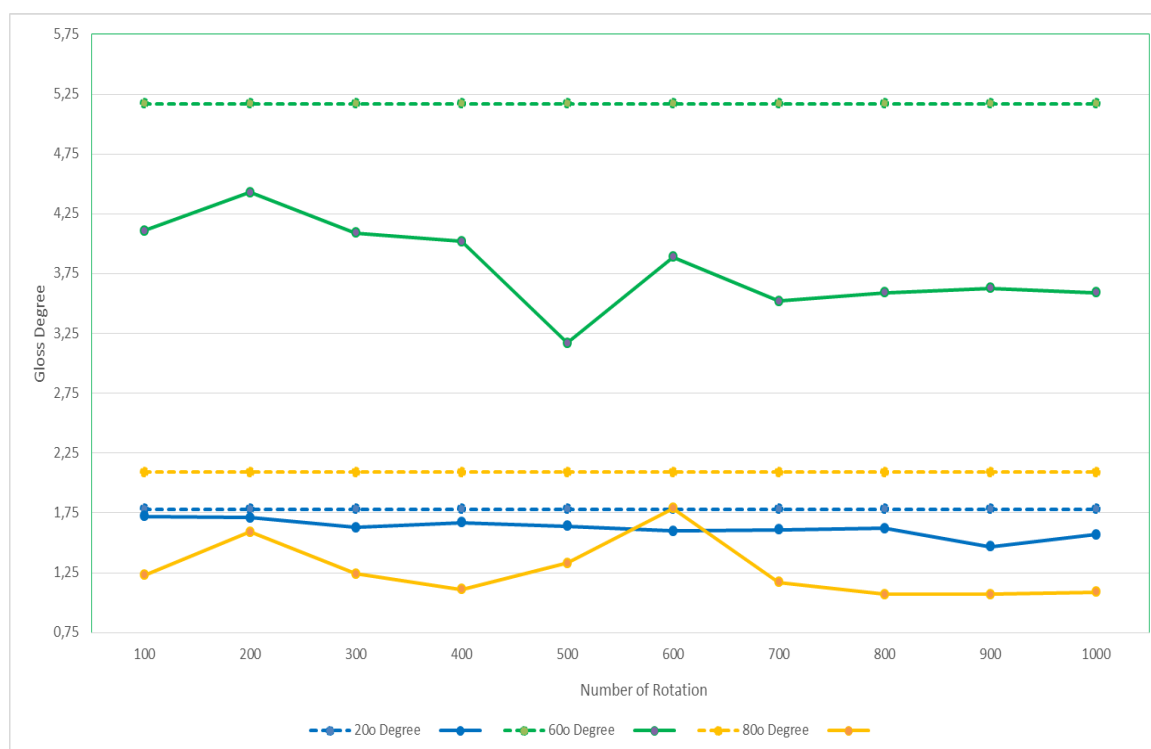


Figure 1: Abrasion and Surface Glossiness Relation on Wood Surface

As it can be seen in Figure 1, an important correlation has been determined between abrasion and glossiness. Abrasion based gloss loss has started significantly at 100 rpm, i.e. 20.5% loss occurred at 60°, and this loss has increased up to 1000 rpm and reached to 30.6%.

The standard deviation among the glossiness data is observed at minimum 20° and at maximum 60° measurements. For example, the standard deviation between the glossiness levels at natural gloss was 0.92 at 60°, it has reduced to 0.62 in average by varying based on abrasion.

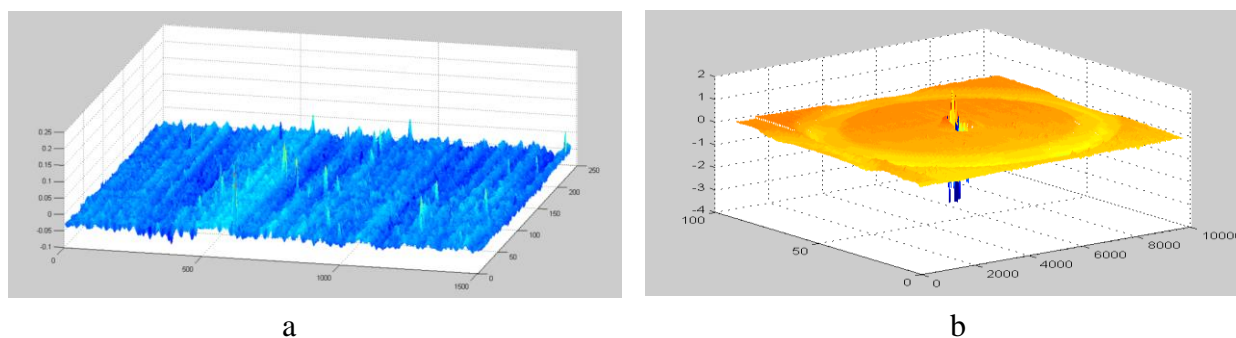


Figure 2: A sample 3D image related to natural (a) and abraded (b) surfaces

Conclusions

In the literature, there are studies evaluating the surface performances of the material through different aging tests. However, these studies are observed to be made generally on the scratching-free, flexibility and abrasion resistances of the surface. No study has been found determining the impact of abrasion on surface glossiness of the wood material as a result of mechanical impacts. This study is considered to reveal the abrasion-glossiness relationship, even at basic level. The results reveal that abrasion significantly affects the glossiness and that this can be digitally modeled if sufficient data is created. Regarding the surface performance, it can be stated that the aesthetic characteristics of the material are significantly affected by abrasion. It's particularly considered that these results can be taken into account in treatments for meeting the increasing visual expectations from the wood material through artificial methods such as aging etc. for example, it is possible to prepare the wood surfaces with mechanical impacts according to the aesthetic expectation (softness feeling, serenity, life experience feeling etc.). Thus, it's been observed in this study that standard deviation in abrasion and glossiness values has reduced significantly. This can be considered as a decrease in heterogeneity on the surface structure.

The study also determines that, in correctly meeting the aesthetic expectations from the wood surfaces, the varnish application applied on the surface significantly increase the glossiness depending to the varnish type and number of layers. This glossiness increase can sometimes be considered as positive, and sometimes as negative. Therefore, the glossiness applications should also be taken into account according to the usage environment in varnish applications. In sum, it's considered that it will be beneficial to perform similar studies multi-directionally for different trees and materials in order to correctly meet the expectations from wood material.

References

- [1] Şanivar, N., 1978. Wood Works Surface Layer Treatments, Publications of National Education, Istanbul, 1978.
- [2] Kurtoğlu, A., 2000. Wood Material Surface Treatments, General Information, Volume 1, Istanbul University, Faculty of Forestry, Department of Forest Industry Engineering, Istanbul, 2000.
- [3] Carter, R., M., 1983. Finishing Eastern Hardwoods, Forest Products Research Society, Madison, Wisconsin, 1983.
- [4] Özen, R., Sönmez, A., 1990. Resistance of Varnishes Used In Wooden Furniture Surfaces against Important Physical and Chemical Impacts, *Doğa Journal* V 14, 1990.
- [5] Ender, H., Koç, K. H., Kurtoğlu, A., 2013. A Sample Application on Evaluating the Aging Techniques and Their Impacts on Wooden Surface, 2nd National Furniture Congress, April 11-13, 2013, p. 27-35
- [6] Hazir, E., 2012. A Modeling Study on Evaluating the Quality of Wooden Surface, Master's Thesis, Istanbul University Institute of Science, Istanbul, 2012.
- [7] Çakicier, N., 2007. Changes Determined on Wooden Material Surface Treatment Layers As A Result of Aging, *Doctoral Thesis*, Istanbul University Institute of Science, Istanbul, 2007.
- [8] Erdin, N., Bozkurt, Y., 2013. Wood Anatomy, Istanbul University Faculty of Forestry, Publication No: 506, ISBN, 2013.
- [9] Sulaiman, O, Hashim, R., Subari, K., Liang, C.K., 2009. Effect of sanding on surface roughness of rubber wood, *Journal of materials processing technology*, 209(2009) 3949-3955
- [10] Kaygin, B., Akgun, E., 2009. A Nano-technological product: An innovative varnish type for wooden surfaces, *Scientific Research and Assay*, Vol. 4(1), pp.001-007, January, 2009, ISSN: 1992-2248
- [11] Irean, S. Andrzej, K. Andrzej, T. Andrzej, C., Anna, R., 2011. Hardness and wear resistance tests of the wood species most frequently used in flooring panels, *Forestry and Wood Technology*, No 76, 2011:82-87
- [12] Tan, P. L., Safian, S., Sudin, I., 2012. Roughness models for sanded wood surface, *Wood Sci Technol.* (2012) 46:129-142
- [13] TS 15185, 2013. Furniture-Assessment of the surface resistance to abrasion, Turkish Standards, Ankara, Turkey
- [14] TS 4318, 1985. Paints and varnishes measurement of specular gloss of non-metallic paints films at 20° 60° and 85°. Turkish Standards, Ankara, Turkey

[15] ASTM D 4060-10, 2013. Standard test method for Abrasion Resistance of Organic Coatings by Taber Abraser, American Society for Testing and Materials, 2013.

[16] TS EN ISO 2813, 2013. Paints and Varnishes-Measurement of Specular Gloss of Non-Metallic Paint Films at 20, 60 and 85 Degrees, Turkish Standards, Ankara, Turkey

Acknowledgement

This study is supported by Scientific Research Projects Coordination Unit of Istanbul University with project no. UDP-42336.

Surface Characteristics of Thermally Modified Plywood Panels

*Zeki Candan, Umit Buyuksari, Suleyman Korkut, Oner Unsal, and
Nevzat Cakicier*

Abstract

As a wood composite, plywood panel is of great importance for furniture production and building construction. Surface characteristics such as surface roughness and surface wettability of wood composites influence different processes including their finishing characteristics and final performance. Surface quality of wood or wood composite panels is affected by thermal modification. The main goal of this work was to determine the surface roughness and surface wettability properties of the thermally modified plywood panels. The experimental panels were provided from a private company. The plywood panel specimens were subjected to thermal modification process at different temperatures for 1 hour. Average surface roughness and maximum surface roughness values were measured to evaluate the surface roughness characteristics of the plywood panels while contact angle values were measured to evaluate wettability property. The surface roughness measurements of the panels were conducted both parallel and perpendicular to the grain using a fine stylus tracing method. The contact angle measurements were carried out using a goniometer system connected to a digital camera and computer system. The results determined in this work clearly indicated that the thermal modification significantly affected the surface roughness and surface wettability values of the plywood panels. The plywood panels modified at 150°C had the smoothest surface. The average surface roughness values of the plywood panels decreased by 7.91% and 4.19% with modification temperature of 150°C and 170°C, respectively. The contact angle values of modified plywood panels increased with increasing the thermal modification temperature. Plywood panels with a hydrophobic property could be acquired with the thermal modification procedure.

Keywords: Plywood panels, thermal modification, surface roughness, surface wettability

Zeki Candan
Department of Forest Products Engineering
Istanbul University
Sariyer 34473, Istanbul, Turkey
Tel: +90-212-226-1100
Fax: +90-212-226-1113
zekic@istanbul.edu.tr

Umit Buyuksari
Department of Forest Products Engineering
Duzce University
81620, Duzce, Turkey
Tel: +90-380-542-1137
Fax: +90-380-542-1136
umitbuyuksari@duzce.edu.tr

*Proceedings of the 57th International Convention of Society of Wood Science and Technology
June 23-27, 2014 - Zvolen, SLOVAKIA*

Suleyman Korkut
Department of Forest Products Engineering
Duzce University
81620, Duzce, Turkey
Tel: +90-380-542-1137
Fax: +90-380-542-1136
suleymankorkut@duzce.edu.tr

Oner Unsal
Department of Forest Products Engineering
Istanbul University
Sariyer 34473, Istanbul, Turkey
Tel: +90-212-226-1100
Fax: +90-212-226-1113
onsal@istanbul.edu.tr

Nevzat Cakicier
Department of Forest Products Engineering
Duzce University
81620, Duzce, Turkey
Tel: +90-380-542-1137
Fax: +90-380-542-1136
nevzatcakicier@duzce.edu.tr

Bio-Friendly Systems for Finishing of Wooden Windows Elements

Tomasz Krystofiak, Stanisław Proszyk and Barbara Lis

Abstract

For production of doors and windows wooden elements are introduced in last years bio-friendly systems to the obtaining of proecological coatings about excellent features within the range functionalities and durability and resistance of obtained surface finishings. The window-joinery is exploited in exceptionally disadvantageous conditions, different from these in which are used the most of wooden products. The durability and the correct performance of windows are dependent mainly from the kind of used wood species, adopted technical solutions, and the surface protection before the influence of biological and atmospheric factors, which one obtain as result of the preservation and the application of suitable lacquer products. A very important issue in the production of the window elements from wood is the selection of the proper lacquer system, providing the obtainment of coatings about the high resistance. A particularly essential matter is also the suitable protection of the wood surface before the influence of biotic and atmospheric factors, what is obtains, both in consequence of the preservation or the use of lacquer products (in the form of ground, bottom and top layers). In the frame of polish-norwegian project "Superior bio-friendly systems for enhanced wood durability" are undertaken studies concentrating on the contribution of wood durability to sustainability through the development of systems for quality assurance and performance classification of eco-friendly treated wood as alternative against traditional preservatives and coatings too. In the work was presented the behavior of lacquer coatings from acrylic dispersions of the new generation, formed on wood surface and surrendered into accelerated aging tests simulate natural weather conditions.

Keywords: window, lacquer coating, durability, aging

Tomasz Krystofiak
Poznan University of Life Sciences
Department of Wood Based Materials
Division of Gluing and Finishing of Wood
Wojska Polskiego Str. 38/42
60-627 Poznan
+48-691-898-220 FAX: +48 61-848-74-32
tomkrys@up.poznan.pl

Sorption Properties of Viscoelastic Thermal Compressed (VTC) Wood

Andreja Kutnar^{1} – Frederick A. Kamke² – Emil Engelund Thybring³*

¹ Assistant Professor, University of Primorska, Andrej Marušič Institute, Faculty of Mathematics, Natural Sciences and Information Technologies, Koper, Slovenia.

** Corresponding author*

andreja.kutnar@upr.si

² Professor, Department of Wood Science and Engineering, Oregon State University, Corvallis OR, USA.

fred.kamke@oregonstate.edu

³ EMPA Cofund Postdoc, ETH Zurich and EMPA, Zurich, Switzerland.

emil.thybring@empa.ch

Abstract

Low-density hybrid poplar (*Populus deltoides* × *Populus trichocarpa*) specimens were densified with Viscoelastic Thermal Compression (VTC) process to three different degrees of densification, 63 %, 98 %, and 132 %. After VTC treatment, control and VTC cuboids of around 20 mg were prepared and sorption measurements at 25 °C were performed using gravimetric sorption analysis (DVS Advantage, Sorption Measurement Systems, London, UK). During the continuous mass measurements, temperature was kept constant while relative humidity was increased from 0 % to 95 % in steps of 5 % and subsequently lowered stepwise with similar step size. The climate conditions at each step were kept constant until the change in mass was less than 0.002 %/minute. The results showed that VTC treatment affects the sorption properties of wood. The equilibrium moisture content of VTC wood at different climate conditions is lower than that of untreated wood, while degree of densification does not influence the sorption properties of VTC wood. However, the degree of densification to some extent affects the time needed for reaching equilibrium.

Keywords: densification, DVS, equilibrium moisture content, relative humidity, sorption analysis.

Introduction

The "green revolution" has increased public awareness regarding the efficient utilization of timber, and the protection of forest lands, particularly of old-growth forests. Consequently, the available resource base is shifting from mature forests to intensively managed forest plantations. Wood from plantations often has inadequate mechanical properties. However, low quality wood can be modified by various combinations of compressive, thermal and chemical treatments. Because most of the mechanical properties of wood are correlated to its density, interest in modification by means of densification has increased in recent years. All forms of densification result in wood that has a lower volume of air space, which increases overall density. A more

thorough understanding and knowledge of the viscoelastic nature of wood tissue enables densification without adding chemical substances or causing fracture of cell walls. Among the emerging eco-friendly methods of modifying wood is the combined application of heat, moisture and mechanical action, so-called Thermo-Hydro-Mechanical (THM) treatments. These treatments result in physical and chemical changes to the wood, reduction in void spaces and compression, or densification (Sandberg et al. 2013). THM processing can improve the intrinsic properties of wood, produce new material and give desired form and functionality without changing wood's eco-friendly characteristics. In addition, densification of wood can be combined with some other processes, like for instance with thermal and resin treatments.

Kamke and Sizemore (2008) developed a method for wood densification using a viscoelastic thermal compression (VTC) process. This process works by mechanically compressing wood to increase its density by between 100 and 300%. The key to the VTC device is the compressing of wood in a high pressure steam environment. This condition prevents the wood cells from fracturing under the extreme load. The compression is then permanently fixed using heat. The wood morphology changes significantly during the VTC process and depends strongly upon the degree of densification (Blomberg et al. 2006; Kutnar et al. 2009; Standfest et al. 2013). Densification is achieved by reducing the void volume (cell lumens) by cell wall buckling, but without destruction of the micro-cellular structure of the wood (Kutnar et al. 2009). The undamaged cell walls, hence, are a major factor for the improved properties of densified wood (Navi and Girardet 2000, Kamke and Sizemore 2008). Kutnar and Kamke (2012) studied the influence of temperature and condition of steam environment during the VTC process on equilibrium moisture content (EMC) of VTC wood. The study concluded that temperature of the treatment significantly affected the EMC. Higher temperature of the compression treatment resulted in lower EMC after conditioning regardless of the steam conditions during treatment. VTC specimens compressed at 170°C had 8% EMC, while untreated specimens had 12% EMC after conditioning at 20°C and 65% relative humidity (RH). Kutnar and Kamke (2012) concluded that the temperature effect on EMC was consistent with thermal degradation expected within the range of temperature studied.

The EMC of wood is controlled by the available hydroxyl group content and their accessibility. During the VTC process wood is exposed to high temperature and steam pressurized environment that causes thermal degradation. Since the close structure of densified wood could affect the accessibility of hydroxyl groups in the densified wood, the aim of this paper was to study the sorption properties of VTC wood of three different degrees of densification by using gravimetric sorption analysis (DVS Advantage, Sorption Measurement Systems, London, UK).

Materials and Methods

Materials. Low-density hybrid poplar (*Populus deltoides* × *Populus trichocarpa*) from a plantation in Northwest Oregon USA was ripped, re-sawn and processed with a planer in order to obtain specimens with a rectangular shape. The width and length of specimens were 56 mm and 170 mm, respectively. The initial thickness of the specimen varied, depending on intended level of densification to be achieved by the VTC process. Thus, specimens having three different initial thicknesses were prepared: 6 mm, 5 mm and 4 mm. Ten specimens with mixed radial and tangential orientation were prepared for each degree of densification, and for the control (undensified specimens). The specimens were free of macroscopic defects (e.g. knots and splits). Special care was taken to ensure that specimens had similar characteristic in terms of density,

ring width and orientation. Before densification with the VTC process, all the specimens were conditioned in a controlled environment with 65 % RH and 20°C in order to obtain constant moisture content (MC) of 12%.

The VTC process. The VTC process consists of the three main phases, which are evident in Figure 1. The initial phase is steaming of the specimen at 860 kPa. The specimens are steamed without compression for three minutes, and for an additional two minutes with a compressive load of 1.38 MPa. After this treatment, the steam pressure is released, and specimen is able to vent for 100 s without compression (phase 2). During the venting period the specimen loses moisture and the temperature drops. Phase 3 begins with an application of a compressive load of approximately 4.48 MPa, which is applied for five minutes. This compression is mostly borne by the mechanical stops that control specimen thickness. The moisture loss during venting induces mechano-sorption effects. During phase 3 the platen temperature is raised from 175°C to 200°C. In the last step specimens are cooled under compression to 100°C. The specimens were compressed to a target thickness of 2.5 mm. Since three different initial thicknesses were used (4, 5 and 6 mm), VTC specimens with three different degrees of densification (63 %, 98 % and 132 %) were created (Table 1).

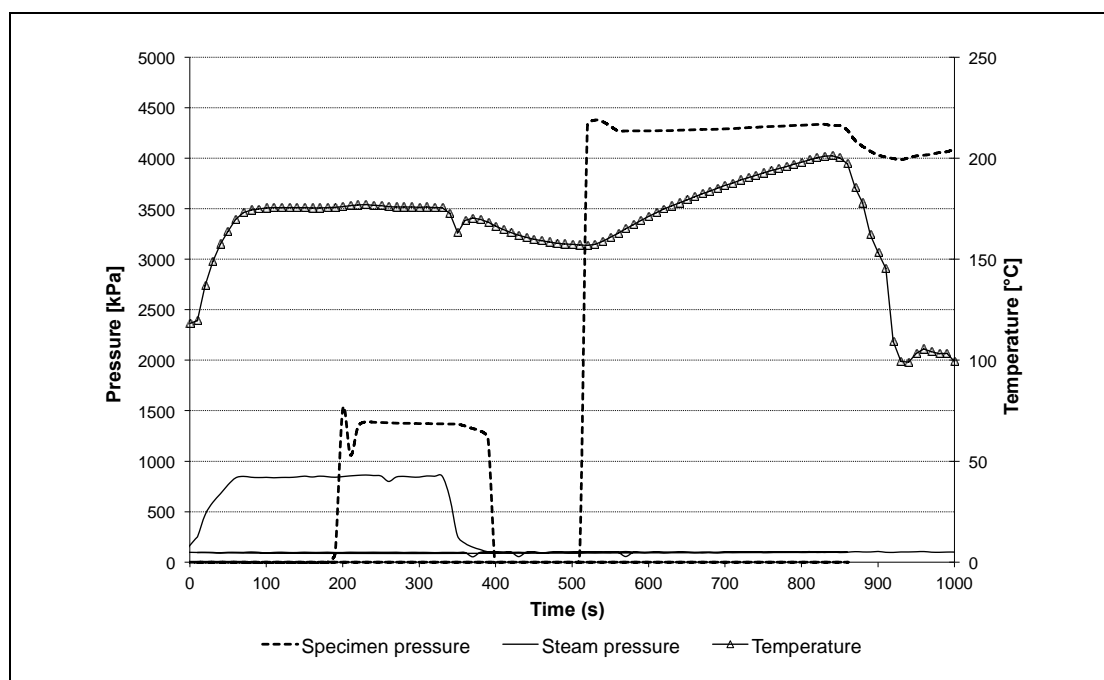


Figure 1: Schedule of the VTC process.

Sorption measurements. The sorption measurements at 25°C were done using Dynamic Vapour Sorption equipment (DVS Advantage, Sorption Measurement Systems, London, UK) located at the Technical University of Denmark, Department of Civil Engineering. During the continuous mass measurements, temperature was kept constant while RH was increased from 0 % to 95 % in steps of 5 % and subsequently lowered stepwise with similar step size. The climate conditions at each step were kept constant until the change in mass was less than 0.002 %/minute. A cuboid of around 20 mg was cut with razor blades from each sample material and used for the measurements.

Table 1: Characteristics of the VTC and control specimens.

Initial thickness (mm)	Initial density (ρ_0) at MC=0% (g cm^{-3})	Density after compression (ρ_c) at MC=0% (g cm^{-3})	Degree of densification $(\rho_c - \rho_0) / \rho_0$ (%)
4	0.339	0.552	63
5	0.341	0.676	98
6	0.340	0.792	132
6 (control)	0.331	0.331	0

Results

The amount of moisture adsorbed is dependent on the relative humidity of air to which wood is exposed or to the availability of water. These relationships are available under the form of sorption curves. Wood exhibits a characteristic sigmoidal sorption isotherm. The EMC of wood depends not only on the climatic conditions, but also on the moisture history. This phenomenon is referred to as sorption hysteresis and can be seen as a difference in EMC after conditioning in similar climate from a higher (via desorption) or lower (via adsorption) moisture content. The results showed that VTC treatment affects the sorption properties of wood. The EMC of VTC wood at different climate conditions is lower than that of untreated wood, while degree of densification does not significantly influence the level of EMC of VTC wood. Also, sorption hysteresis was not affected by the degree of densification.

Results for adsorption and desorption cycles, at 5% RH steps, for control and VTC wood specimens of different degrees of densification at temperature of 25 °C are shown in Figure 2. As the RH of the atmosphere changes, the moisture content of the wood sample changes in response and approaches a new EMC. The result is an asymptotic curve approaching the equilibrium after infinite time of exposure at a given RH. In this study the climate conditions at each step were kept constant until the change in mass was less than 0.002 %/minute. Although a more detailed analysis would be needed, the recorded curves indicate that the approach to EMC of VTC wood specimens progress with the same rate as that of control undensified wood. Thus, even though the closed microstructure of densified wood, along with probable thermal degradation, affects the amount of accessible hydroxyl groups in the densified wood, the approach to EMC is similar. Of course, less moisture is taken up in the VTC wood meaning that the absolute rate of sorption is lower in the modified material.

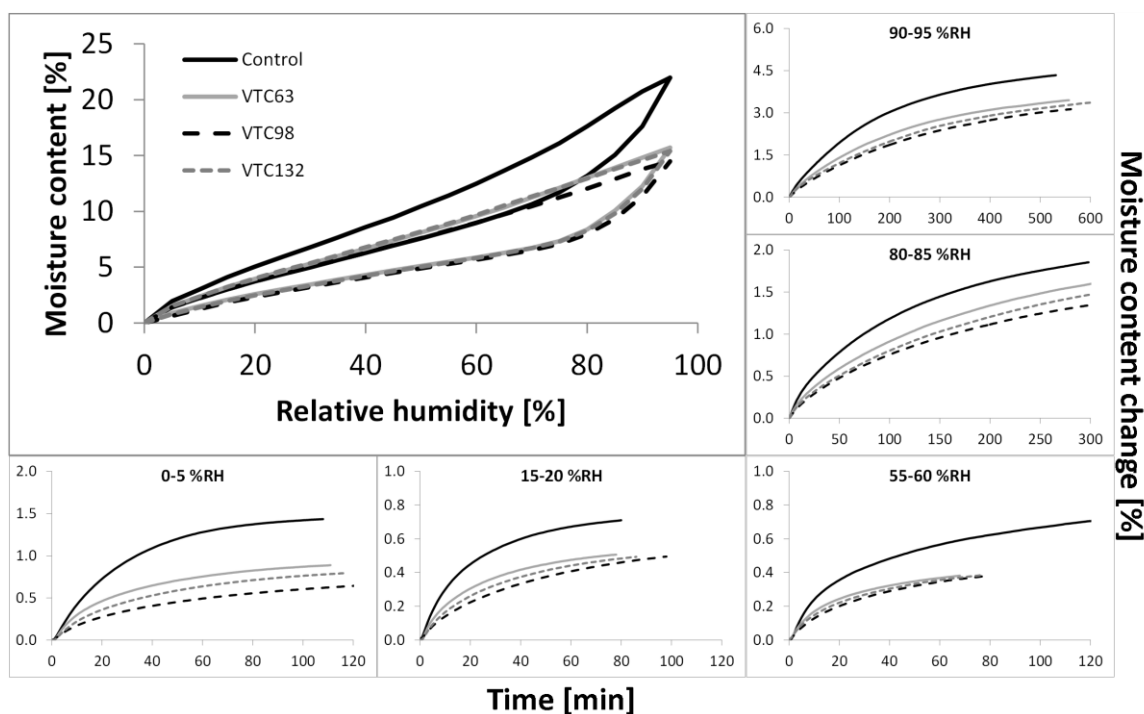


Figure 2: Sorption isotherm at 25 °C run at 5% RH steps for control and VTC wood of different decrease of densification.

During the VTC process the mass of the wood material decreases because of the thermal degradation in the wood cell wall polymers (Kutnar and Kamke, 2012). Borrega and Kärenlampi (2010) showed that the hygroscopicity of wood decreased in proportion to the mass loss as a result of thermal modification. Furthermore, Rautkari et al. (2013) analyzed the accessibility of hydroxyl groups in thermally modified wood by deuterium exchange in the DVS apparatus. They found poor correlation with the EMC, hydroxyl group accessibility, and theoretical hydroxyl group content. Therefore, they concluded that the general explanation that the EMC is controlled by the available hydroxyl group content and their accessibility is not correct, and that besides moisture content, there must to be an additional mechanism.

Conclusion

The sorption properties of control hybrid poplar and densified VTC wood specimens were studied with sorption measurements at 25 °C using Dynamic Vapour Sorption (DVS Advantage) equipment. The results showed that VTC treatment affects the sorption properties of wood. The equilibrium moisture content of VTC wood at different climate conditions is lower than that of untreated wood, while degree of densification does not influence the equilibrium moisture content of VTC wood. However, closed microstructure of densified wood affects the accessibility of hydroxyl groups in the densified wood, which results in slower absolute adsorption and desorption processes. Nonetheless, the approach to equilibrium is fairly similar in both VTC and untreated wood. A more detailed study, however, is needed to confirm the conclusion that close microstructure of VTC wood influences the accessibility of hydroxyl groups

Acknowledgment

Andreja Kutnar would like to acknowledge the Slovenian Research Agency for financial support within the frame of the project Z4-5520.

References

Blomberg, J., Persson, B., Bexell, U. (2006) Effects of semi-isostatic densification on anatomy and cell-shape recovery on soaking. *Holzforschung*, 60: 322–331.

Borrega, M., Kärenlampi, P.P. (2010) Hygroscopicity of heat-treated Norway spruce (*Picea abies*) wood. *European Journal of Wood and Wood Products*, 68(2): 233–235.

Kamke, F.A., Sizemore, H. (2008) Viscoelastic thermal compression of wood. U.S. Patent Application No. US Patent No. 7.404.422.

Kutnar, A., Kamke, F.A., Sernek, M. (2009) Density profile and morphology of viscoelastic thermal compressed wood. *Wood Science and Technology* 43(1): 57–68.

Kutnar A., Kamke FA (2012) Compression of wood under saturated steam, superheated steam, and transient conditions at 150°C, 160°C, and 170°C. *Wood Science and Technology*, 46(1/3): 73–88.

Navi, P., Girardet, F. (2000) Effects of thermo-hydro-mechanical treatment on the structure and properties of wood. *Holzforschung* 54: 287–293.

Rautkari, L., Hill, C.A.S., Curling, S., Jalaludin, Z., Ormondroyd, G. (2013) What is the role of the accessibility of wood hydroxyl groups in controlling moisture content? *Journal of Materials Science*, 48(18): 6352–6356.

Sandberg, D., Haller, P., Navi, P. (2013) Thermo-hydro and thermo-hydro-mechanical wood processing: An opportunity for future environmentally friendly wood products. *Wood Material Science and Engineering*. 8: 64–88.

Standfest, G., Kutnar, A., Plank, B., Petutschnigg, A., Kamke, F.A., Dunky, M. (2013) Microstructure of viscoelastic thermal compressed (VTC) wood using computed microtomography. *Wood Science and Technology*, 47(1): 121–139.

Effect of Microfibrillated Cellulose Content on the Bonding Performance of Urea-Formaldehyde Resin

Jin Heon Kwon¹ – Seung-Hwan Lee² – Nadir Ayrilmis^{3} – Tae Hyung Han⁴*

¹ Professor, Ph.D., ² Assistant Professor, ⁴ Research Scientist
Department of Forest Biomaterials Engineering, College of Forest and
Environmental Sciences, Kangwon National University, 200-701, Chuncheon city,
Republic of Korea

kwon@kangwon.ac.kr, lshyhk@kangwon.ac.kr, thhan212@kangwon.ac.kr

³ Associate Professor, Department of Wood Mechanics and Technology, Forestry
Faculty, Istanbul University, Bahcekoy, Sariyer, 34473, Istanbul, Turkey

nadiray@istanbu.edu.tr

* Corresponding author

Abstract

Microfibrillated cellulose (MFC) was produced from dissolving grade wood pulp by a mechanical homogenization process. Urea-formaldehyde (UF) resin mixtures with a 5% solution of MFC at 0, 1, and 3 wt% based on solid resin were prepared by mixing an aqueous MFC suspension with UF-resin. Beech lamellas with dimensions of 5 mm x 20 mm x 150 mm were prepared from beech lumbers using planer saw. The determination of tensile shear strength of single lap-joint specimens bonded with MFC modified UF-resin was carried out according to EN 205 (2003). The specimens with the modified UF-resin showed better tensile shear strengths as compared to the specimens with the unmodified UF-resin. As compared to the control specimens, the tensile shear strength of the specimens increased by 5.7% as 3 wt% MFC was incorporated into the UF-resin. However, further increment in the MFC content (up to 5 wt%) decreased the tensile shear strength of the specimens (-14.3 of control specimen). The improvement in the bonding performance of the UF-resin indicates that the addition of a certain amount of MFC in the UF-resin improves the mechanical performance of wood resin bonds.

Keywords: Microfibrillated cellulose, Wood, Urea-formaldehyde, Tensile shear strength, Lap-joint test

Introduction

Plant fibers, which are abundant renewable resources, exhibit high specific strength and stiffness, and industrial use of plant fibers as fillers in composites have attracted much interest. Plant fibers are turned into nanofibrous forms by chemical and mechanical treatments. One type of such nanofibers is called microfibrillated cellulose (MFC), which can be obtained by a high pressure

homogenizing treatment (Iwamoto 2014, Jang et al. 2013). Micro/nanofibrils isolated from natural fibers have garnered much attention for the use in composites, coatings, resins, and film because of high specific surface areas, renewability and unique mechanical properties in the past two decades (Spence et al). Microfibrillated cellulose (MFC) was introduced in 1983 (Turbak et al. 1983). The properties of MFC have been previously reviewed by Siro and Plackett (2010). The MFC consists of moderately degraded long fibrils that have greatly expanded surface area. Typically, traditional MFC consists of cellulose microfibril aggregates with a diameter ranging from 20 to even 100 nm with and length of several micrometers, rather than single nanoscale microfibrils (Kettunen 2013). Siro and Plackett (2010) have reviewed the production mechanisms and properties of MFC and reported the following routes of treatments for the production of MFC; Mechanical: refining and high-pressure homogenization, cryocrushing, grinding. Pretreatments: alkaline pretreatment; oxidative pretreatment; enzymatic pretreatment.

Resin is one of the important factors affecting mechanical and physical properties of wood-based composites. Urea-formaldehyde (UF) resin is commonly used in the manufacture of plywood, laminated veneer lumber, particleboard, and fiberboard etc. The advantages of UF resins are low cost, water solubility, easy use (under a wide variety of curing conditions), relatively low cure temperature, microorganisms resistance, low abrasion hardness, excellent thermal properties, and clear or light color (especially of the cured resin) (Nikvash et al. 2013). Due to these advantages, wood-based composite industry utilizes UF as a common resin, worldwide. However, the mechanical performance of resin bonds between the UF and wood is limited, in particular humid conditions. Since the elastic modulus of cured UF bond lines is high, the deformation of the resin layer under mechanical loading is usually small. As a result, stress concentrations along the bond line of a wood resin joint are generated that reduce the overall strength of the joint (Veigel et al. 2012).

UF-resins are a widely used class of low-priced wood resins, which are well known for their pronounced brittleness and their tendency to develop microcracks which limits their mechanical performance. The combination of low price and poor mechanical performance makes UF an ideal candidate for studying the effect of added filler. There are limited studies on the properties of wood composites bonded with MFC filled resins (Veigel et al. 2011 and 2012). The objective of this study was to improve the resin bond strength of UF-resin using at different loading levels of MFC.

Materials and Methods

Materials

Beech lumbers without defects (knot etc.) were supplied from a commercial lumber company in Chuncheon, South Korea. The lamellas with dimensions of 5 mm x 20 mm x 150 mm were prepared from beech lumbers using planer saw. Prior to bonding, all the lamellas were planed in order to ensure smooth and flat surfaces. The lamellas were conditioned in a climate room at 20°C and 65% relative humidity and allowed to reach a nominal equilibrium moisture content of 12%.

A commercial liquid UF-resin (E0 class) with 62.4% solid content was used for the bonding of two beech wood. As a hardener 1% of ammonium chloride solution (20%) based on resin solid content was added into the UF-resin.

The MFC (BiNF_i-s) was purchased from Sugino Machine Ltd. in Japan.

Preparation of UF-resin modified with MFC

UF-resin mixtures with 5% solution of MFC at 0,5, 1, 3, and 5% by weight of solid resin were prepared. The MFC filled UF-resin was mixed with magnetic stirrer for 5 min to achieve a proper distribution of MFC in the UF matrix. As a hardener 1% of ammonium chloride (NH₄Cl) solution with 20 wt% solids content based on the UF-resin solids content was added in to the UF-resin solution.

Bonding of beech lamellas

The preparation of UF-resin bonded single lap-joint specimens was carried out according to EN 205 (2003). Two beech lamellas were bonded together with the UF-resin having different amounts of MFC solution and UF-resin without MFC solution was used for resin application. The resin was applied on one surface (180 g/m²) of the lamella using a rubber roller. Assembling was always performed in parallel grain directions, whereby the panel without resin was always on the bottom, to obtain equal penetration conditions for all specimens. All the specimens were pressed simultaneously in a hydraulic press at 140°C and 1.6 MPa for 8 minutes. Prior to testing test specimens were conditioned at 20 ± 2°C and 65 ± 5% relative humidity for one week. A total of 35 specimens, 7 for each type of UF-resin mixture and control, were produced. The experimental design is presented in Table 1.

Table 1. Composition and properties of UF-resin mixtures.

Resin mixture	Solid resin (%)	MFC (% of solid resin)
Control	61.3	0
N5-0,5	61.3	0.5
N5-1	61.3	1
N5-3	61.3	3
N5-5	61.3	5

MFC, 5% water suspension; Hardener, 1%.

Tensile shear strength test of single lap-joint specimen

Determination of tensile shear strength of the specimens was performed according to EN 205 (2003). The specimen geometry is presented in Figure 1. Lap-joint testing was performed on an Instron universal testing machine with a testing speed of 1 mm/min. The tensile shear strength of lap-joint specimens was calculated as follows:

$$\sigma_s = F_{\max} / A = F_{\max} / a.b \quad (\text{N/mm}^2)$$

Where; σ_s is the tensile shear strength (N/mm²), F_{\max} is the maximum load (N) observed, A is the bonding surface of the specimen in mm² (a is the width of bonded face, and b is the length of bonded face).

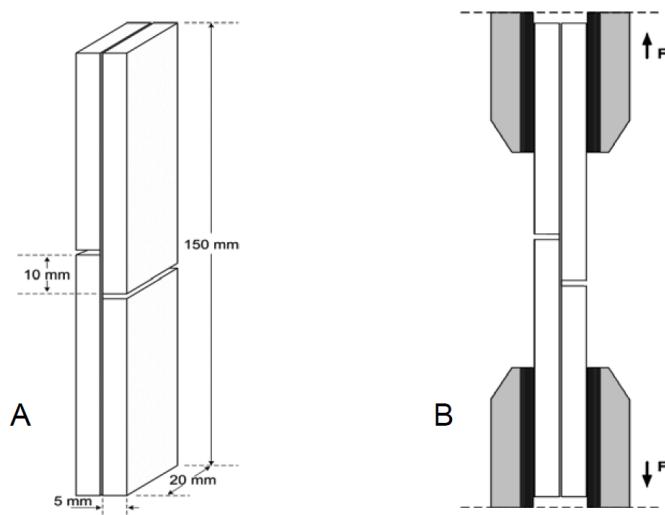


Figure 1. A) Configuration of the test specimen and B) method of loading the specimen in tension.

Measurements

The crystallinity index of MFC was measured by *x-ray diffraction (XRD)*. A disk pellet (1-cm diameter, 0.8-mm thickness, and 0.1-g weight) prepared from a freeze-dried sample was used for

wide-angle X-ray diffraction (WAXD) measurements. Freeze-drying should be used for the preparation of samples instead of oven drying process in order to not affect the WAXD measurements. Measurements were performed using a Rigaku RINT-TTR III diffractometer. Nickel-filtered Cu K α radiation ($\lambda = 0.1542$ nm) was used at 50 kV and 300 mA. The diffraction intensity was determined in the range of $2\theta = 2-60^\circ$ at intervals of 0.02° at a rate of $2^\circ/\text{min}$.

The morphology of MFC was observed using a scanning electron microscope (SEM, S-4800, Hitachi High-Technologies co., Japan). The samples were solvent-exchanged with t-butyl alcohol, then freeze-dried to keep their own morphology. The dried samples were coated with osmium.

Results and Discussion

The results of tensile shear strength of lap-joint specimens are shown in Figure 2. The tensile shear strength of the specimens increased with increasing amount of MFC in the UF-resin. As compared to the control specimens, the tensile shear strength of the specimens increased by 5.7% as 3 wt% MFC (5% suspension in water) was incorporated into the UF-resin. The deformation at failure for the lap-joint specimens increased with the addition of with homogenised MFC, suggesting that the UF-resin was possibly toughened by the addition of fibrillated cellulose. A similar result was found by Veigel et al. (2012). They reported that the vertical cracks in the cured UF bond line were a typical result of the brittleness of this frequently used wood resin. Our findings shows that the MFC reduces the brittleness of the UF-resin. However, the further increment (5 wt%) in the MFC content decreased the tensile shear of the specimens (-14.3 of control specimen).

Based on the findings obtained from the tensile shear strength, it could be said that the improvement in the bonding performance of the UF-resin decreased above a certain amount of MFC. The structure and appearance of the MFC is presented in the SEM image (Fig. 3). The specific surface area of the MFC was measured to be $86 \text{ m}^2/\text{g}$. The specific surface area of the MFC in the UF-resin considerably increased with increasing MFC content. This can be the main reason which is responsible for decreasing bond performance of UF-resin. The X-ray diffraction (XRD) profiles of MFC are presented in Figure 4. Typical cellulose I diffraction pattern with the strong crystalline peak of the 002 crystalline plane of cellulose was shown in Figure 4.

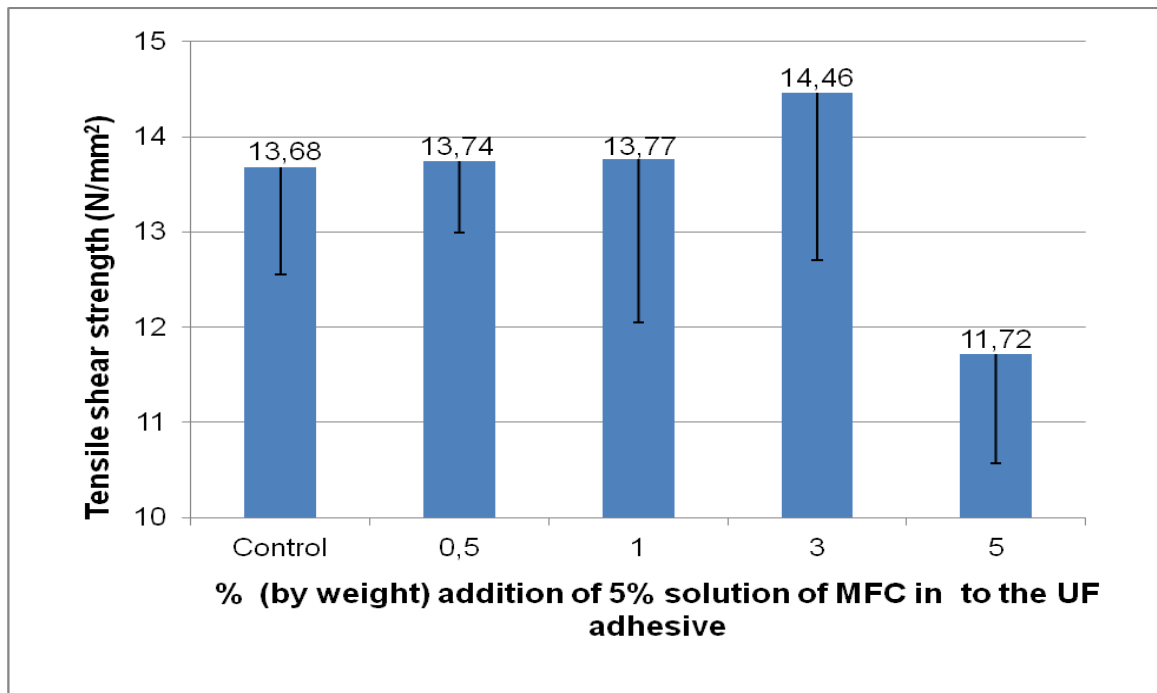


Figure 2. Tensile shear strength of single lap-joint specimens bonded with UF-resin containing MFC.

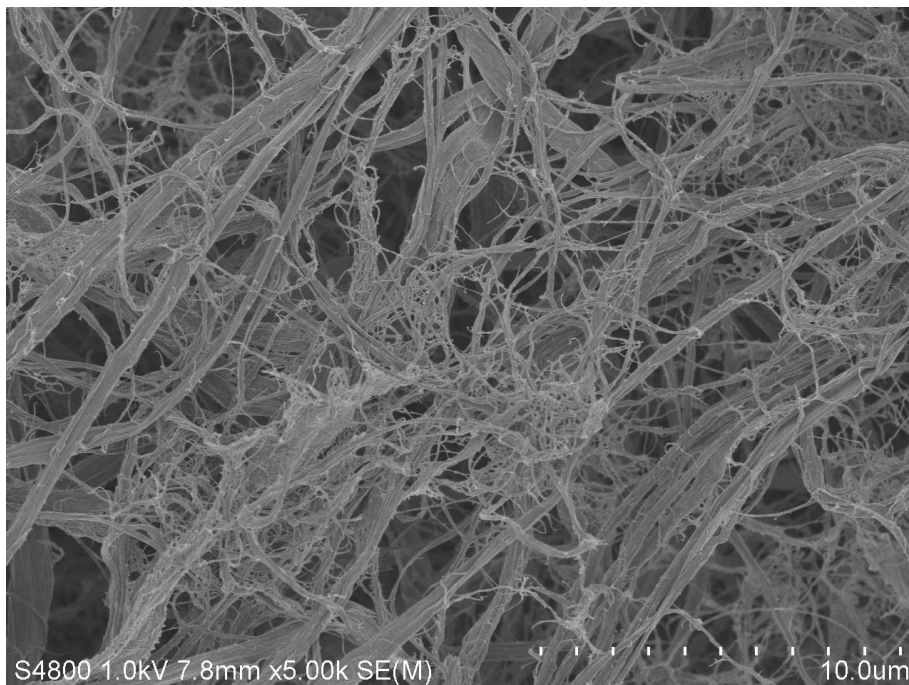


Figure 3. Structure and appearance of MFC by SEM (micro-scale).

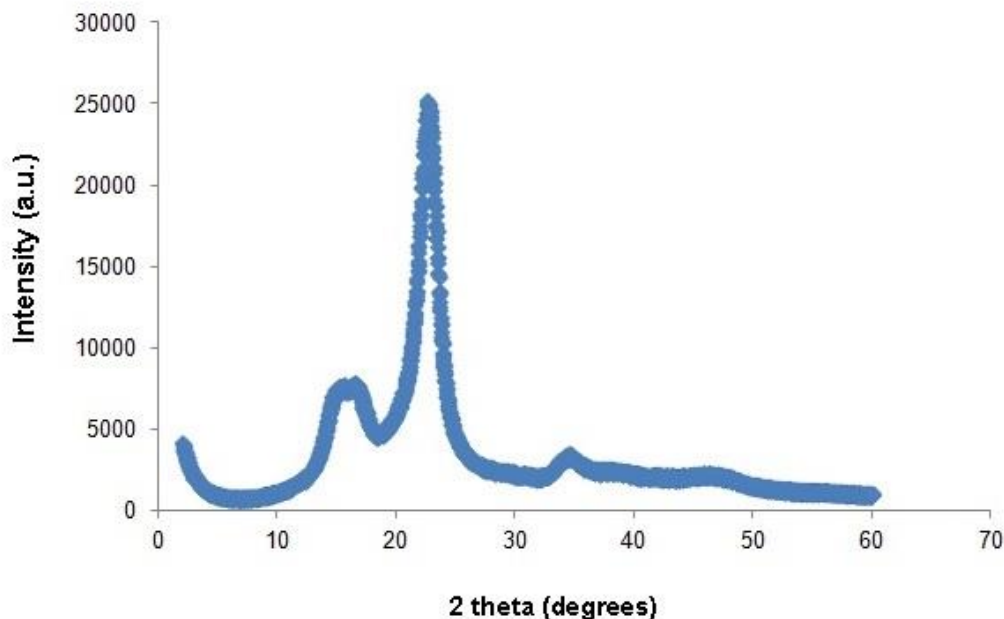


Figure 4. X-ray diffraction patterns of MFC.

Conclusions

UF-resin has the problem to form brittle glue joints when they are cured. The MFC has proven promising in improving the mechanical properties of UF-resin bond lines. The specimens with the modified UF-resin showed better tensile shear strength as compared to the specimens with the unmodified UF-resin. As compared to the control specimens, the tensile shear strength of the specimens increased by 5.7% as 3 wt% MFC (5% suspension in water) was incorporated into the UF-resin. However, further increment in the MFC content (up to 5 wt%) decreased the tensile shear strength of the specimens (-14.3 of control specimen). The improvement in the bonding performance of the UF-resin indicates that the addition of a certain amount of MFC in the UF-resin improves the mechanical performance of wood resin bonds, thus opening up new fields of application for UF, which is currently used only in the non-structural field.

References

- EN 205. 2003. Resins - Wood resins for nonstructural applications - Determination of tensile shear strength of lap-joints. European Committee for Standardization, Brussels, Belgium.
- Jang, J.H., Lee, S.H., Endo, T., Kim, N.H. 2013. Characteristics of microfibrillated cellulosic fibers and paper sheets from Korean white pine. *Wood Science and Technology*. 47: 925–937.
- Iwamoto, S., Yamamoto, S., Lee, S.H., Endo, T. 2014. Mechanical properties of polypropylene composites reinforced by surface-coated microfibrillated cellulose. *Composites Part A: Applied Science and Manufacturing*. 59: 26–29.

Kettunen, M. Cellulose nanofibrils as a functional material. 2013. Doctoral Dissertation. Aalto University, School of Science, Department of Applied Physics Molecular Materials, Helsinki, Finland, 80 p.

Nikvash, N., Euring, M., Kharazipour, A. 2013. Use of MUF Resin for Improving the Wheat Protein Binder in Particle Boards Made from Agricultural Residues. *Journal of Materials Science Research*. 2(2): 126–134.

Siro, I., Plackett, D. 2010. Microfibrillated *cellulose* and new nanocomposite materials: a review. *Cellulose*. 17: 459–494.

Turbak, A.F., Snyder, F.W., Sandberg, K.R. 1983. *Journal of Applied Polymer Science*. 37: 815–827.

Veigel, S., Muller, U., Keckes, J., Obersriebnig, M., Gindl-Altmutter, W. 2011. Cellulose nanofibrils as filler for resins: effect on specific fracture energy of solid wood-resin bonds. *Cellulose*. 18: 1227–1237.

Veigel, S., Rathke, J., Weigl, M., Gindl-Altmutter, W. 2012. Particle board and oriented strand board prepared with nanocellulose-reinforced resin. *Journal of Nanomaterials* Volume 2012. Article ID 158503, 8 pages.

The Application of Canola Straw in the Reduction of the Particleboard Density

Ahmad Jahan Latibari

Professor, Department of Wood and Paper Science, Karaj Branch, Islamic Azad University, Mehrshahr. Eram Blvd. Azadi Ave., Karaj, Iran Postal Code: 3187644511, Corresponding Author; latibari.aj@gmail.com

Hanieh Ghasemi

M.Sc. Student Department of Wood and Paper Science, Karaj Branch, Islamic Azad University, Mehrshahr. Eram Blvd. Azadi Ave., Karaj, Iran Postal Code: 3187644511

Abolfazl Kargarfard

Associate Prof., Wood and Products Research Division, Institute of Forests and Rangeland, Tehran Karaj Freeway. Tehran, Iran

Abstract

The impact of the addition of different amounts of colza straw particles to the composition of the hardwood particles for the production of lower density particleboard was investigated. Canola particles at 0, 15, 30 and 45% of the composition of the particles were added to hardwood particles and the dosage of urea resin was either 10 or 12%. Boards at two densities of 600 and 650 kg/m³ were produced and then the strength and internal bonding and thickness swelling after 2 and 24 hours immersion in water of the produced boards were determined using relevant EN standard test methods. Addition of different amounts of canola straw particle to the hardwood particles did not change either modulus of rupture or modulus of elasticity of the boards, but the internal bonding of the boards was reduced. As the dosage of the canola particles increased in the boards, both water absorption and thickness swelling were reduced. Increasing the dosage of the urea formaldehyde resin improved both the strength and thickness swelling.

Keywords: Canola straw, Particleboard, Density, Strength, Thickness swelling

Introduction

The unique characteristics of particleboard opened its way into various applications and generated interest among different consumer sectors especially cabinet and home furniture. Such interest caused a very fast rate of expansion and implementation of new plants in industrial and developing countries. Therefore, the wood raw material sources were diverted to forest residues as well as chips produced in saw mill operations. As a result, world particleboard production increased to almost 98.5 million m³ in 2012 (FAO, 2013).

However, the developing regions are faced with the severe shortage of wood as the main raw material and therefore these regions such as Iran have been looking for alternative procedures to fulfill the needed wood. Among them plantation of exotic fast growth species such as poplar and eucalyptus trees have been in the central point of research and developments. Therefore, due to the limitation in wood supply, particleboard is forced to find alternative and low cost raw material. In this course, lower quality, uncommon raw material such as agricultural wastes including wheat and rice straw and baggase have been investigated and used not only in fiber deficient regions but also in the industrial world.

Grigoriau and Natalos (1999) have investigated the production of particleboard from corn stalks and agricultural residues including wheat straw as the possible alternative raw material for wood using urea-formaldehyde/isocyanate resin system and expressed concerns on the bonding potential of corn stalks. Hague et al. (1999), and Gu and Gao (2002) also investigated the application of agricultural residues and other non-wood fiber resources for particleboard production and compared the characteristics of the boards with the particleboard from poplar tree small branches. The main limitation and drawback has been the existence of the waxy layer on the surface of the agricultural residues as the barrier for the sufficient bonding. Other research on the utilization of agricultural residues includes Han et al. (1998) who used kenaf and wheat straw and utilized silane coupling agent to facilitate the bonding between urea formaldehyde resin and waxy layer on top of wheat straw. Meinschmidle et al. (2008) has expressed that the thin wall of the agricultural wastes and the expandable cells provide useful characteristics which enables the production of lower density boards.

Mo et al. (2001) and Wang and Sun (2002) have attempted to employ the bulky nature of the non-wood lignocellulosic material to reduce the density of the final board using isocyanate and soy protein glues. Attention has been focused on the reduction of the final board density as the possible way to reduce the raw material requirements. Wang and Sun (2002) utilized wheat straw and corn stalks to produce board of the required quality at lower density. However, the need to use isocyanate resin has limited the application of such material.

The severe shortage of wood raw material has forced the investigators to search and use the alternative, uncommon and unconventional fiber supply especially urban wood residues. The availability of agricultural residues in rural areas and limitations on fiber supply necessitated the investigation to identify the suitability of such material for particleboard production.

Materials and Methods

Material

Canola straw was collected from canola plantation field in the northern city of Gorgan, Gholestan Province. The straw was transferred to Alborz Research Center, wood and paper research laboratory for particle preparation.

Urea-formaldehyde resin was purchased from Fars Chemical Company resin plant, Shiraz. The characteristics of the resin was as follow: gel time; 47 seconds (Bison Cup), density; 1.285, solid content; 63%, pH;7.5 and viscosity; 45 seconds.

Hardener; industrial grade ammonium chloride was used.

Methods

Particle preparation

Canola straw was chipped using laboratory drum chipper, Pallmann PHT 120x430 to obtain suitable chips for particle production. Chips were then flake using Pallmann ring flaker Z8. Flake were dried in a laboratory rotating drum dryer equipped with electrical heating elements to reach final moisture content of 2% (dry basis). The dried particles were screened manually and fine portion was separated. The dried and screened particles were stored in polyethylene bags until used.

Board Making and Testing

Particles were blended with a mixture of 10 or 12 % resin (dry basis) and 1% hardener (based on dry weight of resin) at the concentration of 50%, utilizing rotary drum blender and spray nozzle. Then the blended particles were hand formed using wooden mold. Board target density was varied at 600 and 650 kg/m³ and thickness was selected as 15 millimeters. Homogenous particle mats were pressed in laboratory press (Buerkle L100) applying 30 bar specific pressure, and five millimeters per seconds closing speed. Four boards for each combination of variables and total of 64 boards were produced. All boards were conditioned at 65% relative humidity and 21 °C for 15 days and then test samples were prepared from each board according to relevant EN standards. MOR and MOE was measured according to EN310/1996, Internal bonding (IB), EN319/1996 and dimensional changes, EN 317/1996 standards. For each test, four samples were prepared from each board and tested.

Statistical Analysis

Factorial experimental based on randomized block design was used for statistical analysis of the generated data.

Results and Discussion

The results showed that as the percentage of the canola straw particles in the mixture of the board making particles increases, both the flexural strength and modulus and internal bonding of the boards reduces. MOR varied from the highest value of 9.16 MPa measured on boards produced using 100% hardwood particle and the lowest value of 5.4 MPa for boards having canola straw particles. However, a specific trend was not observed. Similar trend was also observed for MOE. Statistical analysis indicated that the effect of this variable on the measured properties except the MOR of the boards was statistically significant at 99% level. Canola straw produces long and slender particles, which may generate higher flexural strength and modulus, but canola particle like other non-wood particles are inherently weak which impairs the strength of the final product. Furthermore, the canola particles are very thin with higher surface to weight ratio (specific surface) and this shape will consumes higher amount of resin which reduces the internal bonding. The presence of a waxy layer on the surface of canola straw also reduces the bonding potential of the canola straw particle which reduces the internal bonding of the board (Wang and Sun, 2002; Xu et al., 2004; Bekalo and Reinhardt, 2010). However, positive effect of increasing either higher board density or higher dosage of resin was observed. The internal bonding of the boards was higher than anticipated and the highest value of internal bonding was measured on boards with 100% hardwood particles. Even though, the flexural strength and modulus of the boards did not meet the requirements of EN specification, but the internal bonding of the boards produced with either 100% hardwood particle or 85% hardwood particles and 15% canola straw particle and application of 12% resin was sufficient for interior grade particleboards (Table 1).

The thickness swelling of the boards was increased at content of the canola straw particles. Both board density and resin dosage improved the thickness swelling. The lowest values were measured on boards with 100% hardwood particle and the lowest values from boards with higher dosage of canola straw particles. The impact of either variable on the thickness swelling of the boards was statistically significant at 99% confidence level. The thickness swelling of the boards is higher than the requirement of the either Iran or EN standard varying between 16.06-31.22% (2 hours soaking in water) and 18.58-36.5% (24 hours soaking in water) (Table 1). Therefore, special measures must be foreseen to improve the dimensional stability of such boards.

Conclusion

Wood industry is facing sever shortage of wood raw material, and therefore, this industry ought to research for alternative raw material. Different uncommon, unconventional but abundant raw material such as agricultural residue has been investigated. Canola straw can be one raw material with potential to be used in particleboard production. Canola straw is abundant and unlike wheat straw, it can not be used as cattle feed. WE have investigated the properties of laboratory made boards using different ratios of hardwood/canola straw particles. Even though the properties of the boards are not as good as hardwood particles, but different measures such as optimization of the type and dosage of resin and particle generation must be foreseen to improve the properties of the final product.

Table 1- The results of the strength and thickness swelling measurements on particleboards produced using different wood raw material

Wood Chip Composition		Board Density	Resin Dosage				Thickness swelling (%)	
Mixed hardwood	Canola Straw		(%)	MOR MPa	MOE MPa	IB MPa	2 hours	24 hours
100	-	600	10	7.03	918.96	0.513	18.18	23.27
100	-	600	12	7.46	1002	0.496	15.34	18.02
100	-	650	10	7.08	866	0.553	18.29	22.64
100	-	650	12	9.16	1128	0.651	19.71	22.31
85	15	600	10	5.37	747	0.300	20.71	27.11
85	15	600	12	5.99	929	0.363	21.22	24.95
85	15	650	10	5.34	778	0.453	24.01	29.71
85	15	650	12	7.88	1076	0.446	21.40	28.04
70	30	600	10	5.89	875	0.224	23.55	29.35
70	30	600	12	5.40	819	0.234	20.17	35.31
70	30	650	10	7.66	1186	0.395	28.98	37.05
70	30	650	12	8.31	1229	0.476	21.46	29.49
55	45	600	10	5.85	881	0.241	32.34	37.20
55	45	600	12	8.05	1165	0.248	27.11	33.20

55	45	600	10	7.84	1172	0343	31.22	36.50
55	45	600	12	9.05	1290	0.399	24.66	31.17

Acknowledgment

This study was financially and technically supported by Islamic Azad University, Karaj Branch, which would like to express our appreciation.

References

Food and Agriculture Organization Statistics. (2013). Rome, Italy.

European Standard EN 319 (1996) Wood based panels, determination of tensile strength perpendicular to plane of the board. European Standardization Committee, Brussell.

European Standard EN 325-1 (1993) Wood based panels, Sampling, cutting and inspection. Sampling and cutting of test pieces and expression of test results. European Standardization Committee, Brussell.

European Standard EN 326-1 (1993). "Wood based panels, Sampling, cutting and inspection. Sampling and cutting of test pieces and expression of test results." European Standardization Committee, Brussell.

European Standards EN 310. (1996). "Wood based panels, determination of modulus of elasticity in bending and bending strength," European Standardization Committee, Brussell.

Grigouria, H. A, Natalos, A. G. 1999. Agrowaste panel bonded with UF and UF: PMDI resin. Presented at third European panel products symposium.

Meinlschmidt, P. Schirp, A. Dix, B. Thole, V. Brinker, N. 2008. Agricultural Residues with light, parenchyma cells and Expandable filler Materials for the production of light weight particleboards. International Panel Products Symposium; Braunschweig Germany, 179-188

Bekalo, S.A., Reinhardt, H.W. and Riedl, B. 2010. Fibers from coffee husk and hulls for the production of particleboard. *Materials and Structures* 43:1049-1069.

Hague, J., Loxton, C., Quinney, R. and Hobson. 1999. Assessment for the suitability agro-based material for panel products.

Gu, J. and Gao, Z. 2002. A discussion on producing agro-residue composites with isocyanate resin. *Journal of Forestry Research*, 13(1); 74-76.

Xu, J., Sugawara, R., Widyorini, R., Han, G., Kawai, Sh. 2004. Manufacture and properties of low density binderless particleboard from Kenaf core. *J. Wood Sci.* 50:62-67.

Wang, D., and Sun, X.S. 2002. Low density particleboard from wheat straw and corn pith. *Industrial Crops and Products*. 15:43-50.

Han, G., Zhang, Ch., Zhang, D., Umemura, K. and Kawai, Sh., 1998. Upgrading of the urea formaldehyde –bonded reed and wheat straw particleboards using silane coupling agents. *J. Wood Sci.* 4:282-286.

Mo, X., Hu, J., Sun, X.S. and Ratto, J. 2001. Compression and tensile strength of low density straw-protein particleboard. *Industrial Crops and products*, 14; 1-9.

Biotransformation of Geraniol by *Polyporus brumalis*

*Su-yeon LEE*¹ – *Chang-Young Hong*² – *Seon-Hong Kim*³ – *In-Gyu Choi*^{4*}

¹ Ph.D candidate, Department of Forest Sciences, College of Agriculture and Life Sciences, Seoul National University, South Korea.

goodday8508@snu.ac.kr

² Ph.D candidate, Department of Forest Sciences, College of Agriculture and Life Sciences, Seoul National University, South Korea.

ukuk1227@snu.ac.kr

³ Ph.D candidate, Department of Forest Sciences, College of Agriculture and Life Sciences, Seoul National University, South Korea.

Sh98sh08@snu.ac.kr

⁴ Professor, Department of Forest Sciences, College of Agriculture and Life Sciences, Seoul National University, South Korea.

** Corresponding author*

cingyu@snu.ac.kr

Abstract

Biotransformation means that the chemical modification of substrate made by an organism as biocatalyst. In this study, biotransformation of geraniol was carried out by *Polyporus brumalis*. Geraniol is known the monoterpene alcohol compound of essential oil from diverse plants such as geranium and lemon. Also, *Polyporus brumalis* is the white rot fungus of basidiomycetes which live on dead or living timbers. In particular, basidiomycetes widely studied because of their ability to synthesize high-valued compounds. Therefore, in this study, biotransformation of geraniol was performed for synthesizing the high-valued compounds. As the result, geraniol transformed to citronellol, linalool, isopulegol and *p*-menta-3-en-ol by gas chromatography mass analysis. As the results, useful monoterpenoids, *p*-menta-3-en-ol was transformed from geraniol.

Keywords: Geraniol, monoterpenoid, biotransformation, *Polyporus brumalis*

Introduction

Monoterpenoids are especially important flavor and fragrance compounds that have pleasant odors (van der Werf et al., 1997) and are produced by branched chain C-10 hydrocarbons formed from two isoprene units. Geraniol is known the monoterpene precursor which has acyclic monoterpene alcohol can convert into diverse monoterpenoids by cyclization, rearrangement and oxidation. Its natural form occurs in geranium oils in which is widely used as a floral substitute of the rose scent for the perfumery and cosmetic industries (Gomes et al., 2007). Although terpenoids had important means for flavor and fragrance, the conventional method to obtain the 'natural terpenoid' has limits to control weather or season variation, risk of plant diseases and instability of supplying area. Biological technology called biotransformation can be applied

supplemental method to reduce these problems. The purpose of this study is the production of valuable terpenoids. Therefore, biotransformation of monoterpene compounds was performed by whole cell of *Polyporus brumalis*.

Materials and Methods

Materials.

Fungus

Polyporus brumalis was provided from the Korea Forest Research Institute in August 2010. The provided fungus, *P. brumalis*, was pre-inoculated in PDAM (Potato Dextrose Agar Medium) on a stationary incubator at 28°C for 7 days. After fully growing to the edge of the Petri dishes for 7 days, mycelium was separated from the agar medium using platinum wire. It was mixed with distilled water and then homogenized into suspension by ultra-homogenizer (Figure 2-1). The fungal suspension of *P. brumalis* was used as the biocatalyst on biotransformation of monoterpenes. Fungal suspension can use as identical amount by calculating dry weight.

Methods

Biotransformation reaction

Biotransformation was carried out through 3 steps; preparation of substrates and biocatalyst, reaction by substrate addition on fungal culture and identification of transformed metabolites. Especially, reaction was carried out under the liquid culture with a reactor (500 ml Erlenmeyer flask) to obtain the high recovery rates of biocatalyst and transformed product. As the liquid culture, synthetic medium (SM) was proposed. The elements of SM was followed, 1% glucose, 0.02% ammonium tartrate (C_4HCO_6), 0.01% monopotassium phosphate (KH_2PO_4), 0.05% magnesium sulfate ($MgSO_4$) and 0.01% calcium chloride ($CaCl_2$). SM culture was modified from SSC (Shallow Stationary Culture) which was suggested by Kirk et al. for activation of specific enzyme such as ligninolytic enzymes. After preparation of culture, 1 ml of fungal suspension (cell dry weight: 5 mg/ml) was inoculated in 200 ml of SM culture in 250 ml Erlenmeyer flask. The flasks were incubated in a stationary incubator at 28°C for 5 days, during which germination of the spore and mycelia growth took place, to avoid toxic effects of the substrate to the whole cell. After 5 days, 20 μ l geraniol was added to growing cells on the SM culture directly. Then, the flasks are sealed with a rubber stopper and placed on a shaking incubator at 26°C, 80 rpm.

Analysis of products

Transformed products were analyzed by gas chromatography for volatiles. Every 2 days, 5 ml aliquots of culture was extracted from the reaction cultures by ethyl acetate 5 ml by shaking extractor for 3 times with sodium chloride (NaCl) for salting out effects.

Analysis of transformed products was analyzed by gas Chromatography (GC). Qualitative and quantitative analysis was carried out using FID and MS detectors. The stationary phase GC MS was DB-5 column (dimension 30 m \times 0.25 mm, coating thickness of 0.25 μ m) and carrier gas was He at 1 ml/min. The working conditions were 300°C of injection temperature and 250°C detector temperature. The oven temperature was increased from 40 to 280 at 5°C/min, with an initial holding time and a final holding time of 10 min. A split ratio 5:1 and mass range was from 50 to 800 m/z. Peak identification was based upon mass spectra comparison with the NIST 08 (National Institute of Standard and Technology) library and with spectra of injected standards. The identification of retention index of individual compounds was based on comparison of their relative retention times with n-alkane (C8-C30) mixture in DB-5 column.

Also, quantitative analysis of compounds was performed with a Agilent model 6890A gas chromatography equipped with a split injector and FID detector. The stationary phase was a DB-5 column (dimension 30 m × 0.25 mm, coating thickness 0.25 μm) and carrier gas was ultra-pure He at 1 ml/min. The working condition carried out under the same condition of GC MS analysis. Calibration was carried out by using external standard of substrate and product.

Results and Discussion

Biotransformation of geraniol

A geraniol (trans-3,7-dimethyl-2,6-octadien-1-ol, C₁₀H₁₈O) is one of the most important substrate on the biotransformation of monoterpene. Although geraniol isn't classified to MOH like α-pinene, it is known a precursor of FPP and GGPP which can convert into diverse mono-, sesqui- and diterpenoids.

The transformed products, linalool and citronellol, were identified from geraniol in comparison to controls, after 5 days. Two products are known monoterpene alcohol and isomers of geraniol by ionization and reduction. They are not only widely used in flavor and fragrance industry but also distributed widely in various plants. Linalool is present in the essential oils of rosewood, bergamot, rose, jasmine and lavende. Linalool has also a sweet floral taste, and it is often used as an ingredient of perfumes, pesticides, or for the chemical synthesis of vitamins A and E. Citronellol (3, 7-dimethyl-2,6-octadien-1,al) is a major component of lemon scented essential oils extracted from lemon grass, melissa, verbena which are used as a food additive and a fragrance agent in cosmetic industry.

After 10 days, another transformed products, isopulegol and *P*-menthane-3,8-diol (PMD), were identified on the culture of *P. brumalis*, additionally. And no more transformation was identified (Figure 1).

Structurally, isopulegol (2-isopropenyl-5-methyl-cyclohexanol) and *P*-menthane-3, 8-diol are classified to *p*-menthane skeleton with monocyclic ring form (Figure 2). As the results, *P. brumalis* catalyzed cyclization from acyclic structure of geraniol to monocyclic form, *p*-menthane skeletons. A number of *p*-menthane monoterpenoids which is used a flavor or pharmaceutical compounds. Especially, isopulegol (C₁₀H₂₀O) is known important an intermediate in the manufacture of menthol (C₁₀H₂₀O) which has possesses the characteristic peppermint odor and cooling effect. Isopulegol also has been applied to the synthesis of natural products such as pheromone. On the other hand, PMD (*p*-menthane-3,8-diol), another transformed product, is known as an active ingredient used in insect repellents. It smells similar to menthol and has a cooling feel. It was registered as an active ingredient by the U.S. EPA in 2000 and by Canadian Pest Management Regulatory Agency in 2002.

PMD can be synthetically manufactured from citronellal. For cyclization from acyclic form, citronellal, to monocyclic form of PMD, sulfuric acid is used. Despite the heterogeneous catalytic system advantages of performing the cyclisation of citronellal, the methods described involve the use of hazardous solvents, heating, high molar ration of the catalyst, expensive catalyst or the necessity for special treatment for its activation. Also, studies have found that repellents containing synthetic PMD mixtures are not as effective as naturally derived PMD. Therefore, synthesis of PMD by *P. brumalis* could be applied as 'natural PMD'.

In conclusion, biotransformation technology of terpenoids by using white rot fungi could be possible applied for producing valuable compounds in the flavor and fragrance industry.

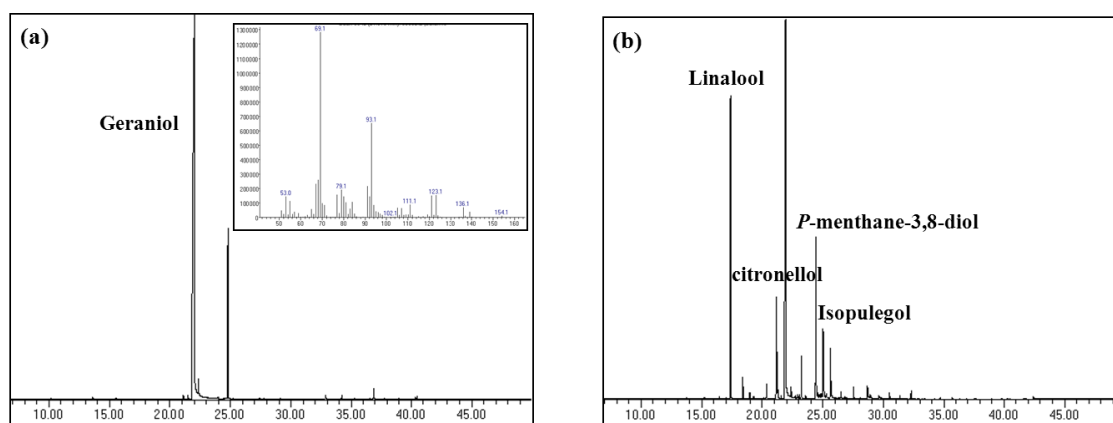


Figure 1. TIC (Total Ion Chromatogram) of transformed products from geraniol by GC MS analysis after 10 days. (a) Geraniol before the biotransformation (b) Biotransformed products from geraniol by *P. brumalis*

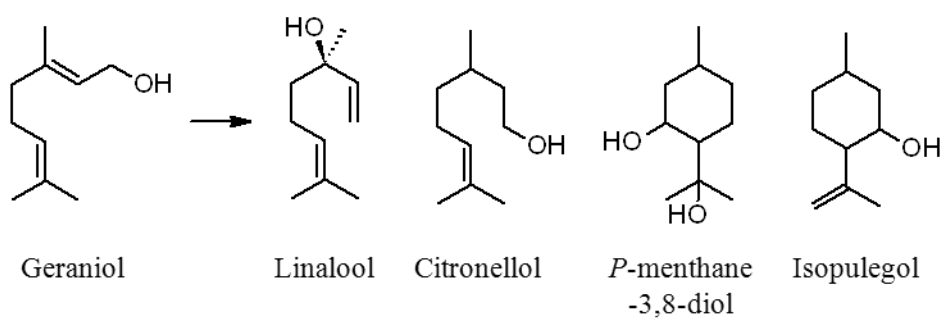


Figure 2. Biotransformation of geraniol by *P. brumalis*, after 15 days

Reference

Gomes PB, Mata VG, Rodrigues AE. Production of rose geranium oil using supercritical fluid extraction. *The Journal of Supercritical Fluids* (2007) 41:50-60.

van der Werf M, de Bont J, Leak D. Opportunities in microbial biotransformation of monoterpenes. *Biotechnology of aroma compounds* (1997):147-177.

Dimensional Responses of Wood Subjected to Cyclical Temperature Changes

Erni Ma^{1} – Junbo Shang² – Yi Shi³*

¹ Ph.D., College of Materials Science and Technology, Beijing Forestry University, Beijing 100083, China

* *Corresponding author*

maerni@bjfu.edu.cn

² Ph.D., College of Materials Science and Technology, Beijing Forestry University, Beijing 100083, China

³ Undergraduate, College of Materials Science and Technology, Beijing Forestry University, Beijing 100083, China

Abstract

Hygroexpansion is a fundamental problem affecting dimensional and shape stability of wood during processing and use. In order to investigate dimensional responses of wood under dynamic temperature condition, poplar (*populus euramericana Cv.*) specimens, 20mm in radial (R) and tangential (T) directions with two thicknesses of 4mm and 10mm along the grain, were exposed to cyclic temperature changes in square wave between 25°C and 40°C at 60% relative humidity (RH) for three different cycling periods of 6h, 12h and 24h. R and T dimensional changes measured during the cycling gave the following results: Transverse dimensional changes of the specimens were generally square but at an opposite phase and lagged behind the imposed temperature changes. The phase lag was inversely correlated with cycling period, but positively related to specimen thickness, while the response amplitude was directly proportional to cycling period, but in a negative correlation with specimen thickness. The specimens showed swelling hysteresis behavior. The heat shrinkage coefficient became greater as cycling period increased or specimen thickness decreased.

Keywords: cyclic temperature changes, dimensional responses, dynamic condition, wood.

Introduction

Wood is a naturally hygroscopic material. Since daily temperature and humidity are hard to keep constant, moisture always moves in and out of wood cell wall, and dimensional changes in wood continually occur as a result (Ma and Zhao 2012). However, previous studies on hygroexpansion of wood were mostly conducted under constant temperature and humidity (static condition). Since the 1950s, various investigations were made on affecting factors (Stevens 1963, Noack et al. 1973, Meylan 1972, Cave 1978, Espenas 1974, Chomcharna and Skaar 1983, Chanhan and Aggarwal 2004, Mcmillen 1955, Espenas 1971, Boyd 1977, Harris and Meylan 1965),

anisotropy and its mechanism of hygroexpansion (Barber and Meylan 1964, Barber 1968, Barret et al. 1972, Cave 1978, Yamamoto 1999, Yamamoto et al. 2001, Gu et al. 2001, Pang 2002). Although static condition can simplify the research method, it is too ideal to provide scientific information for wood utilization.

Therefore, dimensional changes of wood under dynamic condition received specific attentions, which was first carried out by Stevens (1963) and termed “movement” to describe wood dimensional changes caused by changes in RH during atmospheric range. The study suggested that “movement” was considerably smaller than the dimensional changes of wood took place during initial drying from green condition, and it is a useful index for dimensional stability of wood products in service. Chomcharn and Skaar (1983) then subjected wood specimens to sinusoidally varying RH between 77-47% at 25°C. Moisture and transverse dimensional changes were measured during the cyclic process.

In our previous research, Ma et al (2010) exposed Sitka spruce specimens at the size of 20mm×20mm×4mm to sinusoidally RH between 45-75% at 20°C for 1, 6, and 24h, and measured Moisture and R and T dimensional changes during the cycling. The study found that moisture and dimensional changes of the specimens were generally sinusoidal but lagged behind the imposed RH. The phase lag decreased and amplitude increased with increasing cyclic period. Nevertheless, there are few studies available on hygroexpansion of wood under varying temperature condition up to the present. This work subjected wood specimens with two thicknesses to cyclic temperature changes in square wave between 25-40°C at 60% RH, aiming at investigating dimensional responses of wood in dynamic temperature condition. The results from this study could be helpful in grasping the characteristics of wood at temperature non-equilibrium state and enriching wood physics theoretically, as well as improving wood processing and utilization through the regulation of dimensional stability practically.

Materials and Methods

Poplar (*populus euromericana Cv*) was chosen as the study species. The specimens, 20mm in R and T directions with two thicknesses of 4mm and 10mm along the grain, were initially oven-dried at 105°C. After their oven-dry dimensions in the three directions were measured, they were conditioned at 60%RH controlled by saturated salt solution of sodium bromide (Macromolecule Academy 1958) at 25±0.2°C.

They were then moved into a temperature conditioning chamber where RH was kept at 60% throughout the experiment and temperature changed in square wave between 25°C-40°C for periods of 6h, 12h and 24h. The temperature in the chamber was programmed to vary in discrete steps according to a predetermined schedule, and a thermo recorder was placed at the test specimens to ensure the desired conditions. R and T dimensional changes of the specimens in responses to the imposed temperature were recorded by three CCD laser displacement sensors (1 µm) (Ma et al. 2010). In addition, every group had three end-matched specimens for each cycle. The average values of the three tests for dimension of them were taken as the final result.

Results and Discussion

General Dimensional Responses

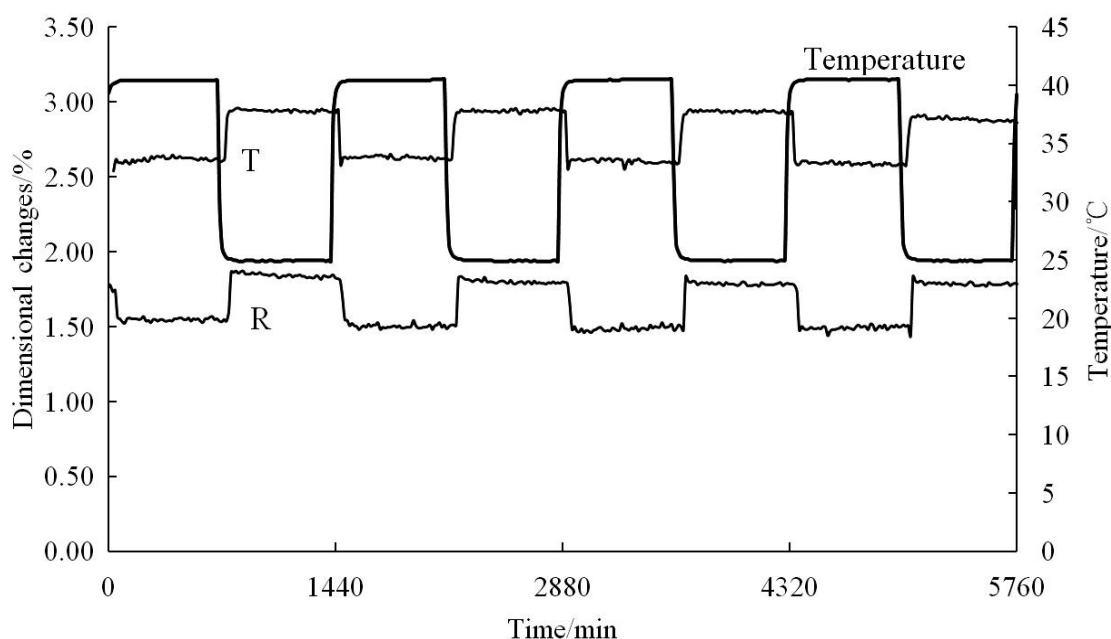


Figure 1 Plots of temperature, tangential (T) and radial (R) dimensional changes against cyclic time for 10mm thick poplar wood (60%RH, cyclic period of 24 h)

Dimensional responses of the specimens to temperature changes in square wave cycled at 24h, as an example, is shown in Figure 1 in which dimensional changes are given in terms of swelling based on oven-dry dimensions. It can be found that R and T dimensional changes were generally in square wave as well. An increase in temperature corresponds to decreased dimensions, leading to an opposite phase between temperature and dimensional changes of the specimens. This is as expected because moisture adsorbed by wood reduced as temperature increased (Cao et al. 1997), which weakened the dimensional responses. Moreover, dimensional changes of the specimens lagged behind the impose temperature slightly.

Amplitude and Phase Lag

Table 1 Amplitude of tangential (T) and radial (R) dimensional response for poplar wood

Thickness /mm	Period /h	Amplitude/%	
		T	R
4	6	0.20	0.14
	12	0.27	0.18
	24	0.32	0.21
10	6	0.17	0.12
	12	0.21	0.15
	24	0.25	0.18

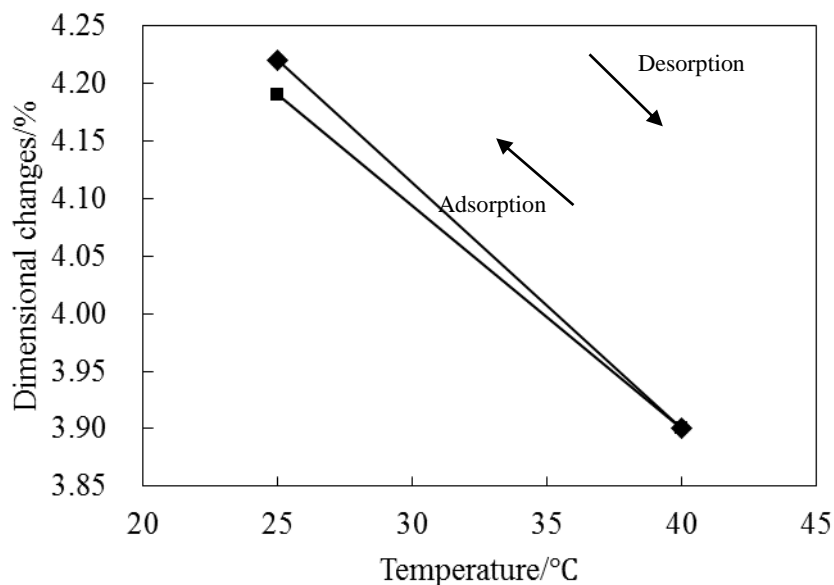
Table 1 lists the amplitude of R and T dimensional responses of different specimen thicknesses for each of the three cyclic periods. It is clear that as the cyclic period increases, the amplitude

increases. This is anticipated because with longer cyclic period, the specimens could more sufficiently respond to the temperature changes and produce higher amplitude as a result. In addition, the amplitude decreases with the increasing thickness of specimens.

Table 2 Phase lags of tangential (T) and radial (R) dimensional responses for poplar wood

Thickness /mm	Period /h	Phase lag/radians	
		T	R
4	6	0.14	0.16
	12	0.13	0.15
	24	0.10	0.11
10	6	0.15	0.17
	12	0.15	0.16
	24	0.11	0.13

Table 2 gives the phase lags of R and T dimensional responses of different specimen thicknesses at each of the three cyclic periods. There is a positive correlation between the phase lag and specimen thickness, namely, thick specimens have greater phase lag values and response to temperature changes slowly. And tangential responses act faster than radial responses to dynamic condition, which may attribute to the ray restraint effect (Liu and Zhao 2004). On the other hand, the phase lag is inversely related to cyclic period, or in other word, specimens cycled at longer period have lower phase lag values due to the fact that their responses could more nearly follow the temperature changes.



Swelling Hysteresis

Figure 2 Plots of tangential dimensional changes against cyclic temperature for the first adsorption-desorption cycle of 10mm thick poplar wood (cyclic period of 24 h)

T dimensional changes against cyclic temperature for 10mm thick specimens cycled during the first adsorption-desorption at 24h is shown in Figure 2 as an example. Swelling hysteresis caused by sorption hysteresis can be clearly observed in the figure.

The slope of the lines in this figure represents variation in wood dimensional change per temperature change, which is defined as heat shrinkage coefficient (HSC) here, an index to reflect dimensional instability of wood by moisture exchange due to atmospheric temperature varying. Table 3 summarizes the dynamic heat shrinkage coefficient in tangential direction of the specimens for different cycle periods. It indicates that the HSC value is proportional to cyclic period, but in negative correlation with specimen thickness.

Table 3 Heat shrinkage coefficient of poplar wood in tangential direction under dynamic condition

Thickness /mm	Period /h	HSC /(%/°C)	Average /(%/°C)
4	6	1.60×10^{-2}	1.82×10^{-2}
	12	1.87×10^{-2}	
	24	2.00×10^{-2}	
10	6	1.18×10^{-2}	1.24×10^{-2}
	12	1.25×10^{-2}	
	24	1.30×10^{-2}	

As shown in Table 3, the HSC value of wood is at the order of magnitude of 10^{-4} , which is different from the thermal expansion coefficient (TEC) resulted directly from temperature increase. Generally, TEC is at the order of magnitude of 10^{-6} - 10^{-5} (Gao et al. 1995, Liu and Zhao 2004), much lower than the HSC. Therefore, the dimensional changes caused by thermal expansion could be negligible in this work. At the same time, dimensional responses owing to water evaporation during heating were more notable than those coming from thermal expansion, which was also the case in previous study (Yin 1996).

Conclusions

Poplar (*populus euramericana* Cv.) specimens with two thicknesses of 4mm and 10 mm along the grain, were exposed to cyclic changes in square wave between 25°C and 40°C at 60% RH. Radial and tangential dimensional changes measured in this study gave the following results:

- 1) Transverse dimensional changes of the specimens were generally square but at an opposite phase.
- 2) Dimensional changes of the specimens lagged behind the imposed temperature changes. The phase lag was inversely correlated with cycling period, but positively related to specimen thickness.
- 3) Response amplitude was directly proportional to cycling period, but in a negative correlation with specimen thickness.
- 4) The specimens showed swelling hysteresis behavior. The heat shrinkage coefficient became greater as cycling period increased or specimen thickness decreased.

References

- Barber, N.F. 1968. A theoretical model of shrinking wood. *Holzforschung*. 22(4): 93-103.
- Barber, N.F. Meylan, B.A. 1964. The anisotropic shrinkage of wood: A theoretical model. *Holzforschung*. 18(5): 146-156.
- Barrett, J.D. Schniewind, A.P. Taylor, R.L. 1972. Theoretical shrinkage model for wood cell walls. *Wood Sci*. 4:178-192.
- Bosshard, H.H. 1956. Bber die anisotropie der holzschwindung. *Holz Roh Werkst*. 14(8): 285-295.
- Boyd, J.D. 1974. Anisotropic shrinkage of wood: Identification of the dominant determinants. *Wood Res. Soc*. 20: 473-482.
- Boyd, J.D. 1977. Relationship between fiber morphology and shrinkage of wood. *Wood Sci Technol*. 11(1): 3-22.
- Browne, F.L. 1957. Swelling of springwood and summerwood in softwood. *For Prod J*. 7(11):416-424.
- Cao, J.Z. Zhao, G.J. Lu, Z.Y. 1997. Thermodynamic Characteristics of Water Absorption of Heat treated Wood. *Journal of Beijing Forestry University*. 19(4): 26-33.
- Cave, I.D. 1978. Modelling moisture-related mechanical properties of wood: Computation of properties of a model of wood and comparison with experimental data. *Wood Sci Technol*. 12(2): 127-139.
- Cave, I.D. 1978. Modelling moisture-related mechanical properties of wood: Properties of the wood constituents. *Wood Sci Technol*. 12(1): 75-86.

- Chanhan, S.S. Aggarwal, P. 2004. Effect of moisture sorption state on transverse dimensional changes in wood. *Holz Roh Werkst.* 62(1): 50-55.
- Chomcharn, A. Skaar, C. 1983. Moisture and transverse dimensional changes during air drying of small green hardwood wafers. *Wood Sci Technol.* 17(3): 227-240.
- Espenas, L.D. 1974. Longitudinal shrinkage of western redcedar, western hemlock, and true fir. *For Prod J.* 24(10): 46-48.
- Espenas, L.D. 1971. Shrinkage of Douglas fir, western hemlock, and red alder as affected by drying conditions. *For Prod J.* 21(6): 44-46.
- Gao, R.T. Xu, Q.G. Su, W. 1995. Study on mechanism of wood thermal expansion. *Journal of Northeast Forestry University.* 23(2): 55-61.
- Gu, H. Zink, S.A. Shell, J. 2001. Hypothesis on the role of cell wall structure in differential transverse shrinkage of wood. *Holz Roh Werkstoff.* 59(6): 436-442.
- Harris, J.M. Meylan, B.A. 1965. The influence of microfibril angle on longitudinal and tangential shrinkage in *Pinus radiata*. *Holzforschung.* 19(5): 144-153.
- Liu, Y.X. Zhao, G.J. 2004. *Wood resources in Materials Science.* China Forestry Publishing House. Beijing. 362pp.
- Ma, E.N. Nakao, T. Zhao, G.J. Ohata, H. Kawamura, S. 2010. Dynamic sorption and hygroexpansion of wood subjected to cyclic relative humidity changes. *Wood Fiber Sci.* 42(2): 229-236.
- Ma, E.N. Zhao, G.J. 2012. *Special topics on wood physics.* China Forestry Publishing House. Beijing. 90pp.
- Macromolecule Academy .1958. *Physical properties of macromolecule.* Kyoritsu Press. Tokyo. 250 pp.
- McMillen, J.M. 1955. Drying stresses in red oak: effect of temperature. *For Prod J.* 5(4): 230-241.
- Meylan, B.A. 1972. The influence of microfibril angle on the longitudinal shrinkage-moisture content relationship. *Wood Sci Technol.* 6(4): 293-301.
- Noack, D. Schwab, E. Bartz, A. 1973. Characteristics for a judgement of the sorption and swelling behavior of wood. *Wood Sci Technol.* 7 (3): 218-236.
- Pang, S. 2002. Predicting anisotropic shrinkage of softwood: Theories. *Wood Sci Technol.* 36(1): 75-91.
- Pentoney, R.H. 1953. Mechanisms affecting tangential vs radial shrinkage. *For Prod Res Soc.* 3(2): 27-321.
- Quirk, J.T. 1984. Shrinkage and related properties of Douglas fir cell walls. *Wood and Fiber Science.* 16(2): 115-133.
- Skaar, C. 1988. *Wood water relations.* Springer Verlag. Berlin. 283 pp.
- Stevens, W.C. 1963. The transverse shrinkage of wood. *For Prod J.* 13(9): 386-389.
- Wang, J.Y. Zhao, G.J. 1999. Mechanism of formation, recovery and permanent fixation of wood set. *Journal of Beijing Forestry University.* 21(3):71-77.
- Yamamoto, H. 1999. A model of the anisotropic swelling and shrinking process of wood: Generalization of Barber's wood fiber model. *Wood Sci Technol.* 33(4): 311-325.
- Yamamoto, H. Sassus, F. Ninomiya, M. Gril, J. 2001. A model of the anisotropic swelling and shrinking process of wood (II): A simulation of shrinking wood. *Wood Sci Technol.* 35 (1-2): 167-181.
- Yin, S.C. 1996. *Science of Wood.* China Forestry Publishing House. Beijing. 272pp.
- Zhang, W.B. Morihiko, T. Takashi, T. Koh, Y. 2006. Effect of Delignifying Treatments on Mechano-sorptive Creep of Wood I. *Journal of Wood.* 52(1): 19-28.

Acknowledgements

The authors would like to thank the National Natural Science Foundation of China (No.31200435) for the financial support.

Spectrophotometric Analysis of the Accelerated Aged Wood Treated with Transparent Coatings for Exterior Constructions

Miroslava Mamoňová^{1} – Ladislav Reinprecht²*

¹Assistant professor, Department of Wood Science
Faculty of Wood Sciences and Technology, Technical University in Zvolen, T. G.
Masyryka 24, Zvolen, Slovakia

** Corresponding author*

mamonova@tuzvo.sk

²Professor, Department of Mechanical Wood Technology
Faculty of Wood Sciences and Technology, Technical University in Zvolen, T. G.
Masyryka 24, Zvolen, Slovakia

reinprecht@tuzvo.sk

Abstract

The aim of this work was to analyse changes in the colour of wood treated with selected transparent coatings after accelerated ageing in Xenotest. Black locust (*Robinia pseudoacacia* L.) heart-wood samples were treated with three transparent coatings recommended for outdoor exposures: PerlColor, Osmo UV-Protection Oil 420 and AquaStop, creating eight coating systems with or without nanoscale particles. Accelerated ageing of the treated and reference samples was performed in the Xenotest Q-SUN Xe-1 Test Chamber by the EN 927-6, in duration of 3, 6, 9 or 12 weeks. Colour changes in the surfaces of aged samples were analysed by the spectrophotometer “Minolta CM2600d” with determination of the differential spectra. The best colour stability had coating systems containing the nanoscale particles (PerlColor), more apparently in combination with the top water-repellent layer (AquaStop).

Keywords: *Robinia pseudoacacia*, Coating Systems, Nanoscale particles, Ageing, Colour, Differential Spectra.

Introduction

Resistance of coatings to ageing is one of the basic requirements for quality finishing of wood, as in terms of aesthetic appearance of the product itself as well as the protective effect of wood (Liptáková & Sedláčik 1989, Reinprecht 2013). Thin stains are the most progressive coating system for finishing of wood products in outdoor exposures. In addition to their good ecological parameters, they are characterized also by the aesthetic quality - maintaining the appearance of natural wood. Coating systems for outdoor exposures should provide protection of wood surfaces against atmospheric agents (UV radiation, humidity, etc.), or also combined protection of wood against the weather and biotic pests. Coatings designed for exterior have to contain particles that

can eliminate the penetration of UV radiation into wood surfaces, further additives with hydrophobic effect and fungicides ([Reinprecht et al. 2011](#), [Reinprecht & Pánek 2013](#)).

Each ageing of wood products treated with coating film or oil raises a number of irreversible chemical and physical changes in structure of wood and also in structure of coating. The most aggressive component of weathering is the UV part of sunlight, which promotes the breakdown of lignin in wood and also of film-forming and other components in coatings with creation of the following defects: - changes in the microstructure of coating (cracks, etc.); - decreases in the thickness of coatings; - changes in the colour of coatings; - changes in the surface structure of wood (Mamoňová & Reinprecht 2008).

Electron-microscopy analyses are convenient for assessing the structure of the coatings and their quality, their penetration into wood, and reveal otherwise hidden defects in individual layers of the coating system and also in the surface of treated wood (Mamoňová & Reinprecht 2008, Kúdela 2009, Mamoňová et al. 2010).

Perception of light and colour by a human sight is individual, psycho-physiological matter. In spectrophotometrical measurement of colours the principle of the method inheres in measurement of particular spectral characteristics of white (composite) light reflected from a sample surface, to be directed to an optical system of spectrophotometer, where it is decomposed in individual wave-lengths (Babiak et al. 2004).

The work is aiming to analyze colour changes of transparent coating systems with or without nanoscale particles (UV absorbers) and top water-repellent layer applied on black locust samples that had been exposed in Xenotest through course of differential spectra. Paper builds on a previous research (Mamoňová et al. 2010), in which micro-structural changes in coatings with similar composition after accelerated ageing were evaluated.

Materials and Methods

Wood

Black locust (*Robinia pseudoacacia* L.) heartwood has yellowish to greenish brown colour caused by number of chemical substances such as robinetin, dihydrorobinetin, etc. (Molnár & Tolvaj 2004, Tolvaj & Németh 2008., Fan et al. 2010., Chen et al. 2012). For the experiment were prepared samples of black locust heartwood with the dimension of 38 mm x 8 mm x 55 mm (RxTxL), which have been grinded along grains with 120-grit sandpaper. The front surfaces of samples were then treated with silicone.

Coatings

For the surface treatment of the black locust samples were used the following three transparent coatings recommended for outdoor exposures: PerlColor (Bomol), Osmo UV-Protection Oil 420, and AquaStop, all supplied by Böhme AG, Switzerland:

PerlColor – transparent stain containing nanoscale particles (UV absorber) and oil-based synthetic resin modified with ASS-Chelat (UV protection), applied as a water system. Additives: IPBC fungicide.

Osmo UV-Protection Oil 420 (OsmoUV) – satin-matt oil, clear finish for exterior application. It is based on natural vegetable oils (sunflower and soyabean oils) in dis-aromatized white spirit (benzene-free), which penetrates deeply into the wood. It is moisture regulating, reduces swelling and shrinking of the wood, and is water and dirt resistant.

AquaStop – clear transparent water-repellent and sunblocker, modified with ASS-Chelat (UV protection), applied as a water system for higher UV, weather and rain protection of wood and basic paints.

From these three coatings were created eight coating systems with determined designation and composition (Tab. 1).

Table 1 *The coating systems (CS) used in the experiment*

Designation	Composition of coating systems (CS)
CS1	One layer of PerlColor
CS2	Two layers of PerlColor
CS3	One layer of PerlColor + One layer of AquaStop
CS4	Two layers of PerlColor + One layer of AquaStop
CS5	One layer of Osmo UV Protection Oil 420
CS6	Two layers of Osmo UV Protection Oil 420
CS7	One layer of Osmo UV Protection Oil 420 + One layer of AquaStop
CS8	Two layers of Osmo UV Protection Oil 420 + One layer of AquaStop
Untreated	Without coating

Accelerated ageing in Xenotest

Tested samples, it means untreated reference and samples treated with coating systems, were undergone to accelerated artificial ageing in the Xenon Test Chamber Q-SUN Xe 1 in 1-weeks intervals, totally lasting 3, 6, 9 or 12 weeks. The ageing process of samples during one week interval is shown in Table 2.

After 3, 6, 9, and 12 weeks of ageing (cycles 1, 2, 3, and 4) the samples were undergone to the spectrophotometric analyses. There from the ends of tested samples were cut also small specimens for microscopic analyses. New ends of samples were then treated with silicone and samples were again put into Xenotest.

Table 2 *Exposure of samples in the Xenotest during the 1-week interval (EN 927-6:2006)*

Duration of 1-week ageing (168 h)		Function in the Xenotest	
1. Step		24 h	Spray off, Temperature 45 ± 3 [°C], UV off
2. Step	A	2.5 h	UV Irradiance 0.55 [$\text{W}\cdot\text{m}^{-2}$] at 340 nm, Temperature 50 [°C]
	B	0.5 h	Water - Spray, Temperature 20 [°C], UV off
	A + B	3 h	
	48 Sub-intervals (A+B) : $48 \times 3 \text{ h} = 144 \text{ h}$		

Notes: According to EN 927-6:2006 the prescribed parameters for test chamber are as follows: Irradiance set point = 0.89 W.m⁻²]; Temperature = 60 ± 3 [°C]). For used Xenotest (Q-SUN Xe-1) the parameters set are upper the limit of the real test chamber.

Colours and differential spectra

Colours of wood treated with coatings were measured with the spectrophotometer type MINOLTA of CM 2600d. With aid of „SpectraMagic“ software we contrived the measurement processes as well as working with measured data (Babiak et al. 2004). To define differential spectra there were performed 20 measurements of each testing sample namely before an exposition (reference samples) and after an exposition of particular cycles.

To delimitate the sample surface to be measured there was used a standard measuring aperture of 8 mm diameter. Illuminating system was set to a measuring mode including scattering components (SCI). We carried out measurements of wave lengths ranging from 360 - 740 nm, with resolution 10 nm, when a xenon discharge tube D65 was used as a source of light.

The spectrometer can measure also a course of spectrum dependent upon reflected wave lengths (Mamoňová 2009). It is measured through “reflectance – reflectiveness” representing an ability of the substance surface to reflect an incident light. It is stated in percentages as a ratio between reflected light (radiation) and an amount of reflected light from a reference surface (a white reference with 100%). So, in this work, within the reflectance were analyzed also the colour changes due to presence of coatings on wood and due to their ageing in whole range of a visible spectrum.

The closer is a course of differential spectra to particular coating systems (they converge) and at the same time they have the higher reflectance, the coating system is at shorter wave lengths more stable and more resistant against photo degradation processes. A positive course of spectrum curve is also just then when they oscillate near around a curve of a spectrum of a reference or a native sample.

Results and Discussion

The differential spectra of the black locust heart-wood samples, the untreated and treated with the eight different coating systems (CS1 – CS8, see Tab. 1), refer about their reflectance and light absorbability at different wave lengths comparing with the non-aged references (Figs. 1-4).

Analyses of differential spectra at individual ageing cycles

Cycle 0:

In the Figure 1 (at Cycle 0 = Reference) we can see almost the same decreased character of the light absorbability in samples treated with coating systems in relation to the untreated samples (see zero value in the all interval of wavelength).

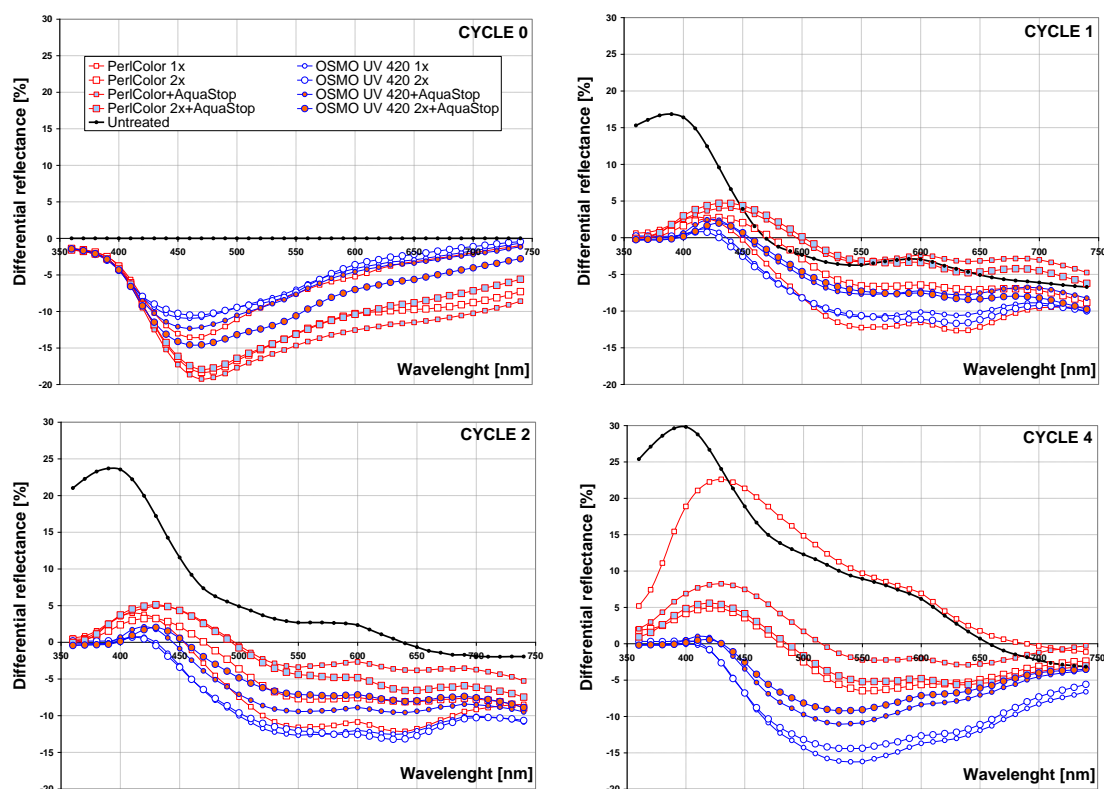


Figure 1 Differential spectra of samples before (Cycle 0) and after ageing in Xenotest (Cycles 1, 2, and 4)

Coating systems CS1 – CS4: The highest absorbability is featured for CS3 (One layer of PerlColor + One layer of AquaStop), whereby the minimum reflectance is achieved only -20% at the wave length 470 nm comparing with a native non-finished surface of black locust wood sample. The least absorbability is featured for CS1 (One layer of PerlColor), at the wave length of 460 nm.

Coating systems CS5 – CS8: The least absorbability is at CS6 (Two layers of Osmo UV Protection Oil 420), which has the minimum reflectance at value of -10% at the wave length of 460 nm. The highest absorbability is surprisingly at CS8 (Two layers of Osmo UV Protection Oil 420 + One layer of AquaStop) at a wave length of 470 nm. A characteristic feature for all coating systems is, that up to a wave length of about 420 nm they show almost the same course of absorbability, then from 420 nm is absorbability of each CS different even when a course of differential spectra has similar course.

Cycle 1:

A course of differential spectra after the 1st cycle of exposition (Fig. 1, cycle 1) shows that all coating systems have once again after the 1st cycle a similar character of a course of light reflectance. The best reflectance showed at the CS4 (Two layers of PerlColor + One layer of AquaStop) at a wave length of 440 nm, +5 %. At the same time paradoxically the minimum reflectance of -13 % was achieved at CS1 (One layer of PerlColor) in area of wave lengths of 550-650 nm comparing with a reference sample. Character of reflectiveness of an original non-treated wood is up to a wave length of 470 nm positive, and then the light is already absorbed. The highest value of a differential reflectance (+17%) for a native non-treated sample was recorded at a wave length of 390 nm.

Cycle 2:

Figure 1 (Cycle 2) shows how the reflectance changed at various wave lengths after the 2nd cycle of samples exposition in the Xenotest in relation with reference samples (Cycle 0). The highest reflectance has got native wood, maximum reflectance +24 % comparing with a reference of a non-treated original sample, ranging from a wave length 640 nm, in area o long waves, a non-treated sample reaches negative values of reflectance.

A course of differential spectra is typical in area of low wave length for all coating systems, when a sample surface has the higher reflectance as reference samples. Especially CS1 – CS4 show a higher reflectance than CS5 – CS8, for which a light absorption is typical.

The best reflectance in short waves and the least absorbability in long wave lengths from coating systems CS5 – CS8 is recorded from CS8 (Two layers of Osmo UV Protection Oil 420 + One layer of AquaStop). The coating system CS3 (One layer of PerlColor + One layer of AquaStop) achieved the best reflectance at short wave lengths and the least absorbability of light at long wave lengths from combination series of coating systems CS1 – CS4.

Differential spectra of untreated black-locust

During individual cycles of ageing in Xenotest from 0 to 4 (Cycle 0 = reference without ageing; Cycle 1 = 3 weeks; Cycle 2 = 6 weeks; Cycles 3 = 9 weeks; Cycle 4 = 12 weeks of ageing) the reflectance of untreated samples increased mainly at the short wave lengths. The differential spectra show almost a regular increase of reflectance at a wave length of 390 nm (Fig. 2). Such high reflectance can be assigned to a surface erosion of a early wood, which has showed significantly lighter colour than a late one. So, we can deduce that at the short wave lengths the most significant erosion occurs on the wood surfaces from the area of a visible spectrum. A maximum reflectance was achieved after the 4th cycle at a wave length of 400 nm (+30%) and it gradually decreased to the length of 660 nm from where the light was absorbed.

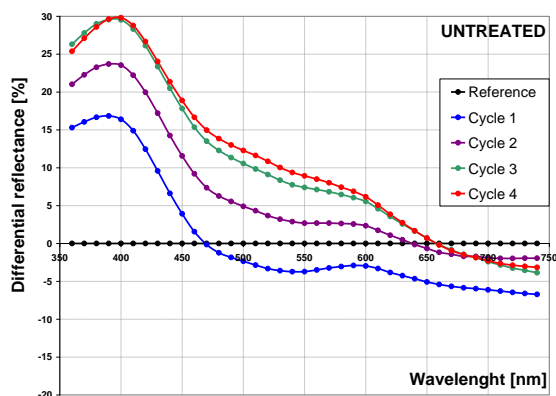


Figure 2 *Differential spectra of native wood for individual cycles of ageing*

Differential spectra of black locust treated with coating systems

In the work were used two basic groups of coating systems (CS), namely: 1st group CS1 – CS4 (PerlColor with nano-particles), and the 2nd group CS5 – CS8 (Osmo UV-Protection Oil 420 without defined presence of nano-particles) – see Tab. 1.

From courses of the differential spectra of particular coating systems (Figs. 3 and 4) we can note, that the composition of coating system influences their reflectance. Mutual comparison of spectra

reports that the both groups of coatings absorb light more (Figs. 3 and 4) than the native wood (Fig. 2). It means that used transparent coating substances changed a colour spectrum of wood towards the more obscure areas. A more absorbed light was recorded for the 1st group of coating systems CS1 – CS4 based on nano-particles (PerlColor in 1 or 2 layers, and its combination with AquaStop) in comparison to the 2nd group CS5 – CS8.

Comparing the differential spectra at short wave lengths there was noted that the reflectance increased with duration of ageing, mainly for the 1st group of coatings (Fig. 3). However, at longer wave lengths of differential spectra the effect of ageing of individual coatings systems was not so clear (Figs. 3 and 4).

Coating systems CS1 – CS4:

Coating system CS4 (Two layers of PerlColor + One layer of AquaStop) appears as the best one, having a same value of light reflectance indeed (+7%) in short wave lengths as coating system CS3 (One layer of PerlColor + One layer of AquaStop), but a course of spectrum curve shows that coating system does not create great differences between cycles. Light reflectance is almost the same during cycles in short wave lengths, however in long wave lengths of a spectra curve they non-significantly differ. Comparing coating systems CS1 – CS4 we suppose that a surface AquaStop layer creates a more stable system against photo degradation processes in treated wood at short wave lengths.

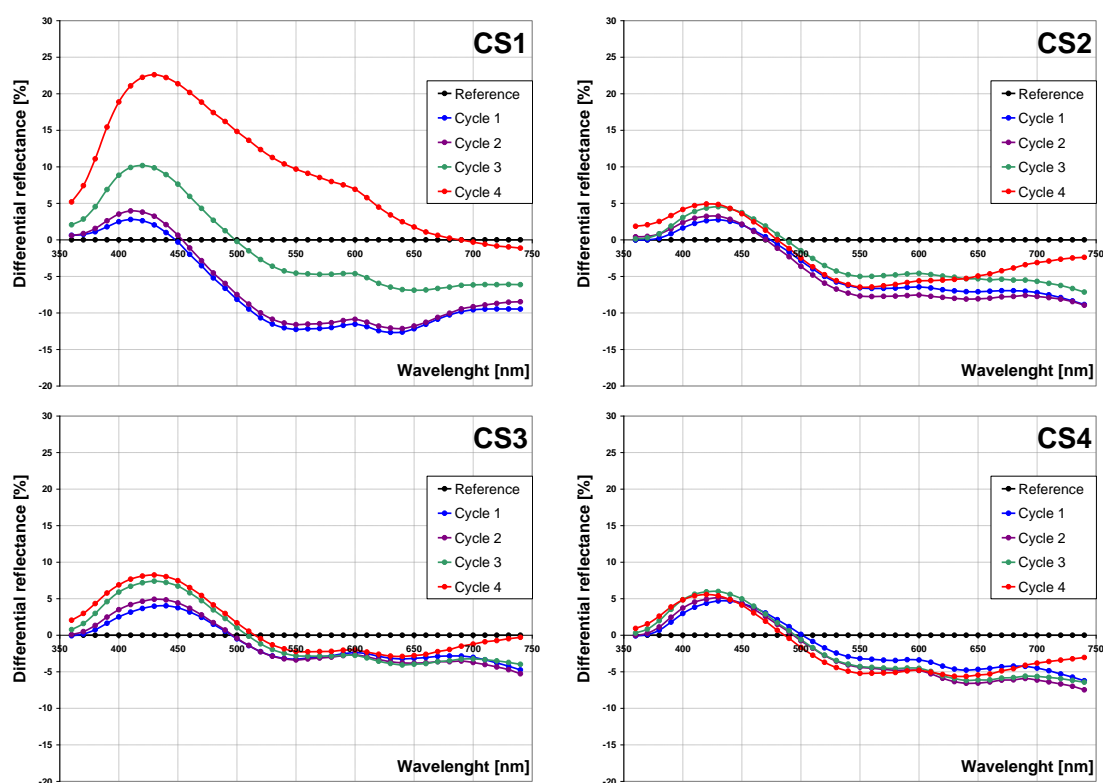


Figure 3 *Differential spectra of wood treated with coating systems with PerlColor (CS1 – CS4) for individual cycles of ageing*

Coating systems CS5 – CS8:

Comparing differential spectra from particular cycles we deduce that the most favorable result have been achieved by the coating system CS8 (Two layers of Osmo UV Protection Oil 420 +

One layer of AquaStop). AquaStop significantly increased the light reflectance in short wave length comparing with the coating system CS6. Two layers of Osmo UV ensured together with AquaStop for a decrease of light absorbability in long wave lengths. Course of spectra curves is almost similar without a significant change comparing with coating system CS7.

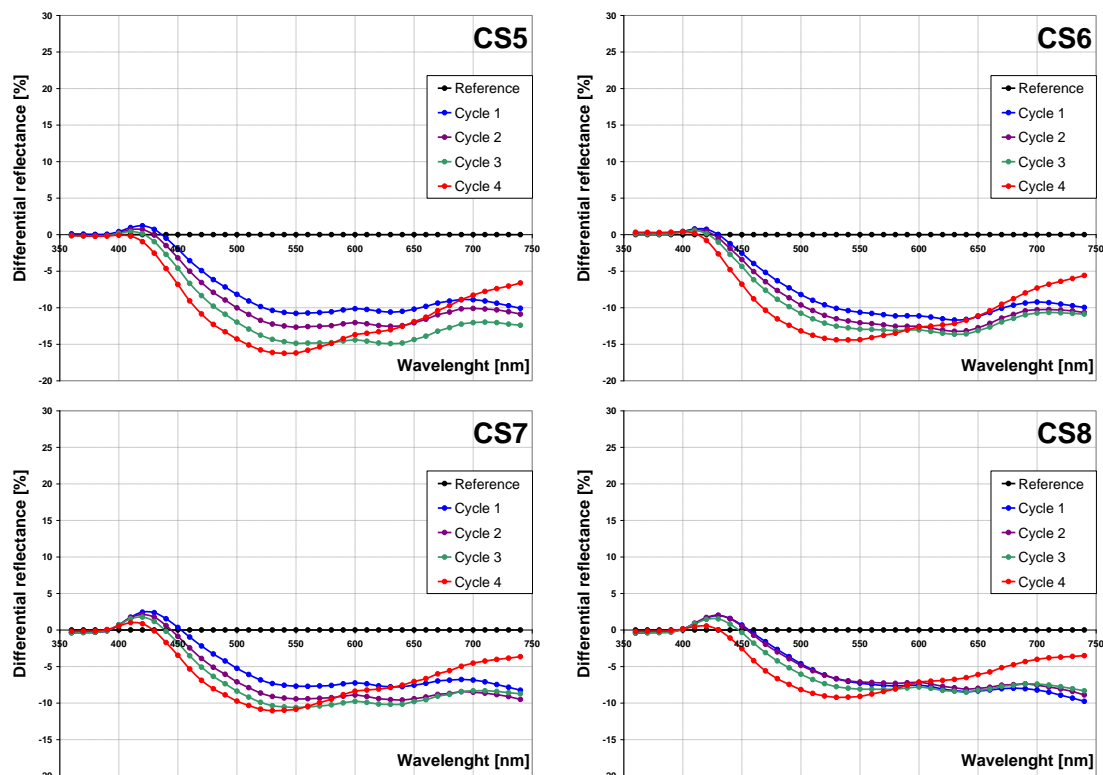


Figure 4 Differential spectra of wood treated with coating systems with Osmo UV-Protection-Oil-420 (CS5 – CS8) for individual cycles of ageing

Conclusions

On the basis of the differential spectra of artificially aged black locust samples treated with eight coating systems can be noted these conclusions:

- 1) Using more layers of coatings (2 of PerlColor, 2 of Osmo UV Protection Oil 420, and combination of these coatings with the water-repellent top layer AquaStop) had a positive effect on the colour stability of wood surfaces at photo-degradation processes.
- 2) Nano-scale particles present in PerlColor caused a higher light reflectance in the range of short wavelengths than reference samples
- 3) The top water-repellent layer AquaStop creates a stability surface protective layer for background layers (PerlColor; Osmo UV Protection Oil 420) and it increases a light reflectance in short wave lengths. Our statements are supported by results of microscopic analyses (Mamoňová et al. 2010) where AquaStop retained its smooth look without significant defects and surfaces resisted to degradation processes.
- 4) Using the method of spectrophotometric analysis can be exactly described the behaviour of advanced coating systems at ageing, e.g. those containing nanoscopical particles.

References

- Babiak, M., Kubovský, I., Mamoňová, M. 2004. Farebný priestor vybraných domácich drevín. [Color space of the selected native wood species]. In: Interaction of Wood with Various Forms of Energy. Zvolen: Technical University in Zvolen. pp.113-117. ISBN 80-228-1429-6.
- EN 927-6: 2006. Paints and varnishes. Coating materials and coating systems for exterior wood. Exposure of wood coatings to artificial weathering using fluorescent UV lamps and water. Part 6.
- Fan, Y., Gao, J, Chen, Y. 2010. Colour responses of black locust (*Robinia pseudoacacia* L.) to solvent extraction and heat treatment. *Wood Science and Technology*, 44(4): 667-678.
- Chen, Y., Gao, J., Fan, Y., Tshabalala, M. A., and Stark, N. M. 2012. Heat-induced chemical and color changes of extractive-free black locust (*Robinia pseudoacacia*) wood. *BioResources*, 7(2): 2236-2248.
- Kúdela, J. 2009. Defekty povrchovej úpravy dreva náterovými látkami. *Stolársky magazín*, 10(5): 4-6. ISSN 1335-7018.
- Liptáková, E., Sedliačik, M. 1989. Chémia a aplikácia pomocných látok v drevárskom priemysle. Alfa Bratislava, 519 p. ISBN 80-05-00116-9.
- Mamoňová, M. 2008. Voľba vhodného náterového systému pre zvláštne kresby dreva pomocou spektrofotometra CM-2600d. [Selection of proper coating system for specific figure in wood using Spectrophotometer CM-2600d]. In: Interaction of wood with various forms of energy, (eds. Dubovský, J., Kúdela, J.), Zvolen, Technical University in Zvolen, pp. 67-73. ISBN 978-80-228-1927-5.
- Mamoňová, M., Reinprecht, L. 2008. Štruktúra a farba akrylátových náterov po ročnej expozícii v exteriéri a interiéri. [Structure and color of acrylate coating after inner and outer yearlong exposition]. In: Interaction of wood with various forms of energy, (eds. Dubovský, J., Kúdela, J.), Zvolen, Technical University in Zvolen, pp. 91-97. ISBN 978-80-228-1927-5.
- Mamoňová, M. 2009. Voľba vhodného náterového systému pre textúry koreníc. [Selection of proper coating system for stump wood figure]. *Acta Facultatis Xylogologiae Zvolen*, 51(2): 39-48. ISSN 1336-3824.
- Mamoňová, M., Pánek, M., Reinprecht, L. 2010. Micro-structural analysis of coatings with nanoscale particles after ageing in Xenotest. In: Wood structure and properties '10 / (eds. Kúdela, J., Lagaňa, R.). Zvolen: Arbora Publishers, p. 209-216. ISBN 978-80-968868-5-2.
- Molnar, S., Tolvaj, L. 2004. Colour homogenisation of different wood species by steaming. In: Interaction of wood with various forms of energy. Zvolen, TU Zvolen. Pp 119-122.
- [Reinprecht, L.](#), Baculák, J., [Pánek, M.](#) 2011. Prirodzené a urýchlené starnutie náterov pre drevené okná. [Natural and accelerated ageing of paints for wooden windows]. *Acta Facultatis Xylogologiae Zvolen*, 53(1): 21-31. ISSN 1336-3824.

Reinprecht, L. 2013. Wood protection. Technical University in Zvolen, 134 p. ISBN 978-80-228-2501-6.

[Reinprecht, L.](#), [Pánek, M.](#) 2013. Vplyv pigmentov v náteroch na prirodzené a urýchlené starnutie povrchov smrekového dreva. [Effect of pigments in paints on the natural and accelerated ageing of spruce wood surfaces]. *Acta Facultatis Xylologiae Zvolen*, 55(1): 71-84. ISSN 1336-3824.

Tolvaj, L., Németh, K. 2008. Correlation between hue-angle and colour lightness of steamed black locust wood. *Acta Silv. Lign. Hung.*, 4: 55-59.

Acknowledgement

The authors would like to appreciate the support of the Slovak Grant Agency to the Project VEGA No. 1/0574/12 in frame of which the research was performed.

A Comparison of Latewood Measurements in Suppressed Douglas-fir

Carl Morrow D.¹ – Thomas M. Gorman^{2} – David E. Kretschmann³*

¹ Postdoctoral Researcher, Department of Forest, Rangeland, and Fire Sciences, University of Idaho, Moscow, ID, USA.

cmorrow@uidaho.edu

² Professor, Department of Forest, Rangeland, and Fire Sciences, University of Idaho, Moscow, ID, USA.

tgorman@uidaho.edu

** Corresponding author*

³ Research General Engineer, USDA Forest Service, Forest Products Laboratory, Madison, WI, USA.

dkretschmann@fs.fed.us

Abstract

Measurements of latewood percentage can be used to infer the physical or mechanical properties of products derived from a given tree or quantify differences in xylem formation processes between trees. Dynamic latewood determination methods have been reported to be more consistent than traditional threshold methods, but the authors of these studies did not specifically identify what characteristic(s) were targeted by the dynamic methods. A clearer understanding of the anatomy at the latewood transition points selected by various latewood measurement techniques would help researchers and forestry professionals determine which method is most appropriate for their projects.

Seven increment cores of varying density from suppressed Douglas-fir (*Pseudotsuga menziesii* var. *glauca*) were scanned using X-ray densitometry. A threshold, a polynomial, and an inflection method were used to determine the location of the earlywood/latewood transition for each annual ring X-ray density profile. The radial dimensions of the tracheid walls and lumen diameter of the at the earlywood/latewood transition were also measured using microscopy.

The threshold method consistently identified a region of the annual ring with a lumen:cell ratio, similar to Mork's definition, of 4.0. The lumen:cell wall ratio of the transition regions identified by the polynomial and inflection methods were variable, but seemed to target the position in the annual ring in which the lumen:cell wall ratio was decreasing the most rapidly. In addition, they seemed to systematically overshoot or undershoot the actual position (as determined by anatomy) of most change based on the average density of the annual ring. This finding suggests that dynamic measures of latewood percentage may appear more consistent because they report shorter than expected latewood percentages in high density rings, and vice versa. This systematic bias could be reduced with a linear correction based on average ring density.

Keywords: A. Douglas-fir, B. Polynomial latewood measurement, C. Inflection latewood measurement, D. Threshold latewood measurement, E. Tracheid anatomy, F. Earlywood/latewood transition.

Introduction

Studies of seasonal xylem formation have identified periods of rapid changes in the xylem formation process (e.g. Cuny et al. 2012; Dodd and Fox 1990) during the transition from earlywood to latewood. These changes include an abrupt decrease in the duration and rate of tracheid expansion and an increase in the duration of secondary wall thickening, and result in progressively denser latewood tracheids as the final stages of the growing season proceed.

Measurements of the percentage of latewood in an annual ring, log, or board can be used to estimate its physical or mechanical properties and can be used as a measurement of wood quality. Some visual grading rules even require a minimum proportion of latewood in the annual rings in a board (SPIB 2012). The proportion and density of latewood can also be used to quantify historic differences in growing conditions or climate for some species (Drew et al. 2012). There may be many reasons to measure latewood, but researchers must also determine which latewood measurement method to use.

Static latewood methods such as Mork's (Mork 1928) or threshold density measurements (e.g. Lasserre et al. 2009; Polge 1978) use a fixed ratio of cell wall to lumen, or density, to distinguish between earlywood and latewood. The underlying assumption for these methods is that the transition from earlywood to latewood is always expressed during the xylogenic process by a specific tracheid geometry. These static measures of latewood may not provide consistent measurements within individuals (e.g. juvenile vs. mature), within a species, or between species (Koubaa et al. 2002).

Dynamic latewood measurement methods have been developed to define the earlywood/latewood transition as the period in which there is the greatest change in tracheid density (e.g. Koubaa et al. 2002; Pernestal et al. 1995). These dynamic latewood measures attempt to identify the tracheids in the annual ring that were formed during the period of rapid xylogenic change described by Dodd and Fox (1990) and Cuny (2012; 2013). Proponents of these methods assert that dynamic latewood measurements should generate more consistent comparisons within and between trees because they attempt to measure the state of the xylem formation process within each annual ring and not use a one-size-fits-all measure of the formation process.

In order for these dynamic measures to be useful, researchers need an improved understanding of their performance and to verify that the region selected as the earlywood/latewood transition coincides with the abrupt change in tracheid diameter and cell wall thickness in an annual ring. The objective of this project was to compare the consistency of a traditional threshold latewood measurement with two dynamic latewood measurements in terms of the anatomy at the selected earlywood/latewood transition and the proximity of the selected transition point to the position at which the tracheid diameter and cell wall thickness change the most.

Materials and Methods

Densitometry

Increment cores from nearly 300 small diameter Douglas-fir were extracted from the Darby Forest Service Ranger District in Western Montana in the summer of 2007. We randomly selected fifty of these increment cores for use in another study, and from these 50, six cores were randomly selected for this study (Trees 1 through 6). The increment cores were machined into 1.5mm strips and scanned using a QMS-QTRX (Quintex Measurement Systems, Knoxville, TN) X-ray densitometer. Annual rings that were incomplete, contained compression wood, or less than 0.4mm in length were omitted. The resulting densitometer data was used to assign the position of the earlywood/latewood transition using the three latewood measurement methods.

Earlywood/Latewood Transitions

Threshold Method

The threshold earlywood/latewood transition position was identified using the QMS software. The raw densitometry data was analyzed using a threshold value of 500 kg/m³ (e.g. Kantavichai et al. 2010) to define the position of the transition from earlywood to latewood for each annual ring. The position of the earlywood/latewood transition for each annual ring was recorded.

Inflection Method

A Microsoft Excel© Macro was written to identify the earlywood/latewood transition as the position at which the second derivative of the density/position curve passed through zero and the first derivative was near its maximum value. The position of the earlywood/latewood transition for each annual ring was recorded.

Polynomial Method

A Matlab© (Matlab 2013, MathWorks Inc. Natick, MA, 2013) script was written to identify the earlywood/latewood transition point similar to that proposed by Koubaa and others (2012). A sixth order polynomial was fit to each annual ring. The earlywood/latewood transition was defined as the root of the second derivative of the polynomial that was: 1) closest to the bark, 2) positioned between 20% and 90% of total ring length, 3) occurred before the (toward the pith) most dense portion of the ring, and 4) the first derivative of the polynomial exhibited a negative slope when read from bark to pith. The position of the earlywood/latewood transition for each annual ring was recorded. Figure 1 shows a polynomial fit to an annual ring, and the four roots of the second derivative of the polynomial identified.

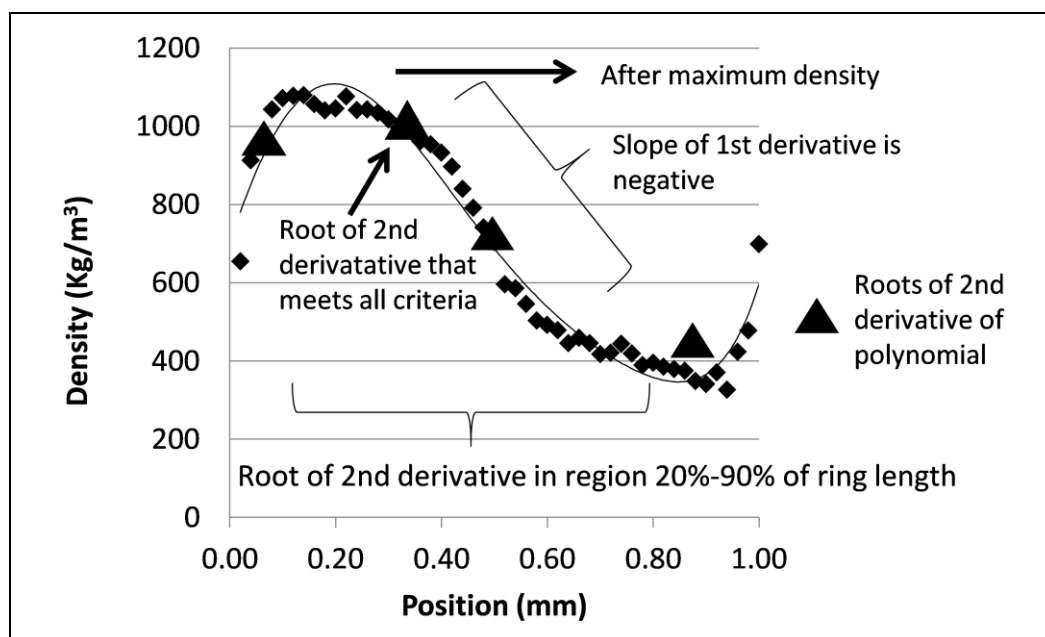


Figure 1. Selection of the earlywood/latewood transition using the polynomial method.

Anatomical Measurements

The six increment cores were sliced using a sliding microtome to produce transverse sections for microscopic analysis. An Olympus BX51 (Olympus America, Center Valley, PA) microscope was used to produce micrographs of the sections, and the Olympus software was used to measure the radial dimensions of the lumen and cell wall for five rows of tracheids in each of the five most recent annual rings. A curve was fit to the cell wall and lumen measurements of the individual radial rows within each annual ring. The locations of the earlywood/latewood transitions determined using densitometry were identified, and the anatomy at those transition points was recorded. After completing the anatomical analysis on the six initial trees, the densest of the remaining 44 trees was added to the data set (Tree 7) and all X-ray and anatomical measurements were collected for it.

Results and Discussion

Figure 2 shows the anatomical measurements from a typical annual ring, and curves fit to the anatomical data. The locations of the earlywood/latewood transitions from the three densitometric techniques are also shown. The threshold method chose a transition just beyond (after) Mork's definition of latewood, and the two dynamic latewood measurements chose earlywood/latewood transition points in the region with the most change in lumen diameter and cell wall thickness. When results from all the rings and trees are combined, the average lumen:cell wall ratio selected by the threshold method was 3.9 (Mork's definition would equal 4.0) with a standard deviation of 0.50, but the lumen:cell wall ratio at the points selected by the dynamic methods were much more variable and seemed to be correlated with average density of the annual ring.

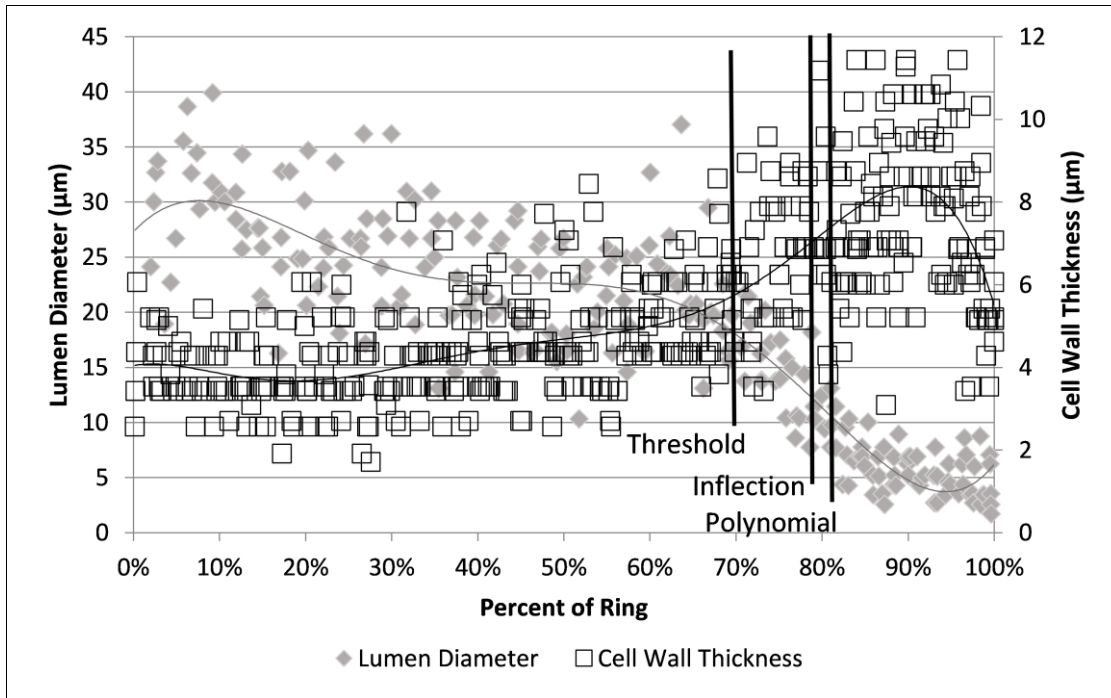


Figure 2. Lumen diameter and cell wall thickness for a typical annual ring with the threshold, inflection, and polynomial latewood transition points identified.

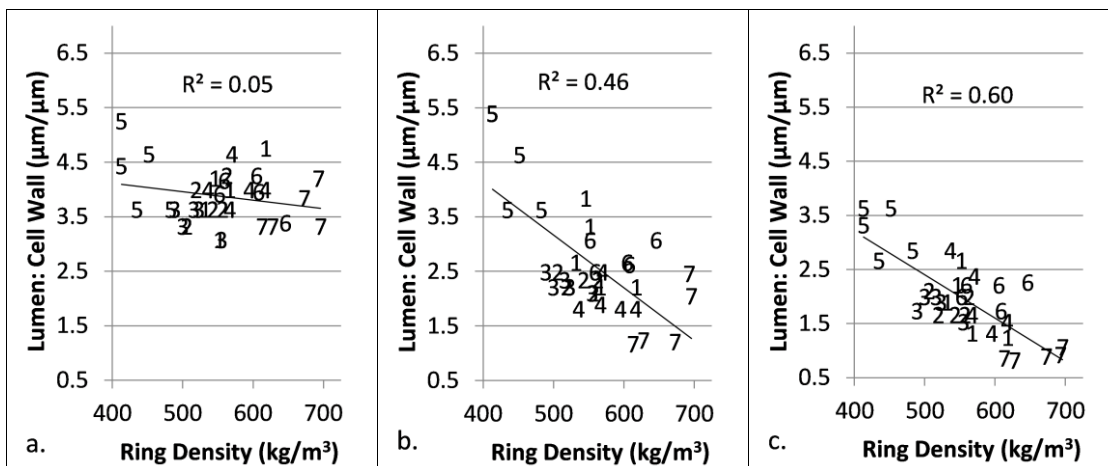


Figure 3. Lumen:cell wall ratio plotted against annual ring density for the threshold (a), inflection (b), and polynomial (c) methods. Symbols indicate tree number.

Figure 3 shows the lumen:cell wall ratio for the three latewood determination methods regressed against average ring density, with the symbols indicating tree number. For the threshold method (Fig. 3a), the lumen:cell wall ratio generally fell between 3.5 and 4.5 and seemed to be consistent across the range of average densities analyzed. The inflection (Fig. 3b) and polynomial (Fig. 3c) methods both exhibited a negative correlation between lumen:cell wall ratio at the transition point and average ring density. Trees One through Six comprised the initial data set, and tree Seven was selected based on its high density to determine if the trend between lumen:cell wall ratio and average ring density for the dynamic latewood methods continued for trees of above average density. Figure 3 suggests that the trends did continue and the inflection and polynomial methods chose earlywood/latewood transitions later in the ring for more dense annual rings, and vice versa.

In order for the dynamic methods to be useful, they need to consistently identify a meaningful portion of the annual ring using densitometry data. The inflection and polynomial method seemed to target the region of the annual ring where the lumen diameter was decreasing the most rapidly, and the cell wall thickness was increasing the most rapidly. To test the consistency of these methods, the distance between the position identified as the earlywood/latewood transition using the densitometry data and the location of most change in lumen diameter and cell wall thickness identified using microscopy were compared for all 35 annual rings. These distances were standardized as a percent of total ring length using Equation (1) (D_{MAXSLP}). A negative value of D_{MAXSLP} meant the densitometer derived earlywood/latewood transition occurred before the position of maximum change in lumen diameter and cell wall thickness.

$$D_{MAXSLP} = \frac{(Pos.ofEW/LW\ Trans.) - (Pos.of\ max\ change\ lumen\ and\ cell\ wall)}{Total\ ring\ length} \quad (Equation\ 1)$$

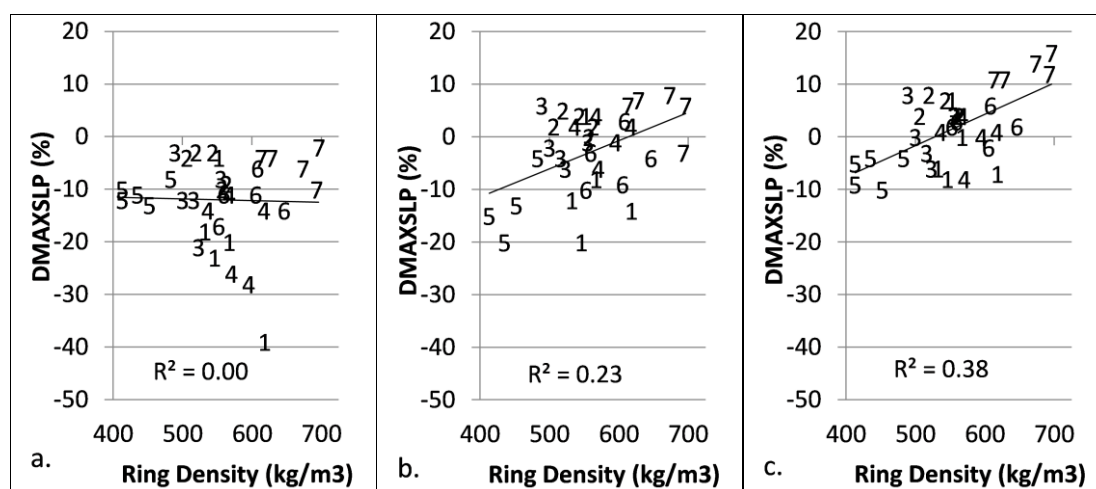


Figure 4. Deviation between the earlywood/latewood transitions determined by densitometry and the position of most change in lumen and cell wall dimensions as determined by microscopy for the threshold (a), inflection (b), and polynomial (c) methods. Symbols indicate tree number.

Figure 4 shows D_{MAXSLP} plotted against annual ring density for the three latewood methods. The threshold method (Fig. 4a) always selected an earlywood/latewood transition before the position of most change in lumen and cell wall. The inflection (Fig. 4b) and polynomial (Fig. 4c) showed a tendency, in low density annual rings, to select a earlywood/latewood transition point before the position of most change in lumen and cell wall, and vice versa in high density annual rings.

The results in Figure 4 indicate that the inflection and polynomial methods did not perform consistently for high and low density rings. High density rings exhibited a positive value for D_{MAXSLP} meaning the latewood measurement methods returned a shorter latewood period than expected for high density rings. Low density rings exhibited negative values for D_{MAXSLP}, indicating the dynamic latewood methods returned a longer than expected latewood period for low density rings. By shortening the latewood period of high density rings, and lengthening the latewood period of low density rings, the dynamic measures appeared to return more consistent latewood percentages, but they did not consistently identify a meaningful feature in the annual ring in the highest and lowest density rings. Figures 4b and 4c indicate that a linear

transformation based on the annual ring density could be used to reduce the systematic portion of this deviation.

Table 1 shows the reduction in the mean and Root Mean Squared Error (RMSE) of DMAXSLP when the linear regressions shown in Figures 4a, 4b, and 4c are used to reduce the systematic portion of the error in the DMAXSLP measurements. As expected, the transformations bring the mean DMAXSLP for all methods to zero, and reduces the RMSE for all methods. The results indicate that if a researcher wanted to use a densiometric measurement to locate the position in the ring with the greatest change in lumen:cell wall ratio, the polynomial method with a transformation to account for the effects of average density would provide the most consistent results.

Method	Values of DMAXSLP (% Ring length)			
	Before transformation		After transformation	
	Mean	RMSE	Mean	RMSE
Threshold	-12.0	14.5	0	8.0
Inflection	-3.1	8.4	0	6.8
Polynomial	1.6	7.0	0	5.4

Table 1. Values of DMAXSLP for the three latewood methods before and after linear transformation.

Conclusion

Latewood measurements need to identify some significant portion of the annual ring consistently in order to be useful for researchers. We compared the two dynamic latewood measurement methods against the traditional threshold measurement method and found that the dynamic methods seemed to target the region of the annual ring where the radial dimensions of the lumen and cell walls changed most rapidly. The threshold method seemed to target a region of the annual ring with a lumen:cell wall ratio of 4.0, similar to Mork's definition of latewood. The dynamic latewood measurements appeared to overestimate the latewood percentage in low density rings, and underestimate the latewood percentage in high density rings. This behavior would return latewood percentages that appear to be more consistent, but may actually reflect inconsistencies in the measurement methods. Our research suggests that a linear transformation based on average ring density could be used to reduce the systematic portion of this error, and that the polynomial method would be the most consistent. Further research is needed to confirm these results on a broader range of trees and species. Researchers interested in using these dynamic latewood measurement methods should assess what is actually being measured and the consistency of the anatomy at the positions identified by the latewood measurement methods.

Acknowledgements

We wish to acknowledge the Coalition for Advanced Wood Structures for providing funds for this work.

References

Cuny H.E., Rathberger C.B.K., Lebourgeois F., Fortin M., Fournier M. 2012. Life strategies in intra-annual dynamics of wood formation: example of three conifer species in a temperate forest in north-east France. *Tree Physiology*. 32(5): 612-625.

- Dodd R.S., Fox P. 1990. Kinetics of tracheid differentiation in Douglas-fir. *Annals of Botany*. 65(6):649-657.
- Drew, D.M., Allen, K., Downes, G.M., Evans, R., Battaglia, M., Baker P. 2013. Wood properties in a long-lived conifer reveal strong climate signals where ring-width series do not. *Tree Physiology*. 33(1): 37- 47.
- Kantavichai R., Briggs D.G., Turnblom E.C. 2010. Effect of thinning, fertilization with biosolids, and weather on interannual ring specific gravity and carbon accumulation of a 55-year-old Douglas-fir stand in western Washington. *Canadian Journal of Forest Research* 40(1): 72-85.
- Koubaa A, Zhang S.Y.T., Makni S. 2002. Defining the transition from earlywood to latewood in black spruce based on intra-ring wood density profiles from X-ray densitometry. *Ann. For. Sci.* 59(5-6): 511-518.
- Laserre J.P., Mason E.G., Watt M.S., Moor J.R. 2009. Influence of initial planting spacing and genotype on microfibril angle, wood density, fibre properties and modulus of elasticity in *Pinus radiata* D. Don corewood. *Forest Ecology and Management* 258(9): 1924-1931.
- Mork E. 1928. Die Qualität des Fichtenholzes unter besonderer Rücksichtnahme auf Schleifuned Papeirholz. *Der Papier-Fabrikant* 26: 741-747.
- Pernestal K., Jonsson B., Larsson B. 1995. A simple model for density of annual rings. Wood Science and Technology. 29(6): 441-449.*
- Polge H. 1978. Fifteen years of wood radiation densitometry. *Wood Science and Technology*. 12(3): 187-196.
- Southern Pine Inspection Bureau. 2012. Standard Grading Rules for Southern Pine Lumber. Pensacola, FL: Southern Pine Inspection Bureau.

Pre-treatment of Surface of Old Wood Structural Elements with Dry Ice

*Pavel Šmíra¹⁾ – Pavel Ihracký²⁾ – Leoš Mrenica²⁾ – Andrea Nasswettrová¹⁾ –
Jozef Kúdela²⁾**

¹⁾ Thermo Sanace Ltd., Ostrava – Kunčičky, Czech Republic

²⁾ Faculty of Wood Sciences and Technology, Department of Wood Science,
Technical University in Zvolen, Slovak Republic

**Corresponding autor*

[*kudela@tuzvo.sk*](mailto:kudela@tuzvo.sk)

Abstract

Wood structural elements in old buildings of notable historic value need protection against attacks by fungi or by wood boring insects. In these cases, protection means applying suitable substances onto contaminated surface, and as such it may be challenging. The cleaning of surface of wood construction elements can be painstaking, and there are sought cleaning methods enabling to reduce the pains and matching strong ecological requirements. One of these methods is cleaning with dry ice (CO₂).

The subject of this work is the change in surface properties of old wood cleaned in this way. The results obtained investigating the surface roughness, colour change and wetting capacity demonstrate that the old wood's treatment with dry ice does not only means effective removal of contaminants from the wood surface but also guarantees proper wetting capacity with polar and apolar-polar liquids – due to the increased wood surface energy. This increase will also enhance the adhesion of these liquids to wood and improve the wood surface quality for subsequent surface treatment, impregnation or gluing.

Keywords: Old wood, Dry ice, Surface properties, Roughness, Colour, Wetting.

Introduction

The study of mechanical properties of structural spruce and fir wood sampled from several historical buildings dated from the 17-th to the 21-th centuries showed that this wood's elasticity and strength were not affected by its natural ageing but by the secondary effects of a range of biotic agents. These effects may vary in their intensity, equally in very old as relatively recent wood (Kúdela and Šmíra 2012, Kúdela *et al.* 2013). We may suggest that old structural wood (not attacked by rot or wood-boring insects) can be re-used for reconstructions of wooden structural elements in historical buildings. Such wooden constructions, however, need protection against biotic agents by using appropriate protective means.

The wood surface in old constructions is generally degraded due to effects of radiation of various types, moisture and heat and their interactions. These factors underlie morphological and

chemical changes to the wood surface during its ageing (Hon 1981, Feist 1990, Williams 2001, Huang *et al.* 2012, Tolvaj *et al.* 2013). In addition, the surface of these constructions (primarily roofs) may be contaminated, to a considerable extent, by dust, bird and bat droppings, and similar. Such pollution lowers the wood surface wetting capacity, and this can play a negative role in wood impregnation with protective substances, gluing and surface treatment. There arises a question of cleaning and preparing the wood surface prior to the treatment with protective liquids.

The bigger is the construction, the more demands are on the labour and time. Therefore, there are sought suitable methods for cleaning such constructions, lower in labour demands and, at the same time, meeting ecological and hygienic criteria. The method using dry ice (impinging CO₂ jet) seems to be a promising one – (Liu 2012, Uhger 2012). This method is flexible, enabling to control its sensitivity, ecological and efficient, and as such, it offers a wide range of implementations in multiple branches. The blasting with dry ice enables cleaning very various construction elements directly *in situ*, without their separation and, eventually, transport.

Each mechanical treatment of wood surface affects its surface properties, primarily morphology. These changes are important to detect and study, as the surface morphology has considerable impact on the surface wetting with liquids.

Wood surface morphology is to assess from the anatomical as well as physical viewpoint. The wood anatomical elements are very various shaped and arranged, and as such they form a complex heterogeneous porous system. The porous character of wood underlies the immense internal surface area and considerable external surface roughness. Consequently, an ideally smooth surface is not possible to obtain in real wood surfaces. In case of a real wood surface, the impact of the treatment tool on the wood surface roughness is to consider too, as this roughness is the result of interactions between the internal wood structure and the mechanical treatment.

Wood ageing induces changes in its colour; the wood is gradually getting dark. Wood surface cleaning comprises also removal of a thin surface layer, therefore, a colour change is necessary to imply.

The aim of this work was to test the using of dry ice as a surface cleaning technology for old wood and to evaluate the impact of this technology on the specific surface properties of the wood treated.

Material and Methods

The equipment we used for wood produced dry ice (solid carbon dioxide) in forms of pellets or nuggets.

Dry ice pellets accelerated in a flow of compressed air attacked the cleaned surface under pressure. The mini-explosions generated at the contact sites removed undesired layers and contaminants from the surface. The dry ice sublimated immediately, so all contaminants were removed without abrasive residuum.

From the cleaned construction elements, there were cut samples 1m long. Up to the mid, the sample surface was left untreated; the other part was treated with dry ice (Fig. 1).

The two parts were examined in their roughness, wetting with liquids and colour changes on their surface



Fig. 1 An old log surface, originally dark, turned into lighter after dry-ice treatment

The roughness was measured with a contact profilometer Surfcom 130A. This parameter was measured on the untreated fir wood and on the same wood treated with dry ice. The measurements were performed parallel to grain and perpendicular to grain.

For each measurement, there was derived sampling length serving for obtaining the basic roughness parameters – mean arithmetical mean of assessed profile (Ra) and the maximum height of profile unevenness (Rz). The arithmetical mean deviation of the assessed profile (Ra) is the mean arithmetical value of absolute deviations of profile $Z(x)$ within the range of basic length, i.e.

$$Ra = \frac{1}{l} \int_0^l |Z(x)| dx ,$$

(1)

where l is the basic length and Z is the distance of the point scanned from the central line of profile at a distance x_i along the basic length.

The maximum height of the profile unevenness (Rz) was determined as the sum of the maximum profile peak height Zp and the maximum profile valley depth Zv within the range of the sampling length.

The wood wetting was performed with two liquids – di-iodomethane and water. Di-iodomethane is an apolar liquid whose apolar component of surface free energy is higher than the disperse component of wood. The second liquid – water is a representative of apolar –polar liquids with their polar surface free energy component higher than the polar component of wood (Table 1).

Table 1 Parameters of the liquids used.

Testing liquid	γ [mJ·m ⁻²]	γ^d [mJ·m ⁻²]	γ^p [mJ·m ⁻²]	η [Pa·s]
water	72.80	21.80	51.00	0.010
di-iodomethane	50.80	50.80	0.00	0.028

The wood surface wetting with the two liquids used in differently treated surfaces was studied and analysed through the static method of a drop placed onto the wood surface – „sessile drop“.

This method enables to obtain chronological patterns of contact angle change from the same liquid.

We studied experimentally the change of shape in drop placed onto the wood surface. The parameters we determined were: the contact angle θ_0 at the beginning of the wetting process and the contact angle θ_u at the moment when the advancing contact angle was turned into the receding one.

The wood wetting process with the liquids was analysed with an Analyser DSA30 Standard equipped with a software package. The liquid was placed onto the wood surface with a dosing unit (syringe) at amounts of 0.002 ml. The transitory drop profile was monitored along the grain, from the moment of the first contact until the complete soaking. The drop was scanned with a camera and displayed on a monitor. At the pre-set time intervals, we measured the drop's height and diameter. The contact angle was calculated according to the equation

$$\operatorname{tg} \theta/2 = 2h/d \quad (2)$$

where h is the drop height and d is the diameter of the contact area between the substrate and liquid along the grain (Fig. 2).

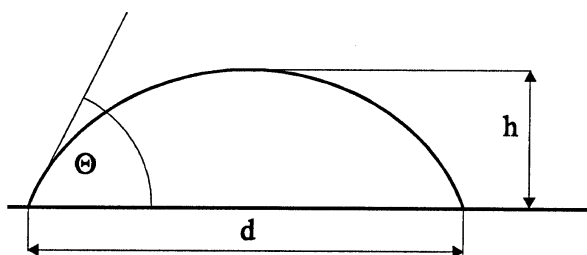


Fig. 2 Drop parameters

Experimentally determined contact angles θ_0 and θ_u were used for determining the contact angle θ_w corresponding to the wood substance with molecular dimensions (Liptáková and Kúdela 1994).

The surface free energy was determined as in NEUMANN *et al.* (1974), according to the equation

$$\cos \theta = \frac{(0,015\gamma_s - 2,00)\sqrt{\gamma_s\gamma_L} + \gamma_L}{\gamma_L(0,015\sqrt{\gamma_s\gamma_L} - 1)} \quad (3)$$

after substituting the contact angle values θ_w . Providing with the values of surface free energy of the substrate γ_s , the surface free energy of the liquid standards γ_L and their disperse and polar components γ_L^d and γ_L^p , we calculated the disperse and polar shares of the surface free energy of wood according to KLOUBEK (1974), using the following equations

$$\sqrt{\gamma_s^d} = \sqrt{\gamma_L^d} \frac{1 + \cos \theta}{2} \pm \sqrt{\gamma_L^p} \sqrt{\frac{\gamma_s}{\gamma_L} - \left(\frac{1 + \cos \theta}{2}\right)^2} \quad (4)$$

$$\sqrt{\gamma_s^p} = \sqrt{\gamma_L^p} \frac{1 + \cos \theta}{2} \mp \sqrt{\gamma_L^d} \sqrt{\frac{\gamma_s}{\gamma_L} - \left(\frac{1 + \cos \theta}{2}\right)^2} \quad (5)$$

The wood colour change in the wood treated with dry ice was evaluated with a spectrophotometer Spectro-guide 45/0 gloss by BYK-Gardner GmbH.

Results and Discussion

The properties of the wood surface-treated with dry ice were compared with the untreated surface. The original fir prisms had been probably treated by axing. The roughness values measured parallel and perpendicular to grain are in (Table 2). The experimental results showed that equally the original as well as dry-ice-treated surfaces were characterised with a coarse topography. The way of wood surface treatment and the anatomical direction along which the roughness was measured have been identified as crucial factors influencing the wood surface roughness. The experimental results manifest a considerable variability in both anatomical directions. The factors influencing the roughness parameters and their variability in fir (Table 2) were: the heterogeneous anatomical structure of this wood at its macro- and micro-scale and the mechanical treatment of the wood surface.

Table 2 Basic statistical characteristics for roughness parameters Ra and Rz for two basic lengths

Treatment mode	Basic statistical characteristics	Roughness parameter			
		l = 0,8		l = 8	
		Ra [µm]	Rz [µm]	Ra [µm]	Rz [µm]
Old surface untreated	Parallel to grain				
	\bar{x} [µm]	4.46	25.01	13.06	84.48
	s [µm]	0.96	5.14	2.57	13.76
	v [%]	21.50	20.50	19.70	16.30
	n	10	10	10	10
	Perpendicular to grain				
	\bar{x} [µm]	11.13	62.11	25.50	192.90
	s [µm]	1.22	5.92	3.04	25.53
	v [%]	11.00	9.50	11.90	13.20
	n	10	10	10	10
Old surface treated with dry ice/adom	Parallel to grain				
	\bar{x} [µm]	8.44	45.73	35.35	280.96
	s [µm]	3.42	15.65	6.88	45.73
	v [%]	40.50	34.20	19.50	16.30
	n	10	10	10	10
	Perpendicular to grain				
	\bar{x} [µm]	19.62	108.9	41.52	284.09
	s [µm]	2.54	13.98	8.63	64.99
	v [%]	12.90	12.80	20.70	22.90
	n	10	10	10	10

l – basic length, n – number of lengths measured

In both anatomical directions, the roughness values measured perpendicular to grain was significantly higher than parallel to grain, mainly due to the arrangement of cell wall elements. The measurement inaccuracies may be considered only of a secondary importance.

The Table 2 shows that the roughness also depended on the sampling length determined in advance. The bigger was this length, the bigger were the roughness parameters.

The enhanced surface roughness of fir-wood treated with dry ice is due to tiny craters excavated by the ice chips hitting the wood surface (Fig. 3). These excavations, comparatively well dispersed especially across the early wood, also reduce the differences in roughness between the two anatomical directions discussed. The size and frequency of these excavations can be controlled through the rate of ice pellets attacking the wood surface.

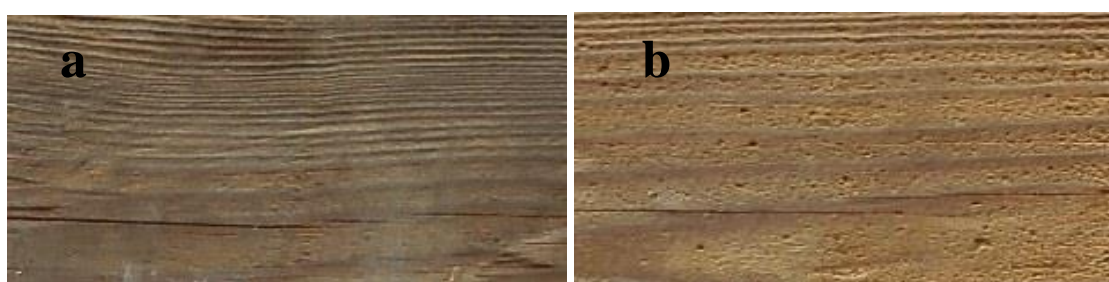


Fig. 3 Morphology of wood surface: a) untreated and b) treated by impinging dry ice jet

In wood wetting process with water and di-iodomethane, we recorded the moment t_u at which the advancing contact angle was turned into the receding one, the time t needed for the complete soaking of the drop into the wood, and we determined the contact angles θ_0 , θ_u and θ_w . The study of the wetting process in old wood demonstrated that the testing liquids were very fast spreading over the wood surface and soaked into the wood inside. The average time of complete soaking was 1 s for water and 0.5 s for di-iodomethane. Also the contact angles were small (Table 3). Compared to the recent wood, with its surface milled, the surface wetting was distinctly more intensive in the old wood. One of possible causes may be the micro-fractures occurring in old wood and the chemical alterations to the old wood surface (Williams 2001, Müller *et al.* 2003, Huang *et al.* 2012 Tolvaj *et al.* 2013). Similar facts were observed by Ihracký (2014) for accelerated ageing of spruce and beech wood surfaces.

The fir-wood surface treated with dry ice was able to soak perfectly (Table 3). The (Table 3) illustrates that this was due to the increase in the polar component we determined based on the wood wetting with water.

The wetting process varied in duration, due to the random drop's placing on the surface and due to the heterogeneity in wood surface structure. This was observed equally in radial and tangential surfaces.

The values of contact angle θ_0 are dependent on the interactions at the phase boundary wood–liquid and on the morphological and chemical properties of the wood surface, while the angle θ_w is exclusively dependent on the wood surface chemistry (Liptáková *et al.* 2000).

The contact angle values θ_w were differing with differently treated surfaces; consequently we may suppose that the chemistry of wood surface treated with dry ice will be different from the original one. Several works (Liptáková *et al.* 1995, Gardner 1996, Kačík and Kubovský 2011) demonstrate that different treated surfaces of the same wood differ in chemical composition at their atomic scale.

The surface free energy determined with the liquids used in our study showed differences in quantity and quality (Table 3). The results revealed that the wood surface free energy values did not only result from the wood surface properties but they also depended on the chemical composition of the liquid standard used. The differences were comparatively big, which is in contradiction with the fact that surface free energy commonly recognised as a material constant of substances.

The surface free energy determined with using the apolar liquid (di-iodomethane) was lower, in fact equal to its disperse component. The polar component was very close to zero. Apolar liquids having their disperse component higher than wood only allow to obtain the disperse component of surface free energy of wood. Therefore, to determine the polar component of surface free energy of wood needs using liquids the surface energy of which is additive. The polar component of surface free energy of wood can be obtained with using water (Kúdela 2014).

The last cited work implies that not any of the liquids used in our work is sufficient alone to determine the surface free energy of wood. The disperse and polar component of wood surface free energy are possible to assess separately by means of a suitable apolar and apolar-polar standard. Considering this belief in case of wood, the disperse component of wood is assessed with di-iodomethane the disperse component of which is supposed higher than the disperse component of wood. The polar component of wood, on the other hand, is determined with the aid of water whose polar component is higher than the polar component of wood. Then the total surface free energy representing the sum of the disperse and polar components obtained in this way is in general higher than the value supposed until now. In our case, the surface free energy of wood treated with dry ice is higher than the energy of the untreated original old surface. This will also naturally entail increments in wood cohesion and its adhesion with liquid and solid materials (Kúdela 2014).

Table 3. Basic statistical characteristics of wetting parameters, wood surface free energy and its components in untreated old fir wood and the same wood treated with dry ice

Treatment mode	Basic statistical characteristics	Time of drop soaking			Contact angle		Surface free energy and its components		
		t	θ_0	θ_u	θ_w	γ_s	γ_s^p	γ_s^d	
		[s]	[°]			[mJ·m ⁻²]			
		Water							
Old surface untreated	\bar{x}	1.23	29.87	21.7	22.41	65.1	37.1	28.0	
	s	0.77	18.81	11.6	12.15	0.91	8	8.62	
	X _{min}	1.00	70.50	38.2	38.2	67.2	49.2	45.2	
	X _{max}	5.00	3.20	3.20	3.2	63.5	21.3	15.4	

Old surface treated with dry ice	v [%]	62.6 0	62.96	53.7 7	54.24	1.39	21.9 3	30.7 5
	n	30	30	30	30	30	30	30
	Di-iodomethane							
	\bar{x}	0.47	16.14	16.1 4	16.14	48.7 1	0.10	48.6 1
	s	0.53	5.37	5.37	5.37	1.26	0.09	1.34
	X _{min}	0.00	27.2	27.2 0	27.2	50.5 7	0.35	50.5 5
	X _{max}	1.80	5.6	5.60	5.6	45.6 8	0.02	45.3 3
	v [%]	112. 00	33.29	33.2 9	33.29	2.58	90.8 6	2.76
	n	30	30	30	30	30	30	30
	Water							
	\bar{x}	0	13.98	10.2 5	10.48	65.2 0	43.5 6	21.6 4
	s	0	16.77	10.2 1	10.52	0.92	8.42	9.11 4
	X _{min}	0	54.6	39.7	39.7	67.6 1	49.5 0	44.0 0
	X _{max}	0	2.1	2.1	2.1	63.1 3	22.5 5	15.2 4
v [%]	0	120.0 1	99.6 2	100.3 8	1.41	19.3 4	42.1 0	
n	30	30	30	30	30	30	30	
Di-iodomethane								
\bar{x}	0	4.62	4.62	4.62	50.5 7	0.02	50.5 5	
s	0	3.24	3.24	3.24	0.42	0.01	0.43	
X _{min}	0	15.7	15.7	15.7	50.7 7	0.06 4	50.7 5	
X _{max}	0	2.3	2.3	2.3	48.9 8	0.01 7	48.9 2	
v [%]	0	70.25	70.2 5	70.25	0.84	51.7 8	0.86	
n	30	30	30	30	30	30	30	

The old logs decontaminated with dry ice also manifested changes in their original colour (Fig. 3). The values of colour coordinates for the surfaces ice-treated are in Table 4.

Table 4 shows that the wood treated with dry ice was lighter in its colour, with the * coordinate shifted towards yellow and the b* coordinate towards red. The most conspicuous change was in the b*coordinate.

Table 4 Basic statistical characteristics of fir wood colour coordinates in the space CIELab

Basic statistical	Colour coordinates in CIELab	
	Original surface	Surface treated with dry ice

characteristic	L*	a*	b*	L*	a*	b*
\bar{x}	47.183	6.169	15.021	49.183	10.004	24.220
s	1.876	0.744	0.860	1.640	0.687	1.529
v	3.9	12.1	5.7	3.3	6.8	6.3
n	50	50	50	50	50	50
	ΔE	ΔL^*	Δa^*	Δb^*		
	10.17	2.000	3.835	9.190		

These changes to the wood surface induced by its treatment with dry ice can be accepted as positive from the viewpoint of wood's impregnation, coating and gluing. Another profit of this technology is no secondary waste. No toxic substances are used in this process, so it is ecological and high efficient.

Conclusion

Old wood surface decontamination with dry ice has been evidenced as suitable for cleaning wooden constructions.

The morphological changes to wood surface mediated by its treatment with dry ice may be considered as positive from the viewpoint of this surface wetting.

The results we obtained for wetting and for surface free energy and its components have revealed that the dry ice treatment not only guarantees effective decontamination of this wood surface but also improves its quality subsequent treatment, impregnation or gluing. In this case, the wood wettability will be good with both apolar and apolar-polar liquids, thanks to the wood surface free energy increased in its polar and disperse component. This increase in surface free energy will also guarantee better adhesion of these materials to wood.

As for the surface colour change, we may conclude that the surface will be "vitalised" also in this aspect.

Acknowledgement

We highly acknowledge the support from the Scientific Grand Agency of the Ministry of Education SR and the Slovak Academy of Sciences (Grant No. 1/0893/13 „Surface properties and phase interface interactions of the wood – liquid system“).

References

- Feist, W. C. 1990. Outdoor wood weathering and protection. In: Rowell, R.M. and Barbour, J.R. (Eds.), *Archaeological Wood Properties, Chemistry, and Preservation*. Washington DC: Advances in Chemistry Series 225. Proceedings of 196th meeting, American Chemical Society.
- Gardner, D. J., Ostmeyer, J. G., Elder, T. J. 1991. Bonding surface activated hardwood, flakeboard with phenol-formaldehyde resin: Part II. Flake surfacechemistry *Holzforschung*, 45(3): 215–222.

- Hon, D. N. 1981. Photochemical degradation of lignocellulosic materials. Grassie, N. (Ed.), *Developments in Polymer Degradation*–3. Essex: Applied Science Ltd. Chapter 8, p. 229–281.
- Huang, X., Kocaefe, D., Kocaefe, Y., Boluk, Y., Pichette, A. 2012. A spectrophotometric and chemical study on color modification of heat-treated wood during artificial weathering. *Applied Surf. Sci.*, 258(14): 5360–5369.
- Ihracký, P. 2014. The effect of accelerated weathering on surface properties of wood. (Doctoral Thesis.) Faculty of Wood Sciences and Technology. Technical University in Zvolen.
- Kloubek, J., 1974. Calculation of surface free energy components of ice according to its wettability by water, chlorobenzene and carbon disulphide. *J. Colloid Interface Sci.* 46(2): 185–190.
- Kačík, F., Kubovský, I. 2011. Chemical changes of beech wood due to CO₂ laser irradiation. *Journal Photochemistry and Photobiology, A: Chemistry.* 222: 105–110
- Kúdela, J. 2014. Wetting of wood surface by liquids of a different polarity. *Wood Research*, 59(1): 11–24.
- Kúdela, J., Šmíra, P. 2012. The effects of age of structural timber from historic buildings on its strength and durability (in Slovak). In: *Drevo – surovina 21. storočia v architecture, stavebníctve a interiéri.* Smolenice – Bratislava: ADAPT, p.17–20.
- Kúdela, J., Šmíra, P., Nasswetrová, A., Štrbová, M. 2013. Quality assessment of wood from historical buildings, performed based on its elasticity and modulus of rupture (in Slovak). *Sanace dřevených konstrukcí.* Ostrava: Šmíra-Print s.r.o., 2013, 146–154.
- Liu, Y. H., Daisuke, H., Shuji, M. 2012. Particle removal process during application of impinging dry ice jet. *Powder Technology* 217: 607–613.
- Liptáková, E., Kúdela, J. 1994. Analysis of the wood – wetting process 1994. *Holzforschung*, 48(2): 139–144.
- Liptáková, E., Kúdela, J., Bastl, Z., Spirovová, I. 1995. Influence of mechanical surface treatment of wood the wetting process. *Holzforschung*, 49(4): 369–375.
- Liptáková, E., Kúdela, J., Sarvaš, J. 2000. Study of the system wood - coating material I. Wood – liquid coating material. *Holzforschung*, 54(2):189–196.
- Mülller, et al 2003. Yellowing and IR-changes of spruce wood as result of UV-irradiation *Journal Photochemistry and Photobiology, B: Biology* 69: 97–105.
- Neumann, A.W., Good, R.J., Hope, C.J., Sejpal, M., 1974. An equation-of-state approach to determine surface tensions of low energy solids from contact angles. *Colloid Interface Sci.* 49(2): 291–303.
- Tolvaj, L., Molnar, Z., Nemeth, R. 2013. Photodegradation of wood at elevated temperature: Infrared spectroscopic study. *Journal Photochemistry and Photobiology, B: Biology* 121: 32–36.
- Unger, A. 2012. Decontamination and “deconsolidation” of historical wood preservatives and wood consolidants in cultural heritage. *Journal of Cultural Heritag.* 13(3):196–202.
- Williams, R. S., Knaebe, M. T., Evans, J. W., Feist, W. C. 2001. Erosion rates of wood during natural weathering: Part III. Effect of exposure angle on erosion rate. *Wood and Fiber Science*, 33(1): 50–57.

Silanes Adhesion Promoters Applied in Furniture Industry

Monika Muszyńska, Tomasz Krystofiak, Stanisław Proszyk and Barbara Lis

Poznan University of Live Sciences, Faculty of Wood Technology,
Department of Wood Based Materials, Division of Gluing
and Finishing of Wood, Poznan, Poland
e-mails: monika.muszynska@up.poznan.pl; tomkrys@up.poznan.pl;
sproszyk@up.poznan.pl; blis@up.poznan.pl

Abstract

Development in adhesives for application in the woodworking industry has enabled introduction to the industrial practice the newer and innovating solutions. On a world furniture market a biggest production concerns plastics, such as laminates, foils, thus modification of their properties has become one of the most important challenges in a field of furniture industry and technology as well. Bearing in mind factors contributing to difficulties in bonding processes for both wood and plastic materials, it is necessary to carry out such technology treatment that adequately prepare the substrate and thus will allow to obtain surface of good adhesion. Among the methods of activating the surface of materials can be distinguished in the following ways: physicochemical or chemical methods, electrical (plasma and corona discharge) and radiation (IR and UV) methods. Some of the above methods of surface activation have been tried to adapt to the wood, the greatest importance in this respect have adhesion promoters commonly known as primers. On the background of other methods they stand out their high efficiency, universality and in particular easy way of application, without incurring the high cost of investment. Scientific data shows that the most important group of adhesion promoters are systems based on silanes. The essence of action the adhesion promoters relies on so-called diffusion affinity to bonded material and creating with it and adhesives various types of physical and chemical interactions. High energy chemical bonds are extremely desirable to contribute to improving the adhesion system. Si-OH groups have the ability to connect with the hydroxyl groups which are present on the surface of plastics and wood. Application of primers causes primarily improvement the wettability and increase surface free energy of materials. Adhesion promoters being developed for the wood industry in particular for the furniture industry are offered only by some specialized manufacturers of adhesives in not too extensive range of products like waterborne systems.

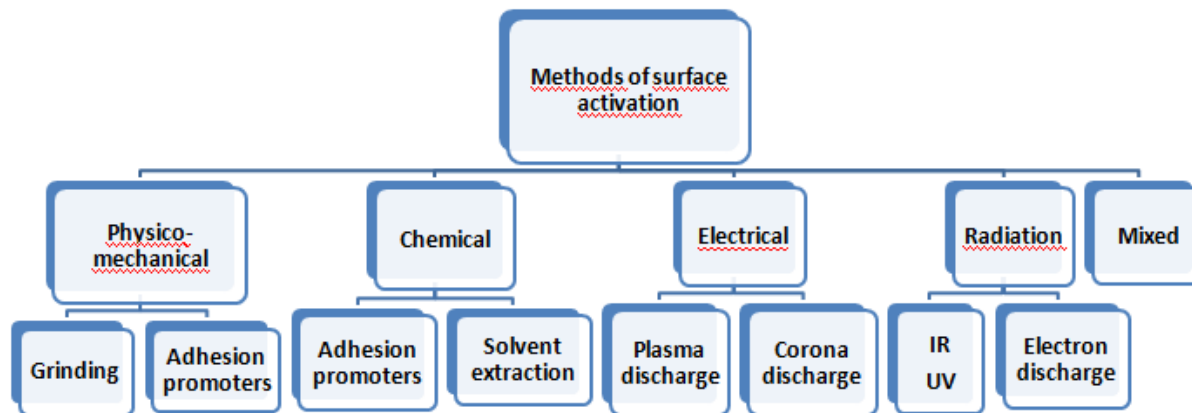
Keywords: adhesion promoter, silanes, wood surface modification

Introduction

Larger consumer demands are forcing the furniture industry and interior design to apply increasingly attractive materials which can cause difficulties during the production process. As mentioned these are all kinds of plastics, foils, tapes, foams and exotic wood. They are characterized by high quality and as substitutes may be used for different forms of surface finishing such as veneers, laminates or finish type foils. Polymeric materials which may create

difficulties during the bonding process include mainly plastic based on i.a. ABS, MUF, PA, PE, PMM, PVC and laminates manufactured in versions CPL, HPL or LPL (Muszyńska et al. 2014). The low surface free energy (LSE), which is at the level of 20 to 40 mJ/m² and the non-porous surface are factors which make mainly difficulties in bonding processes. It is assumed that the surface free energy (γ_s) of plastic should be greater by at least 10 mJ/m² from the LSE of lacquer products and adhesives applied on the material (Żenkiewicz 2000).

Exotic wood is now one of the most desirable raw materials for the furniture industry, which is used by the manufactures of furniture, windows and floors. During the bonding process exotic wood is a material more complicated than native species as a result of the wide variability of their properties. Anatomical structure of wood, density, hardness, moisture, natural defects and damage are just a few of many physical and mechanical properties of wood, which can help or hinder the work of many technologists responsible for different stages of production preparation. Literature data shows that the difference in the chemical composition of exotic wood especially in the content of cellulose, lignin, pentosan and extractives substances plays a huge role during the bonding process (Bodig 1962, Freeman 1960, Freeman and Wangaard 1960, Gray 1962, Zenkteler 1966). Bearing in mind these factors hindering the gluability, it is necessary to carry out such processes that adequately prepare and increase the activity of the surface. Among the methods of surfaces activation of materials can be distinguished following ways: chemical, physicochemical, radiation and electric methods (Fig.1). Some of the above methods of surface activation tried to adapt to the wood, the most important in this regard have adhesion promoters, which stand out against the other ways high efficiency, universality, especially easy applications, without incurring the high cost of investment. The essence of action adhesion promoters lies in the so-called diffusion affinity to the bonded surface of material and formation with adhesives various types of physical and chemical interactions.



Fi

Figure 1. Methods of surface activation (Krystofiak 2002, Żenkiewicz 2002).

The most important and most common group of adhesion promoters are systems based on organofunctional silanes (OSI), (Krystofiak, Lis and Proszczyk 2006). Silane coupling agents have two functional ends, one of them improves the adhesion to metals and inorganic substrates, and the other one is chemically reactive (Sathyanarayana and Yaseen 1995). Si-OH groups have the ability to connect with hydroxyl groups which are present on the surface of plastics, polymers and wood (Sebe and Brook 2001, Mai et al. 2005). The use of adhesion promoters cause the increase of materials's surface free energy and improve their wettability. Adhesion promoters after evaporation of the solvent, formed a protective layer on the substrate, thereby reducing the migration of additional components to the surface (Żenkiewicz 2000). Primers properly selected for specific types of applications, may be applied by any methods in the form of very thin layer

on all surfaces. After application of the agent in a thin layer (monolayer), it is always completely dried up to solidify. In Department of Gluing and Finishing of Wood research was carried out to improve the adhesion of wood and plastics in form of foils and edging tapes.” In research of effects of silane adhesion promoters on the strength and thermoresistance of glue lines in MDF boards finished with PVC foils was found that application of silane promoters improve the quality of glue lines in splitting test and thermal resistance (Krystofiak, Proszyk and Lis 2005)”. „In case of studies of adhesion promoters with the use FTIR spectroscopy it was concluded that increase of temperature and lengthening of the drying up time of primer is causing the increase of contact angle (Kasprzyk, Krystofiak 2000)”.

”In research of influence of dried parameters adhesion promoters on PVC foil on the surface free energy of layers is stated influence of surface polar forces in system PVC foil-adhesion promoter on the surface free energy . The highest value of surface free energy have adhesion promoters dried in temperature 40°C (Krystofiak 2001)”. „Also in tests of relative hardness of PUR and PVAC adhesives layers, where were used adhesion promoters found that primers have various influence on growth of hardness of glue layers. Solvent-borne system showed higher hardness than water-borne systems (Krystofiak 2003)”. The objective of this study was to assess the bonding properties of exotic wood species glued with PVAC adhesives with the use of adhesion promoters.

Materials and Methods

In experimental part 5 exotic wood species were used: acajou (*Khaya ivorensis*), badi (*Nauclea diderichii*), frake (*Terminalia superba*), framire (*Terminalia ivorensis*) and iroko (*Chlorophora exelsa*). In form of squared timber, wood was bought in dimensions 3.00x0.20x0.05 m, the density was in the range 500-800 kg/m³ and value of MC was 12±1%.

On the basis of commercial offers products JOWAT AG company in Detmold, 2 adhesion promoters were selected: solvent-borne (S) and water-borne (W) applied with isocyanate catalyser (5 parts of dry mass per 100 parts of W). For gluing one and two component PVAC adhesives were used. They were catalysed with 20% AlCl₃ and isocyanate (5 and 15 parts of dry mass per 100 parts of adhesive respectively).

For experiments two primers with the following properties were used: one-component solvent-borne adhesion promoter: dynamic viscosity 140 mPas, density 900 kg/m³, solid content 14%, and two-component water-borne primer with: dynamic viscosity 1000 mPas, density 1000 kg/m³, solid content 27%, pH value 7.0.

For splitting strength samples were prepared acc. to PN-EN 205 standard. Strength and resistance of glue lines have been defined acc. to D4 durability class described in PN-EN 204 and WATT'91. For splitting strength of glue lines tests were performed with using MZ prototype testing device.

For the evaluation of effectiveness of adhesion promoters used for examinations a point scale was proposed. After the individual resistance tests determined the ratio of the strength of glue lines in the case of wood with primer to wood without primer. Proposal criteria for evaluation was accepted (after test no. 1 and 6 acc. to PN-EN 204 and WATT'91 procedure):

≥ 120% - 5; ≥ 115% - 4; ≥ 110% - 3; ≥ 105% - 2; ≥ 100% - 1.

Results

In tables 1-2 are summarized the results of the impact of adhesion promoters on splitting strength of glue lines from PVAC adhesives for exotic wood species. As the evaluation criteria the WFP (Wood Failure Percentage) indicator was accepted.

In Tables 3-4 summarizes the results of the analyses the effectiveness of individual adhesion promoters after waterresistance tests (test no.6 acc. to PN-EN 204) and thermoresistance tests (acc. to WATT'91).

Table 1

Influence of kind of adhesion promoter on the formation the splitting strength of glue lines from acajou wood with statistical estimating

Kind of adhesion promoter	Kind of adhesive	Statistical data ^{*)}				WFP
		x_{max}	\bar{x}	x_{min}	N	
		[MPa]			[%]	
control	PVAC 1K	9.78	8.90	7.65	7.93	90
	PVAC 2K (AlCl ₃)	10.46	9.25	7.31	13.26	95
	PVAC 2K (isocyanate)	13.60	11.09	9.61	10.49	90
S	PVAC 1K	12.41	10.10	8.33	12.35	95
	PVAC 2K (AlCl ₃)	13.79	11.27	9.88	13.33	85
	PVAC 2K (isocyanate)	17.66	14.31	11.82	15.60	70
W + 5% catal.	PVAC 1K	13.60	11.09	9.61	9.86	80
	PVAC 2K (AlCl ₃)	13.24	10.76	9.13	10.44	85
	PVAC 2K (isocyanate)	15.51	12.74	10.85	15.98	80

^{*)} \bar{x} -average value, x_{min} -minimum value, x_{max} -maximum value, v -coefficient of correlation, WFP-wood failure percentage

Table 2

Influence of kind of adhesion promoter on the formation the splitting strength of glue lines from frake wood with statistical estimating

Kind of adhesion promoter	Kind of adhesive	Statistical data ^{*)}				WFP
		x_{max}	\bar{x}	x_{min}	v	
		[MPa]			[%]	
control	PVAC 1K	10.37	8.76	6.29	14.83	70
	PVAC 2K (AlCl ₃)	11.82	9.35	8.16	11.12	70
	PVAC 2K (isocyanate)	10.71	8.83	7.48	9.75	80
S	PVAC 1K	10.20	7.83	5.15	18.45	90
	PVAC 2K (AlCl ₃)	9.52	8.61	7.48	7.53	90
	PVAC 2K (isocyanate)	10.97	9.64	7.99	14.38	80
W + 5% catal.	PVAC 1K	8.84	7.02	5.95	10.98	85
	PVAC 2K (AlCl ₃)	9.18	7.77	6.21	8.43	90
	PVAC 2K (isocyanate)	10.03	8.12	6.55	11.27	90

Table 3

Influence of kind of adhesion promoter on the formation of waterresistance of glue lines from exotic wood species (test no. 6 acc. to PN-EN 204)

Kind of adhesion promoter	Kind of adhesive	Kind of wood species					Together
		acajou	badi	frake	framire	iroko	
		Note [points]					
S	PVAC 1K	1	1	2	2	5	11
	PVAC 2K (AlCl ₃)	3	2	2	1	4	12
	PVAC 2K (isocyanate)	2	3	4	5	3	17
W + 5% catal.	PVAC 1K	1	1	3	3	5	13
	PVAC 2K (AlCl ₃)	3	3	1	2	5	14
	PVAC 2K (isocyanate)	1	3	4	4	5	17
		11	13	16	17	27	

Table 4

Influence of kind of adhesion promoter on the formation of thermoresistance of glue lines from exotic wood species (acc. to to WATT'91)

Kind of adhesion promoter	Kind of adhesive	Kind of wood species					Together
		acajou	badi	frake	framire	iroko	
		Note [points]					
S	PVAC 1K	1	5	2	2	4	14
	PVAC 2K (AlCl ₃)	3	3	1	1	2	10
	PVAC 2K (isocyanate)	2	3	1	5	3	14
W + 5% catal.	PVAC 1K	3	5	3	3	5	19
	PVAC 2K (AlCl ₃)	3	3	2	2	5	15
	PVAC 2K (isocyanate)	2	5	2	4	5	18
		16	24	11	17	24	

Analysis of data provided in tables 1-2 shows that the glue lines in temporary conditions were characterized by very high quality advantages, at beneficial values of the WFP indicator in the scope of 70-100 %. Analysing the strength of glue lines from wood not covered with adhesion promoter, can be concluded that the impact of the water in not increased temperature and as well as boiling caused a drastic decline in the value of the different species of wood and adhesive. This effect was observed especially after tests no. 3 and 5 according to PN-EN 204. After the test no. 3 the average degree of delamination of glue lines in wood at failure loads expressed by WFP indicator was very low, being included in the scope of 0-20 %, with the values of the coefficient of correlation on the level 20-25 %. In taking back to the test no.1 glue lines from PVAC 2K (hardened with isocyanate) were characterized by the highest relative strength, a bit lower, although comparable with PVAC 2K (catalyzed by AlCl₃), however the lowest in relation to the PVAC 1K. The lowest results significantly different from the other, obtained for the connections from badi and framire wood. A further decrease in the strength of the glue lines occurred after the test no. 5. Humidification of wood connected with the hydrolysis of wood caused the reduction of glue lines strength by 30% with reference to the test no.1. For glue lines from PVAC 1K and PVAC 2K (hardened with AlCl₃) in case of badi and framire wood, the destruction took place at very low failure loads, and values of the WFP indicator amounted to 0-10%, mostly in the cohesive layers of adhesives. Distinct increase the water resistance of glue lines was achieved by coverage the surface of bonded wood with adhesion promoters. Confirmation of primers' s impacts, solidified on wood with PVAC adhesives, especially 2K(hardened with isocyanate) were glue lines' s strength results after the test no. 6. Drying of previously moistened samples

allowed to obtain glue lines's strength similar to the value after the test no.1. Thanks to the application of adhesion promoters for all variants increase of WFP indicator values even by the 30% have been noted. Generally it was found that adhesion promoters used for testing in the individualized way influenced on the quality of obtained glue lines. It has been shown that a more efficient system in terms of increasing the strength and resistance of glue lines for bonding exotic wood species was water-borne. The greatest efficiency in thermoresistance tests showed badi and iroko wood, then framire and acajou. Whereas in the case of frake wood an influence was not stated

Conclusions

As a result of the conducted studies it can be stated that:

1. Adhesion promoters showed significantly expedient influence on splitting strength of glue lines from PVAC adhesives and exotic wood. In water resistance tests no. 3 and 5 acc. to PN-EN 204 standard the highest advantages were observed. Promoters of adhesion caused the increase of WFP (wood failure percentage) indicator.
2. In case of exotic wood, more efficient system for improvement the strength and resistance of glue lines was water-borne adhesion promoter. This primer showed the highest effectiveness to iroko and badi wood then to framire and acajou wood. The lowest efficiency obtained for frake wood.

References

- Bodig J. 1962. Wettability related to gluabilities of five philippine mahoganies. In: For. Prod. J. 12 (6): 265-270.
- Freeman H.G. 1960. Properties of wood and adhesion. In: For. Prod. J. 10 (12): 451-458.
- Freeman H.G., Wangaard F.F. 1960. Glue-line behavior of two urea resins. In: For. Prod. J. 10 (9): 311-315.
- Gray V.R. 1962. The wettability of wood. In: For. Prod. J. 12 (9): 452-461.
- Kasprzyk H., Krystofiak T. 2000. Studies of adhesion promoters with the use FTIR spectroscopy. In: IIIth International Symposium, Wood Agglomeration, Zvolen 28-30.06-2000.
- Krystofiak T., Lis B., Proszyk S. 2006. Środki wiążące na bazie silanów do zastosowań w technologiach oklejania powierzchni elementów płytowych foliami i taśmami obrzeżowymi w meblarstwie. Maszynopis w Katedrze Klejenia i Uszlachetniania Drewna WTD AR w Poznaniu.
- Krystofiak T., Proszyk S., Lis B. 2005. Effect of silane adhesion promoters on the strength and thermal resistance of glue lines in MDF boards finished with PVC foils. In: XVIIth International Symposium, Adhesives in Woodworking Industry, Zvolen 7-9.09.2005: 162-165.
- Krystofiak, T. 2001. Influence of dried parameters adhesion promoters on PVC foil on the surface free energy of layers. In: Zeszyty Naukowe Politechniki Śląskiej. Chemia z.146:291-294.

Krystofiak, T. 2003. Effects of adhesion promoters on the relative hardness of PUR and PVAC adhesive layers. In: XVIth International Symposium, Adhesives in Woodworking Industry, Zvolen 3-5.09.2003: 140-144.

Mai C., Donath S., Weigenand O., Militz H. 2005: Aspects of Wood Modification with Silicon Compounds. 2nd European Conference on Wood Modification. Göttingen, Germany 6-7th of October 2005.

Muszyńska M., Krystofiak T., Lis B. 2013. Some economic-technological aspects of using adhesion promoters in furniture industry. In: Intercatedra-Scientific Quarterly of the Economics Departments of European Universities 29(4):13-19.

Sathyanarayana M.N., Yaseen M. 1995. Role of promoters in improving adhesion of organic coatings to a substrate. In: Progress in Organic Coatings (26): 275-313.

Sebe G. Brook M.A. 2001. Hydrophobization of wood surfaces: covalent grafting of silicone polymers. In: Wood Science and Technology (35): 269-282.

Zenkter M. (1966): Badania nad podatnością różnych gatunków drewna na klejenie na zimno. Fol. For. Pol. ser. B-Drzewnictwo 7: 5-62.

Żenkiewicz M. 2000. Adhezja i modyfikowanie warstwy wierzchniej tworzyw wielkocząsteczkowych. WNT Warszawa.

Effect of Pretreatment of Rice Husk with Acetic Acid on Properties of Rice Husk/HDPE Composites

Abdollah Najafi

Abstract

In this study, chemical treatments of rice husk flour on physical and mechanical properties of rice husk flour (RH) / high density polyethylene (HDPE) composites were studied. Initially, rice husk was milled and its flour through the sieve of 60 mesh was selected for using. Rice husk flour was subjected to chemical treatment with acetic acid, and then, was mixed with powder of high density polyethylene at weight ratio of 60% filler loading in an internal mixer. After milling, samples of composites were made by injection moulding method. Physical and mechanical properties of treated RH/HDPE composites were compared to untreated RH/HDPE composite and a RH/HDPE composite including a coupling agent (MAPE). FT-IR spectra of chemical treatments of rice flour husks were also investigated to what extent changes in the functional groups being studied. Physical tests like short and long term of water absorption and thickness swelling and mechanical tests such as flexural, tensile and impact resistance tests according to ASTM performed on samples produced and the following results were obtained. In physical properties, composite made of rice flour treated with acetic acid and the composite including the maleic anhydride have less water absorption and thickness swelling. Results showed that high values of flexural strength, maximum bending load and modulus of elasticity (in flexural test), tensile strength, break elongation and break energy (in tensile test) and impact strength in composites made of rice flour treated with acetic acid and the composite including maleic anhydride were seen. Results of FT-IR indicated that the chemical treatments of rice husks led to a change of OH group absorbance on 3430 cm^{-1} was increased by interaction to acetic acid. Also, in rice husk treated with acetic acid a omitted peak in the region of 1741 cm^{-1} related to functional group of C=O that resulting from the removal part of hemicellulose from lignocellulosic material was seen.

Keywords: Chemical treatment, HDPE, Rice husk, Mechanical properties, Physical properties.

Abdollah Najafi
Islamic Azad University,
Faculty of Natural Resources,
Department of Wood and Paper Science and Technology,
Chalous branch, Iran.
Tel: +981912220020 Fax: +981912220536
Email: ab_najafi@yahoo.com

Ozra Maleki
Ministry of Education,
Student's reaserch house
Amol, Iran

Premature Failure of Creosote Treated Electricity Transmission Wood Poles in Zambia

Elisha Ncube^{1} - Donald Chungu² - Phillimon Ng'andwe² - Donatien Pascal*

Kamdem³ – Abel Chongo⁴ - Enock Mwale⁴

¹Senior Lecturer, Department of Biomaterials Science and Technology, Copperbelt University, Riverside, Kitwe, ZAMBIA.

**Corresponding author*

elisha.ncube@cbu.ac.zm or enncube@yahoo.com

²Lecturers/⁴Research Assistants, Department of Biomaterials Science and Technology, Copperbelt University, Riverside, Kitwe, ZAMBIA.

pngandwe2002@yahoo.co.uk; Donald.chungu@cbu.ac.zm

³Professor, Michigan State University, School of Packaging Innovation and Sustainability, East Lansing, MI 48824, USA.

Kamdem@msu.edu

Abstract

Creosote treated *Eucalyptus grandis* wood poles should remain in service for well over 30 years, but most are being replaced after about 15 years in Zambia. The aim of this study was to determine causes of premature failure. Analysis of wood poles replacement frequency was also undertaken during July-December annual maintenance windows in 2010 and 2011 to establish the effect of field conditions. Sixty four wood poles of 0.9 m length and 15 cm to 20 cm in diameter were treated following the Bethel process. Wood shavings were obtained from level 1 and 2 of sapwood. Creosote retention was determined by assay method and extracted on automated soxhlet extraction using dichloromethane. Creosote retention of 60 kg/m³ which was found was significantly lower than the standard 115 kg/m³. The analysis of maintenance records for wood poles power distribution network in Kitwe region revealed that replacements increased with distance from Nkana mine (i.e. Mine township < Kitwe south < Kitwe north) to Kalulushi area with a 0.9 coefficient of determination (R²). In addition, the results showed that the treated poles were amenable to colonization and detoxification by wood degrading fungi in the field. The reduced replacement frequency of wood poles near Nkana mine indicates changes to wood degrading biotic communities in areas close to emission sources.

Keywords: Creosote, *Eucalyptus grandis*, Penetration, Retention, Wood poles, Premature failure.

Introduction

The Copperbelt Forestry Company (CFC) was born out of Government's privatization drive, between 1991 and 2002, of Zambia Forestry and Forest Industries Corporation's (ZAFFICO) production units including the pole production plant at CFC Kafubu sawmill (ZAFFICO 2008). CFC relies on ZAFFICO for supply of eucalypt wood poles from Chati and Lamba plantation blocks. The researchers observed an increased replacement frequency of electricity transmission

wood poles when compared to Zimbabwe Electricity Supply Authority. Zambia Electricity Supply Corporation's (ZESCO) maintenance engineers in Kitwe, Solwezi and Mwinilunga regional offices confirmed that the replacement frequency of wood poles has increased compared to that in the 1980s. ZESCO's power transmission wood poles are being replaced after about 15 years instead of at least 30 years expected for creosote treated wood poles (Becker et al. 2001). Most of the poles being replaced show extensive heartwood degradation by biotic agents. Termites are found in gouged portions of wood poles in the Copperbelt and North-western provinces. The characteristic heartwood gouging is also present in Western and Southern provinces where Kalahari sand soils predominate and termites are absent. This shows that the wood poles being replaced prematurely have not been effectively treated to render them toxic to wood degrading organisms. The effectiveness of a preservative is influenced by the protective value of the preservative chemical method of application and the degree of uptake, penetration and retention in the treated wood, sapwood thickness, heartwood penetrability, wood moisture content prior to treatment, and the propensity of wood species to checking and crack propagation cracks (Labow 2010; Morrel et al.2009).

The objective of this study was to determine the causes of premature failure of creosote treated wood poles in ZESCO's Kitwe region.

Materials and Methods

Materials. *Eucalyptus grandis* Hill ex Maiden wood poles with a butt diameter not exceeding 200 mm and visibly free from surface checks, knots and biological attacks were randomly selected from stock ready for treatment at Copperbelt Forestry Company (CFC) Kafubu sawmill near Kalulushi. Sixty four poles in 150-200 mm diameter range and 0.9 m long were cut from the butt end of untreated and air dry electricity transmission wood poles. Wood shavings were obtained from the sapwood region at 3 mm increment levels and their moisture content determined by oven dry method (ASTM D4442-07 2007). The moisture content was used to predict the oven-dry weight of experimental poles and shavings.

Creosote impregnation. Sixteen poles were randomly selected and impregnated with creosote in a cylinder with a capacity of 23 to 25 wood poles (i.e. 1.8 m diameter and 20.5 m long) in 4 replicate charges spread over two weeks. The treated poles were then discharged and air-dried for 3 to 4 hours.

Preservative uptake and penetration. Differences in the weight of poles before and after treatment provided a measure of uptake (kg/m^3). Treated poles were cross-cut mid-way and sapwood penetration (mm) on 4 equidistant points on the periphery measured and penetration (%) calculated as a fraction of the corresponding sapwood thickness (mm). Full sapwood penetration is realized when 100% of sapwood is penetrated (BS EN 351-2 1992). Measurement of axial penetration on the end grain calculated as a fraction of sapwood thickness provided a relative measure of axial penetration (%).

Creosote retention analysis. Fifteen poles were randomly selected from treated stock while two control poles were obtained from untreated stock. Thirty treated and six untreated wood shavings samples were obtained from three equidistant points on the periphery of each pole at three increment levels_{1...3} using a 12 mm borer. Fourteen wood shaving samples from level 1 and 2 were extracted using an automated soxtecTM 2050 extraction system (Khan et al. 2005). The remaining 16 wood shavings samples plus other 14 from level 3 were not yet analyzed at the

time of reporting. Glass cups and dichloromethane solvent were used with the Soxtec™2050 extractor set at 160°C boiling temperature (Fig. 1).

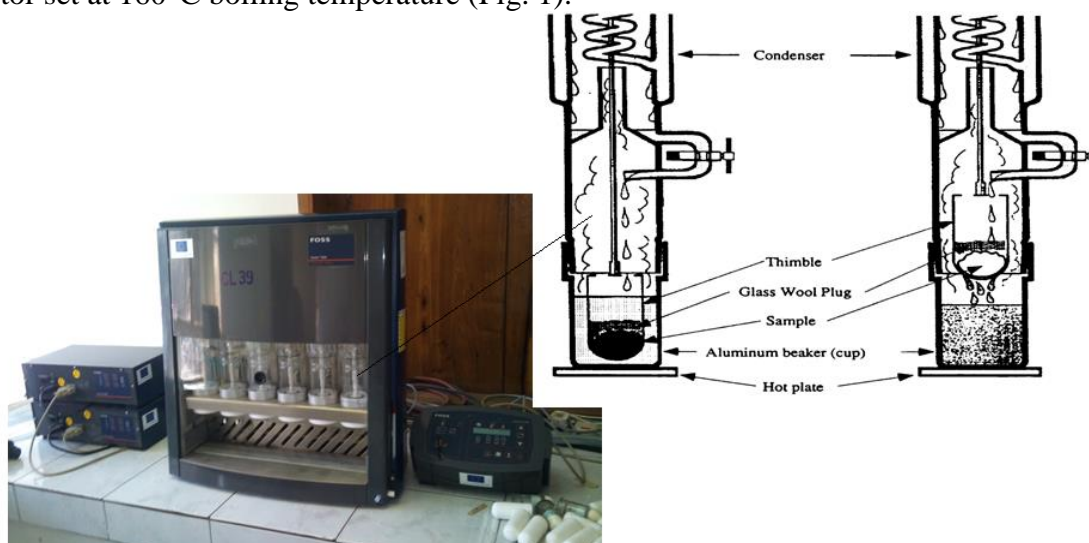


Figure 1: Automated soxhlec™ 2050 extraction system and a close up of extraction during the immersion phase (Left) and rinsing phase (Right)

Initially, the thimbles with wood shavings were immersed in boiling solvent to ensure intimate shavings/solvent contact and rapid extraction of organic analyte over 60 minutes (Method 3541 1994). In stage two, the thimbles were elevated above the solvent, to mimic the rinse-extraction of soxhlet extraction in Method 3540 (1994), and refluxed for an additional 60 minutes. After rinsing, the solvent was evaporated for 10 minutes to leave the extracted creosote compounds in aluminum beakers.

The volume of wood shavings was calculated from the 727.1 kg/m³ (stdev 80.6) air-dry density of *E. grandis*. This density is similar to 750 kg/m³ reported by McMahon et al. (2010) for air-dry *E. grandis* at 12% moisture content. The difference between extracts from treated and untreated samples provided a measure of creosote content (kg) at each zone. Creosote retention (g/cm³) in sapwood was analyzed by assay method to determine the amount of creosote (g) in wood shavings (g) from a specific analytical zone with reference to 115 kg/m³ standard (PIESA 1001 2004).

Replacement of wood poles: Maintenance records for Zambia Electricity Supply Company's (ZESCO) transmission wood poles in Kitwe region were analyzed to determine the replacement quantity, frequency and distribution in Kalulushi, Kitwe North, Kitwe South and Mine Township areas (Fig. 2). This helped establish the effect of different conditions on the activity of wood degrading organisms. The records analyzed were for July-December annual maintenance windows in 2010 and 2011.

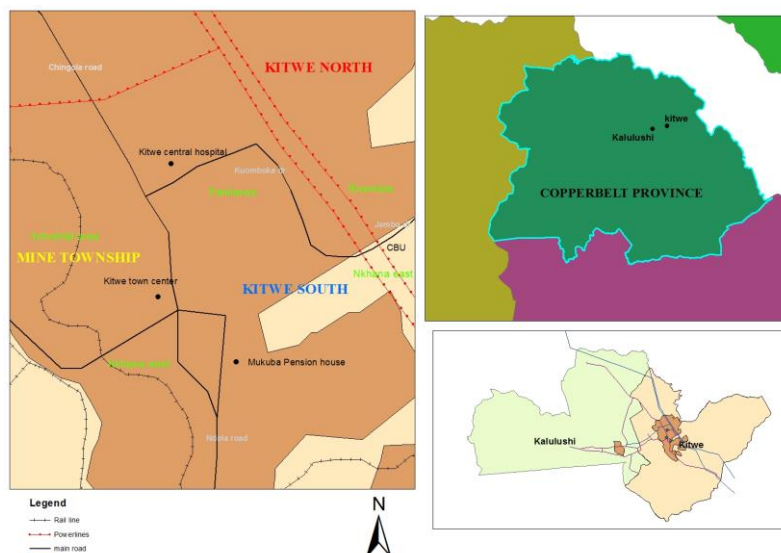


Figure 2: Distribution of Kalulushi, Kitwe North, Kitwe South, and Mine Township areas in Zambia Electricity Supply Company's Kitwe region on the Copperbelt province

Data analysis. Analysis of variance was conducted to find if there was a significant difference in the concentration of creosote at levels 1 and 2. The PIESA standard was used as a reference standard for treated wood poles. A correlation coefficient was used to show if any relationship existed between decay and distance from the mine.

Results and Discussion

Moisture content. A moisture content of 10.42 % (stdev. 0.50%) observed on untreated samples was acceptable as Cookson et al. (2002) also reported a similar level of moisture, i.e. 12%, for the same species after air-drying. Therefore the poles were amenable to preservative penetration and uptake as their moisture levels were much below the recommended upper limit of 25% (Morrison 2012; CEB Standard 081 2001).

Preservative uptake and penetration: Creosote uptake of 3.4 kg/m³ was recorded while sapwood penetration was excellent at 96% (Fig. 3). However, longitudinal penetration from the end grain was very low at 5.48% of sapwood thickness. This may be attributed to presence of tyloses, pit encrustation and presence of very small pit pore sizes (Bamber 1987).

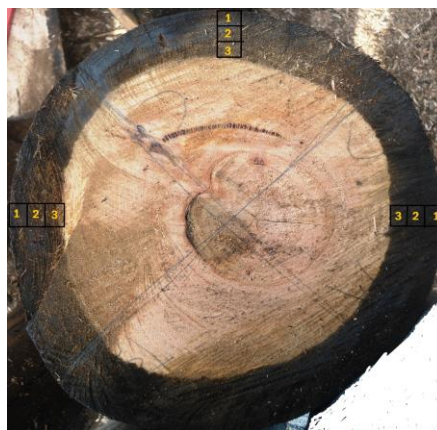


Figure 3: Illustration for 3 incremental levels from which wood shavings were obtained

Extractives content. Untreated shavings recorded extractives content of 0.19% (stdev. 0.08% (from 0.68 g wood shavings). This indicates the amount of natural extractives, i.e. waxes, fats, resins, photosterols and non-volatile hydrocarbons, fraction which was dislodged by dichloromethane (TAPPI T204 cm 1997). The amount of extractives is close to 0.27% found by Nelson, Sefara and Birkett (2004) and Moodley (2011) for *E. grandis*. Morais and Pereira (2012), found higher extractives content of 2.8% for air-dried (15% moisture content) *E. globulus* sapwood powder (3 g) extracted by automated soxhlet extraction using 40 ml of dichloromethane, 1 h extraction and 30 minutes rinsing at 110°C. The discrepancy between what we found and what is reported in literature could be due to the amount of material extracted and the influences of tree provenance and wood variations on diversity and the amount of extractives biosynthesized.

Creosote retention. The data points were below ± 2.5 z-scores which indicated that the measurements obtained had no outliers. Creosote retention in level 1 was 55.9 kg/m³ while that in level 2 was 60.3 kg/m³. These were not significantly different ($F_{calc} 0.14 < F_{crit} 1.841$; P-value of 0.72). However, the student's *t*-test showed that the experimental means were significantly lower than 115 kg/m³ for wood used in hazard class 4 ($|t_{calc} -9.84| > |t_{crit} -2.77|$) service conditions (ZABS DZS 746-6 2010). Hunter (2005) analyzed retention versus failure data of wood poles which had been in the field for 46 to 60 years. He demonstrated that treated wood poles at creosote retention of 60 kg/m³ achieve a service life of 14-15 years while those at 230 kg/m³ could provide a service for about 55 years. This showed that electricity transmission wood poles treated at the CFC Kafubu sawmill are vulnerable to biotic attack at the time of erection in the field. This substandard retention coupled with leaching of creosote from wood poles in service indicates that the active ingredients are low and could be further lowered in the field to levels which are not adequately toxic. Chungu et al. (2012) isolated 13 different types of wood decay fungi from ZESCO's electricity transmission wood poles in Mwinilunga, Mongu and Livingstone urban centers in Zambia. This indicates that some micro organisms thrive in creosote treated wood. *Hormodendrum drumresinae* have been found in creosote treated wood loaded with very toxic substances, such as, phenols and polycyclic aromatic hydrocarbons (Christensen et al. 1942).

The treatability and durability of *E. grandis* heartwood is poor (Ncube et al. 2012) and so any cracks which may develop after treatment and extend into the heartwood provide an avenue for attack by termites (Shultz 2010). Temperature and moisture variations of poles in service initiates cracks which may extend beyond the treated envelope, creating avenues for attack by termites. The entire heartwood portion near the ground line of most poles observed is depleted (Fig. 4).



Figure 4: Typical degradation observed on electricity transmission wood poles

Replacement of wood poles: Fig. 5 shows that proximity of wood poles to the emission source had a direct bearing (R^2 0.9) on the number of poles replaced. A much lower number of wood poles were replaced in areas close to Nkana mine, a flue gas emission source, in Kitwe urban than in Kalulushi area. The ‘direct exposure of decay fungi on the forest floor to air pollutants may alter their growth rate or their ability to decay wood’ (Miller 1977). The results here indicated disturbance of wood degrading biotic agents in areas within the reach of pollutants in flue gases from mining activities.

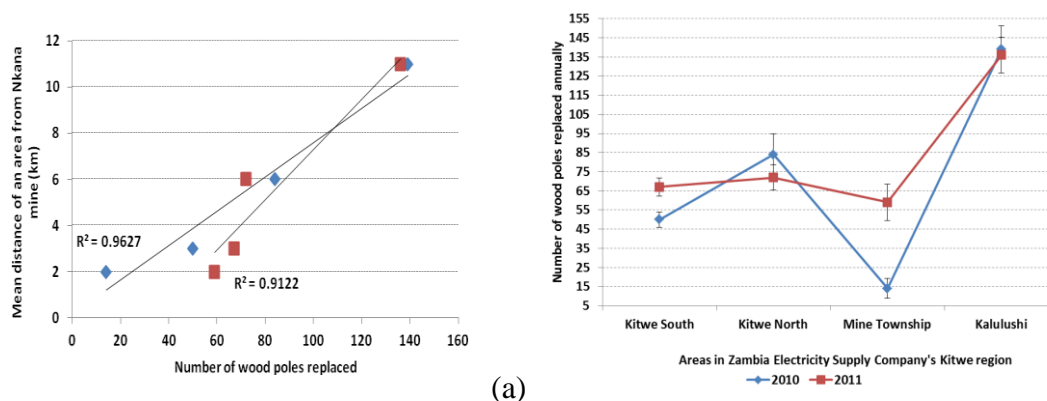


Figure 5: Number of electricity transmission wood poles replaced annually in four areas under Kitwe region of Zambia Electricity Supply Company’s power distribution network boundaries

Conclusions

A creosote retention of 60.3kg/m^3 found in poles treated at CFC Kafubu sawmill was significantly low than the 115kg/m^3 standard recommended by the PIESA for power transmission wood poles. Wood poles treated to this substandard retention last for about 15 years in Zambia just as it has been found by researchers elsewhere. So, degradation of wood poles in service is either initiated by fungus with a capability to detoxify creosote or by splits, which extend beyond the treated sapwood, which provide an avenue for infestation by termites. The results also indicated that the activity of wood degrading biotic agents was lower in areas close to pollution sources such as flue gas from mining activities.

Acknowledgement

The authors acknowledge the Copperbelt Forestry Company for providing the wood samples and availing their creosote pressure impregnation plant for experimentation at Kafubu sawmill, and the Copperbelt University for funding the study.

References

- American Standards Test Method D4442-07 (2007). *Direct moisture content measurement of wood and wood-base materials*. ASTM: West Conshohocken.
- Bamber K (1987). *Sapwood and heartwood*, Forestry Commission of New South Wales, Technical Publication No. 2, ISBN: 07220675.
- Becker L, Matuschek G, Lenoir D, Kettrup A (2001). Leaching behavior of wood treated with creosote. *Chempere*, 42.
- BS EN 351-2 (1992). *Durability of wood and wood-based products. Natural durability of solid wood - Guide to natural durability and treatability of selected wood species of importance in Europe*. BSI: London.
- Ceylon Electricity Board Standard 081 (2001) *Specification for wood poles for overhead low voltage lines*. Sir Chittampalam: Sri Lanka.
- Christensen CM, Kaufert FH, Schimtz H, Allison JL (1942). *Hormoden drumresinae* (Lindau), an inhabitant of wood impregnated with creosote and coal tar. *Am. J. Botany*, 29: 552-558.
- Chungu D, Ncube E, Ng'andwe P (2012). *Biodegradation of Transmission wooden poles by decay organisms in Zambia*, Unpublished report, Copperbelt University.
- Cookson L, McCarthy K, Scown D (2002). *Vineyard posts from Eucalyptus grown on effluent water*. A report for the RIRDC/Land and water Australia/FWRDC joint venture Agro forestry Program, Clayton (Victoria).
- Hunter D, Rossouw P (2005). Motivation for the introduction of a new creosote wood preserve code into the South African market. *Wood preserve paper*, Rev. 00: 1-24.
- Khan Z, Troquet J, Vachelard C (2005). Sample preparation and analytical techniques for determination of polyaromatic hydrocarbons in soil. *Journal of Environmental Science and Technology*, 2: 275-286.
- Labow ST (2010). *Research Forest Products Technologist, General Technical Report FPL-GTR-190*. Madison, WI, USA.
- McMahon L, George B, Hean R (2010). *Eucalyptus grandis, Primefact 1055*. Industry and Investment NSW: Australia.
- Method 3540/3541 (1994). *Automated Soxhlet Extraction*, viewed on 22 August 2013, <<http://www.epa.gov/osw/hazard/testmethods/sw846/pdfs/3541>>.
- Moodley P (2011). *Characterization and quantification of wood extractives and their impact on pitch*. MSc thesis, University of KwaZulu-Natal.
- Morais MC and Pereira H (2012). Variation of extractives content in heartwood and sapwood of *Eucalyptus globulus* trees. *Wood Science and Technology*, 46(4): 709–719.
- Morrel J, Freitag C; Chen H (2009). *Utility pole research corporative 29th Annual Report*, Department of Wood Science and Engineering, Oregon State University.
- Morrison N (2012). *Specification for creosote treated wood poles, cross arms and spacer blocks*. Eskom Rev. 2.
- Miller PR (ed.) (1977). *Photochemical oxidant air pollutant effects on a mixed conifer forest ecosystem – A progress report*. University of California.

- Ncube E, Chungu D, Kamdem PK, Musawa M (2012). Use of a short span field test to evaluate termite resistance of *Eucalyptus grandis* and *Bobgunnia madagascariensis* in a tropical environment. *BioResources*, 7(3): 4098-4108.
- Power Institute for East and Southern Africa 1001 (2004). *Wood poles, cross-arms and spacer blocks*. 2nd edn. South Africa Bureau of Standards: Pretoria.
- Sefara NL, Birkett M (2004). *Development of an alternative solvent to replace benzene in the determination of organic soluble extractives in wood*. African Pulp and Paper Week, viewed on 4 November 2013, <<http://www.tapps.co.za/archive2/>>.
- Shultz TP, Nicholas D (2010). Biocide retention variation and gradients in commercially treated 4 by 4s. *Forest Products Journal*, 60(2): 190-193.
- TAPPI T204 cm (1997). *Solvent extractives of wood and pulp*. Chemical Properties Committee of the Process and Product Quality Division: TAPPI.
- Zambia Bureau of Standards DZS 746-6 (2010). *Rural electrification construction and safety – specification, Part 6: Wood poles, cross-arms and spacer blocks*. ZABS: Lusaka.
- Zambia Forestry and Forestry Industries Corporation (2008). *Plantation management plan 2003-2013*. ZAFFICO: Ndola.

Mechano-sorptive Creep in Reinforced Sitka Spruce

*C. O'Ceallaigh*¹ - A. Harte¹ - K. Sikora¹ - D. McPolin²*

¹ College of Engineering & Informatics, National University of Ireland, Galway,
University Rd., Galway, Ireland.

² School of Planning, Architecture and Civil Engineering, Queen's University
Belfast, University Road, Belfast BT7 1NN, UK

* *c.oceallaigh1@nuigalway.ie*

Abstract

The reinforcement of timber using fibre reinforced polymer (FRP) rods or plates is widely accepted as an effective method of increasing the strength and stiffness of members, while at the same time reducing the variability in properties. The short-term behaviour of these reinforced members is well understood. The long-term or creep behaviour has received less attention. Due to the hygroscopic nature of timber, creep is accelerated by moisture variations, the mechano-sorptive effect. In reinforced timber beams, the influence of the reinforcement and adhesive on the long-term response must be taken into account.

The objectives of the present work are to determine the durability of reinforced timber beams with respect to load duration (viscoelastic creep) and variable climate (mechano-sorptive creep) and to develop appropriate strength modification factors for design purposes. Sitka spruce is the most widely grown species in Ireland and is the timber used in this study. Glued Laminated (Glulam) beams are constructed from Sitka spruce and a proportion of the Glulam beams are reinforced with basalt-fibre reinforced polymer (BFRP) rods. Short-term flexural tests are performed on all unreinforced beams. Six matched groups are created and four of these groups are reinforced and retested. The creep test beams are loaded in bending and the effects of load duration and varying climate are being monitored. One sub-sample of the beams is being tested at constant temperature and relative humidity and a second sub-sample in a climate with varying temperature and relative humidity. This paper contains a description of the test set-up and presents the short-term bending stiffness increase results for reinforced beam groups.

Keywords: Mechano-sorptive Creep, Glued Laminated Timber, Irish Grown Sitka Spruce, BFRP

Introduction

Sitka spruce is the most abundant tree species grown in Ireland. This species has an average rotation length of 30 – 40 years ([Moloney and Bourke 2004](#)) leading to low density, low grade material. This low density timber demonstrates limited capacity to carry substantial loads, however, when combined to create a composite element such as a glued laminated beam, the capacity of this softwood timber may be greatly increased.

Further increases in glulam capacity can be achieved with the addition of FRP reinforcement material. By deploying the reinforcement on the tensile side, the additional capacity of the

timber in the compression zone is utilised and results in much more consistent behaviour as well as significantly increasing the flexural stiffness ([Raftery and Harte 2011](#)). Basalt fibre reinforced polymer (BFRP) is a novel FRP material, which has shown great potential as a reinforcement material for timber elements.

The long-term behaviour of such reinforced glulam beams is of critical importance to structural engineers when designing timber structures. Creep effects must be understood as excessive deflection will result in untimely failure. The creep effect manifests itself as an increase in deflection with time under a sustained load. This time dependent creep is known as viscoelastic creep. Mechano-sorptive creep occurs due to an interaction between stress and moisture content change. Although it occurs simultaneously with viscoelastic creep, it is independent of time. Depending on environmental conditions, this effect can greatly increase the creep deflection of a beam and accelerate the time to failure. To the authors knowledge, only one study addresses these effects on unreinforced and reinforced glulam beams made from Irish grown Sitka spruce ([Gilfillan et al. 2003](#)).

Literature Review

The creep effect is the increase in deflection with time for a given constant stress. Creep within timber structures can be divided into two categories, namely viscoelastic creep and mechano-sorptive creep. Timber is a viscoelastic material so its deformation response is a combination of both elastic and viscous components. Viscoelastic creep is defined as a deformation with time at constant stress and at constant environmental conditions. Mechano-sorptive behaviour is a deformation due to an interaction between stress and change in moisture content due to variations in relative humidity ([Armstrong and Kingston 1960](#); [Armstrong and Christensen 1961](#)). It is independent of time and it does not occur in constant temperature and relative humidity conditions ([Armstrong 1972](#)). Due to the complex nature of timber, and the numerous variables involved, quantifying creep, both viscoelastic and mechano-sorptive, can be difficult.

Creep is quantified by a number of time dependent parameters. The most common are creep compliance and relative creep. Creep compliance may be described by the following formula:

$$C_C(t) = \frac{\Delta\varepsilon(t)}{\sigma_0}$$

Equation (1)

where:

C_C = Creep compliance,

$\Delta\varepsilon = \varepsilon_t - \varepsilon_0$ = Change in strain with time,

σ_0 = Applied constant stress.

Relative creep (C_R) is defined as the increase in deflection at time t, expressed in terms of the initial elastic deflection, as follows:

$$C_R(t) = \frac{\Delta\varepsilon(t)}{\varepsilon_0} = \frac{\varepsilon_t - \varepsilon_0}{\varepsilon_0}$$

Equation (2)

where:

C_R = Relative creep,

ε_0 = Initial strain.

Relative creep has also been expressed as the change in creep compliance ($C_c(t)$) at time t divided by the initial creep compliance (C_{c0}). Changes in the moisture content of timber result not only in mechano-sorptive creep effects but also in dimensional changes in timber. These dimensional changes (shrinkage and swelling (ε_s)) result in increased deflection and must be monitored.

The total measured strain ε_m , may be written as

$$\varepsilon_m = \varepsilon_{vc} + \varepsilon_{ms} + \varepsilon_s$$

Equation (3)

where:

ε_{vc} = Viscoelastic strain,

ε_{ms} = Mechano-sorptive strain,

ε_s = Swelling/shrinkage strain of a matched zero-load control specimen.

The mechano-sorptive component may then be calculated as

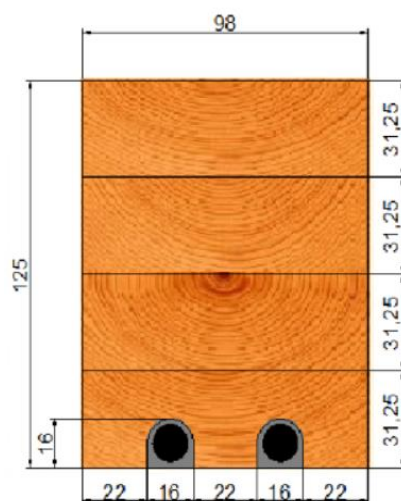
$$\varepsilon_{ms} = \varepsilon_m - (\varepsilon_{vc} + \varepsilon_s)$$

Equation (4)

Mechano-sorptive behaviour has been the focus of many studies due to its ability to increase deflection and cause premature failure of timber elements. There is no defined method for examining creep factors in timber beam elements. This has resulted in many different test methods and test rigs being designed and used to examine creep deflection. Duration of creep tests and moisture cycles also vary considerably in the literature. EN 1156 ([NSAI 2013a](#)) describes procedures for determining the creep factors of wood based panels. It recommends the moisture cycle implemented must be designed to coincide with a Service Class as defined in Eurocode 5 ([NSAI 2005+NA:2010+A1:2013](#)). [Abdul-Wahab et al. \(1998\)](#) performed long-term creep tests on 65 unreinforced glued laminated and solid timber beam specimens under different environmental conditions over an eight year period. The beams were subject to four-point bending. These beams were subjected to three sets of environmental conditions. Although not deliberate, these conditions happened to coincide with Service Classes 1, 2 and 3 as defined in Eurocode 5 ([NSAI 2005+NA:2010+A1:2013](#)). [Abdul-Wahab et al. \(1998\)](#) found that Service Class 3 beams experienced the greatest creep averaging a 285% increase in creep when compared to Service Class 1 beams at constant temperature and relative humidity. Service Class 2 in the variable climate experienced an increase in creep of 165% when compared to the beams at Service Class 1 at constant temperature and relative humidity. These deformations are significant and motivate the need for greater understanding of these effects. The addition of reinforcement, regardless of material type, has been shown to reduce the creep effect within timber elements when compared to unreinforced members ([Davids et al. 2000](#); [Kliger et al. 2008](#); [Lu et al. 2013](#)). BFRP is a novel reinforcement material that has demonstrated 35-42% higher elastic modulus when compared to GFRP ([Lopresto et al. 2011](#)). The long-term effects on timber elements reinforced with BFRP require attention.

Experimental Procedure

This project is designed to study the long-term effects of BFRP reinforced glued laminated manufactured from C16 Irish grown Sitka spruce. Long-term creep tests will be performed under constant variable environmental conditions and appropriate modification factors will be determined for design. This paper details the short-term experiments, which were carried out prior to long-term creep tests. In total, thirty six glulam beams were manufactured in the Engineering Laboratory at the National University of Ireland, Galway. Thirty beams used in the experimental programme will be subject to creep tests and six supplementary beams will be used to monitor shrinkage/swelling and moisture content variations during creep testing. The beams consist of four laminations. Each beam measures 98 mm x 125 mm x 2300 mm. The beams are divided into 2 matched groups, one group will be tested in a controlled climate at $20 \pm 2^\circ\text{C}$ and at a relative humidity of $65 \pm 5\%$ and the other group will be placed in a variable climate chamber. Each beam will be subjected to four-point bending for a period of at least two years to examine the duration of load effects and the creep effects in different climate conditions.



creep beams Long- and purposes. which total, Timber in the tests and variations

Glulam Manufacture. Each laminate was initially strength graded using a mechanical grading machine. Each laminate was ranked accordingly. It was desirable to manufacture thirty six beams of equal properties to create matched groups for comparative studies of long-term effects at a later stage. The beam lay-up was designed by arranging each laminate based on the strength graded data. To create a secure bond at the timber interface, each laminate was knife planed in order to create a smooth surface with which to adhere, free from irregularities and torn grain in accordance with EN 14080 (NSAI 2013b). A 1:1 phenol resorcinol formaldehyde adhesive was used to bond each laminate. Adhesive was applied to the surfaces to be bonded ensuring an even spread of a minimum of 350 g/m^2 . To ensure complete wetting of the bonding surfaces, 200 g/m^2 was applied to each surface using a rubber roller. The beams were clamped in a steel rig applying a minimum pressure of 0.6 N/mm^2 in accordance with EN 14080 (NSAI 2013b). The beams remained in the rig for 24 hours to cure after which they were placed into a conditioning chamber to cure for 5 weeks at $20 \pm 2^\circ\text{C}$ and at a relative humidity of $65 \pm 5\%$ prior to short-term testing.

Reinforced Glulam Manufacture. From the 36 beams created, 20 of the beams were reinforced with BFRP. Two 12 mm BFRP rods were inserted into two circular grooves routed the full length of bottom tensile laminate and centered 30 mm from each edge as shown in Figure 1. The grooves accommodate the BFRP rod plus a 2 mm glue line. The two BFRP rods accumulate to a percentage reinforcement ratio of 1.85%. To guarantee a solid bond, each groove was cleaned using compressed air to ensure it was free from dust and other impurities. A two-part thixotropic structural epoxy adhesive was chosen to bond the reinforcement to the timber as it is specially formulated for the bonding of FRP to timber (Rotafix, 2014). The groove was initially filled to approximately two-thirds of the routed depth. The BFRP rod was then inserted into the groove forcing excess adhesive

Figure 1. Reinforcement

BFRP rod adhesive

around the sides of the rout up to the top of the rod. Additional adhesive was then applied to complete the 2 mm glue line. The beams were then placed in the conditioning chamber with a temperature of 20 ± 2 °C and with a relative humidity of $65 \pm 5\%$, where they remained to cure for a period of 3 weeks prior to short-term testing.

Short-term Testing. The bending test set up is in accordance with EN 408 ([NSAI 2010+A1-2012](#)). The beams were loaded at a constant cross head rate of 0.15 mm/s to a maximum stroke of 15 mm to ensure that the deflection did not exceed the elastic limit of the beam and that the maximum load was less than 40% of the estimated ultimate failure load. The deflection was measure locally and globally at the midspan using two linear variable differential transformers (LVDTs). The local deflection was measured over a gauge length of 625 mm using a hanger suspended to the neutral axis as seen in Figure 2.

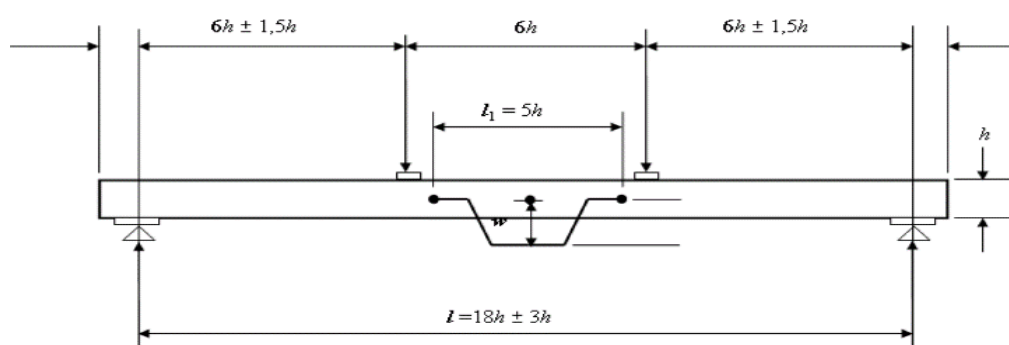


Figure 2. Beam bending set-up ([NSAI 2010+A1-2012](#))

The recorded local and global deflection data was used to obtain the stiffness values. The increment in displacement ($w_2 - w_1$) corresponding to the load increment ($F_2 - F_1$) was substituted into Equations (5) and (6) to obtain the values for local and global stiffnesses, respectively:

$$(EI)_{m,l} = \frac{al_1^2(F_2 - F_1)}{16(w_2 - w_1)}$$

Equation (5)

$$(EI)_{m,g} = \frac{l^3(F_2 - F_1)}{12(w_2 - w_1)} \left[\left(\frac{3a}{4l} \right) - \left(\frac{a}{l} \right)^3 \right]$$

Equation (6)

In these equations a is the distance between the load head and the nearest support, l_1 is equal to the gauge length for local modulus measurement, l is equal to the span and F_1 and F_2 are the loads corresponding to 10% and 40% F_{max} , respectively. Similarly w_1 and w_2 are the deflections corresponding to 10% and 40% F_{max} , respectively. These tests were performed on the unreinforced beams and subsequently on twenty of the reinforced beams. The test set up remained constant throughout allowing the percentage increase in stiffness to be calculated.

Creep Testing. As discussed in the introduction one sub group consisting of 15 beams will be subject to creep testing for at least 2 years in a constant environment and one sub group also consisting of 15 beams will be subject to creep testing in a variable climate. The constant climate

condition will be at $20 \pm 2^\circ\text{C}$ and at a relative humidity of $65 \pm 5\%$ (This will coincide with Service Class 1 as defined in Eurocode 5 (NSAI 2005+NA:2010+A1:2013)). The constant climate conditions will provide data for the analyses of viscoelastic creep. The variable climate condition will encompass viscoelastic creep together with mechano-sorptive creep and strains due to swelling and shrinkage. The test set up will be similar to that in Figure 2. Each beam will be subjected to four-point bending for a period of at least 2 years. Swelling and shrinkage strains will be measured on zero load control beams. Moisture content will be monitored continuously using moisture probes embedded at various depths within the timber to monitor the varying moisture penetration due to the chosen environmental condition. Tensile creep testing of the BFRP rod will be carried out in both controlled and variable environments.

Results

Once the beams had been tested in their unreinforced state, six matched groups were created. Four of these groups were subsequently reinforced as described in the experimental procedure. The average increase in bending stiffness of each reinforced group is calculated relative to the stiffness in its unreinforced state. The results can be seen in Table 1 and Figure 3.

The average increase in the local bending stiffness is 16.30% with a standard deviation of 1.65% and the average increase in global bending stiffness is 8.80% with a standard deviation of 3.65%. Once reinforced the effective local elastic modulus had a mean value of 10727 N/mm^2 and the effective global elastic modulus had a mean value of 9307 N/mm^2 .

GROUP	Average Local EI Increase (%)	Average Global EI Increase (%)
1	15.30%	6.54%
2	17.86%	14.14%
3	14.51%	8.15%
4	17.54%	6.36%
Average	16.30%	8.80%
Standard Dev.	1.65%	3.65%
Median	16.42%	7.34%

Table 19: Group Beam Results

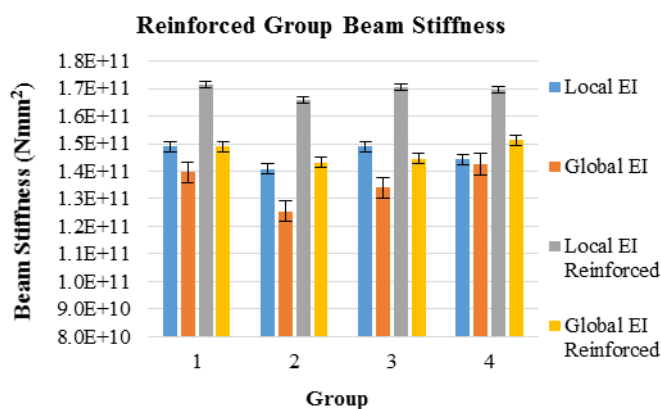


Figure. 3: Group Beam Results

Conclusion

The long-term effects with regards creep effects in timber and the experimental programme have been described. Short-term tests have provided a reliable basis for comparable studies in future work. Flexural tests have demonstrated that the addition of BFRP rod reinforcement in modest quantities can greatly increase the short-term stiffness of glued laminated beams. An average increase in local bending stiffness of 16.3% was observed for a moderate percentage reinforcement of 1.85%.

References

- Abdul-Wahab, H., G. Taylor, W. Price and D. Pope 1998. "Measurement and modelling of long-term creep in glued laminated timber beams used in structural building frames." *Structural Engineer* 76: 271-282.
- Armstrong, L. 1972. "Deformation of wood in compression during moisture movement." *Wood Sci* 5(2): 81-86.
- Armstrong, L. and G. Christensen 1961. "Influence of moisture changes on deformation of wood under stress." *Nature* 191: 869-870.
- Armstrong, L. and R. Kingston 1960. "Effect of moisture changes on creep in wood." *Nature, London* 185(4716): 862-863.
- Davids, W. G., H. J. Dagher and J. M. Breton 2000. "Modeling creep deformations of FRP-reinforced glulam beams." *Wood and Fiber Science* 32(4): 426-441.
- Gilfillan, J. R., S. G. Gilbert and G. R. H. Patrick 2003. "The use of FRP composites in enhancing the structural behavior of timber beams." *Journal of Reinforced Plastics and Composites* 22(15): 1373-1388.
- Kliger, R., M. Al-Emrani, M. Johansson and R. Crocetti 2008. Strengthening timber with CFRP or steel plates - Short and long-term performance. 10th World Conference on Timber Engineering 2008, June 2, 2008 - June 5, 2008, Miyazaki, Japan, Engineered Wood Products Association.
- Lopresto, V., C. Leone and I. De Iorio 2011. "Mechanical characterisation of basalt fibre reinforced plastic." *Composites Part B: Engineering* 42(4): 717-723.
- Lu, W., E.-W. Song, K. Yue and W.-Q. Liu 2013. "Experimental study on creep behavior of FRP-reinforced glulam beam." *Jianzhu Cailiao Xuebao/Journal of Building Materials* 16(2): 294-297.
- Moloney, S. and M. Bourke 2004. Adding value to fast grown Irish Sitka spruce through drying and re-engineering,. Proceedings of the COST E15 Conference, Athens, Greece.
- NSAI. 2005+NA:2010+A1:2013. I.S. EN 1995-1-1. Eurocode 5: Design of timber structures - Part 1-1: General - Common rules and rules for buildings.
- NSAI. 2010+A1-2012. I.S. EN 408 Timber Structures - Structural Timber and Glued laminated timber - Determination of some physical and mechanical properties.
- NSAI. 2013. I.S. EN 1156. Wood-based panels - Determination of duration of load and creep factors.
- NSAI. 2013. I.S. EN 14080 Timber Structures - Glued laminated timber and glued solid timber - Requirements.

Raftery, G. M. and A. M. Harte 2011. "Low-grade glued laminated timber reinforced with FRP plate." *Composites Part B: Engineering* 42(4): 724-735.

Rotafix. 2014, Material Data Sheet. Rotafix House. Abercraf, Swansea, SA9 1UR, U.K., downloaded from www.rotafix.co.uk/ 29th April 2014

Acknowledgments

This work has been carried out as part of the project entitled 'Innovation in Irish Timber Usage' (project ref. 11/C/207) funded by the Department of Agriculture, Food and the Marine of the Republic of Ireland under the FIRM/RSF/COFORD scheme. The authors would also like to thank ECC Ltd. (Earrai Coillte Chonnacht Teoranta) for supplying all the timber used in this project.

Compressive Strength of Cross-Laminated Timber Panel

Jung-Kwon Oh¹ – Jung-Pyo Hong² - Junjae Lee³

¹ Research professor, Research Institute for Agriculture and Life Sciences
Department of Forest Sciences, Seoul National University, Seoul, Korea.

jkoh75@hotmail.com

² Research professor, Research Institute for Agriculture and Life Sciences
Department of Forest Sciences, Seoul National University, Seoul, Korea.

jp.hong@snu.ac.kr

³ Professor, Research Institute for Agriculture and Life Sciences
Department of Forest Sciences, Seoul National University, Seoul, Korea
6221 200Bldng., 599 Gwanak-ro, Gwanak-gu, Seoul, Korea

junjae@snu.ac.kr

** Corresponding author*

Abstract

Compressive strength of cross-laminated timber (CLT) is one of the important mechanical properties which should be considered in the design of mid-rise CLT building because it work to resist a heavy vertical bearing load from the upper level. The CLT panel can be manufactured in various combinations of the grade and dimension of lamina. Therefore, an experimental approach to evaluating the strength of CLT would be expensive and time-demanding. In this paper, lamina-property based models for predicting the compressive strength of CLT panel was studied. Monte Carlo simulation was applied for the model prediction. A set of experimental compression test on CLT panel (short column) was conducted to validate this model. Using this model, the influence of the panel's width on the global CLT compressive strength was investigated. It reveals that the CLT compressive strength increases with the increase in width of the panel (or increase of number of lamina). It can be thought that there is repetitive member effect for the CLT panel wall, which was explained by the decrease of the variation in strength in case of the model simulation. This dependency of the number of lamina needs to be considered when reference design value was determined and very narrow CLT column (Wall) will be designed.

Keywords: Cross laminated timber, Compressive strength,

Introduction

Cross-laminated timber which is an European wood engineered product has a great lateral and vertical load resistance. As the interest of mid-rise wood frame building has increased, this product is regarded as a novel construction material which is appropriate for this tall building.

In low-rise wood frame building, the vertical load resistance of wall and column is not noticed as a critical performance in structural design, because of wood's high compressive strength and relatively low vertical load. However, in mid-rise buildings the walls and columns need to resist much higher vertical load of the upper stories than low-rise building. Cross-laminated timber has shown a great possibility for the use of the mid-rise wood frame construction. The cross laminated timber (CLT) walls in mid-rise building need to resist much heavier vertical load than low-rise buildings.

The walls under vertical load are designed based on compressive strength and elasticity (Euler stress) of CLT panel. As a properties required in wall design, the compressive strength of CLT panel might be one of the critical properties in mid-rise building design. The CLT panel can be manufactured in various combinations of the grade and dimension of lamina. Therefore, an experimental approach to evaluating the strength of CLT would be expensive and time-demanding. The CLT panel needs to be designed by a calculation model based on performance of lamina grade.

Glued engineered wood products, especially glued-laminated timber, also have similar situation to CLT design. They also are manufactured by varied combinations of lamina. Many models have been developed to determine the reference design characteristics depending on the combinations and they are being used for glued-laminated timber design. Foschi and Barrett (1980) developed a model to predict bending strength of glued-laminated timber. After that Bender et al.(1985), Colling (1990), Hernandez et al. (1992), Renaudin (1997), Serrano et al (2001) and Lee et al. (2005) also studied model prediction of the bending strength of glued-laminated beam. For compressive strength of glued-laminated timber, Frese et al. (2012) predicted it by finite element analysis.

Unlike glued-laminated timber, cross-laminated timber is different in several points. CLT is made by gluing laminae crossly; hence cross layers of CLT will be stressed in perpendicular to the grain direction. The perpendicular to the grain compressive strength of wood is approximately 10% of the parallel to grain compressive strength (Barrett and Lau, 1994). Therefore, the contribution of cross layers in the global compressive strength of CLT panel might be very small. Besides, in the process of assembling laminae for CLT panel, edge gluing is not applied in general. This leaves gaps between laminae. Even though there is no gap between laminae by applying edge pressure during assembling and glue curing, the gap between them can progress in service by lamina shrinkage. In general, the design procedure of CLT does not consider the contribution of cross layers to the compressive load resistance (FPinnovations 2013). Also, there may be weak laminating effects because the laminae are not glued together edgewise. In this study, based on the assumption of no contribution of cross layers to the global compressive strength of CLT panel, the prediction of compressive strength of CLT panel was studied and experimentally verified. An adjustment for more accurate prediction was discussed.

Materials and Methods

Compressive strength of lamina Korean Larch (*Larix kaempferi*) was used to produce nominal 100 (width) x 30mm (thickness) x 2,600mm (length) lamstock which was graded according to Korean Standard F 3021-structural glued laminated timber. This standard dictates that, after being passed visual quality checking, laminae should be classified by modulus of elasticity (MOE) measured by an MOE-rating machine, then, each lamina is given a grade which specifies a corresponding minimum MOE to satisfy. For example, Grade E11 of lamina should have the MOE of 11GPa or higher.

Thirty pieces of Grade E11 laminae were prepared for evaluating the compressive strength of lamina. The length of laminae was 2,600mm with the cross section of 30mm by 100mm. Maximum strength reducing defect (MSRD) was identified for the full length. In order to prevent buckling during the compressive test, the lamina specimens were cut into 180mm-length (slenderness ratio, L/r , <17)(short column, ASTM D198) including the identified MSRD (Fig. 1).

The specimens were loaded by universal testing machine in the fiber direction. The maximum load was recorded and the compressive strength was calculated by dividing by the area of cross section.

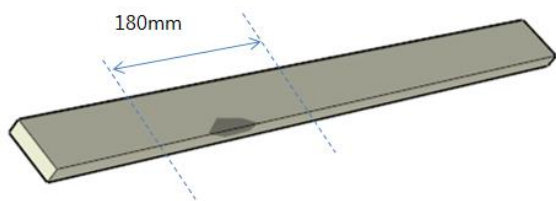


Fig. 1 Preparation of lamina test specimen containing MSRD

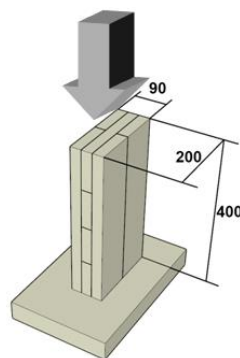


Fig. 2 Compression test specimen for CLT panel

Compressive strength of CLT panel To verify prediction model of compressive strength for CLT panel, 30 pieces of CLT specimens were also prepared.

The MOE-rated laminae of nominal 100 (width) x 30mm (thickness) x 2,600mm (length) were used for manufacturing 3-layer CLT panels with the assembly of Grade E11 laminae at the outer layers and Grade E8 laminae at middle. Thirty pieces of 1,200mm (width) x 90mm (thickness) x 2,400mm (length) CLT panels were manufactured by trimming. Then the full size panels were cut into 200mm by 2400mm strip panels.

In order to prevent buckling at compression test (slenderness ratio, L/r , < 17), the strip panel was cut into 400mm-length test specimens. Unlike the MSRD lamina specimen, the location of MSRD was not considered for the CLT panels; hence, the CLT specimens were randomly cut along the length. Fig. 2 shows a CLT specimen which has four surface E11 laminae in loading direction and four E8 cross laminae in middle. The specimens were loaded by universal testing machine in the fiber direction. The maximum load was recorded and the compressive strength was calculated by dividing by apparent area of cross section.

Prediction of compressive strength for CLT panel Under compressive loading, the cross layers of the CLT panel are loaded in perpendicular to the grain direction. The resistance of compression in perpendicular-to-the-grain direction is only 10% of the parallel to the grain direction. Also, in general the laminae are not glued edgewise. Therefore, in this study, it was assumed that the cross layers do not contribute to the global resistance of the CLT and there is no lamination effect between parallel laminae.

Based on this assumption, the compressive resistance of CLT ($F_{CLT}A_{apparent}$) can be simply calculated by Eq. (1).

$$F_{CLT}A_{apparent} = \sum F_i A_i \quad (1)$$

where,

- F_{CLT} = Compressive strength of CLT panel (MPa)
- F_i = Compressive strength of i^{th} lamina (MPa)
($F_i = 0$ if i^{th} lamina is cross layer)
- A_i = Cross sectional area of i^{th} layers (mm^2)
- $A_{apparent}$ = Cross sectional area of CLT (mm^2)

Before comparing the prediction with the as-measured load resistance of CLT, an adjustment of size effect was made for the CLT. In preparation for the lamina specimens, the cutting location of 180mm long lamina specimen was selected to contain MSRDR. Because all lamina specimens contain MSRDR, the measured compressive strength of the lamina was used for representing that of the 2,600mm full-length lamina. Unlike this lamina test, the location of 400mm-long CLT specimens were randomly chosen in the length direction. So, MSRDR could be excluded in the 400mm-long CLT specimens. Therefore, it is obvious that the probability for this short CLT specimen (400mm-long) to contain MSRDR would be lower than for the full length specimen. To adjust this disagreement, the compressive test results of the CLT specimens were modified by a size factor. Therefore, the compressive load resistance of CLT was adjusted based on Weibull weakest link theory in which 0.1 was used as k factor in Eq. (2) (Madsen 1992).

$$\frac{\sigma_2}{\sigma_1} = \left(\frac{L_1}{L_2} \right)^k \quad (2)$$

where,

- σ = Compressive strength of CLT panel (MPa)
- L = Length of specimen (m)
- k = Length effect parameter (0.1)

For calculation of the 5th percentile strength of the CLT panel, two methods were used in this study; Deterministic method (DM) and Monte Carlo Simulation (MCS). When DM was used, the 5th percentile strength of the CLT panel was calculated with the 5th percentile value of the lamina used, and the average load resistance of the CLT panel can also be done by the corresponding value of the lamina. When MCS was used, the distribution of compressive strength for Grade E11 was input. The compressive strengths of 4 Grade E11 laminae were generated based on the Weibull-fit distribution. With the generated compressive strength, the compressive strength of CLT was calculated by Eq. 1. This procedure was repeated until 3000 CLT panel calculations. Out of 3000 compressive strength results, 5th percentile value was obtained by parametric method (Weibull).

Results and Discussions

For the E11 lamina test and CLT panel, compressive strength was measured and 5% point estimate (PE) was calculated by parametric analysis (3-parameter Weibull). The test results are shown in Table 1 and Fig 3.

Table 1 Statistics of compressive strength for grade E11 lamina and CLT panel

	Compressive strength (MPa)	
	Grade E11 Lamina	CLT
N	39	34
Average	47.93	38.71
St. dev.	5.34	1.56
COV (%)	11.14	4.03
Min	37.19	34.83
Max	59.96	42.29
5% point estimate	39.68	36.32

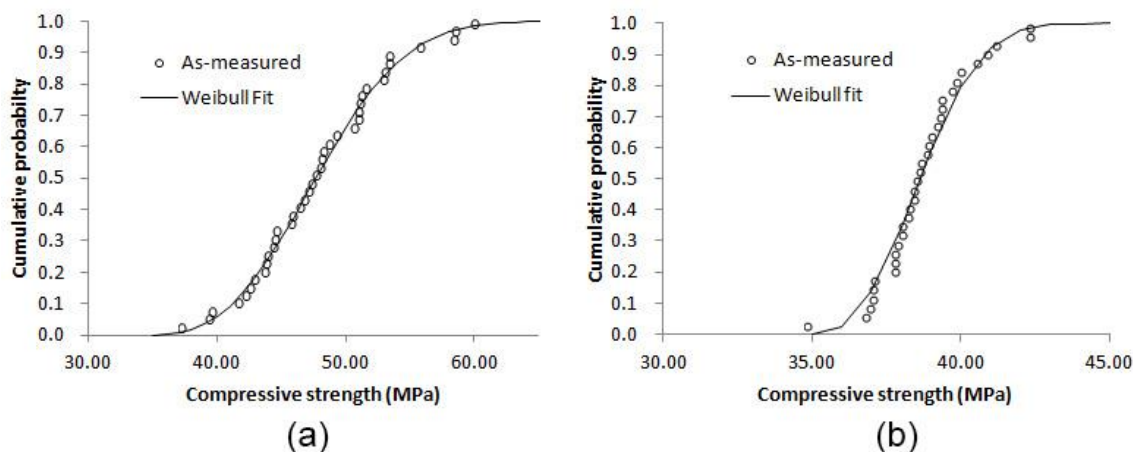


Fig. 3 Compressive strength of Grade E11 lamina and CLT panel. a : Grade E11 lamina, b: CLT panel

Table 2 Results of compressive load resistance for CLT (kN)

	Measured		Predicted			
	Value	Length adjusted	DM		MCS	
			Value	Difference	Value	Difference
Average	676.8	561.3	575.1	+13.8 (+2.46%)	575.3	+14.0 (+2.49%)
5%	653.8	542.2	476.2	-66.0 (12.17%)	524.2	-18.0 (-3.31%)

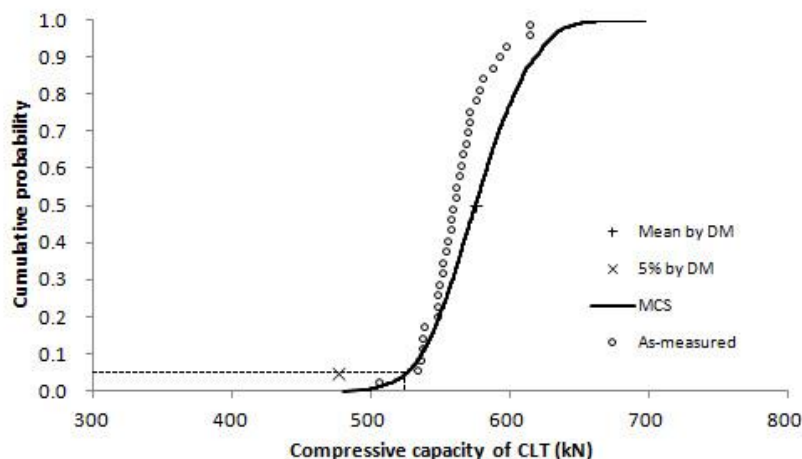


Fig. 4 Comparison of measured CLT compressive load resistance with the predicted values by Monte Carlo simulation.

By the DM, the 5th percentile value and average compressive load resistance of CLT panel was predicted as Table 2 shows. Average compressive load resistance of CLT panel was 575.1kN and 5th percentile value was 476.2kN. In this case, the difference in the 5th percentile load resistance between the measured and predicted values was larger than in the average.

In DM prediction, the 5th percentile value of the lamina specimen was used for the calculation of the 5th percentile compressive load resistance of CLT panel based on an assumption that all laminae have the 5th percentile compressive strength (39.68MPa) simultaneously in the CLT panel. However, the probability that the strength of CLT panel is lower than that CLT in which all laminae have the 5th percentile strength might not be 5%. This difference between the 5th percentile strength to determine and predicted value by DM method may increase as the number of laminae increases. In order to find more accurate 5th percentile value, MCS was used. The MCS was expected to be more likely to reflect the real manufacturing situation in terms of probability calculation. The compressive strengths of all the parallel laminae were randomly generated based on the distribution fit of Grade E11 lamina grade. All laminae are independently generated. With the generated compressive strengths, the compressive load resistance of CLT panel was predicted by Eq. (1) and 5th percentile was calculated from the simulated results by parametric approach of 3-parameter Weibull distribution. As shown in Table 2 shows, the MCS provided a more accurate 5th percentile value than the DM. As Fig. 4 shows, the simulated compressive load resistance was fit very well to the measured result, especially in the lower tail. Based on this comparison between the MCS model and the measured result, it was concluded that the MCS models used in this study can predict the compressive strength of CLT panel and the DM method tends to underestimate the 5th percentile compressive strength.

The 5th percentile value expected to be governed by the number of laminae due to the probability calculation. Using the M.C. model, the influence of CLT's width on the compressive strength of wall width (or the number of laminae in a CLT) was investigated. The number of the parallel lamina will increase (if the lamina's widths are the same) as the width of CLT panel increases. Therefore, the cross section of a lamina was assumed as 30 by 100mm, then the compressive strength according to the number of lamina was calculated by the M.C. model. As Fig. 5a shows, the coefficient of variation (COV) of the compression strength decreased as the number of parallel lamina increases. In other words, with the increase of the wall width, the resistance

against compressive stress has less variation. This results were also applied for 5th percentile compressive strength of CLT panel as the panel width increases. As Fig. 5b shows, the 5th percentile compressive strength of CLT panel has a tendency to increase as the number of laminae in CLT increase. When testing for establishment of the reference design strength, this dependency of the panel width needs to be considered. This implies that the strengths of CLT panel also might be influenced by the repetitive member effect of beam, which explains that the load carrying capacity of individual member is increased by load sharing with adjacent members. It is thought that feasibility of this effect factor for CLT panel needs further study.

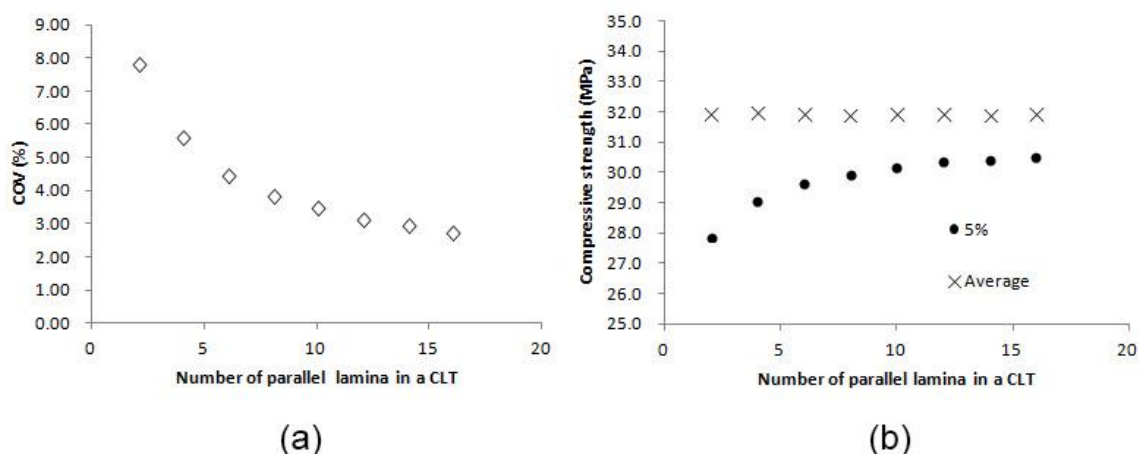


Fig. 5 Change of CLT compressive strength according to the number of parallel lamina used in a CLT. a : Strength variation, b : Average and 5th percentile.

Conclusions

Based on a simple prediction formula for compressive strength, the compressive strength of CLT panel was predicted by the corresponding lamina property. In 5th percentile strength calculation, the DM method has a tendency to underestimate the 5th percentile strength. For more accurate calculation Monte Carlo simulation was applied in this study. A set of experimental study on CLT panel (short column) indicated that the MCS method showed better fit to the experimental result than DM method. Using this model, the influence of panel width on the compressive strength of CLT panel was investigated. Then it showed that the compressive strength increases with the increase in width of CLT panel (number of parallel lamina used). This lamina number dependency needs to be consider in test for determination of allowable strength and CLT wall design.

References

1. Foschi RO, Barrett JD (1980) Glued-Laminated Beam Strength: A Model. J Structural Division, ASCE, 106(8):1735-1754
2. Colling F (1990) Bending strength of laminated timber beams in relation to size effect: Development of a statistical model. Holz Roh-Werkst 48:269-273
3. Bender DA, Woeste FE, Schaffer EL, Marx CM (1985) Reliability formulation for the strength and fire endurance of glued-laminated beams. Research paper FPL460, Forest

Products Laboratory, Madison, WI, USA.

4. Hernandez R, Bender DA, Richbur BA, Kline KS (1992) Probabilistic modeling of glued-laminated timber beams. *Wood and Fiber Science* 24(3):294-306.
5. Renaudin P (1997) Approche probabiliste du comportement mecanique du bois de structure, prise en compte de la variabilite biologique. Doctoral thesis, LMT, ENS Cachan, Paris, France
6. Serrano E, Gustafsson J, Larsen HJ (2001) Modeling of finger-joint failure in glued-laminated timber beams. *J Structural Engineering*, 127(8):pp.914-921
7. Lee JJ, Park JS, Kim KM, Oh JK (2005) Prediction of bending properties for structural glulam using optimized distributions of knot characteristics and laminar MOE. *J wood science* 51(6): 640-647
8. Frese M., Enders-Comberg M, Blass HJ, Glos P (2012) Compressive strength of spruce glulam. *Eur. J. Wood Prod.* 70(6):801-809
9. Barrett JD, Lau W (1994) Canadian lumber properties, Canadian Wood Council p8
10. FPInnovations (2013) CLT Handbook : cross-laminated timber U.S. Edition, FPInnovations. Chapter 3 Structural p7
11. Madsen B (1992) Structural behaviour of timber, Timber Engineering LTD. p278

Accelerated Leaching Test for Estimating Service Life of Preservative Treated Wood in Retaining Wall

Sung-Jun Pang¹ – Jung-Kwon Oh² - Jun-Jae Lee^{3}*

¹ Ph.D Candidate, Dept. of Forest Sciences College of Agriculture & Life Sciences
- Seoul National University, Seoul 151-742, Korea.

pangjungjun@snu.ac.kr

² Research Professor, Dept. of Forest Sciences, Research Institute for Agriculture
and Life Sciences, College of Agriculture & Life Sciences, Seoul National
University, Seoul 151-742, Korea.

³ Professor, Dept. of Forest Sciences, Research Institute for Agriculture and Life
Sciences, College of Agriculture & Life Sciences, Seoul National University, Seoul
151-742, Korea.

junjae@snu.ac.kr

* *Corresponding author*

Abstract

The aim of this study is estimating service life of preservative treated wood at outdoor condition. For using wood in retaining wall, the service life should be lasted at least 50 years in South Korea. Estimating service life by outdoor test, above ground and in ground contact, is the most accuracy and reliable method, but it takes long time. Thus, in this study, the service life of preservative treated wood was estimated by accelerated leaching test.

In order to predict the long-term leaching rate of preservative treated wood, the leaching test was carried out by OECD Emission Scenario Document for Wood Preservatives. The leaching rate of tested specimens was 14.4% for 50 years and 9.16 kg/m³ of preservatives will be remained in the specimens after 50 years. The estimated ACQ (9.16 kg/m³) is higher than the toxic thresholds to fungus (2.4 kg/m³, *I. lacteus*). Thus, the service life of the specimens will be expected at least 50 years.

Keywords: Leaching rate, Preservatives, Service life, Treated wood

Introduction

Using timber as a construction material is often faced with questions about how long a wooden member lasts once it is placed in the structures. Service life of 50 years is required for materials at retaining wall in South Korea.

The wood deterioration is caused by decay, insect, weathering, mechanical damage etc. In case of finishing or interior coating wood, the weathering and ultraviolet rays (UV) should be

considered significantly, because weathering causes the erosion of wood and UV changes the color of wood surface. In case of structural wooden member, however, the important factor for estimating service life is bio-deterioration which can severely degrade a wood in just a few years. The service life of wood in British Standard (BS 8417) related solely to the resistance of the wood to bio-deterioration as well.

For maintaining the structural performance of timber at outdoor condition, the wooden members are usually treated with preservatives. Service life of preservative treated wood can be estimated by outdoor test. For example, the United States Dept. of Agriculture (USDA) assessed the service life of preservative treated pine posts by the 60th percentile of failure point of posts after 53 years. This method is very reliable and accuracy, but it takes long time.

In this study, the alternative method has been considered for estimating the service life of preservative treated wood with some assumptions.

Materials and Methods

Materials. Four length of rounded wood (Ø100×600, Ø100×900, Ø100×1200, Ø100×1800) were treated with Alkaline Copper Quaternary (ACQ) –Type D (Amine based with Cu and DDAC as quat). The species was Korean pine (*Pinus densiflora*) in northeastern South Korea. The moisture content of specimens was about 30% before pressure-treating. The pressure processes are as follows: Pre-vacuum: 700 mmHg for 50 min; Pressure: 18kg/m³ for 300 min; Post-vacuum: 600 mmHg for 30 min. The treated specimens was cured 60°C for 24 hours.

Leaching test. All of the treated specimens were fully dipped in distilled water (Fig. 1) which was adjusted to pH 4.5 by hydrochloric acid for simulating the rain at major city in South Korea. The volume of water was same with the volume of each specimen. For measuring the amount of cooper, leachate solution (50ml) was sampled in 1, 2, 4, 6, 8, 10, 20, 30 days after the beginning of the leaching experiment. After sampling the leachate solution, the remaining water was changed with new distilled water.

Measurement of cooper rate. The samples from leachate solution was Coupled Plassma (ICP).



amount of cooper in measured by Inductively

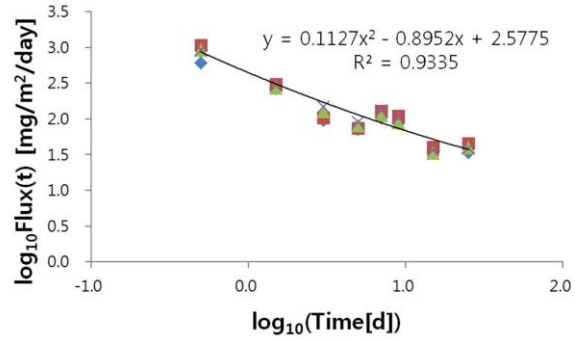
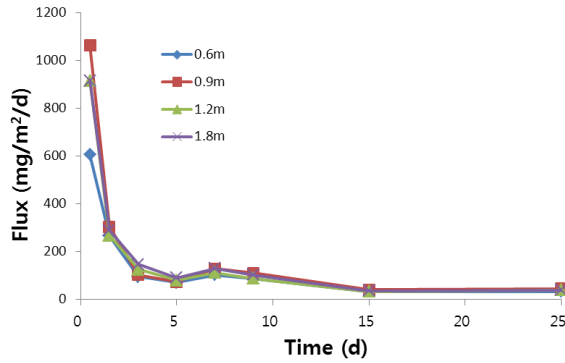
Modeling of wood preservative leaching. Several models for describing a leaching curve of wood preservatives were suggested and the models have advantages and disadvantages. OECD Emission Scenario Document for Wood Preservatives was adopted Panelli's model (Eq. 1) which is based fluxes (leaching rates). In this study, the Panelli's model was used estimating the amount of leached cooper.



on for

$$\log_{10}FLUX(t) = a + b \log_{10}(t) + c \log_{10}(t)^2 \quad \text{Eq. (1)}$$

Assumptions for estimating service life. (1) The service life of wood related solely to the resistance of the wood to bio-deterioration. (2) Unless the preservative retention in wood is less than toxic thresholds, the wood has resistance to the bio-deterioration. (3) The leaching rate of



the components of the preservatives (ACQ) is

same with the leaching rate of cooper. (4) All of cooper is remained in specimens except the leached cooper by water.

Results and Discussions

Penetration and retention of wood preservatives.

The wood preservatives were permeated deeply inside of specimens (Fig. 2). Moreover, the retention of preservatives in 15-50 mm was also higher

than Use Category 4 (ground contact condition, 9.6kg/m³) in American Wood Protection Association (AWPA) Standards as shown in Table 1. Thus, the resistance to bio-deterioration is expected although crack is happened by drying defects.

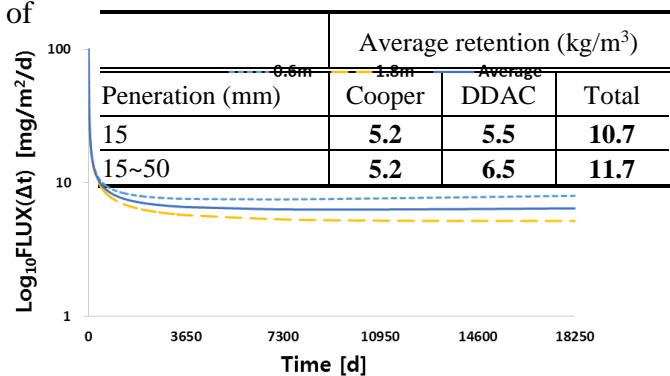


Table 56 Retention of wood preservatives

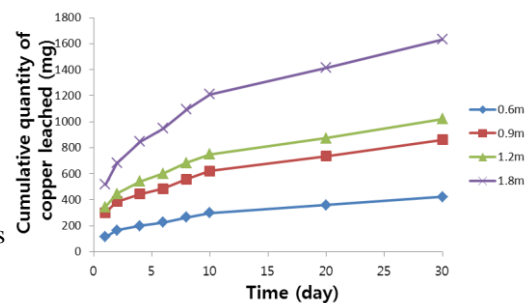


Figure 57 Penetration of wood preservatives

Characteristics of Copper Leaching from ACQ. The cumulative quantity of copper leached as a function of time was more in larger specimens (Fig. 3). However, although the initial fluxes of each specimen were different, over time the flux showed a similar trend regardless of the length of specimens (Fig. 4). It means that the effect of length for leaching rate is small. Thus, the emission equation can be derived for predicting long term leaching quantity regardless of the specimen length.

Estimation of long term leaching rate of copper.

In logarithmic plots (Fig. 5), all measurement points were distributed regularly. Simple polynomial regression of second order derived for estimating the long term leaching



the

was

Figure 5 $\log_{10}FLUX(\Delta t) - \log_{10}(Time[d])$

Figure 6 Long time exposures (50 years)

quantity. The long time exposures (50 years) were plotted by Eq. (1) as shown in Fig. 6. The leaching rate of copper for 50 years was calculated by Eq. (2). As a result, the reaching rate for 50 years was 14.4%.

$$Cu \text{ leaching rate} = [Q_c(t) \text{ (mg/m}^2) \times SA_{\text{unit volume}} \text{ (6m}^2)] / R_{\text{initial of Cu}} \text{ (5.2kg)} \quad \text{Eq. (2)}$$

Where, $Q_c(t)$: total quantity of copper leached out of 1 m² of wood area

$SA_{\text{unit volume}}$: surface area of unit volume

$R_{\text{initial of Cu}}$: initial retention of copper

Comparison of the remaining ACQ with toxic thresholds. The remaining quantities of ACQ were calculated by the leaching rate of copper (Table 2). If the leached ACQ is 14.4%, the remaining quantity of ACQ in wooden member is 9.16 kg/m³. This value is higher than toxic threshold of ACQ (Table 3) which was researched by Archer *et al.* (1995). Thus, the tested specimens will have resistance to bio-deterioration for 50 years.

Table 2 Leaching rate and remaining quantity of ACQ

Time (years)	Leaching rate (%)	Leaching quantity (kg/m ³)	Remaining quantity (kg/m ³)
10	3.6	0.36	10.31
30	9.0	0.96	9.74
50	14.4	1.54	9.16

Table 3 Toxic threshold of ACQ **Conclusion**

ns	Threshold	Fungi
An alternative method for	2.4	<i>I. lacteus</i> (brown-rot)
	1.4	<i>T. versicolor</i> (brown-rot)
	0.7	<i>P. placenta</i> (white-rot)
	0.2	<i>G. trabeum</i> (white-rot)

[Archer *et al.*, 1995] estimating the suggested with some

service life of preservative treated wood was assumptions. A quantity of preservatives remained in specimens was compared with toxic thresholds to bio-deterioration. In the test results, the estimated ACQ in specimens after 50 years was high than the toxic thresholds to fungi. Thus, the service life of the specimens will be expected at least 50 years.

References

- AWPA U1-13. 2013. Use Category System: User Specification for Treated Wood. In American Wood-Preservers' Association.
- Archer, K., Nicholas, D. D., and Schultz, T. P. 1995. Screening of wood preservatives: comparison of the soil-block, agar-block, and agar-plate tests. *Forest products journal* 45(1): 86-89.
- BS 8417. 2011. Preservation of wood. Code of practice : BSI.
- Freeman, M. H., Crawford, D. M., Lebow, P. K., and Brient, J. A. 2005. A Comparison of Wood Preservatives in Posts in Southern Mississippi: Results from a Half-Decade of Testing. *Proceedings, American Wood-Preservers' Association*. 101: 136-143.
- OECD, Emission scenario document for wood preservatives. 2013

Log Homes Mitigate the Global Warming

Zoltán PÁSZTORY

Innovation Center, University of West Hungary,
Sopron, Hungary

Abstract

In this study was enquiring about the wood content of blockhouses regarding the net area of the buildings. It was also defined the carbon-dioxide is needed in order to grow this amount, and finally the effect that blockhouses have favorable impact on our natural environment. To stop the growth of greenhouse gases, it is a good way to increase the number and volume of wood products. Trees and the wood products retain carbon from the atmosphere.

High number of blockhouse layouts was examined from different companies to determine the equivalent CO₂ content of the building. In European Union CO₂-emission of housing sector is about 30% of the total CO₂ emission, so nowadays various studies analyze the opportunities that how our carbon emission can be reduced. One of the possible solutions is to use environmentally friendly building materials. While general materials e.g. concrete, bricks, cement, plastic have fairly high carbon-emissions, wood is a better choice to build our homes.

According to the literature, spruce is the most popular construction wood in Europe and 50% of its absolute dry weight is carbon, so it can determine how many atmospheric CO₂ is bounded into the blockhouses.

By processing of 80 building documents can be declared that an average blockhouse has 110 m² and generally they consist of 30 m³ wood, which means almost 24 tones bounded atmospheric CO₂. It is essential to note down that this value only concerns the walls, not the whole building.

Key words: log homes, blockhouse, carbon storage, CO₂ emission,

Zoltán Pásztor
University of West Hungary
Innovation Center
Sopron 9400 Bajcsy-Zs. u. 4. Hungary
+36-99-518-298
zoltan.pasztor@skk.nyme.hu

Case Study: Exports of U.S. Hardwood Products: Increasing Performance in Asia and Western Europe

*Edgar Arias**
*Henry Quesada-Pineda**
*Robert Smith**

*Department of Sustainable Biomaterials
Virginia Tech
Blacksburg, Virginia, USA

Abstract

The U.S. hardwood industry suffered a continued decline from 1999 through 2009, in part as a consequence of the collapse of the domestic housing market, and the overall economic recession that followed. Despite of the efforts of US government to incentive economic expansion through stimulus spending, the economic growth slowed following cutbacks in the federal government cash infusions. Improvements in the domestic and global economies have led to a slow recovery of the U.S. Hardwood industry, particularly on traditional markets such as pallets and crates, and non-traditional markets, as the exports sector for instance. A comprehensive export performance theory is yet to be defined, and specific aspects of the business such as demand and supply chain management are yet to be studied, particularly, in the hardwood industry. A survey study was implemented between January and May 2014 to explore the importance of export performance factors found in the literature and assess the need of incorporating new ones in a model specifically adapted for the U.S. Harwood Industry. The main goal of this study is to gather insights from companies about the state of the export business, its main drivers, opportunities for growth and challenges. The collection of data and analysis was carried out in two phases. The first phase consisted in a series of interviews with officers of the USDA Foreign Agricultural Service, U.S. Harwood lumber trade associations, and export managers of selected hardwood firms in the Appalachian area. In this phase, semi-structured interviews were applied to capture the respondents' perspectives on key considerations for the success of firms in the export business. The second phase of the study involved applying a survey to hardwood exporting companies. This study built upon previous research by incorporating the revision of commonly accepted export performance factors, but also contributed to the international marketing body of knowledge by exploring the effect of non-traditional factors such as demand management systems, and economic, cultural, social and regulatory factors.

Keywords: International marketing, hardwoods, value-added products

Background

U.S. Harwood Domestic Market

The hardwood industry used to benefit from high production volumes –above 10 million board feet per year –particularly between years 1997 and 2005 (Hornsby, 2012). However, not only the hardwood production, but the entire wood manufacturing industry fell to historically low levels after the collapse in the U.S housing market and the economy meltdown in the final quarter of 2008 (HMR, 2012). The housing starts (**Error! Reference source not found.**, (IBISWorld, 2012), critical hardwood business economic driver, were 554,000 in 2009: this is the lowest level observed in the last 50 years (Woodall et al., 2011) and represents only 27 percent of the housing starts in 2005 (historical maximum), and 40 percent of the average of last 39 years. The Eastern US hardwood production (**Error! Reference source not found.**), which peaked in 1999 at an estimated 12.6 billion board feet (BBF), recorded in 2009 the lowest production since 1960 at 5.73 BBF –a drop of minus 55 percent versus 1999 (Barford, 2012).

International Markets for U.S. Hardwoods

Exports haven't risen to match 2007 records, but they have certainly become a key market for present and short term US hardwood production. The international trade is expected to account for a 13.2 percent of the total industry revenue in 2014 (Goddard, 2014), thereby exports have become the second market in importance for the industry, only after pallets. The value of hardwood exports has increased from 1.89 billion USD in 2009 to 2.99 billion USD in 2013 – almost a 58 percent increase, which also signifies a 2.14 percent increase vs. 2006, the year that held the highest exporting record until now. Even though exports haven't come to raise the industry's total production levels to match 1999 records (14 BBF), but they have certainly become a key market for short and long term growth (HMR, 2012). Hence there is no question as to the growing importance of international markets. International markets are growing in importance and have become a marketing research priority.

Problem statement and goal

The identification and understanding of factors impacting international markets for hardwood products in key US overseas markets is essential for US hardwood producers to shape successful marketing strategies. Even though there has been extensive research on export performance, this field of study of International Business, still characterizes by fragmentation, diversity and inconsistency in results. The purpose of this research is to identify opportunities to increase the export performance of U.S. hardwood firms in Asia and Western Europe by gathering insights from companies, trades associations, and government agencies about the state of the export business, its main drivers, opportunities for growth and challenges. The focus will be hardwood firms located in eastern U.S., and particularly those in the Appalachian region, considering that importance of its contributions to the total of hardwood exports industry.

Literature Review

There have been several studies that have attempted to revise the existing literature on export performance (Leonidou, Katsikeas, & Samiee, 2002; Shaoming & Simona, 1998; Sousa, Martínez-López, & Coelho, 2008). These studies provide a perspective about those factors which have been proposed as determinants of export performance. Sousa, in particular, studied the literature between 1998 and 2005, and developed a framework that condenses the results of

52 papers in the export performance literature. In general, Sousa found that most attempts of developing a framework to explain export performance indicate the presence of at least four elements: internal factors, external factors, control variables and moderating variables. The internal factors relate to multiple dimensions of the firm: firm characteristics (e.g. size, international experience, market orientation, etc.), export marketing strategy (e.g. product, price, promotion, distribution, etc.) and management characteristics (e.g. export commitment and support, education, international experience, etc.). External factors relate to the environment that surrounds the firm, domestically and internationally: foreign market characteristics (e.g. legal and political, environmental turbulence, cultural similarity, etc.) and domestic market characteristics (e.g. export assistance). Control factors (variables) may be either internal or external factors that are of no interest for researcher, but need to be controlled in order to suppress any potential effect in the study. The selection of control variable depends on the research question, so one researcher's internal or external variable can be another researcher's control variable and vice versa. Finally, moderating variables are those that influence the relationship between independent and dependent variables. Not all studies accounted by Sousa's in his literature review include either control or moderating variables.

Even though there has been abundant research on export performance, it has not been the case for the hardwood industry. As a matter of fact, the study developed of by Sousa established that most research has been multi-industry, rather than single industry. He recommends that single-industry-based studies are necessary to procure the advancement in the field since they may provide more significant insights on the determinants of export performance. This would allow having industry as a blocking factor or controlling variable: this means that the differences on the results obtained can't be explained by differences in industries. Considering the fact that previous research revealed clear trends in the export performance literature, and that this research proposal needs to build upon previous inquiries in the hardwood industry to contribute to the body of knowledge, the factors and categories which were proposed will be used to code and classify the data collected in the field work of this case study.

Methodology

A case study took place between January and May 2014, to assess the importance of export performance factors found in the literature from the perspective of U.S. hardwood exporters. For this purpose, the researchers designed an on-line questionnaire consisting in three main sections: "*General Characteristics of the Company*", "*Exporting to Asia*" and "*Exporting to Europe*". In *General Characteristics of the Company*, the respondents were asked to provide basic information about the firm and its performance: location, number of employees, number of facilities (e.g. sawmills), domestic sales, among others. *Exporting to Asia* addressed the characteristics of markets located in East and Southeast Asia, such as: the distribution of exports per country, preferences regarding hardwood species and product types. On this section, respondents were also inquired about general aspects of their firms' marketing strategies in Asia, and the factors they believed were key in achieving a better positioning on the same. Similarly, *Export to Europe* covered the demographics, business strategies and performance drivers in Western Europe. The questionnaire was designed, pre-tested and implemented following the "Tailored Design Method" proposed by Dillman et al. (Dillman, Smyth, & Christian, 2009). The selection of the survey platform was based on the consideration of aspects such as reliability, security, flexibility and availability to the Virginia Tech research community. The research team opted to use the research software suite provided by *Qualtrics*®. A questionnaire consisting in

thirty-seven questions was designed to address the three main areas previously described, which include open-ended and closed-ended questions, most of them categorical. The distribution of the same took place through the National Hardwood Lumber Association (NHLA) electronic newsletter, in three separate issues: one initial request, two subsequent reminders. The final reminder was published on the issue of April 15th. Categorical data analyses (Agresti, 2002) were conducted to explore the behavior of each individual variable and the potential relationships among them; which included contingency tables, Chi-Squared tests for independence of one-way and two-way tables, and Fisher's Exact Test of independence of two-way tables.

Results and Discussion

A total of thirty-one responses were obtained from the members of NHLA. The results to questions eleven and twenty-one, which measure the relevance of export performance factors found in literature review, for Asian and European markets respectively, are the main focus of this technical paper. The analysis and discussion of the remaining twenty-nine variables will be addressed in a further publication. The answers to these two questions, which are depicted in **Figure 58** and **Figure 59**, were intended to quantify the importance of export performance factors in the form of what Hill conceptualized as order winners (Hill, 2000). The *order winners* are those characteristics of either the product, service, etc. that offer additional value to the customer, and therefore may help companies achieving better positioning than competition. Thereby questions eleven and twenty-one are found to be grouped in two main *order winner* categories: *product characteristics* and *service characteristics*, according to the concepts of export performance studied in the literature review. The top four individual order winners in Asia are: *Quality, Packaging, Volume Availability* and *Customer Service*, being the first two product related, and the other four service related. In *Europe Packaging, Quality, Customer Service* and *End-Trimming*, were found to be the main opportunities to add value to customers.

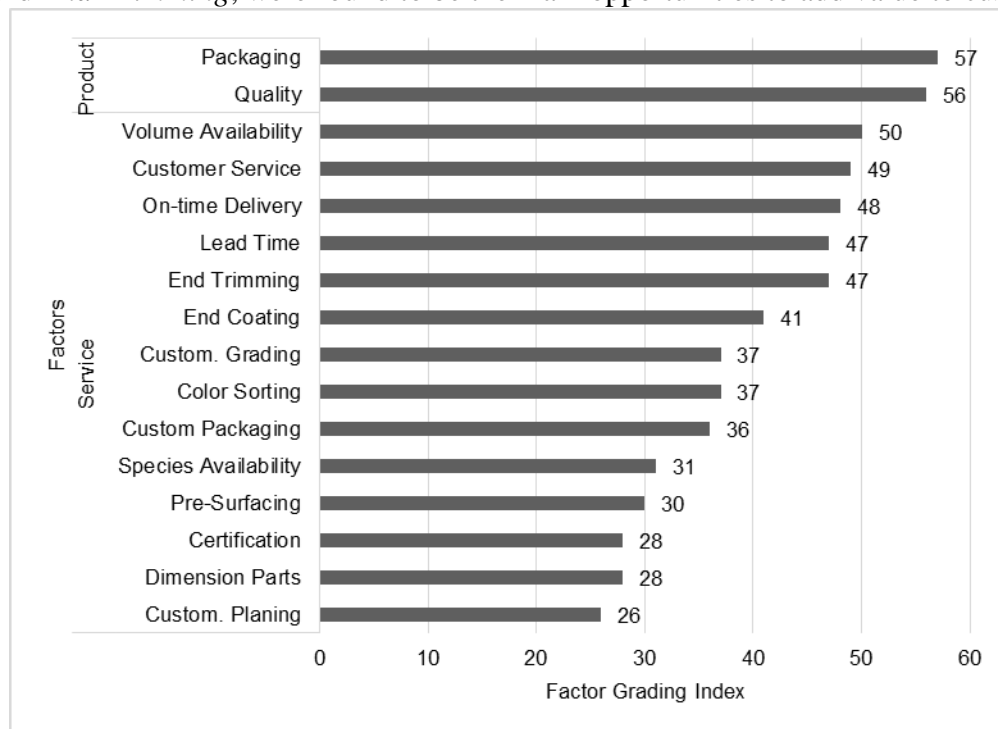


Figure 58 Question 11: Export Performance Factors (Drivers) in Asian Markets

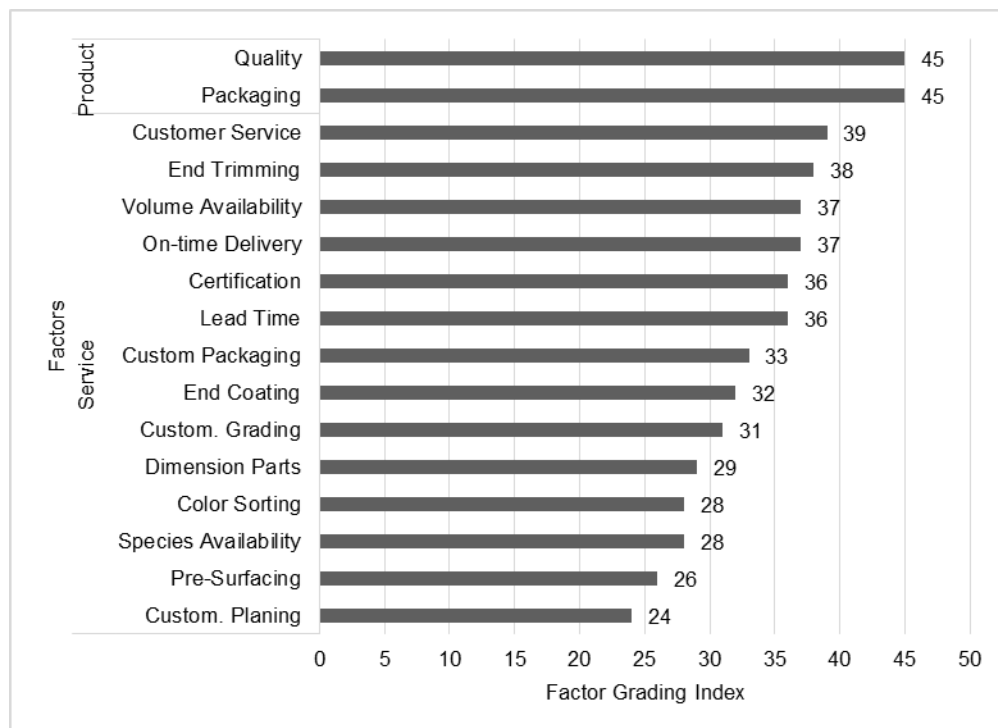


Figure 59 Question 21: Export Performance Factors (Drivers) in European Markets

Conclusions

Exports haven't come to raise the industry's total production levels to match 1999 records (14 BBF), but they have certainly become a key market for short and long term growth (HMR, 2012). Firms need to have a good understanding of the characteristics and dynamics of markets to formulate proper strategies to increase growth and improve profits. Even though there has been extensive research on export performance, this field of study of International Business, still characterizes by fragmentation, diversity and inconsistency in results. The goal of this research is to identify opportunities to increase the export performance of U.S. hardwood firms in Asia and Western Europe. The main goal of this research was to identify the factors that determined the export performance of U.S. hardwood products in Asian and European markets. Previous research demonstrates the importance of these markets for US hardwoods. Therefore, it is critical to find new ways to improve export performance in these markets. Five factors were found to be key drivers of performance: Price, Packaging, Volume Availability and Customer Service, which indicates that any marketing strategy intended to address the international hardwood products markets should include such elements in its core. The theory behind the concept *order winners*, support the notion that certain characteristics of a firm's products and services would only permit former to enter the competition for customer's demand, and other features actually lead the company to create competitive advantage. Hence exporters need also to understand what the customers' basic expectations are. This topic is addressed in the presentation SWST 2014 presentation: "*Factors Impacting the Export of US Hardwoods in Germany, China and Vietnam*".

References

- Barford, M. (2012). The Future of North American Hardwood Lumber. Retrieved 07/02/2012, 2012, from <http://sbio.vt.edu/workshops/ischp/downloads/presentations/Mark%20Barford%20-%20The%20Future%20of%20%20North%20American%20Hardwood%20Lumber.pdf>
- Dillman, D. A., Smyth, J. D., & Christian, L. M. (2009). Internet, Mail, and Mixed-Mode Surveys: The Tailored Design Method (pp. 1-15, 402-440). Hoboken, N.J: Wiley & Sons.
- Goddard, L. (2014). Now boarding: Renewed construction demand will support industry growth *IBISWorld Industry Report 32111 Sawmills & Wood Production in the US* (pp. 1-41): IBISWorld.
- Hill, T. (2000). *Manufacturing strategy: text and cases*. Boston, Mass: Irwin/McGraw-Hill.
- HMR. (2012, January 2012). Wrapping up the North American Hardwood Marketplace for 2011 Part I. *HMR Executive*, 6, 1-10.
- Hornsby, R. (2012). The International Hardwood Trade: All Roads Lead to China. *Hardwood Matters: The Voice of the Hardwood Industry*, 10-13.
- IBISWorld. (2012). IBISWorld Business Environment Profiles: Housing Starts. Retrieved May, Tuesday the 1st, 2012, 2012, from <http://clients1.ibisworld.com.ezproxy.lib.vt.edu:8080/reports/us/bed/default.aspx?entid=2598>
- Leonidou, L. C., Katsikeas, C. S., & Samiee, S. (2002). Marketing strategy determinants of export performance: a meta-analysis. *Journal of Business Research*, 55(1), 51-67. doi: 10.1016/S0148-2963(00)00133-8
- Shaoming, Z., & Simona, S. (1998). The determinants of export performance: a review of the empirical literature between 1987 and 1997. *International Marketing Review*, 15(5), 333-356. doi: 10.1108/02651339810236290
- Sousa, C. M. P., Martínez-López, F. J., & Coelho, F. (2008). The determinants of export performance: A review of the research in the literature between 1998 and 2005. *International Journal of Management Reviews*, 10(4), 343-374. doi: 10.1111/j.1468-2370.2008.00232.x
- Woodall, C. W., Ince, P. J., Skog, K. E., Aguilar, F. X., Keegan, C. E., Sorenson, C. B., . . . Smith, W. B. (2011). An Overview of the Forest Products Sector Downturn in the United States. *61*(8), 595-603.
- http://vt.summon.serialsolutions.com/link/0/eLvHCXMwA20DNjU3N0w2SwH2lc2BrSKTFHMzs1RgzWJpkZxskQSeKkDseEcqzd1EGULcXEOcPXSh9wDopptaGOqmAbvFwIol0dwcdLpcYppZkrFZMuh-iFQjoLEWiRZplknAWtEiDdg6B1ZoyZYGJikmKcBmhXlicmqqaWhGANvImi5eF4JeFtZCt-vip1u3AXuh3dsvCIVw3jyAAB88C_Y

Effect the Indentation of the Annual Growth Rings in Norway Spruce (*Picea Abies L.*) on Shear Strength - Preliminary Study

Vladimír Račko^{1*} – Oľga Mišíková² – Blažej Seman³

¹ Research associate, Department of Wood Science, Technical University Zvolen, T.G. Masaryka 24, Zvolen, SLOVAKIA

* *Corresponding author*

racko@tuzvo.sk

² Research associate, Department of Wood Science, Technical University Zvolen, T.G. Masaryka 24, Zvolen, SLOVAKIA

misikova@tuzvo.sk

³ Associate professor, Department of Chemistry and Chemical Technologies, Technical University Zvolen, T.G. Masaryka 24, Zvolen, SLOVAKIA

xsemab@is.tuzvo.sk

Abstract

Anatomic observation the microstructure of tissue containing indented growth rings indicate high morphological inhomogeneity the tracheides and ray parenchyma cells, which occurred mainly in the peripheral, but also partly in the central zones of indented growth rings. This morphological disproportion compared to normal wood, in the globally, negatively affect on the shear strength of parallel to grain in the radial- longitudinal plane. Although, influence of density was not confirmed, strength decrease was due to hyperplasia and hypertrophy of ray parenchyma. On the other hand, distortion, twist and entanglement of tracheides in marginal zones had partially reinforcing effect. Even though, the structure of indented growth ring tissues had a significant effect on reducing the shear strength, the difference in mean values was small.

Keywords: Norway spruce, Indented growth ring, Normal growth ring, Shear strength, Density.

Introduction

The indentations, which are anatomical anomalies, can be explained by abnormal cambial growth but it is still unclear why and how they are produced (Nocetti and Romagnoli 2008). Indented growth rings (IGRs) were observed in many coniferous species *Picea abies* and *Pinus jeffreyi* (Ziegler and Merz 1961), *Picea sitchensis* (Ziegler and Merz 1961, Fukazawa and Ohtani 1984, Ohtani et al. 1987) and *Pseudotsuga menziesii* (Schultze and Gotze 1986) and *Cedrus libani* (Yaman 2007). Structural changes in morphology wood elements containing IGRs zones predetermine such wood mainly for the production of musical instruments. There were found appropriate acoustic properties such wood, opposite to wood with normal growth rings (NGRs) (Bonamini et al. 1991, Buksnowitz et al. 2012). Bonamini and Uzielli (1998) also presented an innovative easy methods, based on the search of indentations on the bark of the stem. Different fiber orientation in IGRs zones may cause tension during drying and subsequent formation of cracks. IGR impact on the bending strength and bending modules of elasticity has been studied in

the works (Račko and Cunderlík 2007, Buksnowitz et al. 2012). However, the other mechanical properties were not investigated.

The aim of the article was describe differences in the morphology of the wood elements and tissues in IGRs and NGRs and find out the impact of structural changes on shear strength parallel to grain in a radial fracture plane.

Materials and Methods

Samples were chosen from forest stands of the Muraň forest district (the National Park of the Muráňska Planina, Slovak Republic), altitude – 1200 m a.s., forest age – 160 years, subsoil – calcite. From two felled logs (diameter 25 cm, length 3m) were sawn six radial sample boards (thickness of 30 mm). The boards were first air-conditioned under natural environment conditions for 60 days (May-June). Subsequently, there were identified and prepared the samples which contained 83 zones including IGRs and 48 samples including NGRs (dimension 30x30x60mm). Prepared samples were used for investigation of micro anatomy wood tissues, determination of the density and mechanical testing.

Wood anatomy observation - 10 + 10 samples from both zones were used. First part of them was used for preparation of macerates (intended for determination of cell morphology), second part was used for the preparation of micro sections of the wood tissue. Maceration consisted from boiling of blocks (volume 1-2 cm³) in a solution containing of 1 part hydrogen peroxide (H₂O₂) and 1 part concentrated acetic acid. Subsequently, macerate was washed and diluted with distilled water and stained with Safranin. Cell morphology was measured with automated equipment, operating on the principle of image analysis L, W FiberTester with Blend software module (Lorentzen, Wettre Sweden).

First step of slide preparations for transmission optical microscopy in polarized and non-polarized light consisted from slicing of transverse, radial and tangential sections with sledge microtome Recher Austria. Before the slicing, the blocks were impregnated by starch based non-Newtonian fluid (10g cornstarch, 8ml of water and 7g of glycerol) from the reason of preservation the strip off the secondary walls with microtome blade (Schneider and Gärtner 2013). Another steps was washing the slices with distilled water and staining in Astra blue and Safranin solutions. In the case of preparations for polarized microscopy the staining was omitted. Finally, slices were washed again, dehydrated in ethanol (concentrations of 75 and 96%) and mounted with mounting media Euparal (Gärtner and Schweingruber 2013). Macerates and micro slides were observed with the light microscope CarlZeiss AxioLab A1 under magnification of 50, 100, 200 and 400x. The micrographs were taken with attached DSLR camera Canon Eos 600d.

Shear strength and wood density determination - The samples (30x30x60mm) were air-conditioned (t = 20 °C, φ = 65 %) and tested on wood density by gravimetric and volumetric method. Shear modulus of rupture (parallel to grain in radial-longitudinal plane) were tested on the specimens of specific shape (Fig. 1). Specimen preparations were made subsequently, from the samples, after testing of wood density. The specimens were prepared so that the shear plane passed through IGRs zone.

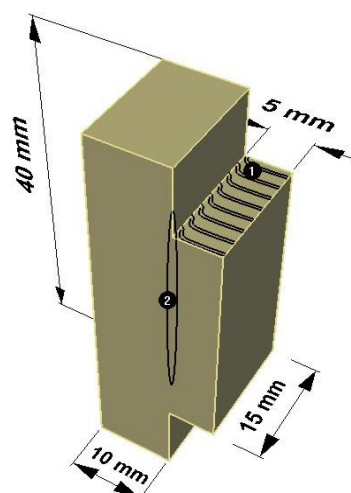


Figure 1 Testing specimens for determination of shear strength (including IGRs). Location of shear plane in the middle IGRs zone - (1) on transverse - (2) on tangential surface

Results were evaluated by Student's t-test.

Results and Discussion

Macroscopic observation of IGRs zones in *Norway spruce* has confirmed earlier findings which has made on *Sitka spruce* by Fukazawa and Ohtani (1984). We agree that IGRs occur continuously in the radial direction for many years. In many cases, they are longitudinally slit-like in tangential section (Fig. 2A) and many of them reach to the cambium, others do not. However, most of our specimens came from juvenile zones and it seems that some of them had an origin in pith, or in first or second annual ring from that. This is contrary to argument that within a trunk, regardless of height level, they only occur in the outer part and not near the pith (Fukazawa and Ohtani 1984).

Microscopic observations of morphology wood tissues confirmed the high frequency and hypertrophy and hyperplasia of ray parenchyma cells in marginal and central zones of IGRs (Figs. 2B, 2C and 3C). Cells were two to three times wider than in the NGR zones and their shape was irregular. The frequency in IGRs zones compared NGRs increased by 5.2%, which represents an relative increase of about 50% (Tab. 1).

Table 1 Test characteristics determining impact of IGRs on the shear strength

	Anatomical characteristics				Physical and mechanical characteristics				
	n	Frequency parenchyma cells [%]	Length of tracheides [mm]*	Width of tracheides [mm]*	n	Wood density [kg·m ⁻³]*	t-test level	Shear strength [N·mm ⁻²]*	t-test level
IGR	20326	15.6	1.47±0.99	25.4±1.67	83	404±17.5	0.5918	6.3±0.68	0.0060
NGR	20295	10.4	2.14±1.22	28.3±3.32	48	406±14.0	ns	6.8±1.17	++
Total	40358	13.0	1.80±1.16	26.9±2.26	131	405±16.2		6.5±0.91	

*mean±standard deviation, ++statistical significance at p=0.01, ns. - non-significant effect

In NGRs zones occurred mostly uni and biseriate rays. However, marginal and central zones of IGRs contained also large multiseriata heterogeneous rays (Fig. 3C) abruptly beginning and during same or next year ending. These zones repeated more or less regularly during next vegetation seasons (Figs. 2B and 2C). Ray height in these regions reaches a few millimeters (Fig.

3B). Similar abnormal forms of biseriate and multiseriate rays in *Chamaecyparis nootkatensis* and *Sitka spruce* observed Bannan (1950, Ohtani et al. (1987). Takizawa et al. (1980) observed that in *Larix leptolepis* within one growth period two closely spaced uniseriate rays became a multiseriate one containing a radial resin canal. Difference in ray frequency of IGRs and NGRs regions in *Picea abies* described Ziegler and Merz (1961). In marginal zones of IGRs the number of rays increased by 40 to 50%, but the cell number of a ray in tangential section is diminished by 10 to 20%. Yaman (2007) also showed in *Lebanon cedar* that average maximum ray height is greater in IGRs than in NGRs.

Morphology of tracheides in IGRs is also different. We found abnormal morphology and arrangement of tracheids in marginal zones, sometimes in central zone of IGRs (Figs. 2C and 3A). Tracheids in this zones were shorter and narrower (tab. 1) and twisted and entangled (Figs. 3A and 3B). Microfibril angle are considerable changed in depend on the shape change of tracheides in radial and tangential direction only in zones with IGRs. The same result also reached authors in *Picea abies* (Schultze and Gotze 1986) in *Pseudotsuga menziesii* (Ohtani et al. 1987), in *Pinus halepensis* (Lev-Yadun and Aloni 1991), in *Cedrus libani* (Yaman 2007). Yaman (2007) also found that lumen diameter and double-wall thickness are wider in IGRs than NGRs zones.

The results showed that between morphology of the IGR and the shear strength paralel to grain in the radial plane is evident relationship (Table 1, Figs. 4 and 5). High content of ray parenchyma in IGRs zones caused lower shear strength. According to Požgaj et al. (1993) the shear strength in the radial plane is 10-30% lower, than the tangential plane. Mean value for spruce is about 6.7 N.mm⁻², which it is identical to our findings. The authors also state that the change of the strength between the two shear planes (radial and tangencial) is caused by low strength of thin-walled parenchyma cells in rays. It is evident that the main changes of direction uniseriate rays in outer marginal zones of IGRs could cause this problem (Fig. 2E). However, more significant role in reducing the strength in IGRs plays presence of large multiseriate ray with hypertrophic parenchyma cells.

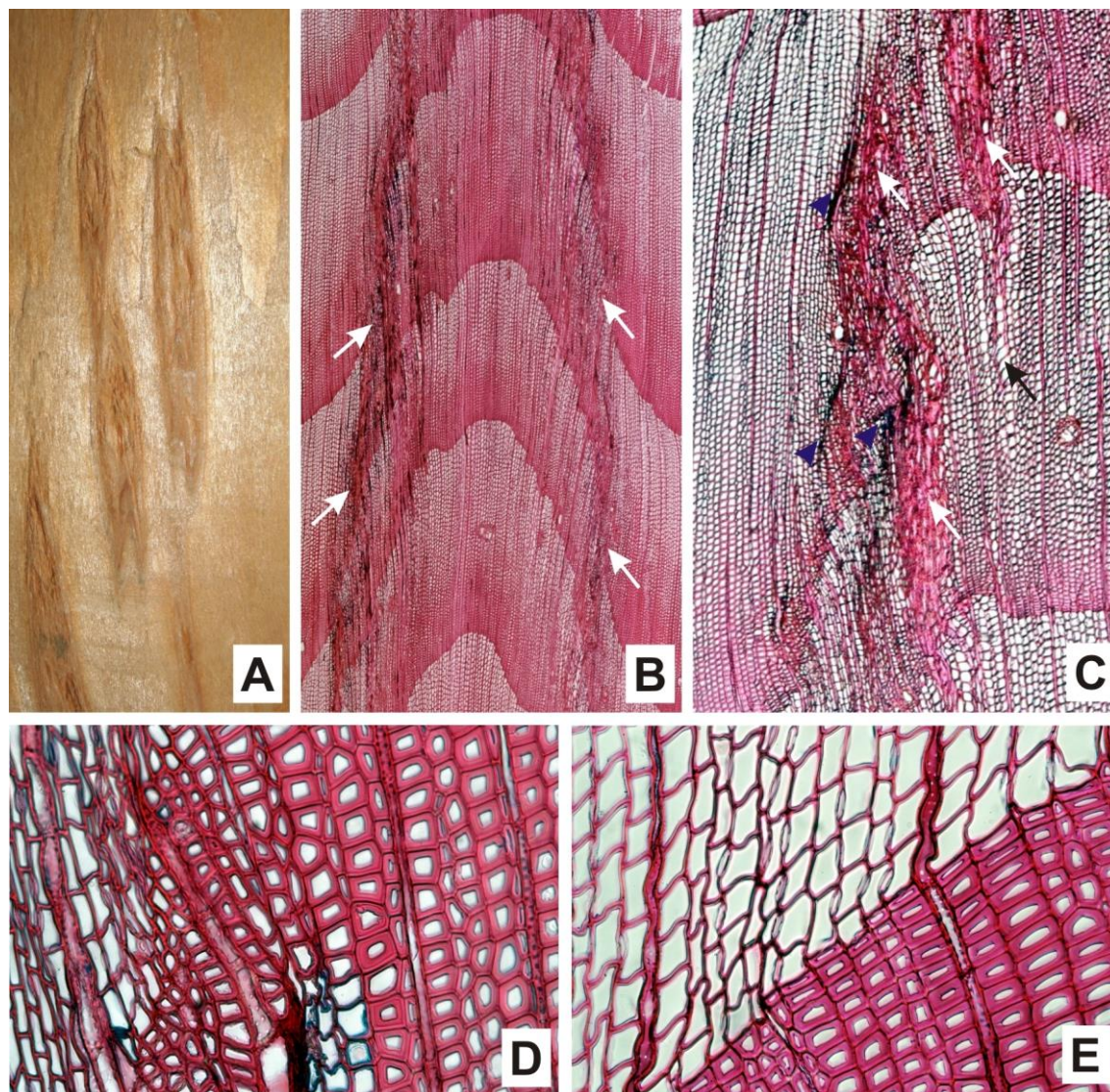


Figure 2 (A) – Macroscopic view of IGR zones on tangential section. (B) – Multiseriate parenchyma rays (white arrow) in marginal zones of IGRs (transverse section, magnification of 40x). (C) – Detail of three multiseriate parenchyma rays (white arrow) in marginal and central zones of IGRs. Hypertrophy of earlywood tracheides (black arrow) in central part of IGR. Unligified sequence of tracheides in marginal zone (blue arrowhead)(transverse section, magnification of 100x). (D) – Alterations of shape, size and number of latewood tracheids in the central part of IGR. Some tracheids have unligified S₂ and S₃ layers (blue color) (transverse section, magnification of 200x). (E) – Alteration of the shape and orientation of tracheids and parenchyma rays at the early/latewood boundary in the marginal zone of IGR (transverse section, magnification of 200x).

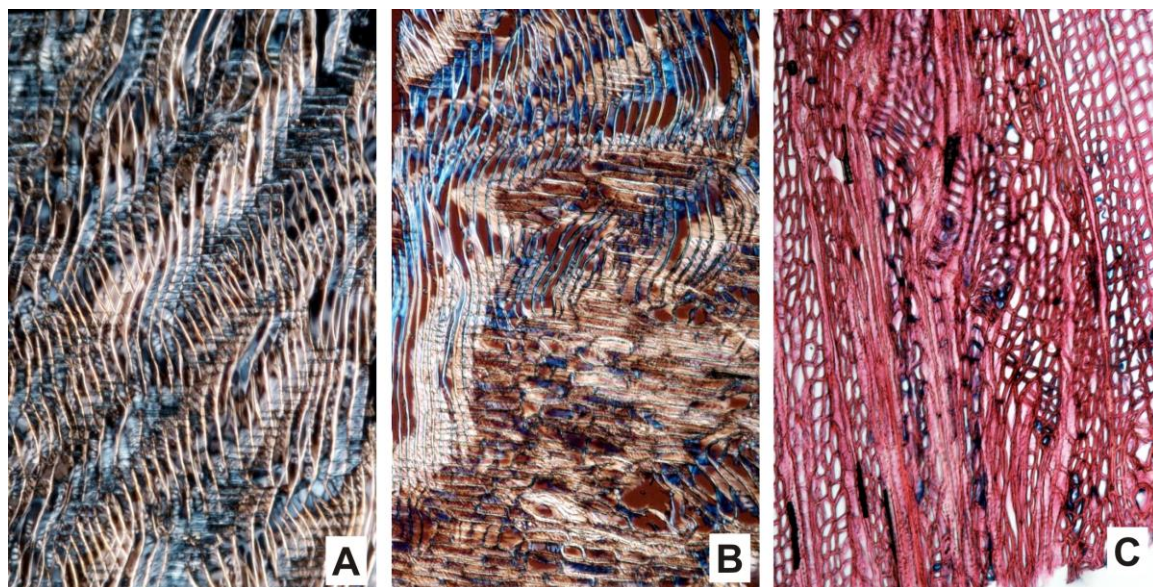


Figure 3 (A) – Micrograph of twisted tracheides in marginal zones of IGR (observed under polarized light, radial section, magnification of 150x). (B) – fragment of abnormal ray parenchyma (brown and white color) and entanglement of twisted tracheides (blue color) in marginal zone of IGR (observed under polarized light, radial section, magnification of 150x). (C) – Multiseriate rays with hypertrophy and hyperplasia of parenchyma cells in central and marginal part of IGR. Blue color indicates unligified regions of tracheide cell walls around rays (transverse section, magnification of 150x).

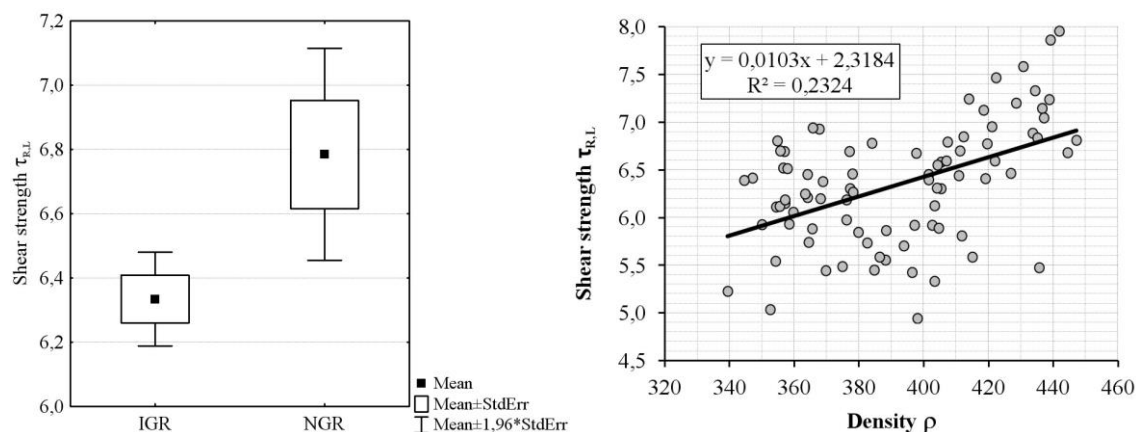


Figure 4 Graphical interpretation of statistical significance the influence of annual growth rings indentation on shear strength (Students t-test)

Figure 5 Dependency between shear strength and wood density

On the other hand, entanglement twisting of tracheides in zones IGRs seems to have a reinforcing effect. Therefore, the difference in strength between IGR and NGR was small, although statistically significant (Table 1, Fig. 4). It can be seen (Table 1) that the density of samples with IGRs and NGRs did not change significantly. However, the shear strength due to density had increased, even though correlation was weak (Fig. 5).

We have to say that local density in IGRs zones were not found out in this study. Therefore, we can not certainty say that it affects on the the shear strength. However, Romagnoli et al. (2003) studied density variations in spruce wood with IGRs and showed that density was greater in indented than in unindented parts.

References

- Bannan, M.W. 1950. Abnormal Xylem Rays in *Chamaecyparis*. American Journal of Botany 37(3): 232-237.
- Bonamini, G., Chiesa, V., Uzielli, L. 1991. Anatomical features and anisotropy in spruce wood with indented rings. *Catgut Acoust Soc J* 8: 12-16.
- Bonamini, G., Uzielli, L. 1998. Non destructive methods for the identification of Norway spruce trees with indented rings / Un semplice metodo non distruttivo per riconoscere in bosco gli abeti rossi cosiddetti di risonanza. *Monti e Boschi (Italy)*.
- Buksnowitz, C., Evans, R., Müller, U., Teischinger, A. 2012. Indented rings (hazel growth) of Norway spruce reduce anisotropy of mechanical properties. *Wood Science, Technology* 46(6): 1239-1246.
- Fukazawa, K., Ohtani, J. (1984) Indented rings in sitka spruce. In: *Proceedings of Pacific Regional Wood Anatomy Conference : Oct 1-7, 1984, Tsukuba, Ibaraki, Japan . Int Assoc of Wood Anatomists*
- Gärtner, H., Schweingruber, F.H. 2013. *Microscopic preparation techniques for plant stem analysis. Remagen-Oberwinter ,Switzerland:Verlag Dr. Kessel.*
- Lev-Yadun, S., Aloni, R. 1991. An experimental method of inducing "Hazel" wood in *Pinus halepensis* (Pinaceae). *IAWA Bulletin n.s.* 12(4): 445-451
- Nocetti, M., Romagnoli, M. 2008. Seasonal cambial activity of spruce (*Picea abies karst.*) with indented rings in the Paneveggio Forest (Trento, Italy). *Acta Biologica Cracoviensia Series Botanica* 50(2): 27-34.
- Ohtani, J., Fukazawa, K., Fukumorita, T. 1987. SEM observations on indented rings. *IAWA Bulletin n.s.* 8(2): 113-124.
- Požgaj, A., Chovanec, D., Kurjatko, S., Babiak, M. 1993. *Štruktúra a vlastnosti dreva. Príroda a.s., Bratislava.*
- Račko, V., Cunderlík, I. 2007 Selected Mechanical Properties of Hazel Wood“ in Norway Spruce (*Picea Abies L.*) In: *Proceedings of 5th International Symposium "Wood Structure and Properties '06" September 03-06, 2006, Sliac, Sielnica, Slovakia. Technical University Zvolen.*

Romagnoli, M., Bernabei, M., Codipietro, G. 2003. Density variations in spruce wood with indented rings (*Picea abies karst*). *Holz als Roh - und Werkstoff* 61(4): 311-312.

Schneider, L., Gärtner, H. 2013. The advantage of using a starch based non-Newtonian fluid to prepare micro sections. *Dendrochronologia* 31(3): 175-178.

Schultze, D.G., Gotze, H. 1986. Abnormal wood structure: 'hazel grain' and wavy grain. *Wood Research* 111: 1-10.

Takizawa, T., Takahashi, M., Kawaguchi, N. 1980. A note on the distribution of radial resin canals in *Larix leptolepis* Gord. *IAWA Bulletin n.s.* (1): 111-112.

Yaman, B. 2007. Anatomy of Lebanon cedar (*Cedrus libani* A. Rich.) wood with indented growth rings. *Acta Biologica Cracoviensia Series Botanica* 49(1): 19-23.

Ziegler, H., Merz, W. 1961. Der Hasel Wuchs. *Holz Roh Werkstoff* (1): 1-8.

Acknowledgments

This paper was processed in the frame of the project No. 1/0163/12 as the result of author's research at significant help of VEGA agency, Slovakia.

Improvement of Properties of Selected Wood Species Using Different Modification Techniques

First Results:

Impregnation of Beech Wood with Robinia Extracts

P. Rademacher , P. Sablík, Z. Paschová, R. Rousek, P. Pařil, J. Baar,
P. Čermák, V. Koiš, J. Dömény*

Mendel University in Brno, Faculty of Forestry and Wood Technology,
Department of Wood Science, Brno, Czech Republic

* Corresponding author

Peter.Rademacher@mendelu.cz

Abstract

Increasing demand for wood may in future be solved by plantations or utilization of lesser used wood species in addition to managed forests of common used species. Currently, wood from fast growing plantations or forest species neglected by industry is mainly used as fuel because of insufficient material properties for more effective use. Wood modification is a suitable tool to improve wood properties of species with low durability, dimensional stability or strength. Especially wood of plantation-grown species like poplar or *Robinia* is suitable to be improved, e.g. by compression-, microwave-, heat- or chemical treatments with natural substances. Whereas few processes are established, a lot of additional trials or substances represent possible targets to establish innovative wood-based materials. Mechanisms of known or new processes are more or less unknown. Investigation aims at gaining additional knowledge about cellular and sub-cellular mode of action of treatments by using structural or chemical analytical methods. The main goal is exposure of correlations between amount, position and function of added or changed molecules at cell wall level and achieved changes of wood properties.

Actual results show very first trials of property improvement of non-durable wood species using the example of beech wood impregnation with native extracts from *Robinia* heartwood or other renewable substances.

Keywords: Beech wood, *Robinia*, extracts, modification, impregnation, microwave, weight-percent-gain, durability, mass-loss, leaching

Introduction

In addition to wood production in natural forests, the establishment of plantations could help to increase the amount of available wood assortments (Murach et al. 2008, Bemmann et al. 2008). The production and utilization of renewable biomass especially from fast growing trees in short rotation plantations (SRPs) have increased during the past ten years and are important for future biomass supply with also options for different usages. Because of low material properties due to fast growing character or low wood-density (Hapla 1992, Niemz 1993) and low incorporation of heartwood-substances (Gierlinger et al. 2003), biomass from central European plantations is mainly used for energy purposes (Murach et al. 2008). First step for an increased material- and reduced energy-use of wood from fast growing plantations or also from lesser used wood species along the utilization chain is deepened knowledge about properties of native wood and their secondary improvement.

Whereas in practical wood protection the use of biocides is increasingly limited by laws, which control application of environmental toxic substances, the innovative process of wood modification works with non-toxic chemicals (Rowell 1983, Militz et al. 1997, Hill 2006), preferring types of native origin (Saxe et al. 2011). Examples are natural oils or technical produced bio-/ pyrolysis-oils as well as native phenols, which are available as extracts from residual materials (Schwager & Lange 1998, Ermeydan et al. 2012, Gierlinger et al. 2003, Grabner et al. 2005). Also utilization of nanoparticles to improve solid wood or smaller wood particles is an upcoming process with a lower chemical input and a small influence on the environment (Rassam et al. 2012). Compared to traditional wood protection with biocide-functional groups in molecule which only react toxic to wood decaying organisms, wood modification deals with changes in wood structure by adding molecules or chemical bonds, leading to higher complexity of wood structure and masked points of attack for wood decaying organisms. Additional to this, the incorporation of nature identical or similar chemical substances into the wood fibrils can also improve further properties, like dimensional stability or strength by masking hydrophilic hydroxyl-groups or stabilizing wood structure (Fengel & Wegener 1989, Grabner et al. 2005, Meier et al. 2001).

Wood assortments which need improvement of properties are wood from non-durable tree species, mostly supplied with a low amount of accessory substances, leading to low durability and low physical and mechanical properties (Gierlinger et al. 2003). Also young trees, e.g. from fast growing plantations, which have no or not finished synthesis and incorporation of heartwood-substances in cell walls and no or lower durability and dimensional stability, have to be improved in case of a higher material use by impregnation with native or close to nature substances or by densification after cell-wall plasticization with steam, heat, or microwave and/ or NH₃-treatment (Stojcev 1979, Pařil et al. 2013).

Based on first modification treatments of beech wood with non-biocide, but native and renewable substances, like extracts from natural high-durable *Robinia*-heartwood, first results of property improvements of treated wood will be shown.

Materials and Methods

Sampling and preparing of wood. Subsamples of heartwood and bark chips were taken randomly from 70- and 30–40-year-old black locust (*Robinia*) trunk and ground using Retsch SM300 mill; final material separation was performed by sifting on a 50-mesh (0.50mm screen). Miniaturized wood block test was used for young *Robinia* samples, native beech and extract efficiency evaluation against wood-rotting fungi (Bravery 1979). Methodology was based on standard EN 113 and employed wood blocks 30 mm long and 10*5 mm² in cross section prepared from reference wood species. Standard size samples with a length of 50 mm and 15*25 mm² in cross section were used for durability test of native older *Robinia* compared to native beech reference according to EN 113.

Extraction. Black locust heartwood and bark as well as African padauk heartwood powder samples with a weight of 10 g ±0.1 g were extracted by the *fexIKA* method (fexIKA 2014). Dry powder was extracted with 100 ml mixture of methanol and distilled water (1:1, v/v). The obtained extract was dried in an oven to constant weight and then cooled in desiccator. Subsequently, the quantitative amount of extractive content was determined gravimetrically from dry weight of original samples as well as specified by HPLC. Extracted compounds were re-dissolved with 100 ml of methanol, filtered and concentrated in ratio 20:1 for impregnation.

Liquid chromatography-mass spectrometry (HPLC-HRMS). LC-MS chromatograms of extracts were obtained using a Dionex Ultimate 3000 HPLC system coupled to a LTQ Orbitrap XL high resolution mass spectrometer equipped with a heated electrospray ionization source.

Impregnation. Impregnation of samples with extract-solution was conducted according to EN 113, treatment was carried out in one step using vacuum (20 kPa) maintained for one hour. Impregnated samples were placed in the conditioning chamber with a temperature of 20 °C and 65 % of rel. humidity.

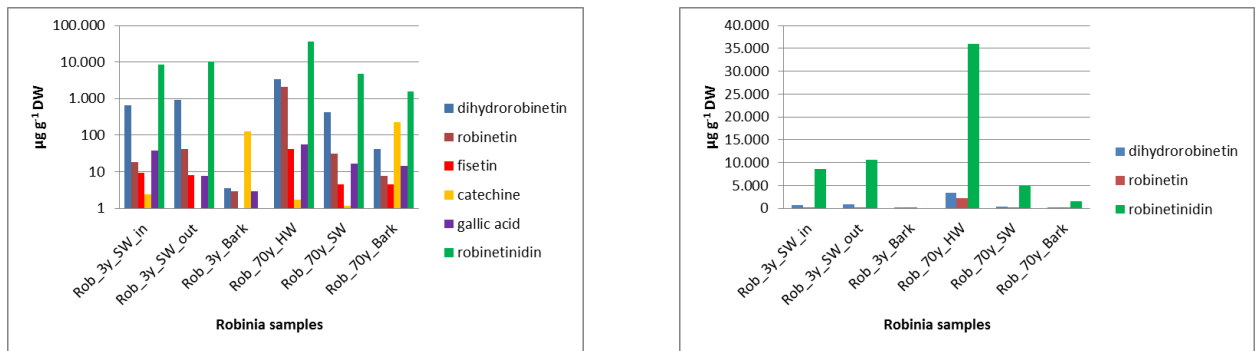
Leaching Test. Impregnated samples were leached in distilled water according to EN 84, using 5 cycles in 192 hrs. and conditioned in the chamber with a temperature of 20 °C and 65 % of relative humidity.

Durability test. Impregnated, native and non-impregnated reference wood samples were sterilized by gamma radiation (28 kGy) and put into Petri dishes (Bravery samples) or Kolle flasks (standard samples) with agar medium covered by *Trametes versicolor* culture. One reference untreated and two treated samples were placed into each dish/flask on stainless mesh. After finishing the durability test (according to EN 113 or the Bravery Test) mass loss was calculated for each sample.

Results and Discussion

Extracts. Extraction process with methanol-water mixture (1:1) resulted in a wide range of

different concentration levels of robinetinidin (RON), dihydrorobinetin (DHR), robinetin (ROB), catechine (CAT), gallic acid (GAC) and fisetine (FIS). Maxima for individual flavonoids were within the range of about 35.000 $\mu\text{g g}^{-1}$ (RON), 3.500 $\mu\text{g g}^{-1}$ (DHR), 2000 $\mu\text{g g}^{-1}$ (ROB), 250 $\mu\text{g g}^{-1}$ (CAT), 50 $\mu\text{g g}^{-1}$ (GAC) and 40 $\mu\text{g g}^{-1}$ (FIS). All named substances showed maximal concentration in older *Robinia* heartwood, with the exception of catechine (CAT), which was more or less only presented in the bark. CAT in old bark (70-year-old) was about twice as much compared to young bark (3-year-old). Also concentration of RON, DHR and FIS was about 3 to 7 times higher in old *Robinia* heartwood compared to young or older sapwood, ROB was detected 50 to 100 times more concentrated in heartwood than in young or old sapwood. Only GAC was of similar concentration in the heartwood of old as well as in older, inner sapwood of young *Robinia*, in younger, outer sap and bark



concentration was about 5-10 times lower (Fig. 1).

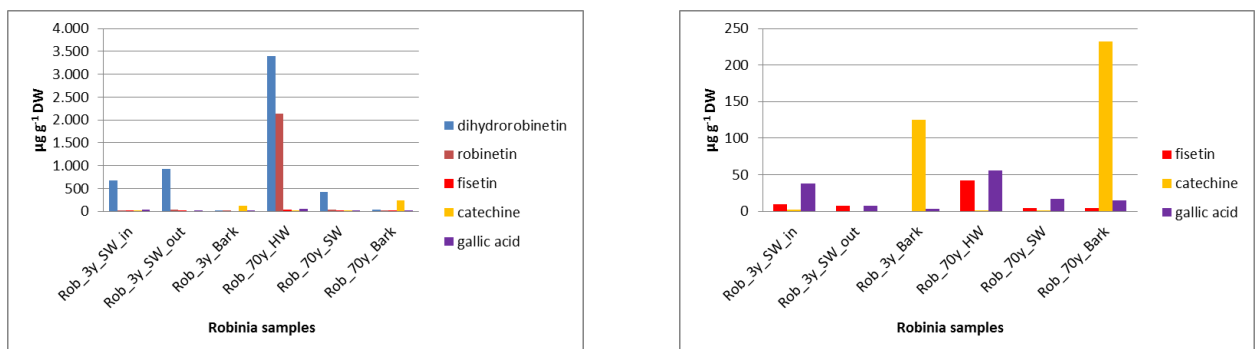


Figure 1: Concentration [$\mu\text{g g}^{-1}$] of robinetinidin (RON), dihydrorobinetin (DHR), robinetin (ROB), catechine (CAT), gallic acid (GAC) and fisetine (FIS) from methanol-water extractions (1:1) of young (3y) and old (70y) *Robinia* (Rob) sapwood (SW, inner [in] and

outer [out]) as well as heartwood (HW) and bark

The high amount of native-biocide extractives in older *Robinia* or other durable heartwoods is responsible for its high durability (Scheffer & Cowling 1966, Wagenführ & Scheiber 1974, Klumpers et al. 1994, Faix 2008); most of the named substances cause damage to wood decaying fungi (Schwager & Lange 1998, Haupt et al. 2003). The sum of only robinetinidin, dihydrorobinetin and robinetin is more than 40.000 $\mu\text{g g}^{-1}$, which is about 4%; related to determined total sum of all extractives in *Robinia* heartwood (8–9%, including sugars and other non-biocide substances), these three substances compose the main portion of the protective potential of *Robinia* extracts.

Weight-Percent-Gain (WPG) and Weight-Percent-Remain (WPR) after Leaching. All beech samples were impregnated with methanol-water extracts of heartwood from *Robinia pseudoaccacia* – compared with high durable African padauk extracts – as well as extracts from *Robinia* bark, using vacuum of 20 kPa in impregnation chamber.

The results show that impregnation with extracts, mainly those originated from *Robinia* heartwood, was quite successful: the increase in weight (weight-percent-gain [WPG]) of more than 4% after drying was about 50% of extract content in native *Robinia*, leading to durability of class 1-2 in natural heartwood. In the case of extracts from *Robinia* bark and African padauk heartwood, the WPG was lower, about 3% and 2%, respectively.

Also the extract remain after leaching with water showed a higher amount of non-leached fraction (about 30-40%) in the case of *Robinia* (and African padauk) heartwood-extract impregnation than in the case of *Robinia* bark, where the remaining fraction was lower after leaching (15-20%).

Differences in leaching ratio between microwave treated (with MW) and non-microwave-treated (without MW) were very small in the case of *Robinia* heartwood extracts, and not determinable in the case of *Robinia* bark and African padauk extracts (Fig. 2).

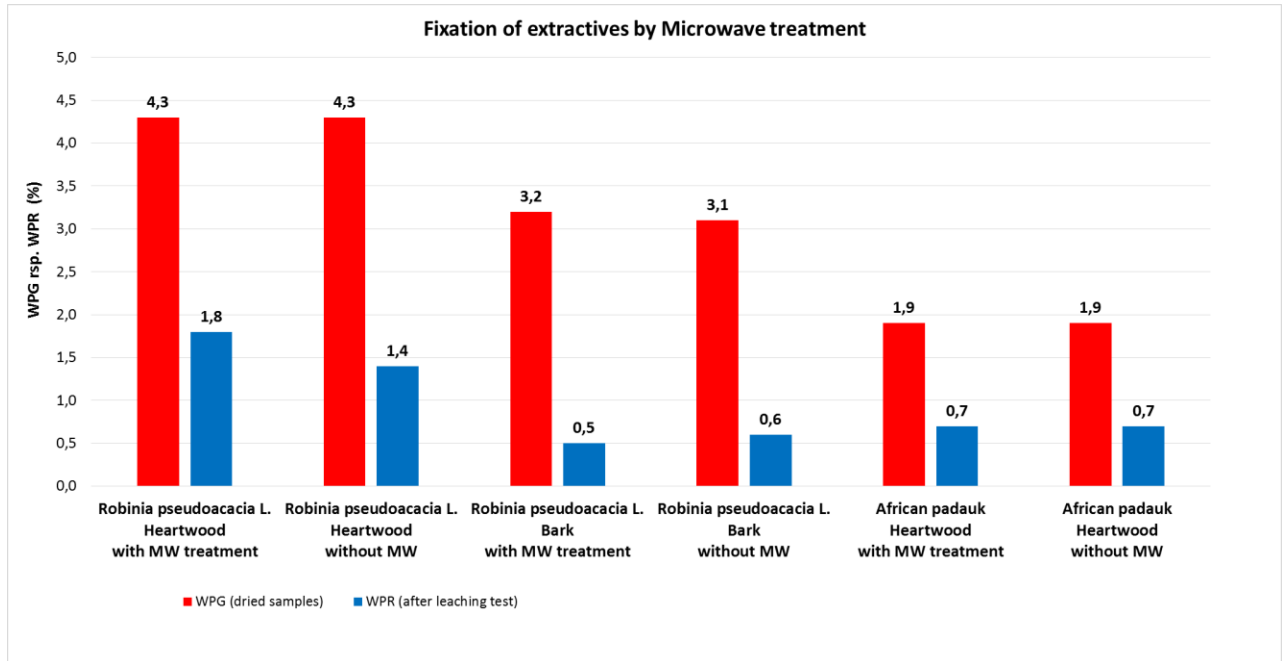


Figure 2: Weight-percent-gain (WPG [%]) of impregnated, dried Bravery beech samples (length 30 mm, cross section 10*5 mm²) and weight-percent-remain (WPR [%]) after leaching with water acc. to EN 84. Samples treated without or with microwave (MW) energy of 1 KW. N=20

Improvements in fixation or enhancements in reaction rates of impregnated substances due to chemical (Ermeýdan et al. 2012) or microwave treatment are known in the case of inorganic (Yu et al. 2010) or organic compounds (Connor & Topsett 2008), but sample size of present impregnation process with actual heartwood or bark extracts seems to be disadvantageous: energy budgets of microwave treatment, using small Bravery samples, was very uneffective, only <50% of energy was absorbed by samples; in the case of standard-sized samples results are very promising, the absorption was more effective (95-98%) and possibilities to form out new bonds between agent and hemicellulose or lignin increased (Yu et al. 2010).

Microscopic view. Microscopic view of UV-light illuminated cross sections of older Robinia heartwood as well as impregnated beech samples showed stronger detection of phenolic compound response in kind of yellow-green shining compared to younger Robinia or non-treated beech samples.

There was a ranking of shining, starting with native beech wood < young Robinia/ outer sapwood < young Robinia/ inner sapwood < Robinia-extract impregnated beech wood < old Robinia heartwood (Fig. 3).

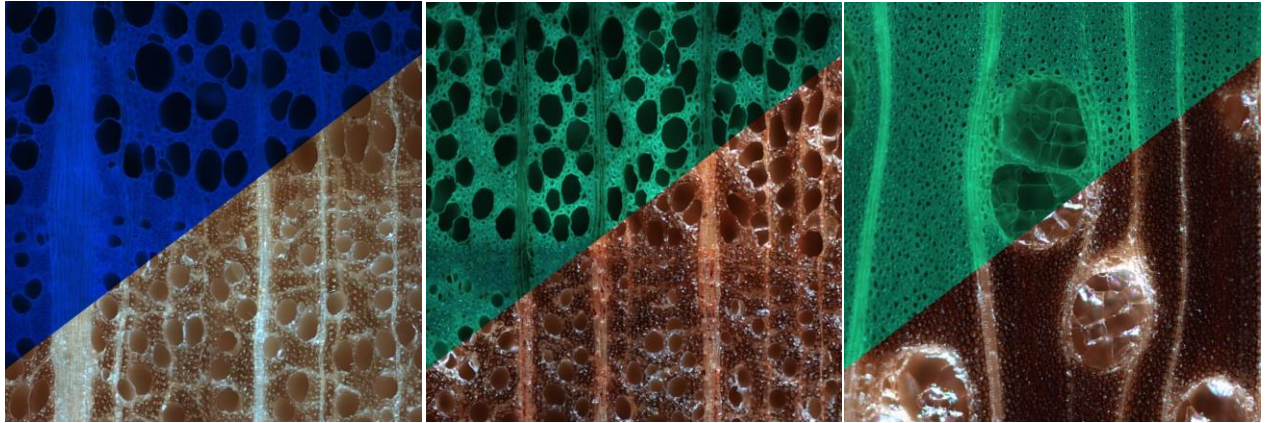


Figure 3: Increase of UV-light induced shining, detecting increasing amount of phenolic compounds in cell walls of native beech (left; upper part of picture: blue = no phenolic compounds), *Robinia*-extract impregnated beech wood (middle) and *Robinia* heartwood (right; upper part of pictures: green = detection of phenolic compounds) compared with normal light (lower part of picture: brown). Each image has dimension 0.9 x 0.9 mm² (magnification = 60x)

Durability. Mass loss due to decay (*Trametes versicolor*) of 70-year-old *Robinia* heartwood (mass loss of about 1.1%) was lower compared to 30-40-year-old heartwood (mass loss of 2.3%)

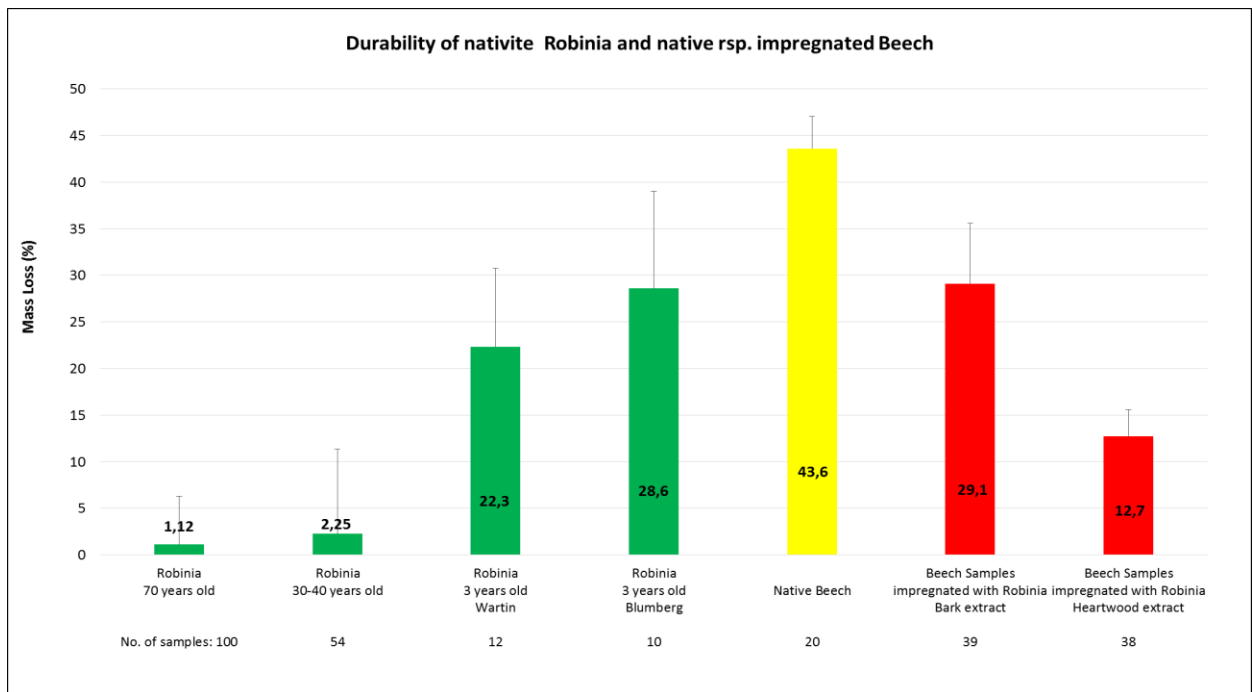


Figure 4: Mass loss (%) of native old (70-year-old, 1 site, 1 tree, 5 stem-heights and different radius-fractions) and median aged (30-40-year-old, 4 sites, each 2 trees) wood from forest located resp. young plantation related stands (3 years old, NE-German short rotation

plantation stands Wartin and Blumberg, 2 sites, each 3 trees) of *Robinia* inner stem wood (green bars) as well as non-treated (native beech, yellow) and treated beech wood, impregnated with extracts from *Robinia* bark or heartwood (red). Durability test based on Bravery test (3yr-old samples and impregnated beech) resp. according to EN 113 (70- and 30-40yr-old). Decay test with *Trametes versicolor* for 6 (Bravery) resp. 16 weeks (EN 113). No of samples: N=10 until 100 (see graphic)

and much lower compared to young plantation *Robinia* sapwood (22–29%, Fig. 4), following the amount of decay-protecting extractives in corresponding wood fractions (Haupt et al. 2003, Klumpers et al. 1994). Native beech, with very low and, due to the missing biocide character, non-protective extracts (Scheffer & Cowling 1966), was decayed by about 44%, whereas impregnation with extracts from *Robinia* bark and heartwood could decrease the amount of mass loss of treated beech wood by about 33% or 70%, respectively (Fig. 4).

Outlook

Results of leaching- and durability-tests only show a very first evaluation of impregnation process with extractives from *Robinia* biomass-assortments. Further investigations have to include leached test-samples based on standard as well as durability tests under equal conditions. However, the results already show at this early stage that durability of native *Robinia* increases with age, in other words, development of native extracts. Also improvements in durability of beech wood after impregnation with *Robinia* extracts, compared to untreated beech, are visible. However, the level of improvement and the amount of fixation of impregnated substances have to be enhanced.

First results of extract-treated beech wood are an introductory step of further treatments of non-durable or non-dimensionally stable wood from lesser used species or trees from fast growing plantations, up to now mainly used for lower valued utilizations or energy use. Upgrading of use and utilization chain is an important goal in economical and ecological use of limited recourses (FAO 2005, Mantau & Bilitewski 2005).

Acknowledgement

This article is supported by the project “The Establishment of an International Research Team for the Development of New Wood-based Materials” Reg. No. CZ/1.07/2.3.00/20.0269 and the Internal Grant Agency (IGA-V) of the Faculty of Forestry and Wood Technology, Mendel University in Brno (IGA-79/2013).

References

Bemmann, A., Pretzsch, J., Schulte, A. 2008. Tree plantations worldwide – an overview. Schw. Z Forstw. 159 (6), 124-132

Bravery A.F. 1979. A miniaturised wood-block test for the rapid evaluation of wood preservative fungicides. Doc. No. IRG/WP 2113, Stockholm: International Research Group on Wood Preservation

Connor, W.C., Tompsett, G.A. 2008. How could and do microwaves influence chemistry at interfaces? J. Phys. Chem. B. 112, 2110-2118

Ermeýdan, M., Cabane, E., Masic, A., Koetz, J., Burgert, I. 2012. Flavonoid insertion into cell walls improved wood properties. Appl. Mater. Interfaces 4: 5782–5789

Faix, O. 2008. Chemie des Holzes. In: A. Wagenführ und F. Scholz (Eds.): Taschenbuch der Holztechnik, Leipzig, 47–74

FAO 2005. Global Forest Resources Assessment 2005. Progress towards sustainable forest management, FAO For. Paper 147

Fengel, D., Wegener, G. 1989. Wood: Chemistry, Ultrastructure, Reactions. Walter de Gruyter Berlin/NY, 613 p.

fexIKA 2014. http://www.ika.de/ika/product_art/manual/ika_fexika_vc.pdf. Called 6.5.2014

Gierlinger, N., Jaques, D., Schwanninger, M., Wimmer, R., Hinterstoisser, B., Paques, L. E. 2003. Rapid prediction of natural durability of larch heartwood using Fourier transform near-infrared spectroscopy. Can. J. For. Res. 33: 1727–1736

Grabner, M., Müller, U., Gierlinger, N., Wimmer, R. 2005. Effects of Heartwood Extractives on mechanical properties of Larch. IAWA Journal 26: 211–220

Hapla, F. 1992. Holzqualität von Kiefern aus einem Waldschadensgebiet nach fünfjähriger Nasslagerung. HRW 50: 268-274

Haupt, M., Leithoff, H., Meier, D., Puls, J., Richter, H. G., Faix, O. 2003. Heartwood extractives and natural durability of plantation-grown teakwood (*Tectona grandis* L.) - a case study. Holz als Roh- u. Werkstoff. 61(6), 473-474

Hill, C. 2006. Wood Modification – Chemical, Thermal and Other Processes. Wiley Series in Renewable Resources, 239 p.

Klumpers, J., Scalbert, A., Janin, G. 1994. Ellagitannins in European Oak Wood: Polymerization during wood ageing. Phytochemistry 36(5), 1249-1252

Mantau, U., Bilitewski, B. 2005. Stoffstrom-Modell-HOLZ: Bestimmung des Aufkommens,

der Verwendung und des Verbleibs von Holzprodukten: Abschlussbericht, Studie im Auftrag des Verbandes Deutscher Papierfabriken e.V. (VDP), 65 p.

Meier, D., Andersons, B., Irbe, I., Tshirkova, J., Faix, O. 2001. Preliminary study on fungicide and sorption effects of fast pyrolysis liquids used as wood preservatives. In: Bridgwater AV, ed. Progress in Thermochemical Biomass Conversion. Vol 2. Abingdon, UK: Blackwell Science; 2001:1550-1563

Militz, H., Beckers, E. P. J., Homan, W.J. 1997. Modification of solid wood: research and practical potential. Stockholm, Inter. Res. Group on Wood Preservation, IRG/WP 97-40098. 19 p.

Murach, D., Knur, L., Schultze, M. 2008. DENDROM-Zukunftsrohstoff Dendromasse. Verlag Kessel, 514 p.

Niemz, P. 1993. Physik des Holzes und der Holzwerkstoffe. DRW-Verlag, 243 p.

Pařil, P., Brabec, M., Rousek, R., Maňák, O., Rademacher, P., Čermák, P., Dejmál, A. 2013. Physical and mechanical properties of densified beech wood plasticized by ammonia. Pro Ligno 9 (4), 195-202

Rassam, G., Ghofrani, M., Taghiyari, H. R., Jamnani, B., Khajeh, M. A. 2012. Mechanical performance and dimensional stability of nano-silver impregnated densified Spruce wood. Eur. J. Wood Prod. 70: 595–600

Rowell, R. M. 1983. Chemical modification of wood. For. Prod. Abstracts 6: 363–382

Saxe, F., Singh, A., Eder, M., Singh, T., Burgert, I. 2011. Micromechanical and structural characterization of chitosan impregnated Radiata pine (*Pinus radiata*) wood. Novel Materials from wood or cellulose; IAWA International Conference 31st August – 2nd September 2011

Scheffer, T. C., Cowling, E. B. 1966. Natural resistance of wood to microbial deterioration. Annual Rev. Phytopath. 4, 147-168

Schwager, C., Lange, W. 1998. Biologischer Holzschutz. Schriftenreihe Nachwachsende Rohstoffe 11, 727 p.

Stojcev, A. 1979. Lignamon – Zušlechtěné dřevo. Výroba, vlastnosti a použití. Práce Vvúd Sv. 22

Wagenführ, R., Scheiber, C. 1974. Holzatlas. VEB Fachbuchverlag, Leipzig

Yu, L., Gao, W., Cao, J., Tang, Z. 2010. Effects of microwave post-treatments on leaching resistance of ACQ-D treated Chinese fir. *For. Stud. China* 12(1), 1-8

CO₂ Balance of Wood Wall Constructions Compared to Other Types of Wall

Péter RÉBÉK-NAGY, Zoltán PÁSZTORY

Innovation Center, University of West Hungary,
Sopron, Hungary

Abstract

Nowadays the CO₂ emission is a highly dealt issue, therefore a lots of efforts were taken to mitigate climate change. This study also tries to give some data for the mentioned pursuit. Twelve wall structures were examined in different versions such as brick, gas concrete, American and European light-frame wood structure, log homes with inner and exterior insulation. Thermal transmittance coefficient of wall structures was chosen to the same value (0.13 W/m²K) for being comparable. That is why the wall structures were adjusted with different insulation thickness. Embodied energy (CO₂ equivalence) was calculated of all elements of wall layers, this is the energy amount of which were consumed during manufacturing process. There are materials containing significant amount of carbon. In this case the equivalent stored CO₂ was calculated too. According to the results three groups were formed. The most unfavorable CO₂ balanced structures were the silicate based walls which causing high amount of CO₂ emission in one square meter wall surface (103-154 kg/m²). Moderately CO₂ balanced were those mixed organic and inorganic structures (0-23 kg/m²). In the third group the CO₂ balance were negative, what means the related emitted CO₂ was less than the stored in the materials built in the wall structure (-162 -0 kg/m²). The numbers shows the emitted and/or stored CO₂ related to one square meter of wall surface. It can be stated that the wood frame and log buildings store more carbon than the CO₂ equivalent embodied energy consequently this type of buildings seem to be the most appropriate regard to the ecological architecture.

Key words: CO₂ balance of wall structures, CO₂ emission, embodied energy, wood frame buildings, log homes,

Péter Rébék-Nagy
University of West Hungary
Innovation Center
Sopron 9400 Bajcsy-Zs. u. 4. Hungary
+36-99-518-226
peter.rebek-nagy@skk.nyme.hu

*Proceedings of the 57th International Convention of Society of Wood Science and Technology
June 23-27, 2014 - Zvolen, SLOVAKIA*

Zoltán Pásztor
University of West Hungary
Innovation Center
Sopron 9400 Bajcsy-Zs. u. 4. Hungary
+36-99-518-298
zoltan.pasztor@skk.nyme.hu

Non-Wood Lignocellulosic Composites

Roman Réh^{1} – Marius C. Barbu² – Ayfer D. Çavdar³*

¹ Associate Professor, Department of Mechanical Technology of Wood,
Faculty of Wood Science and Technology, Technical University in Zvolen,
Zvolen, Slovak Republic.

reh@tuzvo.sk

** Corresponding author*

² Professor, Salzburg University of Applied Sciences, FH-Salzburg,
Kuchl, Austria

marius.barbu@fh-salzburg.ac.at

and

University "Transilvania" Brasov, Faculty for Wood Engineering,
Brasov, Romania.

cmbarbu@unitbv.ro

³ Assistant Professor, Karadeniz Technical University,
Faculty of Architecture, Trabzon, Turkey

adonmez@ktu.edu.tr

Abstract

With appropriate treatment almost any agricultural residue may be used as a suitable raw material for the wood-based panels production. The literature on wood-ligno-cellulose plant composite boards highlights steady interest for the design of new structures and technologies towards products for special applications with higher physical and mechanical properties at relatively low prices. Experimental studies have revealed particular aspects related to the structural composition of lignocellulose materials, such as the ratio between the different composing elements, their compatibility, and the types and characteristics of the used resins. Various technologies have been developed for designing and processing composite materials by pressing, extrusion, airflow forming, dry, half-dry, and wet processes, including thermal, chemical, thermo-chemical, thermo-chemo-mechanical treatments, etc. Researchers have undertaken to determine the manufacturing parameters and the physical and mechanical properties of the composite boards and to compare them with the standard particleboard, medium density fiberboard, hardboard, or softboard made from wood. A great emphasis is placed on the processability of the lignocellulose composite boards by classical methods, by modified manufacturing processes, on the types of tools and processing equipment, the automation of the manufacturing technologies, the specific labor conditions, etc.

Keywords: composites, non-wood lignocellulosic composites, wood based panels.

Flax, Hemp, and Jute

Flax (*Linum usitatissimum* L.), hemp (*Cannabis sativa* L.) and jute (*Corchorus capsularis* L.) are plants with rich content of cellulose both in their wooden parts and in the fibers used for the production of engineered sheet composites flaxboard, hempboard and juteboard. Shives from the stalk of the flax (hemp, jute) plant are in fact by-products of the linen industry. Flaxboard, hempboard and juteboard are non-structural products. The flaxboard industry in Europe (Belgium, France, Sweden, Germany, Slovakia, and Czech Republic) dates from the late nineteen fifties and until recently. Flax shives from the stalk of the flax plant comprise the bulk of flaxboard and are prepared in a mechanical chipper and can also contain other raw materials such as particles of wood (wood, flakes, chips, shavings, saw dust and similar materials). These chips are compressed and are generally bound together with synthetic resin systems such as urea-formaldehyde (UF) or melamine urea-formaldehyde (MUF), though phenol-formaldehyde (PF) and polymeric methylene di-isocyanate (pMDI) by some manufacturers. Another way to utilize flax or hemp shives is their addition to the core layer of particleboard in certain ratios as the substitution of wood. It is possible to consider adjustment of particleboard layers in order to improve their overall properties and they take into account the effect of different hydrophobic agents, fillers, fungicides, insecticides and flame retardants in layers of particleboard. The option of replacing wood chips with hemp shives in the production of particleboard and also the possibility to produce a lightweight board was considering with the idea to reduce density of triple-layer particleboard by using hemp shives.

Bagasse

Bagasse is the residue fiber remaining when sugar cane (*Saccharum officinarum* L.) is pressed to extract the sugar. Some bagasse is burned to supply heat to the sugar refining operation. Some is returned to the fields, and some finds its way into various board products. There is approximately 1.7 billion tons of annual production of sugar cane in the world. Bagasse is composed of fiber and pith. The fiber is thick walled and relatively long (1 – 4 mm). For use in composites, fibers are obtained mostly from the rind, but there are fibrovascular bundles dispersed throughout the interior of the stalk as well. Only bagasse fiber is utilized for the production of high-quality composites. Various schemes are available to separate the bagasse fiber from the pith. The fibers after depithing are more accurately described as fiber bundles that can be used “as is” to make particleboard, or they can be refined to produce fibers for fiberboard.

Cereal Straw

Cereal straw represents another important raw material source (over 500 million tons without rice and maize), successfully used in composites producing. Cereal straw, like bagasse, is an agricultural residue. Unlike bagasse, large quantities of cereal straw are generally not available at one location. Storage is usually accomplished by baling. The bales must then be transported to a manufacturing facility. Straws have a high ash content

thus tending to fill fireboxes in boilers. Their high inherent silica content results in increased tool wear compared to other lignocellulosic composites and could be a problem for further use. Conversely, the high silica content also tends to make them naturally fire-resistant. The manufacturing technology for such composites is similar to that used in the production of particleboard. The alterations are the following:

- The transportation and preparatory operations of raw materials have been simplified and adapted to this category of plants.
- The storage silos for chipping and glued material were over-dimensioned, due to the low bulk density of straw and the massive seasonal accumulation of material.
- The cut-to-size and sanding equipment were provided with abrasion-proof tools specific for this type of boards.

Kenaf

Kenaf (*Hibiscus cannabinus* L.) is a hibiscus, and it has a pithy stem surrounded by fibers. The fibers make up 20 – 25 % of the dry weight of the plant. Mature kenaf plants can be 5 m high. Kenaf has the long aspect ratio of fibers and fiber bundles which is possible to exploit for fiberboard production. After a resin is added to kenaf fibers, they can be pressed into flat panels or molded into shapes, such as interior car door substrates. Kenaf is not abrasive during processing, has a low density and high specific mechanical properties and is biodegradable.

Palm Wood

In warm climate areas, palm wood (*Palmae* spp.) represents an important source of raw material for lignocellulosic composites. In the palm tree cultivation areas located in the southeastern part of Asia biomass quantities as high as about 85 – 90 million tons are achieved by silvicultural operations in plantation or by replacement after the 20 year rotation time. Palm tree trunks weigh 500 kg including 20 % fibers; all the rest is pith and other substances.

Cotton Stalks

The cotton cultures (*Ceiba pentandra* [L.] Gaertn.), specific for areas lacking abundant forest vegetation, are another important source of lignocellulosic raw materials for composites. Cotton is cultivated primarily for textile fibers, and little use is made of the cotton plant stalk. Stalk harvest yields tend to be low and storage can be a problem. The cotton stalk is plagued with parasites, and stored stalks can serve as a breeding ground for the parasites to winter over for next year's crop.

Rice Husks

Rice as a grain plant (*Oryza sativa* L.) is produced in temperate zone reaching an amount of almost 700 million tons in the world. The dominant producers are major world's nations China, India, USA, Bangladesh, Indonesia, Japan, Philippines, Russia, Thailand, and Vietnam. One of the valuable uses of rice straw with high cellulose content is in the panel industry (particleboard, cement bonded boards, and MDF). Production of rice straw boards with performance rivaling wood-based boards at lower production cost utilizing a simpler process is still the main challenge to be addressed on a global scale.

Maize

Maize cultures (*Zea mays* spp.) under all its forms provide raw material (1 billion tons) for composites. Attempts made to produce boards with possible uses for interior applications (particleboard), insulation or in the automobile industry (to replace the use of plastics) open other opportunities for superior uses of maize residues.

Sunflower

Sunflower (*Helianthus* spp.) has low fiber content and therefore develops low strengths in sunflower-based boards. The wood content in the medullar and parenchyma areas of the stalk supports the production of insulating boards that meet the mechanical standards stipulated in the technical standards.

Peanut and Hazelnut

In some countries, peanut husk (*Arachis hypogaea* L.) and residues of nuts represent another valuable source for lignocellulosic composites. Hazelnut husks and shells (*Coryllus arellana* L.) are abundant but they have not drawn much attention as an agricultural residue that can be used in wood processing industry. Turkey is the biggest hazelnut producer and exporter in the world producing 70 % of the amount. Approximately 400,000 – 500,000 tons per year of husk residues are estimated to be burned or left in the field after harvest and there exists no reasonable utilization. Hazelnut husk is a lignocellulosic material and contains 34.5 % cellulose, 20.6 % hemicelluloses and 35.1 % lignin. It was investigated the potential utilization of hazelnut husks in tree-layer particleboard.

Coconut Wood and Husks

Coconut (*Cocos nucifera* L.) is found throughout the tropics and in major parts of the subtropics as an agricultural crop. As usual, every part of the coconut can be used as food, drink, oil, medicine, fiber, timber, thatch, mats, fuel, and domestic utensils. When the production is uneconomical, the trees are felled for replanting.

Other Agricultural Residues

Banana (*Musa* sp.), tea leaves (*Luffa cylindrical* (L.) Roem.), canola/rapeseed (*Brassica napus* L. and *Brassica napus* var. *Oleifera* L.), bamboo (*Bambusa* spp.), reed (*Phragmites communis* Trin.), mace reed (*Polygonum* spp.), maiden grasses (*Miscanthus* spp.), silver grass (*Miscanthus sinensis* Andersson), kiwi prunings (*Actinidia* spp.), grapevine canes (*Vitis* spp.), rhododendron (*Rhododendron ponticum* L.), or papyrus (*Cyperus* spp.) are other lignocellulosic raw material sources.

References

Barbu, M. C. - Réh, R. – Çavdar, A. D.: Non-Wood Lignocellulosic Composites. In: Research Developments in Wood Engineering and Technology, edited by Alfredo Aguilera and J. Paulo Davim. Non-Wood Lignocellulosic Composites, Chapter 8. Hershey PA: IGI Global, 2013, ISBN 978-1-4666-4554-7. pp. 281-319.

Acknowledgements

The research described in the paper presented was supported by grant No. 01/0345/12 from the Slovak Grant Agency (Interaction of the Components of Wood and High Temperatures during Pressing of Wood Composites and its Effect on the Formation of Composites Avoiding the Chemical Changes in Composition of Pressed Wood Particles and Elimination of the Fire Risk). The authors would like to thank the grant agency for the support of this research.

The Role of Fibre Characteristics for Online Process Adaptation in the Manufacturing of MDF

Martin RIEGLER, Martin WEIGL, Ulrich MÜLLER

The characterisation of wooden fibres that are used for producing medium density fibreboards (MDF) is still not routinely implemented in the industrial manufacturing process. However, the knowledge of the interaction between processing parameters, fibre characteristics and final board properties is of major interest, when optimising the production process.

In this study, an easy to apply laboratory approach for characterising the geometry of MDF fibres is presented. In particular, a random sample of fibres was withdrawn from the industrial production process of manufacturing MDF after forming. The sample of fibres were spread onto a black ISO216 A4 sized paper and fixed using a self-adhesive transparency film. Fibres were scanned with a conventional flat bed scanner and analysed using the free image processing software ImageJ. The length of fibres was calculated using a skeletonisation algorithm, which enables an accurate determination of the length of curved particles.

Adding the obtained information of fibre geometry to the multivariate data analysis of manufacturing MDF, the modelling of mechanical properties of boards could be improved. In particular, the fibre length was selected as third most important variable for predicting the internal bond strength of MDF using partial least squares regression, resulting in an error of 4.8 % (mean normalised root mean squared error of prediction).

The presented approach of determining fibre geometry is easy to apply in a laboratory scale, does not require high investment costs and provides a representative overview of the geometry of particles.

Keywords: skeletonisation, ImageJ, multivariate regression analysis, knowledge-based process adaptation

Martin RIEGLER

Wood K plus – Competence Centre for Wood Composites and Wood Chemistry

Konrad Lorenzstraße 24

3430 Tulln, Austria

+43 1 47654-4265

E-Mail: m.riegler@kplus-wood.at

Martin WEIGL

Holzforschung Austria

Franz Grill-Strasse 7

1030 Wien, Austria

+43 1 798 26 23-839

E-Mail: m.weigl@holzforschung.at

Ulrich MÜLLER
Institute of Wood Science and Technology
University of Natural Resources and Life Sciences
Konrad Lorenzstrasse 24
3430 Tulln, Austria
+43 1 47654-4252
E-mail: ulrich.mueller@kplus-wood.at

Introduction

In high technological manufacturing processes, parameters from processes and machines are well recorded and understood. However, raw material parameters are often neglected. In the case of process control of manufacturing fibreboards, morphological parameters of wooden fibres are hardly considered. One reason for this lack of information could be the difficulties that arise when characterising inhomogeneous natural raw materials such as wood. Up to now only few appropriate characterisation devices are available (e.g. Camsizer, FIBERCAM, FibreShape, QIC-PIC, QualScan). Pieper et al. (2011) developed a method to detect shives on the surface of MDF. Based on these findings, Benthien et al. (2014) recently published a device that is able to measure fibre morphology automatically. They state high reproducibility and the possibility of detecting differing process conditions. Plinke (2012) introduced a technique to analyse particles without pre-separation, which would be beneficial for online process control. However, this approach cannot be applied on unseparated fibres but on particles dedicated for manufacturing oriented strand boards.

As wooden fibres, used for MDF, are usually curved, a special algorithm is needed to determine their length and width. One possibility is the medial axis transformation of two-dimensional objects, which is also known as skeletonisation. In past studies, the medial axis transformation was also used to determine the length of cotton fibres (Wang 2007).

The aim of the present study was to establish an easy to apply and low cost intensive approach to determine fibre morphology, using the proposed method of fibre preparation, image analysis and automatic analysis of morphological parameters.

Material and Methods

Wooden fibres, used for the manufacturing of medium density fibreboards (MDF), were withdrawn from the industrial manufacturing process between the forming station and the prepressing of the formed fibre mat. These fibres were already resinated and had a moisture content of 10 % in average. For preservation purposes, the fibres were dried to oven dry weight using a kiln at 103 °C. Per sample, 7 mg of fibres were used for fibre characterisation, which represented a number of fibres between 25,000 and 50,000. In total, 115 batches of fibres were investigated.

The fibres were evenly spread onto a black ISO216 A4 sized paper that was placed within an open-top box, using a sieve with a mesh size of 0.5 mm (Fig. 1). The reason for the black background paper was to avoid the creation of shadows during scanning, as these would have overestimated the size of the fibres. Afterwards, overlapping particles were separated using tweezers. The so positioned fibres were fixed using a self-adhesive transparency film. This prepared sheet was scanned using a flatbed scanner to create a grey scale image with a resolution of 1000 dpi. Images were stored in the tagged image file format (tif). The contrast of the images was set to + 20. To remove artefacts from the transparency film from the edges, the edges were stained black using Adobe Photoshop. The so prepared images were read and analysed by a developed macro written in the software ImageJ. Here, undertaken steps for image analysis were the definition of the scale (25.4 mm = 1000 pixel), the definition of parameters to be analysed (area, perimeter, fit, shape, feret's diameter), the definition of the minimum size of particles to be analysed (0.005 mm² - due to limited processor capacities), the application of the skeletonisation algorithm and saving the results as text file.



Fig. 1 Spreading and separating fibres onto a black background

To detect the realistic length of curved particles, the so-called skeletonisation algorithm introduced by Zhang and Suen (1984) was used, where the medial axis through a particle is determined (Fig. 2). This technique, first described by Blum (1967), enables the detection of the actual length of curved particles. The skeletonisation algorithm initially defines the endpoints of a particle. Afterwards, pixel per pixel is symmetrically removed at the circumference of the particle until only one row of pixels remains in the centre. The length of the particle can easily be calculated by counting the pixels of this single row (black line in Fig. 2). Branches are also detected by the algorithm, but were not considered in the present analysis. The slenderness ratio was determined using the perimeter and the area of particles, according to formula 1. Slender particles would have circularities towards zero and rather circular particles would have circularities towards one.

$$circularity = 4 * \pi * \frac{area}{circumference^2} \quad (1)$$

The width of fibres was determined by dividing the area of one particle by its length, resulting in an average width of the entire fibre. The results obtained from ImageJ, were further analysed in MATLAB to calculate statistics and create plots.



Fig. 2 Curved wooden fibre (grey) with calculated medial axis for determining the actual fibre length (black line) and length of branchings (white)

Results and Discussion

Qualitative comparisons with real measurements have shown, that the real length of fibres could be detected very accurately using the skeletonisation algorithm. The arithmetic mean of the length of all analysed fibres was 0.43 mm (Fig. 3, a), which was highly influenced by the high proportion of short fibres, as 44 % of the fibres were shorter than 0.1 mm (Fig. 3). This right-skewed distribution of fibre lengths was also found in Benthien et al. (2014), who stated that 90 % of their fibres were shorter than 1 mm.

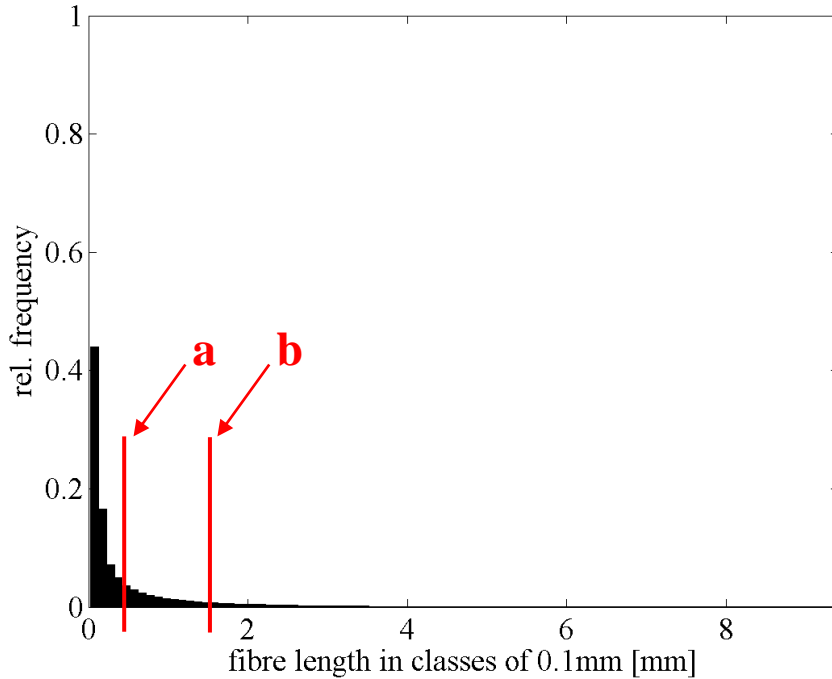


Fig. 3 Frequency of fibre lengths classified in 0.1 mm steps (a = arithmetic mean; b = length weighted mean)

As longer fibres are considered to determine final board properties significantly, an additional statistical parameter was calculated that promotes longer particles. Thus, the length weighted length (lwl) was calculated by summing up the squared lengths of fibres divided by the total sum of fibre lengths (formula 2). This approach is also commonly used in paper industry to determine the technologically important length of paper fibres (Clark 1985). Similarly, Benthien et al. (2014) used a double length-weighted fibre length. In the present study, the average fibre length increased from 0.43 mm to 1.72 mm (Fig. 3, b) by calculating the lwl.

$$lwl = \frac{\sum l^2}{\sum l} \quad [mm], \quad (2)$$

The distribution of the fibre area showed a similar skewness as the distribution of the fibre length (Fig. 4). The high frequency of small fibres could also be seen when comparing with a typical spruce fibre (length: 4 mm, width: 0.04 mm, area: 0.16 mm²). Here, 85 % of the fibres were smaller than this typical softwood fibre, which indicates a high proportion of fibre fracture.

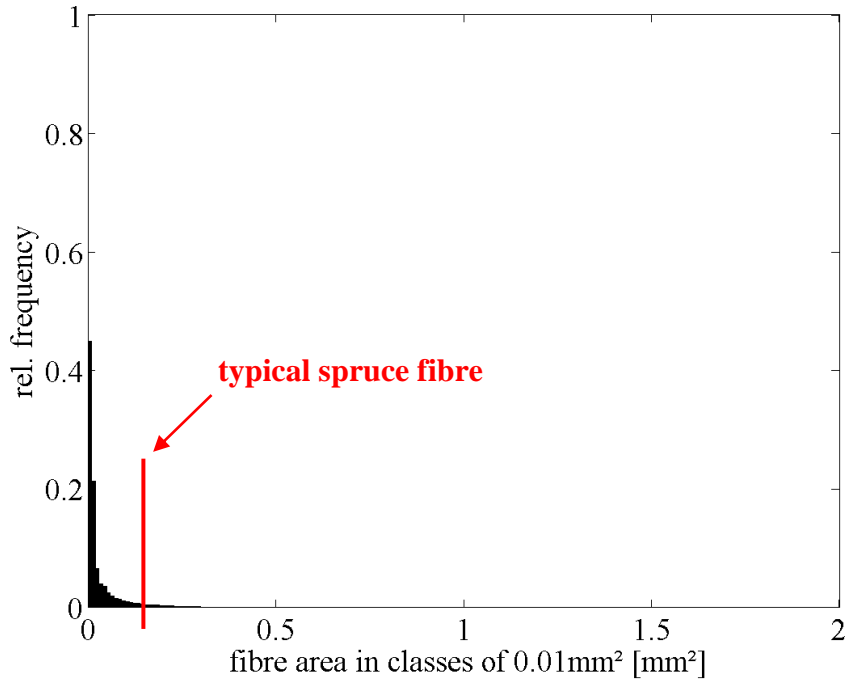


Fig. 4 Frequency of fibre areas with size of a typical spruce fibre

The slenderness ratio of fibres confirmed the findings in fibre length and area, as 30 % of the fibres were rather circular (circularity: 0.9-1) and only 5 % were rather slender (circularity: 0-0.1) (Fig. 5). As small particle fractures usually tend to be rather circular, it can be assumed that a high proportion of fibre fractures occurred during the defibration process.

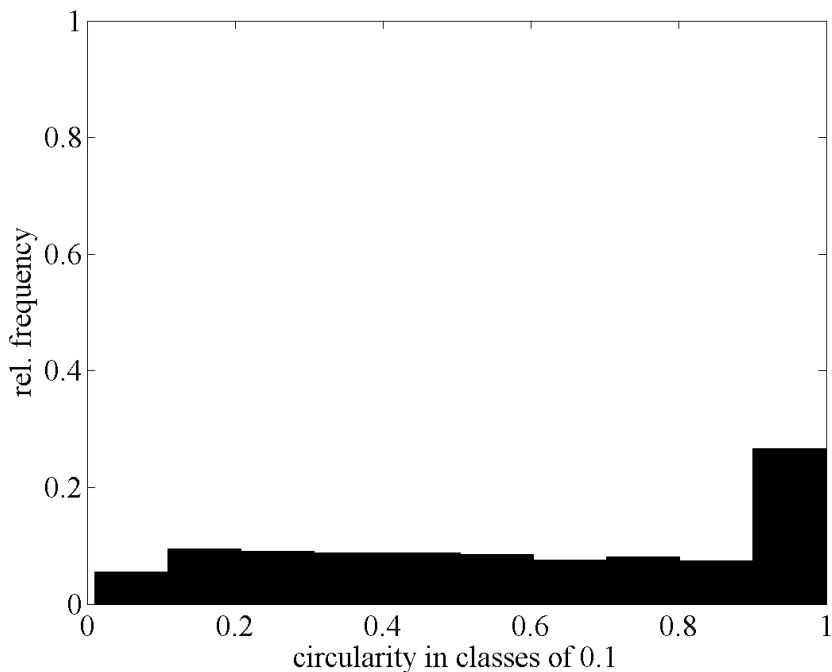


Fig. 5 Distribution of the circularity of fibres (0 means perfectly slender, 1 means perfectly circular)

The above mentioned hypothesis of a high amount of fibre fractures can also be verified when analysing the width of fibres by their class of circularity. There, the average width of rather slender fibres (circularity: 0-0.1) was 0.08 mm, whereas the average width of rather circular fibres (circularity: 0.9-1) was about twice as high (0.17 mm).

The addition of fibre morphology parameters to process data improved the models obtained from multivariate regression analysis. In particular, the fibre length was statistically selected as third most important variable (behind board density and steam consumption for cooking wood chips) for predicting the internal bond strength of MDF using partial least squares regression. In this preliminary test of modelling final board properties, an increased length of slender fibres (circularity: 0.1-0.2) improved the internal bond strength. The resulting mean normalised root mean squared error of prediction (MNRMSEP) was 4.8 %. For comparison, models without considering fibre morphology revealed a significantly higher MNRMSEP of 7.3 %.

Conclusion

The proposed laboratory approach of determining fibre morphology is easy to implement and does not need high investment costs. The amount of fibres analysed per time should be increased by automation, e.g. automatic sample preparation. Due to the scanning technique and the skeletonisation algorithm used, the approach provides accurate results of the fibre length. The possibility of classifying the analysis of fibres regarding their slenderness ratio facilitates the interpretation of fibre characteristics and the underlying process conditions. Additionally, the inclusion of fibre characteristics in PLSR modelling enhanced the predictability of final board properties, which reveals the significant influence of raw material properties in process modelling.

References

- Benthien JT, Bähnisch C, Heldner S, Ohlmeyer M (2014) Effect of fiber size distribution on medium-density fiberboard properties caused by varied steaming time and temperature of defibration process. *Wood and Fiber Science* 46 (2):1-11
- Blum H A Transformation for Extracting New Descriptors of Shape. In: Wathen-Dunn W (ed) *Models for the Perception of Speech and Visual Form*, Cambridge, MA, 1967. MIT Press, pp 362-380
- Clark J (1985) *Pulp technology and treatment for paper*. 2. edn. Miller Freeman Books, San Francisco, Cal.
- Pieper O, Bückner J, Seppke B, Ohlmeyer M, Hasener J Faserinspektion zur Optimierung der Oberflächenqualität. In: *Proceedings of the 8th Fußbodenkolloquium*,

- Dresden, Germany, 10-11 November 2011 2011. Institut für Holztechnologie
Dresden (IHD),
Plinke B (2012) Größenanalyse an nicht separierten Holzpartikeln mit regionenbildenden
Algorithmen am Beispiel von OSB-Strands. Technischen Universität Dresden,
Dresden
Wang HBE (2007) Fiber Property Characterization by Image Processing. Texas Tech
University, Lubbock
Zhang TY, Suen CY (1984) A fast parallel algorithm for thinning digital patterns.
Communications of the ACM 27 (3):236-239

Errors of Sampling Based Moisture Content Measurement of Wood

Ildikó RONYECZ, Kristóf MOHÁCSI, Zoltán PÁSZTORY

Innovation Center, University of West Hungary,
Sopron, Hungary

Abstract

The atro-weight based measurement of wood-assortment in the forest is becoming more prevalent, than the volume based one. The measurement related to absolute dry moisture content has an uncertainty owing to the inhomogeneity of wood. Thus the measuring accuracy getting more and more important at the measurement, since a small difference of percent can cause a large fault in the real wood quantity. Due to the anisotropy and capillary porous nature of wood the moisture content can show serious differences, already in the living tree. These differences can grow further at the case of fell tree. The difference between the chain saw and drill sampling had revealed in our experiment just as the possible sources of errors originated from storing and measuring of wood. In industrial practice the chain saw sampling is wide spread, in which series of error possibilities are emerging. The errors can come from the high revolution number of chain saws under operation and using of chain lubricating oil supplying friction-reducing function. The friction resulted heat can cause evaporation water from sample. During the procedure, the oil splashed to the shavings brings an unknown magnitude and direction of uncertainty in the system. The possible differences in the measured and the real moisture content caused by the depth and the time of sampling and the circumstance of sample's storing were determined. Nowadays to explore the errors of chain saw sampling is important question for the industry. According our results the error can reach even 5-3% of moisture content. The scientific examination of the mentioned errors is required and serves with valuable information.

Keywords: moisture measurement, moisture content of wood, chain saw sampling, errors of moisture content measurement

Ildikó Ronyecz, Kristóf Mohácsi, Zoltán Pásztory
University of West Hungary
Innovation Centre
Bajcsy-Zs. u. 4. 9400 Sopron Hungary
+36-99-518-298
zoltan.pasztory@skk.nyme.hu

Stereomicroscopic Optical Method for the Assessment of Load Transfer Patterns Across the Wood-Adhesive Bond Interphase

Matthew Schwarzkopf

PhD Candidate, Wood Science and Engineering, Oregon State University
173 Richardson Hall
Corvallis, OR 97331
matthew.schwarzkopf@oregonstate.edu

Lech Muszyński

Associate Professor, Wood Science and Engineering, Oregon State University
106 Richardson Hall
Corvallis, OR 97331
lech.muszynski@oregonstate.edu

Abstract

Mechanical performance of wood-based composites is determined by the mechanical properties of their individual components and the effective load transfer between these components. In laminated wood composites the adhesive bond facilitates this load transfer and holds the laminates together. An understanding of how the adhesive contributes mechanically to the bulk composite material will allow adhesive and composite manufacturers to better formulate and construct their products. The experimental methodology developed in this study measures and analyzes full-field deformation and strain distributions across the loaded wood-adhesive interphase at a micro-mechanical level. Optical measurements based on digital image correlation (DIC) principles were taken using a stereomicroscopic camera system. This system allows monitoring of in plane deformations as well as out of plane displacements, providing full-field 3D surface strain maps across the adhesive bond. These measurements can be used to improve the understanding of the load transfer between the adherends and serve as rich quantitative input for numerical modeling and simulations.

Keywords: digital image correlation (DIC); load transfer; micromechanics; optical measurement; adhesive interphase

Introduction

The mechanical performance of adhesive bonded wood-based composites is determined by the mechanical properties of their individual components and the internal bonds

providing effective load transfer between these components. During manufacture, the pre-polymeric adhesive may penetrate into the wood cell wall structure and when cured will form a polymerized adhesive system. The performance of the wood-adhesive system may to some extent be modified by changing the composition and the internal structure of the bond by adjusting certain processing parameters like the resin viscosity, resin spread rates, and bonding pressures. Currently, we lack a quantifying metric of this performance that captures the efficiency of the load transfer across the adhesive bond interphase. One such metric would allow for the comparison and ranking of bonds obtained with various adhesive systems or various bonding parameters.

The study presented in this paper was part of this larger project and was used for the development, optimization, and validation of a multi-modal, morphology specific numerical model. The specific objective of this study was to create a methodology for measuring and assessing the full-field deformation and strain distribution across the loaded wood-adhesive interphase at a micro-mechanical level. Consequently, the objective of this paper is to present methodological aspects of this study with only as much results as was necessary to illustrate the process.

Materials and Methods

The approach of this study was to measure surface displacements and strains across the adhesive bond in small bond specimens subjected to micro-scale lap-shear tests. Three wood species and adhesives were chosen: Douglas-fir (DF), southern yellow pine (SYP), hybrid poplar (HP), and phenol-formaldehyde (PF), polymeric methylene diphenyl diisocyanate (pMDI), and poly (vinyl acetate) (PVAc). The adhesives were prepared with a contrasting agent in order to achieve increased x-ray attenuation in XCT scans. The specific formulations of the doped resins are described in Paris et al.(2014). The specimens of approximately 2 mm x 2 mm x 15 mm (R x T x L) were cut from two-layer laminates in six replicates of each of the selected wood species/adhesive combinations (a total of 54 specimens). Next, one radial-longitudinal plane of each specimen was microtomed to create a flat surface for optical measurements. Finally, a notch was created on each side by removing material using a small file and a razor blade to prepare the specimens for the micro lap shear tests (Figure 60B).

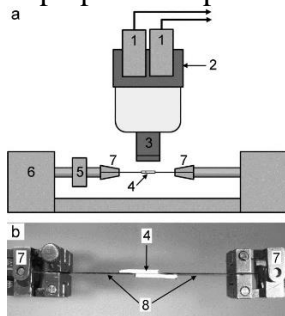


Figure 60. (a) Universal test machine showing lap-shear specimen and DIC optical measurement system; (b) Example of a lap-shear specimen with ends bonded to

graphite-epoxy tabs for attachment to test machine; 1 cameras, 2 beam splitter, 3 microscope objective, 4 specimen, 5 load cell, 6 test frame, 7 grip, 8 graphite-epoxy tab.

At this stage, XCT scans were completed on all of the specimens to record the morphological structure of the bond interphases (Paris et al. 2014). To achieve micron level resolution in the scan data, the total specimen scan volume was limited to 26.2 mm³ which defined the lap shear specimen size. Following the scanning procedure, epoxy-graphite gripping tabs were glued onto the end arms of the specimen, because the shear-lap specimens were too small for direct gripping.

The optical measurement technique based on the DIC principle used in this study required an artificial speckle pattern to be applied to the surface of the test specimen to improve the software's ability to measure surface displacements. Printer toner powder was used in this test based on the success with other small scale DIC measurements (Choi et al. 1991; Zink et al. 1995; Schwarzkopf and Muszyński 2013). A uniform toner pattern was transferred onto the specimens by means of a custom made air deposition apparatus (Schwarzkopf et al. 2013) and fixed on the surfaces by heating in an oven at 103°C for 10 min.

An Instron ElectroPuls E1000 test machine was used for the lap shear tests. The specimens were clamped in place by gripping the attached epoxy-graphite tabs (Figure 60B) in a way that ensured axial loading. The specimens were loaded in displacement control mode at a rate of 0.16 mm/min (strain rate: 0.014 mm/mm per minute) for one minute. The total displacement was chosen as to not break the specimens. The force was measured using an Instron 2518-807 load cell (± 0.02 N). Force and displacement of the cross head were recorded throughout the test. An analog force and position signal was recorded with a data acquisition (DAQ) unit. A nominal average shear stress over the bond plane was used as reference for the strain analysis. During the test, images of the specimen surface showing the bondline (field of view, 3.10 mm x 2.59 mm) were recorded every 1 second for 1 minute (60 images for every test) using the VIC-Micro 3D™ system by Correlated Solutions, Inc (Figure 60A). The basic hardware components for this system consisted of two cameras, a stereomicroscope, and a beam splitter used to split the stereomicroscopic light path into two separate images. The two cameras were synchronized to assure that the two images are acquired at the same time. Image sequences of the tests were processed using VIC-3D 2010 software (by Correlated Solutions, Inc.), which uses the DIC technique to calculate specimen surface coordinates, components of displacement vectors, and surface strain tensors. For each individual test we manually selected an area of interest (AOI) for analysis which included one of the notches and, as far as possible, matched the boundaries of the XCT scanned volume

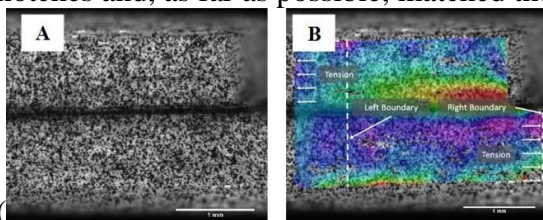


Figure 61B). In this experiment a subset size of 49 and a step size of 5 were used.

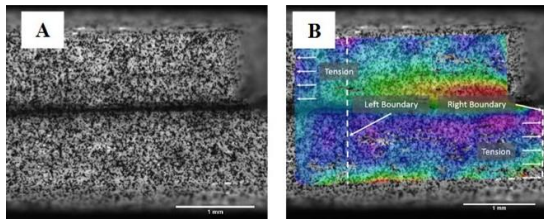


Figure 61. *A: lap shear specimen with toner particle speckle pattern applied; B: lap shear specimen with shear strain plot overlaid on the surface; left and right boundaries of XCT scanned data marked with dotted lines.*

The accuracy and precision of optical measurement systems based on DIC principle depends on a number of factors, which besides the resolution of the camera and the intrinsic robustness of the DIC algorithm include also quality of optics, lighting, focus, speckle pattern, selection of the algorithm options and parameters. Analyzing of all the impacts separately is tedious and impractical. Instead, in this study the accuracy and precision of the system was assessed by statistical analysis of series of displacement and strain maps recorded on undeformed specimens. The expected mean displacements and strains in all directions are zero, and all non-zero values measured can be thought of as the noise of the optical measurement system. The mean displacement and strains recorded for all data points within the AOI provides a convenient measure of accuracy, while standard deviation of the recorded noise provides a measure of the system's precision. These values will be different for each specimen due to different speckle patterns and specimen morphology. As an example, the DIC measurement shown in **Error! Reference source not found.** has an accuracy and precision in x displacements of $0.070 \mu\text{m} \pm 0.045 \mu\text{m}$ and for y displacements, $0.101 \mu\text{m} \pm 0.040$. The principal strain accuracy and precision was $61.366 \mu\text{m}/\text{m} \pm 1.381 \mu\text{m}/\text{m}$.

The numerical data output generated by VIC-Micro 3D™ system was compatible with numerical output of the MPM morphology-based model used to simulate the test in the larger project (Nairn et al. 2013). The numerical output is also used to produce full-field color coded maps of strains and displacements overlaid on the deformed specimen image. These maps allow quick visual inspection of strain distribution, identification of potential stress concentrations, and interactions between components. In the absence of measured volumetric stress or strain data the surface strains measured with the optical system provided unique “thumbprints” of the specimens during testing that will be used for validation of the numerical model used in the larger project (Nairn et al. 2013; Kamke et al. 2014; Muszyński et al. 2014).

Results and Discussion

The test matrix of the larger study included 54 specimens (Nairn et al. 2013; Kamke et al. 2014; Muszyński et al. 2014). As stated above the objective of this paper is to present

methodological aspects of this study with only as much results as was necessary to illustrate the process. Full results will be presented in a separate publication.

Much of the variation observed in the measured strain maps can be attributed to the specimen specific micro-morphology, particularly to anatomical features hidden directly below the surface. These can be investigated using the XCT scans of the specimens. For example, Figure 62 shows a SYP specimen with a PVA type adhesive. This specimen also shows a high magnitude shear strain region in the lower laminate. This strain concentration seems to be connected with a resin canal exposed on the surface. The resin canal is more compliant than the surrounding tracheids and deforms more easily. The XCT scan also revealed a second resin canal in the upper laminate further beneath the surface. This kind of morphological feature would be missed only using optical surface measurements, and would likely confuse the analysis if the surface strains are assumed to be representative of the entire specimen volume. Due to this morphological variation between specimens, qualitative assessments of the measured surface strain patterns alone have a limited value in understanding of the system.

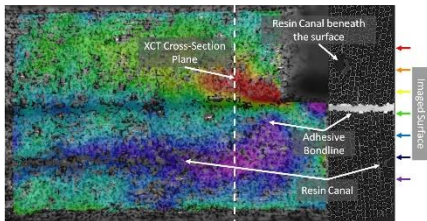


Figure 62. Left: measured shear strain of a southern yellow pine specimen with a PVA type adhesive; Right: XCT scan of the same specimen

For a more reliable analysis of bond efficiency, one would need to include the strain or stress analysis in the entire volume of the specimen. This can be obtained from numerical simulation of the test in three dimensions.

Conclusions

In this paper we have presented a methodology for measuring and assessing the full-field deformations and strains distribution across the loaded wood-adhesive interphase at a micro-mechanical level.

It was found that the measurement of surface displacements and strains was substantially affected by the local morphology unique to the specimen under examination. This morphological variation and its effect on measurements must be taken into account for any analysis of the adhesive bond interphase at this scale. Due to this substantial effect, any analysis of the load transfer behavior would be best conducted in conjunction with predictive modeling tools. The data produced by the methodology described in this paper has been used to verify the reliability of the numerically simulated displacement and strain results that are generated for the entire depth of the specimen Kamke et al.(2014).

A methodology for integration of these optically measured displacements and strains with the simulated results is described in depth by Muszyński et al. (2014).

References

- Choi, D., Thorpe, J.L., Hanna, R.B. 1991. Image analysis to measure strain in wood and paper. *Wood Sci. Techn.* 25: 251-262.
- Kamke, F.A., Nairn, J.A., Muszyński, L., Paris, J.L., Schwarzkopf, M., Xiao, X. 2014. Methodology for micromechanical analysis of wood adhesive bonds using x-ray computed tomography and numerical modeling. *Wood Fiber Sci.* 46(1): 15-28.
- Muszyński, L., Kamke, F.A., Nairn, J.A., Schwarzkopf, M., Paris, J.L. 2013. Integrated Method for Multi-Scale/Multi-Modal Investigation of Micro-Mechanical Wood-Adhesive Interaction. *International Conference on Wood Adhesives, 2013, Toronto, Ontario, Canada.*
- Muszyński, L., Kamke, F.A., Nairn, J.A., Schwarzkopf, M., Paris, J.L. 2014. Integrated Method for Multi-Scale/Multi-Modal Investigation of Micro-Mechanical Wood-Adhesive Interaction. *Forest Prod J Accepted for Publication.*
- Nairn, J.A., Kamke, F.A., Muszyński, L., Paris, J.L., Schwarzkopf, M. 2013. Direct 3D Numerical Simulation of Stresses and Strains in Wood Adhesive Bond Lines Based on Actual Specimen Anatomy from X-Ray Tomography Data. *International Conference on Wood Adhesives, October 9-11, 2013, Toronto, Ontario, Canada; pp. 11.*
- Nairn, J.A., Muszyński, L., Schwarzkopf, M. 2013. Morphology Based Modeling of Micro-Mechanics and Failure Mechanisms in Bio-Materials with Polymer Matrices. *Oregon State University, USDA.*
- Paris, J.L., Kamke, F.A., Mbachu, R., Gibson, S.K. 2014. Phenol formaldehyde adhesives formulated for advanced X-ray imaging in wood-composite bondlines. *J. Mater. Sci.* 49(2): 580-591.
- Schwarzkopf, M., Muszyński, L. 2013. Strain Distribution and Load Transfer at the Polymer-Wood Particle Interphase in Wood Plastic Composites. *Accepted by Holzforschung.*
- Schwarzkopf, M., Muszyński, L., Nairn, J.A. 2013. A Methodology for the Characterization of Micromechanical Load Transfer in the Wood Particle and Matrix Interphase of WPCs. *67th FPS International Convention, 2013, Austin, TX.*
- Zink, A.G., Davidson, R.W., Hanna, R.B. 1995. Strain Measurement in Wood Using a Digital Image Correlation Technique. *Wood Fiber Sci* 27(4): 346-359.

FE model of Oriented Strand Board Made by Two Different Geometry Generation Techniques

Václav Sebera^{1*} – Jan Tippner¹ – Jiří Kunecký² – Lech Muzsyński³, Peter Rademacher⁴

¹ Research assistant, Department of Wood Science, Mendel University in Brno, Brno, Czech Republic.

* Corresponding author

vaclav.sebera@mendelu.cz

jan.tippner@gmail.com

² Researcher, Institute of Theoretical and Applied Mechanics, v.v.i., Academy of Sciences of the Czech republic, Prague, Czech Republic

kunecky@itam.cas.cz

³ Associate professor, Department of Wood Science and Engineering, Oregon State University, Corvallis, USA.

Lech.Muszynski@oregonstate.edu

⁴ Chief researcher, Department of Wood Science, Mendel University in Brno, Brno, Czech Republic.

Peter.Rademacher@hnee.de

Abstract

For finite element modeling of wood-based composites (WBC's) can be used two different approaches. The first one is so-called morphological modeling meaning the WBC is first imaged in 2d or 3d and, then, transformed using empirical laws into FE model. The second approach that is more traditional, is based on a priori knowledge of properties and geometry of the WBC's. The goal of the work was to create parametric finite element model of oriented strand board (OSB) and study an influence of material properties and strands orientations on modulus of elasticity. For these purposes the two different techniques for building the FE model were used. The first model was built via volume entities (OSB_{VOL}), but because of its high errors achieving ci. 600% due to a coupling of strongly heterogeneous meshes, it was rejected in the end. The second model (OSB_{MAT}) was build via mapped finite element mesh using modified algorithm created in the first model. OSB_{MAT} exhibited lower error in terms of modulus of elasticity than OSB_{VOL} (ci. 69% and after the material properties adjustment it was only 1,21%). This proved that it is more suitable to model strand composites such as OSB using the mapped a priori prepared FE mesh.

Keywords: Finite element model, Oriented strand board, composite, .

Introduction

Finite element method is one of the key instrument in a design of structures and assessment of material behavior including the composites based on renewable resources. One of the main advantages of the FE modeling is that it enables to study objects of complicated geometries and complex material properties which includes so called what-if scenarios or virtual prototyping. The FE modeling is preferably accompanied by certain validation either based on analytical calculation, experimental testing or more simple FE simulations known as verification studies. The need for verification of FE model is apparent because too many simplifications must be usually made within a simulation which means the FE model is as precise as we define it and as we want to have it in respect to the aim of the FE analysis. The FE modeling of the materials can be carried out in two different procedures (Muszyński a Launey 2010): a) the FE model is built based on a priori known parameters that might be also randomized (“deterministic” approach); b) the FE model is derived from the real material geometry based on image data such as X-ray CT or MRI (“morphological” modeling). The latter approach is not concerned in this work and was successfully applied on wood (Badel and Perre 2002; Nairn 2006 and 2007; Koňas 2009, Kamke et al. 2014) or OSB material (Sebera and Muszyński 2010).

The first approach of FE modeling of materials is more traditional way due to historical development of CAE software and is well reported in Mackerle (2005). For wood at a cell-wall scale it was demonstrated in Holmberg (1999) and Javořík (2002). The probabilistic approach at a scale of cells and tree-rings was showed in Koňas (2003), similar approach but for strand for OSB production was showed in Hindman and Lee (2007). The use of random generation of wood-based composite was demonstrated in Faessel et al. (2005) and Dai (2007), who used Monte Carlo simulation instead of FEM.

Looking at the OSB material specifically, Shaler and Blankenhorn (1990) used rules of mixtures and Halpin-Tsai theory to predict modulus of elasticity (MOE) of OSB. Triche and Hunt (1993) developed linear FE model that was capable to predict strength and stiffness of PWSC material. Their FE model incorporated the layer of adhesive too and was based on defining of superelements. Wang and Lam (1998) developed 3D nonlinear stochastic FE model of PWSC which was used for prediction of tension strength. Clouson (2001) presented FE model of PSL for its optimization in terms of stiffness and strength while the classical laminate theory was incorporated. The First contact numerical model of pressing of OSB strands was presented by Nairn and Le (2009) who used the material point method (MPM) instead of FEM. Their model considered geometry, adhesion of strands and resulted in prediction of effective material properties. Stürzenbecher et al. (2010) created multiscale model of OSB based on homogenization principles that was capable to predict effective material properties at different scales. Gereke et al. (2012) also applied stochastic modeling on wood strand composites including the effect of resin content on effective elastic moduli. Their numerical prediction achieved higher agreement with experiments than analytical models.

Materials and Methods

In this study, we examined two different finite element models of OSB. The main focus was to compare two different approaches for building their geometries and mutually compared on a basis of common characteristics – modulus of elasticity (MOE). The first FE model was build in scheme that the strand mat was generated through the volume entities. These strands were intersected and subtracted from each other using Boolean algebra to form the mat that consists of particular strands that are glued together. The mat was subsequently cut into the virtual specimen for three-point bending test and meshed using free meshing. The model that was obtained by this way is OSB_{VOL} (see Fig. 1 a-c). Because of complex geometry, the FE mesh was strongly heterogeneous which resulted in a fact that adjacent layers could not be glued using standard procedure. For this reason, the algorithm that coupled degrees of freedom of closest pair of nodes was developed. This enabled to connect all layers together. The second FE model of OSB was created with help of a priori prepared mapped FE mesh, from which the strands were created using ANSYS selection logic (OSB_{MAT}).

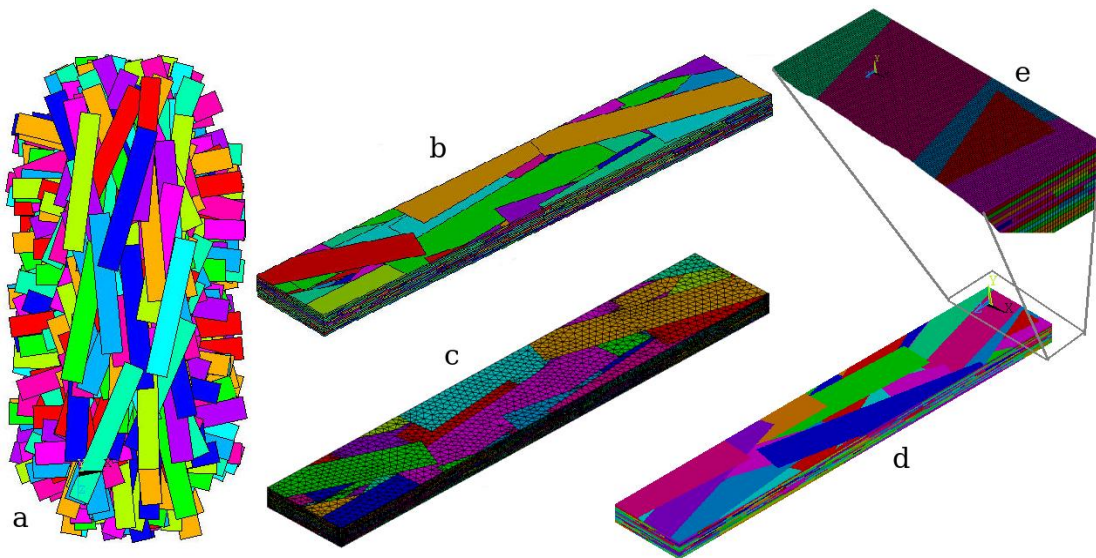


Figure 1. Created FE models of OSB, a) strand mat for creating OSB_{VOL} model, b) geometry of OSB_{VOL} model, c) FE mesh of OSB_{VOL}, d) geometry of OSB_{MAT} model, d) FE mesh of the OSB_{MAT}

Assumptions made in both FE models of OSB are following: a) each strand is only in one layer; b) strands are perfectly bonded together within a layer and adhesive material is not considered; c) orientation of strands is generated following Gauss probability distribution that ranges between -20° and 20° in respect to longitudinal axis of specimen; d) thickness of each strand is 0,8 mm which means that for 15 layered FE model, the thickness is 12 mm; e) one material model, Norway Spruce (NS) was used for all numerical analyses. The properties of NS were taken from the literature that examined NS in Central Europe (Požgaj et al. 1997) and are showed in Table I. The material of adhesive was not considered in the analysis.

Tab. I: Used material model of Norway spruce (*Picea abies* L.) from Požgaj et al. 1997

Species	E_L	E_R	E_T	G_{LR}	G_{LT}	G_{RT}	ν_{LR}	ν_{LT}	ν_{RT}
Norway spruce	1365	789	289	573	53	474	0.48	0.01	0.687
	0						9	4	

E_L, E_R, E_T – normal moduli of elasticity [MPa]; G_{LR}, G_{LT}, G_{RT} – shear moduli of elasticity [MPa]; $\nu_{LR}, \nu_{LT}, \nu_{RT}$ – Poisson's ratios [-]

Results

The model OSB_{VOL} exhibited very high error (about 912 %) compared to a commercially available material OSB/4 in terms of elastic modulus in bending (MOE). The reason for such enormous error is a stiffening of the OSB_{VOL} structure that was caused by added coupling bonds. Those couplings were necessary to be input into the OSB structure since it was only way how to connect strongly heterogeneous meshes in adjacent layers. The problem arose in a situation when two nodes of adjacent layers were at different positions. The prescription forcing them to share their degrees of freedom (DOF's) induced additional stiffness. The stiffening can be seen as unusual behavior of strands resulting in buckling or bending of strands inside the material, as seen in Fig. 2. The coefficient that would reduce such effect is not possible to find due to very heterogeneous and orthotropic structure of composite and variable and different stress states at each point of the material. Because of this error, the model OSB_{VOL} was rejected and another approach had to be found. This led to developing the new strand model (OSB_{MAT}).

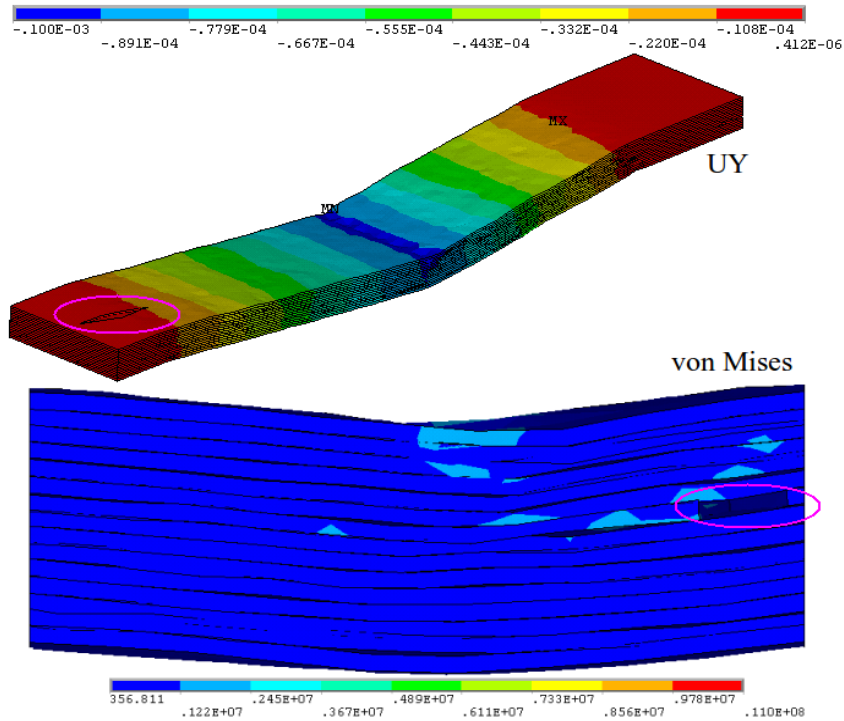


Figure 2. Results of OSB_{VOL}, displacement in Y direction (top), von Mises stress (bottom)

For default material properties of the mapped model (OSB_{MAT}), the model exhibited $MOE = 8,14$ GPa, which meant relative error 69,9% (compared to $OSB/4$). Within the process of fundamental adjustment of this model (in material properties of strands), it was achieved relative error about 1,21%. This was achieved when longitudinal elastic modulus of strands was half of original value ($\lambda = 0,5$). Presented procedure of FE model for an accuracy improvement indicates an optimization character of considered problem. To have such procedure that is fully legitimized, it should, in ideal case, reflect an influence of whole manufacture history on properties of strand-glue complex. Nonetheless, we can conclude that the modeling of OSB using mapped FE models represent more trustworthy and meaningful way of FE modeling than using the generation of OSB via volume entities. To show the complexity of stress state in OSB that is induced by randomized strand orientations, the stress components can be compared to the layered model (“plywood”) that have the same amount of layers as simplified OSB (OSB_{MAT}). This comparison is depicted in Fig. 3.

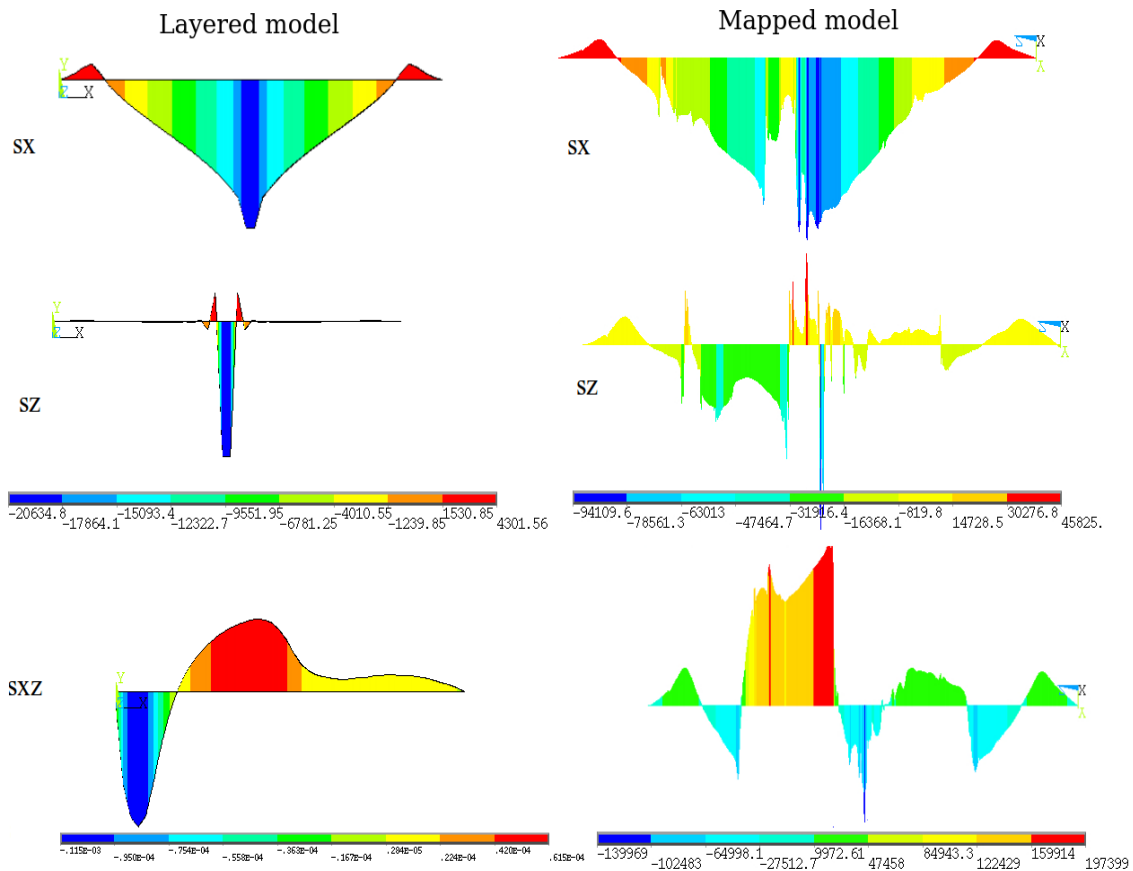


Figure 3. Comparison of stress components of layered model (left column) and OSB_{MAT} (right column). The stress components are mapped onto the line along the specimen length

From the Fig. 3 we may see that layered model consisting of 15 layers (plywood) with same properties as used in OSB simulations, exhibit predictable stress distributions that

could be calculated even using classical laminate theory (CLT). By looking at situation in OSB_{MAT} we can conclude the stress state is more heterogeneous and cannot be predicted by analytical techniques (CLT, homogenization etc.) and, therefore, numerical modeling in general is still only instrument that can evaluate such problems in such complex composites as OSB.

References

- Badel, EA, Perre, P (2002) Predicting oak wood properties using X-ray inspection: representation, homogenisation and localisation. Part I: digital X-ray imaging and representation by finite elements. *Ann. For. Sci.* 59:767–776.
- Clouston, PL. Computational modelling of strand-based wood composites. University of British Columbia 2001, 149 s.
- Dai, Ch (2007) Modeling formation and bonding of wood composites. Presentation presented at FPInnovation – Forintek Division, Vancouver, Canada.
- Faessel, M, Delisee, C, Bos, F, Castera, P (2005) 3D Modelling of random cellulosic fibrous networks based on X-ray tomography and image analysis. *Compos. Sci. Tech* 65:1931–1940.
- Gereke, T, Malekmohammadi, S, Nadot-Martin, C, Dai, C, Ellyin, F, and Vaziri, R. Multiscale Stochastic Modeling of the Elastic Properties of Strand-Based Wood Composites. *Journal of Engineering Mechanics*, 2012, 138(7):791-799
- Hindman, PD, Lee, NJ (2007) Modeling wood strands as multilayer composites: bending and tension loads. *Wood Fiber Science* 39:515–526.
- Holmberg, S, Persson, K, Petterson, H (1999) Nonlinear mechanical behaviour and analysis of wood and fibre materials. *Comput. Struct.* 72:459–480.
- Javořík, J (2002) A numerical model of microstructure of the wood and a structural analysis of the wood. MendelNet conference. MU in Brno. pp. 117–124. [in Czech]
- Kamke, F., Nairn JA., Muzsyński, L., Paris JL, Schwarzkopf M. Xiao, X. (2014) Methodology for micromechanical analysis of wood adhesive bonds using X-ray computed tomography and numerical modeling. *Wood and Fiber Science* 46(1):15-28.
- Koňas, P (2003) General concept of finite element (FE) model based on anatomy structure (Part V – probabilistic FEM model of wood). *Acta Univ. Agric. et Silv. Mendel. Brun.* 1:69–79.
- Koňas, P, Gryc, V, Vavrčík, H (2009) 3D visualization and finite element mesh formation from wood anatomy samples, Part I – Theoretical approach. *Acta Univ. Agric. et Silv. Mendel. Brun.* 1:1–16.
- Mackerle, J(2005) Finite element analyses in wood research: a bibliography. *Wood Sci. Technol.* 39:579–600.
- Muszyński, L, Launey, ME (2010) Advanced imaging techniques in wood-based panels research. In: *Wood-Based Panels – An Introduction for Specialists. State-of-the-Art in Wood-Based Panels Research.* COST Action E49:177–201.
- Nairn, JA (2006) Numerical Simulations of Transverse Compression and Densification in Wood. *Wood Fiber Sci.* 38:576–591.
- Nairn, JA (2007) Material point method simulations of transverse fracture in wood with realistic morphologies. *Holzforschung* 61:375–381.

- Nairn, JA, Le, E. Numerical Modeling and Experiments on the Role of Strand-to-Strand Interface Quality on the Properties of Oriented Strand Board, Proc of 9th Int. Conf. on Wood Adhesives, Lake Tahoe, Nevada, USA, Sept. 28-30, 2009
- Sebera, V, Muszyński, L (2011) Determination of local material properties of OSB sample by coupling advanced imaging techniques and morphology-based FEM simulation. *Holzforschung*. 2011(65)6:811-818. ISSN 0018-3830.
- Shaler, SM, Blankenhorn PR (1990) Composite Model Prediction of Elastic Moduli for Flakeboard. *Wood and Fiber Science*, 22(3), 1990, pp.246-261, ISSN 0735-6161
- Sturzenbecher, R, Hofstetter, K, Schickhofer, G, Eberhardsteiner, J (2010) Development of high-performance strand boards: multiscale modeling of anisotropic elasticity. *Wood Science and Technology* 44:205-223.
- Triche MH, Hunt MO (1993) Modeling of Parallel-Aligned Wood Strand Composites. *Forest Products J.*, 43(11/12), pp. 33-44, ISSN 0015-7473
- Wang YT; Lam, F (1998) Computational Modeling of Material Failure for Parallel-Aligned Strand Based Wood Composites. *Computational Material Science* 11, pp.157-165, ISSN 0927-0256s

Aluminum-laminated Wood Composites: Manufacturing Parameter Optimization

Franz Segovia^{1*} – *Pierre Blanchet*² – *Costel Barbuta*³ – *Robert Beauregard*⁴

¹ PhD Candidate, Université Laval. QC. Canada

* *Corresponding author*

franz.segovia-abanto.1@ulaval.ca

² Associate Professor, NSERC Industrial Research Chair on Ecoresponsible Wood Construction. Université Laval. QC. Canada

Pierre.blanchet@sbf.ulaval.ca

³ Scientist, Secondary Manufacturing. FPIInnovations. QC. Canada.

costel.barbuta@fpinnovations.ca

⁴*Professor. Faculté de Foresterie, géographie et géomatique. Université Laval. QC. Canada.*

robert.beauregard@ffgg.ulaval.ca

Abstract

Wood-based composites were developed with high MOE. Lamination has quickly been identified as the avenue to reach this goal. Several wood-based composites face-laminated with aluminum alloy sheets were manufactured in the laboratory under various pressure conditions, using three types of 9 mm-thick cores (high-density fiberboard, medium-density fiberboard and oriented strand board) and 0.6-mm thick aluminum 3003 alloy sheets as face laminations. The objective of this study was to define the optimal manufacturing pressures and assess the potential of the various wood-based composites as core layer in laminated panels (sandwich panels). The physical and mechanical properties of the laminated panels were evaluated according to ASTM Standard D1037.06a. The tensile strength perpendicular to the surface (surface soundness) was determined according to Standard EN 311:2002. The results demonstrated that face-lamination with aluminum alloy sheets yielded significantly greater bending properties in addition to improving the dimensional stability (thickness swelling, water absorption).of the wood-based composite core.

Keywords: Laminated wood-based composite. Physical properties. Mechanical properties. Aluminum alloy sheets.

Introduction

Wood-based composites are used for a number of structural and non-structural applications. Knowledge of the mechanical properties of these products is of critical importance to their proper use (Cai and Ross 2010). Plywood and oriented strand board (OSB) are used as structural panels for construction and industrial applications. Medium density fiberboard (MDF) is used as an interior wood composite substrate in the manufacture of cabinets and other furniture. Wood-based composites offer good mechanical properties for their main applications, but some weaknesses such as poor water resistance, dimensional stability and durability limit their use in applications involving exposure to wet environment conditions. In the last decades, several studies have aimed to improve the performance and structural efficiency of wood-based composites (Kawasaki et al. 1999, Cai 2006, Mohebbi et al. 2011, Büyüksari et al. 2012, Biblis et al. 1996) by creating sandwich panels that combine the wood-composite used as a core with face laminations that consist of strong, stiff and thin materials bonded onto the top and bottom of the core. These studies reported that wood-based composites laminated with fiberglass or wood veneer sheets tend to show an increase in physical properties (thickness swelling, water absorption). Reinforcing materials such as fiberglass, wood veneer sheets or densified wood veneer sheets compressed yielded even greater increases in mechanical properties (modulus of elasticity, MOE, and modulus of rupture, MOR). The resulting composite sandwich (laminated panel) lends itself to wider utilization where strength, stiffness, dimensional stability and weight efficiency are required, for example, in aircraft, automotive and marine applications. The adhesive type, pressing conditions (specific pressure, temperature and time) and the structural characteristics of the lamination material are among the factors that need to be considered for core-to-face bonding to be optimized (Kiliç et al. 2009). The objective of the study was to determine the optimal specific pressure, as one key manufacturing parameter, and to assess the performance of three wood-based composites as a core layer in laminated panels.

Materials and Methods

Materials. Three types of wood-based composite panels were used as cores, i.e., high-density fiberboard (HDF), medium-density fiberboard (MDF) and oriented strand board (OSB) (Table 1). These panels were obtained on the market as produced by the manufacturers. They were conditioned at 20°C and 50% relative humidity (RH) until constant mass was achieved. The laminating material consisted of aluminum alloy sheets (Alloy-3003) having a thickness of 0.6mm and a nominal density of 2740 kg/m³. A liquid polyurethane adhesive (Macroplast UR-8346) provided by Henkel Canada Corporation was used for bonding.

Table 1: Physical properties of the wood-based composites

Wood-based composites	Symbol	*Moisture content (%)	Thickness (mm)	*Density (kg/m³)
High-density fiberboard	HDF	6	9.742	822
Medium-density fiberboard	MDF	7	9.742	798
Oriented strand board	OSB	8	9.742	673

**Moisture content was determined using ASTM Standard D4442-07 (Method A-Over-Drying), while density was determined according to ASTM Standard D2395-07 (Test Method A- volume by measurement).*

Panel lamination. The wood-based composites and aluminum alloy sheets were sanded with 120- and 150-grit sandpaper respectively. The polyurethane adhesive was applied at a spread rate of 130 g/m². The laminated panels with two aluminum alloy faces were compressed in the laboratory hot press at three pressure levels, i.e.: 138 kPa, 414 kPa and 689 kPa at 120°C for 6 minutes. After pressing, the panels were stored in a conditioning chamber at 20°C and 65% RH until constant mass was achieved.

Determination of physical and mechanical properties. Nine 150x150mm laminated specimens were prepared for water absorption and thickness swelling tests; nine 76x314mm specimens for bending (MOE and MOR) tests; six 51x51mm specimens for internal bond (IB) tests; and eight 50x50mm specimens for tensile strength tests perpendicular to the surface. The thickness swelling, water absorption, bending and internal bond tests were conducted according to ASTM Standard D1037.06a (ASTM International 2012), while the tensile strength perpendicular to the surface was measured according to EN 311:2002 Standard (Wood-based panels-Surface soundness-Test method). Non-laminated wood-based composite specimens were included in the tests for comparison purposes.

An ANOVA using Statistical Analysis System (SAS) software 9.3 (2010) was performed to determine significant differences between laminated panels pressed at three pressure levels.

Results and Discussion

Physical properties

Water absorption (WA) and thickness swelling (TS)

The WA and TS values obtained for the 2-hour and 24-hour water immersion tests are presented in Table 2. The TS values after 24-hour of water immersion ranged from 0.38% to 16.17%, while those for WA ranged from 1.65% to 19.70%. The laminated panels with

MDF core presented the greater TS and WA values after 2-hour and 24-hour water immersion. The WA values after 24-hour of laminated panels does not present significant differences at three pressure levels. The laminated panels with an HDF core presented the lowest TS value in comparisons to laminated MDF- and OSB-core panels mainly by the physical properties of HDF. All laminated specimens exhibited significantly lower TS and WA values after 24-hour water immersion than the wood-based composites without lamination. This decrease in TS and WA was due to reduced water penetration into the wood-based composite due to the aluminum sheet. No delamination between the aluminum alloy sheets and the wood-based composite was observed after 24-hours of immersion.

Table 2. WA and TS average values of aluminum laminated wood-based composites pressed at 138 kPa, 414 kPa and 689 kPa.

Wood-based Composite	Process	Pressing pressure (kPa)	Thickness swelling (%)		Water absorption (%)	
			2-h	24-h	2-h	24-h
HDF	w/o lamination ^a	---	2.95 (0.34) ^b	9.30 (0.21)	3.64 (0.09)	14.04 (0.63)
	Laminated	138	0.27 (0.03)	0.41 (0.03)	0.33 (0.12)	2.45 (0.23)
	Laminated	414	0.21 (0.17)	0.41 (0.02)	0.12 (0.05)	2.43 (0.13)
	Laminated	689	---	0.38 (0.14)	0.45 (0.02)	1.65 (0.08)
MDF	w/o lamination	---	3.17 (0.09)	14.25 (0.25)	4.59 (0.01)	22.05 (0.18)
	Laminated	138	0.10 (0.05)	1.15 (0.03)	5.22 (3.18)	16.33 (2.50)
	Laminated	414	0.29 (0.27)	13.94 (0.58)	1.57 (0.48)	17.77 (0.64)
	Laminated	689	1.05 (0.65)	16.17 (2.57)	2.74 (0.91)	19.70 (2.42)
OSB	w/o lamination	---	3.88 (0.81)	14.81 (1.50)	10.23 (0.42)	35.28 (1.22)
	Laminated	138	0.35 (0.04)	4.54 (2.08)	2.65 (0.48)	14.71 (4.89)
	Laminated	414	0.39 (0.15)	2.21 (0.15)	2.94 (1.57)	11.09 (1.05)
	Laminated	689	0.81 (0.39)	2.46 (0.99)	2.46 (0.99)	11.37 (1.06)

*wood-based composite without lamination

^a values in brackets are standard deviations

Mechanical properties

Modulus of elasticity and modulus of rupture

Both MOE and MOR values were strongly influenced by lamination with aluminum alloy sheets. They increased significantly in relation to the values of the wood-based composites without lamination, as is observed in Figures 1 and 2. The average MOE values of the laminated panels pressed at 689 kPa were greater than those of the laminated panels pressed at 138 kPa and 414 kPa. The laminated MDF- and OSB-core panels showed a densification following pressing at 689 kPa, which explains the observed increase in MOE values. The laminated HDF-core panels did not present any thickness reduction after pressing, nevertheless, MOE values showed an increase following pressing. For example, the average MOE for the laminated HDF-core panels was 8% higher for 689 kPa than for 138 kPa. This can be explained by the mechanical properties of HDF mainly shear strength, although, this can be demonstrated with respective tests. As regards MOR values, there was no significant difference between the three pressure levels. The increase in average MOE and MOR values obtained with the

aluminum alloy laminates proved significantly higher than the gains reported in the literature with other types of laminates such as fiberglass, wood veneer sheets or densified wood veneer sheets (Ayrilmis et al, 2008; Biblis et al, 1996; Cai, 2006). This increase in MOE and MOR values can be explained by the tension and compression strength and by the thickness of aluminum alloy sheets (0.6 mm). The thickness of the aluminum alloy sheet is a key factor for improving MOE and MOR, as has been demonstrated by the results. As in the previous tests, no delamination was observed between the aluminum alloy sheets and the wood-based cores.

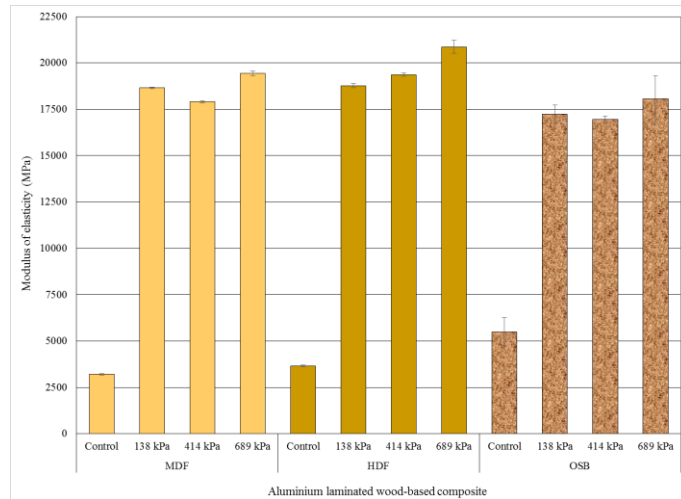


Figure 1. Effects of pressing at 138 kPa, 414 kPa and 689 kPa on MOE in the laminated panels.

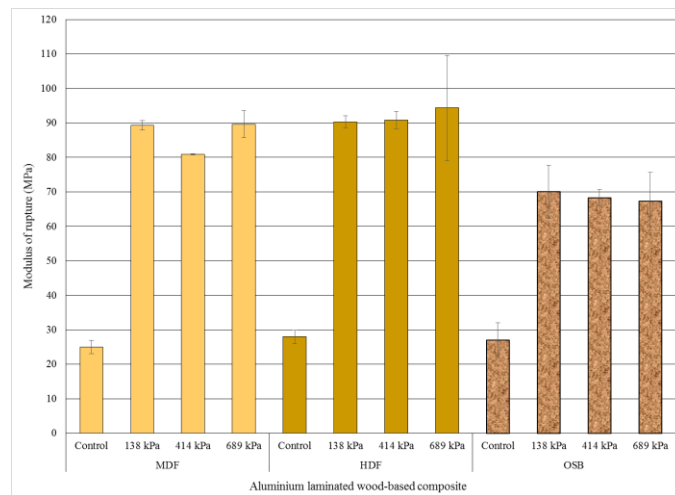


Figure 2. Effects of pressing at 138 kPa, 414 kPa and 689 kPa on MOR in laminated panels.

Internal Bond strength (IB)

The average IB values of the laminated panels tended to be lower than those of the wood-based composites without lamination (Figure 3). The average IB strength of the laminated MDF- and OSB-core panels proved variable. The IB strength of the laminated panels pressed at 689 kPa were significantly lower than those of wood-based composites without lamination. As for the laminated panels pressed at 138 kPa, they presented a non-significant increase in IB, which may be attributed to IB strength variations in the wood-based composite core. It should be noted that a decrease in the thickness of the MDF and OSB core layers was observed after pressing at 689 kPa. One possible explanation is that the compression level may have caused fractures in the core layer, leading to reduced IB strength. As regards the laminated panels with an HDF core, no significant decrease in the average IB strength was observed, irrespective of pressing pressure, by comparison with non-laminated HDF panels. The HDF core experienced no thickness reduction due to pressing. The results of the laminated HDF-core panels can be explained mainly by the greater density values of the HDF panels in comparison to the MDF- and OSB-core panels.

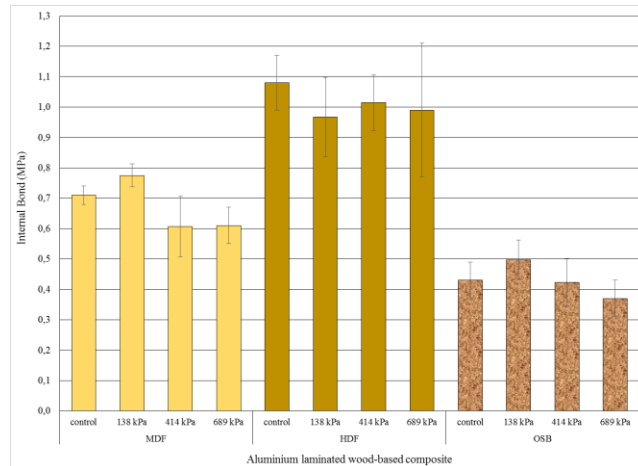


Figure 3. IB strength values of laminated panels pressed at 138 kPa, 414 kPa and 689 kPa.

The results for the MDF and OSB core laminated panels demonstrated the same trends. The best results for the IB tests on the laminated MDF- and OSB-core panels were obtained at pressure levels of 138 kPa and 414 kPa. This contrast with the results the bending tests where the best MOE values were obtained at 689 kPa. Despite the fact that the HDF-core panels were laminated, they did not show any reduction in thickness. Therefore, while the pressure level applied when the laminated panels are pressed depends on several factors, it is mainly determined by the type of wood-based composite used.

All the specimens failed in the wood-based composite core layer, with no occurrence of failure at the interface between the aluminum face and the core. The bonding strength between the wood-based composite and the aluminum face was adequate throughout the

range of tests performed in this study. However, an additional study which focuses on the application rate and the quality of adhesive under difference pressing pressures must be conducted in order to complement this study.

Tensile strength perpendicular to the surface

The tensile strength values perpendicular to the surface are presented in Figure 4. Test failure always occurred on the surface of the wood-based composite cores, which indicated that a) the polyurethane adhesive performed well, and b) the sanding treatment (120-grit sandpaper for the wood-based composites and 150-grit sandpaper for the aluminum alloy sheet) was adequate. Pressing pressure levels did not seem to have any significant effect on the results (Figure 4).

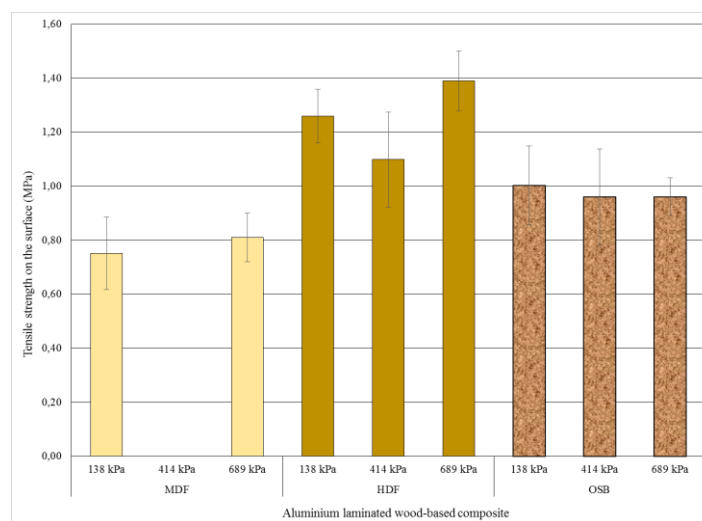


Figure 4. Tensile strength perpendicular to the surface of laminated panels pressed at 138 kPa, 414 kPa and 689 kPa.

Conclusions

The objective of this research was to determine the optimal specific pressure to be used in the manufacture of laminated panels consisting of aluminum alloy faces bonded onto three different wood-based composites (high-density fiberboard (HDF), medium-density fiberboard (MDF) and oriented strand board (OSB)) and to assess the performance of the wood-based composites as a core layer. Irrespective of the manufacturing pressure, the laminated panels showed excellent dimensional stability. Thickness swelling (TS) and water absorption (WA) were clearly reduced as a result of the barrier to water penetration provided by the aluminum alloy sheets. The laminated panels exhibited significantly greater modulus of elasticity (MOE) and modulus of rupture (MOR) values than the equivalent wood-based composites without lamination. A higher manufacturing pressure led to higher MOE gains, this being particularly true with the HDF core. On the other hand, the use of a high pressure (689 kPa) also led to a decrease in IB strength with both

the MDF and OSB cores. With a lower pressure (138 kPa), no such IB reduction was observed, and the laminated HDF panels were not affected, whatever the pressing pressure. The absence of IB failure at the aluminum/wood interface demonstrated the efficacy of the polyurethane adhesive, a result that was confirmed by the tensile strength tests perpendicular to the surface.

References

- ASTM International. (2012). Standard test methods for evaluating properties of wood-based fiber and particle panel materials. ASTM D1037. Vol. 04.10. ASTM International, West Conshohocken, Pennsylvania, USA.
- ASTM International. (2013). Standard test methods for specific gravity of wood and wood-based materials. ASTM D2395-07. ASTM International. West Conshohocken, PA. USA.
- ASTM International. (2013). Standard test methods for direct moisture content measurement of wood and wood-based materials. ASTM D4442-07. ASTM International. West Conshohocken, PA. USA.
- Ayrilmis, N., Candan, Z., Hiziroglu, S. (2008). Physical and mechanical properties of cardboard panels made from used beverage carton with veneer overlay. *Materials and Design*, 29, 1897-1903.
- Biblis, E. J., Grigoriou, A., Carino, H. (1996). Flexural properties of veneer-overlaid OSB composite panels from southern yellow pine. *Forest Prod. J.* 46(4), 59-62.
- Büyüksari, U., Hiziroglu, S., Akkiliç, H., Ayrilmis, N. (2012). Mechanical and physical properties of medium density fiberboard panels laminated with thermally compressed veneer. *Composites: Part B* 43, 110-114.
- Cai, Z. (2006). Selected properties of MDF and flakeboard overlaid with fibreglass mats. *Forest Prod. J.* 56(11/12), 142-146.
- Cai, Z., Ross, R. J. (2010). Mechanical properties of wood-based composite materials. In *Wood Handbook : Wood as an engineering material: chapter 12. Centennial ed. General technical report FPL ; GTR-190.*
- EN 311:2002 (2005). Wood-based panels-surface soundness-test method. European Norm.
- Kawasaki, T., Zhang, M., Kawai, S. (1999). Sandwich panel of veneer-overlaid low-density fiberboard. *J Wood Sci.* 45, 291-298.

Kilic, M., Burdurlu, E., Aslan, S., Altun, S., Tumerdem, O. (2009). The effect of surface roughness on tensile strength of the medium density fiberboard (MDF) overlaid with polyvinyl chloride (PVC). *Material and Design*. 30, 4580-4583.

Mohebby, B., Tavassoli, F. (2011). Mechanical properties of medium density fiberboard reinforced with metal and woven synthetic nets. *Eur. J. Wood Prod.* 69, 199-206.

Development of Ready-to-Assemble Furniture Constructions

Milan Šimek^{1} – Adam Kořený² – Václav Sebera³*

Jan Tippner³ – Zdeněk Dlauhý⁴

¹ Research assistant, Department of Furniture, Design and Habitation – FFWT, Mendel University in Brno-CZECH REPUBLIC.

** Corresponding author*

simek@mendelu.cz

² Researcher, Department of Furniture, Design and Habitation – FFWT, Mendel University in Brno-CZECH REPUBLIC.

³ Research assistant, Department of Wood Science – FFWT, Mendel University in Brno-CZECH REPUBLIC.

⁴ PhD student, Department of Furniture, Design and Habitation – FFWT, Mendel University in Brno-CZECH REPUBLIC.

Abstract

Computer numerical control (CNC) manufacturing technology is being applied in the furniture industry for quite a long time, more widely, and not only for wood and wood composite processing. The current furniture production is more accurate and faster thanks to this technology which also allows the production of joints. The furniture with joints manufactured directly on the CNC machine is in terms of the structure known as ready-to-assemble (RTA) furniture, or as flat pack furniture as well. The aim of our paper is the demonstration of new RTA furniture constructions. The interdisciplinary approaches to the development and testing of mechanical properties of selected types of RTA furniture are presented. The fabrication process of chair and table design manufactured on CNC machines and subsequent testing procedures are described. The standard tests for furniture employing the European Standards are used for further analysis of mechanical behavior in the accredited laboratory. The optical method - Digital Image Correlation (DIC) analyzes displacement and deformation of critical construction parts. The numerical simulation predicts the most loaded joints. The results of experimental tests of chair and table furniture provide specific information about the developing process and enable the optimization of strength properties, both in terms of structure, materials and furniture joints. The presented work highlights the importance of furniture parametrization and application of new methods for testing of industrial products.

Keywords: furniture construction, CNC technology, mechanical properties, testing, ready-to-assemble (RTA)

Introduction

The use of fittings as a traditional approach of European furniture industry is one of the basic principles of furniture constructions. The influence of world used technologies and processes brings new holistic perspective to this field. Dismountable furniture is usually described as a type of construction with a use of knock-down fittings. This construction method is commonly used by large volume producers as well as small carpenters because of its simplicity. The significant advantages are the through-feed lines, production cells or other technologies that can be used for drilling, sawing and routing. Dependence on the fittings and its influence on design, price and quality of final product are the major issues. The “Nesting” technology had an influence on the manufacturing of joints on CNC machines. The RTA furniture construction is the result of such approach. The necessity to eliminate multiple positioning of the part on the machine table leads to new construction and joints development related to the CNC machines. Manufacturing cell is able to produce a complex furniture product which is simple for production as well as for assembly with high accuracy and without any additional material (fittings). Nevertheless, the process depends on manufacturing technology which influences the speed, flexibility and quality. The above mentioned principles excluding their disadvantages and traditional construction concepts can lead to new interesting designs. The nowadays furniture construction and technology development trends and modern methodologies of applied research and development of industrial products enable faster launch of competitive furniture products. The synergic effect of the above described fact is wide cooperation between research and development university departments and commercial sphere.

CNC machining technology has been developed in the 40`s and 50`s of the 20 century in the United States. Main advantages of a CNC technology are automation of the manufacturing process, high accuracy and speed of processing, high reliability and versatility with low maintenance and exclusion of technology breaks for new settings. On the other hand main disadvantages are higher purchasing and operating costs, higher knowledge demands on the operator and lower production speed compared to large series production of the various specialized machines (Higley, 2002). While RTA and/or flat pack furniture has been produced for more than twenty years, experience with constructing it and with its strength properties is still limited. Development of technologies, new materials and informatics not only in production and marketing, but also in furniture design brings many methods which allow engineers and designers to adopt new work approaches. Despite the fact that standardized furniture testing, is not compulsory for producers in most cases, it is commonly implemented. Numerical simulations have been applied by furniture industry in a limited way so far (e.g. Mirra Office Chair; Larder and Wiersma, 2007). However they are supported by research quite significantly. From a large number of works we can mention research on behaviour of constructions of sitting furniture (Prekrat et al., 2012; Horman et al., 2010; Smardzewski and Gawroński, 2003) or box-type furniture (Nicholls and Crisan, 2002; Tankut et al., 2012), as well as the research on behaviour of wood product joints (Mihailescu, 2003; Černok et al., 2004; Prekrat and Smardzewski, 2010). The issue of strength design of furniture and various research methods is rather comprehensively described by Eckelman

(2003) or Smardzewski (2004). The Digital Image Correlation (DIC) methodology in relation to a shape and deformation measurement is described e.g. by Sutton (2008) or Nestorović et al. (2011).

Case study I. – RTA Chair Design

The design was created in the CAD and CAM software. It was made by a CNC machine (with a nesting table) of plywood (12mm thickness), with integrated dovetail not-glued joints. Similar principles of constructing furniture based on rapid manufacturing were described e.g. by Oh et al (2006). The construction of the chair was assembled from six parts while no glue was used. It was designed as self-locking construction (Figure 1). The construction was mechanically loaded in an accredited furniture testing laboratory according to the Czech standard CSN EN 1728, article no. 6.4. Experimental optical measurement was carried out by the digital single lens reflex camera Nikon D5100 (Nikkor 50mm F1,8 AF-S lens) which was set perpendicularly to the examined surface – the side part. To achieve constant intensity of the recorded surface image, it was necessary to keep stable lighting conditions within image acquisition. For this purpose the examined surface of the chair construction was lightened by diffuse lights. The frequency of recording was set up to 1 fps, the bit depth of images was 8-bit. The open-source tethering software DigiCamControl, connected to the camera using the USB port, was used to transfer data to a mobile PC station. Correlation computation of displacement and strain fields was carried out in the Vic-2D software.



Figure 1: Chair design during testing in accredited laboratory

The goal of the work was to compute displacement fields on the chair side surface using the DIC method. The DIC computation brought reliable results which are based both on quantitative (standard deviation was lower than 0.05) and qualitative evaluation (displacement contours follow mechanical behaviour assumptions resulting from a loading mode). The highest absolute value of horizontal displacement was experienced at the top of backrest ($u = 3,9$ mm) and the highest absolute value of vertical displacement was experienced at the front leg ($v = 1,2$ mm). The next step in the analyses was to look at the strain fields computed from displacements. The strain field in horizontal direction

(ϵ_{xx}) is depicted in the Figure 2; the vertical strain component (ϵ_{yy}) is depicted in the Figure 3. The results show that vertical strain is highest in the dovetail connections on top of the chair seat. Nonetheless its highest absolute strain did not exceed $\sim 0,3\%$ so we can affirm that all strains occurring there are elastic – below the proportional limit of all possible loading modes in wood and birch plywood (Bodig and Jayne, 1993; Wood Handbook, 2010). The horizontal strain is the highest in the backrest dovetail connections and its maximal absolute value is $\sim 1,56\%$.

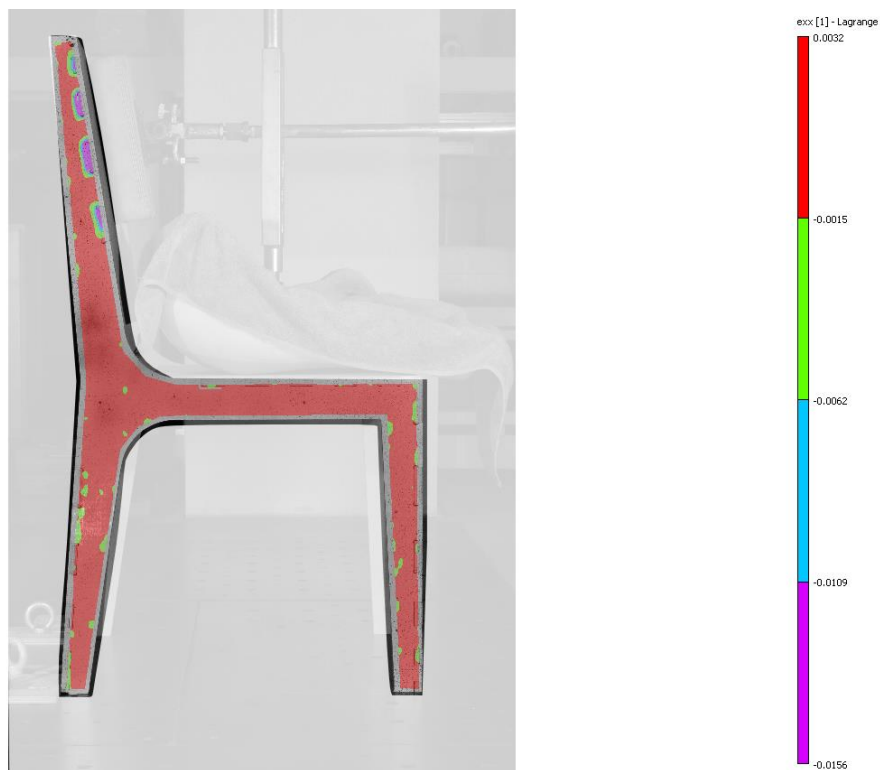


Figure 2: The strain field in horizontal direction (ϵ_{xx})

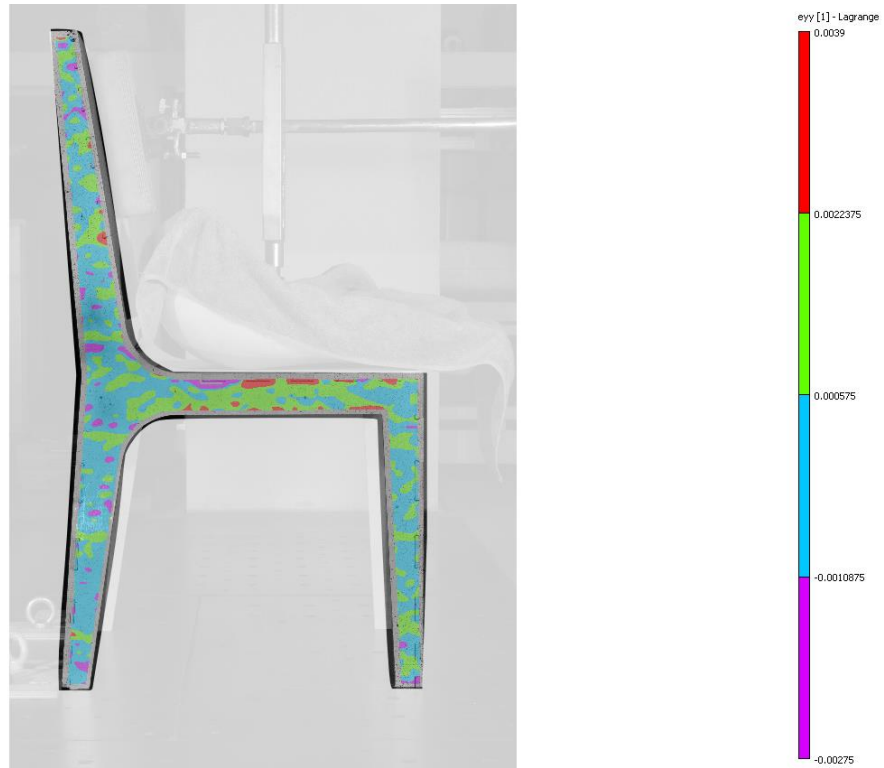


Figure 3: The strain field in vertical direction (ϵ_{yy})

Case study II. – Origami desk

The analysed desk construction (Fig. 4) was produced as a prototype using CNC laser cutting, precise CNC press banding (metal parts – base) and typical furniture production CNC processing (wooden composite materials – desk top). The aim of the study was to establish the probable mechanical behaviour of the office desk, especially the base, in consequence of the defined static loading based on the standards. The study focuses on the analysis of the extreme response (maximum tension) points and the probable breakage points by means of static numerical analysis. These points will be evaluated and based on that we will propose a solution for the achievement of the optimum results.



Figure 4: The desk design

The model of the analysed construction was created in the modelling environment of the CAD software (Autodesk Inventor 2011). The three-dimensional model was parametric (its geometry could be modified anytime during its processing). The strength numerical analysis was carried out in the module Strength Analysis of the used CAD software application by means of the finite element method (FEM).

The model is nonlinear in its geometry and it is made of three different materials. All components were allotted with the appropriate material and the material properties: physical and mechanical properties and constants such as density, Young's modulus of elasticity, Poisson constant, yield points and rupture points in tension were established based on literary sources and standards. The process of ascertaining the size of the affecting force was based on the Czech standard (ČSN EN 527-3) which deals with the methods for the construction stability and mechanical strength establishment. Based on paragraph 5.2 of the standard – Vertical loading test - two points where a loading force of 1 000 N was applied on the construction were selected. The first was the centre of a long apron; the second point was a corner of an apron. The construction of the desk stand was analysed with emphasis on the upper part of the leg. The leg is made of an open profile, therefore, we expected that it will be the most sensitive to loading.

The results of the numerical simulations are presented in a graphical form as pictures showing the progress of the measured quantity by means of colour spectra. The resulting images represent von Mises stress (Figs. 5) and the coefficient of safety (Figs. 6 and 7). The desk top was excluded from the simulation as in the final prototype this is made of anisotropic – laminated chipboard, which would unnecessarily prolong the calculating time. With respect to the focus of the study on the analysis of the stand and the critical points in the upper part of the leg, an inclusion of a desk top would be inefficient. Therefore, when assessing the results of the analysis, we have to take into account that the loading force applied to the desk apron at the given point would be more homogeneously distributed over the entire construction – thanks to the desk top.

According to the analysis, the expected deformations and damage would occur at the points where the upper part of the desk leg is connected to the plate (which ensures the dismantling connection of the desk leg to the apron), specifically at the points of contact between the plate and the edges. Because of the symmetry in the leg geometry and the symmetrical progress of tension in this geometry, the leg was divided by a vertical plane in the axis of symmetry and further we will only concentrate on the results of one half of the model. In Fig. 8 we can see the lowest coefficient of safety of 0.41 in bending inside the open profile. This value says that the equivalent tension at this point is 504.88 MPa, which is approximately 2.5 times higher than the yield point of steel (R_e 207 MPa). According to the numerical analysis, a permanent deformation of the material would appear at this point.

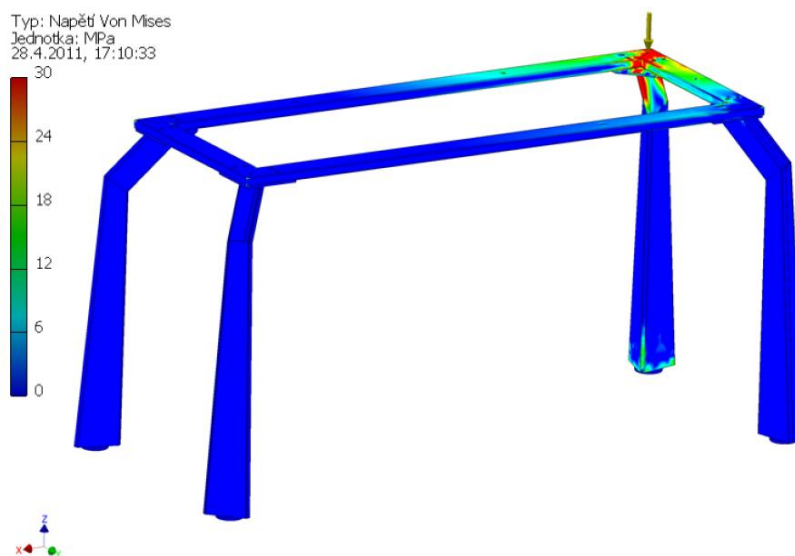


Figure 5: Equivalent tension (von Mises) when the apron is loaded in the corner

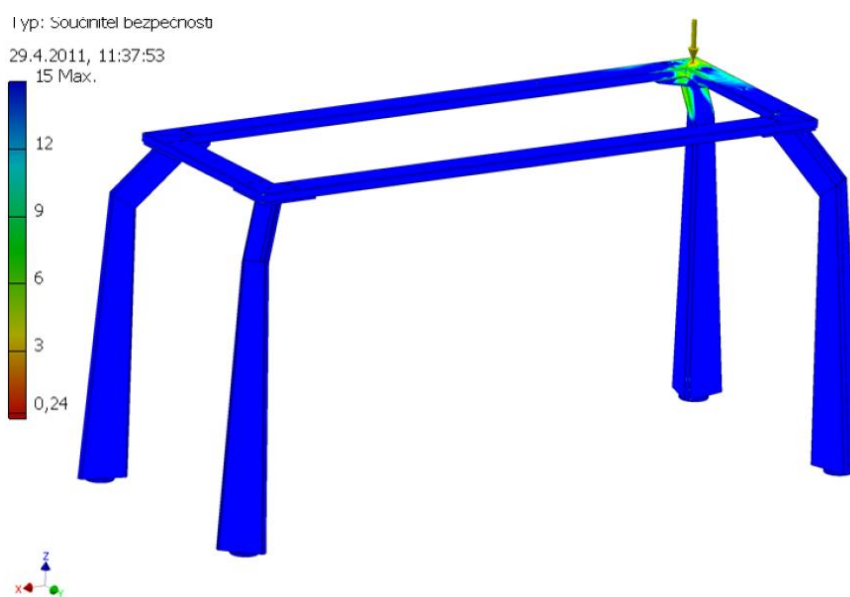


Figure 6: Coefficient of safety when the apron is loaded in the corner

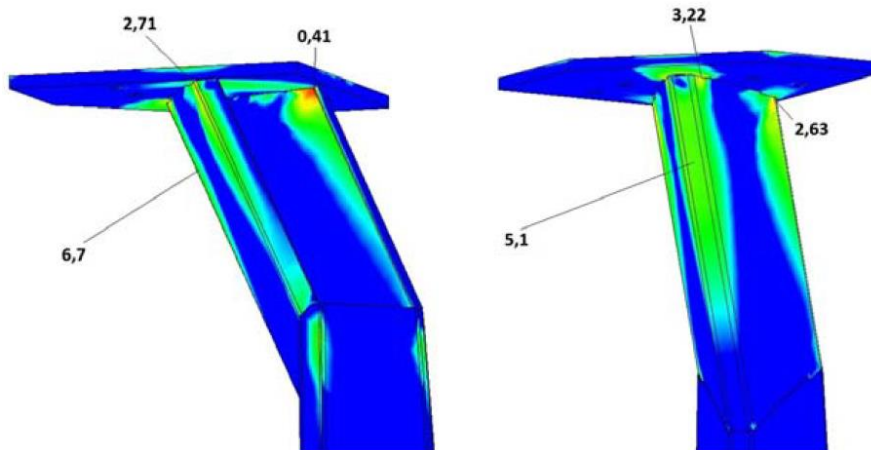


Figure 7: Coefficient of safety – detail of the upper part of desk leg

Conclusion

Our goal was to present a new concept of furniture design based on the connection of modern technologies, recent R&D advances in the field of furniture industry and parametric design. Parametric design currently represents what most industries are trying to achieve – not only does it save resources, but it also increases competitive strength and stimulates innovation (Song and Gazo, 2013). In the furniture industry and timber trade, this tendency may be observed mainly in the field of education and innovation. This is due to the fact that one of the specific features of parametric designs is usually innovative design that is not accepted by every customer. And due also to the fact that furniture, unlike other industrial products, doesn't have such well-developed legislation dealing with the placement of new products on the market, new products struggle to break into the market.

From the applied method point of view, it is possible to say that the DIC is easily applicable to furniture testing due to its relative simplicity and low requirements on employed devices, undemanding data procession and data assessment realized by accredited laboratories or research institutes. Development departments of furniture making companies can apply the methodology to increase their competitiveness and innovation potential. By means of deeper analysis of data it is possible to detect badly dimensioned construction connections or to optimize the construction from the shape or used materials point of view.

Acknowledgements

The authors thank the Internal Grant Agency (IGA) of Mendel University in Brno, Faculty of Forestry and Wood Technology, project IGA 57/2013.

References

- Bodig, J., Jayne, B. A., 1993: Mechanics of wood and wood composites. Malabar, Krieger Publish. Comp., p. 712.
- Černok, A., Joščák, P., Lang, M., 2004: Výpočtový model kolíkového spoja. Nábytok 2004, Faculty of Wood Technology, Technical University in Zvolen, 12 p.
- Eckelman, C., 2003: Product engineering and strength design of furniture. Purdue University, West Lafayette, Indiana, 204 p.
- Higley, J. B. (2002): *CNC applications*. Calumet., Purdue University, Indiana, Available at: <http://technology.calumet.purdue.edu/met/mfet/275/>
- Horman, I., Hajdarević, S., Martinovaić, S., Vukas, N., 2010: Numerical analysis of stress and strain in a wooden chair. *Drvna Industrija*, 61 (3), pp. 151-158
- Larder, L., Wiersma, J., 2007: CEA takes a front seat. *ANSYS Advantage*, Vol. 1/1, 2 p.
- Mihailescu, T., 2003: Finite element analysis of mortise and tenon joint in parametric form. Transilvania University, Faculty of Wood Industry, Brasov, 145 pp.
- Nicholls, T., Crisan, R., 2002: Study of the stress-strain state in corner joints and box-type furniture using Finite Element Analysis (FEA). *Holz als Roh- und Werkstoff*, v. 60, pp. 66–71.
- Nestorović, B., Skakić, D., Grbac, I., 2011: Determining the characteristics of composite structure laminae by optical 3D measurement of deformation with numerical analysis. *Drvna Industrija*, 62 (3), pp. 193-200.
- Oh, Y., Johnson, G., Gross, M.D., Do, E.Y.L., 2006: The designosaur and the furniture factory. International Conference on Design Computing and Cognition, Eindhoven, NL, pp. 123 - 140.
- Prekrat, S., Smardzewski, J., 2010: Effect of gluline shape on strength of mortise and tenon joint, *Drvna Industrija*, 61 (4), pp. 223 – 228.
- Prekrat, S., Smardzewski, J., Brezović, M., Pervan, S., 2012: Quality of corner joints of beech chairs under load. *Drvna Industrija*, 63 (3), pp. 205-210.
- Smardzewski, J., Gawroński, T., 2003: Gradient optimisation of skeleton furniture with different connections. *Electronic Journal os Polish Agricultural Universities*, Vol. 6, Issue 1, Available at: <http://www.ejpau.media.pl/volume6/issue1/wood/abs-01.html>
- Smardzewski, J., 2004: Modelowanie półsztywnych węzłów konstrukcyjnych mebli. Wydawnictwo Akademii Rolniczej im. Augusta Cieszkowskiego w Poznaniu, p. 224., ISBN 83-7160-343-6.
- Song, M.; Gazo, R. (2013): *Competitiveness of US Household and Office Furniture Industry*, International Journal of Economics and Management Engineering, Apr. 2013, Vol.3 (2), pp. 47-55.
- Sutton, M.A., 2008: Digital image correlation for shape and deformation measurements. Springer handbook of experimental solid mechanics. Ed. Sharpe, W.N. Springer-Verlag, Heidelberg. pp. 565–600.
- Tankut, A.N., Tankut, N., Karaman, A., 2012: Creep performance of Ready-to-Assemble (RTA) fasteners in bookcase construction. Proceedings from XXIII. International Conference Ambienta, Zagreb, October 12, 2012, pp. 195-208
- *** 2013: EN 1728 Furniture – Seating furniture – Testing methods for the determination of strength and Durability.

*Proceedings of the 57th International Convention of Society of Wood Science and Technology
June 23-27, 2014 - Zvolen, SLOVAKIA*

- *** ČSN EN 527-3 (911105), 2005: Kancelářský nábytek – Pracovní stoly (Office Furniture – Working Tables) Část 3: Metody zkoušení pro stanovení stability a mechanické pevnosti konstrukce. Český normalizační institut, Praha, 16 p.
- *** 2010: Wood handbook – Wood as an Engineering Material, Centennial edition. USDA Forest Service – FPL, Madison, p. 509.

Defining of Wood Colour

Tomislav Sinković, Slavko Govorčin*, Vlatka Jirouš Rajković*, Tomislav Sedlar*, Josip Miklečić*, Maja Marošan*

*Faculty of Forestry, University of Zagreb, Croatia. tsinkovic@sumfak.hr,
govorcin@sumfak.hr, vjirous@sumfak.hr, tsecllar@sumfak.hr,
mikleccic@sumfak.hr

Abstract

Defining of wood colour with spectral photometer has been used for some time and has become one of the most frequent methods in researching of macroscopic and aesthetical properties of wood. Measuring the colour of wood as a heterogeneous material of biological origin is difficult. The colour of wood is not uniform due to the alternating early wood/late wood colour. The aim of this study was to examine the relationship between the density of wood and early wood/ late wood colour. Sycamore maple species (*Acer pseudoplatanus* L.) was used in this study. It was established that colour parameters L^* , a^* , b^* of early wood zone were not statistically correlated to density. The same result was obtained for late wood of *Acer pseudoplatanus*.

Key words: wood colour, spectral photometer, colour variation, tangential section.

1 Introduction

When we talk about wood colour, it means the natural colour tone of dried wood (Ugrenović, 1950). In the textbooks, wood colour is usually defined descriptively so the description of certain types of wood provide general information, describing the colour of a yellowish, brown, red-brown, etc. (Horvat and Krpan, 1967). This may be in the nature of colour, a large variability in the colour of wood, but also in a difficult notion of technical-measuring values of the wood colour.

When the light affects the surface of the wood, part of the incident light directly reflects from the surface, and the other part enters the surface wood cells. The basic structure of wood (cellulose, lignin and hemicellulose) differently absorbs and reflects light, and pigments absorb certain wavelengths of light. Part of the light that is not absorbed into the cell walls disperses and rejects, and partially passes through the wood substance. Unabsorbed light is recognized as the wood colour, and by nature of wavelength changes we sense specific wood colour of some wood species.

The natural wood colour is specific for each species, and the total number of more than 30000 wood species is the largest source of variability of the wood colours. Growth conditions can also affect the colour variation within the same wood species; growth rate, soil nutrition and the brightness affects the wood colour.

Wood colour is also affected by the physical factors such as the angle of the light falling on the fibres and surface roughness (Nishino *et al.*, 2000). The incidence angle of light on some wood surface shows strong differences in the gloss in direction and perpendicular to the fibres, which affects the impression of colour.

Defining of wood colour with spectral photometer has been used for some time and it has become one of the most frequent used methods in researching of macroscopic and aesthetical properties of wood (Blanchard and Blanchet, 2011; Brischke *et al.*, 2007; Chen, T. *et al.*, 2012; Chen, Y. *et al.*, 2012; Jung *et al.*, 2008; Miklečić *et al.*, 2011; Miklečić *et al.*, 2012; Nemeth *et al.*, 2013; Nishino *et al.*, 1998). Research in the area of early wood density and late wood density and their relationship with the colour has not been done. The aim of this research was to measure and calculate the movement of density and colour of wood in the radial direction. Sycamore maple (*Acer pseudoplatanus* L.) was selected for the investigation.

Attempt was made to contribute to research and better understanding of the changes in colour and differences in density of early and late wood, since maple wood is diffuse porous hardwood. Maple wood is interesting to explore, as a diffuse porous wood species has a uniform structure with slight differences within annual ring and poorly visible annual ring border. The density of wood as a physical property is specific for a certain wood species, but because of biological origin is also highly variable, both among the different species and within the same wood species. In the same way the wood colour varies from species to species. Some species have darker and some have lighter colour, but with measuring and specifying the components we can accurately quantify it.

2 Material and Methods

For investigation were used randomly selected samples from three different maple trees. All three trees came from the same forest unit, which means that they had equal conditions for growth. Bark to bark cores, 70 cm in height were sawn from the trees. After the cores had dried to a water content of about 12%, from the highest part of the core, which was in the area of the chest height (1.3 m), samples of 20 mm × 20 mm × 25 mm were made (Figure 1). The samples were sawn in the radial direction from heart to bark and labelled with markers that indicate from which tree they were sawn, to which side of the world they belong to and the ordinal number from the heart to bark.

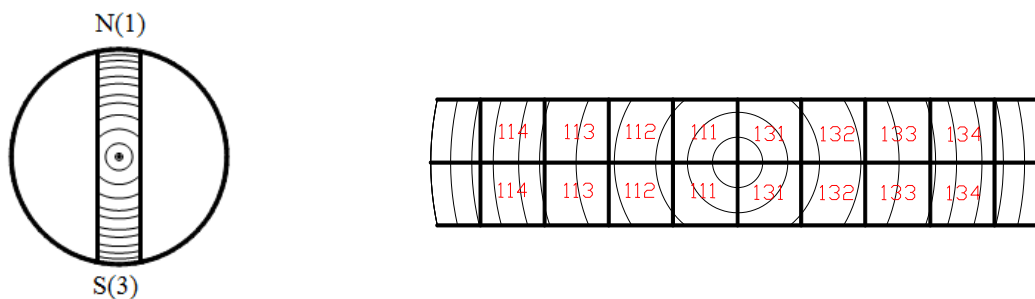


Figure 1 Bark to bark core (North – South) and samples of 20 mm × 20 mm × 25 mm from core.

After making of test samples, those with the widest annual rings were selected. From these samples one annual ring was cut with chisel, meaning wood chips were cut from annual ring from the early wood and late wood zone. Total of 30 wood chips from early wood and 30 wood chips from late wood was made.

To be able to perform spectral photometer colour measurement, after cutting specimens of early and late wood, each sample was sanded with sandpaper granulation 180. Each sample was marked with a number that indicates the number of tree, the side of the world where annual ring was, as well as the number of sample from which it was cut.

Colour measurement was performed with spectral photometer Microflash 100d produced by Datacolor (d/8° measuring geometry, 10° standard observer, D65 standard illuminate).

Due to the 9 mm aperture at the measurement point, it was not possible to measure the colour of early and late wood in radial and cross-sectional area. Aperture of instrument crossed not only the line between early and late wood, but the border between the annual rings as well. For this reason, the measurement was performed on tangential sections and the results are only measuring from the tangential sections.

Measurement was performed for each sample of early and late wood simultaneously. Measuring gave the results of colour values using the CIE $L^*a^*b^*$ colour system, where L^* describes the lightness, and a^* and b^* describe the chromatic coordinates on the green-red and blue-yellow axes. C^* describes colour saturation and h_{ab} describes the colour tone.

Density was measured in addition to colour measuring from each sample of early and late wood. Due to the size and irregularities of samples (wood chips), volume was determined in mercury.

3 Results and Discussion

Table 1 Statistical data for early and late wood

Early wood						Late wood						
h_{ab}	C^*	b^*	a^*	L^*	$\frac{w}{\square}$	$\frac{w}{\square}$	L^*	a^*	b^*	C^*	h_{ab}	
					$\frac{g}{cm^3}$	$\frac{g}{cm^3}$						
30	30	30	30	30	30	COU NT	30	30	30	30	30	

70, 37	14,9 7	14,4 2	3,46	69,26	0,417	MIN	0,44 1	75,3 3	3,87	14,76	15,31	72,2 0
73, 20	17,7 7 ^A	16,9 8 ^A	5,17 A	75,66 A	0,591 A	AVE R	0,64 1 ^A	78,8 1 ^A	4,69 A	16,17 A	16,84 ^A	73,8 7
77, 37	22,2 0	21,1 1	6,96	82,60	0,690	MAX	0,86 0	82,5 8	5,58	18,06	18,89	76,4 1
1,6 2	1,79	1,62	0,91	3,28	0,071	STDE V	0,11 2	1,68	0,51	0,97	1,04	1,11
11, 96	4,33	17,6 6	9,55	10,10	2,22	CV	17,5 1	10,9 2,13	2	5,97	6,18	1,50

Key: pw - density at the time of measurement, L - colour lightness, a* - chromatic coordinate (red - green), b* - chromatic coordinate (blue - yellow), C* - chromatic saturation, h_{ab} - chromatic coordinate, COUNT - number of samples, MIN - minimum value, AVER - mean value, MAX - maximum value, STDEV - standard deviation, CV – coefficient of variation*

^A *Average values identified with the letters A are statistically different at α = 95%, t-test was used.*

Statistical data shows that the mean density of the early and late wood zone varies. Although the maple wood is diffuse porous hardwood species and it is difficult to determine the boundary between the zones of early and late wood, measurement demonstrated that the early wood zone has a lower density than the late wood zone (Table 1) as expected; and the colour composition of early wood and late wood are different. Unexpected is that early wood colour has lower value of L* (lightness) compared to late wood, meaning the early wood zone is slightly darker than the late wood zone.

The average value of the chromatic coordinates a* in early wood zone is slightly higher than the average value of a* in the late wood. The same case is with the average value of chromatic coordinate b*. In the early wood zone, average color saturation C* is slightly higher than in the late wood zone, and the color tone h_{ab} is very similar in the early and late wood zone. All measured values between early and late wood are statistically different (tested with t-test).

Table 2 Pearson's correlation coefficients for the relationship between wood colour parameters and density of early and late wood of *Acer pseudoplatanus*.

	L*	a*	b*	C*	H*
Density of early wood	-0,18 P=0,354	0,13 P=0,505	0,04 P=0,833	0,05 P=0,788	-0,20 P=0,288
Density of late wood	-0,24 P=0,207	0,34 P=0,066	0,29 P=0,123	0,30 P=0,105	-0,28 P=0,136

Correlations are significant at $P < 0,05$

No significant correlation coefficients were found between the density of the early wood zone and colour coordinates L^* , a^* and b^* at 95% confidence level (Table 2).

Figures 1, 2 and 3 show the relationship between density of early wood zone and colour parameters L^* , a^* and b^* of sycamore maple wood. The coefficient of correlation between colour parameters and wood density are detailed in Table 2 for early wood and for late wood of *Acer pseudoplatanus*.

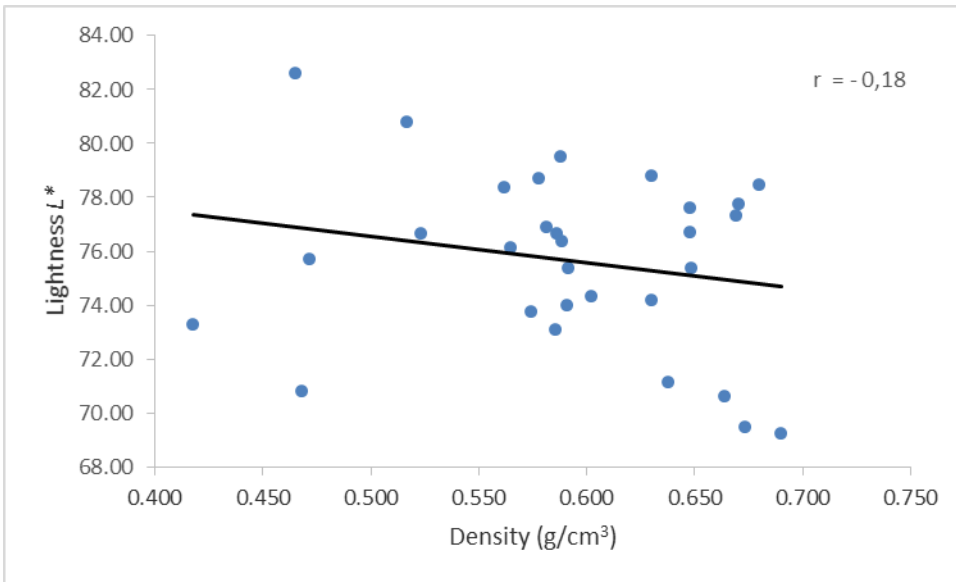


Figure 2 Relationship between density of early wood zone and colour parameter L^* of sycamore maple wood

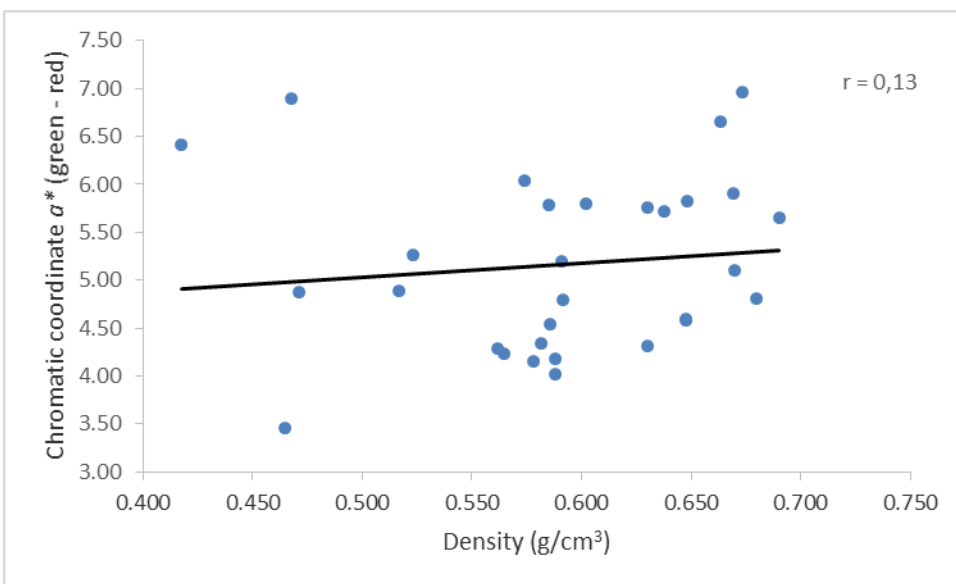


Figure 3 Relationship between density of early wood zone and colour parameter a^* of sycamore maple wood

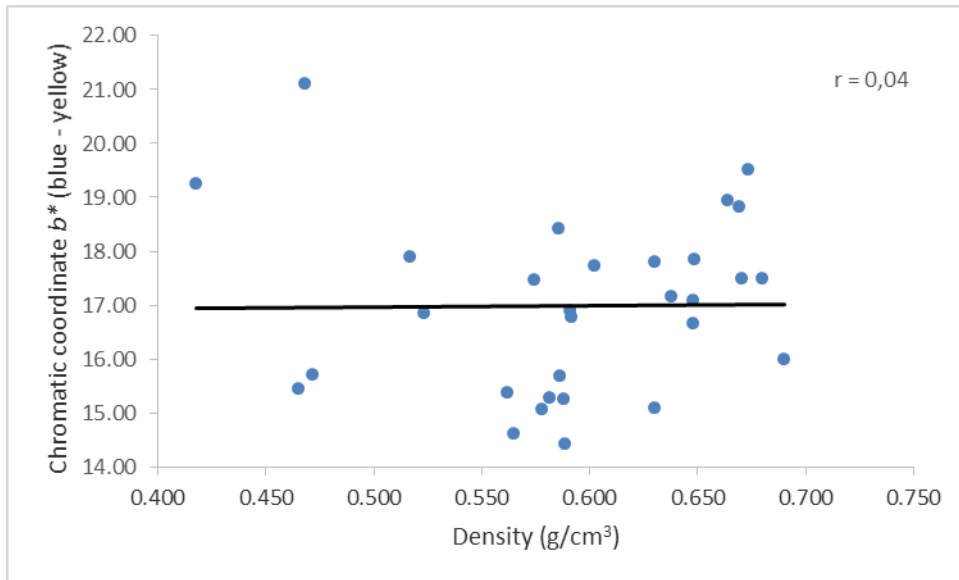


Figure 4 Relationship between density of early wood zone and colour parameter b^* of sycamore maple wood

Figures 4, 5 and 6 show the relationship between density of late wood zone and colour parameters L^* , a^* and b^* of sycamore maple wood.

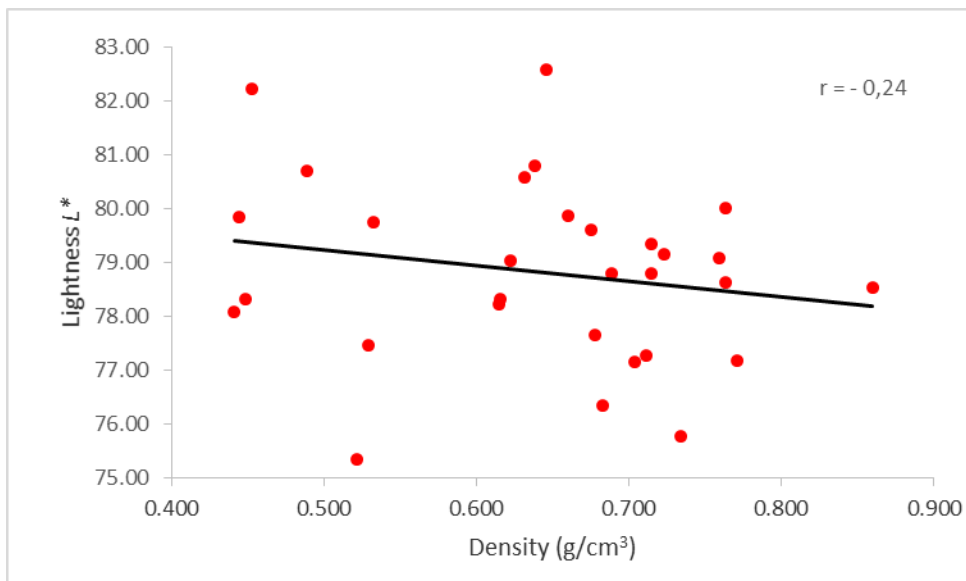


Figure 5 Relationship between density of late wood zone and colour parameter L^* of sycamore maple wood

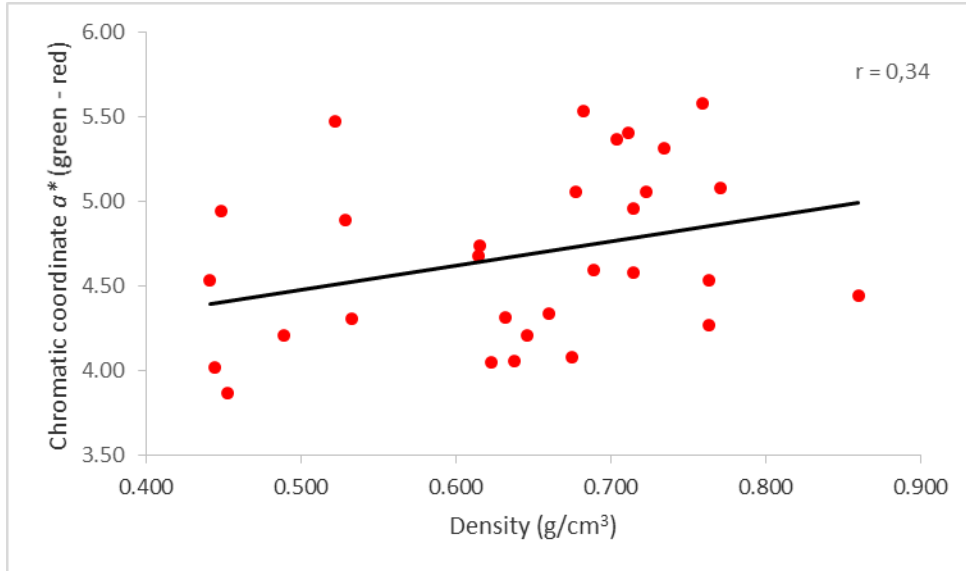


Figure 6 Relationship between density of late wood zone and colour parameter a^* of sycamore maple wood

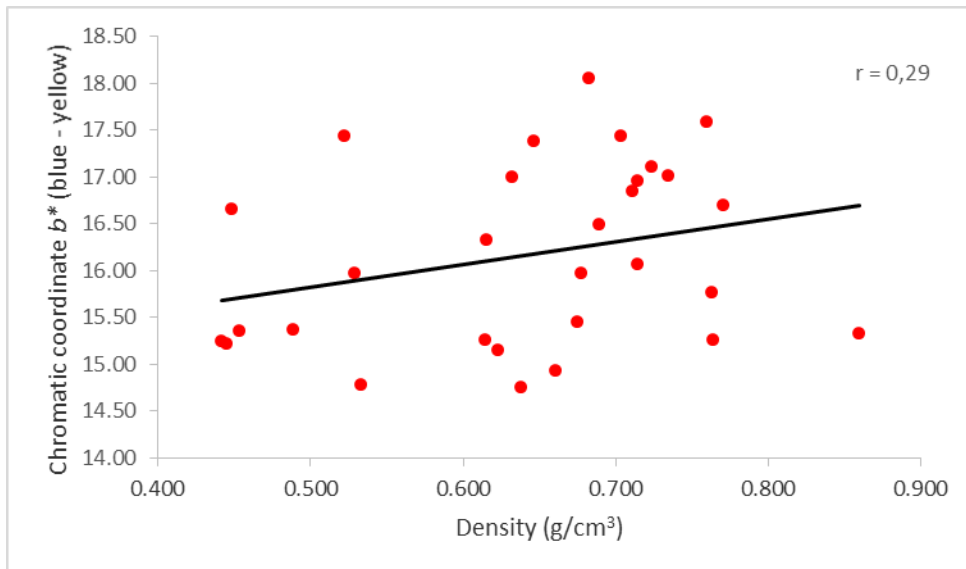


Figure 7 Relationship between density of late wood zone and colour parameter b^* of sycamore maple wood

4 Conclusions

From the analysis of the data obtained in this investigation, the conclusion was that the increase in density of the early wood zone of sycamore maple (*Acer pseudoplatanus* L.)

reduces the colour coordinates L^* , meaning that the wood gets darker tone. The same result was obtained in the early wood and the late wood zone.

With increasing of density in the early and late wood zone, the values of colour coordinates a^* and b^* are growing. Increase in density also leads to an increase in colour saturation in the early and the late wood zone. Slight differences were measured in the average colour saturation C^* and colour tone h_{ab} between early and late wood zones. These results are not statically significant.

Statistically, the mean values of early wood density (0.591 g/cm³) and the mean density of the late wood (0.641 g/cm³) are significantly different.

With this measuring method, on these samples it was not possible to find significant correlation between density of wood and colour of wood.

The unexpected result was obtained by comparing the mean values of the colour coordinates L^* (the lightness of the early and late wood). The average lightness of late wood zone is greater than the average lightness of the early wood zone, meaning that the early wood zone is darker than the late wood zone.

Lack of significant correlation between density and wood colour opens new questions in wood colour measurement. Repeating this measuring method on larger number of specimens, and different wood species could be a good topic for future research.

5 Literature

1. Blanchard, V.; Blanchet, P., 2011: Color stability for wood products during use: Effects of inorganic nanoparticles. *Bioresources*, Volume: 6, Issue: 2, Pages: 1219-1229.
2. Brischke, C.; Welzbacher, C. R.; Brandt, K.; Rapp, A. O., 2007: Quality control of thermally modified timber: Interrelationship between heat treatment intensities and CIE $L^*a^*b^*$ color data on homogenized wood samples. *Holzforschung*, Volume: 61, Issue: 1, Pages: 19-22.
3. Chen, T., 2012: A Study of the Visual Physical Characteristics and Psychological Images of Select Taiwanese Hardwoods. *Forest Products Journal*, Volume: 62, Issue: 1, Pages: 18-24.
4. Chen, Y.; Gao, J.; Fan, Y.; Tshabalala, M. A.; Stark, N. M., 2012: Heat-induced Chemical and Color Changes of Extractive-free Black Locust (*Robinia pseudoacacia*) Wood. *Bioresources*, Volume: 7, Issue: 2, Pages: 2236-2248.
5. Horvat, I.; Krpan, J., 1967: *Drvnoindustrijski priručnik*, Zagreb.
6. Jung, B. W.; Kozak, R. A., 2008: Color testing of four Canadian wood species. *Forest Products Journal*, Volume: 58, Issue: 11, Pages: 84-86.
7. Miklečić, J.; Jirouš-Rajković, V.; Antonović, A.; Španić, N., 2011: Discolouration of thermally modified wood during simulated indoor sunlight exposure. *Bioresources*, Volume: 6, Issue: 1, Pages: 434-446.

8. Miklečić, J.; Španić, N.; Jirouš-Rajković, V., 2012: Wood color changes by ammonia fuming. *Bioresources*, Volume: 7, Issue: 3, Pages: 3767-3778.
9. Nemeth, R.; Ott, A.; Takats, P.; Bak, M., 2013: The Effect of Moisture Content and Drying Temperature on the Colour of Two Poplars and Robinia Wood. *Bioresources*, Volume: 8, Issue: 2, Pages: 2074-2083.
10. Nishino, Y.; Janin, G.; Chanson, B.; Detienne, P.; Gril, J.; Thibaut, B., 1998: Colorimetry of wood specimens from French Guiana. *Journal of Wood Science*, Volume: 44, Issue: 1, Pages: 3-8.
11. Nishino, Y.; Janin, G.; Yamada, Y.; Kitano, D., 2000: Relations between the colorimetric values and densities of sapwood. *Journal of Wood Science*, Volume: 46, Issue: 4, Pages: 267-272.
12. Ugrenović, A., 1950: *Tehnologija drveta*. Nakladni zavod Hrvatske. Zagreb.

CORRESPONDING ADDRESS:

Izv.prof.dr.sc. Tomislav Sinković
University of Zagreb
Faculty of Forestry
Svetošimunska 25, Zagreb, CROATIA
e-mail: tsinkovic@sumfak.hr

Assessment of Drying Quality and Accuracy of Wood Processing

Nikolay Skuratov^{1} – Igor Sapozhnikov²*

¹ Professor, Department of Processes and Apparatuses in Woodworking Industry– Moscow State Forest University. 141005, Mytishi, Moscow Region, RUSSIA.

** Corresponding author*

skuratov@mgul.ac.ru

² Professor, Department of Processes and Apparatuses in Woodworking Industry - Moscow State Forest University. 141005, Mytishi, Moscow Region, RUSSIA.

gosha@mgul.ac.ru

Abstract

Efficiency of woodworking enterprises depends significantly on the quality of drying timber. Usually any batch of dried timber includes some boards with distortions. Practice shows assessment of drying quality of boards with cupping is associated with considerable difficulties. The cross-sectional shape of such boards differs markedly from the rectangular. This creates problems at performance of preparatory procedures and measurements and also complicates the interpretation of results.

For carrying out of experiments pine boards 40x150 mm and alder boards 32x120 mm were dried up to the moisture content of about 8% by low temperature schedules. The drying quality was investigated on the basis of the large number of measurements of wood moisture content and drying stresses. For the measurement of wood moisture content oven dry and electrical resistance methods were used. Residual drying stresses were determined by means of the prong and slicing tests.

Analysis of the data showed that due to the transverse curvature the measurement results are not always correct. This can lead to underestimation or overestimation of drying quality of such boards. Apparently there is a need to clarify the methods for assessment of drying quality of the boards with cupping.

The second purpose of this study was estimation of tendency for cupping when the product is manufactured by resawing dried sawn timber. Attempt to connect indicators of drying quality with possible changes of wood detail sizes in which after drying remained essential moisture content gradients and residual stresses was undertaken. Possibility of

application of specialized computer programs to simulate deformations of cross section of wood details at their asymmetrical processing was estimated.

Keywords: timber drying, drying quality, prong test, slicing test

Introduction

Timber drying is an important procedure in the manufacturing process. Quality products can be made only from good-dried wood. Requirements for the quality of drying depend on the final usage of product made of dried wood. There are rules (recommendations or standards) to evaluate the timber drying quality in different countries (Guiding technical materials 1985, European Drying Group 1994, EN 14298). Typically, the following properties are determined: the average final moisture content, variation of moisture content across the board thickness and within a kiln load. If the limits on the degree of stressed condition are specified, then in addition to the moisture content measurements, the actual drying stresses have to be evaluated. Defects caused by the inherent properties of wood or improper drying condition are also taken into account. The smaller the difference between final moisture content and given one, variation of final moisture content among the board thickness and within a kiln load, the residual drying stresses, the better drying quality.

To determine the average moisture content of wood resistance (Guiding technical materials 1985, EN13183-2) and capacitive (EN 13183-3) moisture meters are widely used. Local moisture content can be measured only by needle resistance moisture meters. In practice, the oven dry method (Guiding technical materials 1985, EN 13183-1) for determining wood moisture content is rarely utilized.

Level of residual stresses in dried timber is evaluated by means of prong test (Guiding technical materials 1985, Denig et al. 2000) and slicing test (ENV 14464). Both methods are based on the measurement of deformations, depending on stress-strain state of wood after drying.

Cupping is a common drying defect associated with nonuniform of transverse wood shrinkage. Practice shows assessment of drying quality of boards with cupping is associated with considerable difficulties. The cross-sectional shape of such boards differs markedly from the rectangular. This creates problems at performance of preparatory procedures and measurements and also complicates the interpretation of results. Also, cupping may occur during mechanical processing of the dried timber. Even though wood is dried out evenly, but the considerable internal stresses remained therein after machining the shape and cross-sectional dimensions of parts can change. Typically these changes are observed at the asymmetric machining of workpieces, which is associated with the redistribution of internal stresses resulting in deformation of their cross sections. Quantitative assessment of changes in the shape and size of the cross sections of timber at drying and machining is of practical interest. Assessment can be made based on both experiments and computations.

There are specialized computer programs for modeling two-dimensional deforming of bodies caused by various reasons (ABAQUS, ANSYS). Many researchers have used specialized software to simulate the behavior of wood when changing temperature and relative humidity of ambient air. Simulation results are useful for analysis of the wood condition at the different technological processes and in operation at variable temperature and relative humidity of ambient.

The objective of this paper is to identify the problems in assessing the drying quality of warped timber and evaluation of the actual deformations of wood pieces at planing.

Materials and Methods

For the experiments seven 40x150mm pine boards and seven 32x120 mm alder boards having cupping were chosen. All boards of length 3-4 m were dried in industrial kilns to the final moisture content of about 8-10% by appropriate low temperature schedules (Guiding technical materials 1985). Drying quality was evaluated by both Russian and European methods. From clear parts of every board no less than 32 sections were cut: 2 sections for measuring average moisture content; 6 sections for measuring moisture gradients; 12 sections for prong tests; 6 sections for slicing tests; 6 sections for measuring cupping after detail processing (Fig. 1).

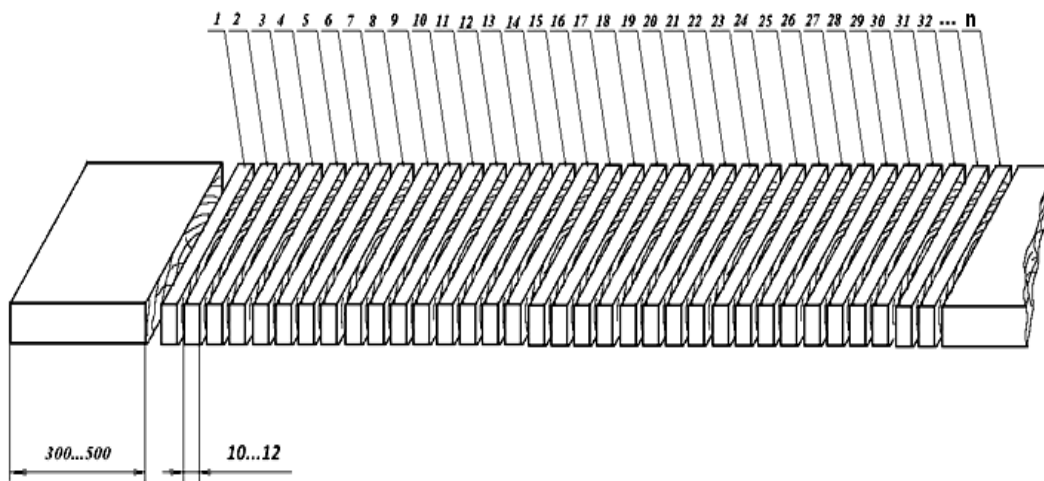


Figure 1. Schematic of cutting sections out of the board

Average wood moisture content was determined by oven dry method for reference purpose (EN 13183-1). For measuring moisture gradients the slicing method was used (Guiding technical materials 1985). Moisture distribution sections were cut into 5 pieces (Fig. 2).

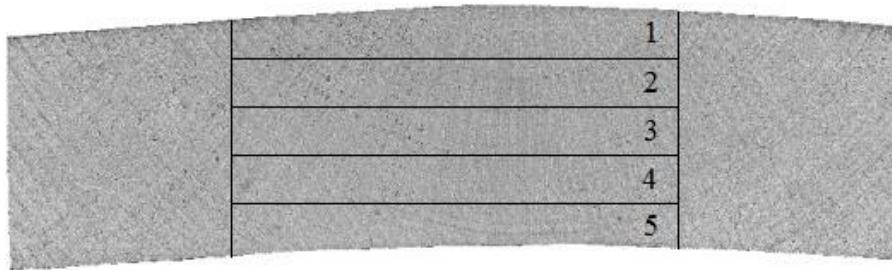


Figure 2. Schematic of cutting section for measuring moisture content gradient

Moisture content gradient was calculated as the difference between the moisture content of the central piece and the average moisture content of the surface pieces. Additionally, the average moisture content in 10 points at the both sides of every board (Fig. 3) was measured by the resistance meter (EN13183-2).

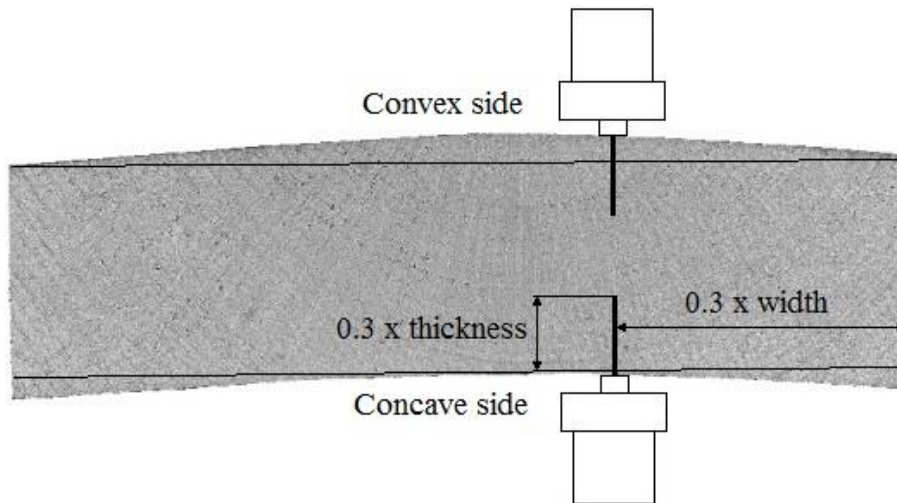


Figure 3. Schematic of cutting moisture distribution sections

Residual stress level was evaluated by both slicing test (ENV 14464) and prong test (Guiding technical materials 1985). In EU countries drying stresses are measured by means of the slicing test. Stress level is determined by the magnitude of the gap between two halves of cross section which was cut to 100 mm and split in half (Fig. 4).

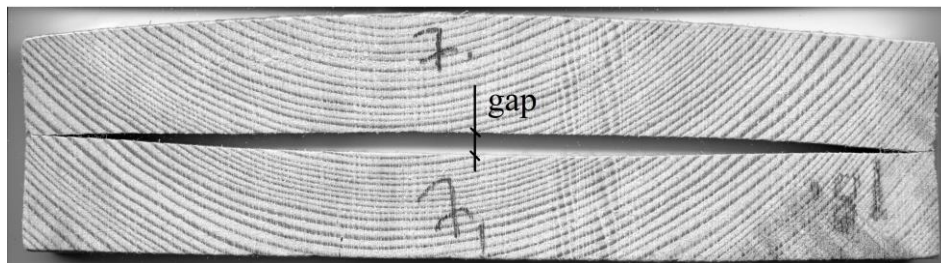


Figure 4. European method of cutting stress section for slicing test

If the actual width of the stress section is smaller than 100 mm, the measured results for the gap opening have to be related to the standard specimen width of 100 mm by using the formula stated below (1). This formula may also be used when a width of section is greater than 100 mm.

$$gap_{100} = gap_{measured} \cdot (100 / width_{actual})^2 \quad (1)$$

In Russia drying stresses are evaluated by relative bending of prongs having a fixed thickness (Fig. 5a). Unfortunately technical literature does not offer recommendations on cutting stress specimens from non-rectangular sections of warped wood. For this reason, two variants of the samples with the rectilinear and curvilinear prongs have been made (Fig. 5 b, c). The residual drying stresses are evaluated by the relative bending of prongs *PR* having a fixed thickness of 5-7 mm.

$$PR = 100 \cdot (T - T_1) / 2 \cdot L \quad (2)$$

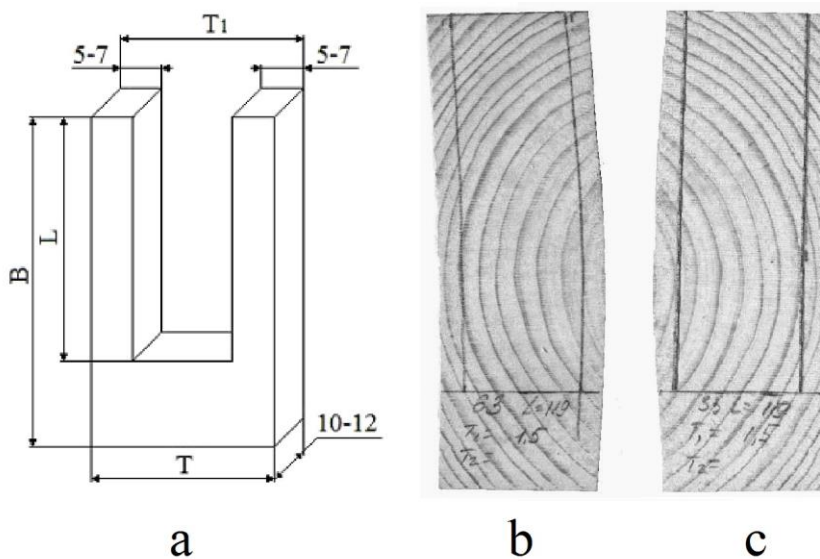


Figure 5. Russian method of cutting stress section for prong test (a) and its application for warped timber when stress specimens with rectilinear (b) and curvilinear (c) prongs may be used. B – board width, T – board thickness, L – prong length, T₁ – distance between the outer prong edges after removing core of the section

To estimate possible cupping which may occur during mechanical processing of the dried timber special samples simulating asymmetrical machining wooden workpieces were prepared (Fig. 6).

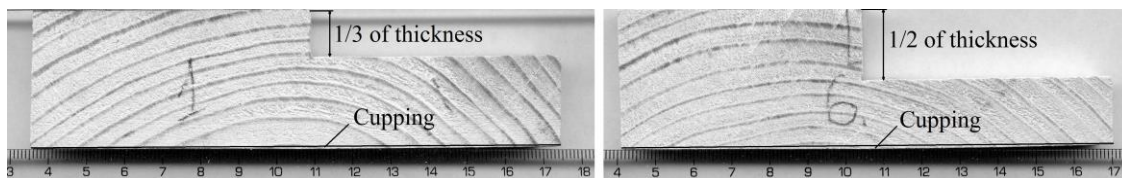


Figure 6. Samples simulating asymmetrical machining wooden workpieces

First, the sections were processed to give them the shape of a regular rectangle. Then given portions of the sections were cut out. It caused cupping opposite side of the sample which was measured. Size of removable portion simulates machining depth. The more size the more depth of machining and workpiece cupping.

Results and discussion

The results of measuring average and local moisture content are shown in the Table 1. Noteworthy is that the moisture content of surface zones measured on the concave side of the boards is higher than on the convex side. Apparently this is due to the different conditions of moisture exchange on different sides of warped boards. Also a small difference is visible from the results of measuring the average moisture content by means of the moisture meter. Measurements on the convex side of the boards were closer to the actual values determined by the oven dry method.

Table 1

MC of layers, MC gradient, average MC based on oven dry method and measured by meter

Board number	MC of board layer, %			MC gradient, %	Average MC, oven dry method, %	Average MC measured by meter, %	
	Concave side	Centre	Convex side			Concave side	Convex side
1 Pine	9.11	11.04	7.83	2.57	9.76	10.4	10.1
2 Pine	8.52	10.65	8.31	2.24	9.53	10.0	9.9
3 Pine	9.06	10.56	8.39	1.83	9.65	10.1	9.8
4 Pine	9.04	10.94	8.26	2.29	9.80	10.3	9.9
5 Pine	9.09	10.99	8.92	1.99	9.99	10.3	10.0
6 Pine	9.61	11.25	8.36	2.27	10.12	10.5	10.2
7 Pine	9.88	11.28	8.72	1.99	10.29	10.7	10.4
1 Alder	7.29	8.81	6.22	2.05	7.79	8.2	7.9
2 Alder	7.24	9.23	7.02	2.10	8.18	8.5	8.2
3 Alder	7.52	8.87	6.90	1.66	8.04	8.3	8.0
4 Alder	7.32	8.76	6.72	1.74	7.89	8.3	8.1
5 Alder	7.50	9.12	7.32	1.71	8.27	8.5	8.3
6 Alder	8.07	9.45	7.02	1.90	8.50	8.9	8.6
7 Alder	8.46	9.65	7.41	1.71	8.70	9.2	8.8

Evaluations of residual drying stresses obtained by European and Russian methods are collected in Table 2. Values of the prong bending for samples with the rectilinear and curvilinear prongs are presented. On average, European method showed the average level of stress, and the Russian - increased. Curvilinear prongs were bent less than rectilinear prongs. Rectilinear prongs bends more because they are thinner at the bottom (Fig. 5).

When evaluating the stress level in warped boards samples with curvilinear prongs should be used.

Table 2

Residual drying stresses evaluated by European and Russian methods

Board number	MC gradient, %	European method. Gap, mm	Russian method. Prong bending, %	
			Rectilinear prongs	Curvilinear prongs
1 Pine	2.57	1.4	3.2	2.9
2 Pine	2.24	1.5	3.3	3.0
3 Pine	1.83	1.4	3.0	2.5
4 Pine	2.29	1.6	2.2	2.0
5 Pine	1.99	1.3	2.9	2.2
6 Pine	2.27	1.5	3.5	2.8
7 Pine	1.99	1.4	3.1	2.6
1 Alder	2.05	1.3	1.5	1.3
2 Alder	2.10	1.2	1.7	1.5
3 Alder	1.66	1.2	1.2	1.0
4 Alder	1.74	1.1	1.3	1.1
5 Alder	1.71	1.2	1.5	1.4
6 Alder	1.90	1.0	1.2	0.9
7 Alder	1.71	1.0	1.6	1.2

Cupping of special samples was measured with help of image scanning. Maximal measured cupping was equal to 1.5 mm. The real relationship between the prong bending and cupping at the different depth of wood machining is shown in Figure 7. The dependence obtained allows to estimate the possible warping of workpieces when asymmetric machining using the prong test results. Relationship between sample cupping and gap width was weak (Fig. 8).

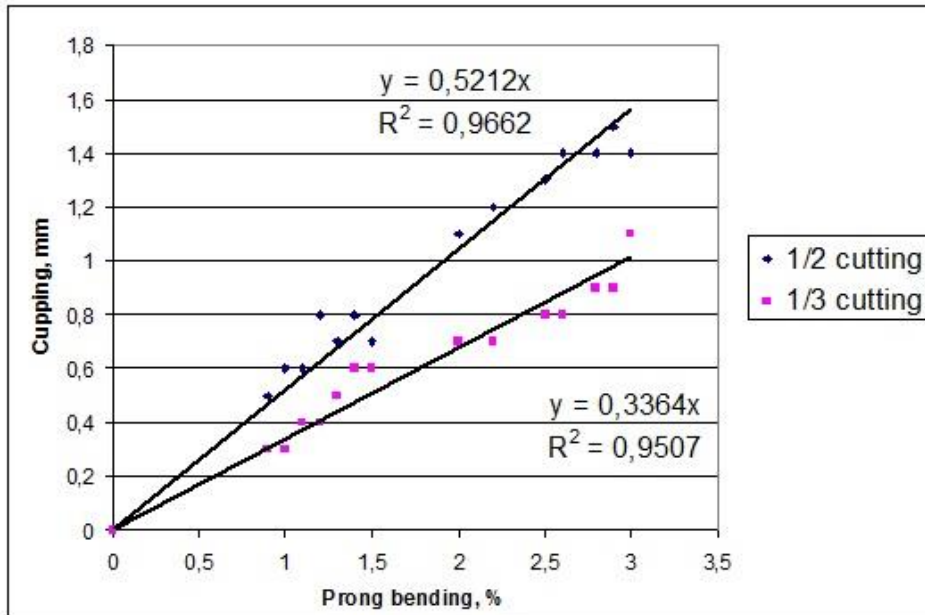


Figure 7. The relationship between the prong bending and cupping at the different depth of wood machining

Perhaps this is due to the lower sensitivity of the slicing test compared to the prong test. Obviously in order to generalize the results and apply them in practice additional researches with the use of computer simulations are needed. To produce reliable quantitative results, computer software should be not only a two-dimensional but also take into account actual heterogeneity and anisotropy of wood as an object of modeling. In addition, the program should allow to change the boundary conditions at the asymmetric machining wooden parts.

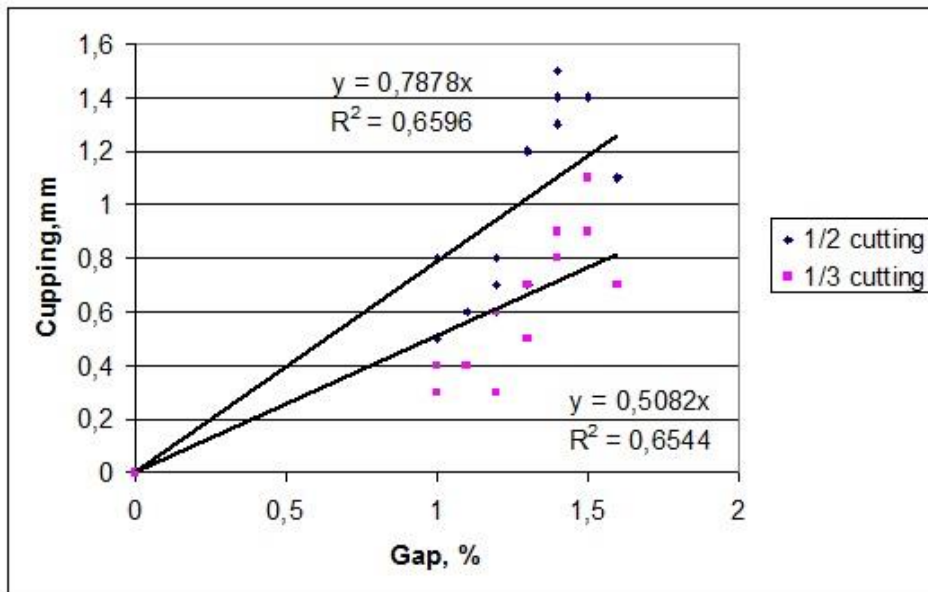


Figure 8. The relationship between the gap and cupping at the different depth of wood machining

Conclusion

Moisture content on the concave and convex sides of warped timber can be different. When measuring the average moisture content using a moisture meter this difference should be taken into account. Perhaps it is advisable to determine the average moisture on the convex side of the warped boards. When evaluated the stress level in warped boards samples with curvilinear prongs should be used. There is dependence between the prong test results and the possible warping of workpieces when asymmetric machining.

References

ABAQUS version 6.6 manual. ABAQUS Inc., 2006.

ANSYS Structural analysis guide section 2.3., 2007.

Denig, Joseph; Wengert, Eugene M.; Simpson, William T. 2000. Drying hardwood lumber. Gen. Tech. Rep. FPL–GTR–118. Madison, WI: U.S. Department of Agriculture, Forest Service, Forest Products Laboratory. 138 p.

ENV 14464. Sawn timber. Method of assessment of case-hardening. 2003:8p.

EN 13183-1 Moisture content of a piece of sawn timber. Part 1: Determination by oven dry method.

EN 13183-3 Part 3: Estimation by capacitance method.

EN 13183-2. Moisture content of a piece of sawn timber. Estimation by electrical resistance method.

EN 14298 Sawn timber – Assessment of drying quality

European Drying Group. 1994. Assessment of Drying Quality of Timber. 27 p.

Guiding technical materials on technology of kiln drying of wood. Arkhangelsk: TSNIIMOD, 1985. 143 p. (in Russian).

Dissertation. Chalmers University of Technology.

Mathematical Modeling of Timber Elastic-Viscous-Plastic Deformation in the Drying Process

Yaroslav Sokolovskyy, Yuriy Prusak, Igor Kroshnyy

Abstract

In the paper there is described solving a current scientific problem of mathematical modeling of heat-mass transfer processes and elastic-viscous-plastic deformation taking into account the mechanics and sorption creep in hygroscopic capillary-porous materials with variable anisotropic heat and mechanics characteristics what is of importance for the rational choice and substantiation of energy conservative technologies of timber drying under the conditions of necessary qualitative production providing. There has been implemented the formulated mathematical model of timber deformation during the drying process which enables to identify two-dimensional intense-deforming state under the conditions of non-isothermal humidity transfer by means of the finite elements method. This method has been developed for the research of the two-dimensional anisotropic intense-deforming state during the capillary-porous materials drying process in an elastic-viscous-plastic area of deformation taking into account the mechanics and sorption creep. There has been elaborated the applied software which consists of the documented classes and provides the possibility to automate the finite-elemental analysis of timber intense-deformation state during drying process.

The problem of timber drying process optimization has been formulated and solved which enables to define the parameters of the drying process conditions taking into consideration the restrictions on the intense-deforming state which does not exceed the solidity limit of the material.

Keywords: mathematical model, the method of finite elements, heat and mass transfer, elastic-viscous-plastic state, drying process.

Ukrainian National Forestry University (UNFU)
Gen. Chupryny Str., 103, Lviv, Ukraine, 79059
Department of Computer Engineering and Modeling of Technological Processes
+38-032-2392795

Prof. Dr.-Ing. Ya. Sokolovskyy
e-mail: sokolowskyyyar@yahoo.com
Postgrad. Yu. Prusak
e-mail: yu.prsk@gmail.com
Assistant Prof. I. Kroshnyy
e-mail: kroshny.igor@gmail.com

Mitigation of End Shakes on Oak Saw Timber as a Result of Storage by Applying Environment-Friendly Methods

Péter Szeles¹ - Szabolcs Komán^{2} - Sándor Fehér³*

¹PhD Student, *Simonyi Károly Faculty of Engineering, Wood Sciences and Applied Arts, Institute of Wood Science, Sopron, Hungary*

peter.szeles@skk.nyme.hu

² Assistant Professor, *University of West Hungary, Simonyi Károly Faculty of Engineering, Wood Sciences and Applied Arts, Institute of Wood Science, Sopron, Hungary*

** Corresponding author*

szabolcs.koman@skk.nyme.hu

³ Associate Professor, *University of West Hungary, Simonyi Károly Faculty of Engineering, Wood Sciences and Applied Arts, Institute of Wood Science, Sopron, Hungary*

sandor.feher@skk.nyme.hu

Abstract

The mitigation of the damages occurring during the storage of saw timber can be solved – based on the current requirements – exclusively by applying environment-friendly methods. For this purpose diverse end grain sealers are available. Their efficiency in case of saw timber protection is however generally unknown or only little information is available for the users. The selection of the appropriate sealer can be performed only within the frame of a complex research program. The research series regarding end grain sealing conducted first at the company Északerdő Forestry PLC. in our country has confirmed that after logging already during the storage it is possible to mitigate the extent and quantity of the developing end shakes and hereby to prevent fungoid and insect pests. The research involved the study of four commercially available end grain sealers of different base. The change in the moisture content of the timbers and the visible shakes appearing on the end grain surfaces of the timbers with their end pointing to the four cardinal points have been continuously observed for a period of six months. The changes to the end grain surfaces have been recorded with photographs and then evaluated. The research supports the idea that the use of the appropriate end grain sealer may significantly mitigate desorption through the end grain surface, which may also have beneficial impact on the number and depth of end shakes.

Keywords: end grain sealing, end-shake, yield, orientation of timber

Introduction

Regarding the activities and economic efficiency of wood-processing businesses, yield is of extreme importance. Within the activities performed in sawmills, the storage of delivered timbers is the first phase of operation where yield can be improved. The quality of the sawmill timber, so the character and quantity of the wood defects in the timber play a very important role in the development of the yield percentage. Following logging, changes may tend to appear on saw timbers as a result of external abiotic and biotic factors. The more efficient the mitigation process is to treat such changes, the higher extent the quality of saw timber can be preserved.

The period and the circumstances of storage play a significant role in the subsequent formation of end shakes on saw timber. End shakes, ripping, lathe checks can easily develop and in this context fungoid and insect pests can appear. There are several methods for mitigation, a part of which can be considered as traditional (e.g. storage in water, spraying, end grain surface shielding). Different environment conditions such as temperature, relative humidity, air flow rate or solar radiation significantly affect end shakes (Yang and Normand 2012). With professional decisions made as to the place of storage, and by taking orientation into consideration, timber quality can be efficiently preserved. According to Shupe and Mills (1997) the East-West orientation is more advantageous due to the stronger solar radiation on the Southern side, however for the mitigation of end shakes different individual protective devices, such as treatment of the end grain surfaces are available.

In total the collective application of these methods will provide us with the optimal solution.

End grain sealing is a very popular method in the preservation of quality. The end-shakes arising on the saw timber are frequent and important timber defects of sawmills processing broad-leaf trees (Wilhelmsen 1969), for this reason it is of great importance primarily in the protection of the finished and semi-finished products issued by sawmill industry, but prospectively its application will be emphasized in the preservation of saw timbers as well.

The end shakes develop as result of the rapid drying, the extent of which is not always unambiguous. Because these end-shakes open and close during the drying process, it is occasionally complicated to detect them. The hair-cracks at the end of materials drying outdoors can be even 30 cm or longer (Murray 2014).

The sealers can be applied cold or warm onto the material to be protected. Cold applicable sealers can be applied easily, while warm applicable sealers can be applied difficult – in case of timber – onto the surface (McMillen 1961).

In Hungary the different oak types are of significant importance both in silviculture and in timber-industry. The “production” of high-quality plate and sawmill timbers is significant for silviculture and timber-industry respectively. It is reasonable to start the quality improvement as soon as possible – already on the log yard. The preservative end-coating is still not spread in timber preservation in our country, so the basic objective of the research was to propose appropriate technology and preservative for the storage of the high-value chestnut oak timber. In our research work the efficiency of four different end grain sealers was determined. During the research series of almost 8 months we have continuously investigated the alteration of the moisture content and end shakes of the timber and we have searched for the answer, whether the orientation of the saw timber during storage affects the tendency to end shakes.

Materials and Methods

As base material of the research project 50 pcs. Sessile oak (*Quercus petraea*) saw timbers were available. The length of the timber was 2,1 m, diameter between 25-50 cm. For the end grain sealing of sawmill materials several wood preservatives are available. Among them we have selected preservatives for the elaboration of the research program, the purchase of which is not complicated on the timber preservative market. For this reason we have considered four different end grain sealers: aqueous paraffin, water based-I, alcohol based and water based-II.

Establishment of research stacks

On the asphalted log yard of a North-East-Hungarian sawmill two research stacks consisting of 25 pcs. each was established. Within the stacks the timber were placed in two rows on each other showing to the 4 main cardinal points with the ends. Accordingly one stack was located in North-South orientation and the other in East-West. The end grain surfaces of the timber were coated with four different end grain sealers. Within the 25-pcs-stacks the oak trunks were arranged by fives. To measure the efficiency of the four preservatives a fifth group – control group – was established, where the investigation was performed without end-coating.

Condition survey

The occurrence of end shakes can be observed mainly on timber felled between April and October, for this reason logging work is recommended for winter (Yang and Beauregard 2001). The alterations arising at the timber ends (end shakes, colouration etc.) were recorded by means of pictures about the end grain surfaces beginning from the establishment of the stacks up to breaking-down. The condition surveys were carried out between April and October, approximately in every 1,5 month, totally 5-times. For the evaluation of end shakes we have started to work on a methodology, by the help of which based on the pictures (Fig. 1) made during the condition surveys the alterations can be numbered, excluding subjective judgements. The essence of the method is that in image analyzing programs it is possible to display diagrams showing the distribution of image tints – alias histograms.

Taking a look at the pictures we wish to analyze it can be seen that the end-shakes appear on the cross-section of the timber in a darker tone (Fig. 1), so they can be clearly separated by an image analyzing program. A divalent black-and-white image shall be established from the photographs (Fig. 2) by means of a limit value correction, in order to have only two tones – black and white – on the histogram received. The limit value shall be selected in a manner, that every end shake becomes black and the body white. Then the percentual value of the end shakes can be read from the statistic data of the histogram.

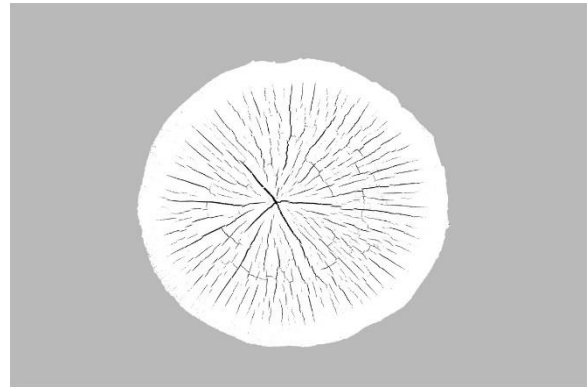


Figure 1. End grain surface for examination *Figure 2. Result of the image conversion*

Alteration of the moisture content

The growing and vital functions of living trees need water, so it is natural, that the fresh logged timber contains significant amount of moisture. Affected by the shape and dimensions of the body it will be equilibrated with its environment only after several months. The equilibrium moisture content of timber is basically determined by the air temperature and relative humidity. As soon as any of these factors changes, these alterations are followed also by the moisture content of timbers. Several environmental effects affect the ambient temperature and the relative humidity of course; among others weather components such as sunshine, precipitation, wind, but also storage conditions, e.g. orientation of timbers or topographic relations (valley, hillside, etc.) have influence on moisture content.

The alteration of the net moisture content of timber was registered by instrumental measuring on every single experimental timber. The measuring was performed 30 and 60 cm from both ends of the saw timber and in the middle respectively, so the alteration of moisture content could be observed on the entire length of the timber.

Results and assessment

The measuring of the water content alterations has coincided with the occasion of making photographs about the end-shakes. During the evaluation of the results the external effects on the timber during the experiment shall be considered in any case. The weather – sunshine, precipitation quantity – affects directly the alteration of moisture content and the cracks and damages respectively. Three seasons – spring, summer and autumn – fell into the examined six-month-period. The different seasonal effects deviating from the

particular year can probably modify the results received to a certain extent. In the year of the investigation the weather of the region has deviated from the previously usual. At the beginning of summer the precipitation was more than expected, the real long-lasting warm period has started only at the end of the season, while autumn earlier with more precipitation has brought drought and higher temperature than usual.

Moisture content

Average moisture content

The chronological alteration of the average moisture content of the experimental items closely correlates with weather parameters. The actual measuring works of the research project have started at the beginning of April (08 April). The first three examinations were carried out by the beginning of July. These measuring results did not demonstrate any excessive deviations owing to the rainy weather. Analyzing the data of Figure 3 it can be well observed that the extent of desorption increases significantly after the third measuring.

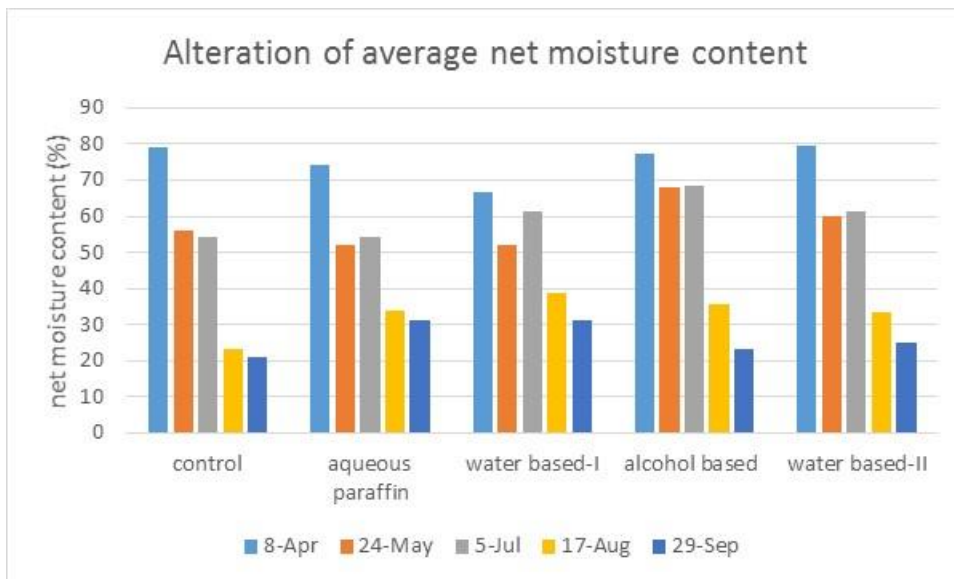


Figure 3. Effect of the end grain sealer to the extent of the average desorption (N-S)

It can be observed that a moisture loss of higher extent occurred at the 4th measuring time. There is a difference in the moisture content of more than 10% between the control and the treated samples, which reduces gradually with time. This period can be observed in the stage of summer, when there were also longer lasting warm periods. At the last indication the average moisture content was indicated between approx. 20 and 30%. It can be also observed that each of the preservatives applied has reduced the extent of desorption, the coated timber have lost their water content more uniform, while the moisture content of the control pieces has fallen under 25% already during the measuring in August. The most uniform desorption has taken place with the application of the preservative water based-I. The experimental timbers have shown almost similar results independent from the orientation.

Desorption

For the examination of the desorption intensity the results of the measuring points indicated 30 cm from the ends were analyzed on the control timbers. Using these data – performing a functional analysis – information about the trend of desorption can be received and the extent of the effect of orientation can be indicated.

The extent and frequency of the end shakes of timber closely correlate with the amount and rate of desorption. The most favourable condition is provided, when both the reduction of water content and its rate are as low as possible. If the desorption rate is represented on a graph and a trend line is put on it, the curve incline refers to the desorption rate. Based on the analysis of the function relationships it can be observed that the connection of the data sets can be optimally described by a power curve. The data and functional relationships of Figure 4 express the information related to the characteristics of desorption on the side corresponding with the individual cardinal points. The value of the moisture content on the Northern, Southern and Western side has reduced under 25% for the last measuring (18-25%), on the contrary the Eastern end has shown a result above 40%. On the foregoing topographic survey the deviation between the East-West and North-East side is around 20% (45,1 and 39,4% and 25,3 and 23,4 resp.) The desorption rate on the Eastern side has a more moderate curve.

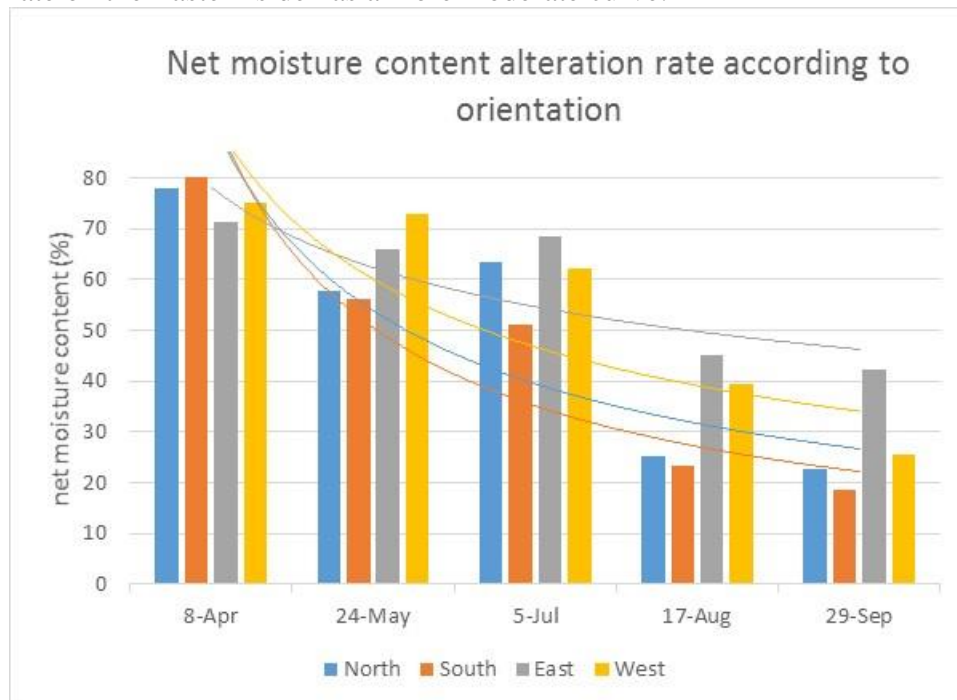


Figure 4. Tendency of desorption depending on the cardinal points

The deviations between the incline of the curves of the diverse cardinal points can be well observed. In order to receive exact data of the desorption tendency; we have summarized the numeric results (Table 1) of the function analyses – the function-related coherences and the r^2 values – because their incline cannot be read from the trend lines of the figures.

		North	South	East	West
Control	function	$y= 91,66x-$	$y= 94,004x-$	$y=78,197x-$	$92,254x-$

		0,767	0,896	0,326	0,619
	r^2	0,7394	0,8499	0,6829	0,7175

Table 1. Result of the function analysis of desorption for every cardinal point

The high amount of the coefficients of determination refers to close fit for every cardinal point, based on which reliable conclusion can be drawn from the investigation results. The most favourable value has come from the Eastern side, where the desorption rate was more moderate than on the other sides, so the probability of end shakes is lower. A significantly higher multiplier factor can be stated than on the other sides, so the tendency of desorption refers to a more intensive drying there, which shows the highest value on the Southern side. It corresponds with the preliminary expectations, according to which the intensive sunshine on the Southern side and the long-lasting strong solar radiation in the afternoon on the Western side can seriously damage the end grain surfaces through similarly more rapid desorption. The examination of the Northern side had an interesting result in the form of a similarly rapid desorption. It refers to the fact that the drying effect of another factor shall be considered, namely intensive desorption caused by windy weather.

End-shakes

The end shakes on the end grain surfaces were visible already during the establishment of the stacks, because the selected timbers were already logged. As the result of the drying their areal ratio has been ranged from 3 to 4%. The further alterations were recorded with photographs made in different times. The end shakes occur due to the intensive desorption of the surfaces, where the moisture content can reach the hygroscopic limit directly on the surface and in its surroundings or even fall below. As a result of this the end shakes develop on account of the stresses arising in the timber.

After the application of the end grain sealers the qualitative and quantitative alteration of end shakes has developed differently in both research stacks. On the Eastern side of the East-West-orientated timber the quantity of end shakes has barely deviated from the 2-5% range, except the application of aqueous paraffin. After the application of aqueous paraffin the amount of end shakes has gradually increased as months gone by, which has almost reached 12% by the end of September? On the Western side similar results were recorded with the deviation that the amount of end shakes has increased after the application of alcohol based. In case of the application of both preservatives – with East-West orientation – the quantitative alteration of end shakes was not considerable against the control timber. This lower result can be also seen on the summarized end shake – area ratio diagram of the four cardinal points (Fig. 5). However it can be also observed that the increase of the end shakes does not coincide with the tendency of control timbers. Despite the relative uniform increase of the control timber the aqueous paraffin shows a higher increase only at the fourth measuring, while alcohol based only at the fifth measuring date, which is maybe in connection with the degradation of the preservatives.

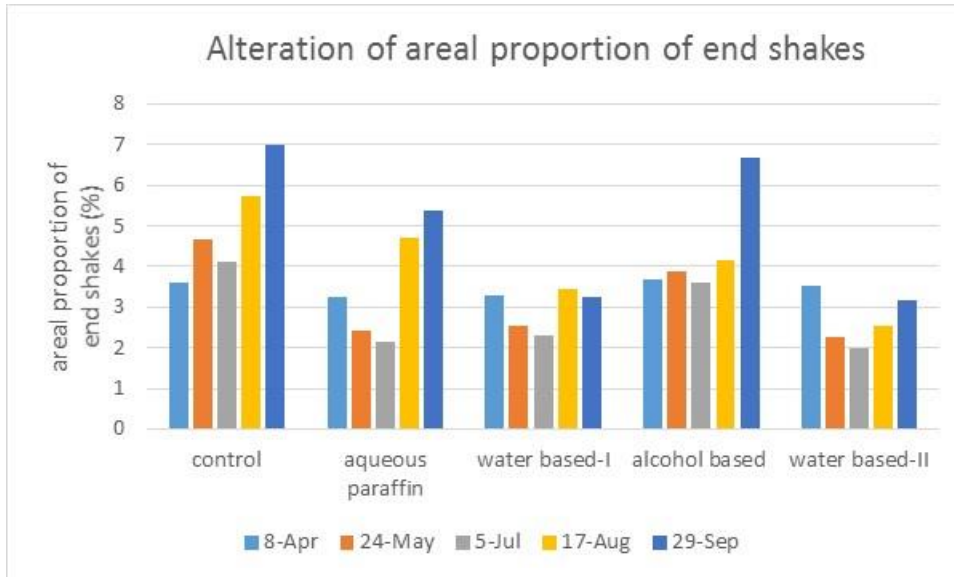


Figure 5. Average areal proportion of the end-shakes additional to the application of individual sealers

The end shake ratio has also significantly increased on the end grain surfaces of the North-West-orientated control timbers – almost to the double on the Northern side and with approx. 25% on the Southern side. Further increase on the Northern side surfaces cannot be demonstrated with the application of preservatives, on the contrary on the Southern side the application of alcohol based did not have adequate result again. Despite the application of this sealer the quantity of end shakes – similar to the Western side – has increased.

Based on the evaluation of the end grain surfaces of the inspected timber – considering all 4 cardinal points – significant difference can be demonstrated among the applied sealers. As indicated in Figure 5 every sealer has moderated the development of end-shakes, however not to the same extent. The end grain sealers water based-I and water based-II have reduced the quantity of the developing end-shakes in case of both orientations; accordingly their efficiency against the other two sealers can be well observed in the summarized diagram.

Summary and Conclusion

By closing the research project we succeeded in improving the quality oak timber processing of the sawmill factory by elaborating a technological step, which can make the economic activity of the factory more competitive. The research results can be summarized in the following points:

The stored timber suffer an intensive desorption during a relative short time, for this reason significant quality loss can be experienced – without end-coating -, which can result serious yield problems.

The orientation of the stored timber is a significant factor among the quality affecting factors. Based on the research work it is reasonable to apply an East-West-orientated stacking system, because desorption rate is more moderate on the end grain surfaces than in case of North-South-orientation.

The investigations support the fact that an appropriate preservative can significantly mitigate desorption through end grain surfaces, so it can favourably affect the amount and extent of the arising end shakes.

All of the end grain sealers applied during the research project has some kind of protective effect, however – based on the results received – significant quality difference can be demonstrated among them.

The application of the end grain sealers water based-I and water based-II has reached an excellent result in the reduction of intensive desorption and moderation of the arising end-shakes.

The end grain sealing ability of the popular aqueous paraffin and alcohol-based fall behind the efficiency of the other two end grain sealers.

Acknowledgements

This study was supported by the Environment conscious energy efficient building TAMOP-4.2.2.A-11/1/KONV-2012-0068 project sponsored by the EU and European Social Foundation

Literature

John M. McMillen. 1961. Coatings for the prevention of end checks in logs and lumber forest products laboratory, Forest Service U. S. Department of Agriculture, Wisconsin.

Shupe, T.F. and R.H. Mills. 1997. Seasoning to prevent defects in green wood. Louisiana State University Agricultural Center. Cooperative Extension Service. Pub. No. 2642. 11 p.

Dian-Qing Yang, Dany Normand. 2012. Best Practices to Avoid Hardwood Checking Part I. Hardwood checking – the causes and prevention.

Wilhemsen, G. 1969. Protection of wood raw material in Scandinavia. *Material und Organismen* 4(3): 201-229.

Yang, D.Q., R. Beauregard. 2001. Check development on jack pine logs in Eastern Canada. *Forest Product Journal* 51 (10): 63-65.

Normann E. Murray. Preventing End Checking in Hardwood Logs & Lumber

*Proceedings of the 57th International Convention of Society of Wood Science and Technology
June 23-27, 2014 - Zvolen, SLOVAKIA*

<http://www.turnstonesingapore.com/files/Preventing%20End%20Checking%20in%20Hardwood%20Logs%20and%20Lumber%20-%20FINAL.pdf> (last download: 10. April 2014).

Effects of Atmospheric Plasma Treatment on Wood Surface

Radovan TINO, Zuzana REPANOVA and Michal JABLONSKY

Abstract

Plasma is a partially or fully ionized gas in which neutral atoms are split into electrons, ions, free radicals and the next elementary parts; it is often referred to as a fourth state of matter. Plasma technologies are often distinguished depending on their temperature (low, high) and pressure (low, atmospheric): in case of high temperature, the ionization is induced thermally whereas in case of low temperature, it is generated by High Voltage electric fields.

By producing high frequency electric discharges, plasma generates ionized gas that can modify the surface properties of the material it is in contact with. Plasma treatment is a versatile and powerful technique commonly used in many industries for materials such as plastics, textiles, glass and metals. Plasma is also used for the sterilization of number products in the food and pharmaceutical industries. Plasma is a versatile technique with number of variable parameters (gas, flow rate, power, pressure, application time, gap, etc.) and electrode set up, that can result simultaneously in various effects for different classes of materials, especially on lignocellulosic materials containing wide range of chemicals, which particles in plasma discharge can react with. In recent years, plasma technologies operating at room temperatures and at atmospheric pressure have emerged. Depending on the treated material, plasma is expected to simultaneously provide a number of effects such as eradication of biological activity of living organisms, surface activation (pre-treatment for coating application), hydrophilization and/or strengthening through thin-film deposition, and material structure strengthening applying plasma assisted treatment. On the other hand, plasma treatment provides a cost-effective, versatile, environmentally friendly, non-thermal treatment system. Presented study will summarize multiple atmospheric plasma effects on the wood surface.

Keywords: plasma, atmospheric, low temperature, treatment, wood

Radovan Tiňo
Slovak University of Technology in Bratislava
Faculty of Chemical and Food Technology
Dept. of Wood, Pulp and Paper
Radlinskeho 9
812 37, Bratislava
Slovakia

*Proceedings of the 57th International Convention of Society of Wood Science and Technology
June 23-27, 2014 - Zvolen, SLOVAKIA*

+421-2-59325 621
radovan.tino@stuba.sk

Probabilistic Numerical Analysis of Quasi-stationary Thermal Measurement of Medium Density Fiberboard

Jan Tippner^{1} – Eva Troppová¹ – Richard Hrčka² – Pavol Halachan² –
Rastislav Lagaňa² – Václav Sebera¹ – Miroslav Trcala¹*

¹ Department of Wood Science, Faculty of Forestry and Wood Technology,
Mendel University in Brno, Zemědělská 3, Brno, Czech Republic

** Corresponding author*
jan.tippner@mendelu.cz

² Department of Wood Science, Faculty of Wood Science and Technology,
Technical University in Zvolen, T. G. Masaryka 2117/24, Zvolen, Slovak
Republic

Abstract

Quasi-stationary thermal analysis of materials is based on time-recording of temperature in the middle of heated block of samples. The method enables determination of heat capacity, longitudinal and transverse thermal conductivity and heat transfer coefficient from a single measurement. All outputs are influenced by many varying factors as for example density, temperature and moisture, heat losses, heterogeneity of structure etc. Theoretical analysis based on verified numerical models streamlines description of variability of results in many of various input combinations. Probabilistic transient finite-element analyses of problem were performed. The Medium Density Fiberboard specimens with 4 different thicknesses were prepared and density profiles of samples were scanned, then thermal parameters were calculated and statistically evaluated. Numerical model of the experimental apparatus consists of two samples described by thermal solid elements. Orthotropic material properties based on experimentally derived data were assigned to the model. A high number of time steps enabled to calculate the temperature increase in the center point between samples and to compare the curve with experimental recording. The numerical and experimental data were in close agreement with each other. Verified model was used for thousands of variable solutions with randomization of each parameter. Factors which significantly affect results include sample properties, boundary conditions and parameters of apparatus.

Keywords: Medium density fiberboard, Quasi-stationary thermal analysis, Finite-element method, Probabilistic analysis

Introduction

Medium density fiberboard (MDF) is widely used composite material made of wood fibers. Its favorable physical and mechanical properties enable usage mainly in furniture and construction production. Many authors described mechanical properties of MDF [1-5], but there are only limited studies on the thermal properties. The knowledge of thermal properties is important especially in the process of drying, thermal modification, hot pressing or general in processes where heat transfer occurs. Thermal properties of wood-based materials as well as wood itself are mainly affected by density, temperature and moisture content [6-8] and vary within each type due to heterogeneity of material. There is a number of ways to measure thermal properties of MDF. The stationary method performs a measurement when the temperature of measured material does not change with time. On the contrary, temperature rise is a function of time in the transient dynamic techniques. A non-stationary method based on principals described by [9-10] was developed at Technical University in Zvolen [11]. A quasi-stationary apparatus is based on the monitoring of temperature changes in the middle of sample and enables simultaneous determination of thermal conductivity, thermal diffusivity and specific heat capacity. Generally, every measuring process is influenced by variety of parameters. Numerical simulations of heat transfer are performed to find the influence of various physical parameters on thermal response of wood and wood-based materials. Parametric studies than predict significance of each parameter. A simulation of heat and mass transfer in wood was carried out by [12-14]. One of the challenging issues remains the description of heat transfer in wood-based materials during measuring process and the evaluation of factors that influence the final temperature increase in time. Data like geometry of samples, material properties, or loads are usually not known perfectly [15]. Therefore, the verification of numerical solution with analytical calculations is needed. The main goal of this article was to establish the thermal properties (thermal conductivity, thermal diffusivity and specific heat capacity) of MDF using the quasi-stationary method. To extend knowledge about this method, a numerical simulation of heat transfer in MDF samples based on and verified by experiment were done and compared with the analytical solution. Parametric sensitivity study was held to find out the influence of parameters on the accuracy of measurement.

Materials and Methods

In this study, the thermal parameters of commercially available MDF boards with different thicknesses and densities were measured and analytically evaluated. Thermal properties were then used as input parameters in the numerical model. The probabilistic analysis showed the main factors influencing measurement of thermal parameters.

Experimental measurement and analytical evaluation of thermal properties.

Medium density fiberboards with four thicknesses: 12, 18, 25 and 38 mm were prepared. Samples with approximate dimension (width and length) of 50x50 mm and 100x100 mm were cut from prepared MDF boards. A density profile from each type of samples was scanned by using an X-ray densitometer with a scanning step length of 0.01 mm (X-RAY

Dense-Lab, Germany) to reach precise density value. A quasi-stationary apparatus consists of a block of eight samples alternately interspersed with 0.01 mm thick NiCr foil, see Figure 1. Both sides of the block were insulated by polystyrene and pertinax to avoid heat losses to the surrounding. As the foil produced heat, the samples warmed up. The average heat flux ranged from 590 to 1760 W.m⁻² at different measurements. The rise in temperature was recorded with a thermocouple placed in the middle of the samples [11]. The two middle samples were changed after each measurement and their averaged thermal properties evaluated. Four arrangements of each MDF types (thickness of 12, 18, 25 and 38 mm) and each size (50x50 mm and 100x100 mm) were measured. Together 32 measurements was held. All samples were conditioned at 20 °C and a relative humidity of 65 % in a Sanyo MTH 2400 air chamber to reach the equilibrium moisture content. The data from the measurements are illustrated as a curve and describe the temperature increase in time in the center of the middle sample. The analytical solution is based on solving the heat transfer equation and interpolation of the curve according the theoretical line[16]. The last square method is used for evaluation of thermal properties.

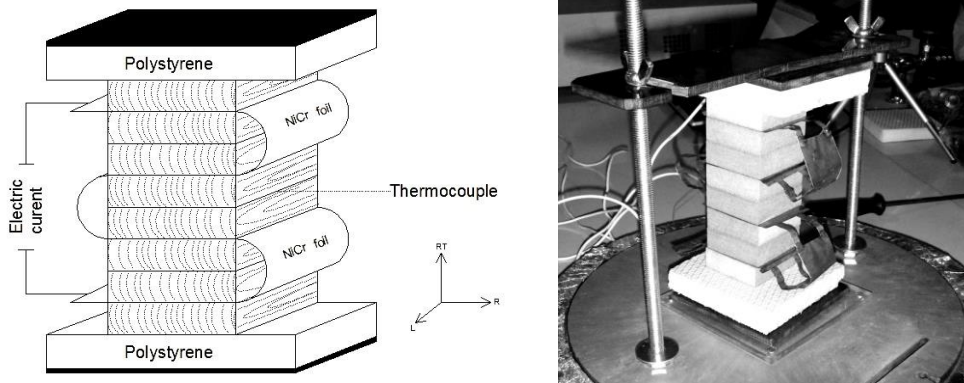


Fig 1. Scheme of the experimental device based on the quasi-stationary method (adopted from [17, 18]).

Numerical simulation and probabilistic study. A finite element numerical model has been developed for the simulation of the quasi-stationary apparatus using Ansys Parametric Design Language. A parametric script was created in Ansys Mechanical APDL 14.5 software. The model including simplified geometry consists of two MDF samples (blocks with dimensions 49.85 x 49.66 x 18.20 mm) in between the temperature increase is calculated. The two blocks are bonded perfectly with no interaction between them. Quadratic hexahedral thermal solid elements (SOLID279) created regular mesh in the model. Experimentally obtained values of density, specific heat capacity and thermal conductivity in both directions (longitudinal and transverse) were specified and assigned to the geometry. Heat transfer is caused by the heat flux (925 W) applied to the upper and lower surface of samples. Heat transfer coefficient (14 W.m⁻².K⁻¹) was assigned to the boundary surfaces. A thermal transient analysis with the end time (20,000 s) was performed. A number of substeps (20,000) enabled to calculate the temperature in the center between the two middle samples every 1 second which is comparable with the experimental recording. The probabilistic analysis was used to predict the behavior of the

measuring device. The Ansys Probabilistic Design System enabled to describe the influence of input parameters (material properties of the sample and the boundary conditions) on the output results (temperature increase in time). The sensitivity of measured outputs was established and described by the correlation coefficients. The Monte Carlo method generation of input parameters with direct sampling in specified range of values with Gaussian distribution was used. This technique randomly samples the variables according to input range defined with Gaussian distribution. The range is set up by average value of parameter and standard deviation (established in accordance to 10% or 20% variance).

Results

The variation of density in the thickness direction is referred to the vertical density profile (VDP) which profoundly affects the mechanical and physical properties of MDF. X-ray densitometry results are presented in Figure 2. All density profiles are symmetrical with high-density faces and slight decrease in density with depth of 2 mm from surface layers. A parabolic density profile describes density distribution in MDF with thickness of 12 and 25 mm. On the contrary, a flat and almost homogeneous densification of fibers in the core of samples is present in MDF with thickness of 18 and 38 mm. Densities vary from cca 600 to 950 [kg.m⁻³]; it makes the density important factor for sensitivity analyzes.

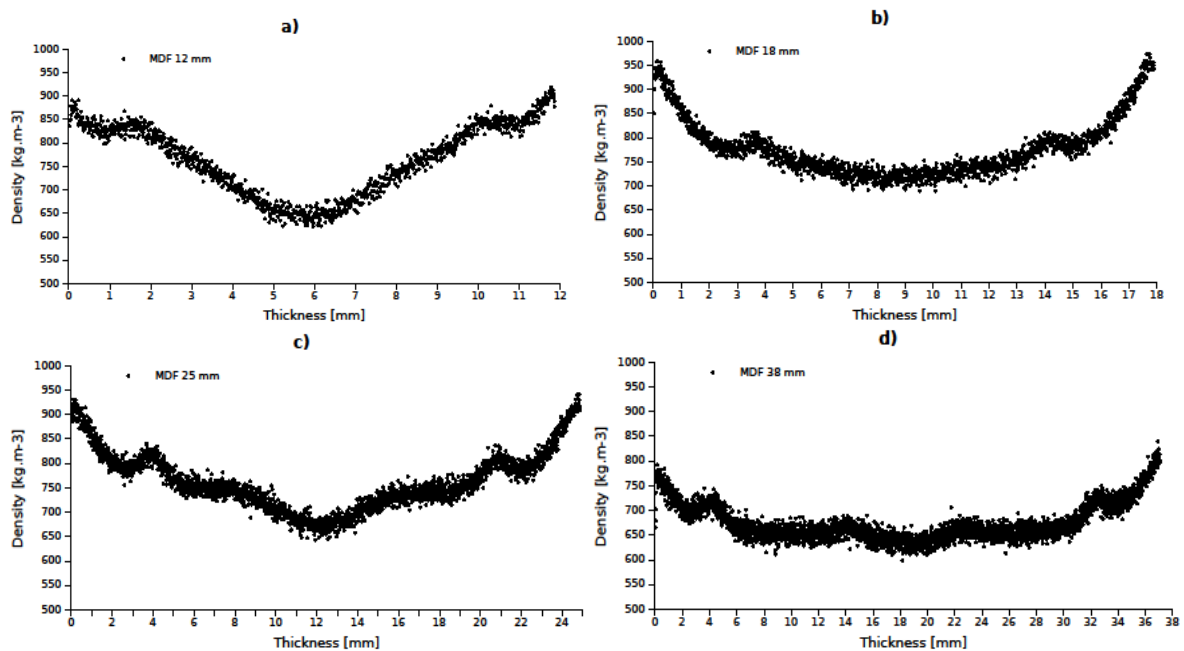


Fig 2. Vertical density profiles of selected MDF samples.

The thermal parameters (thermal conductivity, thermal diffusivity and specific heat capacity) were derived from the quasi-stationary measurements. The results proved that the thermal measurements of MDF samples with dimensions 100 x 100 mm and thicknesses 12 and 18 mm are reliable only, see Table 1. The variation coefficient of measurement is higher for samples with dimensions 100 x 100 mm. This can be caused

by the higher variability of samples, but does not predicate on accuracy of the measuring method. The higher the thickness of MDF sample (25 and 38 mm), the higher were heat losses to the surrounding from lateral surfaces. Proper ratio between thickness and width of the sample lower the influence of heat transfer coefficient on the heat losses through lateral surfaces [11]. Even the ratio 0.24 (samples with width 50 mm and thickness 12 mm) was not sufficient for relevant thermal measurement. The higher density, the higher are values of thermal conductivity (valid only for reliable results). The thickness of samples does not affect thermal diffusivity and specific heat capacity.

MDF samples	Thickness [mm]	Density [kg.m⁻³]	Thermal conductivity [W.m⁻¹.K⁻¹]	Thermal diffusivity [10⁷ m².s⁻¹]	Specific heat [J.kg⁻¹.K⁻¹]
Dimensions 100x100 mm	12	767 (1.4)	0.213 (6.4)	1.144 (3.8)	2426 (2.3)
	18	778 (1.6)	0.223 (10.9)	1.157 (5.1)	2476 (6.5)
	25	753 (0.6)	0.239 (7.5)	1.268 (2.9)	2500 (4.2)
	38	658 (1.1)	0.169 (5.9)	1.428 (4.9)	1803 (9.5)
Dimensions 100x100 mm	12	719 (0.3)	0.147 (9.6)	1.069 (5.8)	1916 (5.2)
	18	739 (0.8)	0.152 (14.0)	1.097 (4.5)	1868 (10.1)
	25	715 (0.6)	0.174 (7.5)	1.139 (4.2)	2132 (3.7)
	38	740 (0.2)	0.294 (33.5)	1.635 (33.6)	2433 (5.3)

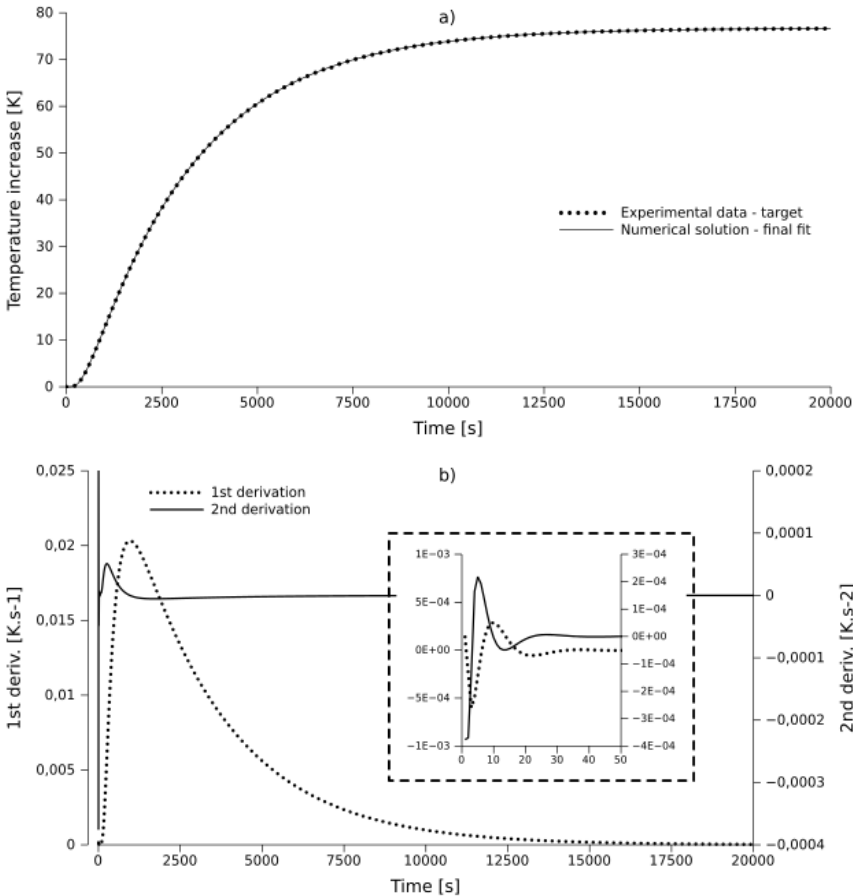
Tab 1. Mean thermal properties of samples measured in the transverse direction (the values in parentheses describe the variation coefficient of measurement)

The comparison of the experimental recording and numerical calculation is obvious in Figure 3a. The numerical and experimental data were in close agreement with each other (differences between temperatures were lower than 0.01 °C in all parts). Testing of mesh density in large range as well as different ANSYS element types used for analyzes didn't influenced results perceptibly; on the contrary time step of transient analysis influenced shape of the curve considerably, especially in first and second part. Very good agreement of model with experiment was obtained by solution with fine time step 1 sec. (Figure 3a) and lower - such well fitted model can be used for sensitivity analyses consequently. The boundary between nonlinear and linear part describes the first derivation of temperature increase in time, see Figure 3b. The first derivate measures the rate of temperature change which is maximal in 966 seconds (maximal first derivation). The rate of change of speed with respect to time indicates the second derivation, see Figure 3b. Maximal values of

second derivate are within first few seconds (see detail in Figure 3b) of the measurement and also in the connection point of first and second part of the curve.

Fig 3.

Results of numerical solution - the case of 50x50 mm specimens; a) temperature increase in time in the middle sample - comparison with measurement, b) first and second derivation of the temperature increase in time with detail graph for first 50 seconds.



Verified model was used for probabilistic analysis based on variable solutions with randomization of main *input variables* (Density, Heat capacity, Longitudinal and Transverse thermal conductivity, Heat transfer coefficient). The outputs from transient solution (Figure 3) were analyzed to compute *output parameters* (Table 2), such as: max. and min. of first and second derivation (*1stDermin*, *1stDermax*, *2ndDermin*, *2ndDermax*), average value of derivation on linear part of temperature increase in time (*Deravg*), time at min. or max. 1st and 2nd derivation (*T@1stDermin*, *T@1stDermax*, *T@2ndDermin*, *T@2ndDermax*), time when the 1st derivation is equal to zero (*T@Der0*). These parameters are instrumental towards describing the modeled curve from the quasi-stationary measurements [16]. The evaluation of the probabilistic sensitivities is based on the correlation coefficients between all random *input variables* and a particular random *output parameters* (Table 2). Spearman rank order correlation coefficients are shown (for the values closer to zero, the two variables are weakly correlated; for the values closer to 1 or -1, the two variables are highly correlated either in positive or negative sense, respectively).

Tab 2. Matrix of correlation coefficients based on ANSYS probabilistic analysis - the case of 50x50 mm specimens. Values in brackets indicate not significant correlation coefficient (a significance level of 2.5 % has been used).

	Long. thermal conductivity	Transv. thermal conductivity	Densit y	Specific heat	Heat transfer coeff.
<i>Deravg</i>	(-0.077)	(0.048)	-0.659	-0.739	(0.001)
<i>IstDermin</i>	0.464	0.500	0.551	0.574	-0.265
<i>IstDermax</i>	(-0.126)	0.014)	-0.659	-0.744	(-0.008)
<i>2ndDermin</i>	0.595	0.821	0.169	0.173	(-0.153)
<i>2ndDermax</i>	(-0.067)	0.089)	-0.651	-0.729	0.140)
<i>T@IstDermin</i>	(-0.124)	-0.401	0.503	0.517	(-0.110)
<i>T@IstDermax</i>	-0.231	-0.347	0.596	0.646	(-0.110)
<i>T@2ndDermin</i>	-0.199	-0.329	0.301	0.406	(-0.021)
<i>T@2ndDermax</i>	-0.180	-0.415	0.534	0.609	(-0.065)
<i>T@Der0</i>	-0.204	(-0.089)	0.591	0.587	-0.431

Conclusion

The numerical model of thermal behavior of MDF was based on measurements (density, thermal conductivity and specific heat in 4 thicknesses of boards) and verified by experiments too (Figure 2); it enables thousands of variable analyzes in realizable time. Relevancy of the model is influenced by time step of analysis, then again the accuracy it's not very affected by mesh density. Both these parameters are important for efficiency of solution - the crucial factor for sensitivity analyzes. Experimental evaluation of thermal properties shown - in addition to properties (Table 1) - that: the higher the thickness of sample, the higher are heat losses to the surrounding; the higher density, the higher are values of thermal conductivity; the thickness of samples does not affect thermal diffusivity and specific heat capacity. The consequent probabilistic analysis describes correlations (Table 2) between input variables (corresponding to evaluated material properties) and output parameters (corresponding to measured time-temperature curve). The analysis shown the significant correlation of longitudinal and transversal conductivity in several cases, the influence of density and specific heat to almost all outputs. The outputs are weakly correlated with heat transfer coefficient. Measured density profiles (Figure 1) are symmetrical with high-density faces and slight decrease in density from surface layers. The future incorporation of realistic density profile into numerical model will improve analyzes, although material model needs extensive experimental evaluation of relationship between density and thermal properties.

Acknowledgement

This article is supported by the project “The Establishment of an International Research Team for the Development of New Wood-based Materials” Reg. No. CZ/1.07/2.3.00/20.0269.

References

- [1] Bodig, J., Jayne, B.A. 1993. Mechanics of Wood and Wood Composites, Malabar: Krieger Publish. Comp. r. 21.
- [2] Cai, Z., Ross, R.J. 2010. Mechanical properties of wood-based composite materials, Wood Handbook: Wood as an engineering material: Forest Products Laboratory 12.1-12.12.
- [3] Ganev, S., Gendron, G., Cloutier, A., Beaugard, R. 2005. Mechanical Properties of MDF as a Function of Density and Moisture Content, Wood and Fiber Sc. 37(2): 314-326.
- [4] Wilczyński, A., Kociszewski, M. 2007. Bending properties of particleboard and MDF layers, Holzforschung 61(11): 717-722.
- [5] Schulte, M., Frühwald, A. 1996. Shear modulus, internal bond and density profile of medium density fibre board (MDF), European J. of Wood and Wood Products 54(1): 49-55
- [6] MacLean, J.D. 1941. Thermal conductivity of wood, Heating, Piping and Air Conditioning 13(6): 380-391.
- [7] Steinhagen, H.P. 1977. Thermal conductive properties of wood, green or dry, from -40 °C to +100°C: a literature review, U.S. Department of Agriculture forest service, Forest products laboratory Madison.
- [8] Suleiman, B.M., Larfeldt, J., Leckner, B., Gustavson, M. 1999. Thermal conductivity and diffusivity of wood, Wood Science and Technology 33: 465-473.
- [9] Clarke, L.N., Kingston, R.S.T. 1950. Equipment for the simultaneous determination of thermal conductivity and diffusivity of insulating materials using a variable state method, Australian Journal of Applied Science 1: 172-187.
- [10] Krischer, O., Esdorn, H. Simple short-term method for the simultaneous determination of thermal conductivity, heat capacity and thermal effusivity of solids, VDI-Forsch.-H. 450 (in German).
- [11] Požgaj, A., Chovanec, D., Kurjatko, S., Babiak, M. 1997. Wood structure and properties, Priroda, 1- 486 (in Slovak).
- [12] Younsi, R., Kocaefe, D., Kocaefe, Y. 2006. Three-Dimensional Simulation of Heat and Moisture Transfer in Wood, Applied Thermal Engineering 26(11): 274-285.
- [13] Gu, H. M. 2001. Structure based, two-dimensional anisotropic, transient heat conduction model for wood, Ph.D. thesis, Dpt. of Wood Sci. & Forest Prods., Virginia Tech. Blacksburg, 1-242.
- [14] Hunt, J.F., Gu, H.M. 2004. Finite element analyses of two dimensional, anisotropic heat transfer in wood, International Ansys Conference, 1-13.

- [15] Čermák, P., Trcala, M. 2012. Influence of uncertainty in diffusion coefficients on moisture field during wood drying, *International Journal of Heat and Mass Transfer*, 55(25-26): 7709-7717.
- [16] Hrčka, R., Babiak, M. 2012. Some non-traditional factors influencing thermal properties of wood, *Wood Research* 57(3): 367-374.
- [17] Hrčka, R. 2010. Variation of thermal properties of beech wood in the radial direction with moisture content and density, *Wood Structure and Properties*, J. Kúdela and R. Lagaňa (eds.), Arbora Publishers, Slovakia.
- [18] Troppová, E., Tippner, J., Hrčka, R., Halachan, P. 2013. Quasi-stationary measurements of Lignamon thermal properties, *Bioresources* 8(4): 6288-6296.

Integrating the Surface Treatment of Monocotyledons into Particleboard Production Process for Providing a Substitute Raw Material

Johann Trischler^{1} – Dick Sandberg²*

¹ PhD student, Linnaeus University, SE-351 95 VÄXJÖ, Sweden

** Corresponding author*

johann.trischler@lnu.se

² Professor of Wood Technology at Luleå University of Technology, SE-931 87 SKELLEFTEÅ, Sweden

Abstract

If monocotyledons are to be used in particleboards, their external surfaces should be modified to increase their wettability by conventional adhesives such as melamine-urea-formaldehyde (MUF). The modification should affect the wax layer of the external surface of monocotyledons. According to the literature, modification by enzymes leads to increased wettability by water-based adhesives. The purpose of this study is to evaluate the integration of surface treatment by enzymes into particleboard production in a way that leads to a value added output. During the pre-treatment process, it can be expected that residues such as fines and organic acids will accumulate. These residues can be used for methane production, and this should increase the efficiency of the process. Once established, the methane production can be extended to include other residues from the wood process, leading to an increased energy production. A residue of this methane process is lignin which is nowadays generally used as a fertilizer and energy source, but research is also focusing on the use of lignin as an adhesive or additive. A SWOT analysis of the literature shows the advantages and disadvantages of integrating a pre-treatment of monocotyledons into the particleboard production process. In addition to a mixture of light-weight raw material for particleboard production, energy and maybe additives for adhesives, this concept also supports the production of panels with a greater range of densities by using different proportions of the different raw materials.

Keywords: Lignocellulosic raw material, Enzymes, Methane.

Introduction

The consumption of wood in Europe, especially for energy purposes, is expected to increase (Mantau 2010; Jonsson et al. 2011; United Nations 2011) and this will lead to greater competition between the particleboard industry, the pulp and paper industry, and the thermal energy recovery industry. Monocotyledons might open an opportunity for the particleboard industry to decrease its competition for wood (Boquillon et al. 2004). As

monocotyledons like straw generally have a higher ash content and a lower ash melting point than wood, they are not the preferential raw material for combustion (Diamantidis and Koukios 2000; Kim and Dale 2004; Greenhalf et al. 2012). Some monocotyledons have fibres which might be suitable for pulp and paper production, but they are not being used in larger quantities yet (Finell 2003; Enayati et al. 2009). Research into the substitution of wood by monocotyledons in particleboards has mainly concentrated on wheat straw (Tröger and Pinke 1988; Wang and Sun 2002; Mo et al. 2003; Boquillon et al. 2004; Frounchi et al. 2007; Azizi et al. 2011) and rice straw (Jarusombuti et al. 2009; Li et al. 2010).

Nevertheless, there are difficulties in including alternative raw materials into the conventional production of particleboards (Müller et al. 2012). For example, both the wettability of the particles and the mechanical properties of the board vary with changes in the anatomical and chemical structure of the wood (Baharoğlu et al. 2013), the thermal treatment of the wood (Sarı et al. 2013) and the moisture content of the wooden particles (Baharoğlu et al. 2012). The monocotyledon raw material has very different physical and chemical properties even within a single species (Pahkala and Pihala 2000; Wiśniewska et al. 2003). Most challenging is the treatment of the external surface of the monocotyledons, because the surface structure consists of cuticles with embedded waxes superimposed by epicuticular waxes (Barthlott et al. 1998; Wiśniewska et al. 2003), also because its design affects the so-called lotus effect (Barthlott and Neinhuis 1997).

The wax layer of the external surface can be modified using lipase or cellulase under anaerobic conditions, with lipase showing the best effect comparable to alkaline treatment with NaOH (sodium hydroxide) but with a longer treatment time (Zhang et al. 2003; Hua et al. 2009; Zheng et al. 2009; Chao et al. 2011; Shen et al. 2011). Lipases act at the interface between the aqueous and non-aqueous phase under mild conditions and catalyse a wide range of reactions (Pandey et al. 1999). These enzymes hydrolyse different components of the wax layer without weakening the rest of the substrate and without affecting the internal layer (Zhang et al. 2003; Feng et al. 2009; Hua et al. 2009). The composition of the wax layer makes conversion of the wax into methane by these enzymes easier and faster possible than the rest of the lignocellulos plant for two reasons: Firstly, the components of the wax layer are built-up of quite small molecules which allow conversion into methane without depolymerisation, and secondly, they are not affected by lignin (Tong and McCarty 1991).

The time needed for the enzymatic process depends on the substrate, the enzyme, the pH value, and the temperature used (Tengborg et al. 2001; Gupta et al. 2004). Lipases in the presence of water hydrolyse fats or esters into their constituent acids and glycerol or alcohol (Gandhi 1997). Hydrolysis results not in methane but in soluble component units which are further fermented into other intermediates (organic acids) and then into acetic acid, hydrogen, and carbon dioxide which are finally converted into methane and CO₂ (Isaacson 1991; Tong and McCarty 1991). This stepwise process of anaerobic digestion (AD) includes three different groups of bacteria, the hydrolytic, transitional, and methanogen, and a water level of at least 75% to transport substrates to and waste

products from the bacteria so that toxic concentrations for the bacteria do not occur (Isaacson 1991). Lignin is usually not more than 10% anaerobically degraded within several weeks by the fermentation process (Tong and McCarty 1991). Compared to the AD process with methane as a product, fermentation for ethanol production needs sugars, starch and cellulose as raw material (Chen and Qiu 2010; Tanjore et al. 2012).

Nevertheless, to avoid contamination within the ethanol production process, the methane production and ethanol production systems can generally be combined (Börjesson et al. 2013). In ethanol production, the polysaccharides, hemicellulose and cellulose of the raw material are hydrolysed to monomeric sugars (Mussatto et al. 2010) which are then fermented by bacteria, yeast or filamentous fungi (Hahn-Hägerdal et al. 2006), and the extractives and organic acids should then go directly to AD so that they do not inhibit the ethanol fermentation (Zaldivar et al. 2001; Börjesson et al. 2013). Hydrolysis and fermentation of the solid fraction for ethanol production can be carried out in a single step, so-called SSF (simultaneous saccharification and fermentation or solid state fermentation), or in two steps, so-called SHF (separate hydrolysis and fermentation) (Tengborg et al. 2001; Olofsson et al. 2008; Ekman et al. 2013).

In summary, to provide a substitute raw material through a value-adding pre-treatment by enzymes, (1) lipolysis can be started during storage (Chow et al. 2004), and (2) continued by AD (Tong and McCarty 1991; Zheng et al. 2009), with an output (a) pre-treated raw material for particleboards (Zhang et al. 2003; Feng et al. 2009; Hua et al. 2009), (b) methane, and (c) lignin as residue (Tong and McCarty 1991).

Objectives

The purpose of this study is to evaluate an integrated surface treatment of monocotyledons by enzymes into particleboard production in a way that leads to a value-added product.

Methods

The literature related to particleboard production, monocotyledons, surface treatment, enzymes, and methane production was studied. Based on this literature, a concept of integrating monocotyledons and their surface treatment is presented by combining descriptive literature data for the different disciplines. The SWOT (strength, weaknesses, opportunities and threats) analysis was chosen, which is one of the most popular methods used for an analysis of a company's strategic position (Hill and Westbrook 1997).

Results and Discussion

The suggested concept integrates the surface treatment of monocotyledons by enzymes into particleboard production and methane production. The output of the process is

methane, probably combine with ethanol, pre-treated raw material for particleboard production, and residual lignin for energy or adhesive purposes.

The SWOT analysis, presented in Table 1, shows the conditions of the combined and value added processes and their interaction with the environment. The strength and opportunities are mainly related to the products and product mix, while the weaknesses and opportunities are economic. Strengths and risks can be mainly allocated to markets and competition, weaknesses and risks are characterized mainly by the low product invention or development as such.

Table 20. *SWOT analysis presenting the conditions of the value added integration of monocotyledons including surface treatment into the particleboard production.*

		INTERN ANALYSIS	
		STRENGTHS	WEAKNESSES
E X T E R N	O P P O R T U N I T I E S	Additional raw material Product diversification (furniture, construction, insulating material) Use of capacity Light-weight-panel production Constant level of raw material by storage Life cycle assessment (LCA) Regional development	Undeveloped process Cost-effectiveness (esp. enzymes) Product diversification (fixed costs) Trade-off of products Logistics (storage, transport distance) Life cycle assessment (LCA)
	A N A L Y S I S	Market (buying patterns) Energy market Integrated process (cheaper) Formaldehyde emission	Investment costs (e.g. effectiveness of chemicals vs. enzymes) Competition of raw material (increasing prices) Change of residuals (ingredients...) The process is value added not the product Change of process parameters Sandwich-Paper panel Formaldehyde problem (unchanged)

Strengths-opportunities-combination: The additional raw material in the form of monocotyledons (Zhang et al. 2003; Hua et al. 2009) creates an opportunity for a product mix in panel production (furniture, construction, insulating material) (Sampathrajan et al. 1992) and an additional energy production. The product diversification can lead to a greater utilisation of capacities when all products are produced in the same production

line (Fine and Freund 1990; Li and Tirupati 1994). According to different sources, monocotyledons might also be suitable for light weight panels (Garcia-Ortuno et al. 2011; Dziurka and Mirski 2013; Shalhafan 2013). This can lead to a greater diversification on the market, which can lower risks for the producer (Fine and Freund 1990). At the same time, it is possible to lower the risks regarding the raw material supply, as a wider range of raw materials can be used. As monocotyledons have to be stored to be available throughout the year, a constant level of raw material is available. It is further expected that the integrated pre-treatment process has a positive impact on the LCA (Pandey et al. 2011). Once this concept is approved and economically interesting, companies might build new sites in agricultural areas, and this would lead to regional development (Thomson and Psaltopoulos 2005).

Strengths-threats-combination: Because of the wider range of products, fluctuations in the market (buyer patterns) lead to lower risks for the production site. The energy production from renewable resources can also be beneficial under recent energy policies (Berndes et al. 2003; Parikka 2004; Obersteiner et al. 2006). The capacity of the production site can also be increased by the greater variety of products which are produced on the same production line (integrated process) (Li and Tirupati 1994; Zheng et al. 2009). The wider product range brings new competitors but weakens the strong completion based on a single type of product. Further, the wider range of raw materials may have a positive impact on the transaction costs. Developments in the adhesive industry to optimize adhesives for particleboards made of monocotyledons might also result in formaldehyde-emission free adhesives (Mo et al. 2003; Boquillon et al. 2004).

Weaknesses-opportunities-combination: The greatest weakness is that it is still an undeveloped process which includes high risks, but once it is working it will increase the capacities of the production line (lower fixed costs), more products, and a wider range of raw materials, but there is a trade-off of raw material for particleboard production and energy (Zheng et al. 2009). Further research in the area of enzymes and lignin is needed. While the costs of enzymes are problematic (Rowell 1998), the lignin requires technical improvements (Pizzi and Mittal 2003; Pizzi 2006), but the solution of these would lead to great opportunities. Logistical factors (Müller et al. 2012; Ekman et al. 2013) such as storage and transport distance must be considered from an economical and LCA point of view.

Weaknesses-threats-combination: The most negative aspect is the economic situation of this project, especially the pre-treatment with enzymes (Shen et al. 2011). The raw material properties after pre-treatment also have to be analysed and the process must be optimized. It is to be expected that the price of the raw material, which is cheap nowadays, will increase with the higher demand (Hall 2002). The raw material properties can underlie a wide range of properties (Youngquist et al. 1993) and the process parameters during production can depart from the parameters for wood panels (Dai et al. 2004). And as it is only a process and not a product development, some problems relating to particleboard like the formaldehyde-emitting adhesives (Dunky 1998) remain, and the large raw material input compared to that with alternative sandwich panels (Barbu et al. 2010) remains to be solved.

Conclusions

An integration of pre-treatment of monocotyledons into particleboard producing process resulting in a value-added process has been evaluated by a SWOT analysis. The output of the process is methane, possibly combined with ethanol, pre-treated raw material for particleboard production, and residual lignin for energy or adhesive purpose. The results and discussion of the SWOT analysis show that it might be possible to include monocotyledons but also that this concept has to be approved, verified, and optimized from technical, environmental, and economic points of view.

References

- Azizi, K., Tabarsa, T., and Ashori, A. 2011. Performance characterizations of particleboards made with wheat straw and waste veneer splinters. *Composites Part B-Engineering* 42(7): 2085-2089.
- Baharoğlu, M., Nemli, G., Sarı, B., Bardak, S., and Ayrılmış, N. 2012. The influence of moisture content of raw material on the physical and mechanical properties, surface roughness, wettability, and formaldehyde emission of particleboard composite. *Composites Part B: Engineering* 43(5): 2448-2451.
- Baharoğlu, M., Nemli, G., Sarı, B., Birtürk, T., and Bardak, S. 2013. Effects of anatomical and chemical properties of wood on the quality of particleboard. *Composites Part B: Engineering* 52(0): 282-285.
- Barbu, M.C., Lüdtke, J., Thömen, H., and Welling, J. 2010. Innovative production of wood-based lightweight panels. In: *Processing Technologies for the Forest and Biobased Products Industries*, M.C. Barbu, ed. 2010. Wien: LIT Verlag: 115-122.
- Barthlott, W., and Neinhuis, C. 1997. Purity of the sacred lotus, or escape from contamination in biological surfaces. *Planta* 202(1): 1-8.
- Barthlott, W., Neinhuis, C., Cutler, D., Ditsch, F., Meusel, I., Theisen, I., and Wilhelm, H. 1998. Classification and terminology of plant epicuticular waxes. *Botanical Journal of the Linnean Society* 126(3): 237-260.
- Berndes, G., Hoogwijk, M., and van den Broek, R. 2003. The contribution of biomass in the future global energy supply: a review of 17 studies. *Biomass and Bioenergy* 25(1): 1-28.
- Boquillon, N., Elbez, G., and Schönfeld, U. 2004. Properties of wheat straw particleboards bounded with different types of resin. *Journal of Wood Science* 50(3): 230-235.
- Börjesson, P., Ahlgren, S., Barta, Z., Björnsson, L., Ekman, A., Erlandsson, P., Hansson, P.-A., Karlsson, H., Kreuger, E., Lindstedt, J., Sandgren, M., Schnürer, A., Trobro, S., Villman, S., and Wallberg, O. 2013. Sustainable performance of lignocellulose-based ethanol and biogas co-produced in innovative biorefinery systems Department of Environmental and Energy Systems Studies Lund, http://www.f3centre.se/sites/default/files/f3_lth_report_2013-87_co-produced_ethanol_and_biogas_130827.pdf, [January, 29 2014].

- Chao, Q., Weihong, W., and Wenjing, L. 2011. A new process for manufacturing straw particleboard by impregnating and enzyme treatment. *Advanced Materials Research* 221(221): 140-145.
- Chen, H., and Qiu, W. 2010. Key technologies for bioethanol production from lignocellulose. *Biotechnology Advances* 28(5): 556-562.
- Chow, T., Fievez, V., Ensberg, M., Elgersma, A., Smet, S.d., Lúscher, A., Jeangros, B., Kessler, W., Huguenin, O., and Lobsiger, M. Year. Fatty acid content, composition and lipolysis during wilting and ensiling of perennial ryegrass (*Lolium perenne* L.): preliminary findings. In: *Proceedings, Land use systems in grassland dominated regions. Proceedings of the 20th General Meeting of the European Grassland Federation, Luzern, Switzerland, 21-24 June 2004.*; Year. vdf Hochschulverlag AG an der ETH Zurich: 981-983.
- Dai, C., Wasylciw, W., and Jin, J. 2004. Comparison of the pressing behaviour of wood particleboard and strawboard. *Wood Science and Technology* 38(7): 529-537.
- Diamantidis, N.D., and Koukios, E.G. 2000. Agricultural crops and residues as feedstocks for non-food products in Western Europe. *Industrial Crops and Products* 11(2-3): 97-106.
- Dunky, M. 1998. Urea-formaldehyde (UF) adhesive resins for wood. *International Journal of Adhesion and Adhesives* 18(2): 95-107.
- Dziurka, D., and Mirski, R. 2013. Lightweight boards from wood and rape straw particles. *Drewno* 56(190): 19-33.
- Ekman, A., Wallberg, O., Joelsson, E., and Börjesson, P. 2013. Possibilities for sustainable biorefineries based on agricultural residues – A case study of potential straw-based ethanol production in Sweden. *Applied Energy* 102(1): 299-308.
- Enayati, A.A., Hamzeh, Y., Ahmad Mirshokraie, S., and Molaii, M. 2009. Papermaking potential of canola stalks. *BioResources* 4(1): 245-256.
- Feng, J., Wang, F., Liu, G., Greenshields, D., Shen, W., Kaminskyj, S., Hughes, G.R., Peng, Y., Selvaraj, G., Zou, J., and Wei, Y. 2009. Analysis of a *Blumeria graminis*-secreted lipase reveals the importance of host epicuticular wax components for fungal adhesion and development. *Molecular Plant-Microbe Interactions: MPMI* 22(12): 1601-1610.
- Fine, C.H., and Freund, R.M. 1990. Optimal Investment in Product-Flexible Manufacturing Capacity. *Management Science* 36(4): 449-466.
- Finell, M. 2003. The use of reed canary grass (*Phalaris arundinacea*) as a short fibre raw material for the pulp- and paper industry, Umeå: Swedish University of Agricultural Sciences.
- Frounchi, M., Dadbin, S., Iahanbakhsh, J., and Janat-Alipour, M. 2007. Composites of Rice Husk/Wheat Straw with pMDI Resin and Polypropylene. *Polymers & Polymer Composites* 15(8): 619-625.
- Gandhi, N. 1997. Applications of lipase. *Journal of the American Oil Chemists' Society* 74(6): 621-634.
- Garcia-Ortuno, T., Andreu-Rodriguez, J., Ferrandez-Garcia, M.T., Ferrandez-Villena, M., and Ferrandez-Garcia, C.E. 2011. Evaluation of the Physical and Mechanical Properties of Particleboard Made from Giant Reed (*Arundo Donax* L.). *BioResources* 6(1): 477-486.

- Greenhalf, C.E., Nowakowski, D.J., Bridgwater, A.V., Titiloye, J., Yates, N., Riche, A., and Shield, I. 2012. Thermochemical characterisation of straws and high yielding perennial grasses. *Industrial Crops and Products* 36(1): 449-459.
- Gupta, R., Gupta, N., and Rathi, P. 2004. Bacterial lipases: an overview of production, purification and biochemical properties. *Applied Microbiology and Biotechnology* 64(6): 763-781.
- Hahn-Hägerdal, B., Galbe, M., Gorwa-Grauslund, M.F., Lidén, G., and Zacchi, G. 2006. Bio-ethanol – the fuel of tomorrow from the residues of today. *Trends in Biotechnology* 24(12): 549-556.
- Hall, J.P. 2002. Sustainable production of forest biomass for energy. *The Forestry Chronicle* 78(3): 391-396.
- Hill, T., and Westbrook, R. 1997. SWOT analysis: It's time for a product recall. *Long Range Planning* 30(1): 46-52.
- Hua, J., Yang, Z., and Xuefei, W. 2009. Effect of lipases on the surface properties of wheat straw. *Industrial Crops & Products* 30(2): 304-310.
- Isaacson, R. 1991. *Anaerobic digestion*, Stanford: Taylor & Francis Group.
- Jarusombuti, S., Hiziroglu, S., Bauchongkol, P., and Fueangvivat, V. 2009. Properties of Sandwich-Type Panels Made from Bamboo and Rice Straw. *Forest Products Journal* 59(10): 52-57.
- Jonsson, R., Egnell, G., and Baudin, A. 2011. *Swedish Forest Sector Outlook Study*. United Nations, Geneva, http://www.unece.org/fileadmin/DAM/timber/publications/DP-58_hi_res.pdf, [March, 18 2014].
- Kim, S., and Dale, B.E. 2004. Global potential bioethanol production from wasted crops and crop residues. *Biomass and Bioenergy* 26(4): 361-375.
- Li, S., and Tirupati, D. 1994. Dynamic Capacity Expansion Problem with Multiple Products: Technology Selection and Timing of Capacity Additions. *Operations Research* 42(5): 958-976.
- Li, X., Cai, Z., Winandy, J.E., and Basta, A.H. 2010. Selected properties of particleboard panels manufactured from rice straws of different geometries. *Bioresource Technology* 101(12): 4662-4666.
- Mantau, U. 2010. *Wood Resource Balance results – is there enough wood for Europe?*, Hamburg, http://ec.europa.eu/energy/renewables/studies/doc/bioenergy/euwood_final_report.pdf, [March, 18 2014].
- Mo, X., Cheng, E., Wang, D., and Sun, X.S. 2003. Physical properties of medium-density wheat straw particleboard using different adhesives. *Industrial Crops and Products* 18(1): 47-53.
- Mussatto, S.I., Dragone, G., Guimarães, P.M.R., Silva, J.P.A., Carneiro, L.M., Roberto, I.C., Vicente, A., Domingues, L., and Teixeira, J.A. 2010. Technological trends, global market, and challenges of bio-ethanol production. *Biotechnology Advances* 28(6): 817-830.
- Müller, C., Schwarz, U., and Thole, V. 2012. Zur Nutzung von Agrar-Reststoffen in der Holzwerkstoffindustrie. *European Journal of Wood and Wood Products* 70(5): 587-594.

- Obersteiner, M., Alexandrov, G., Benítez, P., McCallum, I., Kraxner, F., Riahi, K., Rokityanskiy, D., and Yamagata, Y. 2006. Global Supply of Biomass for Energy and Carbon Sequestration from Afforestation/Reforestation Activities. *Mitigation and Adaptation Strategies for Global Change* 11(5-6): 1003-1021.
- Olofsson, K., Bertilsson, M., and Liden, G. 2008. A short review on SSF - an interesting process option for ethanol production from lignocellulosic feedstocks. *Biotechnology for Biofuels* 1(7): 1-14.
- Pahkala, K., and Pihala, M. 2000. Different plant parts as raw material for fuel and pulp production. *Industrial Crops and Products* 11(2-3): 119-128.
- Pandey, A., Benjamin, S., Soccol, C.R., Nigam, P., Krieger, N., and Soccol, V.T. 1999. The realm of microbial lipases in biotechnology. *Biotechnology and Applied Biochemistry* 29(2): 119-131.
- Pandey, C.N., Nath, S.K., and Sujatha, D. 2011. Wood based panel products: technology road map. *Journal of the Indian Academy of Wood Science* 8(2): 62-67.
- Parikka, M. 2004. Global biomass fuel resources. *Biomass and Bioenergy* 27(6): 613-620.
- Pizzi, A. 2006. Recent developments in eco-efficient bio-based adhesives for wood bonding: opportunities and issues. *Journal of Adhesion Science and Technology* 20(8): 829-846.
- Pizzi, A., and Mittal, K.L. 2003. *Handbook of Adhesive Technology*: M. Dekker.
- Rowell, R.M. 1998. The state of art and future development of bio-based composite science and technology towards the 21st century. USDA, Forest Service, Forest Products Laboratory, Bogor, Indonesia, <http://originwww.fpl.fs.fed.us/documnts/pdf1998/rowel98f.pdf>, [March, 10 2014].
- Sampathrajan, A., Vijayaraghavan, N.C., and Swaminathan, K.R. 1992. Mechanical and thermal properties of particle boards made from farm residues. *Bioresource Technology* 40(3): 249-251.
- Sarı, B., Nemli, G., Ayrilmis, N., Baharoğlu, M., and Bardak, S. 2013. The Influences of Drying Temperature of Wood Particles on the Quality Properties of Particleboard Composite. *Drying Technology* 31(1): 17-23.
- Shalhafan, A. 2013. Investigation of Foam Materials to be Used in Lightweight Wood Based Composites, Staats- und Universitätsbibliothek Hamburg, Hamburg.
- Shen, J.-h., Liu, Z.-m., Li, J., and Niu, J. 2011. Wettability changes of wheat straw treated with chemicals and enzymes. *Journal of Forestry Research* 22(1): 107-110.
- Tanjore, D., Richard, T.L., and Marshall, M.N. 2012. Experimental methods for laboratory-scale ensilage of lignocellulosic biomass. *Biomass and Bioenergy* 47(1): 125-133.
- Tengborg, C., Galbe, M., and Zacchi, G. 2001. Influence of enzyme loading and physical parameters on the enzymatic hydrolysis of steam-pretreated softwood. *Biotechnology Progress* 17(1): 110-117.
- Thomson, K.J., and Psaltopoulos, D. 2005. Economy-wide effects of forestry development scenarios in rural Scotland. *Forest Policy and Economics* 7(4): 515-525.
- Tong, X., and McCarty, P.L. 1991. *Microbial hydrolysis of lignocellulosic materials*, Stanford: Taylor & Francis Group.

- Tröger, F., and Pinke, G. 1988. Beitrag zur Herstellung PMDI-verleimter Spanplatten mit verschiedenen Strohanteilen. *Holz als Roh- und Werkstoff* 46(10): 389-395.
- United Nations. 2011. European Forest Sector Outlook Study II: 2010 - 2030. 978-92-1-117051-1, FAO, Geneva,
http://www.unece.org/fileadmin/DAM/timber/publications/sp-28_01.pdf, [March, 25 2014].
- Wang, D., and Sun, X.S. 2002. Low density particleboard from wheat straw and corn pith. *Industrial Crops and Products* 15(1): 43-50.
- Wiśniewska, S.K., Nalaskowski, J., Witka-Jeżewska, E., Hupka, J., and Miller, J.D. 2003. Surface properties of barley straw. *Colloids and Surfaces B: Biointerfaces* 29(2-3): 131-142.
- Youngquist, J.A., English, B.E., Spelter, H., and Chow, P. 1993. Agricultural fibres in composition panels. Washington State University, WA. Pullman,
<http://www.fpl.fs.fed.us/documnts/pdf1993/young93b.pdf>, [March, 10 2014].
- Zaldivar, J., Nielsen, J., and Olsson, L. 2001. Fuel ethanol production from lignocellulose: a challenge for metabolic engineering and process integration. *Applied Microbiology and Biotechnology* 56(1-2): 17-34.
- Zhang, Y., Lu, X., Pizzi, A., and Delmotte, L. 2003. Wheat straw particleboard bonding improvements by enzyme pretreatment. *Holz als Roh- und Werkstoff* 61(1): 49-54.
- Zheng, Y., Pan, Z., Zhang, R., El-Mashad, H.M., Pan, J., and Jenkins, B.M. 2009. Anaerobic digestion of saline creeping wild ryegrass for biogas production and pretreatment of particleboard material. *Bioresource Technology* 100(4): 1582-1588.

Thermal conductivity and Water Vapor Transmission Properties of Wood-based Fiberboards

Eva Troppová^{1} – Jan Tippner²*

¹ Department of Wood Science, Faculty of Forestry and Wood Technology,
Mendel University in Brno, Zemědělská 3, Brno, Czech Republic

** Corresponding author*
xtroppov@mendelu.cz

² Department of Wood Science, Faculty of Forestry and Wood Technology,
Mendel University in Brno, Zemědělská 3, Brno, Czech Republic

jan.tippner@mendelu.cz

Abstract

Low density fiberboards are wood-based materials widely used in engineering as thermal insulators. Exposure to environment with high temperature and humidity can lead to changes in physical properties of this porous material. Temperature and moisture content are important parameters influencing mainly thermal properties of wood-based materials. Thermal conductivity of commercially available insulation fiberboards was measured by using the stationary measuring device heat-flow meter (HFM 436 Lambda). The relationship between thermal conductivity, temperature (ranging from -10 °C to 60 °C) and moisture content (established gravimetrically at 15 %, 50 % and 85 % of relative humidity) was found. The moisture behavior of the material described by adsorption and desorption isotherms was explained. The sorption models of Hailwood-Horrobin (H-H) and Dent were used and compared with the experimental values. The H-H model was in a closer agreement with the measured data, although the total sorption is equal in both models.

Keywords: Fiberboard, Thermal conductivity, Heat flow meter, Sorption model

Introduction

Low density fiberboards are porous materials with specialized heat insulation properties. They usually refer to thermal insulation boards as they are mainly used as façade insulation in civil engineering. Exposure to high temperature and humidity can cause changes in their physical properties. Varying moisture content leads to dimensional changes and furthermore to accelerated material degradation. Along with the moisture changes, the thermal conductivity may also alter (Steinhagen 1977). Thermal conductivity and water sorption are important characteristic important for physical calculations (Sonderegger and Niemz 2012).

There are a number of possibilities to measure thermal conductivity. The steady state technique performs a measurement where analyzed material is in complete equilibrium (Salmon 2001). Thermal conductivity is then evaluated according to the Fourier's law (Siau 1984). The heat flow meter technique or guarded hot plate method are frequently applied to establish thermal conductivity of commercially produced wood-based boards (Yu et al 2011). Many authors dealt with the influence of moisture content and temperature on the thermal conductivity of insulation fiberboards by heat-flow measurements, as for example (Brombacher *et al.* 2012, Matias *et al.* 1997).

The vapor sorption behavior of wood fibres is comparable to solid wood, as shown by Scheiding (1998). Often applied theories describing sorption of wood are for example Hailwood-Horrobin (H-H) model, Brunauer-Emmett-Teller (BET) theory or Dent model. The H-H model is similar to the BET model in partitioning of the total sorbed water (Simpson 1980). With the H-H model, sorption isotherm of wood and other natural fibers can be characterized (Hill et al. 2009).

More research needs to be done to assess the influence of temperature and moisture on the thermal conductivity of insulation fiberboards to better quantify the insulation performance. The aim of the present study was to obtain accurate parameters suitable for modeling coupled moisture and heat transfer in wooden buildings. The specific research objectives are as followed: a) characterize the influence of temperature and moisture content on thermal conductivity of fiberboards, and b) evaluate the moisture behavior of the material using Hailwood-Horrobin and Dent model.

Materials and Methods

The sorption of six commercially available insulation fiberboards varying in thickness and density from three different companies were investigated. An overview of differences between the investigated boards is in Table 1. Adsorption and desorption isotherms were obtained by testing 20 samples with dimensions of 50mm x 50mm x board thickness per type. Equilibrium moisture contents (EMC) were measured at 20 °C, starting at 10 % up to 90% RH, with 10% RH increments. The specimens were dried at 60 °C before the adsorption tests. The single-hydrate Hailwood-Horrobin (H-H) model (Simpson 1980) comparable with Dent model was used with the equilibrium moisture data at each conditioned climate step. The parameters A, B, C (1) and coefficients of the H-H and Dent model (2) were obtained through fitting a second order polynomial function to the experimental data, following Skaar (1988). The total sorption isotherm (3) was determined from the sum of hydrated (4), and the dissolved (5) water which is equal to the sum of primary (6) and the secondary (7) sorbed water of the Dent model.

$$\frac{RH}{MC} = A + B(RH) - C(RH)^2 \quad (1)$$

$$K_1 = b_2 = \frac{-B + \sqrt{B^2 + 4AC}}{2A} \quad K_2 = 1 + \frac{B}{AK_1} \quad b_1 = \frac{B}{A} + 2b_2 \quad (2)$$

$$M_{total} = M_{hyd} + M_{dis} = M_1 + M_2 \quad (3)$$

$$M_{hyd} = M_0 \left(\frac{K_1 K_2 h}{1 + K_1 K_2 h} \right) \quad M_{dis} = M_0 \left(\frac{K_1 h}{1 - K_1 h} \right) \quad (4, 5)$$

$$M_1 = M_0 \left(\frac{b_1 h}{1 - b_2 h + b_1 h} \right) \quad M_2 = M_0 \left(\frac{b_1 b_2 h^2}{(1 - b_2 h)(1 - b_2 h + b_1 h)} \right) \quad (6, 7)$$

$$M_0 = \frac{100}{\sqrt{B^2 + 4AC}} \quad (8)$$

with MC being the moisture content [-], RH the relative humidity [-], A,B,C the regression fitting constants, K_1 , K_2 the coefficients calculated for the Hailwood-Horrobin model, b_1 , b_2 the coefficients calculated for the Dent model, M_{hyd} the moisture content of hydrated water [%], M_{dis} the moisture content of dissolved water [%], M_1 the moisture content of primary sorbed water [%], M_2 the moisture content of secondary sorbed water [%] and finally M_{total} as the total moisture content [%].

Thermal conductivity was measured across the thickness of the board using the heat-flow meter HFM 436 Lambda by Netzsch®. Ten samples from material 6 (producer B) sized 600 mm x 600 mm x 35 mm were cut, and dried in a Sanyo MTH 2400 chamber at 60 °C until weight constancy (< 0.1 % weight change / 24 hours). The temperature difference between the hot and a cold plate was set to 10 °C. A set of eight temperature points, ranging from -10 °C to +60 °C, at 10 °C increments were used. All samples were conditioned at 20 °C and 15 %, 50 %, 85 % relative humidity (RH), respectively. Samples were wrapped in transparent foils (thickness 0.01 mm) to ensure stable moisture contents.

Table 1. Description of measured insulation fiberboards

Material	Producer	Manufacturing method	Thickness [mm]	Additives	Density [kg.m ⁻³]	Thermal conductivity* [W.m ⁻¹ .K ⁻¹]
1	A	dry process	40	aluminium sulfate	265	0.048
2	A	dry process	40	aluminium sulfate	160	0.039
3	B	wet process	40	paraffin	210	0.044
4	C	dry process	32	PUR + paraffin	270	0.063
5	C	dry process	60	PUR adhesive	230	0.047
6	B	wet process	35	paraffin	260	0.049

*Values given by producers, determined according to EN ISO 10456

Results

The sorption models (H-H model and Dent model) allowed representing the hysteresis for the total RH range. The total sorption of material 6 is shown for adsorption and desorption (Figure 1). The H-H model separates the total moisture sorbed into its monomolecular (expressed in hydrated water) and polymolecular components (dissolved water) (Mantanis and Papadopoulos 2010), which is comparable to primary and

secondary sorbed water of the Dent model. The primary water (M_1) of the Dent model is slightly higher than the hydrated water (M_{hyd}) of the H-H model, see Figure 1. The secondary water of the Dent model (M_2) is slightly lower than the dissolved water (M_{dis}) of the H-H model, which is also confirmed by Sonderegger and Niemz (2012). However, the total sorption isotherm (M_{total}) is equal in both models. Complete monolayer coverage of all available sorption sites is represented by MC 5.56 % corresponding to complete hydration for adsorption and MC 8.11% for desorption. As seen from Figure 1, the values at 100 % RH were lower for desorption than for adsorption. This was caused by the fact that the measurements start and end at 90 % of RH instead of 100 % of RH.

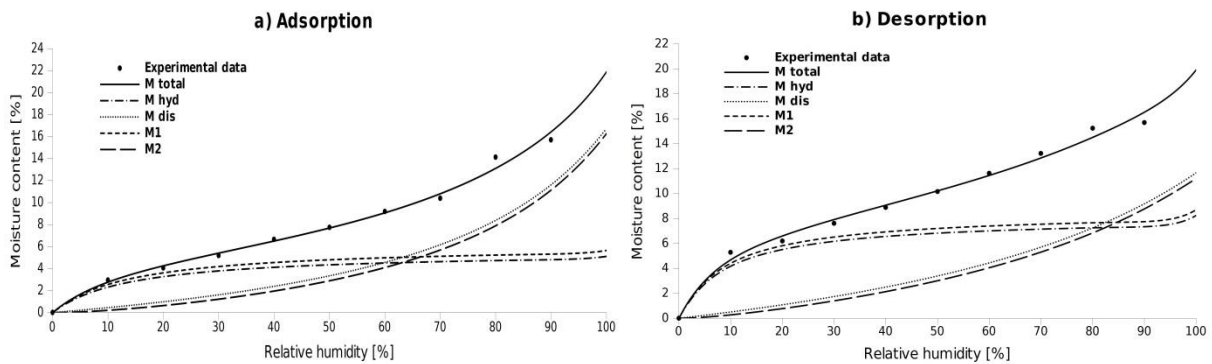


Fig. 1 Sorption isotherms of material 6 ((a) adsorption, (b) desorption) according to the single-hydrate H-H model and Dent model

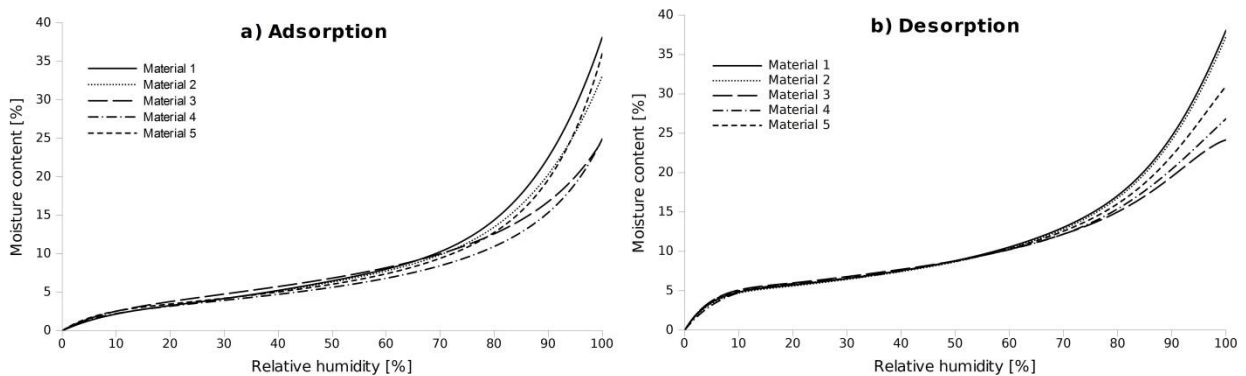


Fig. 2 Adsorption (a) and desorption (b) isotherms of the total sorption (material 1-5) according to the H-H and Dent model

Figure 2 shows the total adsorption and desorption curves of materials 1-5. Sorption isotherm of selected fiberboards (material 1, 2 and 5) rapidly increases above about 80% RH. This effect can be caused due to the absence of additives which are in some cases added during the manufacturing process to improve the water resistance properties. Additives probably change the saturation of water vapor in the air, as discussed by Sonderegger and Niemz (2012), Lesar et al. (2009) or Seifert (1972).

Thermal conductivity data of the measured insulation fiberboards (material 6) at different moisture contents, for the temperature range of -10°C to 60°C, are shown in Table 2. The average EMC after conditioning at 15%, 50%, 85% of RH were gravimetrically determined. Thermal conductivity increased as temperature and moisture content of the wood went up, as also reported by Kühlmann (1962). The higher the moisture content, the higher the thermal conductivity, which is caused by water conduction (Zhou et al. 2013). Thermal conductivity increases almost linearly with moisture content at a given temperature. Further, the higher the temperature, the bigger the differences were between conductivity values at oven-dry condition (increase of 12 %) and at 14.2 % of MC (increase of 61 %). The relationship between thermal conductivity, temperature and MC of samples was found by fitting the data with a second order polynomial function ($R^2=0.958$, formula 9).

$$\lambda = 0.0474 + 5.895e^{-4}w + 1.117e^{-4}T + 6.743e^{-5}w^2 - 1.226e^{-7}T^2 + 2.922e^{-5}wT \quad (9)$$

Table 2. Thermal conductivity of samples measured at different temperatures and moisture contents (the values in parentheses describe the coefficient of variation)

Relative humidity [%]	Moisture content [%]	Temperature [°C]							
		-10	0	10	20	30	40	50	60
		Thermal conductivity [W.m ⁻¹ .K ⁻¹]							
0	0	0.0437 (1.56)	0.0454 (1.46)	0.0475 (2.34)	0.0490 (3.01)	0.0514 (4.30)	0.0531 (6.66)	0.0544 (3.79)	0.0550 (3.61)
15	2.58	0.0445 (0.99)	0.0462 (0.98)	0.0484 (1.10)	0.0511 (2.07)	0.0529 (2.43)	0.0541 (2.46)	0.0549 (1.88)	0.0555 (1.24)
50	7.41	0.0467 (1.32)	0.0483 (1.47)	0.0514 (2.40)	0.0544 (3.76)	0.0568 (4.35)	0.0595 (4.63)	0.0608 (6.81)	0.0595 (4.89)
85	14.29	0.0488 (1.69)	0.0512 (2.31)	0.0553 (4.80)	0.0609 (7.45)	0.0671 (8.79)	0.0735 (10.66)	0.0812 (12.39)	0.0886 (13.92)

Conclusion

The relationship between thermal conductivity, temperature and MC of samples was established and described by fitting the data with a second order polynomial function. The formula describes thermal-moisture behavior of selected fiberboards and can be used as one of parameters suitable for modeling coupled moisture and heat transfer. Thermal conductivity increases almost linearly with MC at a given temperature. The differences between conductivity values at oven-dry conditions and at 85 % of RH increase remarkable with increasing temperature (increase of 61 % at 60 °C). Mean values for experimentally derived EMC at various levels of RH were evaluated. The H-H model and Dent model were used to investigate the water vapor sorption. The expected sorption hysteresis was observed. The manufacturing process and the lack of additives probably lead to increase in sorption of selected fiberboards above 80 % RH.

Acknowledgement

This article is supported by the project “The Establishment of an International Research Team for the Development of New Wood-based Materials” Reg. No. CZ/1.07/2.3.00/20.0269.

References

- Brombacher V., Michel F., Niemz P., Volkmer T. (2012) Investigation of thermal conductivity and moisture behaviour of fiberboards and material combinations, *Bauphysik* 34, 157-169
- Hill CAS, Norton a., Newman G (2009) The water vapour sorption behaviour of natural fibers, *J Appl Polym Sci* 112:1524-1537
- Kühlmann, G. (1962) Investigation of the thermal properties of wood and particleboard in dependency from moisture content and temperature in hygroscopic range, *Holz als Roh- und Werkstoff* 20(7), 259-270
- Lesar B., Gorisek Z., Humar M. (2009) Sorption properties of wood impregnated with boron compounds, sodium chloride and glucose, *Dry Technology* 27(1):94-102
- Mantanis G.I., Papadopoulos A.N. (2010) The sorption of water vapour of wood treated with a nanotechnology compound, *Wood Science and Technology* 44(3), 515-522
- Matias L., Santos C., Reis M., Gil L. (1997) Declared value for the thermal conductivity coefficient of insulation corkboard, *Wood Science And Technology* 31: 355-365
- Salmon D. (2001) Thermal conductivity of insulations using guarded hot plates, including recent developments and source of reference materials, *Measurement Science and Technology* 12, 89-98
- Scheiding W. (1998) Development, production and investigation of major characteristics of water-glass-bonded fiberboards made of spruce. Dissertation, TU Dresden
- Seifert J. (1972) Zur Sorption und Quellung von Holz un Holzwerkstoffen. Erste Mitteilung: Einflusse auf das Sorptionsverhalten der Hlzwerkstoffe, *Holz Roh-Werkst* 30(3):99-111
- Siau J. F. (1984) Transport process in wood, Berlin, Springer-Verlag
- Wu Q., Suchland O., Prediction of a moisture content and moisture gradient of an overlaid particleboard, *Wood And Fiber Science* 28 (1996) 227-239
- Simpson W. (1980) Sorption theories applied to wood, *Wood Fiber* 12(3):183-195
- Sonderegger W., Niemz P. (2012) Thermal and moisture flux in soft fibreboards, *European Journal of Wood and Wood Products* 70: 25-35
- Zhou J., Zhou H., Hu Ch., Hu S. (2013) Measurement of thermal and dielectric properties of medium density fiberboard with different moisture contents, *BioResources* 8(3), 4185-4192

Interconnection of Strength, Porosity and Microstructure of Hardwood

Inna Varivodina, Nikolai Kosichenko, Tamara Starodubtseva

Voronezh State Academy of Forestry and Technologies
Voronezh, Russia

Interconnection of strength, porosity and microstructure of hardwood is studied. It turned out that in diffuse-porous species with an increasing number of annual layers in 1 centimeter, compressive strength along the grain increases, as the proportion of tracheae decreases.

Uniform dispersed distribution of average diameter tracheae is the most favorable for treatment. Drooping birch dries uniformly, it is well-cut and well-soaked. Medullar rays do not differ significantly in width, which contributes to the homogeneity of wood properties.

Representatives of hardwood diffuse-porous species have linear and directly proportional relationship between compressive strength along the grain and the number of annual rings.

English oak wood has inverse nature of the relationship between the studied indicators - dependence is linear and inverse proportional. The decrease of compressive strength indicator along the grain by increasing the number of annual rings in 1cm is because deciduous ring-porous species have genetically unchanged width of early zone. Consequently, the wood with a large number of annual rings will be less strong, dense and solid, but will bend well because the proportion of large tracheae increases in reducing oak annual ring. English oak wood, because of its anatomical structure - the presence of large tracts of fibres of libriform and fiber tracheids in the late zone - is hard to be processed. Oak wood is characterized by high durability and biostability.

Keywords: porosity, strength, rate of growth, histological structure

Wood is a unique natural material used by man since ancient times. Multiple use of wood is explained by rare combination of many valuable properties in this wildlife product. Wood has high physical and mechanical properties due to which it can be processed in different ways - sharpening, planing, cutting; beautiful appearance, allowing its use for the production of artistic products and souvenirs.

Natural, absolutely dry wood (V_0) is porous (capillary) material consisting of the volume of the cell walls ($V_{w.s.}$) and pores between them (V_p) [1]:

$$V_0 = V_{w.s.} + V_n \quad (1)$$

Then indicator of porosity (P) can be expressed by the formula:

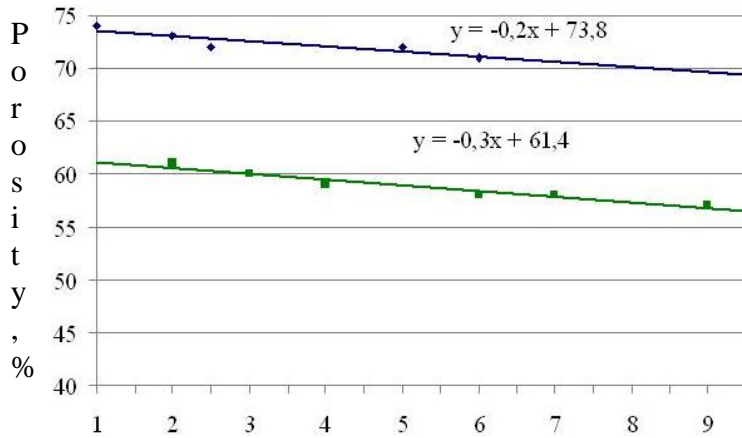
$$P = \frac{V_0 - V_{w.s.}}{V_0} 100 \quad (2)$$

Converting the density, this expression will have the form:

$$P = \left(1 - \frac{\rho_0}{\rho_{w.s.}} \right) 100 \quad (3)$$

where P – wood porosity, %; ρ_0 – wood density in a completely dry condition; $\rho_{w.s.}$ – density of wood substance.

Based on the formula (3), the operation of calculating of porosity is reduced to the determination of basic wood density, because the density of wood substance - constant. But this procedure is time-consuming and energy-intensive process. Experiments were conducted to identify the relationship between the porosity of wood and width of the annual ring in representatives of different groups of wood. At Scientific-experimental forestry of Voronezh State Academy of Forestry and Technologies samples of European aspen *Populus tremula* and silver birch *Betula pendula* as representatives of diffuse-porous hardwoods and English oak *Quercus robur*, European ash *Fraxinus excelsior* and European white elm *Ulmus laevis* as representatives of ring-porous hardwoods were selected. For the study, samples were taken, which represented the entire range of fluctuation of the width of wood annual rings from wide-ringed to close grown wood. Samples were prepared of standard sizes 20x20x30 mm and their density was determined in the dry state according to GOST 16483.1-84, and porosity was calculated by the formula (3). In accordance with GOST 16483.18-72 number of the annual rings in 1 cm (n) was determined. According to studies dependency diagrams of porosity from the number of annual rings in 1 cm was made (Fig. 1).



Number of growth rings in 1 cm

Fig. 1. Dependence of porosity of diffuse-porous hardwoods on the number the annual rings in 1 cm

As can be seen from the Figure 1, the relationship between porosity and the number of annual rings in aspen and birch is linear, inversely. Regression equation of the relationship between the porosity of wood and number of the annual rings in 1 cm has the form:

For aspen $P = 7.8 - 0.2 \cdot n$ (4)

For birch $P = 61.4 + 0.3 \cdot n$ (5)

As can be seen from the Figure 2, the relationship between the porosity of wood and number of annual rings in representatives of ring-porous hardwoods is linear, directly proportional.

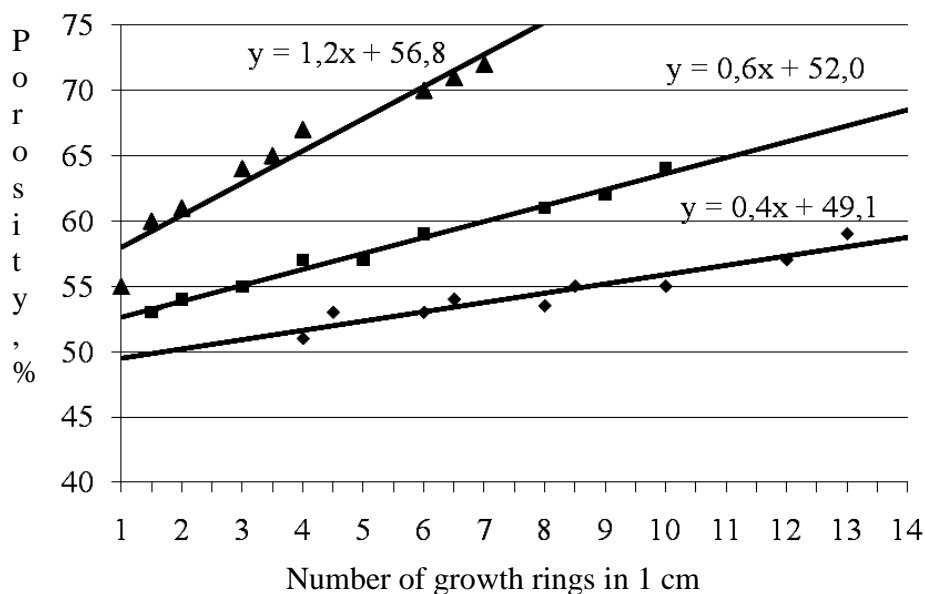


Fig. 2 – Dependence of porosity of ring-porous hardwoods on the number the annual rings in 1 cm

Regression dependence equation has the form:

$$\text{For elm} \quad P = 56.8 + 1.2 \cdot n \quad (6)$$

$$\text{For ash} \quad P = 52.0 + 0.6 \cdot n \quad (7)$$

$$\text{For oak} \quad P = 49.1 + 0.4 \cdot n \quad (8)$$

Explanation of the cause of revealed patterns can be given on the basis of anatomy, genetics, and ecology of plants. It is known that with the age of the tree, reduction of the annual ring takes place. As it is shown by previous studies, in wood species of different levels of evolutionary development this process proceeds differently. Representatives of conifers have age reduction of the annual ring due to reducing the width of the early wood. Width of late wood throughout the whole ontogeny varies slightly and it is under strict genetic control. It should be borne in mind that under the experimental conditions of this environmental law is violated.

Description of the microscopic structure of wood or anatomical characteristic of wood includes typical and stable features that can be used to assess the wood as a structural material. The use of wood as a structural material is due to the ability to resist the action of forces, i.e. mechanical properties.

The most characteristic of the mechanical properties of wood and which are of practical importance is its compressive strength along the fibers.

Compressive deformation along the fibers is expressed in a shortening of the sample. The destruction begins with the lateral deflection of the individual fibers. Wood has a fairly large compressive strength along the fibers.

Experiments were carried out to establish the relationship between the strength of wood and width of the annual ring. According to our experiment dependence diagram of compressive strength along the fibers on the number of annual rings in the 1cm was made ($\sigma_{comp}(n)$)

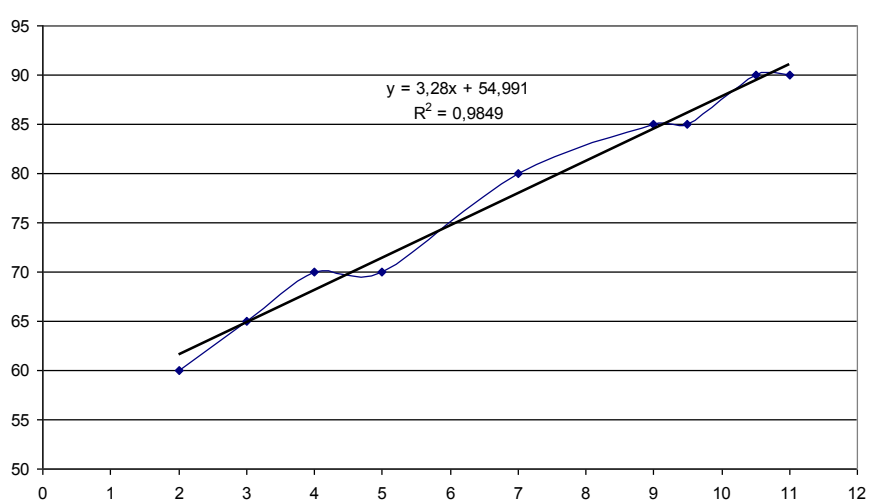


Fig. 3 Dependence of compressive strength along the fibers (σ_{comp} , MPa) of silver birch wood on the number of annual rings in 1cm (n , cm^{-1})

With an increasing number of annual rings in 1cm and compressive strength along the fibers increases, as the proportion of vessels decreases (they perform conductive function). Evenly dispersed distribution of the vessels of the mean diameter is the most favorable for treatment. Silver birch dries uniformly, it is well-cut, soaked. Medullar rays do not have a significant difference between the width ($6.7 \pm 0.16 \mu m$), which contributes to the homogeneity of the properties of wood.

As it is seen in Figure 3, the relationship between the compressive strength along the fibers and the number of annual rings in diffuse-porous hardwood representatives is linear, directly proportional.

The equation of the regression relationship between tensile strength of wood in compression and in a number of annual rings in 1 cm has the form:

For birch
$$\sigma_{comp} = 54.9 + 3.28 \times n, \text{ MPa} \quad (9)$$

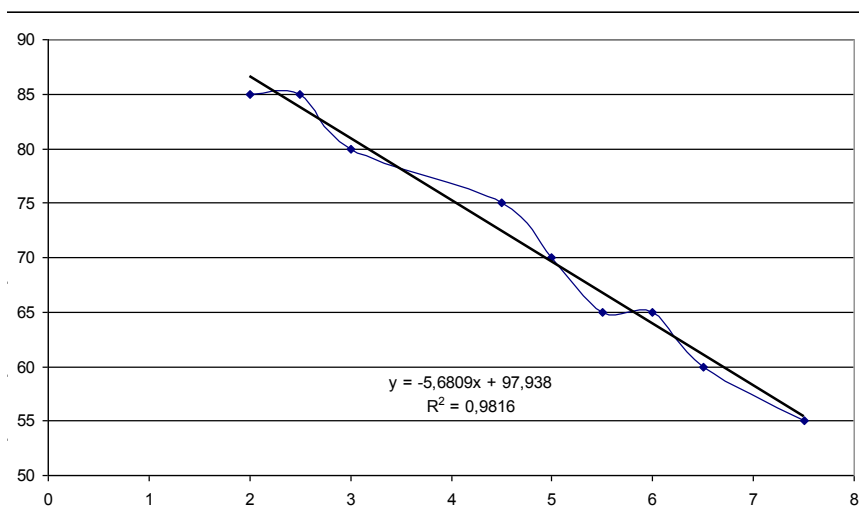


Fig. 4 Dependence of compressive strength along the fibers (σ_{comp} , MPa) of English oak wood on the number of annual rings in 1cm (n , cm^{-1})

In English oak wood nature of the relationship between the studied parameters is linear, inversely proportional. Equation of the linear regression dependence is expressed by:

$$\text{For oak} \quad \sigma_{comp} = 97.9 - 5.7 \times n \quad , \text{MPa} \quad (10)$$

The decrease of compressive strength along the fibers with increasing number of annual rings in 1cm is because width of early zone of deciduous ring-porous woods (English oak) remains genetically unchanged. Consequently, the wood with a large number of annual rings will be less strong, dense, firm, but will bend well as in the oak with annual ring reducing the proportion of large vessels increases.

English oak wood has a number of shortcomings in the machining due to large vessels zone ($293.0 \pm 7.32 \mu\text{m}$) cracks, breaks, lacker breaking. A special form of the structure of beam system - a combination of broad medullar rays ($177.8 \pm 4.44 \mu\text{m}$) with single row ones ($11.5 \pm 0.28 \mu\text{m}$) strongly influence the properties of oak. This is manifested in the heterogeneity of wood at different sites. Large rays become a cause of severe shrinkage, warpage. English oak wood because of its anatomical structure - the presence of large tracts of libriform and fiber tracheids in the late zone (more than 40% of the total composition) - is heavily processed. At this the endings of wood fibers bifurcate and contain teeth that cause high strength of oak wood for break. The presence of gelatinous fibers increases elasticity of the wood - bending strength. Oak wood is characterized by high durability and biopersistence.

Direct functions are clearly expressed and simple equations of functions allow with a sufficient degree of accuracy and reliability, scientifically determine the porosity and strength of wood across the width of annual rings. This study is important for the theory and practice of Wood Science. For theory it reveals the role of phylogenetic specialization of xylem elements, features of combined effects of genotype and environment on the complex processes of formation of high-quality wood. In practical terms, it greatly reduces the labor and energy costs in determining such indicators of wood quality as its porosity, density and strength.

References

1. Ugolev B.N. Wood science with the basics of merchandising: Textbook. - Moscow: SEI HPE MSFU, 2007. -351 p.
2. Varivodina I., Kosichenko N., Varivodin V., Sedliačik J. Interconnections among the rate of growth, porosity and wood water absorption // Wood Research, 2010, 55(1): 59-66.
3. Varivodina I.N., Kosichenko N.E., Nedelina N.Y., Varivodin V.A. Wood porosity of the main ring-porous hardwoods // Adhesives in woodworking industry, XX Symposium, Zvolen, Jun 29-Jul 1, 2011, 255-259.

Cross Industry Innovation Process to Identify “New” Technologies for Mechanical Wood Disintegration

Oliver Vay^{1*} – *Johannes Konnerth*² – *Stephan Frybort*³ – *Thomas Krenke*⁴
– *Alfred Teischinger*⁵ – *Ulrich Müller*⁶

¹ Senior Researcher, Wood K plus – Competence Centre for Wood Composites and Wood Chemistry, Tulln, Austria.

* *Corresponding author*

o.vay@kplus-wood.at

² Associate Professor, Institute of Wood Science and Technology, BOKU – University of Natural Resources and Life Sciences, Vienna, Austria.

³ Senior Researcher, Wood K plus – Competence Centre for Wood Composites and Wood Chemistry, Tulln, Austria.

⁴ Junior Researcher, Wood K plus – Competence Centre for Wood Composites and Wood Chemistry, Tulln, Austria.

⁵ Professor, Institute of Wood Science and Technology, BOKU – University of Natural Resources and Life Sciences, Vienna, Austria.

⁶ Priv.-Doz., Institute of Wood Science and Technology, BOKU – University of Natural Resources and Life Sciences, Vienna, Austria.

ulrich.mueller@boku.ac.at

Abstract

In many fields of industry, the best innovators systematically use existing ideas of other branches as a source for new ones for their own applications. A current study proves that more than 80% of the actual innovations are based on a recombination of existing knowledge.

Normally wood is mechanically disintegrated by tradition based technologies like sawing, peeling, hammer milling, refining and other cutting technologies. However, existing mechanical disintegration technologies are not able to account for the mechanical potential of the raw material because cutting always means a destruction of the natural optimized structure of wood. A couple of these mechanical disintegration technologies work energetically inefficiently and exhibit insufficient yield of high quality material or possess increased abrasive wear of the tools.

We hypothesize that it is possible to mechanically disintegrate and refine wood in a different and also more efficient way. Probably these new methods also include non-cutting technologies.

An interdisciplinary cross-industry innovation process is performed so as to see how existing technologies of other branches could be used to create potentially breakthrough innovations in the field of wood disintegration. In a first step of the innovation process, existing technologies in the wood industry are analyzed with the help of experts from various disciplines from industry and research. This analysis was used to create key words for an extensive patent research to identify “new” technologies. Special innovation techniques were used to create general key words which are independent of the typically branch specific wording.

Keywords: Cross innovation, Patent research, Technology transfer, Wood machining.

Introduction

“I invented nothing new. I simply assembled into a car the discoveries of other men behind whom were centuries of work....Had I worked fifty or ten or even five years before, I would have failed. So it is with every new thing. Progress happens when all the factors that make for it are ready, and then it is inevitable. To teach that a comparatively few men are responsible for the greatest forward steps of mankind is the worst sort of nonsense” (Henry Ford).

Spanning multiple otherwise disconnected industries to see how existing technologies could be used to create breakthrough innovations in your own technological sector is the idea of technology brokering (Hargadon and Sutton 1997). Today innovation has only little do to with a solitary flash of genius. More than 80% of all innovations are based on a recombination of existing knowledge (Figure 1). In all fields, the best innovators systematically use “old” ideas as the raw material for new ones.

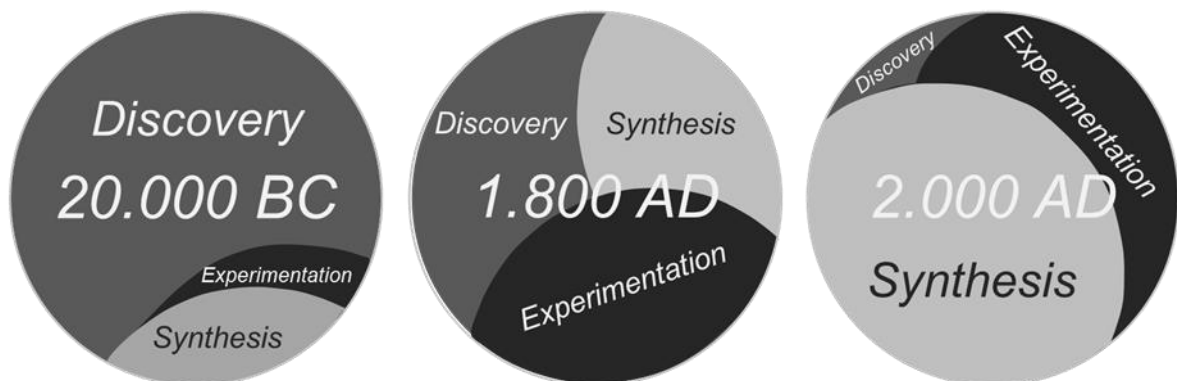


Figure 63. Change over time in use of methods for creating knowledge (Burnett 2009).

Wood is generally disintegrated, fragmented and refined in the first process steps in wood industries. Currently traditional technologies like sawing, peeling, hammer milling, refining and others are applied. Using these existing technologies wooden products are usually not able to tap the full mechanical potential of wood (Teischinger and Patzelt 2006) and current technologies exhibit insufficient yield of high quality material. One can state, that the high mechanical syntheses of nature, implemented in a tree, cannot be

utilized in man-made wood based materials. Moreover, the energy efficiency of the machinery applied is rather low and tools possess abrasive wear. We hypothesize that it is feasible to fractionize wood in a different and also more efficient way. The best innovators have systematized the generation and testing of new ideas (Hargadon and Sutton 1997), so why not following their lines for wood disintegration?

Capturing Good Ideas

To identify “new”, notably “non-cutting based” technologies potentially adaptable in wood industry we followed the approach of an interdisciplinary cross innovation process (Gassmann and Zeschky 2008). The uses of analogies existing apart from one’s own industry is a tool of creative thinking for problem solving (De Bono 1990, Amabile 1996) and thus a source for radical innovation (Gordon 1969, Dahl and Moreau 2002). Knowledge and therefore an analogical technical solution that already exists can be identified by a literature research. The first difficulty that faces this analogizing research is the risk to use only predetermined branch specific keywords. Therefore, a strategy to open up the solution space by creating generalized key words applicable across industry boundaries is required.

Function analysis. As a first step, we analyzed machines or technologies currently used in wood industry (Figure 2).

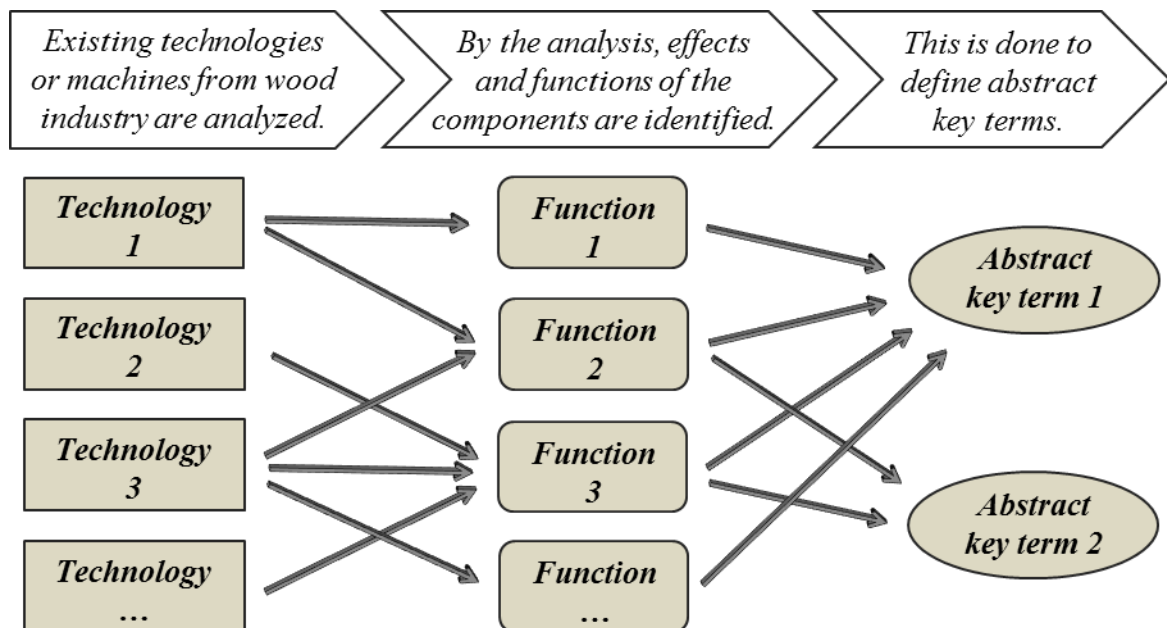


Figure 64. *Function analysis of existing technologies and machines to generate abstract search terms.*

This was done for a deep understanding of the technological function and the interrelation between single components of the processes. Accordingly, the underlying mechanism was identified. Moreover, the function analysis subsequently increased the

degree of abstraction from the original technology and accordingly the wording used to describe the original processes. Thus, by abstracting the technical descriptions to structural functions, the space for potential solutions is opened up (Hentschel et al. 2010, Koltze and Souchkov 2011).

Research methodology. Based on abstract key terms, an intensive patent research was performed. This was done on the premise that no technical field can be excluded. In total, more than 18.000 patents were screened, from which about 250 patents were selected for a detailed inspection. These selected patents provide about 40 “new” ideas involving incremental innovations as well as radical new technologies possibly applicable for wood disintegration.

Ablation technology, which is required in the field of medicine, in particular in the field of cataract extraction, may serve as an example for one alternative method or idea for mechanical fragmentation. An innovative ablation instrument is described by Gluche et al. (2003). The tool, schematically shown in figure 3, can be used for cutting, fragmenting and/or removing material from an object.

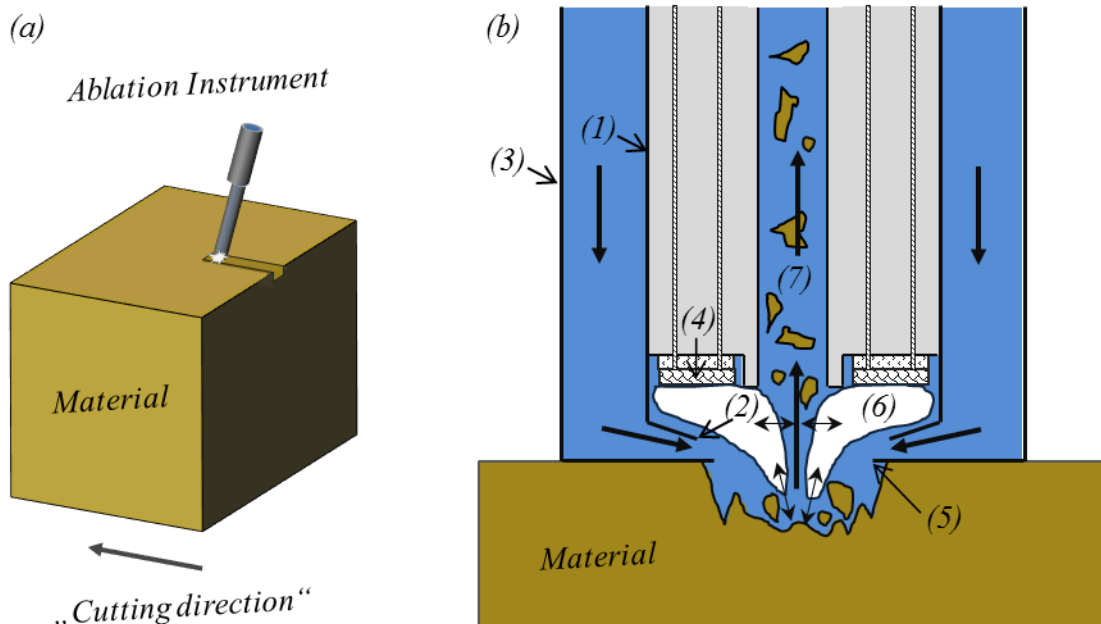


Figure 65. Ablation instrument for cutting, fragmenting and/or removing material from an object. (a) Schematic representation of the tool for cutting material. (b) Detailed representation of the tube according to Gluche et al. (2003). The external wall of the tube (1) narrows in a concentric manner inwardly above the opening (2). The channel between the external wall of the tube and the housing (3) serves for supplying an evaporation medium to the resistance-heated element (4) of the tool. The medium, e.g. water, indicated by the blue colour, flows in the direction of the arrows into the region between the opening (2) and the nozzle opening (5). By heating the element (4), a concentric gas bubble (6) is formed which fragments the material above the nozzle opening. Thus a cavity is formed. Fragments of the material are sucked via the opening (7) in the direction of arrow.

In the nozzle of the tool, a gas bubble is formed which fragments material above the nozzle opening. Due to the fact that the medium to be evaporated, e.g. water, is provided by the tool it is feasible to fragment or cut solid bodies. So could this be a technology for fragmentation or cutting used in wood industry?

Adaptation

To evaluate and filter relevant knowledge and to transfer and adapt ideas or technologies provided by the patent research will be the next step. Therefore, external experts will be integrated. We do not know yet if all selected “new” ideas are reasonably adaptable and applicable in wood industry. Nevertheless we found that the wood industry must be open-minded for external solutions. This approach is considered to be highly beneficial for innovation.

References

Hargadon A., Sutton R.I. 1997. Technology brokering and innovation in a product development firm. *Administrative Science Quarterly*. 42(4): 716-749.

Burnett B. 2009. Building new knowledge and the role of synthesis in innovation. *International Journal of Innovation Science* 1: 13-27.

Teischinger A., Patzelt M. 2006. XXL-Wood. Materialkenngrößen als Grundlage für innovative Verarbeitungstechnologien und Produkte zur wirtschaftlich nachhaltigen Nutzung der österreichischen Nadelstarkholzreserven. *Berichte aus der Energie- und Umweltforschung*, Bundesministerium für Verkehr, Innovation und Technologie, Wien

Gassmann O., Zeschky M. 2008. Opening up the solution space: The role of analogical thinking for breakthrough product innovation. *Creativity and innovation management*. 17(2): 97-106.

De Bono E. 1990. *Lateral Thinking for Management*. Penguin Books. London.

Amabile T.M. 1996. *Creativity in Context*. Westview Press, Boulder, US.

Gordon W.J.J. 1969. *Synergetics – The Development of Creative Capacity*. Harper and Row. New York.

Dahl D.W., Moreau P. 2002. The Influence of Value of Analogical Thinking During New Product Ideation. *Journal of Marketing Research* 39: 47-60.

Hentschel C., Gundlach C., Nähler H.T. 2010. *TRIZ. Innovation mit System*. Hanser Verlag

*Proceedings of the 57th International Convention of Society of Wood Science and Technology
June 23-27, 2014 - Zvolen, SLOVAKIA*

Koltze K., Souchkov V. 2011. Systematische Innovation – TRIZ Anwendung in der Produkt- und Prozessentwicklung. Hanser Verlag

Gluche P., Ertl S., Lingenfelder C., Kohn E. 2003. Ablation instrument and method for cutting, fragmenting and/or removing material. International Publication Number WO03047445A2.

Acoustic Sorting Models for Improved Log Segregation

Xiping Wang^{1*} – *Steve Verrill*² – *Eini Lowell*³ – *Robert Ross*⁴ – *Vicki Herian*⁵

¹ Research Forest Products Technologist
USDA Forest Service, Forest Products Laboratory
Madison, WI, USA

* *Corresponding author*

[*xwang@fs.fed.us*](mailto:xwang@fs.fed.us)

² Mathematical Statistician
USDA Forest Service, Forest Products Laboratory,
Madison, WI, USA

[*sverrill@fs.fed.us*](mailto:sverrill@fs.fed.us)

³ Research Scientist
USDA Forest Service, Pacific Northwest Research Station,
Portland, OR, USA

[*elowell@fs.fed.us*](mailto:elowell@fs.fed.us)

⁴ Project Leader
USDA Forest Service, Forest Products Laboratory,
Madison, WI, USA

[*rjross@fs.fed.us*](mailto:rjross@fs.fed.us)

⁵ Statistician (Retired)
Madison, WI, USA

[*vicki@swst.org*](mailto:vicki@swst.org)

Abstract

In this study we examined three individual log measures (acoustic velocity, log diameter, and log vertical position in a tree) for their ability to predict the average modulus of elasticity (MOE) and grade yield of the structural lumber obtained from Douglas-fir (*Pseudotsuga menziesii*, (Mirb., Franco)) logs. We found that the combinations of log acoustic velocity and log diameter or log acoustic velocity and log position were better predictors of average lumber MOE and lumber visual grade yield than log acoustic velocity alone. For sorting best quality logs, multi-variable models were more effective than the velocity-alone model; however for sorting poorest quality logs, the velocity-alone model was as effective as multi-variable models.

Keywords: Acoustic velocity, log diameter, log position, log sorting, lumber, modulus of elasticity, visual grade.

Introduction

Research has shown that log acoustic measures can be used to predict the strength and stiffness of structural lumber that would be produced from a log (Aratake et al. 1992, Aratake and Arima 1994, Ross et al. 1997, Wang et al. 2004a). Currently, the companies implementing acoustic sorting strategies measure only the velocity of acoustic waves and segregate stems and logs into velocity classes using predetermined cut-off velocity values. Although this simple sorting strategy has been proved somewhat effective by several mill studies (Tsehaye et al. 1997, Carter and Lausberg 2003, Wang et al. 2004a, Carter et al. 2005), the strength of the direct correlation between the acoustic velocity in a particular log and the properties of wood products derived from that log are actually not very strong, with a typical correlation of coefficient (R^2) in the range of 0.38 and 0.54 (Aratake et al. 1992, Farrell and Nolan 2008). While still operationally useful, the precision of acoustic sorting is less than desired. The purpose of this study was to gauge the effect of combining additional variables with acoustic velocity to predict the average modulus of elasticity (MOE) and grade yield of the structural lumber obtained from the logs. Specifically, we examined three individual log measures— acoustic velocity (V), average log diameter (D), and log vertical position in a tree (P)—for their ability to sort logs individually and then developed new acoustic sorting models that used diameter and/or log position as a second variable for improving log sorting precision.

Materials and Methods

Forty eight Douglas-fir (*Pseudotsuga menziesii*, (Mirb., Franco)) trees ranging from 14.2 to 53.3 cm diameter at breast height (dbh) were selected from a 70-year-old stand on Pack Forest, the University of Washington's Research Forest in Eatonville, Washington. The sampled trees were then harvested and bucked into 4.9-m long mill-length logs. Each log was tagged with a number that identified the tree and the position in the tree from which it came. A log position (P) number was assigned to the logs to identify the vertical position in each tree based on the cutting sequence from the ground level ($P = 1 - 6$, with 1 representing the butt log, 2 the second log, and so on). A total number of 171 mill-length logs were obtained. The log position in each tree stem was recorded, and the log length and diameters of both ends of each log were measured.

Each log was nondestructively tested using an acoustic resonance technique to obtain an acoustic velocity for the log. The logs were then sawn into lumber using a Wood-Mizer™ (Wood-Mizer Products, Inc., Indianapolis, IN) at the yard site of Pack Forest. As each piece of lumber was sawn, it was labeled with the sawing number, and its position within the sawing pattern was diagrammed. The lumber pieces produced were predominantly 51-mm dimension (51 by 102-mm, 51 by 152-mm, and 51 by 203-mm) with some 25-mm jacket boards (25 by 102-mm and 25 by 152-mm) sawn from the outer portion of the logs. Green lumber thickness and width were measured on a randomly selected sample. All lumber were kiln dried to below 19% moisture content and surfaced at a local sawmill.

After the sawing and kiln drying, 1,098 pieces of lumber were obtained and evaluated for stiffness and visual grades yield. The dynamic modulus of elasticity (MOE_d) of each piece of lumber was measured using an E-computer (Metriguard Inc., Pullman, WA) according to ASTM standard D 6874-03 (ASTM 2003). All lumber were then visually graded according to Structural Light Framing grading rules (WWPA 1998) under the supervision of a Western Wood Products Association certified lumber inspector.

Data Analysis

We first evaluated log acoustic velocity (V), log diameter (D), and log position (P) as individual predictors of lumber MOE and visual grade yield. We then gauged the effect of combining log diameter and log position with the log acoustic velocity to predict the MOE and grade yield of the lumber. The log diameters used in the analysis were the averages of the large and small end diameters of the logs. For each log, we obtained a simple unweighted average of the MOEs of the lumber extracted from the log. The SAS (SAS Institute Inc., Cary, North Carolina) Version 8 MEANS and UNIVARIATE procedures were used to generate descriptive statistics for log and lumber properties. The SAS REG procedure was used to perform the linear regressions. The simple unweighted average MOE of all of the lumber in a log was the response being predicted.

Results and Discussion

Log and lumber properties

Table 1 provides descriptive statistics for the diameter, acoustic velocity, and average lumber MOE of the Douglas-fir logs. The acoustic velocity of the Douglas-fir logs ranged from 3255 to 4886 m/s with a COV of 7.9%. On a per log basis, the average MOE of the dried lumber for the Douglas-fir logs ranged from 8.9 GPa to 21.6 GPa with a COV of 18.4%. One thousand ninety-eight pieces of lumber were obtained from the logs. Of these, 12.5% were Select Structural (SS), 24.1% No. 1, 57.1% No. 2, and 6.3% No. 3.

Acoustic sorting models

Table 2 shows the results from the regressions of average lumber MOE on log acoustic velocity (V), log diameter (D), log position (P), and on the combinations of log acoustic velocity and log diameter or log acoustic velocity and log position. Prediction equations were derived using the following two functional forms:

$$MOE = \beta_0 + \beta_1 \cdot x_1 \quad (1)$$

$$MOE = \beta_0 + \beta_1 \cdot x_1 + \beta_2 \cdot x_2 \quad (2)$$

where MOE is the average lumber modulus of elasticity being predicted; x_1 and x_2 are predicting variables (log acoustic velocity V , log diameter D , and log position P); β_0 , β_1 , and β_2 are the regression coefficients.

Log acoustic velocity had a positive correlation with lumber MOE, but the relationship was not very strong ($R^2 = 0.40$). Log diameter was found to have a weak relationship with lumber MOE ($R^2 = 0.12$). Although not suited for predicting lumber MOE, log diameter

Table 1. Descriptive statistics of log diameter, log acoustic velocity and average modulus of elasticity of lumber on a per log basis.

Property	Mean	Min.	Max.	COV ^a (%)
Log diameter (cm)	23.5	10.2	40.6	27.4
Log acoustic velocity (m/s)	4212	3255	4886	7.9
Average lumber MOE (GPa)	14.8	8.9	21.6	18.4

^a Coefficient of variation

Table 2. Regressions of average lumber MOE on log acoustic velocity (V), log diameter (D), log position (P) and on the combination of V, D, and P^a.

Predictors		Coefficients						R^2	Adjusted R^2	$RMSE^b$
x_1	x_2	β_0	p -value	$\beta_1(x_1)$	p -value	$\beta_2(x_2)$	p -value			
V	—	-7.70	0.0005	0.001621	0.0001	—	—	0.400	0.396	2.06
D	—	11.37	0.0001	0.374	0.0001	—	—	0.122	0.116	2.49
P	—	18.72	0.0001	-1.48	0.0001	—	—	0.587	0.584	1.70
V	D	-10.39	0.0001	0.001606	0.0001	0.316	0.0001	0.501	0.495	1.88
V	P	6.53	0.0014	0.000823	0.0001	-1.19	0.0001	0.672	0.668	1.52

^aThe average MOE of all of the lumber in a log is the response being predicted. The average coefficients and the $RMSE$ are for MOE measured in GPa.

^b $RMSE$ — root mean squared error.

was found to have a significant effect on acoustic wave propagation (Wang et al. 2004b). In this study, we examined a simple acoustic sorting approach in which the density of the logs was not measured and thus prediction of log MOE through the fundamental wave equation was not considered. However, the effect of log diameter on acoustic wave measures cannot be neglected.

Log vertical position in a tree was found to have a relatively good but negative relationship with lumber MOE ($R^2 = 0.59$). The lumber MOE was highest at the first and the second logs, and decreased with increasing position. This finding is similar to what Iangum et al. (2009) reported for 20 years old Douglas-fir and western hemlock trees, in which they observed that flexural stiffness and strength decreased with increasing vertical position.

Regressions of average lumber MOE on the combinations of log acoustic velocity and log diameter or log acoustic velocity and log position show significant improvement as evidenced by the increase of coefficient of determination (Table 2). Figure 1 plots observed MOE versus predicted MOE for a regression in which MOE is regressed on both log acoustic velocity and log diameter ($R^2 = 0.50$). Figure 2 plots observed MOE versus predicted MOE for a regression in which MOE is regressed on both log acoustic velocity and log position ($R^2 = 0.67$). The results indicated that log acoustic velocity by itself was not as good a predictor as the combination of log acoustic velocity and log

diameter or the combination of log acoustic velocity and log position. The practical implications of these sorting models are illustrated through the following two sorting strategies.

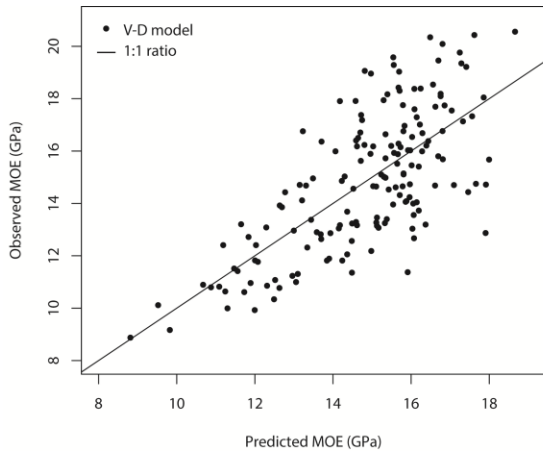


Figure 1. Observed MOE vs predicted MOE for a regression in which MOE is regressed on both log acoustic velocity (V) and log diameter (D).

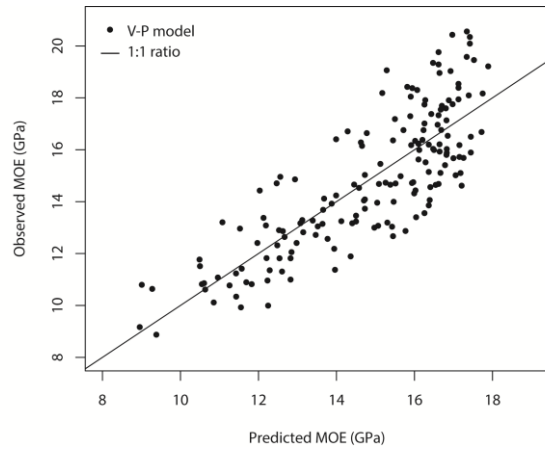


Figure 2. Observed MOE vs predicted MOE for a regression in which MOE is regressed on both log acoustic velocity (V) and log position (P).

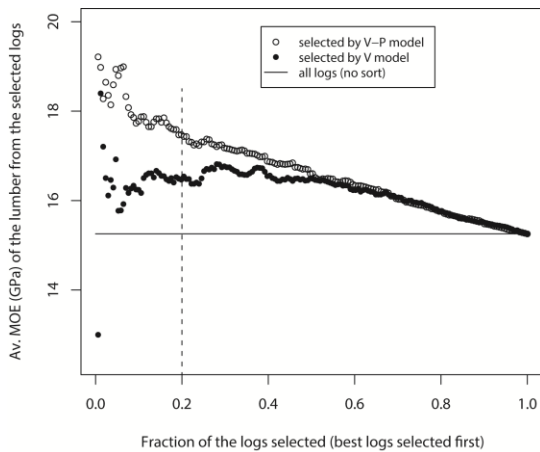


Figure 3. Average MOE of lumber from the selected logs vs fraction of the logs selected (best logs selected first).

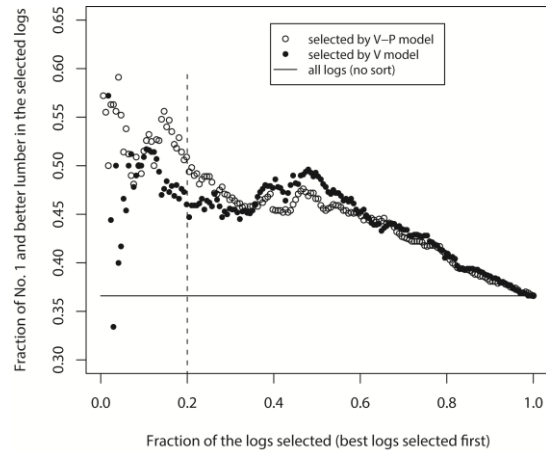


Figure 4. Fraction of No. 1 & Better lumber among lumber produced from selected logs vs fraction of the logs selected (best logs selected first).

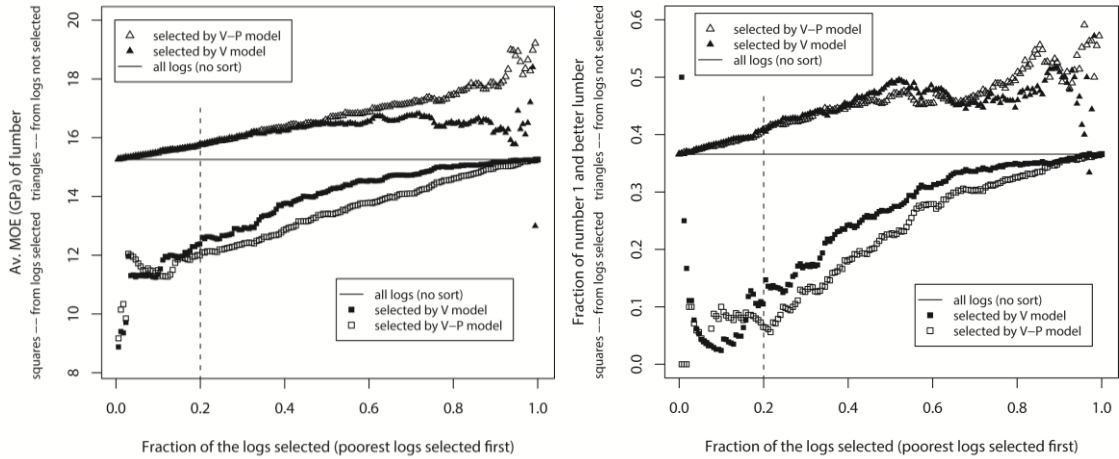


Figure 5. Average MOE of lumber from the selected and unselected logs vs fraction of the logs selected (poorest logs selected first).

Figure 6. Fraction of No. 1 & Better lumber among lumber produced from selected and unselected logs vs fraction of the logs selected (poorest logs selected first).

Illustration of acoustic sorting strategies

In a practical log-sorting process, companies can achieve benefits by implementing one of the following sorting strategies based on log sources and desired end products: 1) Sorting best quality logs; and 2) sorting poorest quality logs.

Sorting best quality logs Figure 3 demonstrates the outcomes of sorting best quality logs in terms of lumber MOE. Suppose we used the regression equation to identify the logs that would produce the lumber with the highest average MOE. If we selected, for example, the predicted top 20% of the logs, the average MOE of the lumber produced from the logs identified by the log acoustic velocity and log position equation (*V-P* model) would be about 17.5 GPa, while the average MOE of the lumber produced from the logs identified by the velocity-alone equation (*V* model) would be about 16.5 GPa. If we used no prediction equation, the resulting average MOE would be about 15.3 GPa. Thus, selection of the “best” 20% of the logs based on the *V-P* and *V* models yield 14.5% and 8% increases in average lumber MOE respectively. When less than 10% of the logs selected, the average lumber MOE for the logs selected by *V*-model showed large variations, which indicated the uncertainties of *V*-model when only a small sample size of logs was selected. *V-P* model, on the other hand, showed a consistent trend in MOE improvement between 0 and 50% log selection.

Figure 4 shows the results of sorting best quality logs in terms of visual grades. The fraction of No. 1 & Better lumber in selected logs fluctuated significantly when log selection was less than 50%. This could contribute to the fact that visual grading is a subjective procedure and does not fully reflect the stiffness of individual pieces of lumber. There seems no difference between *V-P* model and *V* model if less than 10% or higher than 30% of the logs were selected. But the results did show a clear difference of the two acoustic sorting models for log selection between 10% and 30%. For example, if we selected the predicted top 20% of the logs, the fraction of No. 1 & Better lumber in the lumber produced from the logs identified by the *V-P* model would be about 51%, while the fraction of No. 1 & Better lumber in the lumber produced from the logs identified by the *V* model would be about 46%. If we used no prediction equation, the fraction of No. 1 & Better lumber in the lumber produced from the logs would be about 37%. Thus, selections of the “best” 20% of the logs based on the *V-P* and *V* models yield 39% and 26% increases in the fraction of No. 1 & Better lumber respectively.

Sorting poorest quality logs Figures 5 and 6 demonstrate the outcomes of sorting poorest quality logs. Figure 5 plots both the average MOE of the lumber produced from the selected logs and the average MOE of the lumber produced from the logs that are not selected versus the fraction of logs that are selected. If we use the *V-P* model to select the predicted poorest (lowest stiffness) 34 of the 171 logs (the poorest 20%), the average MOE of the resulting lumber is approximately 12.0 GPa. The corresponding average MOE of the lumber from the 137 logs not selected (the remaining 80%) is approximately 15.8 GPa. If we use the *V* model to select the predicted poorest 34 of the 171 logs (the poorest 20%), the average MOE of the resulting lumber is approximately 12.4 GPa. The corresponding average MOE of the lumber from the 137 logs not selected (the remaining 80%) is approximately 15.8 GPa. Thus, sorting out the predicted 20% poorest logs using

either the *V-P* model or the *V* model enhanced the average lumber MOE of the remaining log population by about 3.3% (recall that the average lumber MOE for all logs was approximately 15.3 GPa).

Figure 6 plots the fraction of No. 1 & Better lumber among the lumber produced from the selected and unselected logs versus the fraction of the logs that are selected. Similarly, if we use the *V-P* model to select the predicted poorest 34 of the 171 logs (the poorest 20%), then the fraction of No. 1 & Better lumber in the resulting lumber is approximately 7%. The corresponding fraction of No. 1 & Better lumber in the lumber from the 137 logs not selected (the remaining 80%) is approximately 41%. If we use the *V* model to select the predicted poorest 34 of the 171 logs (the poorest 20%), the fraction of No. 1 & Better lumber in the resulting lumber is approximately 11%. The corresponding fraction of No. 1 & Better lumber in the lumber from the 137 logs not selected (the remaining 80%) is still about 41%. Thus, sorting out the 20% poorest logs using the *V-P* model or *V* model resulted in an increase from 37% to 41% in the fraction of No. 1 & Better lumber in the remaining log population (recall that the average for all logs was about 37%).

Two observations can be made from the above analysis. First, the increase in lumber MOE or visual grade yields as a result of sorting poorest logs might be minimal and could be offset by the prediction errors of the acoustic sorting models. The main benefit of sorting out the poorest quality logs prior to mill process is to avoid cutting low MOE or low grade lumber from the poorest quality logs, thus reducing the cost of misallocation of resources. Second, the effectiveness of *V-P* model and *V* model for sorting the poorest quality logs are about the same, which implies that the simpler *V* model could be used to segregate poorest logs in mill operations.

Conclusions

In this paper, we examined three log measures (acoustic velocity, log diameter, and log position) for their ability to predict the average modulus of elasticity and grade yield of the structural lumber obtained from Douglas-fir logs. Based on the results from this mill study, we conclude the following:

1. The combinations of log acoustic velocity and log diameter or log acoustic velocity and log position were better predictors of average lumber MOE and lumber visual grade yield than log acoustic velocity alone. The log acoustic velocity and log position model performed better than the log acoustic velocity and log diameter model in this study.
2. For sorting best quality logs, multi-variable models were more effective than the velocity-alone model; however for sorting poorest quality logs, the velocity-alone model was as effective as multi-variable models. In the first case, we are focusing on the properties of the 20% of the logs that were selected as best. In the second case, we are focusing on the 80% of the logs that were not selected.
3. In sawmill operations, a real threshold for sorting logs should be determined based on incoming log sources, end products, and the sorting strategy for the specific operation and it can be fine-tuned to maximize the products value.

Acknowledgement

This study was supported in part by funds provided by Michigan Technological University, Houghton, Michigan and Fibre-gen, Inc., Christchurch, New Zealand.

References

- Aratake S, Arima T, Sakoda T, Nakamura Y (1992) Estimation of modulus of rupture (MOR) and modulus of elasticity (MOE) of lumber using higher natural frequency of log in pile of logs – Possibility of application for Sugi scaffolding board. *Mokuzai Gakkaishi* 38 (11): 995-1001.
- Aratake S, Arima T (1994) Estimation of modulus of rupture (MOR) and modulus of elasticity (MOE) of lumber using higher natural frequency of log in pile of logs II – Possibility of application for Sugi square lumber with pith. *Mokuzai Gakkaishi* 40 (9): 1003-1007.
- ASTM (2003) D6874-03. Standard test methods for nondestructive evaluation of wood-based flexural members using transverse vibration. American Society for Testing and Materials, West Conshohocken, PA.
- Carter P, Lausberg M (2003) Application of Hitman[®] acoustic technology – The Carter Holt Harvey Experience. FIEA paper. 6 pp.
- Carter P, Briggs D, Ross RJ, Wang X (2005) Acoustic testing to enhance western forest values and meet customer wood quality needs. PNW-GTR-642, Productivity of Western Forests: A Forest Products Focus. USDA Forest Service, Pacific Northwest Research Station, Portland, OR. Pages 121-129.
- Farrell R, Nolan G (2008) Sorting plantation Eucalyptus nitens logs with acoustic wave velocity. Technical Report: Resource Characterization & Improvement, Project No. PN07.3018. Forest & Wood Products Australia Limited, Victoria, Australia. p27.
- Iangum CE, Yadama V, Iowell EC (2009) Physical and mechanical properties of young-growth Douglas-fir and western hemlock from western Washington. *Forest Products Journal* 59(11/12):37-47.
- Ross RJ, McDonald KA, Green DW, Schad KC (1997) Relationship between log and lumber modulus of elasticity. *Forest Prod. J.* 47(2):89-92.
- Tsehaye A, Buchanan AH, Walker JCF (1997) Log segregation into stiffness classes. Pages 7–10 *in* Ridoutt, B.G., ed., *Managing variability in resource quality*. FRI Bulletin No. 202, Forest Research Institute, Rotorua, New Zealand.
- Wang X, Ross RJ, Green DW, Brashaw B, Englund K, Wolcott M (2004a) Stress wave sorting of red maple logs for structural quality. *Wood Science and Technology* 37: 531-537.
- Wang X, Ross RJ, Brashaw BK, Panches J, Erickson JR, Forsman JW, and Pellerin RF. (2004b). Diameter effect on stress-wave evaluation of modulus of elasticity of small-diameter logs. *Wood and Fiber Science* 36(3): 368-377.

*Proceedings of the 57th International Convention of Society of Wood Science and Technology
June 23-27, 2014 - Zvolen, SLOVAKIA*

WWPA (1998) Western lumber grading rules. Western Wood Products Association, Portland, OR.

Heart Rots Detection by Velocity Difference within a Cross-Section

Kyaw Ko Win¹ - JungKwon Oh² - Jun Jae Lee^{3}*

¹ Master candidate, College of Agriculture and Life Sciences, Department of Forest Sciences, Seoul National University, Seoul, Republic of Korea.

** Corresponding author*

kyawkowin.zeus@gmail.com

² Research Professor, Department of Forest Sciences/Research Institute for Agriculture and Life Sciences, Seoul National University, Seoul, Republic of Korea.

³ Professor, Department of Forest Sciences/Research Institute for Agriculture and Life Sciences, Seoul National University, Seoul, Republic of Korea.

junjae@snu.ac.kr

Abstract

When stress wave CT technique was applied to inspect trees, stress wave velocity can change with the orientation of transducers which are mounted on trees because of anisotropic property of wood. Although CT images of cross-section of a stem can be seen, a deep experience is necessary to guess tree condition by interpreting the images. Heart rots form near the middle of a tree's cross-section. Velocities of stress wave paths passing through the inner and outer zones of cross-sections of 25 sound green discs were measured and calculated the velocity difference percentages. That difference percentages were used as standards to distinguish sound discs and heart rots discs. That index can be used as additional criteria to detect heart rots while using the stress wave CT imaging devices.

Keywords: A. Stress wave CT, B. Transducers' angles, C. Heart rots, D. velocity difference, E. Index.

Introduction

Stress wave method is a well-established technique for nondestructively evaluating the mechanical properties and characterizing natural defects of various wood products (Pellerin *et al.* 2002). Research development showed a very good potential for stress wave technique to be used to assess wood quality of living trees (Wang *et al.* 2007b). Since timber is inhomogeneous in nature, the grain orientation influences the speed of stress wave travel. Stress wave velocity can change according to the angles between transducers because of the annual rings orientation with the wave path and the anisotropic

properties of wood. In the cross-section of a tree stress wave can travel through in three directions; radially (perpendicular to annual ring), tangentially (parallel to annual ring) and across the rings at an angle between 0 and 90 degrees (X. Wang *et al.* 2004). The shortest is in the radial direction; stress wave speed is about 30% faster than that in other directions. These findings are based on the wave paths and the annual rings orientation. In case of inspecting trees, the annual ring angles orientation cannot be identified because the pith location is inconsistent inside the tree. In practical point of view, the angles of transducers mounted on the trunk of a tree can be known. So, it is better to investigate the transducers' angles and their related velocities.

There are some researchers developed the determination criteria to distinguish between sound and unsound specimens. A study conducted by Pellerin *et al.* (1985) demonstrated that a 30% increase in stress wave transmission time implies a 50% loss in strength. A 50% increase in stress wave transmission time indicates severely decayed wood. Oh (1999) concluded that the stress wave time of 12 μ s/cm could distinguish between sound and unsound specimen with the accuracy of 77.5%. Bae (2003) developed a threshold value for stress wave velocity to determine the degree of deterioration. When the accelerometer stress wave velocity was above 2200 μ s/m, the ratio of deterioration was increased above 17%. But for teak trees species, there is no decision making criterion to detect heart rots in the cross-sections.

There are some commercial stress wave CT tomograph instruments in the market to inspect the cross-section of the tree stem. They can provide the cross-section view of the stem with computerized images. The resolution of an image can be increased by using more transducer numbers. However, untrained inspector can misinterpret the CT images in the field because it needs technical and professional knowledge background on it. Therefore, there is still limitation to use these devices for untrained labors. The objective of this study was to develop less complicated indices that could be used to detect the presence of heart rots in green Teak.

Materials and Methods

Materials. Forty six Teak (*Tectona grandis*) trees were selected and felled from a plantation situated at Coupe no.41, Western Mone Reserved Forest at Minbu District, Magway Division in Myanmar. The cross-sections of the felled trees were visually checked. A disc was sliced from each tree stem by a chain-saw. Those forty eight Teak discs were wrapped by plastic bags immediately after being felled to prevent them from being dried. The sizes of these discs were ranging from 200-300 mm in diameter and irregular in shape. Among them, eleven discs had heart rots with various sizes. Those discs were transported to Korea by shipment. After receiving them at Seoul National University, they were kept in a refrigerator.

Velocity measurement. A PiCUS Sonic Tomograph was used for stress wave velocity measurement. "Fig.1 (a)" showed the PiCUS Sonic Tomograph and there were 12 transducers with an electric hammer. A disc to be tested was unpacked from the plastic

bags and weighed. The measuring points were made to locate the positions of transducers around the circumference of a disc. “Fig. 1(c)” showed the locations of the points on the cross-section (from A to H) for 8 transducers test set up and the wave paths from transmitting transducer to receiving transducers. The nails were driven at those points and the transducers were attached to that nails. “Fig.1 (c)” showed the experimental setup of transducers on the disc and the angles between transducers for 8 transducers set up. The angle Θ_r is the angle between transmitter and related receiver. The receivers are set at the receiver angles $\Theta_r=45^\circ$, $\Theta_r=90^\circ$, $\Theta_r=135^\circ$ and $\Theta_r=180^\circ$. The travel time was measured by tapping five times on transmitter A with a hammer. The stress wave, released from transmitting transducer A, was received by 7 receiving transducers (B, C, D, E, F, G and H) and measured the travel times from a transmitter to all receivers. The next tapping was carried out on B transmitter and the other 7 receivers (C, D, E, F, G, H and A) captured the wave from B and recorded the travel time. The same process continued until all the transducers had been tapped five times per each alternately. The wave paths passing through the cross-section of the disc among the transducers were shown in “Fig. 1 (b)”. In this study, three test setups with 8, 10 and 12 numbers of transducers were used. The same procedure was also done for 10 and 12 transducers. After carried out the testing, the number of transducers used and their related angles between transducers were tabled.

..

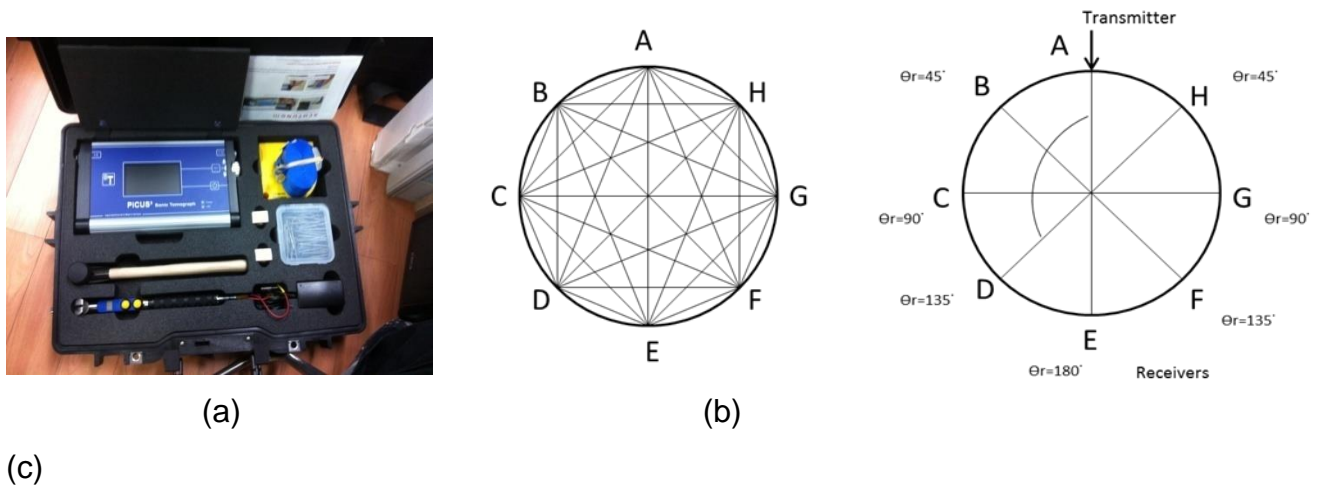


Fig.1 PiCUS Sonic Tomograph (a), wave paths passing through the cross-section (b), Experimental set up of transducers on the circumference with 8 transducers (c).

Table 1. Number of transducers and the angles between transducers for one disc

Number of transducers	Angles between transducers
8	45°, 90°, 135°, 180°
10	36°, 72°, 108°, 144°, 180°
12	30°, 60°, 90°, 120°, 150°, 180°

Index development for detecting heart rots. To study on the velocities of various transducers’ angle orientations, twenty five sound discs were tested. Five impacts were released at each transmitting sensor and the resulting Time-Of-Flight (TOF) were recorded and downloaded to a personal computer. The velocity was calculated for each

wave path by dividing the distance between a transmitter and a receiver by the travel time.

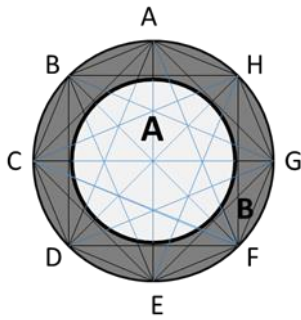


Table. 2 Grouping angles according to their wave

No. of transducers	B-angles	A-angles
8	45°, 90°	135°, 180°
10	36°, 72°	108°, 144°, 180°
12	30°, 60°, 90°	120°, 150°, 180°

Fig. 2. Grouping of angles and their stress wave paths in the cross-section for 8 transducers

When a stress wave was released from a transmitted transducer, it passed through the cross-section in various directions. Some wave paths were passing through the central or near the central part of the cross-section and the others were passing through the outer part as shown in “Fig. 2”. Heart rots usually form in the central part of cross-section. Therefore, the angles of wave paths between transducers were grouped into two, “A-angles” and “B-angles”. A-angles (inner zone) include angles larger than 100°, and B-angles (outer zone) include angles smaller than 100°. The A-angles represent the inner part of the cross-section and the B-angles represent the outer part of the cross-section. Since different experimental set ups were used with three different transducers numbers, “Table. 2” showed their A and B angles according to the number of transducers. Most of the stress wave paths at the smaller angles (B-angles) were closely orientated with the annual rings in tangential directions and most paths at the larger angles (A-angles) orientation with the annual rings were nearer to radial directions. In general, a stress wave travels faster in radial direction than in tangential direction. By comparing the average velocity of all A-angles and B-angles for each number of transducers (8, 10 and 12), the average difference velocity (A_{dv}) percentage could be calculated for each disc by “Equation (1)”.

$$A_{dv} = \frac{V_{b(avg)} - V_{a(avg)}}{V_{a(avg)}} \quad (1)$$

Where,

A_{dv} is the average difference velocity percentage between “B” and “A” angles for one disc

$V_{b(avg)}$ is the average velocity of all the “B” angles of the same disc

$V_{a(avg)}$ is the average velocity of all the “A” angles of the same disc

The rest ten sound discs and thirteen discs with heart rots were classified into two as sound discs and defective discs. Each disk was tested with the same experimental method, calculated the velocities for each angle and averaged. Each disk’s “A” angles and “B” angles’ velocities were calculated and averaged. Then, the A_{dv} was calculated for each transducer number by comparing average angles’ velocities of groups “B” and “A”

by using the “Equation (1)” for each disk. After the A_{dv} calculations for sound and defective discs, an index was established by calibrating on the A_{dv} values.

Results and Discussions

“Fig. 3” showed the measured mean velocities of the different transducers’ angles. The mean velocities at the smaller angles was slower than that at the larger angles as predicted because most of the stress wave paths at the smaller angles were closely orientated with the annual rings in tangential directions and most paths at the larger angles orientation with the annual rings were nearer to radial directions. The amount of velocity difference from 108° to 180° is quite small. However, the velocity decreases significantly starting from the angle 90° to 30° as shown in “Table. 3”.

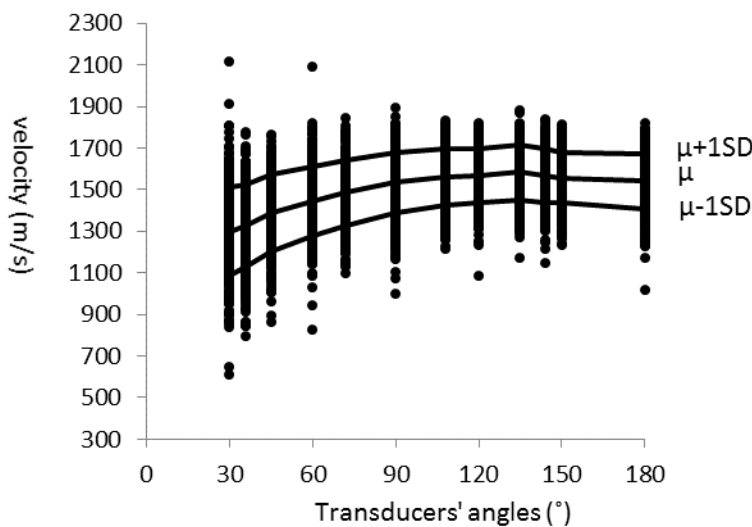


Fig.3. The reference velocity at different transducer angles of 25 sound discs

Table 3. Measured mean velocity of each transducer angle

velocity	Transducers' angles											
	30	36	45	60	72	90	108	120	135	144	150	180
mean	1299	1327	1389	1443	1485	1535	1562	1567	1583	1567	1557	1541
SD*	213	198	187	167	157	147	135	127	133	130	120	131
$\mu+1SD$	1512	1525	1576	1610	1642	1681	1698	1694	1716	1697	1678	1672
$\mu-1SD$	1086	1129	1202	1277	1327	1388	1427	1439	1450	1437	1437	1409
R**	-15.7%	-13.9%	-9.9%	-6.3%	-3.7%	-0.4%	1.4%	1.7%	2.7%	1.7%	1.1%	0.0%

SD* is the standard deviation

R** is the mean velocity difference over the mean velocity at 180°

The calculated A_{dv} for each 8, 10 and 12 transducers of 25 sound discs were shown in “Table. 4”. The mean A_{dv} was found at (-6.4%) for 8 transducers, (-9.7%) for 10 transducers and (-8.3%) for 12 transducers. Those results represented that the average

mean velocities of B-angles are (6.4%), (9.7%) and (8.3%) slower than those of A-angles with 8, 10 and 12 transducer numbers respectively. The mean A_{dv} among each transducer number was different because (a) the calculated A_{dv} was based on the number of transducers' angles and (b) inconsistency pattern of velocity change.

Table.4. Mean A_{dv} (%) and \pm SD of 25 sound discs

$A_{dv}(\%)$ for transducers			
$\mu \pm SD$	8	10	12
$\mu + 3SD$	-3.4	-6.7	-5.3
$\mu + 2SD$	-4.4	-7.7	-6.3
$\mu + 1SD$	-5.4	-8.7	-7.3
μ (%)	-6.4	-9.7	-8.3
$\mu - 1SD$	-7.4	-10.7	-9.3
$\mu - 2SD$	-8.4	-11.7	-10.3
$\mu - 3SD$	-9.4	-12.7	-11.3

In "Table. 5", the calculated A_{dv} for 10 sound and 11 defective discs were shown. The average A_{dv} of all sound discs was quite smaller than that of defective discs.

Table.5. Calculated A_{dv} for 10 sound discs and 11 defective discs with heart rots

Disc no	Sound discs A_{dv} (%)			Disc no	Defective discs A_{dv} (%)		
	No. of Transducers				No. of Transducers		
	8	10	12		8	10	12
S1	-8.2	-11.2	-9.3	D1	7.4	5.1	6.0
S2	-5.0	-8.3	-8.8	D2	-1.0	-3.7	-3.1
S3	-10.6	-10.7	-10.7	D3	-5.1	-8.2	-8.5
S4	-12.9	-16.3	-14.5	D4	-8.6	-9.5	-8.5
S5	-7.2	-9.1	-9.0	D5	0.5	-1.2	-1.1
S6	-10.4	-13.1	-11.8	D6	14.4	8.3	12.5
S7	-5.5	-7.1	-8.7	D7	-5.3	-4.8	-4.4
S8	-1.3	-3.6	-6.5	D8	-5.9	-7.4	-6.3
S9	-10.5	-11.9	-12.1	D9	1.2	0.0	1.6
S10	-6.8	-10.0	-9.6	D10	-2.8	-4.0	-2.5
				D11	-4.3	-4.6	-5.0
Average	-7.8	-10.1	-10.1		-0.9	-2.7	-1.8

By using the mean A_{dv} of 25 reference sound discs, 10 sound discs and 11 defective discs, the results showed that the best indices were found at (-5.4%) for 8 transducers, (-7.7%) for 10 transducers and (-8.3%) for 12 transducers as seen in "Table.6".

Table.6. The best indices for each transducer number with overall accuracy

no. of transducers	A_{dv} (%) index	Accuracy for		
		sound	defective	Overall
8	-5.4	81.8%	80.0%	81.0%
10	-7.7	81.8%	80.0%	81.0%
12	-8.3	81.8%	90.0%	85.7%

Conclusions

This study was carried out to investigate the accuracy of a model developed by the concept of velocity difference between “A” angles and “B” angles of the transducers. The followings were concluded from this study.

1. The velocity pattern change from “B” to “A” angles is one of the indicators to decide the presence of heart rot in Teak.
2. Indices were established for each different transducer number.
3. The accuracy was getting higher when the transducer numbers were increased.
4. The developed indices values can be used additionally as less complicated criteria to detect heart rots while using the stress wave CT devices.

References

1. Bae, M-S. (2003). A thesis of evaluation of deterioration for wooden structural members by nondestructive testing.
2. F. Divos, P. Divos (2006). Resolution of stress wave based acoustic Tomography, NDT. Net Vol. 11, No.4
3. F. Tallavo, G. Cascante, and M.D. Pandey (2012). A novel methodology for condition assessment of wood poles using ultrasonic testing, NDT&E international Vol.52, Pages 149-156
4. H.Zhang, X. Wang, R.J. Ross (2009). Stress wave propagation on standing trees- Part 1. In: Proceedings of the 16th nondestructive evaluation of wood symposium. P. 53-58
5. Oh, J-K. (1999). A thesis of Evaluation of biological deterioration in structural members of ancient wooden structures using stress wave method.
6. Win Myint (2011), An overview of Teak resources and plantations in Myanmar.
7. Wang, X., F. Divos, C. Pilon, B.K. Brashaw, R.J. Ross, and R.F. Pel-lerin. 2004. Assessment of decay in standing timber using stress wave timing nondestructive evaluation tools – A guide for use and interpretation. Gen. Tech. Rep. FPL – GTR–147. .S. Department of Agri-culture, Forest Service, Forest Products Laboratory, Madison, WI. 12
8. Wang, X., P. Carter, R.J. Ross, and B.K. Brashaw. 2007b. Acoustic assessment of wood quality of raw forest materials -A path to increased profitability. Forest Product Journal 57(5): 6-14.

9. Yamamoto, Koichi, Sulaiman, Othman, Hashim, Rokiah (1998). Nondestructive detection of heart rot in *Acacia mangium* trees in Malaysia, *Forest Products Journal*, Vol.48 Issue 3, p83.

Analysis of High Frequency Dielectric Curing of Phenol-Resorcinol Formaldehyde Resin used for Manufacturing Larch Glulam

*Sang-Yun Yang¹, Yeonjung Han¹, Jun-Ho Park¹, Yoon-Seong Chang¹,
Yonggun Park¹, JuHee Lee¹, Se-Jong Kim², Moon-Jae Park²,
Hwanmyeong YEO^{1, 3*}*

¹ Department of Forest Sciences, College of Agriculture & Life Sciences,
Seoul National University, Seoul, Korea

² Korea Forest research Institute, Seoul, Korea

³ Associate Professor, Research Institute of Agriculture and Life Sciences,
College of Agriculture & Life Sciences, Seoul National University, Seoul,
Korea

** Corresponding author*

hyeo@snu.ac.kr

Abstract

For reducing labor and time costs in glulam manufacturing, high frequency (HF) curing technique was analyzed in this study. Heat energy is internally generated by electromagnetic energy dissipation when HF wave passes through a dielectric material. Because both lamina and adhesives have dielectric property, internal heat would be generated when HF wave is applied to glulam. Most room temperature (such as phenol-resorcinol formaldehyde resin, PRF) and thermosetting adhesives which are commonly used for manufacturing glulam, can be cured faster as temperature of adhesives increase. In this study, dielectric properties of larch wood and PRF adhesives were experimentally evaluated, and the HF heating mechanism which leads the fast curing of glue layer in glulam, was theoretically analyzed.

Relative loss factor of PRF resin, which leads heating, was higher than that of larch wood in transversal direction. Also, it showed that density and specific heat of PRF, which are resistance factors of temperature increase, were greater than those of larch wood. These results were expected that the heat generation in PRF resin by HF heating would occur greater than that in larch wood. Through theoretical approach with the experimental results, the ISM band HF electric field strengths to achieve a target heating rate, which is set to increase temperature of glue line up to 80 °C within 10 minutes, were estimated.

Keywords: Dielectric property, High frequency heating, Glulam manufacturing, PRF resin.

Introduction

It is hard to secure large structural lumber because trees in stand practically have small diameter. As alternative, structural engineered wood products have been developed. Among the engineered wood products, glulam has great advantage because it can be manufactured in large member from small lamina (Kim et al. 2009, Kim et al. 2007, Lee et al. 2003).

To produce glulam, adhesives are spread between each side area of lamina. The adhesive layers between each side area of lamina should be pressured during curing process. Phenol-resorcinol formaldehyde (PRF) adhesive used in this study needs curing time more than 24 hours at room temperature (Shim et al. 2005). The long time for curing of adhesives in large pressing facility reduces the productivity of glulam. First of all, in order to solve the productivity problem, curing time of adhesives should be shorten.

In general, PRF can be cured fast in high temperature condition (Pizzi 2003). However, because PRF adhesive layers are located between lamina, the adhesive layers are hard to be heated fast by conductive or convective heat transfer. To heat adhesive layers effectively, high frequency wave (HF) could be hired. When HF is applied to dielectric material, heat is generated internally by dielectric loss. By taking HF dielectric heating which converts from electromagnetic energy to heat energy, the temperature of adhesion layer can be increased (Pereira et al. 2004).

The amount of heat generation per volume, which is defined by power density (PD) over thickness of specimen (d), would be correlated with electric field strength (E), frequency (f) and relative loss factor (ϵ'') as shown in Equation (1) (Zhou and Avramidis 1999).

$$\frac{PD}{d} = (5.56 \times 10^{-11}) E^2 f \epsilon'' \quad \text{Equation (1)}$$

PD	: Power density	(W/m ²)
d	: Thickness of specimen	(m)
E	: Electric field strength	(V/m)
f	: Frequency	(Hz)
ϵ''	: Relative loss factor	

The temperature increase rate with HF heating is correlated with density (ρ) and specific heat (C_p) as shown in Equation (2) (Zhou and Avramidis 1999)

$$\frac{\partial T}{\partial t} = \frac{PD/d}{\rho C_p} \quad \text{Equation (2)}$$

T	: Temperature	(°C)
t	: Time	(s)
ρ	: Density	(kg/m ³)

C_p : Specific heat (J/g °C)

By combining Equations (1) and (2) then using the equation, we could evaluate and/or predict the correlated properties of material to increase the temperature of adhesive layer to target temperature. In this study, we would like to develop the HF dielectric heating technique which could enhance productivity of glulam. The physical properties of components of glulam (lamina and PRF) were evaluated. In result, theoretical electric field strength to reach the target temperature and to shorten curing time was estimated.

Materials and Methods

Materials. Larch (*Larix kaempferi*) wood was prepared for this study. Larch is common species in Korea and widely used to manufacture glulam. As adhesives, PRF (Deernol-No. 40, Oshika Shinko) was used.

Density (ρ) measurement. The specimens for determining density was cut into a rectangular plate with dimensions of 150 X 150 X 20 mm. After humidifying the specimens to 10% moisture content (MC), lengths and weights of each specimen were measured. The density of PRF was measure by liquid substitution method.

Specific heat (C_p) measurement. To measure the specific heat, differential scanning calorimetry (DSC, Q200, TA Instruments) was employed. DSC scans temperature difference ratio and enthalpy difference simultaneously. When putting the data which were acquired from DSC into Equation (3), specific heat of specimens can be measured (Chae 2007, Skoog et al. 2006).

$$C_p = \frac{dH/dt}{dT/dt} \times \frac{1}{m} \quad \text{Equation (3)}$$

dH/dt : Enthalpy differences between air and specimen per second (J/s)

m : Mass of test specimen (g)

Dielectric properties (ϵ_r) measurement. Both wood and adhesives are composed of polar molecules. Also, they have low magnetic characteristic and high dielectric characteristics. To induce the correlation between dielectric characteristics and heat characteristics, HF dielectric behavior should be considered.

In general, Equation (4) is used to explain complex dielectric property (ϵ_r) of material quantitatively in alternative electric field. The equation is composed of relative dielectric constant (ϵ_r') and relative loss factor (ϵ_r'') (Agilent 2006).

$$\epsilon_r = \epsilon_r' - j\epsilon_r'' \quad \text{Equation (4)}$$

Impedance analyzer (E4491A, Agilent) and dielectric material test fixture (16453A, Agilent) were employed to measure relative dielectric constants of specimens. The dielectric properties of specimen put in electromagnetic field having frequency from 1MHz to 100MHz were evaluated.

The dielectric properties test specimens of larch was cut into a small rectangular plate with 3 mm thickness in transversal direction. Liquid PRF resin mixed with hardener (15 parts) was prepared. Because the dielectric material test fixture was for solid specimen, quartz glass containers was prepared. Liquid PRF resin was injected into quartz glass container which was mounted to dielectric material test fixture and complex dielectric properties of the PRF resin were measured

Result and Discussions

Density (ρ). Lamina for manufacturing glulam are recommended to be kiln-dried to 10% MC. The average density of larch specimens dried to 10% MC was 663.5 kg/m^3 . Because the PRFs which were hardened had irregular shapes, density of PRFs was determined by liquid substitution method. The density of PRF was 1043 kg/m^3 .

Specific heat (C_p). Figure 1 shows the result of specific heat of larch wood and PRF. The C_{ps} shown in Figure 1 were determined by Equation 3 and result of DSC. The specific heat of larch increased as its temperature increased. However, the specific heat of PRF increased as its temperature increased until 80°C then decreased with increase of temperature. The average specific heats of larch wood and PRF were $1.67 \text{ J/g}^\circ\text{C}$ and $2.08 \text{ J/g}^\circ\text{C}$

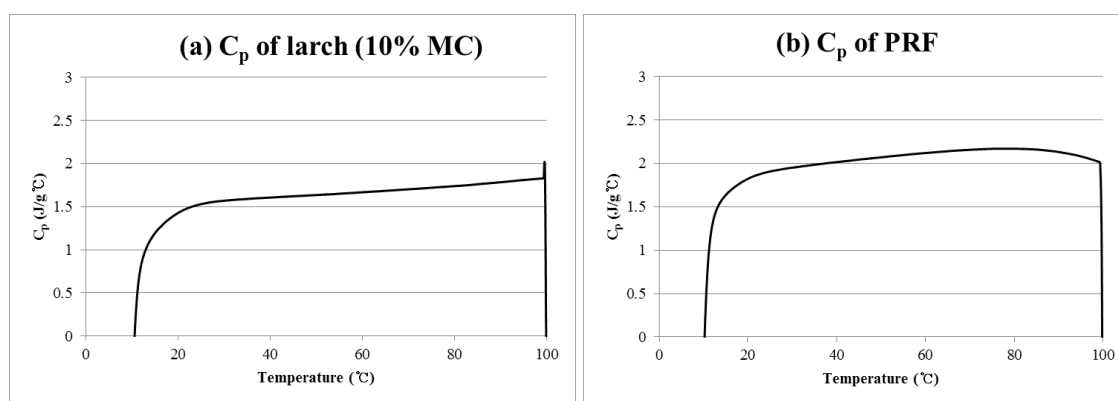


Figure 66 Specific heat of Larch wood and PRF resin determined by DSC: (a) C_p of larch wood, (b) C_p of PRF resin

Dielectric Properties (ϵ_r). The relative dielectric constants of larch and PRF were measured. Due to anisotropic characteristics of wood, relative dielectric constants of wood differ to wood direction. Generally, relative dielectric constant of longitudinal direction is the greatest and those of radial and tangential direction are similar to each

other. This result is correlated with geometric shape of cell in wood. In result, relative dielectric constants of each direction were measured.

As shown in Figure 2(a), relative dielectric constants of all directions of larch wood were decreased as HF frequency increased. The longitudinal relative dielectric constants were in the range from 4 to 5. The radial and tangential relative dielectric constants were similar to each other and those were ranged from 2.5 to 3.5.

As shown in Figure 2(b), relative loss factors of all directions of larch wood were increased as HF frequency increased. It is hard to analyze loss factors of specimens put in the HF field between 1MHz to 5MHz because there was large noise. The longitudinal relative loss factors were ranged from 0.2 to 0.4. The radial and tangential relative loss factors were similar to each other and were ranged from 0.1 to 0.2.

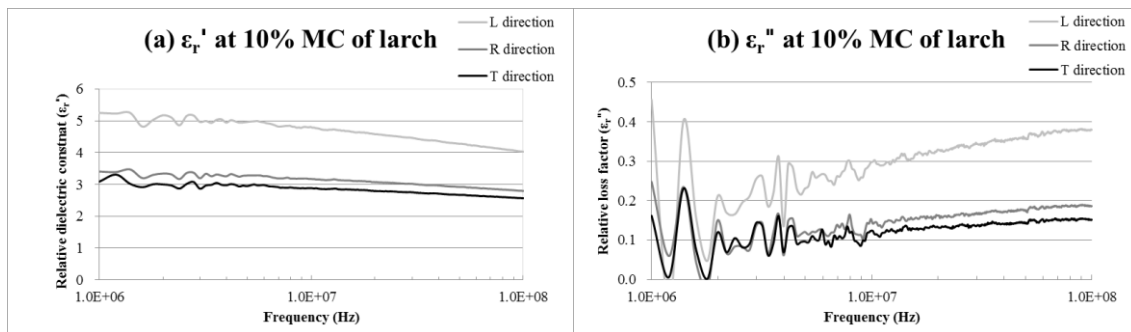


Figure 67 Relative dielectric constant (ϵ_r') and loss factor (ϵ_r'') of larch wood (a) ϵ_r' , (b) ϵ_r''

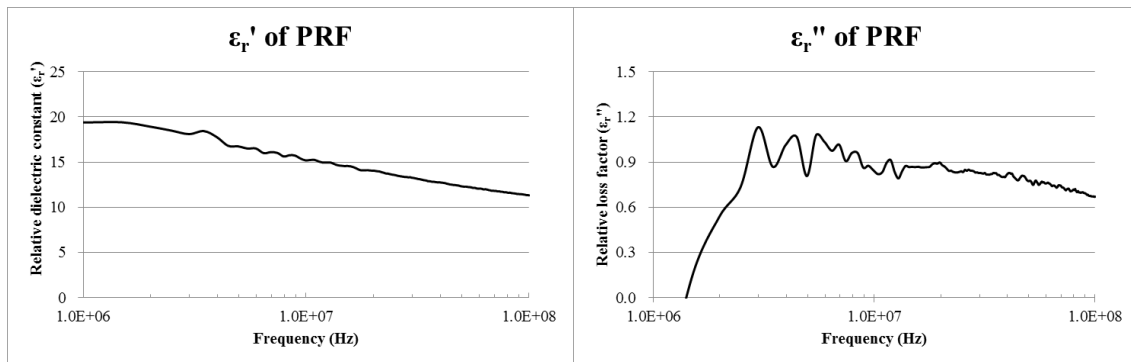


Figure 68 Relative Dielectric constant (ϵ_r') and loss factor (ϵ_r'') of PRF resin (a) ϵ_r' , (b) ϵ_r'' .

As shown in Figure 3, relative dielectric constant and loss factor of PRF were decreased as HF frequency increased. In test frequency, relative dielectric constant of PRF was ranged from 20 to 12 and relative loss factor was ranged from 1.2 to 0.9.

Analysis of time consumption for HF curing. With experimental results analyzed in this study, we would determine the electrical field strength to reach target curing temperature of PRF. For the use of radio frequency energy for industrial, scientific and medical purpose other than telecommunication, specified radio band was reserved and/or

assigned internationally as ISM band. Among the ISM bands in HF band, 13.56, 27.12 and 40.68MHz could be freely used for commercial purpose in HF band. Therefore, HF dielectric heating should be performed using these ISM bands.

In this study, we set a goal temperature of 80 °C to PRF layer curing. The heating condition that temperature increase up to the goal temperature within 10 minutes was assigned as good condition. In result, electric field strengths to achieve a goal condition were estimated.

$$E = \sqrt{\frac{1}{5.56 \times 10^{-11}} \times \frac{\partial T}{\partial t} \frac{\rho C_p}{f \epsilon_r}} \quad \text{Equation (5)}$$

By combining Equations (1) and (2), electric field strength to achieve a goal could be derived to Equation (5). When HF is applied to glulam, both lamina and PRF layer are heated. By inserting experimental data to Equation (5), we could find that temperature increment ratio of PRF layer is higher than that of larch lamina. Thus, temperature gradient between lamina and adhesive layer must be occurred. However, heat transfer caused by the temperature gradient was not considered in this study.

As shown in Table 1, electric field strength decreases as frequency increases. Although relative loss factor of PRF decreased as frequency increases, PD/d increases because frequency increase ratio is bigger than decrease ratio of relative loss factor of PRF.

Frequency (MHz)	Electric Field Strength (kV/m)
13.56	17.7
27.12	12.5
40.68	10.3

Table 21 Estimated electric field strength at each ISM band.

Conclusion

HF dielectric heating has great advantages to increase the temperature of adhesives layers which are located in glulam, indirectly. To perform HF dielectric heating and curing effectively, density, specific heat and relative loss factor of lamina and adhesives should be measured. We investigated HF dielectric heating performance of PRF resin in ISM bands without considering heat transfer to each other component. Consequently, it is expected that PRF layer could reach target temperature (80 °C) in 10 minutes at lower electric field strength as HF frequency increases. However, in this study, heat transfer occurred by temperature gradient between lamina and PRF layer was neglected.

This study is only based on theoretical heating analysis. Thus, the heat transfer mechanism in glulam should be considered in further study. It is expected that this study could be used as a database for dielectric heating facility design and frequency selection.

References

- Agilent Technologies, Inc. 2006. Application note : Basic of measuring the dielectric properties of materials. Agilent Technologies, Inc. USA. pp. 4-6.
- Chae, S. H. 2007. Specific Heat Measurements of Several Polymer Materials. DanKook University Master's Thesis. Korea pp. 26-27
- Kim, K. M., Shim, K. B., Park, J. S., Kim, W. S., Lim, J. A., and Yeo, H. 2007. Development of Pitch Pine Glued Laminated Timber for Structural Use -Improvement of Bending Capacity of Pitch Pine Glulam by Using Domestic Larch Lamina-. *Mokchae Konghak* 35(6): 13-22.
- Kim, K. M., Shim, S. R., Shim, K. B., Park, J. S., Kim, W. S., Kim, B. N., Yeo, H. 2009. Development of Structural Glued Laminated Timber with Domestic Cedar. *Mokchae Konghak* 37(3): 184-191.
- Lee, J. J., Kim, K. M., Han, J. S., Kim, J. K. 2003. Evaluation of the Bending Properties of Glulam with Different Cross-Section. *Mokchae Konghak* 31(5): 65-71.
- Pereira C, Blanchard C, Carvalho L, Costa C. 2004. High frequency heating of medium density fiberboard (MDF): theory and experiment. *Chem. Eng. Sci.* 59(4): 735-745.
- Pizzi A. 2003. *Handbook of Adhesive Technology* 2nd ed. Marcel Dekker Inc., New York.
- Shim, S. R., Yeo, H., Shim, K. B. 2005. Evaluation of Shear Bond Strength and Adhesive Bond Durability of Mixed Species Structural Glued Laminated Timber . *Mokchae Konghak* 33(1): 87-96.
- Skoog D, Holler J, Crouch S. 2006. *Principles of instrumental analysis* 6th ed. Saunders College Publishing, New York. pp. 575-577.
- Zhou B, Avramidis S. 1999. On the loss factor of wood during radio frequency heating. *Wood Sci. Tech.* 33(4): 299-310.

Analysis of Laminar Yield for Manufacturing Cross Laminated Timber

*Yeonjung Han¹ - Yoon-Seong Chang² - Sang-Yun Yang³ - Chul-Ki Kim⁴ -
Gi-Young Jeong⁵ - Jun-Jae Lee⁶ - Hwanmyeong Yeo^{7*}*

¹ Graduate Research Assistant
jack2001@snu.ac.kr

² Graduate Research Assistant
jang646@snu.ac.kr

³ Graduate Research Assistant
sly1357@snu.ac.kr

⁴ Graduate Research Assistant
aries05@snu.ac.kr

⁵ Assistant Professor, College of Agriculture and Life Sciences, Chunnam
National University, Gwangju, Korea
gjeong1@.ac.kr

⁶ Professor, College of Agriculture and Life Sciences, Seoul National
University, Seoul, Korea
junjae@snu.ac.kr

⁷ Associate Professor, College of Agriculture and Life Sciences, Seoul
National University, Seoul, Korea
hyeo@snu.ac.kr

** Corresponding author*

Abstract

The objective of this study was to evaluate the production yield for manufacturing of cross laminated timber (CLT) using domestic larch (*Larix kaempferi*) wood. Each yield of lumbering, planning, cross cutting and finishing was 42.4%, 66.0%, 96.3%, and 85.5%, respectively. The final production yield for manufacturing CLT was 23.2%. In order to analyze the effect of the size reduction of lumbering on the final production yield of CLT, the geometric model was presented to predict the lumbering yield and the number of lamina. The experimental apparatus for control of drying deformation was manufactured to reduce the size of lumbering. Using the experimental apparatus during kiln-drying, cup

and twist were reduced 50% and 90%, respectively. If the width and thickness of 5 mm at each decreased, the production yield for manufacturing of CLT can be increased from 23.2% to 27.6%.

Keywords: Laminar yield, Cross laminated timber, Distortion, Conventional drying.

Introduction

Cross laminated timber (CLT) has been developed and used in Europe, North America, and Japan since the early 2000s. It is engineered lumber which has advantage in construction of high-rise wooden building. Recently, global climate change is making issue of carbon emission. Because carbon emission reduction of wooden building is better than concrete building, Korea has interest in wooden building and materials of wooden building. To activate the wooden building industry, CLT manufactured using domestic tree is required. CLT is the one of the best ways to use domestic wood resources as a value-added product and expand wood frame building for various purposes. However, there is no study on CLT using domestic trees. The objective of this study was to evaluate the production yield for manufacturing of CLT using domestic larch (*Larix kaempferi*) wood. The experimental apparatus for control of drying deformation was manufactured to reduce the size of lumbering. And it was analyzed that change in production yield for manufacturing of CLT by reduction of lumbering dimension.

Materials and Methods

Production yield for CLT. The larch wood used for manufacturing CLT was harvested at Yeongdong-gun, Chuncheongbuk-do. The harvested larch logs were cut into 2.7 m length. With end diameters of 150 mm or more, 87 logs were used for evaluation of the production yield of CLT. The volume of the logs was calculated according to KS F 2163. The below equation was used for calculating the volume of logs.

$$V = D^2 \cdot L \cdot 10^{-6} \quad (1)$$

where, V = volume of log (m^3); D = (small) end diameter of log (mm); L = length of log (m)

The volume of larch wood which was used in this study was 8.85 m^3 . The logs were cut for lamina of CLT ($125 \text{ mm} \times 40 \text{ mm} \times 2.7 \text{ m}$) and louver ($120 \text{ mm} \times 15 \text{ mm} \times 2.7 \text{ m}$). 287 laminas were manufactured from lumbering and were dried with T10-C4 klin-drying schedule. The initial moisture content of laminas were from 40 to 110 %. Oven-dried specific gravity was $0.476 (\pm 0.021)$. The cup, bow, crook, and twist were measured after drying to analyze the relationship between distortion and lumbering yield.

Control of distortion during drying. The drying distortions like cup, bow, crook, and twist must be controlled to use for lamina of CLT. The experimental apparatus to improve the lumbering and planing yield for control of distortion during drying (Fig. 1). It was designed for putting a certain pressure to wood using a spring even if thickness of lamina was reduced.

Estimation of lumbering yield and the number of lamina. The lumbering yield and the number of lamina were estimated by change of small end diameter using geometrical model. In this study, larch wood was cut like in Fig. 2. The laminas of white part in Fig. 2 were cut first, and grey part were cut later. When the end diameter, thickness and width of lamina are Φ , x and y , respectively, the numbers of laminas of white part and grey part were a and b , respectively. a and b were calculated as the following equations.

$$a^2(x+2.5)^2 + y^2 \leq \Phi^2 \quad (2)$$

$$a \leq \frac{\sqrt{\Phi^2 - y^2}}{\sqrt{(x+2.5)^2}} \quad (3)$$

$$b(x+2.5) \leq \frac{\Phi}{2} - \frac{y}{2} - r \quad (4)$$

$$r = \frac{\Phi}{2} - \sqrt{\left(\frac{\Phi}{2}\right)^2 - \left(\frac{y}{2}\right)^2} \quad (5)$$

$$b \leq \frac{\Phi/2 - y/2 - r}{x+2.5} \quad (6)$$

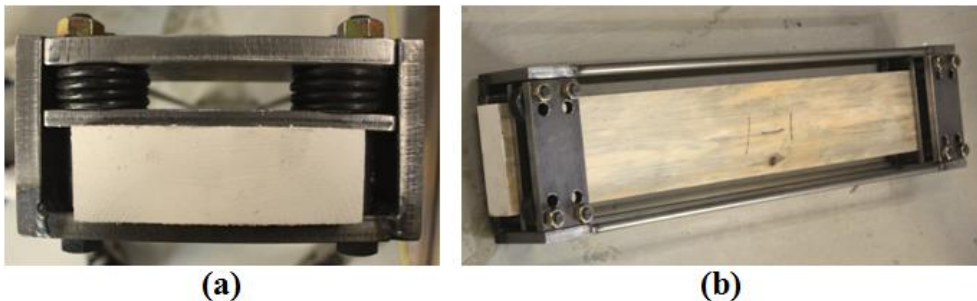


Figure 1. Experimental apparatus for control of cup (a) and twist (b)

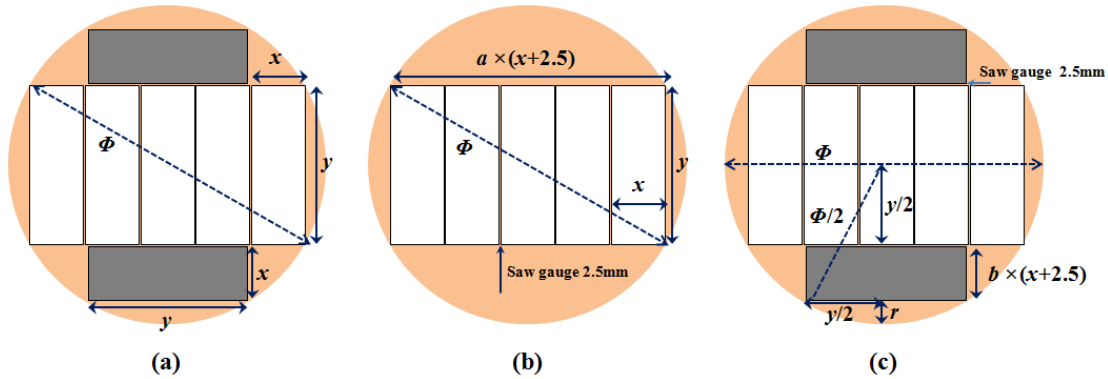


Figure 2. Geometric model for prediction of the lumbering yield and the number of lamina

Using above equations, the total number of laminas was defined as $a + 2b$.

Results and discussion

Production yield for CLT. The lumbering, planing, cross cutting, finishing yields for manufacturing CLT were presented in Table 1. The lumbering, planing, cross cutting, finishing yields were 42.4 %, 66.0 %, 96.3 %, and 86.2 %, respectively. The cumulative yield was 23.2 %, which means 76.8 % of volume of log was not used for manufacturing CLT.

Table 1. Measured production yield for CLT

Classification	Log	Lumbering (125×40×2.7)	Planing (110×30×2.7)	Cross cutting (110×30×2.6)	Finishing plane (110×30×2.4)
Volume (m ³)	8.85	3.75	2.95	2.39	2.05
Process yield (%)	100	42.4	66.0	96.3	86.2
Cumulative yield (%)	100	42.4	28.0	27.0	23.2

Analysis of reduction by control of distortion during drying. Without using the experimental apparatus for control of distortion, cup, bow, crook, and twist were 2.55 mm, 1.44 mm, 1.55 mm, and 11.91 mm, respectively. Using the experimental apparatus, cup was decreased from 2.55 mm to 0.9 mm and reduced more than 50 %, and twist decreased from 11.91 mm to 1.0 mm and reduced more than 90 % (Fig. 3). If this apparatus is applied in wood industry, lumbering dimension of lamina to produce the final dimension of 110 mm × 30 mm × 2.7 m can be reduced from 125 mm × 40 mm × 2.7 m to 120 mm × 35 mm × 2.7 m

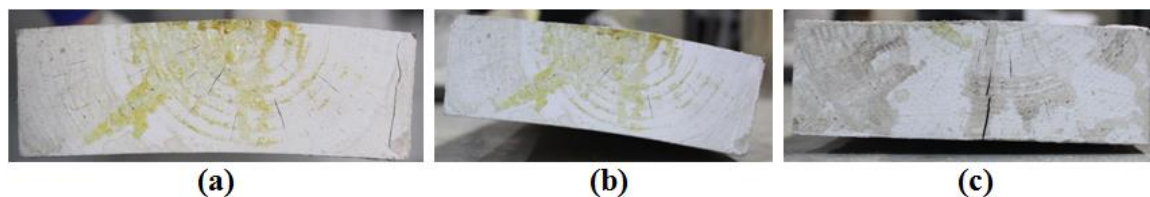


Figure 3. Cup (a) and twist (b) after kiln-drying, and drying distortion using experimental apparatus during drying

Change of production yield of CLT according to the reduction of lumbering

dimension. The measured value of lumbering yield and the number of lamina by small diameter of log was represented in Table 2. From 8.85 m³ larch wood, the lumbering yields of lamina for CLT and louver were 42.4 % (278 of laminas) and 6.2 %, respectively. The lumbering yield was increased with increasing the end diameter of log. When lumbering dimension is 125 mm × 40 mm × 2.7 m, lumbering yield, 58.3 %, was most large at 245 mm of small end diameter. It means that proper small end diameter can be changed by lumbering dimension.

When lumbering dimension is 120 mm × 35 mm × 2.7 m, the estimated values of number of lamina determined by eq. (2) and (5) were represented in Table 3. The number of produced lamina increased 20 % more because of with decrease of lumbering dimension. The change of production yield of manufactured CLT with decreased dimension lumber was represented in Table 4. The lumbering yield was same even though the lumbering dimension decreasing. However, the cumulative yield increased 4.4 % as the planing yield increased from 66.0 % to 78.6 %.

Table 2. Measured value of lumbering yield and the number of lamina by small end diameter of log

Φ (mm)	150	160	170	180	190	200	210	220	230	240	250	260	270	280	290	300	Total
Number of log	9	16	5	7	7	7	1	4	6	3	3	4	1	0	3	2	78
Average number of main product	1.9	1.8	2.2	3.0	3.0	3.0	3.0	4.0	5.0	6.3	5.7	7.0	6.0		7.7	9.0	278
Yield of main product (%)	406	339	395	410	396	365	340	409	465	533	453	513	412		456	500	42.4
Total yield (%)	473	441	434	472	467	496	458	488	551	573	527	525	483		544	572	50.5

Table 3. Calculated value of number of lamina (120 mm × 35 mm × 2.7 m) by small end diameter of log

Φ (mm)	150	160	170	180	190	200	210	220	230	240	250	260	270	280	290	300	Total
Number of log	9	16	5	7	7	7	1	4	6	3	3	4	1	0	3	2	78
Predicted value	2	2	3	3	3	4	6	6	6	7	7	7	8		10	11	303

Table 4. Change of production yield by reduction of lumbering dimension

Classification	Log	Lumbering (120×35×2.7)	Planing (110×30×2.7)	Cross cutting (110×30×2.6)	Finishing plane (110×30×2.4)
Volume (m ³)	8.85	3.75	2.95	2.84	2.45
Process yield (%)	100	42.4	78.6	96.3	86.2
Cumulative yield (%)	100	42.4	33.3	32.1	27.6

Half-Life and Carbon Stock of Harvested Wood Products (HWP) produced by domestic tree in Korea

*Yoon-Seong Chang¹ – Jun-Ho Park² – Whi-Lim Son³ – Joo-Saeng Park⁴ –
Moon-Jae Park⁵ – Hwanmyeong Yeo^{6*}*

^{1,2} Graduate Research Assistant, Dept. of Forest Science, College of Agriculture, Seoul National University, Seoul, South Korea.

[*Jang646@snu.ac.kr*](mailto:Jang646@snu.ac.kr)

³ Researcher, Div. Wood Engineering, Dept. of Forest Products, Korea Forest Research Institute, Seoul, South Korea.

⁴ Research Scientist, Div. Wood Engineering, Dept. of Forest Products, Korea Forest Research Institute, Seoul, South Korea.

⁵ Senior Research Scientist, Div. Wood Engineering, Dept. of Forest Products, Korea Forest Research Institute, Seoul, South Korea.

⁶ Associate Professor, Research Institute of Agriculture and Life Sciences, Dept. of Forest Science, College of Agriculture, Seoul National University, Seoul, South Korea.

** Corresponding author*

[*hyeo@snu.ac.kr*](mailto:hyeo@snu.ac.kr)

Abstract

Global warming is one of the most concerning environmental problems that the whole world has to face. Forests could play an important role in stabilizing global warming as potentially they could reduce a significant amount of carbon dioxide from the atmosphere over the decades to come. After harvesting, because the wood stores carbon for a long period of time, the carbon, until burned or decomposed played a role as components in harvested wood products (HWP), such as wooden buildings and furniture. In order to account for the carbon amounts in HWP, it is necessary to determine the lifespan of the HWP. The time, that carbon can be stored in wood products, can be expressed as the 'half-life', which is the time required for half of the carbon in a wood product to be transformed or eliminated by normal use. The proportion of carbon remaining in different wood product pools depends on their half-lives. Hence, it is difficult to estimate of half-lives of various products accurately. In this study, other countries' methods and conditions for determining the half-life of HWP were investigated. With statistics related to the carbon flow and the type of carbon stocks in domestic HWP, the half-life of HWP in Korea was estimated. The results of this study show that HWP is an important type of carbon storage that should be considered in decisions associated with climate change adaptation and mitigation in Korea.

Keywords: Harvested Wood Products, Half-life, Carbon Storage, Material Flow, Climate change

Introduction

Harvested wood products (HWP) are known as products from the tree such as structural lumber, wooden building and paper. After harvesting, carbon emissions into the air are delayed because almost all of the carbon from forests remains fixed in the HWP. However, recently, a lot of concerns have been focused on carbon accounting for evaluating the eco-friendly value of the harvested wood products and putting the value into national greenhouse gas inventories. The maximization of carbon storage can be achieved only if the use of wood from forests is achieved with replanting and regeneration that exceeds the amounts leaving forests (Perez-Garcia et al. 2005, Hennigar et al. 2008). Also, wood used as structural and interior materials are intended to replace plastic and iron so as to mitigate climate change (Knight et al. 2005, Mahalle and Connor 2009, Lippke et al. 2010).

After the carbon accounting approach for HWP in the IPCC 1996 guidelines was presented, opinions on the carbon storage effect of HWP have continually been raised (Winjum et al. 1998, Lim et al. 1999, Bowyer et al. 2010). Recently, in 17th UN Framework Convention on Climate Change Conference of the Parties (COP) held in Durban, it comes to an agreement that target for accounting domestic carbon amount is only HWP manufactured with domestic harvested tree.

As a result, a quantitative evaluation of the carbon storage effect of domestic HWP is required. Recently, as a factor required for the accounting of carbon in domestic HWP, the half-life of HWP, indicating the carbon emission, has been investigated. In this study, examples of the methods and conditions of other countries for determining the half-life of HWP are analyzed.

Materials and Methods

According to methods pertaining to carbon stocks of HWP, as presented in the 2006 IPCC (Intergovernmental Panel on Climate Change) Guidelines, accounted should be done based on the FAO forest product statistics and IPCC default values if the related country-specific data is not available (Tier 1). However, if there are statistics and associated variable values pertaining to country-specific forest products (Tier 2), and if further accurate estimations that feasibly match the conditions of the country (Tier 3) exist, those are also applied to the methodology (IPCC 2006).

Wooden buildings are a source of HWP, serving as a large and long-term form of carbon storage. Wooden buildings have been considered in attempts to reflect greenhouse gas inventories in countries in North America and Europe and in Japan. The literature on

accounting for carbon in wooden building in foreign countries and the each country's half-life of HWP for determining carbon stocks were investigated for the purposes of this study.

Results

USA. In the United States, most low-rise buildings are built out of wood products. The half-life of sawn wood, mainly used as structural timber, is 40 years. The half-life of structural panels is 45 years and that of non-structural panels is 23 years. The actual half-lives of wooden buildings were determined by investigating how many wooden buildings built in the past year remained in the survey year (Skog and Nicholson 1998).

Table 1 Assumed duration of carbon sequestration in end uses of wood products and wooden building (Skog and Nicholson 1998)

Product	Half-life(years)
Single-family homes (pre-1980)	80
Single-family homes (post-1980)	100
Multi-family homes	70
Mobile homes	20
Nonresidential construction	67
Sawn wood	40
Structural panels	45
Non Structural panels	23

Europe. It is typical in Finland to construct wooden buildings. The statistics pertaining to wooden building stock include information on floor areas in different buildings, which are divided into eight categories (detached houses, attached houses, blocks of flats, free-time buildings, commercial and public buildings, industry buildings and warehouses, agricultural and related buildings, and buildings with no permits). The building stock in the statistics is updated every five years. A reasonable fit to the inventory-based data from calculating the wooden building carbon stock was achieved with a time constant of 39 years (Pingoud et al. 2001).

Other European countries also published the half-lives of HWP as accounted for in industrial statistics pertaining to wood construction and related products (Kloehn and Ciccicarese 2009).

Table 2 Half-lives of different wood products, Construction Sector (Kloehn and Ciccicarese 2009)

Product	Half- life(years)	Country
Construction	60	Germany
Construction	80	UK
Construction wood	30	Netherlands
Building sector	30-50	France
Construction material	80	Norway

Construction	75	Germany
Buildings and other long-life construction work	50	Europe
Construction	35	Italy

Japan. Japanese policy has encouraged the use of domestic wood products in the construction sector and the expansion of the role of HWP as a form of carbon storage. The typical amount of HWP input into the construction sector each year was calculated using national production statistics. It was applied to calculate the ratio of HWP made of domestic wood, excluding pulp and wood chips. The wood density (sawn wood 0.45; wood panel 0.628) and carbon composition (sawn wood 0.5; wood panel 0.468) were determined using the IPCC default values. The half-life of a wooden building was determined to be at 35 years, while that of non-wooden buildings was set to 30 years (Tsunetsugu and Tonosaki 2010).

Korea. For the determination of the carbon stocks of domestic HWP, studies were performed in Korea (Choi and Kang 2007, Choi et al. 2010) using FAO statistics and national statistics. However, the IPCC default values were used because there were no country-specific factors. To solve the problem, a method for determining the half-life of domestic HWP was proposed. As the half-life of the final HWP (e.g., structural lumber and interior material) was assumed with foreign data, these values were multiplied by the proportion of domestic semi-final HWP making up all domestic semi-final products. In addition, estimates of each half-life value for semi-final HWP types (e.g., sawn wood, plywood) were obtained.

Table 3 Half-life of HWP by mass flow of wood industry in Korea

Semi-final products(SP)	Final products(FP)	Ratio (%)	Half-Life (HL) of FP	Conversion (Ratio × HL of FP)	Total (=HL of SP)
Sawn wood	Structural lumber	44	50	22	24
	Furnishing and interior materials	10	16	1.6	
	Structural support materials and Etc.	46	1	0.4	
Plywood	Interior materials	93.9	16	15	15.1
	Structural support materials	6.1	1	0.1	
Particle board	Interior materials	2.9	16	0.5	16
	Furnishing	97.1	16	15.5	
MDF	Interior materials and flooring	38.6	16	6.2	15.2
	Furnishing	55.8	16	8.9	
	Etc.	5.6	1	0.1	

The half-life of the final HWP value was assumed using EFI data (Egger 2002), while the component ratio of wood in the final primary wood determination was calculated by means of a ‘wood utilization actual condition survey’ (Korea Forest Service 2011). It was determined that the half-life of sawn wood is 24 years, that of plywood is 15.1 years, that of particle board is 16 years and that of MDF is 15.2 years.

Conclusion

Wood, as a renewable natural resource, can significantly reduce greenhouse gas emissions when used as a long-term product. In particular, the industrial production of wood products requires less consumption of fossil energy than the production of competing materials such as steel and concrete. It is possible to maximize the mitigating effect. Because there are no reliable statistics on the number of wooden buildings removed or on wooden building construction permits and areas, it is difficult to derive the half-life of HWP from national statistics at present. It is necessary to collect more appropriate national and industrial statistical data for determining the half-life of HWP.

Acknowledgments

This study was carried out with the support of Forest Science & Technology Projects.

References

- Bowyer, J., Bratkovich, S., Howe, J., Fernholz, K. 2010. Recognition of carbon storage in harvested wood products: A post-Copenhagen update. USA. Dovetail Partners Inc.
- Choi, S.I., Kang, H. M. 2007. The changes in carbon stocks and emissions assessment of harvested wood products in Korea. *Journal of Korean Forest Society* 96(6): 644-651.
- Choi, S.I., Joo, R. W., Lee, S. M. 2010. An estimation of the carbon stocks in harvested wood products: accounting approaches and implications for Korea. *Mokchae Konghak* 38(6): 507-571.
- Eggers, T. 2002. The impacts of manufacturing and utilisation of wood products on the european carbon budget. European Forest Institute Internal Report 9. Europe, European Forest Institute.
- Hennigar, C.R., MacLean, D.A., Amos-Binks, L.J. 2008. A novel approach to optimize management strategies for carbon stored in both forests and wood products. *Forest Ecology and Management* 256: 786-797.
- IPCC. 2006. Guidelines for National Greenhouse Gas Inventories. Switzerland. IPCC.
- Kloehn, S., Ciccacese, L. 2009. Applying the IPCC GPG for LULUCF approaches for assessing changes in carbon stocks and emissions of green-house gas for Harvested Wood Products in Italy. Italy. Italian Ministry for Environment and Territory and Sea report.
- Knight, L., Huff, M., Stockhausen, J.I., Ross, R.J. 2005. Comparing energy use and environmental emissions of reinforced wood doors and steel doors. *Forest Product. Journal* 55(6): 48-52.
- Korea Forest Service. 2011. Wood utilization actual condition survey. Korea, Korea Forest Service..
- Lim, B., Brown, S., Schlamadinger, B. 1999. Carbon accounting for forest harvesting and wood products: a review and evaluation of possible approaches. *Environmental Science and Policy* 2: 207-216.

- Lippke, B., Wilson, J., Meil, J., Taylor, A. 2010. Characterizing the Importance of Carbon Stored in Wood Products. *Wood and Fiber Science* 42: 5-14.
- Mahalle, L., Connor, J.O. 2009. Life cycle assessment of western red cedar siding, decking, and alternative products. Canada, FPInnovations..
- Perez-Garcia, J., Lippke, B., Connick, J., Manriquez, C. 2005. An Assessment of carbon pools, storage and wood products market substitution using life-cycle analysis results. *Wood and Fiber Science* 37: 140-148.
- Pingoud, K., Perala, A.L., Pussinen, A. 2001. Carbon dynamics in wood products. *Mitigation and Adaptation Strategies for Global Change* 6: 91-111.
- Skog, K., Nicholson, G.A. 1998. Carbon cycling through wood products: The role of wood and paper products in carbon sequestration. *Forest Product Journal* 48(7): 75-83.
- Tsunetsugu, Y., Tonosaki, M. 2010. Quantitative estimation of carbon removal effects due to wood utilization up to 2050 in Japan: effects from carbon storage and substitution of fossil fuels by harvested wood products. *Journal of Wood Science* 56: 339-344.
- Winjum, J.K., Brown, S., Schlamadinger, B. 1998. Forest harvests and wood products: sources and sinks of atmospheric carbon dioxide. *Forest Science* 44: 272-284.

Wood Quality of Black Walnut Grown in Reclaimed Surface Mine in the Czech Republic

Ales Zeidler^{1} – Vlastimil Boruvka² - Guillermo Garcia Mayoral³*

¹ Associate Professor, Department of Wood Processing, Faculty of Forestry and Wood Sciences, Czech university of Life sciences Prague, Prague, Czech Republic.

* *Corresponding author*

zeidler@fld.czu.cz

² Assistant professor, Department of Wood Processing, Faculty of Forestry and Wood Sciences, Czech university of Life sciences Prague, Prague, Czech Republic.

³ Student, Universidad Politecnica de Madrid, Madrid, Spain.

Abstract

We tested in this study wood quality of black walnut (*Juglans nigra* L.), an American native species, grown in former surface brown coal mine in the Czech Republic. From physical properties wood density and shrinkage were evaluated, from mechanical properties compression strength was tested. Wood density was 578 kg.m⁻³, tangential, radial and volumetric shrinkage was 9.6 %, 5.7 % and 16.2 % respectively, and compression strength was 68.6 MPa. Wood quality is inferior when compared to the native Persian walnut (*Juglans regia* L.). Wood density and shrinkage was also lower compared to that obtained in native areas. Compression strength was higher by contrast. No trend was found for horizontal variability for the tested properties. Compression strength was very little influenced by wood density.

Keywords: Black walnut, Wood, Properties, Density, Shrinkage, Compression strength

Introduction

Northwestern part of the Czech Republic is an industrial area with lots of surface brown coal mines. Lots of them were closed in the second half of the last century and underwent vast and expensive reclamation. This gave rise to an exceptional location, basically artificially created by man. Such sites were mostly afforested with a wide range of species, both native and introduced. Reclaimed dumps unique are absolutely unique habitats, actually huge open air laboratory, allowing to test special silviculture practices and especially to test wood quality and potential to wood processing industry of species that are not indigenous to Europe. One of the species used for afforestation was black walnut.

Black walnut (*Juglans nigra* L.), also called American walnut, is a species native to the central and eastern parts of the United States. Black walnut trees on good sites may reach 30 to 37 m in height and 76 to 102 cm in d.b.h. (Burns and Honkala 1990). Apart from wood the nuts of black walnut are used for many purposes. The sapwood of black walnut is whitish, while the heartwood is light brown to chocolate brown, often with darker streaks. The wood is heavy, hard, and stiff and has high shock resistance. Density for 12% MC is 609 kg.m⁻³, compression strength is 52 MPa, tangential, radial and volumetric shrinkage is 7.8 %, 5.5 % and 12.8 % respectively. Black walnut is easily worked with hand tools and by machine. It finishes beautifully and holds paint well. It also glues and polishes well. It is rated as very resistant to heartwood decay. Wood is used primarily for veneer, also for furniture and interior paneling (Alden 1995).

This paper presents preliminary results of vast study focused on wood quality of various tree species grown in reclaimed surface mines in the Czech Republic. In this case wood quality of black walnut was evaluated. We tested wood density, shrinkage and compression strength, and their radial variability within a stem. Correlation between wood density and compression strength was also assessed.

Materials and Methods

Materials. The testing material used in this study comes from reclaimed surface mine called Uzin, occupying about 82 ha, north-east to Chabarovice town in Usti region, north-western part of the Czech Republic. Sample trees were about 45 years old, the average height of the trees was 16 meters and diameter ranged from 23 to 25 cm. The basal section, representing the most valuable part of a stem, was taken from each sample tree. Central board was cut from these sections and used for preparation of testing samples (Fig. 1).

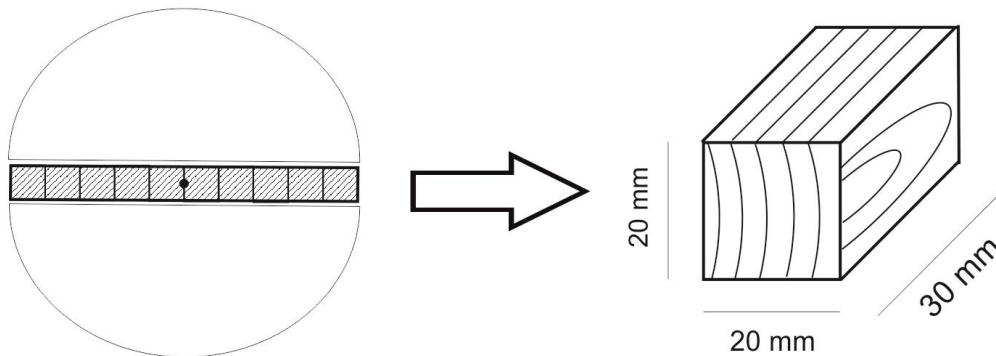


Figure 1 – Sampling of sections

Methods. Wood density, tangential, radial and volumetric shrinkage and compression strength parallel to the grains were tested following Czech standards. Testing samples 20 x 20 x 30 mm were used for all the tests (Fig. 1). Totally 930 samples were used for evaluation of the properties. Wood density and compression strength were set for 12% moisture content.

Results

The results of the tested physical and mechanical of black walnut are given in Table 1. Wood density of 578 kg.m⁻³ is higher than Praus et al. (2004) reported for South Moravia region (535 kg.m⁻³) in Central Europe, but it is little bit lower compared to 609 kg.m⁻³ mentioned by Alden (1995) for native areas or even low compared to value 640 kg.m⁻³ given by Wagenführ (2007). The value is quite low when contrasted to the native Persian walnut 670 kg.m⁻³ (Lexa et al. 1952). The tested wood featured higher values of shrinkage, except for radial shrinkage, when compared to wood from native areas (Tab. 2). The values are also higher contrasted to wood of the native species of walnut (Tab. 3). By contrast compression strength was quite high. It exceeded the value of 52.2 MPa (Alden 1995) from native areas and also value 55,1 MPa reported by Praus et al. (2004) or 54,0 MPa given by Požgaj et al. (1997) for Middle Europe. It is nearly as high as 72 MPa of native Persian walnut (Wagenführ 2007).

Table 1 – Physical and mechanical properties of black walnut grown in the Czech sites

		Mean ± SD	Max	Min	CV (%)
Density	kg.m ⁻³	578 ± 37	673	488	6.4
Shrinkage tangential	%	9.6 ± 1.4	14.0	5.7	14.2
Shrinkage radial	%	5.7 ± 1.0	9,0	3.3	18.1
Shrinkage volumetric	%	16.2 ± 2.3	23.9	10.7	13.9
Compression strength	MPa	68.6 ± 7.1	80.4	42.5	10.4

Based on wood density black walnut can be likened to native commercial species as black alder (*Alnus glutinosa*). It ranks with its volumetric shrinkage among timbers with high shrinkage as native basswood or European beech (*Fagus sylvatica*). On the contrary compression strength outperformed most of the commercial species, even with considerably higher density.

Table 2 – Shrinkage, comparison with native areas

	this study	Glass and Zelinka (2010)
Shrinkage tangential (%)	9.6	7.8
Shrinkage radial (%)	5.7	5.5
Shrinkage volumetric (%)	16.2	12.8

*Table 3 – Comparison of the results with native Persian walnut (*Juglans regia*)*

	Density (kg.m ⁻³)	Shrinkage tangential (%)	Shrinkage radial (%)	Shrinkage volumetric (%)	Compression strength (MPa)
Black walnut	578	9.6	5.7	16.2	68.6
Persian walnut (Wagenführ 2007)	680	7.8	5.5	12.8	72

When horizontal variability of the tested properties in a stem is a concern, the lowest values were obtained in all cases at the position close to the bark (Fig. 2). Although Praus et al. (2004), Boyce et al. (1970) and Panshin and De Zeeuw (1980) mentioned decreasing density from the stem center toward the circumference for black walnut, no other statistically significant pattern of distribution of the properties in radial direction was confirmed. Compression strength turned out to be very little correlated to wood density, although it was statistically significant, as the coefficient of determination was only 0.0164.

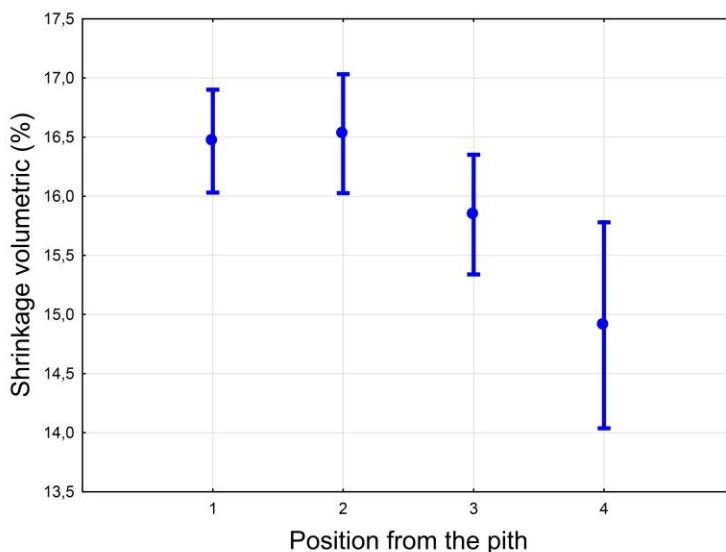


Figure 2 – Radial variability of volumetric shrinkage in black walnut (ANOVA results)

Conclusions

Reforested former surface brown coal mines are quite unique sites in the Czech Republic. Quality of timber coming from those sites is unknown at present. We tested basic physical and mechanical wood properties of black walnut grown in the reclaimed coal mine. Except for compression strength the properties were lower when compared to wood from native areas. Black walnut didn't achieve quality of Czech native walnut. No trend was found in horizontal variability of the tested properties. The impact of wood density on compression strength is low in black walnut.

References

- Alden, H. A. 1995. *Hardwoods of North America*. Madison, WI: U.S.D.A., Forest Service, Forest Products Laboratory. 136 pp.
- Boyce, S. G., Kaeiser, M., Bey, C. F. 1970. Variations of some wood features in five black walnut trees. *Forest Science*. 16(1): 95–100.
- Burns, R. M., Honkala, B. H. 1990. *Silvics of North America, Volume 2. Hardwoods* Washington DC: U.S.D.A. Forest Service Agriculture Handbook 654.
- ČSN 49 0101 1980. Wood. General requirements for physical and mechanical tests. (in Czech)
- ČSN 49 0103 1979. Wood. Moisture content determination for physical and mechanical tests. (in Czech)
- ČSN 49 0108 1993. Wood. Determination of density. (in Czech)
- ČSN 49 0110 1977. Wood. Determination of compression strength parallel to the grains. (in Czech)
- ČSN 49 0128 1989. Shrinkage determination. (in Czech)
- Glass, S. V. Zelinka, S. L. 2010. Moisture Relations and Physical Properties of Wood. In: *Wood handbook - Wood as an engineering material*. General Technical Report FPL-GTR-190. Madison, WI: U.S. Department of Agriculture, Forest Service, Forest Products Laboratory 2.1-2.45.
- Lexa, J., Nečesaný, V., Paclt, J., Tesařová, M., Štofko, J. 1952. *Wood Technology I. Mechanical and Physical Properties of Wood*. Bratislava: Práca. 436 pp. (in Czech)

Panshin, A. J., De Zeeuw, C. 1980. Textbook of Wood Technology. 4.ed. New York: Mc-Graw-Hill. 722 pp.

Požgaj, A., Chovanec, D., Kurjatko, S., Babiak M. 1997. Structure and properties of wood. Bratislava: Príroda. 485 pp. (in Slovak)

Praus, L. Vavrčík, H., Koňas, P. 2006. Wood Properties of Black walnut (*Juglans nigra* L.). In: Proceedings, 5th International Symposium Wood Structure of Properties '06; September 2006; Zvolen: Arbora Publishers; Slovakia.

Wagenführ, R. 2007. Holzatlas. Leipzig: Fachbuchverlag. 816 pp.

Acknowledgments

We would like to express our thanks to Forests of the Czech Republic, state enterprise, for kindly providing us with testing material from their forest stands on the former surface mines.

Student Poster Competition
Session Co-Chairs: *Douglas Gardner, University of
Maine, USA and Jozef Kúdela,
Technical University in Zvolen, Slovakia*

**Effects of Particle Geometry on Dimensional Stability of
Bamboo - Reinforced Cement Composites**

Adesope A.S¹, Olayiwola H.O², Ojo, A.R and Alao, O.J

^{1,3&4}Forestry Research Institute of Nigeria, P.M.B. 5054, Ibadan, Oyo State

² Department of Agric and environmental Engrg, University of Ibadan.

¹E-Mail: adeyinka_sope@yahoo.com. Phone No: +2348060553393

Abstract

A lot of materials, both organic and inorganic, have been combined with cement matrix at different ratio, all in search of materials that are most suitable for a particular end use. This study determined the dimensional stability of bamboo-reinforced cement composites. Cement bonded composites (35mm-cube) were made from particles derived from bamboo (*Bambusa vulgaris*). The proportion of cement, sand, stone-dust and bamboo content was done by weight in a nominal mix of 1:2:4. Bamboo particles and chemical accelerator's substitutions were based on sand and cement proportions respectively. Mean Water Absorption after 2h of immersion in cold water ranged between 11.6 to 24.0% (at 0% CaCl₂) and 10.6 to 18.2% (at 3% CaCl₂). After 24h the range was between 13.1 to 24.4 % (at 0%CaCl₂) and 11.2 to 20.0 % (at 3%CaCl₂). The range of values of mean TS after 2h of immersions was 0.1 to 0.34% and 0.09 to 0.36% following 2h soaking at 0% and 3%CaCl₂ respectively. After 24h of immersion the range was 0.11 to 0.35% at 0%CaCl₂ and 0.10 to 0.37 at 3% CaCl₂. Based on the findings, it was therefore concluded that composites produced with 850µm particle size at 10% particle content and 3%CaCl₂ had less water absorption and thickness swelling potentials.

Keywords: Bamboo particles, dimensional stability, chemical accelerator, thickness swelling and water absorption

Life Cycle Assessment of Exported Torrefied Wood Pellets (TOP) from Maine to the European Union

Melanie Blumentritt^{1*} – *Sasha Howes*² – *Stephen M. Shaler*³

¹ PhD Candidate, School of Forest Resources/ Advanced Structures and Composites Center, University of Maine, Orono ME, USA

* *Corresponding author:*

melanie.blumentritt@maine.edu

² NSF REU Summer Intern at University of Maine
Virginia Tech University, Blacksburg, VA, USA

³ Director and Professor School of Forest Resources, Associate Director
Advanced Structures and Composites Center University of Maine, Orono
ME, USA

shaler@maine.edu

Abstract

Torrefied wood pellets are an energy source that has the potential to partially displace coal use in power plants, reducing the global warming impact of electricity produced from coal. Torrefied wood is produced by heating wood for a short period of time without oxygen at high temperatures (200 - 300°C). The final product is hydrophobic, not subject to biological degradation, has an energy density close to that of coal, and can be ground up easily. These properties allow for high co-firing rates with coal without the need to retrofit existing plants to adjust to a new fuel source. The life cycle emissions of torrefied wood pellets (TOP) produced in a case study plant in Maine and shipped to the European Union (EU) for combustion were accounted for using the LCI modeling software package SimaPro 7.3.3. Environmental impacts were assessed based on the global warming potential (GWP) of carbon dioxide equivalents (CO_{2eq}) over 100 years. Results indicate that the highest impact on GWP is produced by the transportation of TOP from Maine to the EU. Other aspects are the source of electricity at the torrefying and pelletizing facility and whether emissions from burning biomass are included in the calculation. On average, depending on system boundaries and scenarios, 90% net savings of CO_{2eq} of pure TOP compared to pure coal were found.

Keywords: biomass, energy, LCA, pellets, torrefaction

Introduction

As the world's population grows and energy demand rises, the pressure to find renewable and low carbon emitting energy sources increases. Global warming and climate change are issues the world is already feeling the effects of and many countries have implemented measures to combat climate change. The Kyoto Protocol, which was adopted in 1998 by many countries, including most of the European Union (EU), puts various emission limits on its members. By the year 2020, EU countries are expected to reduce their greenhouse gas emissions (GHG) to 20% below the 1990 levels of their respective country. In order to meet these goals without compromising economic gain, energy companies are looking to innovative technologies to use for energy production. Especially, large coal power plants are feeling the pressure to reduce emissions. However, in order to use renewable biomass sources in existing power plants significant changes to the plant need to be made, due to differences in material properties, like particle size, energy density, and storability between coal and biomass. Furthermore, these changes can be costly and difficult to implement in a time efficient manner. One technology that allows for continual co-firing of a renewable resource and coal are torrefied wood pellets (TOP) (Bergman 2005). Torrefaction is a mild pyrolysis taking a biomass resource (e.g. wood chips) and heating them between 250 - 300°C for a short period of time (10 - 30 minutes). During the process the biomass partly decomposes and gives off various volatiles, so called torrefaction gas. 70% of the initial mass is retained in the solid biocoal product, containing 90% of the initial energy content (Bergman 2005, Acharya et al. 2012). Torrefied wood has a variety of benefits, including a lack of biodegradability, hydrophobicity, and an energy density close to that of coal (6.94 MWh/t for coal and 6.67 MWh/t for TOP) (Bergman and Kiel 2005). Torrefaction can also be performed on a variety of biomass feedstocks, including forest residues. The lack of biodegradability and hydrophobicity allow for the torrefied product to be stored outdoors, without loss of product performance (Lipinsky et al. 2002, Bergman 2005, van der Stelt et al. 2011, Acharya et al. 2012, Li et al. 2012, Pirraglia et al. 2012). A new process uses microwave energy to avoid the issue of limited heat conduction of biomass related to particle size for torrefaction. This offers the ability to torrefy wood chips before undergoing a significant size reduction, reducing overall energy consumption. Torrefied wood is easier to grind than green wood chips making it easier to further process the biocoal into TOP and to use these as co-firing fuel for coal plants that use pulverized fuel combustion. TOP have the advantage over loose biocoal in that they can be transported more easily and have a higher bulk density. The emitted torrefaction gas is also suitable for energy conversion, allowing for the emissions from the torrefaction to actually fuel the process by combustion of portions of its own emissions.

Few studies have been performed to analyze the environmental effects of torrefied wood pellets (TOP) (Happonen 2012, Kabir and Kumar 2012). There are some studies looking at the life-cycle of white pellets (WP) produced in North America for European markets which are similar to TOP in regards to transportation and some manufacturing and handling processes (Magelli et al. 2009, Sikkema et al. 2010, Pa et al. 2011, Kabir and

Kumar 2012). In order to fully assess the benefits and issues associated with the production and export of TOP from an environmental impact point of view, a life cycle assessment (LCA) was conducted and modeled using the LCI modeling software package SimaPro 7.3.3. To account for environmental impacts, IPCC 2007 GWP 100a was used. IPCC 2007 GWP models the global warming potential (GWP) of a system for a 100 year time frame. The goal of this LCA study is to analyze the environmental effects of producing and using TOP for electricity production. The process was analyzed based on a case study of the in development start-up plant by Thermogen Industries LLC, located in Millinocket, Maine, USA. The system boundary can be seen in “Figure 1” and is described in the subsequent inventory analysis. A functional unit of one year's worth of TOP produced (100,000 t using 217.724 t biomass) was used. Results of TOP will be compared to coal, since the product is intended to partially displace the use of coal for electricity production.

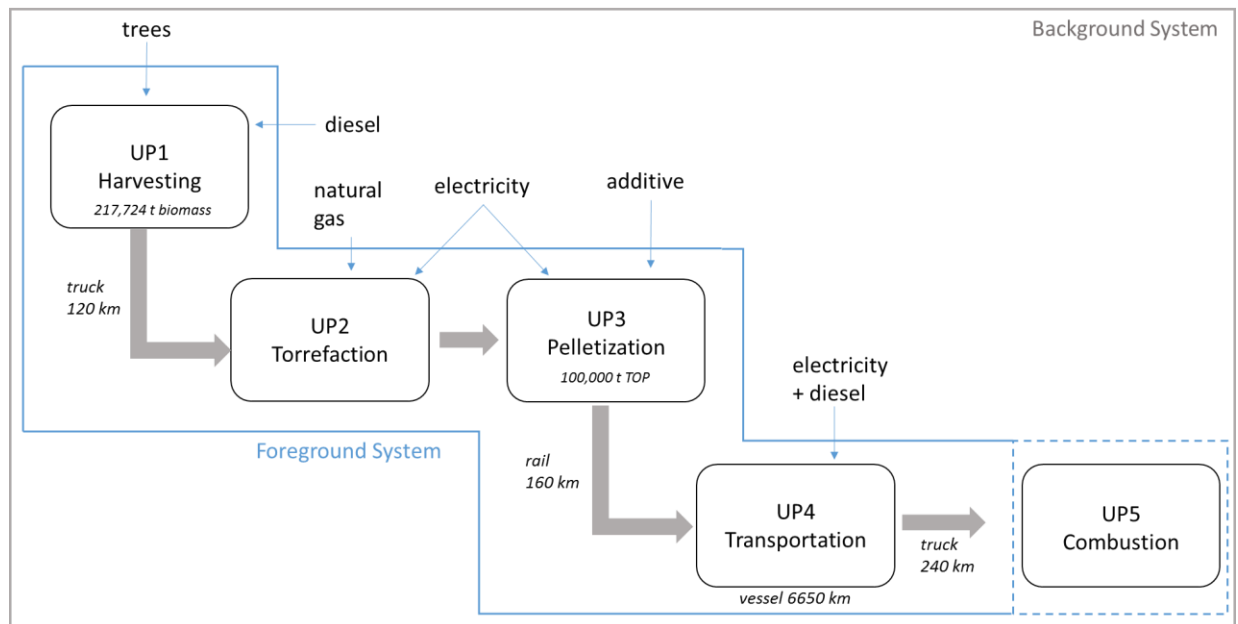


Figure 1 - System boundary and unit processes (UP) of production and transportation logistics of torrefied wood pellets (TOP) from the Maine forest to the European market, including some process flows.

Methods

Inventory analysis

Harvesting and Wood Residue Transportation

The biomass feedstock is forest residue, a combination of branches and foliage often left behind after the harvesting of trees for pulp and lumber, accounting for 30% or more of the harvested biomass. Due to the fact that forest residue is a byproduct of the primary products of pulpwood and sawlogs, all silviculture, and land change effects, as well as the manufacturing and disposal of logging equipment is of out of scope for this study. However, the operation of all equipment was taken into account. Maine operates 80% of

its forest operations using the whole tree model, which was modeled here. This forest operations system is comprised of a feller buncher, grapple skidder, and stroke delimeter bringing the trees roadside. Fuel consumption was calculated based on the average productivity of the respective equipment per hour and mass (Benjamin and Hiesl 2013, Leon and Benjamin 2013). A chipper and loader then chip the residue into large trucks for transportation. Allocations were made to the resource production of forest residue by mass allocation and value allocation based on data of the whole-tree-model and Maine stumpage prices for biomass, sawlogs, and pulpwood (Maine Forest Service 2012). Biomass represents 18.33% of the mass of the total harvested volume and 5.95% of the total estimated value. The effects of carbon removal from the environment was not accounted for. It was assumed that roads were already constructed for the primary products of sawlogs and pulpwood. The operation of the truck carrying the residue chips was accounted for. It was assumed that 217,724 t (240,000 ton, wet basis) of biomass are processed by the facility each year, with each truck carrying 33 t per trip. The average haul distance from the forest to the facility was 120 km (75 miles, one way). Fuel consumption of the truck returning empty to the forest was accounted for.

Torrefaction

Since the project focuses on the production of TOP in a facility in Millinocket, Maine certain site specific features need to be considered. The facility is located on the site of an old pulp and paper mill with existing infrastructure and connection to an on-site hydropower plant. Trucks bring in forest residue chips and load them onto a concrete holding pad. The chips are loaded onto a screen and processed by a hammermill, creating biomass of a uniform upper size. The biomass is then sent to a metering bin and into a rotary dryer, which dehydrates the wood to the level desired for downstream processes. In normal operating conditions, the combustible gases from the thermal oxidizer will provide heat for the dryer, but in startup conditions, the biomass fines from the hammermill will be burned in a biomass suspension burner to provide heat. Exhaust gasses from the dryer are separated from the biomass by a cyclone and treated in a wet electrostatic precipitator before being exhausted to the atmosphere. The torrefaction process uses microwaves and thermal energy in an oxygen starved environment to torrefy the wood to biocoal. The majority of the torrefaction gas is recycled by combustion to provide heat to the system. The remaining gases are sent to a heat exchanger and thermal oxidizer system, which recycles the majority of these gases through the heat exchanger and back to the torrefaction process and the rotary dryer and the remaining gases are combusted in the oxidizer, pass through the heat exchanger for heat recovery and then through a wet electrostatic precipitator (ESP) for emissions control before being released to the atmosphere. After torrefaction, the biocoal is sent through a cooling screw conveyer and sprayed with water, before being pelletized. Since this study considers the process of a proposed plant design, the LCI data largely relies on estimated and modeled data by Thermogen Industries LLC. Energy use, mostly in form of electricity and corresponding emissions, was accounted for. The building infrastructure and manufacturing, use, and disposal of all of the equipment were not included in the analysis.

TOP Production

The torrefied biomass from the processor is ground and then pelletized with a small amount of natural additive that acts as a binder and plasticizer, collected, and cooled via a series of conveyers and a pellet cooler that exhausts through a high efficiency cyclone. Transportation of the additive for the pellets is modeled by truck. Electricity consumption for all equipment and emissions were accounted for. Building infrastructure and manufacturing, use, and disposal of the equipment was modeled based on pellet manufacturing infrastructure processes in databases available in SimaPro with estimated electricity consumptions by Thermogen Industries LLC.

Transportation to the European Union

The finished torrefied pellets are transported in bulk by rail to Searsport, ME, 160 km away from the facility, where they are transferred onto a ship to be transported an estimated 4130 km to a port in the EU (e.g. Rotterdam in the Netherlands). From the European port, it was assumed the torrefied pellets would be transported by truck over 240 km to a power plant. Operation, manufacture, and maintenance of the oceanic and truck transport, electricity for handling equipment at the port, and fuel for the rail transport are included, while recycling and disposal are not, based on available databases in SimaPro data. Location specific data was used where existing.

Use and Disposal

The use of the TOP is as fuel by combustion. Exact emissions are dependent upon specific plant configurations including, type of co-firing, combustion or gasification technologies, and emission control data. Two scenarios were considered a) all emissions from the torrefied wood are biogenic and carbon neutral (van Loo and Koppejan 2008) and therefore not accounted for and b) emissions from burning, except for CO₂, were calculated based on data from Kabir & Kumar (2012). Wood ash can be used for a variety of applications but due to the fact the TOP are assumed to be co-fired with coal, the ash will likely be disposed of with the coal waste. Allocations could be made to the coal waste for use in industry but disposal was not taken into account due to the uneven nature of the ash (Happonen 2012) and unknown conditions of the final combustion process. Emissions associated with infrastructure, supporting equipment, and energy requirements for combustion at the power plant were not accounted for.

Results and Discussion

A cradle-to-gate LCA analysis, based on the LCI results, was carried out with a variety of scenarios. Emissions from burning/ gasifying biomass do not need to be accounted for, based on the carbon neutral properties of biomass. However, there is a growing body of literature questioning carbon neutrality, and corresponding assumed climate neutrality, of using forest harvest residues and biomass in general because the re-sequestration of the combusted carbon takes place over many decades, due to the slow growth rate of trees (Repo et al. 2011, Agostini et al. 2013, Guest et al. 2013). Therefore, a scenario excluding all emissions from burning and gasifying biomass and one including emissions were evaluated.

The location of the case study plant is very unique both in terms of raw material availability in the near surroundings and especially the connection to a low emission power source. In order to better translate results to a different plant site we included scenarios with the average local energy mix from the Maine grid as power supply (EPA 2014). Since emissions from shipping vary greatly by the technology used, a scenario with a low, high, and medium shipping efficiency were considered.

Global Warming Potential 100 Year Model

“Figure 2” gives an overview of the impact on global warming potential of some scenarios per unit process. Among the variety of scenarios analyzed, particular patterns emerged as to what created the best and worst scenarios. The best scenario took into account the value allocation for harvesting, run of the river hydroelectric power and high efficient transatlantic transport, and no emissions from burning/ gasifying biomass (TOP3). On the other hand, the worst scenario took into account mass allocation for harvesting, local electricity usage, low efficient transatlantic transportation and all emissions from burning/ gasifying biomass (TOP4). Scenario TOP1a represents the most likely scenario for this case study with the currently available data. Overall, the biggest contributor to GWP are transatlantic shipping and emissions from burning/ gasifying biomass, if included. There is also a significant difference between the sources of electricity, but only a slight difference between mass and value allocation for harvesting (6.8 compared to 3.8 kg CO_{2eq} t_{TOP}⁻¹, respectively).

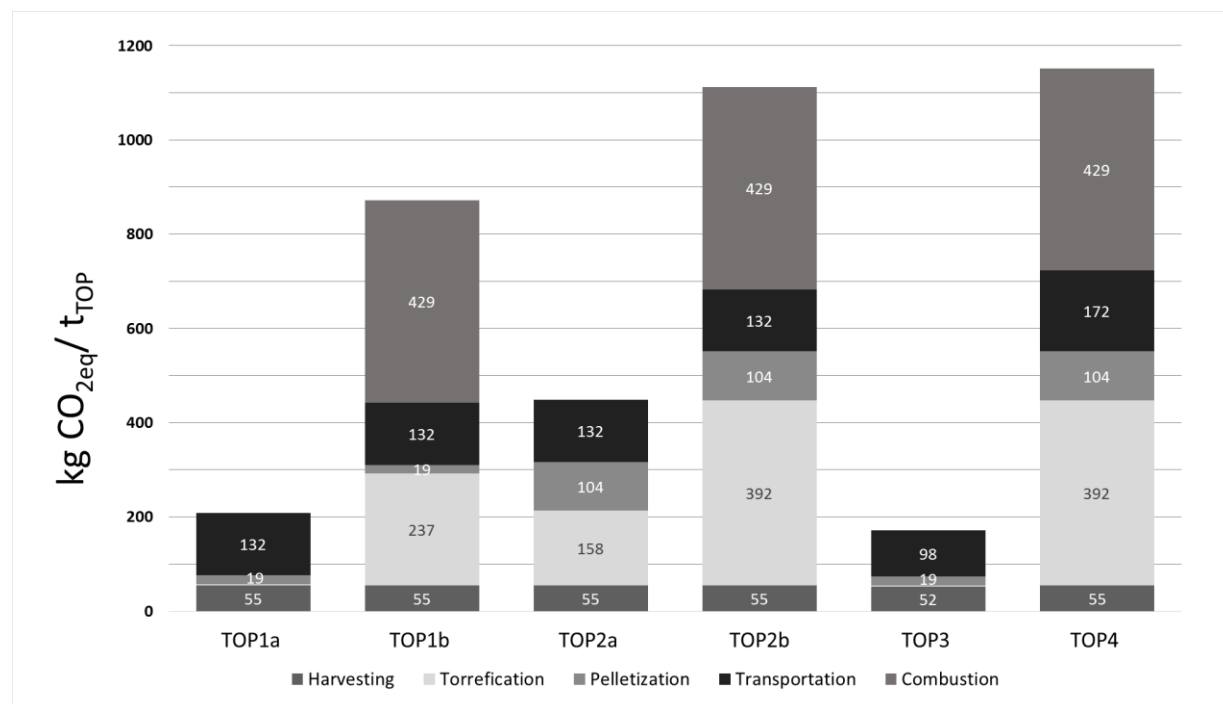


Figure 2 - GWP in kg CO_{2eq} t_{TOP}⁻¹ per unit process for different scenarios. TOP1 with electricity from hydropower and TOP2 with electricity from the Maine grid, a) and b) without and with emissions from biomass. TOP3 represents the best and TOP4 the worst possible scenario.

The best scenario has a 97% GWP reduction from coal, while the worst still has an 82% GWP reduction. The average percent reduction from coal is 90%. This is better than 72% net savings of white pellets from coal found by Dwivedi et al. (2011). However, savings compared to coal (Table 1) depend strongly on used emission values for coal. In this study we based our comparison on 1080 kg CO_{2eq} MWh⁻¹ for coal. This value was calculated based on processes available in databases in SimaPro for the Netherlands and is comparable to the average emissions estimated for coal found in other studies (Spath 1999, Whitaker et al. 2012). As “Table 1” demonstrates, the results for TOP in kg CO_{2eq} MWh⁻¹ and kg CO_{2eq} tonne_{TOP}⁻¹ are within the bounds reported in literature. The energy content of TOP was estimated at 5.84 kWh kg⁻¹. The GWP for TOP products is lower than white pellets due to the fact that TOP is more energy dense, leading to a more efficient use of transportation energy.

Limitations of the Study

All LCAs are defined by their system boundaries and the quality of information they are able to collect. The system boundary for this study did not include the equipment, plant manufacturing or disposal; while some other studies do, leaving a gap of information. Furthermore, the plant is based on plant design estimates rather than an operating facility. Accurate combustion data for the co-firing of torrefied wood pellets were also not available.

Further studies should be performed in the near future once TOP have been established on the market. We also believe that a more thorough investigation of the carbon cycle of wood and possible impacts on GWP should be considered, as well as other pollutants (e.g. particulates) that are not included in the IPCC GWP100 method but are known to cause emissions when burning biomass and coal.

Table 1 - Comparison of GWP in CO_{2eq} per MWh and tonne product

Source		kg CO_{2eq} MWh⁻¹	kg CO_{2eq} t_{product}⁻¹	Product*
This Study	Best	29	172	TOP
	Worst	197	1152	TOP
	Average	113	661	TOP
	TOP1a	36	209	TOP
	Coal	1080		coal
Kabir and Kumar (2012)		169		FR-TOP
		215		WT-TOP
		244		FR-WP
		302		WT-WP
Magelli et al. (2009)		532-723	WP	
Pa et al. (2012)		295	WP	
Happonen (2012)	134		TOP	

*TOP=torrefied wood pellets, FR=forest residue, WT=whole tree, WP= white pellets

Conclusions

This study attempts to quantify the life cycle emissions and global warming potential of a new energy product, torrefied wood pellets (TOP). Torrefied wood has the potential to be co-fired in large coal power plants, to reduce global warming emissions (e.g. CO₂, CH₄, and N₂O) from electricity generation. Scenarios analyzed resulted in an average saving of 90% CO_{2eq} compared to coal. It is evident that torrefied wood pellets, if the forests are managed sustainably, are a significantly better option than coal in terms of global warming potential to produce electricity, especially if they can be produced using a large amount of renewable energy sources. Further studies on the types of torrefaction processes and allocation opportunities in the LCA of torrefaction should be pursued.

References

- Acharya, B., Sule, I. and Dutta, A. 2012. A review on advances of torrefaction technologies for biomass processing. *Biomass Conversion and Biorefinery*. 2(4):349-369.
- Agostini, A., Giuntoli, J. and Boulamanti, L. 2013. Carbon accounting of forest bioenergy—Conclusions and recommendations from a critical literature review. European Commission, Joint Research Centre (JRC) Report, EUR 25354.
- Benjamin, J. and Hiesl, P. 2013. Productivity of whole tree and cut to length harvesting equipment. Personal communication. August 2013.
- Bergman, P.C.A. 2005. Combined torrefaction and pelletisation - The TOP process. ECN Report, ECN-C-073.
- Bergman, P.C.A. and Kiel, J. (2005). Torrefaction for biomass upgrading. In: *Proceedings, 14th European Biomass Conference & Exhibition, Paris, France*. ECNRX-05-180.
- Dwivedi P, Bailis, R., Bush, T.G. and Marinescu, M. 2011. Quantifying GWI of wood pellet production in the Southern United States and its subsequent utilization for electricity production in the Netherlands/Florida. *Bioenergy*. 4:180-192.
- Guest, G., Cherubini, F. and Strømman, A.H. 2013. The role of forest residues in the accounting for the global warming potential of bioenergy. *GCB Bioenergy*. 5(4): 459-466.
- Happonen, K. 2012. Torrefied wood pellets as an alternative fuel to coal: Climate benefits and social desirability of production and use. Master's Thesis, University of Helsinki, Finland.
- Kabir, M.R. and Kumar, A. 2012. Comparison of the energy and environmental performance of nine biomass/coal co-firing pathways. *Bioresource Technology*. 124: 394-405.
- Leon, B. and Benjamin, J.G. 2013. A survey of business attributes, harvest capacity and equipment infrastructure of logging businesses in the Northern forest. *The Northern Forest Logging Industry Assessment*. Orono, ME, University of Maine: 29.

- Li, H., Liu, X., Legros, R., Bi, X.T., Jim Lim, C. and Sokhansanj, S. 2012. Pelletization of torrefied sawdust and properties of torrefied pellets. *Applied Energy*. 93: 680-685.
- Lipinsky, E.S., Arcate, J.R. and Reed, T.B. 2002. Enhanced wood fuels via torrefaction. *Fuel Chemistry division preprints*. 47(1): 408-410.
- Magelli, F., Boucher, K., Bi, H.T., Melin, S. and Bonoli, A. 2009. An environmental impact assessment of exported wood pellets from Canada to Europe. *Biomass and Bioenergy*. 33(3): 434-441.
- Maine Forest Service 2012. 2011 stumpage prices by Maine county/ unit. Department of Agriculture, Maine Forest Service, Forest Policy and Management Division. Augusta, Maine, Maine Government.
- Pa, A., Bi, X.T. and Sokhansanj, S. 2011. A life cycle evaluation of wood pellet gasification for district heating in British Columbia. *Bioresource Technology*. 102: 6167-6177.
- Pirraglia, A., Gonzalez, R., Saloni, D., Wright, J. and Denig, J. 2012. Fuel properties and suitability of *Eucalyptus benthamii* and *Eucalyptus macarthurii* for torrefied wood and pellets. *BioResources*. 7(1): 217-235.
- Repo, A., Tuomi, M. and Liski, J. 2011. Indirect carbon dioxide emissions from producing bioenergy from forest harvest residues. *GCB Bioenergy*. 3(2): 107-115.
- Sikkema, R., Junginger, M., Pichler, W., Hayes, S. and Faaij, A.P.C. 2010. The international logistics of wood pellets for heating and power production in Europe: Costs, energy-input and greenhouse gas balances of pellet consumption in Italy, Sweden and the Netherlands. *Biofuels, Bioproducts and Biorefining*. 4(2): 132-153.
- Spath, P.L., Mann, M.K. and Kerr, D.R. 1999. Life cycle assessment of coal-fired power production, No. NREL/TP-570-25119. National Renewable Energy Lab., Golden, CO.
- United States Environmental Protection Agency (EPA). 2014. "Power profiler, NPCC New England region." Retrieved February 21, 2014, from: http://oaspub.epa.gov/powpro/ept_pack.charts.
- van der Stelt, M., Gerhauser, H., Kiel, J. and Ptasincki, K. 2011. Biomass upgrading by torrefaction for the production of biofuels: A review. *Biomass and Bioenergy*. 35(9): 3748-3762.
- van Loo, S. and Koppejan, J. 2008. *The handbook of biomass combustion and co-firing*, Earthscan.
- Whitaker, M., Heath, G.A., O'Donoghue, P. and Vorum, M. 2012. Life cycle greenhouse gas emissions of coal-fired electricity generation. *Journal of Industrial Ecology*. 16: S53-S72.

Acknowledgements

Funding support for this project was provided by the Northeastern States Research Cooperative (NSRC), a partnership of Northern Forest states (New Hampshire, Vermont, Maine, and New York), in coordination with the USDA Forest Service. <http://www.nsrcforest.org> and by the USDA/NIFA Project 2011-69005-30401.

Changes in the Anatomy of Exposed Roots of Some Hardwood Species

Bryan Dick, Perry Peralta, and Ilona Peszlen

Abstract

Dendrogeomorphology, a subfield of dendrochronology, is a valuable tool for dating and estimating the rates of erosion and deposition of river banks, ephemeral channels, hillslopes, landslides and other mass movements. By determining the initial year of root exposure, exposed tree roots offer a means of determining erosion rates for both riverine and hillslope processes. While dendrogeomorphology is a well-established field, there is very little information available to researchers and practitioners in the way of specific responses of hardwoods by genus or classification of anatomical structure. Macroscopic and microscopic indicators of the date or root exposure include; the occurrence of eccentricity in growth rings, a transition of diffuse to ring porous arrangements of vessels (root-like to stem-like anatomy), a decrease in the size of vessels and fibers, fiber cell wall thickening, the occurrence of gelatinous fibers in tension wood and the occurrence of pith flecks (scarring and wound tissue). The observed macroscopic and microscopic changes in root wood anatomy of exposed roots of sugar maple (*Acer saccharinum*), slippery elm (*Ulmus rubra*) and common hackberry (*Celtis occidentalis*), water oak (*Quercus nigra*), green ash (*fraxinus pensylvannica*), water hickory (*Carya aquatica*), black willow (*Salix nigra*), and eastern cottonwood (*Populus deltoids*) will be presented. The difficulties associated with using some species will also be discussed, in order to assist with the planning of what is best used for future studies of soil erosion using exposed roots.

Keywords: dendrochronology, dendrogeomorphology, exposed roots of hardwoods

Bryan Dick, Ph.D. Student

bmdick@ncsu.edu

Perry Peralta, Associate Professor

+1919-515-5731; Fax: +191-3513-3496

Perry_Peralta@ncsu.edu

Ilona Peszlen, Associate Professor

+1-919-513-1265; Fax: +191-3513-3496

Ilona_Peszlen@ncsu.edu

Department of Forest Biomaterials

North Carolina State University

Campus Box 8005

Raleigh, NC 27695-8005

Understanding the Relationship Between Thermo-mechanical Behavior and Lignin Properties of Genetically Modified *Populus trichocarpa*

Charles Warren Edmunds^{1*}, *Dr. Perry Peralta*², and *Dr. Ilona Peszlen*²

¹ Graduate Research Assistant, Department of Forest Biomaterials – North Carolina State University. 2820 Faucette Dr., Raleigh NC 27695.

² Associate Professor, Department of Forest Biomaterials - North Carolina State University. 2820 Faucette Dr., Raleigh NC 27695.

* *Corresponding author*
cw Edmund@ncsu.edu

Abstract

Delignification of feedstock biomass is required for pulping and biofuels production, and high temperatures are utilized in these processes. Therefore, the thermo-mechanical properties of solid wood are of interest. Genetically altered *Populus trichocarpa* clones which are deficient in several genes controlling lignin synthesis have produced wood with altered lignin content and/or lignin structure. The aim of this work was to study the relationship between lignin content, lignin structure, and the thermo-mechanical properties of solid wood. Cellulose content, hemicellulose content, lignin content, and lignin monomer composition were measured using wet chemistry techniques, and the thermo-mechanical properties, including the storage and loss moduli, tan delta, and glass transition temperature (T_g), were measured using dynamic mechanical analysis. Wildtype and several genetically altered lines had lignin contents ranging from 9.9 % to 22 %, and syringyl/guaiacyl (S/G) lignin monomer ratios ranging from 1.3 to 3.4. A good correlation between the T_g and lignin content, and a poor correlation between T_g and S/G ratio indicates that lignin content, and not lignin structure, is more highly correlated to glass transition temperature. These findings have important implication for utilizing genetically engineered wood for increased processing efficiency for bioenergy and pulp production.

Keywords: Thermo-mechanical, lignin, glass transition temperature, dynamic mechanical analysis, S/G ratio.

Introduction

Biomass processing for applications such as pulping and biofuels production require steps to remove lignin. Elevated temperatures are often utilized in the delignification processes, therefore the thermo-mechanical behavior of wood is important (Back and Salmén, 1982; Baumberger et al., 2002). Genetic engineering of lignin biosynthesis in *P. trichocarpa* allows a unique opportunity to isolate the variable of interest, lignin, and reduce the variation of other factors by producing clones with modified genes and wood samples exhibiting a wide range of lignin properties in the same tree species.

This study utilized wood from genetically modified *Populus trichocarpa* exhibiting altered lignin content and/or lignin composition. Structural carbohydrates (cellulose and hemicelluloses), lignin content, and lignin monomer composition were measured using wet chemistry techniques. Thermo-mechanical properties, including storage and loss moduli, tan delta, and glass transition temperature (T_g) were measured using dynamic mechanical analysis. The objective of this study was to probe the relationship between lignin content, lignin monomer composition, and the thermo-mechanical properties of solid wood.

Materials and Methods

Samples. Genetically modified *Populus trichocarpa* was utilized for this study. Genes responsible for lignin biosynthesis were altered, producing wood with a wide range of lignin content and S/G ratios. All trees were grown in a greenhouse under controlled conditions, and harvested after 6-8 months. Stem samples 0-12 in. from the ground were used for thermo-mechanical analysis, and stem samples greater than 12 in. from the ground were used for chemical analysis.

Chemical Analysis. Modified NREL procedures were used to measure structural carbohydrates (glucan, xylan, galactan, arabinan, and mannan), and lignin content. Nitrobenzene oxidation was used to estimate syringyl (S), guaiacyl (G), and hydroxyphenyl (H) lignin monomer concentrations by measuring the lignin degradation product syringic acid and syringaldehyde, vanillic acid and vanillin, and 4-hydroxybenzaldehyde.

Dynamic Mechanical Analysis (DMA). A microcircular saw was used to cut stem into 25x5x1 mm (longitudinal, tangential, and radial) sections. The wood specimens were saturated in ethylene glycol prior to measurement. A temperature sweep was performed using DMA at a frequency of 0.1 Hz, strain of 0.05 % and thermal ramp from 35 – 95 °C at a heating rate of 2 °C per min. The thermal ramp was performed twice for each specimen, the first run was to remove thermal history, and on the second the storage modulus (E'), loss modulus (E''), and tan delta values were recorded. The glass transition temperature (T_g) was determined from the peak in the tan delta curve.

Statistics. SAS (Cary, NC) statistical software was utilized to perform Analysis of Variance (ANOVA) to test for significant effects for gene modification. Tukey's multiple comparison ($\alpha=0.05$) was utilized for mean separation. To show correlations between variables, scatter plots with least squares error (R^2) for a linear regression line was used.

Results

Chemical Analysis. The wildtype and genetically modified wood samples had lignin contents ranging from ~10% to 22%. The ratio between syringyl (S) and guaiacyl (G) subunits in the lignin fraction, or S/G ratio, is commonly used as a metric for woody biomass recalcitrance, with lower values having greater recalcitrance. There was high variation among the measured S/G ratios, which ranged from ~1.2 - 3.4. In general low lignin content samples had significantly higher amounts of cellulose and hemicelluloses. In addition, some of the genetically modified wood specimens had elevated hydroxyphenyl (H) lignin monomers, which is very unusual for tree species.

Thermo-mechanical Analysis. Compared to WT, all transgenic samples, with the exception of one, displayed significantly reduced glass transition temperatures. Additionally, all transgenic samples had significantly lower storage (E') and loss (E'') moduli compared to WT, which indicates reduced stiffness and strength. Low lignin content samples had significantly increased tan delta values at the glass transition temperature. This indicates that severely reduced lignin content is associated with higher tan delta values and greater viscous behavior. There is a good linear correlation for T_g vs. lignin content; and T_g decreases with decreasing lignin content, while a poor correlation exists between for T_g vs. S/G ratio.

Conclusions. There is a clear linear trend of decreasing T_g with decreasing lignin content, no clear correlation for T_g vs. S/G ratio. This result indicates that the lignin content is more strongly correlated than lignin S/G ratio to the glass transition temperature in solid wood. Previous research comparing hardwood and softwood concluded that lignin composition influences T_g to a greater extent than lignin content (Olsson & Salmén, 1997). However this study demonstrates the opposite, that lignin content is more highly correlated to T_g in solid wood than lignin composition. There may be underlying factors that are influencing the T_g that are caused by low lignin content, and these factors are currently under investigation. These results show that genetic modifications to the lignin biosynthetic pathway can cause significant changes in the chemical and physical properties of solid wood, and demonstrates that, in the future, genetic engineering can be utilized to produce wood with properties tailored to suit a particular process or product, such as pulp and paper, biofuels, or structural timber.

Reference

Back, E L, and L Salmen. 1982. "Glass Transitions of Wood Components Hold Implications for Molding and Pulping Processes." *Tappi* 65: 107–110.

Baumberger, S, P Dole, and C Lapiere. 2002. "Using Transgenic Poplars to Elucidate the Relationship between the Structure and the Thermal Properties of Lignins." *Journal of Agricultural and Food Chemistry* 50 (8): 2450–2453.

Olsson, A. M., & Salmén, L. (1997). The effect of lignin composition on the viscoelastic properties of wood. *Nordic Pulp and Paper Research Journal*, 12.

Acknowledgements

I would like to thank the USDA National Institute of Food and Agriculture (NIFA) National Needs Fellowship program for its financial assistance. Many thanks to Dr. Vincent Chiang and the Forest Biotechnology Group for help and advice concerning chemistry techniques, and for providing wood samples. In addition, special thanks to Zach Miller for help in preparing wood specimens and assistance in chemical characterization.

Rheometer Method to Determine Factors Influencing Sticking Behavior of Aminoplastic Resins

Alexandra Himsel^{1} – Ulrich Müller² – Hendrikus W. G. van Herwijnen³ –
Wolfgang Kantner⁴ – Johann Moser⁵ – Roland Mitter⁶*

¹ M.Sc., Junior Researcher, Competence Centre for Wood Composites and Wood Chemistry, Division Wood Materials Technologies, Tulln, Austria.

** Corresponding author*

a.himsel@kplus-wood.at

² Dr. (habil), University of Natural Resources and Applied Life Science, Institute of Wood Technology and Renewable Resources, BOKU, Vienna, Austria.

³ Dr., Senior Researcher, Competence Centre for Wood Composites and Wood Chemistry, Division Wood Materials Technologies, Tulln, Austria.

⁴ Dr., Product Development Manager & Lab Manager, Metadynea Austria GmbH, Krems, Austria.

⁵ Dr., Product Development Manager & Sales Composite Board Resins, Metadynea Austria GmbH, Krems, Austria.

⁶ Ing., Competence Centre Chemistry, Fritz Egger GmbH & Co OG, Unterradlberg, Austria.

Abstract

By using low emission aminoplastic resin in the production of wood based panels sticking occurs. This kind of tacking behavior which goes along with drying out of the adhesive system leads to an accumulation of resinated particles onto machinery parts, such as blender, conveyor, and forming station. For a better understanding of the processes during drying out of resins a method for testing influencing factors of sticking was invented. This basic understanding allows deriving strategies to prevent sticking in the production process. Therefore a new rheometer installation was built, consisting of a wheel which rotates on a wooden surface. By applying a defined amount of resin on the surface of the plate, the rolling resistance can be measured while the adhesive dries out. The experimental set-up is used to describe the drying out behavior of an adhesive and the adherence to other materials. The method allows describing a various number of influencing factors, such as temperature, humidity, surface roughness, viscosity changes, the use of different materials and variation in behavior according to glue recipe differences. Sticking of glue is mainly influenced by climate conditions. However, changes in the sticking behavior by using different materials, such as stainless steel or polypropylene are tremendous, too. Besides this a dependency of the surface roughness of the wooden plate can be measured. The results provide strong evidence that climate

conditions, surface properties and changes in glue characteristics are significantly influencing the sticking behavior, whereas penetration and wetting are not showing a significant contribution to the sticking phenomenon.

Keywords: low emission aminoplastic resin, sticking, drying out, adhesive properties, adherence to materials

Introduction

Current knowledge on the tacking effect of adhesives refers to the testing of viscosity, wetting, penetration and physical strength. Testing methods can be differed in adhesive characterization such as viscosity, pH-value, percentage of formaldehyde and urea, gelation time and dry matter. In practice measurement methods for tacking properties are the "snowball" method or the determination of the tackiness by means of "finger dipping". Also probe tack testing and rolling ball method are commonly known to determine adhesive properties of a resin (ASTM 3121(1989) and ASTM 2979(1988)). All of these methods describe important properties of the used resins. (Schmidt et al. 2010, Roberts 1997)

Due to changing requirements for emissions of formaldehyde (CARB, F***/****) chemism of adhesives changed. The adaptation of formaldehyde-containing adhesive systems to the guidelines for reduced formaldehyde emissions led to a change in resin formulas. These changes, such as F/U ratio, pH-value, are followed by variations in pot life and adhesive behavior. Therefore agglomerations of resinated particles on machinery within the particle board production (such as transportation belt, conveyor and pre-press) increasingly occur. These deposits must be removed manually in order to ensure continued smooth production. This maintenance work leads to a decrease in production efficiency and an increase in production costs. To understand the process of tacking to the machines, the so-called sticking, the rolling rheometer method was developed. (Himsel et al. 2013)

Materials and Methods

Materials. For the investigation urea-formaldehyde (UF) resin from Metadynea Austria GmbH was used. This resin is used for particle board production to fulfil CARB 2 (0.09 ppm measured according to ASTM 1333 (2010)). The used UF resin was one respectively four weeks old and the viscosity was tested in advance.

As a model of the surface of the wood particles, high density fiber board samples with a well-defined roughness are used as ground plate. The samples were sanded (180 grid) and their surface roughness was measured with a Taylor Hobson Pneumo. After estimating the surface roughness twice in each spatial direction the samples were classified in three roughness classes: even – average – rough. The differentiation was made after comparing the means of the roughness profile deviation. Samples were classified as followed:

- even samples: 2.69 to 3.11 μm

- average samples: 3.21 to 4.87 μm
- rough samples: 5.05 – 5.90 μm

Rheometer method. For a better understanding of the so-called sticking problem, the rolling rheometer method was introduced by Kantner et al. (2009). This method can be used to determine the sticking properties of aminoplastic resins. The principal installation of an enhancement of the method is shown in Himsel et al. (2013) and in Figure 69. To fulfil the sticking test aminoplastic resin is put onto a HDF base plate. While drying out, a wheel moves around a balance point and measures the development of sticking.

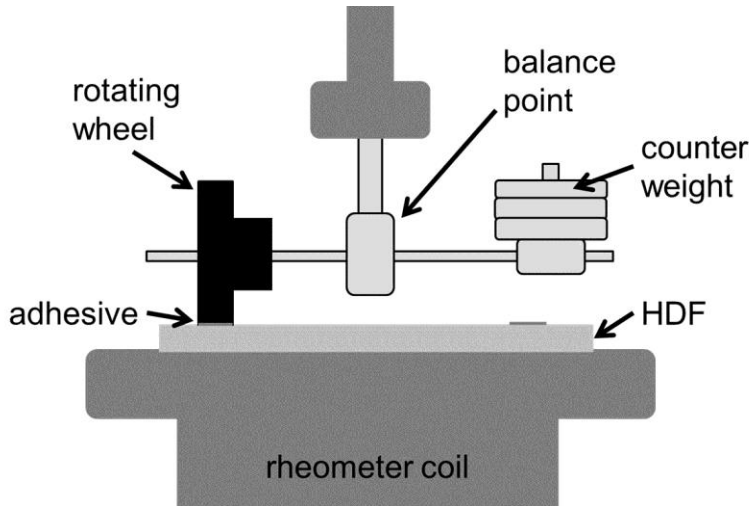


Figure 69: Rheometer method (Himsel et al. 2013)

To measure the influence of the material the rheometer method has been improved and expanded. Different wheel materials have been used. During the investigations, measurements were carried out on the effect of material by using a wheel made of PP and another one made of stainless steel.

Results and discussion

Influence of the surface roughness. Influence of wood surface is estimated as an interaction of sticking and penetration. The amount of resin applied in the rheometer method was equal for every test run. It is assumed, that rougher surfaces show a higher penetration than even surfaces. It is further assumed, that the higher the penetration the lower the moment of torque. The difference between the rough and even surface is shown in Figure 70, proofing lower values for the rough surface.

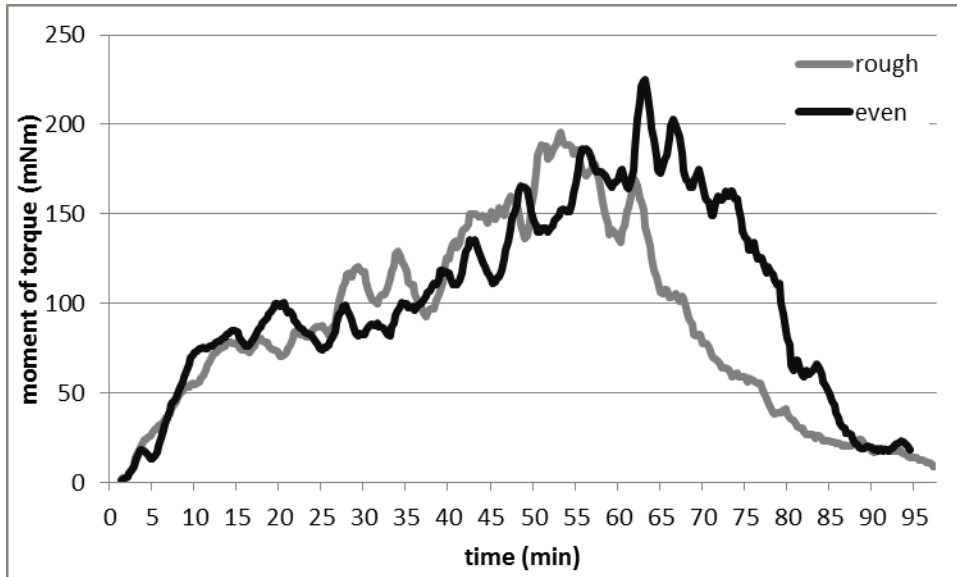


Figure 70: influence of surface roughness on moment of torque at 50% rh and 25°C; resin age: four weeks

The surface roughness influences the moment of torque. Whereas an even surface shows a maximum after 65 minutes, a rough surface already reached the maximum after 50 minutes. Beside the maximum value of moment of torque the rough surface shows the peak value 15 minutes earlier. The results clearly pointed out that surface roughness is a significant parameter influencing the sticking behavior. For that reason the surface of the sanded fiber boards need to be measured before using the rheometer method.

Influence of the wheel material. To prevent that sticking results are biased by the surface roughness of the board samples with an average surface roughness were selected. Sticking with respect to adhesion onto different wheel materials was tested at 50 % relative humidity and a temperature of 25°C. The tests were carried out after storage of the glue for one (Figure 71) and four (Figure 72) weeks, respectively.

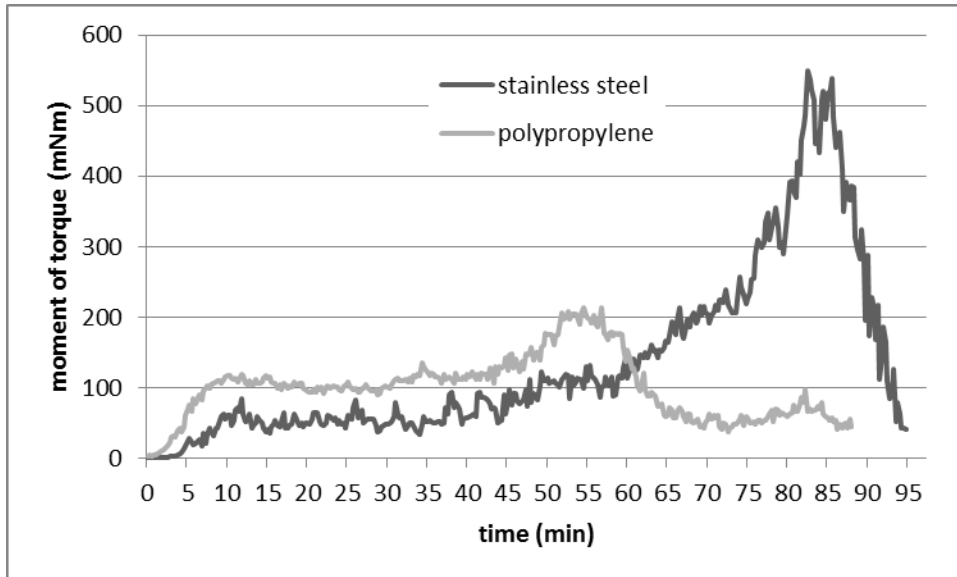


Figure 71: moment of torque with stainless steel and polypropylene wheel at 50 % rh and 25 °C, resin age: one week

Figure 71 shows the difference in the sticking behavior after one week storage of the resin with respect of the wheel material. Polypropylene is characterized by low values with a peak value after 55 min reaching 205mNm. Whereas stainless steel shows a steadily increasing of the moment of torque with a peak value of 550 mNm, which is reached after 85 minutes.

For the resin stored for four weeks the effect of the wheel material is even higher. Tests performed with a polypropylene wheel show a steep increase of the moment of torque just at the beginning of the test run, up to a maximum value of 700 mNm after 10 minutes. Similar behavior up to a running time of 50 minutes can be observed for the stainless steel wheel. However, storage time of four weeks results in a significant reduction of the maximum moment of torque of 220 mNm which is almost 50 % of the fresh resin.

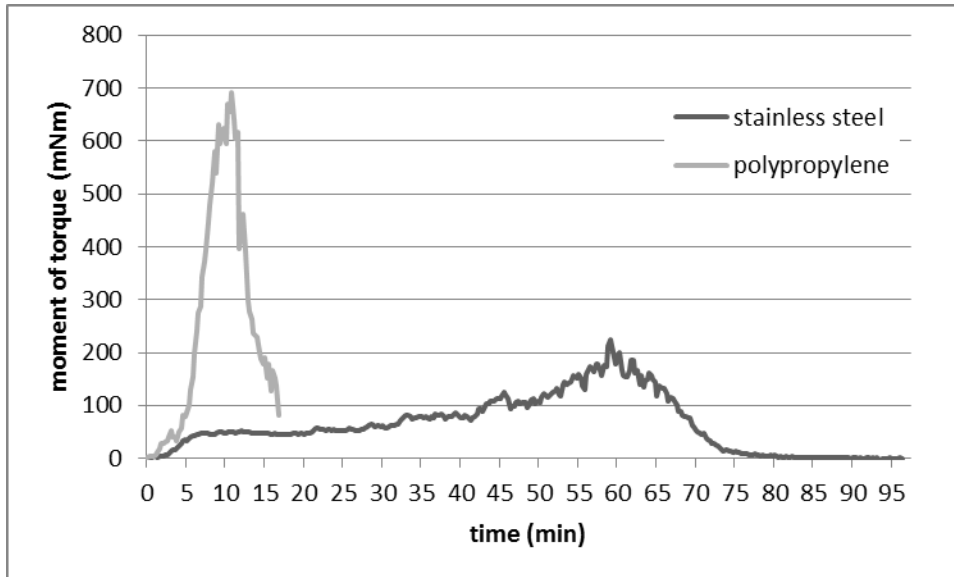


Figure 72: moment of torque with stainless steel and polypropylene wheel at 50 % rh and 25 °C, resin age: four weeks

Results presented clearly point out that the material of the machinery parts (i.e. wheel material) has a significant effect on the sticking behavior.

Conclusion

The sticking test which is presented in Himsel et al. (2013) can easily be varied in order to gain new information on sticking effects. The test sets described here are varied in two points: surface roughness and wheel material. Therefore the surface roughness of the used fiber samples was differed in even – average – rough. By using the same amount of resin for boards with even surface the sticking effect is higher in comparison to rough surfaces. On the other hand, the materials of the machinery parts have a strong effect on the sticking behavior, which was shown by the differences between polypropylene and stainless steel. Beside the surface and material effects a significant change of the sticking behavior is caused by the age of the resin.

The results show that the sticking phenomenon is influenced by a lot of different factors. In summary, the rheometer method developed by Himsel et al. (2013) allows to test the sticking behavior in dependency of surface properties and material effects.

References

ASTM D2979-88. Standard test method for pressure-sensitive tack of adhesives using an inverted probe machine. Annual Book of ASTM Standards. Vol. 15.06.

ASTM D3121-89. Standard test method for tack of pressure-sensitive adhesives by rolling ball. Annual Book of ASTM Standards. Vol. 15.06.

ASTM E1333-10. Standard test method for determining formaldehyde concentrations in air and emission rates from wood products using a large chamber. Annual Book of

ASTM Standards. Vol. 04.10.

Himsel, A., Müller, U., Kantner, W., Moser, J., Mitter, R., and Herwijnen, H.W.G. van. Novel analytical method to determine factors causing unwanted sticking of glued wood particles onto machinery parts. To be published in the Proceedings of the 2013 International Conference on Wood Adhesives.

Kantner, W., Moser, J., Heinemann, C., and Stöckel, F., Novel Analyses of Low Emission Resins, Conference on Wood Adhesives, Lake Tahoe, USA, 2009.

Roberts, R.A. Review of Methods for the Measurement of Tack. [Project PAJ1 - Report]. 1997, [online: <http://www.adhesivestoolkit.com/Docu-Data/NPLDocuments/P%20A%20J/PAJ%20Reports/PAJ1%20Reports/PAJ1%20Report%205.pdf>], 22/08/2013.

Schmidt, M., Knorz, M., and Wilmes, B.. 2010. A novel method for monitoring real-time curing behaviour, Wood Science and Technology 4: 407-420.

Acknowledgements

Funded by EFRE and Land Niederösterreich (project number WST 3-T/-9/021-2012)

Elaboration of Hybrid Materials Based on TEMPO-Oxidized Cellulose Gel and Silica Nanoparticles

Chloé Maury¹; Khalil Jradi^{1,}; Claude Daneault^{1,2}*

¹ Lignocellulosic Material Research Centre, Université du Québec à Trois-Rivières, 3351 Des Forges, Trois-Rivières, Québec G9A 5H7, Canada;

² Canada Research Chair in Value-added Paper, 3351 Des Forges, Trois-Rivières, Québec G9A 5H7, Canada

* Corresponding author: Khalil Jradi (Khalil.jradi@uqtr.ca)

Abstract

In the present study, we report a simple and efficient approach for the fabrication of a hybrid material based on Tempo-oxidized cellulose gel (TOCgel) and silica nanoparticles (SilicaNPs) using the sol-gel process. The advantage in using the TOCgel material is clearly due to the presence of carboxylate (COOH) and hydroxyl (OH) moieties on the surface of TOCgel and also to the nano/micrometric size of their fibers.

In this work, silica NPS were incorporated in the cellulose nanofibers network through two routes: physical and chemical process. In the first one, Silica NPS were physically incorporated in TOCgel fibrous through hydrogen bond. However, the chemical process was accomplished firstly through the use of a cross-link agent (APTES) to realize the covalent coupling (amidation) between the carboxylate moieties of TOCgel and the APTES molecules, and secondly by the in-situ growth of SilicaNPs directly onto the surface of the TOCgel. Resulting composite films (SilicaNPs-TOCgel) were investigated by several techniques including Scanning electron microscopy, FTIR, EDX and XPS spectroscopy, mechanical tests and thermogravimetric analysis. Our results confirmed clearly the grafting state between APTES and TOCgel surface via the formation of amide bond at 1545 cm^{-1} and the strong reduction of the carboxylate moieties of the TOCgel. TGA analysis indicated the presence of silica NPS in the former composite (~ 30 %) for the both process. In the same context, SEM images indicated that the SilicaNPs seemed to be incorporated more homogeneously in the final composite obtained via the chemical process more than that obtained by the physical process. Consequently, mechanical test showed better properties for the former composite obtained through the chemical way than that for the physical one. Finally, because of the good mechanical properties and the well-aligned silica nanoparticles of the SilicaNPs-TOCgel composite films obtained in this work, they can be used as a promising material in applications of sensors, piezo-electric devices.

Keywords: Tempo oxidized cellulose; silica NPS; sol-gel process; amidation; characterization.

Comparing Mechanical and Chemical Properties of Young Transgenic Black Cottonwood Trees Modified for Reduction of Specific Genes in Lignin Biosynthesis

Zachary D. Miller^{1}, Ilona M. Peszlen², Perry N. Peralta²*

¹ PhD Research Assistant, Department of Forest Biomaterials – College of Natural Resources, North Carolina State University, Raleigh NC, USA.

** Corresponding author*

zdmiller@ncsu.edu

² Associate Professor, Department of Forest Biomaterials – College of Natural Resources, North Carolina State University, Raleigh NC,

Abstract

Traditional tree improvement programs are making steady progress towards the enhancement of wood properties but are limited in the time required to make genetic gains. Biotechnology has the potential for making significant genetic improvements to wood properties in a matter of years instead of decades. Recent progress in genetic engineering has been focused on tailor-made trees for specific purposes, such as altered lignin content and structure for more efficient pulping.

In this study, genetically modified six-month-old black cottonwood (*Populus trichocarpa*) clones with modifications to genes located in the lignin biosynthesis pathway were investigated. Black cottonwood was chosen because of its sequenced genome, ease of propagation, fast growth and economic importance. Black cottonwood trees were propagated by rooted cuttings and grown in the Forest Biotechnology greenhouse at NC State. These clones represent a wild type for control and groups that received different genetic modifications based on the steps in the lignin biosynthesis pathway.

The modulus of elasticity (MOE) in three-point bending was measured using a modified micromechanical test method. To study the effect of genetic manipulations on the chemical composition of these clones, sugar and lignin contents were determined using acid hydrolysis. Some clones with severe reductions in MOE values also exhibited severe chemical alterations while MOE reductions of other clones could not be accounted for through sugar and lignin analyses alone.

Keywords: Wood, Lignin, Glucose, Mechanical properties, Chemical properties.

Introduction

Wood, an abundant terrestrial resource, is utilized for a myriad of purposes such as fuel, fibers, building materials, pulp, and a feedstock for biofuels. Research is currently utilizing genetic engineering to modify the composition of wood with particular interest in lignin reduction.

Mechanical Properties

Advances in tree genetic engineering have resulted in trees with different chemical compositions. Wood with reduced lignin content or changed syringyl to guaiacyl ratio can conceivably reduce the chemical input and energy required to break down lignin to access the cellulose (Talukder, 2006). Wood properties that are critical for solid wood applications could be severely affected, however, because lignin imparts compressive support and rigidity. Mechanical testing of transgenic trees with different amounts of lignin is important to determine changes in the structure of the wood.

Standard size specimens have typically been used for mechanical property testing. However, standard size specimens are unobtainable in specimens grown with small diameters. Using micromechanical testing, evaluation procedures have been developed to determine the mechanical properties of small diameter trees (Kasal et al., 2007).

This study's objective was to assess how differing chemical compositions correlate with the wood properties of young (6-month-old) transgenic *P. trichocarpa* with small diameters by analyzing static MOE in three point bending and the sugar/lignin content through acid hydrolysis.

Materials and Methods

Small-diameter black cottonwood *Populus trichocarpa* (Nisqually-1) clones were propagated through rooted cuttings and grown in the Forest Biotechnology Group's greenhouses at North Carolina State University. These sample trees were either a wild type (WT) for control or received genetic modifications in different groups.

Nine sample trees were selected randomly from a group of identical clones and were combined into three groups of biological replicates each containing three specimens. The mean diameter of the stems after the bark was peeled was determined using a digital caliper. The specimens were kept in freezer bags and placed in a freezer to maintain green condition and to prevent fungal degradation. The specimens were removed from the freezer and were defrosted before testing.

Static Modulus of Elasticity Measurements

A modified ASTM D143 standard (Kasal et al., 2007; Horvath et al., 2010) was used to determine static MOE using a 3-point bending test on an MTS mechanical testing machine. A data acquisition system was used to obtain the load-deflection curve. The

diameter of the pith was measured at the point of loading and subtracted from the diameter of the specimen, because it confers no mechanical support to the tree. The 3-point bending mechanism consisted of roller supports to allow for primarily vertical reaction forces at the ends of the specimens. The span was adjusted based on a span-to-diameter ratio of 15 and a specially designed bearing block was used to avoid surface crushing of the specimens.

If the specimen rotated during testing, repositioning of the specimen occurred until no rotation was observed.

Lignin Determination and Sugar Analysis

Specimens were selected for acid hydrolysis based on the results of the mechanical testing. Approximately three biological replicates were milled and combined into one sample for testing and were extracted with benzene/ethanol. The acid-insoluble lignin of the extracted sawdust was determined gravimetrically, while the acid-soluble lignin content was measured by UV-VIS absorption (Sluiter et al. 2010). The concentration of sugars (glucose, xylose, galactose, arabinose and mannose) was quantified by High Performance Liquid Chromatography (Sluiter et al. 2010).

Experimental analysis of data

Two general linear model procedures with descriptive statistics were utilized using SAS® Enterprise Guide 4.2 (SAS Institute Inc., 2009). The clone group means were compared with the wild-type using Dunnett's comparison test at $\alpha=0.05$ within harvest.

Results

Mechanical Properties

The MOE values found in this study are within the range of those found in the literature for similar poplar trees (e.g. Bendtsen and Senft 1986, Peszlen 1998, Xiang 2011). As expected, reported MOE values for mature black cottonwood tested in the green condition (e.g. FPL 1999) are higher than those obtained in this study. However, Bendtsen and Senft (1986) analyzed individual growth rings of 30-yr-old eastern cottonwood and in the first year of growth found MOE values that were comparable to our results.

Chemical Properties

The lignin content of wild-type trees and transgenic trees ranged from ~10% to 22%. The transgenic samples generally had significantly higher glucose contents than the wild-type with values up to ~51%. There was very little correlation between MOE and lignin content and no correlations were found between MOE and the content of hemicelluloses.

Summary and Conclusions

The mechanical properties and chemical composition of five- to six-month-old wild-type and transgenic black cottonwood were studied in this investigation. These results

highlight the importance that the chemical assembly of the wood has on mechanical properties. Modifications that reduce a major cell wall component, whether it be cellulose, hemicelluloses or lignin, have the potential to result in significant reductions in mechanical properties and all components must be present for the cell wall to function properly.

References

Bendtsen, B. A., and Senft, J. (1986). Mechanical and anatomical properties in individual growth rings of plantation-grown eastern cottonwood and loblolly pine. *Wood and Fiber Science*, 18(1):22-38.

FPL (1999). *Wood Handbook-Wood as An Engineering Material*. General Technical Report FPL-GTR-113. USDA Forest Service Forest Products Laboratory, Madison, WI. pp. 4-4.

Horvath, L., Peszlen, I., Peralta, P., Kasal, B., and Li, L. G. (2010). Mechanical properties of genetically engineered young aspen with modified lignin content and/or structure. *Wood and Fiber Science*, 42:310-317.

Kasal, B., Peszlen, I., Peralta, P., and Li, L. (2007). Preliminary tests to evaluate the mechanical properties of young trees with small diameter. *Holzforshung*, 61:390-393.

Peszlen, I. (1998). Variation in specific gravity and mechanical properties of poplar clones. *Drevársky Vyskum*, 43(2), 1-17.

SAS Institute Inc. 2009. *SAS Enterprise Guide 4.2*. SAS Institute Inc., Cary, North Carolina.

Sluiter, A., B. Hames, R. Ruiz, C. Scarlata, J. Sluiter, D. Templeton and D. Crocker (2010). Determination of structural carbohydrates and lignin in biomass: laboratory analytical procedure (LAP); NREL/TP-510-42618. Golden, Colorado, National Renewable Energy Laboratory.

Talukder, K. (2006). Low-lignin wood – a case study. *Nature biotechnology*, 24(4):395-396.

Xiang, Z. (2011). *Effects of Genetic Modification and Drying Stresses on Wood Properties*. M.S. thesis, North Carolina State University, Raleigh, NC. 100 pp.

Novel Imaging and 3D rendering Techniques to Visualise Spiral Grain in *Pinus radiata*

Jimmy Thomas

Central Wood Testing Laboratory, The Rubber Board,
Manganam Post, Kottayam, Kerala, India
woodtechnologist@gmail.com

and,

School of Biological Sciences, University of Canterbury,
Christchurch, New Zealand

David A. Collings

School of Biological Sciences, University of Canterbury,
Christchurch, New Zealand
david.collings@canterbury.ac.nz

We have developed a novel technique to visualise the development of spiral grain in year old *Pinus radiata* trees that is based on tracking the orientation of axial resin canals. 60 µm-thick complete serial transverse sections covering a stem length of nearly 10 mm were imaged at high resolution (2400 dpi) with a professional flatbed scanner using circular-polarised transmitted light. Slides were scanned between linear polarising films oriented at right angles to each other, with these surrounding sheets of quarter wave-retarder film oriented at an angle of 45°. This generated circularly polarised light. Because resin canal parenchyma cells have primary walls that are only mildly birefringent compared to tracheid secondary walls, resin canals appear as black spots against the bright background caused by the birefringent tracheids. Images were aligned with ImageJ macros, and a series of image processing steps were applied to the aligned stack in ImageJ which included thresholding and particle analysis to identify and map the location of the canals. Only resin canals were identified, and these were shown as white dots in the resultant image stack which was used to generate a 3D view of spiral grain using the '3D Viewer' plug-in in ImageJ. The 3D visualisation showed the organisation of resin canals, and thus spiral grain, inside the wood. Imaging confirmed the rapid onset of spiral grain, with a near vertical adjacent to the pith reorienting to a strong left-handed spiral within the first year of growth. Our method should provide new insights in to our understanding on the formation of spiral grain.

Keywords: circular polarised light, image analysis, radiata pine, resin canals, spiral grain

Methods for Observing and Measuring Spiral Grain in Pine and Other Trees

Spiral grain is notorious for its effects in devaluing the wood from pines, as it leads to a reduction in strength of sawn timber (Cown et al., 1991) and has a negative effect on the surface smoothness (Sepúlveda, 2001) which may result in the downgrading in quality and the rejection of large proportions of sawn boards (Johansson et al., 2001). Cown et al. (1996) estimated that over 90% of drying problems in *Pinus radiata* are related to twist which is related to both diameter and spiral grain. In Europe, the annual loss caused by distortion due to spiral grain in dried timber was estimated to nearly €1 billion (Tarvainen, 2005).

To understand how spiral grain forms, it is necessary to investigate grain at the cellular level. Modern approaches to analysing this problem include confocal microscopy (Ogata and Fujita, 2005), computed tomography and digital imaging coupled with image analysis. However, our attempts to image spiral grain with confocal microscopy were unsuccessful for a variety of reasons, notably the limited field of view and depth of laser penetration.

Instead, we imaged the resin canals present within pine wood, and used these as a proxy for grain. Resin canals are the tubular intercellular ducts that occur in most conifers (IAWACommittee et al., 2004). They run parallel to the tracheids and, in transverse sections, are scattered, either solitary or in groups. Because of their large size and length, resin canals are much easier to track than tracheids. Werker and Fahn (1969) found that in *Pinus halepensis* shoots, the pattern and development of the vascular tissues and resin canals were closely related, matching earlier studies from Bannan (1936). Based on further experiments and observations, we hypothesised that the vertical resin canals in radiata pine follow the wood grain and that by measuring their angle of orientation, the spiral grain angle can be assessed. Thus, to study the grain orientation in radiata pine wood, we developed a novel technique involving imaging the transverse sections with circular polarised light followed by 3D reconstruction of the images, using simple image processing tools available in the freeware programme ImageJ (Rasband, 1997-2009).

Materials and Methods

Small stem sections (25 mm in length) were cut from one year old trees and preserved in formaldehyde / acetic acid / alcohol fixative. A score mark was made vertically down the stem to allow for the subsequent aligning of sections. Segments were thoroughly washed in warm water (30°C, 15 min) and 70 or more 60 µm-thick transverse sections (corresponding to 4.5 mm or more of stem) were cut with a sliding microtome (HM400, Microm, Walldorf, Germany). Complete transverse sections, which were up to 10 mm in diameter, were washed in warm distilled water and blotted on a filter paper for few seconds. They were carefully transferred to a microscope slide and mounted in glycerol.

The complete stem transverse sections were imaged with a professional flatbed scanner (Epson Perfection V700 Photo) at 2400 dpi and in 24 bit colour, and saved as TIFF images. For this, slides were placed on a sheet of linear polarising film (polariser) (catalogue number NT38-491, Edmund Optics, Singapore) on the scanner bed and a second sheet of linear polarising film oriented at right angles (analyser) to the polariser to create linear polarised light (Fig. 1a) (Arpin et al., 2002). Two sheets of quarter wave-retarder films (catalogue number NT27-344, Edmund Optics) were added to the optical path on either side of the microscope slides, and at an angle of 45° to the linear polarising sheets. This meant that the wood sections were imaged with circularly polarised light (Fig. 1c) (Higgins, 2010).

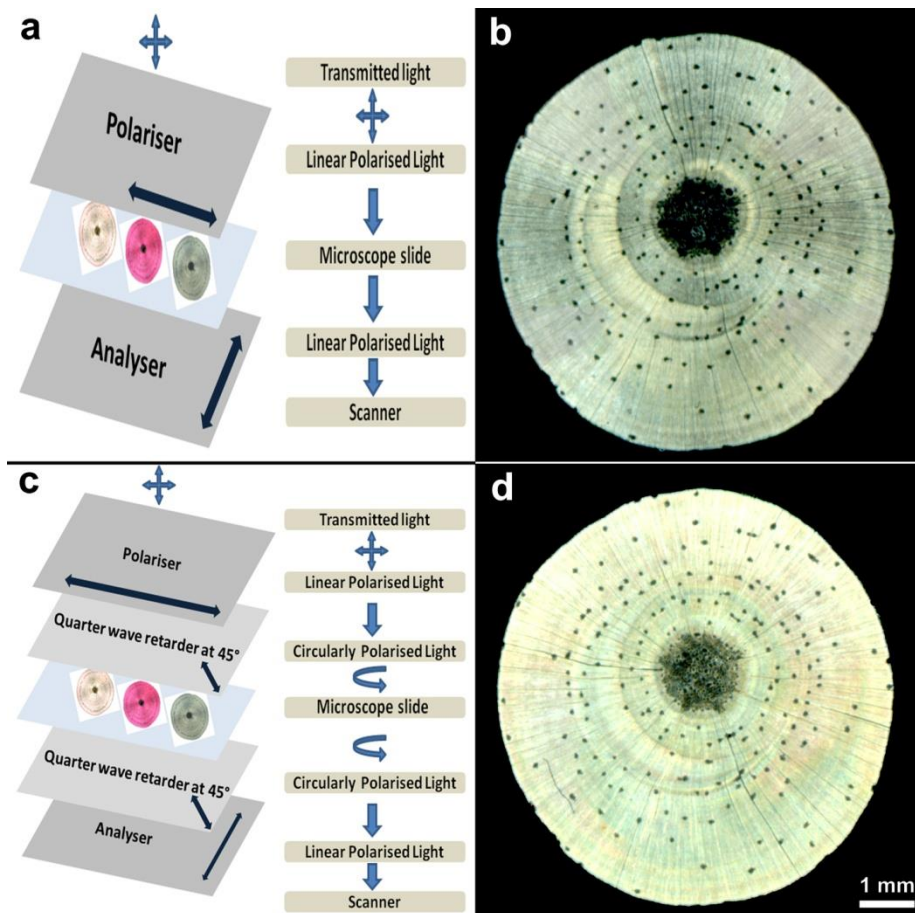


Figure 1 Use of crossed polarisers substantially improved the visibility of resin canals.

- a. Schematic representation of the imaging technique with linear polarised light.
- b. Imaging with linear polarised light. The scan showed the ‘Maltese cross’ effect, with the image being slightly darker in the vertical and horizontal parts.
- c. Schematic representation of the imaging technique with circular polarised light.
- d. Imaging with circular polarised light, demonstrating even lighting across the sample.

Using ImageJ, 3-dimensional reconstruction of the resin canals that had been imaged with circular polarised light resulted in the visualisation of spiral grain. A series of images corresponding to the serial sections through the stem was collated, and the background of each image was filled with white to enable a uniform thresholding. These images were partially aligned manually in Photoshop. Subsequently, the collated images were built into an image stack and processed with ImageJ. Individual images were converted to 8 bit images. Brightness and contrast were standardised within the stack by 'Image' – 'Adjust' – 'Brightness/ Contrast.' (Fig. 2a) The canvas size was then made square by 'Image' – 'Adjust' – 'Canvas size' and the images were aligned using an ImageJ plugin 'StackReg'. Because this plugin defaulted to aligning items within the image, and because the non-birefringent resin canals dominated the image, the 'StackReg' plugin gave straight resin canals and induced a twist within the stem, as judged by the rotation of the vertical score mark. A custom plugin, 'Cumulative Rotation' was used to correct this rotation, and to make the score mark straight within the image stack. Once the stack was aligned, uniform thresholding was applied by 'Image' – 'Adjust' – 'Threshold' and the scale converted from imperial units into metric units (94.49 pixels per mm for a 2400 dpi scanner image) (Fig. 2b). The 'Analyze particles' function detected and measured the location of the resin canals with the following settings: size= 25 - 500 square pixels, circularity= 0.5 to 1.0, and with the option 'Show Masks' selected. The measurements to be collected from the image were set with the 'Analyze' – 'Set measurements' function, and were 'Area', 'Centroid' (that is, where the centre of the object was) and 'Stack position'. The output from the 'Show masks' option was a file that showed the location of all the resin canals detected, with non-measured objects excluded, (Fig. 2c) and this was used to generate a 3D image of spiral grain using the plug-in '3D Viewer.' The canal centroid positions have been used to measure spiral grain angles.

Results

Imaging Stem Transverse Sections with a Flatbed Scanner

Wood transverse sections were imaged with crossed polarisers, and with this arrangement, background light was eliminated by the polariser-analyser duo (Fig. 1b). However, the presence of an anisotropic, birefringent material (the thin section of wood) between the crossed polarisers rotated the plane of polarised light and allowed some light to pass through the analyser. Thus, the cross sections through the stem appeared bright against a dark background. Resin canals, however, being composed of a wall-free duct and parenchyma cells that contain only a thin, unligified cell wall, did not rotate the light as much as the surrounding wood and appeared dark. Subtle variations in secondary wall brightness were apparent, with both ring patterns and darker fringes running horizontally and vertically. This 'Maltese cross' pattern, in which the image is brightest on the diagonals and darkest in the vertical and horizontal directions, is typical of polarised light images (Fig. 1b) (Foster, 1997). However, its presence in the images complicated automated image analysis based on thresholding. To overcome this, a pair of quarter wave retarder-films was added to the light path to give circular polarised light (Fig. 1d) (Foster, 1997; Higgins, 2010). Their addition substantially improved the

visibility of the resin canals, removed the Maltese cross effect and gave more even contrast across image. This made the images suitable for automated analysis.

3-Dimensional Image Reconstructions and Analysis of Grain Orientation

Unlike previously published serial section studies in which the area analysed was limited, 60 µm-thick whole cross sections (8 to 10 mm stem diameter) were analysed, and resin canals were used as a proxy for grain as these cells form from the same fusiform initials as the tracheids and run parallel to them (Bannan, 1936; Werker and Fahn, 1969).

Within individual images, resin canals were arranged in concentric bands around the pith (Fig. 2e). By aligning serial sections (Fig. 2d) and plotting the locations of the canals within these, it was possible to generate a map of spiral grain within the wood piece (Fig. 2f). The canals nearest to the pith nearly straight and those in the outer regions twisted leftwards. As the resin canals follow the tracheids, this twisting of the resin canals demonstrated the rapid and early onset of spiral grain within the first several millimetres of wood formation outside the pith. However, our initial analysis has demonstrated that even though the pattern of resin canal orientation and grain change had some consistency, there were large variations among the different trees in the amount of twisting present.

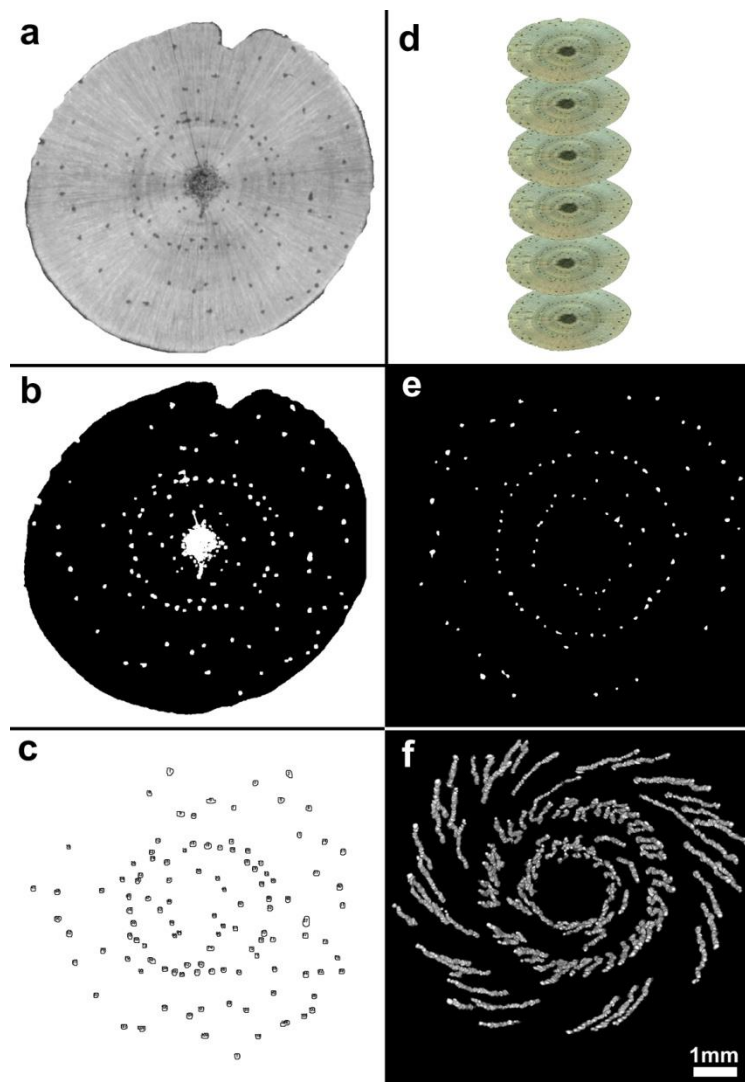


Figure 1 3-dimensional visualisation of spiral grain followed by the detection of canals using ImageJ.

- a.** 8 bit image.
- b.** Transverse section and the resin canals detected.
- c.** Resin canals detected, counted and their area measured.
- d.** Stack of images created with ImageJ.
- e.** Resin canals were arranged in concentric around the pith.
- f.** 3-dimesional visualisation of resin canals and spiral grain using the entire stack.

Discussion

Imaging Stem Transverse Sections with a Flatbed Scanner

The imaging technique employed in this study, using a combination of the polariser films (Arpin et al., 2002) and quarter wave-retarder films (Foster, 1997; Higgins, 2010), is a novel approach to create high-contrast images suitable for any modern image analysis programme. The approach replicates the combination of polariser and the analyser film used in polarised light microscopy but is particularly useful for imaging large areas which can be difficult with conventional microscopy. The addition of correctly-oriented quarter wave-retarder films to the optical path generated circular polarised light and substantially improved the quality of images produced by eliminating the ‘Maltese cross’ effect. Circular polarised light has previously been suggested as a way in which to overcome these image asymmetries (Higgins, 2010). However the use of circular polarised light with automatic image analysis is novel and this new imaging technique is simple to create, convenient to operate and provides better quality images.

Resin Canals as an Indicator of Grain

Resin canals were previously used as markers for spiral grain orientation (Harris, 1989; Koehler, 1955; Noskowiak, 1963) although LaPasha and Wheeler (1990) reported that the orientation of the vertical resin canals is quite straight relative to the long axis of the trunk. Literature reports suggest that resin canals in *Pinus* derive from the same cambial cells as the tracheids (Bannan, 1936), and thus are parallel to the grain. Observations from serial sections and subsequent measurements with X-ray microtomography, have confirmed this (data not shown). These observations coupled with our own findings on the twisted wood samples paved the basis of this new technique and subsequent 3D reconstructions.

For imaging grain across an entire stem, even one as small as 10 mm in diameter as used in this study, tracheids as visualised by light microscopy make a poor target by comparison with resin canals. This is because the tracheids are much shorter by comparison (2-4 mm long, depending on position and age of the tree) and have smaller cross sectional dimensions (average diameter 20-30 μm). The larger dimensions of the canals, with an average diameter of about 100 μm , makes the canals visible even to the naked eye, and they were easy to track along the length of the stem through the serial cross sections when viewed with circular polarised light. This meant that the resin canals provided a much superior target to track changes in grain pattern by image processing and 3D visualisation.

Spiral Grain Develops Rapidly in Young Trees

This study confirmed the early onset of left-handed spiral grain in radiata pine trees, an organisation previously reported (Cown et al., 1991). In general, the resin canals near to the pith showed lower spiralling, being either vertical or sometimes even weakly right-handed, whereas the canals near to the cambium were highly spiralled in a left-handed direction. This technique has provided a novel way to understanding these wood quality issues. Orientation of the resin canals has shown the grain deviation along the length of the stem and hence this 3D reconstruction technique would give a great opportunity to

study the generation and progression of spiral grain in wood. This study is, therefore, the first attempt to look at grain across an entire stem but considering events at a cellular level.

As the visualisation of resin canals inside the wood is now possible, and their orientation was observed to follow the grain, studying the organisation and arrangement of resin canals is an excellent tool to study the occurrence of spiral grain. These experiments were extended to 5 each of tilted and rocked trees, and the same stubs were imaged with X-ray microtomography and fluorescence microscopy and confirmed the methodology.

Acknowledgements

JT gratefully acknowledges funding for his PhD scholarship generously provided by Scion Ltd, Rotorua, New Zealand during this work.

References

- Arpin TL, Mallol C, Goldberg P. Short Contribution: A new method of analyzing and documenting micromorphological thin sections using flatbed scanners: Applications in geoarchaeological studies. *Geoarchaeology: An International Journal* (2002) 17:305-313.
- Bannan MW. Vertical resin ducts in the secondary wood of the *Abietineae*. *New Phytologist* (1936) 35:11-46.
- Cown DJ, Haslett AN, Kimberley MO, McConchie DL. The influence of wood quality on lumber drying distortion. *Annals of Forestry Science* (1996) 53:1177-1188.
- Cown DJ, Young GD, Kimberley MO. Spiral grain patterns in plantation-grown *Pinus radiata*. *New Zealand Journal of Forestry Science* (1991) 21:206-216.
- Foster B. *Optimizing light microscopy for biological and clinical laboratories*. (1997) Dubuque, Iowa, USA.
- Harris JM. *Spiral grain and wave phenomena in wood formation*. (1989) Springer-Verlag, Berlin, Germany.
- Higgins MD. Imaging birefringent minerals without extinction using circularly polarised light. *The Canadian Mineralogist* (2010) 48:231-235.
- IAWA Committee, Richter HG, Grosser D, Heinz I, Gasson PE. IAWA List of microscopic features for softwood identification. *IAWA Journal* (2004) 25:1-70.
- Johansson M, Perstorper M, Klinger R, Johansson G. Distortion of Norway spruce timber Part 2. Modelling twist. *Holz als Roh- und Werkstoff* (2001) 59:155-162.
- Koehler A. *Guide to determining slope of grain in lumber and veneer*. (1955) FPL-1585, US Forest Service Report Madison, Wisconsin, USA.
- LaPasha CA, Wheeler EA. Resin canals in *Pinus taeda*: longitudinal canal lengths and interconnections between longitudinal and radial canals. *IAWA Journal* (1990) 11:227-238.
- Noskowiak AF. Spiral grain in trees - A review. *Forest Products journal* (1963) 13:266-275.

*Proceedings of the 57th International Convention of Society of Wood Science and Technology
June 23-27, 2014 - Zvolen, SLOVAKIA*

- Ogata Y, Fujita M. New anatomical method of grain angles measurement using confocal microscopy and image cross correlation. *Trees* (2005) 19:73-80.
- Rasband WS. ImageJ (1997-2009) Bethesda, MD: National Institute of Health, USA.
- Sepúlveda P. Measurement of spiral grain with computed tomography. *Journal of Wood Science* (2001) 47:289-293.
- Tarvainen V. Measures for improving quality and shape stability of sawn softwood timber during drying and under service conditions - Best practice manual to improve straightness of sawn timber. (2005) VTT Publications Otamedia Oy, Espoo, Finland.
- Werker E, Fahn A. Resin ducts of *Pinus halepensis* Mill. - Their structure, development and pattern of arrangement. *Botanical Journal of the Linnean Society* (1969) 62:379-411.

